

Pertanika Journal of  
**SCIENCE &  
TECHNOLOGY**

**JST**

**VOL. 31 (1) JAN. 2023**



PERTANIKA  
JOURNALS

A scientific journal published by Universiti Putra Malaysia Press

# PERTANIKA JOURNAL OF SCIENCE & TECHNOLOGY

## About the Journal

### Overview

Pertanika Journal of Science & Technology is an official journal of Universiti Putra Malaysia. It is an open-access online scientific journal. It publishes original scientific outputs. It neither accepts nor commissions third party content.

Recognised internationally as the leading peer-reviewed interdisciplinary journal devoted to the publication of original papers, it serves as a forum for practical approaches to improve quality on issues pertaining to science and engineering and its related fields.

Pertanika Journal of Science & Technology is a **quarterly** (*January, April, July, and October*) periodical that considers for publication original articles as per its scope. The journal publishes in **English** and it is open for submission by authors from all over the world.

The journal is available world-wide.

### Aims and scope

Pertanika Journal of Science & Technology aims to provide a forum for high quality research related to science and engineering research. Areas relevant to the scope of the journal include: bioinformatics, bioscience, biotechnology and bio-molecular sciences, chemistry, computer science, ecology, engineering, engineering design, environmental control and management, mathematics and statistics, medicine and health sciences, nanotechnology, physics, safety and emergency management, and related fields of study.

### History

Pertanika Journal of Science & Technology was founded in 1993 and focuses on research in science and engineering and its related fields.

### Vision

To publish a journal of international repute.

### Mission

Our goal is to bring the highest quality research to the widest possible audience.

### Quality

We aim for excellence, sustained by a responsible and professional approach to journal publishing. Submissions can expect to receive a decision within 90 days. The elapsed time from submission to publication for the articles averages 180 days. We are working towards decreasing the processing time with the help of our editors and the reviewers.

### Abstracting and indexing of Pertanika

Pertanika Journal of Science & Technology is now over 27 years old; this accumulated knowledge and experience has resulted the journal being abstracted and indexed in SCOPUS (Elsevier), Clarivate Web of Science (ESCI), EBSCO, ASEAN CITATION INDEX, Microsoft Academic, Google Scholar, and MyCite.

### Citing journal articles

The abbreviation for Pertanika Journal of Science & Technology is *Pertanika J. Sci. & Technol.*

### Publication policy

*Pertanika* policy prohibits an author from submitting the same manuscript for concurrent consideration by two or more publications. It prohibits as well publication of any manuscript that has already been published either in whole or substantial part elsewhere. It also does not permit publication of manuscript that has been published in full in proceedings.

### Code of Ethics

The *Pertanika* journals and Universiti Putra Malaysia take seriously the responsibility of all of its journal publications to reflect the highest in publication ethics. Thus, all journals and journal editors are expected to abide by the journal's codes of ethics. Refer to *Pertanika's Code of Ethics* for full details, or visit the journal's web link at [http://www.pertanika.upm.edu.my/code\\_of\\_ethics.php](http://www.pertanika.upm.edu.my/code_of_ethics.php)

### Originality

The author must ensure that when a manuscript is submitted to *Pertanika*, the manuscript must be an original work. The author should check the manuscript for any possible plagiarism using any program such as Turn-It-In or any other software before submitting the manuscripts to the *Pertanika* Editorial Office, Journal Division.

All submitted manuscripts must be in the journal's acceptable similarity index range:  
**≤ 20% – PASS; > 20% – REJECT.**

### International Standard Serial Number (ISSN)

An ISSN is an 8-digit code used to identify periodicals such as journals of all kinds and on all media—print and electronic.

Pertanika Journal of Science & Technology: e-ISSN 2231-8526 (Online).

### Lag time

A decision on acceptance or rejection of a manuscript is reached in 90 days (average). The elapsed time from submission to publication for the articles averages 180 days.

### Authorship

Authors are not permitted to add or remove any names from the authorship provided at the time of initial submission without the consent of the journal's Chief Executive Editor.

### Manuscript preparation

Most scientific papers are prepared according to a format called IMRAD. The term represents the first letters of the words *Introduction, Materials and Methods, Results, And Discussion*. IMRAD is simply a more 'defined' version of the "IBC" (*Introduction, Body, Conclusion*) format used for all academic writing. IMRAD indicates a pattern or format rather than a complete list of headings or components of research papers; the missing parts of a paper are: *Title, Authors, Keywords, Abstract, Conclusions, References, and Acknowledgement*. Additionally, some papers include *Appendices*.

The *Introduction* explains the scope and objective of the study in the light of current knowledge on the subject; the *Materials and Methods* describes how the study was conducted; the *Results* section reports what was found in the study; and the *Discussion* section explains meaning and significance of the results and provides suggestions for future directions of research. The manuscript must be prepared according to the journal's **Instruction to Authors** ([http://www.pertanika.upm.edu.my/Resources/regular\\_issues/Regular\\_Issues\\_Instructions\\_to\\_Authors.pdf](http://www.pertanika.upm.edu.my/Resources/regular_issues/Regular_Issues_Instructions_to_Authors.pdf)).

### Editorial process

Authors who complete any submission are notified with an acknowledgement containing a manuscript ID on receipt of a manuscript, and upon the editorial decision regarding publication.

*Pertanika* follows a **double-blind peer-review** process. Manuscripts deemed suitable for publication are sent to reviewers. Authors are encouraged to suggest names of at least 3 potential reviewers at the time of submission of their manuscripts to *Pertanika*, but the editors will make the final selection and are not, however, bound by these suggestions.

Notification of the editorial decision is usually provided within 90 days from the receipt of manuscript. Publication of solicited manuscripts is not guaranteed. In most cases, manuscripts are accepted conditionally, pending an author's revision of the material.

As articles are double-blind reviewed, material that may identify authorship of the paper should be placed only on page 2 as described in the first-4-page format in *Pertanika*'s **Instruction to Authors** ([http://www.pertanika.upm.edu.my/Resources/regular\\_issues/Regular\\_Issues\\_Instructions\\_to\\_Authors.pdf](http://www.pertanika.upm.edu.my/Resources/regular_issues/Regular_Issues_Instructions_to_Authors.pdf)).

### The journal's peer review

In the peer-review process, 2 to 3 referees independently evaluate the scientific quality of the submitted manuscripts. At least 2 referee reports are required to help make a decision.

Peer reviewers are experts chosen by journal editors to provide written assessment of the **strengths** and **weaknesses** of written research, with the aim of improving the reporting of research and identifying the most appropriate and highest quality material for the journal.

### **Operating and review process**

What happens to a manuscript once it is submitted to *Pertanika*? Typically, there are 7 steps to the editorial review process:

1. The journal's Chief Executive Editor and the Editor-in-Chief examine the paper to determine whether it is relevance to journal needs in terms of novelty, impact, design, procedure, language as well as presentation and allow it to proceed to the reviewing process. If not appropriate, the manuscript is rejected outright and the author is informed.
2. The Chief Executive Editor sends the article-identifying information having been removed, to 2 to 3 reviewers. They are specialists in the subject matter of the article. The Chief Executive Editor requests that they complete the review within 3 weeks.

Comments to authors are about the appropriateness and adequacy of the theoretical or conceptual framework, literature review, method, results and discussion, and conclusions. Reviewers often include suggestions for strengthening of the manuscript. Comments to the editor are in the nature of the significance of the work and its potential contribution to the research field.

3. The Editor-in-Chief examines the review reports and decides whether to accept or reject the manuscript, invite the authors to revise and resubmit the manuscript, or seek additional review reports. In rare instances, the manuscript is accepted with almost no revision. Almost without exception, reviewers' comments (to the authors) are forwarded to the authors. If a revision is indicated, the editor provides guidelines for attending to the reviewers' suggestions and perhaps additional advice about revising the manuscript.
4. The authors decide whether and how to address the reviewers' comments and criticisms and the editor's concerns. The authors return a revised version of the paper to the Chief Executive Editor along with specific information describing how they have addressed' the concerns of the reviewers and the editor, usually in a tabular form. The authors may also submit a rebuttal if there is a need especially when the authors disagree with certain comments provided by reviewers.
5. The Chief Executive Editor sends the revised manuscript out for re-review. Typically, at least 1 of the original reviewers will be asked to examine the article.
6. When the reviewers have completed their work, the Editor-in-Chief examines their comments and decides whether the manuscript is ready to be published, needs another round of revisions, or should be rejected. If the decision is to accept, the Chief Executive Editor is notified.
7. The Chief Executive Editor reserves the final right to accept or reject any material for publication, if the processing of a particular manuscript is deemed not to be in compliance with the S.O.P. of *Pertanika*. An acceptance letter is sent to all the authors.

The editorial office ensures that the manuscript adheres to the correct style (in-text citations, the reference list, and tables are typical areas of concern, clarity, and grammar). The authors are asked to respond to any minor queries by the editorial office. Following these corrections, page proofs are mailed to the corresponding authors for their final approval. At this point, **only essential changes are accepted**. Finally, the manuscript appears in the pages of the journal and is posted on-line.



Pertanika Journal of

**SCIENCE  
& TECHNOLOGY**

Vol. 31 (1) Jan. 2023



A scientific journal published by Universiti Putra Malaysia Press



## EDITOR-IN-CHIEF

**Luqman Chuah Abdullah**  
*Chemical Engineering*

## CHIEF EXECUTIVE EDITOR

**Mohd Sapuan Salit**

## UNIVERSITY PUBLICATIONS COMMITTEE

### CHAIRMAN

**Nazamid Saari**

### EDITORIAL STAFF

#### Journal Officers:

Kanagamalar Silvarajoo, *ScholarOne*  
Siti Zuhaila Abd Wahid, *ScholarOne*  
Tee Syin Ying, *ScholarOne*  
Ummi Fairuz Hanapi, *ScholarOne*

#### Editorial Assistants:

Ku Ida Mastura Ku Baharom  
Siti Juridah Mat Arip  
Zulinaardawati Kamarudin

#### English Editor:

Norhanizah Ismail

### PRODUCTION STAFF

#### Pre-press Officers:

Nur Farrah Dila Ismail  
Wong Lih Jiu

### WEBMASTER

#### IT Officer:

Illi Najwa Mohamad Sakri

### EDITORIAL OFFICE

#### JOURNAL DIVISION

Putra Science Park  
1<sup>st</sup> Floor, IDEA Tower II  
UPM-MTDC Technology Centre  
Universiti Putra Malaysia  
43400 Serdang, Selangor Malaysia.

Gen Enquiry  
Tel. No: +603 9769 1622 | 1616  
E-mail:  
[executive\\_editor.pertanika@upm.edu.my](mailto:executive_editor.pertanika@upm.edu.my)  
URL: [www.journals-jd.upm.edu.my](http://www.journals-jd.upm.edu.my)

### PUBLISHER

UPM Press  
Universiti Putra Malaysia  
43400 UPM, Serdang, Selangor, Malaysia.  
Tel: +603 9769 8851  
E-mail: [penerbit@putra.upm.edu.my](mailto:penerbit@putra.upm.edu.my)  
URL: <http://penerbit.upm.edu.my>



### ASSOCIATE EDITOR

#### 2021-2023

**Adem Kilicman**  
*Mathematical Sciences*  
Universiti Putra Malaysia, Malaysia

**Miss Laiha Mat Kiah**  
*Security Services Sn: Digital Forensic, Steganography, Network Security, Information Security, Communication Protocols, Security Protocols*  
Universiti Malaya, Malaysia

**Saidur Rahman**  
*Renewable Energy, Nanofluids, Energy Efficiency, Heat Transfer, Energy Policy*  
Sunway University, Malaysia

### EDITORIAL BOARD

#### 2022-2024

**Abdul Latif Ahmad**  
*Chemical Engineering*  
Universiti Sains Malaysia, Malaysia

**Ho Yuh-Shan**  
*Water research, Chemical Engineering and Environmental Studies*  
Asia University, Taiwan

**Mohd Zulkifly Abdullah**  
*Fluid Mechanics, Heat Transfer, Computational Fluid Dynamics (CFD)*  
Universiti Sains Malaysia, Malaysia

**Ahmad Zaharin Aris**  
*Hydrochemistry, Environmental Chemistry, Environmental Forensics, Heavy Metals*  
Universiti Putra Malaysia, Malaysia

**Hsiu-Po Kuo**  
*Chemical Engineering*  
National Taiwan University, Taiwan

**Mohd. Ali Hassan**  
*Bioprocess Engineering, Environmental Biotechnology*  
Universiti Putra Malaysia, Malaysia

#### Azlina Harun@Kamaruddin

*Enzyme Technology, Fermentation Technology*  
Universiti Sains Malaysia, Malaysia

**Ivan D. Rukhlenko**  
*Nonlinear Optics, Silicon Photonics, Plasmonics and Nanotechnology*  
The University of Sydney, Australia

**Nor Azah Yusof**  
*Biosensors, Chemical Sensor, Functional Material*  
Universiti Putra Malaysia, Malaysia

#### Bassim H. Hameed

*Chemical Engineering: Reaction Engineering, Environmental Catalysis & Adsorption*  
Qatar University, Qatar

**Lee Keat Teong**  
*Energy Environment, Reaction Engineering, Waste Utilization, Renewable Energy*  
Universiti Sains Malaysia, Malaysia

**Norbahiah Misran**  
*Communication Engineering*  
Universiti Kebangsaan Malaysia, Malaysia

#### Biswajeet Pradhan

*Digital image processing, Geographical Information System (GIS), Remote Sensing*  
University of Technology Sydney, Australia

**Mohamed Othman**  
*Communication Technology and Network, Scientific Computing*  
Universiti Putra Malaysia, Malaysia

**Roslan Abd-Shukur**  
*Physics & Materials Physics, Superconducting Materials*  
Universiti Kebangsaan Malaysia, Malaysia

#### Daud Ahmad Israf Ali

*Cell Biology, Biochemical, Pharmacology*  
Universiti Putra Malaysia, Malaysia

#### Mohd Shukry Abdul Majid

*Polymer Composites, Composite Pipes, Natural Fibre Composites, Biodegradable Composites, Bio-Composites*  
Universiti Malaysia Perlis, Malaysia

**Wing Keong Ng**  
*Aquaculture, Aquatic Animal Nutrition, Aqua Feed Technology*  
Universiti Sains Malaysia, Malaysia

#### Hari M. Srivastava

*Mathematics and Statistics*  
University of Victoria, Canada

### INTERNATIONAL ADVISORY BOARD

#### 2021-2024

#### CHUNG, Neal Tai-Shung

*Polymer Science, Composite and Materials Science*  
National University of Singapore, Singapore

#### Mohamed Pourkashanian

*Mechanical Engineering, Energy, CFD and Combustion Processes*  
Sheffield University, United Kingdom

#### Yulong Ding

*Particle Science & Thermal Engineering*  
University of Birmingham, United Kingdom

#### Hiroshi Uyama

*Polymer Chemistry, Organic Compounds, Coating, Chemical Engineering*  
Osaka University, Japan

#### Mohini Sain

*Material Science, Biocomposites, Biomaterials*  
University of Toronto, Canada

### ABSTRACTING AND INDEXING OF PERTANIKA JOURNALS

The journal is indexed in SCOPUS (Elsevier), Clarivate-Emerging Sources Citation Index (ESCI), BIOSIS, National Agricultural Science (NAL), Google Scholar, MyCite, ISC. In addition, Pertanika JSSH is recipient of "CREAM" Award conferred by Ministry of Higher Education (MoHE), Malaysia.



**Pertanika Journal of Science & Technology**  
**Vol. 31 (1) Jan. 2023**

**Contents**

Foreword <i>Mohd Sapuan Salit</i>	i
Real-Time Monitoring of Oil Temperature in Distribution Power Transformer by Using Internet of Things <i>Shafrida Sahrani, Nur Darina Ahmad, Ramizi Mohamed, Mohd Aizam Talib and Chaw Jun Kit</i>	1
A Study on Features of Different Tone Quality in a Kenong Set <i>Ahmad Faudzi Musib, Sinin Hamdan and Saiful Hairi Othman</i>	17
Computational Analysis of Polymer Melt Filling in a Medical Mold Cavity During the Injection Molding Process <i>Muhammad Khalil Abdullah, Mohd Syakirin Rusdi, Mohd Zulkifly Abdullah, Abdus Samad Mahmud, Zulkifli Mohamad Ariff, Khor Chu Yee and Mohd Najib Ali Mokhtar</i>	33
Blade Fault Localization with the Use of Vibration Signals Through Artificial Neural Network: A Data-Driven Approach <i>Ngui Wai Keng, Mohd Salman Leong, Mohd Ibrahim Shapiai and Lim Meng Hee</i>	51
<i>Case Study</i> Structural Comparison of Naturally Aspirated and Turbocharged Diesel Engine for Steel and Aluminium Made Radiator: A Finite Element Study <i>Asad Munir, Muhammad Fauzinizam Razali, Nasir Iqbal and Muhammad Tahir Amin</i>	69
The Impacts of Passive Design Strategies on Building Indoor Temperature in Tropical Climate <i>Maryam Qays Olewi and Mohd Farid Mohamed</i>	83
Study of Metabolic Flux Distribution in Rice ( <i>Oryza sativa</i> ) Cultures for Starch Production <i>Nur Aqila Syafiqqa Abdul Nuri, Noor Illi Mohamad Puad, Muhammad Yusuf Abduh and Azlin Suhaida Azmi</i>	109
Prediction of Daily Air Pollutants Concentration and Air Pollutant Index Using Machine Learning Approach <i>Nurul A'isyah Mustakim, Ahmad Zia Ul-Saufie, Wan Nur Shaziayani, Norazian Mohamad Noor and Sofianita Mutalib</i>	123

Real-Time Traffic Sign Recognition Using Deep Learning <i>Ananya Belagodu Shivayogi, Nehal Chakravarthy Matasagara Dharmendra, Anala Maddur Ramakrishna and Kolala Nagaraju Subramanya</i>	137
<i>Review Article</i>	
A Systematic Review on an Optimal Dose of Disaster Preparedness Intervention Utilizing Health Belief Model Theory <i>Mohd Tariq Mhd Noor, Hayati Kadir Shahar, Mohd Rafee Baharudin, Sharifah Norkhadijah Syed Ismail, Rosliza Abdul Manaf, Salmiah Md Said, Jamilah Ahmad and Sri Ganesh Muthiah</i>	149
<i>Review Article</i>	
A Review: Requirements Prioritization Criteria Within Collaboration Perspective <i>Tan Amelia and Rozlina Mohamed</i>	161
Contamination and Human Health Risk Assessment of Toxic Trace Elements in Drinking Water of Gilgit-Baltistan, Pakistan <i>Syed Jarar Hussain, Shaukat Ali, Javid Hussain, Salar Ali, Jamal Hussain, Manzoor Hussain and Ittehad Hussain</i>	187
Development of Flood Hazard Index (FHI) of the Kelantan River Catchment Using Geographic Information System (GIS) Based Analytical Hierarchy Process (AHP) <i>Zulkarnain Hassan and Ain Nihla Kamarudzaman</i>	203
<i>Review Article</i>	
Fibre-Reinforced Soil Mixed Lime/Cement Additives: A Review <i>Sakina Tamassoki, Nik Norsyahariati Nik Daud, Mohammad Nazir Nejabi and Mohammad Jawed Roshan</i>	217
Technology Adoption for STEM Education in Higher Education: Students' Experience from Selected Sub-Saharan African Countries <i>Jumoke Iyabode Oladele, Musa Adekunle Ayanwale and Mdutshekelwa Ndlovu</i>	237
Towards Designing a Framework for Adaptive Gamification Learning Analytics in Quranic Memorisation <i>Siti Hasrinafasya Che Hassan, Syadiah Nor Wan Shamsuddin and Nor Hafizi Yusof</i>	257
<i>Review Article</i>	
A Review of Optical Ultrasound Imaging Modalities for Intravascular Imaging <i>Munyaradzi Charles Rushambwa, Rimer Suvendi, Thanyani Pandelani, Rajkumar Palaniappan, Vikneswaran Vijejan and Fizza Ghulam Nabi</i>	279

Timekeeping and Immediate Monitoring of Employees by Consistently Advocating Time Consciousness and Honesty Using Enhanced Attendance Monitoring System (TIME CATCH Using EAMS) <i>Ronald Bautista Rivera, Maricar Bulan Asis and Oscar Gacutan Bangayan</i>	291
ESS-IoT: The Smart Waste Management System for General Household <i>Shen Yuong Wong, Huashuo Han, Kin Meng Cheng, Ah Choo Koo and Salman Yussof</i>	311
<i>Review Article</i>	
Some Abiotic and Biotic Factors Influencing Firefly Population Abundance in Southeast Asia: A Review <i>Nurhafizul Abu Seri, Azimah Abd Rahman and Nur Faeza Abu Kassim</i>	327
Optimization of the Formulation of Sago Starch Edible Coatings Incorporated with Nano Cellulose Fiber (CNF) <i>Rahmiyati Kasim, Nursigit Bintoro, Sri Rahayoe and Yudi Pranoto</i>	351
<i>Short Communication</i>	
Latent and Manifest Variables of PLS-SEM Model in the Decision Making of PIKNET Sound Wave-Based Attractor Innovation by Fishermen in Bulak Sub-District, Surabaya, Indonesia <i>Nurul Rosana, Nuddin Harahab, Gatot Ciptadi, Andi Kurniawan, Suryadhi, Safriudin Rifandi, Amirul Mukminin and Viv Djanat Prasita</i>	373
The Effect of Varying the HCl Solution on the Purity, Morphological, and Electrical Properties of Silicon Dioxide Extracted from Rice Straw <i>Nazopatul Patonah Har, Endah Kinarya Palupi, Rofiqul Umam, Aminullah, Md Wahadoszamen, Irmansyah and Irzaman</i>	389
Weed Detection in Soybean Crop Using Deep Neural Network <i>Vinayak Singh, Mahendra Kumar Gourisaria, Harshvardhan GM and Tanupriya Choudhury</i>	401
Failure Behavior and Mechanism of Pultruded Kenaf/Glass Hybrid Composite Under Compressive Impact Loading <i>Muhammad Fauzinizam Razali, Sareh Aiman Hilmi Abu Seman, Mohd Syakirin Rusdi and Megat Naiman Megat Anorhisham</i>	425
A Comparative Study on Dengue-related Knowledge, Attitude, and Practice in Hotspot and Non-Hotspot Areas in Selangor <i>Siti Nor Izani Mustapha, Shamarina Shohaimi, Mohd Bakri Adam, Meenakshii Nallappan, Abdul Hafiz Ab Rahman and Nader Salari</i>	437



<i>Review Article</i>	
Review of Window Performance in A Hot and Humid Climate	457
<i>Zinnirah Wellun, Wardah Fatimah Mohammad Yusoff, Mohd Farid Mohamed, Mohd Khairul Azhar Mat Sulaiman and Mohammad Rasidi Mohammad Rasani</i>	
Predicting Students' Inclination to TVET Enrolment Using Various Classifiers	475
<i>Chia Ming Hong, Chee Keong Ch'ng and Teh Raihana Nazirah Roslan</i>	
Water Quality Assessment and Characterization of Rivers in Pasir Gudang, Johor via Multivariate Statistical Techniques	495
<i>Muhammad Syafiq Mohamad Desa, Mohd Aeddy Sulaiman and Shantakumari Rajan</i>	
Ammonia-Nitrogen Reduction in Low Strength Domestic Wastewater by Polyvinyl Alcohol (PVA) Gel Beads	511
<i>Nordin Sabli and Norzarina Zakaria</i>	
Effects of Various Doses of <i>Saccharomyces cerevisiae</i> on the Growth, Survival Rate, and Blood Profile of Saline Red Tilapia ( <i>Oreochromis spp.</i> ) in the Semi-Intensive Culture Conditions	529
<i>Istiyanto Samidjan, Diana Rachmawati, Safar Dody and Putut Har Riyadi</i>	
<i>Review Article</i>	
Chitosan Nanocomposites as Wound Healing Materials: Advances in Processing Techniques and Mechanical Properties	543
<i>Temitope T. Dele-Afolabi, Azmah Hanim Mohamed Ariff, Oluwatosin J. Ojo- Kupiluyi and Ebenezer Oluwatosin Atoyebi</i>	
Brain Tumour Region Extraction Using Novel Self-Organising Map-Based KFCM Algorithm	577
<i>Peddamalla Gangadhara Reddy, Tirumala Ramashri and Kayam Lokesh Krishna</i>	
<i>Review Article</i>	
Reliability Components of Online Teaching and Learning Tools in Lesotho Higher Education Institutions: A Systematic Review	595
<i>Musa Adekunle Ayanwale, Paseka Andrew Mosia, Rethabile Rosemary Molefi and Liapeng Shata</i>	
Alternative Design of One-Sided Shewhart Control Charts for the Multivariate Coefficient of Variation	615
<i>XinYing Chew</i>	

# Foreword

Welcome to the first issue of 2023 for the *Pertanika Journal of Science and Technology (PJST)*!

PJST is an open-access journal for studies in Science and Technology published by Universiti Putra Malaysia Press. It is independently owned and managed by the university for the benefit of the world-wide science community.

This issue contains 35 articles; eight review articles; a case study; a short communication and the rest are regular articles. The authors of these articles come from different countries namely Afghanistan, Bangladesh, China, India, Indonesia, Iran, Japan, Kingdom of Bahrain, Lesotho, Malaysia, Nigeria, Pakistan, Philippines, South Africa and Zimbabwe.

The next article discussed the blade fault localization method centered on time-frequency feature extraction and a machine learning approach. The experiment found that both feature sets can localize the blade fault position. In addition, the classification results too revealed that the Genetic Algorithm-based feature selection method could eliminate unnecessary features and improve classification precision, including network generalization. Finally, the selected features of the statistical and newly proposed features were combined to enhance the diagnosis performance further. As a result, the classification rate for blade fault localization was 83.47%. Details of this study are available on page 51.

An investigation to predict daily air pollutants concentration and air pollutant index using a machine learning approach was conducted by Nurul A'isyah Mustakim and co-researchers from Universiti Teknologi MARA and Universiti Malaysia Perlis, Malaysia. The major air pollutants in Malaysia that contribute to air pollution are carbon monoxide, sulfur dioxide, nitrogen dioxide, ozone, and particulate matter. Predicting the air pollutants concentration can help the government to monitor air quality and provide awareness to the public. This study focuses on an industrial, the Petaling Jaya monitoring station in Selangor. Predictive modeling that can predict the air pollutants concentrations for the next day using a tree-based approach was constructed. From comparing the three models, a random forest is the best-proposed model. Further details of the investigation can be found on page 123.

A regular article titled “Development of Flood Hazard Index (FHI) of the Kelantan River Catchment using Geographic Information System (GIS) based Analytical Hierarchy Process (AHP)” was presented by Zulkarnain Hassan and Ain Nihla Kamarudzaman. This study used the Kelantan River catchment’s flood hazard index (FHI) based on the analytical hierarchy process (AHP) to identify and classify the flood occurrence. According to the AHP model, the annual rainfall was the first ranked parameter in terms of importance weight score. Moreover, Tanah Merah and Jeli were the high-risk areas for floods. Therefore, the present study suggests that the GIS-based AHP can be highly effective for mapping flood hazards and benefit flood management decision-making. Detailed information on this study is available on page 203.

We anticipate that you will find the evidence presented in this issue to be intriguing, thought-provoking and useful in reaching new milestones in your own research. Please recommend the journal to your colleagues and students to make this endeavour meaningful.

All the papers published in this edition underwent Pertanika’s stringent peer-review process involving a minimum of two reviewers comprising internal as well as external referees. This was to ensure that the quality of the papers justified the high ranking of the journal, which is renowned as a heavily-cited journal not only by authors and researchers in Malaysia but by those in other countries around the world as well.

We would also like to express our gratitude to all the contributors, namely the authors, reviewers, Editor-in-Chief and Editorial Board Members of PJST, who have made this issue possible.

PJST is currently accepting manuscripts for upcoming issues based on original qualitative or quantitative research that opens new areas of inquiry and investigation.

**Chief Executive Editor**  
**Professor Ir. Dr. Mohd Sapuan Salit**  
[executive\\_editor.pertanika@upm.edu.my](mailto:executive_editor.pertanika@upm.edu.my)

## Real-Time Monitoring of Oil Temperature in Distribution Power Transformer by Using Internet of Things

Shafrida Sahrani<sup>1\*</sup>, Nur Darina Ahmad<sup>2</sup>, Ramizi Mohamed<sup>3</sup>, Mohd Aizam Talib<sup>4</sup> and Chaw Jun Kit<sup>1</sup>

<sup>1</sup>Institute of IR4.0, Universiti Kebangsaan Malaysia, 43600 UKM, Bangi, Selangor, Malaysia

<sup>2</sup>Centre for Electrical Engineering Studies, Universiti Teknologi MARA, 13500 UiTM, Pulau Pinang, Malaysia

<sup>3</sup>Faculty of Engineering and Built Environment, Universiti Kebangsaan Malaysia, 43600 UKM, Bangi, Selangor, Malaysia

<sup>4</sup>TNB Labs Sdn. Bhd., 43000, Kajang, Selangor, Malaysia

### ABSTRACT

In Malaysia, on-site technical personnel manually inspect power transformers. Some vital condition indicators, such as oil and winding temperatures, are not monitored in real-time. This condition can be hazardous if the transformer gets overheated. Overheating can cause mechanical deformation and insulation degradation if not monitored regularly. Thus, an online monitoring system that meets industry standards is needed to enhance power transformer monitoring and troubleshooting. In this research, the Internet of Things (IoT) based data acquisition (DAQ) system was deployed for real-time oil temperature monitoring and inspection to detect incipient faults in power transformers early. This IoT-based DAQ system was connected to the substation remote terminal unit (RTU) to update real-time data on each power transformer. The long-range (LoRa) technology is proposed for the system to transmit temperature, current, and voltage from the power transformers. The

data transmission from the oil temperature indicator (OTI), network server, and database was monitored and compared. It is observed that the temperature data was transferred from the network server to the database without any transmission delay. The average deviation from the two experiments was 0.006 and 0.003, respectively, compared to the manual reading from the OTI scale meter with a digital reading by the proposed DAQ system. For testing purposes, the alert

### ARTICLE INFO

#### Article history:

Received: 16 February 2022

Accepted: 07 June 2022

Published: 19 August 2022

DOI: <https://doi.org/10.47836/pjst.31.1.01>

#### E-mail addresses:

shafrida@ukm.edu.my (Shafrida Sahrani)

nurdarina9183@uitm.edu.my (Nur Darina Ahmad)

ramizi@ukm.edu.my (Ramizi Mohamed)

aizam.talib@tnb.com.my (Mohd Aizam Talib)

chawjk@ukm.edu.my (Chaw Jun Kit)

\*Corresponding author

module in this system would notify technical personnel if the temperature exceeded +40°C in the power transformers. The proposed system can be used to assist with the upgrade and maintenance of the existing power transformer.

*Keywords:* Data acquisition (DAQ) system, Internet of Things (IoT), LoRa technology, oil temperature indicator (OTI), power transformers, real-time monitoring

---

## INTRODUCTION

Power transformers are vital to enable electrical energy transmission, distribution, and generation in electrical network circuits. Transformers are designed to operate for 20 to 30 years; if properly used, their lifespan may exceed 40 years. Damages or ageing of a power transformer's external or internal part can adversely reduce its efficiency and lifespan (Hernández-Callejo, 2019; Martin et al., 2017). Area blackout may happen if the power transformer fails in its operation. Besides, any faulty is hazardous due to a large amount of oil in direct contact with high voltage (HV) elements (Christian & Gläser, 2017). A higher risk of explosion and fire is deleterious to human safety and surroundings. Such a hazardous event lowers the reliability of the power system and incurs financial damages. Hence, it is crucial to enhance power transformer monitoring and troubleshooting (Wani et al., 2021; Xie et al., 2020).

There are internal and external faults in power transformers. Internal faults, for example, high current flow, can deteriorate the insulation. Mechanical damage can also occur when the cooling mechanism fails to function properly. It may gradually turn into a serious fault, such as overheating, winding failure, and oil contamination (Chandran et al., 2021; Murugan & Ramasamy, 2019). Most of these faults can be prevented through testing and maintenance. An external fault is a damage that cannot be prevented or predicted, such as lightning, earthquakes, or an abnormal tension causing a direct failure. These hazards stress the transformer, which may be of concern and may shorten the transformer's life. In Malaysia, technical personnel manually inspect power transformers on-site. Routine preventative maintenance and testing are executed on a regular basis. However, some vital condition indicators, e.g., oil and winding temperatures, are left unmonitored on a real-time basis (Ghazali et al., 2009). This condition can be hazardous if the transformer's temperature fluctuates and gets overheated. Overheating can occur when temperatures exceed the rating for the insulation system. The insulation will deteriorate and lose its mechanical, electrical, and chemical strength, thereby reducing the lifespan of the transformer or causing early failure (Singh et al., 2020). It can cause more significant damage if it is not monitored regularly. Other methods, such as oil sample quality, dissolved gas, and furfural analyses, are used to check the condition of the power transformer, which requires costly field visits and laboratory sample testing. Thus, a crucial need is emerging for an online monitoring

system in accordance with the industry standards to enhance power transformer monitoring and troubleshooting.

The shifting dynamics in the global power market seek cutting-edge transformer technology. The use of grid sensors contributes to the digital transformation of electrical substations (Liu et al., 2020; Butt et al., 2021; Pong et al., 2021; Raghavan et al., 2021). Smart monitoring via the Internet of Things (IoT) technology offers asset owners access to real-time power transformer conditions regardless of location. Thus, transformer conditions may be assessed without on-site technical personnel, saving precious resources and time. Integrating IoT into transformer technology enhances the basic network of power transmission and its stability (Gajenthiran et al., 2022; Wang et al., 2020). The IoT technology connects node sensors and network devices with power transformers in a flexible, secure, and cost-effective manner. It minimises operational overheads in condition-based maintenance, thus initiating evolution in the energy segment in this digital era.

Several methods have been proposed for power transformer smart monitoring systems. Wireless communication via the ZigBee network was introduced to monitor the frequency of all loads, energy, power, current and voltage in a distribution transformer (Guardarrama et al., 2016). Such real-time monitoring system applies ADE7753 IC and BeagleBone Black with ZigBee Pro S2 as the primary monitoring device. Zigbee covers short-range wireless communication with low energy consumption, thus suitable for urban distribution electric networks. A mobile embedded system for monitoring temperature, oil level, current, humidity, and vibration of a distribution transformer is proposed by Pawar et al. (2017). The PIC18F4550 microcontroller and the Global System for Mobile (GSM) - General Packet Radio Service (GPRS) communication module were used to collect and transmit data. Alert messages were sent via Short Message Service (SMS) when the parameters exceeded predetermined thresholds. However, this monitoring system lacks the server and database modules. The long-range (LoRa) technology implemented with Arduino Uno and selected sensors was used to monitor and diagnose voltage, current, oil and winding temperatures, as well as silica gel status in the breather of distribution transformers (Kumar & Ajitha, 2018). The system displayed continuous monitoring and alerted abnormality. Nonetheless, the database environment was also omitted in this paper.

The field-programmable gate arrays (often shortened to FPGA) embedded controller is introduced for a high-speed IoT-based power transformer monitoring system with a recording function (Zhao et al., 2019). Parameters such as transformer temperatures, circuit breaker status, power, frequency, and voltage are monitored, recorded and stored at network-attached storage (NAS) through the Local Area Network (LAN). The LAN network only covers a small geographical area. A data acquisition (DAQ) system using GPRS and communication with SCADA by DNP3 protocol was initiated for online temperature monitoring systems in power transformers (Kunicki et al., 2020). The system

used Raspberry PI 3B/B+ combined with converters as the basic hardware component. Temperature gradient and ambient temperature were measured in the study. The incorporation of GPRS in the system was limited to power transformers in remote regions. Using satellite communication to monitor power transformers in remote areas without network coverage will be costly. The online monitoring system for distribution transformer based on cloud side end collaboration of IoT is proposed by Zu et al. (2021). The GSM is used as a communication module and the PIC18F458 microcontroller as a core processing chip for hardware. This system can shorten the response time for information status when compared with the existing system. However, GSM technology can only operate in areas with the mobile network coverage. Most cellular operators are retiring GPRS and GSM to make room for Long Term Evolution (LTE) and 5G technologies.

These reviews summarise the identified research gap in the existing power transformer smart monitoring system; the usage of short-range wireless communication, wired network, limited coverage for rural areas and unavailability of the database management system. Based on these findings, a reliable IoT-based DAQ system with LoRa technology for real-time oil temperature monitoring for power transformers is proposed. LoRa is a centralised network that provides a broad range of coverage in urban, rural, and indoor environments with low power consumption.

## METHODOLOGY

The proposed IoT-based DAQ system consists of hardware and software parts in this research. The hardware includes the measurement unit, which is the sensor node, wireless communication, and data transmission modules. The software part is comprised of the diagnostic unit, which is the data processing, communication protocol, and data monitoring modules. This IoT-based DAQ system was designed to enable smart grid initiatives in urban and rural areas or indoor environments in accordance with the industry standards with a reliable database module. The following section discusses the proposed IoT-based DAQ system architecture with LoRa technology.

### System Architecture

Figure 1 presents the block diagram of the proposed IoT-based DAQ system to monitor real-time oil temperature in the power transformer. The system denotes the integration of the LoRa sensor node with a multi-channel LoRaWAN gateway as a measurement unit. This unit will be installed in the selected Remote Terminal Unit (RTU) in Regional Control Centre (RCC) at the substation to gather input and output (I/O) signals from the existing power transformer. First, real-time data such as oil and winding temperature reading were retrieved from the power transformer temperature indicator at RTU. Next, the data were transmitted to the network server, which served as the central data repository. It also functioned as routing IoT data between devices and applications.



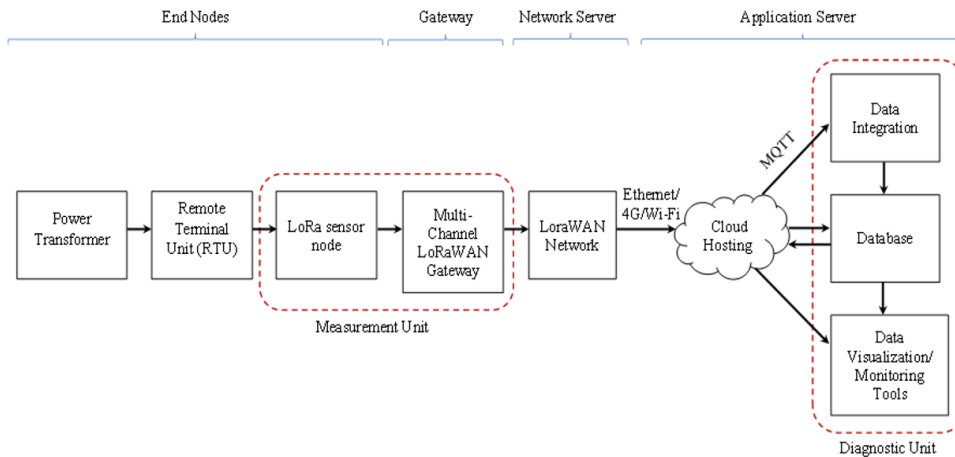


Figure 1. Block diagram of the DAQ system for oil temperature online monitoring in power transformer

The network server was connected to cloud hosting as a storage resource and outsourced data for integration via IoT communication protocol, Message Queuing Telemetry Transport (MQTT). Data were added to the time series database, which could manage massive volumes of data points per second. The time series data may be visualised using analytics platform tools as a diagnostic unit. Such a tool aids technical personnel in analysing and monitoring the pattern of oil temperature data in a power transformer over a certain duration by indicating its location, time, and severity level. This tool can be viewed on any mobile device, tablet, and computer for convenient usage anytime and anywhere.

The alert system module will notify technical personnel if any abnormality is detected in the power transformer. Hence, the technical personnel may take apt measures to hinder failures and power transformer outages. The transformer reliability is also enhanced upon determining the transformer condition in real-time compared to conventional monitoring. Furthermore, immediate corrective/preventive maintenance that increases the lifespan of a power transformer can slash operational costs and resources. Therefore, the proposed system fills the gap in terms of long-range wireless communication and a reliable IoT-based DAQ for the power transformer smart monitoring system. The following section describes the specific equipment and methods utilised in the proposed system.

### Power Transformer Temperature Indicator

Oil and winding temperatures are the critical parameters determined in power transformers. Proper monitoring of these parameters is crucial for electrical asset managers, maintenance teams, and electrical system operators. Two temperature indicators are the oil temperature indicator (OTI) and the winding temperature indicator (WTI). These indicators measure the instantaneous temperature based on the principle of thermal imaging (Askari et al., 2021).

They record the maximum temperature rise of windings and oil in the power transformer. OTI and WTI give alarm and control signals that activate the cooling control systems in a power transformer when the temperature hits a predetermined maximum limit. It can extend the lifespan of a transformer (Patel & Chothani, 2020). Failure or incorrect indication of these devices may have an important impact on transformer ageing. It may also affect the transformer's reliability. Utility experience shows that most transformer maintenance is devoted to OTI/WTI (Sparling, 2017).

Figure 2 illustrates a MESSKO BeTech thermometer—the OTI used in this study to directly display oil temperature measurement from the power transformer. This OTI consisted of a TT version temperature sensor (Figure 3) connected to a measurement unit via a capillary tube. The sensor converted the temperature value to the electrical signal of 4-20 mA and/or 0-5 V DC. Its required power supply was 24V. The OTI/WTI was equipped with a pointer that could turn to display the temperature on a scale. The measuring range for this OTI was 0-150°C. It was also used to measure low voltage (LV) and high voltage (HV) winding temperatures.

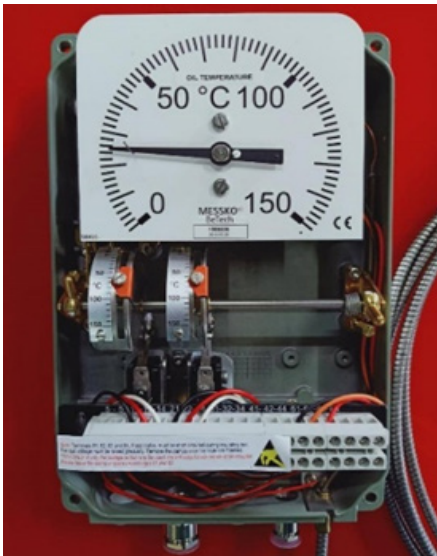


Figure 2. MESSKO BeTech thermometer



Figure 3. TT version sensor

## LoRa Technology

The LoRa radio technology denotes a wireless protocol for long-range transmission with low-power communication (Faber et al., 2020). It is used for Machine-to-Machine (M2M) and IoT applications. The LoRa operates 865-867 MHz and 920-923 MHz bands

in Asia. Wirelessly connects sensors, machines, gateways, and devices to the cloud. LoRa communication protocol uses the unlicensed radio spectrum in the Industrial, Scientific and Medical (ISM) band (Polak & Milos, 2020). The LoRa signal efficiently provides enough coverage for urban, rural and indoor environments with low development costs.

In this paper, LoRaWAN Gateway (Multi-Channel with 4G) was deployed to transmit and receive data from the TT version sensor to the LoRaWAN network. It has a built-in GPS module connected to the SX1308 chip directly for ultra-low power or indoor solution. It is connected concurrently with the LoRa board using 4G, Ethernet or Wi-Fi. This gateway can serve multiple devices simultaneously. It can detect LoRa board input and output (I/O) signals as far as 10 km apart. Thus, this technology can monitor several power transformers within the range.

### **Messaging and Data Exchange for IoT**

MQTT refers to a lightweight messaging protocol with rapid response time (Mishra & Kertesz, 2020; Shanmugapriya et al., 2021). It is based on the subscribe-and-publish model. This protocol can translate messages among devices, servers, and applications. The MQTT can transfer data even with unstable connections. It is an excellent option for sending high volumes of sensor data to cloud solutions and analytics platforms. This protocol is suitable for any small device with low power consumption. It is primarily used for low-bandwidth connections to remote locations. It is also ideal for small devices that require efficient battery usage and bandwidth. Turning to this study, the MQTT was deployed as a light and energy-efficient communication protocol to monitor real-time oil temperature in a power transformer.

### **Measurement Unit**

Figure 4 illustrates a schematic diagram of the measurement unit to retrieve the input and output (I/O) signal from the TT version sensor on the MESSKO BeTech-OTI meter. This study applied the Talk<sup>2</sup> Whisper Node AVR LoRa board, a low-power version of Atmel AVR ATmega328p. It has a built-in LoRa Wireless communication of RFM95/96 sub-GHz module radio (Semtech SX1276). The board can be powered with a minimum of 0.9 V (alkaline battery) or connected to a 5 V power supply. In addition, the W25X40CL 4MBit SPI Flash is attached to the board, suitable to store more data from the power transformer and capable of running for over a year.

The IoT technology used to monitor the condition of real-time power transformer at substation requires continual power. Figure 5 displays the experimental power consumption data for the proposed circuit diagram in its measurement unit. The power consumption is calculated as given in Equation 1 (Patel, 2012):

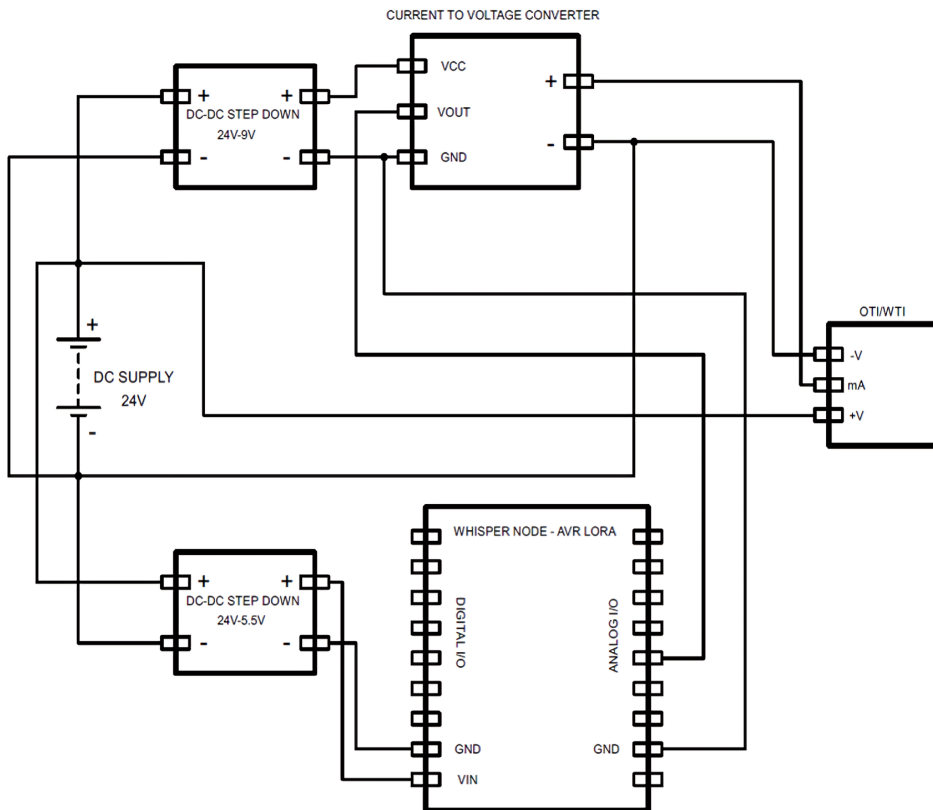


Figure 4. Schematic diagram

$$P_{offset} = V_{cc} \times I_{offset} \tag{1}$$

The power consumption increased to 0.126 watts upon load addition. More power was required as the circuit was connected to the LoRaWAN network, and data were continuously retrieved from the OTI TT version sensor. The proposed system is only suitable for operation in cyclic sleep mode if a battery is used. Battery power limits the system’s capacity and dismisses its viability for emerging IoT devices and sensors with the LoRaWAN network. The use of new or rechargeable batteries and their servicing and replacement has been proven costly (Al Shaqsi et al., 2020).

This research applied two units of DC-DC step-down power converter (24V-9V and 24V-5.5V). They were connected to the Whisper node and OTI/WTI, which demanded a 24V power supply for operation. In actual practice, this measurement unit is installed at the RTU. The temperature data collected by the measurement unit were transferred to the network server via a multi-channel LoRaWAN gateway connected to 4G, Ethernet or Wi-Fi.

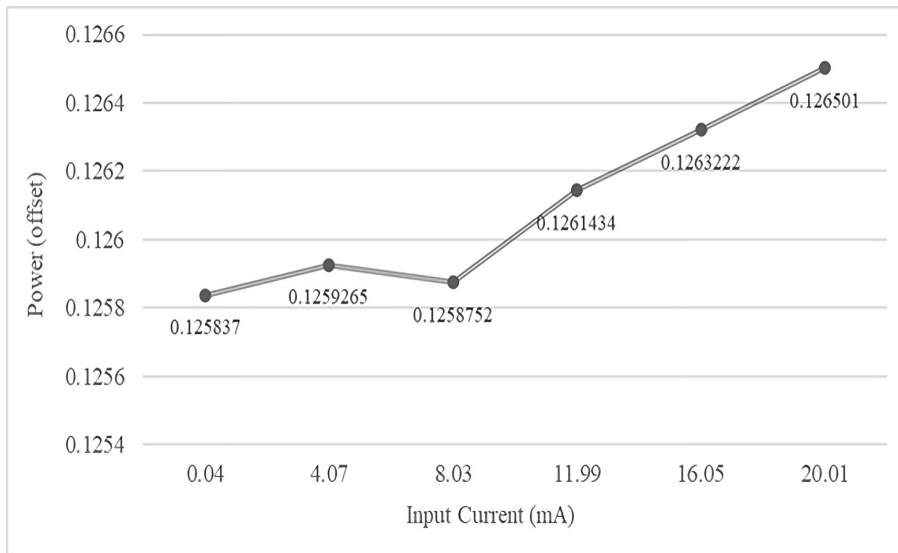


Figure 5. Power consumption

### Diagnostic Unit

Figure 6 portrays the IoT block diagram for oil temperature online monitoring of the power transformer. The data flow from and to the IoT platform using the MQTT protocol. First, data retrieved from the OTI sensor in the measurement unit (Figure 4) were transmitted to the network server; The Things Network (TTN) served as the central repository of data. It also functioned as the routing of IoT data between devices and applications. The TTN was connected to the cloud hosting by Digital Ocean as a storage resource and outsourced the data for integration via the MQTT broker. Node-RED was deployed in this study to wire together the measurement unit, Application Programming Interfaces (APIs), and diagnostic unit to create a smooth data flow in the editor dashboard (Ahmadpanah et al., 2021; Ferencz et al., 2020). Node-RED refers to a JavaScript-based tool built with the Node.js platform. The created flows in Node-RED were stored using JavaScript Object Notation (JSON) format. Next, the data were stored in the InfluxDB database that can manage massive volumes of data points per second. The OTI data stored in InfluxDB can be visualised by using Grafana. This tool indicates a diagnostic unit and can be viewed on all mobile devices, tablets, and computers for convenient usage anytime and anywhere.

Figure 7 illustrates the installation setup in accordance with the schematic and block diagrams. Due to safety concerns, conducting high current experiments on-site with an in-service power transformer is prohibited. In order to make the testing close to the field situation, an electric hot air blower was applied to heat the OTI TT version sensor during the experiment. The electric hot air blower acts as a heat source and is used to emulate the hot temperature of transformer oil in the range of +25°C to +140°C. This situation

is practically identical when the sensor is placed inside the transformer. This laboratory testing is conducted prior to the device being installed on-site.

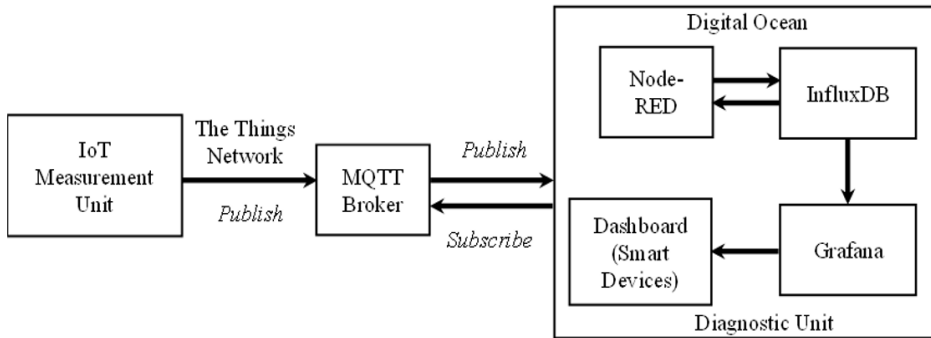


Figure 6. Power transformer oil temperature online monitoring system architecture

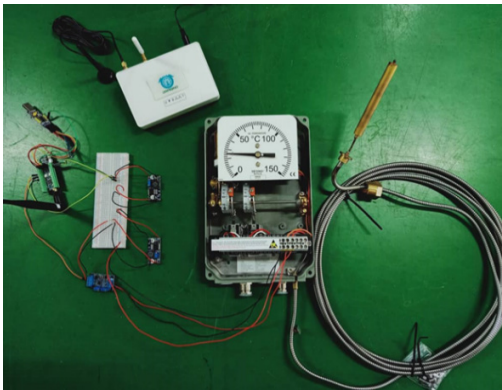


Figure 7. IoT-based DAQ system installation setup

## RESULTS AND DISCUSSIONS

### Temperature Monitoring and Assessment of OTI for Power Transformer

The data transmission from the OTI scale meter, network server TTN and database InfluxDB was monitored and compared. Two cycle readings were taken during the experiment for the temperature ranging between +25°C and +140°C. Table 1 and Table 2 list the readings.

Notably, the temperature data reading was transferred from the TTN network server to the database InfluxDB without transmission delay. The deviation was measured from the manual reading on the OTI scale meter with a digital reading by the proposed DAQ system. The average deviation from the two experiments was found to be 0.006 and 0.003, respectively. The deviation is caused by the capillary tube's response to changes in its surrounding environment by the hot air blower. It is observed that the digital reading by the IoT-based DAQ system is more precise than the analogue OTI scale meter. Figure 8 presented the OTI temperature reading when the system was tested on Grafana at <http://iotsmart.host>. The data recorded and stored in the database could be monitored continuously. Here, the data is stored on a 25GB SSD in Ubuntu 20.04 (LTS) 64bit server.

Table 1

*OTI TT 1<sup>st</sup> cycle sensor reading*

OTI Meter (°C)	TTN (°C)	InfluxDB (°C)	Deviation
26	24.63	24.63	0.0527
30	29.03	29.03	0.0323
40	39.15	39.15	0.0213
50	49.71	49.71	0.0058
60	60.55	60.55	-0.0092
70	70.23	70.23	-0.0033
80	79.32	79.32	0.0085
90	90.76	90.76	-0.0084
100	99.4	99.4	0.0060
110	110.85	110.85	-0.0077
120	119.94	119.94	0.0005
130	132.11	132.11	-0.0162
140	139.29	139.29	0.0051

Table 2

*OTI TT 2<sup>nd</sup> cycle sensor reading*

OTI Meter (°C)	TTN (°C)	InfluxDB (°C)	Deviation
25	24.83	24.83	0.0068
30	29.02	29.02	0.0327
40	39.85	39.85	0.0037
51	49.7	49.7	0.0255
60	60.85	60.85	-0.0142
70	70.03	70.03	-0.0004
80	80.01	80.01	-0.0001
91	90.8	90.8	0.0022
100	99.4	99.4	0.0060
110	110.15	110.15	-0.0014
119	120.14	120.14	-0.0096
130	130.11	130.11	-0.0008
140	140.02	140.02	-0.0001



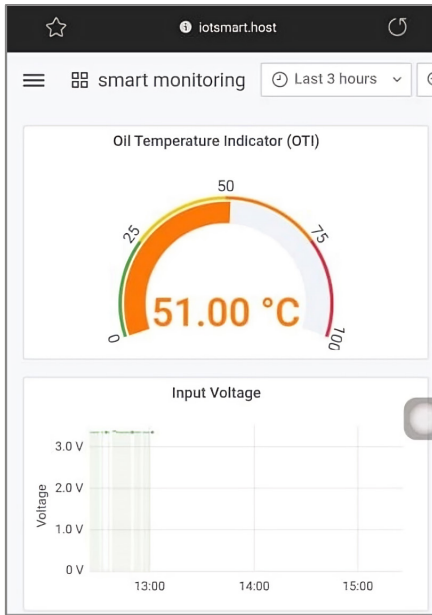


Figure 8. Grafana view for OTI temperature reading

The range of oil temperatures should typically vary between +40°C and +60°C, depending on the operating conditions. These values are based on a maximum ambient temperature of +40°C according to IEEE C57.12.00-2000 standard (IEEE, 2000). The maximum allowable temperature rise for the transformer is usually specified on the transformer nameplate. In this experiment, the notification alert system was set when the temperature exceeded +40°C for testing purposes. In practice, the temperature limit for the on-site alert system will vary based on the requirements of the energy suppliers, as indicated on the transformer’s nameplate. The temperature limit can be determined using the following Equation 2 (Ghosh, 2016):

$$\theta_{top} = \theta_{op} - \theta_{amb} \quad (2)$$

where  $\theta_{top}$  is the top oil temperature rise,  $\theta_{op}$  is the operating temperature, and  $\theta_{amb}$  is the ambient temperature. The notification system is set by using Node-RED as in Figure 9. The alert function would do the operation by sending an e-mail to the person in charge to notify them about the status of the OTI/WTI sensor. The sample for notification alert e-mail is given in Figure 10. Essentially, the proposed IoT-based DAQ system offers a viable solution for real-time online power transformer monitoring.

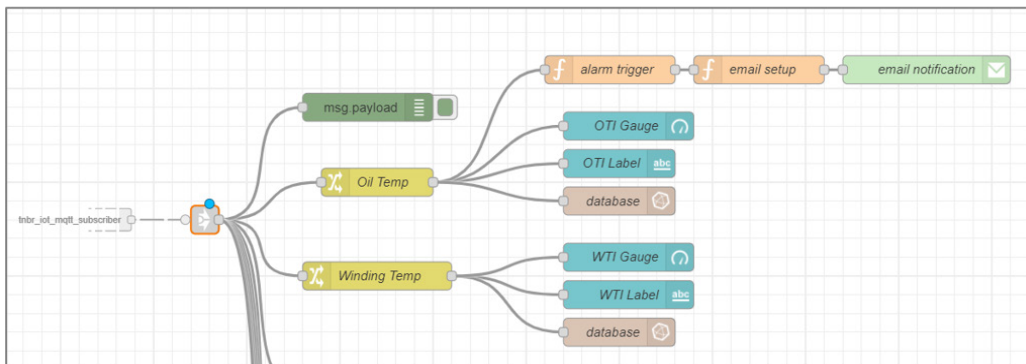


Figure 9. Node-RED flow for alarm trigger and notification

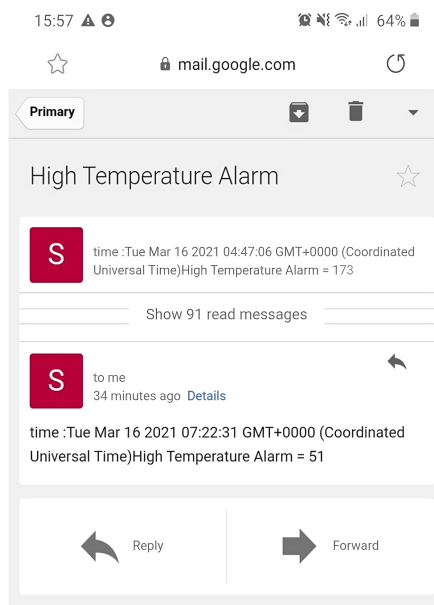


Figure 10. Notification system

## CONCLUSION

This study presents the development and application of an IoT-based DAQ system with LoRa technology for real-time oil temperature monitoring of power transformers. The research was conducted to demonstrate the efficacy of the proposed IoT-based DAQ system. The experimental findings indicate that the temperature data reading was transferred from the network server to the database without any transmission delay. The average deviation from the two experiments was found to be 0.006 and 0.003, respectively, compared to the manual reading from the OTI scale meter with a digital reading by the proposed DAQ system. Thus, it can be used to assist and would give better performance to

monitoring oil temperature as compared to the manual monitoring method. Furthermore, the alert system would notify technical personnel if any abnormality is detected in the distribution power transformer. This system effectively enables asset owners to use the transformers and detect faulty ones prior to catastrophic failure.

## ACKNOWLEDGEMENT

The authors gratefully acknowledge Universiti Kebangsaan Malaysia, TNB Research Sdn Bhd and TNB Labs Sdn Bhd for providing collaboration, laboratory facilities and support throughout the research project.

## REFERENCES

- Ahmadpanah, M. M., Balliu, M., Hedin, D., Olsson, L. E., & Sabelfeld, A. (2021). Securing Node-RED Applications. In D. Dougherty, J. Meseguer, S. A. Mödersheim & P. Rowe (Eds.), *Protocols, strands, and logic* (pp. 1-21). Springer. [https://doi.org/10.1007/978-3-030-91631-2\\_1](https://doi.org/10.1007/978-3-030-91631-2_1)
- Al Shaqsi, A. Z., Sopian, K., & Al-Hinai, A. (2020). Review of energy storage services, applications, limitations, and benefits. *Energy Reports*, 6, 288-306. <https://doi.org/10.1016/J.EGYR.2020.07.028>
- Askari, M. T., Mohammadi, M. J., Pasupuleti, J., Tahmasebi, M., Raveendran, S. K., & Kadir, M. Z. A. A. (2021). Analysis of thermal models to determine the loss of life of mineral oil immersed transformers. *Bulletin of Electrical Engineering and Informatics*, 10(5), 2327-2336. <https://doi.org/10.11591/EEI.V10I5.3131>

- Butt, O. M., Zulqarnain, M., & Butt, T. M. (2021). Recent advancement in smart grid technology: Future prospects in the electrical power network. *Ain Shams Engineering Journal*, *12*(1), 687-695. <https://doi.org/10.1016/J.ASEJ.2020.05.004>
- Chandran, L. R., Babu, G. S. A., Nair, M. G., & Ilango, K. (2021). A review on status monitoring techniques of transformer and a case study on loss of life calculation of distribution transformers. *Materials Today: Proceedings*, *46*, 4659-4666. <https://doi.org/10.1016/J.MATPR.2020.10.290>
- Christian, B., & Gläser, A. (2017). The behavior of different transformer oils relating to the generation of fault gases after electrical flashovers. *International Journal of Electrical Power & Energy Systems*, *84*, 261-266. <https://doi.org/10.1016/J.IJEPES.2016.06.007>
- Faber, M. J., van der Zwaag, K. M., dos Santos, W. G. V., Rocha, H. R. D. O., Segatto, M. E. V., & Silva, J. A. L. (2020). A theoretical and experimental evaluation on the performance of LoRa technology. *IEEE Sensors Journal*, *20*(16), 9480-9489. <https://doi.org/10.1109/JSEN.2020.2987776>
- Ferencz, K., Domokos, J., Jubileumi, X., Konferencia, K., & Domokos, J. (2020). *Using Node-RED platform in an industrial environment*. ResearchGate. <https://www.researchgate.net/publication/339596157>
- Gajenthiran, G., Meyyappan, C., Vishnuprakash, J., Arjun, R., Sena, T. V., Sethu, Y., & Prasanna, R. S. (2022). IoT-based smart monitoring of online transformer. In G. Ranganathan, X. Fernando & F. Shi (Eds.), *Inventive communication and computational technologies* (pp. 951-961). Springer, Singapore. [https://doi.org/10.1007/978-981-16-5529-6\\_72](https://doi.org/10.1007/978-981-16-5529-6_72)
- Ghazali, Y. Z. Y., Talib, M. A., & Rosli, H. A. (2009, June 8-11). TNB experience in condition assessment and life management of distribution power transformers. In *20th International Conference and Exhibition on Electricity Distribution (CIRED 2009)*. Prague, Czech Republic. <https://doi.org/10.1049/CP.2009.0919>
- Ghosh, S. (2016). Calculation of hot spot temperature and aging of a transformer. *International Journal of Technical Research and Applications*, *4*(1), 140-143.
- Guardarrama, J. R., Freire, R. C. S., & Areu, O. H. (2016). A proposed wireless system to real time monitoring in power transformer. *IEEE Latin America Transactions*, *14*(4), 1570-1574. <https://doi.org/10.1109/TLA.2016.7483484>
- Hernández-Callejo, L. (2019). A comprehensive review of operation and control, maintenance and lifespan management, grid planning and design, and metering in smart grids. *Energies*, *12*(9), Article 1630. <https://doi.org/10.3390/EN12091630>
- IEEE. (2000). *C57.12.00-2000 IEEE standard general requirements for liquid-immersed distribution, power, and regulating transformers*. IEEE Publishing. <https://doi.org/10.1109/IEEESTD.2000.91813>
- Kumar, T. A., & Ajitha, A. (2018). Development of IOT based solution for monitoring and controlling of distribution transformers. In *2017 International Conference on Intelligent Computing, Instrumentation and Control Technologies, ICICICT 2017* (pp. 1457-1461). IEEE Publishing. <https://doi.org/10.1109/ICICICT1.2017.8342784>
- Kunicki, M., Borucki, S., Zmarzły, D., & Frymus, J. (2020). Data acquisition system for on-line temperature monitoring in power transformers. *Measurement*, *161*, Article 107909. <https://doi.org/10.1016/J.MEASUREMENT.2020.107909>

- Liu, Y., Li, X., Li, H., Yin, J., Wang, J., & Fan, X. (2020). Spatially continuous transformer online temperature monitoring based on distributed optical fibre sensing technology. *High Voltage*, 7(2), 336-345. <https://doi.org/10.1049/HVE2.12031>
- Martin, D., Marks, J., & Saha, T. (2017). Survey of Australian power transformer failures and retirements. *IEEE Electrical Insulation Magazine*, 33(5), 16-22. <https://doi.org/10.1109/MEI.2017.8014387>
- Mishra, B., & Kertesz, A. (2020). The use of MQTT in M2M and IoT systems: A survey. *IEEE Access*, 8, 201071-201086. <https://doi.org/10.1109/ACCESS.2020.3035849>
- Murugan, R., & Ramasamy, R. (2019). Understanding the power transformer component failures for health index-based maintenance planning in electric utilities. *Engineering Failure Analysis*, 96, 274-288. <https://doi.org/10.1016/J.ENGFAILANAL.2018.10.011>
- Patel, D., & Chothani, N. (2020). Introduction to power transformer protection. In *Digital protective schemes for power transformer* (pp. 1-31). [https://doi.org/10.1007/978-981-15-6763-6\\_1](https://doi.org/10.1007/978-981-15-6763-6_1)
- Pawar, R. R., Deosarkar, S. B., & Member, I. (2017). Health condition monitoring system for distribution transformer using Internet of Things (IoT). In *2017 International Conference on Computing Methodologies and Communication (ICCMC)* (pp. 117-122). IEEE Publishing. <https://doi.org/10.1109/ICCMC.2017.8282650>
- Polak, L., & Milos, J. (2020). Performance analysis of LoRa in the 2.4 GHz ISM band: Coexistence issues with Wi-Fi. *Telecommunication Systems*, 74(3), 299-309. <https://doi.org/10.1007/S11235-020-00658-W>
- Pong, P. W. T., Annaswamy, A. M., Kroposki, B., Zhang, Y., Rajagopal, R., Zussman, G., & Poor, H. V. (2021). Cyber-enabled grids: Shaping future energy systems. *Advances in Applied Energy*, 1, Article 100003. <https://doi.org/10.1016/J.ADAPEN.2020.100003>
- Raghavan, A., Kiesel, P., Teepe, M., Cheng, F., Chen, Q., Karin, T., Jung, D., Mostafavi, S., Smith, M., Stinson, R., Kittrell, B., Shin, J., Lee, S., & Lacarrubba, N. (2021). Low-cost embedded optical sensing systems for distribution transformer monitoring. *IEEE Transactions on Power Delivery*, 36(2), 1007-1014. <https://doi.org/10.1109/TPWRD.2020.2999822>
- Patel, M. R. (2012). *Introduction to electrical power and power electronics*. CRC Press. <https://doi.org/10.1201/B13980>
- Singh, R. P., Sonawane, A. V., Satpute, M. S., Shirsath, D. Y., & Thakre, M. P. (2020). A review on traditional methods of condition monitoring of transformer. In *Proceedings of the International Conference on Electronics and Sustainable Communication Systems, ICESC 2020* (pp. 1144-1152). IEEE Publishing. <https://doi.org/10.1109/ICESC48915.2020.9155858>
- Shanmugapriya, D., Patel, A., Srivastava, G., & Lin, J. C. W. (2021). MQTT protocol use cases in the Internet of Things. In S. N. Srirama, J. C. W. Lin, R. Bhatnagar, S. Agarwal, & P. K. Reddy (Eds.), *Big data analytics* (pp. 146-162). Springer. [https://doi.org/10.1007/978-3-030-93620-4\\_12](https://doi.org/10.1007/978-3-030-93620-4_12)
- Sparling, B. (2017). Improved transformer temperature monitoring. *Transformers Magazine*, 4(4), 58-62.
- Wang, G., Chen, X., Sui, H., Ma, C., Zhang, J., Liu, Y., & Yan, Q. (2020). *Power transformer fault diagnosis system based on Internet of Things*. Research Square. <https://doi.org/10.21203/RS.3.RS-71379/V2>

- Wani, S. A., Rana, A. S., Sohail, S., Rahman, O., Parveen, S., & Khan, S. A. (2021). Advances in DGA based condition monitoring of transformers: A review. *Renewable and Sustainable Energy Reviews*, 149, Article 111347. <https://doi.org/10.1016/J.RSER.2021.111347>
- Xie, B., Zhao, D., & Hong, T. (2020). Transformer monitoring and protection in dynamic power systems - A review. *Frontiers in Energy Research*, 8, Article 150. <https://doi.org/10.3389/FENRG.2020.00150/BIBTEX>
- Zhao, L., Matsuo, I. B. M., Zhou, Y., & Lee, W. J. (2019). Design of an industrial IoT-based monitoring system for power substations. *IEEE Transactions on Industry Applications*, 55(6), 5666-5674. <https://doi.org/10.1109/TIA.2019.2940668>
- Zu, G., Si, W., Yao, Y., Liu, H., Liang, H., & Ji, D. (2021). Design of online monitoring system for distribution transformer based on cloud side end collaboration of Internet of Things. *International Journal of Wireless Information Networks*, 28(3), 276-286. <https://doi.org/10.1007/S10776-021-00521-Y/TABLES/4>

## A Study on Features of Different Tone Quality in a Kenong Set

Ahmad Faudzi Musib<sup>1\*</sup>, Sinin Hamdan<sup>2</sup> and Saiful Hairi Othman<sup>3</sup>

<sup>1</sup>Faculty of Human Ecology, Universiti Putra Malaysia, 43400 UPM, Serdang, Selangor, Malaysia

<sup>2</sup>Faculty of Engineering, Universiti Malaysia Sarawak, 94300 UNIMAS, Kota Samarahan, Sarawak, Malaysia

<sup>3</sup>Institute of Creative Arts and Technology, Universiti Malaysia Sarawak, 94300 UNIMAS, Kota Samarahan, Sarawak, Malaysia

### ABSTRACT

This work discusses how to distinguish kenong frequencies in a signal and the time-localized frequency content for each tone at a given time using an audio-based approach to tuning retrieval where the fundamental and overtone pitch is shown at all frequencies at a given time. The method of temporal localization on the dominant frequency at its unique time for each tone allows for the detection of frequencies present in the signal. Two approaches used in retrieving the harmonic, pitch, and timbre of kenong are Picoscope and Melda analyzer. The audio recording was done using an At4050 microphone and Ur22 audio interface in mono at 24-bit resolution and 48 kHz sampling rate. PicoScope produces the spectrum while the Melda analyzer produces changes in the spectra with time. Kenong D, E, G, A, and C displayed their near overtones at (2:2.8:4.0), (2:3.0:3.9), (2:2.9:3.9), (2:2.6:3.9), and (2:2.6:3.9). Kenong D had a strong fundamental peak at 295Hz. Kenong G keeps the fundamental frequency constant until  $t=5s$ . The basic peak

was maintained by Kenong C. The results reveal that the kenong was properly tuned, although the tuner solely tuned it based on hearing, passed down from generation to generation. The maker's intuition permits him to create a specific 'signature' through sound unique to a given kenong set.

### ARTICLE INFO

#### Article history:

Received: 16 February 2022

Accepted: 24 May 2022

Published: 19 August 2022

DOI: <https://doi.org/10.47836/pjst.31.1.02>

#### E-mail addresses:

[faudzimusib@upm.edu.my](mailto:faudzimusib@upm.edu.my) (Ahmad Faudzi Musib)

[hsinin@unimas.my](mailto:hsinin@unimas.my) (Sinin Hamdan)

[hosaiful@unimas.my](mailto:hosaiful@unimas.my) (Saiful Hairi Othman)

\*Corresponding author

**Keywords:** Acoustic spectra, fundamental frequency, kenong, overtones frequency, sustain fundamental

## INTRODUCTION

### The Motivations of the Studies

It is relatively easy to grasp the theory of gamelan tuning but very hazardous to put it into practice (Sorrell, 1990). It appears to be common practice to copy the tuning of some well-known gamelan. The maker answers the question of what to tune to (since there is no pitch or intervallic structure standardization in Java) in consultation with the purchaser.

Figure 1 shows a typical kenong kettle used in this study. The metallophones produce various and complex shimmering and sparkling timbres. The in-harmonic instruments are tuned to either the pelog (seven-tone) or the slendro (five-tone) scales, which differ from the diatonic scale. The tunings are not exactly in the 2:1 octave and can be slightly larger or smaller than 2:1. The octave of one kenong is unlike the octaves of another kenong. An extensive set of measurements of actual gamelan tunings is given in Sudarjana et al. (1993), which studied more than 30 complete gamelans. They used an analog electronic system. This technique filtered out all higher partials and recorded only the fundamentals. The measurement of the tunings is completely adequate because the fundamentals determined the pitches. Unfortunately, all information regarding timbre (spectra) has been lost. An average slendro tuning (numerically average of all the slendro gamelans) is 0, 231, 474, 717, 955, 1208 (in cents), which has a pseudo-octave stretched by 8 cents. This tuning is close to 5-tet. Some gamelans may deviate from this. An average pelog scale is 0, 120, 258, 539, 675, 785, 943, 1206, which is an unequal tuning (stretched by 6 cents).

This study is conducted to identify the sound produced by a set of kenong by making scales and all aspects of sonic as research data. Accordingly, this study considers



Figure 1. A typical kenong kettle

the configuration procedures of audio equipment, software, and the workflow required for frequency extraction from a kenong set that serves as a musical instrument. This study aims to encourage and expand the approach to working with a variety of approaches in obtaining harmonic contents of metallophones, namely the kenong set through audio signal retrieval via workflows, technologies, and historically as well as culturally recognized music traditions. This research is based on a deep interest in overcoming a kenong set's traditional way of recognizing tunings and scales through a sound recording using various technological and qualitative



methods. That may finally lead to a comprehensive approach to identifying sound characteristics of a kenong set through retrieving tunings by kenong set through tools, devices, and workflow traditionally played in a communal setting representing a local identity. Gamelan music is in *pelog* or *slendro*, and no matter how evocative the piece, the piano cannot reproduce these tunings. These may help discourage the confusion of general orientalism in Western music with specifically Javanese gamelan elements (Sorrell, 1990). The research on retrieving tunings by the kenong set can serve as a pioneering approach to recognition of sound characteristics, perception of tunings through harmonic differences, and construction of audio signal retrieval through workflows. It will enhance information on factors that might have an impact on the characteristics of each kenong instrument, as well as granting useful data on factors that might have contributed to the differences from one set to another. The way of the functioning (a process of sound production from diverse perspectives) and a sound culture within a community allows for the enrichment of a theory based on facts.

Hence, the study will stimulate discussion and generate greater awareness among practitioners and social scientists on the importance of having a working method of identifying sound characteristics of a kenong set through retrieving tunings by kenong set as a framework consisting of effective tools and workflow. This study can therefore also be seen as a model that compensates for limitations in more abstract findings. It can benefit cultural supporters in a broader sense and from a diversity of backgrounds, both internal and external musicians, anthropologists, and social scientists.

### **Statement of the Problem**

Sound analysis and re-synthesis became available for investigating tone systems and tunings of non-Western music cultures (Schneider & Andreas, 1990; Schneider & Beurmann, 1993). The tunings in kenong are different from the Western systems and were difficult to explain in terms of their origins regarding relevant perceptual and cognitive issues (Ellis & Hipkins, 1884; Stumpf, 1901; Kunst, 1934). All the work mentioned above measured the fundamental frequency but did not consider the overtone frequency. As a result, their works are unable to determine the harmonics and sub-harmonics as well as the timbre. This work measures the fundamental and overtone frequency, called timbre. Fourier transformation determines fundamentals, harmonics, and sub-harmonics. The different intensity and harmonics or sub-harmonics (overtones) distinguish each instrument's characteristics. Most importantly, this work showed the range of available frequencies at a specific time.

This research is carried out to classify the sonic properties generated through the kenong by making scales, tuning, and other aspects of sonic. Accordingly, this study considers the configuration procedures of audio equipment, software, as well as workflows that are required for frequency extraction from the individual kenong. This extraction process will

provide an indicator of what sound is appropriate that contributes to what is the preferred sounding of a kenong set. Furthermore, the data collected, which leads to a knowledge of the transformation process factors within the object itself, is important in the production of the kenong set. Therefore, it contributed to the facts of what is preferred sounding kenong.

### **Objectives of the Study**

The main objective of this study is to contribute to tuning and to all facets of sound as research data on the whole sound community of metallophone musical instruments of their high capacity for establishing an independent sound identity, namely kenong, and from the standpoint of retrieving the tunings of the kenong set in field recordings. This contribution helps to clarify further the role of the musical acoustician and his/her relationship to the tuning of metallophones in general. Musical acoustic studies of sound preservation, including a range of responsive viewpoints, would be of growing interest in research projects. Social scientists, audio and sound forensics, technicians, and decision-makers in Malaysian communities are increasingly aware of intangible cultural attributes—focusing on chosen metallophone instruments kenong as the key objects. This study aims to prove the importance of retrieving metallophone tuning through a musical acoustic approach and diversity in sonic studies, that is, through observation and perceptions in the context presented by these instruments' actual meaning. Studies may concentrate on capturing the principles suggested in other metallophone instruments, namely, questionable xylophones and gongs (Schneider, 1988), while checking the applicability of the techniques, instruments, and theoretical views established in the research.

The specific objectives are:

1. To describe the type of kenong set in Malaysia from the perspective of tuning.
2. To describe the kenong set through literature reviews and sound recordings.
3. To describe the tools and devices in retrieving a comprehensive approach to identifying sound characteristics of the kenong set in Malaysia.

**Several Related Works Similar to this Research.** In Indonesia, the instruments are not all tuned to a single standard reference scale, producing many different gamelan tunings (Surjodiningrat et al., 1993). Each instrument is tuned and timbrally adjusted for its orchestral context, where it is created for a single ensemble. Therefore, one gamelan inevitably differs in intonation, tone, and feelings from another. Western diatonic scales are connected to sounds with harmonic spectra. A similar relationship exists between the pelog and slendro scales and the overtone sounds of the saron, bonang, gender, or kenong. The differences between the tunings of various gamelans can be explained by the differences between the spectra of the various instruments. The relation between the spectra and the tunings of the gamelans presents an intriguing challenge. Rossing and Shepherd published

details of the spectra of any gamelan instruments, but this was not a complete study, even of the one gamelan (Rossing & Shepherd, 1982). Only the *jegongan* (a Balinese gender) and the gong are studied, requiring more data.

The metallophones of the gamelan have in-harmonic spectra. Gamelan music scales and tunings are unfamiliar, with the timbre of the instruments unusually bright and harsh. Both the tunings and the timbres are easily quantifiable. The kenong with a larger rim makes a clear and sustained sound. Hence it serves as a primarily rhythmic function. Despite the differences in shape, the spectra of the kenong are like those of the bonang. Figure 2 shows the spectra of 3 typical bonang from Sethares (2005).

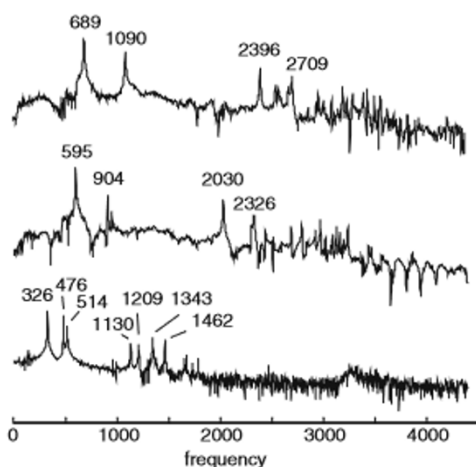


Figure 2. Spectra of 3 typical bonang (Sethares, 2005)

Gamelan has a strong sense of rhythm as it is traditionally played by ear rather as opposed to reading from written musical scores. The beats are clearly audible so that the musical piece can be passed down orally through generations. The significance of beat features shows Gamelan classification compared to Western musical instruments. The first feature of vibration of the kenong is the extraction process, where the whole audio is characterized by a frequency representation (using the Fast Fourier Transform-FFT). This FFT feature clearly showed the whole frequency range after the first beating. With audio data, several studies are also done using the Melda analyzer in Cubase version 9. The significance of

Melda analyzer data features that display the spectra changes with time was investigated, and the characters of the features are discussed. Hamdan et al. (2019) offer a comprehensive discussion on the feature.

## METHODOLOGY

Two approaches suggested in retrieving tunings of kenong via tools, device, and its workflow are shown in Figure 3.

The cast bronze kenong set was chosen from a range of gamelan ensembles available at the Faculty of Applied and Creative Art, Universiti Malaysia Sarawak. The acoustic spectra of the measured sets of 5 just-tuned cast bronze kenong (kenong D, E, G, A, and C), which were made in Indonesia, were captured using PicoScope oscilloscopes and Melda analyzer to investigate the fundamental and the overtone frequencies. Excitation was done

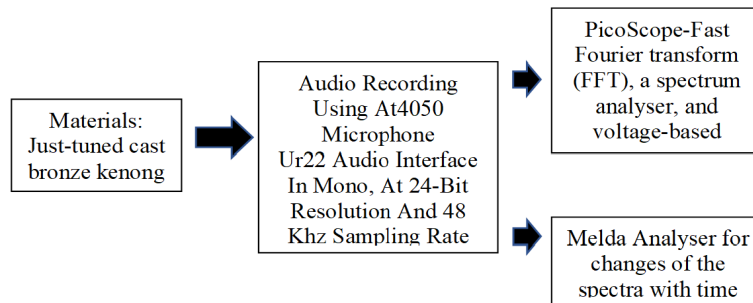


Figure 3. Workflow showing the tools and device for retrieving tunings of kenong

by beating the kenong with padded mallets by an expert kenong player. The Melda analyzer records the sound and plots the intensity versus frequency over time. Various frequencies with differing intensities are presented at any given time. This study gives the intensity versus frequency at 0, 0.5, 1, 2, 3, 4, and 5 seconds. At  $t=0$  s, the fundamental frequency has the highest intensity. This fundamental frequency can no longer be sustained after  $t=0$  s. The analyzer can display how the intensity of the frequency changes over time.

The microphone was held above the top surface along the axis of symmetry of the kenong at about 20 cm (Figure 4). The PicoScope computer software (Pico Technology, 3000 series, Eaton Socon, UK) was used to view and analyze the time signals from PicoScope oscilloscopes (Pico Technology, 3000 series, Eaton Socon, UK) and data loggers for real-time signal acquisition. PicoScope software enables analysis using FFT, a spectrum analyzer, voltage-based triggers, and the ability to save/load waveforms to a disk. Figure 4 shows the schematic diagram of the experimental setup. The kenong was placed where the sound could be captured with minimum interference. The amplifier (Behringer Powerplay Pro XL, Behringer, China) ensured the signal converter's sound capture was loud enough to be detected.

The kenong spectra were also digitally recorded using the Melda analyzer. In this study, the audio signal derived from the striking of the kenong played by an expert kenong player is recorded. The audio signal is recorded in mono, at 24-bit resolution, at a 48 kHz sampling rate. The audio signal is recorded with the aid of a digital audio interface in a .WAV format. Audio signal calibration of the recording system is carried out to ensure the recorded audio signal of the striking of the kenong is at the optimum level. A 1 kHz sine wave test tone is used to calibrate the recording system. Here the 'unity' calibration level is at +4dBu or -10dBV and is read by the recording device at '0 VU'. In this regard, the EBU recommended that the digital equivalent of 0VU is that the test tone generated to the recording device of the experimentation is recorded at -18 dBFS (Digital) or +4dBu (Analog), which is equivalent to 0VU. The amplitude scale of the vertical ruler waveform display is in decibels mode. In this mode, amplitude ranges from -infinity to zero dBFS on a decibel scale. 'FS' stands for 'Full Scale', and 0 dBFS is the highest signal level achieved in a digital audio WAV file.

Higher levels are possible within digital audio workstation software, but 0 dBFS is the highest level in the files that are recorded on the disk. As the signal is either an electronic or digital representation of that sound, variations in signal or sound levels are measured in decibels (dB). In their dB form, decibels do not describe the absolute level of a signal or sound, only any comparison or change in level. 0 dB means no difference in the level or no change in level. Decibels are used to describe differences or changes in level. 0 dB means ‘no change’. Values in dBFS are used to describe signal levels in comparison with the highest level a WAV file can handle. In this thorough calibration procedure, no devices unknowingly boost or attenuate its amplitude in the signal chain when the recording is carried out. The recording apparatus was the Steinberg UR22 mkII audio interface, Audio-Technica AT4050 microphone, XLR cable (balance), with microphone position on axis (<20 cm), and microphone setting with low cut (flat) 0dB.

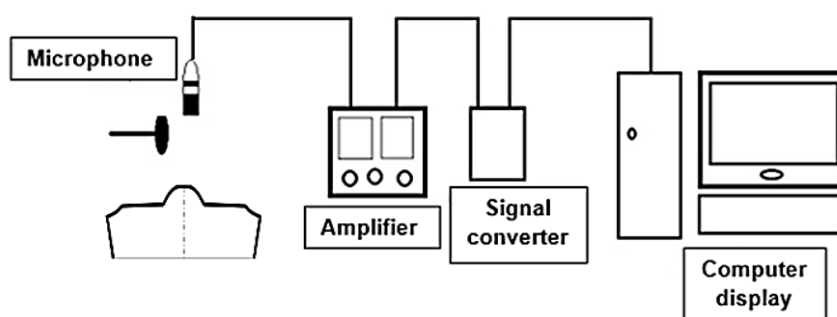


Figure 4. Schematic diagram of the experimental setup

For this investigation, the acoustic signal generated by an experience kenong player striking the kenong was captured. The kenong was struck at a steady rate since the performance was assessed on the rhythm and physiological synchronization of the left and right hands.

## RESULT AND DISCUSSION

Acoustical recordings of metallophones being struck were used to examine ratios of overtone frequencies to the fundamental. Results showed variability in the number and ratios of overtones present. The acoustic spectra for the kenong vary substantially due to variation in shape, size, and dimensional irregularities created during manufacture and while tuning by hand grinding. Figure 5 shows the typical acoustic spectra recorded after excitation of kenong D captured using PicoScope oscilloscopes. The spectrum in Figure 5 is very noisy because the PicoScope captures the whole range of the signal. The peak

picking is not chosen randomly here but based on the highest amplitude. So, the frequencies given in Table 1 are not arbitrarily chosen. Knowing the fundamental frequency of each kenong gives an indicator of the overtone peaks. The spectrum in Figure 6 is captured using the Melda analyzer and displays the signal at  $t=0, 0.5, 1, 2, 3, 4,$  and  $5$  seconds. At one time, such as at  $t=0s$ , the analyzer only displays three significant frequencies  $296, 424,$  and  $1213Hz$ . The signal looks cleaner because the duration of the display is at one time. Although the spectra still depend on the strike, the frequency obtained does not depend on the strike; only the amplitude depends on the strike. Although there is only one example of many possible spectra from one instrument, the author employed a professional player to strike the instrument, and the frequencies are reproducible and repetitive.

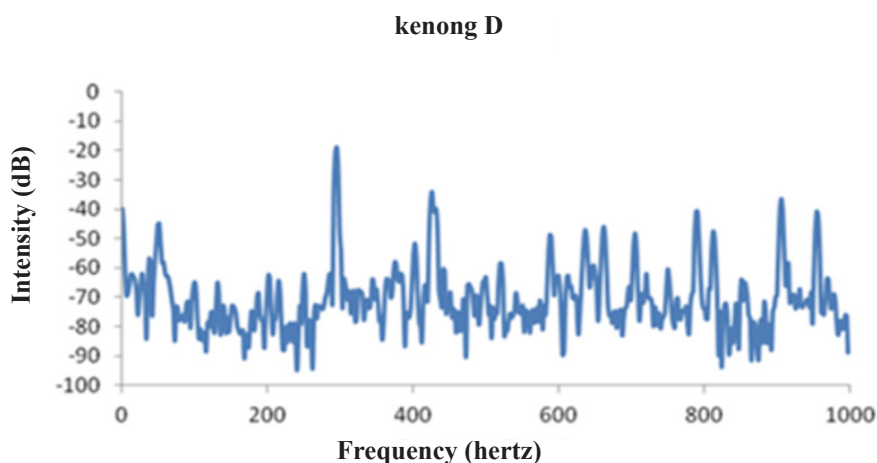


Figure 5. A typical spectrum (kenong D) from PicoScope Oscilloscope

Table 1 shows the fundamental frequency ( $f_0$ ), first overtones ( $f_1$ ), and second overtones ( $f_2$ ) for kenong D, E, G, A, and C. The values in the bracket at the last column based on the equal-tempered scale (ETS) are shown as a reference only. The tuning of kenong cannot be interpreted in a framework of an ETS harmonic or even in the framework of the harmonics of 4 basic waveforms of the square, saw-tooth, triangle, and pulse. These define precisely to decrease amplitude over time. Square wave will have a set of odd-order harmonics determined by the harmonic order and decibel loss per harmonic over time (1, 3, 5, 7, & 9). Saw-tooth is made of odd and even number harmonics 1, 2, 3,4,5, and 6. So kenong is not of these harmonics, and its structure is made of a variety of non-harmonic partials, so the kenong partials were (2:2.89:4.01), (2:3.03:3.90), (2:2.92:3.99), (2:2.67:3.98) and (2:3.12:3.69) for kenong D, E, G, A and C respectively.

Table 1

*Fundamental frequency and overtones for Kenong D, E, G, A and C, Kenong Swastigitha (Sw) and Kenong Kyai KadukManis (Kk) (Hamdan et al., 2019) with the Equal Tempered Scale (ETS) frequencies as a reference*

	$f_0$	$f_1$	$f_2$	$f_0: f_1: f_2$	$f_0$ (Sw)	$f_0$ (Kk)	ETS
<b>D</b>	292.6	423.4	587.2	2:2.894:4.013		242	B3(246) 4(293.7)
<b>E</b>	331.7	503.4	647.7	2:3.035:3.905	375	320	E4(320.6) F4(349)
<b>G</b>	396.0	579.4	790.1	2:2.926:3.990	412	369	F#4(369) G4(392)
<b>A</b>	440.9	589.2	877.9	2:2.673:3.982	472	421	G#4(415) A4(440)
<b>C</b>	518.9	809.7	959.9	2:3.121:3.699	623	478	A#4(466) 5(523.3)
						557	C#5(554)
						623	#5(622)

If a strong fundamental is not essential for perceiving the pitch of a musical tone, the question arises as to which overtones are most important (Sethares, 2005). When the parts of the complex tone are not harmonics, however, the determination of pitch is more subtle. Musical examples of the ability of the auditory system to formulate a pitch from near harmonics in a complex tone are the sounds of bells and chimes.

The manufacturer can bring out the fundamentals for a clearer pitch during the tuning process by raising a small boss at the center of the kenong. Hammering a small boss in a previously un-bossed kenong increases the pitch for the fundamental and most of the higher notes. Progressively enlarging, the boss continues to raise the pitch but more and more slowly. Finally, adding the boss will allow raising the pitch a maximum of a fifth or sixth, typically above that of the original flat disk (Rossing & Peterson, 1982).

The tuning of slendro-kenong of gamelan Swastigitha is 357Hz (F4), 412Hz (G#4), 472Hz (A#4), and 623Hz (D#5). While the tuning of slendro-kenong of gamelan Kyai KadukManis is 242Hz (B3), 320Hz (E4), 369Hz (F#4), 421Hz (G#4), 478Hz (A#4), and 557Hz (C#5) (Hamdan et al., 2019). In this work the spectrum of the respective slendro-kenong as shown in Table 1 are 293Hz (D4) with partial  $f$ , 1.44 $f$ , 2.0 $f$ ; 332Hz (E4) with partial  $f$ , 1.52 $f$ , 1.95 $f$ ; 396Hz (G4) with partial  $f$ , 1.46 $f$ , 1.99 $f$ ; 441Hz (A4) with partial  $f$ , 1.33 $f$ , 1.99 $f$ ; and 519Hz (C5) with partial  $f$ , 1.56 $f$ , 1.85 $f$ .



Table 1 shows that our slendro-kenong is very close to the frequency obtained from the ETS. The kenong from Swastigitha showed a deviation of 7.5% (375-349), 5% (412-392), 1.3% (472-466) and 0.1% (623-622), while kenong from Kyai KadukManis showed a deviation of 1.6% (246-242), 0% (320-320), 0% (369-369), 1.4% (421-415), 2.6% (478-466) and 0.5% (557-554).

Table 1 is reorganized so that the tuning is based on ETS and shows it to the nearest ETS; the reason for such tunings is because tuners were innovative in their client composition. The closeness of the tuning of the measured kenong to ETS was not meant to be intentional. It was given here purely as a reference and comparison. Mixed tuning was developed and created to enrich the color or sonority prior to their compositions. If all tuning is made the same, it will vanish other tunings. Each gamelan is tuned accordingly to a region from where it belongs because it is done purely by listening. If all tuning is the same value as the other tuning, culture will be extinct or write-off. So this must mean that standardizing the tuning is bad. Yes, it is bad because only western tuning will be used and nothing more. Pelog or slendro on gamelan no longer be important because instruments like marimba or xylophone can play it. The same thing applies to the makkam on gambus is no longer important to be played by the gambus because it can be played by guitar. That is a big problem, and all other ethnic instruments will be of no use, for example, samphonton/santur/ sitar and many more.

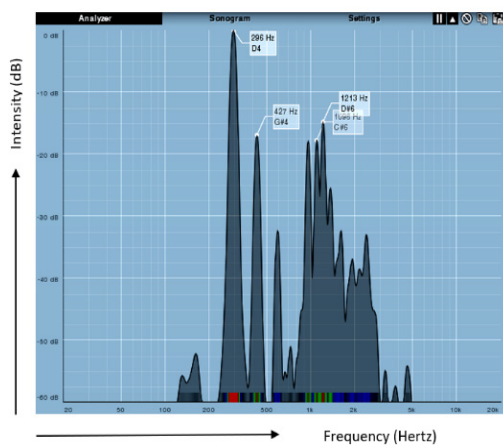
So the acoustician only referred to just the only Western tuning; they are the one who lacks comprehensive knowledge of musical instruments, which we cannot blame because they only have one tuning, and they are also not an ethnomusicologist. There is a variation where some are tuned lower or higher. As a tuner, should the maker consider our tuning reference or use the existing gamelan as a reference?

When the maker makes the gamelan, they will usually be based on the client's request, as our kenong was tuned similar to the ETS. It tells us that there is certain standardization. Each gamelan was developed and constructed accordingly to its tuning standards according to its district. In the past, each kenong was made according to certain standardization of each district. The authors believe that our kenong had been tuned purposely according to the ETS (purchase in 2013) compared to the Swagistitha and Kyai Kayu Manis. To the author's knowledge, the only tuning of the kenong was from Swagistitha and Kyai Kayu Manis (Hamdan et al., 2019).

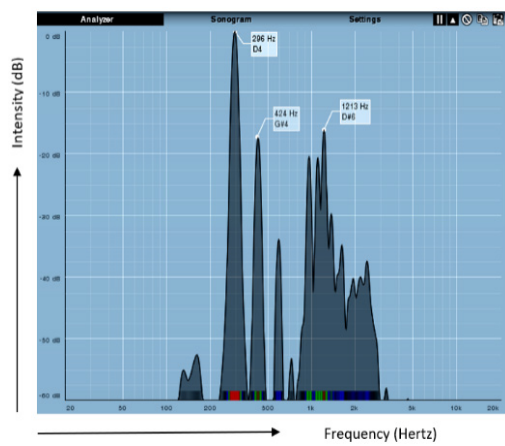
Figure 6 shows the typical sonogram recorded after excitation of kenong D captured using the Melda analyzer. Table 2 showed different peak frequencies for kenong D, E, G, A, and C obtained from the Melda analyzer recorded at  $t=0, 1, 2, 3, 4,$  and  $5s$ . From Table 2, at  $t=0s$ , kenong D showed a high peak at 295Hz (exactly as D4 on ETS) and a second low peak at 425Hz (i.e., A4 on the ETS scale). This 295Hz (D4) peak gradually decays (replaced by  $\sim 425Hz$  (A4) peak) and eventually disappears at  $t=5s$ . It indicates that the overtone



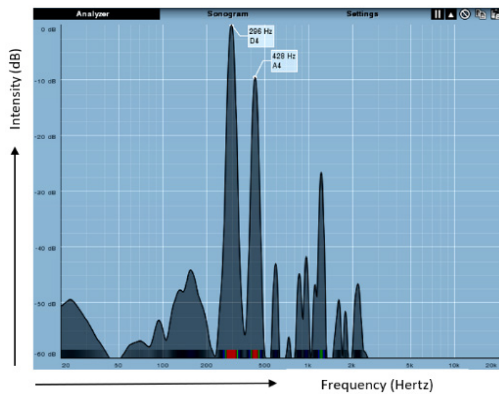
frequency later replaced the fundamental frequency at  $t=0$ s from the second peak at  $t=5$ s, which is the first overtone frequency, i.e., 423.36Hz ( $f_1$ ) as detected by the PicoScope. The fundamental frequency E4 for kenong E disappears at  $t=4$ s and is replaced by B4. Kenong G sustain the fundamental frequency G4 until  $t=5$ s with the overtone G5 increasing from -25dB (at  $t=0$ s) to -9dB (at  $t=5$ s). Kenong A showed a gradually decreasing trend of A4 at -9, -12, -15, -22dB at  $t=2, 3, 4,$  and  $5$ s, respectively, which is replaced by D#5 at  $t=2$ s. Kenong C showed that the fundamental C5 was sustained and maintained the amplitude for 5s. The overtone for kenong C was maintained for the whole 5s.



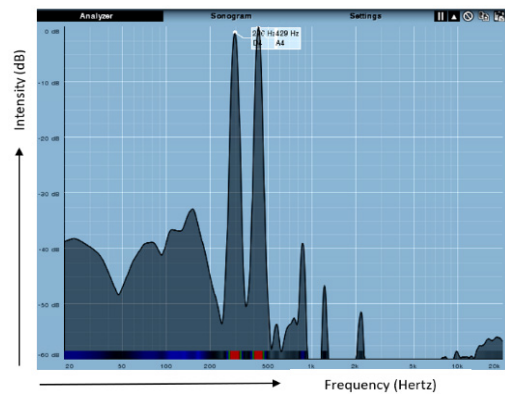
6a.  $t = 0$  seconds



6b.  $t = 0.5$  seconds



6c.  $t = 1$  seconds



6d.  $t = 2$  seconds

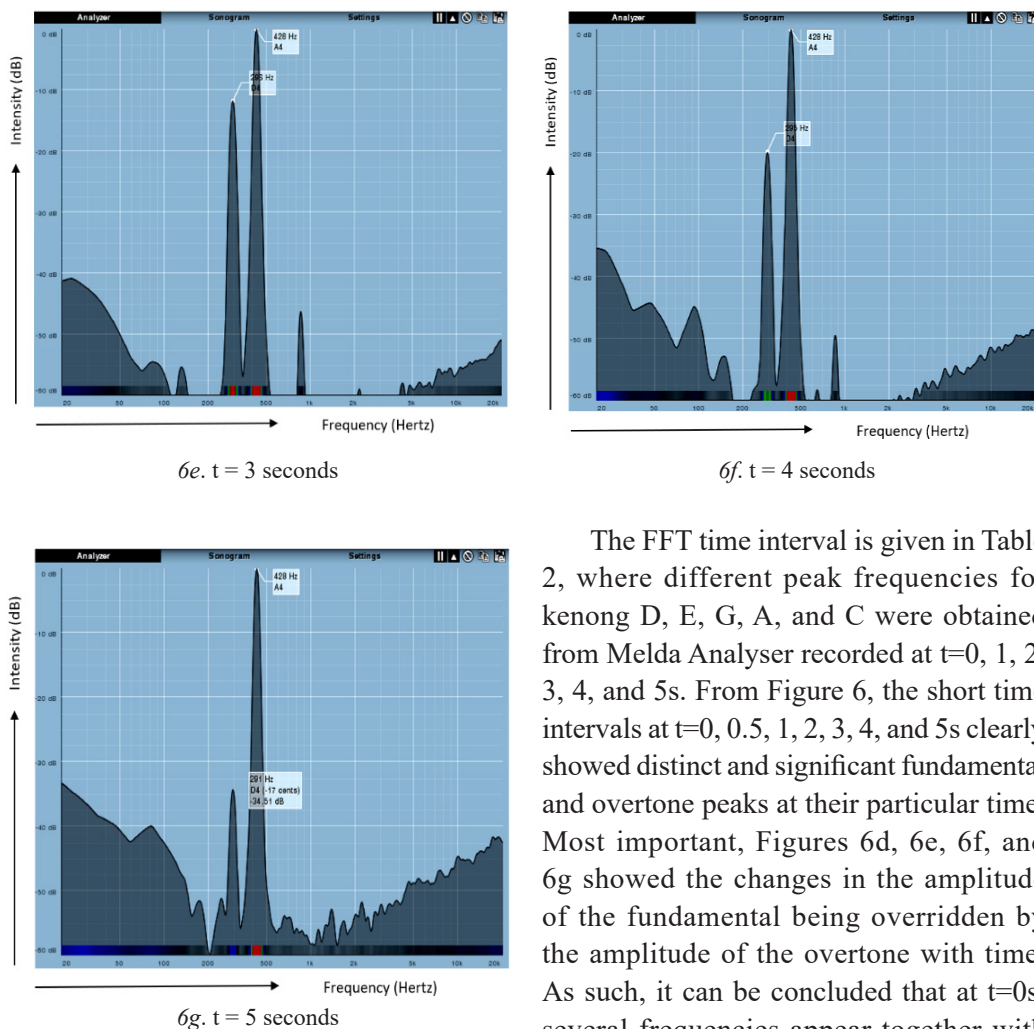


Figure 6. Kenong D at t=0, 0.5, 1, 2, 3, 4, 5 seconds

The FFT time interval is given in Table 2, where different peak frequencies for kenong D, E, G, A, and C were obtained from Melda Analyser recorded at t=0, 1, 2, 3, 4, and 5s. From Figure 6, the short time intervals at t=0, 0.5, 1, 2, 3, 4, and 5s clearly showed distinct and significant fundamental and overtone peaks at their particular time. Most important, Figures 6d, 6e, 6f, and 6g showed the changes in the amplitude of the fundamental being overridden by the amplitude of the overtone with time. As such, it can be concluded that at t=0s, several frequencies appear together with the fundamental, but with time the overtone peak becomes more dominant than the fundamental frequencies.

The precisions of the result of each investigation describe that if all tunings are made the same, other tunings will be lost. Each gamelan is tuned to the region it belongs to because it is solely done by hearing. If all tunings have the same value as the others, culture will become extinct or be forgotten. Therefore, it must imply that standardizing tuning is a poor decision. It is poor because only western tuning will be used, so pelog or slendro on gamelan will no longer be important. It can be played with any instrument, such as a marimba or xylophone. The same is true for the makkam on gambus, which no longer needs to be played by the gambus because it can be played by guitar. That is a major issue; all other ethnic instruments, such as the samphonton/santur/sitar and many more, will be rendered obsolete.

Table 2

*Different peak frequencies for kenong D, E G A C obtained from Melda Analyser recorded at t=0, 1, 2, 3, 4, and 5s*

Kenong	Time Sec	First Peak	dB	Second Peak	dB	f <sub>0</sub>
<b>D</b>	0	f(296D4)	0	1.4f(427G#4)	-19	293
	0.5	f(296D4)	0	1.5f(424G#4)	-19	
	1	f(296D4)	0	1.5f(428A4)	-10	
	2	f(296D4)	0	1.5f(429A4)	0	
	3	f(296D4)	-12	1.5f(428A4)	0	
	4	f(296D4)	-24	1.5f(428A4)	0	
<b>E</b>	5	-	-	1.5f(428A4)	-	332
	0	f(332E4)	0	1.5f(502B4)	-28	
	0.5	f(332E4)	0	1.5f(502B4)	-18	
	1	f(332E4)	0	1.5f(502B4)	-4	
	2	f(332E4)	-18	1.5f(502B4)	0	
	3	f(332E4)	-32	1.5f(502B4)	0	
<b>G</b>	4			1.5f(499B4)	0	396
	5			1.5f(501B4)	0	
	0	f(396G4)	0	1.5f(596D5)	-25	
	0.5	f(396G4)	0	1.5f(596D5)	-25	
	1	f(396G4)	0	1.5f(596D5)	-22	
	2	f(396G4)	0	1.5f(596D5)	-19	
<b>A</b>	3	f(396G4)	0	1.5f(596D5)	-17	441
	4	f(396G4)	0	1.5f(596D5)	-11	
	5	f(396G4)	0	1.5f(596D5)	-9	
	0	f(441A4)	0	1.4f(613D#5)	-12	
	0.5	f(441A4)	0	1.4f(613D#5)	-9	
	1	f(441A4)	0	1.4f(613D#5)	-8	
<b>C</b>	2	f(441A4)	-9	1.4f(613D#5)	0	519
	3	f(441A4)	-12	1.4f(613D#5)	0	
	4	f(441A4)	-15	1.4f(613D#5)	0	
	5	f(441A4)	-22	1.4f(613D#5)	0	
	0	f(519C5)	0	1.5 f(805G5)	-34	
	0.5	f(519C5)	0	1.5 f(805G5)	-34	
<b>C</b>	1	f(519C5)	0	1.5 f(805G5)	-32	519
	2	f(519C5)	0	1.5 f(805G5)	-32	
	3	f(518C5)	0	1.5 f(805G5)	-32	
	4	f(518C5)	0	1.5 f(805G5)	-32	
	5	f(522C5)	0	1.5 f(805G5)	-32	

## CONCLUSION

The spectra recorded by PicoScope oscilloscopes and Melda analyzer were investigated through the vibration overtones. The two-tone quality of the kenong set, namely the kenong of gamelan Swastigitha and Kyai Kaduk Manis, are compared with kenong D, E, G, A, and C from this study with the tuning set to D4, E4, G4, A4, and C5. The kenong of gamelan Swastigitha used their tuning set to F4, G#4, A#4, and D#5. At the same time, the kenong of gamelan Kyai Kaduk Manis are tuned to B3, E4, F#4, G#4, A#4, and C#5. Our study confirms that our *kenong* are well-tuned to the ETS's D4, E4, G4, A4, and C5. Furthermore, this study confirms that one gamelan inevitably differs in intonation, tone, and feelings from another. It is due to the intuitive feeling (listening experience inherited from generation) of the gamelan tuner during the tuning of kenong gamelan Swastigitha and Kyai Kaduk Manis using primitive tools. During a field visit by the authors to Jogjakarta, the tuner only used a pianica and tuned it purely based on his listening. The authors suggest that our instrument results are similar to ETS because it was intended by the purchaser to be tuned according to the ETS, although the tuning tools were primitive.

Hence it proved that these primitive tools could translate the tuning onto the gamelan set. From a field visit to Jogjakarta, the authors were told that the gamelan tuner tuned the gamelan purely based on hearing inherited from generation. The instrument is struck and heard by the tuner based on what he hears from a standard pianica. In our work, this primitive tuning was replaced by reading with PicoScope and Melda analyzer, and it proved that the transmission of the tuner onto the tuning of the gamelan set can be shown on the aspect of intonation, tone, and feels. From the PicoScope data, kenong D, E, G, A, and C showed complex tones with their fundamental equivalent to ETS.

However, kenong's frequency is different when comparing its frequency precision with ETS. Although its frequency accuracy is nearly similar, it differs in the aspect of intonation and tone characteristics. One aspect that needs to be considered in this study is the sound characteristic sense. The sense derived from the maker allowed him to craft a specific 'signature' through the sound characteristic of a particular gamelan set. When kenong is sat in an ensemble of gamelan, the sound stands out as other parts make the sound faculty of the gamelan ensemble unique. It is the peculiarity of gamelan; it is exclusively handmade, produced, and constructed through primitive tools and processing such as hammer, hand file, and ground metal foundry, creating an offset tuning and timbre. The gamelan is the entire instrument. It has a tuning bound to the aesthetics of a group of musicians (of a community in the past, today of some professionally engaged musicians serving the entire sound of the instrument). Destroying this through an imposed "rightful tuning" kills the instrument, especially when people refer to constructed ideas of equidistance tuning. From the Melda analyzer data, at  $t=0s$ , kenong D showed a high peak at 295Hz (exactly as D4 from the ETS) and a second low peak at 425Hz (i.e., A4 from the ETS). This fundamental peak

gradually decayed and was replaced by the first overtone peak and eventually disappeared. It indicates that the overtone frequency later replaced the fundamental frequency. The fundamental frequency for kenong E disappears at  $t=4s$  and is replaced by B4. Kenong G sustain the fundamental frequency (G4) with the overtone (G5) increasing from -25dB (at  $t=0s$ ) to -9dB (at  $t=5s$ ). Kenong A showed a gradually decreasing trend of A4 peak at -9, -12, -15, -22dB at  $t=2, 3, 4,$  and  $5s$ , respectively, which is replaced by D#5 at  $t=2s$ . Kenong C showed that the fundamental C5 peak was sustained and maintained the amplitude for 5s. The overtone for kenong C was maintained for the whole 5s.

## ACKNOWLEDGEMENT

GERAN PUTRA: GP/2017/9561700 funded this research.

## REFERENCES

- Ellis, A. J., & Hipkins, A. J. (1884). II. Tonometrical observations on some existing non-harmonic musical scales. In *Proceedings of the Royal Society of London* (pp. 368-385). The Royal Society Publishing.
- Hamdan, S., Musib, A. F., Musoddiq, I. A., & Wahid, H. A. (2019). Some studies on the understanding the different tones quality in a bonang set. *Journal of Engineering Science and Technology*, 14(4), 1960-1973.
- Kunst, J. (1934). *De Toonkunst van Java* [From toon art to Jawa]. Nijhoff Publishers.
- Rossing, T. D., & Peterson, R. W. (1982). Vibrations of plates, gongs, and cymbals. *Percussive Notes*, 19(3), 31-41.
- Rossing, T. D., & Shepherd, R. B. (1982). Acoustics of gamelan instruments. *Percussive Notes*, 19(3), 73-83.
- Schneider, A. (1988, April 14-17). Psychological theory and comparative musicology. In History of Ethnomusicology Conference (pp. 293-317). University of Illinois, Urbana-Champaign.
- Schneider, A., & Andreas, B. (1990). Okutuusa Amadinda: Zur Frage aquidistanter Tonsysteme und Stimmungen in Afrika [What inspires us Amadinda: To question aquidistanter sound system and moods in Afrika]. In P. Petersen (Ed.), *Musikkulturgeschichte Festschrift für Constantin Floros* [Music culture given to festival for constantin floros] (pp. 493-526). Breitkopf & Haertel Publishing
- Schneider, A., & Beurmann, A. E. (1993). Notes on the acoustics and tuning of gamelan instruments. In B. Arps (Ed.), *PeIfonnance in Java and Bali* (pp. 197-218). School of Oriental and African Studies.
- Sethares, W. A. (2005). *Tuning, timbre, spectrum, scale*. Springer Science & Business Media.
- Sorrell, N. (1990). *A guide to the gamelan*. Faber and Faber Limited.
- Stumpf, C. (1901). *Tonsystem und Musik der Siamesen* [Sound system and music the Siamesen]. *Beitriige zur Akustik und Musik wissenschaft*, 3, 69-146.
- Sudarjana, P. J., Surjodiningrat, W., & Susanto, A. (1993). *Tone measurements of outstanding Javanese gamelans in Yogyakarta and Surakarta*. Gadjah Mada University Press.



## Computational Analysis of Polymer Melt Filling in a Medical Mold Cavity During the Injection Molding Process

Muhammad Khalil Abdullah<sup>1</sup>, Mohd Syakirin Rusdi<sup>2\*</sup>, Mohd Zulkifly Abdullah<sup>2</sup>, Abdus Samad Mahmud<sup>2</sup>, Zulkifli Mohamad Ariff<sup>1</sup>, Khor Chu Yee<sup>3</sup> and Mohd Najib Ali Mokhtar<sup>4</sup>

<sup>1</sup>*School of Materials and Mineral Resources Engineering, Universiti Sains Malaysia, Engineering Campus, 14300 USM, Nibong Tebal, Penang, Malaysia*

<sup>2</sup>*School of Mechanical Engineering, Universiti Sains Malaysia, Engineering Campus, 14300 USM, Nibong Tebal, Penang, Malaysia*

<sup>3</sup>*Simulation and Modelling Research Group (SiMMREG), Faculty of Mechanical Engineering Technology, Universiti Malaysia Perlis, 02100 UniMAP, Perlis, Malaysia*

<sup>4</sup>*Faculty of Manufacturing Engineering, Universiti Teknikal Malaysia Melaka, Hang Tuah Jaya, 76100 Durian Tunggal, Melaka, Malaysia*

### ABSTRACT

This study describes the results of a mold filling simulation analysis of a medical syringe performed during the thermoplastic injection molding process, which was performed using a computational Fluid Dynamic Simulation (CFD) with the Volume of Fluid Method (VOF). ANSYS Fluent was used for analysis and data collection. Medical grade polypropylene (PP) is considered in this study. The studies consider physical parameters (such as inlet position and syringe thickness) of the injection molding process. The outlet vent must be

placed as far away from the inlet as possible to root out entrapped air and allow the molten PP to occupy the mold cavity. The findings revealed that syringe thicknesses ranging from 0.75 mm to 1.00 mm resulted in increased flow velocity, shorter filling time, and faster flow front advancement.

**Keywords:** Injection molding simulation, medical grade polypropylene, plastic flow, syringe

### ARTICLE INFO

#### Article history:

Received: 17 February 2022

Accepted: 20 June 2022

Published: 19 August 2022

DOI: <https://doi.org/10.47836/pjst.31.1.03>

#### E-mail addresses:

[mkhalil@usm.my](mailto:mkhalil@usm.my) (Muhammad Khalil Abdullah)

[syakirin@usm.my](mailto:syakirin@usm.my) (Mohd Syakirin Rusdi)

[mezul@usm.my](mailto:mezul@usm.my) (Mohd Zulkifly Abdullah)

[abdus@usm.my](mailto:abdus@usm.my) (Abdus Samad Mahmud)

[zulariff@usm.my](mailto:zulariff@usm.my) (Zulkifli Mohamad Ariff)

[cykhor@unimap.edu.my](mailto:cykhor@unimap.edu.my) (Khor Chu Yee)

[najibali@utem.edu.my](mailto:najibali@utem.edu.my) (Mohd Najib Ali Mokhtar)

\*Corresponding author



## INTRODUCTION

Despite developing other manufacturing methods and techniques, injection molding is still frequently utilized to create numerous products (Wang et al., 2022; Patil et al., 2021). Intricate forms may be developed using the injection molding method's high pressure (Nagasundaram et al., 2021). Injection molding is now used to make more than one-third of all thermoplastic materials. However, mold fabrication requires a significant amount of time and money. The degree of difficulty is determined by the cavity's design. Additional tooling processes and components are necessary for the complicated shape and distinctive surface cavity. Mold design is typically performed through trial and error, based on years of experience. The fundamental cause and treatment are found via trial and error when a defect develops. If this occurs, the cost and duration of the process, as well as the amount of waste generated by using raw materials, could increase. Due to the high cost of tooling and mold development, conducting a thorough and cost-effective pre-molding analysis is necessary. Alternatively, using simulation modeling tools, the engineer and mold designer may quickly grasp the filling problem and determine the optimal cavity design. Thus, simulations may help accelerate manufacturing and cut testing expenses (Köhn et al., 2021).

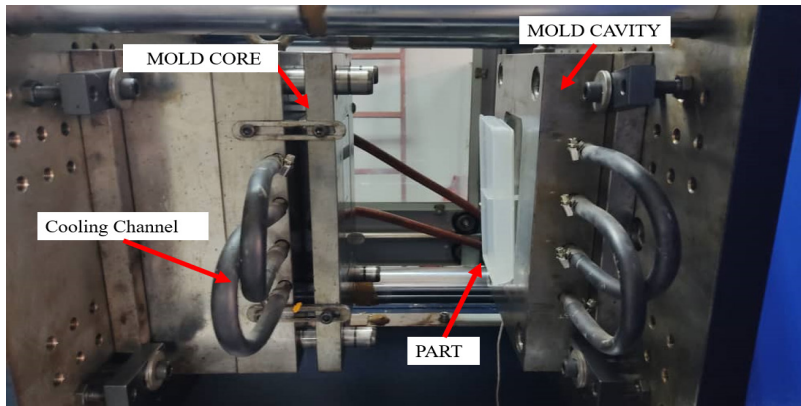


Figure 1. Example of injection molding mold

Rusdi et al. (2016) conducted injection molding simulation using ANSYS FLUENT, the computerized numerical analysis tool for CFD simulation. Injection pressure and temperature were studied. These two process input parameters affect the run time of the mold injection, the advancement of the flow front, and the injection-molding flow.

The ICM process was used in this study by Kwon et al. (2018) for an energy-related application, namely a thin and large polymeric battery case. The mold for the battery case was made using injection molding. The flow of molten polymer into the mold cavity was explored experimentally. To better understand the ICM process, the ICM and traditional injection molding methods were numerically compared. The ICM was determined to



have a low filling pressure, resulting in reduced final product shrinkage and warpage. In addition, the effect of the parting line gap on ICM properties such as filling pressure, filling time, clamping force, warpage, and volumetric shrinkage was investigated using numerical modeling.

A novel constitutive equation for compressing flow, based on the Phan–Thien–Tanner (PTT) model, has been proposed by Cao et al. (2019). This model describes polymers' shear thinning and strain hardening by employing analytical stress solutions for shear and extensional flows. Cao et al. characterize the uniform viscoelastic flow problem for injection/compression in a non-isothermal compressible fluid using a finite element technique. A weak form pseudo-Poisson pressure equation is used to ensure a stable and efficient numerical system. A two-step iterative technique decoupled the velocity, pressure, temperature, and stress. They replicate the benchmark 4:1 contraction flow and compare their results to published findings for validation. Finally, additional injection and compression molding tests are conducted.

Zhang et al. (2019) employed essential microfeatures on a microfluidic flow cytometer chip with a 3:1 aspect ratio as a typical model to establish a suitable approach for describing the filling of the microfeatures using commercial simulation software. Heat transfer coefficients, venting, wall slip, and freeze temperature were all thoroughly researched because they were crucial for micro injection molding but not so for conventional injection molding. A numerical approach for generating material data on thermoset injection molding compounds has been developed by Tran and Gehde (2019), and it has been integrated directly into a simulation program to evaluate its applicability during the thermoset injection molding simulation phase. Also considered during the filling simulation phase was a significant slip phenomenon at the interface of the thermoset melt and the wall surface discovered and observed during injecting molding tests.

Tosello and Costa (2019) did a micro-molding simulation by simulating the real production conditions in the software. Numerous parts of the simulation setup have been investigated to improve the simulation results: the injection rate profile, the injection temperature, the three-mesh specification, and the properties of the molten and solid materials. To make quantitative comparisons, we looked at molding mass, injection pressure, and shot mass. Reducing incidences and uncertainties in experimental data is vital to prevent adding extra uncertainties to simulation computations. Finally, Finkeldey et al. (2020) describe a unique machine learning-based methodology for forecasting the quality attributes of an injection molding process using a mix of simulation and measurement data.

For the low-pressure powder injection molding process, Trad et al. (2020) took an experimental approach of using a cylindrical mold cavity (11.75 mm in diameter and 100 mm long) to validate the numerical modeling of the mold filling stage and component segregation. Autodesk Moldflow Synergy 2019 software was used as a numerical

simulation tool to determine the injected length, filling time, front velocity, shear rate, and pressure, as well as the amount of powder segregation after injection. Aside from that, real measurements of the feedstock's thermal and rheological properties were performed to generate the constitutive equations that would be sent to Moldflow for processing. Finally, a laboratory injection press and real-scale injections (at feedstock temperatures ranging from 80°C to 100°C) were used to validate the findings of the computer models. This study employed a feedstock formulation based on 17-4 PH stainless steel powder (60% vol powder) for experimental characterization and injection.

Trad et al. (2020) were able to duplicate the injection molding process using pvT test equipment and determine the precise fluctuation of a specific volume. There were considerations for the starting temperature and holding pressure, as well as the ending temperature and cooling rate, in addition to the injection temperature and holding time, as well as the cooling rate and holding pressure. Amorphous acrylonitrile-butadiene-styrene (ABS) was used in conjunction with semicrystalline polypropylene (PP). The impact of these parameters on changes in volume during the simulated injection molding cycles was investigated using the design of experiments (DoE) approach.

Sahli et al. (2020) investigated to maximize injection and processing parameters to ensure the molding standard had acceptable properties. Everything of the thermo-rheo-kinetic behavior was determined to accurately predict the entire injection-molding process of curing and cross-linking liquid silicone during the filling stage. Thermal dependence was according to the law of Carreau-Yasuda and Isayev Deng. For the test the thermo-rheo-kinetic behavior and adhesion of liquid silicone during the filling process, Sahli et al. use finite element software (Cadmold 3D).

A collaborative effort between computer scientists, researchers, and technicians has the potential to be critical in the development of simulation software (Khosravani et al., 2022). Effective cooperation is required because of changing client demands and creating new products. This collaboration is possible under specific circumstances, but it is a difficult subject. Despite the many advantages simulation may provide to Industry 4.0, modeling and simulation need further study. The product's geometry, the polymer utilized, the mold, the technical parameters of processing, and the injection molding machine itself all affect the quality of injection molded products (Szabó et al., 2021). Early detection of problems and mold improvement regarding flow simulation can be visualized using simulation models. In this present study, a three-dimensional (3D) mold filling simulation was conducted for the syringe barrel cavity using medical-grade PP material. Additionally, there is a lack of material on the injection molding technique for the medical syringe when medical-grade thermoplastic is used. Thus, this work aims to close this research gap using simulation analysis. The current study made use of CFD software, specifically ANSYS FLUENT 14.0. Rheology experiments were utilized to characterize the rheological properties of PP for use in CFD simulations.

## NUMERICAL SIMULATION METHOD

When explaining thermoplastic flow behavior throughout the injection molding process, the Navier-Stokes equations were applied in the current investigation. This approach is reliant on several assumptions, including the following:

- A non-isothermal process
- Constant density
- It is a three-dimensional, laminar, and incompressible flow
- The fluid (molten PP) is Generalized Newtonian Fluid (GNF)

For injection molding simulation analysis, the governing equations of mass, energy, and momentum describe the flow motion of melt thermoplastic in the mold cavity. The mass conservation or continuity equation applies to incompressible flow (Equation 1):

$$\frac{\partial u}{\partial x} + \frac{\partial v}{\partial y} + \frac{\partial w}{\partial z} = 0 \quad (1)$$

Conservation of momentum in  $i$  th direction in an inertial (Equation 2):

$$\frac{\partial}{\partial t}(\rho u_i) + \frac{\partial u}{\partial x_j}(\rho u_i u_j) = -\frac{\partial P}{\partial x_i} + \frac{\partial \tau_{ij}}{\partial x_j} + \rho g_i + F_i \quad (2)$$

where  $\rho$  is the fluid density,  $u$  is the fluid velocity component,  $P$  is the static pressure,  $\tau_{ij}$  is the viscous stress tensor, and  $g_i$  and  $F_i$  are the gravitational acceleration and external body force in the  $i$  direction, respectively. In the simulation model, the energy equation represents the temperature of the system and fluid. The energy Equation 3 is as follows:

$$\rho c_p \left( u \frac{\partial T}{\partial x} + v \frac{\partial T}{\partial y} + w \frac{\partial T}{\partial z} \right) = k \left( \frac{\partial^2 T}{\partial x^2} + \frac{\partial^2 T}{\partial y^2} + \frac{\partial^2 T}{\partial z^2} \right) + \eta \dot{\gamma} \quad (3)$$

where  $k$  is the thermal conductivity,  $T$  is the temperature,  $\eta$  is the viscosity, and  $\dot{\gamma}$  is the shear rate, respectively.

Viscosity model data is important to simulate molten material (Gou et al., 2011; Koszkuł & Nabialek, 2004). The cross model is the most appropriate for describing the rheological behavior of materials during the injection molding process (Hassan et al., 2010; Khor et al., 2010). The cross model describes the shear rate dependency between the Upper Newtonian and Shear-Thinning Regions. The model, also known as the Cross-Exp model, has an exponential (Exp) dependence on temperature. By employing the Cross model with Arrhenius temperature dependency, we suppose that the molten PP is described as GNF (Equations 4 & 5) (Rusdi et al., 2016).

$$\eta(T, \dot{\gamma}) = \frac{\eta_0(T)}{1 + \left(\frac{\eta_0 \dot{\gamma}}{\tau^*}\right)^{1-n}} \quad (4)$$

with

$$\eta_0(T) = B \exp\left(\frac{T_b}{T}\right) \quad (5)$$

$\tau^*$  is the parameter that describes the transition region between the power-law region and zero shear rate and of the viscosity curve,  $\eta_0$  is the zero-shear viscosity,  $n$  is the power-law index,  $B$  is an exponential-fitted constant, and  $T_b$  is a temperature-fitted constant.

### Volume of Fluid (VOF) and Boundary Conditions

The VOF model's fundamental principle is to track and locate the fluid-fluid contact. The mold cavity's molten PP and the existing air were two fluid phases during the actual injection molding operation. Therefore, the VOF approach detects and creates the liquid phase distribution. This approach assigns a scalar ( $f$ ) to each cell in the computational grid that shows what fraction of the cell's volume is occupied by liquid (Malgarinos et al., 2014). Thus, when the cell contains only molten PP, the value of  $f$  equals one ( $f = 1$ ), when the cell contains no molten PP (or air), the value of  $f$  equals zero ( $f = 0$ ), and when the value is between 0 and 1 ( $0 < f < 1$ ), the cell comprises "interface" cells, also known as the molten PP front. The equation of the melt front with time was determined by the following transport Equation 6:

$$\frac{dF}{dt} = \frac{\partial F}{\partial t} + \nabla \cdot (uf) = 0 \quad (6)$$

The simulation defined molten PP and air as two different fluid phases. While the molten PP fills the cavity during injection, air escapes through the outlet valves. VOF monitored the filling of the melted plastic and the progression of the flow front over time. In the post-processing step, the mobility of molten PP may be viewed. The computational domain of the CFD analysis was defined by the inlet, outlet, and wall boundaries. The boundary conditions defined on the 3D model are depicted in Figure 1. The following are the boundaries and initial conditions:

- a) On mold wall:  $u = v = w = 0$ ;  $T = T_w$
- b) On melt front:  $p = 0$
- c) At inlet:  $p = p_{in}(x, y, z)$ ;  $T = T_{in}$

### Modeling and Mesh Development

SOLIDWORKS software was used to make the model of the medical syringe (Figure 2). The syringe model is considered the cavity in the real injection molding mold. The outer surface of the model is considered the mold wall. The syringe's specifications have a thickness of 0.25 mm, 0.50 mm, 0.75 mm, 1.00 mm, and 1.25 mm. The CFD computational domain was established in ANSYS WORKBENCH based on the dimensions. The mold entry is positioned on the syringe barrel's body, while the air vent is on the syringe barrel's tip. These locations determined the computational domain's inlet and outflow bounds. The syringe cavity is positioned on the y-axis during the injection molding, and molten PP plastic is injected from the inlet (z-axis). Once the model has been exported to ANSYS WORKBENCH, the model will be meshed (Figure 3), applying boundary conditions (such as inlet, outlet, and wall), creating and performing simulations. LyondellBasell 6331 (LB6331) medical-grade polypropylene was used in this investigation, and rheological characterization data were gathered by capillary rheometer experimental work using the GÖTTFERT Rheograph 25 (capillary rheometer machine).

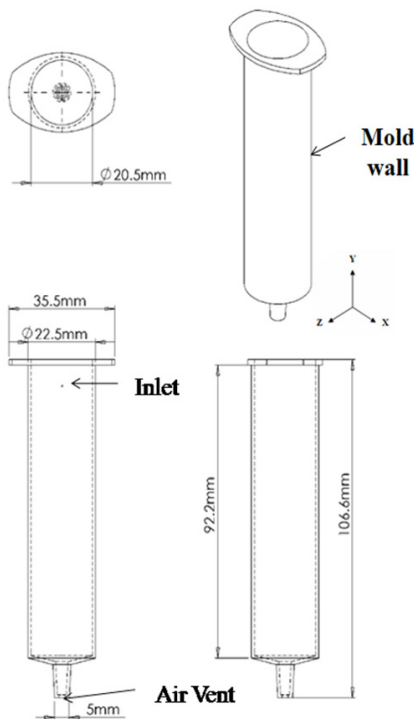


Figure 2. Dimensions and boundary conditions of the syringe barrel mold cavity

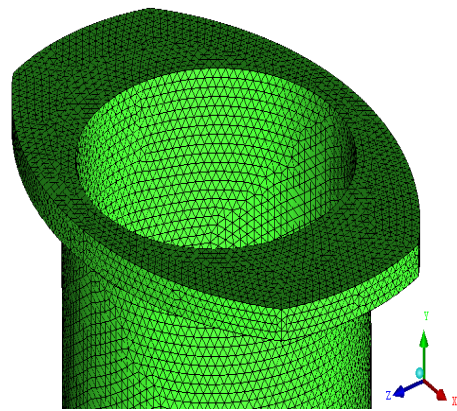


Figure 3. 3-D meshed model for syringe barrel mold cavity

## RESULTS AND DISCUSSION

### Effect of Barrel Thickness for Syringe Barrel Cavity

Cavity thickness is one of the characteristics that affect how molten PP flows. The influence of cavity thickness on velocity profile, flow front advancement, and filling time will be discussed in this section. The thickness ranges between 0.25 mm and 1.25 mm and is

only evaluated for the syringe's thickness up to the tip. The thickness of the flange remains constant. This investigation used a constant system pressure of 5 MPa and a constant melt temperature of 190°C.

**Filling Time.** In Figure 4, a fixed point (Point 1) is depicted in the vicinity of the outlet region. This observation is being made to keep an eye out for the existence of molten PP in the outflow zone. The mold is deemed full when this spot exhibits continuous maximum pressure.

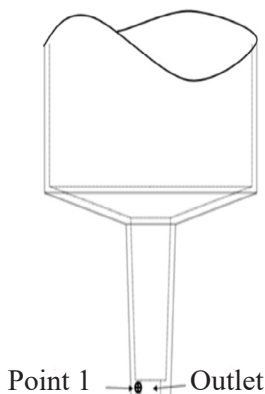


Figure 4. Point where the pressure value was taken

As illustrated in Figure 5, case 0.25 mm could not fill the cavity due to the absence of a maximum pressure plot compared to other thicknesses. The first case fills in 3.99 seconds, followed by case 1.00 mm (4.46 seconds), case 1.25 mm (5.21 seconds), and lastly, the last case 0.5 mm (6.99s), as depicted in Figure 6. When looking at the pressure distribution, the 1.25 mm size had the highest pressure, followed by 1.00 mm, 0.75 mm, and 0.5 mm for the following three sizes, respectively. A bigger thickness results in a greater maximum pressure,

according to the study's results. Because a thick cavity space has a lower barrier to flow and a smaller pressure loss than a thin cavity space, molten polypropylene (PP) may easily fill the gap during the injection molding process. When the system pressure was 5 MPa, and the temperature was 190°C, it was discovered that the molten polypropylene did not have enough energy to fill the cavity gap of Case 0.25 mm in this investigation. Figure 5 illustrates this behavior. At 9 seconds of filling time, the pressure in the 0.25 mm casing is still quite low compared

**Flow Front Advancement.** According to Figure 7, the advancement of the molten PP's flow front was estimated by creating a line in the simulation model (depicted as the red dotted line in Figure 7) through the center of the syringe cavity on the inlet side and the flow front was measured starting from the inlet.

Figure 8 depicts the advancement of the flow front at various thicknesses. Molten polypropylene (PP) in a syringe barrel with a thin cavity flows faster than molten polypropylene in a syringe barrel with a thick cavity at an early stage (0.5s). The flow was close to the entrance when minimal pressure and volumetric loss were critical. Reduced cavity volume necessitates a shorter filling time (rapid filling process) and faster flow front

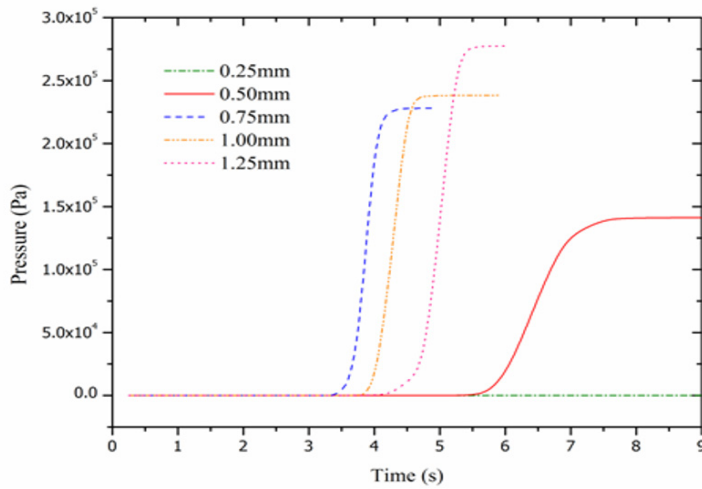


Figure 5. Pressure distribution for different thicknesses

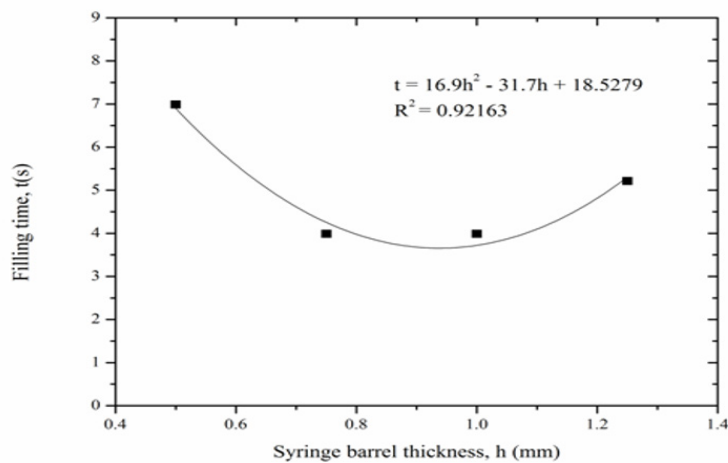


Figure 6. Filling time for different syringe barrel thicknesses

advancement. Because the thick syringe cavity has a larger capacity to fill, the flow front progress is slower than with a narrow cavity. Throughout the filling process, case 0.25 mm flow front advancement becomes slower and practically static, and molten PP ceases to flow into the cavity (Figure 9). The 0.25 mm thickness results in increased flow resistance, which results in increased pressure loss until the pressure is no longer sufficient to propel the flow. However, the thick cavity’s flow front advances smoothly as time passes. At this point, two things are considered: pressure loss and the volume to be filled with air. In addition to having less pressure loss, a thicker cavity also has a larger volume than the melt flow must occupy, as opposed to a thinner cavity. As a result, case 0.75 mm has the fastest



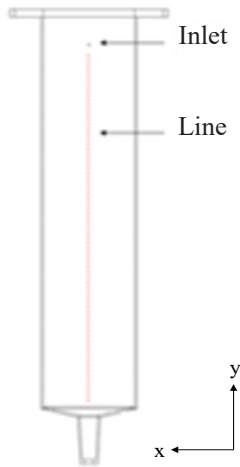


Figure 7. The line for flow front advancement measurement

flow front advancement despite having a greater pressure loss than cases 1.00 mm and 1.25 mm, despite having a higher-pressure loss than the other cases. 0.75 mm thickness provides the best balance between pressure loss and the occupied syringe barrel volume, resulting in the fastest fill time and flow front advancement.

**Velocity.** During the injection molding process, it is difficult to determine the velocity of the molten PP. As a result, the simulation modeling method is critical in providing engineers with a realistic process

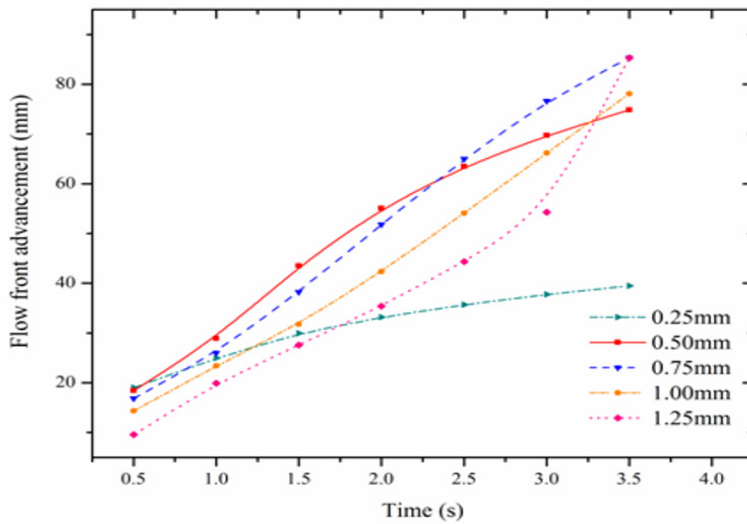


Figure 8. Flow front advancement for different thicknesses

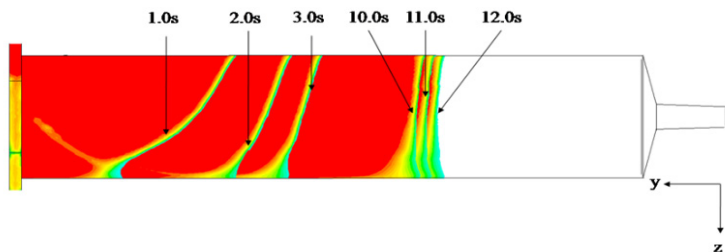


Figure 9. Flow front advancement of case 0.25mm



picture. Additionally, it assists the engineer in comprehending the flow behavior and flowability of the part design. The velocity values of molten PP are estimated at eight sites in this investigation, as seen in Figure 10. The eight locations are positioned 10mm below the inlet (-y-direction).

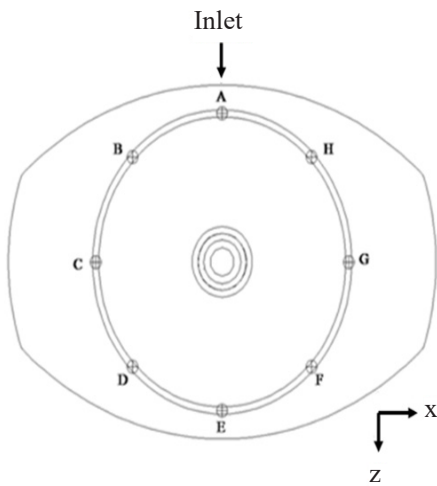


Figure 10. Point where the velocity values were taken

The velocity values for various thicknesses at 2s are displayed in Figure 11. According to expectations, the fastest velocity is found in the thickest layer (0.75mm), which can be found in all locations. In contrast, case 1.25 mm has the highest value at point E due to its smaller size. Furthermore, since Point E is located at the intersection of two directions of flow, it is considered an extreme velocity point since the value was obtained at the point where the two directions of flow meet, resulting in a high flow velocity at the intersection of Point E (Figure 12).

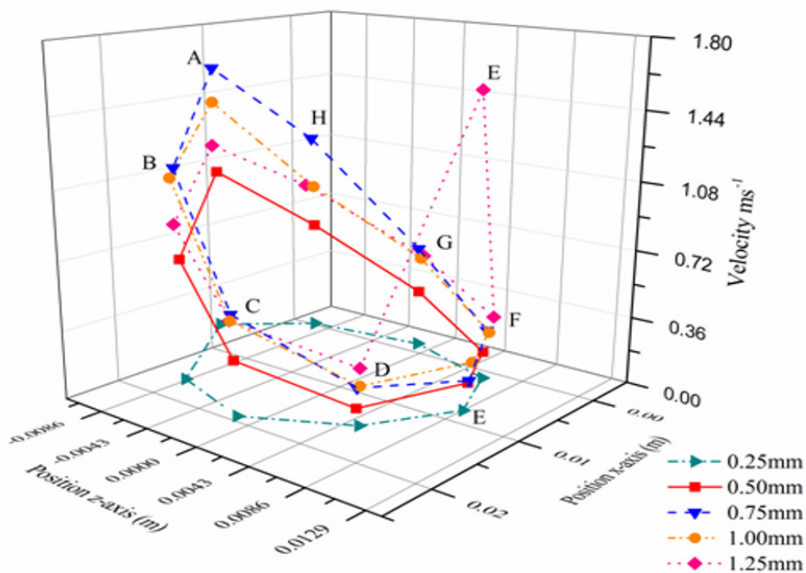


Figure 11. Velocity values for different thicknesses at 2s

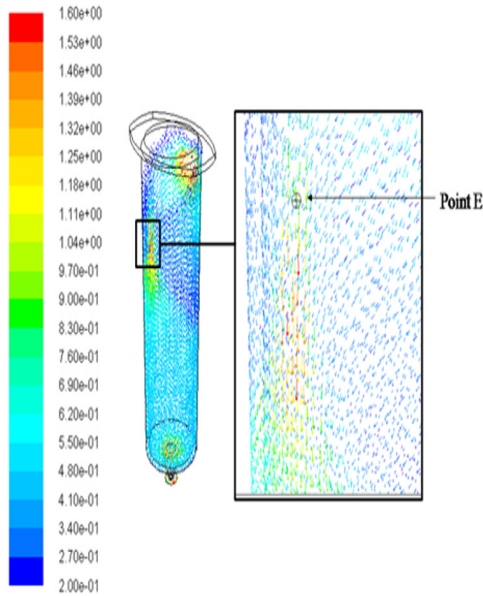


Figure 12. Velocity vector (unit:ms<sup>-1</sup>) at point E for Case 1.25 mm at 2s

As a result, in each example, the highest velocity values were obtained at normal flow at point A. In Figure 13, the greatest velocities were tabulated. A negative quadratic trend can be observed between 0.75 mm and 1.0mm in terms of maximum velocity. The velocity will be extremely low unless the cavity thickness is more than this range. When using 0.75 mm thick syringe cavities, the case 0.75 mm has the highest velocity figures, suggesting that it will fill the syringe the quickest and advance the flow front the fastest. While it has a lower maximum pressure (and therefore more pressure loss) than the 1.00 mm and 1.25 mm, the smaller cavity volume benefits from, the higher velocity profile due to the smaller cavity capacity.

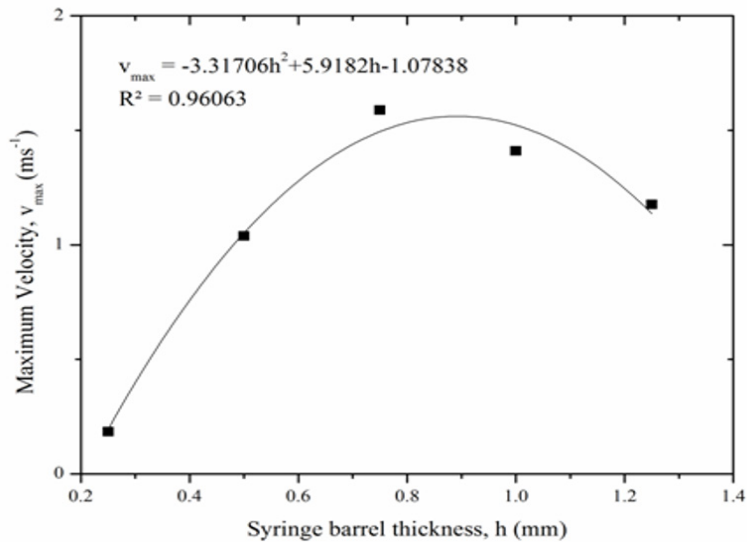


Figure 13. Maximum velocity for different barrel thicknesses

### Effect of Inlet Position for Syringe Barrel Cavity

When the syringe barrel is injection molded, the inlet site is often positioned in the syringe body. Therefore, the location of the inlet was changed in the same y-axis line at five different

locations along this section. The points are located at distances of 6.5 mm to 86.5 mm from the flange, with a 20mm distance between each point. The melt temperature and system pressure were maintained at 5 MPa and 190°C, respectively.

**Cavity Filling.** In order to determine the amount of pressure applied during the injection molding process, two points were used in the experiment. Point 1 was placed closer to the exit, as described in Figure 4, and Point 2 was placed closer to the syringe barrel flange, as illustrated in Figure 14. The first point was used to detect the presence of molten PP in the bottom portion of the syringe cavity, while the second point was utilized to detect the presence of molten PP in the top area of the syringe cavity (flange section). The mold is deemed filled when these spots exhibit the same maximum pressure.

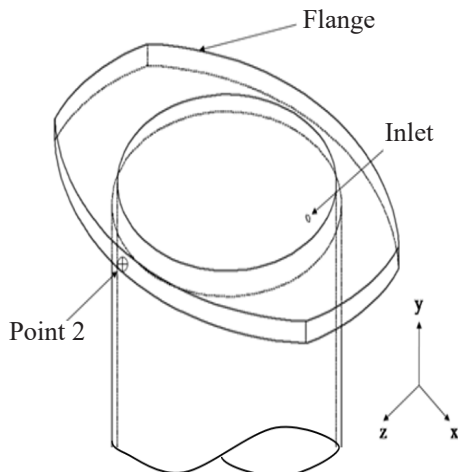


Figure 14. Point 2 location at screw barrel mold cavity

Only the pressures of cases 6.5 mm, 46.5 mm, and 86.5 mm can reach point 1 (Figure 15). However, only case 6.5 mm reached the highest constant pressure curve at point 2 (Figure 16). Based on these two observations, only the case 6.5 mm inlet position can fill the syringe barrel cavity. In other instances, those who were unable to reach one or both locations were deemed to have failed to fill the cavity. The results indicated that the filling of case 86.5 mm with molten PP can only reach point 1 due to its proximity to the outlet and point 1. Its placement also results in unusually high-pressure values when it reaches point 1 at approximately 11.45 MPa, as opposed to 0.14 MPa and 0.18 MPa for cases 6.5 mm and 46.5 mm, respectively.

**Flow Front Advancement.** When five various intake positions are used, only case 6.5 mm fills the cavity, according to the simulation findings. This experiment considered just one exit while designing the syringe barrel cavity. The other examples encountered difficulties because trapped air at the flange part impeded the flow of molten PP. When the molten PP flow from the input side merged with the flow from the backside of the mold cavity, the molten PP flow ceased (Figure 17). The merge entrapped air around the upper side of the cavity (flange portion), preventing it from exiting through the outlet. Even though molten PP does not reach point 2 in cases 26.5 mm, 46.5 mm, and 66.5 mm, these three instances

retain a high-pressure value at point 2 (Figure 16). The pressure values were determined by the pressure of trapped air within the flange section, which prevents the molten PP from filling the flange section.

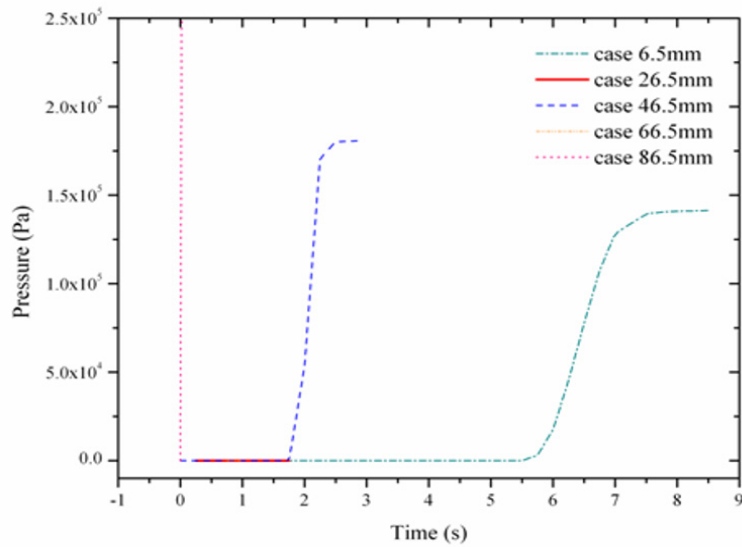


Figure 15. Pressure distribution at point 1

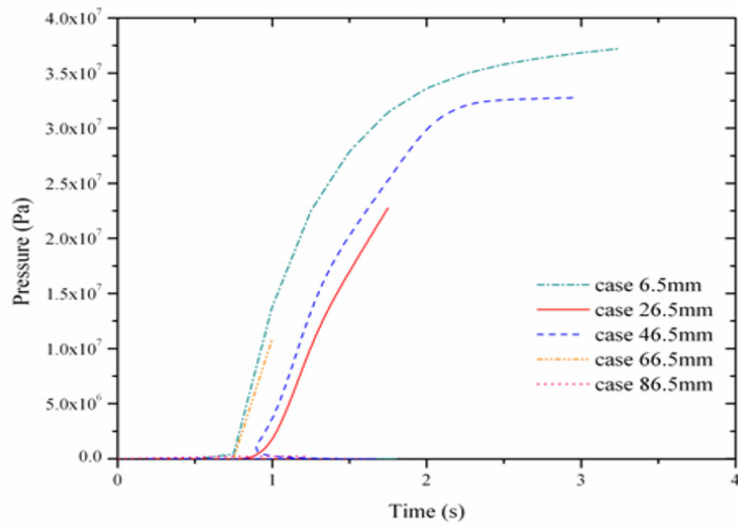


Figure 16. Pressure distribution at point 2

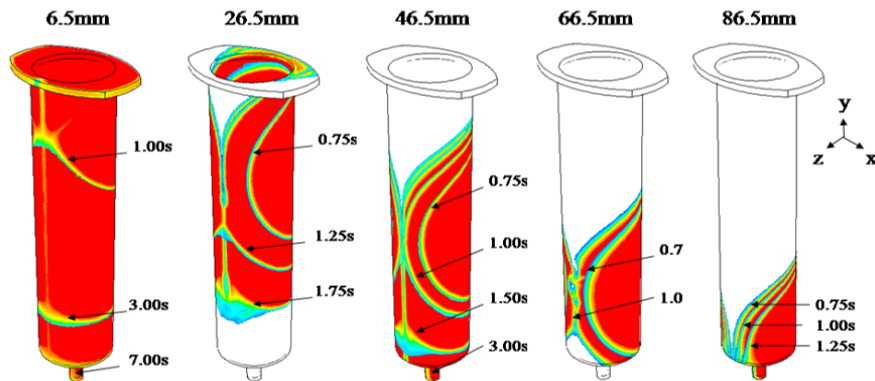


Figure 17. Flow front advancement for different inlet positions

The simulation findings demonstrated that intake position influences pressure and flow front advancement. Additionally, the cavity exit position is crucial for injection molding the syringe barrel. An insufficient exit would result in air entrapment and act as a barrier to the molten PP filling that region. Therefore, it is recommended that the outlet be situated as far away from the intake as practicable. The injection molding procedure must take the output location into account. The outlet is critical for venting air from the mold cavity and facilitating the filling of the cavity with molten PP.

## CONCLUSION

CFD simulations of the syringe barrel were performed, and the barrel was filled with medical-grade PP (LB6331). An appropriate outlet placement must be considered for the injection molding process to be successful. The exit must be as far away from the inlet as possible to properly channel out air and give space for the molten PP to occupy the hollow area. Syringe barrels of varying thickness (0.25 mm, 0.5 mm, 0.75 mm, 1.00 mm and 1.25 mm) exhibit varying flow characteristics. The right thickness must be determined carefully and not simply based on whether a thicker or thinner thickness is acceptable. While thinner thickness results in greater pressure losses than higher thickness, thinner thickness requires less volume to occupy. The range of 0.75 mm to 1.00 mm demonstrated a faster filling time, a faster advancement of the flow front, and a greater flow velocity in the current investigation. These results demonstrated that CFD simulation could simulate capable of simulating the syringe barrel injection molding process.

## ACKNOWLEDGEMENT

The authors acknowledge the support from the Short-Term Research Grant, Universiti Sains Malaysia (304/PMEKANIK/6315569) and the School of Mechanical Engineering, Universiti Sains Malaysia.

## REFERENCES

- Cao, W., Shen, Y., Wang, P., Yang, H., Zhao, S., & Shen, C. (2019). Viscoelastic modeling and simulation for polymer melt flow in injection/compression molding. *Journal of Non-Newtonian Fluid Mechanics*, 274, Article 104186. <https://doi.org/10.1016/j.jnnfm.2019.104186>.
- Finkeldey, F., Volke, J., Zarges, J. C., Heim, H. P., & Wiederkehr, P. (2020). Learning quality characteristics for plastic injection molding processes using a combination of simulated and measured data. *Journal of Manufacturing Processes*, 60, 134-143. <https://doi.org/10.1016/j.jmapro.2020.10.028>.
- Gou, G., Xie, P., Yang, W., & Ding, Y. (2011). Online measurement of rheological properties of polypropylene based on an injection molding machine to simulate the injection-molding process. *Polymer Testing*, 30(8), 826-832. <https://doi.org/10.1016/j.polymertesting.2011.08.005>.
- Hassan, H., Regnier, N., Pujos, C., Arquis, E., & Defaye, G. (2010). Modeling the effect of cooling system on the shrinkage and temperature of the polymer by injection molding. *Applied Thermal Engineering*, 30(13), 1547-1557. <https://doi.org/10.1016/j.applthermaleng.2010.02.025>.
- Khor, C. Y., Ariff, Z. M., Ani, F. C., Mujeebu, M. A., Abdullah, M. K., Abdullah, M. Z., & Joseph, M. A. (2010). Three-dimensional numerical and experimental investigations on polymer rheology in meso-scale injection molding. *International Communications in Heat and Mass Transfer*, 37(2), 131-139. <https://doi.org/10.1016/j.icheatmasstransfer.2009.08.011>.
- Khosravani, M. R., Nasiri, S., & Reinicke, T. (2022). Intelligent knowledge-based system to improve injection molding process. *Journal of Industrial Information Integration*, 25, Article 100275. <https://doi.org/10.1016/j.jii.2021.100275>.
- Köhn, C., van Laethem, D., Deconinck, J., & Hubin, A. (2021). A simulation study of steric effects on the anodic dissolution at high current densities. *Materials and Corrosion*, 72(4), 610-619. <https://doi.org/10.1002/maco.202012051>.
- Koszul, J., & Nabialek, J. (2004). Viscosity models in simulation of the filling stage of the injection molding process. *Journal of Materials Processing Technology*, 157(2), 183-187. <https://doi.org/10.1016/j.jmatprotec.2004.09.027>.
- Kwon, Y. I., Lim, E., & Song, Y. S. (2018). Simulation of injection-compression molding for thin and large battery housing. *Current Applied Physics*, 18(11), 1451-1457. <https://doi.org/10.1016/j.cap.2018.08.017>.
- Malgarinos, I., Nikolopoulos, N., Marengo, M., Antonini, C., & Gavaises, M. (2014). VOF simulations of the contact angle dynamics during the drop spreading: Standard models and a new wetting force model. *Advances in Colloid and Interface Science*, 212, 1-20. <https://doi.org/10.1016/j.cis.2014.07.004>.
- Nagasundaram, N., Devi, R. S., Rajkumar, M. K., Sakthivelrajan, K., & Arravind, R. (2021). Experimental investigation of injection moulding using thermoplastic polyurethane. *Materials Today: Proceedings*, 45, 2286-2288. <https://doi.org/10.1016/j.matpr.2020.10.264>.
- Patil, D. C., Kelageri, N. K., Janawade, S. A., & Mishrikoti, M. S. (2021). Design and analysis of 25 T injection molding machine. *Materials Today: Proceedings*, 46, 2596-2601. <https://doi.org/10.1016/j.matpr.2021.02.262>.

- Rusdi, M. S., Abdullah, M. Z., Mahmud, A. S., Khor, C. Y., Aziz, A., Ariff, Z. M., & Abdullah, M. K. (2016). Numerical investigation on the effect of pressure and temperature on the melt filling during injection molding process. *Arabian Journal for Science and Engineering*, *41*(5), 1907-1919. <https://doi.org/10.1007/s13369-016-2039-0>.
- Sahli, M., Barriere, T., & Roizard, X. (2020). Experimental and numerical investigations of bi-injection moulding of PA66/LSR peel test specimens. *Polymer Testing*, *90*, Article 106748. <https://doi.org/10.1016/j.polymertesting.2020.106748>.
- Szabó, F., Suplicz, A., & Kovács, J. G. (2021). Development of injection molding simulation algorithms that take into account segregation. *Powder Technology*, *389*, 368-375. <https://doi.org/10.1016/j.powtec.2021.05.053>.
- Tosello, G., & Costa, F. S. (2019). High precision validation of micro injection molding process simulations. *Journal of Manufacturing Processes*, *48*, 236-248. <https://doi.org/10.1016/j.jmapro.2019.10.014>.
- Trad, M. A. B., Demers, V., Côté, R., Sardarian, M., & Dufresne, L. (2020). Numerical simulation and experimental investigation of mold filling and segregation in low-pressure powder injection molding of metallic feedstock. *Advanced Powder Technology*, *31*(3), 1349-1358. <https://doi.org/10.1016/j.apt.2020.01.018>.
- Tran, N. T., & Gehde, M. (2019). Creating material data for thermoset injection molding simulation process. *Polymer Testing*, *73*, 284-292. <https://doi.org/10.1016/j.polymertesting.2018.11.042>.
- Wang, J., Hopmann, C., Kahve, C., Hohlweck, T., & Alms, J. (2020). Measurement of specific volume of polymers under simulated injection molding processes. *Materials & Design*, *196*, Article 109136. <https://doi.org/10.1016/j.matdes.2020.109136>
- Zhang, H., Fang, F., Gilchrist, M. D., & Zhang, N. (2019). Precision replication of micro features using micro injection moulding: Process simulation and validation. *Materials & Design*, *177*, Article 107829. <https://doi.org/10.1016/j.matdes.2019.107829>.





## Blade Fault Localization with the Use of Vibration Signals Through Artificial Neural Network: A Data-Driven Approach

Ngui Wai Keng<sup>1\*</sup>, Mohd Salman Leong<sup>2</sup>, Mohd Ibrahim Shapiai<sup>3</sup> and Lim Meng Hee<sup>2</sup>

<sup>1</sup>College of Engineering, Universiti Malaysia Pahang, 26600 UMP, Pahang, Malaysia

<sup>2</sup>Institute of Noise and Vibration, Universiti Teknologi Malaysia, 54100 UTM, Kuala Lumpur, Malaysia

<sup>3</sup>Malaysia-Japan Institute of Technology, Universiti Teknologi Malaysia, 54100 UTM, Kuala Lumpur, Malaysia

### ABSTRACT

Turbines are significant for extracting energy for petrochemical plants, power generation, and aerospace industries. However, it has been reported that turbine-blade failures are the most common causes of machinery breakdown. Therefore, numerous analyses have been performed to formulate techniques for detecting and classifying the fault of the turbine blade. Nevertheless, the blade fault localization method, performed to locate the faulty parts, is equally important for plant operation and maintenance. Therefore, this study will propose a blade fault localization method centered on time-frequency feature extraction and a machine learning approach. The purpose is to locate the faulty parts of the turbine blade. In addition, experimental research is carried out to simulate various blade faults. It includes blade rubbing, blade parts loss, and twisted blade. An artificial neural network model was developed to localize blade fault through the extracted features with newly proposed and selected features. The classification results indicated that the proposed feature set and feature selection method could be used for blade fault localization. It can be seen from the classification rate for blade faultiness localization.

### ARTICLE INFO

#### Article history:

Received: 17 February 2022

Accepted: 21 June 2022

Published: 19 August 2022

DOI: <https://doi.org/10.47836/pjst.31.1.04>

#### E-mail addresses:

wkngui@ump.edu.my (Ngui Wai Keng)

salman.leong@gmail.com (Mohd Salman Leong)

md\_ibrahim83@utm.my (Mohd Ibrahim Shapiai)

limmenghee@gmail.com (Lim Meng Hee)

\*Corresponding author

*Keywords:* Blade fault, classification, localization

### INTRODUCTION

Compressors and turbines are important for extracting energy for petrochemical plants, power generation, and aerospace industries.

The blades of compressors and turbines are the critical parts of their operating system. The failures occurring in compressors and turbines blade result in significant gas turbine damages, catastrophic failure, and financial losses. To illustrate this, Barnard (2006) reported that two catastrophic gas turbine failures account for more than US\$ 25million spent to make up for the production downtime of this equipment.

Moreover, Marsh has testified that turbine and turbine-blade malfunctions continue to be the most typical cause of machinery glitches. It is based on what was experienced by their clients (Marsh, 2016). Therefore, blade fault diagnosis performed on compressors and turbines is essential. The purpose of the diagnosis is to safeguard the safety of this equipment, as well as to prevent significant economic loss. It makes the effective and precise techniques applied for blade fault diagnosis very important.

The singularity discovery approach is the traditional method for blade fault diagnosis, which includes taking a visual depiction of the signal, singularity detection, and the creation of a unique “fingerprint” or “signature.” For example, Peng et al. (2002) applied three distinctive signal processing techniques to determine oil whirl, rotor-to-stator rubbing, and coupling misalignment. The experiment’s results showed that the reassigned wavelet scalogram was a more efficient signal processing method than the frequency spectrum and wavelet scalogram method. In addition, the latest blade fault discovery techniques using time-frequency methods were also anticipated for blade fault diagnosis (Lim & Leong, 2013).

Based on the investigation conducted by Abdelrhman et al. (2014), it was found that wavelet analysis was incapable of separating the frequency components when they were placed close to each other. Two new wavelets were suggested to seek a way out of this problem. According to the findings of the experiment, it was shown that wavelet maps drawn by the suggested new wavelets could not distinguish between the missing blade parts and the defected blade. Besides that, Wang and Chu (2001) recommended a combined wavelet analysis approach and acoustic emission for rubbing fault diagnosis. Chang and Chen (2004) reported that parts in the blade cracks could be localized by applying spatial wavelet analysis. Lim and Ngui (2015) probed the comparison between the effectiveness of the wavelet analysis and vibration spectrum wavelet analysis in diagnosing the blade-related failure. From the experiment, it could be established that both methods are similar for detecting twisted blade conditions. However, a detailed understanding of the vibration spectrum and wavelet map is needed to detect the twisted blade parts.

Overall, most studies mainly focused on detecting blade fault and classifying the fault through the singularity approach. This evaluation approach compares the vibration spectrum or the wavelet map’s amplitudes or patterns. The amplitudes and patterns represent the faulty or healthy condition of a blade. However, there are several challenges and difficulties in deducing the vibration spectrum and wavelet outcomes. Besides, the precision of these

methods depends on the knowledge and individuals' experience in deducing the vibration spectrum and wavelet results.

On the other hand, the artificial intelligence method includes a learning algorithm. With this approach, manual interpretation, which is only subject to the knowledge and the individual's experience, can be relegated. Furthermore, artificial intelligent methods offer automated fault diagnosis (Tiboni et al., 2022; Pang et al., 2020). Previous researchers had also used this method for blade fault diagnosis. The blade features, drawn by vibration signal using frequency domain analysis, were often utilized for blade fault diagnosis. For example, Kuo (1995) studied the occurrence of the wobbly blade, unstable blades, or a blend of these two faults. The defective blades were detected using the aspects drawn from the Fourier analysis as inputs to the ANN. With reference to the investigation, it was clear that the recommended techniques for blade defect classification were workable. Kyriazis et al. (2006) further explored this segment of work. This study investigated the effectiveness of two different models for fusion purposes. Consequently, classification results showed that the information on the recommended combined techniques could be a great instrument utilized for effective blade fault classification. Furthermore, a fault diagnosis method based on ANN was developed. The features extracted from wavelet coefficients as the inputs for ANN were used to classify the blade fault. Consecutively, the proposed techniques were effective for blade fault classification (Ngui et al., 2017). Most of the studies mainly focused on blade fault detection and classification.

For the past few years, numerous studies have been conducted to develop blade fault diagnosis methods. However, there is a limitation in the method for blade fault localization in terms of its ability to locate the blade's faulty parts. Nevertheless, the method for blade fault localization applied to locate the blade's faulty parts is equally important for plant operation and maintenance.

Even though the artificial intelligence method through the machine learning approach was deployed for blade fault diagnosis, its usage was hardly found in the literature. As a result, very few blade fault diagnosis methods are based on machine learning. These methods are developed using the blade features extracted from frequency domain analysis. This process is especially true for blade fault localization. Therefore, this study aims to develop a method that can be utilized for blade fault localization, which is centered on time-frequency feature extraction and machine learning approaches. Several contributions are summarized as follows:

1. The raw vibration signals were analyzed using continuous wavelet transform to extract features as the input for the classifier.
2. A new feature set (blade statistical summation) was proposed to improve the blade fault localization method.
3. A genetic algorithm was used for feature selection.

4. A new blade fault localization method was built based on the extracted features of the recently suggested feature set and feature selection strategy, running on a machine-learning technique.

## MATERIALS AND METHODS

### Experimental Study

Figure 1 illustrates the blade fault test rig employed to simulate numerous blade fault states. The blade fault test rig, which consisted of multi-stages of the rotor blade, possessed 8, 11, and 13. The vibration signals were measured using two accelerometers (Wilcoxon, model 780A). All accelerometers used in the experiment were calibrated with a Rion VE-10 calibration exciter. The Tacho signal was also captured simultaneously using the optical probe with a reflective tape (Compact Instruments, model VLS-DA1-LSR). Ono Sokki CT-742 Digital Tachometer Display was also used in the experiment to verify the operating speed of the experiment further. A handheld digital tachometer was also used to validate the operating speed of the experiment.

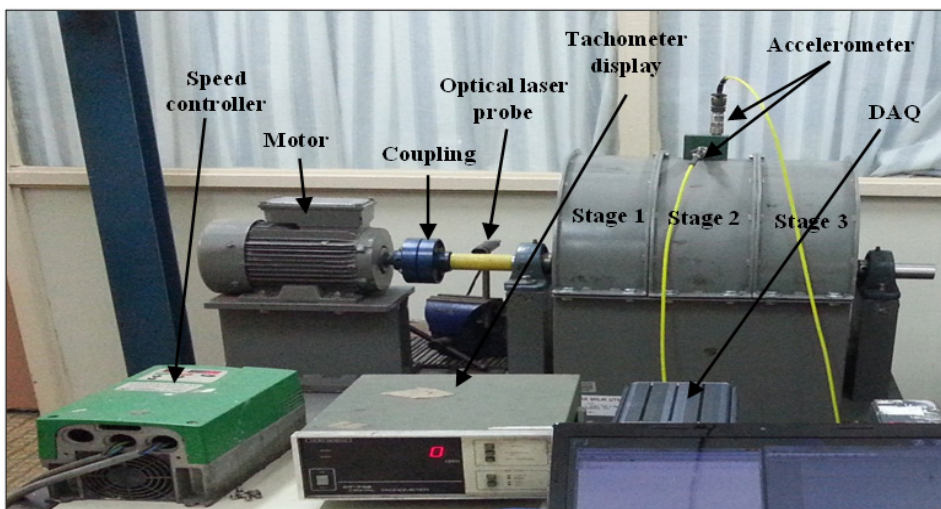


Figure 1. Blade fault test rig

### Experiment Procedure

A three-stage blade fault test rig was adopted in this experiment. First, the blade's initial state (no blade defect) was attained before any blade defect was applied to the test rig. Before the blade defect was applied to the test rig, the tacho and vibration signals for the blade's initial state (no blade defect) were attained. These signals were measured at a steady-state sampling rate of 5 kHz with the test rig's rotating speed set to 1200 rpm. With

a sampling rate of 5 kHz, a total of 250 data points were sampled in just one complete cycle of rotation. It is a reasonably fine sampling resolution and is deemed sufficient to prevent any loss of information. Following that, three different blade faults were applied to various stages of the rotor blade test rig.

Then, the corresponding tacho and vibration signals were acquired. Figure 2 presents the three different blade faults simulated on the test rig, which was done by replacing a normal blade with a prefabricated faulty blade. Blade rubbing was performed by substituting one of the normal blades with a prefabricated blade attached to a sheet metal piece. It was done to the prefabricated blade to lengthen the blade's length. Moreover, the rubbing of a single blade was conducted in a state that the blade's edge must simply be in contact with the rotor casing's internal surface. The loss of the blade defect part was presented in the experiment by substituting one of the standard blades with a manufactured one, which went through a partial loss. Finally, a piece of the standard blade was replaced with another and latched onto the rotor disk backward to gain a twisted blade state. Experimental studies for all blade fault conditions were undertaken in a controlled environment. Various measures were undertaken to reduce rotor dynamics instability effect on the experimental results, such as the rotor system's natural frequencies study, rotor balancing, and rotor alignment prior to the experiment. In order to minimize the random error and reduce the noise in the vibration spectra, Synchronous Time Averaging (STA) method was deployed during the signal processing stage. A total of 21 different blades faulted conditions were examined in this study, as illustrated in Table 1. Figure 3 shows the time domain signals for different blade faulted conditions simulated at stage 3.

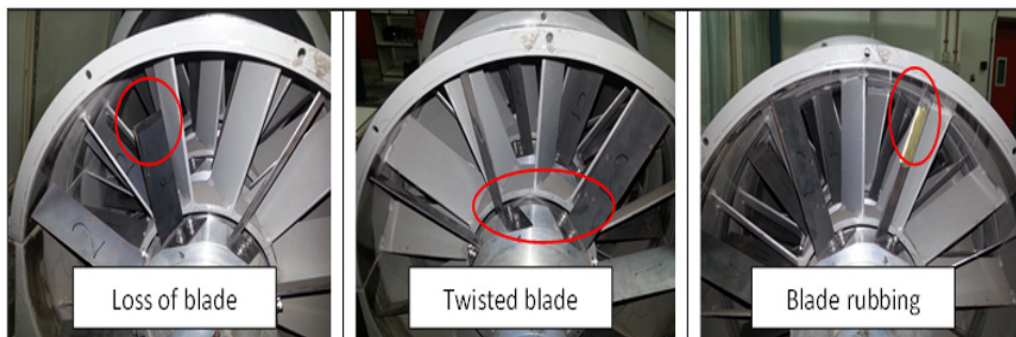
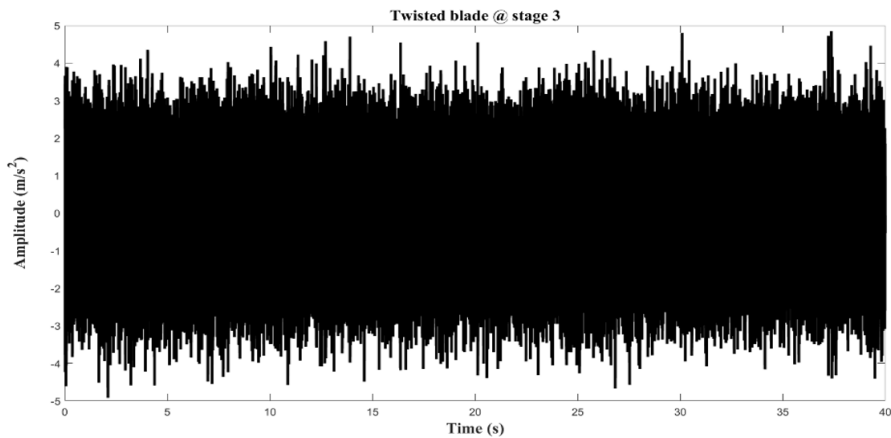


Figure 2. Type of blade faults

Table 1

*Blade conditions*

Blade condition	Fault location
Loss of blade part	Loss of blade part in stage 1
	Loss of blade part in stage 2
	Loss of blade part in stage 3
	Loss of blade part in stages 1 and 2
	Loss of blade part in stages 1 and 3
	Loss of blade part in stages 2 and 3
	Loss of blade part in stages 1, 2, and 3
Twisted blade	Twisted blade in stage 1
	Twisted blade in stage 2
	Twisted blade in stage 3
	Twisted blade in stages 1 and 2
	Twisted blade in stages 1 and 3
	Twisted blade in stages 2 and 3
	Twisted blade in stages 1, 2, and 3
Blade rubbing	Blade rubbing in stage 1
	Blade rubbing in stage 2
	Blade rubbing in stage 3
	Blade rubbing in stages 1 and 2
	Blade rubbing in stages 1 and 3
	Blade rubbing in stages 2 and 3
	Blade rubbing in stages 1, 2, and 3





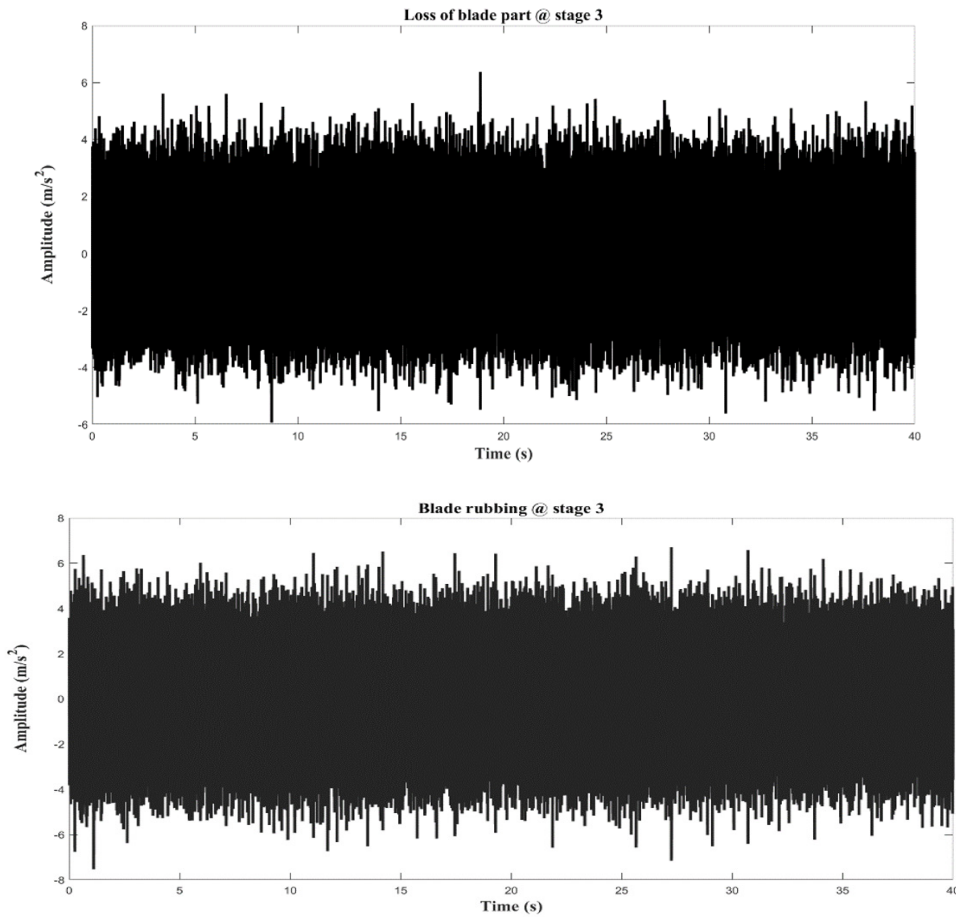


Figure 3. Different blade faulted conditions simulated at stage 3

### Feature Extraction

Based on the proposed feature extraction method, statistical features were extracted for blade fault localizations shown in Figure 4. First, the frequencies were filtered apart from the operating frequency and its conforming blade passing frequencies. The operating frequency was 20 Hz, and the blade passing frequencies for stages 1, 2, and 3 were 160 Hz, 220 Hz, and 260 Hz, accordingly, in this experiment. Next, the filtered signal was transformed from acceleration to velocity mode due to the consistent response of the signals to the frequency range of interest. Then, using the tachometer signal as the marker, the signal was divided into smaller segments (one segment represented one complete cycle of rotation). The STA operation was then applied to every 10th vibration to produce the STA signal, representing the average vibration signal produced by one rotation cycle.

Then, each STA signal was used as the input for the continuous wavelet transform to generate the corresponding wavelet coefficients. The Morlet wavelet was preferred for its ability to achieve better performance, indicating machinery fault problems. An amount of 11 statistical parameters, including energy, variance, mean, crest factor, root mean square, kurtosis, standard deviation, central moment, skewness, energy to Shanon entropy ratio, and the Shanon entropy were counted using the wavelet coefficients of the operating frequency and the blade passing frequencies. Consequently, the statistical features were applied to the classifier’s input features.

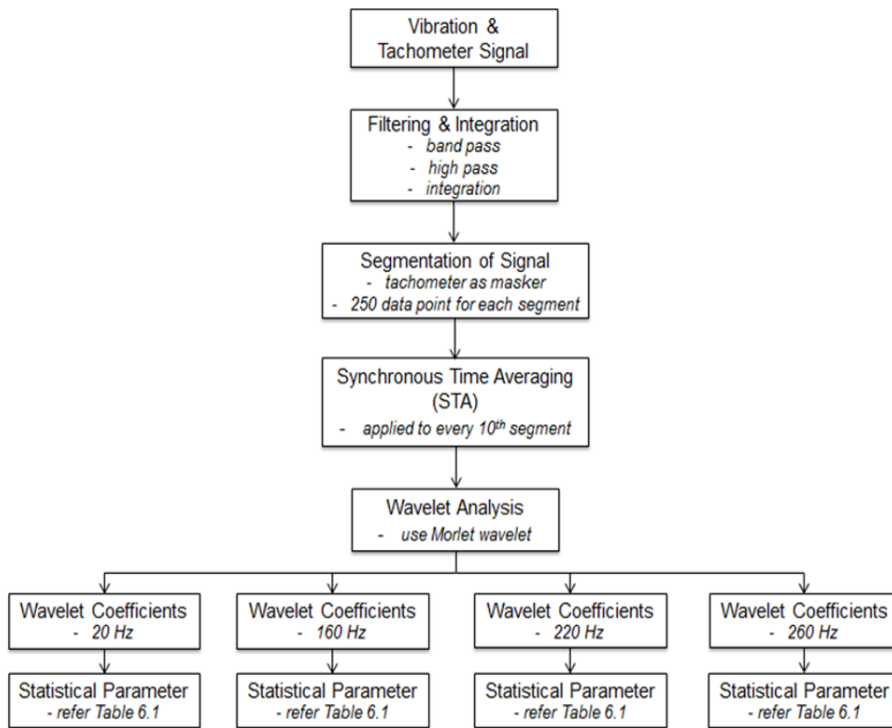


Figure 4. Feature extraction method

### Blade Statistical Summation

Besides the statistical features, a new feature set was proposed to acquire more information on blades and produce a better blade fault classification system. This formula went with the following Equation 1:

$$\text{Blade statistical summation} = \sum_{n=1}^N f(x_n) \quad [1]$$

where

$f(x_n)$ : statistical value

$N$ : number of statistical value, 4



Using the previously computed statistical features, 22 blade statistical summation were computed. Figure 5 shows the calculation of the blade statistical summation feature.

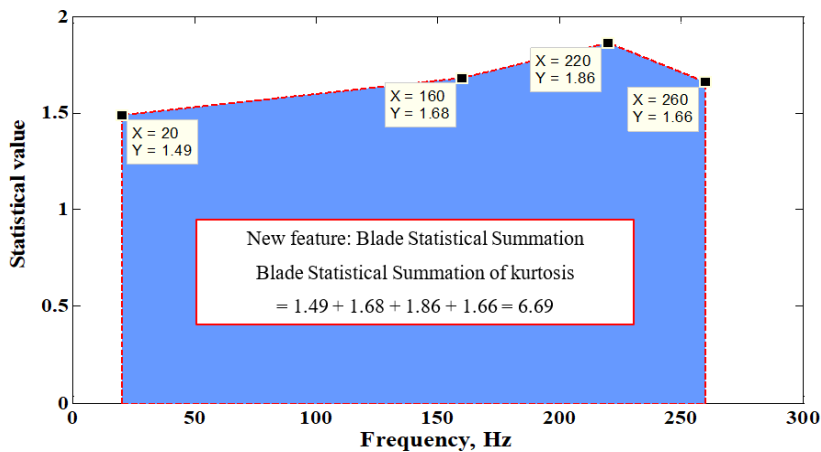


Figure 5. Blade statistical summation

### Features Distribution

For each condition of blade fault, a sum of 78 sets of STA signals was extracted from data set A; hence 78 samples were used for feature selection, training, validation, and testing processes. In addition to data set A, 18 sets of STA signals were extracted from data set B (for each condition of blade fault), and all the 18 samples from data set B were used for testing, as presented in Table 2. In summary, from data set A, 1638 samples (21 conditions x 78 samples) were generated from 21 different blade fault conditions, and each condition contributed to 78 samples. As for data set B, 378 samples (21 conditions x 18 samples) were generated as a new testing dataset.

For blade fault localization, two different feature sets were considered inputs in ANN. The first feature set consisted of statistical features extracted from the operating frequency, and the second set considered only the blade statistical summation features.

Table 2

*Statistical features and blade statistical summation features*

Features	Samples from data set A	Samples from data set B	Total features
Operating frequency (Case A)	1638	378	22
Blade statistical summation (Case B)	1638	378	22

### Genetic Algorithm for Feature Selection

Figure 6 shows the feature selection algorithm architecture. The beginning population was generated at random to start the GA algorithm. The process used a binary representation to create chromosomes that signified a subset of the traits. For example, every chromosome's fitness value  $F(i)$  is presented as Equation 2:

$$F(i) = CE(i) \quad [2]$$

According to Equation 2, when chromosome  $i$  applied a features subset to the training data,  $CE(i)$  denoted the classification error. Classification error means the fraction of the total samples wrongly classified by the classifier. Table 3 summarizes the parameters of GA.

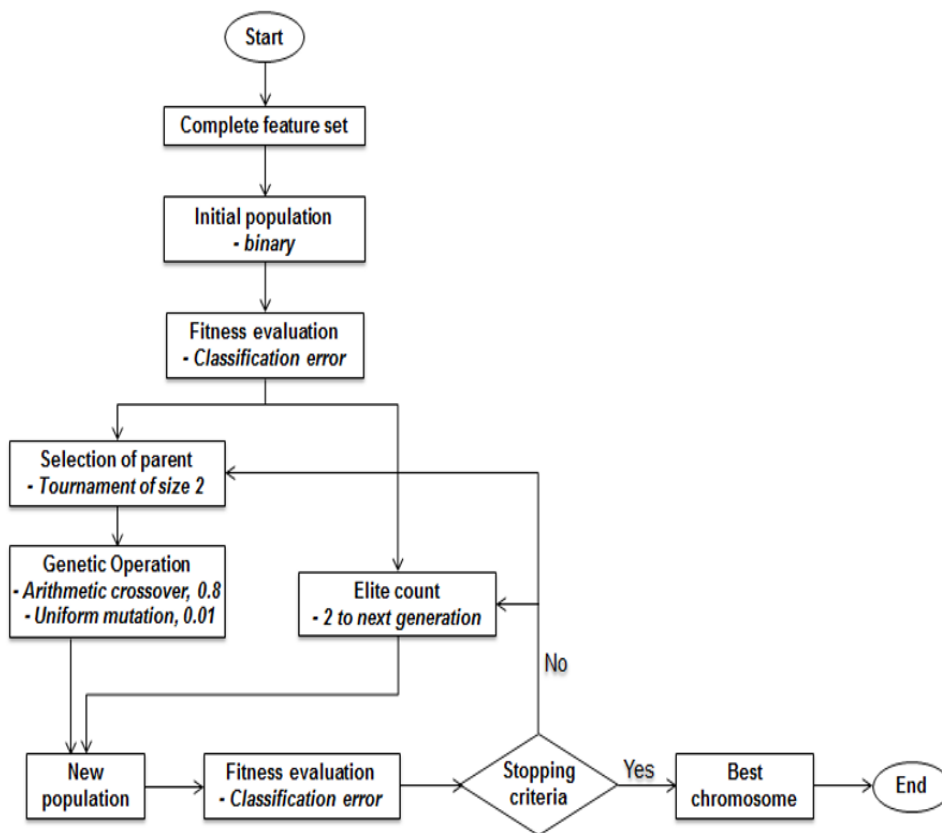


Figure 6. Architecture of feature selection algorithm

Table 3

*Parameter for features selection*

GA parameter	Selected parameter
Number of generations	100
Size	25
Elite count	2
Selection type	Tournament, size = 2
Mutation type	Uniform, rate = 0.01
Crossover type	Arithmetic, rate = 0.8

### ANN Based Blade Faults Localization

A neural network according to a seven-class was created Using the features extracted from the wavelet coefficients and the newly proposed ones. This network aimed to determine the occurrence of blade fault on the parts (stages with blade fault). Seven classes were represented as the parts where blade fault occurred: stage 1, stage 2, stage 3, stages 1 and 2, stages 1 and 3, stages 2 and 3, and stages 1, 2, and 3. This section describes the neural network establishment for blade defect localization. This procedure began by capturing vibration and tacho signals and then was followed by feature selection using the extracted features. The chosen features via GA were then entered into the ANN model for drilling and experimenting. Subsequently, ten-fold cross-validation was performed to train the network with stratified sampling using the selected feature subset. Consequently, the network with the least validation errors was chosen as the last network and administered on the data for testing. Finally, the best subset of chosen statistical feature subsets, as well as of chosen newly proposed feature subsets, are put together and maximized to improve diagnostic performance further and ascertain diagnostic reliability. The purpose of this was to generate the corresponding classification accuracy.

The feed-forward neural network was applied in the present investigation because it performed well when the machinery underwent defects. Also, the number of unseen layers is fixed to two as an increasing number of unseen layers causes overfitting and is time-consuming. Therefore, a neural network with two hidden layers was adequate for mapping the data of arbitrary complexity. Besides that, the number of neurons in the input layer was the same as the number of features. Therefore, the number of neurons in the unseen layer was set at ten. Alternatively, the number of neurons in the output layer was set to seven. Furthermore, the proven ability of the scaled conjugate gradient (trainsig) to solve machinery faults via vibration data was used as the training function in this study. Henceforth, the *tan-sigmoid* function was the switch feature used in each hidden and output layer. Table 4 summarizes the ANN parameters.

Table 4  
*Parameter of the ANN*

Parameter	Selected parameter
Number of neurons in the input layer	Number of selected features
Number of neurons in the hidden layer	10
Number of neurons in the output layer	7
Transfer function	<i>tan-sigmoid</i> function
Training function	Scaled conjugate gradient ( <i>trainsig</i> )

For every class, 180 samples (3 kinds of blade fault x 60 samples) from data set A were utilized for training and tested with 108 samples (3 kinds of blade fault x 18 test samples x 2 data sets) from data sets A and B. In this study, two different feature sets (Case A & Case B) were studied as the inputs in ANN for blade fault localization. The first feature set comprised statistical features extracted from the operating frequency. Meanwhile, only the blade statistical summation feature set was considered for the second feature set.

## RESULTS AND DISCUSSION

### Comparison of Statistical Features and Blade Statistical Summation Features

The newly proposed feature sets and statistical performance for blade fault location were evaluated using two distinctive feature sets as inputs to the ANN. First, the network performance was evaluated using two sets of testing data: A and B. Furthermore, the average accuracy of both testing data sets was represented by their overall accuracy, as shown in Table 5. Based on Table 5, it is apparent that Case A produced the highest overall accuracy in comparison to the two different feature sets. Apart from that, in terms of network generalization, Case A also had the best feature set. Additionally, the newly suggested set of blade statistical sum functions effectively identified blade failures. As a result, the accuracy of the network with the newly proposed feature set was higher than the statistical feature set for the testing data set A. However, this network was less accurate compared to the statistical feature set for the testing data set. Finally, the difference between these two feature sets in terms of the overall accuracy was less than 3%.

Table 5  
*The performance of statistical and newly proposed feature sets*

Case	Testing data A Accuracy, %	Testing data B Accuracy, %	Overall Accuracy, %
Case A	80.95	66.67	73.81
Case B	84.92	57.94	71.43

### Feature Selection Using Genetic Algorithm

The performance of the feature selection method using GA is discussed in this section. A neural network was built using similar ANN architecture and sample amounts for training and testing the data. In addition, the network with the least validation error after the 10-fold cross-validation was chosen. 13 and 10 features were selected from Case A and B, respectively. Figures 7 and 8 show the classification error over generations.

The details regarding the ANNs performance, where the features selected by GA for blade fault localization were included, are shown in Table 6. ANN with the selected features from the statistical feature set displayed the best overall accuracy, with a classification rate of 76.72%. It was followed by the proposed feature set's overall accuracy, with a classification rate of 74.07%. The statistical and newly proposed feature sets are effective for blade fault localization.

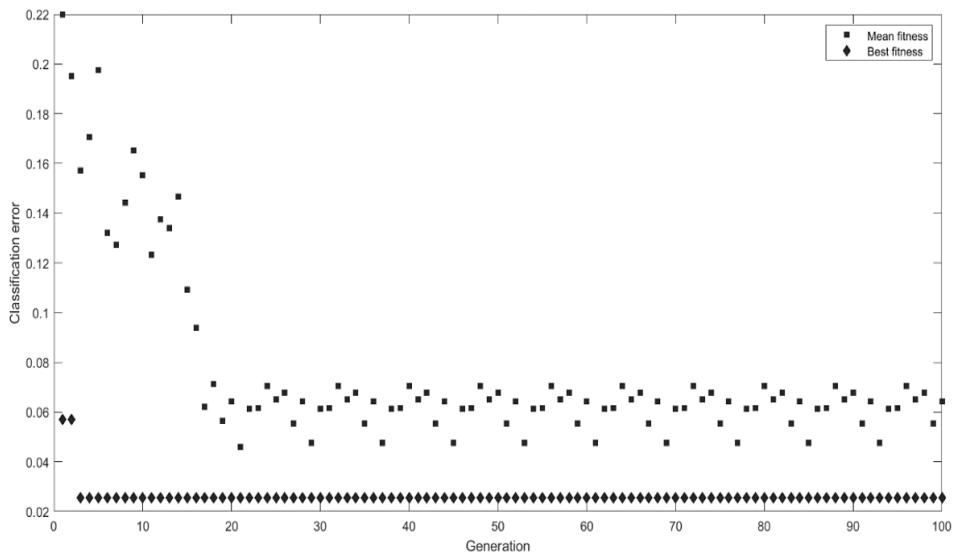


Figure 7. Classification error over generations for Case A

Figure 9 compares the ANNs performance without feature selection and the ANNs performance with feature selection. Based on Figure 9, it can be seen that the ANNs with selected features from GA perform better with fewer features.

According to Table 6 analysis after feature selection, the statistical and newly suggested features are the effective feature subsets in determining blade failure locations. Thus, chosen statistical features and newly suggested features were joined together to improve diagnostic performance further and ascertain diagnostic reliability.

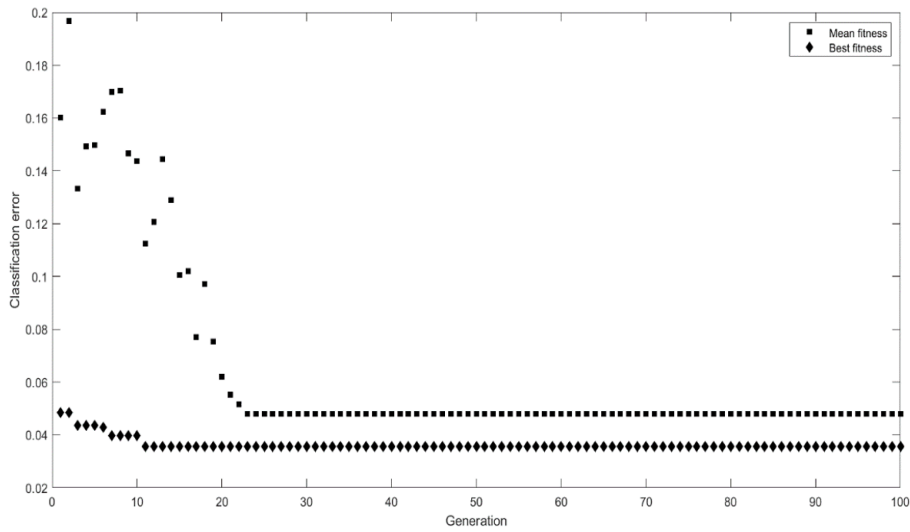


Figure 8. Classification error over generations for Case B

Table 6

Accuracy of different selected feature sets as input for blade fault localization

Feature set	Testing data A Accuracy, %	Testing data B Accuracy, %	Overall Accuracy, %
Statistical feature set	91.80	61.64	76.72
Proposed feature set	89.68	58.47	74.07

The combined feature set was then applied to the proposed algorithm to generate the corresponding classification accuracy. In this instance, 23 features were used as the ANN’s input. On the contrary, the 13 statistical features were from the operating frequency, while the other 10 were the statistical features of the blade. In addition, similar methods elaborated in the previous section were employed to assess the impact of this combined feature set on determining the locations of blade failure. Finally, 10 of the features were removed after the selection feature using GA. Figure 10 shows the classification error over generations.

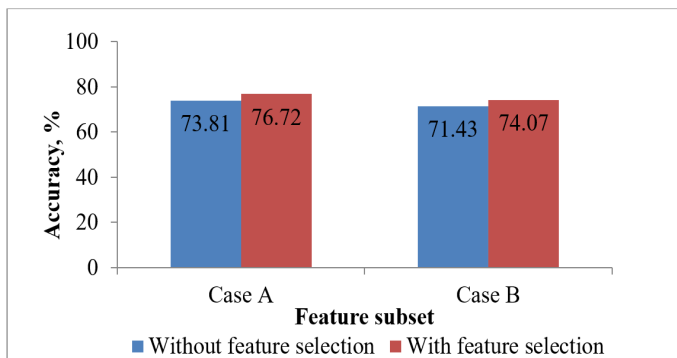


Figure 9. Overall accuracy of blade fault localization for ANNs without feature selection and ANNs with feature selection

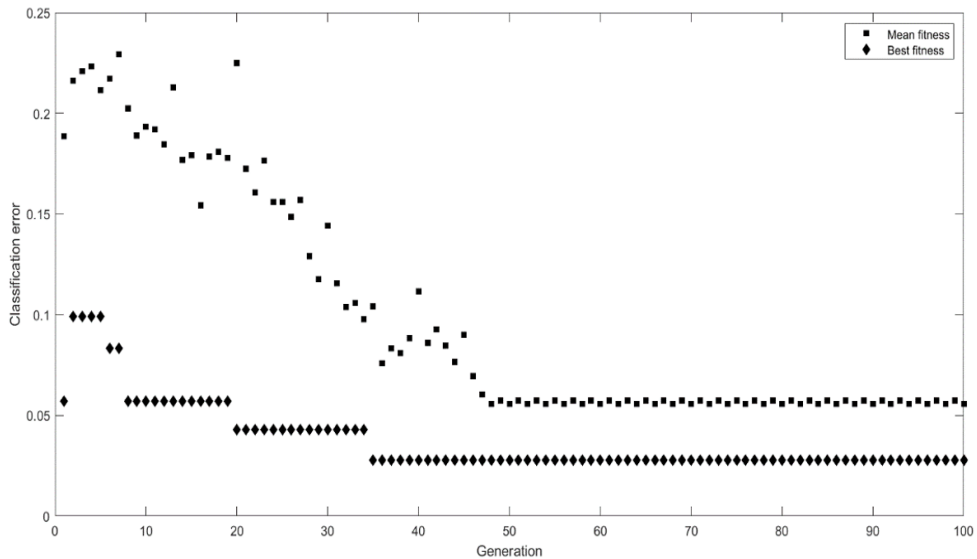


Figure 10. Classification error over generations for the combined feature set

Table 7 illustrates that the combined feature set had produced the utmost testing precision for data set A, testing precision for data set B, and classification precision of all feature sets. Furthermore, not only does the combined feature set after feature selection by GA improve the networks' accuracy, but it also discards unwanted features. Moreover, there was an 11.90% increase in the classification accuracy of testing data set B, from 58.47% to 70.37%. Also, the overall classification accuracy increased between 7% and 9% compared to the overall classification accuracy of ANNs, where only the selected statistical feature subset or newly proposed feature subsets were used as input. Based on the classification results, it was apparent that the extracted features, the proposed new features, and the feature selection method were effective for blade fault localization. Nevertheless, higher accuracy could be attained when the proposed method's statistical features and newly proposed features were applied. Therefore, it can be deduced that the proposed new features and the feature selection method can improve the network generalization capability.

Table 7

*Accuracy of selected features of combined feature set for blade fault localization*

Feature set	Testing data A Accuracy, %	Testing data B Accuracy, %	Overall Accuracy, %
Statistical feature set	91.80	61.64	76.72
Proposed feature set	89.68	58.47	74.07
Combined feature set	96.56	70.37	83.47

A summary of the classification rate of the ANNs for blade fault localization is shown in Figure 11. In this section, several issues were observed, which are as follows:

1. The features drawn from the operating frequencies were efficient in identifying blade defects.
2. The newly proposed blade statistical summation feature set effectively minimized blade fault.
3. Not only did the features selection method using GA remove unwanted features, but it also enhanced the classification accuracy and network generalization.
4. Combining the statistical and newly proposed features could improve the blade fault localization classification rate.

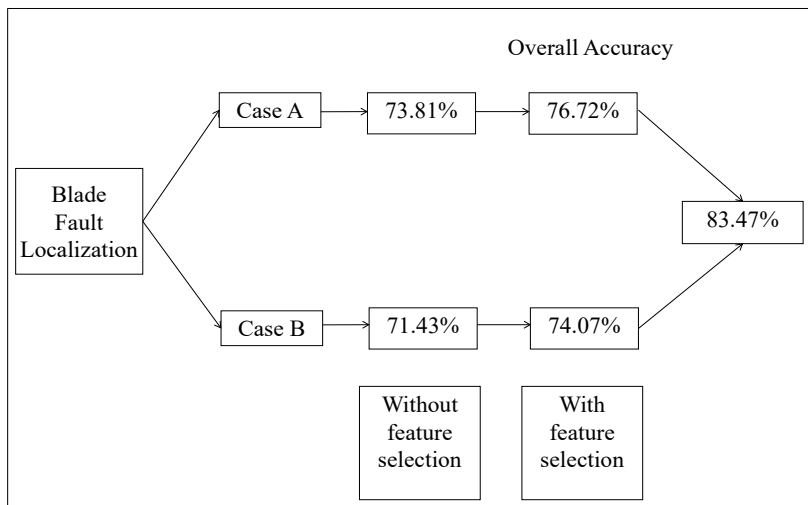


Figure 11. Classification rate

## CONCLUSION

The power generation, petrochemical plants, and aerospace industries require turbines and compressors that use blades to generate energy. Hence, the present study produced a new blade defect locating method by adopting the extracted features using the newly recommended feature set and feature selection technique. The experiment found that both feature sets can localize the blade fault position. In addition, the classification results too revealed that the GA-based feature selection method could eliminate unnecessary features and improve classification precision, including network generalization. The selected features of the statistical and newly proposed features were combined to enhance the diagnosis performance further. As a result, there was an increase in the overall classification accuracy, which was between 7% and 9%, compared to neural networks where only the selected statistical features or selected newly proposed features were used as input. In



general, the features extracted by the recent suggested feature set and feature selection technique work well in identifying the location of blade failure. Nonetheless, if the statistical features and proposed new features were utilized, greater exactness could be achieved. As a result, the classification rate for blade fault localization was 83.47%.

## ACKNOWLEDGEMENTS

The authors thank the Ministry of Higher Education Malaysia for the financial support provided under the Fundamental Research Grant Scheme (FRGS) No. FRGS/1/2018/TK03/UMP/02/24 grant (University reference RDU190157). The authors also acknowledge the Universiti Malaysia Pahang's support through the Postgraduate Research Grants Scheme (PGRS200303). Additional funding for this research also came from the Institute of Noise and Vibration, Universiti Teknologi Malaysia (RDU192303).

## REFERENCES

- Abdelrhman, A. M., Leong, M. S., Hee, L. M., & Hui, K. H. (2014). Vibration analysis of multi stages rotor for blade faults diagnosis. *Advanced Materials Research*, 845, 133-137. <https://doi.org/10.4028/www.scientific.net/AMR.845.133>
- Barnard, I. (2006). Asset management - An insurance perspective. In *Engineering Asset Management* (pp. 44-53). Springer.
- Chang, C. C., & Chen, L. W. (2004). Damage detection of cracked thick rotating blades by a spatial wavelet based approach. *Applied Acoustics*, 65(11), 1095-1111. <https://doi.org/10.1016/j.apacoust.2004.03.006>
- Kuo, R. J. (1995). Intelligent diagnosis for turbine blade faults using artificial neural networks and fuzzy logic. *Engineering Applications of Artificial Intelligence*, 8(1), 25-34. [https://doi.org/10.1016/0952-1976\(94\)00082-X](https://doi.org/10.1016/0952-1976(94)00082-X)
- Kyriazis, A., Aretakis, N., & Mathioudakis, K. (2006). Gas turbine fault diagnosis from fast response data using probabilistic methods and information fusion. In *Turbo Expo: Power for Land, Sea, and Air* (Vol. 42371, pp. 571-579). ASME Publishing.
- Lim, M. H., & Ngui, W. K. (2015, July 12-16). Diagnosis of twisted blade in rotor system. In *22nd International Congress on Sound and Vibration*. Florence, Italy.
- Lim, M. H., & Leong, M. S. (2013). Detection of early faults in rotating machinery based on wavelet analysis. *Advances in Mechanical Engineering*, 2013, Article 625863. <https://doi.org/10.1155/2013/625863>
- Marsh. (2016). *March power and utilities market update*. Marsh LLC. <https://www.marsh.com/pr/en/industries/energy-and-power/insights/marsh-power-and-utilities-market-update-2016.html>
- Ngui, W. K., Leong, M. S., Shapiai, M. I., & Lim, M. H. (2017). Blade fault diagnosis using artificial neural network. *International Journal of Applied Engineering Research*, 12(4), 519-526.
- Pang, S., Yang, X., Zhang, X., & Lin, X. (2020). Fault diagnosis of rotating machinery with ensemble kernel extreme learning machine based on fused multi-domain features. *ISA Transactions*, 98, 320-337. <https://doi.org/10.1016/j.isatra.2019.08.053>

- Peng, Z., Chu, F., & He, Y. (2002). Vibration signal analysis and feature extraction based on reassigned wavelet scalogram. *Journal of Sound and Vibration*, 253(5), 1087-1100. <https://doi.org/10.1006/jsvi.2001.4085>
- Tiboni, M., Remino, C., Bussola, R., & Amici, C. (2022). A Review on vibration-based condition monitoring of rotating machinery. *Applied Sciences*, 12(3), Article 972. <https://doi.org/10.3390/app12030972>
- Wang, Q., & Chu, F. (2001). Experimental determination of the rubbing location by means of acoustic emission and wavelet transform. *Journal of Sound and Vibration*, 248(1), 91-103. <https://doi.org/10.1006/jsvi.2001.3676>

*Case Study*

## Structural Comparison of Naturally Aspirated and Turbocharged Diesel Engine for Steel and Aluminium Made Radiator: A Finite Element Study

Asad Munir<sup>1,2\*</sup>, Muhammad Fauzinizam Razali<sup>1</sup>, Nasir Iqbal<sup>2</sup> and Muhammad Tahir Amin<sup>2</sup>

<sup>1</sup>*School of Mechanical Engineering, Engineering Campus, Universiti Sains Malaysia, 14300 USM, Nibong Tebal, Pulau Pinang, Malaysia*

<sup>2</sup>*Department of Mechanical Engineering, Mirpur University of Science & Technology (MUST), 10250 Mirpur, Azad Kashmir, Pakistan*

### ABSTRACT

The current study is based on the structural analysis of radiators made of different materials to compare their effectiveness in the case of naturally aspirated and turbocharged diesel engines. For the analysis of the radiator structure, ABAQUS software was used. In the ABAQUS, static structural analysis was made to calculate the strength of the radiator. The said software is capable of calculating the strength of the radiator considering the boundary conditions (i.e., fixing at corners) as well as the loading conditions. It was observed that stresses generated while using an aluminium radiator were very high than those produced by steel radiators. According to the study, the following are the key findings for the steel and aluminium radiators. In the first case, while three corners were fixed, the steel radiator showed a deflection of 1.86 mm while aluminium exhibited 5.65 mm. However, in the second case in which the radiator had four fixed corners, the deflection of the steel radiator was 1.10 mm, while that of aluminium was 3.36 mm. Additionally, based on the deflections

obtained from all investigations, it was found that radiators made of aluminium were more sensitive than those made of steel in both naturally aspirated and turbocharged applications. However, due to aluminium's strong thermal conductivity, it is compatible with naturally aspirated engines in terms of thermal capacity. To combat turbocharged engine complications caused by high

#### ARTICLE INFO

*Article history:*

Received: 18 February 2022

Accepted: 18 May 2022

Published: 19 August 2022

DOI: <https://doi.org/10.47836/pjst.31.1.05>

*E-mail addresses:*

asad.me@must.edu.pk (Asad Munir)

mefauzinizam@usm.my (Muhammad Fauzinizam Razali)

enr.norani.me@must.edu.pk (Nasir Iqbal)

ahir.me@must.edu.pk (Muhammad Tahir Amin)

\* Corresponding author

temperatures, such as thermal cracking, engine wear and tear, and so on, a steel-made radiator is more suitable than an aluminium radiator, hence mitigating the issues.

*Keywords:* Aluminium radiator, naturally aspirated, steel radiator, structural analysis, turbocharged

---

## INTRODUCTION

Engine cooling is critical for maintaining the engine's optimal operating temperature for the vehicle's speed and road conditions (Roy et al., 2017a). When engines are driven at high rpm to increase the vehicle's speed, the heat in the engine's components increases dramatically (Sharma et al., 2022). Therefore, it is critical to lower the temperature of a vehicle's internal combustion engine (ICE) by collecting heat and dissipating it into the air. The engine will work optimally with a properly functioning radiator (Habeeb et al., 2020). The radiator is an integral component of the engine cooling system (Wani et al., 2019). It is a heat-type transfer fluid that removes excess heat generated by combustion engines (Elias et al., 2019). Due to rising values of forced convection within radiators, the heat transfer capacity and convective heat transfer coefficient across the radiator rise with increasing water intake velocity and mass flow rate (Dalkilic et al., 2019). Now, a common practice in the manufacture of radiators for automobiles is the use of lightweight materials. Typically, such a structure is constructed of copper and aluminium alloys that are employed as a cooling mechanism for the vehicle engine due to their stainless nature and superior corrosion resistance over iron alloys (Chahardoli et al., 2021).

In recent times, the automobile industry has been striving towards manufacturing components that are smaller in size and lighter in weight for improved fuel efficiency (Zainy, 2021). Lightweight design has attracted extensive attention in the automobile industry to reduce energy consumption and emissions, and decision-making requires a thorough examination of materials, structures, manufacturing, recyclability, and economics (Chu et al., 2019). Furthermore, continuous advancements in manufacturing technology, materials science, and distribution enable the incorporation of novel manufacturing methods and materials into production processes. Radiators are an example of such a product, as they may be made from a variety of materials (cast irons, steels, bronzes, and aluminium alloys) and manufacturing procedures (Pańcikiewicz & Radomski, 2020).

Researchers are continually working to improve the cooling performance of car engine radiators to achieve sustainable and efficient resource utilisation. Throughout this exercise, appropriate material, efficient tube design, and coolant contribute significantly to improving heat exchange and thus radiator efficiency (Arora & Gupta, 2020). Aluminium has recently gained popularity because of the aviation and car sectors' need for lightweight components. These have been utilised to create lightweight transmission cables, heat exchangers, evaporators, cylinder heads, and automobile radiators (Vijayakumar et al., 2020). However, aluminium radiators have the problem of being delicate, as aluminium is a soft metal in

composition, making mechanical damage quite simple. Furthermore, the impact of these radiators on erosion is dependent on the pH of the water; this indicator should be in the range of 7–8 per cent since, at lower levels, this metal frequently fails, erosion occurs, and the radiator eventually fails (Mo'minov & O'tbosarov, 2021). Interestingly steel panel radiators are the most prevalent form of panel radiator used in homes, workplaces, and industrial locations and are typically supplied with natural convection shutters (convectors) to increase heat output (Gelis & Akyurek, 2021). Therefore, it is required to become as familiar with the material as possible to develop this work and to review a large amount of related literature and materials (Ondriga et al., 2021).

The total heat transfer coefficient and entropy generation from panel radiators were investigated, and radiator size increases with increasing flow rate and supply temperature; the total heat transfer coefficient decreases with increasing radiator size and temperature but increases with increasing flow rate (Gelis, 2021). In addition, the most often used radiator tubes have a linear structure and are supported by straight flat plates to offer additional strength to withstand the force of air acting on the tubes, which can cause them to fail (Aravindkumar et al., 2021). In general, in the case of radiators, optimising the temperature distribution on the heater's surface in order to produce the highest potential radiator heat output is vital, but it is only solved once during the radiator's construction (design) and strength of the material (Dzierzowski, 2021).

Recently, emphasis has been placed on optimising cooling efficiency by introducing the thermophysical characteristics of the nanoparticles scattered in the base fluid, and nanofluids are utilised to improve heat transmission in the engine radiator (Ramalingam et al., 2020). Nanofluids have the potential to improve the thermophysical characteristics of heat transfer fluids. Thermal conductivity is critical in applications requiring quick heating and cooling (Ranganathan, 2019). Several failure possibilities include oil leaking at the contact between the radiator element and the plug, element rupture, and plug separation from the bottom opening. The major failure mode is radiator element cracking (Timelli et al., 2019). The finite element model incorporates the stiffness of the entire radiator assembly to accurately simulate the radiator's physical behaviour (Roy et al., 2017b). Different load variations and material changes are utilised to research and suggest a suitable material to sustain structural and dynamic stresses (Gudimetla et al., 2012).

This study's specific objective is to compare the same design radiator made of different materials. For this purpose, radiators made of steel and radiator made of aluminium are selected and analysed with different load cases. Deflection plots, as well as stress plots, are created to compare different parameters of both radiators. Considering the temperature danger posed by turbocharged Diesel engines, a steel-made radiator was considered, and structural analysis was done. Similarly, an aluminium-made radiator was selected for naturally aspirated engines. The study's ultimate objective was to assess the structural strength of both materials.

## MATERIALS AND METHODS

Aluminium and steel were chosen for their distinctive features while keeping in mind the factors contributing to the durability of both types of engines and their adequate cooling supply.

Aluminium is a light metal with a good thermal conductivity ( $200\text{W}\cdot\text{m}^{-1}\cdot\text{K}^{-1}$ ). It has a low emissivity that cannot be increased via heat oxidation in the presence of oxygen. When pure aluminium is exposed to air, the aluminium atoms in the surface layer react rapidly with the oxygen in the air, forming a thin and robust  $\text{Al}_2\text{O}_3$  oxide coating that protects the metal from further oxidation. Anodised coatings withstand temperatures of up to  $300\text{ }^\circ\text{C}$  and have at least five times the heat conductivity of black paints. In addition, anodising simplifies the process of obtaining a high emissivity. It makes aluminium a suitable material for compact, lightweight, portable radiators. Similarly, steel properties are formed by creating an invisible and adherent chromium-rich oxide coating. The protective  $\text{Cr}_2\text{O}_3$  oxide layer forms on the stainless-steel surface at a rate proportional to the temperature, typically to a thickness of 1–3 nm. Due to their superior corrosion resistance, high-chromium austenitic stainless steels are in high demand for high-temperature applications (Bowler, 2016).

A model was designed to test the characteristics of different materials when applied to the same geometric design of the radiator. To do this, we built a middle surface model of the radiator with shell meshing on the surfaces, which enables us to perform finite element analysis on the radiator model.

Two distinct load conditions were applied to the steel radiator. In the first load condition, the model was fixed at all four corners, and a concentrated force was applied to the radiator model's centre. In the second load case type, the model was fixed at three corners and loaded at the fourth corner to determine the model's strength. As indicated previously, the same approach was used to create an aluminium radiator with the same design. Thus, we could compare the findings of the analyses performed on both materials and thus determine which one is stronger.

These are the following six steps involved in the execution of the project:

- i. Geometry Preparation
- ii. Middle Surface Generation
- iii. Mesh Generation
- iv. Analytical Model Preparation
- v. Analysis
- vi. Post Processing

### Geometry Preparation

For the execution of this project, a suitable geometry of a sample radiator having a length and width of 485 mm and 347 mm, respectively, shown in Figure 1, was prepared. First,

the geometric design of the radiator part was designed in the solid works software. Then the model was exported in IGS/STEP format to be readable in the pre-processing software for the analysis.

### Middle Surface Generation

The second phase was creating the centre skin for the available radiator design. First, all features, ribs, pipes, and walls had their middle surfaces constructed, and then an appropriate thickness of 19 mm at the walls and 47 mm at the corners was allocated to the corresponding middle surfaces. These centre surfaces were then linked to form the radiator's original component. Again, we utilised ANSA software for this purpose.

### Mesh Generation

The third phase was critical, as it included meshing the centre surface portion with an average/density of 2.5 mm–3.0 mm in accordance with quality requirements, as illustrated in Figure 2. It is how we transformed our geometric model into finite elements. It enables us to define the analytical model before performing the finite element analysis. We performed all meshing operations in the ANSA programme, which served as a specialised pre-processor for analytical tasks.

### Analytical Model Preparation

After meshing the geometric structure, an analytical model is defined for the analysis. For example, in Figure 2, all four corners of the radiator are fixed to the fixture positions, and a concentrated force of 1 kN is applied in the negative direction of the z-axis to the model's centre.

### Analysis with Four Corners Fixed for Both Steel and Aluminium and Load Applied on Center (Load Case 1)

**Boundary Conditions.** The first load case fixed the radiator model from all four corners. Then, a concentrated load of 1 kN was applied to the radiator's centre to determine the strength of the steel and aluminium radiator, as shown in Figure 3.

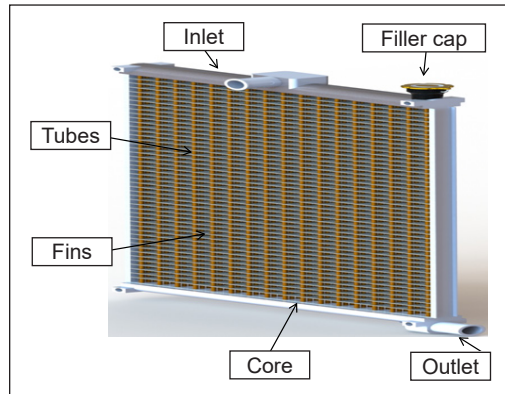


Figure 1. Radiator 3D model

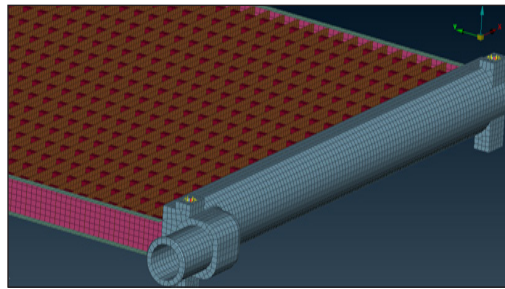


Figure 2. Mesh generation of the radiator



### Analysis with Three Corners Fixed for Both Steel and Aluminium (Load Case 2)

**Boundary Conditions.** In this case, the model was fixed at three corners, and a concentrated load of 40 N was applied to the fourth corner to determine the strength of the aluminium and steel radiator, as shown in Figure 4.

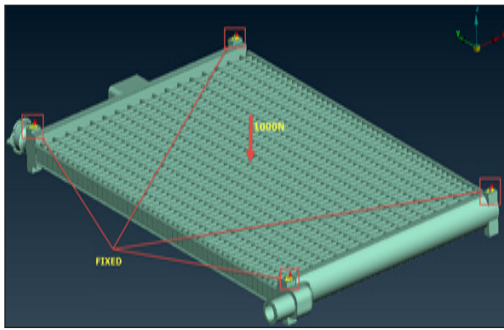


Figure 3. Analytical model for first boundary condition (Load Case 1)

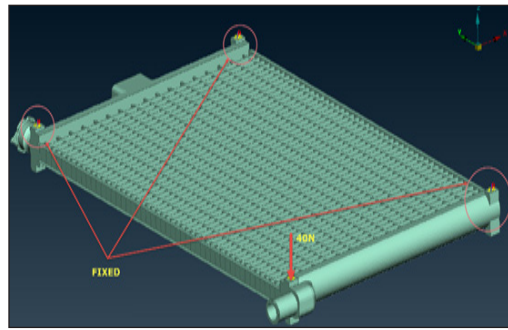


Figure 4. Analytical model for second boundary condition (Load Case 2)

### Analysis

The radiator structure was analysed using the ABAQUS software. First, the strength of the radiator was determined using ABAQUS’s static structural analysis. The software can calculate the radiator’s strength while considering the radiator’s boundary conditions (i.e., corner fixings) and loading circumstances. Two specific load cases were analysed: one with all four corners fixed and one with three corners fixed. Both types of analysis were carried out on the steel and aluminium radiators.

### Post Processing

After running the analysis, results are extracted from the results file generated by the ABAQUS software. With the help of the result file, deformation and stress plots are generated, as discussed in detail below.

### Materials Properties

The analyses were conducted utilising standard material data for both steel and aluminium. The standard values for each material are summarised in Tables 1 and 2.

Table 1  
Materials properties of steel and aluminium

Material	Young’s Modulus of Elasticity (MPa)	Poisson’s Ratio	Density (tonne/mm <sup>3</sup> )
Steel S235JR	210000	0.3	7.85E-9
Aluminium 1100	70000	0.33	2.7E-9



Table 2  
Yield and tensile strength of steel and aluminium

Material	Yield Strength (MPa)	Tensile Strength (MPa)
Steel	235	360-510
Aluminium 1100	105	110

## RESULTS AND DISCUSSION

The following sections discuss the analysis of steel and aluminium radiator load cases in detail.:

### Steel Radiator Analysis with Four Corners Fixed (Load Case 1)

In the first load case, the radiator model was fixed from all four corners, and a concentrated force was applied to the radiator’s centre to determine its strength. Additionally, demonstrate the Von Mises Stress distribution trend across the radiator, with a maximum resulting stress of 387 MPa, as shown in Figure 5.

It represents one of the critical areas of the part. We have very few areas where the stresses are just above the steel yield strength. It also represents the third corner, where we have almost all the fine stresses except the encircled ones.

### Aluminium Radiator Analysis with Four Corners Fixed (Load Case 1)

Similarly, the model was fixed from all four corners for aluminium-made radiators. A concentrated load of 1 kN was applied to the radiator’s centre to determine its strength, as shown in Figure 6.

Following is the resulted deflection plot when the analysis was executed, on the radiator made of aluminium, according to the load case. The maximum deflection was found to be 3.36 mm, which is a much bigger deflection than the radiator made of steel. Also, it has shown the trend of Von Misses Stress distribution throughout the radiator made of aluminium with a maximum resulting in the stress of 388 MPa, which is very high

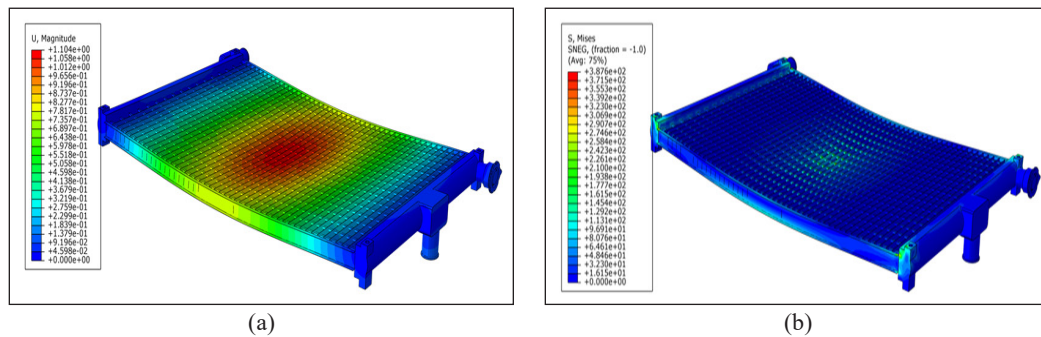


Figure 5. (a) Deflection and (b) stress distribution plot for steel in load case 1

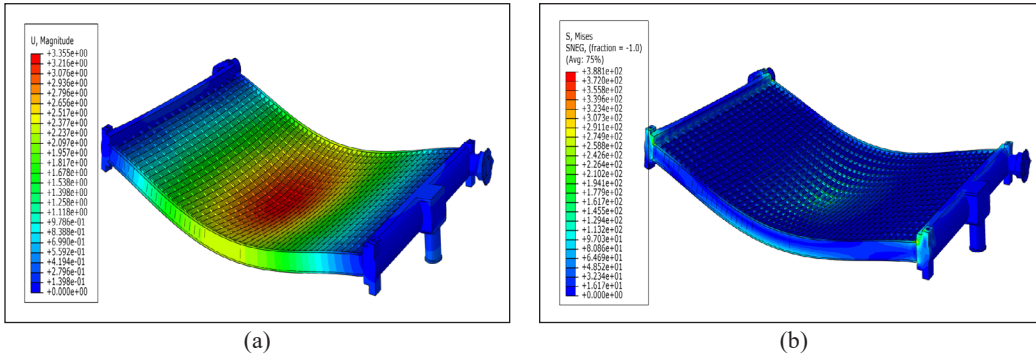


Figure 6. (a) Deflection and (b) stress distribution plot for aluminium in load case 1

considering the strength values of aluminium. Furthermore, it also shows the Von Mises Stress distribution trend throughout the radiator with a three-colour legend maximised at 110 MPa. It is done for a clear understanding of the stress distribution with respect to the yield strength of the aluminium.

### Stress Distribution (Load Case 2)

Figure 7 illustrates the stress distribution at the radiator’s first critical corner for load case 1. because the stresses are significantly less than the yield strength, steel radiator components will not permanently fail or deform in these regions. Also, the Von Mises Stress distribution across the radiator is set to 235 MPa in the colour legend. It is done to ensure a complete understanding of the stress distribution in relation to the steel yield strength, as shown in Figure 8.

The stress distribution at the radiator’s first critical corner is depicted in Figure 9 for load case 2. Since the stresses are significantly less than the yield strength, steel radiator components will not permanently fail or deform in these places. However, the stress distribution at the radiator’s second critical corner is the point at which the aluminium component may break or deform permanently. Since the stress is substantially more than aluminium’s yield and tensile strengths, as seen in Figure 10.

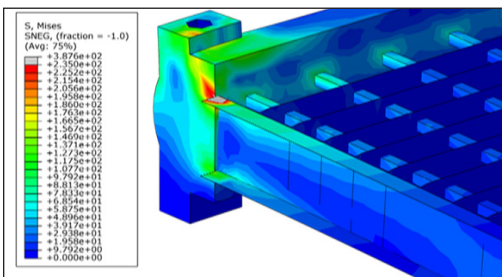


Figure 7. Stress distribution at the critical corners of the radiator for load case 1

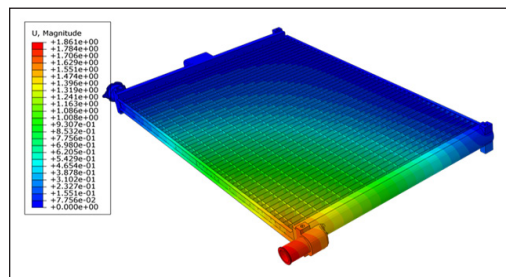


Figure 8. Von Mises Stress distribution throughout the steel radiator

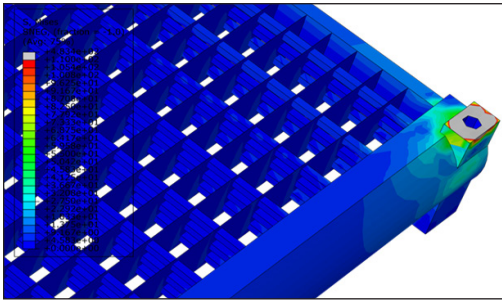


Figure 9. Stress distribution at the first critical corner of the radiator for load case 2

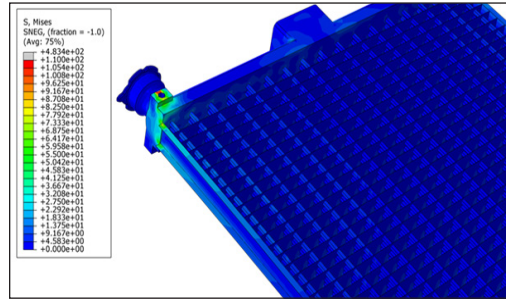


Figure 10. Stress distribution at the second critical corner of the radiator for load case 2

### Graphical Stress Results Comparison

This graph compares the deflection of aluminium and steel for load case 1, in which a 1 kN force was applied at the centre, and the four corners were fixed. As seen in Figure 11, the resultant deflection is 1.104 mm for steel and 3.36 mm for aluminium, nearly three times the deflection for steel.

Similarly, the deflection of aluminium and steel for load case 2, which comprised a 40 N load applied at the corner while three corners were fixed, is shown in this graph. As seen in Figure 12, the resultant deflection is 1.86 mm for steel and 5.652 mm for aluminium, nearly three times the deflection for steel.

Moreover, the yield strength, ultimate tensile strength, and strain generated in steel and aluminium are also shown in the graphs below in Figures 13 and 14, when a 1 kN load is applied centrally. Four corners are fixed, three corners are fixed, and a 40 N load is applied to one end, referred to as case 1 and case 3, respectively. It is worth mentioning that aluminium's yield strength and ultimate tensile strength are quite low when compared to steel. In our analysis, we observed that the strains generated by an aluminium radiator

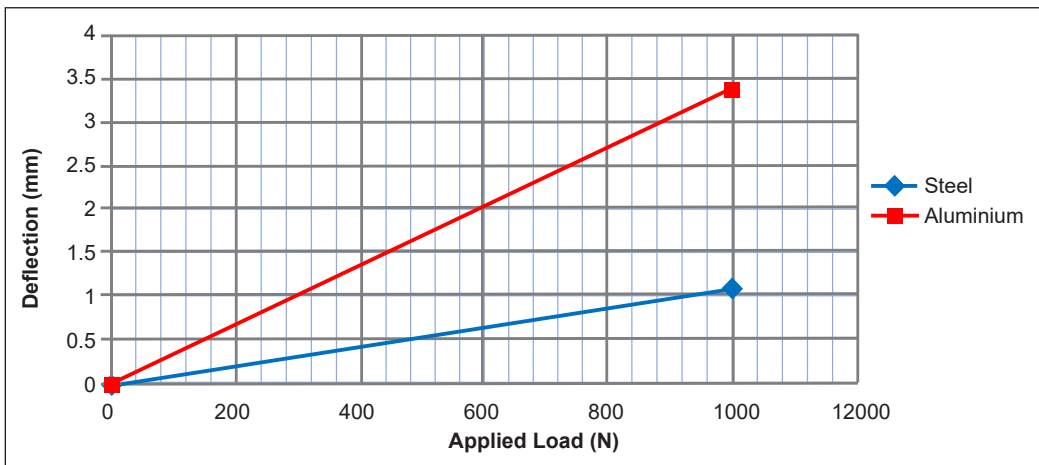


Figure 11. Deflection comparison for both aluminium and steel for load case 1

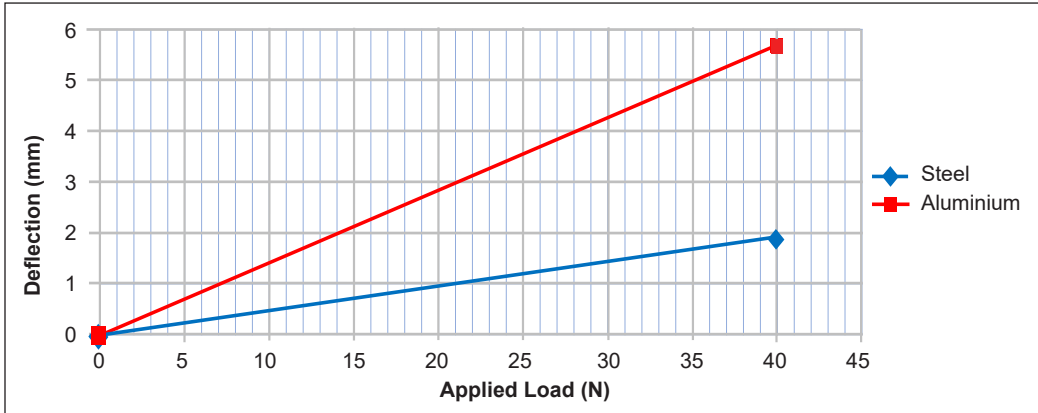


Figure 12. Deflection comparison for both aluminium and steel for load case 2

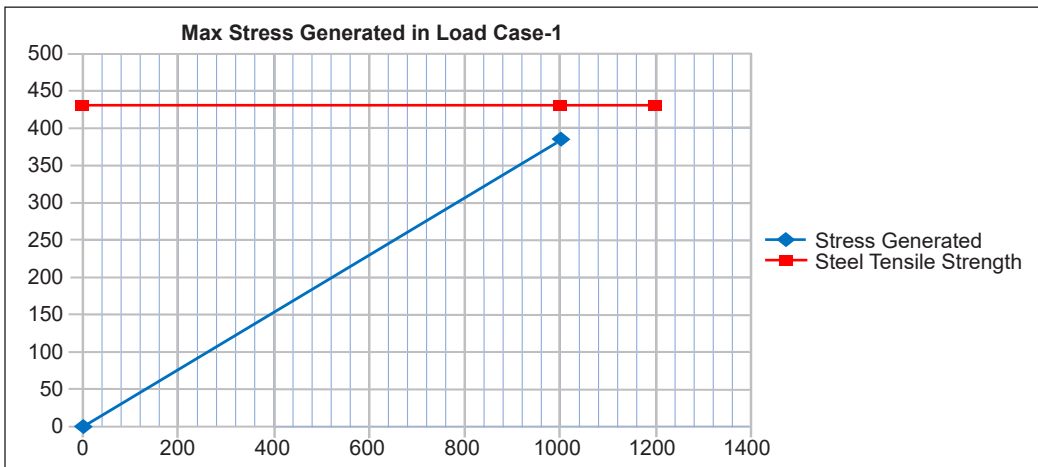


Figure 13. Steel maximum stress generated load case 1

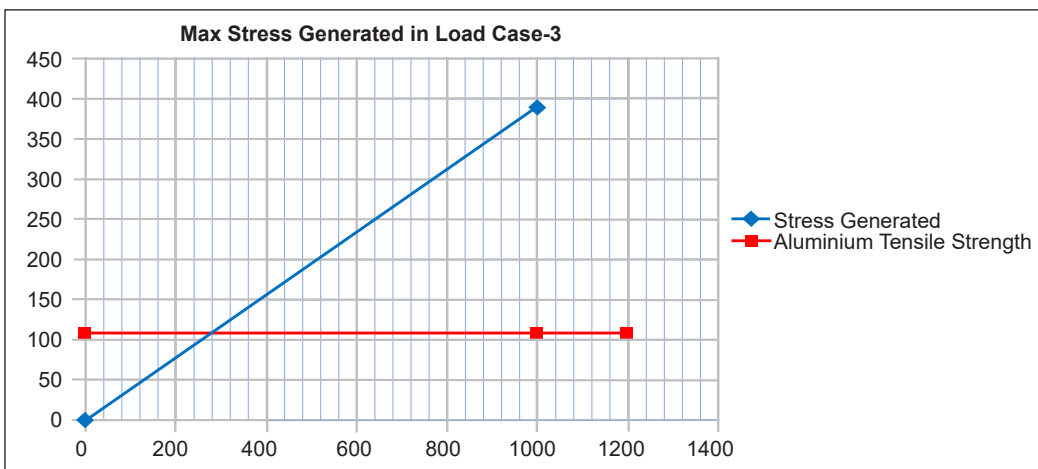


Figure 14. Aluminium maximum stress generated load case 3

were quite high in comparison to their strength. In contrast, the stresses generated by a steel radiator were relatively low.

Looking at the deflections obtained from all analyses, it is evident that the radiator made of steel is more durable than the radiator made of aluminium.

## CONCLUSION

The current study mainly focused on comparing the radiator made of steel and the radiator made of aluminium. The yield strength and ultimate tensile strength of aluminium are low compared to steel's strengths. The radiator made of aluminium material was more sensitive compared to its counterpart material, i.e., steel, in both naturally aspirated as well as in turbocharged cases, as shown from the resulting deflections of the analyses. An aluminium-made radiator is compatible with a naturally aspirated engine as far as thermal capacity is concerned, owing to its high thermal conductivity. On the other hand, a steel-made radiator is more compatible with overcoming the turbocharger engine problems due to high temperatures, such as thermal cracking, engine wear, and tear, compared to its counterpart radiator to reduce the said problems. Structural analysis was carried out using a structural load of 1000 N (load case 1) in the centre and 40 N (load Case) in one corner to estimate the Von Mises stresses, strain, displacement, and deformation.

## ACKNOWLEDGEMENTS

The authors are grateful for the support provided by the Mirpur University of Science and Technology (MUST), 10250 Mirpur, Azad Kashmir, Pakistan.

## REFERENCES

- Aravindkumar, N., Vignesh, S., Kumaran, P., Kumar, C. N., Kumar, K. N., & Navin, B. (2021). Computational and numerical analysis of radiator with different tube structures and nano fluid as coolant. *Materials Today: Proceedings*, 45, 1481-1486. <https://doi.org/10.1016/j.matpr.2020.07.605>
- Arora, N., & Gupta, M. (2020). An updated review on application of nanofluids in flat tubes radiators for improving cooling performance. *Renewable and Sustainable Energy Reviews*, 134, Article 110242. <https://doi.org/10.1016/j.rser.2020.110242>
- Bowler, N. (2016). *Springer series in measurement science and technology measurement and probability* (Vol. 1). Springer.
- Chahardoli, S., Attar, A. A., Ghorbanhosseini, S., & Marashi, S. M. H. (2021). Investigation of the bending and crushing for the light-weight structures used in vehicle's radiator. *Mechanics Based Design of Structures and Machines*, 0(0), 1-17. <https://doi.org/10.1080/15397734.2021.1967165>
- Chu, Y., Sun, L., & Li, L. (2019). Lightweight scheme selection for automotive safety structures using a quantifiable multi-objective approach. *Journal of Cleaner Production*, 241, Article 118316. <https://doi.org/10.1016/j.jclepro.2019.118316>

- Dalkilic, A. S., Acikgoz, O., Ekici, E., & Wongwises, S. (2019). Determination of some domestic radiators' thermal capacity numerically. *Journal of Thermal Engineering*, 5(4), 251-270. <https://doi.org/10.18186/thermal.581754>
- Dzierzgowski, M. (2021). Verification and improving the heat transfer model in radiators in the wide change operating parameters. *Energies*, 14(20), Article 6543. <https://doi.org/10.3390/en14206543>
- Elias, E., Paranjpe, S. R., Krishnasamy, K., Ganguli, D., Sutar, K., & Adimoolam, R. (2019). Study on corrosion inhibitors of eco-friendly radiator coolants. *Journal of Mineral, Metal and Material Engineering*, 5, 58-72. ResearchGate. <https://doi.org/10.31437/2414-2115.2019.05.7>
- Gelis, K. (2021). Factorial experimental design for second law analysis of panel radiators as a function of radiator dimension. *Journal of Building Engineering*, 43, Article 102872. <https://doi.org/10.1016/j.jobe.2021.102872>
- Gelis, K., & Akyurek, E. F. (2021). Entropy generation of different panel radiator types: Design of experiments using response surface methodology (RSM). *Journal of Building Engineering*, 41, Article 102369. <https://doi.org/10.1016/j.jobe.2021.102369>
- Gudimetla, A., Gopinath, C., & Murty, K. L. N. (2012). Failure analysis of radiator fan blade of diesel locomotive engine with reverse engineering. *International Journal of Engineering Research and Technology*, 1(7), 1-10.
- Habeeb, H. A., Mohan, A. E., Norani, N. A. M., Abdullah, M. A., & Harun, M. H. (2020). Analysis of engine radiator performance at different coolant concentrations and radiator materials. *International Journal of Recent Technology and Engineering (IJRTE)*, 8(6), 2664-2669. <https://doi.org/10.35940/ijrte.f7866.038620>
- Mo'minov, O. A., & O'tbosarov, S. R. (2021). Type of heating radiators, principles of operation and theoretical. *JournalNX- A Multidisciplinary*, 7(5), 299-303.
- Ondriga, J., Zvolenský, P., & Hreck, S. (2021). Application of technical diagnostics in the maintenance of the internal combustion engine of diesel multiple units 812 series. *Transportation Research Procedia*, 55, 637-644. <https://doi.org/10.1016/j.trpro.2021.07.030>
- Pańcikiewicz, K., & Radomski, W. (2020). Lack of tightness analysis of concealed welded radiators. *Engineering Failure Analysis*, 114, Article 104579. <https://doi.org/10.1016/j.engfailanal.2020.104579>
- Ramalingam, S., Dhairiyasamy, R., & Govindasamy, M. (2020). Assessment of heat transfer characteristics and system physiognomies using hybrid nanofluids in an automotive radiator. *Chemical Engineering and Processing - Process Intensification*, 150, Article 107886. <https://doi.org/10.1016/j.cep.2020.107886>
- Ranganathan, L. (2019). Enhancement of Heat Transfer Using Nanoadditives in Automobile Radiator. *International Journal of Research in Mechanical, Mechatronics and Automobile Engineering*, 5(2), 76-84.
- Roy, P. R., Hariram, V., & Subramanian, M. (2017a). Probabilistic finite element analysis of a heavy duty radiator under internal pressure loading. *Journal of Engineering Science and Technology*, 12(9), 2438-2452.
- Roy, P. R., Hariram, V., & Subramanian, M. (2017b). Accelerating the product development of a commercial vehicle radiator using finite element analysis. *International Journal of Vehicle Structures and Systems*, 9(1), 7-10. <https://doi.org/10.4273/ijvss.9.1.02>

- Sharma, M., Vishwakarma, P. N., Sharma, A., & Shubham, P. (2022). Performance Investigation of Copper and Aluminium Radiators for Lower HP Tractor Engines. *Journal of Physics: Conference Series*, 2178, Article 012011. <https://doi.org/10.1088/1742-6596/2178/1/012011>
- Timelli, G., De Mori, A., & Haghayeghi, R. (2019). Reliability of a high-pressure die cast Al alloy radiator. *Engineering Failure Analysis*, 105, 87-97. <https://doi.org/10.1016/j.engfailanal.2019.06.002>
- Vijayakumar, M. D., Dhinakaran, V., Sathish, T., Muthu, G., & Ram, P. M. B. (2020). Experimental study of chemical composition of aluminium alloys. *Materials Today: Proceedings*, 37, 1790-1793. <https://doi.org/10.1016/j.matpr.2020.07.391>
- Wani, K., Sose, K., Shitole, M., Kokad, P., & Patil, N. (2019). Basics of Radiator and Improvement Techniques. *International Journal of Innovative Science and Research Technology*, 4(3), 785-787.
- Zainy, M. (2021). *Design of an additively manufactured automotive radiator in formula student*. Bachelor's degree dissertation, Swansea University, United Kingdom. <https://doi.org/10.13140/RG.2.2.21614.95044>





## The Impacts of Passive Design Strategies on Building Indoor Temperature in Tropical Climate

Maryam Qays Oleiwi\* and Mohd Farid Mohamed

*Department of Architecture, Faculty of Engineering and Built Environment, Universiti Kebangsaan Malaysia, 43600 UKM, Bangi, Selangor, Malaysia*

### ABSTRACT

Traditional buildings in Malaysia were developed for hundreds of years to respond to the local climate. Occupants can comfortably occupy the traditional buildings without a mechanical system such as an air conditioning system. However, in many modern buildings, whether houses, mosques or shophouses, similar traditional strategies are not extensively adopted; thus, they are very dependent on the mechanical system to achieve good thermal comfort. Therefore, this study aims to investigate the effect of selected passive cooling strategies on the indoor temperature of a building in a tropical climate. The methodology adopted in this study was computer simulation validated with measured data from a selected case study. The thermal comfort of a case study was examined with different passive cooling strategies that were applied using IES-VE 2019 building simulation software. The simulation was conducted for various design strategies, such as adding shading devices and closing the curtains to decrease the amount of solar radiation that enters the house from the windows, using timber for walls and clay tiles for the roofs and examining seven different orientations to find the best strategy for the house. All these strategies were tested and compared between full-day natural ventilation and without any ventilation. The thermal comfort of these strategies was graphically defined based on the operative temperature. The results of this study revealed that protecting the windows from solar radiation by adding shading devices and closing the curtains had the lowest indoor operative temperature achievement compared to other examined strategies.

### ARTICLE INFO

*Article history:*

Received: 22 February 2022

Accepted: 30 June 2022

Published: 19 August 2022

DOI: <https://doi.org/10.47836/pjst.31.1.06>

*E-mail addresses:*

mar\_mka@yahoo.com (Maryam Qays Oleiwi)

faridmohamed@ukm.edu.my (Mohd Farid Mohamed)

\* Corresponding author

*Keywords:* Building simulation, double storey house, IES-VE software, indoor temperature, shading devices, thermal comfort, timber walls

## INTRODUCTION

Based on modern buildings' current design, occupants must use an air-conditioning system to get thermal comfort. Moreover, the affordability of the mechanical system leads to the perception that designing a building for thermal comfort is less important compared to its aesthetic and cost factors because thermal comfort issues can always be resolved during the occupancy period by installing an air conditioning system, which is now affordable and easily installed as shown in Figure 1. Low electricity tariffs in Malaysia support this trend of controlling indoor thermal comfort. Increasing the use of air conditioning systems with increasing building development in developing nations such as Malaysia will lead to a huge demand for electricity. As Malaysia is still mainly depending on fossil fuels for electricity (Latif et al., 2021; Basri et al., 2021), this will lead to a negative impact on the environment due to factors such as global warming, carbon dioxide emission and air pollution (Imran et al., 2018; SEforALL, 2020; Shafique & Kim, 2017).

Figure 1 shows examples of low-rise and high-density low-cost development in Malaysia, normally occupied by low-income families. Though occupied mostly by low-income families, it is very common to find compressors installed on the façade of the buildings. It is due to various factors such as affordable electricity tariffs as well as less acceptable indoor thermal comfort. Less acceptable indoor thermal comfort in low-cost housing, either low- or high-density housing, is very common as the result of design and cost factors (Amir et al., 2019). For example, greater sun heat penetration is due to poor orientation of the building, unprotected opening and the use of materials, such as sand brick and metal decking.

As the climate change issue becomes critical, the building industry shall look at various strategies to reduce the negative impact of the building sector on the environment. One of the many solutions is to promote buildings with good passive cooling strategies that could contribute to good indoor thermal comfort and are less dependent on mechanical



*Figure 1.* Single story, low-cost detached house with metal decking roof and plastered sand brick wall (Amir et al, 2019) (left), and high-density low-cost housing with air conditioning compressor on the facade (right)

cooling, such as air conditioning systems (Yusoff & Ja'afar, 2019; Yusoff & Mohamed, 2017; Yusoff, 2020). In addition, a lot can be learned from traditional or heritage buildings in Malaysia, whether houses (or palaces), shophouses or mosques.

Traditional buildings in Malaysia have been developed by local builders for hundreds of years and have been responding well to the local climate with various cooling strategies such as large openings (Yusoff & Ja'afar, 2019; Yusoff, 2020). Therefore, traditional buildings, such as houses, shophouses and mosques, do not require mechanical systems such as air conditioning to obtain acceptable indoor thermal comfort. The strategies adopted in these buildings include aspects related to opening, wall, roof, and shading. For example, it is common for traditional mosques and houses in East Cost Malaysia, such as Kelantan and Terengganu, to use thin clay tile known as *singgora* (Husen & Mohamed, 2021) that only store a small amount of heat, which avoids poor indoor temperature during night-time. Using timber as a material also contributes towards good indoor thermal comfort during night-time due to its materiality that does not store heat.

Figures 2, 3, and 4 show some traditional buildings, which are well designed for indoor thermal comfort through various strategies. Generally, it can be clearly observed that the buildings are well ventilated with various strategies. For example, the mosque in Figure 2 shows a large area of openings around the indoor praying area, allowing for good cross ventilation. In the case of a Malay traditional house in Kelantan (Figure 2), fixed decorative openings are provided on a wall for natural ventilation. In the case of the shophouse, Figure 4 shows a shophouse in Malacca City, which has an internal courtyard to solve the ventilation limitation for the long plan intermediate two-storey shophouses. Therefore, the internal courtyard allows for natural ventilation and lighting in the indoor spaces. The internal courtyard of a heritage shophouse could lead to better indoor thermal comfort (Kubota et al., 2014). Some heritage shophouses in Malacca City have more than one internal courtyard. Multiple internal courtyards allow natural lighting and ventilation



Figure 2. Exterior (left) and interior (right) of Kampong Laut Mosque, Kelantan (Mohamed, 2020)



Figure 3. Exterior (left) and interior (right) of Malay traditional house of Kelantan (Mohamed, 2020)

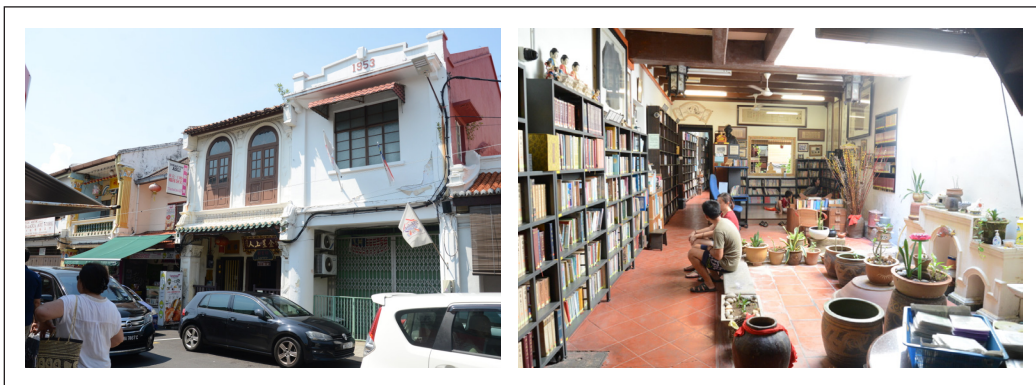


Figure 4. Exterior (left) and interior (right) of heritage shophouse in Melaka City

in a double-storey linked shophouse with a very long depth. More than 200 feet in depth are very common in such heritage shophouses in Malacca City. However, nowadays, such a deep plan is not common in modern linked shophouses.

Other than strategies for natural ventilation and lighting in traditional buildings, many other factors influence the indoor thermal comfort of the buildings—for example, the materials used for the wall and roof. For the traditional Malay house, as in Figure 3, the roof material is thin clay tile known as Singgora, and timber is used for the wall. In the case of the shophouse, as in Figure 4, the roof's material is clay tile, and a thick brick wall is used for the wall. In the case of a traditional mosque (Figure 1), the materials are similar to the traditional Malay house as in Figure 2. However, there are also old traditional mosques in Malaysia that use thick brick walls, such as in Malacca City. The clay tile, timber walls and thick brick walls with a combination of good design strategies in the traditional buildings, such as internal courtyard, large opening, and deep roof overhang, could contribute to better indoor environmental quality (Kubota et al., 2014, Yusoff & Ja'afar, 2019; Yusoff, 2020; Rana et al., 2021).



Nowadays, in many modern buildings, whether houses, mosques or shophouses, similar traditional strategies are not extensively adopted; thus, they are very dependent on the mechanical system to achieve good thermal comfort (Figure 5). Nevertheless, various sustainable or green strategies in traditional buildings can be learned and applied in a modern buildings, leading to greener architecture. In contrast to ‘active’ mechanical cooling devices, passive cooling is typically considered a combination of natural processes and approaches for lowering indoor temperatures (Prieto et al., 2018). Many studies (Mohamed, 2020; Husen & Mohamed, 2021; Oleiwi & Mohamed, 2021; Yusoff, 2020; Yusoff & Mohamed, 2017) have been conducted to identify, outline, or analyse the strategies in traditional buildings. Other than the strategies typically found in traditional buildings, many other passive green strategies are commonly found in modern buildings, such as the introduction of insulation in the roof, roof ventilator and low-emissivity glass. In addition, building designs and methods considering energy consumption can reduce cooling loads (Yeganeh, 2020). The study of Gamero-Salinas et al. (2021) underlined the need for passive cooling and overheating prevention design solutions in tropical regions.

Indoor overheating can be reduced in the tropics if proper building design principles for these climate zones are used (Bhikhoo et al., 2017). Climate change and economic growth will raise cooling energy demand in this region, necessitating immediate adaptation in the building sector to decrease the problems posed by the future rise in cooling energy demand and the increased climatic changes (Santamouris, 2016).

Mirrahimi et al. (2016) conducted a review of prior research on the impact of building envelopes on energy consumption and thermal performance in Malaysia. The study found that passive cooling strategies successfully decreased energy consumption for hot-humid tropical building envelopes. In addition, the study found a substantial link between several architectural components, such as shading devices, external walls, external roofs, external glass, and insulation, and lowering the energy consumed for cooling.



*Figure 5.* Modern mosque at Cyberjaya, Malaysia, has a large opening to optimise natural ventilation and lighting

However, for this study, the investigation was only conducted on a few selected strategies that could potentially affect indoor thermal comfort. Two of the selected strategies are the introduction of shading devices (external) and curtains (internal). Other than that, comparisons were made between a brick wall and timber for wall materials, the clay and concrete tiles for the roof and, finally, the various orientation of the buildings to understand the effects of solar heat. Therefore, this study aims to investigate the effect of the application of selected passive cooling strategies on the indoor temperature and thermal environment of a building located in a tropical climate.

It has been proved that thermal comfort can occur in a narrow range of body temperatures, and the skin moisture is kept low with minimum physiological effort (ASHRAE, 2017). However, occupants in naturally ventilated buildings have a wide range of comfort temperatures, which may exceed the limitations of ASHRAE Standard 55, and a response to local outdoor climate changes (Brager & de Dear, 2000). According to the study of Oleiwi (2020), after calculating the thermal acceptability limits based on the adaptive comfort standard (ACS) that was proposed by Brager and de Dear (2000), it is found that the maximum and minimum temperatures that should not be exceeded are 29.9 and 24.9 °C for 90% acceptability limit and 30.9 and 23.9 °C for 80% acceptability limit respectively in Bangi, Malaysia for April.

It is good to mention that this study only focuses on the aspect of operative temperature and does not look at the other aspects of thermal comforts, such as humidity and air speed. Furthermore, while there are various types of traditional buildings in Malaysia, as an initial study, the investigation was only completed on a double-storey building, which was purposely constructed as a test building for various research.

## **METHODOLOGY**

Studies proved that the energy prediction process could anticipate cooling loads and the effect of passive cooling on lowering interior temperature gains with fair accuracy (Olawale-Johnson et al., 2021). In this study, several design strategies were applied to the tested house (reference case) to investigate the effect of these strategies on the internal thermal environment. The investigation was conducted and compared under two conditions: fully ventilated and without ventilation. Natural ventilation has been proven to be a good strategy to cool the interior spaces down in the tropics; however, allowing the hot air that comes from outdoor to enter the buildings could heat the structure and decrease thermal comfort (Kubota et al., 2009; Oleiwi, 2020). Figure 6 shows the methodology of this study.

The selected approaches are as follows:

- (a) Adding external shading devices and closing the curtains inside the rooms to protect the windows from direct solar radiation.
- (b) Using timber as a construction material for the walls and clay tiles for the roof

to investigate the effects of these materials with different thermal transmittance (U-value).

- (c) Changing the orientation of the house by examining the other seven orientations to find the most thermal comfort orientation.

The tested house was located at the Faculty of Engineering and Built Environment, Universiti Kebangsaan Malaysia (UKM), Bangi, 27 km from Kuala Lumpur, Malaysia’s capital city. Figure 7 shows the double-storey house built using common modern construction materials (sand brick and cement for the walls and concrete roof tiles for the roof). This house was built purposely for research activities. Therefore, easy access to the house enabled the researcher to enter the house easily for site investigation. All the walls were not insulated for heat transmission. The wall structure consists of 114 mm thick sand brick with 19 mm thick cement plastering on the interior and exterior sides. The roof structure consists of concrete grey roof tiles

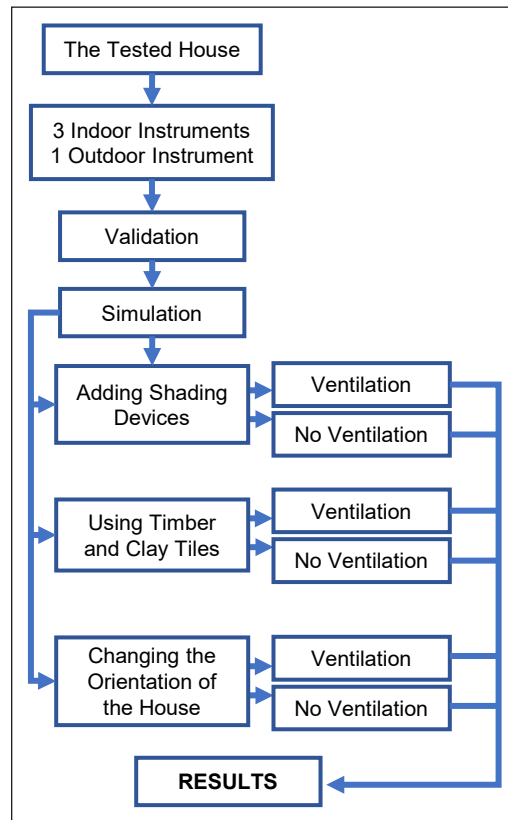


Figure 6. Research methodology diagram

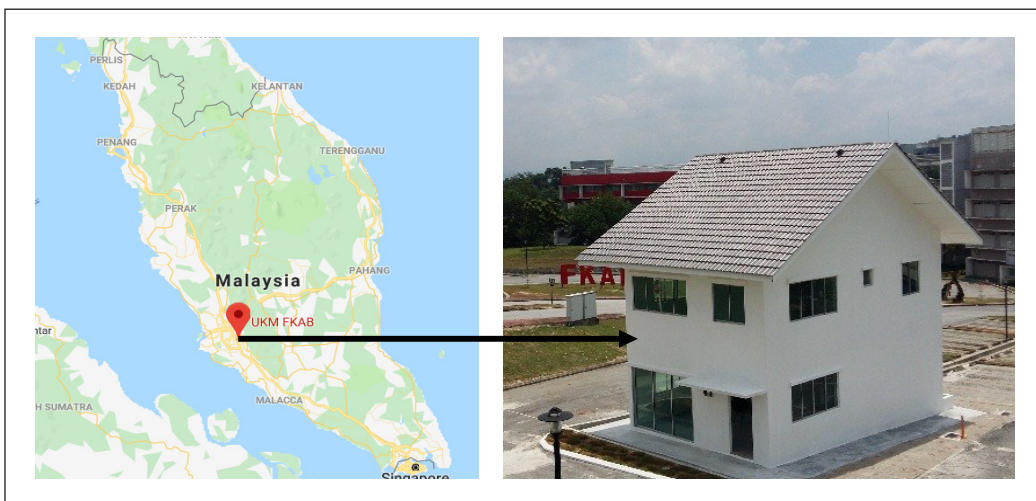


Figure 7. The tested house

with metal roof trusses with double-sided aluminium sisalation and a layer of 3.2 UCO Superflex soffit all around the roof.

The house includes a living room, kitchen, and a bathroom on the ground floor, and three bedrooms and two toilets on the first floor. In this study, Room 1 refers to the living room, Room 2 refers to the secondary bedroom, and Room 3 refers to the master bedroom. The windows of the house faced four directions. Figure 8 shows the ground and first-floor plans of the tested house.

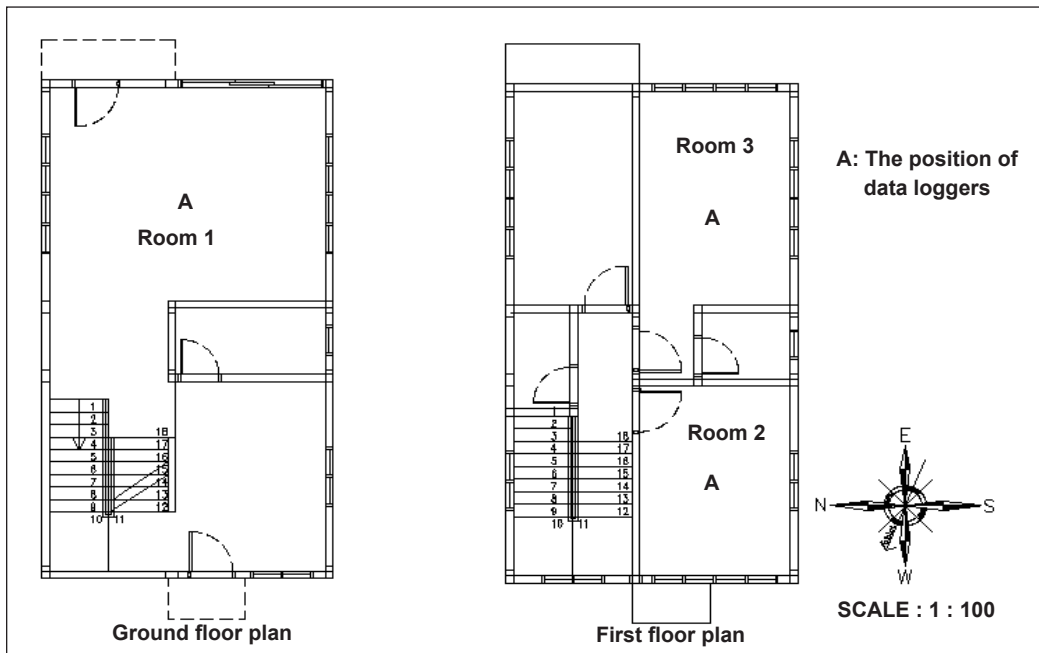


Figure 8. The plans of the tested house

Three sets of Delta Ohm HD32.3 WBGT-PMV thermal comfort instruments were placed indoors, in the centre of the living room (Room 1), the secondary bedroom (Room 2), and the master bedroom (Room 3). The third bedroom was not investigated. The instruments were positioned at 1.5 m above the ground to record the values of air temperature ( $T_a$ ), relative humidity (RH), and mean radiant temperature ( $T_{mrt}$ ) in each room. The data for each room was recorded and obtained using the software DeltaLog10 version 1.30. The list of all instruments is shown in Table 1.

The instruments were set to record data at 10-min intervals for 24 h. The selected measurement periods were from 1 April to 7 May 2018, which falls in the hottest period in the year in Malaysia based on the average monthly data of temperature for 11 years (MMD, 2017; Sulaiman, 2017). Moreover, the rainfall recorded by the MK-III Weather Stations™ was useful for determining whether each day was sunny or rainy. Rainy days were excluded from the study as they do not represent overheated days.



Table 1  
Summary of instruments involved in this study

Instrument	Parameter	Unit	Range
<b>A- Indoor parameters</b>			
AP3203.2 prop, Delta Ohm	- Air temperature (°C)	3	Temperature 0 to 100 °C
HD32.3 PMV data logger	- Air velocity (m/s)		Airspeed 0 to 5 m/s,
TP3276.2 prop, Delta Ohm	- Global temperature (°C)	3	-10 to 100 °C
HD32.3 PMV data logger			
HP3217.2 prop, Delta Ohm	- Air temperature (°C)	3	Temperature -10 °C to 80 °C
HD32.3 PMV data logger	- Relative humidity (%)		The relative humidity is 5% to 98%
<b>B- Outdoor parameters</b>			
MK-III Weather Stations™	Air temperature (°C)	1	-55 to 85°C
	Wind speed (m/s)	1	0 to 67 m/s
	Relative humidity (%)	1	0 to 100%

The geometry of the computational model for the tested house was created using the IES-VE (2019) software. First, the building's geometry, dimensions, and areas of solid and transparent surfaces were defined using [ModellIT]. Next, the location of the house was defined by [APlocate], which was set as Kuala Lumpur suburbs as it was the nearest to the site. Next, window and door openings profiles and window types were set using [MacroFlo]. Then, fabric materials, thermal properties and simulation time were defined using [Apache]. Table 2 shows the construction materials used in the simulation of the tested house.

The simulation was done in the same period of the year of the selected site measurement periods. The weather data of this study were provided by IES-VE, which can be determined according to the nearest location.

Table 2  
Details of construction materials for the tested house

Element	Construction	U-Value (W/m <sup>2</sup> k)
External walls	Cement plaster (19 mm), sand brick with cement (114 mm), cement plaster (19 mm)	3.4
Internal walls	Cement plaster (19 mm), sand brick with cement (114 mm), cement plaster (19 mm)	3.4
Roof (concrete tiles)	Concrete tiles (5 mm), aluminium sisalation (1 mm), UCO Superflex ceiling board (3.2 mm)	6.9
Roof (clay tiles)	Clay tiles (5 mm), aluminium sisalation (1 mm), UCO Superflex ceiling board (3.2 mm)	6.85
Floor	Cast concrete (220 mm)	3.6
Doors	Plywood	2.2

Note. The values are the standard values in the software.

IES-VE simulation software has been chosen for this study as it permits the user to change construction materials, dimensions, thicknesses for all house components (roof, ground, and walls), and windows opening profile.

Before using any building simulation software, the validation of the simulated data should be evaluated by comparing the simulated data with the measured data (Oleiwi et al., 2019). In this study, the simulated indoor air temperature was compared with the one collected from field measurements (during the same period of the year) to ensure the accuracy of the simulation. The validated model would then be used for further simulation. As a result, it is found that the model of this study is valid because the correlation coefficient (R2) of the simulated with measured data was sufficient according to the recommendation of ASHRAE (2009) (R2 of 0.9 or greater), as shown in Figure 9.

To investigate the selected strategies that could affect indoor thermal comfort, firstly, 1-meter depth shading devices have been added above all the windows of the three tested rooms from outside. At the same time, other original conditions of the reference case

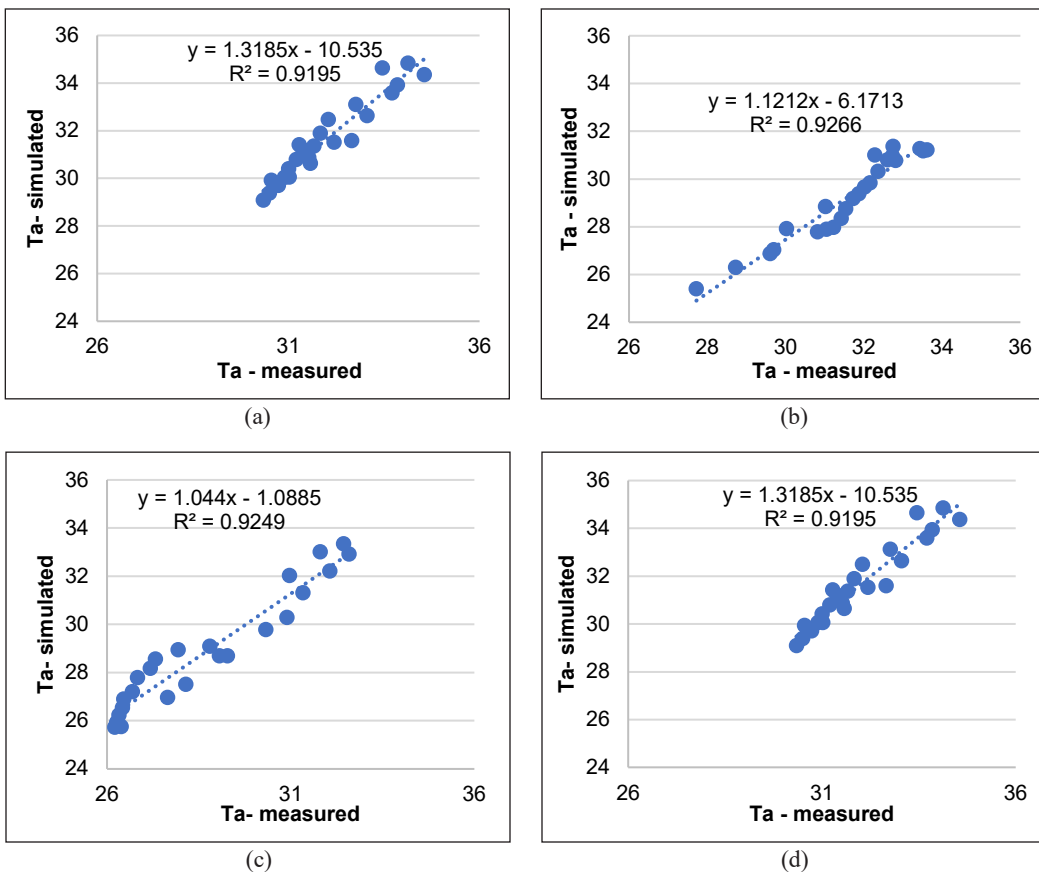


Figure 9. Linear regression analysis (measured versus prediction) for different ventilation conditions of: (a) full-day ventilation; (b) daytime ventilation; (c) night-time ventilation; and (d) no ventilation

remained. The simulation was done with full-day natural ventilation when all windows and internal doors were open for 24 hours and no ventilation when all windows and doors were closed for 24 hours separately. Then, closed curtains were added to the windows of the three tested rooms from the inside to the non-ventilated case to increase the protection of the windows from direct solar radiation.

Secondly, 20mm timber boards have been used as construction material for external and internal walls and flooring, while other original conditions of the reference case remained. Then, the concrete roof tiles were changed to clay roof tiles. Finally, both simulations were done separately with full-day natural ventilation and no ventilation.

Finally, seven orientations have been examined for the tested house, while other original conditions of the reference case remained- to find the most thermal comfort orientation of the house. Changing the orientation was done with full-day natural ventilation and no ventilation separately.

The main simulation output obtained from IES-VE was the indoor air temperature ( $T_a$ ) and the mean radiant temperature ( $T_{mrt}$ ) for the three rooms. The results were converted into Excel sheets to facilitate data analysis.

Operative temperature ( $T_o$ ) was calculated based on Equation 1, which was proposed by ASHRAE (2010):

$$T_o = \frac{(T_a + T_{mrt})}{2} \quad (1)$$

Where  $T_o$  is the operative temperature in °C,  $T_a$  is the air temperature in °C, and  $T_{mrt}$  is the mean radiant temperature in °C.

IES-VE was selected as it is software with a simple input interface that creates the prototype and modifies its layout. Moreover, the output can be easily interpreted and represented in tabular data or graphs. Finally, IES-VE is user-friendly, which makes this software useful for this study. A three-dimensional view of the building modelled in IES-VE is illustrated in Figure 10.

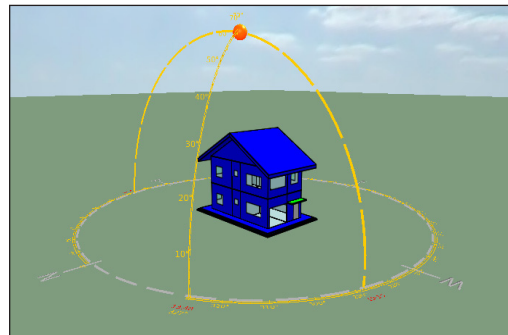


Figure 10. The tested house in IES-VE software

## RESULTS AND DISCUSSION

A comparison of the operative temperature of the simulated cases has been made by applying full-day ventilation (all windows and internal doors were opened for 24 hours) and no ventilation (all windows and doors were closed for 24 hours) to find the best strategy that can achieve thermal comfort for the tested house.

## Shading Devices and Curtains

**Adding Shading Devices with Full-Day Natural Ventilation.** In this case, 1-meter depth shading devices have been added above all the windows of the house from outside to decrease the direct solar radiation that enters the house. Table 3 shows the average operative temperature of April for the simulated cases with full natural ventilation. Figure 11 shows the hourly operative temperature—an average for April, and patterns of the simulated cases with full-day ventilation when shading devices have been added.

By referring to Table 3 and Figure 11, there is a slight reduction in the mean, maximum and minimum operative temperature when adding shading devices and applying 24 hours natural ventilation for all three rooms. The highest reduction happened in the maximum operative temperature of Room 1 (0.45 °C).

As full-day natural ventilation was applied for this case, the outdoor air can enter the rooms and affect the indoor environment. Subsequently, no ventilation strategy was applied by closing all the windows and doors for the same case to remove the effect of outdoor air.

**Adding Shading Devices and Curtains with No Ventilation.** In the previous case, adding closed curtains was not applicable because the windows were opened 24 hours for ventilation purposes, while it could be applied with no ventilation strategy when all the windows and internal doors were closed. Table 4 shows the average operative temperature of April for the simulated cases with no ventilation. Figure 12 shows the average hourly operative temperature for April of the simulated cases with no ventilation.

By referring to Table 4 and Figure 12, a good reduction happened in the mean, maximum and minimum operative temperature when adding shading devices and closing the curtains. At the same time, there was no ventilation in the three rooms. Therefore, the highest reduction was gotten for the maximum operative temperature of Room 1 (the reduction was 2.38 °C), followed by the maximum operative temperature of Room 3 (the reduction was 2.12 °C).

These results can cope with the results of several studies that have been conducted to examine the effect of blocking solar radiation when a shading device was positioned above one of the windows of the building to block sun gain in summer (Taleb, 2014). The results showed that shading had a significant effect on temperature reduction.

In the study of Kim et al. (2015), results showed a 35.1% reduction in the total cooling load caused only by blocking solar radiation due to the external shading added to the tested building.

Moreover, Kim et al. (2017) and Kamal (2010) mentioned that minimising solar radiation by adding external horizontal shading devices for the windows could cool the building effectively and decrease the energy consumption needed.

Regarding closing the curtains, Huang and Kang (2021) concluded that an improvement was achieved in an indoor thermal environment when closing curtains by reducing overheating time to an average of 62.2%. Thus, the comfort time was increased accordingly.

### Using Timber and Clay Roof Tiles

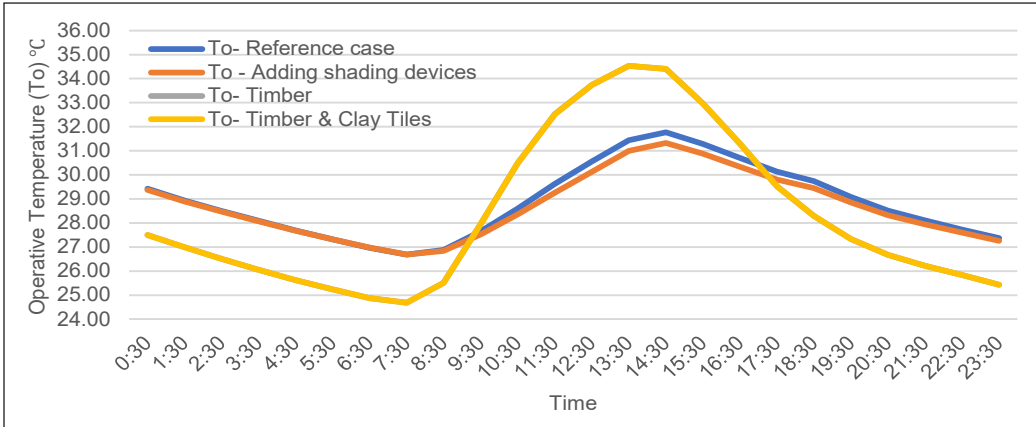
The reference case's external and internal walls and flooring construction material have been changed to timber boards (20mm thickness) for the tested house. In contrast, other original conditions of the reference case remained. Then, the concrete tiles of the roof were changed to clay roof tiles. Both simulations were done with full-day natural ventilation and no ventilation separately.

**Using Timber and Clay Roof Tiles with Full-Day Ventilation.** Table 3 also shows the average operative temperature for April for the simulated cases with full-day ventilation. Figure 11 shows the average hourly operative temperature of April of the simulated cases with full-day ventilation when using timber and clay roof tiles.

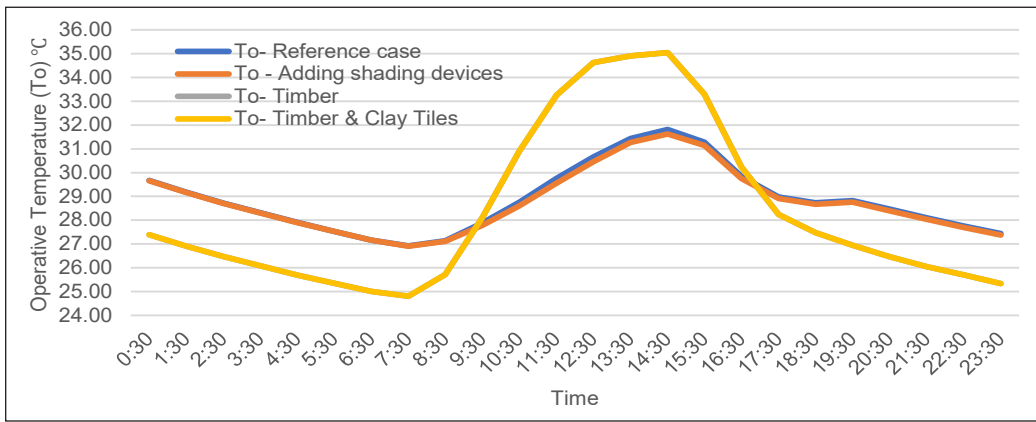
By referring to Table 3 and Figure 11, it can be noticed that using timber only or combining it with clay roof tiles (represented by the grey line in Figure 11, however, it is hidden under the yellow line because they both have similar values) can decrease the indoor operative temperature during night-time and early morning when there is no solar insolation. A good reduction happened in the minimum operative temperature (2.01, 2.11, & 2.20 °C) for Room 1, Room 2 and Room 3 when using only timber or timber and clay roof tiles in the case of full-day ventilation in the three rooms during night-time and early morning. However, using these materials was not significant during the daytime in all three

Table 3  
*Adding shading devices, using timber, and using clay roof tiles with full-day ventilation*

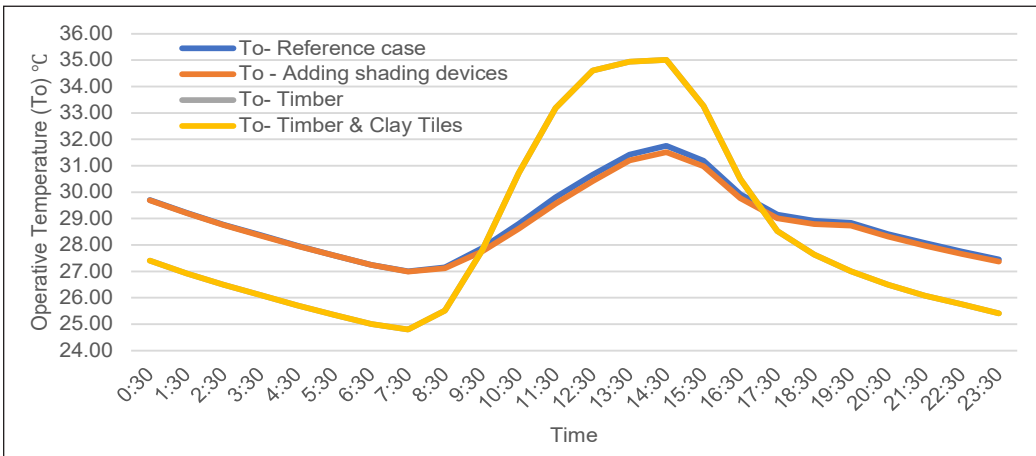
Thermal variables	Statistics	Reference case	Adding Shading Devices	Using Timber	Using Timber & Clay roof tiles
<b>Room 1</b>					
Operative temperature (°C)	Mean	28.87	28.68	28.34	28.34
	Maximum	31.78	31.33	34.54	34.54
	Minimum	26.69	26.59	24.68	24.68
<b>Room 2</b>					
Operative temperature (°C)	Mean	28.84	28.77	28.33	28.33
	Maximum	31.81	31.63	35.04	35.04
	Minimum	26.92	26.91	24.81	24.81
<b>Room 3</b>					
Operative temperature (°C)	Mean	28.88	28.77	28.34	28.34
	Maximum	31.76	31.51	35.01	35.01
	Minimum	27.00	26.90	24.80	24.80



(a)



(b)



(c)

Figure 11. The hourly operative temperature patterns of the simulated cases with full day ventilation strategy when adding shading devices, using timber, and using clay roof tiles: (a) Room 1; (b) Room 2; (c) Room 3

rooms. On the contrary, there was a high increment in the maximum operative temperature (2.76, 3.23 and 3.25 °C) for Room 1, Room 2, and Room 3. These results can cope with the results of Adekunle and Nikolopoulou’s (2016) study, who stated that, while the timber is increasingly being utilised in building construction due to its environmental aspects and capacity to shorten total construction time when compared to conventional materials, the lack of thermal mass and low U-values can be a critical factor in increased overheating.

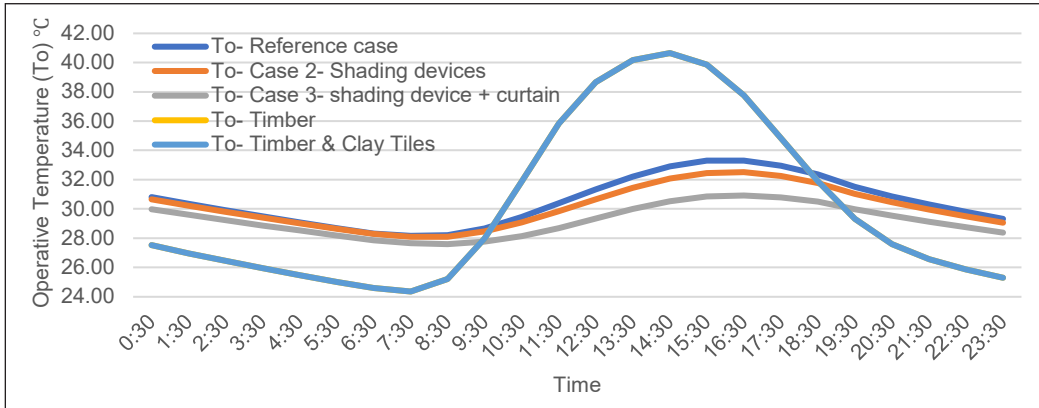
Therefore, using timber only or combining it with clay roof tiles is not significant for the tested house when full-day ventilation is used. Moreover, it is noticed that there was no difference in the mean, maximum and minimum operative temperature between using timber only or combining it with clay tiles for the three rooms due to the approximate u-value of clay roof tiles and concrete roof tiles for the same thickness (Table 2) as previously proved by Oleiwi (2020).

**Using Timber and Clay Roof Tiles with No Ventilation.** Table 4 also shows the average operative temperature of April for the simulated cases with no ventilation. Figure 12 shows the average hourly operative temperature for April of the simulated cases with no ventilation.

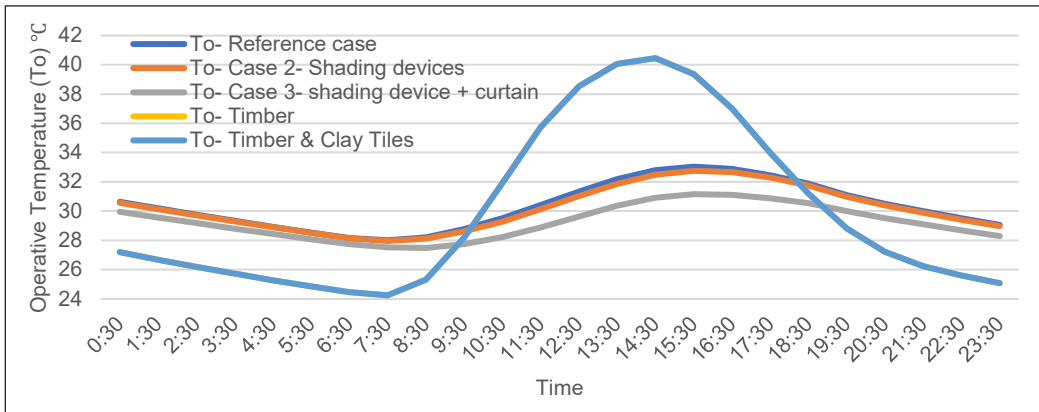
When there is no ventilation, the situation worsens during the daytime because the hot air is trapped inside the rooms. By referring to Table 4 and Figure 12, it can be noticed that a high increment happens when using timber only or combining it with clay roof tiles in the maximum operative temperature (7.35, 7.42 & 7.62 °C) for Room 1, Room 2, and Room 3. However, the situation was different during the night-time. There were decrements in the minimum operative temperature (3.80, 3.77 & 3.89 °C) for Room 1, Room 2 and Room 3.

Table 4  
*Adding shading devices and curtains, using timber; and using clay roof tiles with no ventilation*

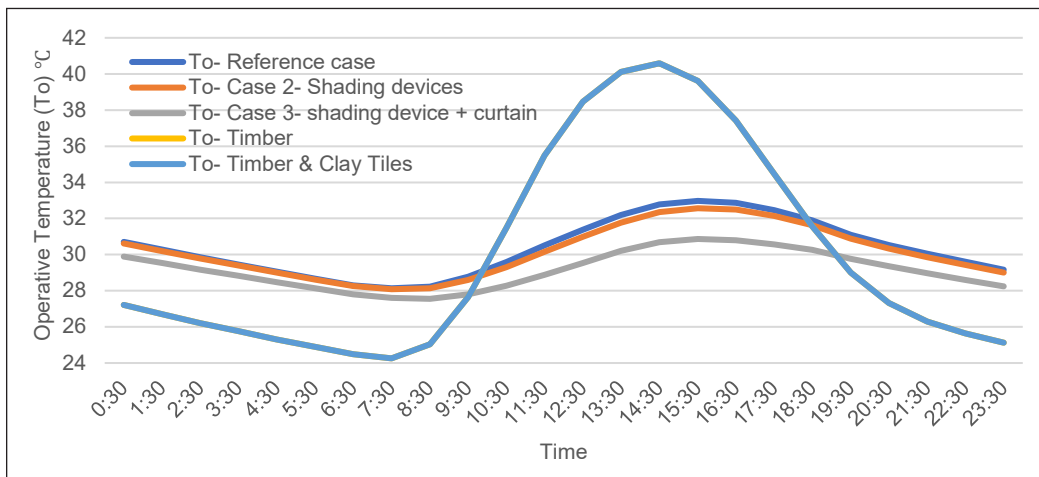
Thermal variables	Statistics	Reference case	Shading Devices	Shading Devices + Curtains	Using Timber	Using Timber & Clay Roof Tiles
<b>Room 1</b>						
Operative temperature (°C)	Mean	30.48	30.11	29.20	30.24	30.24
	Maximum	33.30	32.51	30.92	40.65	40.65
	Minimum	28.15	28.10	27.59	24.35	24.35
<b>Room 2</b>						
Operative temperature (°C)	Mean	30.30	30.16	29.24	29.97	29.97
	Maximum	33.03	32.76	31.15	40.45	40.45
	Minimum	28.01	27.96	27.49	24.24	24.24
<b>Room 3</b>						
Operative temperature (°C)	Mean	30.35	30.15	29.16	30.00	30.00
	Maximum	32.98	32.57	30.86	40.60	40.60
	Minimum	28.14	28.09	27.55	24.25	24.25



(a)



(b)



(c)

Figure 12. The hourly operative temperature patterns of the simulated cases with no ventilation strategy when adding shading devices, adding closed curtains, using timber, and using clay roof tiles: (a) Room 1; (b) Room 2; (c) Room 3



Other studies showed similar results. For example, the study by Dong et al. (2019) proved that using a type of timber (cross-laminated timber (CLT)) in office buildings in China had a significant effect on decreasing energy consumption of heating in the Cold Region and Severe Cold Regions of China; however, the CLT buildings consumed more energy for cooling in the summer. Thus, this type of construction is not suitable for hot regions. In addition, Khavari et al. (2016) concluded that cross-laminated timber generally provides a significant improvement in heating energy efficiency as a heavy and air-tight envelope, but its energy performance efficiency can be affected by weather, building size, internal loading, and HVAC control.

In the North European climate, the results of Kildsgaard et al. (2013) showed that airtight, low-energy apartment buildings could be successfully built with prefabricated timber elements in a cold climate.

### Changing the Orientation of the House

Seven orientations for the angles 45, 90, 135, 180, 225, 270, and 315 degrees have been examined and compared with the reference case, which is considered as zero angle orientation. In contrast, other original conditions of the reference case remained. Figure 13 shows the eight orientations of the tested house. The simulations were done with full-day natural ventilation and no ventilation separately.

**Changing the Orientation of the House with Full-Day Ventilation.** Table 5 shows the average operative temperature for April for the simulated cases with full-day ventilation.

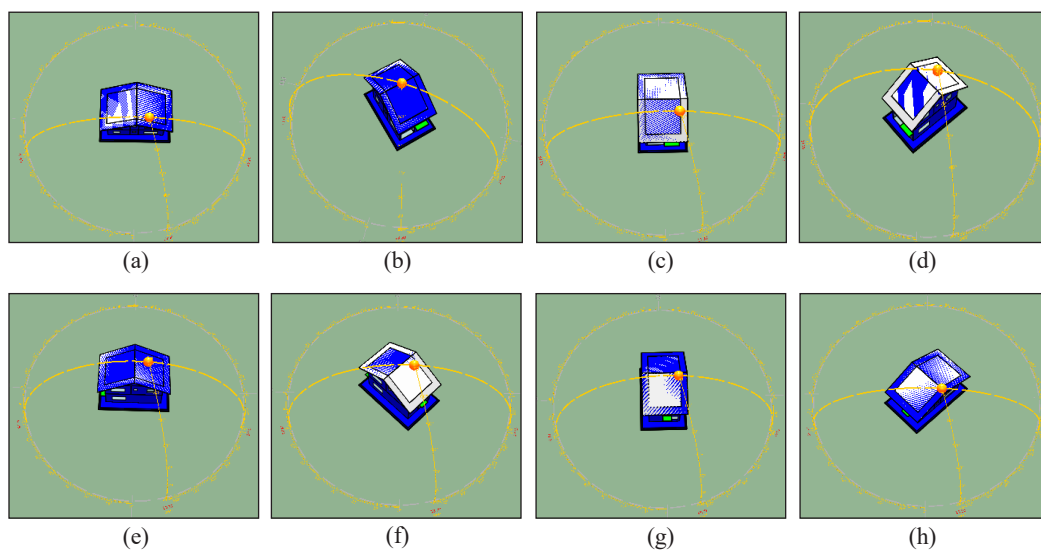
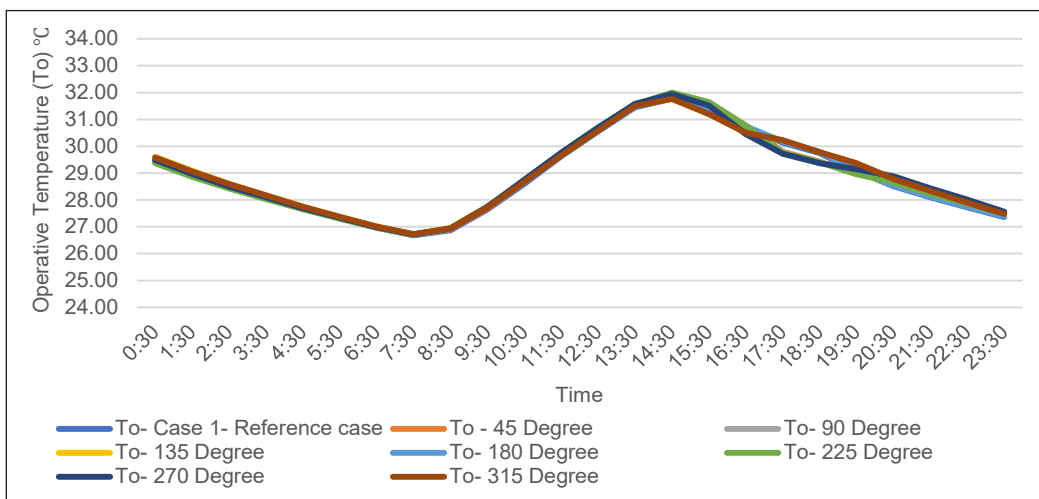


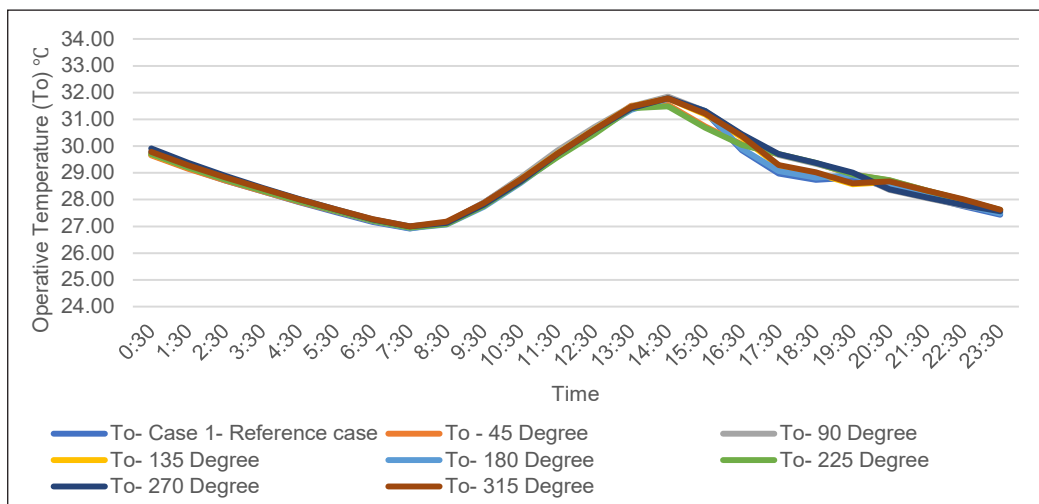
Figure 13. The eight orientations of the tested house: (a) Zero degree; (b) 45 degree; (c) 90 degree; (d) 135 degree; (e) 180 degree; (f) 225 degree; (g) 270 degree; (h) 315 degree

Figure 14 shows the average hourly operative temperature for April of the simulated cases with full-day ventilation.

By referring to Table 5 and Figure 14, it can be noticed that there was no significant difference for all the seven cases compared with the reference case when the full-day ventilation strategy was applied. However, the lowest two directions are 0 and 180 degrees. The main reason for no significant difference could be because the house has big windows from all four sides; thus, it was exposed to solar radiation from all four sides even when the direction of the facades was changed. The other reasons could be that the house is too small with the distance between walls is close to each other, the pure rectangular shape of

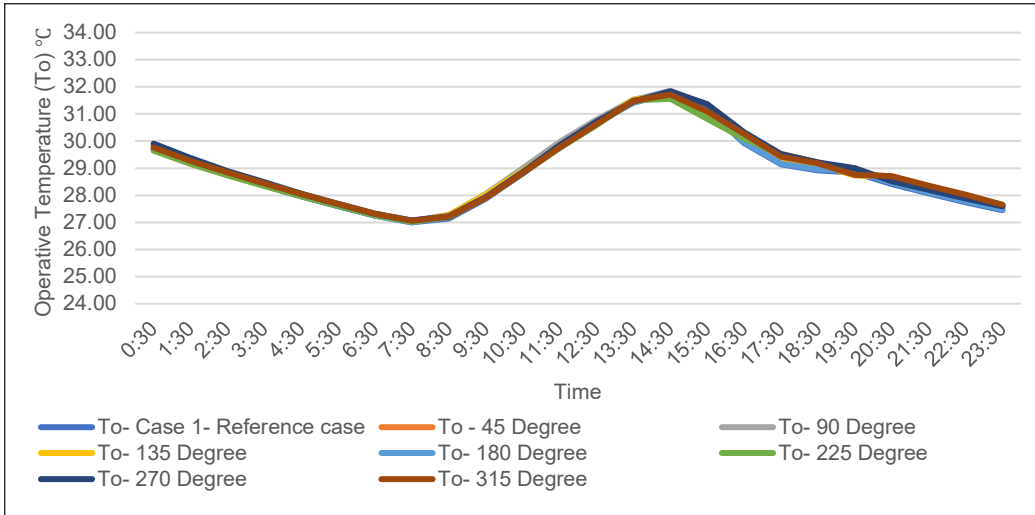


(a)



(b)

Figure 14. The hourly operative temperature patterns of the simulated cases with full day ventilation strategy of the eight orientations: (a) Room 1; (b) Room 2

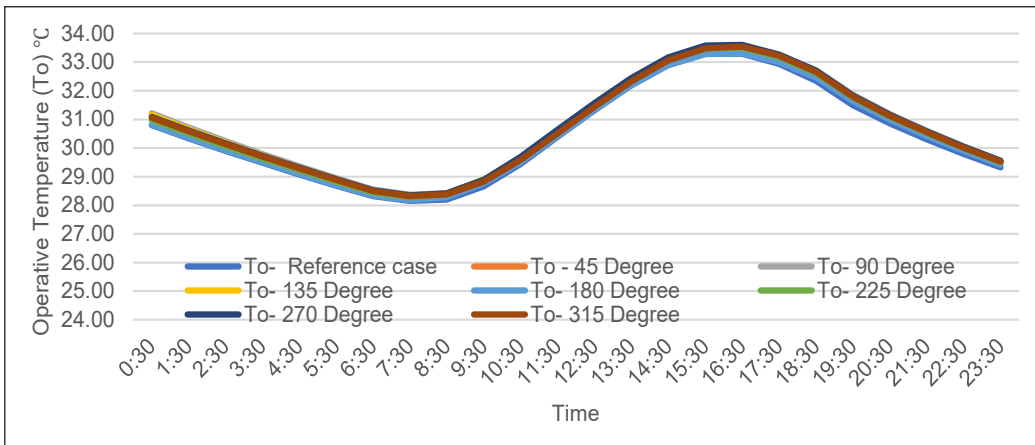


(c)

Figure 14 (continue). The hourly operative temperature patterns of the simulated cases with full day ventilation strategy of the eight orientations: (c) Room 3

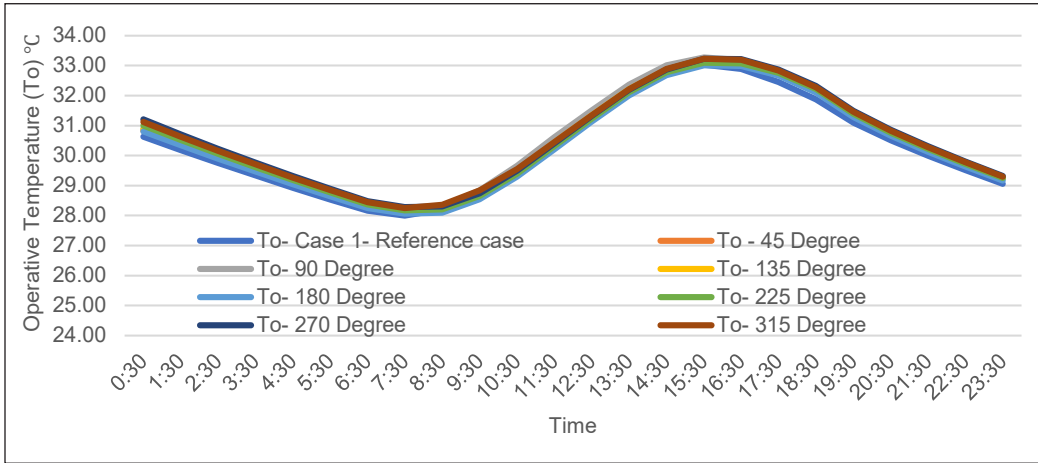
the building (close to being square) and the façade of the building is almost clean without significant protruding elements, which could protect the façade from the sun heat.

**Changing the Orientation of the House with No Ventilation.** Table 6 shows the average operative temperature of the month of April for the simulated cases with no ventilation. Figure 15 shows the average hourly operative temperature for April of the simulated cases with no ventilation.

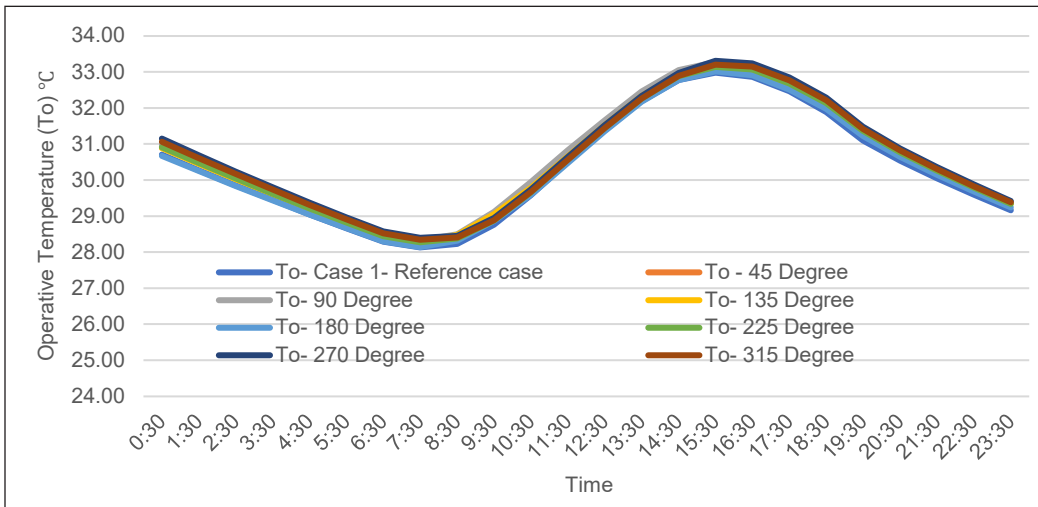


(a)

Figure 15. The hourly operative temperature patterns of the simulated cases with no ventilation strategy of the eight orientations: (a) Room 1



(b)



(c)

Figure 15 (continue). The hourly operative temperature patterns of the simulated cases with no ventilation strategy of the eight orientations: (b) Room 2; (c) Room 3

By referring to Table 6 and Figure 15, it can be noticed that there was no significant difference for all the seven cases compared with the reference case when no ventilation was applied. The reason for that could be the same as when the full-day ventilation strategy was applied.

In Malaysia, it is recommended to expose glazing to the North and South and avoid exposure to the East and West (Tang & Chin, 2013). However, the same study showed that the most significant factor for lowering building energy consumption in a building is decreasing the glazing area. Therefore, removing the windows from two opposite sides is recommended, testing different orientations.

Table 5  
Changing the orientation of the tested house with full-day ventilation

Thermal variables	Statistics	Reference case	45 Degree	90 Degree	135 Degree	180 Degree	225 Degree	270 Degree	315 Degree
Room 1									
Operative temperature (°C)	Mean	28.87	28.89	28.92	28.95	28.89	28.90	28.93	28.95
	Maximum	31.78	31.96	31.89	31.76	31.79	32.01	31.94	31.77
	Minimum	26.69	26.71	26.72	26.72	26.69	26.71	26.72	26.73
Room 2									
Operative temperature (°C)	Mean	28.84	28.91	28.97	28.91	28.85	28.90	28.97	28.95
	Maximum	31.81	31.55	31.85	31.78	31.77	31.48	31.79	31.78
	Minimum	26.92	26.95	26.96	26.96	26.94	26.96	27.00	27.00
Room 3									
Operative temperature (°C)	Mean	28.88	28.95	29.01	28.97	28.89	28.92	29.01	28.97
	Maximum	31.76	31.61	31.86	31.73	31.76	31.57	31.84	31.71
	Minimum	27.00	27.03	27.06	27.05	27.00	27.03	27.07	27.06

Table 6  
Changing the orientation of the tested house with no ventilation

Thermal variables	Statistics	Reference case	45 Degree	90 Degree	135 Degree	180 Degree	225 Degree	270 Degree	315 Degree
Room 1									
Operative temperature (°C)	Mean	30.48	30.48	30.48	30.48	30.48	30.48	30.48	30.48
	Maximum	33.30	33.30	33.30	33.30	33.30	33.30	33.30	33.30
	Minimum	28.15	28.15	28.15	28.15	28.15	28.15	28.15	28.15
Room 2									
Operative temperature (°C)	Mean	30.30	30.47	30.52	30.45	30.34	30.45	30.57	30.55
	Maximum	33.03	33.23	33.28	33.16	33.01	33.10	33.23	33.23
	Minimum	28.01	28.13	28.17	28.14	28.06	28.17	28.28	28.26
Room 3									
Operative temperature (°C)	Mean	30.4	30.57	30.63	30.54	30.39	30.52	30.65	30.58
	Maximum	33.0	33.21	33.27	33.17	33.02	33.14	33.31	33.20
	Minimum	28.1	28.28	28.33	28.28	28.14	28.27	28.40	28.35

## CONCLUSION

In this study, three main passive cooling strategies were applied to the tested house using IES-VE 2019 building simulation software to find the best thermal comfort strategy that can be achieved for a double-storey house in the tropical climate of Malaysia. The first passive cooling strategy was decreasing the direct solar radiation that enters the house from the windows, which was achieved by adding shading devices over the windows and closing the curtains inside the rooms. The second passive cooling strategy examined different construction materials, timber for walls and floors and clay tiles for the roof. The third passive cooling strategy was changing the orientation of the house by examining seven orientations and comparing them with reference cases. All these simulations were tested for full-day natural ventilation and without any ventilation. The thermal comfort of these strategies was defined based on the operative temperature.

Under full-day natural ventilation, the study revealed that adding external shading devices to the windows could decrease the operative temperature inside the three rooms. Moreover, using timber for walls or combining it with clay tiles for the roof was not effective during the daytime; however, the indoor operative temperature was decreased during night-time and early morning when there is no solar insolation. Changing the orientation of the building did not give any significant difference in the indoor operative temperature compared with the reference case when full-day ventilation was applied.

Under conditions without ventilation, the study revealed that adding external shading devices and closing the curtains inside the rooms had the lowest operative temperature compared to other examined strategies. On the other hand, using timber for walls or combining it with clay tiles for the roof was ineffective during the daytime. At the same time, it could decrease the indoor operative temperature during night-time and early morning. Similar to full-day ventilation, no significant difference was noticed in the indoor operative temperature when changing the orientation of the building when all the openings were closed.

Comparing full-day natural ventilation and without any ventilation, the study reveals that protecting the windows from solar radiation by adding external shading devices (when full-day ventilation was applied) and combining them with closing the curtains inside the rooms (when no ventilation was applied) had the lowest indoor operative temperature compared to other examined strategies. The results also showed that using timber for walls and clay tiles for the roof was ineffective during the daytime.

In addition, changing the orientation of the house was not a good suggestion in the case of this building, as no significant decrement happened in the operative temperature inside the three rooms of the house. Nevertheless, it is recommended to examine changing the orientation of the house while removing the windows from the long facades of the house and using other shading strategies, such as using vertical green walls. A further study is

required to investigate the effect of orientation on indoor thermal comfort while avoiding exposure to all the fourth directions.

## ACKNOWLEDGEMENT

The authors want to acknowledge the Ministry of Education, Malaysia, for their support through the Fundamental Research Grant Scheme (FRGS/1/2020/TK0/UKM/02/26—Roof Design in Controlling Mosque's Indoor Thermal Comfort). The authors would also like to thank Universiti Kebangsaan Malaysia (UKM) for the support in completing this research, including allowing access to the test building.

## REFERENCES

- Adekunle, T. O., & Nikolopoulou, M. (2016). Thermal comfort, summertime temperatures and overheating in prefabricated timber housing. *Building and Environment*, *103*, 21-35. <https://doi.org/10.1016/j.buildenv.2016.04.001>
- Amir, A., Mohamed, M. F., Sulaiman, M., & Yusoff, W. F. M. (2019). Assessment of indoor thermal condition of a low-cost single story detached house: A case study in Malaysia. *Alam Cipta*, *12*(1), 80-88.
- ASHRAE. (2009). *ASHRAE handbook of fundamentals*. American Society of Heating, Refrigerating and Airconditioning Engineers. <https://www.pdfdrive.com/2009-ashrae-handbook-fundamentals-si-edition-e169690158.html>
- ASHRAE. (2010). *Standard 55-2010: Thermal environmental conditions for human occupancy*. American Society of heating, Refrigerating and Airconditioning Engineers. [https://www.techstreet.com/ashrae/standards/ashrae-55-2010?product\\_id=1741646](https://www.techstreet.com/ashrae/standards/ashrae-55-2010?product_id=1741646)
- ASHRAE. (2017). *Standard 55-2017: Thermal environmental conditions for human occupancy*. American Society of Heating, Refrigerating and Airconditioning Engineers. [https://www.techstreet.com/ashrae/standards/ashrae-55-2017?gateway\\_code=ashrae&product\\_id=1994974](https://www.techstreet.com/ashrae/standards/ashrae-55-2017?gateway_code=ashrae&product_id=1994974)
- Basri, S., Zakaria, S., & Kamarudina, S. K. J. J. K. (2021). Review on alternative energy education in Malaysia. *Jurnal Kejuruteraan*, *33*(3), 461-472. [https://doi.org/10.17576/jkukm-2021-33\(3\)-08](https://doi.org/10.17576/jkukm-2021-33(3)-08)
- Bhikhoo, N., Hashemi, A., & Cruickshank, H. (2017). Improving thermal comfort of low-income housing in Thailand through passive design strategies. *Sustainability*, *9*(8), Article 1440. <https://doi.org/10.3390/su9081440>
- Bragger, G., & de Dear, R. (2000). *A standard for natural ventilation*. Center for the Built Environment.
- Dong, Y., Cui, X., Yin, X., Chen, Y., & Guo, H. J. A. S. (2019). Assessment of energy saving potential by replacing conventional materials by cross laminated timber (CLT) - A case study of office buildings in China. *Applied Sciences*, *9*(5), Article 858. <https://doi.org/10.3390/app9050858>
- Gamero-Salinas, J., Monge-Barrio, A., Kishnani, N., López-Fidalgo, J., & Sánchez-Ostiz, A. (2021). Passive cooling design strategies as adaptation measures for lowering the indoor overheating risk in tropical climates. *Energy and Buildings*, *252*, Article 111417. <https://doi.org/10.1016/j.enbuild.2021.111417>

- Huang, L., & Kang, J. (2021). Thermal comfort in winter incorporating solar radiation effects at high altitudes and performance of improved passive solar design - Case of Lhasa. In *Building Simulation* (Vol. 14, No. 6, pp. 1633-1650). Tsinghua University Press.
- Husen, N. A., & Mohamed, M. F. (2021). Comparison of green design strategies in five traditional malay houses. *Jurnal Kejuruteraan*, 33(1), 47-53.
- Imran, H. M., Kala, J., Ng, A., & Muthukumaran, S. (2018). Effectiveness of green and cool roofs in mitigating urban heat island effects during a heatwave event in the city of Melbourne in southeast Australia. *Journal of Cleaner Production*, 197, 393-405. <https://doi.org/10.1016/j.jclepro.2018.06.179>
- Kamal, M. A. (2010). A study on shading of buildings as a preventive measure for passive cooling and energy conservation in buildings. *International Journal of Civil Environmental Engineering*, 10(6), 19-22.
- Khavari, A. M., Pei, S., & Tabares-Velasco, P. C. (2016). Energy consumption analysis of multistory cross-laminated timber residential buildings: A comparative study. *Journal of Architectural Engineering*, 22(2), Article 04016002.
- Kildsgaard, I., Jarnehammar, A., Widheden, A., & Wall, M. (2013). Energy and environmental performance of multi-story apartment buildings built in timber construction using passive house principles. *Buildings*, 3(1), 258-277. <https://doi.org/10.3390/buildings3010258>
- Kim, M., Leigh, S. B., Kim, T., & Cho, S. (2015). A study on external shading devices for reducing cooling loads and improving daylighting in office buildings. *Journal of Asian Architecture and Building Engineering*, 14(3), 687-694. <https://doi.org/10.3130/jaabe.14.687>
- Kim, S. H., Shin, K. J., Kim, H. J., & Cho, Y. H. (2017). A study on the effectiveness of the horizontal shading device installation for passive control of buildings in South Korea. *International Journal of Polymer Science*, 2017, Article 3025092. <https://doi.org/10.1155/2017/3025092>
- Kubota, T., Chyee, D. T. H., & Ahmad, S. (2009). The effects of night ventilation technique on indoor thermal environment for residential buildings in hot-humid climate of Malaysia. *Energy and Buildings*, 41(8), 829-839. <https://doi.org/10.1016/j.enbuild.2009.03.008>
- Kubota, T., Toe, D. H. C., & Ossen, D. R. (2014). Field investigation of indoor thermal environments in traditional Chinese shophouses with courtyards in Malacca. *Journal of Asian Architecture and Building Engineering*, 13(1), 247-254. <https://doi.org/10.3130/jaabe.13.247>
- Latif, S. N. A., Chiong, M. S., Rajoo, S., Takada, A., Chun, Y. Y., Tahara, K., & Ikegami, Y. J. E. (2021). The trend and status of energy resources and greenhouse gas emissions in the Malaysia power generation mix. *Energies*, 14(8), Article 2200. <https://doi.org/10.3390/en14082200>
- Mirrahimi, S., Mohamed, M. F., Haw, L. C., Ibrahim, N. L. N., Yusoff, W. F. M., Aflaki, A. (2016). The effect of building envelope on the thermal comfort and energy saving for high-rise buildings in hot-humid climate. *Renewable and Sustainable Energy Reviews*, 53, 1508-1519. <https://doi.org/10.1016/j.rser.2015.09.055>
- MMD. (2017). *General climate of Malaysia*. Malaysia Meteorological Department. <http://www.met.gov.my/en/web/metmalaysia/home>



- Mohamed, M. F. (2020). Sustainable design approaches in Malaysia's traditional mosques and houses. In *Proceeding International Conference on Engineering* (Vol. 1, No. 1, pp. 13-21). Tunas Pembangunan SurakartaUniversity. <https://doi.org/10.36728/icone.v1i1.1263>
- Olawale-Johnson, O. P., Ajwang, P., & Ondimu, S. N. (2021). Reducing cooling demands in Sub-Saharan Africa: A study on the thermal performance of passive cooling methods in enclosed spaces. *Journal of Sustainable Development of Energy, Water and Environment Systems*, 9(4), 1-13. <https://doi.org/10.13044/j.sdewes.d7.0313>
- Oleiwi, M. Q. (2020). *Thermal comfort of residential buildings using industrialised building system through natural ventilation in hot and humid climate of Malaysia* [Doctoral thesis, Universiti Kebangsaan Malaysia, Malaysia]
- Oleiwi, M. Q., & Mohamed, M. F. (2021). An investigation on indoor temperature of modern double storey house with adapted common passive design strategies of Malay Traditional House. *Pertanika Journal of Science Technology*, 29(2). 1135-1157. <https://doi.org/10.47836/pjst.29.2.24>
- Oleiwi, M. Q., Mohamed, M. F., Sulaiman, M. K. A. M., Che-Ani, A. I., & Raman, S. N. (2019). Thermal environment accuracy investigation of integrated environmental solutions-virtual environment (IES-VE) software for double-story house simulation in Malaysia. *Journal of Engineering and Applied Sciences*, 14(11), 3659-3665. <https://doi.org/10.36478/JEASCI.2019.3659.3665>
- Prieto, A., Knaack, U., Auer, T., & Klein, T. (2018). Passive cooling & climate responsive façade design exploring the limits of passive cooling strategies to improve the performance of commercial buildings in warm climates. *Energy and Buildings*, 175, 30-47. <https://doi.org/10.1016/j.enbuild.2018.06.016>
- Rana, M. J., Hasan, M. R., & Sobuz, M. H. R. (2021). *An investigation on the impact of shading devices on energy consumption of commercial buildings in the contexts of subtropical climate*. Emerald Publishing Limited. <https://doi.org/10.1108/SASBE-09-2020-0131>
- Santamouris, M. (2016). Cooling the buildings - Past, present and future. *Energy and Buildings*, 128, 617-638. <https://doi.org/10.1016/j.enbuild.2016.07.034>
- SEforALL. (2020). *Chilling prospects: Tracking sustainable cooling for all - 2020*. <https://www.seforall.org/system/files/2020-07/CP-2020-SEforALL.pdf>
- Shafique, M., & Kim, R. (2017). Application of green blue roof to mitigate heat island phenomena and resilient to climate change in urban areas: A case study from Seoul, Korea. *Journal of Water and Land Development*, 33(1), 165-170. <https://doi.org/10.1515/jwld-2017-0032>
- Sulaiman, M. K. A. M. (2017). *Cooling effect performance of indirect green facade on building in tropical climate of Malaysia* (Doctor of philosophy). Universiti Kebangsaan Malaysia, Malaysia.
- Taleb, H. M. (2014). Using passive cooling strategies to improve thermal performance and reduce energy consumption of residential buildings in UAE buildings. *Frontiers of Architectural Research*, 3(2), 154-165. <https://doi.org/10.1016/j.foar.2014.01.002>
- Tang, C. K., & Chin, N. (2013). *Building energy efficiency technical guideline for passive design*. Public Works Department Malaysia. <http://www.mgbc.org.my/bseep-building-energy-efficiency-technical-guideline-for-passive-design/>

- Yeganeh, M. (2020). Conceptual and theoretical model of integrity between buildings and city. *Sustainable Cities and Society*, 59, Article 102205. <https://doi.org/10.1016/j.scs.2020.102205>
- Yusoff, W. F. M. (2020). The effects of various opening sizes and configurations to air flow dispersion and velocity in cross-ventilated building. *Jurnal Teknologi*, 82(4), 17-28. <https://doi.org/10.11113/jt.v82.14537>
- Yusoff, W. F. M., & Mohamed, M. F. (2017). *Building energy efficiency in hot and humid climate*. Elsevier.
- Yusoff, W. F. M., & Ja'afar, N. H. (2019). Preliminary evaluation of indoor thermal comfort in Malaysia heritage mosque. In *MATEC Web of Conferences* (Vol. 277, p. 02016). EDP Sciences Publishing.

## Study of Metabolic Flux Distribution in Rice (*Oryza sativa*) Cultures for Starch Production

Nur Aqila Syafiqa Abdul Nuri<sup>1</sup>, Noor Illi Mohamad Puad<sup>1\*</sup>, Muhammad Yusuf Abduh<sup>2</sup> and Azlin Suhaida Azmi<sup>1</sup>

<sup>1</sup>Department of Chemical Engineering and Sustainability, Kulliyah of Engineering, International Islamic University Malaysia, P.O. Box 01, 50728, Kuala Lumpur, Malaysia

<sup>2</sup>School of Life Sciences and Technology, Institut Teknologi Bandung, Jalan Ganesha, No. 10, Bandung, 40132 Indonesia

### ABSTRACT

The demand for starch-rich crops remains high due to their wide applications, and one of them is rice (*Oryza sativa*). However, large-scale rice production faces challenges such as unstable productivity, climate changes and excessive use of agrochemicals. Plant cell culture technology is proposed to increase rice yield and produce a drought-resistance variety of rice to sustain its demand. However, the amount of starch in rice cultures is expected to be smaller compared to the planted ones. The main aim of this study is to apply Flux Balance Analysis (FBA) to optimize starch production in rice cultures. This study reconstructed the stoichiometric metabolic model for rice culture based on the published articles. It consists of 160 reactions and 148 metabolites representing rice's main carbon metabolism towards starch production. The model was then formulated in GAMS v31.1.0, and the objective function was set to the maximization of biomass and starch. The selected constraints (sugar uptake rates and cell growth rates) from previous studies were utilized. The simulated starch production rate values were achieved at the highest glucose uptake rates with the value of 0.0544 mol/g CDW.h. The internal metabolic flux distributions demonstrated that the incoming carbon fixes were directed towards the glycolysis pathway, TCA cycle, PPP cycle, and starch biosynthesis reactions. The study results serve as a starting point to further understanding the starch production mechanism in plants known to be complex.

#### ARTICLE INFO

##### Article history:

Received: 25 February 2022

Accepted: 24 May 2022

Published: 19 August 2022

DOI: <https://doi.org/10.47836/pjst.31.1.07>

##### E-mail addresses:

[nuraqilasafiq@gmail.com](mailto:nuraqilasafiq@gmail.com) (Nur Aqila Syafiqa Abdul Nuri)

[illi@iiium.edu.my](mailto:illi@iiium.edu.my) (Noor Illi Mohammad Puad)

[yusuf@sith.itb.ac.id](mailto:yusuf@sith.itb.ac.id) (Muhammad Yusuf Abduh)

[azlinsu76@iiium.edu.my](mailto:azlinsu76@iiium.edu.my) (Azlin Suhaida Azmi)

\* Corresponding author

**Keywords:** FBA, General Algebraic Modeling System (GAMS) software, metabolic flux distribution, rice, starch

## INTRODUCTION

People have utilized starchy materials derived from seeds, roots, and tubers in the past and even today for various purposes. Rice (*Oryza sativa*), the commonly cultivated rice species, is one of the prominent sources of starch used as a source of human food, feed for livestock, and raw materials for chemical, food, and pharmaceutical industries. The most abundant component in rice is carbohydrates consisting of approximately 80% of starch (Marco et al., 2008). Starch is a natural biopolymer consisting of amylose and amylopectin, the polymer type of glucose. The proportions of amylose and amylopectin in rice differ depending on the rice's variety, and these proportions determine the physical properties and functionality of the rice. It has been approximated that the amount of amylose and amylopectin in the rice starch is 15–20% and 80–85%, respectively (Shu et al., 2007).

With the growing demand for rice, many initiatives focus on plant tissue culture to stabilize the demand with the infeasibility of large-scale production, which require several thousand hectares of arable land. Plant tissue culture is known for its ability to produce plants with a higher yield and its flexibility to cultivate the plant *in vitro*, which contributes to overcoming the biotic and abiotic factors affecting the growth of intact plants in the environment. Therefore, many cultures have been used to produce many plants, including rice itself. However, it is expected that the starch content in the plant culture of rice is lesser than the real plant. It is because plant tissue culture involves the growth of a cell, not a whole plant, and certain enzymes or genes may not exist to support starch production.

Flux Balance Analysis (FBA) is a method of metabolic modeling that utilizes a constraint-based approach. The prediction of flux distribution in a metabolic network can be achieved by using this method through maximization and minimization of an objective function through the utilization of experimental data to validate the model predictions (Orth et al., 2010). Through FBA, knowledge about the system's metabolic concentrations and enzyme kinetics is not required as it merely relies on stoichiometric characteristics. Additionally, the assumption of the steady-state system in FBA removes the need to determine rate laws and kinetic parameters, which are commonly difficult to identify (Raman & Chandra, 2009). However, reports on FBA on starch production are still scarce as most studies on FBA focus on optimizing biomass production. Therefore, this study aimed to utilize FBA to optimize starch production in rice plant cell cultures by observing its flux distributions in the constructed metabolic pathway network using GAMS 33.1.0 software.

## METHODS AND MATERIALS

### System Definition

Metabolic networks for rice (*Oryza sativa*) were reconstructed in matrix form by modifying the primary metabolism pathways in Puad (2011), focusing only on the starch metabolism.

The modification was done based on literature reading (Shaw & Kundu, 2015; Zeeman et al., 2010).

### Development of Mass Balance for Each Metabolite

After identifying all metabolites involved in the starch synthesis, mass balances containing all reactions were developed. Mass balances were described using a stoichiometric matrix,  $S$ , and the flux matrix,  $v$ . The stoichiometric representation for each reaction in the form of a numerical matrix, is as shown in Equation 1. Metabolites produced have a positive sign, and the metabolites consumed will have a negative sign.

$$S \cdot v = 0 \quad (1)$$

The assumption in this model was steady-state metabolic flux to ensure the metabolic concentrations remain constant; thus, each metabolite has one linear equation equal to zero (Orth et al., 2010).

### Defining Constraints

Typically, in FBA, there will be more reactions or specific unknown fluxes than the metabolites. Thus, the steady-state solution for the metabolic fluxes is underdetermined. Furthermore, it leads to complexity in the metabolic network, increasing the number of unknown fluxes. Thus, additional constraints are required to ensure a realistic flux distribution can be predicted in FBA (Lularevic et al., 2019). In this study, the experimental constraint was sugar uptake rate by rice cell cultures, while biomass composition was used for biological constraint.

Biomass composition is described in terms of macromolecular components of cells, and the composition is varied for different species, which mainly depends on the growth conditions and environment (Carnicer et al., 2009; Hanegraaf & Muller, 2001). The macromolecular composition of cells can be divided into seven components which are: (1) RNA; (2) DNA; (3) proteins; (4) phospholipids; (5) fatty acids; (6) carbohydrates; (7) starch. Although starch is a polymeric carbohydrate, it is categorized as a storage polysaccharide in the reconstructed metabolic model. At the same time, primary cell wall components (cellulose, hemicellulose, and pectin) contribute to the carbohydrate percentage of 1 g of the cell (Table 1). Due to limited information on 1 g of rice macromolecular cell composition, this model used the macromolecular composition of plant cells collated from different plant types, as summarized in Table 1.

The experimental data for sugar uptake rates were obtained from the initiation of rice cell suspension culture reported in the previous study (Lakshmanan et al., 2013). The rice suspension cultures were established from calli induced by rice seed on an amino acid callus induction medium containing 2,4-dichlorophenoxyacetic acid (2 mg/L), sucrose (30 g/L),

Table 1  
Molecular composition of different plant cells for applications in this model

Macromolecules	gg <sup>-1</sup> cell DW	% of g cell DW	Plant cells	References
RNA	0.03	3	<i>Arabidopsis thaliana</i>	(Poolman et al., 2009)
DNA	0.03	3	<i>Arabidopsis thaliana</i>	(Poolman et al., 2009)
Proteins	0.042	4.2	Rice	(Amthor, 2000)
Phospholipid	0.027	2.7	<i>Catharanthus roseus</i>	(Toivonen et al., 1992)
Fatty acids	0.014	1.4	Rice	(Amthor, 2000)
Carbohydrates	0.55	52	Rice	(Amthor, 2000)
Starch	0.307	33.7	Rice	(Amthor, 2000)

and Gelrite (2 g/L) for two months. The cultures were incubated at 28°C and 120 rpm in a gyratory shaking incubator. Experiments were carried out in 100-mL Erlenmeyer flasks with 30 mL of medium (Lakshmanan et al., 2013). These experimental data are required as the constraints to determine the intracellular flux distribution during the optimization of starch production in rice (Table 2). The data were taken at the stationary phase, from 144 h to 336 h due to sugar uptake rates at these points. In relation to that, these points are required to be fed separately into the model to observe if there is any significant impact on the objective function upon the change in the specific growth rate of rice cultures at different times of the growth curve.

Table 2  
Calculated experimental specific rates for cell suspension culture of rice from a previous study (Lakshmanan et al., 2013) that were used as the constraints for FBA in this study

Time (h)	Specific growth rate, $\mu_{\text{experimental}}$ (h <sup>-1</sup> )	Specific sucrose uptake rate, $q_s$ (mmole sugar per gDW.h)	Specific glucose uptake rate, $q_G$ (mmole sugar per gDW.h)	Specific fructose uptake rate, $q_F$ (mmole sugar per gDW.h)
48	0.00556	0.0325	0	0
96	0.0114	0.2326	0	0
144	0.0052	0.0609	0.0289	0.0289
192	0.0022	0	0.0122	0
240	0.0038	0	0.0105	0.0210
288	0	0	0.0193	0.0289
336	0	0	0	0.0101

### Optimizing Steps and Simulations in GAMS

Numerous objective functions can be set in GAMS; specifically, in this study, they maximized biomass and starch production rates. By clicking the 'Run' button in GAMS, it executes an output file that lists the fluxes' value upon optimizing the objective function. The values are then presented in a metabolic flux map drawn manually in Microsoft Excel 2019.

## RESULTS AND DISCUSSION

### Reconstruction of Plant Primary Metabolic Pathways for Starch Production

For the development of the stoichiometric metabolic model in this study, plant primary metabolic pathways described by Puad (2011) have been used and reconstructed based on the information collected from various sources such as published articles, books, and websites. Upon reconstruction, the developed stoichiometric model for rice consists of 160 reactions and 148 metabolites. From the stoichiometric models, all mass balances developed for each metabolite were formulated in GAMS v33.1.0. The alteration of the plant's primary pathways involved only the addition of the starch metabolism reactions, which is the main objective of this study. The model is composed of central metabolism networks such as glycolysis, Pentose Phosphate Pathway (PPP), and TCA cycle, where these metabolisms take part mainly in the synthesis of biomass such as fatty acids, starch, protein, carbohydrates, amino acid, and phospholipids (Table 3).

Table 3  
*Number of reactions and metabolic pathways involved in this study*

Name of Pathway	Number of Reactions	Name of Pathway	Number of Reactions
Protein Synthesis	58	RNA Synthesis	1
DNA Synthesis	1	Carbohydrate Synthesis	13
Transport Reactions	13	Central Carbon Metabolism	49
Phospholipid biosynthesis	14	Transhydrogenase reactions	2
Biomass constituent	1	ATP consumption for maintenance	1
Fatty acid biosynthesis	6	Carbamoyl phosphate formation	1

### Optimization of Starch Production in Rice Utilizing FBA with Maximization of Biomass and Starch Production Rate as the Objective Function

As discussed previously, this study utilized the experimental data on the initiation of rice cell suspension (Lakshmanan et al., 2013) to simulate the starch production mechanism compared to other types of tissue culture due to the condition for the initiation of the culture itself. A liquid culture system such as cell suspension culture provides a better approach for plant tissue culture processes such as micropropagation and regeneration. Continuous shaking during incubation serves good aeration, oxygen, and nutrient availability. Furthermore, it demonstrates that cells in suspension culture have better contact and a large surface area of the cells directly exposed to the supplied liquid medium. Sucrose uptake rates, glucose uptake rates and fructose uptake rates from Lakshmanan et al. (2013) were fed into the model as the experimental constraints to simulate the starch production mechanism. Since there is a lack of data for other components such as oxygen consumption,

nitrate uptake rates and sulfate uptake rates, they were left as free variables, which GAMS itself determine.

Based on the simulation results, with different objective functions being implemented, the flux distributions were still the same in both cases. Starch is expected to be part of biomass composition (Table 1). The highest values of biomass (0.0135 mmol/g CDW.h) and starch production (0.0041 mmol/g CDW.h) were obtained at 144 h (Day 6) of growth which is during the exponential phase. During this growth period, sugar uptake rates, specifically glucose uptake rates, are at the highest value, which explains the highest value of starch production attained on that day. It is due to the reason that the starch structure is made of a chain of glucosyl compounds as starch is produced from sugars. During photosynthesis, plants will convert light energy into either chemical energy or sugar; this sugar will then either be stored in the form of starch or utilized for respiration and growth. It is reflected in a report where the starch content in callus culture is correlated with the glucose content (Lee & Huang, 2013).

Figure 1 shows the distribution of fluxes in rice cultures for starch and biomass production optimization, where the yellow-colored value shows that no flux was present and the green colored shows the presence of flux. The incoming carbon fluxes from glucose and fructose were directed from glycolysis to the TCA cycle, PPP, carbohydrates biosynthesis, and starch biosynthesis. Based on the flux distributions in Figure 1, fructose 6-phosphate (F6P) is converted to glucose 6-phosphate (G6P) and then glucose 1-phosphate G1P before ADPglucose, which is the precursor to initiating starch biosynthesis, which agrees with Pfister & Zeeman (2016).

Shaw and Kundu (2015) have developed a model for rice leaf metabolism where they emphasized the flux distribution for high and low starch production in the central carbon metabolism. In their study, the maximum and minimum value of starch was obtained using biomass optimization criteria, while in this study, it is for the maximization of starch production. Compared to what was developed in this study, the starch produced is still low compared to the value of starch produced in Shaw and Kundu (2015). It is expected because this study involved the distribution of fluxes in plant cell culture, which is not the whole plant.

Additionally, through the comparison of flux distribution for minimum and maximum starch production, Shaw and Kundu (2015) also mentioned that in the case of maximum starch production, a major fraction of glyceraldehyde 3-phosphate (GL3P) is converted to G6P to overproduce starch, and in the case of minimum starch production, GL3P is converted mostly to 3-phosphoglyceraldehyde (PG3) instead of G6P. G6P is a precursor for G1P production, which is the precursor for ADPglucose production. In contrast with this study, the reaction for the conversion of GL3P to PG3 is active, and there is a lack of reaction for the conversion of GL3P to G6P. Furthermore, our model did not include the





**Table 4**  
*Carbon flux distribution during growth and starch optimization of cell suspension culture of rice*

Time (h)	144	192	240	288	312
$\mu_{\text{experimental}}$ (h <sup>-1</sup> )	0.0052	0.0022	0.0038	0	0
$\mu_{\text{optimized}}$ (h <sup>-1</sup> )	0.0135	0.0028	0.0074	0.0035	0.0007
Total incoming carbon flux (mmole/g CDW h)	0.3468	0.0732	0.189	0.2892	0.0606
Carbon channeled into biomass (%)	84.4143	84.4143	84.4143	84.4143	84.4143
Carbon diverted to PPP (%)	3.2371	3.2371	3.2371	3.2371	3.2371
Carbon diverted to TCA cycle (%)	12.3487	12.3487	12.3487	12.3487	12.3487

Nonetheless, the overall flux distribution did not change significantly from one point of time to another (Table 4), which perhaps indicates that more constraints should be fed into the program, such as specific uptake rates for other nutrients and oxygen consumption, to see the variations in the carbon flux partitioning during the cell growth.

### Specific Nutrient Uptake Rates

Nutrients are supplemented to the plants to ensure good growth and development. It is because the plant that lacks nutrients will not be able to complete its life cycle. For example, a seed may not be able to germinate, and a plant may not be able to develop roots and flowers properly. Moreover, the plant itself will often die upon the unavailability of nutrients. However, an excess amount of nutrients could also cause harm to plants. Thus, nutrient uptakes should be optimized to ensure the good growth of the plant. Besides, a higher biomass formation rate where starch is a part of it will result in a higher uptake rate of nutrients, which makes investigating the nutrient uptake rates important. In relation to that, different types of plants would have different nutrient uptake rates (Tony & McFarland, 2021).

In this study, due to the lack of experimental data on the specific uptake rates for ammonium, nitrate, phosphate, and sulfate, they were set as a free variable which GAMS determined upon optimization. It was observed that cells took up ammonium at the highest rate, followed by phosphate and sulfate (Table 5). It is correlated with a previous study on nutrient uptake in which rice took up nitrogen sources in different forms with ammonium at the highest rate, followed by phosphate (Masni & Wasli, 2019). Apart from that, the planted paddy preferred ammonium rather than nitrate as its main nitrogen source (Wang et al., 1993). Nitrogen is an essential macronutrient for

**Table 5**  
*Fluxes for the inorganic nutrient uptake in cell suspension culture of rice at 144 h of growth*

Nutrient	Flux (mmole/g DW.h)
Ammonium	0.0128
Phosphate	0.0008
Sulfate	0.0002
Nitrate	0

the good growth of rice-cultivar as it increases plant height, panicle number, leaf size, spikelet number, and the number of filled spikelets, which largely determine the yield capacity of rice plant.

### Sensitivity Analysis

In GAMS software, the marginal value of the intermediate metabolites and metabolic fluxes can be determined where it is information about the sensitivity of the optimal value to a change in the objective function. Specifically, in this study, sensitivity analysis allows the determination of significant metabolites that affect the set objective function in which it is represented in the form of marginal values.

Table 6 lists the metabolites that have the most significant effect on each objective function. Generally, both objective functions are highly affected by fatty acids, but they differ in terms of the amount of the marginal value, where marginal values for biomass maximization are higher than starch maximization. It is because starch is a part of biomass composition. Thus, when biomass maximization was set as the objective function, it meant maximization for all components of the biomass, not for the starch alone. Furthermore, although the composition of fatty acids in biomass (Table 1) is low, in the biosynthesis of 1 g fatty acids, 39 mmoles ATP, 44 mmoles AcCoA, and 72 mmoles of NADPH (based on the reconstructed stoichiometric metabolic model) are used which indicate that the energy intensiveness of fatty acids biosynthesis draining these precious resources for a small part of biomass formation (Puad, 2011).

Table 6  
*Sensitivity of the biomass and starch production rate for changes in various metabolites in terms of marginal values*

Metabolite name	Marginal values (Biomass maximization as an objective function)	Marginal values (Starch maximization as an objective function)
Facids	-3.4322	-1.0537
Protein	-1.7020	-0.52257
Chydr	-1.5048	-0.4620
Stearic acid (C180)	-1.0081	-0.3095
Biomass (SS)	-1.0000	-

### CONCLUSION

To conclude, the metabolic model proposed in this study can give exposure to the starch production mechanism in the plant cell culture even though the starch production predicted in this study is still considered to be lower compared to the whole plant. Nevertheless, it has been identified that the sugar uptake rates, specifically glucose, have a major impact on the starch production rate. Thus, it could be proposed that a high glucose uptake rate could contribute to high starch production. Due to that, in terms of the formulation of

the media, higher sugar concentrations should be supplied to achieve a high amount of starch production. However, the limitation of the amount of sugar that should be supplied requires further experimentation. Furthermore, additional constraints other than sugar uptake rates could give a different result because this study only relies on it as a constraint. Therefore, based this study's findings, further improvements should be made to develop a better model for the rice cultures, specifically in terms of the experimental data and the metabolic pathways. Lastly, supposed validation of the FBA results could be done through experimentation. In that case, the simulated results could be applied to the metabolic engineering of the plant to enhance starch production and even explain the interactions between pathways.

## ACKNOWLEDGEMENTS

The authors are grateful to the management of International Islamic University Malaysia for a research fund (RMCG20-018-0018) for this work. Department of Chemical Engineering and Sustainability, Kulliyah of Engineering, IIUM, for providing the laboratory facilities to conduct this study.

## REFERENCES

- Amthor, J. S. (2000). The McCree–de Wit–Penning de Vries–Thornley respiration paradigms: 30 years later. *Annals of Botany*, *86*(1), 1-20.
- Carnicer, M., Baumann, K., Töplitz, I., Sánchez-Ferrando, F., Mattanovich, D., Ferrer, P., & Albiol, J. (2009). Macromolecular and elemental composition analysis and extracellular metabolite balances of *Pichia pastoris* growing at different oxygen levels. *Microbial Cell Factories*, *8*, 1-14. <https://doi.org/10.1186/1475-2859-8-65>
- Hanegraaf, P. P. F., & Muller, E. B. (2001). The dynamics of the macromolecular composition of biomass. *Journal of Theoretical Biology*, *212*(2), 237-251. <https://doi.org/10.1006/jtbi.2001.2369>
- Lakshmanan, M., Zhang, Z., Mohanty, B., Kwon, J. Y., Choi, H. Y., Nam, H. J., Kim, D. Il, & Lee, D. Y. (2013). Elucidating rice cell metabolism under flooding and drought stresses using flux-based modeling and analysis. *Plant Physiology*, *162*(4), 2140-2150. <https://doi.org/10.1104/pp.113.220178>
- Lee, S. T., & Huang, W. L. (2013). Cytokinin, auxin, and abscisic acid affects sucrose metabolism conduce to *de novo* shoot organogenesis in rice (*Oryza sativa* L.) callus. *Botanical Studies*, *54*(1), 1-11. <https://doi.org/10.1186/1999-3110-54-5>
- Lularevic, M., Racher, A. J., Jaques, C., & Kiparissides, A. (2019). Improving the accuracy of flux balance analysis through the implementation of carbon availability constraints for intracellular reactions. *Biotechnology and Bioengineering*, *116*(9), 2339-2352. <https://doi.org/10.1002/bit.27025>
- Marco, C., Pérez, G., León, A. E., & Rosell, C. M. (2008). Effect of transglutaminase on protein electrophoretic pattern of rice, soybean, and rice-soybean blends. *Cereal Chemistry*, *85*(1), 59-64. <https://doi.org/10.1094/CCHEM-85-1-0059>

- Masni, Z., & Wasli, M. E. (2019). Yield performance and nutrient uptake of red rice variety (MRM 16) at different NPK fertilizer rates. *International Journal of Agronomy*, 2019, Article 5134358. <https://doi.org/10.1155/2019/5134358>
- Orth, J. D., Thiele, I., & Palsson, B. O. (2010). What is flux balance analysis? *Nature Biotechnology*, 28(3), 245-248. <https://doi.org/10.1038/nbt.1614>
- Pfister, B., & Zeeman, S. C. (2016). Formation of starch in plant cells. *Cellular and Molecular Life Sciences*, 73(14), 2781-2807. <https://doi.org/10.1007/s00018-016-2250-x>
- Poolman, M. G., Miguet, L., Sweetlove, L. J., & Fell, D. A. (2009). A genome-scale metabolic model of Arabidopsis and some of its properties. *Plant Physiology*, 151(3), 1570-1581. <https://doi.org/10.1104/pp.109.141267>
- Puad, N. (2011). *Modelling the Metabolism of Plant Cell Culture (Arabidopsis)* (PhD thesis). The University of Manchester, UK.
- Raman, K., & Chandra, N. (2009). Flux balance analysis of biological systems: Applications and challenges. *Briefings in Bioinformatics*, 10(4), 435-449. <https://doi.org/10.1093/bib/bbp011>
- Shaw, R., & Kundu, S. (2015). Flux balance analysis of genome-scale metabolic model of rice (*Oryza sativa*): Aiming to increase biomass. *Journal of Biosciences*, 40(4), 819-828. <https://doi.org/10.1007/s12038-015-9563-z>
- Shu, X., Jia, L., Gao, J., Song, Y., Zhao, H., Nakamura, Y., & Wu, D. (2007). The influences of chain length of amylopectin on resistant starch in rice (*Oryza sativa* L.). *Starch/Staerke*, 59(10), 504-509. <https://doi.org/10.1002/star.200700640>
- Toivonen, L., Laakso, S., & Rosenqvist, H. (1992). The effect of temperature on hairy root cultures of *Catharanthus roseus*: Growth, indole alkaloid accumulation and membrane lipid composition. *Plant Cell Reports*, 11(8), 395-399. <https://doi.org/10.1007/BF00234368>
- Tony, L. P. A., & McFarland, L. M. (2021). *Essential nutrients for plants - How do nutrients affect plant growth?* Texas A&M Agrilife Extension. <https://agrilifeextension.tamu.edu/library/gardening/essential-nutrients-for-plants/>
- Wang, M. Y., Siddiqi, M. Y., Ruth, T. J., & Glass, A. D. (1993). Ammonium uptake by rice roots (II. Kinetics of  $^{13}\text{NH}_4^+$  influx across the plasmalemma). *Plant Physiology*, 103(4), 1259-1267. <https://doi.org/10.1104/pp.103.4.1259>
- Zeeman, S. C., Kossmann, J., & Smith, A. M. (2010). Starch: Its metabolism, evolution, and biotechnological modification in plants. *Annual Review of Plant Biology*, 61, 209-234. <https://doi.org/10.1146/annurev-arplant-042809-112301>

## ABBREVIATIONS

Ac	Acetate	GMP	Guanosine monophosphate
Ade	Adenosine	GTP	Guanosine triphosphate
ADP	Adenosine 5'-diphosphate	H <sub>2</sub> S	Hydrogen sulfide
Ala	L-Alanine	Hcellulose	Hemicellulose
AMP	Adenosine monophosphate	Hcys	Homocysteine
Arg	L-Arginine	His	Histidine
Asn	L-Asparagine	HSer	Homoserine
Asp	L-Aspartate	ICit	Isocitrate
ASPSA	Aspartate Semialdehyde	IGP	Indoleglycerolphosphate
C160	Palmitic acid	Ile	L-Isoleucine
C181	Oleic acid	ISMP	Inosinic acid (inosine monophosphate)
C182	Linoleic acid	Ino	Inosol
C183	Linolenic acid	KG	a-Ketoglutarate
CaP	Carbamoyl phosphate	Kval	Ketoisovalarate
CDP	Cytidine diphosphate	Leu	Leucine
CDPDG	CDP-diacylglycerol	Lys	Lysine
Chor	Chorismate	Mal	Malate
Cit	Citrate	Met	Methionine
Citr	Citrulline	MeTHF	N <sup>5</sup> -N <sup>10</sup> -methyl-THF
CL	Cardiolipin	MetTHF	N <sup>5</sup> -N <sup>10</sup> -methylene-THF
CMP	Cytidine monophosphate	MGDG	Monogalactosyl diacylglycerol
CO <sub>2</sub>	Carbon dioxide	MTHF	N <sup>5</sup> -methyl-THF
CO <sub>2</sub> _exp	Exported carbon dioxide	MTR	methylthioribose
CTP	Cytidine triphosphate	NAD_plus	Nicotineamide-adeninenucleotide
Cys	L-cysteine	NADH	Nicotineamide-adeninenucleotide (reduced)
dADP	deoxy-adenosine diphosphate	NADHm	Nicotineamide-adeninenucleotide mitochondrion (reduced)
dCDP	deoxy-cytidine diphosphate	NADP_plus	Nicotineamide-adeninenucleotide phosphate
DG	diacylglycerol	NH <sub>3</sub> _imp	Imported ammonium
DGDG	digalactosyl diacylglycerols	NH <sub>3</sub>	Ammonium
dGDP	deoxy-guanosine diphosphate	NO <sub>3</sub> _imp	Imported nitrate
DHAP	dihydroxyacetone phosphate	NO <sub>3</sub>	Imported nitrate
DHF	7,8 Dihydrofolate	OA	Oxaloacetate
dTMP	deoxy-thymidine monophosphate	OBJECTIVE	Objective function
E4P	Erythrose 4-phosphate	Orn	Ornithine
Ethn	Ethanol	Oxy_imp	Imported oxygen
Ethn_exp	Exported ethanol	Oxy	Oxygen
F10THF	N <sup>10</sup> -Formyl-THF	PA	Phosphatidic acid
FbP	Fructose 1,6-biphosphate	PC	Phosphatidylcholine
FADH <sub>2</sub>	Flavine adenine dinucleotide	PE	Phosphatidylethanolamine
Frc_med	Fructose in medium	Pect	Pectin
Frc	Fructose	PEP	Phosphoenolpyruvate
Fum	Fumarate	PG	Phosphoglycol
GDP	Guanosine diphosphate	Phe	L-phenylalanine
GDPGlc	GDP-glucose	Pi_imp	Imported inorganic orthophosphate
Glc_med	Glucose in medium	Pi	Inorganic orthophosphate
Glc	Glucose	PIIno	Phosphatidylinositol
Gln	L-Glutamine	PPi	Inorganic pyrophosphate
Glox	Gloxylate	PRAIC	5'-Phosphoribosyl-5-amino-4-imidazole carboxamide
Glu	L-Glutamate		
Gly	Glycine		
Gly3P	Glycerol-3-phosphate		

Flux Distribution in Rice Cultures for Starch Production

Pro	L-Proline
PRPP	5-Phosphoribosyl-pyrophosphate
PS	Phosphatidylserine
Pyr	Pyruvate
Ri5P	Ribose 5-phosphate
Ru5P	Ribulose 5-phosphate
S7P	Sedoheptulose 7-phosphate
SAH	S-adenosyl-homocysteine
SAM	S-adenosyl-methionine
Ser	L-serine
SO4	Sulphate
Succ	Succinate
SuccCoA	Succinate Coenzyme A
THF	Tetrahydrofolate
Thr	L-Threonine
Trp	L-Tryptophan
Tyr	L-Tyrosine
UDP	Uridine diphosphate
UDPGal	UDP-Galactose
UDPGlc	UDP-Glucose
UDPGlcA	UDP-Glucuronic acid
UDPXy	UDP-Xylose
UMP	Uridine monophosphate
UTP	Uridine triphosphate
Val	L-Valine
Xyl5P	Xylulose 5-phosphate
Plipids	Phospholipids
dAMP	deoxy-adenosine monophosphate
dCMP	deoxy-cytidine monophosphate
dGMP	deoxy-guanosine monophosphate





## Prediction of Daily Air Pollutants Concentration and Air Pollutant Index Using Machine Learning Approach

Nurul A'isyah Mustakim<sup>1</sup>, Ahmad Zia Ul-Saufie<sup>1\*</sup>, Wan Nur Shaziayani<sup>2</sup>,  
Norazian Mohamad Noor<sup>3</sup> and Sofianita Mutalib<sup>1</sup>

<sup>1</sup>Faculty of Computer and Mathematical Sciences, Universiti Teknologi MARA, 40450 UiTM, Shah Alam, Selangor, Malaysia

<sup>2</sup>Department of Computer and Mathematical Sciences, Universiti Teknologi MARA, Cawangan Pulau Pinang, Permatang Pauh Campus, 13500 UiTM, Permatang Pauh, Penang, Malaysia

<sup>3</sup>Faculty of Civil Engineering Technology, Universiti Malaysia Perlis, Kompleks Pengajian Jejawi 3, 02600 UniMAP, Arau, Perlis, Malaysia

### ABSTRACT

The major air pollutants in Malaysia that contribute to air pollution are carbon monoxide, sulfur dioxide, nitrogen dioxide, ozone, and particulate matter. Predicting the air pollutants concentration can help the government to monitor air quality and provide awareness to the public. Therefore, this study aims to overcome the problem by predicting the air pollutants concentration for the next day. This study focuses on an industrial, the Petaling Jaya monitoring station in Selangor. The data is obtained from the Department of Environment, which contains the dataset from 2004 to 2018. Subsequently, this study is conducted to construct predictive modeling that can predict the air pollutants concentrations for the next day using a tree-based approach. From the comparison of the three models, a random forest is a best-proposed model. The results of PM<sub>10</sub> concentration prediction for the random

forest is the best performance which is shown by RMSE (15.7611–19.0153), NAE (0.6508–0.8216), and R<sup>2</sup> (0.346–0.5911). For SO<sub>2</sub>, the RMSE was 0.0016–0.0017, the NAE was 0.7056–0.8052, and the R<sup>2</sup> was 0.3219–0.4676. The RMSE (0.0062–0.0075), the NAE (0.7892–0.9591), and the R<sup>2</sup> (0.0814–0.3609) for NO<sub>2</sub>. The RMSE (0.3438–0.3975), NAE (0.7387–0.9015), and R<sup>2</sup> (0.2005–0.4399) for CO were all within acceptable limits. For O<sub>3</sub>, the RMSE

### ARTICLE INFO

#### Article history:

Received: 26 February 2022

Accepted: 05 July 2022

Published: 19 August 2022

DOI: <https://doi.org/10.47836/pjst.31.1.08>

#### E-mail addresses:

nurulaisyahmustakim@gmail.com (Nurul A'isyah Mustakim)

ahmadzia101@uitm.edu.my (Ahmad Zia Ul-Saufie)

shaziayani@uitm.edu.my (Wan Nur Shaziayani)

norazian@unimap.edu.my (Norazian Mohamad Noor)

sofi@fskm.uitm.edu.my (Sofianita Mutalib)

\* Corresponding author

was 0.0051–0.0057, the NAE was 0.8386–0.9263, and the  $R^2$  was 0.1379–0.2953. The API calculation results indicate that  $PM_{10}$  is a significant pollutant in representing the API.

*Keywords:* data mining, decision tree, gradient boosted trees, Modeling,  $PM_{10}$ , random forest

---

## INTRODUCTION

The Malaysian Department of Environment (DOE) plays a vital role by providing real-time Air Pollutant Index (API) readings on the Air Pollutant Index Management System (APIMS) website. It can help people to know the actual situation of air quality status. However, people can only find out the current and past API readings. People need to cancel plans for outdoor activities immediately if the air quality status is unhealthy or worse. It would be better if people could find the air quality status for the next few days, like the weather forecast (Ul-Saufie et al., 2012). Therefore, this study will predict the API for the next day.

Furthermore, there are many studies on the prediction of air pollutants concentration. However, most studies only focus on predicting one pollutant or a few pollutants only such as (Hamid et al., 2017; Shaadan et al., 2019; Alias et al., 2021; Shaziayani et al., 2021), and there is limited study on predicting all pollutants concentration in a study. Thus, this study will predict the concentration of all major air pollutants: ozone, carbon monoxide, nitrogen dioxide, sulfur dioxide, and particulate matter less than 10 micrometers ( $PM_{10}$ ). Besides, there is limited study on predicting API since most researchers only predict the concentration of air pollutants. Therefore, this study has continued to predict API after predicting air pollution concentrations.

Additionally, most researchers use artificial neural networks (ANN) to predict the concentration of air pollutants. The researchers also always predict only one or a few air pollutants in a study, as shown in Table 1. In Malaysia, there are limited studies on the prediction of air pollution concentrations using a tree-based approach and limited studies to predict all major air pollution concentrations. Furthermore, the tree-based approach is suitable to be applied to air pollution data, given that the data is not normally distributed, which can be handled using this method. However, a haze event will result in extreme air pollutants concentration distribution values. The extreme values will affect the normality of the distribution. Therefore, a method with a non-normality assumption is needed to predict the concentration.

Therefore, decision trees, random forests, and gradient boosted trees were used in this study to predict the air pollution concentrations for the next day. Thus, tree-based modeling is chosen to predict the air pollutants concentration because the models are not sensitive and affected by extreme values or outliers (Hu et al., 2018). The study of predicting air pollutants concentration using tree-based models is also limited, given that most researchers focus on regression-based models and time series.

Table 1  
*The summary of methods used in previous studies*

Authors	MLR	ANN	DT	RF	GBT
Thomas & Jacko (2007)	√	√			
Cai et al. (2009)		√			
Moustris et al. (2010)		√			
Arhami et al. (2013)		√			
Rahman et al. (2013)		√			
Sekar et al. (2016)		√	√		
Moazami et al. (2016)		√			
Masih (2019)			√	√	
Qadeer & Jeon (2019)					√
Watson et al. (2019)	√	√		√	√
Alpan & Sekeroglu (2020)			√	√	
Shams et al. (2020)	√	√			
Lu et al. (2021)				√	
Shaziayani et al. (2021)					√

\*Abbreviations of the methods: MLR: Multiple Linear Regression, ANN: Artificial Neural Networks, DT: Decision Tree, RF: Random Forest, GBT: Gradient Boosted Trees.

## MATERIALS AND METHODS

The secondary data is obtained from the Department of Environment (DOE), which contains the data from 2004 to 2019 for the Petaling Jaya air monitoring station (CA0016). Petaling Jaya is an industrial area, and the station is located at Sri Petaling Primary School (N03° 06.612, E101° 42.274'). The number of observations for the dataset is 5763. In addition, the data for each variable is the daily average data to predict the next day's air pollutant concentration. Therefore, each variable in the dataset is very important to understand. It is to get an overview of the data that will potentially be useful for moving on to steps in the data analysis process. At this stage, the data would be evaluated in every way, such as quality, accuracy, and the representative of the data. The variables included in the study for predicting the air pollutants concentration in Petaling Jaya are carbon monoxide (CO), particulate matter 10 microns or less in diameter (PM<sub>10</sub>), nitrogen dioxide (NO<sub>2</sub>), sulfur dioxide (SO<sub>2</sub>), ozone (O<sub>3</sub>), temperature, and relative humidity. Dedovic et al. (2016) mentioned that temperature is an important meteorological parameter in the formation of secondary PM<sub>10</sub>. The relative humidity is also a strong predictor of PM<sub>10</sub> concentration and was used to replace the rainfall parameter because DOE does not measure the data. At the same time, PM<sub>2.5</sub> is not considered in the prediction because PM<sub>2.5</sub> monitoring in Malaysia started in mid-2017, while the report on PM<sub>2.5</sub> was only available in 2018. Table 2 shows the summary of sample size for the dataset. The numbers of missing values for all variables are below 0.6%.

Table 2  
*Summary of dataset sample size*

Variables	Number of Samples	Non-Missing Values	Missing Values	Percentage of Missing Values
O <sub>3</sub>	5398	5372	26	0.48%
CO	5398	5371	27	0.50%
NO <sub>2</sub>	5398	5369	29	0.54%
SO <sub>2</sub>	5398	5366	32	0.59%
PM <sub>10</sub>	5398	5397	1	0.02%
Temperature	5398	5397	1	0.02%
Relative Humidity	5398	5397	1	0.02%

## Model Development

Three models were used in predicting the air pollution concentration. The models are Decision Tree (DT), Random Forest (RF), and Gradient Boosted Trees (GBT). Besides, in the process of model development, model prediction, and model evaluation, RapidMiner Studio was used to predict the air pollution concentration.

Decision Tree (DT) is a popular machine learning algorithm that can solve the problem by transforming the data into a tree representation. DT algorithms can be used to solve both regression and classification problems. In addition, DT can work well with both nominal and numeric data types. The structure of DT consists of nodes, edges or branches and leaf nodes. The nodes represent a test for the values on a certain attribute. Each edge or branch represents a test's outcome and connects to the next node or leaf. Each leaf node (or terminal node) holds a class label that predicts the outcome. In the simplest and most frequent case, each test considers a single attribute, such that the instance space is partitioned according to the attribute's value. DT algorithm splits data into subsets based on an attribute value. The process continues for each consequent subset until the target is found.

Random forest (RF) determines variable importance by randomly permuting (shuffling) a given variable. In this way, the variable should have no relationship with the response. RFs are one of the methods for assembling a collection (or forest) of decision trees with the bagging technique. It trains many trees concurrently and uses the majority judgment developed in DTs as the RF model's final decision. The difference in accuracy in the random forest using the original data and the random forest predictions using the shuffled variable is then calculated. Next, a single variable importance measure is computed as the average of these differences across every tree in the forest (Breiman et al., 2002). Finally, a single variable importance measure is computed as the average of these differences across every tree in the forest.

Boosted regression tree models are developed by integrating two algorithms; Decision trees are used as the main methods for classifying the datasets through a supervised method,

and then boosting is used to aggregate their outputs to obtain the total prediction. Common boosting algorithms applied are Adaboost and gradient boosting. The gradient boosting trees (GBT) method is slightly different from Adaboost. Instead of using the weighted average of individual outputs as the final outputs, GBT uses a loss function to minimize loss (as an optimization function) and converge upon a final output value. Moreover, gradient boosting uses short, less-complex decision trees instead of decision stumps. A larger number of gradient boosting iterations reduces training set errors. However, raising the number of gradients boosting iterations too high will increase the overfitting. So, monitoring the error of prediction from a distinct validation data set can help choose the optimal value for the number of gradients boosting iterations.

The year 2004 to 2018 will be divided into two parts which are 70% of the data for model training and another 30% for model testing, as suggested by Arabameri et al. (2019). Then the results of each model were compared to find the best-proposed model for predicting each air pollutant. Finally, the best-proposed model was applied to the dataset for the year 2019 to calculate the air pollutant index.

Table 3 shows the general model of DT, RF and GBT in predicting air pollutants concentration. The predicted value is represented by  $\delta$  while the observed value is represented by  $D$ . Each method (DT, RF, and GBT) is used to predict the next day's concentrations for each pollutant with CO, PM<sub>10</sub>, NO<sub>2</sub>, SO<sub>2</sub>, O<sub>3</sub>, T, and RH of the current day as predictors.

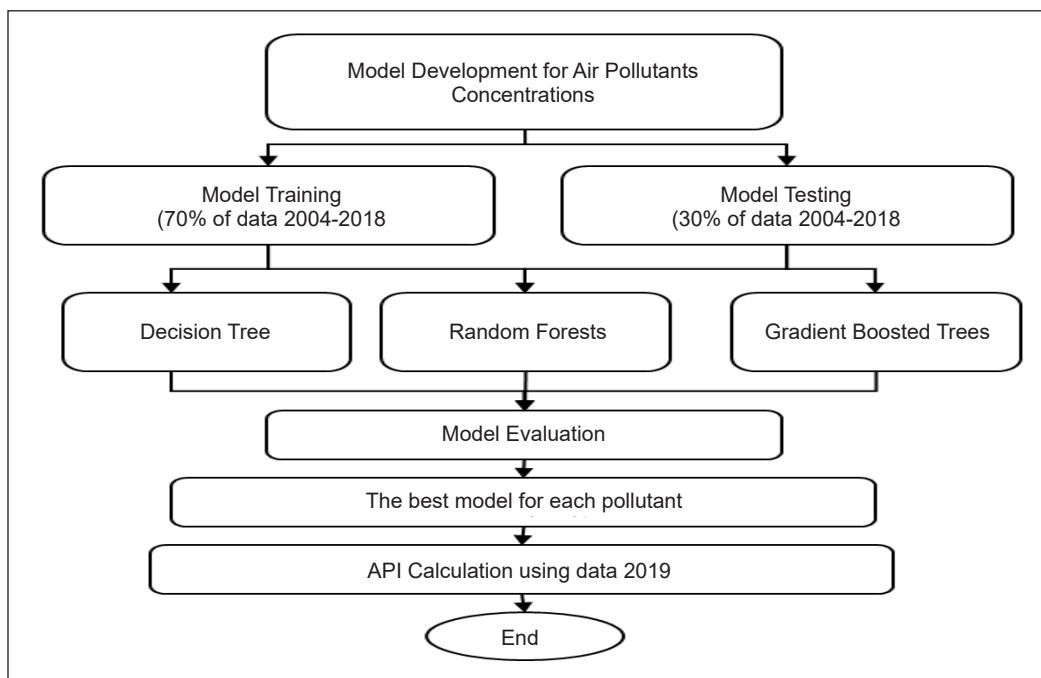


Figure 1. Model prediction workflow

Table 3  
General model for the next day's prediction

Prediction	Model
Next day ( $\delta+1$ )	CO ( $\delta + 1$ ) ~ DT [CO <sub>(D)</sub> , PM <sub>10(D)</sub> , NO <sub>2(D)</sub> , SO <sub>2(D)</sub> , O <sub>3(D)</sub> , T <sub>(D)</sub> , RH <sub>(D)</sub> ]
	CO ( $\delta + 1$ ) ~ RF [CO <sub>(D)</sub> , PM <sub>10(D)</sub> , NO <sub>2(D)</sub> , SO <sub>2(D)</sub> , O <sub>3(D)</sub> , T <sub>(D)</sub> , RH <sub>(D)</sub> ]
	CO ( $\delta + 1$ ) ~ GBT [CO <sub>(D)</sub> , PM <sub>10(D)</sub> , NO <sub>2(D)</sub> , SO <sub>2(D)</sub> , O <sub>3(D)</sub> , T <sub>(D)</sub> , RH <sub>(D)</sub> ]
Next day ( $\delta+1$ )	PM <sub>10</sub> ( $\delta + 1$ ) ~ DT [CO <sub>(D)</sub> , PM <sub>10(D)</sub> , NO <sub>2(D)</sub> , SO <sub>2(D)</sub> , O <sub>3(D)</sub> , T <sub>(D)</sub> , RH <sub>(D)</sub> ]
	PM <sub>10</sub> ( $\delta + 1$ ) ~ RF [CO <sub>(D)</sub> , PM <sub>10(D)</sub> , NO <sub>2(D)</sub> , SO <sub>2(D)</sub> , O <sub>3(D)</sub> , T <sub>(D)</sub> , RH <sub>(D)</sub> ]
	PM <sub>10</sub> ( $\delta + 1$ ) ~ GBT [CO <sub>(D)</sub> , PM <sub>10(D)</sub> , NO <sub>2(D)</sub> , SO <sub>2(D)</sub> , O <sub>3(D)</sub> , T <sub>(D)</sub> , RH <sub>(D)</sub> ]
Next day ( $\delta+1$ )	NO <sub>2</sub> ( $\delta + 1$ ) ~ DT [CO <sub>(D)</sub> , PM <sub>10(D)</sub> , NO <sub>2(D)</sub> , SO <sub>2(D)</sub> , O <sub>3(D)</sub> , T <sub>(D)</sub> , RH <sub>(D)</sub> ]
	NO <sub>2</sub> ( $\delta + 1$ ) ~ RF [CO <sub>(D)</sub> , PM <sub>10(D)</sub> , NO <sub>2(D)</sub> , SO <sub>2(D)</sub> , O <sub>3(D)</sub> , T <sub>(D)</sub> , RH <sub>(D)</sub> ]
	NO <sub>2</sub> ( $\delta + 1$ ) ~ GBT [CO <sub>(D)</sub> , PM <sub>10(D)</sub> , NO <sub>2(D)</sub> , SO <sub>2(D)</sub> , O <sub>3(D)</sub> , T <sub>(D)</sub> , RH <sub>(D)</sub> ]
Next day ( $\delta+1$ )	SO <sub>2</sub> ( $\delta + 1$ ) ~ DT [CO <sub>(D)</sub> , PM <sub>10(D)</sub> , NO <sub>2(D)</sub> , SO <sub>2(D)</sub> , O <sub>3(D)</sub> , T <sub>(D)</sub> , RH <sub>(D)</sub> ]
	SO <sub>2</sub> ( $\delta + 1$ ) ~ RF [CO <sub>(D)</sub> , PM <sub>10(D)</sub> , NO <sub>2(D)</sub> , SO <sub>2(D)</sub> , O <sub>3(D)</sub> , T <sub>(D)</sub> , RH <sub>(D)</sub> ]
	SO <sub>2</sub> ( $\delta + 1$ ) ~ GBT [CO <sub>(D)</sub> , PM <sub>10(D)</sub> , NO <sub>2(D)</sub> , SO <sub>2(D)</sub> , O <sub>3(D)</sub> , T <sub>(D)</sub> , RH <sub>(D)</sub> ]
Next day ( $\delta+1$ )	O <sub>3</sub> ( $\delta + 1$ ) ~ DT [CO <sub>(D)</sub> , PM <sub>10(D)</sub> , NO <sub>2(D)</sub> , SO <sub>2(D)</sub> , O <sub>3(D)</sub> , T <sub>(D)</sub> , RH <sub>(D)</sub> ]
	O <sub>3</sub> ( $\delta + 1$ ) ~ RF [CO <sub>(D)</sub> , PM <sub>10(D)</sub> , NO <sub>2(D)</sub> , SO <sub>2(D)</sub> , O <sub>3(D)</sub> , T <sub>(D)</sub> , RH <sub>(D)</sub> ]
	O <sub>3</sub> ( $\delta + 1$ ) ~ GBT [CO <sub>(D)</sub> , PM <sub>10(D)</sub> , NO <sub>2(D)</sub> , SO <sub>2(D)</sub> , O <sub>3(D)</sub> , T <sub>(D)</sub> , RH <sub>(D)</sub> ]

### Model Evaluation

The performance of the models is evaluated using statistical comparisons, which were root mean square error (RMSE), normalized absolute error (NAE), and squared correlation ( $R^2$ ). The  $R^2$  is used to assess the model's accuracy; values closer to 1 imply more accuracy. While to quantify a model's error, the RMSE and NAE are used; a value close to 0 indicates a minimal error. The models that provide the best prediction values were selected as the best-proposed models for predicting the concentration of air pollutants. Below is the Equations 1-3 for each indicator:

$$NAE = \frac{\sum_{i=1}^n |P_i - O_i|}{\sum_{i=1}^n |\bar{O} - O_i|} \tag{1}$$

$$RMSE = \left( \frac{1}{N} \sum_{i=1}^N [P_i - O_i]^2 \right)^{\frac{1}{2}} \tag{2}$$

$$R^2 = \left[ \frac{\sum_{i=1}^N [(P_i - \bar{P})(O_i - \bar{O})]}{N \sigma_P \sigma_O} \right]^2 \tag{3}$$

where,

$N$  = Total number of sample size;



$O_i$  = Observed values of i-th day

$P_i$  = Predicted values of i-th day

$\overline{P}$  = Mean of the predicted values of one set of daily monitoring records

$\overline{O}$  = Mean of the observed values of one set of daily monitoring records

$S_P$  = Standard deviation of the predicted values of one set of daily monitoring records

$S_Q$  = Standard deviation of the observed values of one set of daily monitoring records

The results of RMSE, NAE, and  $R^2$  for the three models were compared to determine the best model. First, the lowest value of RMSE and NAE was ranked as 1, the second lowest value was ranked as 2, and the highest was ranked as 3. For  $R^2$ , the method for ranking is the opposite of RMSE and NAE. The highest value of  $R^2$  was ranked as 1, the second highest value was ranked as 2, and the lowest was ranked as 3. Then, the ranked values for RMSE, NAE, and  $R^2$  were summed up to find the lowest total ranking values among the three models, which indicate the best (Shaziyani et al., 2021).

### API Calculation

The first step to calculating the air pollution index (API) is the sub-index for each pollutant. The predicted values of air pollutant concentration were used to calculate the sub-index. Table 4 shows the formulas used by the Department of Environment (DOE) in calculating the sub-index. Let X represent predicted concentration and Y represent the index.

Then, the highest sub-index among the air pollutants was chosen as the API for the predicted day. Figure 2 shows the determination of API calculation. After calculating the sub-index for all pollutants, the sub-index results were compared, and the highest was chosen as a maximum index, API.

Table 4  
Equations of sub-index calculation

Air Pollutants	Values of Predicted Concentration (X)	Formula of Sub-Index (Y)
Carbon Monoxide (CO)	$X < 9$ ppm	$Y = X \times 11.11111$
	$9 < X < 15$ ppm	$Y = 100 + [(X - 9) \times 16.66667]$
	$15 < X < 30$ ppm	$Y = 200 + [(X - 15) \times 6.66667]$
	$X > 30$ ppm	$Y = 300 + [(X - 30) \times 10]$
Ozone (O <sub>3</sub> )	$X < 0.2$ ppm	$Y = X \times 1000$
	$0.2 < X < 0.4$ ppm	$Y = 200 + [(X - 0.2) \times 500]$
	$X > 0.4$ ppm	$Y = 300 + [(X - 0.4) \times 1000]$
Nitrogen Dioxide (NO <sub>2</sub> )	$X < 0.17$ ppm	$Y = X \times 588.23529$
	$0.17 < X < 0.6$ ppm	$Y = 100 + [(X - 0.17) \times 232.56]$
	$0.6 < X < 1.2$ ppm	$Y = 200 + [(X - 0.6) \times 166.667]$
	$X > 1.2$ ppm	$Y = 300 + [(X - 1.2) \times 250]$

Table 4 (continue)

Air Pollutants	Values of Predicted Concentration (X)	Formula of Sub-Index (Y)
Sulfur Dioxide (SO <sub>2</sub> )	$X < 0.04$ ppm	$Y = X \times 2500$
	$0.04 < X < 0.3$ ppm	$Y = 100 + [(X - 0.04) \times 384.61]$
	$0.3 < X < 0.6$ ppm	$Y = 200 + [(X - 0.3) \times 333.333]$
	$X > 0.6$ ppm	$Y = 300 + [(X - 0.6) \times 500]$
Particulate Matter (PM <sub>10</sub> )	$X < 50$ µg/m <sup>3</sup>	$Y = X$
	$50 < X < 150$ µg/m <sup>3</sup>	$Y = 50 + [(X - 50) \times 0.5]$
	$150 < X < 350$ µg/m <sup>3</sup>	$Y = 100 + [(X - 150) \times 0.5]$
	$350 < X < 420$ µg/m <sup>3</sup>	$Y = 200 + [(X - 350) \times 1.4286]$
	$420 < X < 500$ µg/m <sup>3</sup>	$Y = 300 + [(X - 420) \times 1.25]$
	$X > 500$ µg/m <sup>3</sup>	$Y = 400 + (X - 500)$

Source. Department of Environment (1997)

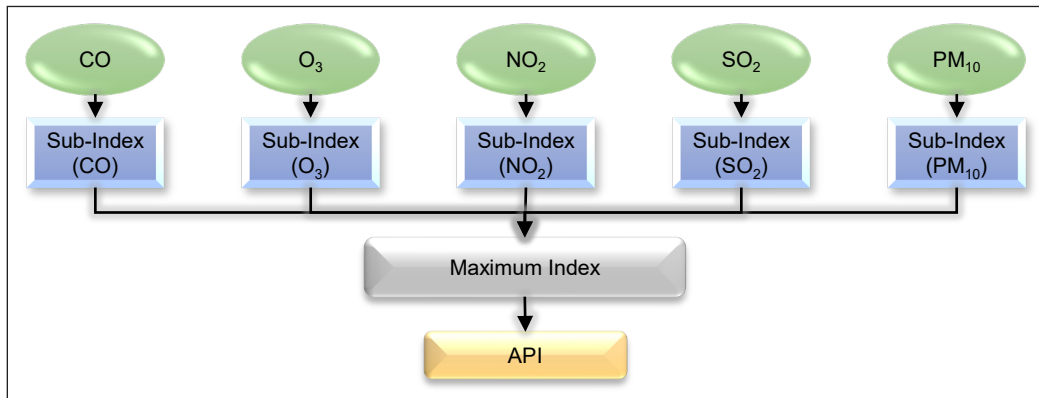


Figure 2. Diagram of API calculation  
Source. Department of Environment (2017)

## RESULTS AND DISCUSSION

The central tendency and dispersion measures are shown in Table 5 from 2004 to 2018. This research focuses on five major air pollutants at Petaling Jaya station, namely O<sub>3</sub>, CO, NO<sub>2</sub>, SO<sub>2</sub>, and PM<sub>10</sub>. From this study, PM<sub>10</sub> is the one with the most unstable data as it has many outliers compared to others. O<sub>3</sub>, CO, NO<sub>2</sub>, and SO<sub>2</sub> also have outliers but not as much as PM<sub>10</sub>. Besides, PM<sub>10</sub> has the highest standard deviation, which means that PM<sub>10</sub> concentrations are far from the mean of the set and spread over a wider range. Meanwhile, the standard deviation for O<sub>3</sub>, CO, NO<sub>2</sub>, and SO<sub>2</sub> are all less than one, which means the values tend to be close to the set mean.

The highest concentration of PM<sub>10</sub> was recorded in Petaling Jaya on August 11, 2005. According to Shahrudin and Noorzuan (2006), massive fires caused by agricultural activities in Kampar, Pelalawaan, Indragiri Hulu, and Bengkalis provinces, as well as

peat forest fires in Rokan Hulu and Rokan Hilir, were the main sources of PM<sub>10</sub> emissions entering the Malaysian atmosphere from 10–12 August 2005.

Lastly, it reveals that all the variables are not normally distributed because the skewness is not equal to zero. Furthermore, besides the skewness results, it indicates that O<sub>3</sub>, CO, SO<sub>2</sub>, and PM<sub>10</sub> are skewed right because the values are positive, while NO<sub>2</sub>, temperature, and relative humidity are skewed left because the values are negative. Thus, the non-normal distribution data reinforces the reason it is necessary to use the tree-based approach because the approach does not require assumptions of normality (Elith et al., 2008).

Table 5  
Summary of dataset statistic

Variables	Mean	Median	Standard Deviation	Skewness	Maximum
O <sub>3</sub>	0.0142	0.0130	0.0063	0.6269	0.0420
CO	1.3201	1.2660	0.4664	1.1080	6.7730
NO <sub>2</sub>	0.0285	0.0280	0.0079	-0.0313	0.0610
SO <sub>2</sub>	0.0041	0.0040	0.0021	1.0787	0.0240
PM <sub>10</sub>	48.1261	43.5830	24.9671	4.9070	482.2080
Temperature	27.0160	28.0279	5.3528	-4.1983	33.1370
Relative Humidity	71.6447	73.0000	9.4837	-2.2168	94.2071

### Prediction Model

The results of RMSE, NAE, and R<sup>2</sup> in predicting air pollution concentrations using DT, RF, and GBT are shown in Table 6. First, the best-proposed model is chosen by choosing the lowest RMSE, lowest NAE, and highest R<sup>2</sup>. Next, the RMSE, NAE, and R<sup>2</sup> were ranked to make it easier. The best performance was ranked 1, followed by 2 and 3. After that, the ranks were summed up to choose the best-proposed model. It is revealed that the random forest is the best-proposed model for predicting PM<sub>10</sub> concentration because it has the lowest RMSE, NAE, and second highest R<sup>2</sup> in predicting the next day's air pollution concentration.

Next, the results also show that random forest is the best-proposed model for predicting SO<sub>2</sub>, NO<sub>2</sub>, O<sub>3</sub>, and CO concentrations for the next day since it has the lowest error and highest accuracy, with a total of rank values of 4 for NO<sub>2</sub> and 3 for SO<sub>2</sub>, O<sub>3</sub>, and CO. These results are similar to Alpan and Sekeroglu (2020), where the RF model achieved the best results in predicting air pollution concentration compared to the other two models in their study.

### Air Pollutant Index

The best-proposed model, the random forest, is applied to the dataset for the year 2019 to predict the air pollution concentration. As shown in Table 7, the predicted air pollution concentration is used to calculate the sub-index, and the maximum sub-index is chosen as

Table 6  
Model evaluation of PM<sub>10</sub> concentration prediction

Air pollutants	Model	Model Evaluation			Rank			
		RMSE	NAE	R <sup>2</sup>	RMSE	NAE	R <sup>2</sup>	Sum
PM <sub>10</sub>	Decision tree	17.4991	0.7098	0.4790	2	2	3	7
	<b>Random forest</b>	<b>15.7611</b>	<b>0.6508</b>	0.5764	1	1	2	<b>4</b>
	Gradient boosted tree	19.2405	0.7895	<b>0.5911</b>	3	3	1	7
SO <sub>2</sub>	Decision tree	0.0017	0.7642	0.3685	2	2	3	7
	<b>Random forest</b>	<b>0.0016</b>	<b>0.7056</b>	<b>0.4676</b>	1	1	1	<b>3</b>
	Gradient boosted tree	0.0018	0.8350	0.4620	3	3	2	8
NO <sub>2</sub>	Decision tree	0.0072	0.9161	0.2507	3	3	3	9
	<b>Random forest</b>	<b>0.0062</b>	<b>0.7892</b>	0.3587	1	1	2	<b>4</b>
	Gradient boosted tree	0.0067	0.8610	<b>0.3609</b>	2	2	1	5
O <sub>3</sub>	Decision tree	0.0056	0.9072	0.2161	3	3	3	9
	<b>Random forest</b>	<b>0.0051</b>	<b>0.8386</b>	<b>0.2953</b>	1	1	1	<b>3</b>
	Gradient boosted tree	0.0055	0.8963	0.2877	2	2	2	6
CO	Decision tree	0.4108	0.8567	0.2896	3	3	3	9
	<b>Random forest</b>	<b>0.3438</b>	<b>0.7387</b>	<b>0.4399</b>	1	1	1	<b>3</b>
	Gradient boosted tree	0.3901	0.8434	0.4243	2	2	2	6

Table 7  
API calculation of next day

ID	Date	Sub-Index (PM <sub>10</sub> )	Sub-Index (SO <sub>2</sub> )	Sub-Index (NO <sub>2</sub> )	Sub-Index (O <sub>3</sub> )	Sub-Index (CO)	API (Max Sub-Index)	Pollutant of Max Sub-Index
1	2019.01.01	31.6825	3.4266	13.5366	15.2291	13.1300	31.6825	PM <sub>10</sub>
2	2019.01.02	30.7458	3.4560	13.6141	11.1102	13.9577	30.7458	PM <sub>10</sub>
3	2019.01.03	35.2744	3.6125	13.9373	16.4702	12.3811	35.2744	PM <sub>10</sub>
4	2019.01.04	35.9763	3.9619	13.8152	15.1340	13.4098	35.9763	PM <sub>10</sub>
5	2019.01.05	38.3268	4.3707	14.9920	16.6031	13.2073	38.3268	PM <sub>10</sub>
6	2019.01.06	35.7925	3.4983	13.3914	16.5355	13.0631	35.7925	PM <sub>10</sub>
7	2019.01.07	31.0234	4.2816	12.3576	10.2682	13.0592	31.0234	PM <sub>10</sub>
8	2019.01.08	35.9258	4.3158	15.2095	14.1415	14.8572	35.9258	PM <sub>10</sub>
9	2019.01.09	35.6401	3.9545	13.4431	14.4477	14.8709	35.6401	PM <sub>10</sub>
10	2019.01.10	31.2531	3.9623	12.6887	12.0756	13.1288	31.2531	PM <sub>10</sub>

the next day's air pollution index (API). In this section, only 10 observations are shown from 365 days in 2019 as an example of results in calculating and selecting the API index. For instance, on January 1, 2019, the highest value for the sub-index was PM<sub>10</sub> concentration. Therefore, PM<sub>10</sub> was selected as the API for this date. Overall, the results showed that all APIs selected PM<sub>10</sub> because the index of PM<sub>10</sub> is the highest among the air pollutants.

## CONCLUSION

The main finding showed that the random forest was chosen as the best-proposed model for predicting the concentrations of O<sub>3</sub>, CO, NO<sub>2</sub>, SO<sub>2</sub>, and PM<sub>10</sub> for next-day prediction. The random forest has the best performance and is compared using RMSE, NAE, and R<sup>2</sup>. Then, the best random forest model is applied to the dataset for the year 2019. The predicted air pollutants concentrations for 2019 are used to calculate the sub-index. Then, the maximum sub-index was chosen as API. From the results of API calculation, all data of the maximum sub-index represent by PM<sub>10</sub>. It indicates that PM<sub>10</sub> is a significant pollutant in calculating the API.

The main contribution of this study is that, besides using this tree-based model to predict air pollution concentration, this study also converted air pollution prediction concentration to sub-index API. This procedure will help the local authorities to make predictions on air pollutants in Malaysia and as a tool for the early warning system.

## ACKNOWLEDGEMENT

The Ministry of Science, Technology & Innovation (MOSTI) under Technology Development Fund 1(TDF04211363) funded this research. Thanks to the Faculty of Computer and Mathematical Sciences, Universiti Teknologi MARA, for their support and the Department of Environment Malaysia for providing air quality monitoring data.

## REFERENCES

- Alias, S. N., Hamid, N. Z. A., Saleh, S. H. M., & Bidin, B. (2021). Predicting carbon monoxide time series between different settlements area in Malaysia through chaotic approach. *Journal of Science and Mathematics Letters*, 9, 45-54. <https://doi.org/https://doi.org/10.37134/jsml.vol9.sp.6.2021>
- Alpan, K., & Sekeroglu, B. (2020). Prediction of pollutant concentrations by meteorological data using machine learning algorithms. *International Archives of the Photogrammetry, Remote Sensing and Spatial Information Sciences - ISPRS Archives*, 44(4/W3), 21-27. <https://doi.org/10.5194/isprs-archives-XLIV-4-W3-2020-21-2020>
- Arabameri, A., Pradhan, B., & Lombardo, L. (2019). Comparative assessment using boosted regression trees, binary logistic regression, frequency ratio and numerical risk factor for gully erosion susceptibility modelling. *Catena*, 183(6), Article 104223. <https://doi.org/10.1016/j.catena.2019.104223>
- Arhami, M., Kamali, N., & Rajabi, M. M. (2013). Predicting hourly air pollutant levels using artificial neural networks coupled with uncertainty analysis by Monte Carlo simulations. *Environmental Science and Pollution Research*, 20(7), 4777-4789. <https://doi.org/10.1007/s11356-012-1451-6>
- Breiman, L., Culter, A., Liaw, A., & Wiener, M. (2002). Classification and regression by random forest. *R News*, 2, 18-22.
- Cai, M., Yin, Y., & Xie, M. (2009). Prediction of hourly air pollutant concentrations near urban arterials using artificial neural network approach. *Transportation Research Part D: Transport and Environment*, 14(1), 32-41. <https://doi.org/10.1016/j.trd.2008.10.004>

- Dedovic, M. M., Avdakovic, S., Turkovic, I., Dautbasic, N., & Konjic, T. (2016). Forecasting PM10 concentrations using neural networks and system for improving air quality. In *2016 xi international symposium on telecommunications (bihtel)* (pp. 1-6). IEEE Publishing. <https://doi.org/10.1109/BIHTEL.2016.7775721>
- Department of Environment. (1997). *A guide to air pollution index in Malaysia (API)*. Ministry of Science, Technology and the Environment. <https://aqicn.org/images/aqi-scales/malaysia-api-guide.pdf>
- Department of Environment. (2017). *AIR pollutant index (API) calculation*. Ministry of Environment and Water. [http://apims.doe.gov.my/public\\_v2/pdf/API\\_Calculation.pdf](http://apims.doe.gov.my/public_v2/pdf/API_Calculation.pdf)
- Elith, J., Leathwick, J. R., & Hastie, T. (2008). A working guide to boosted regression trees. *Journal of Animal Ecology*, 77(4), 802-813. <https://doi.org/10.1111/j.1365-2656.2008.01390.x>
- Hamid, H. A., Japeri, A. Z. U. S. M., & Ahmat, H. (2017). Characteristic and prediction of carbon monoxide concentration using time series analysis in selected urban area in Malaysia. In *MATEC Web of Conferences* (Vol. 103, p. 05001). EDP Sciences.. <https://doi.org/10.1051/mateconf/201710305001>
- Hu, Y., Scavia, D., & Kerkez, B. (2018). Are all data useful? Inferring causality to predict flows across sewer and drainage systems using directed information and boosted regression trees. *Water Research*, 145, 697-706.
- Lu, J., Zhang, Y., Chen, M., Wang, L., Zhao, S., Pu, X., & Chen, X. (2021). Estimation of monthly 1 km resolution PM2.5 concentrations using a random forest model over “2 + 26” cities, China. *Urban Climate*, 35, Article 100734. <https://doi.org/10.1016/j.uclim.2020.100734>
- Masih, A. (2019). Application of random forest algorithm to predict the atmospheric concentration of NO<sub>2</sub>. In *2019 Ural Symposium on Biomedical Engineering, Radioelectronics and Information Technology (USBEREIT)* (pp. 252-255). AIP Publishing LLC. <https://doi.org/10.1063/1.5137947>
- Moazami, S., Noori, R., Amiri, B. J., Yeganeh, B., Partani, S., & Safavi, S. (2016). Reliable prediction of carbon monoxide using developed support vector machine. *Atmospheric Pollution Research*, 7(3), 412-418. <https://doi.org/10.1016/j.apr.2015.10.022>
- Moustris, K. P., Ziomas, I. C., & Paliatsos, A. G. (2010). 3-day-ahead forecasting of regional pollution index for the pollutants NO<sub>2</sub>, CO, SO<sub>2</sub>, and O<sub>3</sub> using artificial neural networks in athens, Greece. *Water, Air, and Soil Pollution*, 209(1-4), 29-43. <https://doi.org/10.1007/s11270-009-0179-5>
- Qadeer, K., & Jeon, M. (2019). Prediction of PM10 concentration in South Korea using gradient tree boosting models. In *PervasiveHealth: Pervasive Computing Technologies for Healthcare* (pp. 1-6). ACM Publishing. <https://doi.org/10.1145/3387168.3387234>
- Rahman, N. H. A., Lee, M. H., Latif, M. T., & Suhartono, S. (2013). Forecasting of air pollution index with artificial neural network. *Jurnal Teknologi*, 63(2), 59-64. <https://doi.org/10.11113/jt.v63.1913>
- Sekar, C., Gurjar, B. R., Ojha, C. S. P., & Goyal, M. K. (2016). Potential assessment of neural network and decision tree algorithms for forecasting ambient PM2.5 and CO concentrations: Case study. *Journal of Hazardous, Toxic, and Radioactive Waste*, 20(4), 1-9. [https://doi.org/10.1061/\(asce\)hz.2153-5515.0000276](https://doi.org/10.1061/(asce)hz.2153-5515.0000276)
- Shaadan, N., Rusdi, M. S., Azmi, N. N. S. N. M., Talib, S. F., & Azmi, W. A. W. (2019). Time series model for Carbon Monoxide (CO) at several industrial sites in Peninsular Malaysia. *Malaysian Journal of Computing (MJoC)*, 4(1), 246-260.

- Shaharuddin, A., & Noorazuan, M. H. (2006). Kebakaran hutan dan isu pencemaran udara di Malaysia: Kes jerebu pada Ogos 2005 [Forest fires and air pollution issues in Malaysia: The case of haze on August 2005]. *UKM Journal Article Repository*, 1(1), 1-19.
- Shams, S. R., Jahani, A., Moeinaddini, M., & Khorasani, N. (2020). Air carbon monoxide forecasting using an artificial neural network in comparison with multiple regression. *Modeling Earth Systems and Environment*, 6(3), 1467-1475. <https://doi.org/10.1007/s40808-020-00762-5>
- Shaziayani, W. N., Ul-Saufie, A. Z., Ahmat, H., & Al-Jumeily, D. (2021). Coupling of quantile regression into boosted regression trees (BRT) technique in forecasting emission model of PM10 concentration. *Air Quality, Atmosphere and Health*, 14, 1647-1663. <https://doi.org/10.1007/s11869-021-01045-3>
- Thomas, S., & Jacko, R. B. (2007). Model for forecasting expressway fine particulate matter and carbon monoxide concentration: Application of regression and neural network models. *Journal of the Air and Waste Management Association*, 57(4), 480-488. <https://doi.org/10.3155/1047-3289.57.4.480>
- Ul-Saufie, A. Z., Yahaya, A. S., Ramli, A., & Hamid, H. A. (2012). Performance of multiple linear regression model for long-term PM10 concentration prediction based on gaseous and meteorological parameters. *Journal of Applied Sciences*, 12(14), 1488-1494.
- Watson, G. L., Telesca, D., Reid, C. E., Pfister, G. G., & Jerrett, M. (2019). Machine learning models accurately predict ozone exposure during wildfire events. *Environmental Pollution*, 254, Article 112792. <https://doi.org/10.1016/j.envpol.2019.06.088>





## Real-Time Traffic Sign Recognition Using Deep Learning

Ananya Belagodu Shivayogi<sup>1</sup>, Nehal Chakravarthy Matasagara Dharmendra<sup>1\*</sup>,  
Anala Maddur Ramakrishna<sup>2</sup> and Kolala Nagaraju Subramanya<sup>3</sup>

<sup>1</sup>Department of Computer Science, R. V. College of Engineering, Bangalore, 560059 India

<sup>2</sup>Department of Information Science, R. V. College of Engineering, Bangalore, 560059 India

<sup>3</sup>R. V. College of Engineering, Bangalore, 560059 India

### ABSTRACT

Traffic Sign Recognition (TSR) is one of the most sought-after topics in computer vision, mostly due to the increasing scope and advancements in self-driving cars. In our study, we attempt to implement a TSR system that helps a driver stay alert during driving by providing information about the various traffic signs encountered. We will be looking at a working model that classifies the traffic signs and gives output in the form of an audio message. Our study will be focused on traffic sign detection and recognition on Indian roads. A dataset of Indian road traffic signs was created, based upon which our deep learning model will work. The developed model was deployed on NVIDIA Jetson Nano using YOLOv4 architecture, giving an accuracy in the range of 54.68–76.55% on YOLOv4 architecture. The YOLOv4-Tiny model with DeepStream implementation achieved an FPS of 32.5, which is on par with real-time detection requirements.

*Keywords:* DeepStream, Indian traffic sign dataset, NVIDIA Jetson Nano, traffic sign detection, YOLOv4

### ARTICLE INFO

*Article history:*

Received: 26 February 2022

Accepted: 31 May 2022

Published: 19 August 2022

DOI: <https://doi.org/10.47836/pjst.31.1.09>

*E-mail addresses:*

ananyabs.cs18@rvce.edu.in (Ananya Belagodu Shivayogi)

nehalcmd.cs18@rvce.edu.in (Nehal Chakravarthy Matasagara Dharmendra)

analamr@rvce.edu.in (Anala Maddur Ramakrishna)

subramanyakn@rvce.edu.in (Kolala Nagaraju Subramanya)

\* Corresponding author

### INTRODUCTION

The Traffic Sign Recognition System is part of a bigger set of features called the Advanced Driver Assistance System (ADAS). ADAS plays a key role in the working of driverless or self-driving cars. With the help of data accumulated from various sensors and cameras, driverless vehicles make certain decisions that a typical driver takes. Besides self-driving cars, a TSR system can help drivers avoid road

accidents by minimising human errors. Traffic signs have been installed on the streets to give the necessary information that drivers have to follow, but often drivers tend to miss or ignore traffic signs while trying to focus on the road. A Traffic Sign Recognition System thus assists the driver by providing information about the traffic signs without the need for the driver to have a look at them.

Traffic sign detection and recognition in computer vision have recently been an active research topic. Initial research (Ellahyani et al., 2016) concentrated on the most important traffic signs, such as mandatory, prohibitory sign classification using colour and shape features. Before Convolutional Neural Networks (CNN) became popular, classical detection techniques for object detection like Histogram of Gradient (HOG) combined with Support Vector Machine (SVM) were widely used (Muthukumaresan et al., 2016; Do et al., 2017).

The recognition of a traffic sign from an image comprises two steps: localisation and classification. Object detectors such as the Faster-RCNN, Region-based Fully Convolutional Networks (R-FCN), and Feature Pyramid Networks (FPN) are region-based object detectors. On the other hand, one-stage detectors such as SSD-ResNet (Lu et al., 2019), MobileNet-SSD and YOLO perform object detection in a single step and are usually faster but at the cost of accuracy. YOLOv2 algorithm is used for Traffic Sign Recognition (Zhang et al., 2017), and high precision and low latency results were noted, despite the usage of a small number of traffic signs of different categories. The YOLO algorithm was analysed and considered a powerful object detection technique for real-time implementation (Oltean et al., 2019). In particular, YOLOv3 was used to balance between accuracy and speed properly. The implementation in this paper uses the YOLOv4 model (Bochkovskiy et al., 2020), as real-time implementation demands faster execution.

Many proposed systems are just limited to the classification of traffic sign instances captured by a camera (Tabernik & Skocaj, 2020; Luo et al., 2018). However, for real-time implementation, environmental parameters like cloudy and rainy conditions can influence the detection of traffic signs to a large extent (Tabernik & Skocaj, 2020; Sari & Cibooglu, 2018); hence an accurate object detection model using deep learning is required, which is not prone to scale changes (Hasegawa et al., 2019). Therefore, this paper proposes a system to recognise a traffic sign by adapting to various environmental conditions.

Through the course of this study, an Indian road traffic sign dataset is created, upon which the implementation of the TSR system will work. Most practical implementations convey the information by displaying an image of the sign on the dashboard. However, it further requires the driver to take his eyes off the road and look at the alert on the dashboard. Hence, an audio message would be a safer and much better way to convey the information. This paper describes a practical implementation of a TSR system on the NVIDIA Jetson Nano, which can detect Indian road traffic signs in real-time and give out audio alert messages as output. Table 1 consolidates the features of similar works conducted in this direction.

Table 1  
Related work

Author(s) & Year	Feature extraction algorithm	Classifier	Dataset	Recognition rate	Comments
Lu et al (2019)	HOG and LSS	Random Forest classifier	Swedish Traffic Signs Data set includes more than 20,000 images	96%	Difficulty in recognising signs with motion blur.
Bochkovskiy et al. (2020)	HOG Feature Extraction	SVM classifier	Image database created by capturing in streets of Ho Chi Minh City	98%	Detection and recognition of speed limit traffic signs with high accuracy are seen even in conditions with complex backgrounds.
Luo et al. (2018)	Mask R-CNN	Fast R-CNN	A novel dataset containing thirteen thousand traffic signs and seven thousand high-resolution images	2-3% error rate	A deep learning method for traffic sign detection, with signs with intra-category variation in appearance, is proven to be adequate for real-time deployment.
Sari and Ciboglu (2018)	Maximally Stable Extremal Regions (MSERs)	Multi-task CNN	Street view images and synthesised traffic sign images from standard sign templates	87.3%	Recognition of traffic sign images with distortion, rotation and blur is good.
Hasagawa et al. (2019)	Edge Detection and Contour Detection	CNN	German Traffic Signs Recognition Benchmark (GTSRB)	87.36 %	Colour filtering method cannot be relied upon in lighting and other complex conditions in the test environment.
Zoph et al. (2019)	YOLOv2, which in turn utilises an FCN	YOLOv2	Novel dataset containing 16 traffic sign classes, including a total of 7160 images	66.39%	Training the model with images of varying sizes and data augmentation effectively handles scale and contrast changes.
Zhong et al. (2020)	An end-to-end convolutional network that YOLOv2 inspires	YOLOv2	CCTSDB - Changsha University of Science and Technology Chinese traffic sign detection benchmark	95.31%	Detection of small-sized traffic signs is not achieved and needs to be improved.
Islam (2019)	HSV colour space with masking	CNN based on the LeNet architecture	U.K. traffic signs image database, which has around 40000 images, including both positive and negative images	90%	Real-time detection and recognition remain a challenge and need to be implemented.
Koresh (2019)	Hough transform	Capsule neural network	Indian traffic sign data set	15% higher accuracy than CNN and RNN	Efficiency of CapsNet is more due to the ability to identify pose and spatial variance better than CNNs.
Hegadi (2011)	Shape and colour-based detection	Pre-trained CNN	German Traffic Signs Recognition Benchmark (GTSRB)	96%	Traffic sign recognition system for driver assistance is deployed on the NVIDIA Jetson TX1.

## METHOD

The methodology can be divided into four phases: data collection, annotation, training, and implementation. The series of steps involved is shown in Figure 1.

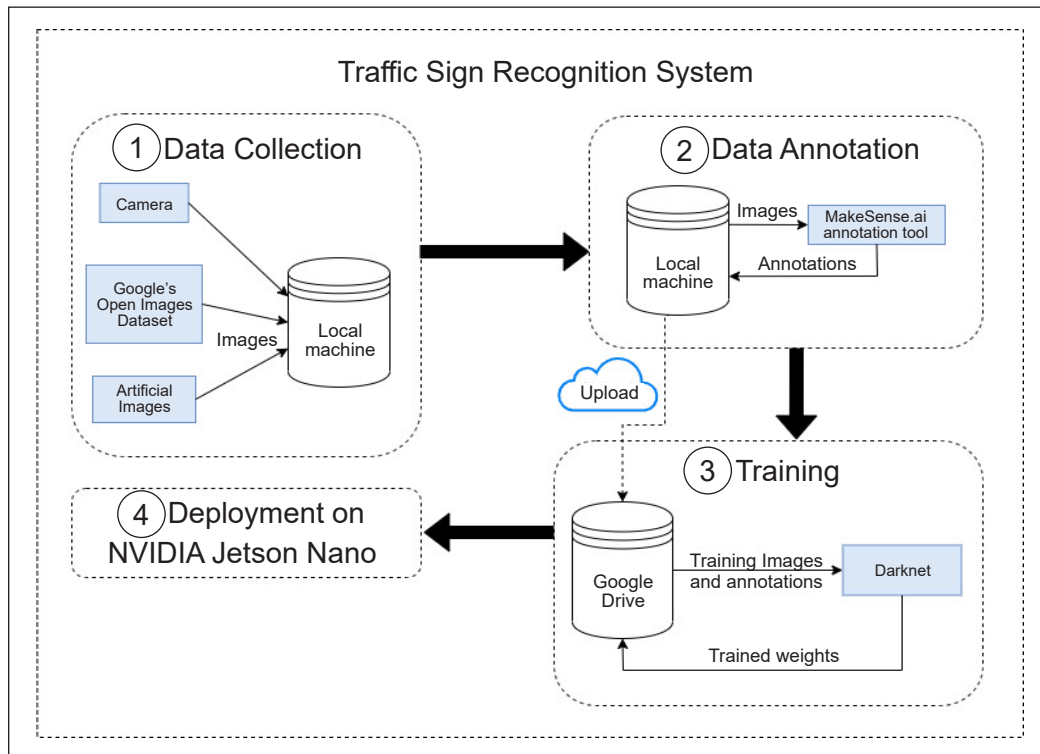


Figure 1. Traffic Sign Recognition System

### Data Collection and Annotation

The study is focused on Indian road traffic signs. Due to the non-availability of a public dataset on Indian road traffic signs, a dataset of about 5800 images across 30 classes is created by capturing images and videos using mobile phones. Among the 30 classes, the 10 most commonly found classes with a sufficient number of images are considered for our study. The various classes considered for the study and the number of images are summarised in Table 2.

### Training

The images are annotated manually according to the YOLO format and split at a ratio of 75:25 into training and validation sets. In addition, YOLOv4 performs data augmentation during the training process by varying image parameters such as saturation, exposure, and hue (known as colour jittering), as shown in Figure 2.

Table 2  
Classes, their corresponding traffic sign image, and the number of images











Traffic Sign	Class Name	Number of images	Traffic Sign	Class Name	Number of images
	Stop	425		Speed Limit 20 km/h	285
	Left Curve	401		Speed Limit 30 km/h	332
	Right Curve	434		Speed Limit 40 km/h	305
	No Parking	376		Speed Limit 50 km/h	320
	No U-Turn	385		Speed Limit 60 km/h	325



Figure 2. Data augmentation by colour jittering

Further, Mosaic data augmentation is performed, as shown in Figure 3, which combines four training images into one at certain ratios (Zoph et al., 2019). It encourages the model to learn how to detect traffic signs at different positions of the frame and on a smaller scale than usual.

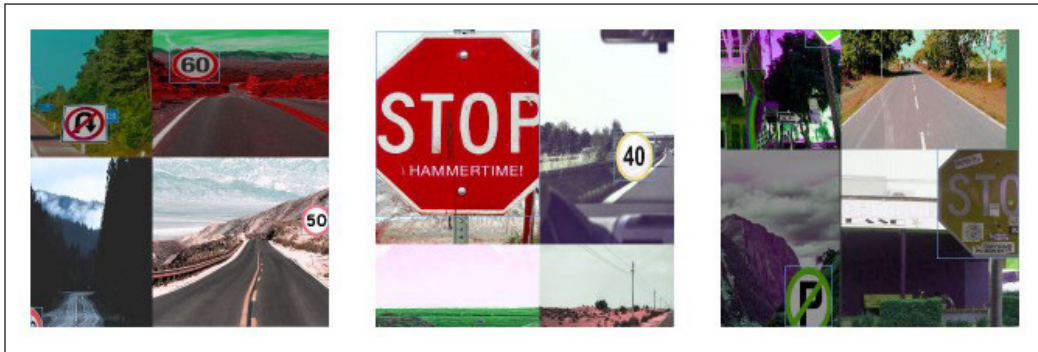


Figure 3. Mosaic augmentation of training images in YOLOv4

## System Design

The proposed design of the system is shown in Figure 4. First, a live video feed of the road is continuously captured by a camera fixed to the moving vehicle. Then, each frame that is captured by the camera is fed into the YOLOv4 detection module, deployed on the Jetson Nano. The detection module detects the traffic sign, if any, in the input frame. Next, the class name of the detected traffic sign is extracted and provided as input to the Text-to-Speech module, which generates an audio message that is given as output.

The YOLOv4 object detection model is trained on GPU, using the Darknet framework. The training is performed for 5000 epochs, and a mAP (mean Average Precision) of 87.22% is achieved on the validation set. The trained model is deployed on the NVIDIA Jetson Nano developer kit. YOLOv4 is computationally intensive and requires high-end GPUs for better performance. Even though YOLOv4-Tiny is lighter than YOLOv4, the obtained frame rate was far from real-time performance standards. Thus, Darknet implementation is not ideal for deployment on edge computing devices.

A TensorRT engine with FP16 precision is generated for the trained model for TensorRT acceleration. FP16 precision is chosen over FP32 since it would improve speed (TFLOPS), performance and reduce memory usage. With the help of TensorRT acceleration, the frame rate obtained is higher than that obtained using Darknet. However, it is insufficient for deployment in real-time use case. For example, TensorRT engines for YOLOv4-Tiny did not perform better than Darknet and showed a drop in the FPS values.

The model was deployed using the NVIDIA DeepStream 5.1 SDK to achieve real-time inference. DeepStream provides extensive support for object detection and segmentation



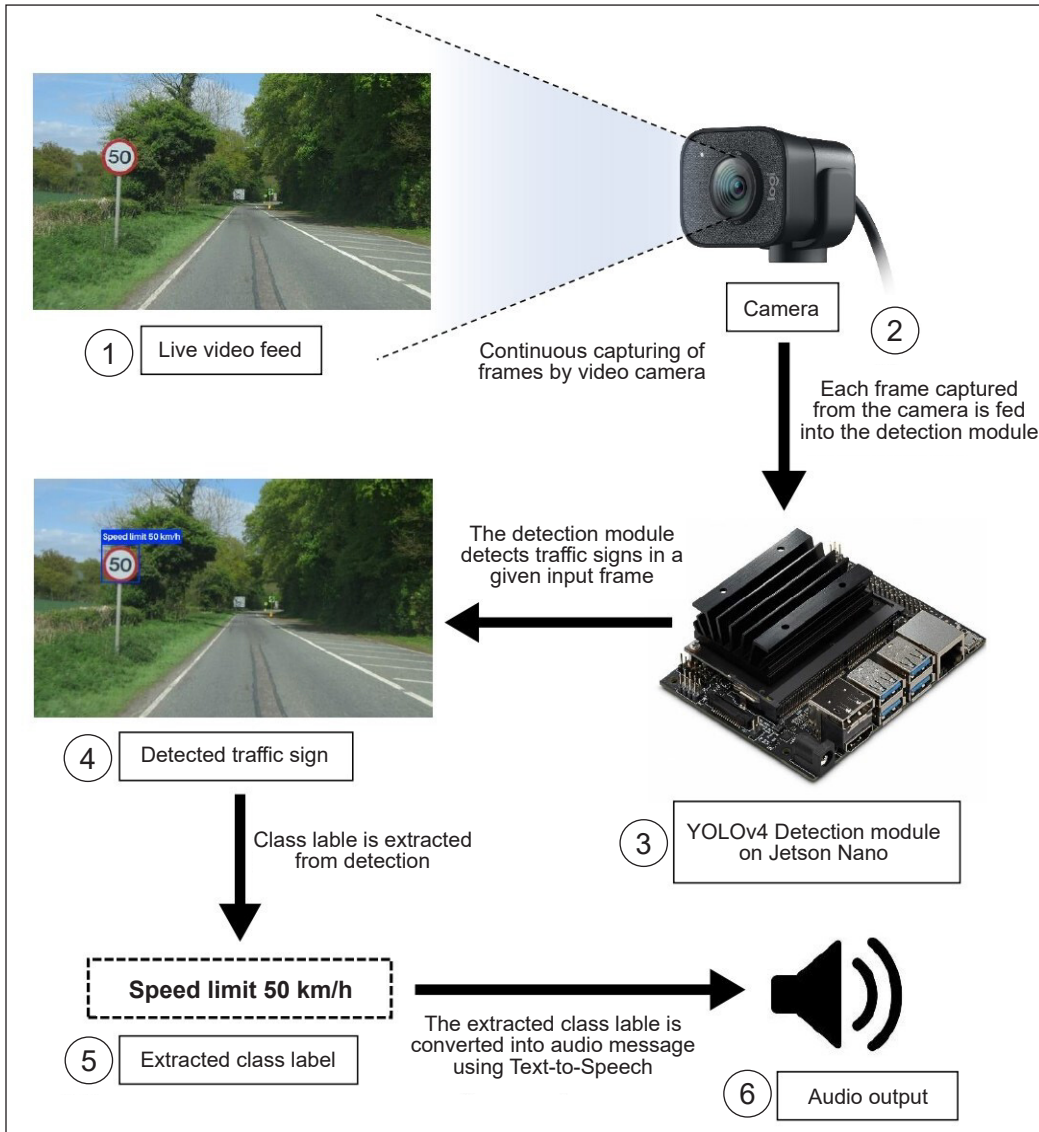


Figure 4. Proposed system design

models and offers exceptional throughput. Even though the frame rate of the YOLOv4 model is moderate, the YOLOv4-Tiny gave exceptional results. The frame rate obtained using YOLOv4-Tiny is on par with the real-time implementation requirements; hence DeepStream performs better than Darknet and TensorRT.

The next step is to translate the detected traffic signs into audio messages. The audio message corresponding to the detected traffic sign would be loaded from the secondary storage when a detection occurs and is given as output. It reduces the overhead of generating audio during execution, slowing down the processing of each frame.

## RESULTS AND DISCUSSION

The model was tested with multiple network resolutions of  $320 \times 320$ ,  $416 \times 416$ ,  $512 \times 512$  and  $608 \times 608$ . Mean Average Precision (mAP) is chosen as the performance evaluation metric, which is a precision averaged over all classes of traffic signs. The mAP values were obtained by testing the model on a test set of 297 images. Table 3 shows comparative results of mAP and frame rate for various network resolution sizes using Darknet, TensorRT and DeepStream 5.1.

Table 3  
*Performance comparison in terms of mAP and frame rate of different models*

Model	Network Resolution	mAP <sup>50</sup>	Frame rate (FPS)		
			Darknet	TensorRT	DeepStream
YOLOv4	$320 \times 320$	67.83	2.4	4.9	7.5
YOLOv4	$416 \times 416$	70.82	1.6	3.6	4.9
YOLOv4	$512 \times 512$	72.65	1.3	3.0	4.0
YOLOv4	$608 \times 608$	68.80	0.8	2.1	2.5
YOLOv4-Tiny	$320 \times 320$	54.68	12.4	11.2	53.7
YOLOv4-Tiny	$416 \times 416$	67.82	11.5	10.2	38.2
YOLOv4-Tiny	$512 \times 512$	71.21	10.5	9.3	32.5
YOLOv4-Tiny	$608 \times 608$	76.55	7.3	7.6	20.5

From analysing the results, it is seen that the mAP value of the model increases as the network resolution size increases. We observe a deviation from this trend for the highest resolution of YOLOv4 at  $608 \times 608$  due to an increase in false positives because of duplicate bounding boxes. The highest mAP value achieved is 76.55% by YOLOv4-tiny at  $608 \times 608$ . The frame rate gradually decreases for both models as the network resolution increases. The reason behind this trend is that many features in the input image reduce the speed. However, the accuracy is better for higher input sizes.

An optimal architecture can be chosen depending on the practical TSR application requirements. For example, if faster processing is required, Tiny YOLOv4 architecture can be preferred over YOLOv4 architecture as it utilises less memory. However, if accuracy is an important criterion, YOLOv4 architecture can be preferred over Tiny YOLOv4. The memory consumption in YOLOv4 is quite high as it is computationally intensive but gives better accuracy. In this study, the focus is on building a real-time system. Thus, considering the importance of processing speed in this case, YOLOv4-Tiny architecture using DeepStream at  $512 \times 512$  is chosen as the optimal architecture, which gives a mAP of 71.21% and 32.5 FPS, yielding about three times better frame rate than Darknet and TensorRT.

Even though the model is trained on limited data, it performs well in challenging conditions, as depicted in Figure 5. The sign in Figures 5(a) and 5(b) have been detected



with good accuracy despite occlusion and deterioration of the traffic signs. The model also performs well at night as well as in rainy conditions, as shown in Figures 5(c) and 5(d), 5(e) and 5(f), respectively.

However, the model does not perform very well in detecting traffic signs that are small and far away, and the samples for the same condition are shown in Figure 6. The detector shows a moderate performance for the speed limit traffic signs in comparison with the other five classes, as seen in Figure 6(a). It is because classes of speed limits are very



Figure 5. Detection samples: (a) and (b) are in dim lighting conditions; (c) and (d) are during night-time; (e) and (f) are in rainy weather conditions

similar to each other. Thus, with training images as low as 300, the model has difficulty distinguishing the speed limit signs.

Due to the fairly small size and distant image of the traffic sign, detection is either missed, as in the case of Figure 6(c) or resulted in false detection, as seen in Figure 6(b). Deterioration of the traffic sign, as seen in Figure 6(d), makes it difficult for the detector to detect the sign; hence a missed detection is observed. Despite some failed detections, the model performs well in many complex conditions and is robust against scale changes. The attempt to provide output in the form of audio messages was also feasible. Thus, the model can detect 10 classes of urban traffic signs at a decent accuracy in real-time and provide audio alerts to the driver.



Figure 6. Detection samples: (a) and (b) are wrong class predictions; (c) and (d) are no class predictions

## CONCLUSION

This paper discusses the implementation of a Traffic Sign Recognition System for Indian roads on the NVIDIA Jetson Nano using YOLOv4 architecture. The proposed solution is a good choice to be used as a Traffic Sign Recognition System as a part of ADAS, where it gives accuracy in the range of 54.68–76.55% for different input network resolutions. This module is integrated with the audio module to give the final output as an audio message.

The YOLOv4-Tiny model with DeepStream implementation was able to achieve an FPS of 32.5, which is on par with real-time detection requirements. However, despite its good overall performance, the ideal performance is yet to be achieved due to some missed and false detections. It can be improved by fine-tuning the neural network and expanding the training dataset. Furthermore, the designed system can be integrated with other subsystems like lane detection, navigation system, and obstacle detection with hardware assistance to form a complete ADAS.

## ACKNOWLEDGEMENTS

The authors thank NVIDIA pvt Ltd. for donating the Jetson Nano Developer kit used to conduct this project.

## REFERENCES

- Bochkovskiy, A., Wang, C. Y., & Liao, H. Y. M. (2020). *YOLOv4: Optimal speed and accuracy of object detection*. arXiv Preprint. <http://arxiv.org/abs/2004.10934>
- Do, H. N., Vo, M. T., Luong, H. Q., Nguyen, A. H., Trang, K., & Vu, L. T. K. (2017). Speed limit traffic sign detection and recognition based on support vector machines. In *2017 International Conference on Advanced Technologies for Communications (ATC)* (pp. 274-278). IEEE Publishing. <https://doi.org/10.1109/ATC.2017.8167633>
- Ellahyani, A., El Ansari, M., El Jaafari, I., & Charfi, S. (2016). Traffic sign detection and recognition using features combination and random forests. *International Journal of Advanced Computer Science and Applications*, 7(1), 686-693. <https://doi.org/10.14569/IJACSA.2016.070193>
- Hasegawa, R., Iwamoto, Y., & Chen, Y. W. (2019). Robust detection and recognition of japanese traffic sign in the complex scenes based on deep learning. In *2019 IEEE 8th Global Conference on Consumer Electronics (GCCE)* (pp. 575-578). IEEE Publishing. <https://doi.org/10.1109/GCCE46687.2019.9015419>
- Hegadi, R. S. (2011). Automatic traffic sign recognition. In *Proceedings of International Conference on Communication, Computation, Management & Nanotechnology* (pp. 1-5). REC Bhalki.
- Islam, M. T. (2019). Traffic sign detection and recognition based on convolutional neural networks. In *2019 International Conference on Advances in Computing, Communication and Control (ICAC3)* (pp. 1-6). IEEE Publishing. <https://doi.org/10.1109/ICAC347590.2019.9036784>
- Koresh, M. H. J. D. (2019). Computer vision based traffic sign sensing for smart transport. *Journal of Innovative Image Processing*, 1(1), 11-19. <https://doi:10.36548/jiip.2019.1.002>
- Lu, X., Kang, X., Nishide, S., & Ren, F. (2019). Object detection based on SSD-ResNet. In *2019 IEEE 6th International Conference on Cloud Computing and Intelligence Systems (CCIS)* (pp. 89-92). IEEE Publishing. <https://doi.org/10.1109/CCIS48116.2019.9073753>
- Luo, H., Yang, Y., Tong, B., Wu, F., & Fan, B. (2018). Traffic sign recognition using a multi-task convolutional neural network. *IEEE Transactions on Intelligent Transportation Systems*, 19(4), 1100-1111. <https://doi.org/10.1109/TITS.2017.2714691>

- Muthukumaresan, T., Kirubakaran, B., Kumaresan, D., Satheesan, A., & Prakash, A. J. (2016). Recognition of traffic sign using support vector machine and fuzzy cluster. *International Journal of Science Technology & Engineering*, 2(10), 190-197.
- Oltean, G., Florea, C., Orghidan, R., & Oltean, V. (2019). Towards real time vehicle counting using YOLO-Tiny and fast motion estimation. In *2019 IEEE 25th International Symposium for Design and Technology in Electronic Packaging (SIITME)* (pp. 240-243). IEEE Publishing. <https://doi.org/10.1109/SIITME47687.2019.8990708>
- Sari, A., & Cibooglu, M. (2018). Traffic sign detection and recognition system for autonomous RC cars. In *2018 6th International Conference on Control Engineering & Information Technology (CEIT)* (pp. 1-5). IEEE Publishing. <https://doi.org/10.1109/CEIT.2018.8751898>
- Tabernik, D., & Skocaj, D. (2020). Deep learning for large-scale traffic-sign detection and recognition. *IEEE Transactions on Intelligent Transportation Systems*, 21(4), 1427-1440. <https://doi.org/10.1109/TITS.2019.2913588>
- Zhang, J., Huang, M., Jin, X., & Li, X. (2017). A real-time Chinese traffic sign detection algorithm based on modified YOLOv2. *Algorithms*, 10(4), Article 127. <https://doi.org/10.3390/a10040127>
- Zhong, Z., Zheng, L., Kang, G., Li, S., & Yang, Y. (2020). Random erasing data augmentation. *Proceedings of the AAAI Conference on Artificial Intelligence*, 34(07), 13001-13008. <https://doi.org/10.1609/aaai.v34i07.7000>
- Zoph, B., Cubuk, E. D., Ghiasi, G., Lin, T. Y., Shlens, J., & Le, Q. V. (2019). *Learning data augmentation strategies for object detection*. arXiv Preprint.



*Review Article*

## **A Systematic Review on an Optimal Dose of Disaster Preparedness Intervention Utilizing Health Belief Model Theory**

**Mohd Tariq Mhd Noor<sup>1</sup>, Hayati Kadir Shahar<sup>1,2\*</sup>, Mohd Rafee Baharudin<sup>1</sup>, Sharifah Norkhadajah Syed Ismail<sup>1</sup>, Rosliza Abdul Manaf<sup>1</sup>, Salmiah Md Said<sup>1</sup>, Jamilah Ahmad<sup>3</sup> and Sri Ganesh Muthiah<sup>1</sup>**

<sup>1</sup>*Department of Community Health, Faculty of Medicine and Health Sciences, Universiti Putra Malaysia, 43400 UPM, Serdang, Selangor, Malaysia*

<sup>2</sup>*Malaysian Research Institute of Ageing (MyAgeing), Universiti Putra Malaysia, 43400 UPM, Serdang, Selangor, Malaysia*

<sup>3</sup>*School of Communication, Universiti Sains Malaysia, 11800 USM, Pulau Pinang, Malaysia*

### **ABSTRACT**

Disaster preparedness is an issue that receives little attention in the community. Communities must take preventative measures to overcome obstacles and improve community preparedness. This review identifies the optimal dose of disaster preparedness intervention in the community. A systematic literature search was conducted to examine a study about the optimal dose of disaster preparedness intervention developed for implementation at a community level. A scoping review based on the PRISMA diagram was conducted from four databases. A combination of keywords was adapted for each database. Inclusion and exclusion criteria were applied. A total of eight articles were

synthesized based on the intervention dose of disaster preparedness among community interventions. The summarized studies provided evidence that the optimal dose for disaster preparedness intervention in the community can be prevented with an educational intervention program with a minimal dosage of intervention. The Health Belief Model Theory was the most often cited theory by researchers. The best dose for disaster preparedness intervention in a community can be mitigated with a single dose of education. Nonetheless, we cannot

#### **ARTICLE INFO**

*Article history:*

Received: 26 July 2021

Accepted: 09 May 2022

Published: 21 October 2022

DOI: <https://doi.org/10.47836/pjst.31.1.10>

*E-mail addresses:*

drariq84@gmail.com (Mohd Tariq Mhd Noor)

hayatik@upm.edu.my (Hayati Kadir Shahar)

mohdrafee@upm.edu.my (Mohd Rafee Baharudin)

norkhadajah@upm.edu.my (Sharifah Norkhadajah Syed Ismail)

rosliza\_abmanaf@upm.edu.my (Rosliza Abdul Manaf)

salmiahms@upm.edu.my (Salmiah Md Said)

jahmad@usm.my (Jamilah Ahmad)

sriganesh@upm.edu.my (Sri Ganesh Muthiah)

\* Corresponding author

disregard alternative disaster preparedness theories because each has its advantages and disadvantages.

*Keywords:* Community, disaster preparedness, flood, health belief model, health education, intervention, optimal dose, theory

---

## **BACKGROUND**

Three hundred thirty-five natural disasters struck 95.6 million people in 2017, killing up to 9,697 and causing \$335 billion in damage. With 44% of all disastrous occurrences, 58% of deaths, and 70% of persons affected by events worldwide, Asia is the most disastrous continent for disasters like floods and storms. For example, between 1998 and August 2018, a period of two decades, Malaysia was hit by 51 natural disasters (MERCY Malaysia, 2019). During that time, 281 people perished, almost 3 million people were harmed, and approximately \$2 billion worth of damage was caused (MERCY Malaysia, 2019). A disaster is an occurrence that occurs when a significant number of people are exposed to hazards to which they are vulnerable, resulting in injury and death, as well as property destruction. According to United Nations Office for Disaster Risk Reduction research, China had the most catastrophes with 286 from 2005 to 2014, followed by the United States with 212 and the Philippines with 181 disasters (United Nations, 2015).

### **Problem Statement**

One of the crucial decisions investigators must make when creating a behavioral intervention is selecting the best dose of the intervention in terms of duration, frequency, and volume (Voils et al., 2014). According to interventional researchers, optimizing prospective behavioral intervention theories is a good goal. Alternatively, the researcher must consider how the improved intervention will promote public health by reaching more people and providing more significant and long-term benefits to those who receive it. Optimized interventions also contribute to the body of knowledge by producing meaningful studies with higher statistical power to discover the true treatment effect. Although there is no commonly agreed process for optimizing intervention and delivery, investigating individual and component operations rather than the entire requires an efficient and scientific method (Voils et al., 2014). As a result, if this intervention proves beneficial, it will help improve the community's current disaster readiness.

### **Significance of Study**

The optimal dose for multiple behavior treatments considerably impacts public health more than single-behavior interventions. The comparison of theories and substantial behavior studies, on the other hand, creates several additional issues. Among these are

adopting standard measures across behaviors, enhancing treatment fidelity, and finding novel strategies to promote recruitment and retention, particularly among diverse groups. In addition, it may improve behavioral change measurement and assessment and expand the reach and translation of practical intervention approaches (Nigg et al., 2002). As a result, to scientifically improve the influence of the outcome, it is necessary to establish the ideal dose in the behavioral intervention study. Individuals, health care providers, and the government rarely address disaster preparations in the community until issues develop. The community is ignorant that vulnerable people, such as women, children, and the elderly, require special consideration in disaster planning (Luna, 2001).

## **MATERIALS AND METHODS**

The systematic review was conducted by searching available electronic databases and published research and review bibliographies. First, the databases were thoroughly searched, beginning with generic terms to identify relevant search terms. The PRISMA (Preferred Reporting Items for Systematic Review and Meta-Analysis) acronym stands for “Preferred Reporting Items for Systematic Review and Meta-Analysis” (Schulz et al., 2010).

### **Data Extraction and Quality Assessment**

This systematic review used PubMed, Science Direct, Medline, and CINAHL databases. In addition, a comprehensive literature search was conducted systematically through an electronic database; PubMed, Ovid, ScienceDirect and Scopus. The articles reported for the past ten years were searched with the terms: “disaster preparedness,” “disaster preparedness intervention theory,” “disaster preparedness,” and “theory.” Boolean operator combined these exact phrases “and.” The literature searched was limited to articles and reports in the English language.

The study titles were initially screened, and the abstracts were analyzed to determine their relevance to this systematic review. The full text of the articles was then obtained, and only the studies that met the inclusion and exclusion criteria were chosen. The study’s population was a community. The respondents were divided into two groups: those who received the intervention and those who did not. The outcome was those who had increased their level of disaster preparedness. The systematic review included only experimental studies, randomized control trials (RCT) or quasi-experiments.

### **Inclusion and Exclusion Criteria**

The systematic review used English full-text availability and was conducted among the community as inclusion criteria. Exclusion criteria included duplication of studies or studies



conducted among different groups. In addition, the author names, titles, and sample sizes of duplicate publications were compared. The details extracted include the author's name, the year of publication, and the research's location. Other information includes publication details (trial, acronym, enrollment period, year of publication), study design, sample size, inclusion and exclusion criteria, intervention used, and study outcome. Any disagreements among the reviewers were settled by consensus.

### Search Result and Study Description

After removing duplicated studies, the electronic search strategy yielded 60 articles. Following a review of the title and abstract, twenty articles were removed. Twenty articles were obtained and reviewed for eligibility. After reviewing full articles, 15 articles that met the inclusion and exclusion criteria were reviewed for secondary screening. Eight articles were included in the systematic review after full articles were reviewed depicted in Figure 1. Seven papers were excluded due to duplicates, non-randomized studies, inappropriate control groups, and outcomes. The lack of quantitative evidence from local studies was a major issue due to the limited availability of databases with a wide scope.

### RESULTS

After reviewing the complete text, more than 60 results were returned, eight relevant to this study. Next, the principal researcher reviewed all the full text to ensure its relevance,

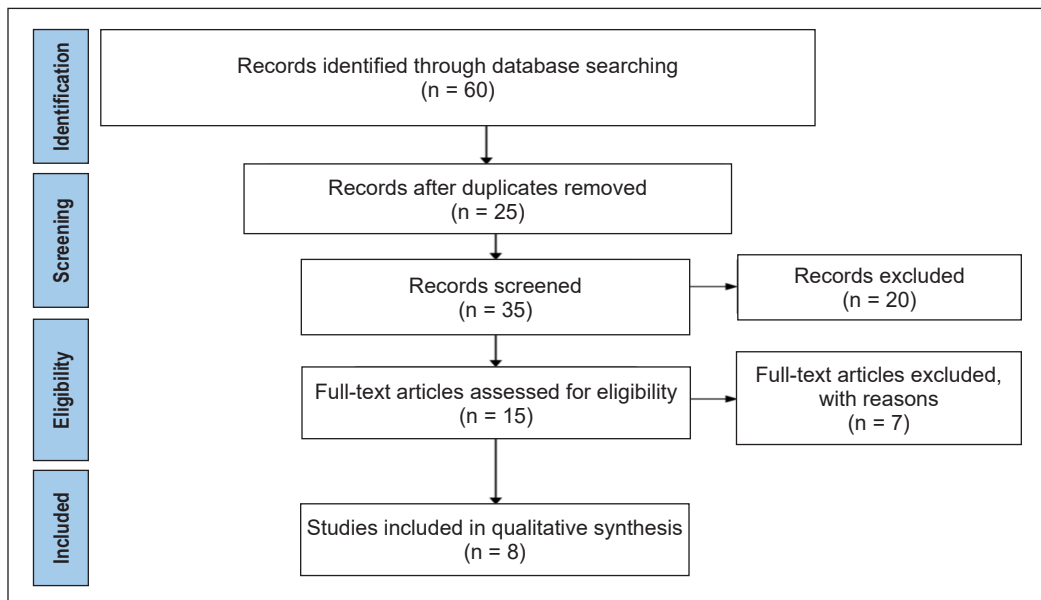


Figure 1. PRISMA Diagram of article reviews for the Optimal Dose of Disaster Preparedness Intervention Utilising Health Belief Model Theory

Source: Moher et al. (2009). For more information, visit [www.prisma-statement.org](http://www.prisma-statement.org).

Table 1  
Dose and theory intervention of disaster preparedness

No.	Authors	Type of Study	Intervention's implementation, duration, follow-ups, and delivery	Theory	Intervention Dose	Results, Attrition rates, Intervention vs. Control
1	(Ardalan et al., 2013)	RCT	A controlled community intervention (health education) trial with pre-and post-assessments was conducted in 2011 in 3 provinces of Iran. In each province, two areas were chosen and randomly selected as an intervention or control group.	Community risk perception changes (Health Belief Model Theory)	One dose of intervention and post-assessment have given after three months of intervention. The total study duration of 6 months.	There were relative changes in awareness in intervention and control areas $p < 0.01$ . Relative changes for readiness scores were 5.52 in intervention areas and 0.56 in control areas ( $P < 0.01$ ). The result was significantly correlated with a community's baseline risk perception and previous experience with natural disasters ( $P < 0.01$ ).
2	(Ebi & Semenza, 2008)	RCT	Divided into urban intervention and rural intervention.	Community-based adaptation (Health believes model)	One dose of intervention but not mentioned duration post-assessment and the study duration.	Improvements in mental health ( $p = 0.03$ ), a greater sense of community ( $p < 0.01$ ), expansion of social interactions ( $p = 0.06$ ), and total growth of social capital ( $p = 0.01$ ) were all significant differences in the urban intervention. The adjusted odds ratio for participation in an evacuation drill in the intervention area in post-assessment compared with pre-assessment was 29.05 (95% confidence interval [CI]: 21.77-38.76), whereas in the control area, it was 2.69 (95% CI: 1.96-3.70) with $p < 0.01$ .
3	(Ardalan et al. 2010)	RCT	Fifteen intervention villages and 16 control villages in Golestan province of Iran.	Health belief model (for perception component)	One dose of intervention and post-assessment have given after three months of intervention. 6-month study duration.	

Table 1 (continue)

No.	Authors	Type of Study	Intervention's implementation, duration, follow-ups, and delivery	Theory	Intervention Dose	Results, Attrition rates, Intervention vs. Control
4	(Pesiridis et al., 2015)	RCT	Two hundred seven hospital-based nurses were randomly assigned into intervention ( $n = 112$ ) and original control ( $n = 95$ ) groups.	Knowledge, Attitudes and Practices Theory	One dose of intervention and post-assessment was given immediately after training and six months later 6 months, the study duration.	The intervention increased nurses' knowledge and self-confidence but had no significant effect on behavioral intentions. The mean knowledge score increased significantly in both groups at times two and three as compared to time one [pre-test: 6.43 (2.8); post-test: 16.49 (1.7); follow-up test: 13.5 (2.8)], ( $P < 0.002$ ). Between the intervention and control groups, changes in knowledge were significantly different ( $P < 0.001$ ) and had a large effect size (eta-squared = 0.8). The overall model shows a moderate degree of significance [ $F(9,177) = 6, P < 0.000$ , adjusted $r^2 = 0.23$ ] for changes in decision-making for the communication plan. Findings for changes in decision-making stages for disaster supplies are barely significant. The only significant predictor has perceived self-efficacy, with a marginal $P$ -value.
5	(Glik et al., 2014)	RCT	Between 2006 and 2007, the study was done in Los Angeles in a low-income neighborhood with a high concentration of Latino residents. Only one adult per family was eligible, and 242 respondents were recruited in the initial sample. Once enrolled in the study, each participant was randomized to a block of six to ten persons depending on their zip code. A computer-generated random number determined which arm of the experiment they were randomly assigned to.	Precaution adoption process model	One dose of intervention and a questionnaire gave after three months of intervention. 6-month intervention.	

Table 1 (continue)

No.	Authors	Type of Study	Intervention's implementation, duration, follow-ups, and delivery	Theory	Intervention Dose	Results, Attrition rates, Intervention vs. Control
6	(Eisenman et al., 2009a)	RCT	This study was a community-based, randomized, longitudinal cohort design with two groups. Assessments were made at baseline and three months.	Health belief model (for perception component)	Two doses of intervention with pre-assessment at baseline, three months, and post-assessment at 6-month after the intervention. A total of 9-month study duration.	There was a significantly different before and after intervention through media education ( $p < 0.01$ ).
7	(Thomas et al., 2018)	RCT	Two hundred eight respondents were included in this study, embarking on preparedness interventions that optimize the potential for individuals to adopt preparedness behavior.	Health believes model	Two doses of intervention with pre-assessment at baseline, three months, and post-assessment at 6-month after the intervention. A total of 9-month study duration.	Results suggest that the intervention was effective in improving participants' household disaster preparedness knowledge ( $P < 0.01$ ), attitudes ( $P < 0.01$ ), and community resiliency.
8	(James, et al., 2019)	RCT	The research included 480 randomly selected community members drawn from three disaster-affected communities. Randomize allocation to the control and intervention groups.	Community-based intervention with mental health intervention using a theoretical model (HBM)	Three doses of intervention with pre-assessment at baseline, three months, and post-assessment at 3-month after the last intervention. A total of 9-month study duration.	The intervention increased disaster preparedness, reduced symptoms associated with depression, post-traumatic stress disorder, anxiety, and functional impairment, and increased peer-based help-giving and help-seeking.

including bibliographic references and conducted critical author and grey literature searches. It proved an effective complementary approach to the original review, and the search was reverted to the original. This method resulted in a total of eight relevant full-text results. Table 1 summarizes the intervention dose for a health education-based intervention for disaster preparedness. Most studies were randomized controlled trials.

## **DISCUSSION**

### **Assessment Gap**

Five of the eight articles used intervention only once during the study, two used interventions twice, and one used them extensively. As a result, most studies used a single intervention that lasted six months and was carried out concurrently. Most results are similar to the findings of the article study in Iran. The four research projects involved in the study included three provinces in Iran and analysis of urban and rural areas in countries such as the United States. The study was carried out in a remote city in Golestan, and the study was carried out in Los Angeles (Ardalan et al., 2010; Ebi & Semenza, 2008; Glik et al., 2014). All four of these studies found that there was still a significant level change for the researcher's items three months after the intervention.

Moreover, a similar intervention dose was studied with a six-month assessment gap showed a significant change immediately after the study and six months later. Finally, it demonstrated that an intervention dose with a study gap of six to nine months still shows significant changes in items measured compared to the study's control sample (Bostick et al., 2017; Pesiridis et al., 2015).

### **Theories**

All five articles from a single dose intervention concerning disaster preparedness at the community level apply specific theories. Of the five articles, three used HBM theory, one used the precaution adoption process model, and one used the Theoretical model for KAP theory. Most articles use HBM theory to plan disaster intervention using a single intervention dose in the community. Among the articles that used HBM theory is the Republic of Iran, which used six months of intervention by developing intervention modules based on HBM theory. The research has found that community preparedness was highly significant before and after six months of the intervention program, with  $p < 0.01$  for each component in the intervention module (Ardalan et al., 2010).

### **Intervention Dose**

Two separate studies on two doses of intervention, one conducted on Latinos in Los Angeles and another on homemakers in the United States, lasted nine months (Chandler

et al., 2016; Eisenman et al., 2009). These studies were evaluated three to six months after the intervention, and both showed significant changes in the assessed things. As a result, even though the studies were conducted in two different locations, the differences measured revealed significant differences.

Furthermore, two doses of intervention were carried out for research in a Los Angeles community with 231 participants via social media and small group discussion. The study used the perceived concept from the HBM component. The small group discussion intervention based on HBM theory significantly improved disaster preparedness more than the social media arm (Eisenman et al., 2009). In other research, such as in Atlanta, an intervention involving the community and civil service exhibited a significant improvement in disaster preparedness after applying module and intervention components based on HBM theory with two doses of intervention (Thomas et al., 2018). Other studies, such as one conducted in Atlanta, which involved the community and civil service, revealed a significant improvement in disaster preparedness after implementing a module and intervention component based on HBM theory with two doses of intervention.

In addition, a study in Haiti explains three doses of interventions using the Health Belief Model Theory, with an assessment three months after the intervention. This study found that there were significant changes in the variables studied. As a result, if we look at all the interventions carried out, we can see that the intervention findings remained significant even though the dose varied. Furthermore, these articles demonstrated that even six months after the intervention, the assessment still revealed significant changes (Glik et al., 2014; James et al., 2019).

## CONCLUSION

Each author or researcher provided evidence of a post-intervention assessment conducted within six months of the intervention. However, no author demonstrated or evaluated the intervention after one year, two years, or longer. As a result, the outcome may be unpredictable. Meanwhile, module characteristics and research location played a significant role in determining the estimated result because they influenced respondents' decision to use or not use the intervention. Nonetheless, most of the publications examined demonstrate that the authors' incorporated modules and components from HBM theory when developing modules and implementing the intervention.

Additionally, the investigation's findings indicate that all articles exhibited behavioral changes. It indicates that a single dose of disaster preparedness intervention can significantly alter an individual's behavior from unprepared to prepared. Nonetheless, we cannot dismiss alternative theories and methods for disaster preparedness because each has unique advantages and applicability in a community. The optimal dose for each intervention was generally irrelevant to the end result, whether one dose, two doses, or three doses or more.

Dose determination is difficult due to a lack of a dose framework and dose selection guidelines. Additional variables such as quantity, exposure, and engagement must be considered when assessing the effectiveness of subsequent interventions presented to the respondent. Community knowledge, skills, and preparedness significantly increased regardless of the methodology used. Thus, investigators should develop a strategy for assessing intervention quality prior to conducting research, which should include determining the number of intervention contacts and the duration of each contract.

Finally, this literature review demonstrates that research is being conducted to ascertain the optimal dose. It is well established that interventions focused on health education and utilizing HBM improve community knowledge, skills, and preparedness. A single treatment dose resulted in statistically significant changes in pre- and post-treatment periods. Future research may examine additional behavioral theories pertaining to community education interventions and their effectiveness. A complex program can be evaluated using the HBM theoretical framework. The determined intervention doses may be particularly advantageous in comparative trials. This information is valuable if a deviation from the protocol results in variation in outcomes both within and across treatment arms and trials using similar interventions.

## ACKNOWLEDGEMENTS

The authors appreciate the guidance and help given by the Department of Community Health, Faculty of Medicine, Universiti Putra Malaysia, Malaysian Research University Network grant for sponsoring this study [Grant number MRUN Grant PT.S(BPK)2000/09/01/046(51)], all the project Members from Universiti Putra Malaysia (UPM), Universiti Teknologi Malaysia (UTM), Universiti Kebangsaan Malaysia (UKM), Universiti Sains Malaysia (USM) and Research Management Centre, UPM.

## REFERENCES

- Ardalan, A., Naieni, K. H., Mahmoodi, M., Zanganeh, A. M., Keshtkar, A. A., Honarvar, M. R., & Kabir, M. J. (2010). Flash flood preparedness in Golestan province of Iran: A community intervention trial. *American Journal of Disaster Medicine*, 5(4), 197-214. <https://doi.org/10.5055/ajdm.2010.0025>
- Bostick, T. P., Holzer, T. H., & Sarkani, S. (2017). Enabling stakeholder involvement in coastal disaster resilience planning. *Risk Analysis*, 37(6), 1181-1200. <https://doi.org/10.1111/risa.12737>
- Chandler, T., Abramson, D. M., Panigrahi, B., Schlegelmilch, J., & Frye, N. (2016). Crisis decision-making during hurricane sandy: An analysis of established and emergent disaster response behaviors in the New York Metro Area. *Disaster Medicine and Public Health Preparedness*, 10(3), 436-442. <https://doi.org/10.1017/dmp.2016.68>
- Ebi, K. L., & Semenza, J. C. (2008). Community-based adaptation to the health impacts of climate change. *American Journal of Preventive Medicine*, 35(5), 501-507. <https://doi.org/10.1016/J.AMEPRE.2008.08.018>



- Eisenman, D. P., Glik, D., Gonzalez, L., Maranon, R., Zhou, Q., Tseng, C.H., & Asch, S. M. (2009). Improving Latino disaster preparedness using social networks. *American Journal of Preventive Medicine*, 37(6), 512-517. <https://doi.org/10.1016/J.AMEPRE.2009.07.022>
- Glik, D. C., Eisenman, D. P., Zhou, Q., Tseng, C. H., & Asch, S. M. (2014). Using the precaution adoption process model to describe a disaster preparedness intervention among low-income Latinos. *Health Education Research*, 29(2), 272-283. <https://doi.org/10.1093/her/cyt109>
- James, L. E., Welton-Mitchell, C., Noel, J. R., & James, A. S. (2019). Integrating mental health and disaster preparedness in intervention: A randomized controlled trial with earthquake and flood-affected communities in Haiti. *Psychological Medicine*, 50(2), 342-352. <https://doi.org/10.1017/S0033291719000163>
- Luna, E. M. (2001). Disaster mitigation and preparedness: The case of NGOs in the Philippines. *Disasters*, 25(3), 216-226. <https://doi.org/10.1111/1467-7717.00173>
- MERCY Malaysia. (2019). *Malaysia: Disaster management reference handbook (June 2019) Malaysia*. ReliefWeb. <https://reliefweb.int/report/malaysia/malaysia-disaster-management-reference-handbook-june-2019>
- Moher, D., Liberati, A., Tetzlaff, J., & Altman, D. G. (2009). Preferred Reporting Items for Systematic Reviews and Meta-Analyses: The PRISMA Statement. *PLoS Med* 6(7): e100097. doi:10.1371/journal.pmed100097
- Nigg, C. R., Allegrante, J. P., & Ory, M. (2002). Theory-comparison and multiple-behavior research: Common themes advancing health behavior research. *Health Education Research*, 17(5), 670-679. <https://doi.org/10.1093/her/17.5.670>
- Pesiridis, T., Sourtzi, P., Galanis, P., & Kalokairinou, A. (2015). Development, implementation and evaluation of a disaster training programme for nurses: A switching replications randomized controlled trial. *Nurse Education in Practice*, 15(1), 63-67. <https://doi.org/10.1016/J.NEPR.2014.02.001>
- Schulz, K. F., Altman, D. G., & Moher, D. (2010). CONSORT 2010 statement: Updated guidelines for reporting parallel group randomized trials. *Annals of Internal Medicine*, 152(11), 726-732. <https://doi.org/10.7326/0003-4819-152-11-201006010-00232>
- Thomas, T. N., Sobelson, R. K., Wigington, C. J., Davis, A. L., Harp, V. H., Leander-Griffith, M., & Cioffi, J. P. (2018). Applying Instructional design strategies and behavior theory to household disaster preparedness training. *Journal of Public Health Management and Practice*, 24(1), e16-e25. <https://doi.org/10.1097/PHH.0000000000000511>
- United Nations. (July 29, 2015). *World population projected to reach 9.7 billion by 2050*. United Nations Department of Economic and Social Affairs. <http://www.un.org/en/development/desa/news/population/2015-report.html>
- Voils, C. I., King, H. A., Maciejewski, M. L., Allen, K. D., Yancy, W. S., & Shaffer, J. A. (2014). Approaches for informing optimal dose of behavioral interventions. *Annals of Behavioral Medicine*, 48(3), 392-401. <https://doi.org/10.1007/s12160-014-9618-7>



*Review Article*

## A Review: Requirements Prioritization Criteria Within Collaboration Perspective

Tan Amelia<sup>1,2\*</sup> and Rozlina Mohamed<sup>1</sup>

<sup>1</sup>Faculty of Computing, Universiti Malaysia Pahang, UMP 26600 Pekan, Pahang, Malaysia

<sup>2</sup>Department of Information System, Universitas Dinamika, 60298 Surabaya, Jawa Timur, Indonesia

### ABSTRACT

The attributes or criteria used in the requirements prioritization process become an essential reference in calculating priorities. Most of the techniques are used to increase the value impacting business success. On the contrary, there are limitations on cost, time, and resources for developing software. Therefore, the requirements prioritization process often requires collaboration from the perspectives involved. So far, the pattern and basis have not been seen in the criteria used in the requirements prioritization process. Consequently, there need to be other factors that become a reference so that the selection of criteria is appropriate. This study identifies criteria based on the categorized perspectives of requirements prioritization. A systematic literature review presents criteria for prioritizing requirements from multiple collaborative perspectives. Findings show that the criteria in requirements prioritization can be classified into beneficial and non-beneficial, where business value and development cost are the most frequently used criteria. Furthermore, the involvement of multiple perspectives in requirements prioritization focuses on the client's and developer's perspectives. The findings also reveal that some of the challenges in the requirements prioritization process are biases by stakeholders, reducing pairwise comparison, and scalability. In the future, it will be investigated whether the selection of criteria correlated with stakeholder perspectives will increase the accuracy of priorities. Thus, the contribution of this paper is to recommend criteria from stakeholders' perspectives.

#### ARTICLE INFO

*Article history:*

Received: 03 December 2021

Accepted: 24 May 2022

Published: 21 October 2022

DOI: <https://doi.org/10.47836/pjst.31.1.11>

*E-mail addresses:*

[meli@dinamika.ac.id](mailto:meli@dinamika.ac.id) (Tan Amelia)

[rozlina@ump.edu.my](mailto:rozlina@ump.edu.my) (Rozlina Mohamed)

\* Corresponding author

*Keywords:* Aspects, client's perspective, cost-value approach, developer's perspective requirements, models, methods, prioritization criteria, techniques

## INTRODUCTION

A software requirement is a service that must exist to solve software user problems. The requirements life cycle consists of five stages: trace, maintain, prioritize, assess, and approve. These stages aim to ensure that businesses, stakeholders, and the requirements and design of a solution align (IIBA, 2015). Requirements engineering is the first step in the software development process. Play an important role so that software developers can understand the needs of stakeholders and can economically create high-quality software (Dabbagh et al., 2014). Requirements that have passed the assessment and approval stage will then enter the management process, which consists of trace, maintain, and prioritize stages. Requirements prioritization is assessing the value, urgency, and risk associated with specific requirements and designs to ensure that analysis or work is carried out at the most fundamental level on time. Limited time and resources to fulfill the requirements are important factors in the requirements prioritization process (Babar et al., 2011; Riegel, 2012; Thakurta, 2016).

In Agile requirements engineering, the value-driven approach is emphasized for product development (Schön et al., 2017). Due to increased competition, focusing on user requirements and essential delivery has become important in product development. However, the decision to carry out prioritization requirements will be more difficult when many stakeholders are involved— because different stakeholders have different perspectives. In general, the perspective on seeing requirements is based on the point of view of clients and developers (Danesh et al., 2016; Gupta & Gupta, 2018; Idrus et al., 2011; Narendhar & Anuradha, 2016). Requirements are also prioritized by looking at the relationship between benefits and costs. By calculating the cost-benefit ratio, it can be seen how much the company will pay for the features that must be made. (Torrecilla-Salinas et al., 2015). Addedly, requirements prioritization techniques are based on business and technical aspects. (Sher et al., 2019, 2014).

The process of prioritizing requirements has two sides. On the one hand, it must be fast and straightforward, and on the other hand, it must produce accurate and reliable results. Stakeholders play an essential role in the priority process. As cited in Karlsson and Ryan (1997), there are three factors in stakeholder satisfaction mentioned by Shoji Shiba and his colleagues: cost, quality, and delivery. Software project success depends on the ability to minimize costs, on time and maximize quality.

Karlsson and Ryan use relative value and cost in prioritizing requirements called the cost-value approach. This approach builds customer satisfaction from values in potential candidate requirements. In contrast, costs are expenses incurred to produce candidate requirements (Karlsson & Ryan, 1997). Requirements cannot be completely collected at the start of the project due to various factors. Therefore, continuous interaction with

clients is critical to achieving the correct requirements. The agile manifesto emphasizes collaboration among the project team and stakeholders (Sverrisdottir et al., 2014).

In software development, the popular models that have been widely used are agile development methods. One of the agile approaches is delivering value and quality within the project development budget. This objective is highly appropriate for the cost-value approach to the requirement prioritization process that compares the value and cost of software implementation. Besides the presented perspective of the agile approach, compatibility of agile and cost-value can be observed from one of the agile manifestos, which highlights “how can we honestly say that our backlog is prioritized based on what delivers VALUE for our customer?” as well as agile principles, which declare that “business people and developers must work together daily throughout the project.” This harmony rises because, in the cost-value approach, the product owner is the one who will oversee determining relative values for candidate requirements. At the same time, the software development team is assigned relative costs for implementing each one of the candidate requirements.

One of the important aspects of the requirements prioritization process is determining the criteria used. The criteria in the prioritization process will affect the success of software development. According to Sher et al., requirements prioritization aspects are categorized into three groups: technical, business, and client (Sher et al., 2019). Most requirements prioritization techniques support these aspects since they influence decision-making in requirements prioritization. However, today’s trend shows that most techniques are not scalable and less supportive of business or client aspects. Riegel & Doerr divides the criteria into six main categories: Benefits, Technical Context & Requirement Characteristics, Risks, Costs, Penalties & Avoidance, and Business Context (Riegel & Doerr, 2015). Odu and Charles-Owaba believe all criteria are divided into beneficial and non-beneficial aspects. Each criterion valued is related to the pre-assigned weightage. The value is considered positive strength for the beneficial criteria and negative for the non-beneficial (Odu & Charles-Owaba, 2013).

The systematic literature review in this study focuses on the requirements prioritization domain. The nature of the project that uses requirements prioritization under study is bespoke software with medium-level requirements (number of requirements between 20 and 50). The motivation of this study is to investigate the correlation of attributes or criteria for prioritization requirements in a cost-value approach from a collaboration perspective. The collaboration perspective is the point of view of stakeholders involved, especially clients and developers. The contribution of this study is to find the criteria used with a cost-value approach in the requirements prioritization process from the perspective of the client and developer. The following paper is organized into materials, methods, results, discussion, and conclusions.

## MATERIALS AND METHODS

The correlation of attributes or criteria for requirements prioritization in a cost-value approach is investigated from a client’s and developer’s perspective. From the existing literature, the SLR is carried out based on the guidelines from Kitchenham (Kitchenham & Charters, 2007; Kitchenham et al., 2009).

Figure 1 shows the design review protocol for performing SLRs. The protocol review consists of six research phases:

research questions, search strings; resources; inclusion and exclusion criteria; quality assessment criteria; data collection and synthesis. The review methods process begins with the first phase, formulating a set of research questions to answer the research objectives. The second phase is to design a search strategy according to the research question, identify search terms and select literature data sources. The third phase is to extract the data that has been collected and assess the quality of the selected data. Finally, the fourth phase analyzes the data to answer the research objectives.

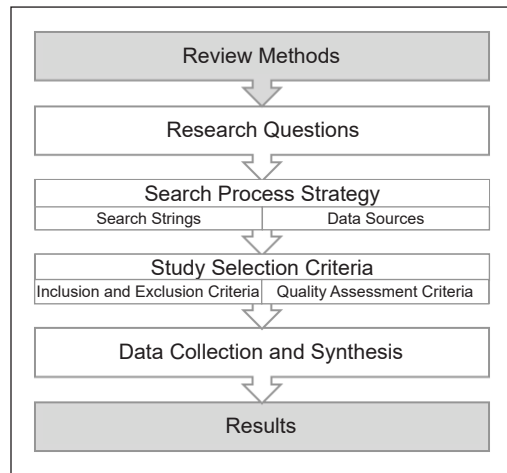


Figure 1. Review protocol

### Research Questions

The primary purpose of this study is to investigate the existing research on attributes or criteria in requirements prioritization. This research is also related to the perspectives of the requirements prioritization process, the stakeholders involved, and the mapping of criteria in perspective. The following is the formulation of the questions in this study:

- RQ1. What attributes or criteria are used in the requirements prioritization process?
- RQ2. What perspectives are involved in requirements prioritization, and how do we classify the requirements prioritization criteria based on view?
- RQ3. Who are the stakeholders that belong to each perspective?
- RQ4. How are the attributes or criteria grouped in each perspective?
- RQ5. What are the recommended improvements for the specified limitations or challenges?

RQ1 investigates the attributes or criteria used in requirements prioritization research. This investigation aims to find operational definitions of attributes or criteria in requirements prioritization and their popularity in the literature. RQ2 finds out what perspective is used in the requirements prioritization process and its effect on criteria. RQ3 looks for stakeholders involved in each perspective. RQ4 does a mapping between attributes or criteria with

perspectives in requirements prioritization. Finally, RQ5 provides recommendations on possible future trends in addressing the identified requirements prioritization challenges.

### **The Search Process Strategy**

The search for papers related to this research is carried out comprehensively. The search process is carried out online in digital libraries to find papers that have been published since 2010. The following is a step-by-step procedure for conducting a search based on a predefined research question:

1. First, identify critical terms based on research questions.
2. Second, find alternative synonyms and spellings of the primary terms.
3. Third, verify the search terms of the relevant studies.
4. Finally, use the Boolean OR/AND operator to combine search terms.

### **Search Strings**

The search string is developed in this study. The list of search strings used is as follows:

- Requirements Prioritization Models OR Framework OR Methods OR Techniques
- Cost-Value Approach for Requirements Prioritization Techniques OR Models OR Framework OR Methods
- Requirements Prioritization within Stakeholders OR Clients OR Developers Perspective OR View
- Collaborative Approach in Requirements Prioritization
- Requirements Prioritization in Agile
- Requirements Prioritization Criteria OR Attribute OR Parameter OR Aspect OR Element OR Factor
- Challenges OR Limitations OR Issues of Requirements Prioritization Models

### **Resources**

Literature resources used in searches using the above keywords are IEEE Xplore, Elsevier, ACM Digital Library, Springer, ScienceDirect, and Google Scholar.

Based on the selected data sources, the following are the study's search and selection process steps, as illustrated in Figure 2.

Search Stage 1: In the initial stage of the search process, 360 probable selected papers are collected. The results from 6 online databases are journal articles and conference proceedings.

Search Stage 2: The merge from all resources probably has the duplicate paper, i.e., title and authors. Duplicate papers are then excluded from making sure all of them are unique. The results are 342 papers.



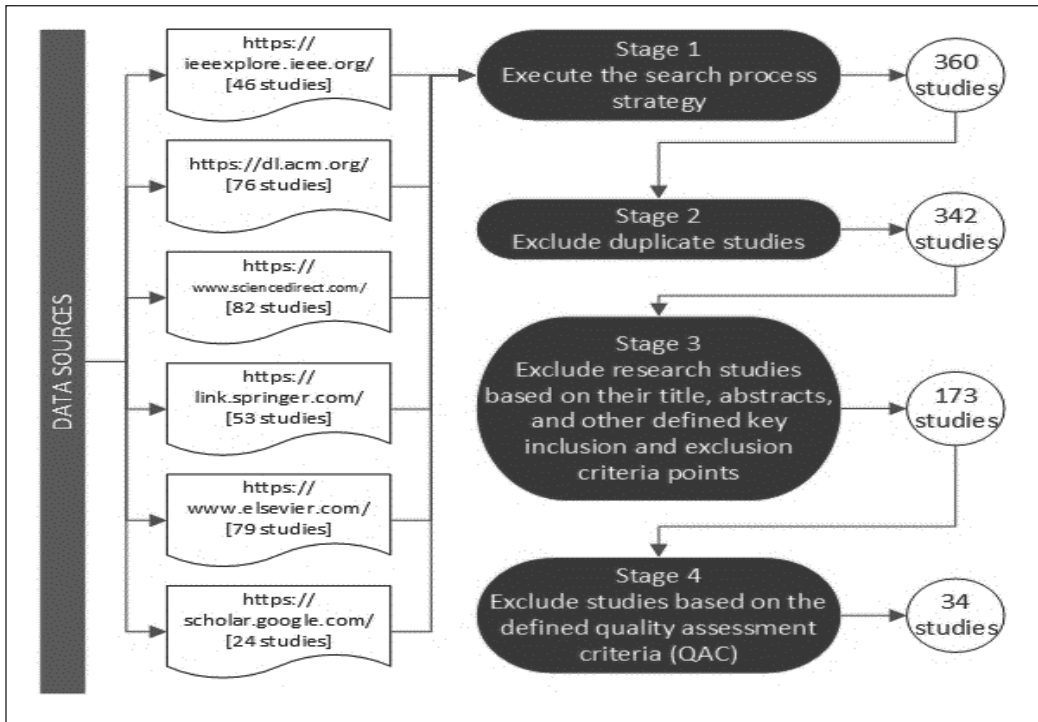


Figure 2. Stages of search and selection process

Search Stage 3: The relevant papers from the previous stage are concisely studied for their titles, abstracts, and contents. After the inclusion and exclusion are executed, 173 papers are selected.

Search Stage 4: Finally, the question or quality assessment criteria are applied to the papers selected from the previous stage. At the end of the exercise, 34 papers are selected and are considered qualified to provide answers to the research questions formulated.

### Study Selection Criteria

Study selection criteria are run to identify the primary studies that directly support the research question. This strategy is to decide which literature will be included or excluded. This study is divided into two subcategories: inclusion and exclusion criteria and quality assessment criteria selected relevant.

### Inclusion and Exclusion Criteria

Three hundred sixty studies are collected during the initial search process. First, the title and abstract are read carefully, and then studies not related to requirements prioritization are excluded. If there are several similar studies, the study that discusses it in full will be

taken. The studies taken are in English and have been published since 2010. The detailed inclusion and exclusion criteria used in this SLR are shown in Table 1.

Table 1  
*Inclusion and exclusion criteria*

INCLUSION CRITERIA	EXCLUSION CRITERIA
<ul style="list-style-type: none"> <li><input type="checkbox"/> Research work focuses on requirements prioritization criteria OR perspective.</li> <li><input type="checkbox"/> Studies included those whose title corresponded with the research topic with a keyword related in a formulated search string.</li> <li><input type="checkbox"/> All studies have the prospect of answering at least one research question.</li> <li><input type="checkbox"/> Relevant studies have been published since 2010.</li> <li><input type="checkbox"/> All studies are published in the English language.</li> </ul>	<ul style="list-style-type: none"> <li><input type="checkbox"/> Studies that are unrelated to the research questions</li> <li><input type="checkbox"/> Duplicate studies, only the newest and most complete, will be included. The rest are excluded.</li> <li><input type="checkbox"/> Studies that are not written and published in English.</li> <li><input type="checkbox"/> All studies are considered grey and do not have bibliographic details such as publication type/date.</li> </ul>

**Quality Assessment Criteria**

Quality Assessment Criteria (QAC) help assess the quality of the selected topic. The assessment of the selected topic was carried out based on QAC quality questions that are related to the domain of this study. The QAC checklist consists of six questions. These questions are presented in Table 2. The answer to each question can be ‘Yes,’ ‘Partially,’ or ‘No.’ The values are 1, 0.5, and 0.

To ensure the reliability of the study, studies that obtained a quality score of more than or equal to three, which is half of the total scores, will be used (6). As a result, from 173, only 34 studies are finally selected as relevant studies. The results of the quality scores of each study are shown in Figure 3.

Table 2  
*Quality assessment criteria*

ID	QUESTION
QAC1	Are the review’s inclusion and exclusion criteria represented and suitable?
QAC2	Does the study focus on the requirements prioritization domain?
QAC3	Does the study illustrate the requirements prioritization criteria?
QAC4	Is the proposed model/solution/ technique clearly described?
QAC5	Were the basic data/studies sufficiently explained?
QAC6	Is the result of the research clearly stated?

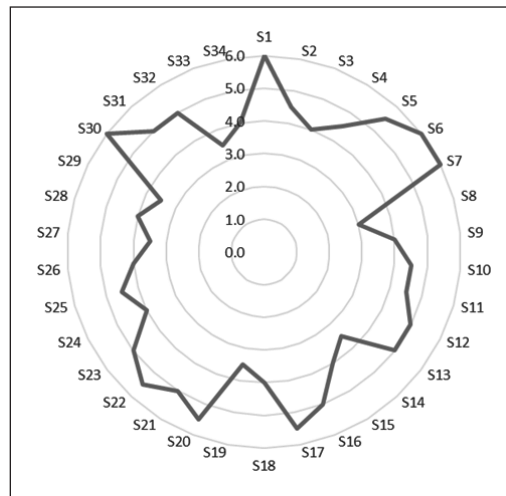


Figure 3. The results of quality scores from the selected studies

Based on Figure 3, from a score of 0 to a score of 6, only one paper, S8, gets a score of 3, while others get higher than 3. Figure 4 shows the number of studies that have answered yes, part or no to each question in QAC.

From 34 studies selected, only QAC1 and QAC5 questions have the “No” (0) result. These results mean that most of the papers can meet the questions of quality assessment criteria.

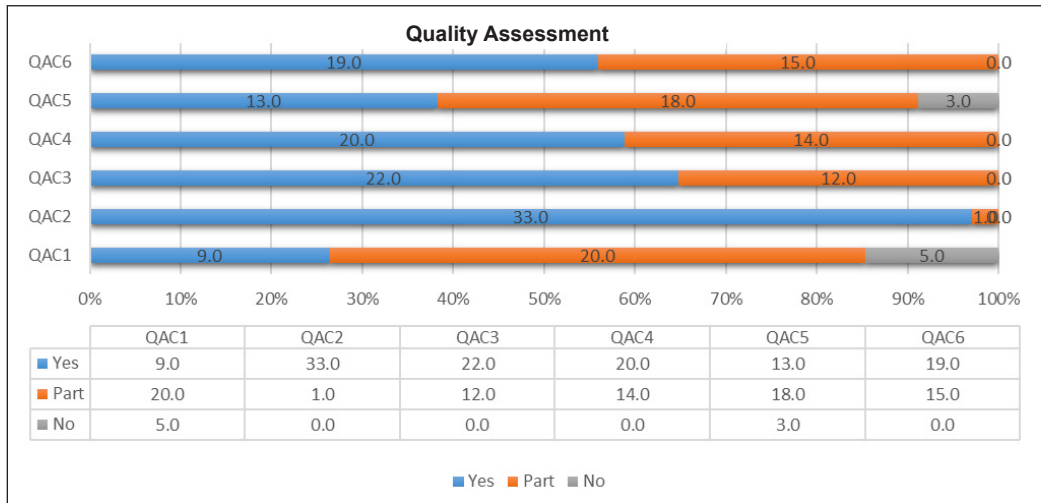


Figure 4. Quality assessment

### Data Collection and Synthesis

From 34 selected papers, the main data extracted are: title, year of publication, authors, criteria/ parameter/ aspect/ element/ factor. In this process, the difficulty encountered is that the names of different criteria are often encountered but have the same meaning. The problem with clarifying criteria is to explore whether these different criteria names have the same understanding or are different in prioritization.

In data synthesis, quantitative and qualitative data analysis approaches are used. The data that have been collected are analyzed by focusing on research questions. RQ1 explores the criteria used in the requirements prioritization process. Then to answer RQ2, look for the perspective used in the paper and its effect on the criteria used. The stakeholders involved are then explored to be able to answer RQ3. Furthermore, to answer RQ4, map or group the criteria based on perspective. The last is to do a resume to answer RQ5 regarding the recommended improvements in the process of requirements prioritization criteria.

### RESULTS AND DISCUSSIONS

Based on 34 identified papers, Figure 5 shows the number of papers published each year. Two papers present the SLR results to find the criteria used in the prioritization

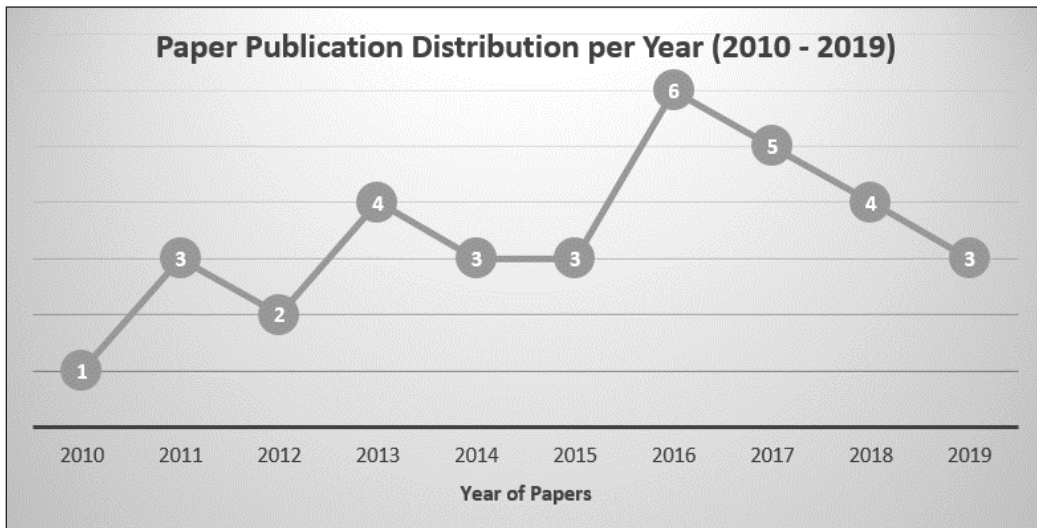


Figure 5. Papers published by year

requirements: Riegel and Doerr (2015) and Hujainah et al. (2018). Only the top ten criteria are taken from the study from these two papers.

### **(RQ1) What are the Attributes or Criteria Which are Used in the Requirements Prioritization Process?**

Some attributes or criteria are mentioned or used in papers that meet the requirements. Of the 38 identified criteria, several criteria have different names but have the same meaning and purpose. For example, the criteria for “business value” are also called: “value,” “customer value,” and “value to user.” “Development cost” is also called: “development effort,” “cost,” and “budget.” “Time to market” is also known as: “release date,” “time,” and “timely delivery.” “Available of resources” is also called: “resource availability,” “human resources,” and “manpower.” Table 3 shows all the criteria found and their operational definitions.

The frequency of the criteria used or mentioned in the SLR paper can be seen in Figure 6. The frequency here indicates the number of papers in this study that use these criteria. The use of criteria in the requirements prioritization process is very diverse. Thus, many criteria are used in the literature when collected. This study finds 38 criteria, from the few frequencies (only once or twice mentioned) to the favorite criteria, such as business value and development cost. The business value has been mentioned 30 times, development cost has been mentioned 23 times, risk has been mentioned 16 times, and time to market has been mentioned 15 times. Furthermore, dependency has been mentioned nine times, followed by available resources, effort estimation/size measurement, and schedule, which have been mentioned eight times. The criteria with a frequency of seven

Table 3  
*The criteria of requirements prioritization*

<b>ID</b>	<b>CRITERIA</b>	<b>CITATION</b>	<b>OPERATIONAL DEFINITION</b>
C1	<b>Business Value</b>	Al-Ta'ani & Razali, 2016; AL-Ta'ani & Razali, 2013; Alawneh, 2018; Albuga & Odeh, 2018; Alkandari & Al-Shammeri, 2017; Anand & Dinakaran, 2017; Asghar et al., 2017; Devulapalli et al., 2016; Devulapalli & Khare, 2014; Gupta & Gupta, 2018; Hujainah et al., 2018; Khan et al., 2016; Kukreja, 2013; Kukreja et al., 2012; Narendhar & Anuradha, 2016; Racheva et al., 2010; Rahim et al., 2018; Riegel & Doerr, 2015; Sheemar & Kour, 2019; Sher et al., 2019; Sufian et al., 2019; Sureka, 2014; Thakurta, 2012; Torrecilla-Salinas et al., 2015; Viswanathan et al., 2016	Business value is the entire value that delivers profit to the organization to increase revenue, improve service, or avoid costs.
C2	<b>Development Cost</b>	Al-Ta'ani & Razali, 2016; AL-Ta'ani & Razali, 2013; Alawneh, 2018; Alkandari & Al-Shammeri, 2017; Amiri & Golozari, 2011; Anand & Dinakaran, 2017; Asghar et al., 2017; Bajaj & Arora, 2013; Devulapalli & Khare, 2014; Hujainah et al., 2018; Idrus et al., 2011; Kukreja, 2013; Kukreja et al., 2012; Narendhar & Anuradha, 2016; Rahim et al., 2018; Riegel & Doerr, 2015; Samarakoon & Ratnayake, 2015; Sher et al., 2019; Sufian et al., 2019; Sureka, 2014; Thakurta, 2012; Torrecilla-Salinas et al., 2015; Viswanathan et al., 2016	The cost an organization incurs while developing a software product.
C3	<b>Time To Market</b>	Alkandari & Al-Shammeri, 2017; Amiri & Golozari, 2011; Asghar et al., 2017; Bajaj & Arora, 2013; Devulapalli et al., 2016; Devulapalli & Khare, 2014; Idrus et al., 2011; Khan et al., 2016; Sheemar & Kour, 2019; Sher et al., 2014; Sufian et al., 2019; Svensson et al., 2011; Tahvili et al., 2015; Viswanathan et al., 2016	During the period needed, the development team does every task until it is released to the market.
C4	<b>Risk</b>	AL-Ta'ani & Razali, 2013; Alkandari & Al-Shammeri, 2017; Amiri & Golozari, 2011; Anand & Dinakaran, 2017; Asghar et al., 2017; Hujainah et al., 2018; Khan et al., 2016; Narendhar & Anuradha, 2016; Racheva et al., 2010; Rahim et al., 2018; Sufian et al., 2019; Svensson et al., 2011; Tahvili et al., 2015; Thakurta, 2012; Viswanathan et al., 2016	Risk is the probability of software failure. It refers to the business and technical risks associated with implementing the requirements in the given scenario.

Table 3 (continue)

ID	CRITERIA	CITATION	OPERATIONAL DEFINITION
C5	<b>Dependencies</b>	Al-Ta'ani & Razali, 2016; AL-Ta'ani & Razali, 2013; Anand & Dinakaran, 2017; Asghar et al., 2017; Gupta & Gupta, 2018; Hujainah et al., 2018; Riegel & Doerr, 2015; Sureka, 2014; Viswanathan et al., 2016	Requirements dependency is the relationship between requirements that depends on the others.
C6	<b>Available of Resources</b>	AL-Ta'ani & Razali, 2013; Alkandari & Al-Shammeri, 2017; Anand & Dinakaran, 2017; Danesh et al., 2016; Devulapalli et al., 2016; Devulapalli & Khare, 2014; Riegel & Doerr, 2015; Sureka, 2014	Availability of development resources, knowledgeable in domain/ technology/ skill.
C7	<b>Effort Estimation/ Size Measurement</b>	Al-Ta'ani & Razali, 2016; Alkandari & Al-Shammeri, 2017; Bajaj & Arora, 2013; Danesh et al., 2016; Hujainah et al., 2018; Kukreja et al., 2012; Racheva et al., 2010; Torrecilla-Salinas et al., 2015	In the effort process, estimation difference is computed between total available effort and effort required for software releases, and this job is done by technical and development teams.
C8	<b>Schedule</b>	Al-Ta'ani & Razali, 2016; AL-Ta'ani & Razali, 2013; Alkandari & Al-Shammeri, 2017; Kukreja, 2013; Kukreja et al., 2012; Samarakoon & Ratnayake, 2015; Sureka, 2014; Torrecilla-Salinas et al., 2015	The project schedule is a project's timeframe. It includes start and finish dates, activities, and deliverables and lists all project-related milestones.
C9	<b>Volatility</b>	AL-Ta'ani & Razali, 2013; Alkandari & Al-Shammeri, 2017; Anand & Dinakaran, 2017; Devulapalli & Khare, 2014; Rahim et al., 2018; Riegel & Doerr, 2015; Svensson et al., 2011	Requirements Volatility is frequent changes to the requirements over time.
C10	<b>Implementation Effort</b>	Devulapalli et al., 2016; Devulapalli & Khare, 2014; Khan et al., 2016; Riegel & Doerr, 2015; Sureka, 2014; Tahvili et al., 2015; Viswanathan et al., 2016	Costs are needed for implementation until the source code commit.
C11	<b>Importance</b>	AL-Ta'ani & Razali, 2013; Alkandari & Al-Shammeri, 2017; Asghar et al., 2017; Danesh et al., 2016; Hujainah et al., 2018; Sureka, 2014; Svensson et al., 2011	The important requirements are functions that bring an organization business value.
C12	<b>Stakeholder Satisfaction</b>	Hujainah et al., 2018; Narendhar & Anuradha, 2016; Riegel & Doerr, 2015; Sher et al., 2014; Svensson et al., 2011; Tahvili et al., 2015; Viswanathan et al., 2016	Fulfill the expectations of stakeholders that can achieve their personal goals and objective.
C13	<b>Complexity</b>	AL-Ta'ani & Razali, 2016; AL-Ta'ani & Razali, 2013; Anand & Dinakaran, 2017; Asghar et al., 2017; Tahvili et al., 2015	The complexity and interdependencies to streamline product development with challenges complicate the selection.

Table 3 (continue)

ID	CRITERIA	CITATION	OPERATIONAL DEFINITION
C14	<b>Quality</b>	Amiri & Golozari, 2011; Idrus et al., 2011; Sheemar & Kour, 2019; Tahvili et al., 2015; Torrecilla-Salinas et al., 2015	Quality refers to a capability that must be present in a requirement. Quality represents what is needed to validate the successful completion of a project deliverable.
C15	<b>Penalty</b>	Asgar et al., 2017; Hujainah et al., 2018; Svensson et al., 2011; Thakurta, 2012	The customer or business will likely experience penalties if specific requirements are not included in the scenario.
C16	<b>Authority</b>	AL-Ta'ani & Razali, 2013; Anand & Dinakaran, 2017; Samarakoon & Ratnayake, 2015; Sher et al., 2014	The requirements priorities are best determined by clients who have dominion over the system.
C17	<b>Learning Experience</b>	AL-Ta'ani & Razali, 2013; Alkandari & Al-Shammeri, 2017; Racheva et al., 2010	The learning experience is risky because the developer will need more time to learn new technology.
C18	<b>Impact</b>	Devulapalli et al., 2016; Devulapalli & Khare, 2014	The impact of the characteristics of the product or service on the intended beneficiaries.
C19	<b>External Change</b>	Racheva et al., 2010; Alkandari & Al-Shammeri, 2017	External changes are the "events that occur during the project and impact the company, the business environment or the product under development."
C20	<b>Knowledge</b>	AL-Ta'ani & Razali, 2013; Anand & Dinakaran, 2017	Stakeholders must have significant knowledge of development and customer needs and interest.
C21	<b>Strategic</b>	Sher et al., 2014; Svensson et al., 2011	A strategic requirement is something an organization sets out to achieve.
C22	<b>Scalability</b>	Sher et al., 2014; Asghar et al., 2017	The ability to appropriately handle increasing (and decreasing) requirements.
C23	<b>Usability</b>	Hujainah et al., 2018; Sheemar & Kour, 2019	Usability refers to producing systems that are easier to use and matching them more closely to user requirements.
C24	<b>Technical Feasibility</b>	Kukreja et al., 2012; Samarakoon & Ratnayake, 2015	Technical feasibility also implicates evaluating the proposed system's hardware, software, and other technical requirements.
C25	<b>Customer Input</b>	Sher et al., 2019	To use client input as criteria for prioritization.
C26	<b>Performance</b>	Bajaj & Arora, 2013	Requirement performance represents how well a process is to be executed or performed or how well it is accomplished.
C27	<b>Uncertainties</b>	Devulapalli & Khare, 2014	Changes imminent.
C28	<b>Easy Use</b>	Sher et al., 2014	How easily users can use a product.
C29	<b>Accuracy</b>	Sher et al., 2014	The provision of right or effects attributes or agreed results.



Table 3 (continue)

ID	CRITERIA	CITATION	OPERATIONAL DEFINITION
C30	<b>Developers' Input</b>	Alkandari & Al-Shammeri, 2017	How easily users can use a product.
C31	<b>Negative Value</b>	Alkandari & Al-Shammeri, 2017	The 'negative' value thus is equivalent to a loss of importance or damage to the business.
C32	<b>Visibility</b>	Al-Ta'ani & Razali, 2016	A lack of visibility prevents teams from taking appropriate action, leading to uncontrollable impediments later in the sprint.
C33	<b>Trust</b>	AL-Ta'ani & Razali, 2013	Stakeholders must have direct communication to achieve trust.
C34	<b>Sales</b>	Sher et al., 2014	Sales Impact.
C35	<b>Marketing</b>	Sher et al., 2014	Most aspects of your business depend on successful marketing.
C36	<b>Applicability</b>	Samarakoon & Ratnayake, 2015	Applying or capable of being applied.
C37	<b>Reliability</b>	Samarakoon & Ratnayake, 2015	This quality attribute defines how likely the system would run without failure.
C38	<b>Urgency</b>	Gupta & Gupta, 2018	Urgency of implementation.

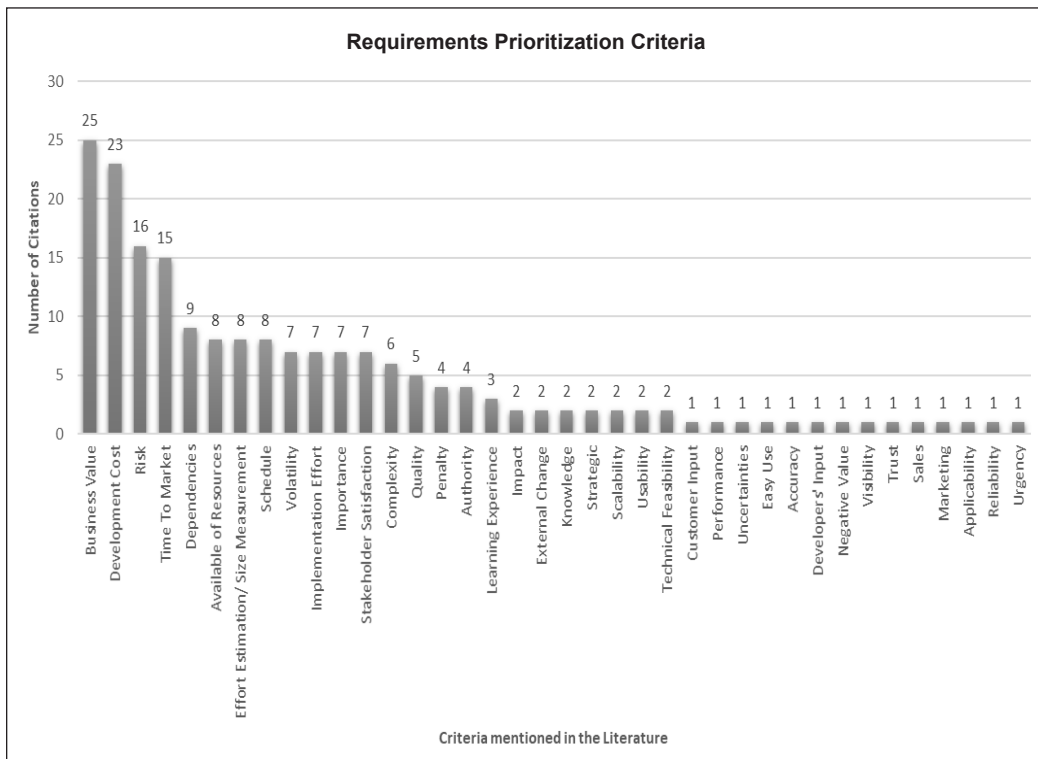


Figure 6. The usage frequency of requirements prioritization criteria

consist of volatility, implementation effort, importance, and stakeholder satisfaction. In addition, quality was mentioned five times, penalty and authority were mentioned four times, followed by learning experience, which was mentioned three times. The criteria mentioned twice are impact, external change, knowledge, strategy, scalability, usability, and technical feasibility. Finally, the remaining criteria show a frequency of 1: customer input, performance, uncertainties, ease of use, accuracy, developer’s input, negative value, visibility, trust, sales, marketing, applicability, reliability, and urgency.

**(RQ2) What are the Perspectives Involved in Requirements Prioritization, and How to Classify the Requirements Prioritization Criteria Based on View?**

Requirements from stakeholders represent the needs from an individual point of view. The term perspective emphasizes that there is no simple relationship between requirements and people or between requirements and roles. A perspective is an area of knowledge that is internally consistent. Perspectives usually have an identifiable focus of attention, the motivational concern of the requirements they represent (Easterbrook, 1991).

In software development projects, there are many people along with roles that have perspectives, respectively. The success of a requirements engineering project depends on an accurate analysis of this perspective for incompleteness and inconsistency. Many papers mention that the involvement of perspectives is very important and affects the requirements prioritization process (Alkandari & Al-Shammeri, 2017; Gupta & Gupta, 2018; Ibriwesh et al., 2019; Idrus et al., 2011; Madi et al., 2013; Narendhar & Anuradha, 2016; Schön et al., 2017; Sher et al., 2019, 2014; Wohlin & Aurum, 2005).

As for the perspectives used by SLR, most do not explicitly mention the view used. For example, there are only eight papers identified mention the perspective used in the study (Alkandari & Al-Shammeri, 2017; Danesh et al., 2016; Gupta & Gupta, 2018; Idrus et al., 2011; Narendhar & Anuradha, 2016; Sher et al., 2019, 2014; Torrecilla-Salinas et al., 2015). To expand the extent to which the use of perspective in the requirements, Table 4 shows the addition of a source of books on engineering requirements.

The influence of perspective on the criteria used in the requirements prioritization process is closely related to the point of view. There are big groupings in perspective, namely, the client’s perspective and the developer’s perspective.

Table 4  
*Requirements prioritization perspective*

#	PERSPECTIVE	DEFINITION	TYPE OF CITATION	
			PAPER	BOOK
<b>GROUP OF CLIENTS' PERSPECTIVES</b>				
1	Clients	The product, according to the client's needs	Gupta & Gupta, 2018; Danesh et al., 2016; Idrus et al., 2011	

Table 4 (continue)

#	PERSPECTIVE	DEFINITION	TYPE OF CITATION	
			PAPER	BOOK
2	Customers	Care about the user/customer value to determine whether they describe the desired functions and qualities of the system	Alkandari & Al-Shammeri, 2017	Aurum & Wohlin, 2005; Wiergers, 2009
3	User	Comparable to the owner's view of a house		Pohl & Rupp, 2015; Wieringa, 1996
4	Stakeholders	State what the stakeholders are required to achieve by the system	Narendhar & Anuradha, 2016	Hull et al., 2011
5	Top Manager	It represents the product idea		Wieringa, 1996
6	Business	To decide whether the business really needs the system	Sher et al., 2014; Sher et al., 2019	Sommerville, 2016
<b>GROUP OF DEVELOPERS' PERSPECTIVES</b>				
7	Developers	Know about the technical difficulties	Gupta & Gupta, 2018; Danesh et al., 2016; Idrus et al., 2011; Narendhar & Anuradha, 2016; Alkandari & Al-Shammeri, 2017	Aurum & Wohlin, 2005
8	Software Architect	To ascertain if they contain all necessary information for architectural design		Pohl & Rupp, 2015
9	Analyst	State abstractly what the system will do to fulfill the stakeholder requirements		Hull et al., 2011
10	Designer	State how the specific design will fulfill the system requirements. Comparable to the specification delivered by the architect for the designer		Hull et al., 2011; Wieringa, 1996
11	Technical	To assess the quality of the application software and the system's support software and hardware	Sher et al., 2014; Sher et al., 2019	Wiergers, 2009; Sommerville, 2016
12	Builder	The technology model		Wieringa, 1996
13	Tester	To establish whether they contain the information necessary to derive test cases from the requirements		Pohl & Rupp, 2015
14	Financial Representative	Know and manage budgetary limitations and risks		Aurum & Wohlin, 2005

### **(RQ3) Who are the Stakeholders that Belong to Each Perspective?**

Stakeholders of the system are people or organizations that directly or indirectly affect the system requirements. To obtain requirements, stakeholders are one type of requirements source other than documents and systems in operation (Pohl & Rupp, 2015). Therefore, identifying relevant stakeholders is important in requirements engineering. If stakeholders are not recognized will result in a significant negative impact on the success of the project. In practice, there may be many stakeholders involved. Still, Requirements Prioritization should differentiate the involvement of stakeholders, whether only being affected by the project or being a collaborator (integrated and responsible with stakeholders). The list of stakeholders involved in requirements prioritization can be seen in Table 5.

### **(RQ4) How are the Attributes or Criteria Grouped in Each Perspective?**

RQ4 aims to classify the attributes or criteria obtained from the RQ1 results. The cost-value approach is a process of prioritizing software requirements to maximize quality, minimize costs, and the shortest possible delivery time, according to the relative value and cost based on the Analytic Hierarchy Process (AHP) analysis tool (Amelia & Mohamed, 2018; Karlsson & Ryan, 1997; Karlsson et al., 1997; Sie, 2016). AHP and TOPSIS are methods in Multi-Criteria Decision Making (MCDM) that are often used and combined.

The attributes or criteria in the MCDM are divided into two types: beneficial and non-beneficial. For example, attributes whose value must be kept low are non-beneficial attributes, and other attributes which must have higher value are beneficial attributes. Another name for beneficial attributes is favorable indicators, while non-beneficial attributes are unfavorable indicators. If related to the criteria, use the beneficial attributes from the client's perspective and the developer's perspective using non-beneficial attributes.

Table 3 is based on the cost-value approach, which is classified as beneficial attributes and non-beneficial attributes, with the results shown in Table 6. In the process of priority needs, the attributes or criteria used in most of the papers are non-beneficial rather than beneficial attributes.

The criteria in the prioritization requirements are grouped into project constraints in some literature (AL-Ta'ani & Razali, 2013; Alkandari & Al-Shammeri, 2017; Nurdiani et al., 2016). Project constraints are constraints on specific parameters that affect the results (Thakurta, 2016). Some studies include "project constraints" as one of the criteria, which is ambiguous. For example, the development cost is a criterion that limits the project because of the different abilities of each project owner to cover the costs. On the other side, the business value is not a project constraint because this criterion does not restrict the development of a project. In addition, most of the criteria used in beneficial attributes are not project constraints.

Table 5  
Stakeholders in a requirements prioritization process

#	STAKEHOLDERS OF CLIENTS' PERSPECTIVE	CITATION	#	STAKEHOLDERS OF DEVELOPERS' PERSPECTIVE	CITATION
1	End Users	Shukla & Auriol, 2013; Lim et al., 2013; Hujainah et al., 2018; Pohl & Rupp, 2015); Hull et al., 2011; Chemuturi, 2013; Wieggers, 2009); Wieringa, 1996; Laplante, 2017; Sommerville, 2016)	1	Developers	Kaiya et al., 2005; Bendjenna et al., 2012); Heikkila et al., 2015; Lim et al., 2013; Hujainah et al., 2018; Sadiq & Jain, 2013; Pohl & Rupp, 2015; Aurum & Wohlin, 2005; Chemuturi, 2013; Wieggers, 2009; Wieringa, 1996; Laplante, 2017
2	Operators	Sadiq & Jain, 2013; Pohl & Rupp, 2015	2	Software Architects	Dos Santos et al., 2016; Heikkila et al., 2015; Hujainah et al., 2018; Pohl & Rupp, 2015; Sommerville, 2016)
3	Customers / Sponsor	Dos Santos et al., 2016; Kaiya et al., 2005; Bendjenna et al., 2012; Heikkila et al., 2015; Lim et al., 2013; Hujainah et al., 2018; Sadiq & Jain, 2013; Pohl & Rupp, 2015; Aurum & Wohlin, 2005; Chemuturi, 2013; Wieggers, 2009); Laplante, 2017; Sommerville, 2016	3	Technical Engineer	Shukla & Auriol, 2013; Hujainah et al., 2018; Wieringa, 1996; Laplante, 2017; Sommerville, 2016
4	Business Analyst	Shukla & Auriol, 2013; Hujainah et al., 2018; Kukreja et al., 2012	4	System Designers	Hujainah et al., 2018; Wieringa, 1996; Laplante, 2017
5	Managers	Hujainah et al., 2018; Hull et al., 2011; Sommerville, 2016	5	Requirements analysts	Dos Santos et al., 2016; Hujainah et al., 2018; Wieggers, 2009
6	Financial Representatives	Sadiq & Jain, 2013; Aurum & Wohlin, 2005	6	Programmers	Hujainah et al., 2018; Wieringa, 1996; Laplante, 2017
7	Maintenance and service staff	Hull et al., 2011; Laplante, 2017	7	Project managers	Heikkila et al., 2015; Hujainah et al., 2018; Kukreja et al., 2012; Wieggers, 2009; Wieringa, 1996
8	Sales and Marketing	Hujainah et al., 2018; Hull et al., 2011; Chemuturi, 2013; Wieggers, 2009	8	Business Engineer	Hujainah et al., 2018
9	Government	Hull et al., 2011; Laplante, 2017	9	Testers	Pohl & Rupp, 2015; Wieggers, 2009
10	Organizational Standards Group	Hull et al., 2011; Laplante, 2017			
11	Regulatory authorities	Lim et al., 2013; Hull et al., 2011			

Table 6  
*The correlation attributes based on perspectives*

CLIENTS PERSPECTIVE		
<b>BENEFICIAL ATTRIBUTES</b> (37%)	<b>Project Constraints (No)</b>	Business Value, Importance, Stakeholder Satisfaction, Authority, Knowledge, Strategic, Usability, Customer Input, Performance, Easy Use, Accuracy, Customer Input, Visibility, Sales, Marketing, Applicability, Reliability, Urgency
	<b>Project Constraints (Yes)</b>	Quality, Impact, Scalability, Trust
DEVELOPERS PERSPECTIVE		
<b>NON-BENEFICIAL ATTRIBUTES</b> (63%)	<b>Project Constraints (No)</b>	Effort Estimation/ Size Measurement, Penalty, Learning Experience, External Change, Technical Feasibility, Uncertainties, Developers' Input, Negative Value
	<b>Project Constraints (Yes)</b>	Development Cost, Risk, Time to Market, Dependencies, Available of Resources, Schedule, Volatility, Implementation Effort, Complexity

**(RQ5) What are the Recommended Improvements for the Specified Limitations or Challenges?**

The requirements prioritization process involving many parties has challenges: inaccuracy, time consumption, and ease of use. However, there are open opportunities to improve the weaknesses that still exist with the increase in requirements prioritization models. Some points that issues can add to the requirements prioritization domain include:

- Bias issues by stakeholders due to the many stakeholders involved, without considering the perceptions of stakeholders (Philip et al., 2014; Babar et al., 2015; Bakhtiar et al., 2015; Hannan et al., 2015; Khan et al., 2016; McZara et al., 2015). The result of requirements prioritization can perform accuracy using fuzzy numbers and give proper weighting based on stakeholders' perceptions.
- Requirements Prioritization must address the issue of reducing pairwise comparisons to minimize time consumption (Gambo et al., 2018; Karlsson et al., 1998). AHP only provides attribute weighting, while TOPSIS is used to calculate alternatives to facilitate pairwise comparison.
- Attribute weighting while calculating alternatives using TOPSIS.
- Scalability issues related to the ease of prioritization requirements should be further improved, regardless of the requirements (Achimugu et al., 2014; Achimugu et al., 2016; Babar et al., 2015; Duan et al., 2009; Gambo et al., 2018; Khan et al., 2016; Lim & Finkelstein, 2012; Veerappa, 2012). Meanwhile, prioritization can be done by making tools to facilitate the needs.

## CONCLUSION

Attributes or criteria in the prioritization requirements are fundamental things that must be selected. This study conducted a comprehensive investigation on the criteria that are widely used in the prioritization requirements. The resulting criteria can help researchers or practitioners to choose criteria that suit their needs and increase the accuracy of the chosen ones so that the results of the requirements prioritization can be more accurate. The involvement of stakeholder perspectives in the requirements prioritization process is a collaboration between the client's and the developer's perspectives. The findings suggest that future research needs to consider the selection of criteria from stakeholders' perspectives.

## ACKNOWLEDGEMENT

This publication supported by The Center for Research and Community Service of Universitas Dinamika.

## REFERENCES

- Achimugu, P., Selamat, A., & Ibrahim, R. (2014). A clustering based technique for large scale prioritization during requirements elicitation. In T. Herawan, R. Ghazali & M. Deris (Eds), *Recent Advances on Soft Computing and Data Mining* (pp. 30-39). Springer. <https://doi.org/10.1007/978-3-319-72550-5>
- Achimugu, P., Selamat, A., & Ibrahim, R. (2016). ReproTizer: A fully implemented software requirements prioritization tool. In N. T. Nguyen & R. Kowalczyk (Eds), *Transactions on Computational Collective Intelligence XXII* (Vol. 9655, pp. 80-105). Springer. <https://doi.org/10.1007/978-3-662-49619-0>
- Al-Ta'ani, R. H., & Razali, R. (2016). A framework for requirements prioritisation process in an agile software development environment: Empirical study. *International Journal on Advanced Science, Engineering and Information Technology*, 6(6), 846-856. <https://doi.org/10.18517/ijaseit.6.6.1375>
- AL-Ta'ani, R. H., & Razali, R. (2013). Prioritizing requirements in agile development: A conceptual framework. *Procedia Technology*, 11, 733-739. <https://doi.org/10.1016/j.protcy.2013.12.252>
- Alawneh, L. (2018). Requirements prioritization using hierarchical dependencies. In S. Latifi (Ed.), *Information Technology-New Generations. Advances in Intelligent Systems and Computing* (Vol. 558, pp. 459-464). Springer <https://doi.org/10.1007/978-3-319-54978-1>
- Albuga, S., & Odeh, Y. (2018). Towards prioritizing software business requirements in startups. In *2018 8th International Conference on Computer Science and Information Technology (CSIT)* (pp. 257-265). IEEE Publishing. <https://doi.org/10.1109/CSIT.2018.8486216>
- Alkandari, M., & Al-Shammeri, A. (2017). Enhancing the process of requirements prioritization in agile software development - A proposed model. *Journal of Software*, 12(6), 439-453. <https://doi.org/10.17706/jsw.12.6.439-453>



- Amelia, T., & Mohamed, R. B. (2018). Review on cost-value approach for requirements prioritization techniques. In *2018 5th International Conference on Information Technology, Computer, and Electrical Engineering (ICITACEE)* (pp. 310-314). IEEE Publishing. <https://doi.org/doi: 10.1109/ICITACEE.2018.8576908>
- Amiri, M., & Golozari, F. (2011). Application of fuzzy multi-attribute decision-making in determining the critical path by using time, cost, risk, and quality criteria. *International Journal of Advanced Manufacturing Technology*, *54*, 393-401. <https://doi.org/10.1007/s00170-010-2928-4>
- Anand, R. V., & Dinakaran, M. (2017). Handling stakeholder conflict by agile requirement prioritization using Apriori technique. *Computers and Electrical Engineering*, *61*, 126-136. <https://doi.org/10.1016/j.compeleceng.2017.06.022>
- Asgar, A. R., Tabassum, A., Bhatti, S. N., & Jadi, A. M. (2017). Impact and challenges of requirements elicitation & prioritization in quality to agile process: Scrum as a case scenario. *International Conference on Communication Technologies, ComTech 2017* (pp. 50-55). IEEE Publishing. <https://doi.org/10.1109/COMTECH.2017.8065749>
- Aurum, A., & Wohlin, C. (2005). *Engineering and Managing Software Requirements*. Springer-Verlag.
- Babar, M. I., Ghazali, M., Jawawi, D. N. A., Shamsuddin, S. M., & Ibrahim, N. (2015). PHandler: An expert system for a scalable software requirements prioritization process. *Knowledge-Based Systems*, *84*, 179-202. <https://doi.org/10.1016/j.knosys.2015.04.010>
- Babar, M. I., Ramzan, M., & Ghayyur, S. A. K. (2011). Challenges and future trends in software requirements prioritization. *International Conference on Computer Networks and Information Technology* (pp. 319-324). IEEE Publishing. <https://doi.org/10.1109/ICCNIT.2011.6020888>
- Bajaj, P., & Arora, V. (2013). Multi-person decision-making for requirements prioritization using fuzzy AHP. *ACM SIGSOFT Software Engineering Notes*, *38*(5), 1-6. <https://doi.org/10.1145/2507288.2507302>
- Bakhtiar, A., Hannan, A., Basit, A., & Ahmad, J. (2015, August 25-27). Prioritization of value-based services of software by using AHP and fuzzy kano model. In *International Conference on Computational and Social Sciences* (Vol. 8, pp. 48-56). Selangor, Malaysia.
- Bendjenna, H., Charre, P. J., & Zarour, N. E. (2012). Using multi-criteria analysis to prioritize stakeholders. *Journal of Systems and Information Technology*, *14*(3), 264-280.
- Chemuturi, M. (2013). *Requirements Engineering and Management for Software Development Projects*. Springer. <https://doi.org/10.1007/978-1-4614-5377-2>
- Dabbagh, M., Lee, S. P., & Parizi, R. M. (2014). Application of hybrid assessment method for priority assessment of functional and non-functional requirements. In *5th International Conference on Information Science and Applications*, (pp. 1-4). IEEE Publishing. <https://doi.org/10.1109/ICISA.2014.6847365>
- Danesh, A. S., Ahmad, R., Shamshirband, S., & Zargarnataj, S. M. (2016). Towards a highly customizable framework for release planning process. *Tehnicki Vjesnik (Technical Gazette)*, *23*(6), 1777-1785. <https://doi.org/10.17559/TV-20150311144435>
- Devulapalli, S., & Khare, A. (2014). A framework for requirement prioritization for software products. *IJUM Journal of Management*, *2*(1), 35-41.

- Devulapalli, S., Rao, O., & Khare, A. (2016). Requirements prioritization: Parameters of relevance - An empirical Study across 3 datasets. In *Proceedings of the Second International Conference on Information and Communication Technology for Competitive Strategies* (pp. 1-5). ACM Publishing. <https://doi.org/10.1145/2905055.2905340>
- Dos Santos, J. R. F., Albuquerque, A. B., & Pinheiro, P. R. (2016). Requirements prioritization in market-driven software: A survey based on large numbers of stakeholders and requirements. In *10th International Conference on the Quality of Information and Communications Technology, September 2016* (pp. 67-72). IEEE Publishing. <https://doi.org/10.1109/QUATIC.2016.020>
- Duan, C., Laurent, P., Cleland-Huang, J., & Kwiatkowski, C. (2009). Towards automated requirements prioritization and triage. *Requirements Engineering*, 14(2), 73-89. <https://doi.org/10.1007/s00766-009-0079-7>
- Easterbrook, S. (1991). *Elicitation of requirements from multiple perspectives* (Doctoral dissertation). University of London, UK. [https://www.researchgate.net/profile/Steve-Easterbrook/publication/2822954\\_Elicitation\\_of\\_Requirements\\_from\\_Multiple\\_Perspectives/links/5735e81b08ae9f741b29c558/Elicitation-of-Requirements-from-Multiple-Perspectives.pdf](https://www.researchgate.net/profile/Steve-Easterbrook/publication/2822954_Elicitation_of_Requirements_from_Multiple_Perspectives/links/5735e81b08ae9f741b29c558/Elicitation-of-Requirements-from-Multiple-Perspectives.pdf)
- Gambo, I. P., Ikono, R. N., Achimugu, P. O., & Iroju, O. G. (2018). A ranking model for software requirements prioritization during requirements engineering: A case study. *International Journal of Computer Science and Information Security (IJCSIS)*, 16(4), 255-268.
- Gupta, A., & Gupta, C. (2018). CDBR: A semi-automated collaborative execute-before-after dependency-based requirement prioritization approach. *Journal of King Saud University - Computer and Information Sciences*, 34(2), 421-432. <https://doi.org/10.1016/j.jksuci.2018.10.004>
- Hannan, A., Ahmad, J., & Basit, A. (2015). Value-based requirements classification of software product using Fuzzy Kano Model. *New Horizion*, 83, 48-56.
- Heikkila, V. T., Paasivaara, M., Rautiainen, K., Lassenius, C., Toivola, T., & Jarvinen, J. (2015). Operational release planning in large-scale scrum with multiple stakeholders - A longitudinal case study at F-secure corporation. *Information and Software Technology*, 57(1), 116-140. <https://doi.org/10.1016/j.infsof.2014.09.005>
- Hujainah, F., Bakar, R. B. A., Abdulgabber, M. A., & Zamli, K. Z. (2018). Software requirements prioritisation: a systematic literature review on significance, stakeholders, techniques and challenges. In *IEEE Access* (Vol. 6, pp. 71497-71523). IEEE Publishing. <https://doi.org/10.1109/ACCESS.2018.2881755>
- Hull, E., Jackson, K., & Dick, J. (2011). *Requirements Engineering* (3rd Ed.). Springer. <https://doi.org/10.1007/978-1-84996-405-0>
- Ibriwesh, I., Ho, S. B., Chai, I., & Tan, C. H. (2019). Prioritizing solution-oriented software requirements using the multiple perspective prioritization technique algorithm: An empirical investigation. *Concurrent Engineering: Research and Applications*, 27(1), 68-79. <https://doi.org/10.1177/1063293X18808559>
- Idrus, A., Sodangi, M., & Husin, M. H. (2011). Prioritizing project performance criteria within client perspective. *Research Journal of Applied Sciences, Engineering and Technology*, 3(10), 1142-1151.

- IIBA. (2015). *A guide to the business analysis body of knowledge (BABOK Guide) Version 3.0* (3rd Ed.). International Institute of Business Analysis. <https://www.iiba.org/career-resources/a-business-analysis-professionals-foundation-for-success/babok/>
- Kaiya, H., Shinbara, D., Kawano, J., & Saeiki, M. (2005). Improving the detection of requirements discordances among stakeholders. *Requirements Engineering*, 10, 289-303. <https://doi.org/10.1007/s00766-005-0017-2>
- Karlsson, J., & Ryan, K. (1997). A cost-value-approach for prioritizing requirements. In *IEEE Software* (Vol. 14, pp. 67-74). IEEE Publishing. <https://doi.org/10.1109/52.605933>
- Karlsson, J., Olsson, S., & Ryan, K. (1997). Improved practical support for large-scale requirements prioritising. *Requirements Engineering*, 2, 51-60. <https://doi.org/10.1007/BF02802897>
- Karlsson, J., Wohlin, C., & Regnell, B. (1998). An evaluation of methods for prioritizing software requirements. *Information and Software Technology*, 39(14-15), 939-947. [https://doi.org/10.1016/S0950-5849\(97\)00053-0](https://doi.org/10.1016/S0950-5849(97)00053-0)
- Khan, S. U. R., Lee, S. P., Dabbagh, M., Tahir, M., Khan, M., & Arif, M. (2016). RePizer: A framework for prioritization of software requirements. *Frontiers of Information Technology & Electronic Engineering*, 17, 750-765. <https://doi.org/10.1631/FITEE.1500162>
- Kitchenham, B., & Charters, S. (2007). *Guidelines for performing systematic literature reviews in software engineering version 2.3* (EBSE Technical Report). Keele University and University of Durham. [https://www.elsevier.com/\\_data/promis\\_misc/525444systematicreviewsguide.pdf/1134285.1134500](https://www.elsevier.com/_data/promis_misc/525444systematicreviewsguide.pdf/1134285.1134500)
- Kitchenham, B., Pearl Brereton, O., Budgen, D., Turner, M., Bailey, J., & Linkman, S. (2009). Systematic literature reviews in software engineering - A systematic literature review. *Information and Software Technology*, 51(1), 7-15. <https://doi.org/10.1016/j.infsof.2008.09.009>
- Kukreja, N. (2013). Decision theoretic requirements prioritization a two-step approach for sliding towards value realization. In *International Conference on Software Engineering* (pp. 1465-1467). IEEE Publishing. <https://doi.org/10.1109/ICSE.2013.6606746>
- Kukreja, N., Boehm, B., Payyavula, S. S., & Padmanabhuni, S. (2012). Selecting an appropriate framework for value-based requirements prioritization. In *20th IEEE International Requirements Engineering Conference (RE)* (pp. 303-308). IEEE Publishing. <https://doi.org/10.1109/RE.2012.6345819>
- Laplante, P. A. (2017). *Requirements Engineering for Software and Systems* (3rd Ed.). Taylor & Francis Group.
- Lim, S. L., & Finkelstein, A. (2012). StakeRare: Using social networks and collaborative filtering for large-scale requirements elicitation. In *IEEE Transactions on Software Engineering* (Vol. 38, pp. 707-735). IEEE Publishing. <https://doi.org/10.1109/TSE.2011.36>
- Lim, S. L., Harman, M., & Susi, A. (2013). Using genetic algorithms to search for key stakeholders in large-scale software projects. In I. Mistrik, A. Tang, R. Bahsoon & J. Stafford (Eds.), *Aligning Enterprise, System, and Software Architectures* (pp. 118-134). IGI Global. <https://doi.org/10.4018/978-1-4666-2199-2.ch007>
- Madi, T., Dahalin, Z., & Baharom, F. (2013). Towards a user value co-creation model for agile web development approach. *Science International*, 25(4), 1137-1143.

- McZara, J., Sarkani, S., Holzer, T., & Eveleigh, T. (2015). Software requirements prioritization and selection using linguistic tools and constraint solvers - A controlled experiment. *Empirical Software Engineering*, 20, 1721-1761. <https://doi.org/10.1007/s10664-014-9334-8>
- Narendhar, M., & Anuradha, K. (2016). Different approaches of software requirement prioritization. *International Journal of Engineering Science Invention*, 5(9), 38-43.
- Nurdiani, I., Borstler, J., & Fricker, S. A. (2016). The impacts of agile and lean practices on project constraints: A tertiary study. *Journal of Systems and Software*, 119, 162-183. <https://doi.org/10.1016/j.jss.2016.06.043>
- Odu, G. O., & Charles-Owaba, O. E. (2013). Review of multi-criteria optimization methods - Theory and applications. *IOSR Journal of Engineering*, 3(10), 1-14. <https://doi.org/10.9790/3021-031020114>
- Pohl, K., & Rupp, C. (2015). *Requirements Engineering Fundamentals* (2nd Ed.). Rocky Nook.
- Racheva, Z., Daneva, M., Herrmann, A., & Wieringa, R. J. (2010). A conceptual model and process for client-driven agile requirements prioritization: Results of a case study. In *Proceedings the 2010 ACM-IEEE International Symposium on Empirical Software Engineering and Measurement* (pp. 1-4). ACM Publishing. <https://doi.org/10.1145/1852786.1852837>
- Rahim, M. S., Chowdhury, A. Z. M. E., & Das, S. (2018). Rize: A proposed requirements prioritization technique for agile development. In *5th IEEE Region 10 Humanitarian Technology Conference 2017, R10-HTC 2017* (pp. 634-637). IEEE Publishing. <https://doi.org/10.1109/R10-HTC.2017.8289039>
- Riegel, N. (2012). Model-based prioritization in business-process-driven software development. In *20th IEEE International Requirements Engineering Conference* (pp. 349-352). IEEE Publishing. <https://doi.org/10.1109/RE.2012.6345836>
- Riegel, N., & Doerr, J. (2015). A systematic literature review of requirements prioritization criteria. In S. Fricker & K. Schneider (Eds.), *Requirements Engineering: Foundation for Software Quality. REFSQ 2015. Lecture Notes in Computer Science* (Vol. 9013). Springer. [https://doi.org/10.1007/978-3-319-16101-3\\_22](https://doi.org/10.1007/978-3-319-16101-3_22)
- Sadiq, M., & Jain, S. K. (2013). A fuzzy-based approach for requirements prioritization in goal-oriented requirements elicitation process. In *International Conference on Software Engineering and Knowledge Engineering*, (pp. 54-58). ResearchGate.
- Samarakoon, S. M. K., & Ratnayake, R. M. C. (2015). Strengthening, modification and repair techniques' prioritization for structural integrity control of ageing offshore structures. *Reliability Engineering and System Safety*, 135, 15-26. <https://doi.org/10.1016/j.ress.2014.10.023>
- Schön, M., Thomaschewski, J., & Escalona, M. J. (2017). Agile Requirements Engineering: A systematic literature review. *Computer Standards & Interfaces*, 49, 79-91. <https://doi.org/10.1016/j.csi.2016.08.011>
- Schön, E., Winter, D., Escalona, M. J., & Thomaschewski, J. (2017). Key challenges in agile requirements engineering. In *International Conference on Agile Processes in Software Engineering and Extreme Programming* (Vol. 283, pp. 37-51). Springer. [https://doi.org/10.1007/978-3-319-57633-6\\_3](https://doi.org/10.1007/978-3-319-57633-6_3)
- Sheemar, H., & Kour, G. (2019). Enhancing user-stories prioritization process in agile environment. In *International Conference on Innovations in Control, Communication and Information Systems, ICICCI 2017* (pp. 1-6). IEEE Publishing. <https://doi.org/10.1109/ICICCI.2017.8660760>

- Sher, F., Jawawi, D. N. A., Mohamad, R., & Babar, M. I. (2014). Requirements prioritization techniques and different aspects for prioritization a systematic literature review protocol. In *2014 8th Malaysian Software Engineering Conference (MySEC)* (pp. 31-36). IEEE Publishing. <https://doi.org/10.1109/MySec.2014.6985985>
- Sher, F., Jawawi, D. N. A., & Mohammad, R. (2019). Requirements prioritization aspects quantification for value-based software developments. *Journal of Theoretical and Applied Information Technology*, *97*(14), 3969-3979.
- Shukla, V., & Auriol, G. (2013, December 4). Methodology for determining stakeholders' criteria weights in systems engineering [Conference session]. In *Proceedings of the Posters Workshop at CSD&M*. Paris, France.
- Sie, A (2016). *Cost-value Requirements Prioritization in Requirements Engineering Student*. Semantic Scholar.
- Sommerville, I. (2016). *Software Engineering* (10th Ed.). Pearson.
- Sufian, M., Khan, Z., Rehman, S., & Haider Butt, W. (2019). A systematic literature review: Software requirements prioritization techniques. In *Proceedings - 2018 International Conference on Frontiers of Information Technology, FIT 2018* (pp. 35-40). IEEE Publishing. <https://doi.org/10.1109/FIT.2018.00014>
- Sureka, A. (2014). Requirements prioritization and next-release problem under non-additive value conditions. In *Proceedings of the Australian Software Engineering Conference, ASWEC* (pp. 120-123). IEEE Publishing. <https://doi.org/10.1109/ASWEC.2014.12>
- Svensson, R. B., Gorschek, T., Regnell, B., Torkar, R., Shahrokni, A., Feldt, R., & Aurum, A. (2011). Prioritization of quality requirements: State of practice in eleven companies. In *Proceedings of the 2011 IEEE 19th International Requirements Engineering Conference, RE 2011* (pp. 69-78). IEEE Publishing. <https://doi.org/10.1109/RE.2011.6051652>
- Sverrisdottir, H. S., Ingason, H. T., & Jonasson, H. I. (2014). The role of the product owner in scrum-comparison between theory and practices. *Procedia - Social and Behavioral Sciences*, *119*, 257-267. <https://doi.org/10.1016/j.sbspro.2014.03.030>
- Tahvili, S., Saadatmand, M., & Bohlin, M. (2015, 15-20 November). Multi-criteria test case prioritization using fuzzy analytic hierarchy process [Conference session]. In *Tenth International Conference on Software Engineering Advances*. Barcelona, Spain.
- Thakurta, R. (2012). A framework for prioritization of quality requirements for inclusion in a software project. *Software Quality Journal*, *21*, 573-597. <https://doi.org/10.1007/s11219-012-9188-5>
- Thakurta, R. (2016). Understanding requirement prioritization artifacts: A systematic mapping study. *Requirements Engineering*, *22*, 491-526. <https://doi.org/10.1007/s00766-016-0253-7>
- Torrecilla-Salinas, C. J., Sedeño, J., Escalona, M. J., & Mejías, M. (2015). Estimating, planning and managing agile web development projects under a value-based perspective. *Information and Software Technology*, *61*, 124-144. <https://doi.org/10.1016/j.infsof.2015.01.006>
- Veerappa, V. (2012). *Clustering methods for requirements selection and optimisation* (Doctoral dissertation). University College London, UK. <https://discovery.ucl.ac.uk/id/eprint/1386661/>

- Viswanathan, A., Nair, S. R., & Krishnan, S. M. (2016). Solution model for requirement prioritization. *International Journal of Control Theory and Applications*, 9(15), 7489-7496.
- Wieggers, K. E. (2009). *Software Requirements* (2nd Ed.). Microsoft Press.
- Wieringa, R. J. (1996). *Requirements Engineering: Frameworks for Understanding*. Wiley.
- Wohlin, C., & Aurum, A. (2005). What is important when deciding to include a software requirement in a project or release? In *International Symposium on Empirical Software Engineering* (pp. 246-255). IEEE Publishing. <https://doi.org/10.1109/ISESE.2005.1541833>





## Contamination and Human Health Risk Assessment of Toxic Trace Elements in Drinking Water of Gilgit-Baltistan, Pakistan

Syed Jarar Hussain<sup>1,2</sup>, Shaukat Ali<sup>1\*</sup>, Javid Hussain<sup>3</sup>, Salar Ali<sup>4</sup>, Jamal Hussain<sup>5</sup>, Manzoor Hussain<sup>6</sup> and Ittehad Hussain<sup>7</sup>

<sup>1</sup>Department of Environmental Sciences, Karakoram International University, Gilgit, 15100, Pakistan

<sup>2</sup>Gilgit-Baltistan Environmental Protection Agency Gilgit, 15100, Pakistan

<sup>3</sup>Department of Environmental Sciences, Balochistan University of Information Technology, Engineering and Management Sciences, Quetta, 87100, Pakistan

<sup>4</sup>Department of Environmental Sciences, University of Baltistan, Skardu, Pakistan

<sup>5</sup>Department of Economics, Karakoram International University, Gilgit, 15100, Pakistan

<sup>6</sup>Department of Chemistry, Karakoram International University, Gilgit, 15100, Pakistan

<sup>7</sup>Research Center for Eco-Environmental Sciences, Chinese Academy of Sciences, Beijing, 100085, People's Republic of China

### ABSTRACT

This study investigated the contamination level and risk associated with toxic trace elements in springs' water from Gilgit-Baltistan, Pakistan. Toxic trace elements, including Hg, As, and Zn, were analyzed by metalizer, HM 2000 serial no. MY-011-006, while elements such as Cr, Al, B, Ni, Cu, Mn, and Fe were analyzed using Metalometer HM 2000 serial no. MM005-007, the United Kingdom. The mean concentrations of TTEs in water samples from Skardu were ordered as, Mn < Cu < Fe < Zn < Al < Cr < As < Ni < Hg, in Gilgit, Mn

< Cu < Zn < Ni < B < Cr < Fe < As < Hg, in Ghizer Cu < Mn < Zn < Ni < Cr < Fe < As < Hg, while in Nagar the concentration of TTEs in water samples were ordered as Cu < Mn < Fe < Ni < Al < Cr < Zn < As < Hg. Results obtained from this study showed that the concentrations of As, Hg, Ni, Cr, Al, and Mn in some water samples were higher than the limits recommended by WHO and Pak-NDWQS. However, the chronic daily intake indices (CDIs) and health risk index (HRI) in all samples were found below the US-EPA standards. The correlation analysis revealed a positive association among

### ARTICLE INFO

#### Article history:

Received: 15 December 2021

Accepted: 24 May 2022

Published: 21 October 2022

DOI: <https://doi.org/10.47836/pjst.31.1.12>

#### E-mail addresses:

jarar.gbepa@gmail.com (Syed Jarar Hussain)

dr.shaukat@kiu.edu.pk (Shaukat Ali)

Javid.hussain@buitms.edu.pk (Javid Hussain)

salar.ali@uobs.edu.pk (Salar Ali)

Jamal.hussain@kiu.edu.pk (Jamal Hussain)

manzoor.hussain@kiu.edu.pk (Manzoor Hussain)

ittehad.hussain12@gmail.com (Ittehad Hussain)

\* Corresponding author

different elements, which revealed that the sources of TTE<sub>s</sub> in water samples were mainly geological strata and anthropogenic activities.

*Keywords:* Correlation analysis, Gilgit-Baltistan, Pakistan springs water, risk assessment, toxic trace elements

---

## INTRODUCTION

Naturally, heavy metals in the aquatic environment are very small amounts, mainly released from the natural weathering of rocks and soils (Dessie et al., 2021). However, it is clear that metal enters the aquatic system from multiple sources, both point and non-point and can be easily transported from the abiotic to the biotic system (Khan, 2011).

Currently, the effect of heavy metal pollution on human beings is becoming critical. Heavy metals are classified as essential and nonessential or toxic depending on their toxicity and nutritional value. Cu, Mn, Fe, Zn, and Co are needed in minute quantities for living beings' normal function and survival (Muhammad et al., 2019). Toxic trace elements can follow multiple pathways to enter the body, e.g., skin contact, taking foods, drinking, and breathing (Ali & Rubina, 2018). Though some trace elements are necessary for metabolic activities at small concentrations (Mohmand et al., 2015), a higher concentration may cause havoc on human health.

The most abundant toxic trace elements in the environment are Cd, Pb, Cr, As, Cu, Zn, Ni, and Pb, and prior studies have highlighted that their exposure can cause various poisoning influences on the human body because it can damage the kidney function, circulatory system, and nervous system (Yang & Massey, 2019; Zhang et al., 2015). Moreover, agglomeration of the toxic trace elements in the body brings about various ailments, while their synergistic may even cause death (Huma-Khan et al., 2016; Rasool et al., 2016). For example, zinc helps in body growth and is necessary for the normal functions of living organisms, and its deficiency causes poor wound healing, anorexia, hair loss, immune dysfunction, diarrhea, and dermatitis (Stephanie, 2010). In the same way, Alzheimer's and Manganism are the top diseases caused by prolonged exposure to a high concentration of Mn and Cu in drinking water (Dieter et al., 2005; Muhammad Tahir et al., 2020). Furthermore, the high concentration of Mn in drinking water is perilous to children's intellectual functions (Wasserman et al., 2006).

Several previous studies in different countries assessed the heavy metal contamination in different environmental samples such as water, sediment, soil, and foodstuff (Ali et al., 2019; Dessie et al., 2021; Jiang et al., 2018). Furthermore, the health risk assessment of heavy metals in tap water/drinking water has been conducted in different parts of the world, such as carcinogenic and non-carcinogenic health risk assessments in Iran (Alidadi et al., 2019; Mohammadi et al., 2019; Saleh et al., 2019), compositional and health risk assessment in Pakistan (Muhammad et al., 2011; Murtaza et al., 2020), and water quality

and human health risk assessment in China (Ji et al., 2020). Therefore, it is good to conclude by stating the two sides of the study outcomes: some with low risk and some with alarmingly high risk.

Around two million people of Gilgit-Baltistan are at risk due to the lack of safe drinking water, clear air, and hygienic food products. The number of prevailing diseases, including cardiovascular, upper respiratory tract index, cancer, hepatitis, and many more, are distressing to the public. The rapidly increasing contaminations in the northern part of Pakistan due to the growing population and unplanned infrastructures pose threats to the water quality requiring deep study.

According to our knowledge, there is limited data available on toxic trace element concentrations and their sources in the drinking water of Gilgit-Baltistan. Our studies on toxic trace element concentrations in drinking water sources are extremely important to prevent water contamination and its effects on humans in Pakistan and as well as in other countries. This study attempts to investigate the contamination level of toxic trace elements and their potential health risk in drinking water sources of Gilgit-Baltistan, Pakistan.

## MATERIALS AND METHODS

### Study Area

Gilgit-Baltistan is spread over an area of about 72,500 km<sup>2</sup> and is in northern Pakistan over the Himalayas, Karakoram, and Hindukush Mountains. The climate of Gilgit-Baltistan varies spatially; the complex topography of mountains is responsible for the substantial variability. The eastern part (western Himalayas) is relatively moist, while the climate becomes considerably drier in the Karakoram and Hindukush mount ranges (WWF, 2009). The tectonic setting of the area is highly complex, and the rocks are tremendously deformed. The Indian plate contributed mostly to the exposed rocks, made up of ultramafic and mafic rocks, i.e., greenschist, serpentinite, meta basalt, and schist (Arif et al., 2011; Muhammad et al., 2010). Due to the collision of the Indian and Eurasian plates, different metamorphosed rocks are formed. The primary rocks include peridotite, dunite, gabbros, gabbronorite, pegmatite, quartz vein, basalt, diorite, granodiorite, hornblendite, and granite. Metamorphic rocks are phyllite, schist, gneiss, quartzite, and granulite structurally (A. Khan et al., 2015). Rocks begin to change chemically at temperatures above 200°C. At these temperatures, the crystalline structures of the minerals in the rock are broken down and transformed using different combinations of the available elements and compounds (Pidwirny, 2006), thus creating minerals. Gilgit-Baltistan is divided into three divisions and ten districts, including Gilgit, Hunza, Nagar, Skardu, Shigar, Khapulo, Ghanche, Astore, Diamer, and Ghizer. The present study was conducted in four districts, including Gilgit, Skardu, Ghizer, and Nagar, as shown in Figure 1.

### Sampling Procedure

Four districts, i.e., Gilgit, Skardu, Nagar, and Ghizer, were selected for the springs' water sampling based on tectonic and geologic settings. Thirty-six triplicate samples were collected through random sampling: ten were collected from district Skardu, seven from Gilgit, twelve from Ghizer, and seven from Nagar in June, July and August 2018. The water samples were collected from the targeted sampling locations with a clean polyethylene plastic bottle. Before the sampling, bottles were pre-washed with 20% nitric acid (HNO<sub>3</sub>) and double-distilled water. Samples were filtered and acidified with HNO<sub>3</sub> before transferring them to the laboratory. All the samples were stored at 4°C in a refrigerator (USEPA, 2003). A geographical position system (GPS) was used to record the coordinates of sampling sites. The study area map and sampling sites are shown in Figure 1.

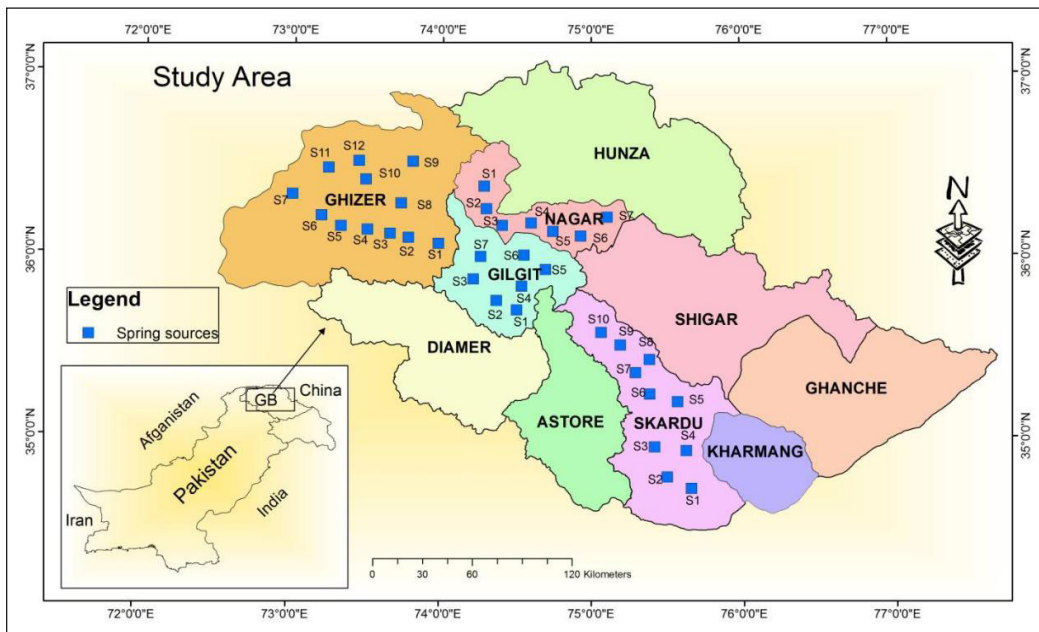


Figure 1. Study area map showing sampling sites in Gilgit-Baltistan, Pakistan

### Chemical Analysis

Water samples were analyzed in a laboratory at Gilgit-Baltistan Environmental Protection Agency (GB-EPA). The concentration of TTEs, including Hg, As, and Zn, were analyzed using Metalyzer HM 2000 Serial No. MY-011-006, while Cr, Al, B, Ni, Cu, Mn, and Fe were analyzed by Metalometer HM 2000 Serial No. MM 005-007, the United Kingdom. The lower and upper instrumental detection limits of Hg, As, and Zn were 5 µg/L and 500 µg/L, respectively. Similarly, the detection limits of Cr, Al, B, Ni, Cu, Mn, Fe were 0.02, 0.01, 0.1, 0.01, 0.05, 0.1, 0.02 mg/L and 2, 0.25, 2, 10, 5, 18, 3 mg/L, respectively.

## Human Health Risk Assessment

Among several pathways through which TTEs enter the body, oral intake is substantial (Lambert et al., 2000). Therefore, the chronic daily intakes (CDIs) of TTEs via water ingestion were calculated using Equation 1 (Krishna et al., 2009; Lambert et al., 2000).

$$CDI = C_m \times L_w / W_b \quad (1)$$

Where  $C_m$ ,  $W_b$ , and  $L_w$  are the TTEs concentration ( $\mu\text{g/l}$ ), average body weight, and daily water intake, respectively. An average  $L_w$  is 2 l/day (adult) or 1 l/day (child), whereas an average  $W_b$  is 72 kg (adults) or 32.7 kg (child), as reported (Alina et al., 2012; Sharma et al., 2008). The health risk index (HRI) was calculated using Equation 2 (Krishna et al., 2009).

$$HRI = CDI/RfD \quad (2)$$

Where  $RfD$  is the value of oral toxicity, reference dose ( $\mu\text{g/kg}^{-1}\text{day}^{-1}$ ). According to the US-EPA database, the  $RfD$  values for Zn, Cr, Mn, Cu, and Ni are  $3.0\text{E} + 02$ ,  $1.5\text{E} + 03$ ,  $1.4\text{E} + 02$ ,  $3.7\text{E} + 01$ , and  $2.0\text{E} + 01$ , respectively (Krishna et al., 2009). It is reported that if the HRI is  $< 1$ , it is considered a safe limit (Sharma et al., 2008).

## Statistical Analysis

Descriptive statistical analysis was performed by using MS Excel 2016 and OriginLab, 2019. In addition, a statistical one-way ANOVA analysis was performed for the correlation among elements using SPSS software V-17. Finally, the spatial distribution of TTEs in water samples was estimated based on the inverse distance weighted (IDW) interpolation method by using ArcGIS.

## RESULTS AND DISCUSSION

### Mean Concentrations of TTEs

The mean concentrations of TTEs in water samples collected from Skardu were ordered as,  $\text{Mn} < \text{Cu} < \text{Fe} < \text{Zn} < \text{Al} < \text{Cr} < \text{As} < \text{Ni} < \text{Hg}$ , in Gilgit as,  $\text{Mn} < \text{Cu} < \text{Zn} < \text{Ni} < \text{B} < \text{Cr} < \text{Fe} < \text{As} < \text{Hg}$ , in Ghizer  $\text{Cu} < \text{Mn} < \text{Zn} < \text{Ni} < \text{Cr} < \text{Fe} < \text{As} < \text{Hg}$ , while in Nagar the concentrations were ordered as,  $\text{Cu} < \text{Mn} < \text{Fe} < \text{Ni} < \text{Al} < \text{Cr} < \text{Zn} < \text{As} < \text{Hg}$ . The mean concentrations of Hg in Skardu, Gilgit, Ghizer, and Nagar districts were measured as  $0.0107 \pm 0.0075$ ,  $0.0005 \pm 0.0002$ ,  $0.002 \pm 0.0007$ , and  $0.0007 \pm 0.0007$  mg/L, respectively as shown in Table 1. The higher concentration of Hg in spring water sources might be due to leaching or weathering of ultramafic and mafic rocks as well as mining/anthropogenic activities (Hussain et al., 2019). The mean concentrations of As in water samples collected from Skardu, Gilgit, Ghizer, and Nagar districts were measured as  $0.0296 \pm 0.0101$ ,  $0.011$

$\pm 0.0030$ ,  $0.011 \pm 0.0033$ , and  $0.01 \pm 0.0038$ , respectively. The highest concentration of As ( $0.18 \text{ mg/L}$ ) was measured in water samples from Skardu, which might be due to weathering/leaching of ultramafic and mafic rocks. The mean concentrations of Cr in Skardu, Gilgit, Ghizer, and Nagar districts were  $0.03 \pm 0.0557$ ,  $0.02 \pm 0.0054$ ,  $0.032 \pm 0.0050$ , and  $0.014 \pm 0.0041 \text{ mg/L}$ , respectively.

The highest concentrations of Cr were detected in Skardu and Ghizer ( $0.07 \text{ mg/L}$ ). Cr is used extensively in industrial activities, such as cement dyeing, metal cleaning, leather tanning, and electroplating. Moreover, agricultural activities and weak and corrosive plumbing may have added Cr into the environment (Kisku et al., 2011). It is reported that a certain quantity of Cr is necessary for growth and different functions; however, the high concentrations of Cr are genotoxic, carcinogens, and cause liver and kidney ailments (Huma-Khan et al., 2016). The mean concentrations of Ni in Skardu, Gilgit, Ghizer, and Nagar were as,  $0.029 \pm 0.0073$ ,  $0.057 \pm 0.0176$ ,  $0.075 \pm 0.0200$  and  $0.03 \pm 0.018 \text{ mg/L}$  respectively. The highest concentration of Ni  $0.3 \text{ mg/L}$  was found in water samples from Ghizer. The highest concentration of Ni in spring water sources could be because of dissolution from nickel ore-bearing rocks in the area. The mean concentrations of Mn were  $1.76 \pm 0.3438$ ,  $0.87 \pm 0.3139$ ,  $0.177 \pm 0.0408$ , and  $0.187 \pm 0.0643 \text{ mg/L}$ . The highest concentration of Mn was detected in water samples collected from Skardu ( $4.3 \text{ mg/L}$ ), which might be due to the direct interconnection between water ultramafic and mafic rocks in the area (Huma-Khan et al., 2016).

The concentration of Al in water samples from the Gilgit and Ghizer districts was not detected. In contrast, the mean concentration of Al in water samples collected from the Skardu and Nagar districts were  $0.045 \pm 0.0167 \text{ mg/L}$  and  $0.018 \pm 0.0138 \text{ mg/L}$ , respectively. Similarly, the concentration of B in water collected from Skardu, Ghizer, and Nagar was not detected, whereas, in water samples collected from the Gilgit district, the mean concentration of B was detected as  $0.042 \pm 0.0244 \text{ mg/L}$ . The mean concentrations of Fe and Cu in the study area are shown in Table 1, which were found within the permissible limits recommended by Pak-EPA. The mode of occurrence of Fe and Cu in spring water source samples are due to geogenic and anthropogenic activities in the form of mining, weathering, leaching of rocks, water passing through geological strata, agriculture activities like the use of pesticides and industrial flushing (Hussain et al., 2019).

Similar to this study's results, the study of Kosovo showed the highest mean concentration levels for Fe, Al, and Mn heavy metals; these three metals exceeded the safety limit for drinking water in some samples (Malsiu et al., 2020). Also, in Tamil Nadu, India, among sixteen analyzed heavy metals, Fe, AL, B, Cu, Cd, Ag, Pb, Ni, and Mn concentration levels were higher than their permissible limits (Vetrimurugan et al., 2017). On the other hand, the results of some studies conducted in Germany, Jordan, Malaysia, the USA, and Turkey highlighted that the heavy metal concentration in their drinking water

was lower than allowed and permissible limits (Alidadi et al., 2019) and higher than the standard limits from Pakistan (Ahmed et al., 2019; Habib et al., 2020; Islam et al., 2020; S. Khan et al., 2016), Nigeria (Maigari et al., 2016), India (Vetrimurugan et al., 2017), Ghana (Bortey-Sam et al., 2015), and Iran (Sadeghi et al., 2020).

Table 1

Mean concentrations (mg/L) of selected metals in drinking water samples in the study area ( $n^a = 36 \times 3$ )

Parameter	Statistics	Skardu n=10	Gilgit n=7	Ghizer n=12	Nagar n=7	PAK <sup>b</sup> - NDWQS	WHO <sup>c</sup> Guidelines
Hg	Range	0-0.07	0-0.003	0-0.01	0-0.004	≤0.001	0.001
	Mean	<b>0.0107</b>	0.0005	<b>0.002</b>	0.0007		
	Std Error	±0.0075	±0.0002	±0.0007	±0.0007		
As	Range	0-0.19	0-0.05	0-0.062	0-0.05	≤0.05	0.05
	Mean	0.0296	0.011	0.011	0.01		
	Std Error	±0.0101	±0.0030	±0.0033	±0.0038		
Zn	Range	0-0.23	0-0.41	0-0.37	0-0.07	5.0	3
	Mean	0.047	0.077	0.128	0.013		
	Std Error	±0.0122	±0.0306	±0.0441	±0.0049		
Cr	Range	0-0.08	0-0.07	0-0.09	0-0.05	≤0.05	0.05
	Mean	0.03	0.02	0.032	0.014		
	Std Error	±0.0557	±0.0054	±0.0050	±0.0041		
Ni	Range	0-0.1	0-0.3	0-0.4	0-0.1	≤0.02	0.2
	Mean	<b>0.029</b>	<b>0.057</b>	<b>0.075</b>	<b>0.03</b>		
	Std Error	±0.0073	±0.0176	±0.0200	±0.018		
Fe	Range	0-0.4	0-0.3	0-0.06	0-0.9	---	--
	Mean	0.055	0.012	0.011	0.128		
	Std Error	±0.0199	±0.0139	±0.0064	±0.0704		
Al	Range	0-0.3			0-0.1	≤0.2	0.2
	Mean	0.045	ND <sup>d</sup>	ND	0.018		
	Std Error	±0.0167			±0.0138		
B	Range		0-0.4			0.3	0.3
	Mean	ND	0.042	ND	ND		
	Std Error		±0.0244				
Mn	Range	0-4.5	0-3.6	0-0.8	0-0.84	≤0.5	0.5
	Mean	<b>1.76</b>	<b>0.87</b>	0.177	0.187		
	Std Error	±0.3438	±0.3139	±0.0408	±0.0643		
Cu	Range	0-2.2	0-0.4	0-1.9	0-1.5	2	2
	Mean	0.45	0.1	0.358	0.412		
	Std Error	±0.1244	±0.0305	±0.0943	±0.1173		

Note. <sup>a</sup>number of samples; <sup>b</sup> source: Pakistan National Drinking Water Quality Standards, 2008; <sup>c</sup> World Health Organization (WHO, 2008); <sup>d</sup> not detected



**Human Health Risk Assessment**

**Chronic Daily Intake Indices.** According to the results, obtained from the human health risk analysis the Chronic daily intake indices (CDIs) for adults and children were calculated in water samples from Skardu were ordered as, Mn < Cu < Fe < Zn < Al < Cr < As and Ni < Hg , in Gilgit as, Mn < Cu < Zn < Ni < B < Cr < Fe < As < Hg , in Ghizer as, Cu < Mn < Zn < Ni < Cr < Fe < As < Hg, and in Nagar as, Cu < Al < Mn < Fe < Cr < Zn < Ni < As < Hg. The CDIs of B in water samples from Gilgit, Ghizer, and Nagar districts and Al in all water samples collected from four districts were not calculated for adults and children because their concentrations were found below the detection limit. Overall the CDIs in the study area were within the permissible limits recommended by USEPA (USEPA, 2005).

The high concentration of TTEs in the springs’ water is generally controlled by drainage basin, lithology, and hydrodynamic features of aquifers (Hussain, 2019). However, the availability of high concentrations in drinking water may cause various health problems. The chronic daily intake through drinking water is presented in Table 2.

Table 2  
*Chronic daily intake (CDIs mg/lkg-1day-1) through drinking water (n<sup>a</sup> = 36×3)*

Parameter	Individuals	Skardu n=10	Gilgit n=7	Ghizer n=12	Nagar n=7
Hg	Adults	0.00027	1.39E-05	5.56E-05	1.94E-05
	Children	0.0003	1.53E-05	6.12E-05	2.14E-05
As	Adults	0.0008	0.0003	0.00028	0.00027
	Children	0.00088	0.00033	0.0003	0.0003
Zn	Adults	0.0013	0.0021	0.00035	0.00038
	Children	0.0014	0.0023	0.0039	0.00039
Cr	Adults	0.00083	0.00055	0.00088	0.00039
	Children	0.00091	0.00061	0.00097	0.00042
Ni	Adults	0.0008	0.0015	0.002	0.00038
	Children	0.00088	0.0017	0.0022	0.00091
Fe	Adults	0.0015	0.00033	0.00032	0.0035
	Children	0.0016	0.00036	0.00033	0.0039
Al	Adults	0.0012	ND	ND	0.00051
	Children	0.0013	ND	ND	0.00055
B	Adults	ND	0.0011	ND	ND
	Children	ND	0.0012	ND	ND
Mn	Adults	0.048	0.024	0.0049	0.0051
	Children	0.053	0.026	0.0054	0.0057
Cu	Adults	0.012	0.0027	0.0099	0.011
	Children	0.013	0.003	0.01	0.012

Note. n = number of water samples; ND = not detected

**Health Risk Index.** The calculated health risk indices (HRIs) for adults and children in Skardu were ordered as, Mn < Cu < Ni < Zn < Cr, in Gilgit as, Mn < Ni Cu < Zn < Cr, in Ghizer as, Cu < Ni < Mn < Zn < Cr and in Nagar as Cu < Mn < Ni < Zn < Cr. HRIs of Zn for adults in Skardu, Gilgit Ghizer, and Nagar were calculated as 0.0043, 0.007, 0.0011, and 0.0012 for children of Skardu, Gilgit, and Ghizer, respectively and Nagar were calculated as, 0.0046, 0.0076, 0.0013, and 0.0013. The HRIs of Cr were 0.00055, 0.00036, 0.00058, and 0.00026 for adults and 0.0006, 0.0004, 0.00064 and 0.00028 for children in Skardu, Gilgit, Ghizer, and Nagar, respectively. The HRIs of Ni ranged from 0.01 to 0.075 for adults and from 0.011 to 0.085 for children. The HRIs of Mn were 0.34, 0.171, 0.035 and 0.036 for adults and were 0.37, 0.18, 0.038 and 0.04 for children, whereas the HRIs of Cu were 0.32, 0.072, 0.26 and 0.29 for adults and 0.35, 0.081, 0.27 and 0.32 for children in Skardu, Gilgit, Ghizer, and Nagar. The HRIs of Hg, As, Al, B, and Fe were not calculated because there is no reference dose for these elements. The HRI values ranged between safe limits (HRI < 1) in Gilgit-Baltistan, as shown in Table 3, suggesting that, at present, there is no risk associated with TTEs to the health of adults and children.

Table 3  
Health risk indexes (HRIs) through drinking water (n= 36×3)

Parameter	Individuals	Skardu n=10	Gilgit n=7	Ghizer n=12	Nagar n=7
Hg	Adults	NC	NC	NC	NC
	Children				
As	Adults	NC	NC	NC	NC
	Children				
Zn	Adults	0.0043	0.007	0.0011	0.0012
	Children	0.0046	0.0076	0.0013	0.0013
Cr	Adults	0.00055	0.00036	0.00058	0.00026
	Children	0.0006	0.0004	0.00064	0.00028
Ni	Adults	0.04	0.075	0.01	0.019
	Children	0.044	0.085	0.011	0.045
Fe	Adults	NC	NC	NC	NC
	Children				
Al	Adults	NC	ND	ND	NC
	Children				
B	Adults	ND	NC	ND	ND
	Children				
Mn	Adults	0.34	0.171	0.035	0.036
	Children	0.37	0.18	0.038	0.04
Cu	Adults	0.32	0.072	0.26	0.29
	Children	0.35	0.081	0.27	0.32

Note. n = number of water samples: NC = not calculated: ND = not detected

### Spatial Distribution of TTEs

Spatial variations based on the concentration of different elements were found in the study area, as presented in Figure 2. The post hoc or Tukey test highlighted that the concentration of Hg was higher ( $P < 0.05$ ) in Skardu compared to Gilgit and Nagar, as shown in Figure 2. It was reported that the high concentration of Hg in water mostly evolved from mining wastes (Hussain et al., 2019). The mean concentration of Zn was significantly higher ( $P < 0.05$ ) in Ghizer compared to Skardu and Nagar. Fe concentration was found to be

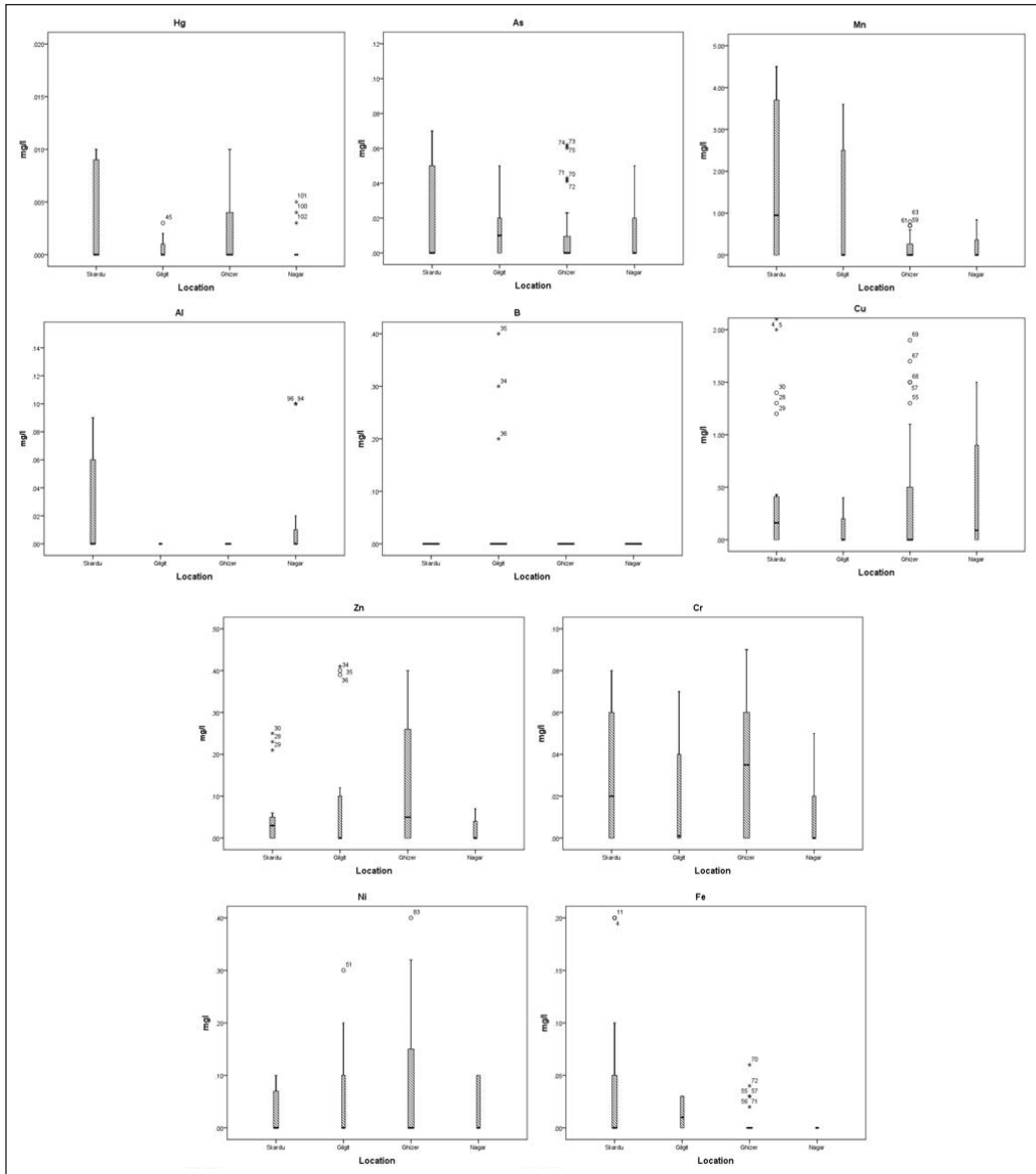


Figure 2. One-way ANOVA box plot comparison of selected TTEs with sampling locations

significantly higher in water from the Nagar than in Ghizer. The concentration of Al in water samples collected from the Skardu was considerably higher than in Gilgit and Ghizer. Similarly, the concentration of B in water samples collected from Gilgit was significantly higher than the concentrations measured in water samples collected from Ghizer Nagar and Skardu. The concentration of Mn in Skardu was higher than in Gilgit, Ghizer, and Nagar. An insignificant difference ( $P > 0.05$ ) was observed among As, Cr, Ni, and Cu in the analyzed water samples. Geologically, these elements can be evolved by reaction with passing through various rock strata and can behave similarly/differently from one another (Kavcar et al., 2009).

### Correlation Analysis

One-way ANOVA analysis for correlations among elements was performed using SPSS software V17. The correlations among different elements provide very useful evidence of the concentrations and pathways of TTEs (Huma-Khan et al., 2016). Based on the results obtained from our study, very strong correlation was found among different elements, such as Hg-As ( $r = 0.983$ ,  $P > 0.05$ ), Hg-Al ( $r = 0.884$ ,  $P > 0.05$ ), Hg-Mn ( $r = 0.852$ ,  $P > 0.05$ ), As-Al ( $r = 0.905$ ,  $P > 0.05$ ), As-Mn ( $r = 0.921$ ,  $P > 0.05$ ), Cr-Zn ( $r = 0.669$ ,  $P > 0.05$ ), and Zn-Ni ( $r = 0.945$ ,  $P > 0.05$ ). However, in some water samples, strong negative correlations were observed, such as Zn-Fe ( $r = -0.878$ ), Ni-Al ( $r = -0.816$ ), and Cu-B ( $r = -0.971$ ). The positive correlation between Mn and Zn represents the intimate source of domestic and agricultural activities (Hussain et al., 2019). The correlation matrix has pointed to two elements with the same sources of agricultural activities, industrial and sewage effluents, and geogenic origin from weathering of sulfide-bearing minerals (Huma-Khan et al., 2016). Correlation matrixes of selected TTEs in water samples are shown in Table 4.

Table 4  
Correlation matrixes of selected TTEs in water samples ( $n = 36 \times 3$ )

	Hg	As	Zn	Cr	Ni	Fe	Al	B	Mn	Cu
Hg	1									
As	<b>0.983</b>	1								
Zn	-0.152	-0.259	1							
Cr	0.582	0.462	0.699	1						
Ni	-0.465	-0.554	<b>0.945</b>	0.432	1					
Fe	-0.0163	0.017	<b>-0.878</b>	-0.65	-0.785	1				
Al	<b>0.884</b>	<b>0.905</b>	-0.586	0.166	<b>-0.816</b>	0.437	1			
B	-0.413	-0.285	0.146	-0.314	0.276	-0.479	-0.493	1		
Mn	<b>0.852</b>	<b>0.921</b>	-0.215	0.347	-0.467	-0.17	0.741	0.108	1	
Cu	0.56	0.463	-0.321	0.259	-0.479	0.562	0.682	<b>-0.971</b>	0.088	1

Note. n = number of water samples

## CONCLUSION

The present study investigated the contamination and human health risks in four districts, including Gilgit, Skardu, Ghzer and Nagar of Gilgit-Baltistan, Pakistan. This study's results revealed that the present Hg, As, Cr, Ni, Al, and Mn levels in springs' water from Gilgit-Baltistan are higher than the permissible limits of WHO, and Pak-NDWQS. Meanwhile Fe and Cu concentrations were under the safe limits. Overall, no risks to human health were detected ( $HRI < 1$ ), but in the near future, the increasing concentration may reach to HRI level recommended by US-EPA. One-way ANOVA showed significant positive/negative correlations among different elements. The positive correlations revealed that the mode of occurrence of TTEs is lithological and anthropogenic. The results of this study provide useful information for policymakers and local administration to control TTE<sub>s</sub> pollution to provide safe drinking water to the residents of Gilgit-Baltistan, Pakistan.

## ACKNOWLEDGMENTS

The authors acknowledge the GB-EPA for providing the laboratory facility for analyzing heavy metals.

## REFERENCES

- Ahmed, N., Bodrud-Doza, M., Islam, A. R. M. T., Hossain, S., Moniruzzaman, M., Deb, N., & Bhuiyan, M. A. Q. (2019). Appraising spatial variations of As, Fe, Mn and NO<sub>3</sub> contaminations associated health risks of drinking water from Surma basin, Bangladesh. *Chemosphere*, 218, 726-740. <https://doi.org/10.1016/j.chemosphere.2018.11.104>
- Ali, S., & Rubina, S. H. (2018). Assessment of freshwater springs, associated diseases and indigenous perception in Ghizer, Gilgit-Baltistan, Pakistan. *Pakistan Journal of Medical Sciences*, 34(1), 121-124.
- Ali, U., Batool, A., Ghufran, M., Asad-Ghufran, M., Sabahat-Kazmi, S., & Hina-Fatimah, S. (2019). Assessment of heavy metal contamination in the drinking water of muzaffarabad, Azad Jammu and Kashmir, Pakistan. *International Journal of Hydrology*, 3(5), 331-337. <https://doi.org/10.15406/ijh.2019.03.00196>
- Alidadi, H., Tavakoly Sany, S. B., Zarif Garaati Oftadeh, B., Mohamad, T., Shamszade, H., & Fakhari, M. (2019). Health risk assessments of arsenic and toxic heavy metal exposure in drinking water in northeast Iran. *Environmental Health and Preventive Medicine*, 24, Article 59. <https://doi.org/10.1186/s12199-019-0812-x>
- Alina, M., Azrina, A., Yunus, A. M., Zakiuddin, S. M., Effendi, H. M. I., & Rizal, R. M. (2012). Heavy metals (mercury, arsenic, cadmium, plumbum) in selected marine fish and shellfish along the Straits of Malacca. *International Food Research Journal*, 19(1), 135-140.
- Arif, M., Henry, D., & Moon, C. (2011). Host rock characteristics and source of chromium and beryllium for emerald mineralization in the ophiolitic rocks of the Indus Suture Zone in Swat, NW Pakistan. *Ore Geology Reviews*, 39(1-2), 1-20.

- Bortey-Sam, N., Nakayama, S. M., Ikenaka, Y., Akoto, O., Baidoo, E., Mizukawa, H., & Ishizuka, M. (2015). Health risk assessment of heavy metals and metalloids in drinking water from communities near gold mines in Tarkwa, Ghana. *Environmental Monitoring and Assessment*, 187, Article 397. <https://doi.org/10.1007/s10661-015-4630-3>
- Dessie, B. K., Gari, S. R., Mihret, A., Desta, A. F., & Mehari, B. (2021). Determination and health risk assessment of trace elements in the tap water of two Sub-Cities of Addis Ababa, Ethiopia. *Heliyon*, 7(5), Article e06988. <https://doi.org/10.1016/j.heliyon.2021.e06988>
- Dieter, H. H., Bayer, T. A., & Multhaup, G. (2005). Environmental copper and manganese in the pathophysiology of neurologic diseases (Alzheimer's disease and Manganism). *Acta hydrochimica et hydrobiologica*, 33(1), 72-78. <https://doi.org/10.1002/ahch.200400556>
- Habib, M. A., Islam, A. R. M. T., Bodrud-Doza, M., Mukta, F. A., Khan, R., Siddique, M. A. B., Phoungthong, K., & Techato, K. (2020). Simultaneous appraisals of pathway and probable health risk associated with trace metals contamination in groundwater from Barapukuria coal basin, Bangladesh. *Chemosphere*, 242, Article 125183. <https://doi.org/10.1016/j.chemosphere.2019.125183>
- Huma-Khan, N., Nafees, M., & Bashir, A. (2016). Study of heavy metals in soil and wheat crop and their transfer to food chain. *Sarhad Journal of Agriculture*, 32(2), 70-79. <http://dx.doi.org/10.17582/journal.sja/2016/32.2.70.79>
- Hussain, R., Wei, C., & Luo, K. (2019). Hydrogeochemical characteristics, source identification and health risks of surface water and groundwater in mining and non-mining areas of Handan, China. *Environmental Earth Sciences*, 78, Article 402. <https://doi.org/10.1007/s12665-019-8350-9>
- Islam, A. R. M. T., Islam, H. T., Mia, M. U., Khan, R., Habib, M. A., Bodrud-Doza, M., Siddique, M. A. B., & Chu, R. (2020). Co-distribution, possible origins, status and potential health risk of trace elements in surface water sources from six major river basins, Bangladesh. *Chemosphere*, 249, Article 126180. <https://doi.org/10.1016/j.chemosphere.2020.126180>
- Ji, Y., Wu, J., Wang, Y., Elumalai, V., & Subramani, T. (2020). Seasonal variation of drinking water quality and human health risk assessment in Hancheng City of Guanzhong Plain, China. *Exposure and Health*, 12, 469-485. <https://doi.org/10.1007/s12403-020-00357-6>
- Jiang, Z., Xu, N., Liu, B., Zhou, L., Wang, J., Wang, C., Dai, B., & Xiong, W. (2018). Metal concentrations and risk assessment in water, sediment and economic fish species with various habitat preferences and trophic guilds from Lake Caizi, Southeast China. *Ecotoxicology and Environmental Safety*, 157, 1-8. <https://doi.org/10.1016/j.ecoenv.2018.03.078>
- Kavcar, P., Sofuoglu, A., & Sofuoglu, S. C. (2009). A health risk assessment for exposure to trace metals via drinking water ingestion pathway. *International Journal of Hygiene And Environmental Health*, 212(2), 216-227. <https://doi.org/10.1016/j.ijheh.2008.05.002>
- Khan, S., Rauf, R., Muhammad, S., Qasim, M., & Din, I. (2016). Arsenic and heavy metals health risk assessment through drinking water consumption in the Peshawar District, Pakistan. *Human and Ecological Risk Assessment: An International Journal*, 22(3), 581-596. <https://doi.org/10.1080/10807039.2015.1083845>

- Khan, T. A. (2011). Trace elements in the drinking water and their possible health effects in Aligarh City, India. *Journal of Water Resource and Protection*, 3(7), 522-530. <https://doi.org/doi:10.4236/jwarp.2011.37062>
- Khan, A., Ahmad, I., Waqarullah, ul Zia, I., & Zakirullah. (2015). *Field report of Gilgit-Baltistan*. <https://pdfcookie.com/documents/geological-field-report-of-gilgit-baltistan-by-arsalan-khan-51q3yxmqd8v7>
- Kisku, G. C., Pandey, P., Negi, M. P. S., & Misra, V. (2011). Uptake and accumulation of potentially toxic metals (Zn, Cu and Pb) in soils and plants of Durgapur industrial belt. *Journal of Environmental Biology*, 32(6), 831-838.
- Krishna, A. K., Satyanarayanan, M., & Govil, P. K. (2009). Assessment of heavy metal pollution in water using multivariate statistical techniques in an industrial area: A case study from Patancheru, Medak District, Andhra Pradesh, India. *Journal of Hazardous Materials*, 167(1-3), 366-373. <https://doi.org/10.1016/j.jhazmat.2008.12.131>
- Lambert, M., Leven, B., & Green, R. (2000). *New methods of cleaning up heavy metal in soils and water*. Hazardous Substance Research Centres. <https://cfpub.epa.gov/ncer/abstracts/index.cfm/fuseaction/display.files/fileID/14295>
- Maigari, A., Ekanem, E., Garba, I., Harami, A., & Akan, J. (2016). Health risk assessment for exposure to some selected heavy metals via drinking water from Dadinkowa dam and river gombe abba in Gombe state, Northeast Nigeria. *World Journal Analytical Chemistry*, 4(1), 1-5.
- Malsiu, A., Shehu, I., Stafilov, T., & Faiku, F. (2020). Assessment of heavy metal concentrations with fractionation method in sediments and waters of the Badovci Lake (Kosovo). *Journal of Environmental and Public Health*, 2020, Article 3098594 <https://doi.org/10.1155/2020/3098594>
- Mohammadi, A. A., Zarei, A., Majidi, S., Ghaderpoury, A., Hashempour, Y., Saghi, M. H., Alinejad, A., Yousefi, M., Hosseinholizadeh, N., & Ghaderpoori, M. (2019). Carcinogenic and non-carcinogenic health risk assessment of heavy metals in drinking water of Khorramabad, Iran. *MethodsX*, 6, 1642-1651. <https://doi.org/10.1016/j.mex.2019.07.017>
- Mohmand, J., Eqani, S. A. M. A. S., Fasola, M., Alamdar, A., Mustafa, I., Ali, N., Liu, L., Peng, S., & Shen, H. (2015). Human exposure to toxic metals via contaminated dust: Bio-accumulation trends and their potential risk estimation. *Chemosphere*, 132, 142-151. <https://doi.org/10.1016/j.chemosphere.2015.03.004>
- Muhammad, S., Shah, M. T., & Khan, S. (2010). Arsenic health risk assessment in drinking water and source apportionment using multivariate statistical techniques in Kohistan region, northern Pakistan. *Food and Chemical Toxicology*, 48(10), 2855-2864. <https://doi.org/10.1016/j.fct.2010.07.018>
- Muhammad, S., Shah, M. T., & Khan, S. (2011). Health risk assessment of heavy metals and their source apportionment in drinking water of Kohistan region, northern Pakistan. *Microchemical Journal*, 98(2), 334-343. <https://doi.org/10.1016/j.microc.2011.03.003>
- Muhammad, S., Ullah, R., & Jadoon, I. A. (2019). Heavy metals contamination in soil and food and their evaluation for risk assessment in the Zhob and Loralai valleys, Baluchistan province, Pakistan. *Microchemical Journal*, 149, Article 103971. <https://doi.org/10.1016/j.microc.2019.103971>
- Muhammad Tahir, S., Suleman, M., Abdul Baqi, S., Sattar, A., & Khan, N. (2020). Determination of heavy metals in drinking water and their adverse effects on human health. A review. *Pure and Applied Biology (PAB)*, 9(1), 96-104. <http://dx.doi.org/10.19045/bspab.2020.90012>



- Murtaza, B., Amjad, M., Shahid, M., Imran, M., Shah, N. S., Abbas, G., & Naeem, M. A. (2020). Compositional and health risk assessment of drinking water from health facilities of District Vehari, Pakistan. *Environmental Geochemistry and Health*, *42*, 2425-2437. <https://doi.org/10.1007/s10653-019-00465-6>
- Pidwirny. (2006). *Characteristics of Metamorphic Rocks*. Physical Geography.net. <http://www.physicalgeography.net/fundamentals/10g.html>
- Rasool, A., Xiao, T., Farooqi, A., Shafeeqe, M., Masood, S., Ali, S., Fahad, S., & Nasim, W. (2016). Arsenic and heavy metal contaminations in the tube well water of Punjab, Pakistan and risk assessment: A case study. *Ecological Engineering*, *95*, 90-100. <http://dx.doi.org/10.1016/j.ecoleng.2016.06.034>
- Sadeghi, P., Loghmani, M., & Frokhzad, S. (2020). Human health risk assessment of heavy metals via consumption of commercial marine fish (*Thunnus albacares*, *Euthynnus affinis*, and *Katsuwonus pelamis*) in Oman Sea. *Environmental Science and Pollution Research*, *27*, 14944-14952. <https://doi.org/10.1007/s11356-020-07907-0>
- Saleh, H. N., Panahande, M., Yousefi, M., Asghari, F. B., Oliveri Conti, G., Talae, E., & Mohammadi, A. A. (2019). Carcinogenic and non-carcinogenic risk assessment of heavy metals in groundwater wells in Neyshabur Plain, Iran. *Biological Trace Element Research*, *190*, 251-261. <https://doi.org/10.1007/s12011-018-1516-6>
- Sharma, R. K., Agrawal, M., & Marshall, F. M. (2008). Heavy metal (Cu, Zn, Cd and Pb) contamination of vegetables in urban India: A case study in Varanasi. *Environmental Pollution*, *154*(2), 254-263.
- Stephanie, S. (2010). Trace elements. *Current Anaesthesia & Critical Care*, *21*(1), 44-48. <https://doi.org/10.1016/j.cacc.2009.08.004>
- USEPA. (2003). *Technical Standard Operating Procedure (SOP EH- 01)*. United States Environmental Protection Agency. <https://www.epa.gov/risk/guidelines-carcinogen-risk-assessment>
- USEPA. (2005, March). *Guidelines for carcinogen risk assessment (EPA/630/P-03/001F)*. United States Environmental Protection Agency. <https://www.epa.gov/risk/guidelines-carcinogen-risk-assessment>
- Vetrimurugan, E., Brindha, K., Elango, L., & Ndwandwe, O. M. (2017). Human exposure risk to heavy metals through groundwater used for drinking in an intensively irrigated river delta. *Applied Water Science*, *7*, 3267-3280. <https://doi.org/10.1007/s13201-016-0472-6>
- Wasserman, G. A., Liu, X., Parvez, F., Ahsan, H., Levy, D., Factor-Litvak, P., Kline, J., Geen, A. V., Slavkovich, V., Lolocono, N. J., Cheng, Z., Zheng, Yan., & Graziano, J. H. (2006). Water manganese exposure and children's intellectual function in Arai hazar, Bangladesh. *Environmental Health Perspectives*, *114*(1), 124-129. <https://doi.org/10.1289/ehp.8030>
- WWF. (2009). *Climate Change Resilience in Gilgit*. [https://www.wwfpak.org/our\\_work\\_/climate\\_and\\_energy\\_/climate\\_change\\_resilience\\_in\\_gilgit/](https://www.wwfpak.org/our_work_/climate_and_energy_/climate_change_resilience_in_gilgit/)
- Yang, F., & Massey, I. Y. (2019). Exposure routes and health effects of heavy metals on children. *Biometals*, *32*, 563-573. <https://doi.org/10.1007/s10534-019-00193-5>
- Zhang, Y., Sillanpää, M., Li, C., Guo, J., Qu, B., & Kang, S. (2015). River water quality across the Himalayan regions: Elemental concentrations in headwaters of Yarlung Tsangbo, Indus and Ganges River. *Environmental Earth Sciences*, *73*, 4151-4163.



## Development of Flood Hazard Index (FHI) of the Kelantan River Catchment Using Geographic Information System (GIS) Based Analytical Hierarchy Process (AHP)

Zulkarnain Hassan<sup>1,2\*</sup> and Ain Nihla Kamarudzaman<sup>1</sup>

<sup>1</sup>Faculty of Civil Engineering Technology, Universiti Malaysia Perlis, 02600 Arau, Perlis, Malaysia

<sup>2</sup>Centre of Excellence Water Research and Environmental Sustainability Growth (WAREG), Universiti Malaysia Perlis, 02600 Arau, Perlis, Malaysia

### ABSTRACT

Kelantan has been facing several cases of catastrophic flooding, causing significant damage to this area. Heavy monsoon rainfall is believed to trigger those floods. This study aims to identify and classify the flood occurrence using the Kelantan River catchment's flood hazard index (FHI) based on the Analytical Hierarchy Process (AHP). This study developed the FHI using the AHP based on spatial analysis in the geographic information system (GIS) environment. Six physical parameters were selected: annual rainfall, slope, river density, land use and land cover (LULC); elevation; and soil permeability. According to the AHP model, the annual rainfall was the first ranked parameter in terms of importance weight score. Moreover, Tanah Merah and Jeli were the high-risk areas for floods. The present study suggests that the GIS-based AHP method can be highly effective for mapping flood hazards and benefit flood management decision-making.

*Keywords:* Analytical Hierarchy Process, flood hazard index, geographic information system, multi-criteria decision analysis

### ARTICLE INFO

*Article history:*

Received: 20 January 2022

Accepted: 24 May 2022

Published: 21 October 2022

DOI: <https://doi.org/10.47836/pjst.31.1.13>

*E-mail addresses:*

[zulkarnainh@unimap.edu.my](mailto:zulkarnainh@unimap.edu.my) (Zulkarnain Hassan)

[ainnihla@unimap.edu.my](mailto:ainnihla@unimap.edu.my) (Ain Nihla Kamarudzaman)

\* Corresponding author

### INTRODUCTION

Flooding is one of the most common and destructive natural hazards, posing a serious threat to society due to its devastating effects on human lives and socio-economic conditions (Qi & Altinakar, 2011). Furthermore, flooding problems are getting more severe as a result of environmental changes such as land-use change (Du et

al., 2015), fast urbanisation (Suriya & Mudgal, 2012), and climate change, regardless of topographical and meteorological circumstances (Detrembleur et al., 2015). Therefore, a flood risk assessment is required to be conducted before deploying mitigation strategies to mitigate or control the flood hazard (Tariq et al., 2020; Green et al., 2000).

In general, flood risk can be developed using two approaches: the flood simulation approach utilising numerical modelling (such as the hydrological and hydrodynamic models) and the index-based approach using various parameters that control floods. In this study, the index-based approach is focused on. The selected approach uses various parameters based on derived information from the digital elevation model (DEM) and raster images, economic activity, infrastructure, demographic aspects, and mitigation policy and rehabilitation issues (Burby et al., 2000). Therefore, calculating the danger using this approach is particularly useful for creating and implementing a catastrophe mitigation strategy.

Many studies have used multiple-criteria decision analysis (MCDA) to estimate index-based flood hazards and risk (Wu et al., 2015; Xiao et al., 2016). In addition, MCDA has been integrated with GIS to organise the criteria hierarchically through spatial analysis effectively. Meanwhile, the AHP calculates the relative weights, relevance, or worth of each important component to the problem once the criteria have been aggregated and classified within the MCDA. From their literature review, de Brito and Evers (2016) found that the AHP in MCDA is quite popular in Asian and European countries, contributing to 72% of the studies. Mudashiru et al. (2022) also found that the AHP can be adopted as a tool for effective flood decision-making over Peninsular Malaysia.

Various techniques have been used to develop the AHP for flood hazard and risk, and the number of parameters used varies from one study to another (Chen et al., 2015; Kazakis et al., 2015). For example, Seejata et al. (2018) prepared the FHI of the lower part of the Yom River basin in Thailand using six parameters: slope, elevation, river density, land use, rainfall intensity, and soil permeability. Meanwhile, Sharir et al. (2019) identified the flood susceptibility level (FSL) of a small area in Sabah, Malaysia, using eight parameters: rainfall, drainage, flow accumulation, land use, elevation, slope gradient, soil texture, and slope curvature.

The Kelantan River catchment in Malaysia is a large catchment with a tendency to experience extreme flooding (Fadhliani et al., 2021; Jaafar et al., 2016). Saadatkhah et al. (2016) revealed a significant impact of land use on the flood experience of the catchment: a 13.7% decrease in forest land and a 6.2% increase in oil palm plantations. Therefore, these reports have garnered the attention of experts to study flood modelling and risk in the area. However, most of the studies adopted numerical modelling to study flood risk. This study attempts to adapt the AHP method to an index-based approach. Hence, the effectiveness of the AHP application can be evaluated for this catchment compared to previous studies that used numerical modelling for flood risk.

Therefore, the objectives of this study are to develop the FHI using the AHP method for the Kelantan River catchment. Six parameters are used in the development: annual rainfall, slope, river density, LULC, elevation, and soil permeability. In the following sections, the methods are presented, followed by the results and discussion. Then, the conclusion is elaborated.

## MATERIAL AND METHODS

### Study Area and Data

The catchment of the Kelantan River is in north-eastern Peninsular Malaysia. It is one of the major rivers in Malaysia and the longest river in the state of Kelantan. It is 248 km long and covers an area of 13,100 km<sup>2</sup>, as shown in Figure 1. The elevation of the catchment ranges from 8 to 2,174 m above the mean sea level and mountains in the west and southwest regions. The mean annual rainfall and temperature of the catchment are more than 2,500 mm and about 27.5°C, respectively (Tan et al., 2017). During the northeast monsoon, between November and January, the river's catchment frequently experiences flood events (Bronstert et al., 2002). Recent flood events in 2014 and 2017 caused immense losses in agricultural production, lives, and property (Alias et al., 2020; Nashwan et al., 2018). Therefore, assessing the flood risk of the catchment is crucial because it can identify the pattern and location of the flood. The outcome of this study can be used as a guideline for the local authorities in providing potential flood mitigation.

The secondary sources in this study were collected from different sources, as shown in Table 1. This study used satellite images from Advanced Spaceborne Thermal Emission and Reflection Radiometer (ASTER) at a 30 m resolution to derive the DEM and produce the map of LULC. The ASTER data are freely available via the Internet from the United States Geological Survey (USGS) Center for Earth Resources Observation and Science (EROS) (see <http://earthexplorer.usgs.gov>). The soil map was derived from the Food and Agriculture Organization (FAO)-UNESCO (1990). The data were obtained from the Department

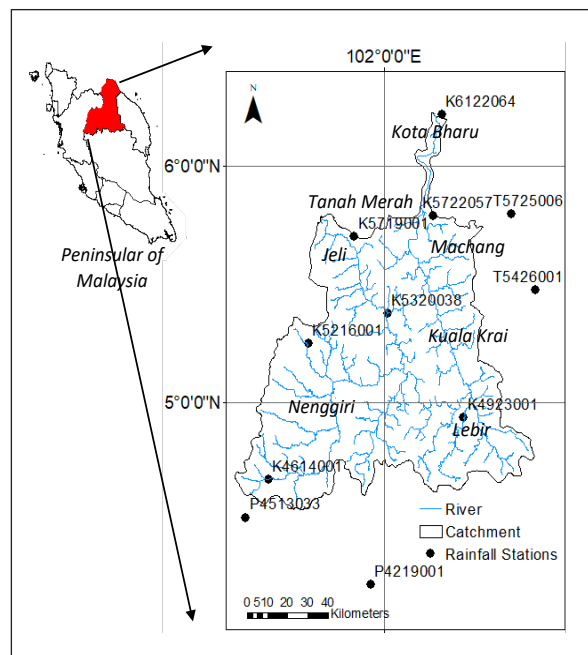


Figure 1. Location of the study area

of Irrigation and Drainage Malaysia in terms of rainfall. Daily rainfall data for 2014 at several rainfall stations (refer to Table 2) were selected, and the data were aggregated to the annual rainfall.

### Analytical Hierarchy Process (AHP)

AHP is a value-judgement approach for semi-quantitative decision-making that serves the decision maker's goals (Razandi et al., 2015). This method allows planners to use their experience and knowledge to break down a problem into a hierarchical structure and solve it using the AHP (Murali et al., 2013; Sar et al., 2015). The method also normalises controlling factor weights (as shown in Table 3) and selects the best alternatives by considering objective and subjective factors.

This study used the AHP approach to appoint weights for flood hazard factors. First, pairwise comparisons were deployed for all parameters of flood hazard. In this study, several parameters were selected since they are major contributors to floods (Wang et al. 2020): Annual rainfall, slope, river density, LULC, elevation, and soil permeability. Those parameters were assigned their relative importance values ranging between 1 and 9 in Table 4. Second, with a comparison matrix, priority vectors or the normalised Eigenvectors of the matrix could be calculated (see Table 5). Third, calculations were made by dividing each column by its corresponding amounts. In the last step, the mean values of each row were calculated and used as a weight in the objective hierarchy to evaluate the flood hazard, as recorded in Table 5.

The Eigenvector of a matrix will have its consistency checked using the consistency ratio (CR) as Equation 1:

Table 1  
*Sources of studied data input*

Data	Sources
Soil Map	FAO-UNESCO (1990)
Land Use and DEM	USGS Center for EROS
Rainfall Data	Department of Irrigation and Drainage Malaysia
Historically Flooded Map	Alias et al., 2020; DID, 2014

Table 2  
*Rainfall stations*

Station	Long(°)	Lat (°)
K4614001	101.485	4.676
K4923001	102.353	4.938
K5216001	101.663	5.251
K5320038	102.015	5.378
K5719001	101.867	5.701
K5722057	102.219	5.788
K6122064	102.257	6.217
T5426001	102.675	5.476
T5725006	102.565	5.797
P4219001	101.940	4.233
P4513033	101.383	4.517

Table 3  
*Scale of preference among parameters (Saaty, 1980)*

Intensity of Importance	Description
1	Equal importance
3	Moderate importance
5	Strong importance
7	Very strong importance
9	Extreme importance
2, 4, 6, 8	Intermediate values

$$CR = \frac{CI}{RI} \tag{1}$$

Table 4  
Comparison matrix of flood hazard parameters

Parameters	Annual Rainfall	Slope	River Density	LULC	Elevation	Soil Permeability
Annual Rainfall	1	3	3	7	5	5
Slope	1/3	1	1/3	3	3	3
River Density	1/3	3	1	7	3	5
LULC	1/7	1/3	1/7	1	1/3	1/3
Elevation	1/5	1/3	1/3	3	1	3
Soil Permeability	1/5	1/3	1/5	3	1/3	1

Table 5  
Normalised matrix of flood hazard parameters, where  $W_i$  is the weight of each parameter

Parameters	Annual Rainfall	Slope	River Density	LULC	Elevation	Soil Permeability	Mean	$W_i$
Annual Rainfall	0.45	0.38	0.60	0.29	0.39	0.29	0.40	4.0
Slope	0.15	0.13	0.07	0.13	0.24	0.17	0.15	1.5
River Density	0.15	0.38	0.20	0.29	0.24	0.29	0.26	2.6
LULC	0.06	0.04	0.03	0.04	0.03	0.02	0.04	0.4
Elevation	0.09	0.04	0.07	0.13	0.08	0.17	0.10	1.0
Soil Permeability	0.09	0.04	0.04	0.13	0.03	0.06	0.06	0.6

CI is the consistency index, and RI is the random index (Kaoje et al., 2021). Therefore, CI can be defined as Equation 2:

$$CI = \frac{\lambda_{max} - n}{n - 1} \tag{2}$$

The RI is referred to in Table 6, and in this study, the number of parameters, n and the RI was 6 and 1.25, respectively.

Using Equation 1, the CR is 0.087 if the  $\lambda_{max}$  is 6.55, reporting a CR value lower than the threshold of 0.1. Hence, the consistency of weights in Table 5 was affirmed.

After determining the  $W_i$  and the rating ( $r_i$ ) of each parameter, the parameters were classed as shown in Table 7. Next, the FHI in Equation 3 was developed using the Raster Calculator tool in ArcGIS through a combination of parametric input maps. Finally, the values of the FHI raster were grouped into five classes to obtain the hazard zones.

$$FHI = \sum_{i=1}^n r_i \cdot W_i \tag{3}$$



Table 6  
*RI used to compute CR (Saaty, 1980)*

n	1	2	3	4	5	6	7	8	9	10
RI	0.00	0.00	0.55	0.89	1.11	1.25	1.35	1.40	1.45	1.49

Table 7  
*r<sub>i</sub> of the parameters and their W<sub>i</sub>*

Parameters	Class	r <sub>i</sub>	W <sub>i</sub>	r <sub>i</sub> ·W <sub>i</sub>
Annual Rainfall (mm)	>3,200 mm	10	4.0	4.00
	2,500–2,700 mm	8		3.60
	2,700–2,900 mm	6		3.20
	2,500–2,700 mm	4		2.80
	<2,500 mm	2		2.40
Slope	0–1°	10	1.5	1.46
	1–2°	8		1.17
	2–3°	6		0.88
	3–5°	4		0.58
	>5°	2		0.29
River Density	Very High	10	2.6	2.57
	High	8		2.06
	Medium	6		1.54
	Low	4		1.03
	Very Low	2		0.51
LULC	Water Bodies	10	0.4	0.37
	Built-Up	8		0.30
	Agriculture	6		0.22
	Forest	2		0.07
Elevation	0–200 m	10	1.0	0.96
	200–400 m	8		0.77
	400–600 m	6		0.58
	600–800 m	4		0.38
	>800	2		0.19
Soil Permeability	Low	8	0.6	0.51
	Medium	6		0.38
	High	4		0.25

## RESULTS AND DISCUSSION

### Spatial Variations of Flood Parameters

Figure 2 presents the thematic map of flood parameters prepared for each pixel/cell of the Kelantan River catchment in the ArcGIS environment. For rainfall intensity, as illustrated in Figure 2(a), the distribution of the annual rainfall in 2014 at 12 stations of the studied

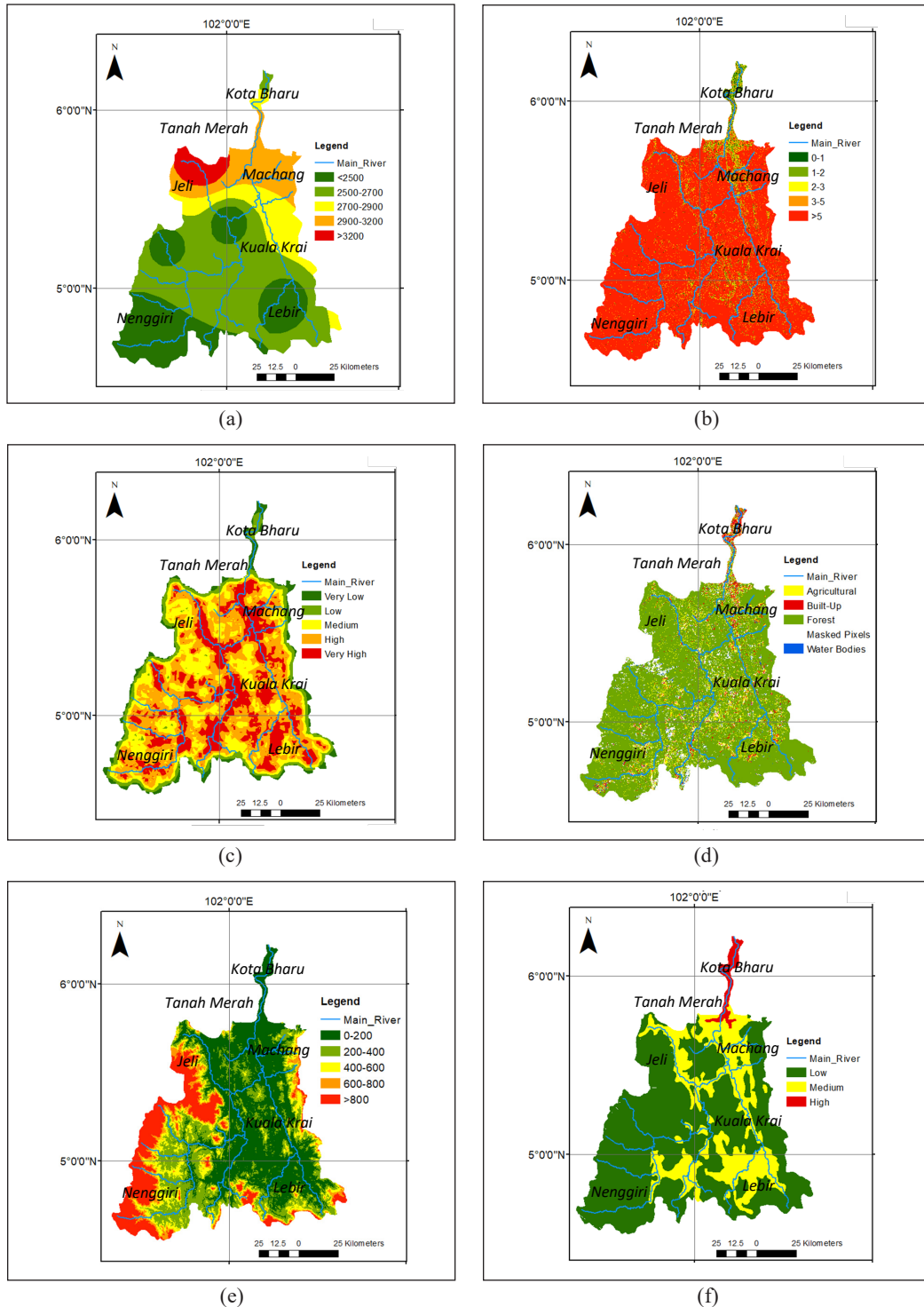


Figure 2. Thematic maps of parameters, used for MCDA, such as of (a) annual rainfall (mm); (b) slope ( $^{\circ}$ ); (c) river density; (d) LULC; (e) elevation (m); and (f) soil permeability

catchment was generated using the Kriging interpolation method. The spatial annual rainfall ranged from 2,500 to 3,200 mm. Figure 2(a) shows that the area near Jeli and Tanah Merah received the highest annual rainfall, over 3,200 mm. However, the amount of annual rainfall decreased towards the southern part of the catchment, such as Nenggiri and Lebir, in which annual rainfall was recorded to be less than 2,700 mm. Rainfall was the most important parameter for the FHI, and a higher rainfall amount usually increases the chance of floods. Hence, the areas of Tanah Merah and Jeli would face frequent flood events during the rainy season at the end of the year. In general, the annual rainfall of the catchment in 2014 was slightly higher than the mean annual rainfall of Peninsular Malaysia, around 2,300 mm, as reported by Wong et al. (2009).

The surface slope of the Kelantan River catchment is presented in Figure 2(b), with 1.45% of the area being categorised as 0–1°, 2.79% as 1–2°, 3.27% as 2–3°, 6.52% as 3–5°, and 85.97% as more than 5°. Most low gradients (less than 3°) were distributed downstream of the catchment (near Kota Bharu and Tanah Merah) and along the river line. It is because the area at the slope is usually low, and rain or excessive water from the river always gathers in this area (Ouma & Tateishi, 2014). Therefore, the possibility of a flood occurring is high. However, most of the upstream areas of the catchment, such as Nenggiri and Lebir, had high gradients (greater than 3°). Thus, the high slopes help to drain water quickly (Seejata et al., 2018).

In terms of river density, the results in Figure 2(c) suggested that a higher drainage density can be seen near the river line. Most high and very high river densities could be derived near the river line. This observation indicated that the area near the catchment's river line is prone to erosion, resulting in sedimentation at the lower grounds. This finding is consistent with other studies, such as Sharir et al. (2019), which found that the drainage density or river density is highest in the areas near the river. River density was one of the important hazard-controlling factors in this study that indicated the nature and properties of the soils.

The catchment is 80.7% surrounded by tropical rainforests, followed by 9.7% agricultural sites (such as rubber and oil palm plantations), 3.5% built-up (residential, commercial, and industrial buildings), and 1.2% water bodies, as illustrated in Figure 2(d). It is evident that the study area has not been extensively explored for development and agricultural activities. Most of the exploration occurred downstream of the catchment, such as in the areas near Kota Bharu and Machang. Rapid exploration without control of slope cutting can trigger flash floods in urban areas. The surrounding forest usually allows a higher infiltration rate than the urban area or pastureland (Seejata et al., 2018). The LULC is one of the significant concerns in flood hazards and was selected as a parameter in this study. The LULC reflected the current use and infiltration of the land.

Figure 2(e) shows the elevation of the catchment. It is considered the fourth important parameter of the weight scores of the AHP (see Table 7). Figure 2(e) depicts that most areas

of the catchment had an elevation of 0–200 m, while high elevations (greater than 600 m) were found in the eastern and western regions near Nenggiri and Lebir. Low elevations would indicate flat areas usually prone to flood occurrences, such as Kota Bharu, Tanah Merah, and Kuala Krai. Most of the previous flood events occurred in those areas with low elevations (Jaafar et al., 2016; Tan et al., 2017). Therefore, elevation became a significant parameter for the development of the FHI in this study.

For soil permeability, as presented in Figure 2(f), the soil type was reclassified into three classes based on the water permeability following the FAO's soil map. In this study, high soil permeability, in which water easily infiltrates the soil, could be found in the mountainous ranges in the eastern and western regions (composed of silt soils). On the other hand, low soil permeability, in which the soil is impermeable, could be identified downstream of the catchment (made of clay and granite soils).

### **Spatial Variations of FHI**

Figure 3(a) shows the FHI prepared for each pixel/cell of the Kelantan River catchment in the ArcGIS environment based on particular features, each criterion's weight and normalised rank (refer to Table 7) calculated using the AHP approach. From Figure 3(a), the spatial variability of the index within the entire district could be obtained and was categorised into five levels of risk, namely very low (<2 FHI), low (2–5 FHI), medium (5–7 FHI), high (7–8 FHI), and very high (>8 FHI) flood zones using Equation (3). The finding showed a very high FHI covering 1,207.6 km<sup>2</sup> or 9.4% of the catchment area. The areas near Tanah Merah and Jeli were mainly part of the very high flood zone. It is because those areas are flat in slope and at low elevations. The areas also intersect two main rivers, the Galas and Lebir Rivers, at the left and right sides of the catchment, respectively. Both rivers contribute a high-water volume to the river downstream during the rainy season. This situation worsens due to the higher rainfall intensity in those areas, proven by the parameter of rainfall density achieving the first objective hierarchy rating score in the FHI development.

The study also discovered that high to extremely high FHI levels were found around the Kelantan River catchment's river line. It is because most of the runoff will flow to the river from high to low elevations, increasing the risk of flooding near the riverbanks (Ologunorisa & Abawua, 2005). The increased flood risk in the riverbanks is due to land use development in low-lying areas. Low-lying areas are undeniably more vulnerable to floods, but whether the soil facilitates or hinders water infiltration depends on the soil's texture. Land use development in low-lying areas, such as the construction of buildings or roads, exacerbates the situation by requiring clearing vegetation, slope cutting, and applying impermeable materials to the surface. As a result, the area becomes increasingly vulnerable to flooding. Meanwhile, the study found that low FHI levels were recorded at high elevations, such as at Nenggiri and Lebir.

The FHI in Figure 3(a), developed from the AHP method, was validated with the historically flooded areas in Figure 3(b) modified from the Department of Irrigation and Drainage Malaysia (DID, 2014) and Alias et al. (2020). The comparison revealed that most historical floods had occurred in zones with very high FHI levels, especially Tanah Merah, Jeli, Gua Musang, and Kuala Krai. Therefore, those areas closely matched the historic floods. However, the area between Tanah Merah and Kota Bharu, mainly classified as having a medium FHI, is not as frequently hit by floods as in historical flood areas. The finding is consistent with Roslan et al. (2019), who also evinced that the area near Kota Bharu is low-risk, based on their flood risk map. The findings showed that the estimated FHI matched the historical flood areas.

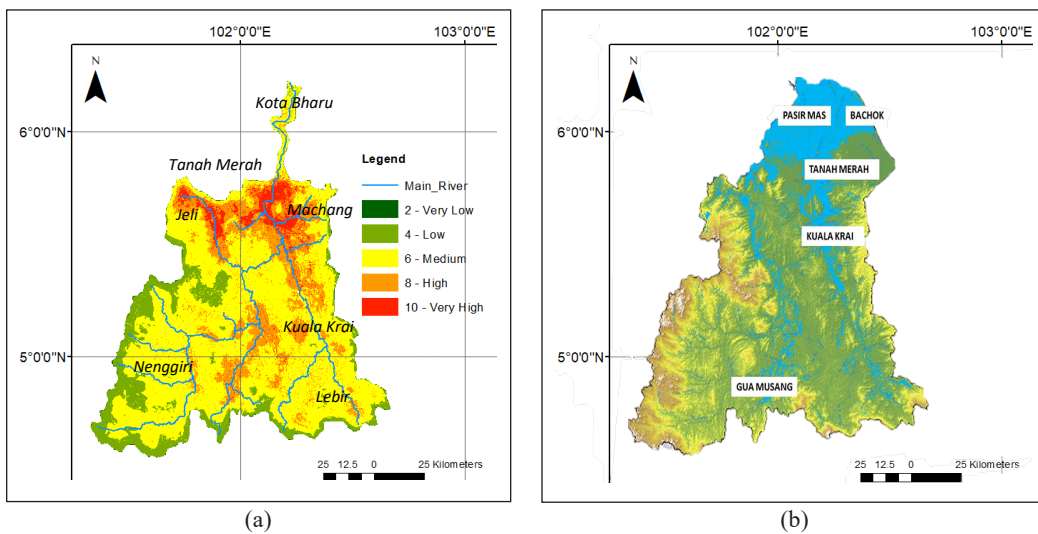


Figure 3. Distribution of (a) FHI derived from AHP and (b) historically flooded areas in Kelantan (Alias et al., 2020; DID, 2014)

## CONCLUSION

The main objective of this study is to identify the FHI areas in the Kelantan River catchment, Malaysia. The weight of the relative importance of six flood parameters was identified using the pairwise matrix comparison. The results showed that very high-risk flood-prone areas with the highest FHI values were Tanah Merah and Jeli. Those areas were susceptible to flood mainly because of the highest annual rainfall in 2014; the annual rainfall generated the highest score from the AHP. Most of the flood areas' spatial patterns derived using the AHP model were similar to the historical flood map.

For future work, it is suggested to evaluate the inclusion of other parameters in developing the FHI value. For example, the weighing of relative importance should be revised due to changes in the parameters. In addition, incorporating comprehensive field

data such as soil parameters, groundwater depth, and local drainage would improve the accuracy of the current approach.

## ACKNOWLEDGMENT

The Ministry of Education Malaysia financially supported this work under the Fundamental Research Grant Scheme (FRGS) (Ref. No.: FRGS/1/2019/TK01/UNIMAP/02/4). In addition, the authors want to thank the Department of Irrigation and Drainage Malaysia (DID) for providing data and technical support.

## REFERENCES

- Alias, N. E., Salim, N. A., Taib, S. M., Yusof, M. B. M., Saari, R., Ramli, M. W. A., Othman, I. K., Annammala, K. V., Yusof, H. M., Ismail, N., Yuzir, A., & Blenkinsop, S. (2020). Community responses on effective flood dissemination warnings - A case study of the December 2014 Kelantan Flood, Malaysia. *Journal of Flood Risk Management*, 13(S1), Article e12552. <https://doi.org/10.1111/jfr3.12552>
- Bronstert, A., Niehoff, D., & Bürger, G. (2002). Effects of climate and land-use change on storm runoff generation: Present knowledge and modelling capabilities. *Hydrological Processes*, 16(2), 509-529. <https://doi.org/10.1002/hyp.326>
- Burby, R. J., Deyle, R. E., Godschalk, D. R., & Olshansky, R. B. (2000). Creating hazard resilient communities through land-use planning. *Natural Hazards Review*, 1(2), 99-106. [https://doi.org/10.1061/\(ASCE\)1527-6988\(2000\)1:2\(99\)](https://doi.org/10.1061/(ASCE)1527-6988(2000)1:2(99))
- Chen, H., Ito, Y., Sawamukai, M., & Tokunaga, T. (2015). Flood hazard assessment in the Kujukuri plain of Chiba prefecture, Japan, based on GIS and multicriteria decision analysis. *Natural Hazards*, 78(1), 105-120. <https://doi.org/10.1007/s11069-015-1699-5>
- de Brito, M. M., & Evers, M. (2016). Multi-criteria decision-making for flood risk management: A survey of the current state of the art. *Natural Hazards and Earth System Sciences*, 16(4), 1019-1033. <https://doi.org/10.5194/nhess-16-1019-2016>
- DID. (2014). *Laporan Banjir Negeri Kelantan*. Department of Irrigation and Drainage Malaysia.
- Detrembleur, S., Stilmant, F., Dewals, B., Erpicum, S., Archambeau, P., & Piroton, M. (2015). Impacts of climate change on future flood damage on the river Meuse, with a distributed uncertainty analysis. *Natural Hazards*, 77, 1533-1549. <https://doi.org/10.1007/s11069-015-1661-6>
- Du, S., Shi, P., Van Rompaey, A., & Wen, J. (2015). Quantifying the impact of impervious surface location on flood peak discharge in urban areas. *Natural Hazards*, 76, 1457-1471. <https://doi.org/10.1007/s11069-014-1463-2>
- FAO-UNESCO. (1990). *FAO-Unesco soil map of the world*. World Soil Resources Report 60/ISRIC. [https://www.isric.org/sites/default/files/ISRIC\\_TechPap20.pdf](https://www.isric.org/sites/default/files/ISRIC_TechPap20.pdf)
- Green, C. H., Parker, D. J., & Turnstall, S. M. (2000). *Assessment of flood control and management options*. World Commission on Dams. <https://citeseerx.ist.psu.edu/viewdoc/download?doi=10.1.1.467.4860&rep=rep1&type=pdf>

- Jaafar, A. S., Sidek, L. M., Basri, H., Zahari, N. M., Jajarmizadeh, M., Noor, H. M., Osman, S., Mohammad, A. H., & Azad, W. H. (2016). An overview: Flood catastrophe of Kelantan watershed in 2014. In W. Tahir, S. H. A. Bakar, M. A. Wahid, S. R. M. Nasir & W. K. Lee (Eds.), *ISFRAM 2015* (pp. 17-29). Springer. [https://doi.org/10.1007/978-981-10-0500-8\\_2](https://doi.org/10.1007/978-981-10-0500-8_2)
- Kaoje U. I., Rahman, M. Z. A., Idris, N. H., Razak, K. A., Rani, W. N. M. W. M., Tam, T. H., & Salleh, M. R. M. (2021). Physical flood vulnerability assessment using geospatial indicator-based approach and participatory Analytical Hierarchy Process: A case study in Kota Bharu, Malaysia. *Water*, *13*(13), Article 1786. <https://doi.org/10.3390/w13131786>
- Kazakis, N., Kougiass, I., & Patsialis, T. (2015). Assessment of flood hazard areas at a regional scale using an index-based approach and Analytical Hierarchy Process: Application in Rhodope-Evros region, Greece. *Science of the Total Environment*, *538*, 555-563. <https://doi.org/10.1016/j.scitotenv.2015.08.055>
- Mudashiru, R. B., Sabtu, N., Abdullah, R., Saleh, A., & Abustan, I. (2022). A comparison of three multi-criteria decision-making models in mapping flood hazard areas of Northeast Penang, Malaysia. *Natural Hazards*, *112*, 1903-1939. <https://doi.org/10.1007/s11069-022-05250-w>
- Murali, M. R., Ankita, M., Amrita, S., & Vethamony, P. (2013). Coastal vulnerability assessment of Puducherry Coast, India, using the analytical hierarchical process. *Natural Hazards and Earth System Sciences*, *13*(12), 3291-3311. <https://doi.org/10.5194/nhess-13-3291-2013>
- Nashwan, M. S., Ismail, T., & Ahmed, K. (2018). Flood susceptibility assessment in Kelantan River basin using copula. *International Journal of Engineering and Technology*, *7*(2), 584-590.
- Ologunorisa, T. E., & Abawua, M. J. (2005). Flood risk assessment: A review. *Journal of Applied Sciences and Environmental Management*, *9*(1), 57-63.
- Ouma, Y., & Tataeishi, R. (2014). Urban flood vulnerability and risk mapping using integrated multi-parametric AHP and GIS: Methodological overview and case study assessment. *Water*, *6*(6), 1515-1545. <https://doi.org/10.3390/w6061515>
- Qi, H., & Altinakar, M. S. (2011). A GIS-based decision support system for integrated flood management under uncertainty with two dimensional numerical simulations. *Environmental Modelling and Software*, *26*(6), 817-821. <https://doi.org/10.1016/j.envsoft.2010.11.006>
- Razandi, Y., Pourghasemi, H. R., Neisani, N. S., & Rahmati, O. (2015). Application of Analytical Hierarchy Process, frequency ratio, and certainty factor models for groundwater potential mapping using GIS. *Earth Science Informatics*, *8*, 867-883. <https://doi.org/10.1007/s12145-015-0220-8>
- Roslan, R., Omar, R. C. Hara, M., Solemon, B., & Baharuddin, I. N. Z. (2019). Flood insurance rate map for non-structural mitigation. *E3S Web of Conferences*, *76*, Article 03002. <https://doi.org/10.1051/e3sconf/20197603002>
- Saadatkah, N., Tehrani, M. H., Mansor, S., Khuzaimah, Z., & Kassim, A. (2016). Impact assessment of land cover changes on the runoff changes on the extreme flood events in the Kelantan River basin. *Arabian Journal of Geosciences*, *9*, Article 687. <https://doi.org/10.1007/s12517-016-2716-z>
- Saaty, T. L. (1980). *The Analytic Hierarchy Process: Planning, priority setting*. McGraw-Hill.



- Sar, N., Chatterjee, S., & Adhikari, M. D. (2015). Integrated remote sensing and GIS based spatial modelling through Analytical Hierarchy Process (AHP) for water logging hazard, vulnerability and risk assessment in Keleghai River basin, India. *Modeling Earth Systems and Environment*, 1, Article 31. <https://doi.org/10.1007/s40808-015-0039-9>
- Seejata, K., Yodying, A., Wongthadam, T., Mahavik, N., & Tantanee, S. (2018). Assessment of flood hazard areas using Analytical Hierarchy Process over the Lower Yom Basin, Sukhothai Province. *Procedia Engineering*, 212, 340-347. <https://doi.org/10.1016/j.proeng.2018.01.044>
- Sharir, K., Rodeano, R., & Mariappan, S. (2019). Flood susceptibility analysis (FSA) using Analytical Hierarchy Process (AHP) model at The Kg. Kolopis area, Penampang, Sabah, Malaysia. *Journal of Physics: Conference Series*, 1358(1), Article 012065. IOP Publishing. <https://doi.org/10.1088/1742-6596/1358/1/012065>
- Suriya, S., & Mudgal, B. V. (2012). Impact of urbanisation on flooding: The Thirusoolam sub watershed - A case study. *Journal of Hydrology*, 412, 210-219. <https://doi.org/10.1016/j.jhydrol.2011.05.008>
- Tan, M. L., Yusop, Z., Chua, V. P., & Chan, N. W. (2017). Climate change impacts under CMIP5 RCP scenarios on water resources of the Kelantan River basin, Malaysia. *Atmospheric Research*, 189, 1-10. <https://doi.org/10.1016/j.atmosres.2017.01.008>
- Tariq, M. A. U. R., Farooq, R., & van de Giesen, N. (2020). A critical review of flood risk management and the selection of suitable measures. *Applied Sciences*, 10(23), Article 8752. <https://doi.org/10.3390/app10238752>
- Wang, J., Hu, C., Ma, B., & Mu, X. (2020). Rapid urbanization impact on the hydrological processes in Zhengzhou, China. *Water*, 12(7), Article 1870. <https://doi.org/10.3390/w12071870>
- Wong, C., Venneker, R., Uhlenbrook, S., Jamil, A., & Zhou, Y. (2009). Variability of rainfall in Peninsular Malaysia. *Hydrology Earth System Science Data Discussions*, 6(4), 5471-5503. <https://doi.org/10.5194/hessd-6-5471-2009>
- Wu, Y., Zhong, P. A., Zhang, Y., Xu, B., Ma, B., & Yan, K. (2015). Integrated flood risk assessment and zonation method: A case study in Huaihe River basin, China. *Natural Hazards*, 78, 635-651. <https://doi.org/10.1007/s11069-015-1737-3>
- Xiao, Y., Yi, S., & Tang, Z. (2016). GIS-based multi-criteria analysis method for flood risk assessment under urbanisation. In *2016 24th International Conference on Geoinformatics* (pp. 1-5). IEEE Publishing. <https://doi.org/10.1109/GEOINFORMATICS.2016.7578963>
- Zulkafli, Z., Yusuf, B., & Nurhidayu, S. (2021). Assessment of streamflow simulation for a tropical forested catchment using dynamic TOPMODEL - Dynamic fluxEs and Connectivity for predictions of Hydrology (DECIPHeR) framework and generalised likelihood uncertainty estimation (GLUE). *Water*, 13, Article 317. <https://doi.org/10.3390/w13030317>



*Review Article*

## **Fibre-Reinforced Soil Mixed Lime/Cement Additives: A Review**

**Sakina Tamassoki<sup>1,2</sup>, Nik Norsyahariati Nik Daud<sup>1\*</sup>, Mohammad Nazir Nejabi<sup>2</sup> and Mohammad Jawed Roshan<sup>2,3</sup>**

<sup>1</sup>*Department of Civil Engineering, Faculty of Engineering, Universiti Putra Malaysia, 43400 UPM, Serdang, Selangor, Malaysia*

<sup>2</sup>*Faculty of Transportation Engineering, Kabul Polytechnic University, Kabul 1001, Afghanistan*

<sup>3</sup>*Department of Geotechnics and Transpiration, Universiti Teknologi Malaysia, 81310 UTM, Johor Bahru, Malaysia*

### **ABSTRACT**

Soil modification is a technique for improving poor soil properties to make them suitable for engineering projects. Regarding the previous studies, various types of stabilisations were used to improve mechanical properties in soil. Several methodologies and experimental tests were used to study the positive and negative effects of utilising fibre on lime/cement-modified soil. This paper reviews the strength behaviour and microstructural properties of Fibre-Reinforced Lime Stabilised (FRLS) soil and Fibre-Reinforced Cement Stabilised (FRCS) Soil. First, the impact of FRLS/FRCS soil on strength behaviour under freeze-thaw conditions, the California Bearing Ratio (CBR) value, and compression/tensile strength are all examined. Then synthetic and natural fibres are compared at the microstructure level. FRCS/FRLS soil has been studied for its influence on geotechnical characteristics such as peak strength, residual strength, ductility, bearing capacity, stiffness, and settlement values. In addition, the micro-level evidence demonstrates that lime/cement affects the interlocking between soil particles and fibre. Although lime/cement improves soil strength by making it solid and compact, it makes stabilised soil brittle. Fibre as reinforcement in lime/cement stabilised soil transforms the brittleness of the soil into ductility.

Hence building various infrastructures on poor soils is possible if fibre with lime/cement is used as an improvement method. Here, these three most used soil additive materials are investigated in terms of strength, microstructural, mineralisation, and some open issues are suggested for further research.

*Keywords:* Brittleness, cement, fibre, lime, microstructure, reinforced, stabilized, strength behaviour

### ARTICLE INFO

*Article history:*

Received: 09 February 2022

Accepted: 31 May 2022

Published: 20 October 2022

DOI: <https://doi.org/10.47836/pjst.31.1.14>

*E-mail addresses:*

[s.tamassoki86@gmail.com](mailto:s.tamassoki86@gmail.com) (Sakina Tamassoki)

[niknor@upm.edu.my](mailto:niknor@upm.edu.my) (Nik Norsyahariati Nik Daud)

[m.n.nejabi@kpu.edu.af](mailto:m.n.nejabi@kpu.edu.af) (Mohammad Nazir Nejabi)

[mj.roshan@kpu.edu.af](mailto:mj.roshan@kpu.edu.af) (Mohammad Jawed Roshan)

\*Corresponding author

## INTRODUCTION

Soil stabilisation and soil reinforcement improve weak soils' shear strength, plasticity, durability, permeability, and density. Generally, soil stabilisation increases the elastic modulus of soil used to construct infrastructure. To improve stability, understanding the properties of the soil and choosing the appropriate modification form is essential. In addition, Atterberg limits, soil mineralogy and composition, required engineering characteristics, stabilisation mechanism, environmental concerns, and budget constraints should be addressed when selecting an additive type (Little & Nair, 2009).

Fibre-reinforced soils have become more popular recently due to their superior strength and ductility compared to parent soils. It improves railway substructure and slope stability (Roshan et al., 2022) while reducing pavement thickness (Valipour et al., 2021). Compared to geosynthetic layers in the soil, using fibre as reinforcement has numerous advantages, for example, fewer catastrophic failures, more utility in complex geometries and constrained places, less chance of weak planes forming, higher ductility and deformability, and more inexpensive pricing than geosynthetics (Han, 2015). Fibres used as reinforcement in soils are categorised into synthetic (polypropylene, polyethylene, glass, polyester, steel, and carbon) and natural (palm, coir, sisal, jute, wheat, and bagasse). Although natural fibres are cheaper and more tolerant than synthetic fibres, synthetic fibres are more resilient and durable when exposed to environmental changes (Hejazi et al., 2012).

In geotechnical engineering, soil stabilisation by chemical admixtures such as lime/cement has recently gained popularity (Petry & Little, 2002). Increased modulus of elasticity and resilient modulus under static loading (Yi et al., 2022) or even cyclic loading (Du et al., 2021), strength properties, reduced plasticity index, permeability, decreased swelling potential and volume instability, deformation and settlement, and improved durability are only a few benefits of lime/cement as stabilisation materials (Behnood et al., 2018). However, they are not used in high-velocity rail substructures because their mechanical fatigue behaviour is unknown and undetermined (Preteville & Lenoir, 2016). Furthermore, although lime has been proved to be an effective binder in soil stabilisation, utilising low lime concentration to improve the geotechnical properties of soil is not an effective strategy since the swelling potential of soil is not greatly diminished (Rosone et al., 2018).

On the other hand, adding lime to expansive clay soils, such as black cotton soil, is beneficial because cation exchange closes clay particles and forms flocs. Flocculation is responsible for improving and modifying the engineering properties of expansive clays when treated with lime (Ghobadi et al., 2014). The Application of lime as a stabiliser agent is not helpful in some cases where soil bearing capacity, density, and hydraulic conductivity are very low (Osinubi et al., 2009). Workability, durability, compressibility, and soil strength are increased by lime stabilisers, while lime has varying effects on permeability. Moreover, sulfate attack, carbonation, and environmental influences are disadvantages of using lime/cement as soil stabilisation.

As a reinforcement, synthetic and natural fibre increases tensile strength, improves stability (Tamassoki et al., 2022a) and reduces soil lateral deformation/settlement (He et al., 2021). Furthermore, adding fibre to lime/cement-stabilised soil can reduce the brittleness of treated soil (Hamidi & Hooresfand, 2013). Fibre also minimises the risk of lime/cement stabilisation causing brittle failure. In soil stabilisation with cement, PP fibres increase tensile strength, density, and initial elastic modulus. Fibre added to cement-stabilised clay soil enhances tensile strength and reduces swelling potential, shrinkage, and crack width (Kumar et al., 2016). Fibre positively impacts the flexural behaviour of cement-based soil stabilisation (Jamsawang et al., 2015). In sandy soil, discarded tire textile fibres were used to improve the damping ratio, resilient modulus, and permanent strain (Narani et al., 2020). Fibre content and aspect ratio reduced critical confinement stress and enhanced shear strength in sandy soil (Ranjan et al., 1994; Zhao et al., 2021). Furthermore, using fibre improved the safety factor, strength, and stability of slopes in embankments filled with fibre-reinforced soil (Ramkrishnan et al., 2018). Similarly, when fibre-reinforced soil was exposed to freeze-thaw cycles, SEM pictures revealed that the fibres remained intact despite the repeated freeze-thaw (Kravchenko et al., 2019).

Combining the chemical binder with a different kind of fibre significantly changes the mechanical behaviour of soils. Therefore, many research works investigated fibre reinforcement, lime/cement stabilisation, and the combination of fibre with lime/cement as practical methods for improving the soil. This review paper studies the geotechnical behaviour of FRLR and FRCR soil; first, the impact of fibre, lime, and cement on strength behaviour under freezing and thawing conditions, pavement subgrade, and compression tensile strength is discussed. Then the synthetic and natural fibre at the microstructural level is compared. Finally, the effect of lime/cement on soil improvements is investigated at the mineralisation level.

## **STRENGTH BEHAVIOUR OF FIBRE REINFORCEMENT STABILISED SOIL**

### **Under Freezing and Thawing Conditions**

Previous research works widely studied the advantages of incorporating FRLS/FRCS soil. Here are a few of these studies. Climatic conditions of a place and high-temperature variation can substantially affect soil stability. When the soil layer is continuously frozen and thawed, attention must be paid to enhancing soil resistance to the freeze-thaw response. Soil geotechnical properties alter when exposed to freezing-thawing cycles. Glaciers create and freeze water into smaller gaps when huge voids inside fine-grained soils are exposed to cold temperatures. When water freezes, its volume increases by 9%, resulting in crack formation in the soil (Yldz & Soğanc, 2012). Several types of research were conducted to decrease the adverse impacts of freezing and thawing on the physical properties of soils.

Lime additive is a common approach for chemically converting weak soils into structurally safe building foundation materials. This approach is particularly suitable for modifying base materials, subbase materials, and subgrade soils in road building. The freeze-thaw cycle does not affect the pozzolanic reaction following the lime-water reaction. Nonetheless, the process is delayed in lime-treated clay soil. So, lime treatment is advantageous for clay soils throughout the cold season.

Fibre is another alternative that can improve soil properties, especially tensile strength. Nevertheless, an increase in the number of freeze-thaw cycles results in a 20–25% reduction in the UCS of PP fibre-reinforced and unreinforced clay soil specimens (Ghazavi & Roustaie, 2010).

Roustaie et al. (2015) found that increasing the amount of PP fibre in clay soil does not mitigate the impact under freeze-thaw conditions. PP fibres are a tensile element in the clay soil matrix during the freeze-thaw action. An increasing number of freeze-thaw cycles decreases cohesion, the only component that holds PP fibres and soil particles together and declines the fibre's influences as a tensile element (Roustaie et al., 2015).

Moreover, Boz and Sezer (2018) presented that adding lime, basalt, and PP fibre decreases mass loss in soil under freezing-thawing cycles while increasing it in untreated soil. In this regard, polypropylene FRLS kaolin clay soil was more efficient than basalt fibre (Boz & Sezer, 2018).

Although cement inclusion can increase the strength of clay to a certain level (Wahab, Rashid et al., 2021) cement-treated clay's low frost resistance is one downside. In addition, the mechanical properties of this type of foundation alter significantly during freeze-thaw cycles, resulting in significant freeze-thaw damage and subsequent differential settlement and instability. Ding et al. (2018) illustrated that adding just cement in clay soil with low plasticity increased the dimension shrinkages and expansive ratio in FRCS clay with increasing freeze-thaw cycles and cement content. Furthermore, the freeze-thaw cycle exacerbates the development of existing cracks in cemented clay and results in new fractures (Ding et al., 2018).

In contrast, Tajdini et al. (2018) demonstrated that the fibre type on the corresponding strain and compressive strength is more pronounced in terms of performance and ductility index. Güllü and Khudir (2014) looked at how freezing and thawing cycles affected low-plasticity silt soil reinforced with jute fibre, steel fibre, and lime. Shear strength and UCS testing were carried out with varying concentrations of lime and fibres in different freezing-thawing cycles ranging from 0 to 3. The results showed that after the freeze-thaw cycle, the UCS values of FRLS soil rose (Güllü & Khudir, 2014). Also, Jafari and Esna-ashari (2012) found that tire cord fibre increased lime-stabilised soil's durability and strength under freeze-thaw cycles. However, adding fibre before freezing-thawing and after one cycle did not significantly increase stiffness, stiffness rose after two cycles (Jafari & Esna-ashari, 2012).

Moreover, Saygili and Dayan (2019) showed that the mixture of kaolinite, lime, synthetic fibre, and silica fume boosted the strength and durability of the material under freezing-thawing conditions. Similarly, Thanushan and Sathiparan (2022) presented that banana fibre in cement stabilised soil improved residual compression strength while coconut coir fibre indicated better residual flexural strength. Both fibres increased cement-stabilised soil resistance to freeze-thaw weathering, wet-dry weathering, and alkali/acid attack. Furthermore, compared to the specimen reinforced with banana fibres, the specimens reinforced with coconut coir were more durable (Thanushan & Sathiparan, 2022).

The compound of FRLS/FRCS is more effective than just lime or fibre in clay soil. Most studies employed synthetic fibre as a soil stabilising reinforcement due to durability and loss of water absorption. Natural fibre has more degradation than synthetic fibre under temperature change. However, the lack of investigation of natural fibres is visible and suggested for future research. It is also considerable that freeze-thaw cycles do not affect the pozzolanic reaction in lime/cement-treated soil. Adding cement in low plasticity soil is ineffective due to the negative impact of soil shrinkage and the developing existing crack in soil.

### **Improve Pavement Subgrade**

Subgrade preparation is critical in constructing highways since it is the foundation for flexible pavement. The subgrade may be fully exploited if compacted soil; the subgrade strength is proportional to the CBR value. Subgrades with poor soils have less than 2% CBR value and must be replaced with suitable soil for subgrade construction (Praveen et al., 2020). Significant research has been conducted over the last few decades, and different optimisation approaches have been developed to improve the CBR values of soft soils. For the first time, Little and Nair (2009) selected the effective soil stabiliser based on particle size analysis and Atterberg limits (Plasticity index), as shown in Figure 1 (Board et al., 2009). Although lime/cement is a common method to stabilise base and subbase materials (Senanayake et al., 2022), FRLS/FRCS soil effectively improves weak subgrade soil. However, when fibre reinforcement is used in lime-stabilised soil, it impacts the stability of subgrade material and pavement thickness (Moghal et al., 2018; Boobalan & Sivakami Devi, 2022). The behaviour of discrete plastic FRLS clay soil was studied by Dhar and Hussain (2019). The results showed that discrete plastic fibre on lime-stabilised soil increased toughness, young's modulus, peak strength, CBR value, and secant modulus values, achieved residual strength and changed the behaviour of soil stabilisation failure from fragile to flexible (Dhar & Hussain, 2019).



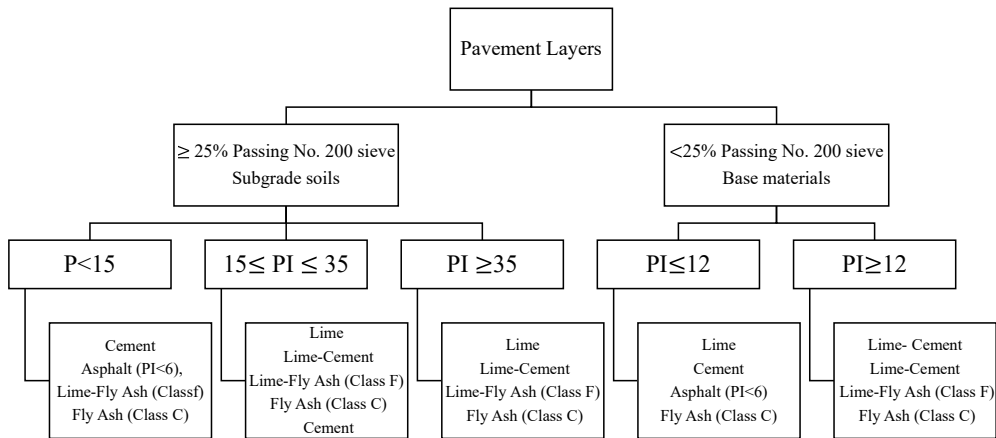


Figure 1. Determination of the appropriate stabiliser based on the plastic index and per cent smaller than 75 µm (Board et al., 2009)

Tiwari and Satyam (2020) investigated expansive soil improved with silica fume, lime, and coir geotextile. Expansive soils exhibit significant shrinkage and swelling characteristics and low shear strength (Punthutaecha et al., 2006). The lime-modified coir geotextile reduced swelling potential and improved the shear resistance and bearing capacity of costly soil, reducing the thickness of the base course layer and subbase in the pavement (Tiwari & Satyam, 2020). Moreover, Praveen et al. (2020) demonstrated that the CBR values had increased dramatically for a mixture of steel fibre, fly ash, and cement, effective for subgrade in country roads with low traffic flow (Praveen et al., 2020). Mishra and Gupta (2018) investigated the effects of PET fibre on fly ash-stabilised clay soil. Although the composite containing fly ash and PET fibre improved shear strength and CBR, the plasticity index deteriorated (Mishra & Gupta, 2018).

Additionally, Otoko and Pedro (2014) showed that adding waste shredded rubber FRCS clayey laterites soil enhanced UCS and CBR values. Although the highest CBR values were obtained after 14 days of curing, this is not attributed solely to cement. Fibre addition created an interlocking effect on the soil (Otoko & Pedro, 2014). Fibre positively impacts the CBR values and increases toughness because of fibre’s energy absorption capacity under tension that the length of fibre crossover the weak zones (Onyejekwe & Ghataora, 2014). Increasing the toughness of fibre-reinforced stabilised soil has significant practical implications for pavement performance, such as strength to fatigue failure and extending their service life.

The effect of lime and cement on elastic modulus and CBR values are significant (Rizal et al., 2022) while fibre has a minor influence on CBR values. In contrast, fibre increases residual strength, so lime/cement does not contribute to this. Consequently, combining fibre with lime/cement in various weak soil increases CBR values, such as in expansive and lateritic soil.

## Compression and Tensile Strength

Compared to unreinforced stabilised soil, using fibre as reinforcement in stabilisation soils reduces soil stiffness while increasing flexible behaviour, ductility, and toughness (Ateş, 2016). Due to the brittle nature of lime/cement stabilised soil- which shows no evidence of failure- the rapid collapse of structures happens when stability is slightly greater than the failure limit (Abdi et al., 2021). However, the UCS increases with increasing lime/cement percentages and curing time (Eskisar, 2015; Yoobanpot et al., 2020). According to Sobhan (2008), chemically stabilised soil is resistant to compression but makes a negligible contribution to tensile strength. It becomes a significant issue when a tensile crack occurs in the soils due to shrinkage, and the stabilisation is supposed to resist it. As a result, it is essential to enhance the tensile strength, hardness, and ductility of lime-treated soil with fibre reinforcement (Sobhan, 2008). Wang et al. (2019) and Li et al. (2012) discovered that incorporating wheat straw fibres and lime into soil increased strain-softening behaviour, secant modulus, and shear strength. Furthermore, when added as reinforcement, fibre improves samples' ductility and strength (Kafodya & Okonta, 2018).

Marine soil characteristics vary significantly between wet and dry soils. When lime-treated coconut fibre was combined with high-salinity marine clay soil, an improvement in strength was seen. It implies that saltwater improved the flexural stiffness of the treated coir fibre in cemented soil (Anggraini et al., 2017). Moreover, Kamaruddin et al. (2020) found that adding coir fibre boosted compressive strength, and tensile strength. Labiad et al. (2022) also found that sisal fibres in cement stabilised compressed earth blocks (produce brick waste and clay) improved tensile strength. Moreover, marginal soil modified with coir fibre, fly ash, and cement exhibited higher shear strength (1.5 to 2 times) than unmodified marginal soil (Praveen & Kurre, 2020). According to the results, coir fibre combined with cement and fly ash promoted interlocking between soil particles, and the UCS value for this composite was the greatest. Additionally, Tamassoki et al. (2020) exhibited coir fiber in activated carbon stabilised lateritic soil improved shear strength, post-peak residual strength, compressive strength, and Elastic Modulus (Tamassoki et al., 2022b).

Furthermore, Sukontasukkul and Jamsawang (2012) investigated using PP and steel FRCS soil. Although PP fibre outperformed the steel FRCS soil in flexural performance, fibre and cement enhanced the flexural performance of modified soil, which exhibited more significant peak and residual strengths (Sukontasukkul & Jamsawang, 2012). Moreover, Tharani et al. (2021) show that CBR, UCS, and Direct shear values were enhanced when PP fibre, basalt, and lime were added to black cotton soil. In contrast, Oliveira et al. (2016) found that utilising PP fibre and steel fibre as reinforcement on cement stabilised soft soil (OH) had a negative impact on UCS values (17–32%), only employing steel FRCS soil increased STS values, while PP fibres did not affect it.

One of the common failure modes of transportation infrastructure is fatigue. Fatigue is a term that refers to the gradual, permanent internal structural changes which occur in a material under repetitive loads (Lee & Barr, 2004). These repetitive loadings cause repetitive tensile stress at the bottom of the layers for hydraulic materials employed in the layers of transportation infrastructures (Preteuille et al., 2013). Therefore, it appears appropriate to include fibres in the materials to improve cement-modified soils' fatigue and tensile strength performance (Consoli et al., 2011). The surface kenaf fibre is pitted and grooved, so cement materials easily adhere to them and increase their friction with soil particles. Hence, the tensile tension in kenaf FRCs sand soil increased as the kenaf fibre length increased (Ghadakpour et al., 2020). However, Lenoir et al. (2016) showed that the initial elasticity modulus does not affect the flexural strength of FRCS sandy clay soil.

In comparison, the flexural stress was lowered by FRCS coarse-grained with a tiny percentage of clay (Ghadakpour et al., 2020). Furthermore, microcracks decreased in FRCS sandy clay soil and were ineffective in FRCS coarse-grained soil when both soils were subjected to cyclic loading (Lenoir et al., 2016). Moreover, Kutanaei and Choobbasti (2017) used several tests to investigate the influence of randomly distributed polyvinyl alcohol fibre, nano-silica, and cement on the mechanical properties of sandy soil. They found that adding fibres to the sandy soil reduces the modulus of elasticity but enhances the energy absorption capacity.

Since the tensile strength and seismic reactivity are strongly associated as severe issues with RE structures, limiting their practical applicability. Zare et al. (2020) studied cement stabilised RE reinforced with Waste Tire Textile Fibres. Due to improved cohesion between soil and fibre, STS values and ductility rose when fibre was added to cement-stabilised soil (Tang et al., 2007). FRCS soil's tensile behaviour mobilised tensile strength and prevented abrupt failure. When the fibre content increases, the abrupt strength loss between the first peak and strength restoration is significantly reduced (Zare et al., 2020). In addition, Shen et al. (2021) confirmed that cement enhanced peak strength more than lime, while residual strength increased similarly for both FRLS and FRCS soils.

However, Consoli et al. (2002) presented that increasing the length of PET fibres had no significant influence on the tensile strength impelled by the splitting tensile test and attributed this to a lack of friction between the cement matrix and the fibres due to smooth surface of the fibres. Also, some research found that employing FRCS clay soil can lower UCS and shear strength values (Correia et al., 2015).

Although using FRLS/FRCS improves the compression and tensile strength in diverse poor soil types, such as clay, marine, and expansive soils, they create minor enhancements in the strength of coarse-grained soil. The surface and length of fibre impact better interlocking particles in the mixture. Improving in UCS value happens due to lime and cement, while fibre is the cause of enhancing tensile strength.

### Microstructure of FRLS/FRCS Soils

Microstructure analysis is a powerful tool for uncovering more objective evidence in changed soil at the micro-level. For example, Mobini et al. (2015) demonstrated that by adding synthetic fibres (steel and PP) into concrete mixtures, a dense zone between the fibres and the concrete matrix is created, which increases the flexural and tensile strengths of concrete samples. In contrast, Rivera-Gómez (2014) showed that when natural fibre (jute) is added to soil, this connection is not created, resulting in a more uncomplicated fracture under tension. It is because natural fibres have greater moisture absorption capacity when compared to synthetic fibres. Figure 2 compares moisture absorption between some natural and synthetic fibres (Rivera-Gómez et al., 2014).

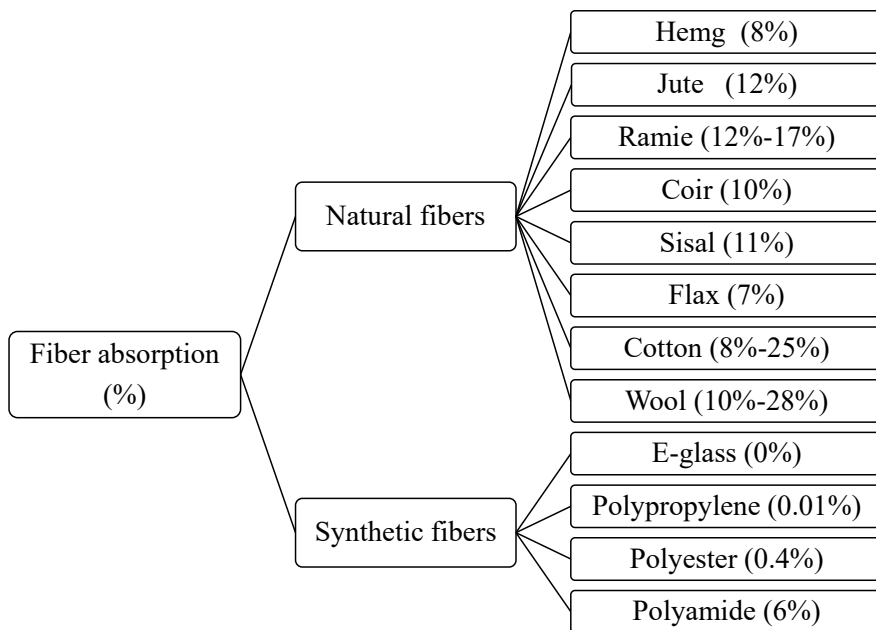


Figure 2. Comparison of moisture absorption between some natural and synthetic fibres (Rivera-Gómez et al., 2014)

Due to absorbing water during the thawing stage, lime-stabilised clayey soil reinforced with waste tire fibre loses 62% of its strength after just one freeze-thaw cycle (Jafari et al., 2012). In addition, Miller and Rifai (2004) showed that PP is a hydrophobic and chemically ineffective polymer. This substance is impervious to soil moisture and leachates and does not absorb or react with them (Miller & Rifai, 2004).

In contrast, Wang et al. (2019) showed honeycomb pattern of wheat fibres created a practical situation in lime-stabilised soil. Due to the water channels provided by the

surfaces and honeycomb structure of wheat straw fibres, the chemical reaction between lime and water proceeds was quicker, resulting in a greater secant modulus than just adding lime (Wang et al., 2019). Cai et al. (2006) also demonstrated that the contact area of fibre with lime-stabilised soil is higher than with un-stabilised soil because lime reduces the pores between clay particles. Lime-soil reactions caused soil particles and the pores in the soil to become smaller and more detached (Cai et al., 2006). Also, soil-fibre contact is exceptionally minimal due to the low frictional properties and smooth surface of PP fibres. Forming cementitious chemicals in lime-stabilised clays binds soil particles and fibres with clay that tensions the fibres and gradually enhances the shear strength in the mixture (Abdi et al., 2021).

Yoobanpot et al. (2020) discovered that increasing curing time in dredging sediments stabilisation with cement and fly ash increases the concentration of CSH, CAH, and CASH. Because of the CSH gel-filled voids and gaps, the proportion of micropores in the treated soil was lower than in untreated. It was discovered that pore spaces were reduced due to better pozzolanic reactions in amended soil (Yoobanpot et al., 2020). Chemical components of modified soil with lime and coir fibre are different in the range of zero to 28 days curing period, according to Jairaj et al. (2020). When the soil was treated with coir fibre and lime, the temperature rose to 38 degrees Celsius, while there was no increase in temperature when the soil was only treated with coir fibre without lime. It was discovered that a pozzolanic reaction generated the heat of hydration in soil treated with lime and fibre. It influenced coir fibre surface properties, and the degradation of coir fibres reduced the UCS value for more than seven days of curing (Jairaj et al., 2020). According to Boz et al. (2018), PP fibre drew out of the soil due to weaker superficial adhesion on the soil-fibre interaction surface, resulting in a gap between soil and fibre. The interlocking and bonding between soil particles and basalt fibre improved when basalt fibre was used as reinforcement in lime-stabilised soil. The energy-dispersive spectroscopy results revealed that Si, Al, O, and Ca were all made up of soil and the presence of water, kaolin, and lime (Boz et al., 2018).

Saygili and Dayan (2019) evaluated the influence of freezing-thawing cycles on silica FRLS soil. The findings showed that CSH gel filled the holes before freezing-thawing cycles, resulting in better durability and strength in treated soil. Increased cracking and gaps in modified soil caused by freezing and thawing cycles, on the other hand, decreased UCS values (Saygili & Dayan, 2019).

Ghadakpour et al. (2020) demonstrated that increasing kenaf fibre concentration increased heterogeneity in cement-treated soil, resulting in various UWV findings. Fibre generated heterogeneity when the percentage of fibre in specimens rose. As a result, the waves diverged and could not travel through the samples, resulting in UWV errors (Ghadakpour et al., 2020).

After employing lime/cement as a stabilising agent, the CSH gel is the primary substance that fills holes and gaps between soil particles. Microstructure studies revealed that lime/cement alone impacts to soil, resulting in improved interlocking between soil particles. Figure 3 illustrates the reasons that cause cracks and gaps in FRLS/FRCS soils.

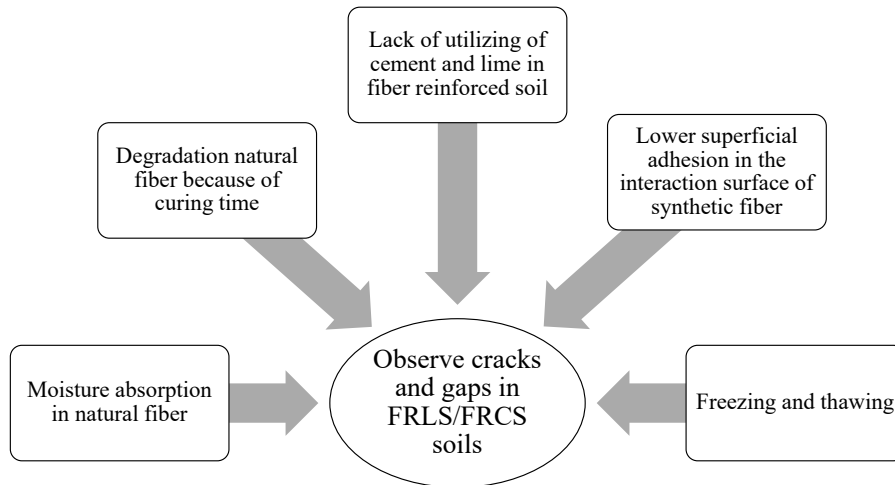


Figure 3. Causes for observing cracks and gaps in FRLS/FRCS soils

### Impact of Lime/Cement on Soil in Terms of Mineralisation

Although cement and lime differ in their chemical nature, they can provide calcium to stabilise different soil types. By adding lime to the soil, an elementary environment ( $\text{pH} > 12$ ) is created in the pore fluid, allowing the Alumina ( $\text{Al}_2\text{O}_3$ ) and Silica ( $\text{SiO}_2$ ) in the soil to dissolve gradually. The dissolved Alumina and Silica form a cementitious gel (similar to CSH and CAH) that covers the coarser particles and creates a strong bonding between them, improving strength and increasing the brittleness of the mixture. Moreover, adding more lime have a negative effect on strength. Strength declines in higher content of lime (9%); this reduction in strength might be caused by an excessive amount of lime ( $\text{CaO}$ ), which produces a large number of calcium ions ( $\text{Ca}^{2+}$ ) and cling to the clay surface. As a result of these ions altering the surface charge to a high positive net charge, osmosis occurs in the pore fluid system. The flocculated structure of the clay particles disperses due to the osmosis process. This structure has negligible compressive resistance and decreasing strength with greater lime concentration (Dhar & Hussain, 2019).

Cement addition alters the structure of lateritic soil. Lateritic soil mainly consists of  $\text{SiO}_2$  and  $\text{Al}_2\text{O}_3$ , whereas cement mainly consists of calcium ions. The CASH, CSH, and CAH are formed because of the pozzolanic interaction between the soil's alumina-silica in soil and the calcium ions of the cement in the presence of water. Pore and crack sizes were reduced, suggesting improved mechanical characteristics (Wahab, Roshan et al., 2021). According to research by Broderick and Daniel (1990), organic compounds in concentrated form have significantly increased the hydraulic conductivity of compacted clay. Lime/cement stabilised soils are less sensitive to organic chemical attacks than untreated soils (Broderick & Daniel, 1990).

When cement reacts with water, calcium ions ( $\text{Ca}^{2+}$ ) are released onto the surface of soil particles and raise the soil pH value (Chew et al., 2004). The pH value continuously lowers in lime/cement stabilised soil as cure time increases regardless of binder amount. The cement dropped its pH value significantly within the first 28 days. It is due to the increased CSH and CAH components resulting from hydration and pozzolanic processes (Al-Jabban et al., 2019). In this respect, accelerated curing guarantees a rapid pH decrease due to the formation of pozzolanic products (CAH and CSH) at high temperatures (Al-Mukhtar et al., 2010).

When soil with a pH value is smaller, it needs more cement content to improve soil strength (Al-Jabban et al., 2019). Because of significant hydration products formed (such as CAH, CSH, and hydrated lime), lime/cement stabilisation decreases volume change and Atterberg limits of soils. Still, it increases the strength and shrinkage limit of the soil-cement matrix (Chen & Wang, 2006).

The most often recurring issue, particularly in cement stabilisation, is sulfate attack caused by the deposition of ettringite. When lime/cement-treated soils with a certain quantity of gypsum or the treated soil are exposed to sulfated waters, sulfate attacks have frequently weakened the soil and resulted in the enlargement of the soil layer. As a result, lime/cement stabilisations have several disadvantages, including damage to the environment and groundwater and a high degree of brittleness. For example, making one ton of cement leads to around 1.3 tons of  $\text{CO}_2$  emission, one of the primary disadvantages of the cement stabilisation process (Ta'negonbadi & Noorzad, 2017).

## CONCLUSION

This literature review investigates the effects of adding lime, cement, and fibre on weak soil enhancements from different aspects. The following is a summary of the important points:

- i. The fibre in lime/cement stabilized soil improves peak strength, residual strength, and stiffness and changes failure behaviour from brittle to ductile. Although several elements are considered under this circumstance, such as the length, percentage, and type of fibre, the percentages of lime/cement and the water ratio are most important.



Depending on the amount of water, it has both good and negative impacts on tensile strength and USC values. In contrast, when frost heave develops, friction between the matrix and fibre is a restraining force against expansion. The fibre will be ineffective if the natural soil is vulnerable to freeze-thaw and saturation. The load-transfer mechanism operates more efficiently in lime/cement stabilised soil, and adding fibre increases soil strength.

- ii. The CSH gel is the major substance that fills holes and gaps between soil particles in FRLS/FRCS soils, while fibres create bridges between soil particles and restrict matrix cracks and gaps after forming gels. So, additional pressures and energy are necessary to pull out the fibres to deflect further. Apart from protecting the soil's integrity, this procedure enhances the bearing capacity of the soil.
- iii. Although one reason to observe gaps and cracks is water absorption in natural fibres, rough surfaces in natural fibre help the reaction between cement/lime and water proceed more quickly. Still, natural fibre degradation may occur in stabilised soil due to hydration and curing time heat. Also, absorbing water during the thawing stage creates gaps in FRLS/FRCS soils, mainly in the bonding zone.

## ACKNOWLEDGEMENT

The authors are grateful to the Government of Malaysia, the Ministry of Education, and Universiti Putra Malaysia for supporting starting of this study. Universiti Putra Malaysia has supported this study under Project Code: GP-IPS/2021/9701400, Type of grant: Geran Inisiatif Putra Siswazah (GP-IPS).

## REFERENCES

- Abdi, M. M. R., Ghalandarzadeh, A., & Chafi, L. S. (2021). An investigation into the effects of lime on compressive and shear strength characteristics of fiber-reinforced clays. *Journal of Rock Mechanics and Geotechnical Engineering*, 13(4), 885-898. <https://doi.org/10.1016/j.jrmge.2020.11.008>
- Al-Jabban, W., Laue, J., Knutsson, S., & Al-Ansari, N. (2019). A Comparative evaluation of cement and by-product Petrit T in soil stabilization. *Applied Sciences*, 9(23), Article 5238. <https://doi.org/10.3390/app9235238>
- Al-Mukhtar, M., Lasledj, A., & Alcover, J. F. (2010). Behaviour and mineralogy changes in lime-treated expansive soil at 50°C. *Applied Clay Science*, 50(2), 199-203. <https://doi.org/10.1016/j.clay.2010.07.022>
- Anggraini, V., Asadi, A., Syamsir, A., & Huat, B. B. K. (2017). Three point bending flexural strength of cement treated tropical marine soil reinforced by lime treated natural fiber. *Measurement*, 111, 158-166. <https://doi.org/10.1016/j.measurement.2017.07.045>
- Ateş, A. (2016). Mechanical properties of sandy soils reinforced with cement and randomly distributed glass fibers (GRC). *Composites Part B: Engineering*, 96, 295-304. <https://doi.org/10.1016/j.compositesb.2016.04.049>

- Behnood, A. (2018). Soil and clay stabilization with calcium- and non-calcium-based additives: A state-of-the-art review of challenges, approaches and techniques. *Transportation Geotechnics*, 17(Part A), 14-32. <https://doi.org/10.1016/j.trgeo.2018.08.002>
- Boobalan, S. C., & Devi, M. S. (2022). Investigational study on the influence of lime and coir fiber in the stabilization of expansive soil. *Materials Today: Proceedings*, 60(Part 1), 311-314 <https://doi.org/10.1016/J.MATPR.2022.01.230>
- Boz, A., & Sezer, A. (2018). Influence of fiber type and content on freeze-thaw resistance of fiber reinforced lime stabilized clay. *Cold Regions Science and Technology*, 151, 359-366. <https://doi.org/10.1016/j.coldregions.2018.03.026>
- Boz, A., Sezer, A., Özdemir, T., Hızal, G. E., & Dolmacı, Ö. A. (2018). Mechanical properties of lime-treated clay reinforced with different types of randomly distributed fibers. *Arabian Journal of Geosciences*, 11(6), Article 122. <https://doi.org/10.1007/s12517-018-3458-x>
- Broderick, G. P., & Daniel, D. E. (1990). Stabilizing compacted clay against chemical attack. *Journal of Geotechnical Engineering*, 116(10), 1549-1567. [https://doi.org/10.1061/\(ASCE\)0733-9410\(1990\)116:10\(1549\)](https://doi.org/10.1061/(ASCE)0733-9410(1990)116:10(1549))
- Cai, Y., Shi, B., Ng, C. W. W., & Tang, C. S. (2006). Effect of polypropylene fibre and lime admixture on engineering properties of clayey soil. *Engineering Geology*, 87(3-4), 230-240. <https://doi.org/10.1016/j.enggeo.2006.07.007>
- Chen, H., & Wang, Q. (2006). The behaviour of organic matter in the process of soft soil stabilization using cement. *Bulletin of Engineering Geology and the Environment*, 65(4), 445-448. <https://doi.org/10.1007/s10064-005-0030-1>
- Chew, S. H., Kamruzzaman, A. H. M., & Lee, F. H. (2004). Physicochemical and engineering behavior of cement treated clays. *Journal of Geotechnical and Geoenvironmental Engineering*, 130(7), 696-706. [https://doi.org/10.1061/\(ASCE\)1090-0241\(2004\)130:7\(696\)](https://doi.org/10.1061/(ASCE)1090-0241(2004)130:7(696))
- Consoli, N. C., De Moraes, R. R., & Festugato, L. (2011). Split tensile strength of monofilament polypropylene fiber-reinforced cemented sandy soils. *Geosynthetics International*, 18(2), 57-62. <https://doi.org/10.1680/gein.2011.18.2.57>
- Consoli, N. C., Montardo, J. P., Prietto, P. D. M., & Pasa, G. S. (2002). Engineering behavior of a sand reinforced with plastic waste. *Journal of Geotechnical and Geoenvironmental Engineering*, 128(6), 462-472. [https://doi.org/10.1061/\(ASCE\)1090-0241\(2002\)128:6\(462\)](https://doi.org/10.1061/(ASCE)1090-0241(2002)128:6(462))
- Correia, A. S. A. S., Oliveira, P. J. V., Odio, D. G. C., Oliveira, P. J. V., & Custódio, D. G. (2015). Effect of polypropylene fibres on the compressive and tensile strength of a soft soil, artificially stabilised with binders. *Geotextiles and Geomembranes*, 43(2), 97-106. <https://doi.org/10.1016/j.geotexmem.2014.11.008>
- Dhar, S., & Hussain, M. (2019). The strength behaviour of lime-stabilised plastic fibre-reinforced clayey soil. *Road Materials and Pavement Design*, 20(8), 1757-1778. <https://doi.org/10.1080/14680629.2018.1468803>
- Ding, M., Zhang, F., Ling, X., & Lin, B. (2018). Effects of freeze-thaw cycles on mechanical properties of polypropylene Fiber and cement stabilized clay. *Cold Regions Science and Technology*, 154, 155-165. <https://doi.org/10.1016/j.coldregions.2018.07.004>

- Du, J., Liu, B., Wang, Z., Zheng, G., Jiang, N. J., Zhou, M., & Zhou, H. (2021). Dynamic behavior of cement-stabilized organic-matter-disseminated sand under cyclic triaxial condition. *Soil Dynamics and Earthquake Engineering*, *147*, 106777. <https://doi.org/10.1016/J.SOILDYN.2021.106777>
- Eskisar, T. (2015). Influence of cement treatment on unconfined compressive strength and compressibility of lean clay with medium plasticity. *Arabian Journal for Science and Engineering*, *40*, 763-772. <https://doi.org/10.1007/s13369-015-1579-z>
- Ghadakpour, M., Choobbasti, A. J., & Kutanaei, S. S. (2020). Investigation of the kenaf fiber hybrid length on the properties of the cement-treated sandy soil. *Transportation Geotechnics*, *22*, Article 100301. <https://doi.org/10.1016/j.trgeo.2019.100301>
- Ghazavi, M., & Roustaie, M. (2010). The influence of freeze-thaw cycles on the unconfined compressive strength of fiber-reinforced clay. *Cold Regions Science and Technology*, *61*(2), 125-131. <https://doi.org/10.1016/j.coldregions.2009.12.005>
- Ghobadi, M. H., Abdilor, Y., & Babazadeh, R. (2014). Stabilization of clay soils using lime and effect of pH variations on shear strength parameters. *Bulletin of Engineering Geology and the Environment*, *73*, 611-619. <https://doi.org/10.1007/S10064-013-0563-7>
- Güllü, H., & Khudir, A. (2014). Effect of freeze-thaw cycles on unconfined compressive strength of fine-grained soil treated with jute fiber, steel fiber and lime. *Cold Regions Science and Technology*, *106-107*, 55-65. <https://doi.org/10.1016/j.coldregions.2014.06.008>
- Hamidi, A., & Hooresfand, M. (2013). Effect of fiber reinforcement on triaxial shear behavior of cement treated sand. *Geotextiles and Geomembranes*, *36*, 1-9. <https://doi.org/10.1016/j.geotextmem.2012.10.005>
- Han, J. (2015). *Principles and practice of ground improvement*. John Wiley & Sons.
- He, S., Wang, X., Bai, H., Xu, Z., & Ma, D. (2021). Effect of fiber dispersion, content and aspect ratio on tensile strength of PP fiber reinforced soil. *Journal of Materials Research and Technology*, *15*, 1613-1621. <https://doi.org/10.1016/J.JMRT.2021.08.128>
- Hejazi, S. M., Sheikhzadeh, M., Abtahi, S. M., & Zadhoush, A. (2012). A simple review of soil reinforcement by using natural and synthetic fibers. *Construction and Building Materials*, *30*, 100-116. <https://doi.org/10.1016/j.conbuildmat.2011.11.045>
- Jafari, M., & Esna-ashari, M. (2012). Effect of waste tire cord reinforcement on unconfined compressive strength of lime stabilized clayey soil under freeze-thaw condition. *Cold Regions Science and Technology*, *82*, 21-29. <https://doi.org/10.1016/j.coldregions.2012.05.012>
- Jairaj, C., Kumar, M. T. P., & Ramesh, H. N. (2020). Effect of addition of lime on coir fiber admixed BC soil. *Innovative Infrastructure Solutions*, *5*, Article 49. <https://doi.org/10.1007/s41062-020-00300-3>
- Jamsawang, P., Voottipruex, P., & Horpibulsuk, S. (2015). Flexural strength characteristics of compacted cement-polypropylene fiber sand. *Journal of Materials in Civil Engineering*, *27*(9), Article 04014243. [https://doi.org/10.1061/\(ASCE\)MT.1943-5533.0001205](https://doi.org/10.1061/(ASCE)MT.1943-5533.0001205)
- Kafodya, I., & Okonta, F. (2018). Effects of natural fiber inclusions and pre-compression on the strength properties of lime-fly ash stabilised soil. *Construction and Building Materials*, *170*, 737-746. <https://doi.org/10.1016/j.conbuildmat.2018.02.194>

- Kamaruddin, F. A., Nahazanan, H., Huat, B. K., & Anggraini, V. (2020). Improvement of marine clay soil using lime and alkaline activation stabilized with inclusion of treated coir fibre. *Applied Sciences*, *10*(6), Article 2129. <https://doi.org/10.3390/app10062129>
- Kravchenko, E., Liu, J., Krainiukov, A., & Chang, D. (2019). Dynamic behavior of clay modified with polypropylene fiber under freeze-thaw cycles. *Transportation Geotechnics*, *21*, Article 100282. <https://doi.org/10.1016/j.trgeo.2019.100282>
- Kumar, A., & Gupta, D. (2016). Behavior of cement-stabilized fiber-reinforced pond ash, rice husk ash-soil mixtures. *Geotextiles and Geomembranes*, *44*(3), 466-474. <https://doi.org/10.1016/j.geotexmem.2015.07.010>
- Kutanaei, S. S., & Choobasti, A. J. (2017). Effects of nanosilica particles and randomly distributed fibers on the ultrasonic pulse velocity and mechanical properties of cemented sand. *Journal of Materials in Civil Engineering*, *29*(3), Article 4016230.
- Labiad, Y., Meddah, A., & Beddar, M. (2022). Physical and mechanical behavior of cement-stabilized compressed earth blocks reinforced by sisal fibers. *Materials Today: Proceedings*, *53*(Part 1), 139-143. <https://doi.org/10.1016/J.MATPR.2021.12.446>
- Lee, M. K., & Barr, B. I. G. (2004). An overview of the fatigue behaviour of plain and fibre reinforced concrete. *Cement and Concrete Composites*, *26*(4), 299-305. [https://doi.org/10.1016/S0958-9465\(02\)00139-7](https://doi.org/10.1016/S0958-9465(02)00139-7)
- Lenoir, T., Preteseille, M., & Ricordel, S. (2016). Contribution of the fiber reinforcement on the fatigue behavior of two cement-modified soils. *International Journal of Fatigue*, *93*(Part1), 71-81. <https://doi.org/10.1016/j.ijfatigue.2016.08.007>
- Li, M., Chai, S. X., Zhang, H. Y., Du, H. P., & Wei, L. (2012). Feasibility of saline soil reinforced with treated wheat straw and lime. *Soils and Foundations*, *52*(2), 228-238. <https://doi.org/10.1016/j.sandf.2012.02.003>
- Little, D. N., & Nair, S. (2009). *Recommended practice for stabilization of subgrade soils and base materials*. National Academies Press. <https://doi.org/10.17226/22999>
- Miller, C. J., & Rifai, S. (2004). Fiber reinforcement for waste containment soil liners. *Journal of Environmental Engineering*, *130*(8), 891-895.
- Mishra, B., & Gupta, M. K. (2018). Use of randomly oriented polyethylene terephthalate (PET) fiber in combination with fly ash in subgrade of flexible pavement. *Construction and Building Materials*, *190*, 95-107. <https://doi.org/10.1016/j.conbuildmat.2018.09.074>
- Mobini, M., Khaloo, A., Hosseini, P., & Esrafil, A. (2015). Mechanical properties of fiber-reinforced high-performance concrete incorporating pyrogenic nanosilica with different surface areas. *Construction and Building Materials*, *101*(Part 1), 130-140. <https://doi.org/10.1016/j.conbuildmat.2015.10.032>
- Moghal, A. A. B., Chittoori, B. C. S., & Basha, B. M. (2018). Effect of fibre reinforcement on CBR behaviour of lime-blended expansive soils: Reliability approach. *Road Materials and Pavement Design*, *19*(3), 690-709. <https://doi.org/10.1080/14680629.2016.1272479>
- Narani, S. S., Abbaspour, M., Hosseini, S. M. M. M., & Nejad, F. M. (2020). Long-term dynamic behavior of a sandy subgrade reinforced by Waste Tire Textile Fibers (WTTFs). *Transportation Geotechnics*, *24*, Article 100375. <https://doi.org/https://doi.org/10.1016/j.trgeo.2020.100375>

- Oliveira, P. J. V., Correia, A. A. S., Teles, J. M. N. P. C., & Custódio, D. G. (2016). Effect of fibre type on the compressive and tensile strength of a soft soil chemically stabilised. *Geosynthetics International*, 23(3), 171-182. <https://doi.org/10.1680/jgein.15.00040>
- Onyejekwe, S., & Ghataora, G. S. (2014). Effect of fiber inclusions on flexural strength of soils treated with nontraditional additives. *Journal of Materials in Civil Engineering*, 26(8), Article 4014039.
- Osinubi, K. J., Ijmdiya, T. S., & Nmadu, I. (2009). Lime stabilization of black cotton soil using bagasse ash as admixture. *Advanced Materials Research*, 62-64, 3-10. <https://doi.org/10.4028/www.scientific.net/amr.62-64.3>
- Otoko, G. R., & Pedro, P. P. (2014). Cement stabilization of laterite and Chikoko soils using waste rubber fibre. *International Journal of Engineering Sciences & Research Technology*, 3(10), 130-136.
- Petry, T. M., & Little, D. N. (2002). Review of stabilization of clays and expansive soils in pavements and lightly loaded structures - History, practice, and future. *Journal of Materials in Civil Engineering*, 14(6), 447-460. [https://doi.org/10.1061/\(ASCE\)0899-1561\(2002\)14:6\(447\)](https://doi.org/10.1061/(ASCE)0899-1561(2002)14:6(447))
- Praveen, G. V., & Kurre, P. (2020). Influence of coir fiber reinforcement on shear strength parameters of cement modified marginal soil mixed with fly ash. *Materials Today: Proceedings*, 39(Part 1), 504-507. <https://doi.org/10.1016/j.matpr.2020.08.238>
- Praveen, G. V, Kurre, P., & Chandrabai, T. (2020). Improvement of California bearing ratio (CBR) value of steel fiber reinforced cement modified marginal soil for pavement subgrade admixed with fly ash. *Materials Today: Proceedings*, 31(Part 1), 639-642. <https://doi.org/10.1016/j.matpr.2020.08.814>
- Preteseille, M., & Lenoir, T. (2016). Structural test at the laboratory scale for the utilization of stabilized fine-grained soils in the subgrades of high-speed rail infrastructures: Experimental aspects. *International Journal of Fatigue*, 82(Part 3), 505-513. <https://doi.org/https://doi.org/10.1016/j.ijfatigue.2015.09.005>
- Preteseille, M., Lenoir, T., & Hornych, P. (2013). Sustainable upgrading of fine-grained soils present in the right-of-way of high speed rail projects. *Construction and Building Materials*, 44, 48-53. <https://doi.org/10.1016/j.conbuildmat.2013.03.022>
- Punthutaecha, K., Puppala, A. J., Vanapalli, S. K., & Inyang, H. (2006). Volume change behaviors of expansive soils stabilized with recycled ashes and fibers. *Journal of Materials in Civil Engineering*, 18(2), 295-306.
- Ramkrishnan, R., Sruthy, M. R., Sharma, A., & Karthik, V. (2018). Effect of random inclusion of sisal fibres on strength behavior and slope stability of fine grained soils. *Materials Today: Proceedings*, 5(11, Part 3), 25313-25322. <https://doi.org/10.1016/j.matpr.2018.10.334>
- Ranjan, G., Vasan, R. M., & Charan, H. D. (1994). Behaviour of plastic-fibre-reinforced sand. *Geotextiles and Geomembranes*, 13(8), 555-565. [https://doi.org/https://doi.org/10.1016/0266-1144\(94\)90019-1](https://doi.org/https://doi.org/10.1016/0266-1144(94)90019-1)
- Rivera-Gómez, C., Galán-Marín, C., & Bradley, F. (2014). Analysis of the influence of the fiber type in polymer matrix/fiber bond using natural organic polymer stabilizer. *Polymers*, 6(4), 977-994. <https://doi.org/10.3390/polym6040977>
- Rizal, N. H. A., Hezmi, M. A., Razali, R., Wahab, N. A., Roshan, M. J., Rashid, A. S. A., & Hasbollah, D. Z. A. (2022). Effects of lime on the compaction characteristics of lateritic soil in UTM, Johor. In *IOP Conference Series: Earth and Environmental Science*, 971(1), Article 012031. IOP Publishing. <https://doi.org/10.1088/1755-1315/971/1/012031>

- Roshan, M. J., A Rashid, A. S., Abdul Wahab, N., Tamassoki, S., Jusoh, S. N., Hezmi, M. A., Nik Daud, N. N., Mohd Apandi, N., & Azmi, M. (2022). Improved methods to prevent railway embankment failure and subgrade degradation: A review. *Transportation Geotechnics*, 37, Article 100834. <https://doi.org/10.1016/J.TRGEO.2022.100834>
- Rosone, M., Ferrari, A., & Celauro, C. (2018). On the hydro-mechanical behaviour of a lime-treated embankment during wetting and drying cycles. *Geomechanics for Energy and the Environment*, 14, 48-60. <https://doi.org/10.1016/j.gete.2017.11.001>
- Roustaei, M., Eslami, A., & Ghazavi, M. (2015). Effects of freeze–thaw cycles on a fiber reinforced fine grained soil in relation to geotechnical parameters. *Cold Regions Science and Technology*, 120, 127-137. <https://doi.org/10.1016/j.coldregions.2015.09.011>
- Saygili, A., & Dayan, M. (2019). Freeze-thaw behavior of lime stabilized clay reinforced with silica fume and synthetic fibers. *Cold Regions Science and Technology*, 161, 107-114. <https://doi.org/10.1016/j.coldregions.2019.03.010>
- Senanayake, M., Arulrajah, A., Maghool, F., & Horpibulsuk, S. (2022). Evaluation of rutting resistance and geotechnical properties of cement stabilized recycled glass, brick and concrete triple blends. *Transportation Geotechnics*, 34, 100755. <https://doi.org/10.1016/J.TRGEO.2022.100755>
- Shen, Y., Tang, Y., Yin, J., Li, M., & Wen, T. (2021). An experimental investigation on strength characteristics of fiber-reinforced clayey soil treated with lime or cement. *Construction and Building Materials*, 294, Article 123537. <https://doi.org/10.1016/j.conbuildmat.2021.123537>
- Sobhan, K. (2008). Improving the tensile strength and toughness of a soil-cement-fly ash pavement subgrade with recycled HDPE strips. In *GeoCongress 2008: Geosustainability and Geohazard Mitigation* (pp. 1065-1072). American Society of Civil Engineers. [https://doi.org/10.1061/40971\(310\)133](https://doi.org/10.1061/40971(310)133)
- Sukontasukkul, P., & Jamsawang, P. (2012). Use of steel and polypropylene fibers to improve flexural performance of deep soil-cement column. *Construction and Building Materials*, 29, 201-205. <https://doi.org/10.1016/j.conbuildmat.2011.10.040>
- Tajdini, M., Bonab, M. H., & Golmohamadi, S. (2018). An experimental investigation on effect of adding natural and synthetic fibres on mechanical and behavioural parameters of soil-cement materials. *International Journal of Civil Engineering*, 16(4), 353-370. <https://doi.org/10.1007/s40999-016-0118-y>
- Tamassoki, S., Norsyahariati, N., Daud, N., Jakarni, F. M., Kusin, F. M., Safuan, A., Rashid, A., & Roshan, M. J. (2022a). Compressive and shear strengths of coir fibre reinforced Activated Carbon stabilised lateritic soil. *Sustainability*, 14(15), 9100. <https://doi.org/10.3390/SU14159100>
- Tamassoki, S., Norsyahariati, N., Daud, N., Jakarni, F. M., Kusin, F. M., Safuan, A., Rashid, A., & Jawed Roshan, M. (2022b). Performance evaluation of lateritic subgrade soil treated with lime and coir fibre-Activated Carbon. *Applied Sciences*, 12(16), 8279. <https://doi.org/10.3390/APP12168279>
- Ta'negonbadi, B., & Noorzad, R. (2017). Stabilization of clayey soil using lignosulfonate. *Transportation Geotechnics*, 12, 45-55. <https://doi.org/10.1016/j.trgeo.2017.08.004>
- Tang, C., Shi, B., Gao, W., Chen, F., & Cai, Y. (2007). Strength and mechanical behavior of short polypropylene fiber reinforced and cement stabilized clayey soil. *Geotextiles and Geomembranes*, 25(3), 194-202. <https://doi.org/10.1016/j.geotexmem.2006.11.002>



- Thanushan, K., & Sathiparan, N. (2022). Mechanical performance and durability of banana fibre and coconut coir reinforced cement stabilized soil blocks. *Materialia*, 21, 101309. <https://doi.org/10.1016/J.MTLA.2021.101309>
- Tharani, K., Selvan, G. P., Senbagam, T., & Karunakaran, G. (2021). An experimental investigation of soil stabilization using hybrid fibre and lime. *Materials Today: Proceedings*, 1-4. <https://doi.org/10.1016/J.MATPR.2021.03.380>
- Tiwari, N., & Satyam, N. (2020). An experimental study on the behavior of lime and silica fume treated coir geotextile reinforced expansive soil subgrade. *Engineering Science and Technology, an International Journal*, 23(5), 1214-1222. <https://doi.org/10.1016/j.jestch.2019.12.006>
- Valipour, M., Shourijeh, P. T., & Mohammadinia, A. (2021). Application of recycled tire polymer fibers and glass fibers for clay reinforcement. *Transportation Geotechnics*, 27, Article 100474. <https://doi.org/10.1016/j.trgeo.2020.100474>
- Wahab, N. A., Rashid, A. S. A., Roshan, M. J., Rizal, N. H. A., Yunus, N. Z. M., Hezmi, M. A., & Tadza, M. Y. M. (2021). Effects of cement on the compaction properties of lateritic soil. In *IOP Conference Series: Materials Science and Engineering*, 1153(1), Article 012015. IOP Publishing. <https://doi.org/10.1088/1757-899X/1153/1/012015>
- Wahab, N. A., Roshan, M. J., Rashid, A. S. A., Hezmi, M. A., Jusoh, S. N., Norsyahariati, N. D. N., & Tamassoki, S. (2021). Strength and durability of cement-treated lateritic soil. *Sustainability*, 13(11), Article 6430. <https://doi.org/10.3390/su13116430>
- Wang, Y., Guo, P., Li, X., Lin, H., Liu, Y., & Yuan, H. (2019). Behavior of fiber-reinforced and lime-stabilized clayey soil in triaxial tests. *Applied Sciences*, 9(5), 900. <https://doi.org/10.3390/app9050900>
- Yi, Y., Jiang, Y., Tian, T., Fan, J., Deng, C., & Xue, J. (2022). Mechanical-strength-growth law and predictive model for ultra-large size cement-stabilized macadam based on the vertical vibration compaction method. *Construction and Building Materials*, 324, Article 126691. <https://doi.org/10.1016/J.CONBUILDMAT.2022.126691>
- Yldz, M., & Soğanc, A. S. (2012). Effect of freezing and thawing on strength and permeability of lime-stabilized clays. *Scientia Iranica*, 19(4), 1013-1017. <https://doi.org/10.1016/J.SCIENT.2012.06.003>
- Yoobanpot, N., Jamsawang, P., Poorahong, H., Jongpradist, P., & Likitlersuang, S. (2020). Multiscale laboratory investigation of the mechanical and microstructural properties of dredged sediments stabilized with cement and fly ash. *Engineering Geology*, 267, Article 105491. <https://doi.org/10.1016/j.enggeo.2020.105491>
- Zare, P., Narani, S. S., Abbaspour, M., Fahimifar, A., Hosseini, S. M. M. M., & Zare, P. (2020). Experimental investigation of non-stabilized and cement-stabilized rammed earth reinforcement by Waste Tire Textile Fibers (WTFs). *Construction and Building Materials*, 260, Article 120432. <https://doi.org/10.1016/j.conbuildmat.2020.120432>
- Zhao, Y., Yang, Y., Ling, X., Gong, W., Li, G., & Su, L. (2021). Dynamic behavior of natural sand soils and fiber reinforced soils in heavy-haul railway embankment under multistage cyclic loading. *Transportation Geotechnics*, 28, Article 100507. <https://doi.org/10.1016/J.TRGEO.2020.100507>





## Technology Adoption for STEM Education in Higher Education: Students' Experience from Selected Sub-Saharan African Countries

Jumoke Iyabode Oladele\*, Musa Adekunle Ayanwale and Mdutshekela Ndlovu

*Department of Science and Technology Education, Faculty of Education, University of Johannesburg, Auckland Park, 2006, Gauteng, South Africa*

### ABSTRACT

Challenges of a lack of formal technology-embedded teacher training, collaborative learning models, adequate technology know-how, and internet access are barriers to adopting technological-enabled teaching and learning STEM subjects in the African context. This study examined technology adoption for STEM in higher education while evaluating students' experiences with evidence and implications for less developed countries. The survey research design was adopted for the study. The study population was students in higher learning institutions in selected countries in the sub-Saharan African region using a multi-stage sampling procedure consisting of convenience and purposive sampling techniques. A self-developed questionnaire titled Technology Adoption for Teaching and Learning Questionnaire "TATLQ" premised on the unified theory of acceptance and use of technology (UTAUT) model was used for data collection. The instrument had an overall reliability coefficient of 0.96. The collated data were analysed using descriptive of the median and a network chart to answer the research questions. In contrast, the inferential statistics of t-test and Analysis of Variance statistics were used to test the hypothesis generated for the study and implemented in the psych package of R programming language version 4.0.2 software. Findings revealed that students had a positive experience

with online teaching and learning and concluded that technology adoption for STEM education online teaching and learning is feasible in sub-Sahara Africa, with the need for improvements in internet access and technical support on the basis for which recommendations were made.

*Keywords:* Higher education, online teaching and learning, STEM education, students' experiences, technology adoption

### ARTICLE INFO

#### *Article history:*

Received: 23 February 2022

Accepted: 07 June 2022

Published: 20 October 2022

DOI: <https://doi.org/10.47836/pjst.31.1.15>

#### *E-mail addresses:*

[jumokeo@uj.ac.za](mailto:jumokeo@uj.ac.za) (Jumoke Iyabode Oladele)

[ayanwalea@uj.ac.za](mailto:ayanwalea@uj.ac.za) (Musa Adekunle Ayanwale)

[mndlovu@uj.ac.za](mailto:mndlovu@uj.ac.za) (Mdutshekela Ndlovu)

\*Corresponding author

## INTRODUCTION

The world is changing exponentially with technological innovations. These changes require training to acquire a new skill set for problem-solving while grasping the available print and digital information. While these changes have become inevitable, Kärkkäinen and Vincent-Lancrin (2013) highlighted the lack of formal teacher training, peer learning and adequate professional development as barriers to adopting technological-centred teaching models and resources. Furthermore, technological difficulties, time management issues, and a lack of readiness for online learning are weaknesses of technology-integrated teaching aggravated by digital inequalities among different groups and a lack of personal support (Oladele et al., 2021; Lee et al., 2021). These challenges are not without implications for Science, Technology, Engineering, and Mathematics (STEM) education (Vahidy, 2019). STEM education is a teaching approach that integrates all four disciplines into a single, multidisciplinary, cross-disciplinary, and transdisciplinary program that offers real-world instruction using appropriate teaching methods (Dalton, 2019; Hasanah, 2020). Understanding these four disciplines is considered a precondition or enabling factor for 21st-century economic development, international competitiveness and job creation which necessitates an improvement in the quality of education delivered as STEM (Ismail, 2018; Schwab, 2016). LaForce et al. (2016) employed a “bottom-up” approach for deriving a theoretical framework of eight elements that represent the common goals and strategies employed for inclusive STEM in schools which were personalisation of Learning; Problem-Based Learning; Rigorous Learning; Career, Technology, and Life Skills; School Community and Belonging; External Community; Staff Foundations; and External Factors. Technology is fast becoming relevant for teacher training in developing countries. Also employing the bottom-top approach, Ayanwale and Oladele (2021) examined online learning indicators and learners’ satisfaction during the COVID-19 pandemic revealing a passive to interactive shift in instructional activities through student-teacher collaboration. This utility-centred approach creates an enabling learning environment for students and instructors to co-create and consolidate knowledge while leveraging technologies for STEM education. This is the gap this study aims to fill (Ismail, 2018).

## CONCEPTUALISING STEM EDUCATION

STEM education means a variety of perspectives considering its widespread among stakeholders such as politically and societally, personally, and interactively. Politically and societally, constituting a primary motivation for educational policy, leading to heavy investments in the field in curriculum developments and research policy inherently concerned with axiological objectives (Chesky & Wolfmeyer, 2015). Personal conception deals with the individual opinion of people on STEM, with no wrong or the right type of individual opinions. This perspective of STEM education as a unit is driven by integrating

Science, Technology, Engineering and Mathematics disciplines to solve emerging challenges. Kubat and Guray (2018) further stressed the need for STEM education as a discipline rather than teaching these four disciplines independently. STEM education as the integration of disciplines can be seen in reform initiatives needed for producing a skilled workforce (Chesky & Wolfmeyer, 2015; Siekmann, 2016). For this study, STEM is conceptualised as a discipline. This stance is premised on a review by Hasanah (2020), revealing that most authors conceptualise STEM as an integrated discipline and a fundamental definition of STEM education.

Thus, acceptance of the STEM element in the process is crucial. The unified theory of acceptance and use of technology (UTAUT) was adopted in this study (Venkatesh et al., 2003). This theory is a full-grown and intensive model to examine users' ability to accept technology and their experience in adopting new technologies. The UTAUT theory has underlying constructs such as performance and effort expectancy, social impact, ease of deployment and behavioural objectives. Venkatesh et al. (2003) described performance expectancy as the benefits of technology in terms of performance enhancement in line with user expectations, while effort expectancy relates to ease of use. Social impact speaks to how users engage technology and its continuity, depending on the available organisational and technical infrastructure, and behavioural objectives are seen as users' intent and decisions on the use of technology. In this study, among these constructs outlined by Venkatesh et al. (2003), performance expectancy described the significance of this study by establishing the students' experience with online teaching and learning. Consequently, items developed for this study were tailored toward this direction.

## LITERATURE REVIEW

STEM education equips learners with problem-solving skills and helps them become knowledge creators, composed, analytical thinkers, and technologically literate (Stohlmann et al., 2011). STEM education drives skills such as tenacity, collaboration, and knowledge application to careers requiring versatility as determinants of success and economic competitiveness in the global market (Boe et al., 2011; Bailey et al., 2015; Tanenbaum, 2016). In addition, STEM education helps to adequately equip students with attributes for the future, such as problem solvers, innovators, inventors, self-confident, logical thinkers, and technology literacy (Hasanah, 2020). According to Dogan and Robin (2015), advances in computer and network technologies aid cooperative learning among students while providing constructivist feedback, enhancing constructivist learning models in education.

Furthermore, the integration and effective use of technology is vital to enhancing learning STEM subjects which have completely changed the way teachers and students communicate and collaborate using various online interaction platforms, enabling students to experience phenomena they normally would not be able to experience first-hand through

simulations, teachers can involve students in the process as well as give them a wider understanding of a particular topic using augmented and virtual reality. Also, gaming for learning puts the students in control, offers incremental difficulty levels, provides instant and ongoing feedback, and creates community by allowing for multiplayer participation (Kärkkäinen & Vincent-Lancrin, 2013; Vahidy, 2019). This process necessitates a strong STEM education from the grassroots, recognised as a key driver of opportunities. The literature on gender disparities within STEM education reveals that in sub-Saharan Africa, females have less access to STEM education at the higher education level, with statistics revealing less than average female participation in STEM-related studies at the tertiary level of education (Ismail, 2018). Gender has continued to be one of the factors in the adoption and use of e-learning systems with various applications (Abahussain, 2017). Eliminating gender imbalance in technical education and training is one of the Sustainable Development Goal 4 targets, which further points to the importance of gender in research and largely contributes toward strategic development at the country level (UNESCO et al., 2015; Oladele et al., 2021). The response to issues relating to gender gaps and mainstreaming in STEM education are geared towards addressing inequalities (IOS, 2017).

Amid these efforts comes the COVID-19 pandemic with the potential of further straining the meagre opportunities for STEM education. In addition, digital literacy has become more prominent concerning 4IR since 2016. The rationale for investment in STEM education relates mainly to acquiring new skill sets required for the 21<sup>st</sup> Century job market with increasing emphasis on technology skills and gender equity in Africa (Ismail, 2018). Therefore, STEM education is a priority for medium to low-income countries. Stemming from this rationale, some benefits of STEM education are improved teacher professional development, enhanced meeting of 21<sup>st</sup> Century workplace demands, and sustainable work. Similarly, the mastery of STEM is correlated to secondary school enrolment and retention, innovation leading to economic prosperity, national peace and international competitiveness (Breiner et al., 2012; Chesky & Wolfmeyer, 2015; Hasanah, 2020).

The COVID-19 pandemic has necessitated electronic instruction (e-learning) to adhere to the COVID-19 safety protocols while leading to the rapid growth in online education (Widodo et al., 2020; Ramírez-Hurtado et al., 2021). This learning model allows students to learn virtually while leveraging online teaching and learning. Electronic instruction leverages the internet. E-learning is the umbrella term for learning across distances, not in a traditional classroom (Kessler, 2018). Forson and Vuopala (2019) described four generations of online teaching and learning, starting from the era of correspondence courses to that of the internet-driven solutions adopted by many universities in developed countries. For Barr and Miller (2013), online teaching and learning focus on a wide range of technological-based platforms for delivering the curriculum. Learning management systems (LMS) such as Blackboard, Moodle, MS Teams, Zoom, Google Meet, Google

Classroom, and Sakai, among others, encourages knowledge diversification and self-driven learning engagements allowing for a flexible implementation framework (Sabharwal et al., 2018; Kessler, 2018; Škobo, 2020; Alturki & Aldraiweesh, 2021). While these are some of the benefits of technology in teaching STEM subjects, the success of instruction driven by digital resources is premised on effectively adapting these resources to attain learning goals (Drijvers et al., 2019). Also, instructors must either create their “virtual classrooms” from scratch or leverage existing LMS software with low-cost alternatives and open sources.

While the COVID-19 pandemic has had its downside for higher education, the digital revolution has enabled instructional delivery modes for inclusiveness while technological affordances beg for answers (Ndlovu & Mostert, 2018; Forson & Vuopala, 2019). Also, how these technologies can aid teaching is germane in mathematics education (Drijvers et al., 2019). Teaching in a web environment comes with tons of requirements, like students’ and teachers’ readiness (preparedness) (Qazaq, 2012; Fakinlede et al., 2014; Rasouli et al., 2016; Ndlovu & Meyer, 2019). Instructors must also have a positive attitude, while the institution must provide supporting resources. As a sequel to the present, education instructors may need difficulties handling online teaching and learning; they will experience discomfort when handling technology-embedded classrooms and related issues (Palloff & Pratt, 2013). Technology users should also be interested in using technology as a learning tool and teaching platform for strengthening the education system globally (Forson & Vuopala, 2019; Ndlovu & Meyer, 2019; UNESCO, 2021). The availability and use of technology in teaching practices are essential in the COVID-19 era, while it remains essential to research students’ preparedness for online teaching and learning (Oladele et al., 2021; Kamaruzaman et al., 2021). These constitute an element to be considered if the goals of STEM education are achieved through online teaching.

The COVID-19 pandemic necessitated an unplanned transition to online teaching and learning. STEM education geared towards acquiring required skills and mindsets for lifelong learning while adopting learning technologies must be adequately evaluated for success. Many countries are committed to improving its quality, considering the importance of STEM for 21<sup>st</sup> Century economies’ development (Hasanah, 2020). Related STEM education studies have been carried out concerning skills needed by teachers at all levels to be intimately familiar with the interrelationships within the STEM disciplines (Breiner et al., 2012); Integrative STEM education is seen as a viable endeavour (White, 2014); the potential of LMS for blended learning with a focus on Moodle (Ndlovu & Mostert, 2018); lecturers’ preparedness for transition to teaching online courses (Lichoro, 2015); readiness of students in applying e-learning (Fakinlede et al., 2014; Rasouli et al., 2016) and teacher readiness on technology integration for teaching Mathematics (Qazaq, 2012; Ndlovu & Meyer, 2019) among others. The current COVID-19 pandemic, which has resulted in institutions taking to online teaching and learning, urges students’ preparation

and experience with STEM instruction to be investigated. This study aims at mirroring students' experiences with online learning to aid improvements where needed. Specifically, the objectives of this study were to:

1. examine students' preparedness for online teaching and learning;
2. examine students' experience with online teaching and learning;
3. assess the quality of lectures deployed via the online platform;
4. find out new skills acquired by students exposed to online teaching and learning; and
5. ascertain if there are significant differences in students' experiences based on selected variables.

The above-stated objectives were further translated to research questions and hypothesis below:

1. What is the level of students' preparedness for online teaching and learning?
2. What are the students' experiences with online teaching and learning?
3. What is the quality of lectures deployed via online platforms?
4. What are the new skills acquired when exposed to online teaching and learning?
5. Is there any difference in students' experience with online teaching for STEM education across gender, age, disciplines and level?

**H<sub>01</sub>:** There is no significant difference in students' experience with online teaching for STEM education across gender, age, disciplines and level of study (graduate/postgraduate).

## METHODOLOGY

The non-experimental design of the survey research type was adopted for the study. The study population was students in higher learning institutions in the sub-Saharan African region, while the target population experienced online teaching and learning due to the pandemic. A multi-stage sampling procedure consisted of convenience sampling and purposive sampling techniques. Four universities were selected using the convenience sampling technique: one each from Nigeria (West Africa), South Africa, Uganda (East) and Algeria (North Africa) was premised on access, while students from the selected universities were sampled purposively to include STEM education learners. A self-developed questionnaire titled Technology Adoption for Teaching and Learning Questionnaire "TATLQ" was used for data collection. The instrument was developed with the UTAUT model suitable for examining users' ability to accept and adopt new technologies and their experience in the adoption process (Venkatesh et al., 2003). Hinged on this model, the instrument consisted of two sections.

Section one presented brief background information on the study. In contrast, section two consisted of seven loose items with corresponding response formats and three themed items on Student preparedness for online teaching and learning with 14 items, Student



experience with online teaching and learning with 21 items and rating the quality of lecture with 11 items on a four Likert response scale of Strongly Agree, Agree, Disagree and Strongly Disagree. The instrument was face and content validated by educational measurement experts. Its reliability was established using the Ordinal Alpha method for determining the instrument's internal consistency applied to the themed items in Sections B. Ordinal reliability coefficients of 0.95, 0.95 and 0.99 were obtained with an overall reliability coefficient of 0.96. The instrument was deployed via Google forms to students in the selected Universities to ensure adherence to the social distancing measure for curbing the spread of the Corona Virus. The collated data were analysed using descriptive of the median and a network chart to answer the research questions and inferential statistics of t-test and Analysis of Variance to test the hypothesis generated for the study, which was implemented in the psych package of R programming language version 4.0.2 software.

## RESULTS

### Data Handling

Responses to the questionnaire were used to answer the questions/hypotheses posed for the study. Data integrity was ensured by handling the missingness and outliers evident in the dataset. Also, a preliminary analysis was conducted to check for assumptions (such as normality, heterogeneity of variance, and sample size adequacy) that underlie the statistical tools employed in this study. The results from Shapiro-Wilk's test ( $W = 0.98$ ,  $p = 0.19$ ) revealed that the dataset followed a normal distribution, thereby not violating the normality assumption. Levene test ( $F = 0.32$ ,  $df = 1,193$ ,  $p = 0.57$ ) was used to assess variance heterogeneity at a significance level of 0.05; it was remarked that equality of variance existed among the subjects used for this study.

### Answering Research Questions

The median statistics describe students' preparedness for online teaching and learning to answer research question one. It provides more information about the sample than the mean, which many researchers in the literature predominantly reported. Also, the measurement scale is ordinal, whereby there is no standard scale on which the difference in each rating is measured. There is a clear order to these categories, but we cannot say that the difference between "strongly agree" and "agree" is the same as that between "disagree" and "strongly disagree." For easy interpretation of the question, a median value less than 2.5 signifies that half of the sample rated the item below 2.5, indicating a 'low level' of participants' preparedness for online teaching. Also, a median value greater than 2.5 signifies that half of the sample rated the item above 2.5, indicating a 'high level' of participants' preparedness for online teaching. Table 1 presents the result.

Table 1  
*Level of students' preparedness for online and teaching*

Statement	Median	Remarks
I have a personal computer	4	High
I have access to the internet	4	High
I have access to an uninterrupted power supply	2	Low
I am experienced with using google collaboration tools	3	High
I have experience participating in zoom meetings before the class starts for the contact session	3	High
I have a functional email address	4	High
I am conversant in using email for communication	4	High
I am used to surfing the internet for required contents	4	High
I have other devices/gadgets for effective participation in online teaching and learning aside from my computer	3	High
I have dedicated enough time to participate in online teaching and learning fully	3	High
I have prepared the cost implication(s) on the data bundle for seamless participation in online teaching and learning	3	High
I have experience in using the chatbot and other facilities of different platforms	3	High
I have used other platforms aside from zoom for meetings before the commencement of class for the contact session	3	High
Learning online sounds like a good idea	3	High

Table 1 presented median values for each item on the scale. It was revealed that most sampled subjects showed high enthusiasm towards items measuring their preparedness for online learning. However, access to an uninterrupted power supply was low, contributing to the participant's level of preparedness. Overall, students were adequately ready and prepared for online learning, especially with the upsurge of COVID-19, which necessitated the teaching-learning process to be migrated online.

Also, research question two was answered using descriptive statistics of the median, and classification of positive and negative was done regarding research question one. The result is presented in Table 2.

Table 2 depicts the values of median descriptive statistics for each item describing students' experience with online teaching and learning. The result showed that participants displayed their experience on each item, measuring the scale above 2.5. They had divergent views on a few items (browsing data and technical availability support during online classes), with a median value below the cut-off of 2.5. The result implies that students'

Table 2

*Level of students' experience in online teaching and learning*

Statement	Median	Remarks
I am conversant with WhatsApp as a mobile technology	4	Positive
I am skilled in using google forms for taking assessments	3	Positive
I am skilled in using google docs for submitting assessments	3	Positive
The school provided the data I used to join classes	2	Negative
I financed the data used to join online classes	4	Positive
I am skilled in using functions from different platforms while in class	3	Positive
I could resolve my internet issues while connecting to online classes	3	Positive
I had technical support during online classes	2	Negative
I had access to clear and legible presentations during my classes	3	Positive
I had ample time to jot down points during online classes	3	Positive
I had the opportunity to ask questions during online classes	3	Positive
Access to lecture playbacks aided the online learning process	3	Positive
The use of technology hampered my learning	3	Positive
Lecture information was effectively disseminated during the class	3	Positive
I could surf the internet for content to support learning	3	Positive
I took online assessments with ease	3	Positive
I got timely feedback after taking my online assessment	3	Positive
I had direct access to the lecturer before and after classes	3	Positive
I had ease of access to course materials before the class	3	Positive
I had educative and informative interactions and discussions with other students	3	Positive
It improves my self-discipline to work independently	3	Positive

experience with online teaching and learning was largely positive. The positive students' experiences being considered, online teaching and learning generally serve as a responsive model to the emergent needs of the student.

Furthermore, research question three on the quality of lecture deployed was assessed using descriptive statistics to depict high or low quality based on the median benchmark of value less than 2.5 and greater than 2.5 on each item. Table 3 presents the result.

Table 3  
*Quality of lecture deployed through online teaching and learning*

Statement	Median	Remarks
Timely commencement of the lecture	3	High
Access to lecture slides	3	High
Clear presentation of lecture content	3	High
Good communication skills	3	High
Adequate course content coverage	3	High
The lecture was revised before taking the final examinations	3	High
Availability of learning resources to support the class	3	High
Engaging lecture presentations (With suitable images and backgrounds)	3	High
Room for feedbacks	3	High
Contents are disseminated in simple and clear terms	3	High
Support for accomplishing class tasks	3	High
Courteous interaction during online classes	3	High

Table 3 remarked that participants from STEM disciplines rated each item above the cut-off of 2.5. This finding implies that students were satisfied with the quality of online teaching and learning content. Also, their responses might be because lecturers were digitally competent at adapting to their wishes and needs regarding teaching; contents are synchronously deployed and enhance their collaboration, especially during a Covid-19 pandemic.

A network chart of skills acquired during online teaching for STEM education was mapped to answer research question four, as shown in Figure 1.

Figure 1 depicts diverse skills acquired during online teaching for STEM education, some of which were typing, time management, problem-solving, PowerPoint presentation, self-development, online research, self-dependence, note-taking, time management, critical thinking, commitment, using LMS, commitment, animation and editing, internet proficiency and safety, cognitive reasoning, self-discipline, graphic design, listening, and collaboration, among others. This finding reveals that students acquired various skills to cope with online teaching and learning.

### Hypotheses Testing

The research hypotheses posed for the study were tested at a significance level of 0.05 after establishing the assumptions of statistical tools, such as independent sample t-test and one-way analysis of variance (ANOVA). Table 4 presents the sample t-test on students' experience with online teaching for STEM education based on gender.

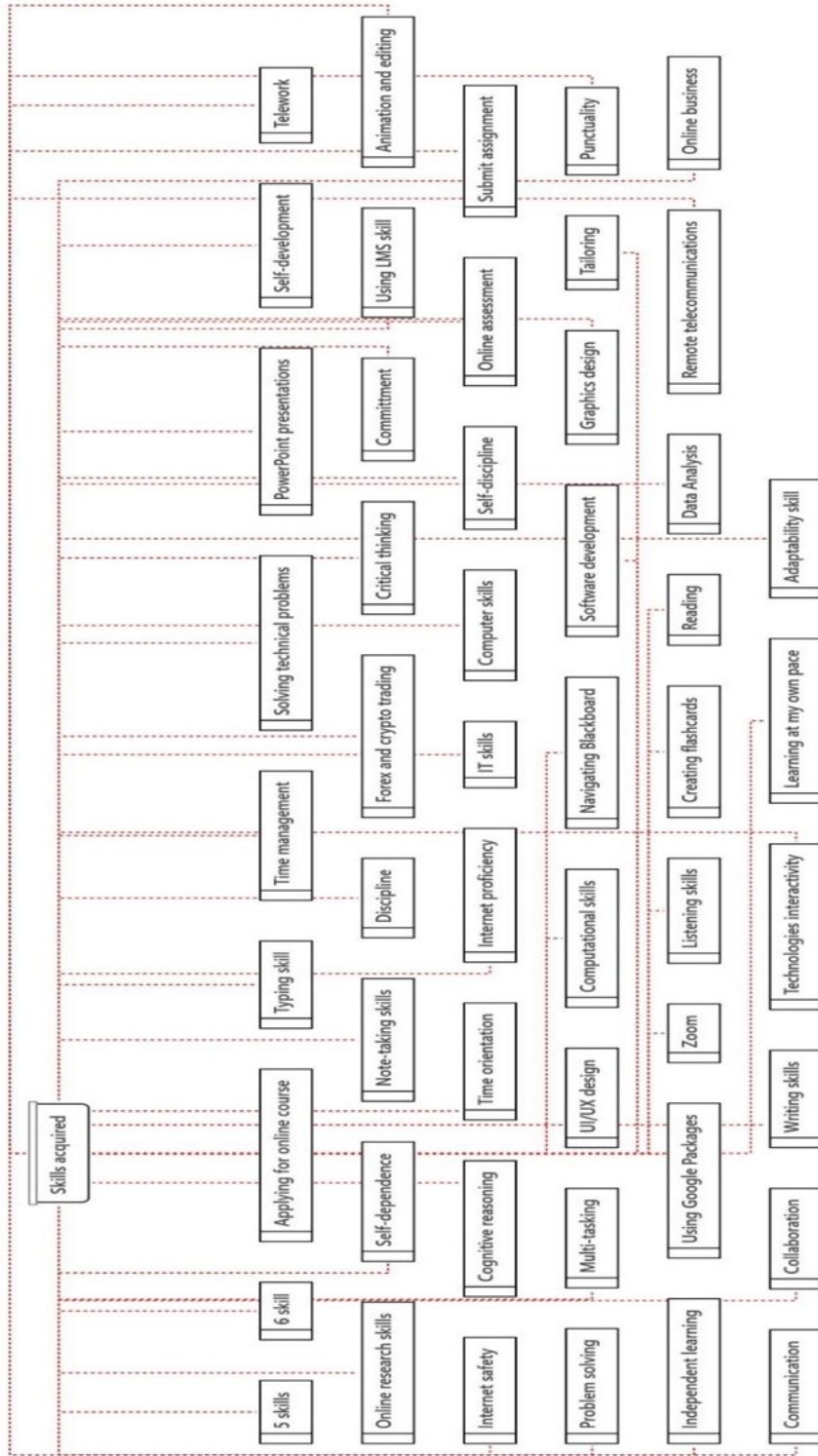


Figure 1. Network of skills acquired during online teaching for STEM education

Table 4

*T-test summary of experience with online teaching for STEM education based on gender*

Gender	Mean	SD	Statistic	df	P
Male	65.8	9.57	1.98	193	0.04
Female	62.9	10.5			

Table 4 showed that male students across the STEM education had higher mean score of (M = 65.8, SD = 9.57) compare with their female counterparts with (M = 62.9, SD = 10.5). This finding shows that male students had a better experience with online teaching and learning than female students. Also, an independent sample t-test was conducted to assess the observed difference in the students’ experience with online teaching; the result yielded a statistically significant difference between the male and female experience with (t = 1.98, df = 193, p = 0.04). Thus, the null hypothesis was rejected. This decision implies that the acquired skills and experience during online teaching differ between male and female students. This outcome might allude to the fact that male students develop more interest in technology-driven teaching than female colleagues.

Also, the hypothesis stated no significant difference in the students’ experience with online teaching for STEM education concerning age group was conducted using one-way ANOVA. The result is presented in Table 5.

Table 5

*ANOVA summary of experience with online teaching for STEM education based on age group*

Age group	Mean	SD	F	df1	df2	p
18-25	65.5	10.05	1.83	3	191	0.14
26-32	61.60	8.94				
33-39	62.60	11.07				
40 and above	62.00	14.28				

Table 5 depicts that age group 18–25 across the STEM education had higher mean score of (M = 65.5, SD = 10.05), followed by 33–39 age group with (M = 62.6, SD = 11.07), next to above 40 with (M = 62, SD = 14.28) and age group 26–32 with (M = 61.6, SD = 8.94) respectively. More so, one-way ANOVA was used to establish whether there was a difference in their mean scores or not. The result remarked a non-statistical significant value with (F<sub>3,191</sub>) = 1.83, p = 0.14). Consequently, the null hypothesis was not rejected. This finding implies that the students’ age groups have nothing to contribute to acquiring skills for online teaching for STEM education.

Also, the hypothesis stated that no significant difference in the students' experience with online teaching for STEM education in disciplines was conducted using one-way ANOVA. The result is presented in Table 6.

Table 6

*ANOVA summary of experience with online teaching for STEM education based on disciplines*

Discipline	Mean	SD	F	df1	df2	p
Engineering	67.80	9.34	0.99	3	191	0.40
Science	63.60	10.75				
Technology	64.00	9.55				
Mathematics	66.90	11.25				

Table 6 remarked that engineering as a discipline had higher mean score of ( $M = 67.80$ ,  $SD = 9.34$ ), followed by Mathematics with ( $M = 66.90$ ,  $SD = 11.25$ ), followed by Technology with ( $M = 64$ ,  $SD = 9.55$ ) and Science with ( $M = 63.60$ ,  $SD = 10.75$ ) respectively. Meanwhile, one-way ANOVA was used to establish a difference in their mean scores. The result showed that the mean difference was not statistically significant ( $F_{3,191} = 0.99$ ,  $p = 0.40$ ). Therefore, the null hypothesis was not rejected. This decision implies that irrespective of the student's discipline has no contribution to experience with online teaching for STEM education.

Furthermore, the hypothesis that there is no significant difference in the students' experience with online teaching for STEM education at the study level was conducted using one-way ANOVA. The result is presented in Table 7.

Table 7

*ANOVA summary of experience with online teaching for STEM education based on the study level*

Study level	Mean	SD	F	df1	df2	p
Graduate	64.5	10.61	0.95	2	192	0.39
Honours	62.2	9.66				
Postgraduate	65.5	8.98				

Table 7 remarked that postgraduate level had higher mean score of ( $M = 65.5$ ,  $SD = 8.98$ ), followed by graduate with ( $M = 64.5$ ,  $SD = 10.61$ ), and honours with ( $M = 62.2$ ,  $SD = 9.66$ ). However, one-way ANOVA was conducted to compare mean differences. The result showed that the mean difference was not statistically significant with ( $F_{2,192} = 0.95$ ,  $p = 0.39$ ). Therefore, the null hypothesis was not rejected. This finding implies that the students' study level has no contribution to experience with online teaching for STEM education.



## DISCUSSION

This study aims at mirroring students' experiences with online learning to aid improvements where needed. Considering that COVID-19 was an emergency where online learning was adopted with little or no preparation, the study surveyed students' level of preparedness for online learning as a precursor to their experiences. The study revealed that students were adequately prepared for teaching online, especially with the upsurge of COVID-19, which necessitated the teaching-learning process to be migrated online. This finding may be because the target population of this study were students enrolled in STEM subjects who are conversant with personalisation of learning; problem-based learning; rigorous learning; career, technology, and life skills; school community and belonging; external community; staff foundations; and external factors being the elements of inclusive STEM education (LaForce et al., 2016). This finding aligns with Forson and Vuopala (2019) and Kamaruzaman et al. (2021), revealing that students had a positive attitude towards online learning. Ndlovu and Meyer (2019) stressed that preparedness is a major requirement for meaningful learning in an online environment. Parkes et al. (2015) gave a divergent view that while students were perceived as technology-ready, there is a need for improvement with synthesising ideas, implementing learning strategies, intellectual rationalisations when necessary and collaboration. However, the finding of this study concerning preparedness can be regarded as superseding that of Parkes et al. (2015), considering that it was premised on real students' experiences.

This study also reported a positive experience with online teaching and learning. In essence, online teaching and learning education generally serves as a responsive model to the emergent needs of the student. Learning is now diversified and deployed innovatively through internships and volunteer activities. The positive experiences recorded might come from personal development and exposure to various online teaching platforms such as zoom, Ms teams, blackboard, smart Board, google meet, LMS canvas, and google classroom. Worthy of note are the areas of browsing data and technical support needs during online classes where students' experiences were negative. This finding aligns with Vahidy (2019) and Oladele et al. (2021) that the high cost of the internet and a dearth of technical assistance while interacting with online learning platforms have been a major challenge in sub-Saharan Africa. This submission is strengthened by a report on internet penetration in South Africa stood at 64.0% (Kemp, 2021).

Similarly, Adegoke (2017) reported that internet delivery is slower, more unreliable, and expensive and stressed the need to build the internet sector considered critical for development and improved efficiency and productivity gains in the educational sector in Africa. Access to browsing data and related technical support can be the gateway to online learning. These submissions magnify the urgent need for solutions to sustain students' high experience with online teaching and learning fast becoming the new normal.

Furthermore, the findings on students' rating of the quality of lectures deployed via the online mode revealed that they gave lectures a high rating. Their responses might be because lecturers were digitally competent at adapting to their wishes and needs regarding teaching; contents are synchronously deployed and enhance their collaboration, especially during a COVID-19 pandemic. This finding correlates with a study by Junus et al. (2021) that lecturers have strong baseline technical skills to use e-learning platforms for online courses, with quick adaptivity capabilities to using a Learning Management System (LMS). Lecturers are an important factor in teaching as learning is described as a social activity strengthened when an instructor carefully facilitates instruction. Considering the need for carefully designed content to suit students' needs, an effective instructor (in this case, the lecturer) is needed to enhance corrective feedback and encouragement while motivating students to be committed to a given task(s) to achieve the learning objectives. Therefore, a symbiotic relationship between students and lecturers is required to learn the online teaching-learning process (Young, 2006).

Furthermore, the findings from the study revealed that students developed an array of skills from online teaching and learning believed to help enhance the student's academic excellence. While this finding resonates with Forson and Vuopala (2019), preparedness, a major requirement for online learning, is influenced by appropriate strategies for independent learning, such as self-regulation, direction, and motivation (Fakinlede et al., 2014). Conducting online teaching on various courses makes learning more flexible, and they can work at their own pace, promoting better learning for the students. Students cultivate time management, and schedules can be more accurately planned, and one activity will not affect the execution of another. Their online research skills were sharpened as students had more time to get information on topics of interest by reading extensively on the same issue in different parts of the world. More knowledge of the usage of teleconferencing software was also improved during online teaching.

Some soft skills are also improved during the period, such as communication skills, including writing, reading, and speaking skills. Also, problem-solving skills were improved in some students. Some also improve discipline and self-dependency. Of course, these will aid better achievement in their academic endeavour in STEM. This finding revealed that the elements of inclusive STEM education derived by LaForce et al. (2016) were much present in the crop of students surveyed in this study. This finding aligned with Forson and Vuopala's (2019) study, which revealed that students possessed skills relevant to the world of work and life-long learning. Also, information technology skills regarded as necessary to success were improved as some learned data analysis, some went into software development, and some went into building an application. This finding aligns with The Glossary of Education (2014), which stressed that new technologies have diversified learning in a dependent, interdependent and self-paced leveraging of technology. After

their studies, these skills will help the students apply knowledge gained in work life. This benefit is particularly important for the 21<sup>st</sup> Century, which is fast, self-paced, and apt for STEM disciplines to solve real-world problems (Chesky & Wolfmeyer, 2015; Ismail, 2018; Alturki & Aldraiweesh, 2021).

All tested hypotheses were accepted for students' age groups, discipline, and study level except for gender, which was rejected. The non-significance concerning students' age groups, discipline, and study level may result from an array of free technology platforms readily accessible via the internet during the COVID-19 pandemic, which coincided with the Fourth Industrial Revolution (4IR). This assertion is strengthened by Aikman (2017), who submitted that the 4IR waves of transformation systems are empowering and carefully designed solutions to enrich human dignity. Therefore, there is no gain-saying that 4IR is an improvement that engages smart technologies that blur the virtual, visible, and botanical spaces in time (Marwala, 2020). On the other hand, the significance with respect to gender implies that the acquired skills and experience during online teaching differ between male and female students. This finding is congruent with Oladele et al. (2021) that a significant difference exists along the gender divide. This finding reveals a persistent inequity in access, participation, and success in STEM subjects, threatening any nation's ability to a technology-driven economy and close the poverty gaps through education (UNESCO et al., 2015; Tanenbaum, 2016).

## CONCLUSION AND RECOMMENDATIONS

This study concluded that online teaching and learning is a plausible direction for STEM education in sub-Saharan Africa. At the same time, internet access and technical support need to be enhanced to improve students' experiences. Some recommendations made based on this conclusion were that the Government should provide enabling business environment for telecommunication companies to subsidise the data cost, data support to higher institutions should be a priority to all societal stakeholders ranging from governmental and non-governmental organisations and civil societies, investments should be increased in the training of technical experts to meet this area of need, and relevant stakeholders should hold the reins of promoting gender equity in technology development, innovation, and problem-solving.

Considering that this study was focused on Technology Adoption for STEM Education in Higher Education while surveying the skills acquired during the COVID-19 pandemic, the quality of these skills concerning producing STEM graduates is essential to the world of work in the 21<sup>st</sup> Century premised on the fourth Industrial way. As such, assessing the acquired skills would constitute a direction for further research.

## ACKNOWLEDGEMENT

The authors would like to thank the universities that approved the survey. We are also grateful to all the students who found the time to fill out this survey.

## REFERENCES

- Abahussain, M. M. (2017). *Examining gender differences toward the adoption of online learning and predicting the readiness of faculty members in a Middle-Eastern recently established public university* (Doctoral dissertation). Northern Illinois University, USA. [https://commons.lib.niu.edu/bitstream/handle/10843/20740/Abahussain\\_niu\\_0162D\\_12948.pdf?sequence=1&isAllowed=y](https://commons.lib.niu.edu/bitstream/handle/10843/20740/Abahussain_niu_0162D_12948.pdf?sequence=1&isAllowed=y)
- Adegoke, Y. (2017). *Africa's internet economy needs more data servers on the continent*. Quartz Africa. <https://qz.com/africa/1138104/africas-internet-economy-needs-more-content-data-servers-on-the-continent/>
- Aikman, D. (2017). *The fourth industrial revolution*. World Economic Forum. [https://www.jmfrii.gr.jp/content/files/Open/2017/20171130\\_Isynpo/AM1%20Mr.%20David%20Aikman\\_presentation.pdf](https://www.jmfrii.gr.jp/content/files/Open/2017/20171130_Isynpo/AM1%20Mr.%20David%20Aikman_presentation.pdf)
- Alturki, U., & Aldraiweesh, A. (2021). Application of learning management system (LMS) during the COVID-19 Pandemic: A sustainable acceptance model of the expansion technology approach. *Sustainability*, 13(19), 10991. <https://www.mdpi.com/2071-1050/13/19/10991/pdf>
- Ayanwale, M. A., & Oladele, J. I. (2021). Path modeling of online learning indicators and learners' satisfaction during COVID-19 pandemic. *International Journal of Innovation, Creativity and Change*, 15(10), 521-541. [https://www.ijicc.net/images/Vol\\_15/Iss\\_10/151038\\_Ayanwale\\_2021\\_E1\\_R.pdf](https://www.ijicc.net/images/Vol_15/Iss_10/151038_Ayanwale_2021_E1_R.pdf)
- Bailey, A., Kaufman, E., & Subotić, S. (2015). *Education technology and the 21st-century skills gap*. Boston Consulting Group. <https://www.bcg.com/publications/2015/public-sector-education-technology-21st-century-skill-gap>
- Barr, B. A., & Miller, S. F. (2013). *Higher education: The online teaching and learning experience*. Online Teaching and Learning.
- Boe, M. V., Henriksen, E. K., Lyons, T., & Schreiner, C. (2011). Participation in science and technology: Young people's achievement-related choices in late-modern societies. *Studies in Science Education*, 47(1), 37-72. <https://doi.org/10.1080/03057267.2011.549621>
- Breiner, J. M., Harkness, S. S., Johnson, C. C., & Koehler, C. M. (2012). What is STEM? A discussion about conceptions of STEM in education and partnerships. *School Science and Mathematics*, 112(1), 3-11.
- Chesky, N. Z., & Wolfmeyer, M. R. (2015). *Philosophy of STEM education: A critical investigation*. Springer.
- Dalton, W. (2019). *What is STEM?* Pearson. <https://pearsonaccelerated.com/blog/stem>
- Dogan, B. & Robin, B. (2015). *A practice-based model of STEM Teaching: STEM students on the stage*. Springer.
- Drijvers, P., Gitirana, V., Monaghan, J., Okumus, S., Besnier, S., Pfeiffer, C., Mercat, C., Thomas, A., Christo, D., Bellemain, F., Faggiano, E., Orozco-Santiago, J., Ndlovu, M., van Dijke-Droogers, M., da Silva Ignacio, R., Swidan, O., Filho, P. L., de Albuquerque, R. M., Hadjerrouit, S., ... & Rodrigues, A. (2019). Transitions Toward Digital Resources: Change, Invariance, and Orchestration. In *The 'Resource' Approach to Mathematics Education* (pp. 389-444). Springer. [https://doi.org/10.1007/978-3-030-20393-1\\_12](https://doi.org/10.1007/978-3-030-20393-1_12)

- Fakinlede, C. O., Yusuf, M. O., Mejabi, O. V., & Adegbiya, V. M. (2014). Readiness for online learning in higher education: A mixed-methods assessment of students at a Nigerian university. *Malaysian Journal of Distance Education*, 16(1), 37-57.
- Forson, I. K., & Vuopala, E. (2019). Online learning readiness: Perspective of students enrolled in distance education in Ghana. *The Online Journal of Distance Education and e-Learning*, 7(4), 277-294.
- Hasanah, U. (2020). Key definitions of STEM education: Literature review. *Interdisciplinary Journal of Environmental and Science Education*, 16(3), 1-7. <https://doi.org/10.29333/ijese/8336>
- IOS. (2017). *Evaluation of UNESCO's Programme Interventions on Girls' and Women's Education*. Internal Oversight Service. [www.unesco.org/.../PI\\_165\\_Rev\\_Evaluation\\_of\\_UNESCOS\\_Programme\\_Intervention](http://www.unesco.org/.../PI_165_Rev_Evaluation_of_UNESCOS_Programme_Intervention)
- Ismail, Z. (2018). Benefits of STEM education. [https://opendocs.ids.ac.uk/opendocs/bitstream/handle/20.500.12413/14258/418\\_Benefits\\_of\\_STEM\\_Education.pdf?sequence=1](https://opendocs.ids.ac.uk/opendocs/bitstream/handle/20.500.12413/14258/418_Benefits_of_STEM_Education.pdf?sequence=1)
- Junus, K., Santoso, H. B., Putra, P. O. H., Gandhi, A., & Siswantining, T. (2021). Lecturer readiness for online classes during the Pandemic: A survey research. *Education Sciences*, 11(3), Article 139. <https://doi.org/10.3390/educsci11030139>
- Kamaruzaman, F. M., Sulaiman, N. A., & Shaid, N. A. N. (2021). A study on perception of students readiness towards online learning during Covid-19 Pandemic. *International Journal of Academic Research in Business and Social Sciences*, 11(7), 1536-1548. <http://dx.doi.org/10.6007/IJARBS/v11-i7/10488>
- Kärkkäinen, K., & Vincent-Lancrin, S. (2013). *Sparkling innovation in STEM education with technology and collaboration: A case study of the HP Catalyst Initiative*. Centre for Educational Research and Innovation. [https://www.oecd.org/education/cei/OECD\\_EDU-WKP\(2013\)\\_%20Sparkling%20Innovation%20in%20STEM%20education.pdf](https://www.oecd.org/education/cei/OECD_EDU-WKP(2013)_%20Sparkling%20Innovation%20in%20STEM%20education.pdf)
- Kemp, S. (2021). *Digital 2021: South Africa*. Data Reportal. <https://datareportal.com/reports/digital-2021-south-africa>
- Kessler, G. (2018). Introduction to teaching and technology. In *The TESOL Encyclopedia of English Language Teaching* (pp. 1-2). John Wiley & Sons. <https://doi.org/10.1002/9781118784235.eeltv06b>
- Kubat, U., & Guray, E. (2018). To STEM or not to STEM? That is not the question. *Cypriot Journal of Educational Sciences*, 13(3), 388-399.
- LaForce, M., Noble, E., King, H., Century, J., Blackwell, C., Holt, S., Ibrahim, A. & Loo, S. (2016). The eight essential elements of inclusive STEM high schools. *International Journal of STEM Education*, 3(1), 1-11. <https://doi.org/10.1186/s40594-016-0054-z>
- Lee, K., Fanguy, M., Bligh, B., & Lu, X. S. (2021). Adoption of online teaching during the COVID-19 pandemic: A systematic analysis of changes in university teaching activity. *Educational Review*, 74(3), 460-483. <https://doi.org/10.1080/00131911.2021.1978401>
- Lichoro, D. M. (2015). *Faculty preparedness for transition to teaching online courses in the Iowa Community College Online Consortium* (Doctoral dissertations). Iowa State University, USA. <https://lib.dr.iastate.edu/etd/14376>
- Marwala, T. (2020). *Closing the gap: The fourth industrial revolution in Africa*. Macmillan.

- Ndlovu, M. C., & Mostert, I. (2018). Teacher perceptions of Moodle and throughput in a blended learning programme for in-service secondary school mathematics teachers. *Africa Education Review*, 15(2), 131-151. <https://doi.org/10.1080/18146627.2016.1241667>
- Ndlovu, M., & Meyer, D. (2019). *Readiness of teachers to teach mathematics with technology: A case study of a school in Gauteng*. Academia.
- Oladele, J. I., Koledafe, O. S., & Daramola, D. S. (2021). Prospects for online instructional delivery using google classrooms: Implications for higher education in sub-Saharan Africa. *Journal of Digital Learning and Education*, 1(3), 92-108. <http://dx.doi.org/10.52562/jdle.v1i3.227>
- Palloff, R. M., & Pratt, K. (2013). *Lessons from the virtual classroom: The realities of online teaching*. John Wiley & Sons.
- Parkes, M., Stein, S., & Reading, C. (2015). Student preparedness for university e-learning environments. *The Internet and Higher Education*, 25, 1-10. <https://doi.org/10.1016/j.iheduc.2014.10.002>
- Qazaq, M. N. A. (2012). *A study on readiness and implementation of e-learning among academic staff at Jordanian Institutions of Higher Education* (Doctoral dissertation). Universiti Utara Malaysia, Malaysia. [http://etd.uum.edu.my/2975/3/Mahmoud\\_Nayif\\_Ali\\_Qazaq.pdf](http://etd.uum.edu.my/2975/3/Mahmoud_Nayif_Ali_Qazaq.pdf)
- Ramírez-Hurtado, J. M., Hernández-Díaz, A. G., López-Sánchez, A. D., & Pérez-León, V. E. (2021). Measuring online teaching service quality in higher education in the COVID-19 environment. *International Journal of Environmental Research and Public Health*, 18(5), Article 2403. <https://doi.org/10.3390/ijerph18052403>
- Rasouli, A., Rahbania, Z., & Attaran, M. (2016). Students' readiness for e-learning application in higher education. *Malaysian Online Journal of Educational Technology*, 4(3), 51-64. <https://files.eric.ed.gov/fulltext/EJ1106478.pdf>
- Sabharwal, R., Chugh, R., Hossain, M. R., & Wells, M. (2018). Learning management systems in the workplace: A literature review. In *2018 IEEE International Conference on Teaching, Assessment, and Learning for Engineering (TALE)* (pp. 387-393). IEEE Publishing.
- Schwab, K. (2016). *The fourth industrial revolution*. World Economic Forum. <https://bit.ly/3Aypuf5>
- Siekmann, G. (2016). *What Is STEM? The need for unpacking its definitions and applications*. National Centre for Vocational Education Research (NCVER). <https://files.eric.ed.gov/fulltext/ED570651.pdf>
- Škobo, M. (2020). Modern technologies in teaching literature. In *Sinteza 2020 International Scientific Conference on Information Technology and Data Related Research* (pp. 86-92). Singidunum University.
- Stohlmann, M., Moore, T. J., McClelland, J., & Roehrig, G. H. (2011). Year-long impressions of a middle school STEM integration program. *Middle School Journal*, 43, 32-40.
- Tanenbaum, C. (2016). *STEM 2026: A vision for innovation in STEM education*. US Department of Education, Washington, DC. <https://www.air.org/system/files/downloads/report/STEM-2026-Vision-for-Innovation-September-2016.pdf>
- The Glossary of Education. (2014). *Learning Experience*. <https://www.edglossary.org/learning-experience/>
- UNESCO. (2021). *Qingdao declaration promotes use of ICT to achieve education targets in new sustainable development goals*. <https://en.unesco.org/news/qingdao-declaration-promotes-use-ict-achieve-education-targets-new-sustainable-development>

- UNESCO, U., UNPFA, U., UNICEF, U., & UN, W. (2015). *Incheon Declaration and Framework for Action for the Implementation of Sustainable Development Goal 4*. [http://uis.unesco.org/sites/default/files/documents/education-2030-incheon-framework-for-action-implementation-of-sdg4-2016-en\\_2.pdf](http://uis.unesco.org/sites/default/files/documents/education-2030-incheon-framework-for-action-implementation-of-sdg4-2016-en_2.pdf)
- Vahidy, J. (2019). *Enhancing stem learning through technology*. Press Books.
- Venkatesh, V., Morris, M. G., Davis, G. B., & Davis, F. D. (2003). User acceptance of information technology: Toward a unified view. *Management Information Systems Quarterly*, 27(3), 425-478. <https://doi.org/10.2307/30036540>
- White, W. D. (2014). What is STEM education, and why is it important? *Florida Association of Teacher Educators Journal*, 1(14), 1-9.
- Widodo, S. F. A., Wibowo, Y. E., & Wagiran, W. (2020). Online learning readiness during the COVID-19 pandemic. *Journal of Physics: Conference Series*, 1700(1), 012-033. <https://doi.org/10.1088/1742-6596/1700/1/012033>
- Young, S. (2006). Student views of effective online teaching in higher education. *The American Journal of Distance Education*, 20(2), 65-77. [https://doi.org/10.1207/s15389286ajde2002\\_2](https://doi.org/10.1207/s15389286ajde2002_2)



## Towards Designing a Framework for Adaptive Gamification Learning Analytics in Quranic Memorisation

Siti Hasrinafasya Che Hassan<sup>1,2\*</sup>, Syadiah Nor Wan Shamsuddin<sup>2</sup> and Nor Hafizi Yusof<sup>3</sup>

<sup>1</sup>Faculty of Computer and Mathematical Sciences, Universiti Teknologi MARA, Kelantan Branch, Bukit Ilmu, 18500 UiTM, Machang, Kelantan, Malaysia

<sup>2</sup>Faculty of Informatics, Universiti Sultan Zainal Abidin, Tembila Campus, 20300 UnisZA, Terengganu, Malaysia

<sup>3</sup>Faculty of Islamic Contemporary Studies, Universiti Sultan Zainal Abidin, Tembila Campus, 20300 UnisZA, Terengganu, Malaysia

### ABSTRACT

The difficulty of sustaining and preserving the quality of Quranic memorisation is still an unsolved problem. Motivation and engagement are the most desired experiential qualities to memorise the Quran. This paper presents a framework for introducing adaptive gamification technology (integrated into the student learning experiences) by providing appropriate personalised formative memorising activities. A methodology that follows the three stages, which are analysis, design, and evaluation, was implemented in this study. A validation process by experts was conducted to get the relevant criticisms and recommendations for further improvement of the proposed framework. The results demonstrated that all components are compatible and usable for developing a prototype application specifically for self-learning Quranic memorisation. With proper integration of gamification in learning and assessment activities, a positive impact on the memorisation process can be achieved, such as higher satisfaction, motivation and greater achievement of students through appropriate learning analysis. Therefore, the proposed conceptual

framework known as Gamification Learning for Al-Quran Memorisation (GLAM-Q) is expected to contribute significantly and be a reference model in developing a Quranic memorisation application.

*Keywords:* Adaptive gamification, game aesthetics, game dynamics, game mechanics, learning analytics, Quranic memorisation, self-regulated learning

### ARTICLE INFO

#### Article history:

Received: 09 March 2022

Accepted: 24 May 2022

Published: 20 October 2022

DOI: <https://doi.org/10.47836/pjst.31.1.16>

#### E-mail addresses:

hasrina581@uitm.edu.my (Siti Hasrinafasya Che Hassan)

syadiah@unisza.edu.my (Syadiah Nor Wan Shamsuddin)

nhafizi@unisza.edu.my (Nor Hafizi Yusof)

\*Corresponding author

## INTRODUCTION

Memorising the Quran may be a great challenge to non-Arabic speakers because they lack mastery of Arabic vocabulary and grammar (Dzulkifli et al., 2014; Salehuddin et al., 2019). Nevertheless, Muslims worldwide have engaged in a concerted effort to understand and preserve the Quran by memorising it (Zakariah et al., 2017). In recent years, studies in the Quranic field in Malaysia, such as by Yusoff et al. (2018), are getting more encouraging responses from communities. This situation can be seen with the increasing number of Tahfiz schools established by the government and private sector (Ibrahim et al., 2018).

However, due to face-to-face learning constraints during this pandemic, online class becomes preferable to adapt to the new normal. Nevertheless, the learning time session between students and a qualified Quran teacher is insufficient and ineffective in sustaining and preserving memorisation quality for an extended time. It is because memorising the Quran to achieve a certain target number of Surah within some period requires much motivation (Aziz et al., 2019; Mustafa & Basri, 2014a; Mustafa & Basri, 2014b) and a good and strong memory to abide by the specific rules (Ariffin et al., 2013; Aziz et al., 2019; Rosmansyah & Rosyid, 2017). Hence, it has been admitted that the process is not easy, and the duration of memorisation depends on the memory retention ability of the students (Aziz et al., 2019). For example, Hashim (2015) reported that in the retention strategy of the Tahfiz learning style, students did not complete memorisation of the Quran revision (Khatam) according to schedule and were less steadfast in following the revision memorisation schedule. Ambo and Mokhsein (2019) reported that many students could not memorize all 30 constituencies within 3 years. In a previous study, Ismail et al. (2017) mentioned that 60% of students could not complete Quran memorisation according to the prescribed schedule of 30 constituencies within 6 semesters. Besides, other statistics showed that the percentage of students who did not manage to recite the Quran according to the prescribed constituencies is high (Yusuf et al., 2019); only 63% of students in National Religious Secondary Schools (SMKA) and Fully Residential Schools (SBP) managed to complete their memorisation phased over 5 years.

In addressing the above issues, Industrial Revolution 4.0 (IR4.0) has introduced gamification technology that could be applied in Tahfiz Higher Religious Institutions (HRIs) to respond to Gen Z students' learning preferences by giving them appropriate assessments to monitor their progress. Therefore, the objective of this study is to propose a new conceptual framework for self-regulated Quranic memorisation using specific learning strategies and some gamification elements. The rest of this paper is organised as follows. At first, this research provides a quick overview of the related works in literature. Afterwards, it presents a research methodology that follows three activities: analysis, design, and evaluation. The next section explains the details of the conceptual framework that consists of learning theories, learning techniques used in memorisation strategy, and

three gamification elements (game mechanics, game dynamics and game aesthetics) with learning analytics used in assessment modules. The last section discusses the analysis result from the expert reviews based on the proposed framework.

### **Quran Memorisation Techniques**

Quran memorisation refers to memorising every verse of the Quran, which should be accompanied by the pure intention of preserving the Quran verses from any alterations, either in the form of elimination or manipulation of the verses (Shukri et al., 2020). The method is essential for students to learn and practice memorising the Quran. However, it is not easy to memorise blindly because it is ineffective, boring, and prone to fail (students forget what they had previously memorised). Saleem (2018) revealed that before starting the actual memorisation, memorisers are taught Arabic letters and their sounds. At this stage, they are only concerned with how to pronounce or read out the ‘words,’ whereby learners internalize the phonotactics of classical Arabic without reference to meaning.

Once the memorisers have completed their ‘reading’ of the text, they embark on memorisation proper. The practice of Quran memorisation is in line with ‘guided repetition’, which involves modelling by an expert, imitation by a novice, and rehearsal and performance by the novice. Nafi et al. (2019) mentioned that there are two main ways to memorise the Quran easily for beginners, which are memorised per page by reading one page 3 to 10 times (or more, which depends on the memoriser’s capability) in Tartil before proceeding to the next page when the reading is smooth and memorise per verse by reciting one verse 3 to 10 times (or more, which depends on the memoriser’s capability) in Tartil before moving to the next verse in the same way. This technique is known as Murajaah, a traditional method that directs students to memorise gradually by dividing chapters and increasing repeatability (Purbohadi et al., 2019).

In memorising the Quran verses, there are three levels of allegiance, namely memorising the new verses (Hifz Jadid), the repeating stage of the last memorisation (Sabaq), and the level of maintaining the existing memorisation (Murajaah) (Abdullah et al., 2003; Abdullah & Muda, 2004). The failure of students to master these three major processes results in the students failing to memorise the Quran at a maximum level (Abdullah et al., 2003). Literature suggested that several prominent Quranic memorisation models highlighted memorising strategies used in memorising the Quran. Through the analysis of previous studies, such as by Dzulkifli and Solihu (2018), there are at least 12 basic methods and approaches to memorising the Quran that have practically been used by most Tahfiz schools in Malaysia and were brought in from Indonesia, Mecca, India (Deobandy method) and Pakistan (Panipati method).

## Adaptive Gamification

Gamification is defined by Lavoué et al. (2019) in Deterding et al. (2011) as the use of game design elements (e.g. mechanics, dynamics and aesthetics) to motivate user behaviour in non-game contexts. It has recently attracted much discussion and research as a promising value in transforming student behaviour towards learning engagement, motivation and performance (Ofosu-Ampong, 2020).

Gamification was first introduced in the application of Islamic learning, *Al-Furqan*, by Bakri et al. (2014). It was a gameplay interactive learning that integrated graphics, sound, and text for children's learning; unfortunately, it was not specifically for memorising. Subsequently, more game mechanics have introduced for Quran memorisation in 2016 and 2017, such as points (Adhoni et al., 2013; Moulana, 2017; Rosmansyah & Rosyid, 2017; Senan et al., 2017; Shamsuddin et al., 2016), achievements (e.g. badges, trophic, rewards/gifts) (Rosmansyah & Rosyid, 2017; Shamsuddin et al., 2016), levels (Adhoni et al., 2013; Adhoni et al., 2014; Moulana, 2017; Rosmansyah & Rosyid, 2017; Senan et al., 2017; Shamsuddin et al., 2016), challenges (Moulana, 2017), progress bar (Rosmansyah & Rosyid, 2017), leaderboard (Rosmansyah & Rosyid, 2017), and so on. However, in 2018, comprehensive studies into gamification in memorising the Quran became less attractive to researchers. There are some reasons for this decline in interest, as concluded by Morschheuser et al. (2018), who posited that gamification is challenging to design because 1) Games are complex, multifaceted, and therefore, difficult to holistically transfer to other environments, 2) Gamification entails the understanding of motivational psychology, and 3) The purpose of gamification usually also influences the behaviour that adds another layer into the scope of the gamification design.

To our knowledge, there are no studies (in the memorisation of the Quran) that adapt the game's features to the students' profiles. Thus, even though gamification can help increase learning motivation, it is important to know the characteristics of each individual. Unfortunately, most game systems incorporate game elements under the standard 'one measure fits all' approach to the standard gamification concept without considering the user's individual preferences, styles, needs and abilities (Alomair & Hammami, 2020). Therefore, to improve the conventional gamification approach, we have proposed adaptive gamification, a more user-centred design to accommodate various characteristics of different users and contexts (Böckle et al., 2018). In personalised learning, the content displayed can be tailored to suit each individual's profile (such as age, gender and motivation), learning style (which is obtained from interaction learners with the system), behaviour and skill/knowledge (namely beginner, intermediate and advanced levels) so that each student is presented with learning activities based on what they know and what they need to know (Rozi et al., 2019).

## Learning Analytics

Learning Analytics (LA) can be defined as measuring and collecting data on students and learning processes to improve the teaching and learning processes through visualisations and data processing (Rosmansyah et al., 2017). The data interpretation activity related to students is required during the educational activity to predict the performance of the overall learning system, support the decision-making process, and detect potential problems or recognise in advance the signs of failure that may arise in the future. It borrows from different related fields (e.g. academic analytics, personalised adaptive learning) to collect, analyse, and report data about learners in specific contexts to understand and optimise learning and the environments in which it occurs (Chatti et al., 2012). Unfortunately, LA in Quranic memorisation is not well addressed in the literature. It was found that most research in Quranic memorisation does not directly mention the implementation of learning analytics research in students' assessment, probably because such assessment requires longitudinal studies. The LA dashboard plays a performance indicator where different topics are visualised and can be adjusted by the learner. It can be used as a Quranic language-learning application that tracks the results of exercises to visualise learners' progress. This dashboard relies on time spent, score, and some assessment at the end of every game for immediate reflection and feedback on the learner's performance that is tracked from the learning environment (Verbert et al., 2013). The feedback provided through progression enables learners to get an insight into their goals and track their advancement in the course over time (Hassan et al., 2021).

LA can be integrated with gamification to acquire data in real-time such as time spent without achieving a goal (i.e., time viewing a tutorial), total time played, number of attempts before completing a task, or users' progression between the first session played and the subsequent sessions (Cano et al., 2016). In another study, Cariaga and Feria (2015) presented other different kinds of information about LA, such as the number of times the learner logs into the system, number of times the learner plays the game, number of questions that are correctly answered, time spent in response to the activity, time spent prior to the first use of a hint, number of mistakes, and number of times a hint is pressed. It is hoped that the information collected could give us an overview of the learning process of the learners and their engagement, the effectiveness of the learning design, and the validity of the user requirements described.

## RESEARCH METHODOLOGY

This study proposes a conceptual framework specifically for self-learning in Quranic memorisation using gamification elements and learning analytics. Therefore, the three phases below were conducted to achieve the objective of this research.

## Phase 1: Analysis

In the first stage, three things have been analysed: 1) Issues or problems faced by Tahfiz students; 2) Comparative studies from related Quran mobile applications and literature; 3) Learning theories related to the learning techniques/strategies used in memorisation.

### Issues or Problems Faced by Tahfiz Students

When memorising the Quran, Tahfiz students face many issues or problems. Based on the problem analysis, researchers conclude that there are three main problems faced by Tahfiz students, which are:

- a. Difficulty in permanent memory retention: Many Quran learners find it difficult to maintain the quality of memorisation once the memorisation is completed (Shukri et al., 2020; Yusuf et al., 2019), despite them having spent time reciting it for numerous repetitions (Abro et al., 2012; Almosallam et al., 2015). Although the method of repetition is a common practice used in Tahfiz schools, it cannot guarantee that all students can memorise easily through the same method applied to all students (Zaki et al., 2019). Therefore, the question arises about the level of mastery of students' Quran memorisation because they are given a short time to complete the memorisation of 30 Juzuk of the Quran, ranging from only 2 to 5 years.
- b. Lack of interest and motivation: According to (Abdullah et al., 2003; Purbohadi et al., 2019; Rosmansyah & Rosyid, 2017; Shukri et al., 2020), one of the obstacles in memorising the Quran is a lack of interest and motivation among the younger generation of Tahfiz students to learn and memorise the Quran traditionally. In addition, some students only joined the Madrasah due to their parent's wishes. Therefore, students tend to be bored when they need to memorise different verses or pages daily for an extended time (Sabbri, 2016; Mustafa & Basri, 2014a; Priatna et al., 2020).
- c. Absence of multiple learning styles: Mustafa et al. (2019) have found that issues of poor student achievement are due to the absence of good memorisation techniques based on student VARK learning styles. As mentioned by Muluk et al. (2020), students apply more than one learning style to assist them in understanding the materials and actively exchange the learning style based on their needs. It shows that combining the learning styles may help the students speed up their memorisation process.

Based on the three problems mentioned above, the next sections will discuss memorisation techniques (or strategies) that have been applied in related applications and literature. Subsequently, the gamification elements were adapted to a holistic user-

centred approach to increase the memorisers' interest, motivation, attention and learning performance, as Rozi et al. (2019) mentioned. In addition, multi-sensory learning styles were emphasized to capture learners with different abilities and characteristics for memorising the Quran. Finally, all relevant learning theories, learning techniques/strategies and game elements with adaptive gamification aspects, including player/learner profiles, learning styles, behaviours and skills/knowledge, have been described as the proposed framework in the design stage.

### **Comparative Studies from Related Applications and Literature**

Recently, many applications support memorisation features and use different methods to implement them. Therefore, a preliminary study was implemented by observation and comparative studies on the existing Quranic mobile applications available in the market, such as Juz30, Hifdh, King Saud University Electronic Quran, and House of Quran portal.

Based on the observation, most applications currently are based on the following criteria:

- a. Repetition: Many products employ repetition of the recitation either for a specific Quranic verse or for the whole section (set of verses) with a specified number of times.
- b. Memorisation progress: Some products review the progress of memorisation. Generally, the review involves different sections that need to be memorised and is used to manage and evaluate each user's memorisation level.
- c. Memorisation test: Two common tests have been used to verify the memorisation accuracy and evaluate its quality. The methods are explained below:
  - i. Recording: Users can confirm their memorisation by recording their recitation and then listening to the recording to discern any errors and correct them.
  - ii. Filling in: The Quranic or section may be shown for a given time to the user before they are asked to fill in a few words or the whole section to confirm their memorisation. Therefore, the user cannot skip any word or section without being sure of their spelling.

In addition, comparative studies from the existing literature were gathered. These comprise journal articles, dissertations, books, and reliable online materials. Finally, according to the analysis, some additional memorising techniques are commonly applied as follows:

- a. Repeats (Takrir) the memorisation of the Ayah several times. For example, the minimum number of repetitions that have been suggested is five times (Shamsuddin et al., 2016), and the maximum number of repetitions is 60 times (Senan et al., 2017).
- b. Systematically organises and meaningfully divides or breaks down the memorised Surah into several segments of Ayah, pages, or the smallest meaningful



parts. There is a significant impact in understanding, memorising and practising as needed when the main topics from a Surah in the Holy Quran are summarised and visualised coherently, such as chunking/breaking down verses into the smallest meaningful parts (Moulana, 2017; Shamsuddin et al., 2016), and visually displaying verses or Surahs in mind maps according to their topics (Böckle et al., 2018; Shamsuddin et al., 2016).

- c. Promotes multi-sensory learning styles such as verbal/textual, auditory/sound and visual/image as the main criteria used to capture the learners' interest and attention to memorise. For example, some previous research, such as by Ahmad et al. (2018), Hamiz et al. (2014) and Moulana (2017), used mnemonics (either Loci or sign language or any navigation cues) to facilitate students with different verbal, auditory and visual abilities, especially among elderly learners and learners with disability.

### **Learning Theories Related to the Learning Techniques/Strategies Used in Memorisation**

The method of memorising the Quran is a series of structured and systematic actions that aim to achieve learning objectives with steps structured in short time blocks. The idea to adapt some of the traditional methods suggested by Darul Quran, JAKIM in Yaacob et al. (2019) into a proposed framework is illustrated in Figure 1 with some learning theories such as:

- a. Dual-Coding theory: The multi-sensory approaches promote variegation regarding the learning styles, teaching and learning methods. It can be done by combining written and pictorial annotations and will have a differential effect on the learning performance of students with different verbal and visual abilities.
- b. Rote Learning theory: Saleem (2018) claimed that students repeat and rehearse the recitation of the Quran to preserve and maintain it in memory because they do not understand the 'meaning' to assist them in memorisation.
- c. Self-Determination theory (Intrinsic Motivation): A metatheory of human personality and motivation concerned with how the learner interacts with learning subjects for a certain period. It defines intrinsic and extrinsic motivation (Böckle et al., 2018). Thus, it is required to motivate learners to keep repeating their memorisation (Murajaah).
- d. Constructivism Learning theory (Active Learning): The basis for using educational games to enhance learning is supported by the ideas of constructivism. Constructivism learning theory is based on the idea that learning is an active process in which the learner builds new knowledge based on prior understanding and experience (Rouse, 2013).
- e. Self-Monitoring theory: This is one of the strategies involved in a self-regulatory learning process. Two essential criteria for self-monitoring are regularity and proximity

(Schunk, 2012). Regularity means monitoring behaviour continuously rather than intermittently. Proximity means that behaviour is observed during the incident and not soon after. In conclusion, monitoring activities include the following activities such as checking the level of understanding, predicting outcomes, evaluating the effectiveness of effort, planning activities, deciding how to estimate learning time, revising, or switching to other activities to overcome difficulties. Hence, it could allow students to improve their work (e.g., revise work for a better grade), use different evaluation forms, and conduct assessments privately.

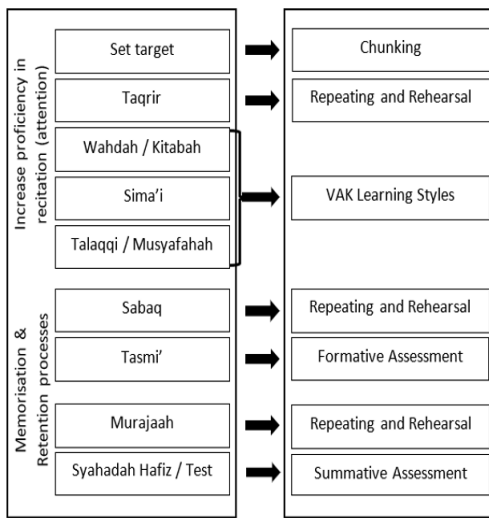


Figure 1. The illustration of Quranic memorisation processes

Figure 1 illustrates the Quran memorisation processes that use common practical techniques in the Malaysian Model of Al-Quran Memorisation Method (Ahmad et al., 2019). The process begins with the ‘attention’ process to the achievable target of memorising parts of the Surah which will later accumulate to completing all 30 Juzuk of the Quran. The determination of memorisation rates and limits depends on the students’ varied abilities that require chunking as one of the most used learning strategies to maximise memory function. It involves organising information according to specific criteria in a meaningful way that could enhance the ability of the mind to process the

information consecutively, as noted by Frankenmolen et al. (2018) in Shukri et al. (2020). ‘Attention’ in Quranic memorisation refers to the focus given to the information that is kept in the memory through visual, auditory, and kinesthetic (VAK) sensory senses, which is crucial in ensuring the accuracy of the processed information when transferred to Long Term Memory (Shukri et al., 2020). It includes reciting the verses fluently and correctly (according to Tajweed rules) before memorising, writing the verses on paper before memorising, reciting the verses with others and teachers, and listening to the verses from the cassette, CD or MP3 before memorising (Yaacob et al., 2019). All these processes are repeated (Taqrir) as often as possible to increase the proficiency of recitation during the memorisation process later.

Repetition and rehearsal are inherent parts of memorisation. Anwar (2019) explained that repetition of the Quran verses has three forms: 1) repetition of new verses (Sabaq); 2) repetition of old verses (Murajaah); and 3) overall repetition of the memorised verses

(Syahadah) in two ways: Syafawi (oral) and Tahriri (writing). Rehearsing information keeps it in Working Memory (WM) but does not necessarily elaborate. Hence, a distinction can be drawn between maintenance rehearsal (repeating information over and over) and elaborative rehearsal (relating the information to something already known) (Schunk, 2012). Besides, the emphasis on the role of repetition and rehearsal in memorising the Quran is in keeping with the claim that repetition of sequences in Short-Term Memory (STM) is necessary for chunking in phonological Long-Term Memory (LTM) as consolidation of information in LTM.

Lastly, formative and summative assessments evaluate the performance or progression of students' memorisation. Formative activity is assumed as similar to the Tasmi' test. At the same time, Syahadah (as the final evaluation) is considered a summative evaluation after the summative assessments are completed. The student's progression is evaluated based on certain levels, from the easier to the difficult stages, according to students' abilities.

## **Phase 2: Design**

In the second stage, a conceptual framework named Gamification Learning for Al-Quran Memorisation (GLAM-Q) was designed based on the memorisation techniques, learning strategies and adaptive gamification elements. The game mechanics must be designed with structured learning activities that include summative and formative assessments to capture the learning analysis in memorising the Quran. The summative evaluation provides information on activities such as assessments or certification. Meanwhile, formative assessment consists of learning activities in which students act (e.g., respond to questions) and receive feedback on the quality of their efforts. It provides students with direct information about their learning and performance and direction for improvement (to tell them what they can do to improve their learning).

A variety of methods exist to conduct formative evaluations during the learning process. In this study, the researchers proposed three categories of assessment methods: 1) Fill in the blank; 2) Sort; 3) Guess the location. The goal is to monitor student learning and to provide ongoing feedback that can be used to improve their Quranic memorisation. This study used game mechanics, dynamics and aesthetic elements in formative assessment activities. All game components have been applied to make the GLAM-Q application more engaging and entertaining. Table 1 shows the details of the mechanics, dynamics and aesthetic components. In addition, these formative assessments were classified into three difficulty levels: easy, intermediate, and challenging, as shown in Table 2.

Table 1

*Summary of game mechanics, game dynamics and game aesthetics used*

Game Mechanics	Game Dynamics	Game Aesthetics	Purpose
Point/Score/ Badges	Reward	Achievement/ Motivation	Scoring offers learners clear feedback on how well/poorly they are learning. It ties to their progress in learning. Learners with the best scores receive rewards such as badges, achievements, or redeemable rewards to boost their motivation in learning activities.
Level/ Challenge	Feedback/ Restrictions	Status/ progression	Learners are challenged to complete the first level of memorisation to continue to the next stage. It indicates that an individual has achieved better achievement and progression. In addition, the level is used to identify the achievement status of a particular learning task.

This study accepts the MDA (mechanics-dynamics-aesthetics) framework as a model of the main structural components of gamification as it has been seen as a common framework for in-game system design and gamification (Sezgin & Yüzer, 2020). Game mechanics are basic functional components that include actions, behaviours, and controls used to ‘gamify’ learning activities to stimulate certain emotions of learners. Meanwhile, game dynamics result from desires and motivations that reflect the emotions stimulated by the game mechanics. Feedback and support, restrictions, and progressions are among these dynamics. Finally, aesthetics emphasizes students’ feelings during and at the end of the memorization process, such as feelings of achievement, joy or happiness for achieving the desired target.

Table 2

*Framework*

Difficulty Level	Formative Activity	Purpose
Easy	Fill in the blank	Completing the unknown verses in the correct order
Intermediate	Sort	Arranging the order of unsorted verses according to their location numbers
Difficult	Guess the location	Randomly guessing the verses according to the given location number

The conceptual framework named Gamification Learning for Al-Quran Memorisation (GLAM-Q) for designing and modelling a Quran Memorisation application is shown in Figure 2. It was designed based on the relevant learning theories (as discussed above), learning techniques/strategies (such as chunking, mnemonic and mind map) and gamification elements (namely game mechanics, game dynamics and game aesthetics) used for the assessment in formative and summative activities (as explained in the previous section).

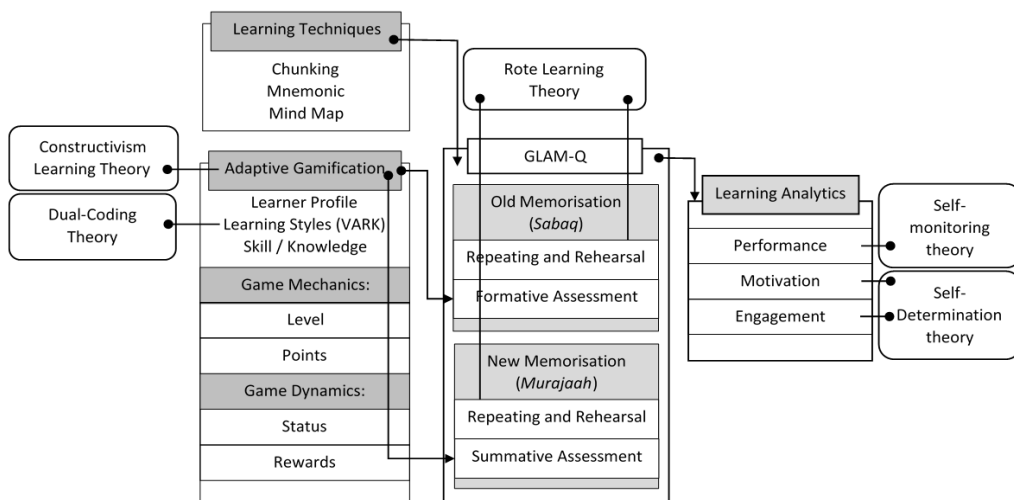


Figure 2. The conceptual framework of GLAM-Q

## RESULTS AND DISCUSSION

### Phase 3: Evaluation

In the third stage, a proposed conceptual framework was evaluated to get experts' relevant criticism and recommendations from multiple areas of expertise. The experts were selected based on several criteria as follows:

1. Expertise either in Instructional Design or User Experience (UX) or Mobile Application or Multimedia or Computer Science (CS) or any related areas, and/or
2. Have been researching Quranic memorisation and/or
3. Have been doing research in gamification or game-based learning and/or
4. Have been doing research/teaching in Multimedia, IT, or CS areas for at least 5 years.

Eight experts from multiple fields reviewed the proposed conceptual framework to collect the relevant criticisms and recommendations for improving the conceptual framework. The evaluation emphasized the personal opinions of experts and their perceptions using a 5-point Likert Scale: Strongly Disagree, Disagree, Somewhat Agree, Agree, and Strongly Agree. The analysis for each component is interpreted in Figures 3 to 7.

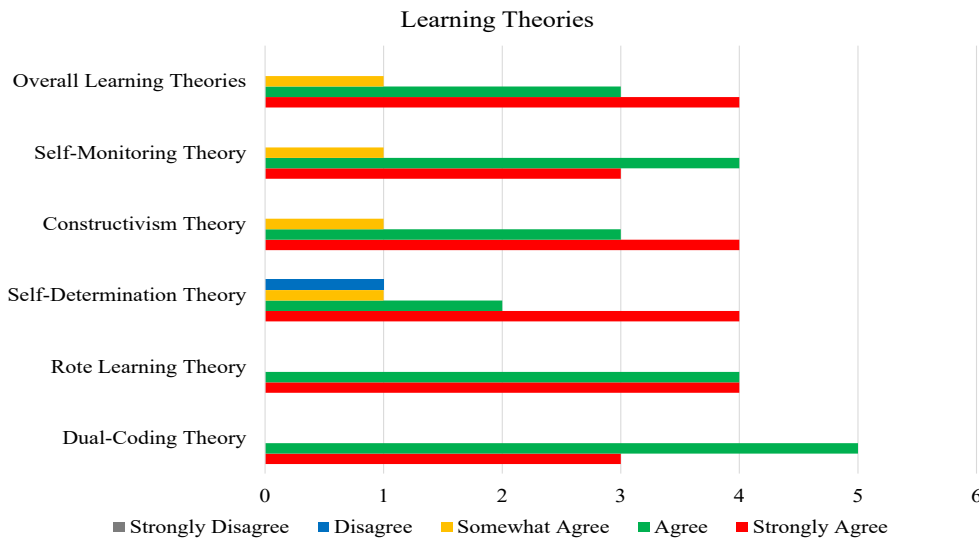


Figure 3. Learning theories

The underpinning theories that support Quranic memorisation through gamification application ensure that learners can improve their learning performance. Five underpinning theories have been focused on: Dual-Coding theory, Rote Learning theory, Self-Determination theory, Constructivism theory, and Self-Monitoring theory. Figure 3 shows the expert review analysis of learning theories applied in a conceptual framework. The overall result concludes that 50% (four experts) strongly agreed, 37.5% (three experts) agreed, and 12.5% (one expert) somewhat agreed with the proposed learning theories. Expert 1 commented that she strongly agreed if theories related to attitudes and behaviours were considered in improving student performance to be more positive-minded and enthusiastic in memorising. Meanwhile, Expert 3, who gave a response of somewhat agreed, mentioned that the proposed theories should align with the needs of education and gamification. Besides, she suggested it is unnecessary to include many learning theories in the framework. Nevertheless, all experts agreed that all these theories should not be removed from the framework.

The learning techniques summarise and visualise the Quran verses coherently, which will significantly impact understanding, memorising, and practising them as needed. Three learning techniques were recommended in memorising the Quran: chunking, mnemonic and mind map. Most of the experts agreed that the learning techniques in the proposed conceptual framework were compatible and relevant, except for Expert 6, a Quran teacher who was not sure how these techniques would be applied later. Statistically, Figure 4 shows the expert review analysis of learning techniques applied in a conceptual framework. The overall result concludes that 37.5% (three experts) strongly agreed, 50% (four experts)

agreed, and 12.5% (one expert) somewhat agreed. In addition, Expert 1 suggested storytelling as an additional method to attract student interest and improve the students' retention in memorising.

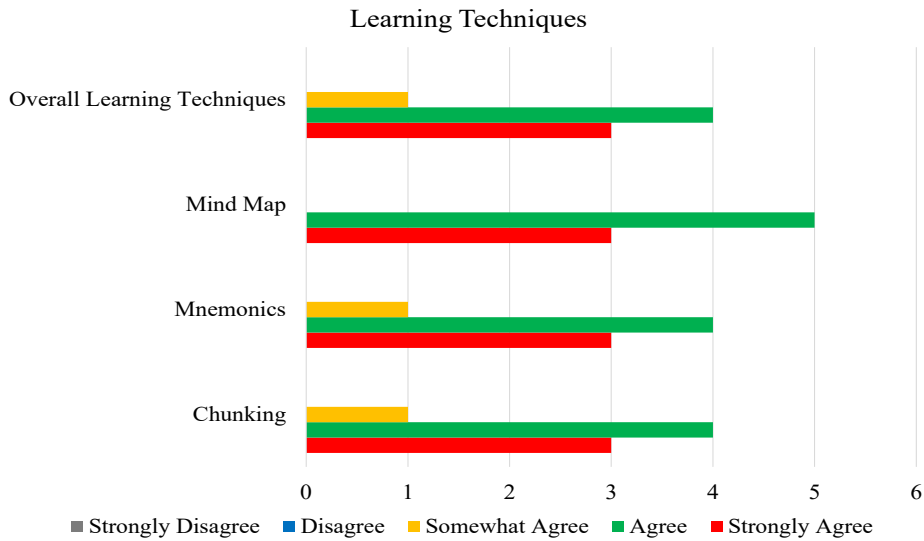


Figure 4. Learning techniques

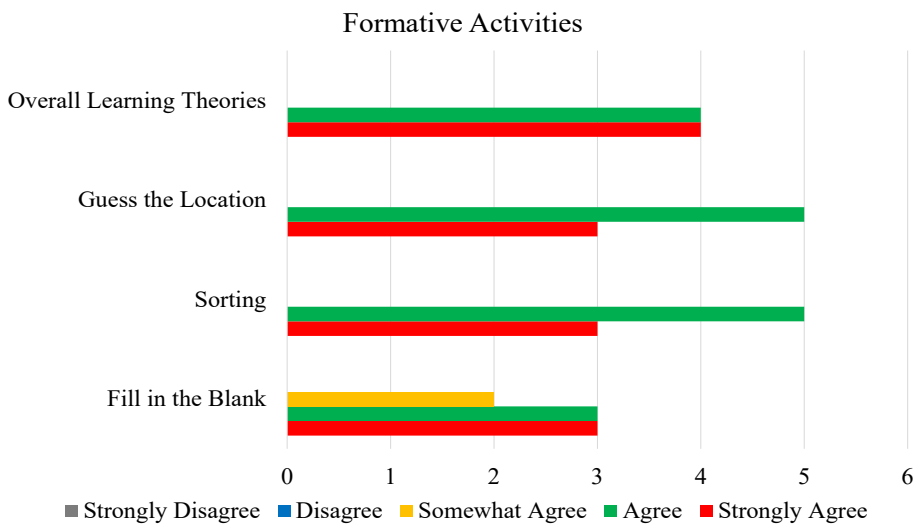


Figure 5. Formative activities



Various methods are applied to conduct formative evaluations during the learning process. The goal is to monitor student learning and to provide ongoing feedback that can be used to improve their Quranic memorisation. The formative assessment was classified into three difficulty levels: easy, intermediate, and difficult. Three formative activities have been proposed in the three assessment levels: completing the unknown verses in the correct order (fill in the blank), arranging the order of unsorted verses according to their location numbers, and randomly guessing the verses according to the given location number. Expert 1 suggested that rewards should be given to encourage students' motivation in each activity. Figure 5 shows the expert review analysis of formative activities suggested in a conceptual framework. The overall result concludes that 50% (four experts) strongly agreed and agreed that the activities were compatible and relevant to the framework. In addition, none of the experts agreed that assessment activities should be excluded from the framework. Nevertheless, Expert 3 suggested that the interface design should conform to human-computer interaction principles emphasising usability and user experience.

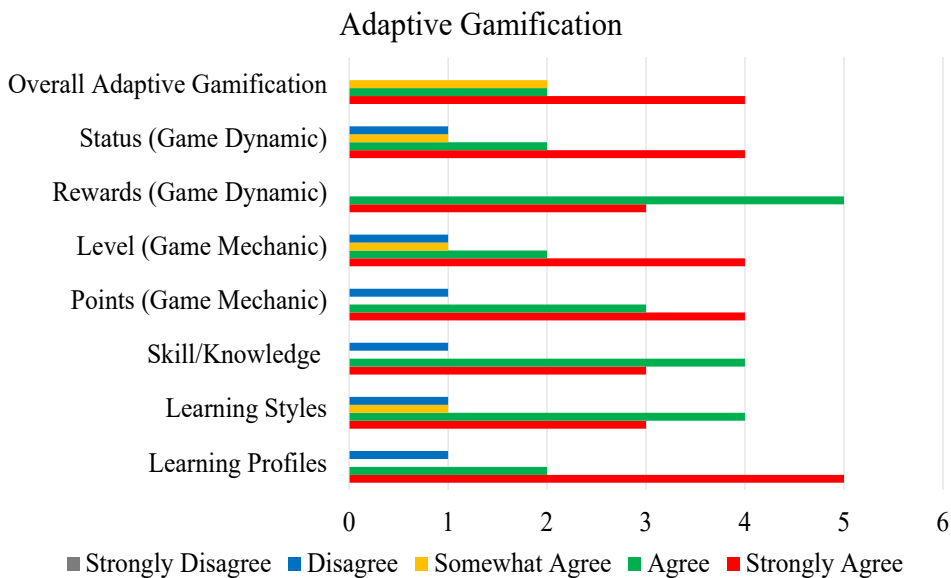


Figure 6. Adaptive gamification

Adaptive gamification addresses personalised incentive mechanisms tailored to particular characteristics of different users and contexts in order to optimise gamification effects. Three input components were considered, which are learner profile (e.g., age and gender), learning style (e.g., visual and auditory) and skill/knowledge (e.g., beginner, intermediate and advanced). Meanwhile, game mechanics are the actions, behaviours, and controls used to ‘gamify’ learning activities to stimulate certain emotions in the

learner. Game mechanics must be designed with structured learning activities that include summative and formative assessments. Lastly, game dynamics result from desire and motivation that reflect the emotions stimulated by the game mechanics above. Figure 6 shows the expert review analysis of adaptive gamification suggested in a conceptual framework. The overall result concludes that 50% (four experts) strongly agreed, 25% (two experts) agreed and somewhat agreed, respectively. The experts who answered somewhat agreed and advised that the mechanic and dynamic elements should further clarify their significance in this study.

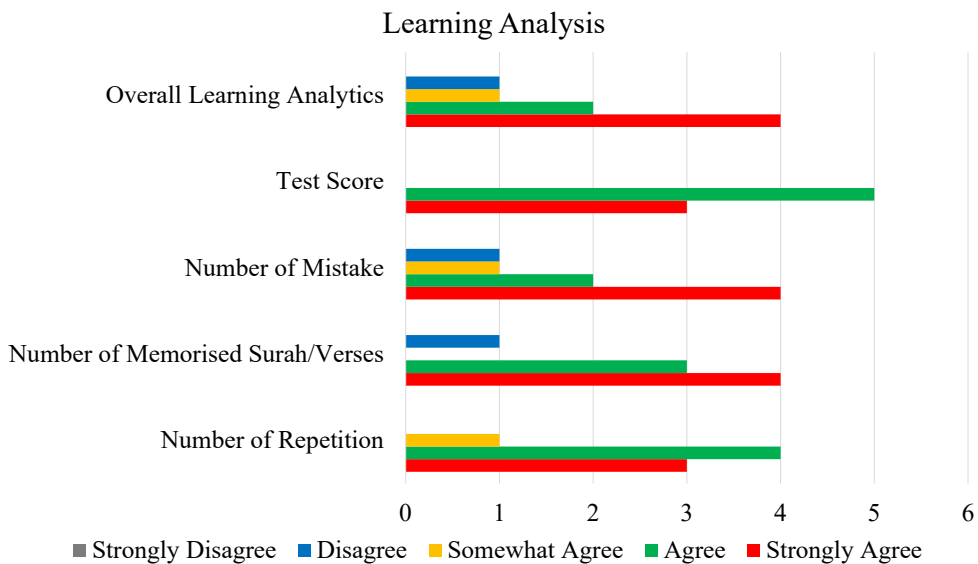


Figure 7. Learning analysis (for motivation and progression)

Dashboard analysis relies on time spent, score, and some assessment at the end of each game for immediate reflection and feedback on the student’s performance that is tracked from the learning environment. The four parameters that will be captured during the memorisation process are as follows: 1) the statistics of rote memorisation (the number of repetitions), 2) the number of memorised Surah/verses, 3) the number of mistakes, and 4) test score (or the overall progression of summative assessment). Figure 7 shows the expert review of learning analysis parameters suggested in a conceptual framework. The overall result concludes that 50% (four experts) strongly agreed, 25% (two experts) chose to agree, and 12.5% (one expert each) evaluated somewhat agreed and disagreed, respectively. Based on the review, none of the experts agreed that assessment activities should be excluded from the framework. In addition, Expert 2 commented that there was a need to add the parameters of learning analysis because of its relevance to the periodic monitoring of student progress.

As a conclusion to the overall results obtained, the authors have concluded the following points:

- 1) All of the reviewers agreed that the connections and flows of all five components are understandable to describe the overall structure of the conceptual framework.
- 2) The conceptual framework proposed is usable for developing prototype applications specifically for self-learning Quranic memorisation.
- 3) None of the components proposed in the conceptual framework need to be removed. However, a reviewer suggested that it is crucial to ensure that only essential theories are applied.
- 4) Fun (aesthetic in gamification) is relevant to make Tahfiz students enjoy themselves and not under pressure when learning the Quran. Nevertheless, most reviewers emphasized the learning engagement and motivation (LEM) of students to keep students' positive attitude in memorising. In addition, they proposed to consider the aspect of usability (e.g., ease of use, learnability, efficiency, and satisfaction) and user experience (e.g., motivation, enjoyment, and pleasure).
- 5) Memorisation requires high imagination. Therefore, it requires additional formative activities (such as filling in the blanks, sorting, and guessing the verse locations).

## CONCLUSION

This article briefly introduced the exciting new class of Quranic memorisation applications with effective memorisation strategies and gamification elements. Due to face-to-face constraints during this pandemic, a GLAM-Q conceptual framework specifically for self-learning is an alternative solution that can be used in Quranic memorisation to improve learning motivation and interest among the younger generation. The gamification elements must be designed with structured learning activities that include summative and formative assessments, which allow students to receive instant feedback about their progress to capture the learning analysis in memorising the Quran. We are very excited about the impact and potential that such a dashboard provides to increase motivation and encourage the learning activities to be more fun and interesting. Therefore, the next step of this research will be to design a prototype that captures learning analysis in memorising the Quran. It is important to realise that future analysis to understand and obtain useful results should focus on usability issues and seriously investigate the users' motivation or interest in engaging with this new technology.

## ACKNOWLEDGMENTS

The Geran Dalaman Dana Universiti Teknologi MARA Cawangan Kelantan (600-TNCPI 5/3/DDN (03) (010/2020), 2020) supported this research.

## REFERENCES

- Abdullah, A. H., Safar, A., Mustari, M. I., Muhammad, A., & Ismail, I. (2003). *Keberkesanan kaedah hafazan di Pusat Tahfiz (Laporan penyelidikan)* [The effectiveness of the memorization method at the Tahfiz Center]. Pusat Pengajian Islam & Pembangunan Sosial, Universiti Teknologi Malaysia.
- Abdullah, A. H., & Muda, H. H. (2004, December 7-9). Kaedah hafazan Al-Qur'an yang sistematik dan praktikal dalam melahirkan para Huffaz yang Rasikh [A systematic and practical method of Al-Qur'an memorization in producing Rasikh Huffaz]. In *International Seminar On Islamic Thoughts Proceeding* (pp. 93-102), Universiti Kebangsaan Malaysia, Malaysia.
- Abro, B., Naqvi, A. B., & Hussain, A. (2012). Qur'an recognition for the purpose of memorisation using speech recognition technique. In *15th International Multitopic Conference (INMIC)* (pp. 30-33). IEEE Publishing. <https://doi.org/10.1109/inmic.2012.6511440>
- Adhoni, Z. A., Al Hamad, H., Siddiqi, A. A., & Adhoni, Z. A. (2014). An instant-based Qur'an memorizer application interface. In *2013 International Conference on Information Science and Cloud Computing Companion* (pp. 382-387). IEEE Publishing. <https://doi.org/10.1109/ISCC-C.2013.14>
- Adhoni, Z. A., Al Hamad, H., Siddiqi, A. A., Parvez, M., & Adhoni, Z. A. (2013). Cloud-based online portal and mobile friendly application for the Holy Qur'an. *Life Science Journal*, *10*, 524-538.
- Ahmad, H., Zainuddin, N. M. M., Ali, R., Maarop, N., Yusoff, R. C. M., & Hassan, W. A. W. (2018). Augmented reality to memorize al-Quran for hearing impaired students: A preliminary analysis. *Journal of Fundamental and Applied Sciences*, *10*(2S), 91-102. <https://doi.org/http://dx.doi.org/10.4314/jfas.v10i2s.8>
- Ahmad, N., Yaacob, M. T., Suratman, M. N., Shuib, S., Samsungei, M. A., Azali, M. F. M., Manaf, A. J. A., Abdullah, I., Sood, Z. M., Rahim, M. M. A., Sulaiman, S., Mudeen, N. S. N., Dahalan, S. B., Sham, N. H. M., Sidek, M. A. R., Zain, A. R. M., Muda, O., Zin, N. M., & Mansor, A. H. (2019). *Kaedah hafazan Al-Quran model Malaysia* [The Malaysian model Al-Quran memorization method]. Darul Quran JAKIM.
- Almosallam, E., Alawadh, M. M., Alhasani, R. S., Almansour, S. M., Altamimi, W. A., & Altujjar, Y. R. (2015). ITQAN: A mobile based assistant for mastering quran memorization. In *5th International Conference on E-Learning (ECONF 2015)* (pp. 349-352). IEEE Publishing. <https://doi.org/10.1109/ECONF.2015.42>
- Alomair, Y., & Hammami, S. (2020). A Review of Methods for Adaptive Gamified Learning Environments. In *2020 3rd International Conference on Computer Applications and Information Security (ICCAIS)* (pp. 0-5). IEEE Publishing. <https://doi.org/10.1109/ICCAIS48893.2020.9096871>
- Ambo, N. F., & Mokhsein, S. E. (2019). Trend and issue in learning strategy of Tahfiz Model Ulul Albab (TMUA). *International Journal of Academic Research in Business and Social Sciences*, *9*(7), 1418-1426. <https://doi.org/10.6007/ijarbss/v9-i7/6789>
- Anwar, M. A. (2019). Revitalizing the method of repetition in the recitation of the Qur'an. *Istawa: Jurnal Pendidikan Islam (IJPI)*, *4*(2), 156-167. <https://doi.org/10.24269/ijpi.v4i2.1995>
- Ariffin, S., Abdullah, M., Suliaman, I., Ahmad, K., Deraman, F., Shah, F. A., Zulkifli, Y., Yusoff, M., Munirah, M., Razzak, A., Murshidi, M., Noor, M., Meftah, J. T., Kasar, A. K., Amir, S., Roslan, M., & Nor, M. (2013). Effective techniques of memorizing the Quran: A study at Madrasah tahfiz Al-quran, Terengganu, Malaysia. *Middle-East Journal of Scientific Research*, *13*(1), 45-48. <https://doi.org/10.5829/idosi.mejsr.2013.13.1.1762>

- Aziz, M. M., Abdullah, W. M., Ahmad, A. M., Mushim, M. A. A., & Shahrudin, M. S. (2019). Comparison between conventional method and modern technology in Al-Qur'an memorization. *International Journal of Recent Technology and Engineering*, 8(1), 289-294.
- Bakri, A., Zakaria, N. H., Zainuldin, S. N. M., & AbuSafia, A. H. (2014). A Conceptual model of Al-Furqan courseware using persuasive system design for early learning childhood. In *8th Malaysian Software Engineering Conference (MySEC)* (pp. 336-341). IEEE Publishing.
- Böckle, M., Micheel, I., Bick, M., & Novak, J. (2018). A design framework for adaptive gamification applications. In *Proceedings of the 51st Hawaii International Conference on System Sciences* (pp. 1227-1236). University of Hawaii.
- Cano, A. R., Fernández-manjón, B., & García-Tejedor, Á. J. (2016). Downtown, a subway adventure: Using learning analytics to improve the development of a learning game for people with intellectual disabilities. In *2016 IEEE 16th International Conference on Advanced Learning Technologies (ICALT 2016)* (pp. 125-129). IEEE Publishing. <https://doi.org/10.1109/ICALT.2016.46>
- Cariaga, A. A., & Fera, R. (2015). Learning Analytics through a Digital Game-Based Learning Environment. In *6th International Conference on Information, Intelligence, Systems and Applications (IISA)* (pp. 1-3). IEEE Publishing. <https://doi.org/10.1109/IISA.2015.7387992>
- Chatti, M. A., Dyckhoff, A. L., Schroeder, U., & Thüs, H. (2012). A reference model for learning analytics. *International Journal of Technology Enhanced Learning*, 4(5-6), 318-331. <https://doi.org/10.1504/IJTEL.2012.051815>
- Deterding, S., Dixon, D., Khaled, R., & Nacke, L. (2011). From game design elements to gamefulness: Defining "gamification". In *Proceedings of the 15th International Academic MindTrek Conference on Envisioning Future Media Environments* (pp. 9-15). ACM Publishing. <https://doi.org/10.1145/2181037.2181040>
- Dzulkifli, M. A., Rahman, A. W. A., Solihu, A. K. H., & Ahmed, J. (2014). Optimizing human memory: An insight from the study of Al Huffaz. In *The 5th International Conference on Information and Communication Technology for the Muslim World (ICT4M)* (pp. 1-4). IEEE Publishing. <https://doi.org/10.1109/ICT4M.2014.7020624>
- Dzulkifli, M. A., & Solihu, A. K. H. (2018). Methods of Qur'anic memorisation (Hifz): Implications for learning performance. *Intellectual Discourse*, 26(2), 931-947.
- Frankenmolen, N. L., Overdorp, E. J., Fasotti, L., Claassen, J. A. H. R., Kessels, R. P. C., & Oosterman, J. M. (2018). Memory strategy training in older adults with subjective memory complaints: A randomized controlled trial. *Journal of the International Neuropsychological Society*, 24(10), 1110-1120. <https://doi.org/10.1017/S1355617718000619>
- Hamiz, M., Bakri, M., Haron, H., Sabri, S. M., & Jamil, N. (2014). Repetitive memorization mobile application development for elderly memory recall. In *2014 IEEE Conference on e-Learning, e-Management and e-Services (IC3e)* (pp. 150-155). IEEE Publishing. <https://doi.org/10.1109/IC3e.2014.7081258>
- Hashim, A. (2015). Correlation between strategy of Tahfiz learning styles and students performance in Al-Qur'an memorization (Hifz). *Mediterranean Journal of Social Sciences*, 6(2), 85-92. <https://doi.org/10.5901/mjss.2015.v6n2s5p85>

- Hassan, M. A., Habiba, U., Majeed, F., & Shoaib, M. (2021). Adaptive gamification in e-learning based on students' learning styles. *Interactive Learning Environments*, 29(4), 545-565. <https://doi.org/10.1080/10494820.2019.1588745>
- Ibrahim, F. W., Rahman, N. F. A., Rahman, S. A., Warif, N. M. A., Harun, D., Ghazali, A. R., Yahya, H. M., Ariffin, F., Mohamad, S., & Ishak, I. (2018). Dietary intake, levels of trace elements and intelligence quotient ( IQ ) among Huffaz students from selected Tahfiz schools in Selangor. *Jurnal Sains Kesihatan Malaysia Isu Khas 2018*, 129-136. <https://doi.org/http://dx.doi.org./10.17576/JSKM-2018-18>
- Ismail, M. J., Mohamad, S., Puji, T. T., & Yusof, N. H. (2017). Strategi kecemerlangan Institusi Pendidikan Tahfiz Al-Quran di Malaysia: Satu tinjauan literatur [The excellence strategy of Tahfiz Al-Quran educational institutions in Malaysia: A literature review]. *Jurnal Islam Dan Masyarakat Kontemporari*, 15, 55-65.
- Lavoué, E., Monterrat, B., Desmarais, M., & George, S. (2019). Adaptive gamification for learning environments. *IEEE Transactions on Learning Technologies, Institute of Electrical and Electronics Engineering*, 12(1), 16-28. <https://doi.org/10.1109/TLT.2018.2823710>
- Morschheuser, B., Hassan, L., Werder, K., & Hamari, J. (2018). How to design gamification? A method for engineering gamified software. *Information and Software Technology*, 95, 219-237. <https://doi.org/http://dx.doi.org/10.1016/j.infsof.2017.10.015>
- Moulana, S. J. (2017). *Synergy : Game Design + Qur'an Memorization* (Master thesis). Virginia Commonwealth University, USA. <https://doi.org/10.25772/JT9P-WA53>
- Muluk, S., Habiburrahim, H., & Rechal, S. R. (2020). Students' awareness and perception towards learning styles. *Jurnal Ilmiah Didaktika: Media Ilmiah Pendidikan dan Pengajaran*, 20(2), 143-164. <http://dx.doi.org/10.22373/jid.v20i2.5229>
- Mustafa, N. M., & Basri, M. (2014a). A preliminary study on mobile Quranic memorization for remote education learning using RFID technology: KUIS as a case study. *GLIT E-Journal Language Practice & Information Technology*, 45-50.
- Mustafa, N. M., & Basri, M. (2014b, June 9-10). Perbandingan kaedah hafazan al-Quran tradisional dan moden: Satu kajian awal. In *Proceeding of the Social Sciences Research ICSSR 2014* (pp. 827-834). Sabah, Malaysia.
- Mustafa, N. M., Zaki, Z. M., Mohamad, K. A., Basri, M., & Ariffin, S. (2019). The design of Quran memorization tool using low-fidelity prototype. *Advancing Technology Industrialization through Intelligent Software Methodologies, Tools and Techniques*, 318, 430-443. <https://doi.org/10.3233/FAIA190069>
- Nafi, N. M., Mokhtar, W. K. A. W., & Imas, M. M. (2019). The Holy Quran memorization in globalization era. *International Journal of Academic Research in Business and Social Sciences*, 9(11), 588-596. <https://doi.org/10.6007/IJARBS/v9-i11/6579>
- Ofosu-Ampong, K. (2020). The shift to gamification in education: A review on dominant issues. *Journal of Educational Technology Systems*, 49(1), 113-137. <https://doi.org/10.1177/0047239520917629>
- Priatna, T., Nurhamzah, N., Suryana, Y., & Nurdiansah, N. (2020). Developing management of Quran memorization institutions through the web system. *International Journal of Advanced Trends in Computer Science and Engineering*, 9(1), 465-468. <https://doi.org/10.30534/ijatcse/2020/63912020>

- Purbohadi, D., Rahmawati, B. R. N., & Setiawan, H. (2019). Development of Qur'an memorization learning model based on mobile learning. In *Journal of Physics: Conference Series*, 1381(1), 012029. IOP Publishing. <https://doi.org/10.1088/1742-6596/1381/1/012029>
- Rosmansyah, Y., Kartikasari, N., & Wuryandari, A. I. (2017). A learning analytics tool for monitoring and improving students' learning process. In *2017 6th International Conference on Electrical Engineering and Informatics (ICEEI)* (pp. 1-5). IEEE Publishing. <https://doi.org/10.1109/ICEEI.2017.8312462>
- Rosmansyah, Y., & Rosyid, M. R. (2017). Mobile learning with gamification for Alquran memorization. In *2017 International Conference on Information Technology Systems and Innovation (ICITSI)* (pp. 378-383). IEEE Publishing. <https://doi.org/10.1109/ICITSI.2017.8267974>
- Rouse, K. E. (2013). *Gamification in science education: The relationship of educational games to motivation and achievement* (Doctoral dissertation). The University of Southern Mississippi, USA.
- Rozi, F., Rosmansyah, Y., & Dabarsyah, B. (2019). A systematic literature review on adaptive gamification: Components, methods, and frameworks. In *2019 International Conference on Electrical Engineering and Informatics (ICEEI)* (pp. 187-190). IEEE Publishing. <https://doi.org/10.1109/ICEEI47359.2019.8988857>
- Sabbri, F. S. M. (2016). *Exploring student motivation and challenges in Tahfiz class in selected private Islamic secondary schools in Selangor: A case study* (Doctoral dissertation). International Islamic University Malaysia, Malaysia.
- Saleem, A. (2018). Memorization without comprehension: A window onto the 'extremities' of the capability of human brain. *Al-Idah*, 36(1), 25-40.
- Salehuddin, K., Shahimim, M. M., Sulaiman, M. Z., & Zolkapli, R. B. M. (2019). Heat maps and scan paths: Qualitative eye-tracking evidence on how the Qur'an is memorized through reading. *Journal of Nusantara Studies*, 4(2), 318-334. <https://doi.org/http://dx.doi.org/10.24200/jonus.vol4iss2pp318-334>
- Schunk, D. H. (2012). *Learning theories: An educational perspective* (6th Ed.). Pearson Education, Inc.
- Senan, N., Aziz, W. A. W. A., Othman, M. F., & Suparjoh, S. (2017). Embedding repetition (Takrir) technique in developing Al-Quran memorizing mobile application for autism children. In *MATEC Web of Conferences* (Vol. 135, p. 00076). EDP Sciences. <https://doi.org/10.1051/mateconf/201713500076>
- Sezgin, S., & Yüzer, T. V. (2020). Analysing adaptive gamification design principles for online courses. *Behaviour and Information Technology*, 41(3), 485-501.
- Shamsuddin, S. N. W., Bakar, N. F. A., Makhtar, M., Isa, W. M. W., Rozaimée, A., & Yusof, N. (2016). A framework for designing mobile Quranic memorization tool using multimedia interactive learning method for children. *Journal of Theoretical and Applied Information Technology*, 92(1), 20-27.
- Shukri, N. H. A., Nasir, M. K. M., & Razak, K. A. (2020). Educational strategies on memorizing the Quran: A review of literature. *International Journal of Academic Research in Progressive Education and Development*, 9(2), 632-648. <https://doi.org/10.6007/ijarped/v9-i2/7649>
- Verbert, K., Duval, E., Klerkx, J., Govaerts, S., & Santos, J. L. (2013). Learning analytics dashboard applications. *American Behavioral Scientist*, 57(10), 1500-1509. <https://doi.org/10.1177/0002764213479363>



- Yaacob, M. T., Suratman, M. N., Shuib, S., Samsungei, M. A., Azali, M. F. M., Manaf, A. J. A., & Abdullah, I. (2019). Kaedah hafazan Al-Quran model Malaysia teras panduan penghafaz Al-Quran [Al-Quran memorization method Malaysian model core Al-Quran memorization guide]. In A. H. H. Salihin, S. Ghazali, R. A. Latif, O. Muda & M. Z. Ismail (Eds.), *Darul Quran Selangor, JAKIM* (2019th Ed.). Darul Quran JAKIM.
- Yusoff, H., Anuar, A., Asmuni, A., & Arif, I. (2018). Characteristics of effective assatizah in higher religious institutions (HRIs). *International Journal of Academic Research in Business and Social Sciences*, 8(11), 168-180. <https://doi.org/10.6007/ijarbss/v8-i11/4893>
- Yusuf, S. A. M., Noh, M. A. C., & Razak, K. A. (2019). Tahfiz teachers ability in teaching of the subject Hifz Quran in implementing integrated curriculum Tahfiz (KBT) secondary schools. *International Journal of Academic Research in Business and Social Sciences*, 9(5), 836-850. <https://doi.org/10.6007/IJARBSS/v9-i5/6010>
- Zakariah, M., Khan, M. K., Tayan, O., & Salah, K. (2017). Digital Quran computing: Review, classification, and trend analysis. *Arabian Journal for Science and Engineering*, 42(8), 3077-3102. <https://doi.org/10.1007/s13369-017-2415-4>
- Zaki, Z. M., Mohamad, K. A., & Basri, M. (2019). *Kaedah hafalan Al-Quran berasaskan kecenderungan gaya pembelajaran VARK (Quran memorization method based on vark learning style)*. USIM. <https://doi.org/10.13140/RG.2.2.15097.21605>

Review Article

## A Review of Optical Ultrasound Imaging Modalities for Intravascular Imaging

Munyaradzi Charles Rushambwa<sup>1</sup>, Rimer Suvendi<sup>2</sup>, Thanyani Pandelani<sup>3</sup>, Rajkumar Palaniappan<sup>4\*</sup>, Vikneswaran Vijejan<sup>5</sup> and Fizza Ghulam Nabi<sup>6</sup>

<sup>1</sup>Electronic Engineering, Harare Institute of Technology, Harare, 277 Zimbabwe

<sup>2</sup>Department of Electrical and Electronic Engineering Science, Faculty of Engineering, and the Built Environments, University of Johannesburg, P.O. Box 524, Auckland Park, 2006, Johannesburg, South Africa

<sup>3</sup>Biomedical Engineering, Council for Scientific and Industrial Research (CSIR), 254 South Africa

<sup>4</sup>College of Engineering, Department of Mechatronics Engineering, University of Technology Bahrain, 18041 Kingdom of Bahrain

<sup>5</sup>BioSIM Group, Sport Engineering Research Centre, Universiti Malaysia Perlis, 02600 UniMAP, Arau, Perlis, Malaysia

<sup>6</sup>Department of Industrial Engineering and Management, University of the Punjab, Lahore, 54590 Pakistan

### ABSTRACT

Recent advances in medical imaging include integrating photoacoustic and optoacoustic techniques with conventional imaging modalities. The developments in the latter have led to the use of optics combined with the conventional ultrasound technique for imaging intravascular tissues and applied to different areas of the human body. Conventional ultrasound is a skin contact-based method used for imaging. It does not expose patients to harmful radiation compared to other techniques such as Computerised Tomography (CT) and Magnetic Resonance Imaging (MRI) scans. On the other hand, optical Ultrasound (OpUS) provides a new way of viewing internal organs of the human body by using skin and an eye-safe laser range. OpUS is mostly used for binary measurements since they do not require to be resolved at a much higher resolution but can be used to check

for intravascular imaging. Various signal processing techniques and reconstruction methodologies exist for Photo-Acoustic Imaging, and their applicability in bioimaging is explored in this paper.

#### ARTICLE INFO

*Article history:*

Received: 10 March 2022

Accepted: 24 May 2022

Published: 20 October 2022

DOI: <https://doi.org/10.47836/pjst.31.1.17>

*E-mail addresses:*

[mrushambwa@hit.ac.zw](mailto:mrushambwa@hit.ac.zw) (Munyaradzi Charles Rushambwa)

[suwendir@uj.ac.za](mailto:suwendir@uj.ac.za) (Rimer Suvendi)

[thanyanip@gmail.com](mailto:thanyanip@gmail.com) (Thanyani Pandelani)

[prkmeect@gmail.com](mailto:prkmeect@gmail.com) (Rajkumar Palaniappan)

[vicky.86max@gmail.com](mailto:vicky.86max@gmail.com) (Vikneswaran Vijejan)

[enfr.fizza@yahoo.com](mailto:enfr.fizza@yahoo.com) (Fizza Ghulam Nabi)

\*Corresponding author

**Keywords:** Imaging, intravascular, optoacoustic, photoacoustic, reconstruction, ultrasound

*Current affiliation*

**Thanyani Pandelani**

Department of Electrical and Electronic Engineering

Science, Faculty of Engineering, and the Built

Environments, University of Johannesburg, P.O. Box 524,

Auckland Park, 2006, Johannesburg, South Africa

## INTRODUCTION

Although ultrasound (US) has been used over decades as real-time imaging technology, using high-frequency sound waves generated by a piezoelectric transducer, it has its shortcomings (Wissmeyer et al., 2018). The shortcomings of the US are not limited to image variability introduced due to body-probe movements, low image spectra and the inability to be used for burnt victims or children. Nevertheless, it is possible to view the internal anatomical structure of human beings and see the movements of internal organs and blood flow using the US by reconstructing the amplitude and time of flight of the reflected acoustic waves into an image that can be displayed, stored, or analysed. Apart from the shortcomings of the US that arise from the movement in the contact of the surfaces, there is also limited signal quality due to the attenuation of the sound waves by air (Omidi et al., 2018). However, this is overcome by using a coupling medium (gel) between the probe and the contact skin. It is not the same as Laser Ultrasound (LUS), as it employs a different signal acquisition mechanism, which uses the light of two or more powered lasers that are transmitted in the air as they measure the acoustic vibrations.

As a result, LUS is applied as a technology that provides a non-contact mechanism and thus can be applied in situations where skin contact must be avoided, such as burn victims or children. We can apply LUS to expose human tissues using acoustic detectors and sources by having adequate resources and applying necessary optical designs and interferometry. The penetration and standoff distance from the target surface depends upon the imaging application and can be incorporated into the design (Berlet et al., 2014). Another optical imaging technology is Photoacoustic Computed Tomography (PACT) which is mainly a soft tissue imaging modality that uses optical contrast mechanism in combination with the conventional ultrasound detection mechanism (Chao et al., 2013). Photoacoustic Imaging (PA) imaging has been employed for the different optical spectra wavelengths ranging from X-Ray to Infrared, with Infrared (IR) having the least bandwidth and the least penetration (Hafizah et al., 2010).

The setup of the basic photoacoustic imaging system is almost the same. It consists of a transducer that transmits the laser pulses and, in turn, acquires the ultrasonic signals that have been reflected. These signals are used to reconstruct an image that will reflect the photoacoustic signals. For this kind of setup, there exist 2 kinds of OpUs interferometry and refractometry (Canagasabey et al., 2011). Interferometry can be realised using Michelson Interferometry (MI), Mach-Zehnder Interferometry (MZI), doppler or the resonator method. MI and MZI use a 2-beam technique in which a laser beam goes through 2 independent paths, one that is the US excited. The other path is used as a reference path, and the change that happens to the path taken by light is caused by the pressure received and instantiates a corresponding change in the beam intensity at the interferometer output. In contrast, in the doppler method, a doppler shift of the received US waves is measured and used to

reconstruct the signal. The resonator method is similar to the 2-beam technique, but the difference is that it uses an optical resonator to detect the US waves (Zhang et al., 2021).

## RELATED WORKS

There have been many approaches and advances in the fields of photoacoustic and optoacoustic imaging necessitated by the need to have 1) more volumetric approaches, 2) non-contact methods, and 3) remote scanning of images using the different photoacoustic and optoacoustic imaging techniques (Demian et al., 2014). US methods have produced more volumetric images of human tissues than other imaging modalities like MRI and CT. However, their geometry makes it difficult to use the US for a wider range of applications in terms of where they can be used on a human body. There has been slow progress in research using or adopting LUS as a novel technique for imaging due to its complexity and high cost involved in setting up the equipment required. In published and known research, LUS has been used in non-destructive testing and demonstrated tissue-mimicking phantoms.

Recently there has been progress in the use of LUS for in vivo human imaging by a team from MIT led by Zhang et al. (2019). Zhang et al. (2019) used 1,550 nanometres of two pulsed lasers of equal wavelength that turned the sound waves as they were reflected from a distance. They used one of the lasers from their setup for motion indication caused by sound waves, combining it with a mechanical laser scanning system, thus making it easy to generate images without any contact with the human subject. They did *ex vivo* tests using a gelatine-based phantom on pig tissue and four human subjects and compared their images with those from the standard ultrasound technique. In their evaluation, they noted that the images they obtained could not match the conventional US but noted that there is room to improve the image quality. Zhao et al. (2019) published a review article on optical ultrasound generation and detection for intravascular imaging. They reviewed recent developments in optical sound transmitters, detectors and all other optical ultrasound imaging systems applied to intravascular imaging. In their review, they highlighted the importance of having an all-optical based ultrasound imaging system and noted that it could be a breakthrough in imaging technologies. Of importance in their work is that they pointed out the need to have better performing all-optical imaging techniques where a varying pulse laser can be used since the generated ultrasound frequencies depend on the excitation light's pulse width.

The team also noted that various tissues exhibit individual optical absorption spectra; thus, using variegated wavelengths could be useful for profiling several tissue structures. Thompson et al. (2020) designed a laser-induced synthetic aperture ultrasound imaging system and took images using a breast-mimicking phantom. Comparing their results with those obtained using conventional ultrasound, they concluded that the difference between the images they took to those of the mimicking phantom was the contrast due

to the difference in the spectral absorption properties of the tissues under investigation. Finally, DiMarzio and Murray (2003) reviewed the different medical imaging techniques that combine light and ultrasound. Their research highlighted the importance of combining light and ultrasound as applied to spectroscopy and the ability to measure blood volume and blood oxygen, even though this might not yield good results since most biological tissues are highly scattering and their respective spatial resolution is not satisfactory.

In contrast, the use of US provided a better resolution, although not so satisfactory on soft tissues; they highlighted and concluded by recommending the need to combine the two techniques to be explored for different imaging tissues. Research by Halani et al. (2018) did not focus on laser ultrasound but used infra-red-based US imaging to diagnose and manage cutaneous diseases. The goal of combining the two modalities suggested a novel approach to diagnosing and managing skin lesions in a non-invasive manner (Halani et al., 2018). Their work focused on infrared compared to the LUS since there was no need for skin penetration; hence, they used infrared. However, the infrared-based method would offer low spatial resolution and might not produce better results if used for intravascular imaging. Colchester et al. (2019) focused on all-optical ultrasound imaging, where they used light to scan and synthesise an imaging aperture. They designed a handheld probe that provided video-rate imaging, and it was demonstrated *in vivo* on human tissue. It was accomplished using a single optic fibre US detector paired with discrete fibre optic US sources, as images were captured.

Zhang et al. (2019) characterised the sources of US signals as applied to biological tissues for imaging applications. In their work, they used a laser source of 800 to 2000 nm to generate LUS at the surface of the biological tissue. Their observation was that the LUS's energy in biological tissue was between 0.5 and 3 MHz, which led to increased acoustic energy as the optical absorption coefficient increased. The different wavelengths from 800 nm to 2000 nm were used to generate different images. They concluded that LUS has greater potential to be used as an effective imaging modality. Thompson et al. (2020) also concluded that the optical inhomogeneity nature of the biological tissues reduces the signal amplitude that happens because of reduced absorption and increased optical scattering. However, clinical iterations of LUS will require multipoint optical transmission and detection to amplify the acoustic source amplitudes and reduce the data acquisition time.

In their work on reconstruction methodologies, Burgholzer et al. (2008) described laser ultrasonics as having high absorption and penetration of the samples. They conducted this study to determine the contrast by varying acoustic impedance. Other research outputs were directed toward using fibre optics instead of the generated laser. As presented by Colchester et al. (2019), they worked on an optical fibre that produced pulsed excitation light in combination with a photo-acoustically excited coating for the generation of the US beam; using the Fabry-Perot setup, and they investigated the capabilities of imaging intraluminal

carotid arteries. Colchester et al. (2019) used the conventional signal processing technique involving depth-dependent filtering of the acquired image data followed by a fourth-order high pass Butterworth filter. Nuster et al. (2013) worked on a hybrid photoacoustic, and US imaging with optical US detection and images were acquired using the inverse Radon transform. They used phantoms to simultaneously get PA and US images by focusing the detectors onto a selected plane (Nuster et al., 2013).

## REVIEW METHODOLOGY

The search protocol used to obtain research information about optical ultrasound technologies is using “optical” AND ‘ultrasound’ AND ‘imaging’ yielding a total of 58 360 results with 37 603 publications done in the last 10 years. The search criteria show that the area of optical ultrasound is a very novel area considering that an estimated 64 per cent of the research has been done in the last 10 years from 1990. Narrowing the search to ‘reconstruction’ AND ‘algorithms’ yielded 44 results of publications in the last 10 years, including books, documents, journals, conference articles and theses. Of the 44 results, only 20 were reviewed and considered significant to this review. In the reviewed articles, we looked at the optical imaging techniques, application domain, signal processing and reconstruction methodologies and finally, the challenges and research opportunities addressed by the published research.

## SIGNAL PROCESSING AND RECONSTRUCTION METHODS

For the conventional US, there exist many reconstruction and visualisation techniques. 2D and 3D methods have been used in the past, with 3D methods including mechanical scanning, 2D array, positional tracking based free hand and untracked based free hand being preferred. For example, the most used 3D reconstruction methods are pixel-based, volume-based, and function-based method are the most used 3D reconstruction methods. Several signal processing and reconstruction methodologies exist for PA imaging. This chapter explores the signal processing techniques and the corresponding reconstruction methods used in this paper’s work. The Synthetic Aperture Focusing Technique (SAFT) is the most commonly used method for reconstruction since it is a low-cost and less complex technique (Trots et al., 2011; Kim et al., 2020). In this method, an image is simultaneously acquired from signal lines one frame at a time. The SAFT reduces the data bandwidth and system complexity by using low-rate sampling with signals transmitted to a computational backend computer that can sequentially perform beam forming as it reconstructs each signal to have B-mode images. The SAFT method is a Fourier domain reconstruction method that requires interpolation for spatial discretization (Trots et al., 2011 ). It is not possible to use the SAFT algorithm for signal processing but rather for optimal performance, to locate the

photoacoustic signals in the sample, time domain delay and sum-focused beam foaming techniques are mostly used. When time delay is used, backpropagation can usually be used for reconstruction, but this causes the introduction of artefacts due to a limited number of view angles. Ultrasound Brightness (US-B) mode images are taken from beamforming, and this technique is used to provide high spatial resolution and better image quality. Other signal processing techniques used with the SAFT algorithm include envelope detection and log compression; both can be used at the backend before reconstruction. In the US-B mode, the image processing steps are reversed to recover the US-post beam foamed Radio frequency (RF) data. The US post-beam foamed RF data is recovered using log compression and convolving the acoustic impulse response and the frequency information using B-mode images as the input. As reviewed in this chapter, several other reconstruction methods have been proposed and used in research. Recent advances in medical imaging research have shown machine learning and artificial intelligence being used for image reconstruction. One such method is using a deep learning algorithm as a reconstruction method, as proposed by Kim et al. (2020) and Peyton et al. (2018). Kim et al. (2020) worked on deep convolutional neural networks to overcome the issue of limited bandwidth and detection views, leading to severe structural loss and low image contrast. The advantage of using deep learning techniques is that they can be used for real-time clinical applications and can be trained. There is evidence from Kim et al. (2020) that if trained, deep learning techniques provide better reconstruction than conventional reconstruction methods, including delay and sum, minimum variance, delay multiply and sum and the iterative methods with compressed sensing. These mentioned methods are computationally complex to be applied for real-time image processing.

Kruizing et al. (2013) proposed a PA image reconstruction method that uses information from US and PA images to simulate the full PA pressure field. The algorithm developed focused on image completion and boundary suppression for the reconstruction. Their approach was similar to the iterative time reversal method that uses the K-wave but different in that the image completion method estimates the spectral proportion of each independent image data. Vu et al. (2018) proposed an image reconstruction algorithm for PA that uses MATLAB/CUDA-without-C++ code (MCC), MATLAB/C++/CUDA code (MCCC) and MATLAB-without-GPU code (MWGC) techniques to compare processing time and image quality using a cross-platform based on MATLAB and CUDA. The approach significantly reduces the reconstruction time by 5 times using the focal time-based backpropagation. Similarly, Nuster et al. (2013) used a method of integrating detectors for image reconstruction. However, they used A-waves are focused on a detecting area that has a size which is greater than the phantom size.

Zhang et al. (2014) proposed a joint variation and Lp-norm-based image reconstruction algorithm where the reconstructed image is updated by computing the sum of the image



variation values and the Lp-nom value. The iterations are used for an operator splitting framework using the Bazilai-Borwein step size selection method. The setup effectively reduced the image scanning time and improved the quality of the PA image.

## APPLICATION DOMAIN

A review from previous research showed that PA imaging could be applied for both deep penetration and lower penetration. The applications picked from the review mainly include brain imaging, tissue and vascular imaging and dermatology. The international society of optics and photonics through the work being done by Huang et al. (2013) on a new Ultrasound Computed Tomography (USCT) and PACT reconstruction mechanisms for transcranial brain imaging. This collaboration's main goal is to develop a better image reconstruction algorithm that produces better image quality to compensate for the noise introduced by the vibrations from acoustic aberrations. PA imaging has also been used to detect neurological disorders like stroke, tumour, and Alzheimer's. It was validated by Chen et al. (2021) using the Fabry Perot Interferometry (FPI) mesoscope for cerebrovascular mouse brain imaging using a photothermally tuneable FPI ultrasound sensor.

Another application for PA imaging is tissue and vascular imaging. For this application, novel applications involved using catheters embedded with LUS probes for tissue imaging. For example, a team at UCL developed an imaging probe that visualises tissues (Zhao et al., 2019). The transmission and detection of the US in their design are done using optical fibres, mainly designed for visualisations during clinical applications. Similarly, for tissue imaging. Little et al. (2020) evaluated the use of optical US for real-time visualisations of the coronary vasculature. Their method was intravascular and validated the application of optical imaging for vascular tissues. Little et al. (2020) also applied US imaging for intracoronary imaging, where pulsed OpUS transducers generate the US using the interferometry method to generate images. High-resolution images of less than 60  $\mu\text{m}$  axial and imaging depths of greater than 2 cm were realised using fibre optic transducers with a pressure of 21.5 MPa and bandwidth of 39.8 MHz.

The third most applied domain of PA is dermatology, where PA is used to image the skin and its properties. To validate the applicability of optical US imaging for dermatology, Csány et al. (2021) designed a device based on the optical US for imaging various skin pathogens. Their setup included a handheld device that combines optics and US to record images of various types of skin lesions. IR-based photoacoustic techniques have also been used for preclinical research to image the skin and skin lesions. Duric et al. (2013) used a waveform-based method to reconstruct breast images. As a follow-up to their recommendation in Huang et al. (2013), they are currently working on a new USCT and PACT reconstruction mechanism for transcranial brain injury.

## CHALLENGES AND RESEARCH OPPORTUNITIES

The conventional US uses a probe placed on the subject's surface whose biological tissues are under examination. It is not always desirable for children and burns victims because of the pressure required to maintain acoustic distance between the probe and the tissues. The probe consists of a transducer array and is pressed against the skin using a coupling gel to transmit the waves into the tissue. Apart from the pain added to the burn victims due to contact, contact-based US also cause image variability due to contact and movements introduced by both the subject and the physician. The conventional US has a low degree of reproducibility since the user has to define the image orientation and field of view by manually adjusting the transducer placements resulting in acquiring patients' images at different times, making it difficult to compare the images taken. Light ultrasound can be used to tackle the problems of using the conventional US. Another alternative would be to use photoacoustic imaging, but with this method, the light is attenuated by the biological tissue; hence, the laser's penetration is needed for intravascular imaging. One would also note that from the work done so far, there is a need for high accuracy in research. Huang et al. (2013) presented the necessity to compensate for time structures by proposing a hybrid imaging system that makes use of PACT and USCT PA imaging has proved to be able to produce high-quality images with better contrast and high spatial resolution. However, for the materials used, in comparison with other techniques, optical US detection techniques have higher sensitivity over a wider bandwidth. It is easier to miniaturize optical transducers and expand the field of application. For high accuracy, Huang et al. (2013) proposed the necessity for compensating time structures by proposing a hybrid system that uses PACT and USCT. Another challenge of PA imaging, as highlighted by Chen et al. (2019), is that most clinical US systems do not have an interface for synchronising channel data from optoacoustic images. Manwar et al. (2020) noted that optical US detection methods are relatively slow, complex and costly to set up. Continuous-wave lasers in such setups make the system more sensitive to temperature changes and vibrations (Manwar et al., 2020). For the evaluation of the refractometry and the interferometry method, research shows that the phase-sensitive refractometry method has a higher bandwidth than the corresponding MZI and doppler counterparts.

Among other benefits, LUS can help remote imaging without contact with the body surface. Body surfaces can add harmful toxins to patients' skin, which is not always feasible for burnt patients and infants. By using LUS, physicians can image different positions since light can penetrate all directions. In addition, LUS has greater bandwidth and thus can be used to image tissues of different optical spectra. Without contact, there is no damage to the skin since light is used, and a safe range of Laser is used and has no radiation effects.

## CONCLUSION AND DISCUSSION

Most research in Photoacoustic Imaging (PAI) has been done using laser and fibre optic cables because of their higher bandwidths and applicability for intravascular imaging. 2 different methods have been reviewed in this paper the Interferometry method and the Refractometry method for the setup of the optical design. In addition, different signal processing techniques and reconstruction methodologies have been reviewed, with the SAFT being the most commonly used reconstruction method. Various application domains for PA have been identified, and it can be concluded that brain imaging, vascular and tissue imaging and dermatology are the main application areas for PAI. Several challenges and opportunities have been presented by different authors in previous research and should be used to perfect research in PAI. The ability to use both PACT and USCT present novel techniques for optical bioimaging using the conventional hardware permitting multimodal imaging that produces high quality images. Optical Coherence Tomography (OCT) has been used as an alternative to LUS but uses ballistic photons for detection.

In contrast, PAI has deeper penetration since it uses diffused photons to provide greater resolution at the end. Therefore, it can be concluded that optical ultrasound has a greater potential in clinical imaging. However, the future use of the technique depends on the changes in data acquisition, laser techniques and the transducer technology based on the application domain.

## ACKNOWLEDGEMENT

The writers would like to acknowledge the Electrical and Electronic Engineering department of the University of Johannesburg for providing resources and facilitating this collaborative research. In addition, much gratitude is given to the Department of Electronic Engineering at Harare Institute of Technology for their profound willingness to work on collaborative research. Finally, extended gratitude goes to the department of Mechatronics Engineering at the University of Technology Bahrain for providing necessary library information services for conducting this research.

## REFERENCES

- Berlet, T., Fehr, T., & Merz, T. M. (2014). Current practice of lung ultrasonography (LUS) in the diagnosis of pneumothorax: A survey of physician sonographers in Germany. *Critical Ultrasound Journal*, 6(1), 16-16. <https://doi.org/10.1186/s13089-014-0016-y>
- Burgholzer, P., Berer, T., Reitinger, B., Nuster, R., & Paltauf, G. (2008). Photoacoustic imaging and laser-ultrasonics using Fourier domain reconstruction methods. *The Journal of the Acoustical Society of America*, 123(5), 3156-3156. <https://doi.org/10.1121/1.2933188>
- Canagasabay, A., Michie, A., Canning, J., Holdsworth, J., Fleming, S., Wang, H. C., & Åslund, M. L. (2011). A comparison of Michelson and Mach-Zehnder interferometers for laser linewidth measurements. In *Conference on Lasers and Electro-Optics/Pacific Rim* (p. C428). Optical Society of America.

- Chao, H., Kun, W., Lihong, V. W., & Mark, A. A. (2013). Image reconstruction in photoacoustic tomography with heterogeneous media using an iterative method. In *Photons Plus Ultrasound: Imaging and Sensing 2013* (Vol. 8581, pp. 37-44). SPIE Publishing.
- Chen, Y., Chen, B., Yu, T., Yin, L., Sun, M., He, W., & Ma, C. (2021). Photoacoustic mouse brain imaging using an optical fabry-pérot interferometric ultrasound sensor. *Frontiers in Neuroscience*, 15, Article 672788. <https://doi.org/10.3389/fnins.2021.672788>
- Chen, Z., Mu, X., Han, Z., Yang, S., Zhang, C., Guo, Z., Bai, Y., & He, W. (2019). An optical/photoacoustic dual-modality probe: Ratiometric *in/ex vivo* imaging for stimulated H<sub>2</sub>S upregulation in mice. *Journal of the American Chemical Society*, 141(45), 17973-17977. <https://doi.org/10.1021/jacs.9b09181>
- Colchester, R. J., Little, C., Dwyer, G., Noimark, S., Alles, E. J., Zhang, E. Z., Loder, C. D., Parkin, I. P., Papakonstantinou, I., Beard, P. C., Finlay, M. C., Rakhit, R. D., & Desjardins, A. E. (2019). All-optical rotational ultrasound imaging. *Scientific Reports*, 9(1), Article 5576. <https://doi.org/10.1038/s41598-019-41970-z>
- Csány, G., Gergely, L. H., Szalai, K., Lőrincz, K. K., Strobel, L., Csabai, D., Hegedüs, I., Marosán-Vilimszky, P., Füzési, K., Sárdy, M., & Gyöngy, M. (2021). *First clinical experience with a novel optical-ultrasound imaging device on various skin pathologies*. medRxiv Preprint. <https://doi.org/10.1101/2021.06.28.21259325>
- Demian, D., Duma, V. F., Sinescu, C., Negrutiu, M. L., Cernat, R., Topala, F. I., Hutiu, G., Bradu, A., & Podoleanu, A. G. (2014). Design and testing of prototype handheld scanning probes for optical coherence tomography. *Journal of Engineering in Medicine*, 228(8), 743-753. <https://doi.org/10.1177/0954411914543963>
- DiMarzio, C. A., & Murray, T. W. (2003). Medical imaging techniques combining light and ultrasound. *Subsurface Sensing Technologies and Applications*, 4(4), 289-309. <https://doi.org/10.1023/a:1026300631323>
- Duric, N., Littrup, P., Roy, O., Schmidt, S., Li, C., Bey-Knight, L., & Xiaoyang, C. (2013). Breast imaging with ultrasound tomography: Initial results with SoftVue. In *2013 IEEE International Ultrasonics Symposium (IUS)* (pp. 382-385). IEEE Publishing. <https://doi.org/10.1109/ULTSYM.2013.0099>
- Hafizah, M., Kok, T., & Spriyanto, E. (2010, May 29-31). 3D ultrasound image reconstruction based on VTK. In *Proceedings of the 9th WSEAS International Conference on Signal Processing* (pp. 102-106). Catania, Italy.
- Halani, S., Foster, F. S., Breslavets, M., & Shear, N. H. (2018). Ultrasound and infrared-based imaging modalities for diagnosis and management of cutaneous diseases. *Frontiers in Medicine*, 5, 115-115. <https://doi.org/10.3389/fmed.2018.00115>
- Huang, C., Wang, K., Nie, L., Wang, L. V., & Anastasio, M. A. (2013). Full-wave iterative image reconstruction in photoacoustic tomography with acoustically inhomogeneous media. *IEEE Transactions on Medical Imaging*, 32(6), 1097-1110. <https://doi.org/10.1109/tmi.2013.2254496>
- Kim, M., Jeng, G. S., Pelivanov, I., & O'Donnell, M. (2020). Deep-learning image reconstruction for real-time photoacoustic system. *IEEE Transactions on Medical Imaging*, 39(11), 3379-3390. <https://doi.org/10.1109/tmi.2020.2993835>
- Kruizinga, P., Mastik, F., Koeze, D., de Jong, N., van der Steen, A. F., & van Soest, G. (2013). Ultrasound-guided photoacoustic image reconstruction: image completion and boundary suppression. *Journal of Biomedical Optics*, 18(9), 1-10. <https://doi.org/10.1117/1.jbo.18.9.096017>

- Little, C., Colchester, R. J., Manmathan, G., Rakhit, R. D., & Desjardins, A. E. (2020). All-optical ultrasound: A new platform for intracoronary imaging. *Journal of the American College of Cardiology*, 75(11), 1348-1348. [https://doi.org/10.1016/s0735-1097\(20\)31975-6](https://doi.org/10.1016/s0735-1097(20)31975-6)
- Manwar, R., Kratkiewicz, K., & Avnaki, K. (2020). Overview of ultrasound detection technologies for photoacoustic imaging. *Micromachines*, 11(7), Article 692. <https://doi.org/10.3390/mi11070692>
- Nuster, R., Schmitner, N., Wurzing, G., Gratt, S., Salvenmoser, W., Meyer, D., & Paltauf, G. (2013). Hybrid photoacoustic and ultrasound section imaging with optical ultrasound detection. *Journal of Biophotonics*, 6(6-7), 549-559. <https://doi.org/10.1002/jbio.201200223>
- Omidi, P., Zafar, M., Mozaffarzadeh, M., Hariri, A., Haung, X., Orooji, M., & Nasiriavanaki, M. (2018). A novel dictionary-based image reconstruction for photoacoustic computed tomography. *Applied Sciences*, 8(9), Article 1570. <https://doi.org/10.3390/app8091570>
- Peyton, G., Boutelle, M. G., & Drakakis, E. M. (2018). Comparison of synthetic aperture architectures for miniaturised ultrasound imaging front-ends. *BioMedical Engineering OnLine*, 17(1), Article 83. <https://doi.org/10.1186/s12938-018-0512-6>
- Thompson, D., Kruit, H., Gasteau, D., & Manohar, S. (2020). Laser-induced synthetic aperture ultrasound imaging. *Journal of Applied Physics*, 128(16), Article 163105. <https://doi.org/10.1063/5.0023412>
- Trots, I., Nowicki, A., Lewandowski, M., & Tasinkevych, Y. (2011). Synthetic aperture method in ultrasound imaging. In M. Tanabe (Ed.), *Ultrasound Imaging* (pp. 37-56). IntechOpen.
- Vu, T., Wang, Y., & Xia, J. (2018). Optimizing photoacoustic image reconstruction using cross-platform parallel computation. *Visual Computing for Industry, Biomedicine, and Art*, 1(1), 1-6. <https://doi.org/10.1186/s42492-018-0002-5>
- Wissmeyer, G., Pleitez, M. A., Rosenthal, A., & Ntziachristos, V. (2018). Looking at sound: Optoacoustics with all-optical ultrasound detection. *Light: Science & Applications*, 7(1), Article 53. <https://doi.org/10.1038/s41377-018-0036-7>
- Zhang, C., Zhang, Y., & Wang, Y. (2014). A photoacoustic image reconstruction method using total variation and nonconvex optimization. *BioMedical Engineering OnLine*, 13(1), Article 117. <https://doi.org/10.1186/1475-925x-13-117>
- Zhang, J., He, Q., Xiao, Y., Zheng, H., Wang, C., & Luo, J. (2021). Ultrasound image reconstruction from plane wave radio-frequency data by self-supervised deep neural network. *Medical Image Analysis*, 70, Article 102018. <https://doi.org/https://doi.org/10.1016/j.media.2021.102018>
- Zhang, X., Fincke, J. R., Wynn, C. M., Johnson, M. R., Haupt, R. W., & Anthony, B. W. (2019). Full noncontact laser ultrasound: First human data. *Light: Science & Applications*, 8(1), Article 119. <https://doi.org/10.1038/s41377-019-0229-8>
- Zhao, T., Desjardins, A. E., Ourselin, S., Vercauteren, T., & Xia, W. (2019). Minimally invasive photoacoustic imaging: Current status and future perspectives. *Photoacoustics*, 16, Article 100146. <https://doi.org/https://doi.org/10.1016/j.pacs.2019.100146>



## Timekeeping and Immediate Monitoring of Employees by Consistently Advocating Time Consciousness and Honesty Using Enhanced Attendance Monitoring System (TIME CATCH Using EAMS)

Ronald Bautista Rivera<sup>1\*</sup>, Maricar Bulan Asis<sup>2</sup> and Oscar Gacutan Bangayan<sup>3</sup>

<sup>1</sup>Department Isabela State University-Angadanan Campus, San Fabian, Echague, Isabela 3309, Philippines

<sup>2</sup>Human Resource Management Office, Isabela State University-Angadanan Campus, Echague, Isabela 3309, Philippines

<sup>3</sup>Office of the Campus Administrator, Isabela State University-Angadanan Campus, Echague, Isabela 3309, Philippines

### ABSTRACT

Attendance management methods that use QR codes and face recognition technology to identify and verify an individual's features are widely used in many aspects of people's lives nowadays, notably in pandemic situations where contact-less systems are used. In this paper, the development of enhanced attendance monitoring system using was introduced. The Isabela State University Angadanan Campus has implemented a biometric attendance monitoring system. However, it is limited to the number of employees' registrations, leave management and generation of Daily Time Record. The biometric system can only store 60 employees in every device, leave application and credits cannot be catered by the system and the Daily Time Record is not auto-generated and auto-formatted. For this reason, an enhanced attendance monitoring system was developed. The system uses a camera and QR Code reader to take attendance electronically, and the attendance

records be saved in a database. It can store multiple number of employees, process leave application, manage remaining leave credits, and provide auto-generated Daily Time Record. This method, on the other hand, reduces the requirement for fixed materials and employees to retain records. From the developed system and the gathered data, it has addressed the problem of the conventional way of checking employee's

### ARTICLE INFO

#### Article history:

Received: 13 October 2021

Accepted: 18 April 2022

Published: 09 November 2022

DOI: <https://doi.org/10.47836/pjst.31.1.18>

#### E-mail addresses:

[ronald.b.rivera@isu.edu.ph](mailto:ronald.b.rivera@isu.edu.ph) (Ronald Bautista Rivera)

[maricar.b.asis@isu.edu.ph](mailto:maricar.b.asis@isu.edu.ph) (Maricar Bulan Asis)

[oscar.g.bangayan@isu.edu.ph](mailto:oscar.g.bangayan@isu.edu.ph) (Oscar Gacutan Bangayan)

\*Corresponding author



attendance. The general mean of 4.72 shows that the software quality of the system based on ISO 25010 is found to be functional that the users have strongly agreed on the different characteristics of the system as it addresses the issues in the current attendance monitoring system of ISU.

*Keywords:* Attendance, QR code, face recognition

---

## INTRODUCTION

During the pandemic, government agencies were urged to cease the usage of the Biometric Fingerprint Attendance Monitoring system. As a result, the use of biometrics as a prerequisite for employee attendance is being phased out to stop the spread of the coronavirus disease. Temporarily, employees have to sign in a logbook located in their respective offices. However, logbooks are not a viable way to guarantee employee safety and capture employee logs since human contact with surfaces contaminated with the COVID19 virus is one exposure route in the transmission of infectious diseases (Hale & Song, 2020).

The Isabela State University-Angadanan Campus has also implemented a biometric system as a basis for employees' attendance. Because the system uses biometric fingerprint verification technology, it is not recommended to be used because employees are still prone to contacting the biometric device that other employees use. More specifically, the system is limited to the number of registered employees, requiring them to provide additional sets of biometric devices for casting attendance logs. Occasionally, the biometric system is incapable of capturing/recognizing fingerprints, necessitating the manual entry of time logs on printed sheets of paper. In the case of Daily Time Record rendering, the system can only export attendance logs in the form of excel files, which necessitates the in-charge downloading and reformatting logs at the end of each month, which consumes a significant amount of preparation time. Another issue is leave management; because the biometric system can only capture attendance logs, leave credits must be manually managed and kept by the Human Resource Management Office. Explicitly, there are flaws in the biometric system's efficiency report on matters pertaining to the attendance system.

TIME CATCH using EAMS was developed to enhance the system to address issues in Timekeeping and Immediate Monitoring of Employees' attendance while implementing contactless transactions. EAMS (Enhanced Attendance Monitoring System) is a network-based system that uses Face recognition and QR code technology for employees' contactless transactions. It is also capable of (1) Registration of employees with an auto-generated ID system, (2) Face Recognition and QR Code Casting employees' attendances, (3) Automatic Generation of DTR, (4) Automatic Management of Employees' Leaves and (5) Live Dashboard for Immediate Monitoring. Using the developed system, the Isabela State University-Angadanan Campus can ensure TIME CATCH (Timekeeping and Immediate

Monitoring of Employees logs by Consistent Advocating Time Consciousness and Honesty) even during this time of the pandemic.

## MATERIALS AND METHODS

This study’s main concern is attaining the objective by following the processes to create a successful project. Therefore, the researcher used the Rapid Application Development Approach, where sequences and various phases were determined, followed, and stated for the accomplishment of the research project, illustrated in Figure 1.

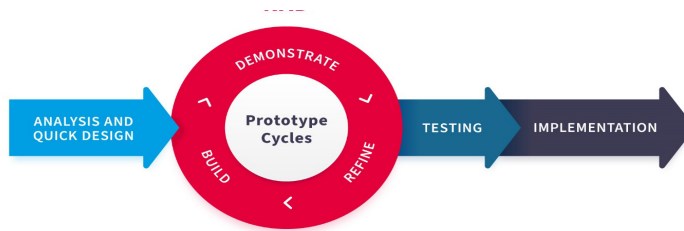


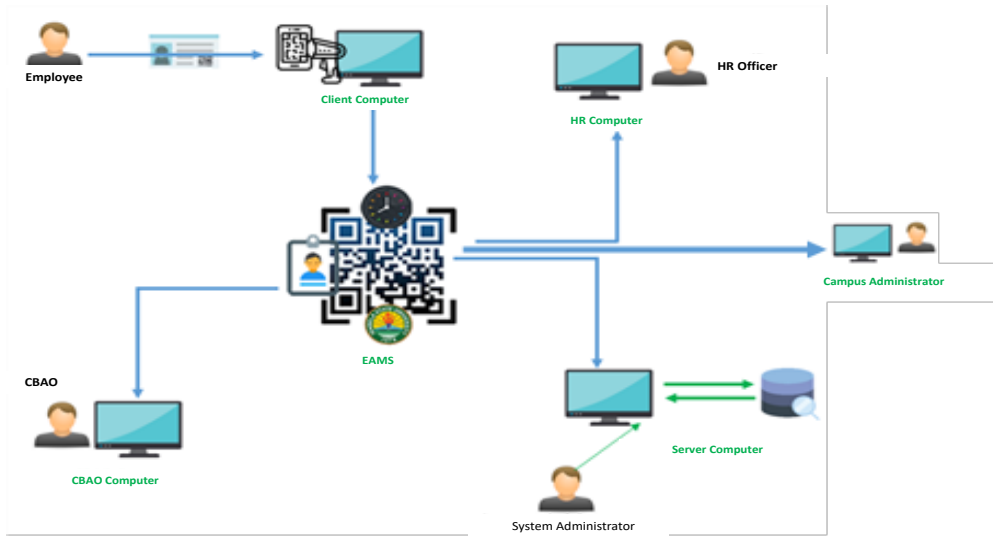
Figure 1. Software development model

### Analysis and Quick Design

To determine the essential features that will be added to the study, the researchers contacted the concerned staff or ended users for features and add-ons to be incorporated into the system. Furthermore, as a foundation for report automation, the researchers gathered HR reports such as the leave form and the DTR. After the collection of data, the system design was created.

### System Design

Figure 2 explains the system design. Employee attendance is recorded by scanning their QR code and using facial recognition software. After the verification and identification processes, if an employee’s QR code and Image model are validated and present in the database, his or her attendance will be updated. The HR is the only user with the sole authority to update employee information and issue auto-generated Daily Time Record (DTR). The campus administrator can monitor the live dashboard of the system, viewing and printing reports links, overall employee matter list, and the employees per department. Meanwhile, the Campus Business Affairs Office (CBAO) is responsible for printing Employees’ QR Code cards. Finally, the System Administrator sets the overall system settings and configurations.



-1

Figure 2. System architecture

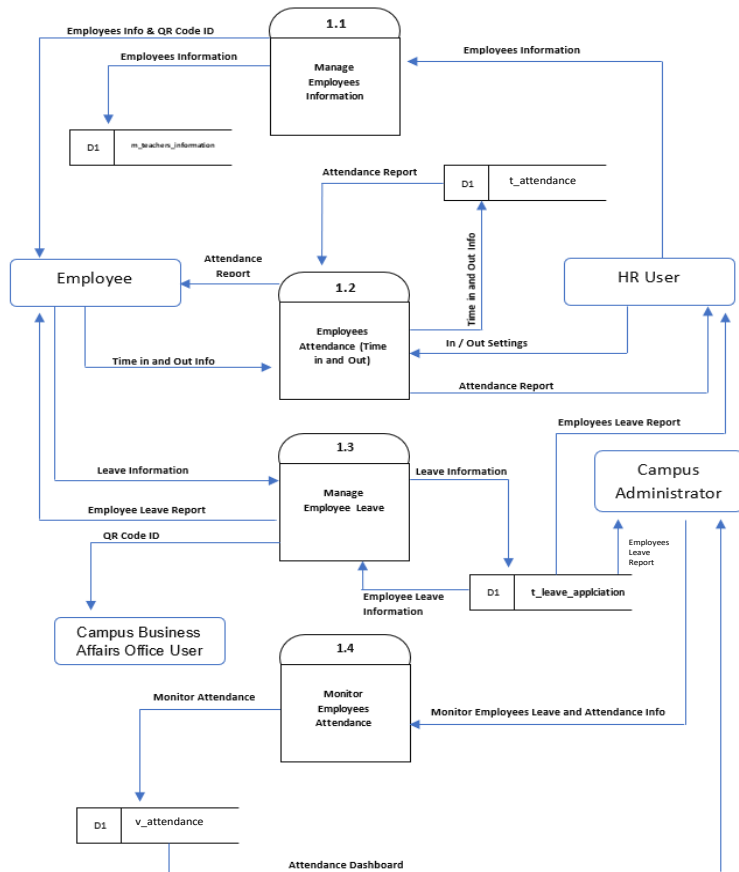


Figure 3. Data flow diagram of the developed system

Figure 3 shows the Data Flow Diagram of the developed TIME CATCH (Timekeeping and Immediate Monitoring of Employees by Consistently Advocating Time Consciousness and Honesty) using EAMS (Enhanced Attendance Monitoring System). The first process begins with the HR User registering each employee’s information. Next, a QR code ID printed by the Campus Business Affairs Office user shall be given to each employee. Finally, employees cast their attendance using their QR codes and captured images. Employees can also file their leave application reflected in the live dashboard monitoring of both HR and Campus Administrator Users. The Figure 4 shows the entity relationship of diagram of the developed system it illustrates the connection of every table in the database.

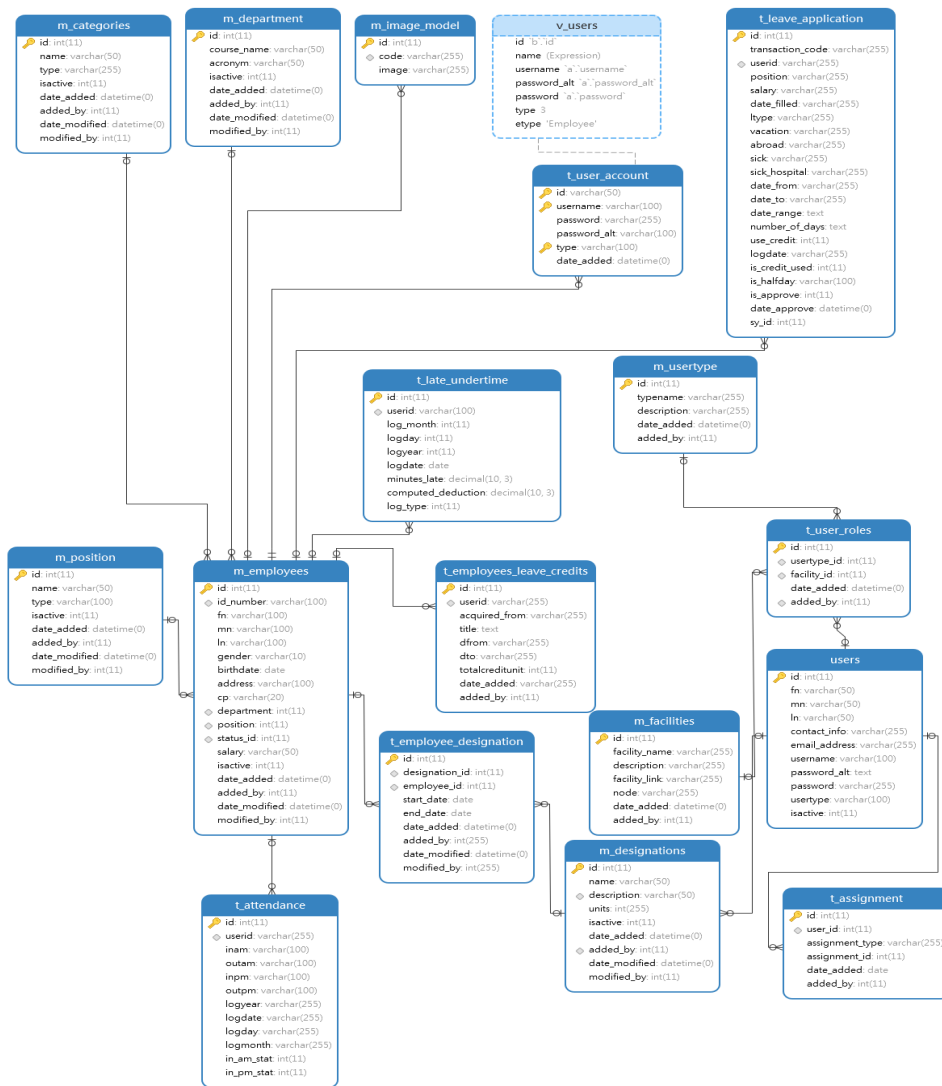


Figure 4. The entity relationship diagram of the developed system

**Prototyping.** Prototyping and actual programming were used to create the program's working interface. The following software was used during the development phase:

- Visual Studio 2010—The client module/attendance window is a window-based application invoked every time the client's computer runs. Visual Studio 2010 was used to develop the attendance window because of its capability to create compiled window-based applications. Moreover, the class libraries of face recognition and QR Code are supported by VB2010.
- PHP—PHP was used as the programming language in constructing the administrator module, particularly in writing server-side scripting language that communicates the UI (User Interface) elements to the database.
- MySQL—served as the database engine of the system. SQL Queries were also used to transact data from the system user's UI (User Interface) to the Database Tables. SQL was also used to extract and visualize data coming from the database. These data were the employee's information, attendance information and leave information.
- Bootstrap 2.4 AdminLTE—Bootstrap is an HTML, CSS and JS Library used to simplify the development of a responsive website. Bootstrap 2.4 AdminLTE is a bootstrap template used to design the system's UI (User Interface) using cards, panels, grids, form elements, navigation, tables and modals.

**Alpha Testing.** The researchers used it to test for faults and other technical issues that could emerge during the creation of a system.

**Beta Testing.** It tested and deployed the system to users (Employees, HR officers and the Systems Administrator).

**System Implementation.** It was done to see how the program complies with the set requirements. The implementation phase is covered by the methods listed below:

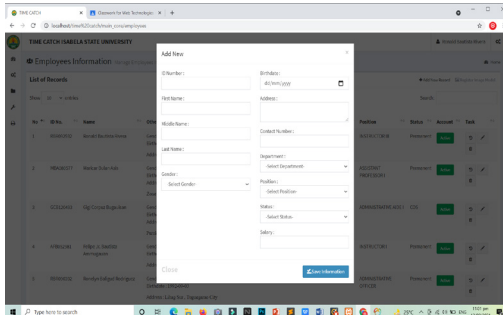
### **Employees Registration**

Employee information is entered in the appropriate field by entering the employee's ID number, name, birthdate, contact number, address, department, job status, and salary (Figure 5). The employee information is then registered. The CBAO (Campus Business Affairs Office) prints the QR Code card once registration is complete.

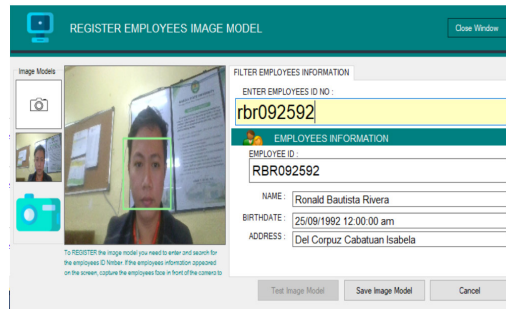
### **Casting of Attendance Logs**

The attendance window is used in casting employee logs, where attendance is taken by scanning the employee's QR code and capturing their face through facial recognition for verification purposes (Figure 6). Employee attendance is automatically recorded in the database once an account has been verified.

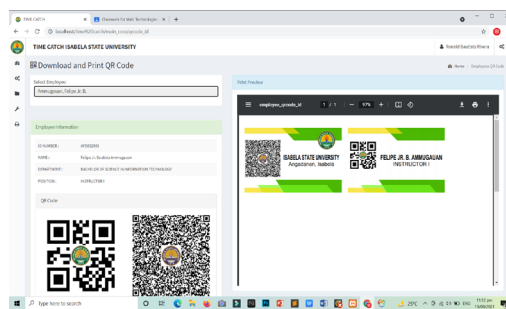
Timekeeping and Immediate Monitoring of Employees by Using EAMS



(a)

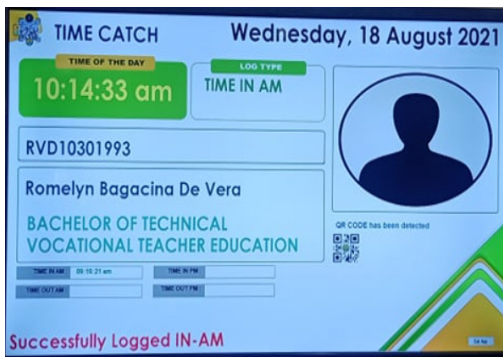


(b)

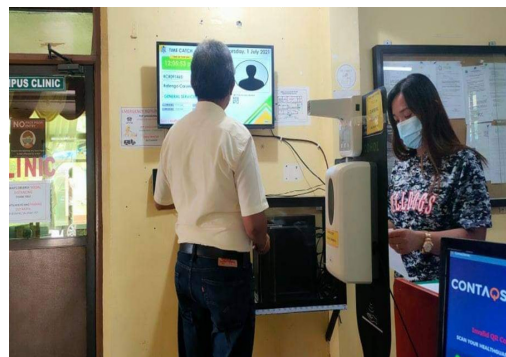


(c)

Figure 5. Employees registration



(a)



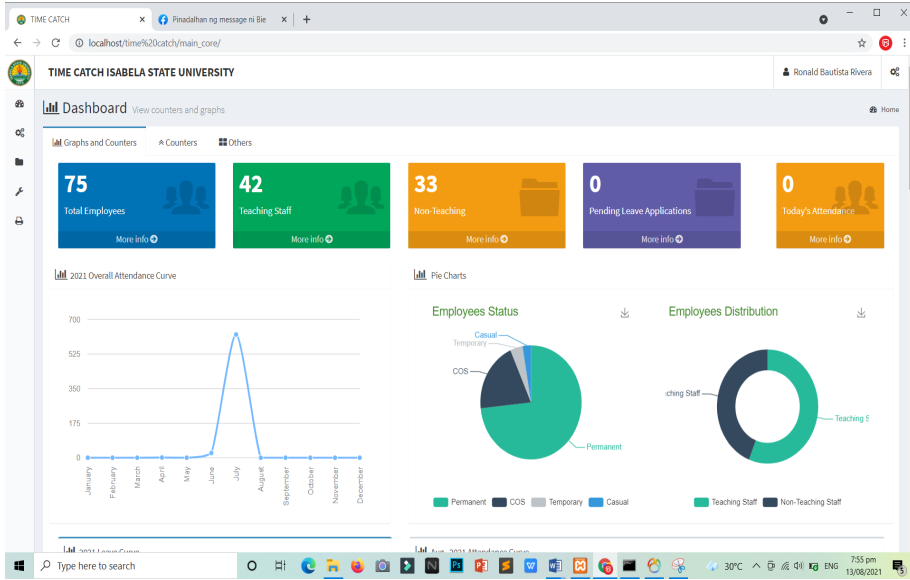
(b)

Figure 6. Casting of attendance logs

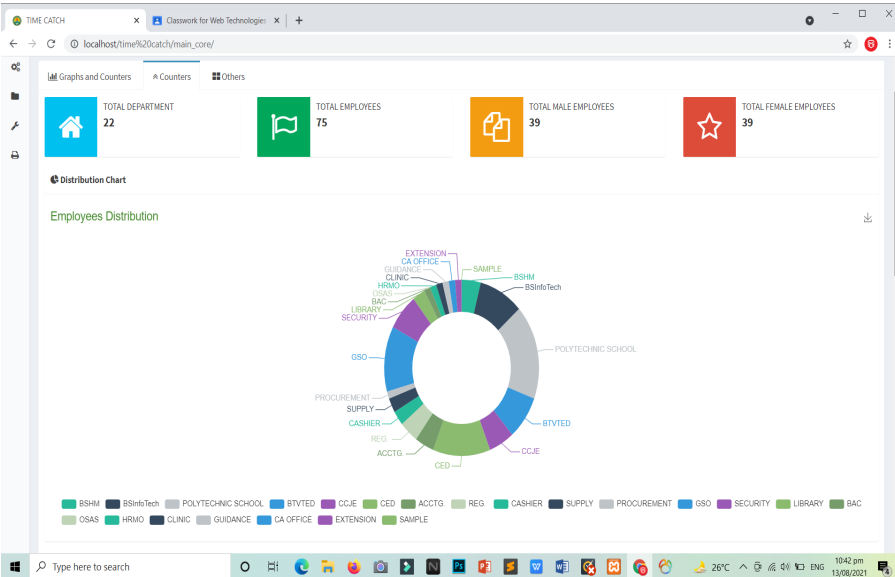
The Monitoring Dashboard

The Monitoring and Dashboard module (Figure 7) lets users view the system’s live dashboard. The module includes counters which can view the number of teaching and non-teaching staff, the total number of employees, pending leave applications and the number of attendances on the current date. The module also includes graphs for attendance, employees’ status pie chart, leave and attendance curve, and employees distribution graph.

The monitoring dashboard module can be viewed by the campus administrator, the Human Resource Officer and the Program Chairs or Deans of Isabela State University.



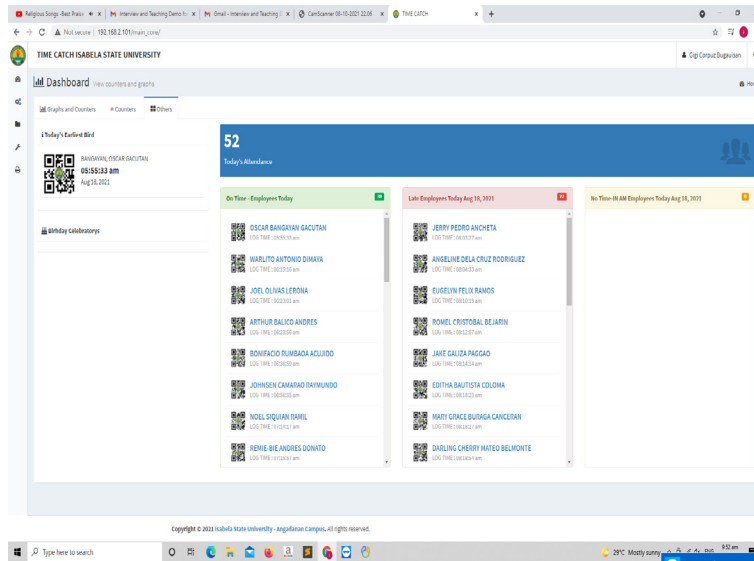
(a)



(b)



## Timekeeping and Immediate Monitoring of Employees by Using EAMS

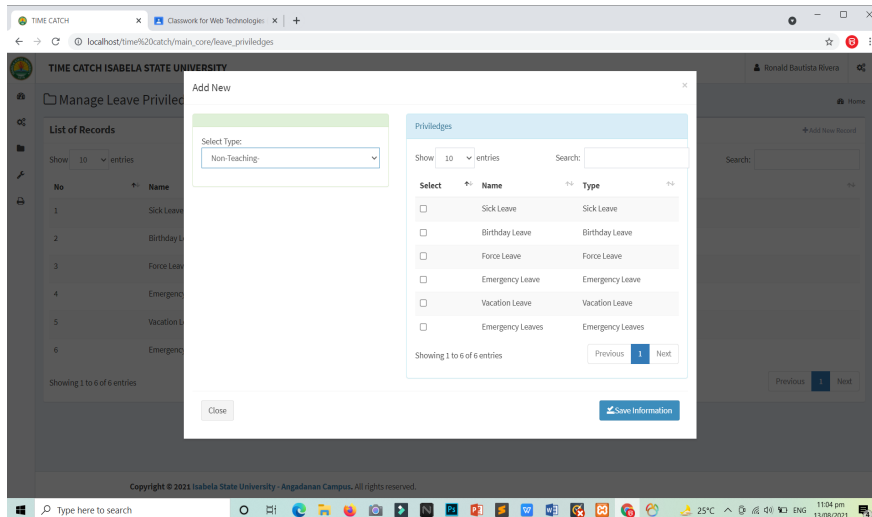


(c)

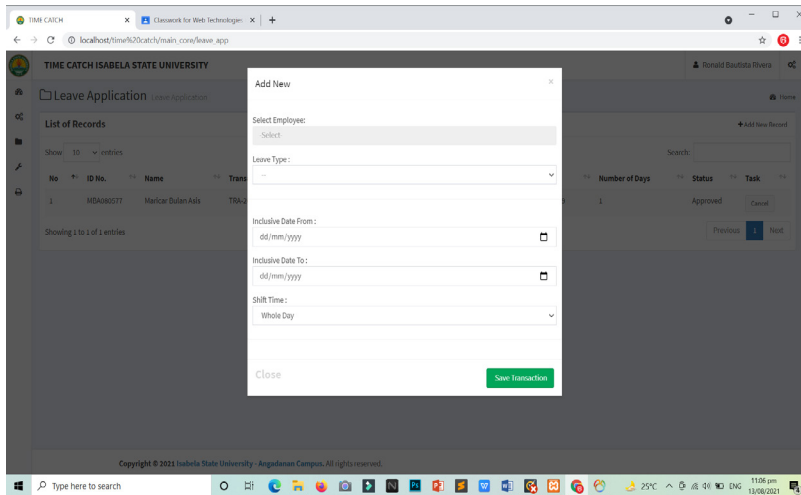
Figure 7. The monitoring dashboard

## The Leave Application

Employees use the Leave Application Module (Figure 8) to submit a leave request. It begins with the processing of leave entitlements by the Human Resource Officer. Next, the various leave entitlements applicable to each type of job are labeled. Finally, every employee's leave request must be reviewed and approved by their immediate supervisor's account (Program Chair/Dean Account). If the leave application is approved, a leave application form is printed. Otherwise, a leave request will be marked as declined.



(a)



(b)



(c)

Figure 8. The leave application module: (a) Manage leave privileges; (b) Add leave application; (c) Leave form

### The Credit Units Manager

The credit unit manager module manages an employee’s credit units. The user will simply add an employee’s credit unit, tag the source from which the credit unit was obtained, encode the inclusive dates, and save it (Figure 9).

## Timekeeping and Immediate Monitoring of Employees by Using EAMS

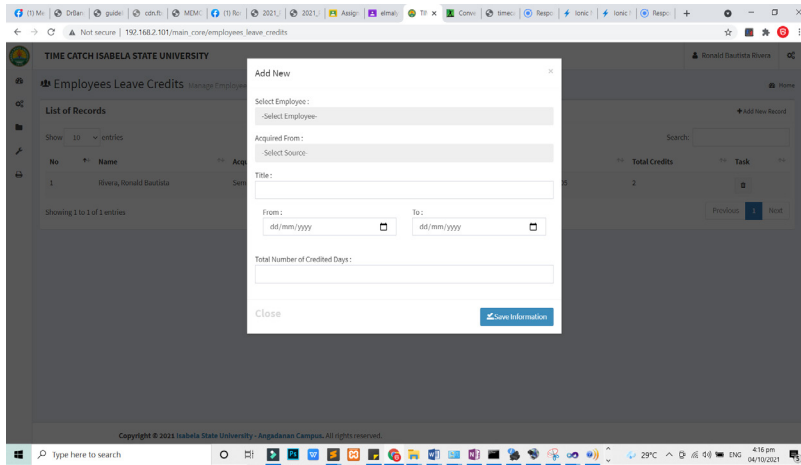


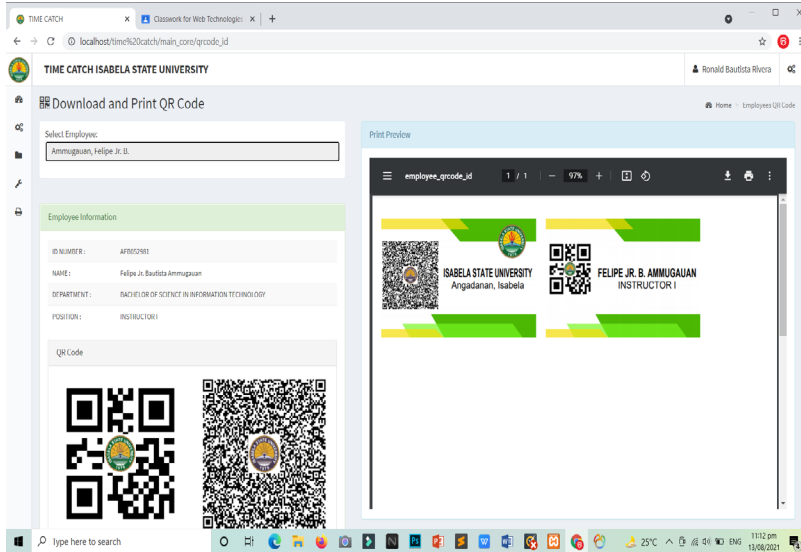
Figure 9. Credit units manager

## Report Generation

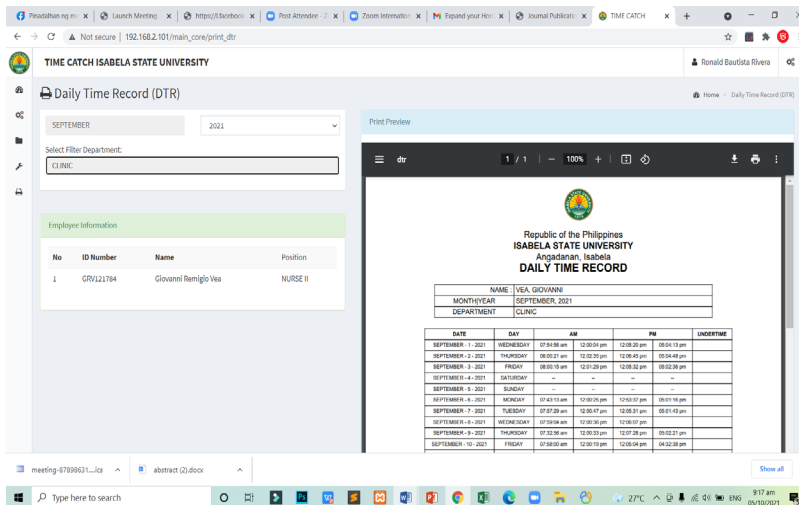
The system generates reports such as the master list of employees, the leave application form, the QR Code ID for casting attendances, the Daily Time Record (DTR), and the Remaining Leave Credits. Figure 10 shows the screenshots of the auto-generated reports.

ID NO	NAME	BIRTHDATE	GENDER	CP NO.	POSITION	DEPARTMENT
1	APATA100285	1985-10-02	Male	0957841460	ADMINISTRATIVE AIDE I	GENERAL SERVICES OFFICE
2	AFB020281	1991-05-29	Male	0917940979	INSTRUCTOR I	BACHELOR OF SCIENCE IN INFORMATION TECHNOLOGY
3	FBA020874	1974-02-08	Male	08274166530	ADMINISTRATIVE AIDE I	GENERAL SERVICES OFFICE
4	RDA040784	1984-04-07	Female	09496052281	INSTRUCTOR III	BACHELOR OF SCIENCE IN INFORMATION TECHNOLOGY
5	SPA100389	1969-10-03	Female	09166501257	ASSISTANT PROFESSOR IV	BACHELOR OF SCIENCE IN INFORMATION TECHNOLOGY
6	LSA091457	1957-09-14	Female	09951812796	ASSISTANT PROFESSOR IV	COLLEGE OF CRIMINAL JUSTICE EDUCATION
7	WDA041761	1961-04-17	Male	09152048835	ASSOCIATE PROFESSOR V	POLYTECHNIC SCHOOL
8	JNA091993	1993-09-19	Male	09958920205	INSTRUCTOR I	BACHELOR OF SCIENCE IN HOSPITALITY MANAGEMENT
9	CPA010282	1982-01-22	Female	09097413308	ADMINISTRATIVE OFFICER	CASHIER OFFICE
10	MSA000277	1977-08-05	Female	09272198909	ASSISTANT PROFESSOR I	BACHELOR OF SCIENCE IN INFORMATION TECHNOLOGY
11	MMB0100158	0098-10-01	Female	09054891148	ADMINISTRATIVE AIDE III	CASHIER OFFICE
12	AA0070159	1990-01-01	Male	09159095141	ADMINISTRATIVE AIDE I	GENERAL SERVICES OFFICE
13	OCB0701763	1963-07-07	Male	09175185887	PROFESSOR III	POLYTECHNIC SCHOOL

(a)



(b)



(c)

Timekeeping and Immediate Monitoring of Employees by Using EAMS

Republic of the Philippines  
**ISABELA STATE UNIVERSITY**  
 ANGADANAN CAMPUS  
 Coruzo II, Angadanan, Isabela

**APPLICATION OF LEAVE**

**BENFOTECI** 1. (Division/Office)      **ASIS** 2. (Last Name)      **MARICAR** (Given Name)      **BULAN** (M)

**2021-07-28 04:28:16** 3. (Date of Filing)      **ASSISTANT PROFESSOR I** 4. (Position)      **23875** 5. (Salary)

**A. TYPE OF LEAVE**  
 Vacation  
 to seek employment  
 Others pls specify \_\_\_\_\_  
 Sick Leave  
 Maternity  
 Others pls specify \_\_\_\_\_  
**BIRTHDAY LEAVE**

**B. WHERE WILL BE SPENT**  
 1. In case of vacation leave  
 In the Philippines  
 Abroad (pls specify) \_\_\_\_\_  
 2. In case of sick leave  
 In hospital (pls specify) \_\_\_\_\_  
 Others pls specify \_\_\_\_\_

**C. NUMBER OF WORKING DAYS** 1  
 Inclusive Dates : 2021-08-29 - 2021-08-29

**D. COMMULATIVE**  
 Requested     Not Requested

Signature of Applicant \_\_\_\_\_

**DETAILS OF APPLICATION OF LEAVE**

**C a. CERTIFICATION OF LEAVE CREDITS**      **b. RECOMMENDATION**  
 BALANCE      VACATION      SICK       Approval       Disapproval

(d)

TIME CATCH ISABELA STATE UNIVERSITY

Employees Leave Credits view and Print Employees Leave Credits

Filter Report

Select Employee: **Rivera, Ronald Bautista**

Employees Information

NAME	Rivera, Ronald Bautista
GENDER	Male
BIRTHDATE	1992-09-25
ADDRESS	Del Corpuz Cabatuan Isabela
CP NUMBER	09973376876
DEPARTMENT	BACHELOR OF SCIENCE IN INFORMATION TECHNOLOGY
POSITION	INSTRUCTOR III
SALARY	30799

**REMAINING CREDIT UNIT**

NAME : RIVERA, RONALD BAUTISTA      DEPARTMENT : BACHELOR OF SCIENCE IN INFORMATION TECHNOLOGY  
 GENDER : MALE      POSITION : INSTRUCTOR III  
 BIRTHDATE : 1992-09-25  
 ADDRESS : DEL CORPUZ CABATUAN ISABELA

LEAVE APPLICATIONS						
NO	LEAVE TYPE	DATE RANGE	DAYS	DATE FILLED	STATUS	USED CREDIT
ACCRUED LEAVE :						0
CREDITED LEAVE :						0

LEAVE CREDITS				
NO	ACQUIRED FROM	TITLE	INCLUSIVE DATES	TOTAL
1	Seminar Workshop / Training	The Potters Way	2021-10-04 - 2021-10-05	2
TOTAL LEAVE CREDITS :				2

**REMAINING CREDITS**  
 TOTAL REMAINING CREDITS : 2

(e)

Figure 10. Auto-generated reports: (a) Master list of employees; (b) QR code ID; (c) Daily time record; (d) Leave application form; (e) Remaining credit units

**Evaluation**

**Respondents of the Study.** Purposive Sampling was used to identify the respondents of the study (Table 1).

Table 1  
*The respondents of the study*

Type of Respondent	Number of Respondents
Non-Teaching Staff	10
Teaching-Staff	18
<b>Total Respondents</b>	<b>28</b>

**Questionnaire.** The researchers used a questionnaire to gather data from the respondents based on ISO 25010, which was adopted from the study of Atanacio and Lacatan (2019) entitled Development and Evaluation of Rural Health Unit Record Management System with Data Analytics for Municipality of Bay, Laguna using ISO 25010.

**Statistical Treatment.** Data were analyzed utilizing mean distribution. The following arbitrary scale in Table 2 was applied to determine the functionality of the system.

Table 2  
*Equivalent weighted mean and interpretation of scale on the evaluation of TIME CATCH using EAMS*

Scale	Weighted Mean	Interpretation
5	4.51-5.00	Strongly Agree
4	3.51-4.50	Agree
3	2.51-3.50	Neutral
2	1.51-2.50	Disagree
1	1.00-1.50	Strongly Disagree

In finding the weighted mean in the presentation, analysis and interpretation of data, the researchers used Equation 1:

$$W = \frac{\sum_{i=1}^n w_i X_i}{\sum_{i=1}^n w_i} \tag{1}$$

- W = weighted average
- n = number of terms to be averaged
- w<sub>i</sub> = weights applied to x values
- X<sub>i</sub> = data values to be averaged

The interpretation of the scale was adopted from the study of Joshi et al. (2015) entitled Likert Scale: Explored and Explained. British Journal of Applied Science & Technology.

## RESULTS AND DISCUSSION

The evaluation result from the participants is based on ISO 25010 Standards in terms of Functionality, Efficiency, Usability, Reliability, Security, Maintainability, and Portability.

Table 3

*Mean rating and qualitative description of respondents on functional suitability of the Developed Attendance Monitoring System (TIME CATCH using EAMS)*

Functionality	Mean	Qualitative Description
The software performs the tasks required	4.71	Strongly Agree
The results expected were delivered	4.92	Strongly Agree
The system can interact with another system	4.93	Strongly Agree
The software prevents unauthorized access	4.88	Strongly Agree
Category mean	4.86	Strongly Agree

Table 3 shows that the system's users strongly agree with the functional characteristics of the systems, as revealed by the category mean of 4.86. Specifically, the participants have shown strong agreement that the system can perform the required task, deliver expected results, interact with another system, and prevent unauthorized access, as indicated by the mean of 4.93, 4.92, 4.88, and 4.71, respectively.

Table 4

*Mean response and qualitative description of the respondents in evaluating the efficiency of the Developed Attendance Monitoring System (TIME CATCH using EAMS)*

Efficiency	Mean	Descriptive Interpretation
The system responds quickly in all its functionality and operation	4.96	Strongly Agree
The system utilizes all its resources efficiently	4.80	Strongly Agree
The users can go directly to the desired function/operation or use a structured navigational menu	4.74	Strongly Agree
The system is demonstrably effective with the intended audience, including people of varying abilities and experiences	4.75	Strongly Agree
Category mean	4.81	Strongly Agree



The analysis in Table 4 shows that the participants strongly agree on the 4.74-4.96 efficiency of the developed system, as indicated by the category mean of 4.81. Further analysis shows that the system responds quickly in all its functionality and operation, utilizes all its resources efficiently, and has the choice of going directly to desired function/operation or using a structured navigational menu. The system is demonstrably effective with the intended audience, including people of varying abilities and experiences, with a mean ranging from 4.74-4.96, qualitatively described as strongly agreed by the participants.

Table 5  
*Mean response and descriptive interpretation of the respondents in measuring the reliability of the Developed Attendance Monitoring System (TIME CATCH using EAMS)*

Reliability	Mean	Descriptive Interpretation
Most faults in the software have been eliminated over time	4.74	Strongly Agree
The software was capable of handling errors	4.75	Strongly Agree
If the program creates a permanent record for a user, that record is secure and confidential. There is a provision for erasing the record when the information is no longer valuable in providing services	4.85	Strongly Agree
Category mean	4.78	Strongly Agree

In terms of measuring the reliability of the developed system (Table 5), the participants strongly agree that the program creates a permanent record for a user and that the record is secure and confidential. Furthermore, there is a provision for erasing the record when the information is no longer valuable in providing services, with a mean of 4.85. Moreover, the participants strongly believed that the software was capable of handling errors, and most of the faults in the software have been eliminated over time with a mean of 4.75 and 4.74, respectively.

Results further show that the participants strongly agree with the reliability characteristics of the system, as revealed by the category mean of 4.78.

Table 6  
*Mean response and descriptive interpretation of the respondents in assessing the usability of the Developed Attendance Monitoring System (TIME CATCH using EAMS)*

Usability	Mean	Descriptive Interpretation
The user easily understands/comprehend how to use the system	4.50	Strongly Agree
The user learns to use the system easily	4.41	Agree

Table 6 (Continue)

Usability	Mean	Descriptive Interpretation
The user uses the system without much effort	4.32	Agree
The interface looked good and attractive	4.86	Strongly Agree
The organization is clear, logical, and effective, making it easy for the intended audience to understand	4.74	Strongly Agree
The individual can operate the system independently	4.45	Agree
Category mean	4.55	Strongly Agree

It is reflected in Table 6 that the participants have a strong agreement regarding the usability of the developed system, as shown by the category mean of 4.55. However, three out of the six sub-characteristics of usability have only been rated agree by the users. It involves the characteristic that the individual can operate the system independently (4.45), the user learns to use the system easily (4.41), and the user uses the system without much effort (4.32).

On the other hand, the participants strongly agree that the user easily understands/comprehend how to use the system, the organization is clear, logical, and effective, making it easy for the intended audience to understand, and the interface looked good and attractive with means of 4.50, 4.74 and 4.86, respectively.

Table 7

*Mean response and descriptive interpretation of the employees in assessing the maintainability of the Developed Attendance Monitoring System (TIME CATCH using EAMS)*

Maintainability	Mean	Descriptive Interpretation
Faults and errors can be easily diagnosed	4.50	Strongly Agree
The software can be easily modified in accordance with what the user needs	4.50	Strongly Agree
The software continues functioning when modifications/changes are made	4.55	Strongly Agree
The software can be tested easily	4.60	Strongly Agree
Category mean	4.54	Strongly Agree

In terms of the maintainability of the system (Table 7), the participants strongly agree that the Software can be tested easily, the Software continues functioning when modifications/changes are made and the software can be easily modified in accordance with what the user needs and faults and errors can be easily diagnosed with means ranging from 4.50-4.60.

The category means of 4.54 further indicates strong agreement of the participants in terms of the system’s maintainability.

Table 8  
*Mean response and descriptive interpretation of the respondents in assessing the portability of the Developed Attendance Monitoring System (TIME CATCH using EAMS)*

Portability	Mean	Qualitative Description
The software can be easily moved from one to another environment	4.73	Strongly Agree
The software is installed easily	4.84	Strongly Agree
The software complies with portability standards	4.80	Strongly Agree
The software can replace other software	4.70	Strongly Agree
Category mean	4.76	Strongly Agree

Table 8 reflects the mean of the participant’s responses regarding the portability of the developed system. The users have shown strong agreement regarding the portability characteristics, gleaned from the category mean of 4.76. The users believed the software could be installed easily, complied with the portability standards, and easily moved from one environment to another. In addition, the software can replace other software, as indicated by the mean greater than 4.50.

Table 9  
*Summary of category mean and qualitative description of respondents on the characteristics of the Developed Attendance Monitoring System (TIME CATCH using EAMS) based on ISO 25010*

System’s Quality Indicators	Weighted Mean	Qualitative Description
Functionality	4.86	Strongly Agree
Efficiency	4.81	Strongly Agree
Usability	4.55	Strongly Agree
Reliability	4.78	Strongly Agree
Maintainability	4.54	Strongly Agree
Portability	4.76	Strongly Agree
General mean	4.72	Strongly Agree

The results in Table 9 show that the respondents firmly agreed that the established system based on ISO 25010 is good quality, as indicated by the general mean of 4.72. Furthermore, the functional characteristics of the system have the highest mean rating, followed by efficiency, reliability, portability, usability, and maintainability.

## CONCLUSION

In conclusion, the developed system addresses the issue of manually or conventionally checking employees' attendance and promotes reducing paper-based work. It also saves the time of preparation of employees' DTR (Daily Time Record), leaves application management, and provides contactless attendance monitoring for employees.

Therefore, the quality/functionality of the developed system can be used as a tool in implementing TIME CATCH (Timekeeping and Immediate Monitoring of Employees by Consistently Advocating Time Consciousness and Honesty) among the employees of Isabela State University-Angadanan Campus.

## ACKNOWLEDGEMENTS

The authors want to thank Mr. Oscar G. Bangayan, Ph.D., the campus administrator, for assisting in the design, development and implementation of this innovation. His continuous encouragement and reminders are extremely beneficial to our career and personal development. Thanks to Almighty God for the wisdom and knowledge, as well as the colleagues and other employees of Isabela State University who were highly involved in executing the enhanced attendance monitoring system.

## REFERENCES

- Abdulkadhim, E. G. (2021). Design and develop an attendance system based on fingerprint and arduino board. In *Journal of Physics: Conference Series* (Vol. 1804, No. 1, p. 012011). IOP Publishing. <https://doi.org/10.1088/1742-6596/1804/1/012011>
- Adewole, K. S., Abdulsalam, S. O., Babatunde, R. S., Shittu, T. M., & Oloyede, M. O. (2014). Development of fingerprint biometric attendance system for non-academic staff in a tertiary institution. *Computer Engineering and Intelligent Systems*, 5(2), 62-70.
- Atanacio, M. L., & Lacatan, L. L. (2019). Development and evaluation of rural health unit record management system with data analytics for municipality of Bay, Laguna using ISO 25010. *International Journal of Recent Technology and Engineering*, 8(3), 3915-3919. <https://doi.org/10.35940/ijrte.C5133.098319>
- Hale, R. C., & Song, B. (2020). Single-use plastics and COVID-19: Scientific evidence and environmental regulations. *Environment Science Technology*, 54(12), 7034-7036. <https://doi.org/10.1021/acs.est.0c02269>
- Joshi, A., Kale, S., Chandel, S., & Pal, D. K. (2015). Likert scale: Explored and explained. *British Journal of Applied Science & Technology*, 7(4), 396-403. <https://doi.org/10.9734/BJAST/2015/14975>

- Mohamed, B. K., & Raghu, C. V. (2012). Fingerprint attendance system for classroom needs. In *2012 Annual IEEE India Conference (INDICON)* (pp. 433-438). IEEE Publishing. <https://doi.org/10.1109/INDCON.2012.6420657>
- Shoewu, O., & Idowu, O. A. (2012). Development of attendance management system using biometrics. *The Pacific Journal of Science and Technology*, *13*(1), 300-307.

## ESS-IoT: The Smart Waste Management System for General Household

Shen Yuong Wong<sup>1\*</sup>, Huashuo Han<sup>1</sup>, Kin Meng Cheng<sup>2</sup>, Ah Choo Koo<sup>2</sup> and Salman Yussof<sup>3</sup>

<sup>1</sup>Department of Electrical & Electronics Engineering, Xiamen University Malaysia, 43900 Sepang, Selangor, Malaysia

<sup>2</sup>Faculty of Creative Multimedia (FCM), Multimedia University, 63100 Cyberjaya, Selangor, Malaysia

<sup>3</sup>Institute of Informatics and Computing in Energy, Universiti Tenaga Nasional, 43000 Kajang, Selangor, Malaysia

### ABSTRACT

With the urban population's growth, unethical and unmanaged waste disposal may negatively impact the environment. In many cities, a massive flow of people in municipal buildings or offices has generated vast amounts of waste daily, which correlates to the enormous expenses of waste management. The critical issue for better waste management is waste collection and sorting. In this study, the Electronic Smart Sorting- Internet of Things (ESS-IoT) is proposed to assist people in better waste management. The ESS-IoT system uses Raspberry Pi 4b as the microcontroller with three modules, and it is designed with two main functions: waste collection and waste classification. The two main functions have been deployed separately in the literature, while this study has combined both functions to achieve a more comprehensive smart bin waste disposal solution. Waste collection is

triggered by the overflow alarm mechanism that employs ultrasonic and tracker sensors. On the other hand, the waste classification is implemented using two classification algorithms: Random Forest (RF) prediction model and Convolutional Neural Network (CNN) prediction model. An experiment is conducted to evaluate the accuracy of the two classification algorithms in classifying various types of waste. The waste materials under investigation can be classified into

### ARTICLE INFO

#### Article history:

Received: 05 December 2021

Accepted: 11 February 2022

Published: 09 November 2022

DOI: <https://doi.org/10.47836/pjst.31.1.19>

#### E-mail addresses:

shenyuon.wong@xmu.edu.my (Shen Yuong Wong)

eee1709121@xmu.edu.my (Huashuo Han)

tidusnjay@gmail.com (Kin Meng Cheng)

ackoo@mmu.edu.my (Ah Choo Koo)

salman@uniten.edu.my (Salman Yussof)

\*Corresponding author

four categories: kitchen waste, recyclables, hazardous waste, and other waste. The results show that CNN is the better classification algorithm between the two. Future work proposes the research extension by introducing an incentive mechanism to motivate the household communities using a cloud-based competition platform incorporated with the ESS-IoT system.

*Keywords:* IoT, machine learning, overflow mechanism, waste collection, waste classification, waste management

---

## INTRODUCTION

With the advancement of modern society, waste management has gradually become a costly issue worldwide. Solid waste has also become a global issue concerning economic sustainability and environmental pollution (Ferronato & Torretta, 2019). One-third of the waste (34%) comes from high-income countries with growing populations. By the middle of the 21st century, the world's waste production is expected to reach 27 billion tons, of which 1/3 will come from Asia ("Global waste," 2018). In Asia, China and India generate more than 90% of the waste generated in the continent. India generates 133,700 tons of waste daily, where approximately only 91,572 tons are collected. The Indian government has paid a lot of money for recycling (Rana R, 2015). More than two-thirds of the cities in India are surrounded by garbage. Urban garbage dumps across the country have occupied 550,000 square kilometers of land. A quarter of the cities no longer have suitable places to stack garbage.

China's 40,000 townships and nearly 600,000 administrative villages generate more than 280 million tons of domestic waste each year. As a result, domestic waste in China has exceeded 8 billion tons. In Malaysia, economic growth has caused environmental burdens, including waste generation, greenhouse gas emissions from the energy system, and open burning (Nanda & Berruti, 2021). Aja and Al-Kayiem (2014) forecasted that Malaysia's solid waste had reached 33,000 tonnes per day, and expectedly 51,655 tonnes of waste per day will be generated by 2025 (Department of Statistics Malaysia, 2020).

This paper proposes an IoT-enabled smart waste management system, Electronic Smart Sorting-Internet of Things (ESS-IoT). Firstly, the system provides a solution to the waste disposal responsibility of waste in general household areas. Although 100,000 free dustbins were given to each household in several cities in Malaysia, the public still disposed of their waste irresponsibly. Only 24% was recycled or separated, and 76% of the waste was sent to landfills. Moreover, the waste overflow problem frequently happens due to the uncollected waste on time, which causes air pollution; wild insects and animals will consume and collect the overexposed waste, including different types of organic and inorganic waste that are potentially hazardous to the environment and public health



(Ivan, 2021). Secondly, the waste sorting problem is among Malaysian problems in waste disposal decisions. The assortment of waste is essential to avoid contamination, where the effectiveness depends on the behavior that requires education and cultivation (Low et al., 2016). Besides, people also face the problem of waste classification on municipal solid waste, which is one of the leading causes of environmental issues (Rana, 2015). To better understand the responsibility of waste disposal, people must learn the types of waste for better classification. However, achieving effective waste sorting and classification takes longer without a smart solution to detect waste disposal materials.

The proposed ESS-IoT system mainly has two main functions. The first is to improve existing waste collection procedures to minimize the hazards of hazardous waste accumulation and reduce the cost of waste collection. The system will collect the waste only if the capacity is up to 80%. The system also functions as a reminder for waste sorting or cleaning and clearing the waste before it overflows (Kumar et al., 2016). Secondly, to help residents sort waste when discarding it through visual imagery analysis with machine learning. This feature can also help reduce the workload of waste collection staff when sorting waste. Different types of waste can be handled in different ways more efficiently and reduce the cost of waste collection from the waste collection companies from sending unmanaged waste to landfills.

Sustainable waste management requires a long-term commitment from the public to establish a good habit of their waste disposal. The proposed ESS-IoT system will only focus on the technical side of waste bin management. Therefore, the motivation to use the ESS-IoT system is crucial for users to apply it in their homes. Any smart system assisting waste or resource separation should be a better move. Separation using manual or labor force should be assisted with innovative systems or fully through smart facilities. Any smart recognition system can be used at the household bins facilities for monitoring and reviewing the type of waste disposed of. Warning or alarms can be triggered when improper management or disposal of recyclable resources or materials to the garbage bins.

## **RECENT TECHNOLOGIES IN WASTE MANAGEMENT**

Recently, many scholars have researched waste disposal technology (Dugdhe et al., 2016), but the research on waste bin monitoring is somewhat lacking. However, some of the technologies proposed by the previous researchers have good application prospects in this regard. Furthermore, in recent research, material waste collection and classification have been done individually (Al-Masri et al., 2019; Mirchandani et al., 2018), whereas both are yet to be combined.

Anagnostopoulos et al. (2020) proposed the city's smart waste bin project supported by the Internet of Things (IoT). Sushmitha et al. (2018) have considered bins with Wi-Fi-based sensors, and Fachmin et al. (2015) proposed a smart bin system to detect if the trash bin is

full. The smart bin system collects data through multiple sensors transmitted via the Internet to detect waste overflow that may cause garbage toxicity and pollute the air if it does not collect. In some cases, the trash bin may not be full, but the trash in the bin has generated harmful gas. If this happens, the trash bin must be cleaned in advance (Anagnostopoulos et al., 2020). With a more efficient detection of waste overflow, a more organized duty cycle technique is also applied in the waste collection system to reduce power consumption and maximize the working time of the system. Therefore, collecting the waste is important as the application of a smart bin system with sensors has been proposed in several studies to encourage the participation of citizens (Pelonero et al., 2020).

The data collected by these sensors is sent to a central server via WiFi. Therefore, it needs internet services to function as it is. First, the communication mode of this system is based on WiFi, which means that the application scope of this system is relatively small, and it is unlikely to be widely used in a modern city. Besides, waste classification with the captured camera has been carried out by Al-Masri et al. (2019). Classification has been used on two types of smart bins to identify the waste: an artificial intelligence tool to label images based on a given trained set, and Microsoft's Custom Vision was used to classify the waste. A practical classification with IoT and modules is believed to be an advantage in overcoming waste classification caused by urbanization.

Wahab et al. (2014) proposed a collection monitoring system that rewards users based on the type and weight of waste in the trash bin. This system can encourage residents to sort garbage. If the user puts the wrong type of trash in a trash bin, the user's score will be deducted. However, this system is somewhat conceptual. Some aspects can be improved, such as multi-sensor systems or computer vision detecting garbage types. Besides, Fachmin et al. (2015), Chandra and Tawami (2020) have implemented the waste collection design. Ruiz et al. (2019) and Hanbal et al. (2020) have focused on waste image classification. However, the literature mentioned above shows only collection or classification; in other words, both works have been done separately. On the contrary, in this study, we combine both mechanisms of collection and classification to create an ESS-IoT smart bin that turns out to be a complete solution to fit our real-world daily waste disposal scenario. Besides, this study also proposes the potential of incorporating a reward system in future research to maximize the efficiency and participation of the citizens in recycling and therefore create a more comprehensive and smarter household waste management. Not only that, but this study also aims to motivate the community to recycle by creating a combined mechanism of collection and classification by skipping the hassle of checking the type of waste and the type of bins for different types of waste.

## METHODOLOGY

The ESS-IoT system has two main functions, waste collection and waste classification. With respect to waste collection, trash bins in public places need to be cleaned up before the waste overflows. The overflow of waste in the trash bin will cause health problems for citizens and environmental problems. We apply and compare the performance of the Random Forest (RF) prediction model and Convolutional Neural Network (CNN) prediction model regarding waste classification. The RF algorithm builds multiple decision trees and merges them to get a more accurate and stable prediction (Hanbal et al., 2020). It is a supervised learning methodology for splitting, association, regression, and other assignments by influencing multiple decision trees during the training and testing process, then analyzing which class represents the mode of classification or predictive regression of decision trees. As a deep learning approach, the Convolutional Neural Network (CNN) has been widely used in image processing and classification tasks (Zeiler et al., 2014; Akshaya & Kala, 2020). Its effectiveness exceeds the expectation of enhancing feature representation capacity (Lim & Chuah, 2018) and quality prediction promotion (Shaily & Kala, 2020). More explanation of the theoretical aspects of RF and CNN can be found in Wu et al. (2021).

The ESS-IoT system consists of three modules: control, sensor, and servomotor. Figures 1 and 2 show the prototype of ESS-IoT. The control module comprises Raspberry Pi 4b and its extended board. The Raspberry Pi 4b has a Broadcom BCM2711, Quad-core Cortex-A72 (ARM v8) 64-bit SoC @ 1.5GHz, 4Gb LPDDR4-320 SDRAM has a built-in power supply system, an additional power supply module is not essential, and it is running Raspberry Operating System (OS). The Raspberry pi camera v2 camera module has a Sony IMX219 8-megapixel sensor. The camera module can be used to shoot high-definition video and still photos. The primary function of the control module is to process the information collected by the sensors and give commands to the servomotor module based on this information.

The sensor module comprises a camera, a display screen and four tracker sensors. The primary function of the sensor module is to collect data for the control module to process through the camera and sensor. It can be said that the system relies entirely on sensor modules to obtain external information. For example, tracker sensors are used to detect the fullness of trash bins. A tracker sensor is an infrared tracking sensor often used to make tracking smart cars. The tracker sensor uses ITR20001/T infrared reflection sensor. The infrared emitting diode of the ITR2001/T sensor continuously emits infrared rays. When objects reflect the emitted infrared rays, they are received by the infrared receiver and output analog values. The output simulation value is related to the distance of the object and the color of the object. By calculating the analog value of five outputs, the position of the trace line can be judged.

The servomotor model is SG90 which has an operating voltage ranging from 4.8V to 6V, operating speed is 0.1s/60° and works on brushed DC motor type. The module comprises a servomotor, trash bins and several wires. The main function of this part is to execute the commands issued by the control module to control the opening and closing of the trash bin lid. Servomotors are divided into two major categories: DC and AC servo motors. The main feature of this device is that there is no rotation when the signal voltage is zero. The waste materials were fresh and from the researchers' household disposal during the usual condition and activities at home.

At first, the trash can is tested with the waste collection. Then, the depth of the trash bin is measured if the trash bin is over 7 cm, 6 cm, 4 cm or below 3 cm. Figure 3 explains the flowchart of ESS-IoT waste collection. After testing out the overflow mechanism in the phase of waste collection, the ability of ESS-IoT on waste classification is tested using the solid waste from the household residential areas. In order to assimilate the real-world domestic waste disposal scenario, we collect many different types of materials for classification. As an example, for domestic kitchen waste, we carry out single-type classification and mixed kitchen waste classification. It is because, in actual life, residents usually dispose of kitchen waste by placing all the kitchen waste together, which is more similar to mixed kitchen waste. The same methodology goes to classifying other categories of waste, where materials are classified on their own or mixed, as reported in Tables 2, 3 and 4.

The waste classification feature in the ESS-IoT system is implemented using two different techniques, which are the Convolutional Neural Network (CNN) and Random Forest (RF) classifier. An experiment was carried out to evaluate the performance of these two techniques. A one-dimensional 9-layer CNN is considered in the experiment. CNN is a network that consists of the input layer, convolution layer, pooling layer, fully-connected layer, and output layer. On the other hand, the RF builds many decision trees and randomly selects attributes from random samples. Data samples of each waste material are split into 60% training and 40% testing. In the phase of waste classification, the average classification performance of 100 trials is recorded.

For all the experiments, the lids of the different color trash bins will open based on the classification result of the object. As illustrated in Figure 2, a green bin is dedicated to kitchen waste, a blue bin for recyclable waste, a red for hazardous waste, and a grey for other waste.

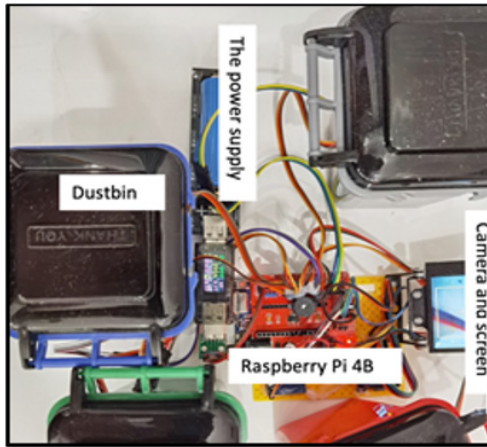


Figure 1. The prototype of the ESS-IoT system (Top view)



Figure 2. The prototype of the ESS-IoT system during the classification test (Front view)

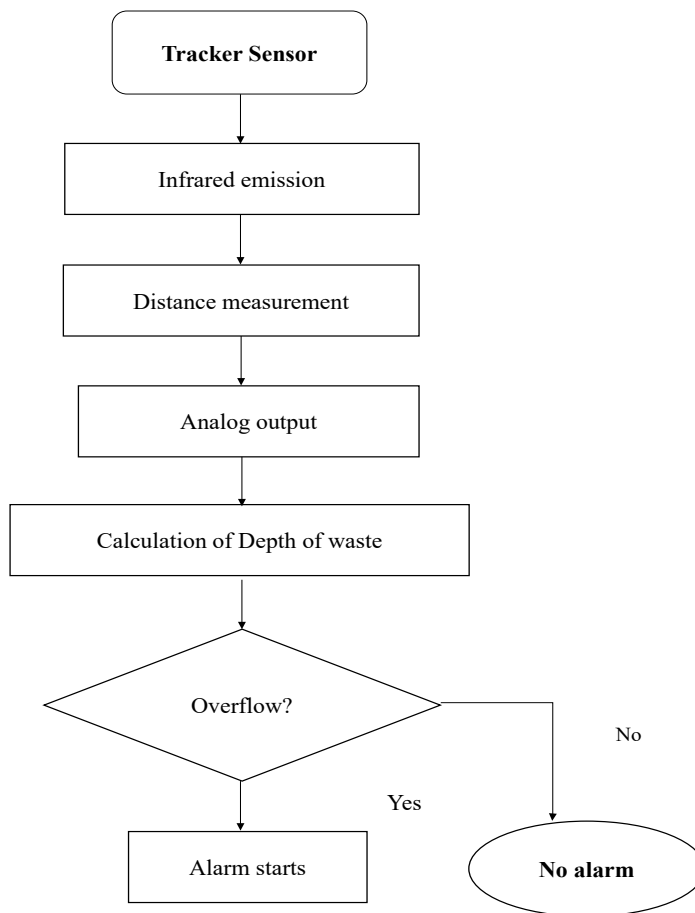


Figure 3. Flowchart of the ESS-IoT system algorithm for waste collection

## RESULTS

### Trash Overflow Alarm

One of the core functions of the ESS-IoT system is to trigger waste collection via an overflow alarm mechanism, which exists to detect whether there is too much garbage in the trash bin. When rubbish piles up in the trash bin, it will produce unpleasant odors and produce many bacteria in the trash bin. In addition, the mosquitoes and flies produced in trash bins can spread pathogens of infectious diseases and endanger the health of residents. This mechanism will notify and remind relevant personnel to dispose of the overflowing garbage bin as soon as possible, ensuring a cleaner and healthier living environment for residents. The realization of this function mainly depends on the tracker sensor. Table 1 shows the results of the overflow mechanism of 5 distances of depth from the sensor, less than or equal to 3 cm, 4 cm, 5 cm, 6 cm and more than or equal to 7 cm. The ESS-IoT system misses two alarms out of 20 tests when the test condition is five centimeters away, which is the critical distance. Overall, the performance is excellent, with close to 100% accuracy.

Table 1

*Results of overflow alarm mechanism*

Distance	Test count	Number of alarms	Accuracy
Greater than or equal to 7 cm	20	0	100%
6 cm	20	0	100%
5 cm	20	18	90%
4 cm	20	20	100%
Less than or equal to 3 cm	20	20	100%

### Waste Classification

The waste classification feature in the ESS-IoT system is implemented using two different techniques, which are the Convolutional Neural Network (CNN) and Random Forest (RF) classifier. The dataset under investigation can be classified into four categories: kitchen waste, recyclables, hazardous waste, and others. The data samples comprise various melon peels, leftovers, and mixed kitchen waste for the kitchen waste category. The data samples for the recyclable waste category include plastic bottles, glass bottles, scrap metal, scrap paper, and other forms of plastics commonly used daily. The data samples for the hazardous waste category consist of ordinary hazardous wastes such as batteries, fluorescent tubes, wastewater silver thermometers, and expired medicines. These kinds of wastes require special safe treatment. Other waste includes bricks, ceramics, muck, porcelain fragments,

animal excrement, disposable items and other wastes that are difficult to recycle. The images are captured by placing the object on a white poster board and using sunlight or room lighting. All the images have been resized to a spatial resolution of  $512 \times 384$ . The results are recorded in Table 2 for kitchen waste, Table 3 for recyclables, Table 4 for hazardous waste, and Table 5 for other types of waste.

Table 2

*Classification result of kitchen waste (green bin)*

Category: Kitchen Waste		CNN Classification		RF Classification	
Type	Material	Average Accuracy	Average Responses Time (s)	Average Accuracy	Average Responses Time (s)
Peel	Watermelon rind	94%	1.72	64%	3.55
	Durian skin	89%	1.69	58%	4.32
	Banana peel	90%	1.70	61%	4.17
Leftovers	Gruel	87%	1.65	69%	3.89
	Rice	82%	1.74	48%	3.55
	Chicken bone	91%	1.68	57%	4.03
Mixed kitchen waste	Peel and gruel	89%	1.78	49%	4.34
	Peel and rice	82%	1.69	67%	3.98
	Peel and chicken bone	92%	1.74	73%	4.12

The study demonstrates the ability of ESS-IoT to handle different categories of waste. Table 2 shows the types of kitchen waste used for classification and how they are applied (single type or mixed waste) during the classification process. Table 2 reports the classification results of CNN and RF classifiers in terms of average accuracy and average response time of ESS-IoT. It can be observed that peel wastes are more correctly classified than leftovers. It could be due to the appearance of leftovers being a bit slimy and different textures that render the classification task more challenging. Using a CNN classifier, the classification accuracy rate can vary between 82% to 94% depending on materials for kitchen waste. In actual life, residents usually dispose of kitchen waste by placing all the kitchen waste together, which is more similar to mixed kitchen waste. ESS-IoT is also applied to classifying mixed kitchen waste to assimilate a real-world scenario. The results are reasonably impressive, with an average accuracy rate of 87.7%.



Table 3

*Classification result of recyclables (blue bin)*

Category: Recyclables		CNN Classification		RF Classification	
Type	Material	Average Accuracy	Average Responses Time (s)	Average Accuracy	Average Responses Time (s)
Metal	Can	96%	1.59	62%	4.61
	Iron sheet, iron nail	84%	1.64	54%	4.32
	Copper wire	87%	1.70	63%	4.75
Wastepaper	Book	94%	1.70	73%	3.90
	Newspaper	96%	1.74	71%	4.51
	Wrapping paper	90%	1.69	54%	3.74
Plastic	Plastic bags or plastic packaging	97%	1.75	78%	4.35
	Mineral water bottles	95%	1.72	76%	4.66
	Plastic toys	87%	1.64	43%	3.41
Waste glass	Glass cup	95%	1.69	65%	4.96
	Glass bottle	96%	1.78	69%	4.81
	Mirror, lens	90%	1.67	50%	3.79

In the second category, which is the recyclables, Table 3 shows that the CNN model has a high accuracy rate (an average of 89% or higher) in identifying recyclables. However, the model has relatively low accuracy in identifying iron nails and copper wires. The reason could be due to the small size of this waste or its slender shape so that the control module cannot extract the necessary information from the photos.

Table 4

*Classification result of hazardous waste (red bin)*

Category: Hazardous Waste		CNN Classification		RF Classification	
Type	Material	Average Accuracy	Average Responses Time (s)	Average Accuracy	Average Responses Time (s)
Used batteries	Button batteries	79%	1.77	68%	4.32
	Lithium battery	89%	1.72	60%	4.61
	Power bank	82%	1.64	54%	4.17

Table 4 (Continue)

Category: Hazardous Waste		CNN Classification		RF Classification	
Type	Material	Average Accuracy	Average Responses Time (s)	Average Accuracy	Average Responses Time (s)
Expired drugs	Capsule	93%	1.79	36%	4.64
	Pill	85%	1.58	45%	4.33
	Medical gauze	91%	1.65	48%	3.79
End-of-life mercury measuring instruments	Mercury thermometer	94%	1.69	58%	4.21
	Mercury sphygmomanometer	96%	1.70	65%	4.29
Waste fluorescent tube	Fluorescent tube	95%	1.63	72%	3.98
	Halogen lamp	96%	1.71	64%	4.07

Table 5

Classification result of other waste (grey bin)

Category: Other Waste		CNN Classification		RF Classification	
Material	Average Accuracy	Average Responses Time (s)	Average Accuracy	Average Responses Time (s)	
Brick and Ceramics	89%	1.63	65%	4.39	
Muck	94%	1.73	72%	4.16	

Table 4 compares the classification accuracy of CNN and RF classifier in identifying the various hazardous wastes. The classification accuracy rate of the used batteries is slightly lower than that of the other types of items in the category, with an average of 83.33%. On the other hand, the CNN classifier shows excellent accuracy in end-of-life mercury measuring instruments and fluorescent tubes, with an average accuracy of close to 95%. Last but not least, in terms of other waste, it can be observed from Table 5 that the CNN model shows a much better classification rate for identifying other waste which is not fit into any of the three categories mentioned above; the average accuracy rate ranges from 89 % to 94%. Thus, it can be concluded that ESS-IoT can perform well in real-life applications.

## DISCUSSION

### Discussion and Implication

The bigger issue of the waste problem is separation at the source. Not all residents or populations practice this habit. Technology-based assistance such as the one proposed in this study that can be developed to curb the issue of waste separation will be highly demanded, especially when the volume of recycled items is in piles and unmanaged. Smart systems would contribute to better waste management since manual separation is time and labor-intensive. On the waste collection aspect, ESS-IoT has the detection of waste overflow that has an accuracy of 90 – 100% that will notify the waste collection party to change the route of waste collection, the reduction of frequency in traveling around the household area can reduce the cost associated to fuel consumption (Bansode et al., 2021). We believe appropriately planned waste collection save waste not only collection costs but also labor cost. In the long run, a smart overflow detection mechanism assists the public in deciding on waste disposal and controlling the animals from fetching and scattering the waste that may be an extra cost to the municipalities.

The ESS-IoT system uses IoT and machine learning for waste collection and classification tasks. IoT has enabled sensors to track the depth of waste and cameras to shoot high-resolution images for visual imagery analysis for waste classification by CNN and RF classifiers. Experimental result has shown the effectiveness of the proposed system with an accuracy of 90 - 100% to detect five different garbage levels in a trash bin and give an alarm if the bin is full.

In terms of waste classification, the CNN classifier shows higher accuracy than the RF classifier. CNN classifier shows a better classification rate. However, CNN training requires a significant amount of labeled data to be trained. Collecting labeled data is costly. Furthermore, the labeling criteria may differ from dataset to application, even for the same applications. It is critical to reduce the amount of data to be labeled and allow CNN training with partially and flexibly labeled data. Shifting from heavily supervised to weakly supervised learning is recommended to make CNN more applicable to the ESS-IoT system (Wang et al., 2020).

### Limitation and Future Works

This study only tested five different garbage levels in a trash bin. Alarms are triggered on almost all 20 tests, except for the two tests of 5cm distance from the detector. Nevertheless, the test shows promising results, which bodes well for the future of the proposed system.

The ESS-IoT system has several limitations on the classification of the materials. First, up to the current stage of the study, the ESS-IoT only focuses on four categories, 13 types and 31 kinds of materials closely related to general household waste, which are

different from commercial and industrial waste that contain highly contaminated chemical substances, heavy metal, radioactive substances and toxic fumes and smoke.

General household waste also leads families in the municipalities to practice ethics and manage household waste disposal that could be brought to the workplace culture and the industry. Therefore, the ESS-IoT system is proposed to extend its future works to the general household with an integration of a cloud-based community incentive system where families around the different households (i.e., terrace, semi-detached, condominium, flat and bungalow communities) can gather and compete with each other to receive incentives or rewards. It is aimed to develop a sustainable habit within the community through extrinsic motivation.

## CONCLUSION

The ESS-IoT system uses IoT and machine learning for waste collection and classification tasks. Experimental result has shown the effectiveness of the proposed system in waste management, i.e., overflow mechanism to properly trigger waste collection and disposal according to waste type classification. There are still many areas to explore with the possibilities of the microcontroller nowadays that could extend to numerous versatile modules that effectively solve daily activities. The incorporation of machine learning, like the proposed ESS-IoT, has also extended the potential of analysis from the gathered data. It has also fulfilled the demand of current data-centric fast-growing cities.

## ACKNOWLEDGEMENT

This work was supported by Xiamen University Malaysia Research Fund under Grant XMUMRF/2021-C8/IECE/0023.

## REFERENCES

- Aja, O. C., & Al-Kayiem, H. H. (2014). Review of municipal solid waste management options in Malaysia, with an emphasis on sustainable waste-to-energy options. *Journal of Material Cycles and Waste Management*, 16, 693-710. <https://doi.org/10.1007/s10163-013-0220-z>
- Al-Masri, E., Diabate, I., Jain, R., Lam, M. H., & Reddy, N. S. (2019). Recycle.io: An IoT-enabled framework for urban waste management. In *Proceedings. 2018 IEEE International Conference on Big Data, Big Data* (pp. 5285-5287). IEEE Publishing. <https://doi.org/10.1109/BigData.2018.8622117>
- Anagnostopoulos, T., Zaslavsky, A., Ntalianis, K., Anagnostopoulos, C., Ramson, S., Shah, P., Behdad, S., & Salmon, I. (2020). IoT-enabled tip and swap waste management models for smart cities. *International Journal of Environment and Waste Management*, 28(4), 521-539. <https://doi.org/10.1504/IJEW.2021.10042472>

- Akshaya, B., & Kala, M. T. (2020). Convolutional neural network based image classification and new class detection. In *Proceedings of 2020 IEEE International Conference on Power, Instrumentation, Control and Computing* (pp. 1-6) IEEE Publishing. <https://doi.org/10.1109/PICC51425.2020.9362375>
- Bansode, P., Rasal, P. V., Waste, S., & City, S. (2021). Smart waste management for smart city using IoT. *Journal of Science and Technology*, 6(1), 53-58.
- Chandra, R. P., & Tawami, T. (2020). Design of smart trash bin. In *IOP Conference Series: Materials Science and Engineering: Material Science Engineering* (Vol. 879, p. 012155). IOP Publishing Limited. <https://doi.org/10.1088/1757-899X/879/1/012155>
- Department of Statistics Malaysia. (2020, November 27). *Compendium of Environment Statistics, Malaysia 2020* (Press Release). Department of Statistics Malaysia. <https://www.dosm.gov.my/v1/index.php?r=column/pdfPrev&id=TjM1ZlFxb3VOakdmMnozVms5dUIKZz09>
- Dugdhe, S., Shelar, P., Jire, S., & Apte, A. (2016). Efficient waste collection system. In *Proceedings of the International Conference on Internet of Things and Applications (IOTA)* (pp. 143-147) IEEE Publishing. <https://doi.org/10.1109/IOTA.2016.7562711>
- Fachmin, F., Low Y. S., & Yeow W. L. (2015). Smartbin: Smart waste management system. In *IEEE Tenth International Conference on Intelligent Sensors, Sensor Networks and Information Processing (ISSNIP)* (pp. 1-2). IEEE Publishing. <https://doi.org/10.1109/ISSNIP.2015.7106974>
- Ferronato, N., & Torretta, V. (2019). Waste mismanagement in developing countries: A review of global issues. *International Journal of Environmental Research and Public Health*, 16(6), Article 1060. <https://doi.org/10.3390/ijerph16061060>.
- Hanbal, I. F., Jeffrey, S. I., Neal, A. O., & Hu, Y. (2020). Classifying wastes using random forests, gaussian naïve bayes, support vector machine and multilayer perceptron. *International Conference Series: Material Science Engineering*, 803, Article 012017. <https://doi.org/10.1088/1757-899X/803/1/012017>.
- Ivan, L. (April 07, 2021). Council to give out free rubbish bins to residents *The Star*. <https://www.thestar.com.my/metro/metro-news/2021/04/07/council-to-give-out-free-rubbish-bins-to-residents>
- Kumar, N. S., Vuayalakshmi, B., Prarthana, R. J., & Shankar, A. (2016). IoT based smart garbage alert system using Arduino UNO. In *Proceedings of 2016 IEEE Region 10 Conference (TENCON)* (pp. 1028-1034). IEEE Publishing. <https://doi.org/10.1109/TENCON.2016.7848162>
- Lim, M. G., & Chuah, J. H. (2018). Durian types recognition using deep learning techniques. In *Proceedings of the 9th IEEE Control and System Graduate Research Colloquium (ICSGRC)* (pp. 183-187). IEEE Publishing. <https://doi.org/10.1109/ICSGRC.2018.8657535>
- Low S. T., Tee S. Y., & Choong W. W. (2016). Preferred attributes of waste separation behaviour: An empirical study. *Procedia Engineering*, 145, 738-745. <https://doi.org/10.1016/j.proeng.2016.04.094>
- Mirchandani, S., Wadhwa, S., Wadhwa, P., & Joseph, R. (2018). IoT enabled dustbins. In *Proceedings of the 2017 International Conference on Big Data, IoT and Data Science* (pp. 73-76). IEEE Publishing. <https://doi.org/10.1109/BID.2017.8336576>
- Nanda, S., & Berruti, F. (2021). Municipal solid waste management and landfilling technologies: A review. *Environmental Chemistry Letters*, 19(2), 1433-1456. <https://doi.org/10.1007/s10311-020-01100-y>

- Pelonero, L., Fornaia, A., & Tramontana, E., (2020). From smart city to smart citizen: Rewarding waste recycle by designing a data-centric IoT-based garbage collection service. In *Proceedings of 2020 IEEE International Conference on Smart Computing (SMARTCOMP)* (pp. 380-385). IEEE Publishing. <https://doi.org/10.1109/SMARTCOMP50058.2020.00081>
- Rana, R., Ganguly, R., Ashok, K. G., (2015). An Assessment of solid waste management in Chandigarh City, India. *Electronic Journal of Geotechnical Engineering*, 20, 1547-1572.
- Ruiz, V., Sanchez, A., Velez, J. F., & Raducanu, B. (2019). Automatic image-based waste. In J. M. F. Vicente, J. R. A. Sanchez, F. D. L. P. Lopez, J. T. Moreo & H. Adeli (Eds), *From Bioinspired Systems and Biomedical Applications to Machine Learning* (pp. 422-431). Springer Nature. <https://doi.org/10.1007/978-3-030-19651-6>
- Shaily, T., & Kala, S. (2020). Bacterial image classification using convolutional neural networks. In *Proceedings of the IEEE 17th India Council International Conference (INDICON)* (pp. 1-6). IEEE Publishing. <https://doi.org/10.1109/INDICON49873.2020.9342356>
- Sushmitha, N., Veena, R. C., Ajay, K., Ajith, D., & Yasarwi, K. (2018). An IoT based waste management system for smart cities. *International Journal of Emerging Technologies and Innovative Research*, 5(12), 202-205.
- The World Bank. (2018, September 20). *Global waste to grow by 70 percent by 2050 unless urgent action is taken: World Bank report*. (Press Release). <https://www.worldbank.org/en/news/press-release/2018/09/20/global-waste-to-grow-by-70-percent-by-2050-unless-urgent-action-is-taken-world-bank-report>
- Wahab, M. H. A., Kadir, A. A., Tomari, M. R., & Jabbar, M. H. (2014). Smart recycle bin: A conceptual approach of smart waste management with integrated web based system. In *Proceedings of 2014 International Conference on IT Convergence and Security (ICITCS)* (pp. 1-4 ). IEEE Publishing. <https://doi.org/10.1109/ICITCS.2014.7021812>
- Wang, S., Chen, W., Xie, S. M., Azzari, G., & Lobell, D. B. (2020). Weakly supervised deep learning for segmentation of remote sensing imagery. *Remote Sensing*, 12(2), Article 207. <https://doi.org/10.3390/rs12020207>
- Wu, M., Lu, Y., Yang, W., & Wong, S. Y. (2021). A study on arrhythmia via ECG signal classification using the convolutional neural network. *Frontiers in Computational Neuroscience*, 14, 1-10. <https://doi.org/10.3389/fncom.2020.564015>
- Zeiler, M. D., & Fergus, R. (2014). Visualizing and understanding convolutional networks. In D. Fleet, T. Pajdla, B. Schiele & T. Tuytelaars (Eds.), *Computer Vision-ECCV 2014, Lecture Notes in Computer Science*, (Vol. 8689). Springer. [https://doi.org/10.1007/978-3-319-10590-1\\_53](https://doi.org/10.1007/978-3-319-10590-1_53)





Review Article

## Some Abiotic and Biotic Factors Influencing Firefly Population Abundance in Southeast Asia: A Review

Nurhafizul Abu Seri<sup>1</sup>, Azimah Abd Rahman<sup>1\*</sup> and Nur Faeza Abu Kassim<sup>2</sup>

<sup>1</sup>Geoinformatic Unit, Geography Section, School of Humanities, Universiti Sains Malaysia, 11800 USM, Pulau Pinang, Malaysia

<sup>2</sup>School of Biological Sciences, Universiti Sains Malaysia, 11800 USM, Pulau Pinang, Malaysia

### ABSTRACT

This paper reviews biotic and abiotic factors that influence the life cycle of fireflies. This review paper has screened and chosen articles by using Preferred Reporting Items for Systematic Reviews and Meta-Analyses (PRISMA) from two databases: Semantic Scholar (n = 1080) and Google Scholar (n = 2280). From this review, generally, abiotic factors, i.e., water level in soil, air temperature, air humidity, rainy season, altitude, water salinity (NaCl), wind direction, wind speed, dissolved oxygen (DO), biochemical oxygen demand (BOD), chemical oxygen demand (COD), ammonia nitrogen (NH<sub>3</sub>-N) and maximum air pollution index (API) were most likely influenced the population abundance and distribution of the fireflies in Southeast Asia. Biotic factors include the presence of *Cyclotropis carinata* snails, vegetation health, tree suitability (leaf size, density, arrangement of leaves, tree location), insecticides (Saponins) in some vegetation species, plant structural architecture, and food (nectar and sap) were the most likely to influence the presence of fireflies species even though synchronous firefly of Southeast Asia were found in other vegetation species, *Sonneratia caseolaris* (Berembang) still the most preferred display tree. From this

review, we also found that Malaysia has the highest reported findings on firefly studies in this region. To conclude, numerous abiotic and biotic elements should be researched further to determine their relationship to firefly populations and other vertebrate - invertebrates in their natural environment.

**Keywords:** Abiotic, biotic, fireflies, mangrove, Southeast Asia

### ARTICLE INFO

*Article history:*

Received: 07 December 2021

Accepted: 27 April 2022

Published: 09 November 2022

DOI: <https://doi.org/10.47836/pjst.31.1.20>

*E-mail addresses:*

[nurhafizul.abuseri97@gmail.com](mailto:nurhafizul.abuseri97@gmail.com) (Nurhafizul Abu Seri)

[azimahrahman@usm.my](mailto:azimahrahman@usm.my) (Azimah Abd Rahman)

[nurfaeza@usm.my](mailto:nurfaeza@usm.my) (Nur Faeza Abu Kassim)

\*Corresponding author

## INTRODUCTION

There are generally various species of fireflies that can be found in all parts of the world. They are mainly distributed in the tropical areas of Southeast Asia (Branham, 2002), with eleven species of the *Pteroptyx* genus identified in Southeast Asia (Ballantyne, 2001). Terrestrial arthropods, insects, and beetle species may be found worldwide in a wide range of biogeographical locations (Table 1). It is estimated that around 15% of insect species are in the north temperate region, while the remainder lives in the tropics and south temperate regions. The neotropics may have more than 1.6 million insect species, with comparable counts for the Australasian and Indo-Malayan areas combined and fewer than a million species for the Afrotropical region (Table 1) (Stork, 2018). Insect species are likely to experience a variety of conditions as they spread across different biogeographical regions. Because abiotic factors are variable in different climates, these species will have distinct abiotic factor requirements. There are around 5.5 million insects, 1.5 million beetles, and 7 million terrestrial arthropods species known worldwide (Stork, 2018), with about 2000 known species of fireflies (Coleoptera: Lampyridae) all around the globe (Lewis et al. 2020). The Lampyridae consists of non-luminous adults, flightless female fireflies, and lightning insects (Lewis et al., 2020). According to Matalin and Wiesner (2006), Latreille (1817) established and defined fireflies as insects belonging to the family Lampyridae of the Coleoptera order. Since then, many new species have been described, and some significant range extensions have been reported. In addition, fireflies can be found in temperate to tropical regions (Chan, 2012).

Thailand, Malaysia, Cambodia, Indonesia, the Philippines, New Guinea, and Sulawesi are among the tropical climate countries where fireflies are extensively spread, and various firefly species exist (Ballantyne & McLean, 1970; Ballantyne & Lambkin, 2001; Nuranca et al., 2013; Jusoh et al., 2018; Sartsanga et al., 2018). In Southeast Asia and the Indo-Pacific region, over 400 species have been identified, most of which are members of the Luciolinae family (Ballantyne et al., 2015). Seri and Rahman (2021) successfully identified 145 firefly species across Southeast Asian countries (including Malaysia, the Philippines, Indonesia, Cambodia, Myanmar, Singapore, Sri Lanka, Papua New Guinea, Laos, Thailand, and Vietnam). At the same time, the authors were also unsuccessful in locating studies in Brunei. Additionally, they noted that data on firefly species found in countries such as the Philippines, Indonesia, Cambodia, Myanmar, Singapore, Sri Lanka, Papua New Guinea, Laos, and Vietnam is extremely outdated due to the country's lack of research (Seri & Rahman, 2021). Regretfully, there has been a decline in the distribution and abundance of numerous firefly species during the previous few decades (Lauff, 2017; Lloyd, 2018). However, since 2007, the firefly population in Kampung Kuantan, Kuala Selangor, Selangor has decreased by 42% in ten years as a result of riverbank cleaning (Nadirah et al., 2020).

Table 1

*Estimated numbers of terrestrial arthropods, insects, and beetle species in various biogeographic areas (Stork, 2018)*

Region	Number of arthropod species	Number of insect species	Number of beetle species
Australasia	890,799	720,521	196,515
Afrotropical	1,205,639	975,179	265,971
Central America	760,240	614,918	167,713
Indo-Malayan	908,479	734,822	200,416
North America	142,800	115,503	31,502
Neotropics	2,003,279	1,620,348	441,935
Oceanic	240,720	194,706	53,104
Palaearctic	648,040	524,165	142,961
Total	648,040	5,500,163	1,500,118

Fireflies produce synchronized spectacle light when congregating in colonies on certain trees. They are commonly seen on Berembang trees (*Sonneratia caseolaris*) (Nada & Kirton, 2004). The most well-known genus due to its spectacular synchronized flashing is *Pteroptyx* fireflies. They are native to coastal areas and riverbanks in Southeast Asia (McKenna & Farrell, 2009). Various techniques have been used to monitor changes in the abundance of *Pteroptyx* species in particular locations, such as the use of land-use spatial analysis of satellite images (Jusoh et al., 2009; Jusoh et al., 2012); non-destructive estimation methods (i.e., a percentage cover chart based on firefly flashing; visual method) (Jusoh et al., 2010a; Shahara et al., 2017); visual counting methods (Prasertkul, 2018); and digital night photography and image analysis digital night photography of the vegetation (non-destructive method) (Khoo et al., 2012). Meanwhile, several studies examining the habitat requirements of fireflies and the factors affecting their abundance have been conducted using a variety of techniques, including photo visual analysis using a high-resolution camera (720 pixels HD) (Faudzi et al., 2021); sweep-netting sampling (Abdullah et al., 2019; Hazmi & Sagaff, 2017); combination between visual counting and sweep net (Jaikla et al., 2020) and visual assessment and aerial net sampling (Foo & Mahadimenakbar, 2015). However, these studies have limitations and should be improved to understand better how specific factors affect the population abundance of these fireflies and their ecological requirements. For example, based on the findings of previous studies, many studies focus exclusively on the short adult phase life cycle of fireflies, although the most prolonged development period happens below the soil surface (especially the stage). Thus, this paper

review aims to evaluate experimental findings on the influence of various biotic and abiotic factors on firefly populations (Coleoptera: Lampyridae) throughout Southeast Asia.

## METHODOLOGY

This study employed a systematic literature review; journal articles were sourced from two of the largest online databases: Semantic Scholar (n = 1080) and Google Scholar (n = 2280). Both review and empirical studies included in the literature review were from the reputable journals, primarily indexed by SCOPUS, and some by Web of Science, namely the *Biodiversity Data Journal*, *International Journal of Tropical Insect Science*, *Oriental Insects*, *Transactions of the American Entomological Society*, *Insects*, *Raffles Bulletin of Zoology*, *BioRisk*, *Sepilok Bulletin*, *Journal of Tropical Biology & Conservation*, *Ecology and General Biology*, *Royal Society Open Science*, *Journal of Asia-Pacific Biodiversity*, *Malaysian Applied Biology*, *Wetlands Ecology and Management*, *Lampyrid*, *Zootaxa*, *Environment and Natural Resources Journal*, *Chemosphere*, *BioScience*, *Journal of Insect Conservation*, *Biodiversity*, *Aquatic Botany*, *Modern Applied Science*, *Science Report of the Yokosuka City Museum*, *Journal of Natural Remedies*, *Pertanika Journal of Tropical Agricultural Science*, *The Coleopterists Bulletin*, *Journal of Insect Behavior*, *Malayan Nature Journal*, *Annual Review of Entomology* and *NU International Journal of Science*.

The Preferred Reporting Items for Systematic Reviews and Meta-Analyses (PRISMA) technique was used to methodically pick relevant research from the available literature in this paper review writing. Four phases need to be followed using the PRISMA method: identification, screening, eligibility, and inclusion (Figure 1). Among the keywords used when searching journal articles from the database are: “Fireflies,” “Fireflies in Southeast Asia,” “Abiotic,” “Biotic,” “Mangrove,” “*Pteroptyx* fireflies,” “Life Cycle,” and “Water Quality.”

## RESULTS AND DISCUSSION

According to previous studies, the most frequently employed approach was sweep-netting sampling, as in the study by Wattanachaiyingcharoen et al. (2011); Shahara et al. (2017); Jusoh et al. (2010a); Abdullah et al. (2019); Abdullah et al. (2020); Hazmi and Sagaff (2017); Badruddin and Ballantyne (2020); Sriboonlert et al. (2015) Sulaiman and Abdullah (2017); and Wattanachaiyingcharoen et al. (2011); Wattanachaiyingcharoen et al. (2016); Wijekoon et al. (2012); Asri et al. (2020). Additionally, some studies combine visual counting and sweep net sampling, as shown in the study by Jaikla et al. (2020), and visual evaluation with aerial net sampling, as indicated in a study by Foo and Mahadimenakbar (2015). In addition, other methods were used in previous studies, such as visual counting (Prasertkul, 2018; Khoo et al., 2012; Faudzi et al., 2021) and aerial net (Sulaiman et al., 2017).

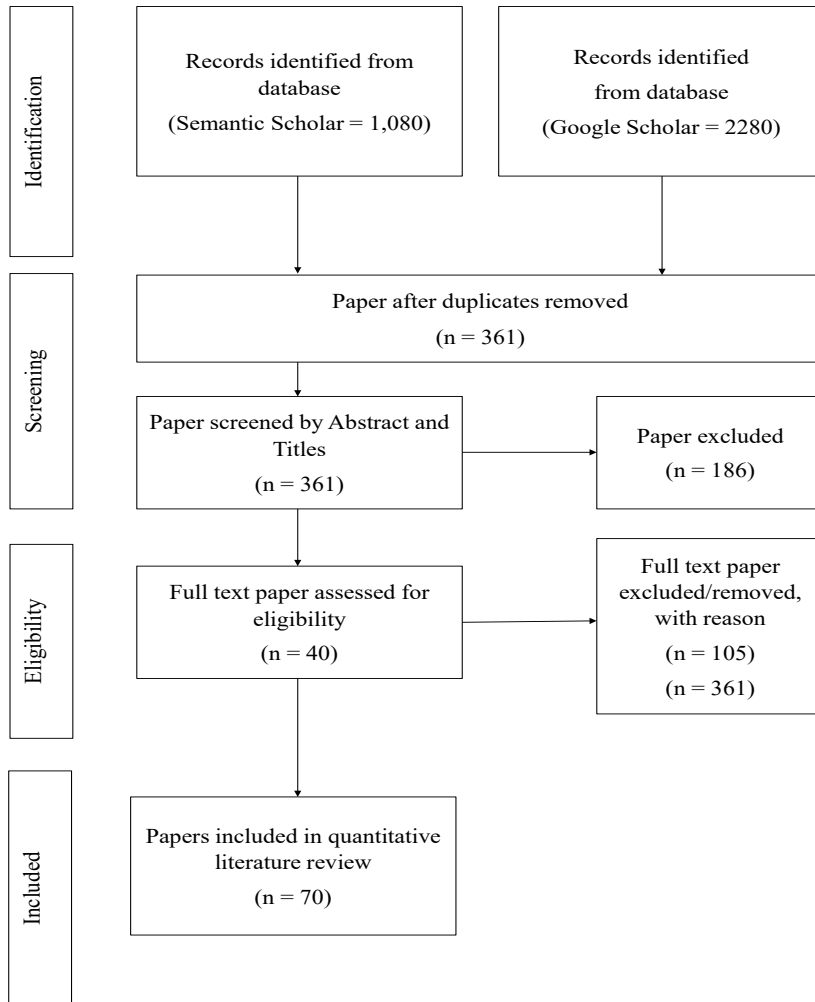


Figure 1. PRISMA methodology flowchart

Previous researchers preferred sweep nets because they are usually made of heavy material that can be dragged through dense vegetation without damage. This sweep net has the advantage of sweeping through vegetation to capture random insects that are not apparent, which is very useful when capturing adult fireflies at night. Meanwhile, aerial nets are rarely used, probably due to their durability; they are composed of several types of netting material and usually have a lightweight handle. Due to its lightweight feature and not being as thick as a sweep net, an aerial net is easily damaged if used in areas with dense vegetation.

DeWalt et al. (2015) suggested that sweep nets with a 38-cm net ring, 91-cm handle, and white muslin bag are highly suitable for sweeping insects out of riparian vegetation.

Sweep net sampling is excellent for determining species' existence and abundance in the field, but it does not provide a reliable estimate of larval density (Edde, 2022). In addition, the weakness in terms of methods applied by previous researchers was the relatively short study period. Ideally, a relatively long study period that may be more than six months to one year is very rational to do to be able to compare the population abundance of fireflies in each different year. So, the researcher will get complete data for one year and cover for each season within that year.

Not many past studies have used the Geographic Information Systems (GIS) and Spatial Analysis approach. Most only used the Global Positioning System (GPS) to mark a congregating station/vegetation of fireflies. Some previous studies use very simple mapping techniques, such as Wijekoon et al. (2012); Wattanachaiyingcharoen et al. (2011); Sartsanga et al. (2015); Jusoh et al. (2010b); Jusoh et al. (2011); Asri et al. (2020); Prasertkul (2018); and Shahara et al. (2017). All the mapping shows the sampling area and the species found there. A study can be said to be more advanced in the mapping technique compared to other previous studies by Jusoh et al. (2012). In the study, they used the land-use spatial analysis of satellite images to investigate the changes taking place to the mangroves on which the fireflies depend. The study conducted by Abdullah et al. (2020) should apply the inverse distance weighting (IDW) technique to obtain a more precise and more exciting data presentation on the relationship between water quality parameters and firefly population.

Several GIS techniques can be used to show the population density of fireflies. First, the hotspot technique shows which area (display tree, sampling point) is the hotspot area (focus) of fireflies, as well as which vegetation species is the primary choice of fireflies to be selected as a display tree. Second, buffering analysis. Buffering can be used to determine the area covered by fireflies in a particular location by indicating at what distance can affect the population distribution of fireflies. As for water quality, among the GIS techniques used is inverse distance weighting (IDW). This technique has been used to delineate groundwater pollutants' area distribution and obtain the spatial dissemination of water quality parameters of the river near the firefly habitat. Finally, data visualization in mapping is easy to comprehend and interpret. Thus, it is suggested that more techniques than GIS applications be used in studies related to the population abundance of fireflies.

Furthermore, the data analysis techniques used in the study of Shahara et al. (2017), i.e., Percentage Cover Estimation (PCE), provide an abundance index (Jusoh et al., 2010b; Nada et al., 2012; Shahara et al., 2017), but it does not indicate how many males are present in each congregation. Digital night photography-image analysis (Khoo et al., 2012) and photo visual analysis using a high-resolution camera (720 pixels HD) (Faudzi et al., 2021) may provide a more reliable estimate. However, it requires meticulous setups on a well-positioned platform that may not be available for every congregation. Another disadvantage of using this technique (Prasertkul, 2018) is that long-exposure photography is sensitive

to movement. So, it will be hard to get a clear picture when the fireflies are moving, or the trees sways. Therefore, manual flash counting was still ideal for studies involving fireflies.

### **Biotic Factors**

Several biotic factors can influence the abundance of fireflies. Human activities or natural calamities, for example, might endanger the snail the firefly larvae feed on (Foo & Mahadimenakbar, 2015). These are because certain riparian vegetation species, such as *Sonneratia caseolaris*, *Hibiscus tiliaceus*, *Nypa fruticans*, *Acrostichum aureum*, *Areca cathechu*, *Oncosperma tigillarum*, and *Ficus* sp., are frequently found in riparian habitats and are associated with fireflies in Peninsular Malaysia and Thailand (Khoo et al., 2012; Prasertkul, 2018; Juliana et al., 2012). The larvae of fireflies are predators of the tiny snails *Cyclotropis carinata* that inhabit the riverbanks (Nada & Kirton, 2004). Their larvae can be found in mangroves and mangrove fringes where *Acrostichum aureum*, *Acanthus ebracteatus*, and *ilicifolius* are present. *Colophotia praeusta*, on the other hand, is a scrubland species. Their adults are found in damp places with few trees and dense grass, among grasses and weeds. Meanwhile, *Pyrocoelia* sp., *Stenocladus* sp., and *Diplocladon* sp. were discovered in secondary forests in Singapore. Adult *Pyrocoelia* sp. likes to visit forest edges in open and closed areas (Chan, 2012). However, in northern Thailand, one species of firefly, *Asymmetricata circumdata* (Motsch.), can be found in disturbed regions such as urban and cultivated areas, but the population is still limited in comparison to natural environments (mixed deciduous forests) (Wattanachaiyingcharoen et al., 2011).

Most *Pteroptyx* spp. have a riparian environment supporting mangroves but not necessarily a mandatory association with mangroves or any particular species. For example, *Pteroptyx galbina* was found up to 30 km from the sea, whereas *P. bearni* Olivier is found in mangroves and other riverside flowering plants (Jusoh et al., 2018). It has been found that most species of firefly prefer to display trees along riverbanks in mangrove zones (Jusoh et al., 2011). Nevertheless, these species' selection of display trees is not necessarily from the same species (Chey, 2004; Ohba & Wong, 2004) since firefly species were discovered to appear in other vegetations species in Sabah's riparian area, including *Rhizophora apiculata*, *Clerodendrum inerme*, *Glochidion littorale*, *Bruguiera parviflora*, and *Excoecaria indica* (Chey, 2004; Mahadimenakbar & Fiffy Hanisdah, 2016). It was demonstrated in a study by Li et al. (2013), who discovered significant differences in the richness and abundance of ground-dwelling arthropods beneath various shrub species. The general impression was that *Sonneratia caseolaris* (L.) Engl. was the mangrove tree. (Sonneratiaceae) was much preferred as a display tree, but it depends on the health condition of this vegetation (Shahara et al., 2017).

While according to Chey (2004), *P. tener* is not specific to which tree it roosts; rather than specificity, its preference is determined by tree suitability. Additionally, Ohba and



Wong (2004) stated that *Pteroptyx* congregations do not require a specific plant species because leaf size, density, and arrangement of leaves, as well as tree location, are potential considerations in display tree selection. In the investigation that has been done on the foliage of the firefly trees, scars, lesions, and tunnels were visible on several leaves, which could have been made during adult firefly feeding (Othman et al., 2018). Klias River (Malaysia Borneo, Sabah) has some trees covered in sparkling fireflies. The trees include the Dungun tree, the mangrove tree Bangkita, and the *Rhizophora apiculata* Bl. (Rhizophoraceae), and the *Excoecaria indica* (Willd.) Muell. Arg. (Euphorbiaceae) tree, also known as the Ligura (Chey, 2004). Chey (2004) also noted the presence of nipa and sago trees near the Klias River, ideal habitats for firefly larvae. The higher firefly larval density in Sago palm groves than in oil palm plantations has been attributed to several factors: 1) The sago patch was cooler, more humid, and shaded; 2) The orchard and oil palm plantation had higher mean air temperatures and lowered mean relative humidity than the sago patch; 3) The orchard had significantly higher soil temperature at a depth of 5 cm than the oil palm plantation and sago patch; and 4) The orchard had the highest photon flux density and the sago patch had the lowest (Kirton et al., 2006). It shows the interconnectedness between the firefly and the river ecosystem. Other possible explanations include the likelihood that the Chukai River in Terengganu, Malaysia, has a low insect population due to the vegetation, *B. racemosa*, that dominates the Chukai River's banks. This plant species is known to contain insecticides (Saponins) capable of repelling insects' presence (Osman et al., 2017).

Most fireflies have been found in *Sonneratia caseolaris* (L.) Engl., (Jusoh et al., 2011), but this species was also found on other display tree species, including *Gluta velutina* Blume, *Hibiscus tiliaceus* L., *Xylocarpus granatum* J. König, *Avicennia alba* Blume, *Rhizophora apiculata* Blume, *Excoecaria agallocha* L., *Barringtonia racemosa* (L.) Spreng., *Bruguiera gymnorhiza* (L.) Lam. and *Nypa fruticans* Wurmb. However, in Peninsular Malaysia, oil palm plantations are encroaching on riverbanks, posing a threat to firefly habitat (Jusoh & Hashim, 2012). Because biotic factors such as mangrove assemblages have a close relationship with firefly abundance, it is critical to protect mangrove swamp ecosystems to maintain their ecosystem functions (Jusoh et al., 2010a). In Thailand, habitat fragmentation is assumed to be responsible for the decline in the population size or local extinction of *Luciola aquatilis* Thancharoen fireflies, as it restricts the firefly dispersal range (Thancharoen, 2007). In addition, several studies conducted in Sabah, Malaysia, such as those conducted on Sakar Island off the coast of Lahad Datu Sabah, found that two firefly species, *Pteroptyx bearni* and *Pteroptyx gelasina*, selected *Scyphiphora hydrophyllacea*, *Rhizophora apiculata*, *Rhizophora mucronata*, and *Rhizophora stylosa* as their display trees (Chey, 2011). In the Garama River, Beaufort fireflies *Pteroptyx bearni*, *Pteroptyx malaccae*, and *Pteroptyx tener* prefer *Rhizophora apiculata*, *Ficus microcarpa*, and *Clerodendrum inerme*, respectively (Chey, 2010); however, in the Klias River, Beaufort, these three

species of fireflies are only found in two types of vegetation, namely *Rhizophora apiculata* and *Glochidion littorale* (Chey, 2010). *P. gelasina* and *P. bearni* in Trayong, Tuaran, chose to be in *Scyphiphora hydrophyllacea* and *Lumnitzera littorea* vegetation (Chey, 2009). Finally, *P. gelasina* and *P. bearni* species discovered in the Sepilok Forest Reserve, Sandakan, chose *Lumnitzera littorea*, *Rhizophora apiculata*, *Scyphiphora hydrophyllacea*, and *Rhizophora mucronata* vegetation as their habitat (Chey, 2008).

Meanwhile, because mangroves provide an essential ecosystem for larvae that feed on snails in the intertidal zone, fireflies and mangroves are closely associated (Nagelkerken et al., 2008). *Pteroptyx* species are classified as semi-aquatic fireflies since they spend their larval stage on muddy riverbanks and may survive for a short period underwater (Thancharoen, 2007). For instance, the snail *Cyclotropis carinata* (Assimineidae) is the primary prey for the firefly larvae, which can be found in tidally inundated areas of riverbanks. Besides entering the shells of the snails and injecting a paralyzing toxin and an enzyme into their soft body tissues to aid in feeding, these larvae are also capable of entering their prey shells (Nagelkerken et al., 2008). It is proven that the prey of snails inhabiting damp areas in mangrove swamps is crucial for the survival of fireflies in the larval stage. This larval stage is the most vital and essential stage for fireflies because they spend a significant amount of time in this stage, which is 97.83 days, dependent on the river water (Loomboot et al., 2007). Near Nipah and Sago palm trees, the larvae, which eat river snails, are often found 5 to 30 meters away from the display trees (Loomboot et al., 2007). Firefly larval density was more significant in Sago palm groves than in oil palm stands, owing to the supply of food (*Cyclotropis carinata* snails) in the patches of sago, compared to few or no snails in oil palm plantations (Kirton et al., 2006). According to Cheng et al. (2017), the adult firefly will also travel further inland, searching for food sources (*Heritiera littoralis*). Overall, the life cycle of *Pteroptyx malacca* Gorham species lasted about 12.15 days during eggs, larvae (97.83 days), pupae (9.83 days), and adults (12.33 days) (Loomboot et al., 2007). *Pteroptyx* larvae feed on mangrove snails, and after they fully develop, the larvae will construct a tiny cell in the mud for pupation (Loomboot, 2007; Loomboot, 2008). *S. caseolaris*, which can be found in the riparian area, has unique and different structural architecture; its complex structure and larger-sized vegetation can provide more resources in the form of leaves and litter for insects to thrive on, particularly food sources (Abdullah et al., 2019).

As for the *Pteroptyx valida*, their life span ranges from 107–228 days, with lasted about 16–25 days during eggs, larvae (76–168 days), pupae (5–13 days), and adults (6–15 days) (Jaikla et al., 2020). Their larvae and some snails that they feed on brackish water are favored in the intertidal zone (Chan, 2012) (Figure 2). The preference for *S. caseolaris* could be explained by the nectaries found on young *S. caseolaris* trees, which supply nutrition for adult fireflies (Juliana et al., 2012; Nallakumar, 2003) and catalyze a series

of chemical reactions within the firefly's body, resulting in photon flashes (synchronous flashing) (Nallakumar, 2003). Adult fireflies, for example, use the *S. caseolaris* trees that line the Selangor River's riverbanks as mating places and food sources due to the presence of sugar in the sap of these trees (Nada et al., 2009). Othman et al. (2018) discovered a unique food canal running from the tip to the end of *P. tener*'s mandible, which confirms it. The mandible tip may be used as piercing equipment by *P. tener* to suck plant sap for food. Additionally, evidence from this species' digestive tract revealed that these species have a tiny crop, a large ventriculus, and a long intestinal tract, all suited for a liquid feeder insect. To sum up, *S. caseolaris* (Berembang) was the most preferred display tree in Peninsular Malaysia by the *Pteroptyx tener* (Jusoh et al., 2010a; Jusoh et al., 2010b).

At Mae Wong National Park and in the evergreen forests of Thailand, *Asymmetricata circumdata* have been found, which are favorite places to find land snails, earthworms, and soft-bodied insects that could be a helpful food supply for firefly larvae (Wattanachaiyingcharoen et al., 2011). In Singapore, mangroves are home to the *Pteroptyx valida*. Adults of this species prefer *Avicennia alba* mangroves, but they can also be found in *Rhizophora apiculata* and *Sonneratia alba* mangroves. In the mangrove area of Nakhon Sri Thammarat, Thailand, which is closer to Malaysia and linked to Surat Thani, no *Pteroptyx tener* was found. It is probably due to the lack of ecological linkages in coastal habitats suitable for fireflies, owing to the fragmentation of mangrove areas in this country, which has influenced the occurrence trend of *P. tener* (Sriboonlert et al., 2015). The study by Jaikla et al. (2020) shows that display trees with open canopies located at river bends are prominent features for fireflies.

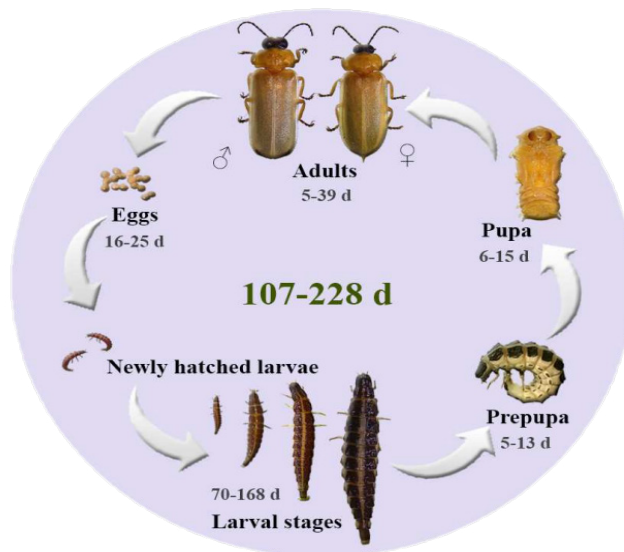


Figure 2. Life cycle of *Pteroptyx valida* in Thailand (Jaikla et al., 2020)

### Abiotic Factors

Wind speed is one of the abiotic factors that influence the firefly population. According to a study by Asri et al. (2021), wind speed significantly impacted the temporal variation of fireflies. They also discovered that the population size of fireflies in Sungai Rembau in Negeri Sembilan, Malaysia, decreased from January to April 2018 and varied due to wind speed changes. Their findings are similar to those of Abdullah et al. (2019), who reported that wind speed had influenced the population size of fireflies at the same study area (i.e., Rembau River). Conversely, in the same study, Abdullah et al. (2019) also discovered that wind speed had a significant negative association with insect abundance and diversity in the Sepetang River and Chukai River. The difference may be due to geographical factors of the study area where Sungai Rembau Negeri Sembilan was exposed to Southwest monsoon types with a wind speed of 15 knots stronger than the wind in the Sepetang River and Chukai River (Asri et al., 2021). The study by Jaikla et al. (2020) on the influence of wind direction and speed on the horizontal distribution of *Pteroptyx* spp. in Thailand.

Bang Bai Mai, Surat Thani; Phetchaburi River, Phetchaburi; Khae, Khlong Thom, Krabi; and Pak Phanang, Bang Kong Khong, Nakhon Si Thammarat) revealed that firefly species preferred to perch on tree areas facing away from the current wind direction (Figure 3). 85% of this firefly species sat more than 45° to either side of the wind direction. 13.1% of the fireflies perched closer to the current wind direction (within 45° on both sides), and 1.9% of the fireflies perched directly facing the wind.

Next, in terms of the soil condition, female fireflies usually fly to the muddy cliffs behind the vegetation after mating and laying their eggs in damp soil (Nada et al., 2008). Therefore, it is suggested that to lay eggs, female fireflies require damp soil. According to Ohba and Sim (1994), excessive water is beneficial to the larvae of the *Pteroptyx Valida* and encourages the population to increase. In addition, firefly eggs require moist soil and shaded areas, such as those provided by *Rhizophora* sp., to ensure that the eggs will not become damaged when exposed to high temperatures and dry conditions (Jusoh et al., 2010a). *Pteroptyx valida* larvae were found in the mangrove area of Singapore, where they preferred moist, wet soil and damp leaf litter composed primarily of *Hibiscus tiliaceus* leaves. *Pyrocoelia* sp., *Stenocladus* sp., and *Diplocladon* sp. larvae preferred moist, wet soil and leaf litter on forest fringes (Chan, 2012). The *P. tener* Thailand was only spotted in a brackish river along the Tapi River in Phunpin district, Surat Thani. *Pteroptyx* fireflies in this area were present throughout the year, with the most significant proportion of adult fireflies seen in October and December (Sriboonlert et al., 2015).

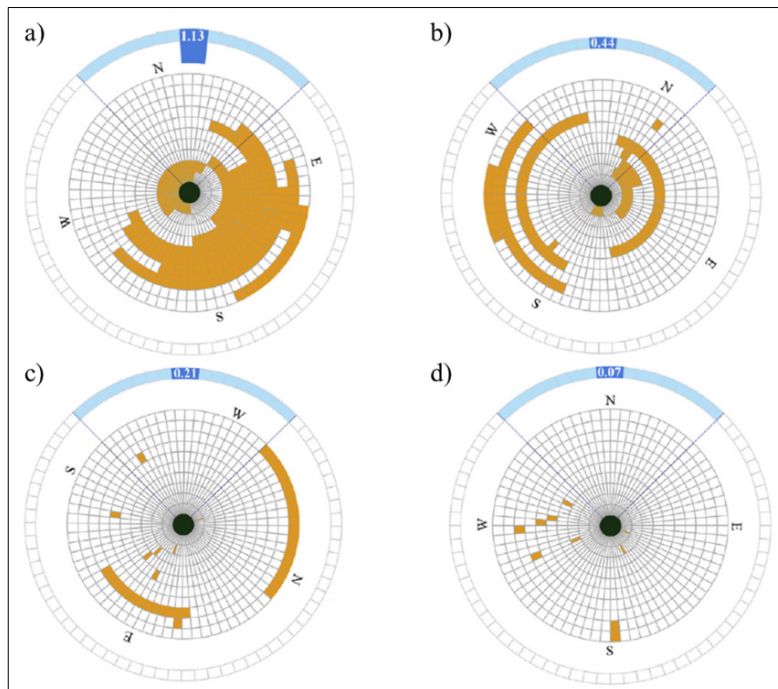


Figure 3. The effect of wind direction on the perching position of *Pteroptyx* spp. in Thailand: a) Bang Bai Mai, Surat Thani; b) Phetchaburi River, Phetchaburi; c) Khae, Khlong Thom, Krabi; and d) Pak Phanang, Bang Kong Khong, Nakhon Si Thammarat (Jaikla et al., 2020)

Notes: Concentric Circles - Display Trees; Orange Bands - *Pteroptyx* Spp. Perching Positions; Dark Blue Bands (In the Outermost Circle) - Wind Direction and Wind Speed; Taller Blue Bands Indicate Stronger Wind Speed

Air temperature has also been proven to have a spatial impact on firefly populations. The size of the firefly population has been reported to have decreased and varied as a result of temperature changes (Asri et al., 2021). The flash interval of fireflies is greatly influenced by air temperature; the flash interval increases when the air temperature falls. Furthermore, the regressions of flash interval on air temperature changed considerably between locations but not between years (Iguchi, 2002). According to Abdullah et al. (2020), ambient air temperature negatively correlates with firefly abundance in Sungai Niah and Sungai Sibuti, Miri, Sarawak, Malaysia, indicating that the firefly is susceptible to higher temperatures. The ambient air temperature in these areas ranged from (24.0°C to 27.9°C). About 2000 fireflies from the beetle order Coleoptera and Lampyridae families are consistently found in varied temperate and tropical climates worldwide (Wang et al., 2007). Hermann et al. (2016) found a trend in firefly activity, indicating that temperature accumulation is indeed a driver of firefly activity. The temperature accumulation of roughly 800 degrees (base 10°C) is where activity peaks. The model also reveals that precipitation



extremes delay thermally moderated firefly activity. As for the firefly larvae, the optimal temperature for larval activity is 18-30°C (Wang et al., 2007). Air temperature ( $27.6 \pm 0.7^\circ\text{C}$ ) and relative humidity ( $82.7 \pm 3.2\%$ ) were found to be important in determining the abundance of the firefly population along the Sungai Sepetang riverbanks in Kampung Dew, Perak, Malaysia, particularly at night (Sulaiman et al., 2017). Although most fireflies are found in areas with high humidity, one species is known to live in the desert, namely the (Lampyridae: *Microphotus Octarthrus* Fall) which can be found in pinyon-juniper and juniper-oak ecosystems between 500 and 2,000 meters in Arizona, New Mexico, West Texas, and Utah (Usener & Cognato, 2005).

Conversely, the low temperature resulted in a large distribution of fireflies. It was attributed to the most significant number of fireflies collected at the sampling station at  $27.3^\circ\text{C}$  and  $28.8^\circ\text{C}$  compared to the sampling station with the highest mean temperature value of  $29.95 \pm 0.65^\circ\text{C}$  (Faudzi et al., 2021). Firefly Percentage Cover Estimation (PCE) of both the right and left riverbanks in Bernam River, Selangor, Malaysia, was shown to have weak and insignificant associations with the abiotic parameters (temperature, relative humidity, wind speed, water salinity, total dissolved solids, conductivity) (Shahara et al., 2017).

Firefly larvae are discovered hiding in cracks or under emarcid leaves, with the head retracted inside the pronotum and using the caudal grasping organ to cling to the substrate or plants during the day- an indication that they prefer low temperatures and high humidity. Then, the larvae began to crawl slowly after sunset (7 p.m. to 8 p.m.) (Wang et al., 2007). On the other hand, adults hide in tiny holes on the ground or perch at the bottom of leaves to escape sunlight throughout the day. Adults began to glow at sunset when the ambient light intensity was reduced. Glowing activity peaked around 1 hour later, when ambient light intensity was about 0 Lux, and generally ceased at 5:00 a.m. the next day. A study conducted in mainland China in 2003-2005 by Wang et al. (2007) showed that the glowing activity of fireflies decreased when there was bright moonlight and intense artificial light or windy, rainy, or cooler.

Meanwhile, it was in contrast to the findings of Foo and Mahadimenakbar (2015). They found that moonlight intensity does not influence on firefly abundance in Teratak River, Sabah, Malaysia, during the full moon and the night of the new moon. Similar to Shahara et al. (2017) findings, there are no statistically significant differences in firefly abundance between the full moon and new moon phases in Bernam River, Selangor, Malaysia. The differences in the study's findings may be because the study period used by Foo and Mahadimenakbar (2015), which was March to April 2014 (two months), and Shahara et al. (2017), which was February to April 2015 (three months), is comparatively short and insufficient to comprehend and make comparisons firefly abundance during the full moon and new moon nights. In opposition to Wang et al. (2007), field observations were made

over a more extended period, from 2003 to 2005, including daily visits during the summer and autumn. The difference may also be influenced by ambient light intensity since even when the full moon occurs, the light intensity may be obscured by thick and dark clouds and haze and smoke in the atmosphere.

The rainy season is ideal for firefly larvae and snails to grow and develop. This condition would increase the population of these species in the months following the rainy season (Nada et al., 2012). In northern Thailand, firefly diversity was influenced by seasonal variation. Some of them appeared during the winter when the temperature was lower at high altitudes (*Luciola* sp.3). It implied that fireflies could survive at high altitudes (Wattanachaiyingcharoen et al., 2016). *Luciola nicollieri* in colder, wetter regions of Uva, Sabaragamuwa, and the North-Western Province of Sri Lanka are evidence that firefly species favor cold climates with high rainfall distribution. Rainfall in Sri Lanka may significantly impact the diversity and abundance of firefly species (Wijekoon et al., 2012). *Luciola chinensis* (under the *Luciola praeusta* complex) was also found in the Southern, Uva, and Sabaragamuwa Provinces, which favored wet climates. However, *L. chinensis* was rarely reported in heavily urbanized areas (Western and Central regions), despite the area being likewise wet (Wijekoon et al., 2012). Meanwhile, *Pteroptyx asymmetria* is restricted on both coasts of southern Thailand, which shares a similar climate with Malaysia (Jaikla et al., 2020) with this species has been documented only in western Peninsular Malaysia (Jusoh et al., 2018).

Wattanachaiyingcharoen et al. (2016) stated that Northern Thailand's highlands were home to numerous fireflies. The seasonal appearance of these firefly species from the Subfamily Lampyrinae and Subfamily Luciolinae can be seen in Table 2. According to the evidence collected by Wattanachaiyingcharoen et al. (2016) in their study (Table 2), some fireflies had seasonal specificity. For instance, the *Diaphanes* sp. 3 and *Luciola* sp. 3 species only appeared in winter. *Pyrocoelia* sp. 2 and *Luciola trilucida*, on the other hand, appeared only during the wet (rainy) seasons. In addition, some firefly species in Northern Thailand, such as *Pyrocoelia analis* and *Luciola indica*, have a broader adult seasonal appearance, appearing from summer to rainy seasons. This record demonstrates a species preponderance in ambient environments, particularly *Pyrocoelia* sp. 2 and *L. trilucida*, that tend to appear in wet conditions. Another study found similar results, showing that *Asymmetricata circumdata* fireflies were found in various habitats in the north of Thailand between the end of April and the beginning of August. However, from the end of April to mid-May, when the weather was most likely to be rainy, the most significant number of fireflies were spotted (Wattanachaiyingcharoen et al., 2011).



Table 2

*The seasonal appearance of firefly species was found in 83 study sites in the highland areas of Northern Thailand (Wattanachaiyingcharoen et al., 2016)*

Species	Seasonal Appearance
<b>Subfamily Lampyrinae</b>	
<i>Diaphanes</i> sp.2	Early Rainy (Late May)
<i>Diaphanes</i> sp.3	Winter (December–February)
<i>Diaphanes</i> sp.4	Mid-winter (January)
<i>Lamprigera yunnana</i>	Late Rainy—Winter (October–January)
<i>Pyrocoelia analis</i>	Late Summer—Rainy (Early May–September)
<i>Pyrocoelia</i> sp.1	Winter (December–February)
<i>Pyrocoelia</i> sp.2	Rainy (June–September)
<b>Subfamily Luciolinae</b>	
<i>Abscondita anceyi</i>	Summer—Early Rainy (March–May)
<i>Abscondita chinensis</i>	Rainy—Winter (June–December)
<i>Asymmetricata circumdata</i>	Summer—Rainy (March–September)
<i>Asymmetricata ovalis</i>	Rainy (June–September)
<i>Curtos cerea</i>	Rainy (June–September)
<i>Luciola curtithorax</i>	Rainy (June–September)
<i>Luciola indica</i>	Late Summer—Rainy (Early May–September)
<i>Luciola triluclida</i>	Rainy (June–September)
<i>Luciola</i> sp.3	Winter (December–February)
<i>Pygoluciola</i> sp.1	Early Rainy (Late May)
<i>Trisinuata</i> sp.2	Late Summer—Rainy (Early May–September)
Unknown genus and species	Late Winter (January–February)

Temperature and humidity did not demonstrate a significant association with insect communities, according to a study by Abdullah et al. (2019); however, warmer and less humid environments can contribute to insect mortality. Over three years, from January 2006 to April 2008, the relatively consistent and slightly varying average monthly temperature and relative humidity did not appear to alter the increasing trend of the adult firefly population. During that period, the temperature ranged between 26.4–28.4°C, while the relative humidity was between 78.3–85.7% (Khoo et al., 2012). Meanwhile, Nada et al. (2012) discovered a remarkably steady average monthly temperature (26.4–28.4°C), relative humidity (78.6–84.9 %), and water quality [68 (slightly polluted) - 86 (clean)] with little variability from January 2006 to April 2007, seemingly scarcely affecting any trend in the adult firefly population. It was also discovered that air humidity geographically

affected the firefly population. Temperature variations have been seen to cause a reduction and fluctuation in the population size of fireflies (Asri et al., 2021). For firefly larvae, 90% or higher relative humidity is ideal for larval activity (Wang et al., 2007). It is also supported by Nada and Kirton (2004), who argued that humid environments might benefit larval growth and the host snail population. It is because the life cycle of *Pteroptyx tener* is expected to take around three months to complete.

Table 3

*Specimens of Pteroptyx species collected in Thailand during the period 2012 to 2015 (Sartsanga et al., 2018)*

Region	Number of specimens			
	<i>Pteroptyx asymmetria</i>	<i>Pteroptyx malaccaae</i>	<i>Pteroptyx valida</i>	<i>Pteroptyx tener</i>
East (Thai Gulf)	0	118	72	0
Central (Thai Gulf)	0	51	30	0
South (Thai Gulf)	22	128	43	30
South (Andaman)	65	2	5	0

Sartsanga et al. (2018) reported that only *P. malaccaae* and *P. valida* were present in East and Central Thailand, and no *P. asymmetria* was identified in those regions (Table 3). In contrast to the firefly species found in the South, *P. asymmetria* was the only species. The capability of *P. malaccaae* and *P. valida* to tolerate lower humidity and more fluctuating temperature conditions in the eastern and central areas (winter, hot, and rain) than in the south (rain and heat) may explain their prevalence in the East and Central areas. The most abundant *Asymmetricata circumdata* species in Thailand was found in the mixed deciduous forest of Mae Wong National Park at an altitude of 289 MSL (Mean Sea Level), with a population of more than 1,000 individuals per site. The evergreen forests in the country with an altitude of 950 MSL had an average firefly population of 100 individuals per site. This firefly species have also been found in evergreen forests throughout the year. It could be because the temperature is favorable throughout the year. As a result, food sources are available for the larvae of this species of fireflies, particularly in forest areas with less pesticide accumulation and less electric light. These are the factors that contribute to the natural reproduction of this firefly species. Compared to lowland and disturbed habitats, such as urban and agricultural areas, fewer individual species are reported (Wattanachaiyingcharoen et al., 2011). Furthermore, electric lights in metropolitan areas can disrupt firefly sexual communication (Thancharoen, 2007). It is supported by Thancharoen (2001), who found *A. circumdata* in the tropical rain forest of Pha Kluai Mai Waterfall, Khao Yai National Park, Thailand, at approximately 680 meters MSL.

In addition, water salinity (NaCl) can alter the soil where fireflies lay eggs and hatch as larvae (Abdullah et al., 2019). In Sungai Rembau, Malaysia, the water salinity indicated only a marginally negative association with firefly abundance spatially and temporally. The firefly population in this area had an optimal level of water salinity, which peaked in January 2018 to March 2018 and June 2018 to August 2018. In line with this event, the population of fireflies likewise peaked in the downstream area of the river (Asri et al., 2021). The salinity of the water is significant for the growth of aquatic and semi-aquatic insects, including the population of fireflies. A relative trend of rising insect abundance with decreasing salinity value has been seen in Malaysia's Sungai Sepetang, Sungai Rembau, and Sungai Chukai. As most larval growth occurs in the water, the river's salinity must be maintained within a tolerable limit (Abdullah et al., 2019). By contrast, Khoo et al. (2012) found that a significant rise in salinity in Selangor River, Malaysia, did not affect the population of fireflies residing in *Sonneratia caseolaris* along the riverbank. In addition, salinity may impact the soil where fireflies lay their eggs and hatch as larvae. However, the direct effect of salinity on the firefly has never been investigated before (Abdullah et al., 2019).

Faudzi et al. (2021) researched in March 2019 to investigate the association between seven water quality parameters and the abundance of firefly populations in the Cherating River, Pahang, Malaysia. According to the study's findings, two parameters, namely the potential of hydrogen (pH) and suspended solids (TSS), had no association with the firefly population. Aside from that, other parameters showed a correlated association between firefly abundance and water quality parameters. For example, there was a strong positive correlation between dissolved oxygen (DO) and the firefly population. Meanwhile, there was a strong negative correlation between the firefly population and water temperature, biochemical oxygen demand (BOD), chemical oxygen demand (COD), and ammonia nitrogen (NH<sub>3</sub>-N). It implied that five water quality parameters, namely water temperature, DO, BOD, COD, and ammonia nitrogen, appeared to impact the firefly population abundance in the Cherating River. The study also found that the higher the temperature in a waterbody, the fewer fireflies in a particular region (Faudzi et al., 2021).

Meanwhile, the Sepetang River in Kampung Dew, Taiping, Perak contains a high concentration of heavy metals, which causes the river's water quality to deteriorate, which subsequently interrupts the life cycle of fireflies (Nada & Kirton 2004; Hazmi et al., 2017). Pollution and dam and embankment construction operations farther upstream, according to Nada and Kirton (2004), are among the causes of changes in the river water quality. These activities can eventually impair the survival of snails and riverbank plants near the firefly habitat. It suggests that water quality is one of the abiotic factors indirectly associated with firefly survival. The moderate decline in water quality in the Selangor River in December 2006 and December 2008 did not appear to affect the adult firefly population

in the following months (Khoo et al., 2012). It suggests that a moderate decline in water quality may not affect the population of fireflies, but a significant decrease in water quality or contamination may cause a decrease in the population of fireflies. Leong et al. (2007) similarly addressed the effect of water quality on fireflies, emphasizing pesticide residues. Pesticide residues can also be toxic and have a detrimental impact on firefly larvae when they reside in intertidal zones on riverbanks flooded by river water during high tide. The levels of downstream pesticides in the Selangor River in 2002 and 2003 surpassed the US Environmental Protection Agency (EPA) guidelines for freshwater aquatic animals (Leong et al., 2007).

Figures 4 and 5 compare the monthly firefly abundance index at the Selangor River to the monthly maximum air pollution index (API) from May 2006 to April 2009. Figures 4 and 5 show that from 2006 to 2009, the month of October 2006 had the most petite firefly population sizes, disregarding the air quality levels. The high air pollution index (API) alone cannot explain this month's low population of fireflies. It may have influenced the population at its lowest in October 2006, when the API was unhealthy (Figure 5) (Khoo et al., 2012).

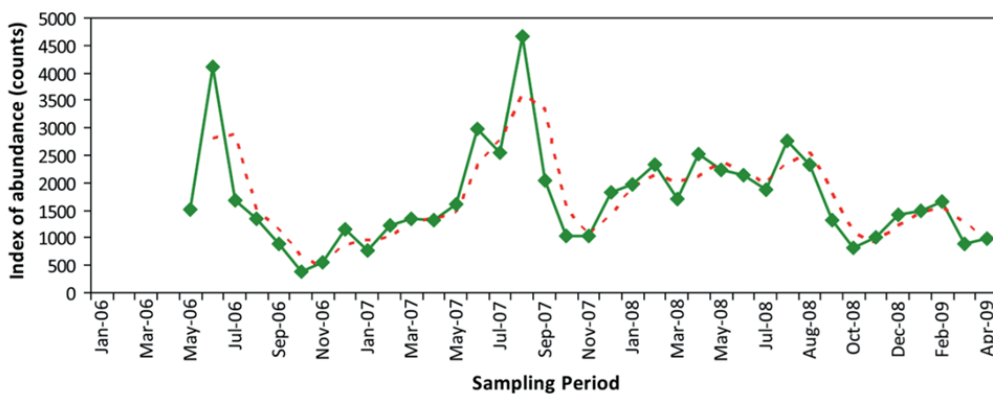


Figure 4. The overall monthly firefly population index for all locations from May 2006 to April 2009 (solid line) and a two-month interval moving average (dotted line) (Khoo et al., 2012)

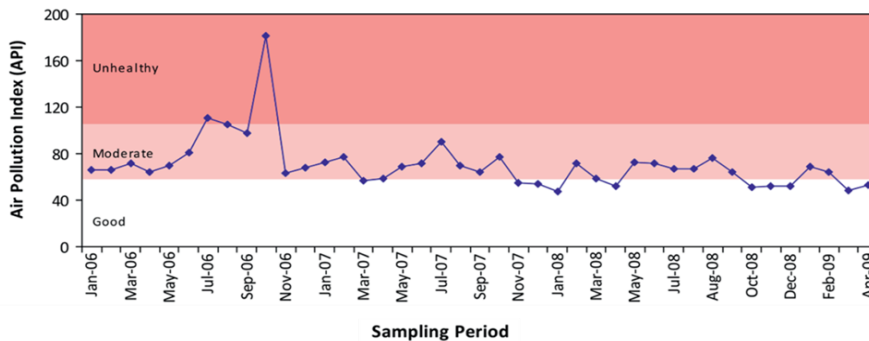


Figure 5. Monthly maximum air pollution index (API) in Selangor River (Khoo et al., 2012)

## CONCLUSION

This study found that several abiotic factors are most likely to affect the population abundance of fireflies in Southeast Asia. Among them is water level in soil, air temperature, water humidity, rainy season, altitude, water salinity (NaCl), wind direction, wind speed, dissolved oxygen (DO), biochemical oxygen demand (BOD), chemical oxygen demand (COD), ammonia nitrogen (NH<sub>3</sub>-N) and maximum air pollution index (API). However, few studies have focused on the specific parameters affecting this firefly species. Therefore, it is suggested that future studies focus more on how ecologically fireflies are affected as a result of environmental changes that affect abiotic in fireflies' habitat. This paper review also found that *Sonneratia caseolaris* (Berembang) remains the most preferred display tree because of many factors. Among them are 1) Display the tree's proximity to the water's edge; 2) appropriate arrangement of the leaf for mating purposes; 3) Presence of sap or nectar in the tree as a food source; 4) Display the tree's proximity to prey and food plants for larvae; and 5) Display tree's overall health (Jusoh et al., 2010b). Therefore, we suggest that more studies focus on the tree architecture of plant species in riparian zones or display trees.

## ACKNOWLEDGEMENTS

The Ministry of Higher Education Malaysia financed this research under the Fundamental Research Grant Scheme with project code: FRGS/1/2020/SS0/USM/02/.

## REFERENCES

- Abdullah, N. A., Asri, L. N., Radzi, S. N. F., Musbah, M., Hazmi, I. R., & Sulaiman, N. (2020). Abiotic factors influencing diversity and abundance of congregating fireflies (Coleoptera: Lampyridae) in Miri, Sarawak, Malaysia. *Oriental Insects*, 55(2), 149-164. <https://doi.org/10.1080/00305316.2020.1757529>
- Abdullah, N. A., Radzi, S., Asri, L. N., Idris, N. S., Husin, S., Sulaiman, A., Khamis, S., Sulaiman, N., & Hazmi, I. R. (2019). Insect community in riparian zones of Sungai Sepetang, Sungai Rembau and Sungai Chukai of Peninsular Malaysia. *Biodiversity Data Journal*, 7, Article e35679. <https://doi.org/10.3897/BDJ.7.e35679>
- Asri, L. N., Abdullah, N. A., Sulaiman, A., Asri, M. H. M., Sulaiman, N., Satiman, E. M. F. E. N., Husin, S. M., Shukor, A. M & Darbis, N. D. A. (2021). Abundance and species composition of synchronous flashing firefly at Sungai Rembau, Negeri Sembilan, Malaysia. *International Journal of Tropical Insect Science*, 41, 1095-1106. <https://doi.org/10.1007/s42690-020-00295-5>
- Badruddin, N., & Ballantyne, L. (2020, December 16-17). Fireflies (Coleoptera: Lampyridae) of Fraser's Hill, Pahang, Malaysia. In *Fraser's Hill Symposium 2020* (pp. 86-90). Selangor, Malaysia.
- Ballantyne, L. A. (2001). The bent winged fireflies of Cambodia, Indonesia, Malaysia, Philippines and Thailand (Coleoptera: Lampyridae: Luciolinae: Luciolini). *Serangga*, 6(1), 51-95.
- Ballantyne, L. A., & Lambkin, C. (2001). A new firefly, *Luciola* (*Pygoluciola*) *kinabalua*, new species (Coleoptera: Lampyridae), from Malaysia, with observations on a possible copulation clamp. *Raffles Bulletin of Zoology*, 49(2), 363-378.

- Ballantyne, L. A., & McLean, M. R. (1970). Revisional studies on the firefly genus *Pteroptyx olivier* (coleoptera: lampyridae: Luciolinae: Luciolini). *Transactions of the American Entomological Society*, 96(2), 223-305.
- Ballantyne, L., Lambkin, C. L., Boontop, Y., & Jusoh, W. F. A. (2015). Revisional studies on the Luciolinae fireflies of Asia (Coleoptera: Lampyridae): 1. The genus *Pyrophanes olivier* with two new species. 2. Four new species of *Pteroptyx o* and 3. A new genus *Inflata boontop*, with redescription of *Luciola indica* (Motsch.) as *Inflata indica* comb. nov. *Zootaxa*, 3959(1), 1-84. <https://doi.org/10.11646/zootaxa.3959.1.1>
- Branham, M. A. (2002). *The evolution of Lampyridae, with special emphasis on the origin of photic behavior and signal system evolution (Coleoptera: Lampyridae)* (Doctoral dissertation). The Ohio State University, USA. <https://www.proquest.com/pagepdf/305559117?accountid=27932>
- Chan, S. H. (2012). *Special Ecology Feature: Habitat Enhancement for Fireflies*. A Centre for Urban Greenery and Ecology Publication. [https://www.nparks.gov.sg/-/media/cuge/ebook/citygreen/cg4/cg4\\_15.ashx?la=en&hash=7864FDE4256090D472BC53EB2982EF0D61E45FAC](https://www.nparks.gov.sg/-/media/cuge/ebook/citygreen/cg4/cg4_15.ashx?la=en&hash=7864FDE4256090D472BC53EB2982EF0D61E45FAC)
- Cheng, S., Chan, K. M., Ishak, S. F., Khoo, V., & Chew, M. Y. (2017). Elucidating food plants of the aggregative, synchronously flashing Southeast Asian firefly, *Pteroptyx tener olivier* (Coleoptera, Lampyridae). *BioRisk*, 12, 25-39. <https://doi.org/10.3897/biorisk.12.14061>
- Chey V. K. (2009). *Fireflies of Tuaran*. Sepilok Bulletin, Sabah Forestry Department. <http://www.forest.sabah.gov.my/docs/frc/Sepilok%20Bulletin%20Vol.%2010.pdf>
- Chey, V. K. (2004). *Fireflies of Sungai Klias and their display trees*. Sepilok Bulletin, Sabah Forestry Department. <http://www.forest.sabah.gov.my/docs/frc/Sepilok%20Bulletin%20Vol.%201.pdf>
- Chey, V. K. (2008). *Fireflies of Sepilok*. Sepilok Bulletin, Sabah Forestry Department. <http://www.forest.sabah.gov.my/docs/frc/Sepilok%20Bulletin%20Vol.%209.pdf>
- Chey, V. K. (2010). *Fireflies of Beaufort with special reference to Sungai Garama and Sungai Klias*. Sepilok Bulletin, Sabah Forestry Department. <http://www.forest.sabah.gov.my/docs/frc/Sepilok%20Bulletin%20Vol.%2012.pdf>
- Chey, V. K. (2011). *Fireflies of Pulau Sakar*. Sepilok Bulletin, Sabah Forestry Department. <http://www.forest.sabah.gov.my/docs/frc/Sepilok%20Bulletin%20Vol.%2013%20&%20Vol.%2014.pdf>
- DeWalt, R. E., Kondratieff, B. C., & Sandberg, J. B. (2015). Order Plecoptera. In *Thorp and Covich's Freshwater Invertebrates: Ecology and General Biology: Fourth Edition* (Vol. 1, pp. 933-949). Elsevier Inc. <https://doi.org/10.1016/B978-0-12-385026-3.00036-X>
- Edde, P. A. (2022). Arthropod pests of rapeseed (canola) (*Brassica napus* L.). In *Field Crop Arthropod Pests of Economic Importance* (pp. 933-949). Elsevier Inc. <https://doi.org/10.1016/B978-0-12-818621-3.00004-5>
- Faudzi, R., Abas, A., Othman, N. W., & Mazlan, S. M. (2021). Effect of water quality on the abundance of firefly populations at Cherating River, Pahang, Malaysia. *EnvironmentAsia*, 14(1), 69-79. <https://doi.org/10.14456/ea.2021.8>
- Foo, K., & Mahadimenakbar, M. D. (2015). Diversity of fireflies (Coleoptera: Lampyridae) of Sungai Teratak, Sabah, Malaysia. *Journal of Tropical Biology & Conservation (JTBC)*, 12, 1-11.
- Hazmi, I. R., & Sagaff, S. A. S. (2017). Fireflies population and the aquaculture industry (Coleoptera: Lampyridae) of the Sungai Sepetang, Kampung Dew, Perak, Malaysia. *Serangga*, 22(2), 217-237.



- Hermann, S. L., Xue, S., Rowe, L., Davidson-Lowe, E., Myers, A., Eshchanov, B., & Bahlai, C. A. (2016). Thermally moderated firefly activity is delayed by precipitation extremes. *Royal Society Open Science*, 3(12), Article 160712. <https://doi.org/10.1098/rsos.160712>
- Iguchi, Y. (2002). The influence of temperature on flash interval in the Genji-firefly *Luciola cruciata* (Coleoptera: Lampyridae). *Entomological Review of Japan*, 57, 119-122.
- Jaikla, S., Lewis, S. M., Thancharoen, A., & Pinkaew, N. (2020). Distribution, abundance, and habitat characteristics of the congregating firefly, *Pteroptyx olivier* (Coleoptera: Lampyridae) in Thailand. *Journal of Asia-Pacific Biodiversity*, 13(3), 358-366. <https://doi.org/10.1016/j.japb.2020.06.002>
- Juliana, W. W., Shahril, M. M., Rahman, N. N. A., Nurhanim, M. N., Maimon, A., & Norela, S. (2012). Vegetation profile of the firefly habitat along the riparian zones of Sungai Selangor at Kampung Kuantan, Kuala Selangor. *Malaysian Applied Biology*, 41(1), 55-58.
- Jusoh, W. F. A. W., & Hashim, N. R. (2012). The effect of habitat modification on firefly populations at the Rembau-Linggi estuary, Peninsular Malaysia. In *Lampyrid*, (Vol. 2, pp. 149-155). Brazen Head Publishing.
- Jusoh, W. F. A. W., Hashim, N. R., & Ibrahim, Z. Z. (2009). Distribution, abundance and habitat characteristics of congregating fireflies (Luciolinae: Lampyridae) in Rembau-Linggi Estuary, Peninsular Malaysia. In *Proceedings of Postgraduate Qolloquium* (pp. 331-336). Bangi, Malaysia.
- Jusoh, W. F. A. W., Hashim, N. R., & Ibrahim, Z. Z. (2010a). Firefly distribution and abundance on mangrove vegetation assemblages in Sepetang estuary, Peninsular Malaysia. *Wetlands Ecology and Management*, 18, 367-373. <https://doi.org/10.1007/s11273-009-9172-4>
- Jusoh, W. F. A. W., Hashim, N. R., & Ibrahim, Z. Z. (2010b). Distribution and abundance of *Pteroptyx* fireflies in Rembau-Linggi estuary, Peninsular Malaysia. *Environment Asia*, 3(special issue), 56-60. <https://doi.org/10.14456/EA.2010.40>
- Jusoh, W. F. A. W., Wong, C. H., & Hashim, N. R. (2011). Zonation of firefly species and their display trees along Kerteh River, Terengganu. *Serangga*, 16(2), 59-66.
- Jusoh, W. F., Ballantyne, L., Lambkin, C. L., Hashim, N. R., & Wahlberg, N. (2018). The firefly genus *Pteroptyx* Olivier revisited (Coleoptera: Lampyridae: Luciolinae). *Zootaxa*, 4456(1), 1-71. <https://doi.org/10.11646/zootaxa.4456.1.1>
- Khoo, V., Nada, B., Kirton, L. G., & Phon, C. K. (2012). Monitoring the population of the firefly *Pteroptyx tener* along the Selangor River, Malaysia for conservation and sustainable ecotourism. In *Lampyrid*, (Vol. 2, pp. 162-173). Brazen Head Publishing.
- Kirton, L. G., Nada, B., Tan, S. A., Ang, L. H., Tang, L. K., Hui, T. F., & Ho, W. M. (2006). *The Kampung Kuantan firefly project: A preliminary assessment of the habitat requirements of Pteroptyx tener* (Coleoptera: Lampyridae). Forest Research Institute Malaysia. [https://www.researchgate.net/profile/B-Nada/publication/237235622\\_The\\_Kampung\\_Kuantan\\_Firefly\\_Project\\_A\\_Preliminary\\_Assessment\\_of\\_the\\_Habitat\\_Requirements\\_of\\_Pteroptyx\\_tener\\_Coleoptera\\_Lampyridae/links/59930313aca272ec9084b5af/The-Kampung-Kuantan-Firefly-Project-A-Preliminary-Assessment-of-the-Habitat-Requirements-of-Pteroptyx-tener-Coleoptera-Lampyridae.pdf](https://www.researchgate.net/profile/B-Nada/publication/237235622_The_Kampung_Kuantan_Firefly_Project_A_Preliminary_Assessment_of_the_Habitat_Requirements_of_Pteroptyx_tener_Coleoptera_Lampyridae/links/59930313aca272ec9084b5af/The-Kampung-Kuantan-Firefly-Project-A-Preliminary-Assessment-of-the-Habitat-Requirements-of-Pteroptyx-tener-Coleoptera-Lampyridae.pdf)
- Lauff, R. (2017). "Fireflies, glow-worms, and lightning bugs: Identification and natural history of the fireflies of the Eastern and Central United States and Canada" by Lynn Frierson Faust, 2017. *The Canadian Field-Naturalist*, 131(2), 191-192. <https://doi.org/10.22621/cfn.v131i2.2002>



- Leong, K. H., Tan, L. L., & Mustafa, A. M. (2007). Contamination levels of selected organochlorine and organophosphate pesticides in the Selangor River, Malaysia between 2002 and 2003. *Chemosphere*, 66(6), 1153-1159. <https://doi.org/10.1016/j.chemosphere.2006.06.009>
- Lewis, S. M., Wong, C. H., Owens, A., Fallon, C., Jepsen, S., Thancharoen, A., Wu, C., De Cock, R., Novak, M., Lopez-Palafox, T., Khoo, V., & Reed, J. M. (2020). A global perspective on firefly extinction threats. *BioScience*, 70(2), 157-167. <https://doi.org/10.1093/biosci/biz157>
- Li, F. R., Liu, J. L., Liu, C. A., Liu, Q. J., & Niu, R. X. (2013). Shrubs and species identity effects on the distribution and diversity of ground-dwelling arthropods in a Gobi desert. *Journal of Insect Conservation*, 17(2), 319-331.
- Ohba, N., & Wong, C. H. (2004). External morphology and ecological study of the firefly, *Pteroptyx tener* at Kampong Kuantan, Selangor, Malaysia. *Science Report of Yokosuka City Museum*, 51, 1-33.
- Osman, N. I., Sidik, N. J., & Awal, A. (2017). Ethnobotanical profiles and phytochemical constituents of *Barringtonia racemosa* L. for potential scrutiny of bioactive compounds through plant biotechnology. *Journal of Natural Remedies*, 17(2), 57-68. <https://doi.org/10.18311/jnr/2017/15945>
- Othman, N. W., Sulaiman, N., Abdullah, N. H., & Ramli, R. (2018). Mouthpart and digestive tract morphology of the synchronised firefly, *Pteroptyx tener* (Coleoptera: Lampyridae). *Serangga*, 23(2), 170-182.
- Prasertkul, T. (2018). Characteristics of *Pteroptyx* firefly congregations in a human dominated habitat. *Journal of Insect Behavior*, 31, 436-457. <https://doi.org/10.1007/s10905-018-9687-8>
- Sartsanga, C., Swatdipong, A., & Sriboonlert, A. (2018). Distribution of the firefly genus *Pteroptyx olivier* and a new record of *Pteroptyx asymmetria* Ballantyne (Coleoptera: Lampyridae: Luciolinae) in Thailand. *The Coleopterists Bulletin*, 72(1), 171-183. <https://doi.org/10.1649/0010-065X-72.1.171>
- Seri, N. A., & Rahman, A. A. (2021). Fireflies in South East Asia: Species diversity, distribution, and habitat (2015-2021). *Pertanika Journal of Tropical Agricultural Science*, 44(4), 713-743. <https://doi.org/10.47836/pjtas.44.4.02>
- Shahara, A., Nura, A. M. R., Maimon, A., & Norela, S. (2017). Assessment of firefly abundance at a new ecotourism site of Sungai Bernam, Selangor, Malaysia. *Malayan Nature Journal*, 69(2), 67-74.
- Sriboonlert, A., Swatdipong, A., Wonnapijij, P., Teerasak, E., & Thancharoen, A. (2015). New record of *Pteroptyx tener olivier* (Coleoptera: Lampyridae: Luciolinae) in Thailand. *The Coleopterists Bulletin*, 69(2), 332-336. <http://dx.doi.org/10.1649/0010-065X-69.2.332>
- Stork, N. E. (2018). How many species of insects and other terrestrial arthropods are there on Earth? *Annual Review of Entomology*, 63, 31-45. <https://doi.org/10.1146/annurev-ento-020117-043348>
- Sulaiman, N., Loo, M. C., & Abdullah, M. (2017). Association between the firefly population and some biotic and abiotic factors along the Sungai Sepetang river banks at Kampung Dew. *Malayan Nature Journal*, 69(3), 110-118.
- Thancharoen, A. (2007). *The biology and mating behavior of an aquatic firely species, Luciola Aquatilis Sp. Nov. Thancharoen (Coleoptera: Lampyridae)* (Doctoral dissertation). Mahidol University, Bangkok.
- Thancharoen, A., & Kitthawee, S. (2001, October 8-11). *Diversity of firefly populations in highland and lowland habitats* [Conference session]. In *5th BRT Annual Conference*. Udon Thani, Thailand.

- Usener, J. L., & Cognato, A. I. (2005). Patterns of mitochondrial diversity among desert firefly populations (Lampyridae: *Microphotus octarthrus* Fall). *The Coleopterists Bulletin*, 59(3), 361-367. <https://doi.org/10.1649/796.1>
- Wang, Y., Fu, X., Lei, C., Jeng, M. L., & Nobuyoshi, O. (2007). Biological characteristics of the terrestrial firefly *Pyrocoelia pectoralis* (Coleoptera: Lampyridae). *The Coleopterists Bulletin*, 61(1), 85-93. <https://doi.org/10.1649/907.1>
- Wattanachaiyingcharoen, W., Nak-eiam, S., & Thancharoen, A. (2011). Distribution and habitat of the firefly, *asymmetricata circumdata* (Motsch.) (Coleoptera: Lampyridae: Luciolinae) in the North of Thailand. *NU International Journal of Science*, 8(2), 12-18.
- Wattanachaiyingcharoen, W., Nak-eiam, S., Phanmuangma, W., Booninkiaew, S., & Nimlob, N. (2016). Species diversity of firefly (Coleoptera: Lampyridae) in the highlands of Northern Thailand. *NU International Journal of Science*, 13(2), 24-32.
- Wijekoon, W. M. C. D., Wegiriya, H. C. E., & Bogahawatha, C. N. L. (2012). Regional diversity of fireflies of the subfamily luciolinae (Coleoptera: Lampyridae) in Sri Lanka. *Lampyrid*, 2, 138-141.



## Optimization of the Formulation of Sago Starch Edible Coatings Incorporated with Nano Cellulose Fiber (CNF)

Rahmiyati Kasim<sup>1</sup>, Nursigit Bintoro<sup>1\*</sup>, Sri Rahayoe<sup>1</sup> and Yudi Pranoto<sup>3</sup>

<sup>1</sup>Department of Agricultural Engineering and Biosystem, Gadjah Mada University, 55281 Yogyakarta, Indonesia

<sup>3</sup>Department of Food and Agricultural Product Technology, Gadjah Mada University, 55281 Yogyakarta, Indonesia

### ABSTRACT

This study aimed to produce new edible coatings based on the mixture of sago starch, cellulose nanofiber (CNF), glycerol, and tween-80. The effect of sago starch (5–10 g of starch/100 ml of distilled water), CNF (0.5–20% w/w), glycerol (10–30% w/w), and tween-80 (0.5–10% w/w) based on sago starch concentration on contact angle (CA), water vapor permeability (WVP), oxygen permeability (PO<sub>2</sub>) and tensile strength (TS) properties of the edible coatings were optimized using factorial experimental design (2k). The result showed that the linear model for all independent variables was significant ( $P < 0.05$ ) on all responses (dependent variable). The sago starch concentration depicted a significant ( $p < 0.001$ ) positive effect on contact angle; CNF showed a statistically significant effect on WVP, PO<sub>2</sub>, and TS; tween-80 showed a significant effect on all dependent variables, whereas glycerol only affected WVP. The optimum concentrations of sago starch, CNF, glycerol, and tween-80 were predicted to be 5 g/100 ml distilled water, 20% w/w, 10% w/w, and 0.5% w/w based on sago starch, respectively to obtain the minimum contact angle, WVP, PO<sub>2</sub>, and the maximum TS. The predicted data for the optimized coating formulation were in good agreement with the experimental value. This work revealed that the potential of sago

starch/CNF based coating formulation could be effectively produced and successfully applied for coating of food.

*Keywords:* CNF, coatings, film, sago starch

### ARTICLE INFO

#### Article history:

Received: 03 January 2022

Accepted: 18 April 2022

Published: 09 November 2022

DOI: <https://doi.org/10.47836/pjst.31.1.21>

#### E-mail addresses:

[rahmiyatikasim@ugm.ac.id](mailto:rahmiyatikasim@ugm.ac.id) (Rahmiyati Kasim)

[nursigit@ugm.ac.id](mailto:nursigit@ugm.ac.id) (Nursigit Bintoro)

[yayoe\\_sri@yahoo.com](mailto:yayoe_sri@yahoo.com) (Sri Rahayoe)

[pranoto@ugm.ac.id](mailto:pranoto@ugm.ac.id) (Yudi Pranoto)

\*Corresponding author

### INTRODUCTION

The edible coating is a postharvest technology that can preserve fresh products by modifying the internal atmosphere of the fruit or vegetables by creating a semi-

permeable barrier to gases ( $O_2$  and  $CO_2$ ), moisture content, and movement of solids, consequently slowing the respiration rate and quality changes during storage (Deng et al., 2018). The effectiveness of edible coating in extending the shelf life of fruits and vegetables is determined, among others, by high barrier characteristics, suitable mechanical properties, high wettability, and good sensory qualities (Lopez-Polo et al., 2020; Sapper et al., 2019). The function and performance of the edible coating are influenced by the composition of the raw materials, the manufacturing process, and the method of application (Andrade et al., 2014).

Sago starch is a type of polysaccharide that has the potential to be used as material for making edible coatings because of its abundant availability, low cost, and higher productivity compared to other types of starch such as cassava starch, corn starch, and rice starch and contains high amylose approximately  $\pm 28.84\%$  (Karim & Tie, 2008; Zhu, 2019). Edible starch coatings have good gas barrier characteristics, produce a thin and transparent film, colorless and tasteless, and adhere well to the surface of fruit or vegetables (Punia et al., 2022; Thakur et al., 2019). However, the hydrophilic nature and high amylose content of starch cause the film or edible coating to be sensitive to high water content, thus affecting the water barrier properties and its mechanical properties become low, high water absorption (Shih & Zhao, 2021; Syafri et al., 2019) and low wettability coefficient of coating solution (Basiak et al., 2017). To overcome these, using cellulose nanofiller-reinforcement to the starch-based polymer has been confirmed as a new way for improving mechanical strength, gas permeability, and water barrier resistance properties (Bangar & Whiteside, 2021b; Shih & Zhao, 2021).

The development of edible coatings with the addition of nano reinforcement such as cellulose nanofiber (CNF) as a filler in a biopolymer matrix such as starch is very promising because it has good barrier properties, is small (diameter  $<100$  nm) and uniform particle size, has high mechanical characteristics, water binding ability, has the same chemical structure as starch and is safe for health (Azeredo et al., 2017; Deng et al., 2017a). In recent years, CNF has been extensively studied and demonstrated to be effective to enhance the performance of biopolymer edible coatings/films such as chitosan (Ghosh et al., 2021), tapioca, potato and corn starch (Shih & Zhao, 2021), potato starch, tapioca starch, and chitosan (Gopi et al., 2019), banana starch (Tibolla et al., 2019), mango seed starch (Silva et al., 2019). Meanwhile, the addition of nano cellulose at high concentrations causes agglomeration in the coating solution.

Glycerol as a plasticizer is added to the starch coating and film to reduce the intermolecular forces of the polymer chains to reduce brittleness and increase the flexibility of films and coatings. However, the addition of glycerol ( $>33\%$ ) can increase water vapor permeability and decrease the mechanical characteristics of the film and coatings (Santacruz et al., 2015; Syafri et al., 2019; Thakur et al., 2019a). A surfactant (i.e. tween-80) is also

added to the coating material formula to increase the wettability and result in lower surface tension values (Santacruz et al., 2015). According to (Deng et al., 2017b), the addition of 10% (w/w dry basis) surfactant to the polymeric matrix materials produced good wettability of coating formulation to the surface of fruits. Therefore, for the enhancement of functional properties of the coating, it is necessary to optimize the ingredients formula of coating.

To the best of our knowledge, no previous research has been conducted to prepare sago starch in combination with CNF or optimization of coating materials. The objective of this study was to optimize the coating material formula (sago starch, cellulose nanofiber (CNF), glycerol, and surfactant concentration) to produce an edible coating with low permeability value (WVP and  $O_2$ ), low contact angle, and high tensile strength. In addition, this work would produce new information about the interaction between sago starch, CNF, glycerol, and surfactant concentrations on properties of coatings and films and produce a high-quality edible coating that is more environmentally friendly and competitive with wax coating materials.

## MATERIALS AND METHODS

### Materials

Sago starch produced by HD (HD Micro, Small and Medium Enterprises (MSME) Yogyakarta, Indonesia), 3% cellulose nanofiber (CNF) high fine slurry was obtained from the Process Development of the Maine University (ME, USA), mature green “Mas” bananas (*Musa acuminata* ‘Lady Finger’) fruits were harvested from a local farmer (Sleman, Yogyakarta, Indonesia), technical glycerol and distilled water purchased from Progo Mulyo CV (Yogyakarta, Indonesia), Tween-80 (Merck, Germany) obtained from Chemmix Pratama CV (Yogyakarta, Indonesia).

### Preparation of Sago Starch and CNF Edible Coatings and Films

Sago starch and CNF nanocomposite edible coating were produced by the casting method according to the previous research method, with some modification (Balakrishnan et al., 2017; Meneguín et al., 2017; Tibolla et al., 2019; Widaningrum et al., 2015). Sago starch as a matrix (5–10 g) was diluted with 100 mL of distilled water while stirring at 700 RPM for 10 minutes at room temperature. Simultaneously, the CNF as a reinforcing agent (0.5–20% w/w) based on sago starch weight was dispersed in 50 ml of distilled water using a digital overhead stirrer (MULAB Type MS-40) at 700 RPM for 10 minutes. After that, the starch solution was added with the cellulose nanofiber (CNF) suspension, and the mixture was agitated by a digital overhead stirrer at 750 RPM for 20 minutes at room temperature. The mixture solution was then heated to 65°C and added tween-80 ( $C_{64}H_{124}O_{26}$ ) as a surfactant material at varying concentrations (0.5–10% w/w of sago starch) while being stirred at a

speed of 750 RPM. After the temperature of the solution reaches 70°C, different amounts of glycerol (C<sub>3</sub>H<sub>8</sub>O<sub>3</sub>) (10 - 30% w/w), based on sago starch weight, as the plasticizer, was added to the solution and continuously heated for 25 minutes while being stirred to obtain the film-forming and coating solutions. 60 ml of the coating solution at a temperature of 60°C was poured onto acrylic plates (20 cm x 20 cm) and dried at room temperature for 2–3 days. The concentrations were chosen based on preliminary experiments. The resulting film was stored for five days at room temperature before testing. For the measurement of the contact angle, it was done by applying the coating solution directly to the banana's peel then measured using a digital microscope.

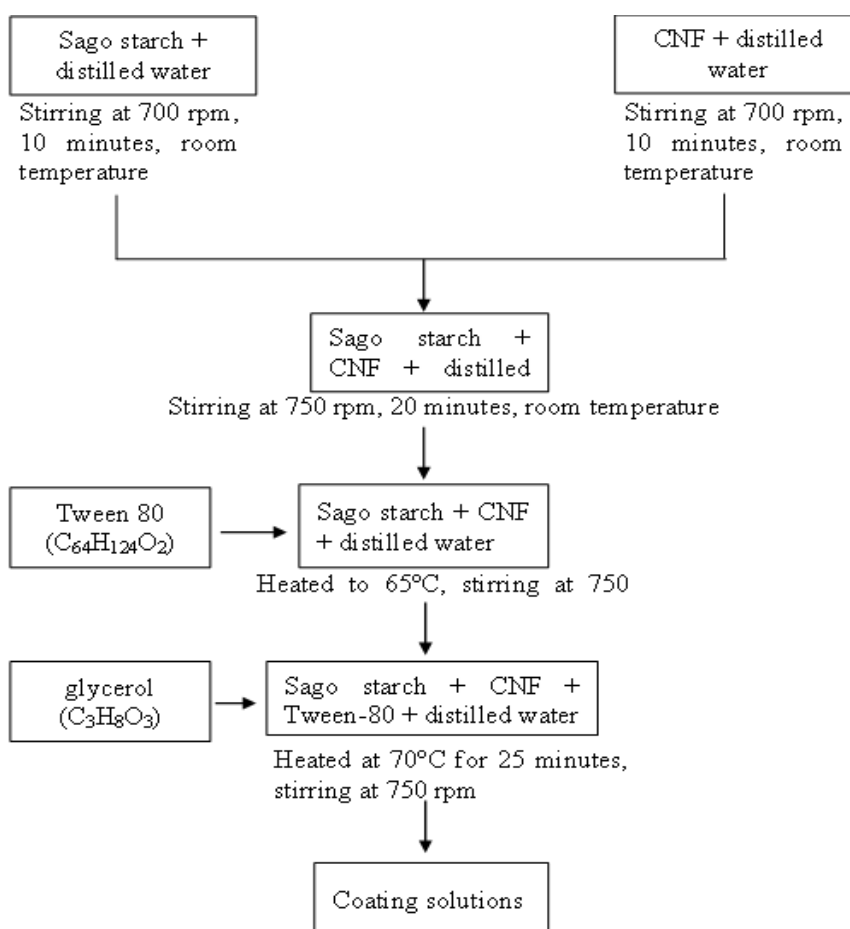


Figure 1. Schematic representation of preparation of sago starch (SS)-CNF nanocomposites



### Characterization of the Coating and Film

**Contact Angle (CA).** The measurement of the contact angle is based on the method used by Deng et al. (2017b) and Rahayoe (2015). The coating solution was taken using a 500  $\mu\text{l}$  syringe, then dripped from a height of 10 mm horizontally on the surface of a banana skin. After 30 seconds, the coating layer on the banana's peel was taken using a digital microscope (Dino-Lite AM2111 series). The results of these images were analyzed using Image J software to determine the contact angle between the droplets of the coating solution on the surface of banana skins. Measurement of contact angle was conducted at 3 points of each part of a banana's peel.

**Water Vapor Permeability (WVP).** The WVP of films was determined by the water desiccant method based on ASTM E 96 (1995). First, a circular-shaped edible film of 30 mm diameter was placed at the top of the WVP bottles containing 10 g of silica gel. Then, the WVP bottles were placed in a desiccator containing distilled water to produce RH 90 %. Finally, WVP bottles were weighed using an analytical balance (OHAUS) every hour for 8 hours of observation. As a result, the WVP is determined from Equations 1, 2, and 3, respectively:

$$\text{WVT} = \frac{\left(\frac{G}{t}\right)}{A} \quad (1)$$

$$\text{Permeance} = \frac{\text{WVT}}{\Delta P} = \frac{\text{WVT}}{S(R_1 - R_2)} \quad (2)$$

$$\text{WVP} = \text{Permeance} \times \text{thickness} \quad (3)$$

Where WVT is the water vapor transmission rate ( $\text{g}/\text{hour} \cdot \text{m}^2$ ), G is the change in weight (from a straight line, g), t is time (hours),  $G/t$  = slope of a straight line ( $\text{g}/\text{hour}$ ), A is the area of the mouth of the bottle ( $\text{m}^2$ ),  $\Delta P$  is the difference in water vapor pressure, mm Hg ( $1.333 \times 10^2$  Pa), S is the saturated vapor pressure at the test temperature, mm Hg ( $1.333 \times 10^2$  Pa),  $R_1$  is the relative humidity in the bottles samples, while  $R_2$  is the relative humidity of the environment, WVP is water vapor permeability ( $\text{g}/\text{m s Pa}$ ).

**Oxygen Permeability ( $\text{PO}_2$ ).** Permeability measurement of edible coating and film to oxygen was determined by the method proposed by Kubík and Zeman (2013) with slight modifications. The film to be tested was fixed between two acrylic chamber boxes with adhesive glue at the lips of the boxes. Then, the two chambers' boxes were fixed firmly using screws. The box was made from acrylic with the size of 15 x 15 x 15 cm with a hole at the base or the top of the boxes with a size 10 cm x 10 cm to regulate the initial oxygen concentration in the boxes. The upper chamber was filled with pure oxygen with a concentration of about 50–80%, while the bottom chamber was flushed using nitrogen

to lower oxygen concentration to around 18%. The changes in the oxygen concentration in the bottom box were measured every 10 minutes for 1.5 hours. Oxygen permeability is calculated according to the Equation 4 of Kubík and Zeman (2013) as follows:

$$P_x = \frac{\Delta \rho_p V M}{\Delta t S \rho_i^2 R T} \quad (4)$$

Where  $P_x$  is the film permeability ( $\text{m}^3/\text{m}^2 \cdot \text{s} \cdot \text{Pa}$ );  $\rho$  is the oxygen density in the bottom box ( $\text{kg}/\text{m}^3$ );  $\rho_i$  is the initial oxygen density in upper box ( $\text{kg}/\text{m}^3$ );  $M$  is the molecular weight mass of the oxygen ( $\text{kg}/\text{mol}$ );  $V$  is the volume of the chambers box ( $\text{m}^3$ );  $R$  is the universal gas constant 8314 ( $\text{J}/\text{k mol K}$ );  $T$  is the temperature ( $\text{K}$ );  $t$  is the time of the observation ( $\text{s}$ ), and;  $S$  is the area of the film ( $\text{m}^2$ ).

**Film Thickness Measurement and Mechanical Properties.** The film thickness was measured using a digital micrometer (Mitutoyo, Co., Code No.293–236, Japan) with an accuracy of  $\pm 0.001$  mm. Measurements were taken from 8 different positions for each film sample (R. Thakur et al., 2018). The thickness measurement results are then averaged.

The tensile strength (TS) of the film was tested using the universal testing machine Zwick type Z0.5. The measurement method was based on (ASTM D882, 2010) with several method modifications from Cazón et al. (2018) and Ventura-Aguilar et al. (2018). The film was cut with a dumbbell with a size of 150 mm x 50 mm. Prior to measurements, the films were preconditioned at  $\pm 55\%$  RH at  $25^\circ\text{C}$  in a desiccator containing sodium nitrate for five days. The measurement began with the film being clamped between the grips, with an initial distance between the grips being 50 mm at a speed of 10 mm/minute. Measurements were repeated two times for each sample. The value of tensile strength (MPa) of the film could be directly obtained from the measurement results.

### Experimental Design and Optimization

In this study, a factorial experimental design (2k) was performed to assess the individual and combined effects of the main component of coating, namely the concentration of starch ( $X_1$ ), CNF ( $X_2$ ), glycerol ( $X_3$ ), and tween-80 ( $X_4$ ) on the contact angle, WVP, oxygen permeability ( $\text{PO}_2$ ) and tensile strength, as responses variable. Construction of experimental factorial designs and data analysis was performed using Design Expert Software (Version 12.0.3.0, Stat-Ease Inc., Minneapolis, MN). The experimental design included different combinations of two levels (i.e., high (+1) and low levels (-1)) of four independent variables and six additional replicates at the center point, leading to the 22 runs experimental design (Kania et al., 2021; Lavecchia et al., 2015). The minimum and maximum levels of each independent variable were determined based on recommendations from previous researchers (Deng et al., 2017a; Tibolla et al., 2019; Widaningrum et al., 2015).

The factors, levels, and responses values are presented in Table 1. To estimate the significance of the model, an analysis of variance (ANOVA) was undertaken with confidence levels higher than 95%. Pareto charts were also constructed to project the significance of factors  $X_1$ ,  $X_2$ ,  $X_3$ , and  $X_4$  or the collective effect of factors; 3-D response surface plots were prepared to reveal the relationship and interactions between the four independent variables and responses. The optimization was based on the following combination: minimizing contact angle, WVP,  $PO_2$ , while maximizing TS. The numerical optimization to achieve the optimum concentrations of four independent variables ( $X_1$ : sago starch,  $X_2$ : CNF,  $X_3$ : glycerol, and  $X_4$ : tween-80) and to obtain the best nanocomposite coating/film properties including contact angle, WVP,  $PO_2$ , and TS were utilized. For validation of the regression models, the experimental data and fitted values predicted by the models were compared and percent error (PE) was calculated for each response.

## RESULTS AND DISCUSSIONS

### Interaction Effects of Coating Formulations on Contact Angle (CA)

In this study, the wettability of the coating was determined by the contact angle ( $\theta$ ) of the coating solution onto the banana skin surface. The value of CA of the coating formulation on a banana epicarp in a range from 18.08° to 88.29° is shown in Table 1. It is noted that to gain the best coating; it is important to select a coating formulation with a low contact angle ( $\theta$ ) to generate closer to completely wetting, strong adhesion, weak cohesion, and a lipophilic condition (Andrade et al., 2014; Deng et al., 2017a). The significance of each model, independent variables, and interactions to the responses were evaluated based on the  $p$ -value, in which a  $p$ -value less than 0.05 was considered statistically significant (Kania et al., 2021). The analysis of variance (ANOVA) evaluation (Table 2) for CA showed the linear model term was significant ( $p$ -value < 0,005). In order to evaluate the goodness of fit of the model, different parameters including the coefficient of determination ( $R^2$ ), the lack of fit F value, and the adequate precision were performed. In this study, the value of  $R^2$  was 0.9384, the adequate precision was 20.4057 (< 4), and the lack of fit values was non-significant ( $p$ -value > 0,005), which indicate an adequate of the applied model and shows model can be used the prediction of contact angle of the coating solution. Moreover, Table 2 also represents that the contact angle of the coating formulation was influenced significantly ( $P < 0,005$ ) by the linear effect of sago starch ( $X_1$ ) and tween-80 ( $X_4$ ) concentrations. However, CNF, glycerol levels and other combinations did not show a significant effect on contact angle value. The relation between and independent variables and the response can be expressed by Equation 5:

$$CA = 51,94 + 25,55 X_1 - 6.51 X_4 \quad (5)$$

Equation 5 shows that starch concentration had more influence than the tween-80 concentration on the contact angle, as the coefficients are 25.55 and 6.51, respectively. A positive coefficients value of the starch concentration means that the response (contact angle) is increased when the sago starch level increases.

The importance of significant main factors and interactions can be presented in the Pareto chart shown in Figure 2a. As shown in the Pareto chart, the factorial effects of very important main factors (above Bonferroni limit) were found to be in the following order: sago starch > tween-80. In order to show the combined effect of independent variables on the contact angle of the coating formulation, 3D response surfaces plots have been presented (Figure 2b). It was observed that the decline of contact angle was a function of starch and tween-80 concentration. The minimum amount of contact angle value could be observed at the low level of starch and higher tween-80 concentration (see Figure 2b). It may be associated with an increased contact angle as results of high starch concentration was due to an increase in viscosity of coating solution, which influences the amount of the materials adhered to the fruit surface and was difficult to spread on a solid surface (Soto-Muñoz et al., 2021; Soradech et al., 2017). Whereas, the addition of tween-80 resulted in a lower contact angle, probably due to it was might be caused by the humectant impact of surfactant and the hydrophobic chain of tween-80 could not interact with the polymers rich in polar groups; thus the film became hydrophilic (Stachowiak et al., 2020). In addition, several previous studies reported that surfactant diminished cohesion forces, hence decreasing the surface tension and increasing the wettability (Deng et al., 2017a; Riva et al., 2020; Sun et al., 2021). Thus, this surfactant improved compatibility between the solution and the fruit skin surface (Vieira et al., 2016). The lower contact angle indicated the higher interaction between coating solution and skin of surface, better hydrophilicity of the surface, and high degree wetting generates coating solution spreads easily on the fruit skin (Patil et al., 2021).

Table 1

*The factorial experimental design (2<sup>4</sup>) results*

No	Run	Independent variables				Responses			
		Starch (% w/v)	CNF (% w/w)	Glycerol (% w/w)	Tween-80 (%w/w)	Contact Angle (°)	WVP x10 <sup>-11</sup> (g/Pa s m)	PO <sub>2</sub> (cm <sup>3</sup> /m <sup>2</sup> . day Pa)	TS (MPa)
1	16	5 (-1)	0.5 (-1)	10 (-1)	0.5 (-1)	24.88	0.859	1314.77	23.15
2	15	10 (1)	0.5 (-1)	10 (-1)	0.5 (-1)	86.29	4.845	939.114	3.29
3	19	5 (-1)	20 (1)	10 (-1)	0.5 (-1)	35.44	0.607	745.268	25.56
4	2	10 (1)	20 (1)	10 (-1)	0.5 (-1)	88.29	1.032	982.803	26.65
5	18	5 (-1)	0.5 (-1)	30 (1)	0.5 (-1)	29.22	0.341	2228.03	10.38
6	26	10 (1)	0.5 (-1)	30 (1)	0.5 (-1)	87.66	1.090	2763.47	6.17

Table 1 (Continue)

No.	Run	Independent variables				Responses			
		Starch (% w/v)	CNF (% w/w)	Glycerol (% w/w)	Tween-80 (%w/w)	Contact Angle (°)	WVP x10 <sup>-11</sup> (g/Pa s m)	PO <sub>2</sub> (cm <sup>3</sup> /m <sup>2</sup> . day Pa)	TS (MPa)
7	30	5 (-1)	20 (1)	30 (1)	0.5 (-1)	30.41	0.653	4235.97	13.61
8	28	10 (1)	20 (1)	30 (1)	0.5 (-1)	85.38	1.797	786.182	6.05
9	10	5 (-1)	0.5 (-1)	10 (-1)	10 (1)	18.08	5.058	28769.9	2.36
10	4	10 (1)	0.5 (-1)	10 (-1)	10 (1)	66.58	5.651	21260.9	0.77
11	13	5 (-1)	20 (1)	10 (-1)	10 (1)	25.35	2.289	3181.23	3.66
12	11	10 (1)	20 (1)	10 (-1)	10 (1)	73.52	1.70 1	7503.29	9.08
13	14	5 (-1)	0.5 (-1)	30 (1)	10 (1)	19.08	3.504	4824.51	1.69
14	7	10 (1)	0.5 (-1)	30 (1)	10 (1)	69.53	2.902	24692	1.85
15	3	5 (-1)	20 (1)	30 (1)	10 (1)	28.65	0.534	2426.95	6.33
16	1	10 (1)	20 (1)	30 (1)	10 (1)	62.67	0.592	4011.19	12.13
17	27	7.5 (0)	10.25 (0)	20 (1)	5.25 (0)	29.68	0.587	8083.38	10.37
18	29	7.5 (0)	10.25 (0)	20 (1)	5.25 (0)	47.45	1.664	8899.55	5.19
19	5	7.5 (0)	10.25 (0)	20 (1)	5.25 (0)	61.73	0.312	5637.9	14.39
20	8	7.5 (0)	10.25 (0)	20 (1)	5.25 (0)	49.27	1.944	6582.57	18.55
21	6	7.5 (0)	10.25 (0)	20 (1)	5.25 (0)	49.27	0.214	5009.85	11.15
22	22	7.5 (0)	10.25 (0)	20 (1)	5.25 (0)	50.96	0.652	15539.1	12.95

Table 2

Significance level (P) calculated for investigating the effect of sago starch (X<sub>1</sub>), CNF (X<sub>2</sub>) glycerol (X<sub>3</sub>), and tween-80 concentration (X<sub>4</sub>) into composite coatings and films the model fitting

Independent Variable	CA	WVP	PO <sub>2</sub>	TS
Model Linear	<0.0001*	0.0025*	0.0075*	0.0121*
X <sub>1</sub> (starch)	<0.0001*	0.0642 <sup>ns</sup>	0.3737 <sup>ns</sup>	0.2423 <sup>ns</sup>
X <sub>2</sub> (CNF)	0.524 <sup>ns</sup>	0.0005*	0.0046*	0.0117*
X <sub>3</sub> (glycerol)	0.893 <sup>ns</sup>	0.0042*	0.2796 <sup>ns</sup>	0.0582 <sup>ns</sup>
X <sub>4</sub> (tween-80)	0.010*	0.0035*	0.0009*	0.0016*
X <sub>1</sub> X <sub>2</sub>	0.518 <sup>ns</sup>	0.2072 <sup>ns</sup>	0.5598 <sup>ns</sup>	0.1029
X <sub>1</sub> X <sub>3</sub>	0.766 <sup>ns</sup>	0.2870 <sup>ns</sup>	0.2128 <sup>ns</sup>	0.5942 <sup>ns</sup>
X <sub>1</sub> X <sub>4</sub>	0.312 <sup>ns</sup>	0.0343*	0.2233 <sup>ns</sup>	0.0397*
X <sub>2</sub> X <sub>3</sub>	0.570 <sup>ns</sup>	0.0413*	0.3279 <sup>ns</sup>	0.3220 <sup>ns</sup>
X <sub>2</sub> X <sub>4</sub>	0.900 <sup>ns</sup>	0.0104*	0.0050*	0.7975 <sup>ns</sup>
X <sub>3</sub> X <sub>4</sub>	0.974 <sup>ns</sup>	0.2051 <sup>ns</sup>	0.0930 <sup>ns</sup>	0.0183*

Table 2 (Continue)

Independent Variable	CA	WVP	PO <sub>2</sub>	TS
X <sub>1</sub> X <sub>2</sub> X <sub>3</sub>	0.801 <sup>ns</sup>	0.0631 <sup>ns</sup>	0.0638 <sup>ns</sup>	0.1573 <sup>ns</sup>
X <sub>2</sub> X <sub>3</sub> X <sub>4</sub>	0.901 <sup>ns</sup>	0.2118 <sup>ns</sup>	0.1280 <sup>ns</sup>	0.1272 <sup>ns</sup>
R <sup>2</sup>	0.9384	0.9282	0.9030	0.8888
Adjusted R <sup>2</sup>	0.9276	0.8205	0.7576	0.7220
Adequate Precession	20.4057	10.8625	8.7020	8.6262
Lack of fit	0.9959 <sup>ns</sup>	0.6405 <sup>ns</sup>	0.3757 <sup>ns</sup>	0.6406 <sup>ns</sup>

Note. \* Significant; <sup>ns</sup> Not significant

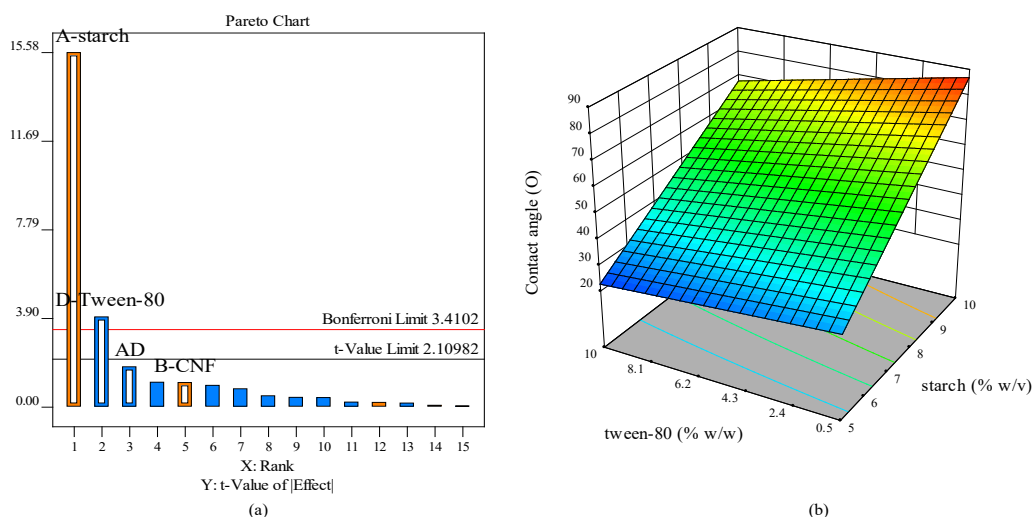


Figure 2. Analysis of (a) Pareto chart, (b) response surface of contact angle (CA) as a function of sago starch-tween-80

### Interaction Effects of Coating Formulation on Water Vapor Permeability (WVP)

In the present study WVP values of the coating were in the range from  $0.214 \times 10^{-11}$  to  $5.651 \times 10^{-11}$  g/ Pa s m (Table 1). The model P-value of 0.0025 implies the linear model was significant (Table 2). As shown in Table 2, a high R<sup>2</sup> value ( $R^2 > 85$ ) and close to the value of adjusted R<sup>2</sup> indicates that the model adequately represented the real relationship between the response and independent variables and is reliable for the prediction of WVP properties of the nanocomposite films and coatings as a function of tested variables (sago starch, CNF, glycerol and tween-80). The adequate precision value was greater than 4 (10.8625), and the lack of fit was non-significant ( $p = 0,6405$ ) indicating an adequate signal and the model fit the test well with a small error. Furthermore, the statistical model reveals that WVP was affected significantly (95%) by the individual factor, namely CNF

concentration ( $X_2$ ), glycerol concentration ( $X_3$ ), tween-80 concentration ( $X_4$ ), and by the interaction between factor (starch-tween 80 concentrations ( $X_1X_4$ ), CNF-glycerol ( $X_2X_3$ ), and CNF-tween 80 ( $X_2X_4$ ). The relationship between responses (WVP) and independent variables was obtained as follows:

$$WVP (x10^{-11}) = 2.09 - 0.9403 x_2 - 0.6644 x_3 + 0.6880 x_4 - 0.4278 x_1x_4 + 0.4077 x_2x_3 - 0.5596 x_2x_4 \quad (6)$$

Equation 6 indicates that the CNF concentration had more impact than glycerol concentration on reduction of WVP, as coefficients are 0.9403 and 0.6644, respectively. Moreover, the value of positive coefficients of tween-80 concentration represents an increase of WVP. It is well known that better coating formulation had low WVP.

The factorial effects of very important main factors and their interactions were found to be in the following order: CNF > tween-80 > glycerol > CNF-tween > starch-tween > CNF-glycerol, as presented in the Pareto chart in Figure 3a. The evolution of WVP as a function of sago starch, CNF, glycerol, and tween-80 concentrations was presented in the 3D response surfaces plot in Figure 3b-d. It can be seen that the WVP value was reduction when CNF and glycerol concentrations were increased (Figure 3b and d), and the interaction starch of tween-80 (Figure 3b) was low concentration coating formulation. The lowest WVP ( $0.214 \times 10^{-11}$  g/Pa s m) was obtained in the coating formula with a composition of 7.5% (w/v) starch, 10.25% (w/w) CNF, 20% (w/w) glycerol, and 5.25% (w/w) tween-80. The WVP value in this study was lower when compared to previous studies, such as those reported by Soofi et al. (2021) in lemon waste powder film incorporated with 6% CNF ( $1.12 \pm 0.09 \times 10^{-7}$  g/Pa h m or  $3.11 \pm 0.09 \times 10^{-11}$  g/Pa s m), Kim et al. (2021) in films based on TEMPO-oxidized CNF and sodium carboxymethyl cellulose (CMC) ( $0.77 \times 10^{-9}$  g/Pa s m) & Yuan and Chen. (2021) in the corn starch-nanocellulose composite films ( $4.41 \times 10^{-4}$  g/Pa h m or  $1.22 \times 10^{-7}$  g/Pa s m). It indicates that the coating formulation in this study has an excellent barrier of water vapor.

The effect of reducing WVP as a result of added CNF on composite films and coating can be related to the following reasons: (1) The shape of cellulose fibers reduces the free space in the polymer matrix, obstructing the passage of water vapor through the surface film. Furthermore. nanocellulose interfaced with the glycerol in the film acts as a water vapor barrier (Da Silva et al., 2015). (2) The reduction in free hydrophilic groups (OH) and the matrix cohesiveness as a result of the formation of hydrogen bonds between CNF and biopolymer matrix implies a strong interaction between CNF and biopolymer matrix (Da Silva et al., 2015; Soofi et al., 2021). (3) The CNF leads to the formation of the long and zigzag pathways and acts as an obstacle to the extent of the diffusion path of water vapor transmission rate through the surface of the film (Bagheri et al., 2019; Paula et al., 2019; Soofi et al., 2021). (4) The CNF filling of void spaces between biopolymer chains reduces the mobility of chains. consequently decreasing the diffusion rate of water molecules and resulting in lower permeability (Bagheri et al., 2019; Soofi et al., 2021). (5) The high



crystalline properties of CNF restricted the passage of water vapor, resulting in a slower diffusion process and lower permeability (Xu et al., 2019). Likewise, in our, work increased glycerol in the starch and CNF composite film formulation decreased WVP. It may be due to the reduced density of the starch matrix, slow crystallization kinetics, and low glass transition temperature as a result of increased glycerol content in starch film (Thakur et al., 2019a). According to Da Silva et al. (2015), nano cellulose combined with glycerol acts as a barrier, thereby reducing water vapor permeability. Similar observations were reported by Thakur et al. (2019a), who indicated that the WVP value diminished at 20% (w/w of total starch) glycerol concentrations, but increased at 40% (w/w of total starch). Tween-80 has a HLB number of 15, indicating that it is readily soluble in water. Hydrophilic part of the tween-80 contributes to the increasing in WVP (Maniglia et al., 2019).

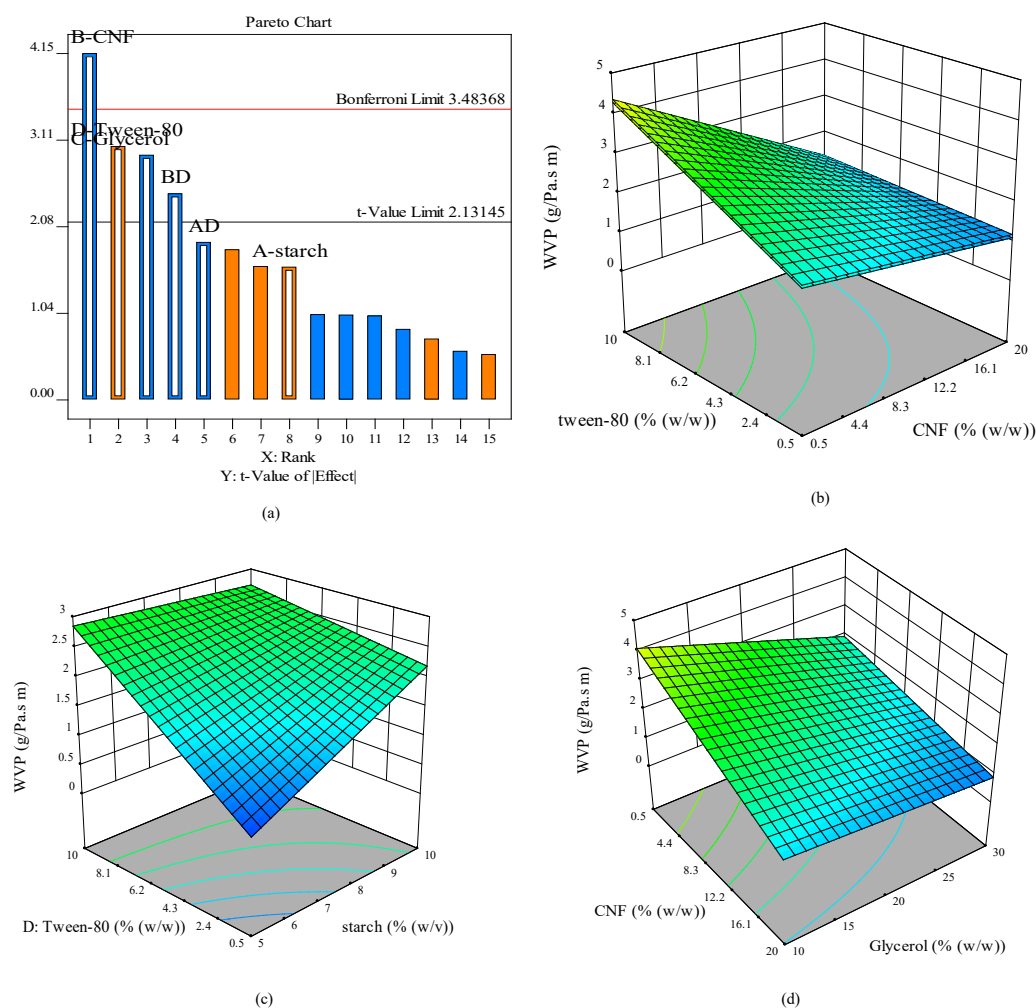


Figure 3. Analysis of (a) Pareto chart, (b) response surface of WVP as a function of CNF-tween-80, (c) starch-tween-80, and (d) CNF-glycerol concentration

## Interaction Effects of Coating Formulation on Oxygen Permeability

Table 1 shows oxygen permeability changes with variation of formulation of coating. As can be seen from Table 2 for the  $PO_2$ , the  $p$ -value of less than 0.05 shows linear terms is acceptable (significant). Moreover, the high determination coefficients ( $R^2$ ) value ( $>85\%$ ), the “adeq. Precision” more than 4, and a non-significant lack of fit indicate that the model can be used to navigate the design space. The factors, namely CNF ( $X_2$ ), tween-80 ( $X_4$ ) concentration, and interaction of these factors ( $X_2, X_4$ ) are statistically significant to the model ( $p$ -value  $\leq 0.05$ ), while the remaining factors are not significant. Linear equation of the oxygen permeability as a function of factors of CNF( $X_2$ ), and tween-80 ( $X_4$ ) is given by Equation 7:

$$PO_2 = 6916.60 - 3932.49 X_2 + 5167.15 X_4 - 3870.60 X_2 X_4 \quad (7)$$

The value of negative coefficients of CNF (Equation 7) represents that low  $PO_2$  can be achieved by using a high concentration of CNF.

The factorial effects of the main important factors and their interactions were found to be in the following order: tween-80 > CNF > CNF-tween-80, as presented in the Pareto chart in Figure 4(b). In order to visualize the effect of interactions of independent variables on  $PO_2$ , 3D response surface plots were depicted Figure 4. In general, a decrease in  $PO_2$  of edible films was obtained with the increases in CNF concentration and low concentration of tween-80 (Figure 4b). The lowest  $PO_2$  ( $745.268 \text{ cm}^3/\text{m}^2 \text{ day Pa} = 0.0087 \text{ cm}^3/\text{m}^2 \text{ s Pa}$ ) was reached at the highest of CNF (20% w/w) and lowest tween-80 concentration (0.5).  $PO_2$  value in this work was lower than  $PO_2$  ( $0.65 \times 10^{13} \text{ cm}^3/\text{m}^2 \text{ s Pa}$ ) of corn starch film reported by Ribeiro et al., (2007). The fact that CNF has good oxygen barrier properties can be due to several reasons, as follows: (1) The dense network structure is formed by nanofibrils with more complexity, smaller pores, and more uniform particle size. Considering this fact, a complex, dense network increases the tortuosity for the diffusion of gases. Consequently, oxygen gas was compelled to diffuse through a more tortuous pathway throughout the film. It increases the time for the gas to navigate macroscopically throughout the film, thereby decreasing the permeability within the films. (2) The CNF films have higher entanglements within the film, which improve the tortuosity or extended the diffusion path; thereby, the oxygen molecules penetrate more slowly through the CNF films. (3) The high crystalline structure and a network structure held together via strong inter and intramolecular hydrogen bonds within the nanofibrils contribute to the gas barrier properties (Bangar & Whiteside. 2021a; Ferrer et al.. 2017; Siti Hajar et al.. 2021; Serpa & Vel. 2016). Furthermore, the present work has the same result as that reported by Ortega-toro et al. (2014), who found that  $PO_2$  increased when surfactants were incorporated into the corn starch film. Whereas, the oxygen permeability is not much affected with the addition of varying the amount of plasticizer, as observed in previous works (Agarwal, 2021).

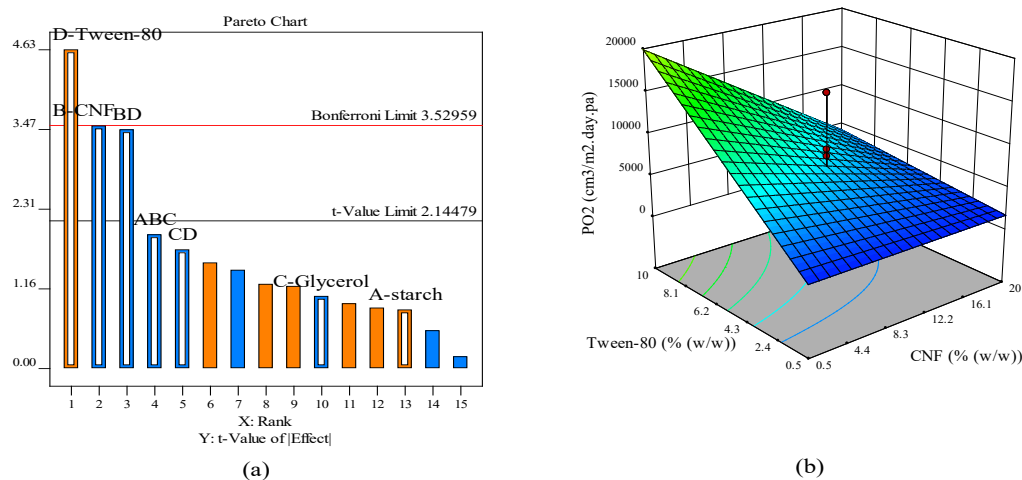


Figure 4. Analysis of (a) Pareto chart, (b) response surface of PO<sub>2</sub> as a function of CNF-tween-80

### Interaction Effects of Coating Formulation on Tensile Strength

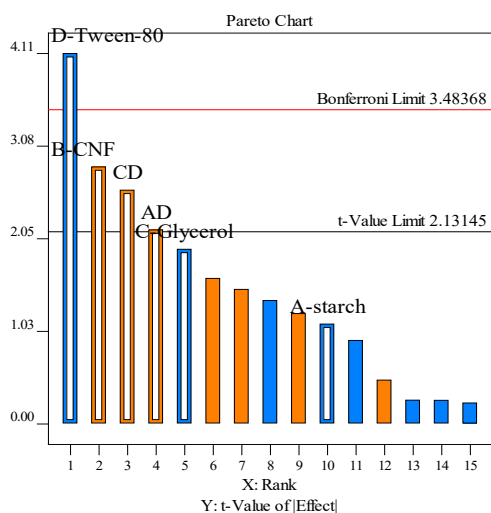
The result of the tensile strength test of varying formulas of the film (0.77 to 26.65 MPa) is displayed in Table 1. As observed in Table 2, it was found that *p*-values of tensile strength for the linear model were significant. The value of *R*<sup>2</sup> was 0.89, the adequate precision was 8.626 (< 4), and the lack of fit values was non-significant (*p*-value > 0,005), indicating adequate signal. It was also reported that the tensile strength of the composite film in the present study was significantly influenced by individual factors (CNF (X<sub>2</sub>) and tween 80 concentration (X<sub>4</sub>)) and combination by factors (starch-tween (X<sub>1</sub>X<sub>4</sub>) and glycerol-tween-80 (X<sub>3</sub>X<sub>4</sub>)). The linear equations for tensile strength as a function of the four independent variables was given below (Equation 8):

$$TS = 9.55 + 3.34x_2 - 4.81 x_4 + 2.52 x_1x_4 + 3.04 x_3x_4 \quad (8)$$

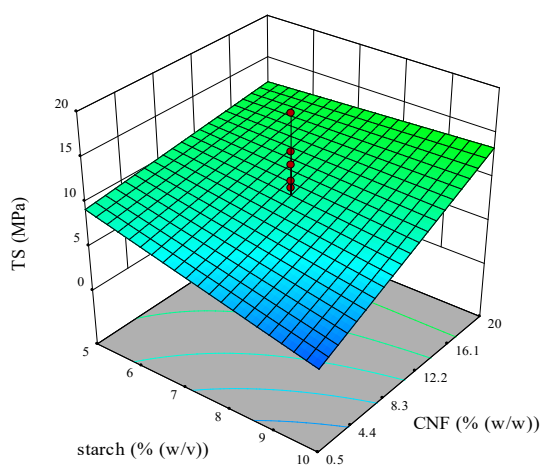
The positive coefficients value of CNF concentration (3.34) in equation 8 indicated enhancement of TS. Whereas the value of the negative coefficient of tween-80 concentration showed diminished TS of starch film or coating.

As can be seen in the Pareto chart in Figure 5a, the factorial effects of very important main factors and their interactions (above Bonferroni limit) were found to be in the following order: tween-80 > CNF > glycerol-tween > starch-tween-80. The 3D response surface in Figure 5b-c depicts that the addition of 5–20% CNF significantly improved TS (Figure 5b). A Similar result regarding the effect of CNF of TS has been described by previous authors (Li et al., 2018b; Xu et al. 2019). As can be seen in Figure 5c and d, the opposite effect was observed with the addition of tween-80, which reduced

TS value obviously at all starch concentrations and high CNF concentration, respectively. Several past studies supported this result (Li et al., 2018a; Xu et al., 2019). The highest TS value (26.65 MPa) in our work was obtained at high CNF concentration (20%) and low Tween 80 (0.5) in sago starch film/coating formulation (Table 1). TS value in this work was higher than that reported by a previous study (Shih & Zhao., 2021) in the film of tapioca starch incorporated 20% CNF (24.32 MPa) and the film is based on potato starch with 10% CNF (19.13 MPa). Several reasons have been argued for increasing the TS value of film by CNF: 1. Similar chemical structures of CNF and starch lead to a strong interaction between CNF and sago starch through the intermolecular hydrogen reaction, and CNF can be uniformly dispersed in the starch matrix, causing the compatibility between starch and CNF and efficient stress transfer from matrix to CNF (Li et al. 2018; Soofi et al., 2021), TS of films is directly associated with dispersion, compatibility, and hydrogen bonding between starch and nano cellulose (Bangar & Whiteside, 2021a), 2. The presence of CNF in void spaces between polymer chains caused decreasing mobility of chain and related with the change of crystalline is and the high mechanical strength of CNF (Hajar et al., 2021; Soofi et al., 2021), 3. Nano-sized CNF promoted strong intermolecular force, resulting in the rigidity enhancement of the films and, therefore high TS (Siti Hajar et al., 2021). In addition, it could be related to that surfactant are small size molecules that could persist between starch chains, like glycerol, increasing even more chain mobility and enhancing the initial plastic effect. The higher hydrophile-lipophile balance (HLB) value of tween 80 could interact with glycerol or water, facilitating its presence between starch chains which weaken the intermolecular hydrogen bonding. Therefore, resulting in the decrease of mechanical properties (Rodriguez et al., 2006).



(a)



(b)

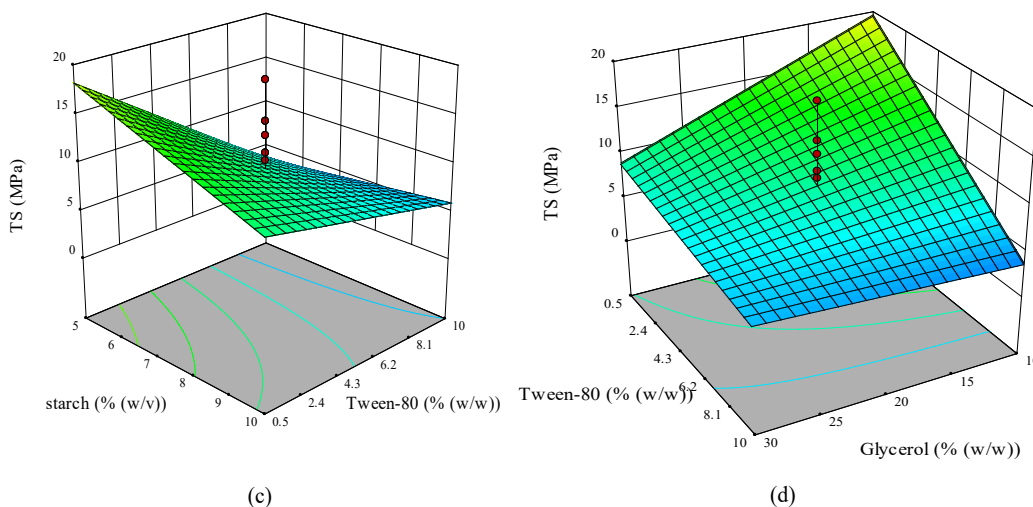


Figure 5. Analysis of (a) Pareto chart, (b) response surface of tensile strength as a function of starch-CNF, (c) starch-tween-80, and (d) tween-glycerol

### Optimization of Coating Formulation

The optimization of the formulation of the coating solution was based on the four criteria: (1) minimizing contact angle; (2) minimizing water vapor permeability; (3) minimizing oxygen permeability; (4) maximizing tensile strength. Also, the importance value of 4 (++++) was selected for all criteria. The optimum concentration for producing the best characterization of starch and CNF coating was obtained with the addition of sago starch (5% w/v), CNF (20% w/w), and glycerol (10% w/w), and tween-80 (0.5% w/w) with maximum desirability 90%. The high desirability value in this work indicates that this formula is suitable for use.

### Verification Experiments and Validation of the Model Equations

Verification experiments were conducted on the central points of the factorial design (7.5% w/v), CNF (10.25% w/w), glycerol (20% w/w), and tween-80 (5.25 % w/w) to validate the equations model adequacy and the result of film characterization compared to the predicted data. Table 3 shows the experimental and predicted value for the dependent variables at the center point. The percentage error (PE) was used for the evaluation of prediction accuracy. A small percentage error value indicated that the accuracy of response surface equations was better and the experimental values were close to the predicted values. From Table 3 it could be observed that the percentage error of the prediction equations differed according to the predicted parameters. The values of percentage error ranged from 8–15% with the smallest value was for WVP and the largest was for tensile strength. It meant that the most accurate prediction was for WVP with the percentage accuracy of around 92% and the least accurate was for tensile strength with the accuracy of around 85%.

Table 3  
*Predicted ad experimental data for the responses at optimum formulation*

Responses	Predicted value	Experimental value	Percentage error (PE)
Contact Angle (°)	53.514	49.1	8.27
WVPx10 <sup>-11</sup> (g /s Pa m)	1.944	1.90	4.68
PO <sub>2</sub> (cm <sup>3</sup> /m <sup>2</sup> day Pa)	6930.304	6763.966	11.147
Tensile strength (MPa)	11.147	9.68	15.18

## CONCLUSION

The optimization of the coating formula was carried out to obtain the minimum value of the contact angle, oxygen permeability, water vapor permeability, and strong tensile strength. The value of contact angle depends on starch and tween-80 concentration. The reduction of WVP is influenced by the amount of CNF, glycerol, and tween-80. The addition of CNF in coating solution affects permeability (WVP and O<sub>2</sub>) and tensile strength. The best film and coating characteristics were obtained in the formulation containing 5% (w/v) starch, 20% (w/w) CNF, 10% (w/w) glycerol, and 0.5% (w/w) tween-80. Verification model were performed on the central points of the factorial design (7.5% w/v), CNF (10.25% w/w), glycerol (20% w/w), and tween-80 (5.25 % w/w) resulted in the value contact angle (49.1°), WVP (1.90 x10<sup>-11</sup> (g/s Pa m), PO<sub>2</sub> (6763.966 cm<sup>3</sup>/m<sup>2</sup> day Pa), and TS (9.68 MPa) respectively.

## ACKNOWLEDGEMENTS

The highest appreciation is given to the educational fund development institution (LPDP). Indonesia which has financed this research

## REFERENCES

- Agarwal, S. (2021). Major factors affecting the characteristics of starch based biopolymer films. *European Polymer Journal*, 160, Article 110788. <https://doi.org/10.1016/j.eurpolymj.2021.110788>
- Andrade, R., Skurtys, O., Osorio, F., Zuluaga, R., Gañán, P., & Castro, C. (2014). Wettability of gelatin coating formulations containing cellulose nanofibers on banana and eggplant epicarps. *LWT-Food Science and Technology*, 58(1), 158-165. <https://doi.org/10.1016/j.lwt.2014.02.034>
- ASTM D882. (2010). Standard test methods for tensile properties of thin plastic sheeting, *Annual Book of ASTM Standards*, 87(Reapproved), 3-5. <https://doi.org/10.1520/D0882-10>
- ASTM E 96 (1995). Standard test methods for water vapor transmission of materials. ASTM International. <https://doi.org/10.1520/E0096-00E01>
- Azeredo, H. M. C., Rosa, M. F., Henrique, L., & Mattoso, C. (2017). Nanocellulose in bio-based food packaging applications. *Industrial Crops & Products*, 97, 664-671. <https://doi.org/10.1016/j.indcrop.2016.03.013>



- Bagheri, V., Ghanbarzadeh, B., Ayaseh, A., Ostadrahimi, A., Ehsani, A., Alizadeh-Sani, M., & Adun, P. A. (2019). The optimization of physico-mechanical properties of bionanocomposite films based on gluten/carboxymethyl cellulose/cellulose nanofiber using response surface methodology. *Polymer Testing*, *78*, Article 105989. <https://doi.org/10.1016/j.polymertesting.2019.105989>
- Balakrishnan, P., Sreekala, M. S., Kunaver, M., Huskić, M., & Thomas, S. (2017). Morphology, transport characteristics and viscoelastic polymer chain confinement in nanocomposites based on thermoplastic potato starch and cellulose nanofibers from pineapple leaf. *Carbohydrate Polymers*, *169*, 176-188. <https://doi.org/10.1016/j.carbpol.2017.04.017>
- Bangar, S. P., & Whiteside, W. S. (2021). Nano-cellulose reinforced starch bio composite films-A review on green composites. *International Journal of Biological Macromolecules*, *185*, 849-860. <https://doi.org/10.1016/j.ijbiomac.2021.07.017>
- Basiak, E., Lenart, A., & Debeaufort, F. (2017). Effect of starch type on the physico-chemical properties of edible films. *International Journal of Biological Macromolecules*, *98*, 348-356. <https://doi.org/10.1016/j.ijbiomac.2017.01.122>
- Cazón, P., Vázquez, M., & Velazquez, G. (2018). Novel composite films based on cellulose reinforced with chitosan and polyvinyl alcohol: Effect on mechanical properties and water vapour permeability. *Polymer Testing*, *69*, 536-544. <https://doi.org/10.1016/j.polymertesting.2018.06.016>
- Da Silva, J. B. A., Nascimento, T., Costa, L. A. S., Pereira, F. V., Machado, B. A., Gomes, G. V. P., Assis, D. J., & Druzian, J. I. (2015). Effect of source and interaction with nanocellulose cassava starch, glycerol and the properties of films bionanocomposites. *Materials Today: Proceedings*, *2*(1), 200-207. <https://doi.org/10.1016/j.matpr.2015.04.022>
- Deng, Z., Jung, J., Simonsen, J., & Zhao, Y. (2017). Cellulose nanomaterials emulsion coatings for controlling physiological activity, modifying surface morphology, and enhancing storability of postharvest bananas (*Musa acuminata*). *Food Chemistry*, *232*, 359-368. <https://doi.org/10.1016/j.foodchem.2017.04.028>
- Deng, Z., Jung, J., Simonsen, J., & Zhao, Y. (2018). Cellulose nanocrystals pickering emulsion incorporated chitosan coatings for improving storability of postharvest bartlett pears (*Pyrus communis*) during long-term cold storage. *Food Hydrocolloids*, *84*, 229-237. <https://doi.org/10.1016/j.foodhyd.2018.06.012>
- Ferrer, A., Pal, L., & Hubbe, M. (2017). Nanocellulose in packaging: Advances in barrier layer technologies. *Industrial Crops & Products*, *95*, 574-582. <https://doi.org/10.1016/j.indcrop.2016.11.012>
- Ghosh, T., Nakano, K., & Katiyar, V. (2021). Curcumin doped functionalized cellulose nanofibers based edible chitosan coating on kiwifruits. *International Journal of Biological Macromolecules*, *184*, 936-945. <https://doi.org/10.1016/j.ijbiomac.2021.06.098>
- Gopi, S., Amalraj, A., Jude, S., Thomas, S., & Guo, Q. (2019). Bionanocomposite films based on potato, tapioca starch and chitosan reinforced with cellulose nanofiber isolated from turmeric spent. *Journal of the Taiwan Institute of Chemical Engineers*, *96*, 664-671. <https://doi.org/10.1016/j.jtice.2019.01.003>
- Hajar, O. S., Nordin, N., Ayuni, N., Azman, A., Sya, I., Amin, M., & Kadir, R. (2021). Effects of nanocellulose fiber and thymol on mechanical, thermal, and barrier properties of corn starch films. *International Journal of Biological Macromolecules*, *183*, 1352-1361. <https://doi.org/10.1016/j.ijbiomac.2021.05.082>



- Kania, D., Yunus, R., Omar, R., Abdul, S., & Mohamed, B. (2021). Physicochemical and engineering aspects rheological investigation of synthetic-based drilling fluid containing non-ionic surfactant pentaerythritol ester using full factorial design. *Colloids and Surfaces A: Physicochemical and Engineering Aspects*, 625, Article 126700. <https://doi.org/10.1016/j.colsurfa.2021.126700>
- Karim, A. A., & Tie, A. P. (2008). Starch from the sago (*Metroxylon sagu*) palm tree - Properties, prospects, and challenges as a new industrial source for food. *Comprehensive Reviews in Food Science and Food Safety*, 7(3), 215-228. <https://doi.org/10.1111/j.1541-4337.2008.00042.x>
- Kim, H., Roy, S., & Rhim, J. (2021). Effects of various types of cellulose nanofibers on the physical properties of the CNF-based films. *Journal of Environmental Chemical Engineering*, 9(5), Article 106043. <https://doi.org/10.1016/j.jece.2021.106043>
- Kubik, E., & Zeman, S. (2013). Determination of oxygen permeability of polyethylene and polypropylene nonwoven fabric foils. *Research in Agricultural Engineering*, 59(3), 105-113.
- Lavecchia, R., Medici, F., Piga, L., & Zuorro, A. (2015). Factorial design analysis of the recovery of flavonoids from bilberry fruit by-products. *International Journal of Applied Engineering Research*, 10(23), 43555-43559.
- Li, M., Tian, X., Jin, R., & Li, D. (2018). Preparation and characterization of nanocomposite films containing starch and cellulose nanofibers. *Industrial Crops and Products*, 123, 654-660. <https://doi.org/10.1016/j.indcrop.2018.07.043>
- Lopez-Polo, J., Silva-Weiss, A., Zamorano, M., & Osorio, F. A. (2020). Humectability and physical properties of hydroxypropyl methylcellulose coatings with liposome-cellulose nanofibers: Food application. *Carbohydrate Polymers*, 231, Article 115702. <https://doi.org/10.1016/j.carbpol.2019.115702>
- Maniglia, B. C., Denise, Laroque, D. A., de Andrade, L. M., Carciofi, B. A. M., Tenorio, J. A. S., & de Andrade, C. J. (2019). Production of active cassava starch films; effect of adding a biosurfactant or synthetic surfactant. *Reactive and Functional Polymers*, 144, Article 104368. <https://doi.org/10.1016/j.reactfunctpolym.2019.104368>
- Meneguim, A. B., Ferreira Cury, B. S., dos Santos, A. M., Franco, D. F., Barud, H. S., & da Silva Filho, E. C. (2017). Resistant starch/pectin free-standing films reinforced with nanocellulose intended for colonic methotrexate release. *Carbohydrate Polymers*, 157, 1013-1023. <https://doi.org/10.1016/j.carbpol.2016.10.062>
- Ortega-toro, R., Jiménez, A., Talens, P., & Chiralt, A. (2014). Effect of the incorporation of surfactants on the physical properties of corn starch films. *Food Hydrocolloids*, 38, 66-75. <https://doi.org/10.1016/j.foodhyd.2013.11.011>
- Rodriguez, M., Oses, J., Ziani, K., & Mate, J. I. (2006). Combined effect of plasticizers and surfactants on the physical properties of starch based edible films. *Food Research International*, 39(8), 840-846. <https://doi.org/10.1016/j.foodres.2006.04.002>
- Patil, S., Bharimalla, A. K., Mahapatra, A., Dhakane-Lad, J., Arputharaj, A., Kumar, M., Raja, A. S. M., & Kambl, N. (2021). Effect of polymer blending on mechanical and barrier properties of starch-polyvinyl alcohol based biodegradable composite films. *Food Bioscience*, 44(Part A), Article 101352. <https://doi.org/10.1016/j.fbio.2021.101352>

- Paula, A., Lamsal, B., Luiz, W., Magalhães, E., & Mottin, I. (2019). Cassava starch films reinforced with lignocellulose nanofibers from cassava bagasse. *International Journal of Biological Macromolecules*, *139*, 1151-1161. <https://doi.org/10.1016/j.ijbiomac.2019.08.115>
- Punia, S., Scott, W., Dunno, K. D., Armstrong, G., Dawson, P., & Love, R. (2022). Starch-based bio-nanocomposites films reinforced with cellulosic nanocrystals extracted from Kudzu (*Pueraria montana*) vine. *International Journal of Biological Macromolecules*, *203*, 350-360. <https://doi.org/10.1016/j.ijbiomac.2022.01.133>
- Rahayoe, S. (2015). *Control of characteristics of chitosan film as fruit coating with the variation of types and additive compositions in making coating solutions* (Doctoral dissertation). Gadjah Mada University, Indonesia. <https://lib.ugm.ac.id/>
- Ribeiro, C., Vicente, A. A., Teixeira, J. A., & Miranda, C. (2007). Optimization of edible coating composition to retard strawberry fruit senescence. *Postharvest Biology and Technology*, *44*(1), 63-70. <https://doi.org/10.1016/j.postharvbio.2006.11.015>
- Riva, S. C., Opara, U. O., & Fawole, O. A. (2020). Recent developments on postharvest application of edible coatings on stone fruit: A review. *Scientia Horticulturae*, *262*, Article 109074. <https://doi.org/10.1016/j.scienta.2019.109074>
- Santacruz, S., Rivadeneira, C., & Castro, M. (2015). Edible films based on starch and chitosan. Effect of starch source and concentration, plasticizer, surfactant's hydrophobic tail and mechanical treatment. *Food Hydrocolloids*, *49*, 89-94. <https://doi.org/10.1016/j.foodhyd.2015.03.019>
- Sapper, M., Bonet, M., & Chiralt, A. (2019). Wettability of starch-gellan coatings on fruits, as affected by the incorporation of essential oil and/or surfactants. *LWT*, *116*, Article 108574. <https://doi.org/10.1016/j.lwt.2019.108574>
- Serpa, A., & Vel, J. (2016). Vegetable nanocellulose in food science: A review. *Food Hydrocolloids* *57*, 178-186. <https://doi.org/10.1016/j.foodhyd.2016.01.023>
- Shih, Y. T., & Zhao, Y. (2021). Development, characterization and validation of starch based biocomposite films reinforced by cellulose nanofiber as edible muffin liner. *Food Packaging and Shelf Life*, *28*, Article 100655. <https://doi.org/10.1016/j.fpsl.2021.100655>
- Silva, A. P. M., Oliveira, A. V., Pontes, S. M. A., Pereira, A. L. S., Souza Filho, M. de sá M., Rosa, M. F., & Azeredo, H. M. C. (2019). Mango kernel starch films as affected by starch nanocrystals and cellulose nanocrystals. *Carbohydrate Polymers*, *211*, 209-216. <https://doi.org/10.1016/j.carbpol.2019.02.013>
- Soofi, M., Alizadeh, A., Hamishehkar, H., Almasi, H., & Roufegarinejad, L. (2021). Preparation of nanobiocomposite film based on lemon waste containing cellulose nanofiber and savory essential oil: A new biodegradable active packaging system. *International Journal of Biological Macromolecules*, *169*, 352-361. <https://doi.org/10.1016/j.ijbiomac.2020.12.114>
- Soradach, S., Nunthanid, J., Limmatvapirat, S., & Luangtana-anan, M. (2017). Utilization of shellac and gelatin composite film for coating to extend the shelf life of banana. *Food Control*, *73*(Part B), 1310-1317. <https://doi.org/10.1016/j.foodcont.2016.10.059>

- Soto-Muñoz, L., Palou, L., Argente-Sanchis, M., Ramos-López, M. A., & Pérez-Gago, M. B. (2021). Optimization of antifungal edible pregelatinized potato starch-based coating formulations by response surface methodology to extend postharvest life of 'Orri' mandarins Lourdes SotoMun. *Scientia Horticulturae*, 288, Article 110394. <https://doi.org/10.1016/j.scienta.2021.110394>
- Stachowiak, N., Kowalonek, J., & Kozłowska, J. (2020). Effect of plasticizer and surfactant on the properties of poly(vinyl alcohol)/chitosan films. *International Journal of Biological Macromolecules*, 164, 2100-2107. <https://doi.org/10.1016/j.ijbiomac.2020.08.001>
- Sun, X., Wu, Q., Picha, D. H., Ferguson, M. H., Ndukwe, I. E., & Azadi, P. (2021). Comparative performance of bio-based coatings formulated with cellulose, chitin, and chitosan nanomaterials suitable for fruit preservation. *Carbohydrate Polymers*, 259, Article 117764. <https://doi.org/10.1016/j.carbpol.2021.117764>
- Syafri, E., Jamaluddin, Wahono, S., Irwan, A., Asrofi, M., Sari, N. H., & Fudholi, A. (2019). Characterization and properties of cellulose microfibrils from water hyacinth filled sago starch biocomposites. *International Journal of Biological Macromolecules*, 137, 119-125. <https://doi.org/10.1016/j.ijbiomac.2019.06.174>
- Thakur, R., Pristijono, P., Golding, J. B., Stathopoulos, C. E., Scarlett, C. J., Bowyer, M., Singh, S. P., & Vuong, Q. V. (2018). Development and application of rice starch based edible coating to improve the postharvest storage potential and quality of plum fruit (*Prunus salicina*). *Scientia Horticulturae*, 237, 59-66. <https://doi.org/10.1016/j.scienta.2018.04.005>
- Thakur, Rahul, Pristijono, P., Scarlett, C. J., Bowyer, M., Singh, S. P., & Vuong, Q. V. (2019). Starch-based films: Major factors affecting their properties. *International Journal of Biological Macromolecules*, 132, 1079-1089. <https://doi.org/10.1016/j.ijbiomac.2019.03.190>
- Tibolla, H., Pelissari, F. M., Martins, J. T., Lanzoni, E. M., Vicente, A. A., Menegalli, F. C., & Cunha, R. L. (2019). Banana starch nanocomposite with cellulose nanofibers isolated from banana peel by enzymatic treatment: *In vitro* cytotoxicity assessment. *Carbohydrate Polymers*, 207, 169-179. <https://doi.org/10.1016/j.carbpol.2018.11.079>
- Ventura-Aguilar, R. I., Bautista-Baños, S., Flores-García, G., & Zavaleta-Avejar, L. (2018). Impact of chitosan based edible coatings functionalized with natural compounds on *Colletotrichum fragariae* development and the quality of strawberries. *Food Chemistry*, 262, 142-149. <https://doi.org/10.1016/j.foodchem.2018.04.063>
- Vieira, J. M., Flores-López, M. L., de Rodríguez, D. J., Sousa, M. C., Vicente, A. A., & Martins, J. T. (2016). Effect of chitosan-Aloe vera coating on postharvest quality of blueberry (*Vaccinium corymbosum*) fruit. *Postharvest Biology and Technology*, 116, 88-97. <https://doi.org/10.1016/j.postharvbio.2016.01.011>
- Widaningrum, W., Miskiyah, M., & Winarti, C. (2015). Edible coating berbasis pati sago dengan penambahan antimikroba minyak sereh pada paprika: Preferensi konsumen dan mutu vitamin C [Sago starch-based edible coating with antimicrobial addition of lemongrass oil to peppers: Consumer preferences and vitamin c]. *Agritech Journal*, 35(1), 53-60. <https://doi.org/10.22146/agritech.9419>
- Xu, J., Xia, R., Zheng, L., Yuan, T., & Sun, R. (2019). Plasticized hemicelluloses/chitosan-based edible films reinforced by cellulose nano fiber with enhanced mechanical properties. *Carbohydrate Polymers*, 224, Article 115164. <https://doi.org/10.1016/j.carbpol.2019.115164>

- Yuan, Y., & Chen, H. (2021). Preparation and characterization of a biodegradable starch-based antibacterial film containing nanocellulose and polyhexamethylene biguanide. *Food Packaging and Shelf Life*, 30, Article 100718. <https://doi.org/10.1016/j.fpsl.2021.100718>
- Zhong, Y., & Li, Y. (2011). Effects of surfactants on the functional and structural properties of kudzu (*Pueraria lobata*) starch/ascorbic acid films. *Carbohydrate Polymers*, 85(3), 622-628. <https://doi.org/10.1016/j.carbpol.2011.03.031>
- Zhu, F. (2019). Food Hydrocolloids Recent advances in modifications and applications of sago starch. *Food Hydrocolloids*, 96, 412-423. <https://doi.org/10.1016/j.foodhyd.2019.05.035>

*Short Communication*

## **Latent and Manifest Variables of PLS-SEM Model in the Decision Making of PIKNET Sound Wave-Based Attractor Innovation by Fishermen in Bulak Sub-District, Surabaya, Indonesia**

**Nurul Rosana<sup>1\*</sup>, Nuddin Harahab<sup>2</sup>, Gatot Ciptadi<sup>2</sup>, Andi Kurniawan<sup>2</sup>, Suryadhi<sup>3</sup>, Safriudin Rifandi<sup>3</sup>, Amirul Mukminin<sup>3</sup> and Viv Djanat Prasita<sup>3</sup>**

<sup>1</sup>*Department of Fisheries, Faculty of Engineering and Marine Science, Universitas Hang Tuah, Surabaya, Indonesia*

<sup>2</sup>*Postgraduate Environmental Science, Doctorate Program, Brawijaya University, Malang, Indonesia*

<sup>3</sup>*Faculty of Engineering and Marine Science, Universitas Hang Tuah, Surabaya, Indonesia*

### **ABSTRACT**

A study of the diffusion process of sound wave-based attractor innovation in fishing groups needs to be done because the application of innovation requires an adaptation process so that one can adopt the new subject through the established stages. The innovation-decision process is a mental process by which a person or institution goes from initial knowledge about an innovation. This research aims to analyze the measurement model and the relationship between variables in the decision-making of Piknet innovation by fishermen in Bulak Surabaya. SEM PLS data analysis was used to determine the relationship between latent and manifest variables. The test results showed that the CR value is above 0.7; therefore, it can be said that the variable has been met. The AVE values for X1-X5,

Y1 and Y2 are above 0.5. Therefore, each latent variable has a valid measurement model. The conclusions from the research are as follows: (1) The analysis results of the measurement model met the requirements with good characteristics. Therefore, it can be continued to the next stage of structural model analysis; (2) Furthermore, 11 eliminated indicator variables did not meet the standard requirements of the outer loading value ; (3) A significant relationship was found in the latent variables of X1-X5,

#### ARTICLE INFO

*Article history:*

Received: 04 January 2022

Accepted: 21 April 2022

Published: 09 November 2022

DOI: <https://doi.org/10.47836/pjst.31.1.22>

*E-mail addresses:*

[nurul.rosana@hangtuah.ac.id](mailto:nurul.rosana@hangtuah.ac.id) (Nurul Rosana)

[marmunnuddin@ub.ac.id](mailto:marmunnuddin@ub.ac.id) (Nuddin Harahab)

[ciptadi@ub.ac.id](mailto:ciptadi@ub.ac.id) (Gatot Ciptadi)

[andi\\_k@ub.ac.id](mailto:andi_k@ub.ac.id) (Andi Kurniawan)

[suryadhi@hangtuah.ac.id](mailto:suryadhi@hangtuah.ac.id) (Suryadhi)

[safriudin.rifandi@hangtuah.ac.id](mailto:safriudin.rifandi@hangtuah.ac.id) (Safriudin Rifandi)

[amirul.muminin@hangtuah.ac.id](mailto:amirul.muminin@hangtuah.ac.id) (Amirul Mukminin)

[viv.djanat@hangtuah.ac.id](mailto:viv.djanat@hangtuah.ac.id) (Viv Djanat Prasita)

\* Corresponding author

Y1 and Y2; (4) Indicator variables related to the latent variable are X1.4, X2.1, X3.2, X4.1-X4.3, X5.1, X5.2, Y1.1-Y1.3 and Y2.1,-Y2.3. To develop this research, continuous research is needed by examining each of the variables used in depth.

*Keywords:* Attractor, fishermen, innovation, Piknet

---

## INTRODUCTION

In general, gill net fishers in Bulak District, Surabaya City, are traditional fishermen with education levels ranging from elementary to high school. The level of education affects the ability to access changes in the surroundings, especially those related to technological changes. Therefore, the application of technology given to gill net fishermen must pay attention to aspects of education and local culture in their environment. One factor influencing fishery resources' sustainability is applying environmentally friendly technology for fishermen and assisting so that fishermen can operate them. The innovation offered to the gill net fishermen is a fish caller device called an attractor, designed based on sound waves with a wave range of 500-1000 Hz, named Piknet.

A study of the diffusion process of sound wave-based attractor innovation in fishing groups needs to be done because the application of innovation requires an adaptation process so that one can adopt the new subject through the established stages. The innovation-decision process is a mental process by which a person or institution goes from initial knowledge about innovation to forming an attitude towards the innovation, implementing the new idea, and confirming the decision (Rogers, 2003).

The sound wave-based attractor innovation from research by Rosana et al. (2018) describes testing a sound wave-based fish calling device called Piknet. The experiment was carried out to see the fish's response to the sound coming out of the tool. Rosana and Muminin (2019) explained the difference in the number of catches of "*Bulu Ayam*" fish (*Oxyporhamphus micropterus*) using a sound wave-based attractor compared to not using a tool. Rosana et al. (2019) explained efforts to introduce sound wave-based attractors to fishermen in *Bulak* District, Surabaya, in their Analysis of the Difference in Frequency Sound Waves to the Catch of Gulamah Fish (*Johnius trachycephalus*) Using a Trammel Net in the Coastal Area of Surabaya. Rosana et al. (2021) explained the results of the trial of Piknet with the catch of gulamah fish, where there was a difference in the number of catches compared to not using Piknet.

This research examines the innovation of a Piknet sound wave-based attractor tested by a group of fishermen in the Bulak Sub-district, Surabaya. In principle, the Piknet attracts the attention of the fish to the gill fishing net gear because of the sound emitted by the tool. Fish that respond to the sound will approach, crash, and then become entangled in the body of the net. In the early stages of testing the Piknet, socialization regarding the

purpose, benefits, and methods of use was conducted on groups of gillnet fishermen. The responses include the ease of use when operated in the waters, changes in the number of catches obtained, the presence of several attracted fish species, and the desire to use Piknet, as well as the suitability of the fishing gear used (Rosana et al., 2019).

In this research, the innovation diffusion concept from Rogers (2003) was used as a latent variable consisting of five aspects, including the innovation characteristics, communication channels, certain periods, social systems, as well as knowledge and persuasion. Meanwhile, the innovation decision-making process uses the adoption and implementation stages as well as confirmation and support. Furthermore, the innovation of fishing gear showed the need to further research the diffusion process to its target users (gill net fishermen group in Bulak Sub-district, Surabaya) by analyzing the factors that influence the fishermen's decision to adopt Piknet. Therefore, this research aims to analyze the measurement model (outer model) and the relationship between variables in the decision-making of Piknet innovation by fishermen in the Bulak Sub-district.

## MATERIALS AND METHODS

This research used a variant-based Partial Least Square (PLS)-Structural Equation Modeling (SEM) approach based on exogenous, endogenous latent, and indicator variables (Mun'im, 2015). Suitably, a measurement model was used to describe the relationship between latent/construct variables and their indicators, also known as outer relations (Jaya & Sumertajaya, 2008).

The measurement model described the relationship between the latent variable and its indicator variable (manifest), also known as the outer relation or measurement model. This model consisted the formative indicator model and the reflective indicator model. The reflective model can occur if the latent variable influences the manifest variable. The formative model explained that the manifest variable affects the latent variable with the direction of causality flowing from the manifest variable to the latent variable. Equations 1 and 2 show the reflective model (Haryono, 2016):

$$x = \Lambda x \xi + \delta \quad (1)$$

$$y = \Lambda y \eta + \varepsilon \quad (2)$$

Where  $x$  and  $y$  are indicators for exogenous ( $\xi$ ) and endogenous ( $\eta$ ) latent variables,  $\Lambda x$  and  $\Lambda y$  are loading matrices describing a simple regression coefficient that relates the latent variable to the indicator. Residuals are measured by  $\delta$  and  $\varepsilon$  and can be interpreted as measurement error or noise.

The formative indicator model can be written as Equations 3 and 4 (Haryono, 2016):

$$\xi = \Pi_{\xi} X_i + \delta \quad (3)$$



$$\eta = \Pi_{\eta} Y + \varepsilon \tag{4}$$

Where  $\xi$ ,  $\eta$ ,  $X$ , and  $Y$  are the same as the previous equation. Where  $\Pi_{\xi}$  dan  $\Pi_{\eta}$  are like multiple regression coefficients of the latent variable on the indicator, while  $\delta$  dan  $\varepsilon$  are the residuals of the regression.

The latent/construct variable consisted of seven variables (5 exogenous ( $X_1$ - $X_5$ ) and two endogenous ( $Y_1$  and  $Y_2$ )). Meanwhile, the manifest/indicator variable consisted of 24 variables (Table 1).

Table 1  
*Exogenous, endogenous latent, and manifest variables with PLS-SEM*

Latent/construct variables	Manifest/indicator variables	Symbol
Innovation characteristics		X1
• Schiffmen & Kanuk (2010)	Relative advantage	X1.1
• Tjiptono & Chandra (2012)	Suitability	X1.2
• Mardikanto (2007)	Complexity	X1.3
• Kusdibyo & Leo (2018)	Testable	X1.4
	Observable	X1.5
Communication Channels		X2
• Leeuwis (2004)	Interpersonal/local with discussion	X2.1
• Septiani & Esfandari (2018)	Cosmopolitan/outside the local system using electronic media	X2.2
• Indraningsih (2011)		
• Warnaen & Cangara (2013)	Cosmopolitan/outside the local system using print media	X2.3
Certain periods		X3
Adianto (2018)	Taking 1–4 months for adoption	X3.1
	Taking 5–8 months for adoption	X3.2
	Taking 9–12 months for adoption	X3.3
Social Systems		X4
Amanah (2006)	Actively participating in fisherman group organization	X4.1
	Actively participating in counseling	X4.2
	Actively participating in training	X4.3
Knowledge and persuasion		X5
Adianto (2018)	Being aware and knowing innovation	X5.1
	Being interested and actively seeking information	X5.2
	Having guidance in the understanding process	X5.3
Adoption and implementation		Y1
• Adianto (2018)	Adopted by individual/own initiative	Y1.1
• Pannell et al. (2006)	Adopted by group	Y1.2
• Warnaen & Cangara (2013)	Implementing innovation continuously	Y1.3
	Implementing innovation occasionally	Y1.4
Support and Confirmation		Y2
Rogers (2003)	Having the support of the closest people	Y2.1
	Having support from community leaders/role models	Y2.2
	Having support from local regional officials (village head)	Y2.3

The variable indicators used based on quantitative analysis were expressed in statements, which are scored in numbers ranging from strongly disagree to strongly agree with a score of 1 to 5. A purposive sampling method was used by considering the criteria of fishermen in the Bulak Sub-district, Surabaya. They operated gill net fishing gear and participated in the Piknet sound wave-based attractor trial. The number of samples used was 50, following the research conducted by Sholihin and Ratmono (2013). In addition, the minimum number of samples used is 45 respondents, while the maximum number of arrows to the latent variable is 5, with a significance of 0.1. Data in qualitative form were analyzed using SEM-PLS with the student version of the Smart PLS tool.

The research was conducted in Bulak Sub-district, Surabaya, East Java, especially in the group of gillnet fishermen in the area, and the map of the research location is shown in Figure 1.

The outer model assessment test (indicator test) was conducted using the criteria in Table 2, including convergent validity (individual reliability), discriminant validity (internal consistency), average variance extracted (AVE), and composite reliability (discriminant validity).

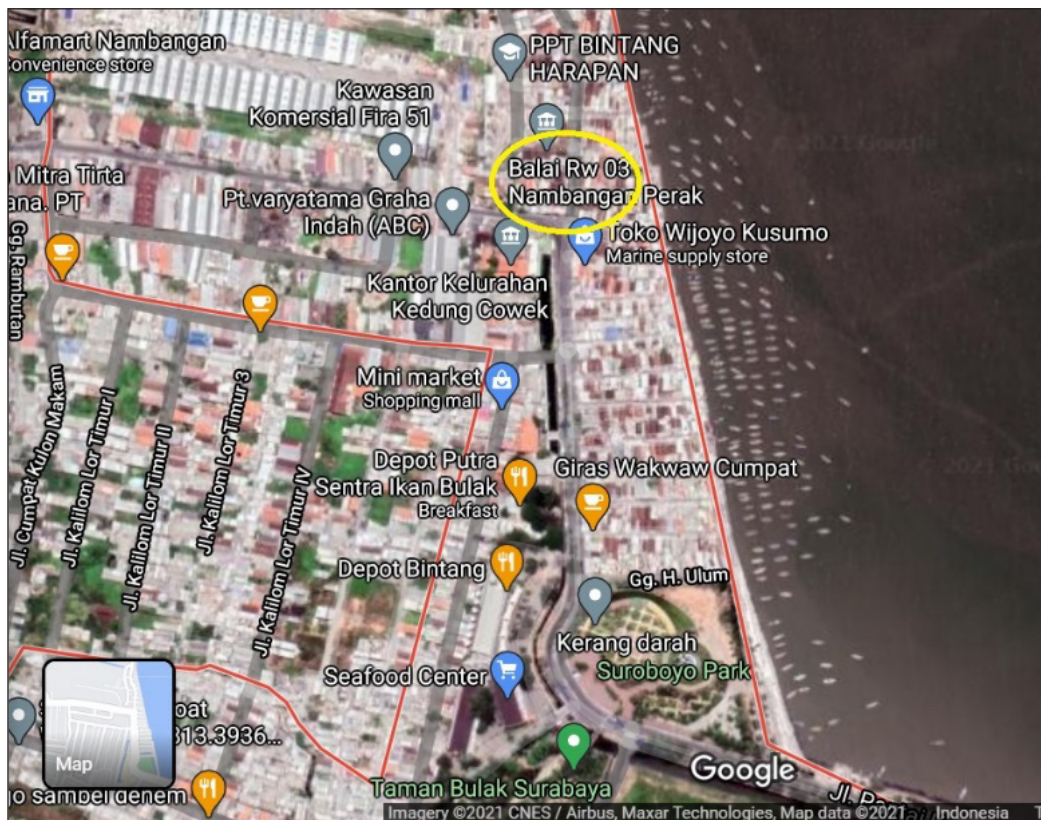


Figure 1. Research location, Bulak Sub-district, Nambangan Perak Village, Surabaya

Table 2  
Model assessment criteria

Model Test	Output PLS	Criteria
Outer Model (Indicator Test)	a. Convergent validity test (individual reliability) b. Discriminant validity test (internal consistency) c. Average Variance Extracted d. Composite reliability test (discriminant validity)	a. Load factor above 0.7 b. Cross-loading correlation > correlation to other latent variables c. AVE > 0.5 d. CR ≥ 0.7

This research was part of a research on the adoption of an attractor innovation model based on the Piknet sound wave for fishermen in Bulak District, Surabaya. The innovation-decision process used the elements of innovation, such as characteristics of tools, communication channels, a certain period and social systems. At the same time, in the stages of the innovation-decision process, the factors used were knowledge and persuasion, adoption and implementation and confirmation (Rosana et al., 2021). The conceptual framework can be seen in Figure 2, and the research flow can be seen in Figure 3.

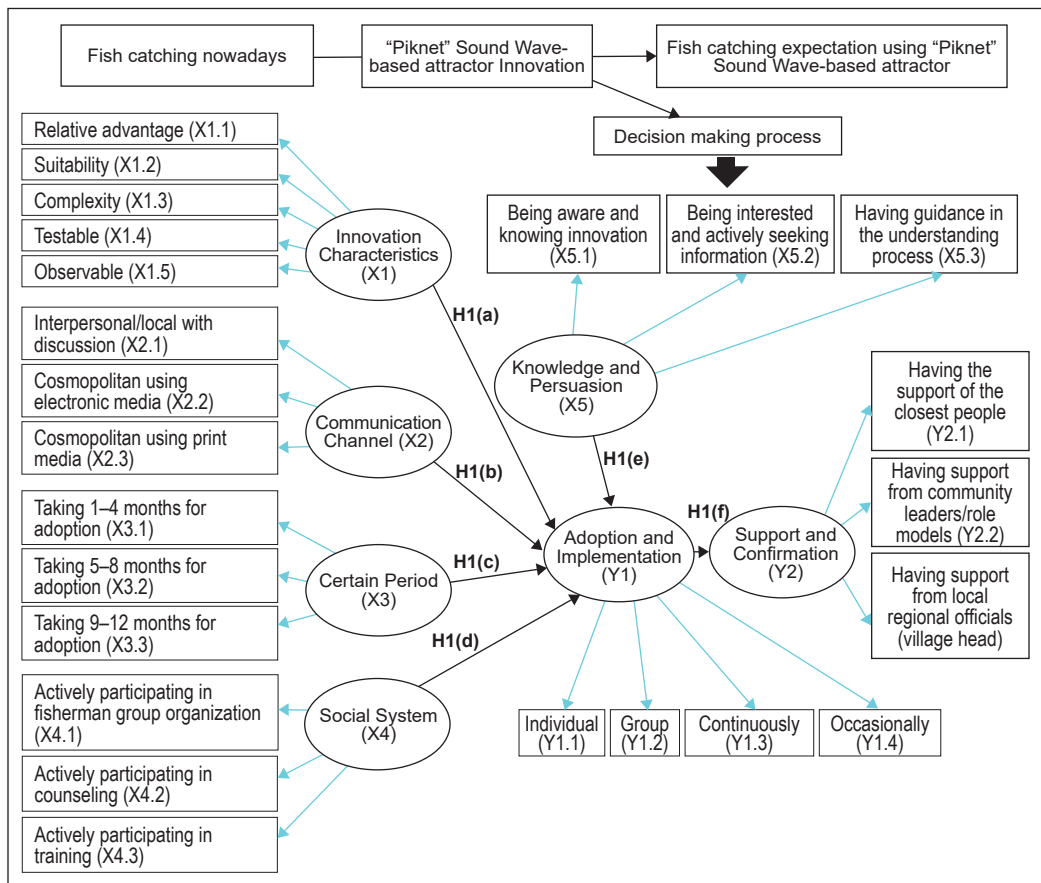


Figure 2. Conceptual framework

## RESULTS AND DISCUSSIONS

### Measurement Model Analysis Results

The measurement or outer model determines the relationship between latent variables and their indicators or manifestations (Nurwulan & Suharno, 2015). Furthermore, the analysis of the outer model was conducted with four stages of testing, namely individual reliability, internal consistency reliability, average variance extracted (AVE), and discriminant validity. The test was carried out on 24 indicator variables shown in Figure 4.

The initial stage in determining the relationship between the latent variable and the indicator variable is explained by describing the relationship as a whole according to the concept of the innovation diffusion process (Figure 4), followed by analyzing the magnitude of the relationship between the latent variable and its indicator variable using the individual

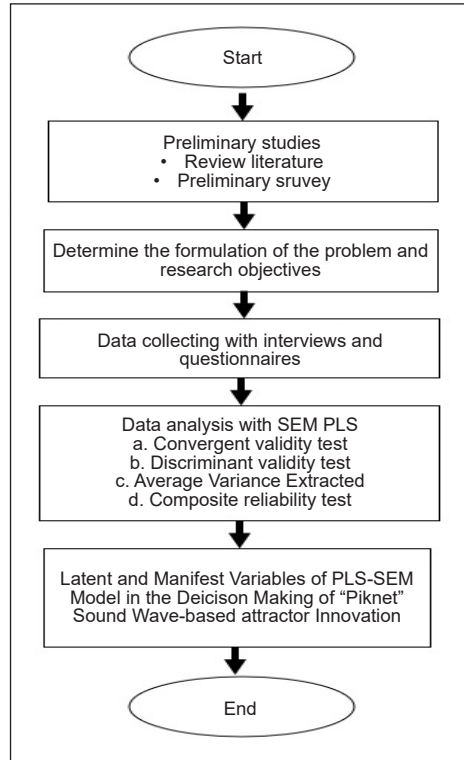


Figure 3. Research flowchart

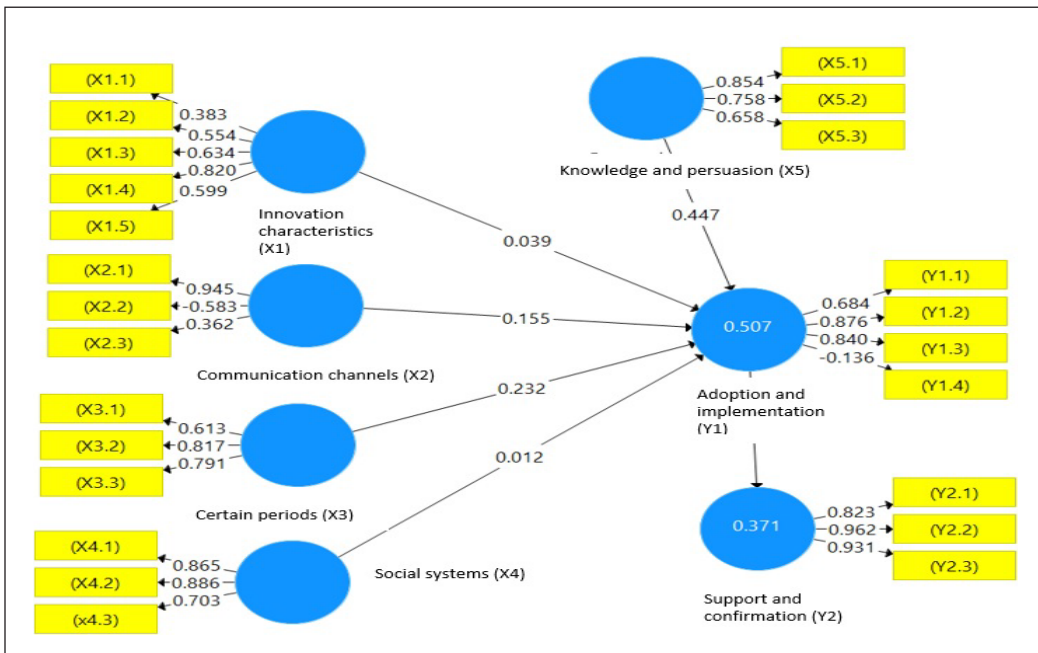


Figure 4. Initial outer model

reliability test so that from the test it can be seen several indicator variables that do not meet the requirements and are eliminated from the model. This stage is described in the individual reliability test sub-section and is depicted in Figure 5.

**Individual Item Reliability Test.** Individual item reliability testing was conducted by investigating the loading factor value, which explains the magnitude of the relationship between latent variables and their indicators. The loading factor is good above 0.7 because it can measure or explain the latent variable. After obtaining the loading factor, the indicators with a value less than 0.7 are eliminated, such as relative advantage (X1.1), suitability (X1.2), complexity (X1.3), observable (X1.5), cosmopolitan/outside the local system with print media (X2.3), taking 1–4 months for adoption (X3.1), having guidance in the understanding process (X5.3), and implementing innovation occasionally (Y1.4). The variable elimination results are shown in Figure 5.

The reliability test results (loading factor) are shown in Table 3, where the variable with the gray block was eliminated due to a loading factor below 0.7.

**Internal Consistency Reliability Test.** The internal consistency reliability test was conducted using the composite reliability value with a threshold of 0.7 (Hair et al., 2011). In addition, composite reliability measures internal consistency reliability compared to Cronbach’s alpha because it does not assume a similarity between all indicator variables. The test results showed that the CR value is above 0.7; therefore, it can be said that the variable has been met. The CR results are shown in Table 4 and Figure 6 below.

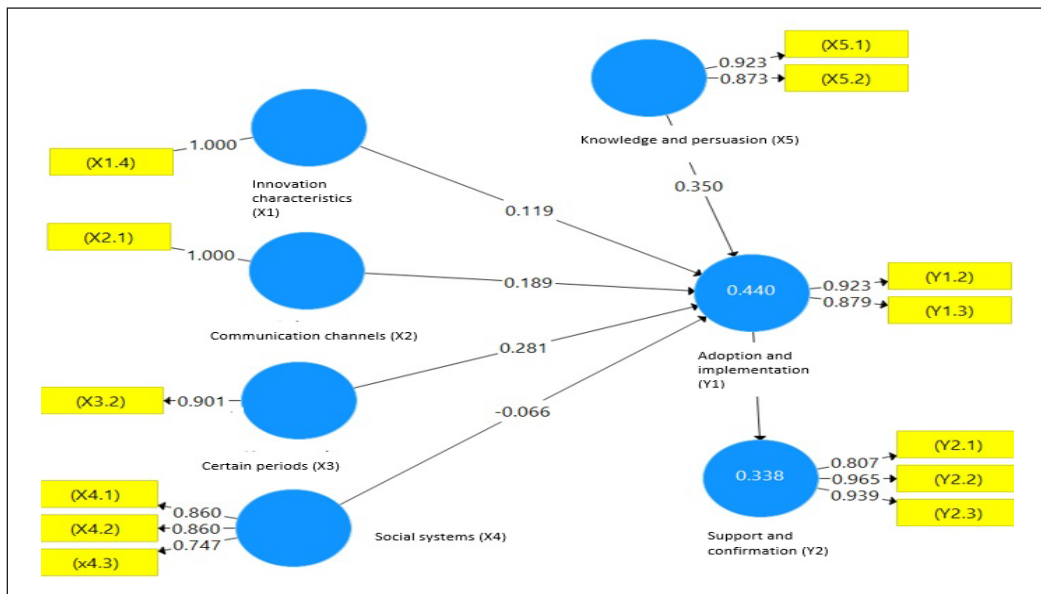


Figure 5. Outer model results with tested loading factor values

Table 3  
The loading factor test results after eliminating several indicator variables

Indicator Variables	Latent Variables						
	Innovation characteristics (X1)	Communication channels (X2)	Certain periods (X3)	Social systems (X4)	Knowledge and persuasion (X5)	Adoption and implementation (Y1)	Support and confirmation (Y2)
X1.1							
X1.2							
X1.3							
X1.4	1.00						
X1.5							
X2.1		1.00					
X2.2							
X2.3							
X3.1							
X3.2			0.901				
X3.3			0.854				
X4.1				0.840			
X4.2				0.840			
X4.3				0.707			
X5.1					0.923		
X5.2					0.873		
X5.3							
Y1.1							
Y1.2						0,923	
Y1.3						0,879	
Y1.4							
Y2.1							0,807
Y2.2							0,965
Y2.3							0,939

Table 4  
Composite reliability (CR) test results

Code	Variable	Composite Reliability (CR)	Result
X1	Innovation characteristics	1.000	Reliable
X2	Communication channels	1.000	Reliable
X3	Certain periods	0.870	Reliable
X4	Social systems	0.863	Reliable
X5	Knowledge and persuasion	0.893	Reliable
Y1	Adoption and implementation	0.897	Reliable
Y2	Support and confirmation	0.932	Reliable



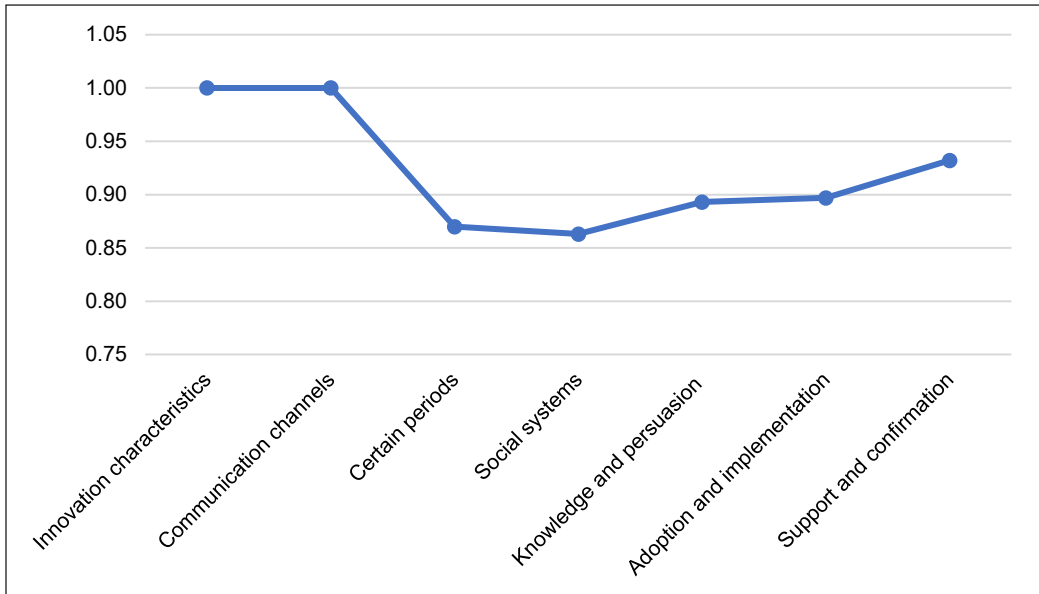


Figure 6. Value of Composite Reliability (CR)

**Average Variance Extracted Test.** The Average Variance Extracted (AVE) test showed a value above 0.5 for each variable. Therefore, the requirements were fulfilled. Also, the AVE value states the variance or diversity of the indicator/manifest variables owned by the latent construct. The greater the variance or diversity of the manifest variables that can be contained by the latent construct, the greater the representation of the latent construct.

Fornell and Larcker (1981) stated that the AVE value is used to assess convergent validity (as cited in Ghozali, 2014). A value of at least 0.5 indicates a good measure of convergent validity. Therefore, the latent variable can explain the average of more than half the variance of the indicators. The AVE values for X1, X2, X3, X4, X5, Y1, and Y2 are above 0.5. Therefore, each latent variable has a valid measurement model, as shown in Table 5 and Figure 7.

Table 5  
Average Variance Extracted (AVE) test results

Code	Variable	Average Variance Extracted (AVE)
X1	Innovation characteristics	1,000
X2	Communication channels	1,000
X3	Certain periods	0,777
X4	Social systems	0,679
X5	Knowledge and persuasion	0,807
Y1	Adoption and implementation	0,812
Y2	Support and confirmation	0,822



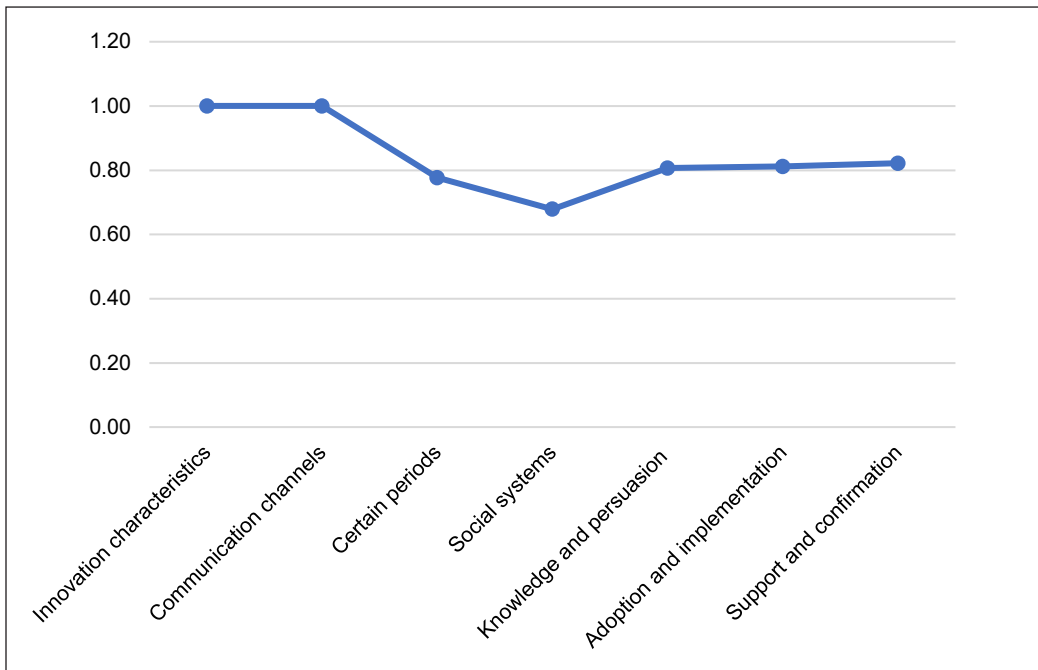


Figure 7. Value of Average Variance Extracted (AVE)

**Discriminant Validity Test.** The discriminant validity test determines the correlation between latent variables, where the value of the AVE root should be greater than this correlation. The test is conducted in two stages, analyzing the value of cross-loading between indicator variables, as well as Fornell Lacker's cross-loading. Furthermore, the correlation between the indicator variables and their constructs should be higher than the correlations with other block constructs, which indicates that the construct can predict the size of the block better than others (Tables 6 and 7).

In research conducted by Schiffman and Kanuk (2010), the general analysis results of the relationship between the construct/latent variables and the indicator/manifest variables were the innovation characteristic variable (X1) used to measure perceptions. It consists of benefits obtained, conformity with adopters, level of complexity, the possibility of being able to try, and ease of observing. In this research, the innovation characteristic variable was closely related to the testable indicator variable (X1.4). Communication channels are part of the decision-making process, where according to Leeuwis (2004), dissemination of innovation to users is conducted between actors involved in innovation, seen as a feedback mechanism. According to Septiani and Esfandari (2018), innovation in the fisheries sector should be conducted by holding meetings and direct guidance with groups of fishermen in the field to smoothly run the process of implementing innovation. Furthermore, the communication channel (X2) and indicator variables are closely related, such as interpersonal and discussion (X2.1).

Table 6  
Discriminant Validity Test (cross-loading)

Indicator Variables	Latent Variable						
	Adoption and implementation (Y1)	Support and confirmation (Y2)	Innovation characteristics (X1)	Certain periods (X3)	Knowledge and persuasion (X5)	Communication channel (X2)	Social system (X4)
X1.4	0.452	0.555	1.000	0.542	0.404	0.354	0.428
X2.1	0.403	0.501	0.354	0.342	0.275	1.000	0.316
X3.2	0.505	0.341	0.507	0.901	0.455	0.178	0.546
X3.3	0.421	0.299	0.441	0.854	0.335	0.448	0.500
X4.1	0.366	0.483	0.278	0.457	0.474	0.315	0.860
X4.2	0.366	0.483	0.375	0.457	0.546	0.315	0.860
X5.1	0.536	0.487	0.345	0.400	0.923	0.343	0.477
X5.2	0.422	0.459	0.388	0.424	0.873	0.127	0.612
Y1.2	0.923	0.548	0.483	0.532	0.540	0.452	0.457
Y1.3	0.879	0.497	0.316	0.413	0.421	0.255	0.285
Y2.1	0.371	0.807	0.505	0.278	0.406	0.323	0.427
Y2.2	0.585	0.965	0.566	0.295	0.507	0.552	0.444
Y2.3	0.585	0.939	0.456	0.413	0.507	0.453	0.479
X4.3	0.305	0.228	0.419	0.582	0.449	0.132	0.747

Table 7  
Discriminant Validity Test (cross-loading Fornell Lacker)

Latent variable	Latent Variable						
	Adoption and implementation (Y1)	Innovation characteristics (X1)	Support and confirmation (Y2)	Certain periods (X3)	Knowledge and persuasion (X5)	Communication channels (X2)	Social systems (X4)
Adoption and implementation (Y1)	0,901						
Innovation characteristics (X1)	0,452	1,000					
Support and confirmation (Y2)	0,581	0,555	0,906				
Certain periods (X3)	0,530	0,542	0,366	0,878			
Knowledge and persuasion (X5)	0,539	0,404	0,526	0,455	0,8990		
Communication channel (X2)	0,403	0,354	0,501	0,342	0,275	1,000	
Social systems (X4)	0,421	0,428	0,494	0,597	0,595	0,316	0,824

The certain periods variable (X3) is related to the need for an adoption time of 5–8 months (X3.2), where according to Adianto (2018), the decision to be taken by a person is within a certain period. The social system variable is based on the activeness of fishermen in the organization by actively participating in counseling and training. According to Amanah (2006), the activities aim to increase their understanding. Furthermore, there was a close relationship between actively participating in fisherman group organizations (X4.1), actively participating in counseling (X4.2), and actively participating in training (X4.3) with the latent variable of the social system (X4).

Knowledge and persuasion variables are a phase where individuals begin to analyze something that has been learned to decide on accepting an innovation with several steps, such as success, ease of access, and guidance (Adianto, 2018). Therefore, the indicator variables: knowledge of innovation (X5.1) and being interested and actively seeking information (X5.2), have a close relationship with the latent variables of knowledge and persuasion (X5).

The adoption and implementation variable (Y1) is the decision-making process to accept or reject an innovation (Adianto, 2018). Meanwhile, Pannell et al. (2006) stated that adoption is utilizing and implementing innovations to meet needs. In addition, Warnaen and Cangara (2013) stated that the first fishermen to implement innovation are the administrators and group leaders in a community. Therefore, the indicator variables having a close relationship with the construct are individual adoption (Y1.1), group adoption (Y1.2), and continuous application of innovation (Y1.3).

The confirmation variable is expected to determine the support from other parties for the innovation decision taken by the adopter (Rogers, 2003), such as the fishermen group. Furthermore, the confirmation and support variables (Y2) have a close relationship with the indicators, namely having support from the closest people (Y2.1), community leaders (Y2.2), and local regional officials (Y2.3). It is hoped that the research results can be used as the basis for carrying out the process of diffusion of Piknet innovations to fishermen and can be adopted and used in fishing operations to increase catches.

## CONCLUSION

The conclusions from the research has achieved all the objectives and can be explained, as follows: (1) The analysis results of the measurement model (outer model) met the requirements with good characteristics, therefore, it can be continued to the next stage of structural model analysis (inner model); (2) Furthermore, 11 eliminated indicator variables did not meet the standard requirements of the outer loading value; (3) A significant relationship was found in the latent variables of innovation characteristics (X1), communication channels (X2), certain periods (X3), social systems (X4), knowledge and persuasion (X5), adoption and implementation (Y1) as well as confirmation and support (

Y2); (4) Indicator variables related to the latent variable are testable (X1.4), interpersonal with discussion (X2.1), taking 5–8 months (X3.2), actively participating in fisherman group organizations (X4.1), actively participating in counseling (X4.2), actively participating in training (X4.3), being aware and having knowledge of innovation (X5.1), being interested and actively seeking information (X5.2), adopted by individuals (Y1.1), adopted by groups (Y1.2), implementation of continuous innovation (Y1.3), supported by the closest people (Y2.1), supported by community leaders (Y2.2), and having support from local regional officials (Y2.3).

To develop this research, continuous research is needed by examining each of the variables used in depth. Some recommendations for future research are related to the addition of other variables, improving the quality of Piknet as an attractor for fishing and the effectiveness of using Piknet for fishermen.

## ACKNOWLEDGEMENTS

The authors are grateful to the promoters and co-promoters from Brawijaya University for providing guidance, input, and suggestions as well as support in completing this research, and to the Rector of Hang Tuah University for supporting the facilities and infrastructure to complete this research properly. Furthermore, they are grateful to the team of lecturers, students, and groups of gillnet fishermen in Bulak Sub-District, Surabaya, for their cooperation during the activity.

## REFERENCES

- Adianto. (2018). Proses adopsi inovasi lokal terhadap peningkatan kesejahteraan masyarakat di kawasan Minapolitan Desa Koto Mesjid Provinsi Riau [The Process of Adopting Local Innovations for Improving Community Welfare in the Minapolitan Area, Koto Mesjid Village, Riau Province]. *Jurnal Sosio Konsepsia*, 7(2), 1-30. <https://doi.org/10.33007/ska.v7i2.1144>
- Amanah, S. (2006). Penyuluhan perikanan [Fisheries Counseling]. *Jurnal Penyuluhan*, 2(4), 62-69. <https://doi.org/10.25015/penyuluhan.v2i4.2117>
- Hair, J. F., Ringle, C. M., & Sarstedt, M. (2011). PLS-SEM: Indeed a silver bullet. *Journal of Marketing Theory and Practice*, 19(2), 139-152. <https://doi.org/10.2753/MTP1069-6679190202>
- Indraningsih, K. S. (2011). Pengaruh penyuluhan terhadap keputusan petani dalam adopsi inovasi teknologi usaha tani terpadu [The Effect of Extension on Farmers' Decisions in Adopting Integrated Farming Technology Innovations]. *Jurnal Agro Ekonomi*, 29(1), 1-24.
- Ghozali, I (2014). *Structural equation modeling, metode alternatif dengan partial least square* [Structural Equation Modeling, Alternative Method with Partial Least Square]. Badan Penerbit Universitas Diponegoro.
- Haryono, S. (2016). *Metode SEM untuk penelitian manajemen dengan AMOS 22.00, LISREL 8.80 dan Smart PLS 3.0* [SEM method for management research with AMOS 22.00, LISREL 8.80 and Smart PLS 3.0]. Badan Penerbit PT.

- Jaya, I. G. N. M., & Sumertajaya, I. M. (2008). Pemodelan persamaan structural dengan partial least square [Structural equation modeling with partial least square]. *Prosiding Semnas Matematika dan Pendidikan Matematika, 1*, 118-132.
- Kusdibyo, L., & Leo, G. (2018, October). Adopsi e-learning di perguruan tinggi [Adoption of e-learning in universities]. In *9th Industrial Research Workshop and National Seminar* (Vol. 9, pp. 371-379). <https://doi.org/10.35313/irwns.v9i0.1125>
- Leeuwis, C. (2004). *Communication for rural innovation: Rethinking agricultural extension*. Wiley Publishers.
- Mardikanto, T. (2007). *Redifinisi dan revitalisasi penyuluhan pertanian* [Redefinition and Revitalization of Agricultural Extension]. PUSPA.
- Mun'im, A. (2015). Analisa usaha petambak garam dan perannya dan perkonomian tahun 2012 (Studi kasus Petambak Garam PUGAR) [Analysis of salt farmers business and its role and the economy in 2012: Case study of PUGAR salt farmers]. *Jurnal Sosial dan Ekonomi Kelautan Perikanan, 10*(2), 217-228. <http://dx.doi.org/10.15578/jsekp.v10i2.1261>
- Nurwullan, E., & Suharno, N. T. (2015). Aplikasi partial least square dalam pengujian implikasi jaringan kerjasama dan inovasi usaha mikro kecil pengolahan kedelai [Partial least square application in testing the implications of network cooperation and innovation for soybean processing micro and small enterprises]. *Jurnal Informatika Pertanian, 24*(2), 205-214.
- Pannell, D. J., Marshall, G. R., Barr, N., Curtis, A., Vanclay, F., & Wilkinson, R. (2006). Adoption of conservation practices by rural landholders. *Australian Journal of Experimental Agriculture, 46*(11), 1407-1424. <https://doi.org/10.1071/EA05037>
- Rogers, E. M. (2003). *Diffusion of innovations*. Free Press.
- Rosana, N., & Muminin A. (2019). Effect of the difference in sound wave-based attractor frequency on the catch of halfbeak fish (*Oxyporhamphus micropterus*) using trammel net at Surabaya Coast. *International Journal of Advanced Research, 7*(9), 1352-1356. <http://dx.doi.org/10.21474/IJAR01/9790>
- Rosana, N., Harahab, N., Ciptadi, G., Kurniawan, A., Supartono, Prasita, V. D., Suryadhi, Rifandi, S., & Muminin, A. (2021). Analysis of the difference in frequency sound waves to the catch of gulamah fish (*Johnius trachycephalus*) using a trammel net in the coastal area of Surabaya. In *International Conference on Innovation and Technology (ICIT 2021)* (pp. 70-74). Atlantis Press. <https://dx.doi.org/10.2991/aer.k.211221.009>
- Rosana, N., Sofijanto, M., & Suryadhi. (2019). Assistance on the use of sound wave attractor to increase fishermen's number of catches Bulak District Surabaya. *International Journal of Advanced Research, 7*(8), 324-327. <http://dx.doi.org/10.21474/IJAR01/9507>
- Rosana, N., Suryadhi, & Rifandi, S (2018). Trial test of fish attractor "Piknet" device in saltwater fish tank. *MATEC Web of Conferences, 177*, Article 01021. <https://doi.org/10.1051/mateconf/201817701021>
- Schiffman, L. G., Kanuk, L. L., & Wisenblit, J. (2010). *Consumer Behavior* (10th Ed.). Pearson College Div.
- Septiani, T., & Esfandari, D. A. (2018). Difusi inovasi sistem teknologi inovasi tata niaga perikanan PT Aruna Jaya Nuswantara di Desa Tanjung Baru, Kalimantan Timur [Diffusion of technology innovation

system for fishery trading system innovation of PT Aruna Jaya Nuswantara in Tanjung Baru Village, East Kalimantan]. *Prosiding Konferensi Nasional Komunikasi*, 2(1), 696-707.

Sholihin, M., & Ratmono, D. (2013). *Analisa SEM-PLS dengan Warppls 3.0 untuk hubungan nonlinear dalam penelitian sosial dan bisnis* [SEM-PLS analysis with Warppls 3.0 for nonlinear relationships in social and business research]. Penerbit Andi.

Tjiptono, F., & Chandra, G. (2012). *Pemasaran global: Konteks offline dan online* [Global marketing: Offline and online context]. STIM YKPN.

Warnaen, A., & Cangara, H. (2013). Faktor-faktor yang menghambat inovasi pada komunitas petani dan nelayan dalam meningkatkan kesejahteraan masyarakat di Kabupaten Takalar [Factors that hinder innovation in farming and fishing communities in improving people's welfare in Takalar Regency]. *KAREBA: Jurnal Ilmu Komunikasi*, 2(3), 241-250.

## The Effect of Varying the HCl Solution on the Purity, Morphological, and Electrical Properties of Silicon Dioxide Extracted from Rice Straw

Nazopatul Patonah Har<sup>1\*</sup>, Endah Kinarya Palupi<sup>2</sup>, Rofiqul Umam<sup>2</sup>, Aminullah<sup>3</sup>, Md Wahadoszamen<sup>4</sup>, Irmansyah<sup>1</sup> and Irzaman<sup>1</sup>

<sup>1</sup>Department of Physics, Faculty of Mathematics and Natural Sciences, IPB University, Bogor 16680, Indonesia

<sup>2</sup>School of Science and Technology, Kwansei Gakuin University, Japan

<sup>3</sup>Department of Food Technology and Nutrition, Djuanda University, Bogor 16720, Indonesia

<sup>4</sup>Department of Physics, University of Dhaka, Dhaka 1000, Bangladesh

### ABSTRACT

Rice straw is a waste product from rice manufacturing that contains cellulose (32–47%), hemicellulose (19–27%), lignin (5–24%), and ash (13–20%). The ash form consists of a large percentage of silicon dioxide (SiO<sub>2</sub>) with widespread use in the industrial field. The extraction of silicon dioxide has been conducted using the sol-gel and ashing method combined with the leaching process using an acid solution such as hydrochloric acid (HCl) at a concentration of 3%. In using HCl with a concentration of 3%, impurities are often found in the SiO<sub>2</sub> sample. Therefore, this study uses the leaching method with HCl of several variations (3%, 5%, and 7%). By raising the concentration of HCl in this process, the quality of SiO<sub>2</sub> without impurities is increased. The results indicate that increasing

the concentration of HCl can significantly lower the sample's impurity content. In the 3% treatment, impurities were found in the form of Carbon and Calcium. The treatment obtained no impurities using 5% and 7% HCl concentrations. As a result, the highest purity of SiO<sub>2</sub> obtained was 89.31% in the 5% HCl treatment. The sample treated with 5% HCl was in the semiconductor region and exhibited an amorphous structure.

**Keywords:** Electrical, morphological, purity, rice straw, silicon dioxide

### ARTICLE INFO

#### Article history:

Received: 19 January 2022

Accepted: 04 April 2022

Published: 09 November 2022

DOI: <https://doi.org/10.47836/pjst.31.1.23>

#### E-mail addresses:

[nazopatul@gmail.com](mailto:nazopatul@gmail.com) (Nazopatul Patonah Har)

[endahkinarya@gmail.com](mailto:endahkinarya@gmail.com) (Endah Kinarya Palupi)

[rofiqulumam.geoscience@gmail.com](mailto:rofiqulumam.geoscience@gmail.com) (Rofiqul Umam)

[aminullah@unida.ac.id](mailto:aminullah@unida.ac.id) (Aminullah)

[wahado.phy@du.ac.bd](mailto:wahado.phy@du.ac.bd) (Md Wahadoszamen)

[irmansyah@apps.ipb.ac.id](mailto:irmansyah@apps.ipb.ac.id) (Irmansyah)

[irzaman@apps.ipb.ac.id](mailto:irzaman@apps.ipb.ac.id) (Irzaman)

\* Corresponding author



## INTRODUCTION

The availability of biomass in Indonesia is significant, including sources from agriculture and plantations such as oil palm, rice, maize, and others (Kurniawan et al., 2019). Generally, biomass is used as fuel (biofuel) (Yusof et al., 2018) and raw material for various alternative products such as biomaterial (Rohaeti et al., 2010; Aminullah et al., 2015), biochemistry (Davis et al., 2018), bioadsorbent (Aichour et al., 2018; Zainal et al., 2018), and biosurfactant (Ebrahimi et al., 2019).

Biomass from rice farming in rice straw has not been maximally utilized in Indonesia. Rice straw ash contains a high percentage of silicon dioxide ( $\text{SiO}_2$ ), ranging from 61.39% to 84.60% (Nandiyanto et al., 2016; Jenkins et al., 1998; Khorsand et al., 2013).  $\text{SiO}_2$  is a material with widespread use in the industrial field, and one of its applications is in silica gel (Sabara et al., 2022a), which reduces humidity. It is used in glass, cement, electronics, ceramics, and other industries (Abdurrahman et al., 2019). However, utilizing  $\text{SiO}_2$  in natural minerals is highly inefficient and might result in environmental problems when stored indefinitely (Abdurrahman et al., 2020). Therefore,  $\text{SiO}_2$  from plant materials is in great demand for natural mineral

Several studies related to the extraction of  $\text{SiO}_2$  from biomass using rice husks (Sintha et al., 2017; Irzaman et al., 2020; Casnan et al., 2019), rice straw (Nazopatul et al., 2018; Hapsari et al., 2020), bamboo leaves (Irzaman et al., 2018; Aminullah et al., 2018), bagasse (Adli et al., 2018), and coir coconut (Anuar et al., 2020) have been reported. The sol-gel method extracted  $\text{SiO}_2$  in those studies, followed by hydrolysis and subsequent condensation operations. By employing this method (Nandiyanto et al., 2016),  $\text{SiO}_2$  of purity of 68% can be extracted from rice straw. Several studies reported the extraction of  $\text{SiO}_2$  by adopting a simpler method consisting of combustion of biomass (forming charcoal) (Sabara et al., 2022b), leaching (using acid), and ashing (Rohaeti et al., 2010; Aminullah et al., 2015; Adli, 2018). This method has been used to extract  $\text{SiO}_2$  from rice husk biomass, with a purity of 99% (Sintha, 2017; Irzaman et al., 2020). The test results revealed the minor presence of many other elements such as carbon, calcium, and others as impurities (Palupi et al., 2020). Then, in another study by (Hapsari et al., 2020),  $\text{SiO}_2$  was extracted using rice straw biomass with variations in the combustion temperature and a purity value approaching 99%. However,  $\text{SiO}_2$  contained many other potassium, calcium, chlorine, and sodium elements, significantly affecting the sample's electrical characteristics. To reduce the impurity in the extracted  $\text{SiO}_2$ , the study (Nazopatul et al., 2019) modified the extraction method (Husna et al., 2020) by washing rice straw before the combustion process. Treatment of gray temperature variations was implemented to obtain purer  $\text{SiO}_2$ . The results show that this method extracts  $\text{SiO}_2$  with reduced impurity content compared to other methods (Palupi et al., 2019a; Palupi et al., 2019b). The purity value reaches 85.41% at a combustion temperature of 800°C. It turns out that by modifying the system,

the effects of contaminants can be mitigated (Sabara et al., 2022b). However, the calculated purity value is lower than the previous method; therefore, further studies are still needed.

Based on some references, this study aims to modify the extraction method by leaching rice straw biomass before burning and measuring the samples' purity, electrical, morphological, and structural properties. The treatment is different from previous studies by taking the variations in the concentration of acid solutions in the leaching process. The concentrations of HCl utilized vary between 3%, 5%, and 7%. Based on the treatment, it is reasonable to assume that using a more significant concentration of HCl increases SiO<sub>2</sub> purity.

## EXPERIMENTAL PROCEDURES

The extraction process included leaching the rice straw, making charcoal, and ashing the charcoal of the rice straw. First, the rice straw is cut into small pieces with a size of ± 5cm, then weighed as much as 100 g. Next, rice straw is soaked with technical grade HCl concentrations of 3%, 5%, and 7% heat for 2 hours. Samples were washed using distilled water until the pH reached 6.5–7 and then dried. After that, the samples were burned in an open space without adding fuel. The rice straw charcoal was burned in a furnace initially at 400 °C for 2 hours and subsequently at 800°C for 1 hour to obtain the ash. The sample structure was then determined by using X-Ray Diffraction (XRD) technique. Spectroscopy Scanning Electron Microscopy (SEM) technique was employed to determine the surface morphology of the sample using a magnification of 5000 and 15000. Energy Dispersive X-Ray Spectroscopy (EDS) was used to determine chemical constituents such as silicon, oxygen, carbon, and others contained in a sample. The purity of SiO<sub>2</sub> was determined based on the percentage of Si (silicon) atoms and calculated by Equation 1:

$$SiO_2(\%atom) = 3 \times (\%atom Si) \quad (1)$$

An Inductance, Capacitance & Resistance (LCR) meter was used to determine some electrical properties of a material, such as electrical conductance, dielectric constant, and impedance. One of the parameters detected in the LCR meter characterization results is the conductance to calculate the material's electrical conductivity. The conductivity values of materials can be categorized into three parts: insulators, semiconductors, and conductors. This study is expected to obtain a semiconductor sample because the results from SiO<sub>2</sub> will be reduced to Si and can be used as a base material for sensor manufacture.

## RESULTS AND DISCUSSION

### Composition Analysis of SiO<sub>2</sub>

The composition analysis of SiO<sub>2</sub> determines the elements contained in the sample. The effect of HCl concentration on the purity of SiO<sub>2</sub> was conducted by testing the

elemental composition at 800°C with HCl concentrations of 3%, 5%, and 7%. Table 1 shows the value of the purity of SiO<sub>2</sub> calculated based on the results of EDS.

The data shows that the sample in the 3% HCl treatment has a purity of 85.41% but still contains calcium and carbon impurities. Meanwhile, the sample obtained with the treatment of 5% HCl has no impurities, and the purity is 89.31%. HCl solution is an effective acid to remove metal

impurities such as Ca. The Cl<sup>-</sup> ions from HCl will bind with Ca<sup>2+</sup> ions from the sample and form CaCl<sub>2</sub> salt. Since salt is soluble in water, it will be lost during infiltration. The purity result of treatment with 7% HCl is 82.86% (which is lower compared to 3% and 5% of HCl), even though no impurities were found. The effect of the sample coating caused the gold element in these results during the characterization process. Therefore, leaching rice straw with HCl concentrations above 5% is not recommended for extracting the desired SiO<sub>2</sub>. The same method applied to rice husk material (Sintha et al., 2017) also shows that HCl concentrations above 5% yield decreased purity of SiO<sub>2</sub>. The study (Lu & Hsieh, 2012) indicated a difference in purity of approximately 1.49% more than the results from this investigation. In addition, the acid concentration is increased to 10% H<sub>2</sub>SO<sub>4</sub>.

Table 1  
*The value of the purity of SiO<sub>2</sub> calculated based on EDS results*

Element	Atom (%)		
	3%	5%	7%
Oxygen (O)	63.83	69.31	71.44
Silicon (Si)	28.47	29.77	27.62
Carbon I	7.51	–	–
Calcium (Ca)	0.19	–	–
Gold/Aurum (Au)	–	0.92	0.94
Purity of SiO <sub>2</sub>	85.41	89.31	82.86

### Morphological Analysis of SiO<sub>2</sub>

Surface morphological analysis of SiO<sub>2</sub> samples extracted from rice straw illustrated in Figure 1 was observed at a magnification of 5.000 and 15.000. The surface morphology obtained with the treatment of 3%, 5%, and 7% HCl are shown in Figures 1 (a), (b), and (c), respectively. The surface structure of the 3% HCl sample has a distribution of fairly homogeneous grain shapes with a relatively larger grain density.

The treatment of 5% HCl produces morphology with a more acceptable surface shape composed of a distribution of heterogeneous grain shapes. The ideal surface shape may be connected to the highest purity of SiO<sub>2</sub> extracted with the treatment of 5% HCl. Meanwhile, the concentration treatment of HCl 7% in Figure 1 (c) has a surface morphology with more uniform and larger grain shapes.

### Structure Analysis of SiO<sub>2</sub>

The structure of SiO<sub>2</sub> extracted from rice straw was analyzed at an angle of 10° to 80°, as shown in Figure 2. The figure shows the structural phase of SiO<sub>2</sub> samples extracted upon leaching with variable (3%, 5%, and 7%) HCl concentrations. The diffraction pattern

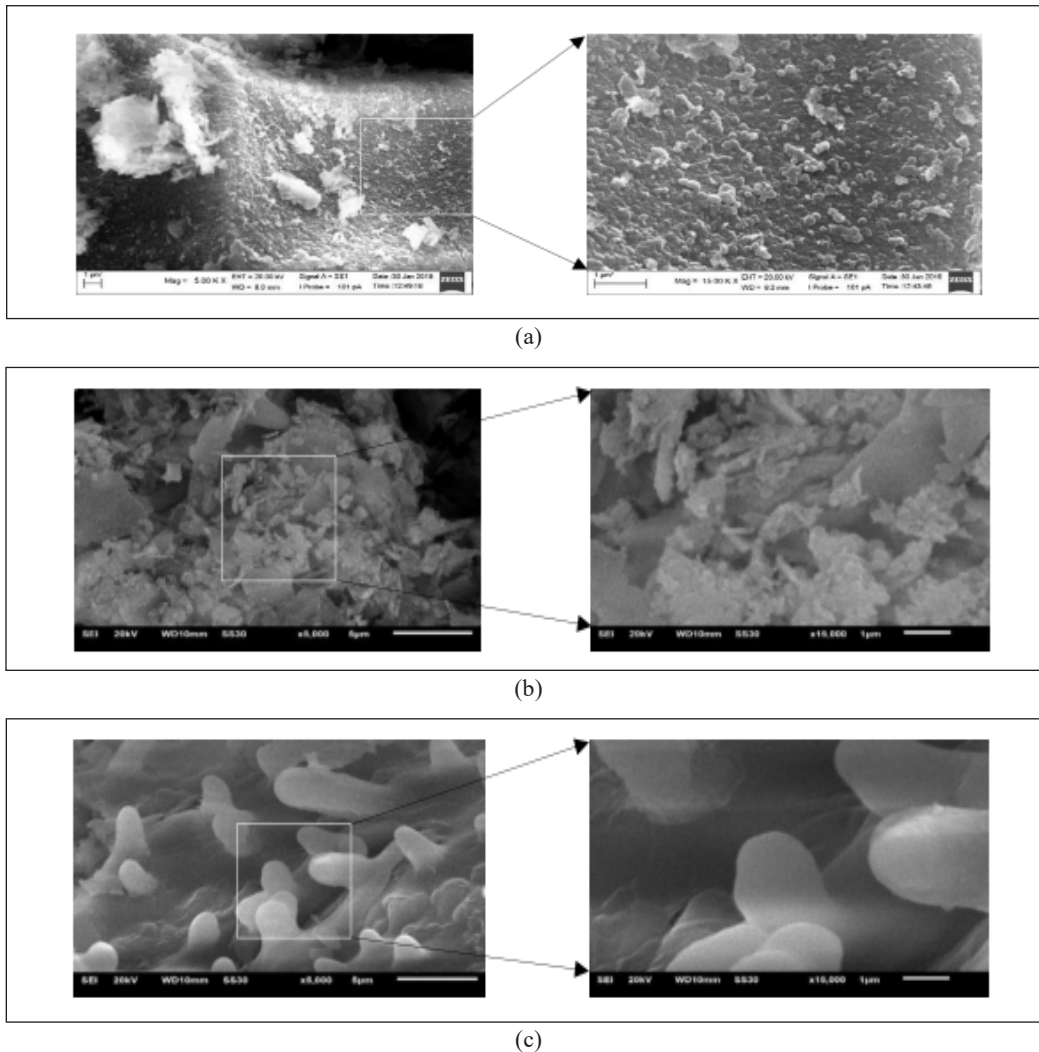


Figure 1. Results of SiO<sub>2</sub> morphological analysis of rice straw using SEM at variations of: (a) HCl 3%; (b) HCl 5%; and (c) HCl 7%.

obtained with the treatment of 3% HCl gives the highest peak at an angle of 21.96°. Compared with JCPDS data, the diffraction pattern gives the highest peak at an angle of 21.98°. Meanwhile, SiO<sub>2</sub> samples obtained from 5% and 7% HCl treatment give the diffraction patterns with the highest peak value at an angle of 21.80°. Based on the results in Figure 2 (Khorsand et al., 2013), SiO<sub>2</sub> from rice straw has an amorphous structure compared with the results of previous studies. Note that the amorphous form of SiO<sub>2</sub> is more utilized than SiO<sub>2</sub> in crystals form. For example, amorphous SiO<sub>2</sub> ash is useful as a substitute for cement additives (Oyekan & Kamiyo, 2011) in zeolite production (Cheng et al., 2012) and other ceramic applications (Sembiring et al., 2014).

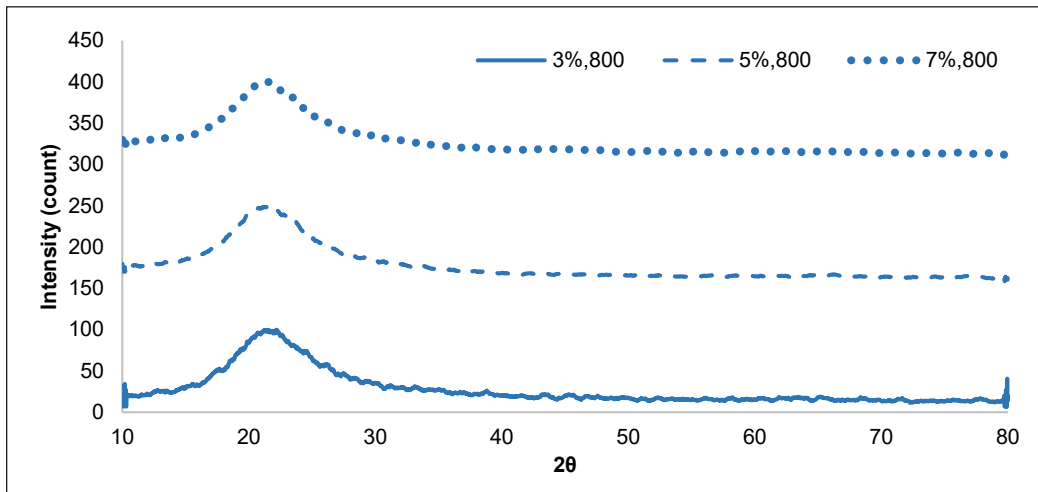


Figure 2. XRD analysis of SiO<sub>2</sub> on variations of HCl 3%, 5%, and 7%

### Electrical Properties of SiO<sub>2</sub>

The electrical properties' measurements aim to determine the electrical characteristics of extracted SiO<sub>2</sub> sample. Furthermore, the electrical conductivities of the SiO<sub>2</sub> were recorded at different frequencies. This study collected data at 200 points within a frequency range of 50 Hz to 5 MHz to cover both the low and high-frequency regimes. Based on electrical conductivity value, a material can be categorized into insulator, semiconductor, and conductor. This study obtains semiconductor properties with conductivity values ranging from 10<sup>-8</sup> S/cm to 10<sup>3</sup> S/cm (Kwok, 1995).

The graph of the relationship between electrical conductivity and frequency is shown in Figure 3. In the figure, the electrical conductivity of each sample increases steadily with increasing frequency. It is entirely consistent with the fact that increasing the frequency increases the kinetic energy of the particles in the sample, resulting in a significant amount of charge transfer between the capacitor plates. The increase in HCl leaching concentration value also causes the value of the electrical conductivity to increase. At frequencies of 50 Hz and below, the electric conductivity value is relatively the same for all the samples. However, at frequencies above 50 Hz, the highest electrical conductivity values were obtained for the sample upon leaching with 3% HCl. It is because, at higher frequencies, the content of the minority atoms also vibrates and impacts the conductance values. The EDS data in Table 2 shows that the treatment of 3% HCl has the highest impurity than the other samples due to the most significant conductivity values compared to the treatments of 5% and 7% HCl. Interestingly, the 5% HCl-leached SiO<sub>2</sub> sample gave the lowest conductivity values with a maximum value of 5.28 × 10<sup>-6</sup> S/cm, a typical semiconducting material value.

An analysis of the capacitance also shows the ability of a material to store electric charge. Based on the capacitance value, the dielectric constant of the sample can be

Table 2

Electrical conductivity values at 800°C with HCl concentrations of 3%, 5%, and 7%

Frequency (Hz)	Electrical conductivity (S/cm)		
	HCl 3%	HCl 5%	HCl 7%
(100-800)	$7.46 \times 10^{-10}$ - $2.90 \times 10^{-8}$	$6.72 \times 10^{-10}$ - $2.03 \times 10^{-8}$	$5.17 \times 10^{-10}$ - $2.51 \times 10^{-8}$
(10000-40000)	$8.77 \times 10^{-8}$ - $2.45 \times 10^{-7}$	$2.16 \times 10^{-8}$ - $5.58 \times 10^{-8}$	$3.04 \times 10^{-8}$ - $9.33 \times 10^{-8}$
(>1000000)	$2.51 \times 10^{-6}$ - $5.82 \times 10^{-6}$	$4.99 \times 10^{-8}$ - $1.67 \times 10^{-6}$	$4.46 \times 10^{-7}$ - $2.87 \times 10^{-6}$

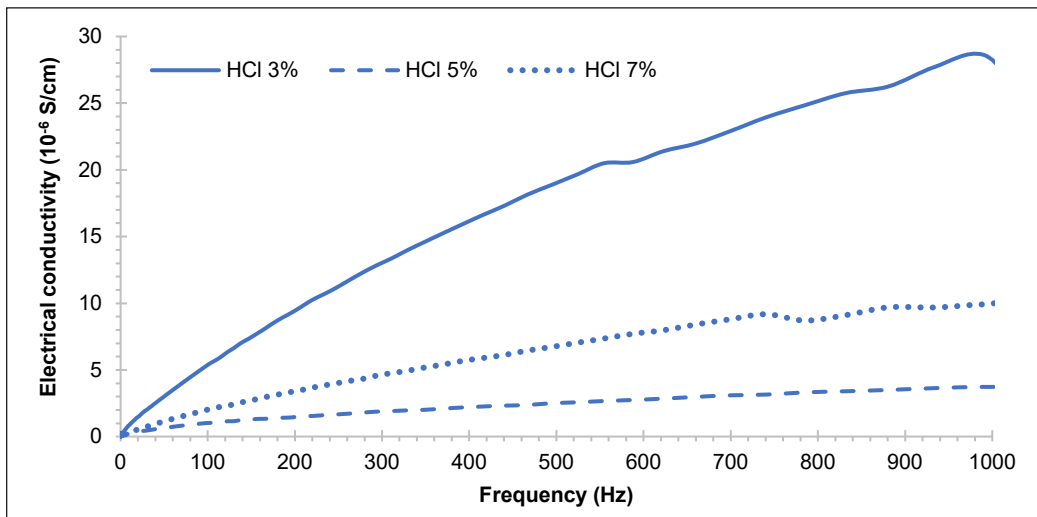


Figure 3. Results of electrical conductivity to the frequency of SiO<sub>2</sub> from rice straw in the treatment of HCl 3%, 5%, and 7%

determined. The results of data analysis of the dielectric constant values are shown in Figure 4. The frequency dependence shows that the frequency is inversely proportional to the dielectric constant value. All the SiO<sub>2</sub> samples showed a decreasing dielectric constant with increasing frequency but with different values. Each sample exhibits a high dielectric constant at frequencies less than 50 Hz and a low dielectric constant above 50 Hz. Therefore, SiO<sub>2</sub> obtained with treatment of 3% HCl gave the highest dielectric constant value compared to 5% and 7% HCl.

The effect of frequency on the electrical impedance value of SiO<sub>2</sub> samples from rice straw is shown in Figure 5. Electrical impedance is a measure of resistance at an alternating current source. It is the electrical resistance of an electronic component to the flow of current in a series at a specific frequency (Giancoli, 2020). The amount of electrical resistance that yields the impedance of a capacitive component is frequency-dependent. Therefore, the resistance of such a component will vary depending on the signal's frequency. The effect on the impedance of the capacitive electrical component SiO<sub>2</sub> samples from rice straw is shown in Figure 5. The graph displays the impedance-to-frequency relationship

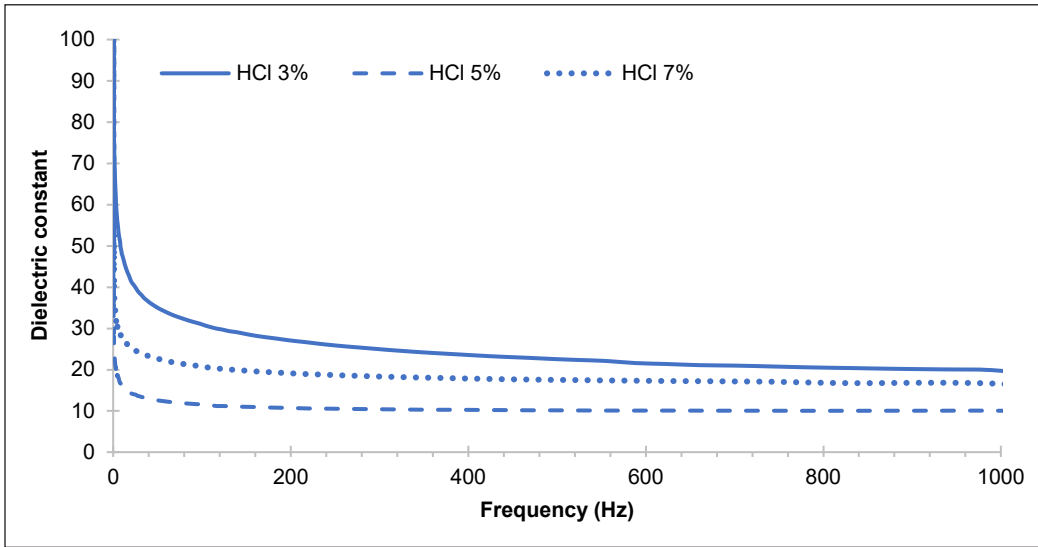


Figure 4. Dielectric constant values of samples at treatments of HCl 3%, 5%, and 7%

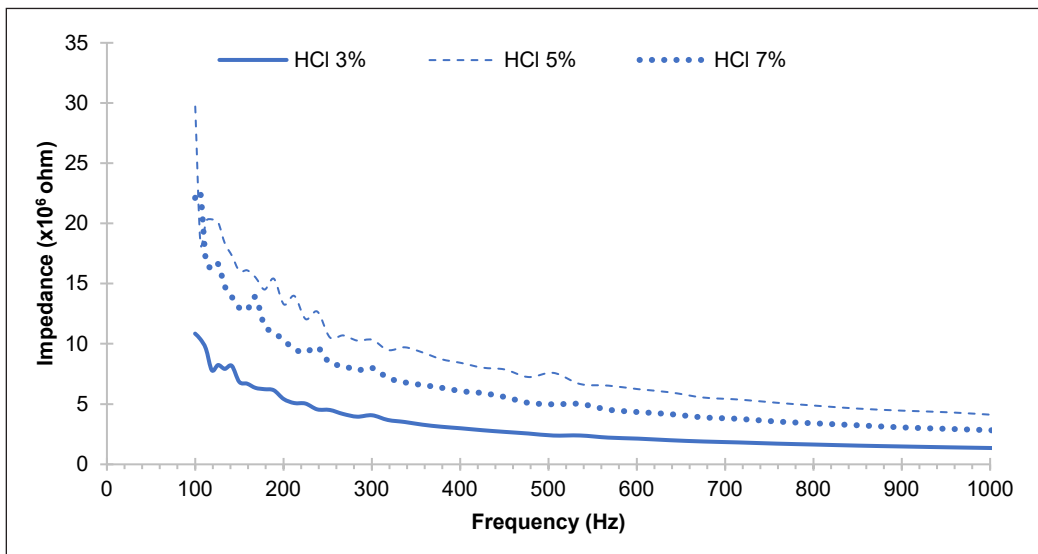


Figure 5. Impedance values of samples at treatments of HCl 3%, 5%, and 7%

in the frequency range 50 Hz to 1000 Hz. The frequency is inversely proportional to the impedance value. Therefore, sample impedance values below 100 Hz frequency are still volatile. Above 100 Hz, the impedance value decreases exponentially for all the SiO<sub>2</sub> samples. SiO<sub>2</sub> extracted with 3% HCl treatment has lower impedance values. The SiO<sub>2</sub> samples at 5% HCl treatment have higher values, while the sample extracted with 7% HCl showed impedance between the 3% and 5% samples. This value is supported by the



electrical conductivity data of the sample. 5% HCl treatment samples gave the lowest electrical conductivity values. It means that such samples can inhibit the most significant electric current. The value of the electrical impedance is higher than the sample in the HCl treatment of 3% and 7%.

## CONCLUSION

Based on the results obtained, it can be concluded that a higher concentration of HCl can increase the value of SiO<sub>2</sub> purity and can remove impurities. This result was supported by structural characteristics, which indicate the amorphous phase of SiO<sub>2</sub>. Furthermore, based on electrical analysis, SiO<sub>2</sub> extracted from straw was in the range of semiconductor materials.

## ACKNOWLEDGMENTS

A Master's Thesis Research (PTM) grant from the Directorate General of Research and Development Strengthening Ministry of Research and Technology of the Republic of Indonesia with contract number: 3/E1/KP.PTNBH/2019, dated March 29, 2019, supported this study.

## REFERENCES

- Abdurrahman, A., Umam, R., Irzaman, I., Palupi, E. K., Saregar, A., Saregar, A., Syazali, M., Junaidi, R., Wahyudianto, B., & Adi, L. C. (2019). Optimization and interpretation of heat distribution in sterilization room using convection pipe. *Indonesian Journal of Science and Technology*, 4(2), 204-219.
- Abdurrahman., Irwansyah, R. F., Umam, R., Syazali, M., Junaidi, R., Palupi, E. K., & Irzaman. (2020). Biomass (rice husk) as a fuel for sterilizing oyster mushrooms: A case study of fuel efficiency comparison, temperature distribution and production effectiveness. In *IOP Conference Series: Earth and Environmental Science* (Vol. 460, No. 1, p. 012041). IOP Publishing. <https://doi.org/10.1088/1755-1315/460/1/012041>
- Adli, M. Z., Sari, Y. W., & Irzaman. (2018). Extraction silicon dioxide (SiO<sub>2</sub>) from charcoal of baggase (*Saccharum officinarum* L). In *IOP Conference Series: Earth and Environmental Science* (Vol. 187, p. 012004). IOP Publishing. <https://doi.org/10.1088/1755-1315/187/1/012004>
- Aichour, A., Boudiaf, H, Z., Iborra, C. V., & Polo, M. S. (2018). Bioadsorbent beads prepared from activated biomass/alginate for enhanced removal of cationic dye from water medium: Kinetics, equilibrium and thermodynamic studies. *Journal of Molecular Liquids*, 256(1), 533-540. <https://doi.org/10.1016/j.molliq.2018.02.073>
- Aminullah, Rohaeti, E., Yulianto, B., & Irzaman. (2018). Reduction of silicon dioxide from bamboo leaves and its analysis using energy dispersive x-ray and fourier transform-infrared. In *IOP Conference Series: Earth and Environmental Science* (Vol. 209, p. 012048). IOP Publishing. <https://doi.org/10.1088/1755-1315/209/1/012048>

- Aminullah, Rohaeti, E., & Irzaman. (2015). Reduction of high purity silicon from bamboo leaf as basic material in development of sensors manufacture in satellite technology. *Procedia Environmental Sciences*, 24, 308-316. <https://doi.org/10.1016/j.proenv.2015.03.040>
- Anuar, M. F., Fen, Y. W., Zaid, M. H. M., & Omar, N. A. S. (2020). Optical studies of crystalline ZnO-SiO<sub>2</sub> developed from pyrolysis of coconut husk. *Material Research Express*, 7(5), Article 055901. <https://doi.org/10.1088/2053-1591/ab8a81>
- Casanan, C., Noor, E., Hardjomidjojo, H., Irzaman, I., & Rohaeti, E. (2019). Scalling up of the pyrolysis to produce silica from rice husk. *Journal Engineering Technology*, 51(6), 747-761.
- Cheng, Y., Lu, M., Li, J., Su, X., Pan, S., Jiao, C., & Feng, M. (2012). Synthesis of MCM-22 zeolite using rice husk as a silica source under varying temperature conditions. *Journal of Colloid and Interface Science*, 369, 388-39. <https://doi.org/10.1016/j.jcis.2011.12.024>
- Davis, R. E., Grundl, N. J., Tao, L., Bidy, M. J., Tan, E. C., Beckham, G. T., Humbrid, D., Thompson, D. N., & Roni, M. S. (2018). *Process Design and economic for the conversion of lignocellulosic biomass to hydrocarbon fuels a coproduct: 2018 Biochemical design case update; biochemical deconstruction and conversion of biomass to fuels and products via integrated biorefinery pathways*. United States. <https://doi.org/10.2172/1483234>
- Ebrahimi, S., Jalili, H., Khajeh, K., Noghabi, K. A., Ebrahimi, M. T., & Amrane, A. (2019). Production and characterization of biosurfactants using bacteria isolated from acidic hot springs. *Applied Food Biotechnology*, 6(2), 127-138.
- Giancoli, D. C., (2020). *Physics for scientists and engineering with modern physics* (3rd Ed.). Prentice Hall.
- Hapsari, I. L., Irzaman, & Indro, M. N. (2020). Extraction of silicon dioxide from rice straw (*Oryza sativa*) with variation ignition temperature. In *IOP Conference Series: Earth and Environmental Science* (Vol. 460, p. 012024). IOP Publishing. <https://doi.org/10.1088/1755-1315/460/1/012024>
- Husna, I., Setyaningrum, E., Handayani, T. T., Kurnia, Y., Palupi, E. K., Umam, R., & Andriana, B. B. (2020). Utilization of basil leaf extract as anti-mosquito repellent: A case study of total mosquito mortality (*Aedes aegypti* 3rd Instar). *Journal of Physics: Conference Series*, 1467, Article 012014. <https://doi.org/10.1088/1742-6596/1467/1/012014>
- Irzaman, I., Cahyani, I. D., Aminullah, A., Maddu, A., Yulianto, B., & Siregar, U. (2020). Biosilica properties from rice husk using various HCl concentrations and frequency sources. *Egyptian Journal of Chemistry*, 63(2), 363-371. <https://dx.doi.org/10.21608/ejchem.2019.8044.1679>
- Irzaman., Oktaviani N., & Irmansyah. (2018). Ampel bamboo leaves silicon dioxide (SiO<sub>2</sub>) extraction. In *IOP Conference Series: Earth and Environmental Science* (Vol. 141, p. 012014). IOP Publishing. <https://doi.org/10.1088/1755-1315/141/1/012014>
- Jenkins, B. M., Baxter, L. L., Miles Jr, T. R., & Miles, T. R. (1998). Combustion properties of biomass. *Fuel Processing Technology*, 54, 17-46. [https://doi.org/10.1016/S0378-3820\(97\)00059-3](https://doi.org/10.1016/S0378-3820(97)00059-3)
- Khorsand, H., Krayee, N., & Masooperast, A. H. (2013). Optimization of amorphous silica nanoparticles synthesis from rice straw ash using design of experiment technique. *Particulate Science and Technology*, 31(4), 366-371. <https://doi.org/10.1080/02726351.2012.755587>

- Kurniawan, B., Rudiyanto, W., Mutiara, H., Stefani, A., Umam, R., & Jermisittiparsert, K. (2019). Correlation between parasitemia with hemoglobin levels in malaria patients at Hanura Health Center working Area Pesawaran District, Lampung, Indonesia. *Systematic Reviews in Pharmacy*, *10*(2), 297-302.
- Kwok, K. N., (1995). *Complete Guide to Semiconductor Device*. McGraw-Hill.
- Lu, P., & Hsieh, Y. L., (2012). Highly pure amorphous silica nano-disk from rice straw. *Powder Technology*, *225*, 149-155. <https://doi.org/10.1016/j.powtec.2012.04.002>
- Nandiyanto, A. B. D., Rahman, T., Fadhlulloh, M. A., Abdullah, A. G., Hamidah, I., & Mulyanti, B. (2016). Synthesis of silica particles from rice straw waste using a simple extraction method. In *IOP Conference Series: Materials Science and Engineering* (Vol. 128, p. 012040). IOP Publishing. <https://doi.org/10.1088/1757-899X/128/1/012040>
- Nazopatul, P. H., Irmansyah, & Irzaman. (2018). Extraction and characterization of silicon dioxide from rice straw. In *IOP Conference Series: Earth and Environmental Sciences* (Vol. 209, p. 012013). IOP Publishing. <https://doi.org/10.1088/1755-1315/209/1/012013>
- Nazopatul, P. H., Irzaman, & Irmansyah. (2019). Crystallinity and electrical properties of silicon dioxide (SiO<sub>2</sub>) from rice straw. In *AIP Conference Proceedings* (Vol. 2202, p. 020028). AIP Publishing LLC. <https://doi.org/10.1063/1.5141641>
- Oyekan, G. L., & Kamiyo, O. M. (2011). A study on the engineering properties of sandcrete blocks produced with rice husk ash blended cement. *Journal of Engineering and Technology Research*, *3*(3), 88-98.
- Palupi, E. K., Nazopatul, P. H., Umam, R., Bibin, A. B., Sato, H., Alatas, H., & Irzaman. (2020). Molecular functional group and optical analysis on chlorophyll of green choy sum and cassava leaves extracts. In *IOP Conference Series: Earth and Environmental Science* (Vol. 460, p. 012030). IOP Publishing. <https://doi.org/10.1088/1755-1315/460/1/012030>
- Palupi, E. K., Irzaman, Alatas, H., Yulianto, B., Umam, R., Andriana, B. B., & Sato, H. (2019a). Analysis of spectroscopy: Mustard greens leaf of chlorophyll as a Ba<sub>0.2</sub>Sr<sub>0.8</sub>TiO<sub>3</sub> (barium strontium titanate) film dopant. *Integrated Ferroelectrics*, *201*(1), 75-85.
- Palupi, E. K., Umam, R., Andriana, B. B., Sato, H., Alatas, H., & Irzaman. (2019b). Fabrication and analysis phonon mode of barium strontium titanate-chlorophyll thin film (chlorophyll extract: Green spinach, cassava, green choy sum). In *AIP Conference Proceedings* (Vol. 2202, No. 1, p. 020018). AIP Publishing. <https://doi.org/10.1063/1.5141631>
- Rohaeti, E., Hikmawati, & Irzaman. (2010). Production of semiconductor materials silicon from silica rice husk waste as alternative silicon. *Materials Science and Technology*, 265-272.
- Sabara, Z., Anwar, A., Yani, S., Prianto, K., Junaidi, R., Umam, R., & Prastowo, R. (2022a). Activated carbon and coconut coir with the incorporation of ABR system as greywater filter: The implications for wastewater treatment. *Sustainability*, *14*(2), Article 1026. <https://doi.org/10.3390/su14021026>.
- Sabara, Z., Mutmainnah, A., Kalsum, U., Afiah, I. N., Husna, I., Saregar, A., Irzaman, & Umam, R. (2022b). Sugarcane bagasse as the source of nanocrystalline cellulose for gelatin-free capsule shell. *International Journal of Biomaterials*, *2022*, Article 9889127. <https://doi.org/10.1155/2022/9889127>

- Sembaring, S., Simanjuntak, W., Manurung, P., Asmi, D., & Low, J. (2014). Synthesis and characterisation of gel-derived mullite precursors from rice husk silica. *Ceramics International*, 40(5), 7067-7072. <https://doi.org/10.1016/j.ceramint.2013.12.038>
- Sintha, I., Dahrul, M., Ismawati, S. S., Kurniati, M., Irmansyah, & Irzaman. (2017). Optimization of silicon extraction from husk ashes by excessive magnesium addition on increasing rate of temperature reduction. In *IOP Conference Series: Earth and Environmental Science* (Vol. 65, p. 012032). IOP Publishing. <https://doi.org/10.1088/1755-1315/65/1/012032>
- Yusof, S. J. H. M., Roslan, A. M., Ibrahim, K. N., Abdullah, S. S. S., Zakaria, M. R., Hassan, M. A., & Shirai, Y. (2018). Environmental performance of bietanol production from oil palm frond petiole sugars in an integrated palm biomass biorefinery. In *IOP Conf. Series: Material Science and Engineering* (Vol. 368, p. 012004). IOP Publishing. <https://doi.org/10.1088/1757-899X/368/1/012004>
- Zainal, N. H., Aziz, A. A., Idris, J., Jalani, N. F., Mamat, R., Ibrahim, M. F., Hassan, M. A., & Aziz, S. A. (2018). Reduction of POME final discharge residual using activated bioadsorbent from oil palm kernel shell. *Journal of Cleaner Production*, 182, 830-837. <https://doi.org/10.1016/j.jclepro.2018.02.110>

## Weed Detection in Soybean Crop Using Deep Neural Network

Vinayak Singh<sup>1</sup>, Mahendra Kumar Gourisaria<sup>1\*</sup>, Harshvardhan GM<sup>1</sup> and Tanupriya Choudhury<sup>2</sup>

<sup>1</sup>School of Computer Engineering, KIIT Deemed to be University, Bhubaneswar, Odisha 751024, India

<sup>2</sup>Department of Informatics, School of Computer Science, University of Petroleum and Energy Studies, Dehradun, India

### ABSTRACT

The problematic and undesirable effects of weeds lead to degradation in the quality and productivity of yields. These unacceptable weeds are close competitors of crops as they constantly devour water, air, nutrients, and sunlight which are helpful for the maturation of crops. For better cultivation and good quality production of crops, weed detection at the appropriate time is an essential stride. In recent years, various state-of-the-art (SOTA) architectures were proposed to detect weeds among crop yields, but they lacked computational cost. This paper mainly focuses on proposing a customized state-of-the-art (SOTA) architecture and comparative study with transfer learning models for detecting and classifying weeds among soybean crops by concentrating on the low computational cost. The selected SoTA is beneficial for detecting weeds on a large scale with very low computational costs. In terms of selection, Maximum Validation Accuracy (MVA), Least Validation Cross-Entropy Loss (LVCEL), and Training Time (TT) were considered for proposing an objective function value system. In total, 15 proposed CNNs with 18 Transfer learning models were analyzed with the help of objective function value and various metric evaluations for finding the best and optimal architecture for weed classification. Experimentation and analysis resulted in C<sub>13</sub> being robust and optimal architecture which

outperformed every CNNs and Transfer learning model by achieving the highest accuracy of 0.9458 with an objective function value of 5.9335 and ROC-AUC of 0.9927 for the classification of weeds from soybean crops.

#### ARTICLE INFO

##### Article history:

Received: 22 January 2022

Accepted: 24 May 2022

Published: 09 November 2022

DOI: <https://doi.org/10.47836/pjst.31.1.24>

##### E-mail addresses:

vinayaksooryavanshi@gmail.com (Vinayak Singh)

mkgourisaria2010@gmail.com (Mahendra Kumar Gourisaria)

harrshvardhan@gmail.com (Harshvardhan GM)

tanupriya1986@gmail.com (Tanupriya Choudhury)

\* Corresponding author

**Keywords:** Agriculture, ANN, CNN, deep learning, image recognition, machine learning, transfer learning

## INTRODUCTION

China, the United States of America (USA), Brazil, and India are major agricultural-producing countries worldwide. Agricultural activities play an important role in the world's economy, majorly for developing nations, as agriculture is the primary source of employment, income, and food. So, agriculture needs a major improvement for fruitful results. Farmers are willing to have less investment and high yielding of crops. So major problem faced by almost every farmer is weed detection problems which are unwanted crops that reduce the growth of crops.

Weed detection in yields is the major reason behind the high cost of crops. They have been a constant threat to the agricultural sector for decades as many techniques have failed to detect weeds at the right time. For the growth of crops, water, air, nutrients, and sunlight are major components, but weeds outgrow and consume a major portion of these which causes losses in crop production every year. Reduction in quality, quantity, and production rate with high prices are major effects of improper growth of crops with weeds.

Majorly this paper will focus on the Soybean crop, which is largely grown in Brazil and consumed by both *Homo sapiens* and *Animalia*. Soybean is a widely grown edible oilseed, and they are in the family of Fabaceae, and they also belong to *Glycine* and *Plantae* in terms of genus and kingdom, respectively. Animal consumes it through soybean meal, and human consumes it as oil. According to the stats collected by Soystats, soybean is a major crop, with 341.8 million Metric Tons of production in 2019. Brazil is the world's major soybean producer, sharing 126 million Metric Tons (Soystats, 2020). Soybean shares almost 25% of our edible oil in the global world. These salient features are likely to be highly rich in fibers, protein, phytoestrogens, low saturated fat, free from cholesterol and lactose, a source of antioxidants, and a good source of omega-3 fatty acids. Weeds are unwanted plants that grow with crops. They are a close competitor for nutrients, space, sunlight, and water with crops, which results in harvesting difficulties, decrement in the quality of crops, and crop diseases, due to which cost of production increases, the risk for pests degrade the rate of production, impurity with moisture in the grains and commercial value of cultivated land is decreased. Weed removal includes various processes like weed removal manually, a sprinkling of pesticides, and many more. Leaves of weeds can be classified into weeds and grasses, where weeds are broadleaf weeds grown between crops. About 40% of global harvesting losses have been caused due to weeds and their damage, besides pests.

Nowadays, farmers are facing problems in growing crops as the input costs are high, but the results of the production of crops are not up to a satisfactory level due to the unwanted growth of weeds. So, machine learning and deep learning will play a crucial role in properly classifying weeds from soybean crops, which will lead to excellent growth of crops, and the quality of crops will be better in terms of earlier stages where weeds were indulged

for sharing nutrients. Manually handling weeds is difficult as it has high labor costs and is not an efficient method for detecting newly growing weeds. Due to weeds, farmers use herbicides that cause crop damage and may lead to various human diseases.

Many researchers have already contributed to this agricultural sector for weed detection as (Aravind et al., 2020) discussed four major crops where ten different crop diseases were included and models that were used pre-trained models like VGG-16, VGG-19, and four more where they gained the highest accuracy of 97.3%. Classification and detection of soybean crops were done by (Ahmad et al., 2021) by using pre-trained VGG-16 for classification and YOLOv3 for localization and identification of weeds, where VGG-16 scored an accuracy of 98.80 and had an F1 score of 99%, whereas YOLOv3 had mAP score of 54.3%. All these implementations were also compared in terms of libraries, namely Keras and Pytorch. In 2017, (Ferreira et al., 2017) used ConvNets (CNNs) and proposed a Convolutional Neural Network Architecture for classifying weeds among soybean crops with an accuracy of 98% and distributed them into 4 classes.

Canny edge detection was used by (Badage, 2018) to detect plant-related diseases. The paper focused on two phases. The first process concentrated on training the model, and the second phase concentrated on monitoring the crop activity and finding whether they are healthy or not. Tang et al. (2017) classified weeds in soybean crops using Convolutional neural networks with an unsupervised technique, i.e., the K-mean feature as the pre-trained process, which achieved an accuracy of 92.89%.

Similarly, (Veeranampalayam et al., 2021) compared object detection using UAV imagery where a Single-shot detector and Faster RCNN were used for weed detection and had IoU of 0.85 for Faster RCNN and 0.84 for Single Shot Detection. Chen et al. (2018) used pre-trained deep learning models such as VGG16 and VGG-19 for detecting diseases in vegetables and fruits like cucumber, rice, wheat, grapes, and many more. The implementation was based on a total of 15000+ images, and the authors created the dataset. Finally, Etienne et al. (2019) proposed the site-specific Weed Management procedure, an automated weed detection system for four common types of weeds. Their proposed methodology consisted of four primary steps: a collection of multispectral and colored images from UAV-based sensors in soybean and cornfields, creation of normalized differential vegetation index (NDVI), image smoothing and thresholding to NDVI imagery, and drawing the bounding boxes with data labeling then the architecture was trained on the various growth stage of crops.

Maximum likelihood classification was used by Asad et al. (2020) to remove the background of images. Further, they labeled the data, and that labeled data was used for training semantic segmentation models and classifying crops. Various deep learning architectures like SegNet and UNet were compared, and ResNet50-based SegNet showed the best result. Similarly, deep convolutional neural networks like VGGNet and GoogleNet



were used by Yu et al. (2019) for weed detection among turf grass, where VGGNet had the highest F1 score, which was above 0.95. On the other hand, DetectNet gained an F1 score of 0.99 for detecting weeds growing in dormant Bermuda grasses. Table 1 shows the tabular representation of five related works with their advantages and disadvantages.

Table 1  
*Tabular representation of various related work*

<b>Author Name and Year</b>	<b>Techniques</b>	<b>Advantage</b>	<b>Disadvantage</b>
<b>Aravind et al. (2020)</b>	VGG-16, VGG19, DenseNet201, GoogleNet, ResNet101	Google Net was the best performer, with the highest accuracy of 97.3%. A good comparative study.	Only pre-trained architectures were compared. No proposed system or customized architectures were proposed.
<b>Badage, (2018)</b>	Canny Edge Detection	Proposed a phase-based system for plant disease detection system. Used Gaussian filter for removing noise from images. Pre-processing was good before training.	No classification process was included. No comparative study with other related works.
<b>Ahmad et al., (2021)</b>	Yolov3, VGG-16	Used VGG-16 for classification and Yolov3 for detection and identification of weeds. The results achieved were outstanding	No comparative study. No customized and proposed neural networks. Only pre-trained networks were considered for classification.
<b>Tang et al. (2017)</b>	CNNs, K-mean	The highest accuracy achieved was 92.89%. Used K-means with CNN architectures for training and pre-processing.	Lacked in comparison with other models and related works
<b>Asad et al. (2020)</b>	Maximum likelihood classification, VGGNet, SegNet	Maximum Likelihood classification was used for background removal. Pre-trained architectures were used for semantic segmentation	The results gained were not good. No comparison with other related works.

Most papers focused on detecting weeds, but in a few articles, the results were not satisfactory. Few lacked a comparison study of architectures, and most of them had used pre-trained architectures. However, this article is especially related to the cultivation of soybean and the classification of weeds from soybean. This paper emphasizes pre-trained not only models but also includes various state-of-the-art architectures. This paper broadly focuses on classifying weeds among soybean crops using Machine learning and deep learning techniques via customized and proposed CNN architectures and transfer learning models. Different configurations of proposed CNNs were compared, and optimal architecture was selected based on a maximum objective function focused on all three domains of maximum validation accuracy, least validation cross-entropy loss, and training time. Best CNN was

selected and was compared with existing transfer learning models in terms of all metrics evaluation. In total, 18 different transfer learning models came into play, and 15 different parameterized CNN architectures were compared. The performance analysis consisted of all the domains of metrics evaluation, including objective function value and AUC- ROC.

This real-time deployment of architectures and transfer learning techniques will help detect weeds. Therefore, it can help farmers greatly by reducing the usage of herbicides and increasing soybean crop health and production of soybeans. The paper's next sections are Materials and Methods, Results, Conclusion and Future Direction. We evaluated all transfer learning models and ANN and CNN architectures to find the best technique and ideal model with maximum objective value function for the dataset of weed detection in soybean crops used in Section 3.

## MATERIALS AND METHODS

This section will focus on the methodology used for classifying weeds from soybean. Weeds like Broadleaf and Grasses can be easily differentiated from our soybean crops, and the technology used for computational work and experimentation is specified in this section. This section is further divided into Dataset Collection, Convolutional Neural Network (CNN), Transfer Learning and Software and Hardware.

### Dataset Collection

The dataset used consisted of 15,336 images which were collected from Mendeley data, and the dataset was deployed by Federico Peccia and Group, which captured all the images consisting of four people, namely Alessandro dos Santos Ferreira, Hemerson Pistori, Daniel Matte Freitas, and Gercina Gonçalves da Silva (Ferreira et al., 2017). These images were from Campo Grande, Mato Grosso do Sul, Brazil, from a soybean plantation area captured from the Phantom DJI 3 Professional drone. For our experimentation, we have removed the soil class from the dataset and converted it into a binary class with a total image of 12,087.

The modified dataset has been classified into two parts: soybean and weeds, which contain Grass and Broadleaf. A sample of images from the dataset for classification among both categories is shown in Figure 1. Table 2 shows the distribution of the dataset among three categories, i.e., Training, Testing, and Validation.

### Convolutional Neural Network (CNN)

ConvNet (CNN) is a basic operational neural network that is a backbone in deep learning, contributing to diagnoses and recalling visual imagery. There is a wide range of CNN applications, such as classification

Table 2  
*Dataset distribution into three categories*

	Soybean	Weeds
<b>Training</b>	4426	2827
<b>Testing</b>	1475	942
<b>Validation</b>	1475	942
<b>Total</b>	7376	4711

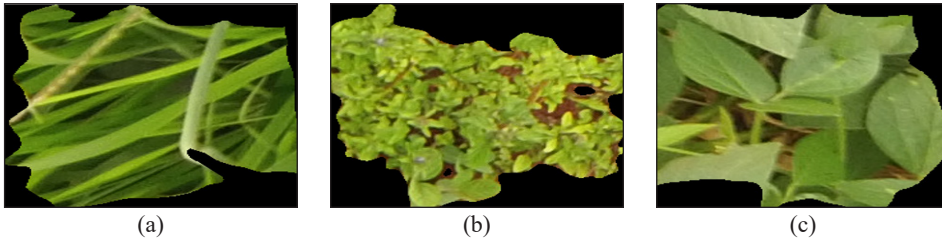


Figure 1. (a) Grasses (b) Broadleaf (c) Soybean leaf

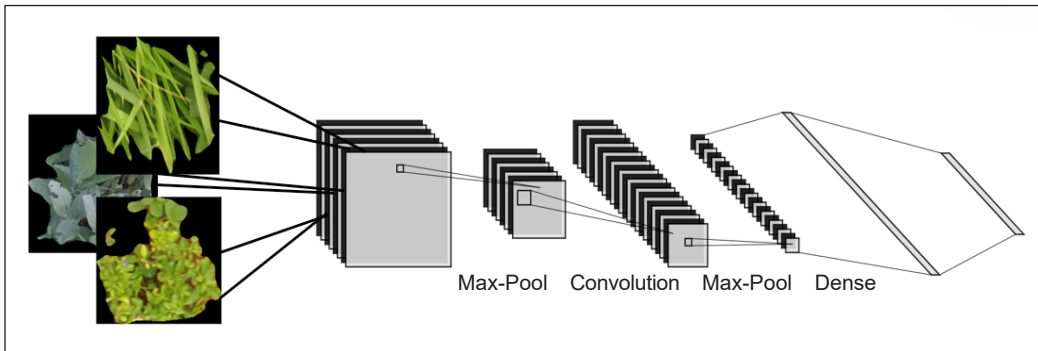


Figure 2. Convolutional Neural Networks (CNN)

of Brain Tumor (Singh et al., 2022a), tuberculosis detection and classification using CXR images (Al-Timemy et al., 2021; Singh et al., 2022b, retinal disease detection and classification (Rajagopalan et al., 2021; Sarah et al., 2021), face recognition (Khalajzadeh et al., 2014), and diagnosis and classification of skin cancer (Sannigrahi et al., 2021 ), sperm classification (Chandra et al., 2021), ductal carcinoma (GM et al., 2022) and arrhythmia detection (Alfaras et al., 2019; Gourisaria et al., 2021). These neural networks are highly interactive with imagery, where they assume and learn the patterns associated with the images. CNN frameworks are composed of 4 layers: Convolution layer, Max-pooling, Flattening, and Full Connection. Figure 2 shows the basic block diagram for CNN.

The convolutional layer is the initial and primary layer of the Convolutional neural network. This network follows the convolutional theorem, which states that a property of equivariant is equivariant to the translation operations. Mathematically, the convolutional theorem can be represented as Equation 1:

$$x ( y ( n ) ) = y ( x ( n ) ) \tag{1}$$

Where n-various input images, x is the convolutional operation, and y is the image translation operation.

The pooling layer is the second layer associated with CNNs, where they provide us the facility to reduce feature maps retrieved from the convolutional layer. These pooling layers

play an important role while reducing the dimensions and extracting the major features from an input image. This layer provides the ability to down-sample the feature map via spatial variance. The pooling layer can be classified into two categories: Average-Pooling and Max-Pooling. In our case, Max-pooling was considered for the implementation of CNN architectures. Output dimension can be calculated by using Equation 2:

$$Dimension_{output} = \frac{(m - f + 1) \times (n - p + 1)}{q(q \times o)} \quad (2)$$

Where  $m$  represents height (feature map),  $n$  represents width (feature map),  $o$  represents channel (feature map),  $p$  represents the filter size (feature map), and  $q$  represents stride length (feature map).

After multi-dimension output retrieval, these features are passed through the flattening layer, which converts the output of the max-pooling layer into a 1-D array, an input for the last fully connected layer. Finally, various operations are performed on a 1-D array received from the flattening layer in a fully connected layer, which turns into output per requirements.

In terms of depth, if the neural network is shallow, then there might be a chance of under-fitting. So variation in the depth of the convolutional layer plays a vital role in proposing a better classification architecture. In terms of depth, CNN architectures get enriched in parameters, and deep neural networks are capable of training on multiclass and heavy datasets for better and good computational results. Subsequently, various optimizers such as softmax and sigmoid play an important role during the operation by efficiently optimizing the output and helping in categorization or classification. In our case, softmax was considered with the binary number of outputs.

So, mathematically we can say in Equation 3:

$$\underbrace{A * A * A \dots \dots * A * A}_n = A^n \quad (3)$$

Where  $A$  is a single convolutional layer with different parameters and  $n$  is the number of layers implemented by users.

Our approach proposed customized CNN architectures based on parameters like Input Sizes of Images, Pooling Size, Feature Detection, L1, L2, Dropout and Batch Normalization, Number of Convolution layers, Artificial layer, and Kernel Size. As a result, CNN architectures' parameters varied within the most suitable range for finding the best architecture with suitable parameters. Furthermore, regularization conditions were closely enclosed with heavy architectures, which prevented them from overfitting the dataset.

### Transfer Learning

Transfer learning architectures are complex CNNs and highly enriched in parameters and layers. Some transfer learning models used for classifications are Inception, MobileNet, VGG, DenseNet, ResNet, EfficientNet, Xception, and NASNet. These models have come up with better accuracy when compared with normal ConvNet architectures. Initially, all these architectures are proposed in a yearly competition known as ImageNet, where all these architectures are trained in thousands of classes. The standard input image size is set to be (224, 224, 3) for RGB images and (224, 224, 1) for black and white images, respectively.

Majorly they are used as pre-trained models where these architectures are imported, and the last layer is trained according to the various dataset by the user.

Transfer learning can be implemented as a heterogeneous method in various states, whether on text and image connections or performing computational matrix calculations. Transfer learning connects various fields and has various applications like text classification, text clustering, image and clustering, sentiment classification, and metric learning. Table 3 shows the configuration of all the used transfer learning models.

Domain and tasks can be used as terms to explain transfer learning mathematically.

Let domain X consists of  $\mathbb{A} \rightarrow$  feature space &  $P(A) \rightarrow$  Marginal Probability Distribution where

$$A = \{a_1, a_2, a_3 \dots a_N\} \in \mathbb{A}$$

Let specific domain  $X = \{\mathbb{A}, P(A)\}$ . It has 2 parts, i. e.,  $Y \rightarrow$  Label Space and  $\{f: \mathbb{A} \rightarrow Y\}$ , i. e., an objective predictive function

For new instances, a function f is used for predicting  $f(a)$ , i. e., the corresponding label.

Now in Equation 4:

$$K = \{Y, f(a)\} \tag{4}$$

where K is the task that is learned for the pair, i.e.  $\{a_a \in A\}$ ,  $\{y_a \in Y\}$  is part of training

Table 3  
*Different models with size and parameters*

Model	Size	Parameters (millions)
<b>Xception</b>	88 MB	22.91
<b>VGG16</b>	528 MB	138.35
<b>VGG19</b>	549 MB	143.66
<b>ResNet50</b>	98 MB	25.63
<b>ResNet101</b>	171 MB	44.70
<b>ResNet152</b>	232 MB	60.41
<b>ResNet50V2</b>	98 MB	25.61
<b>ResNet101V2</b>	171 MB	44.67
<b>ResNet152V2</b>	232 MB	60.38
<b>InceptionV3</b>	92 MB	23.85
<b>InceptionResNetV2</b>	215 MB	55.87
<b>MobileNet</b>	16 MB	4.25
<b>MobileNetV2</b>	14 MB	3.53
<b>DenseNet121</b>	33 MB	8.06
<b>DenseNet169</b>	57 MB	14.30
<b>DenseNet201</b>	80 MB	20.24
<b>NASNetMobile</b>	23 MB	5.32
<b>NASNetLarge</b>	343 MB	88.94

data  $X_s \rightarrow$  Source domain (given),  $K_s \rightarrow$  Learning task,  $X_t \rightarrow$  Target domain, and  $K_t \rightarrow$  Learning task.

Where in Equation 5:

$$\begin{aligned} X_s &\neq X_t \\ K_s &\neq K_t \end{aligned} \quad (5)$$

Where, target predictive function  $f_t(\cdot)$  in  $K_t$  will be able to improve its learning when transfer learning is implemented with the help of knowledge in  $X_s$  &  $K_s$ .

These architectures are quite heavy and can easily and efficiently handle large datasets. We have used them with an Adam optimizer to compare and find the most suitable architecture for weed detection among soybean leaves.

### Software and Hardware

All the models trained during the experiment were completed using Python-based programming with Keras and Tensorflow libraries on the Jupyter notebooks. The hardware system was configured with i5 8<sup>th</sup> Generation and 16GB RAM.

## RESULTS AND DISCUSSION

In this section, we provide every detail regarding performance analysis and evaluation and a full comparison between different models that are trained on the weed dataset, and we selected the best CNN architecture model for comparing it with various transfer learning models for finding an optimal architecture for detection of weeds from soybean leaves. We divide this section into Experiments and Analysis, Transfer Learning Models, and Result of Selected Architecture versus Transfer Learning.

### Experiments and Analysis

This section provides detailed knowledge about the structures of all the CNN models. It helps us find the optimal CNN architecture based on various parameters, including maximum objective function value. Various architectures were trained on different regularization conditions. For implementation, we had different regularization parameters like L1, L2, Dropout and Batch Normalization, Number of Convolution layer, Artificial layer, Input Sizes of Images, Pooling Size, Feature Detection, and Kernel Size and selection of the best architecture was based on Objective Function Value (OFV) where it was calculated by using 3 parameters that were Maximum Validation Accuracy (MVA), Least Validation Cross-Entropy Loss (LVCEL) and Training Time (TT). Objective Function Value can be expressed as Equation 6:

$$\frac{\text{MVA}}{\text{LVCEL} + \text{TT}} = \text{Objective Function Value} \quad (6)$$

All the information regarding all the 15 different CNN and ANN architectures with their MVA, LVCEL, and TT (in seconds) are included in Table 5. Table 4 contains the meaning of all the abbreviations used in Table 5. Figure 3 tells us about the structure of each architecture based on LVCEL, MVA, and TT. Figure 4 plots the training accuracy, and Figure 5 plots the cross-entropy loss of each architecture per epoch. From Table 5, we observed that architectures 9 and 8 performed very poorly concerning MVA and LVCEL as they had the least objective function values of 0.36000 and 0.39843, respectively. It might happen due to L2 and Batch Normalization as these parameters are responsible for the reduction in training time, which resulted in low MVA, led to a fall in objective function value, and further restricted the model from building a good connection with the dataset.

From Table 5, we can develop a relationship between the input image size and training time where TT is directly proportional to input image size as we can notice that if the size of the image is (64, 64), it takes much less time when compared to (128,128) input size of images. Architecture 5, 6, and 13 were fed with (64 and 64), and the rest were on (128,128), which can be observed in Table 5. From Figure 3, training time drastically changed in architectures where (64 and 64) were used as input image sizes. Architecture 9 took 4864 seconds to train the model, but it achieved an accuracy of 0.6103 due to the implementation of the L2 regularization condition. Architecture 8, 9, 10, and 11 show that the models were not performing well as the MVA was only 0.6103. It was due to L1, L2,

Table 4  
Abbreviations used in Table 5

Abbreviation	Meaning
<b>CL</b>	The number of CNN Layers in an architecture.
<b>AL</b>	The number of ANN Layers in an architecture.
<b>L1</b>	Level 1 regularizations
<b>L2</b>	Level 2 regularizations
<b>BN</b>	Batch Normalization
<b>DO</b>	Dropout
<b>IS</b>	Input Size of image (64x64 or 128x128)
<b>FD</b>	Feature detected in a convolutional layer, layer-wise.
<b>KS</b>	Kernel Sizes for each convolutional layer, layer-wise.
<b>PS</b>	Pooling Sizes followed by every convolutional layer are always assumed to be a square matrix.
<b>TT</b>	Time taken in seconds to train the model.
<b>LVCEL</b>	Least Validation Cross-Entropy Loss achieved during training.
<b>MVA</b>	Maximum Validation Accuracy was achieved during training.



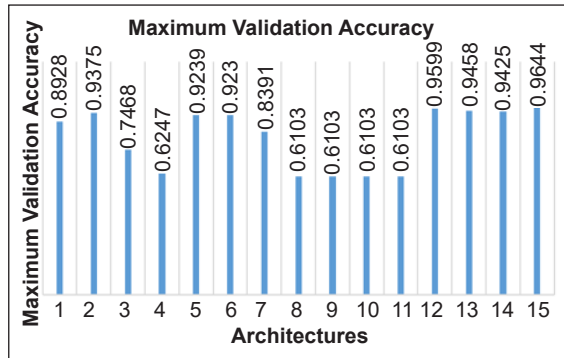
Table 5  
Performance of 15 different CNN architectures on various parameters

S. No.	CL	AL	Regularizations			IS	FD	KS	PS	LVCEL	MVA	TT (in seconds)
			L1	L2	BN							
1	2	3	X	X	X	(128,128)	{64,32}	{9,3}	{4,2}	0.2170	0.8928	3260
2	2	4	X	X	X	(128,128)	{64,32}	{9,3}	{4,2}	0.1808	0.9375	3756
3	2	4	X	X	✓	(128,128)	{64,32}	{9,3}	{4,2}	0.5747	0.7468	4846
4	2	4	X	X	✓	(128,128)	{64,32}	{9,3}	{4,2}	0.6097	0.6247	3791
5	2	4	X	X	X	(64,64)	{64,32}	{9,3}	{4,2}	0.2172	0.9239	960
6	2	2	X	X	X	(64,64)	{64,32}	{9,3}	{4,2}	0.2149	0.9230	1007
7	2	3	X	X	✓	(128,128)	{64,32}	{9,3}	{4,2}	0.3601	0.8391	3611
8	3	4	X	X	✓	(128,128)	{128,64,32}	{9,6,3}	{4,2,2}	0.6686	0.6103	4295
9	3	5	X	✓	X	(128,128)	{128,64,32}	{9,6,3}	{4,2,2}	0.6687	0.6103	4864
10	4	4	✓	X	X	(128,128)	{128,64,32,16}	{9,6,3,3}	{4,2,2,2}	0.6687	0.6103	1183
11	4	5	✓	✓	X	(128,128)	{128,64,32,16}	{9,6,3,3}	{4,2,2,2}	0.6693	0.6103	1439
12	4	5	X	X	X	(128,128)	{128,64,32,16}	{9,6,3,3}	{4,2,2,2}	0.1184	0.9599	1512
13	4	5	X	X	X	(64,64)	<b>{64,32,32,16}</b>	<b>{9,6,3,3}</b>	<b>{2,2,2,2}</b>	<b>0.1594</b>	<b>0.9458</b>	<b>503</b>
14	5	5	X	X	X	(128,128)	{128,64,64,32,16}	{9,6,6,3,3}	{2,2,2,2,2}	0.1645	0.9425	1592
15	5	6	X	X	X	(128,128)	{128,64,64,32,16}	{9,6,6,3,3}	{2,2,2,2,2}	0.1042	0.9644	1557

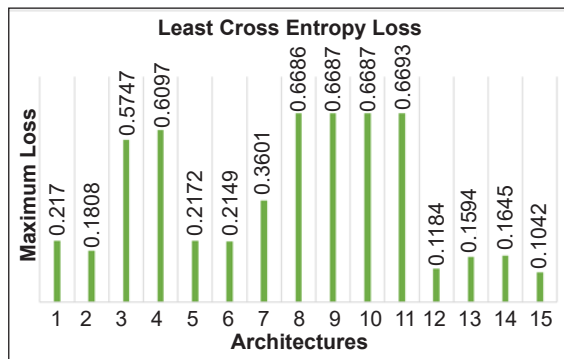
and BatchNorm conditions which led them to an overfitting condition.

However, the maximum objective function value of 5.93 was achieved by Architecture 13 ( $C_{13}$ ). By this, we can conclude that simple architecture with a small input image performs better and is more stable and reliable. Various aspects such as Maximum Validation Accuracy (MVA), Least Validation Cross-Entropy Loss (LVCEL), Training Time (TT), and Objective Function Value (OFV) were considered for the selection of the best state-of-the-art architecture as the main motive for finding the best and optimal CNN architecture with the lowest computational cost for classification of weeds. For Further comparison and consideration, we have taken Architecture 13 as an ideal model to evaluate model performance and comparing with transfer learning models. Therefore, we will call architecture 13  $C_{13}$  for comparing and further considering on weed detection dataset.

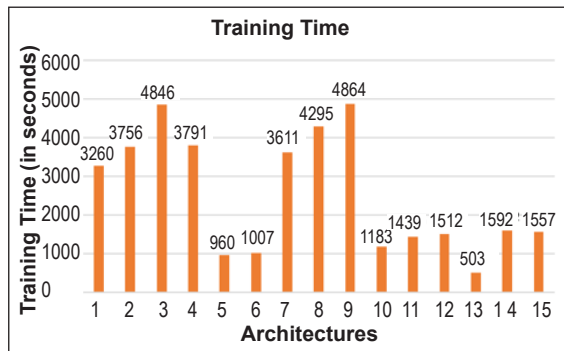
From Table 5, it was also observed that architecture fed with (64, 64) was providing better results when compared with (128, 128) fed architectures as they were less complex and computational power of convolutional neural networks were efficiently working with (64, 64) image size. Furthermore, it was noticed that all 3 architectures of (64, 64) gained accuracy above 0.90 and had less training time compared with (128,128) as the complexity increases as the image size increases. In our case, (64, 64) architectures performed very well as  $C_{13}$  was the best architecture when compared with



(a)



(b)



(c)

Figure 3. (a) Maximum Validation Accuracy (MVA) for each architecture. (b) Least Cross-Entropy Loss (LVCEL) for each architecture. (c) Training Time (TT) for each architecture

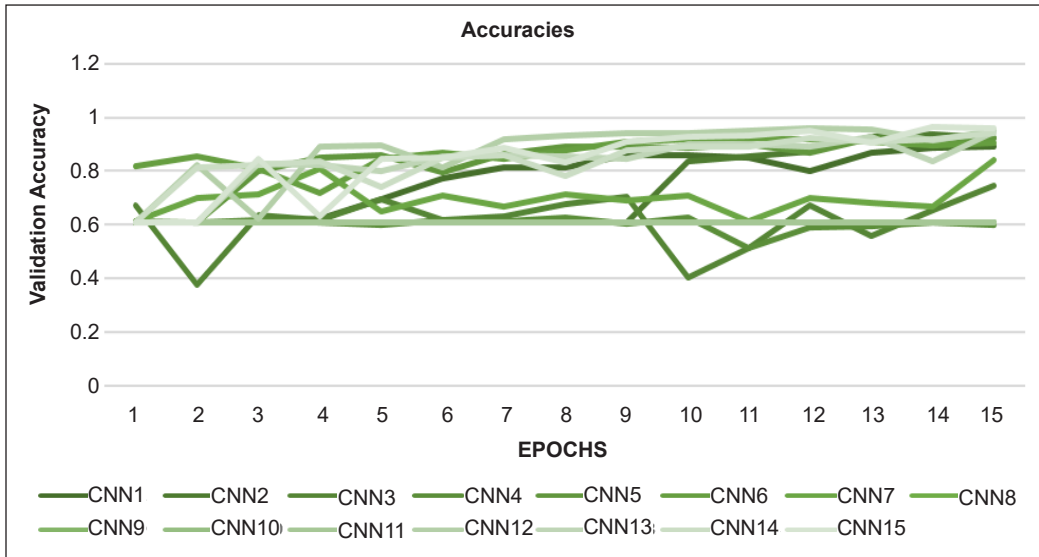


Figure 4. Validation accuracy training curve for each architecture per epoch

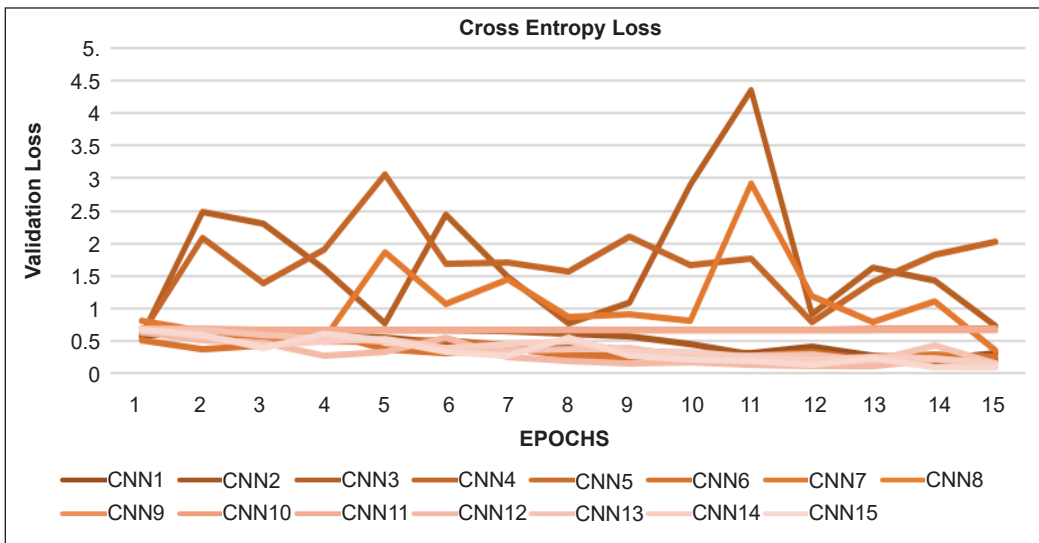


Figure 5. Validation cross-entropy loss training curve for each architecture per epoch

other models in terms of all the metrics where this architecture was balanced in terms of all three categories of maximum validation accuracy (MVA), least validation cross-entropy loss (LVCEL), and training time (TT). These three parameters led to the development of an objective function where our Architecture 13 outperformed all other CNN models.

Heavy architectures were considered with L1, L2, Batch Normalization, and Dropout to avoid the overfitting condition and the major concentration depended on proposing a low computational architecture for classification. Most architectures were trained on

128 × 128 image size. However, the objective function value was unsatisfactory as training time was greater than the time taken by architectures fed with 64 × 64 image size.

### Transfer Learning Models

We have trained different transfer learning models on our dataset to compare our best CNN architecture and considered LVCEL, MVA, and TT for comparison and metric calculations. These architectures are pre-trained on large ImageNet data and heavily enriched parameters. Transfer learning architectures have dense layers of the convolutional network. All the information regarding MVA, LVCEL, and TT (in seconds) of the transfer learning model is provided in Table 6. Abbreviations used in Table 6 are given in Table 4. Figures 6, 7, and 8 discuss every transfer learning model’s LVCEL, MVA, and TT.

From Table 6, we can notice that VGG-19 and NASNetLarge took 35800 and 30869 seconds, respectively, as they are highly rich in parameters, but they took approx. Nine hours of training which is very high. Xception performed pretty well as it achieved high accuracy but has taken less time compared to other architectures like VGG-16, VGG-19, and NASNetLarge. It performed well as a balanced model. MobileNet and MobileNetV2 are light architecture and performed well by achieving accuracy above 90%. The training time of these models was also less when compared to all other transfer learning models.

Table 6  
*Performance of various transfer learning models*

S. No.	Transfer Learning Model	MVA	LVCEL	TT (in seconds)
1	Xception	0.9872	0.0698	11554
2	VGG-16	0.9888	0.0250	29989
3	VGG-19	0.9897	0.0325	35800
4	ResNet50	0.8540	0.4460	5924
5	ResNet101	0.8577	0.5327	15383
6	ResNet152	0.8531	0.6926	22447
7	ResNet50V2	0.8904	0.3341	8744
8	ResNet101V2	0.8635	0.3666	14092
9	ResNet152V2	0.8771	0.3301	21839
10	InceptionV3	0.8713	0.3547	6179
11	InceptionResNetV2	0.8577	0.3633	13421
12	DenseNet121	0.8093	0.4398	11063
13	DenseNet169	0.8395	0.4235	12217
14	DenseNet201	0.8448	0.4344	16676
15	MobileNet	0.9156	0.3418	3318
16	MobileNetV2	0.9090	0.3203	3279
17	NASNetLarge	0.7530	0.4860	30869
18	NASNetMobile	0.7815	0.5135	6564

They have taken only 3318 and 3279 seconds, respectively. NASNetLarge performed badly compared with other transfer learning architectures as the accuracy was only 75.30%, and its training time was 30869 seconds which was very high. Figure 8 shows that if transfer learning models have heavy parameters, they will take much more training time. The training time of transfer learning models was very high due to their high complexity compared with our state-of-the-art architectures.

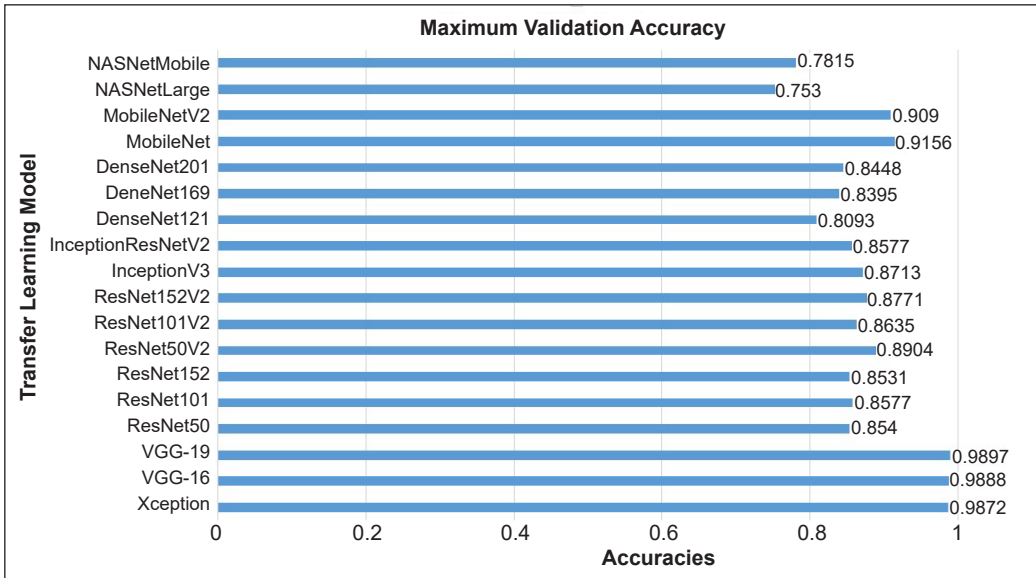


Figure 6. Maximum Validation Accuracy (MVA) for each transfer learning model

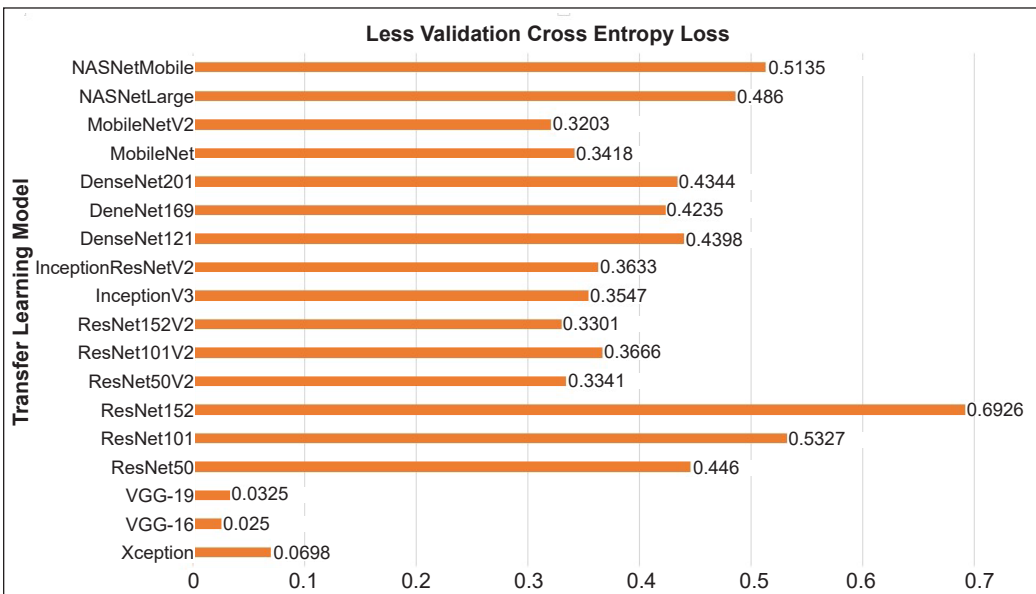


Figure 7. Least Cross-Entropy Loss (LVCEL) for each transfer learning model

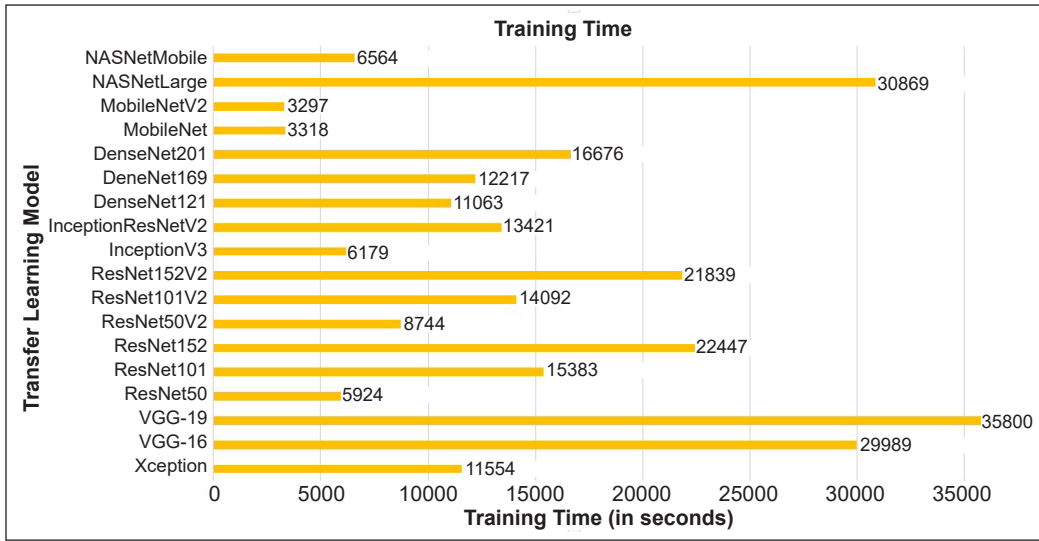


Figure 8. Training Time (TT) for each transfer learning model

While considering only the MVA, it was observed that 5 models gained MVA above 0.90, but when the time taken was considered, they had training time greater than CNN models as they were heavy in configuration, so training time was high. So, in terms of complexity and computational cost, these architectures were not much efficient when compared with models.

However, in the next section, we will compare all transfer learning models with our selected CNN architecture, i. e.,  $C_{13}$  has achieved an objective function value of 5.93, and will judge all the models based on metric calculations performed in the next section.

### Result of Selected Architecture versus Transfer Learning

In this section, our CNN architecture  $C_{13}$  will be compared with various transfer learning models based on various metric calculations. We have calculated all the metrics of the  $C_{13}$  and transfer learning models, which are mentioned in Table 7. Equations 7, 8, 9, 10, 11 and 12 represent the formula for the calculation of various performance metrics. Table 7 shows that Xception, VGG-16, and VGG-19 were strong competitors to  $C_{13}$  architecture. VGG-19 achieved the highest accuracy of 0.9897 and scored 0.9868 in MCC, which was the highest among all the models. Similarly, VGG-16 performed outstandingly in sensitivity and F1-score and achieved the highest metric calculation of 0.9978 and 0.9855, respectively. Xception was the best model in all the transfer learning architectures, and it also performed well in Specificity and Precision calculation, with a score of 0.9972 and 0.9958.

$$\text{Accuracy} = \frac{(TP + TN)}{(TP + TN + FP + FN)} \quad (7)$$

$$\text{Sensitivity} = \frac{TP}{(TP + FN)} \quad (8)$$

$$\text{Specificity} = \frac{TN}{(FP + TN)} \quad (9)$$

$$\text{Precision} = \frac{TP}{(TP + FP)} \quad (10)$$

$$\text{F1 Score} = \frac{2TP}{(2TP + FP + FN)} \quad (11)$$

$$\text{MCC} = \frac{TP \times TN - FP \times FN}{\sqrt{((TP + FP) \times (TP + FN)) \times ((TN + FP) \times (TN + FN))}} \quad (12)$$

Further, if we notice NASNetMobile did not perform well and was not able to establish the relationship between dataset and model. So, NASNetMobile scored low in almost all the fields of metric calculations like Accuracy, Specificity Precision, F1 score, and MCC. The sensitivity of ResNet152 was not so good. According to the calculation, it was found to be only 0.7651, but in other fields, ResNet152 worked well in building the connection between the dataset and the model. Our C<sub>13</sub> performed very well in all metric sections by achieving all the results above 89%.

From Table 7, we can see that Xception was the best in all the transfer learning models. Further, for more clarification, we plotted the AUC-ROC curve for all the architectures, calculated the Area under the Curve and Objective Function Value of all the transfer learning models, and compared it with our C<sub>13</sub>. All details of the AUC score and OFV are mentioned in Table 8. Our architecture C<sub>13</sub> outshined and gained a high AUC of 0.9927, as shown in Figure 8. Objective Function Value was calculated by comparing all the architectures using LVCEL, TT, and MVA, where C<sub>13</sub> achieved an Objective Function Value of 5.9335, which is very high compared to all other transfer learning models. Xception performed very well and gained a value of 2.5788. VGG-16 and VGG-19 performed very well in all the domains. However, heavy parameters took much time for training, and this was the main reason behind the declination in objective function value, where the VGG-19 took almost 35800 seconds for training. Figure 9 shows the graphical comparison between C<sub>13</sub> and all transfer learning architectures.

So, we can see that small architecture can perform well in less training time. Xception had a validation accuracy of 98% for every epoch, which was very good. Figure 10 shows all the ROC curve plotting where Xception, VGG-16, and VGG-19 were close competitors for C<sub>13</sub> architecture, but our architecture had an AUC of 0.9927, which was better than other models. For the selection of the optimal architecture, all evaluation metrics were considered. However, majorly maximum objective function was considered as the paper mainly focuses on proposing a classification model of weed with a low computational cost.



Table 7  
Metric calculation of selected CNN architecture and transfer learning models

Model Name	Accuracy	Sensitivity	Specificity	Precision	F1 Score	MCC	Confusion Matrix	
<b>C<sub>13</sub></b>	0.9458	0.9242	0.9642	0.9448	0.9344	0.8919	890	52
							73	1402
<b>Xception</b>	0.9872	0.9720	0.9972	0.9958	0.9837	0.9733	938	4
							27	1448
<b>VGG-16</b>	0.9888	0.9978	0.9833	0.9735	0.9855	0.9766	917	25
							2	1473
<b>VGG-19</b>	0.9897	0.9852	0.9925	0.9883	0.9783	0.9868	931	11
							14	1461
<b>ResNet50</b>	0.8540	0.9177	0.8277	0.6868	0.7857	0.6947	647	295
							58	1417
<b>ResNet101</b>	0.8577	0.9211	0.8313	0.6943	0.7918	0.7027	654	228
							56	1419
<b>ResNet152</b>	0.8531	0.7651	0.9275	0.8992	0.8267	0.7076	847	95
							260	1215
<b>ResNet50V2</b>	0.8904	0.9734	0.8555	0.7389	0.8401	0.7757	696	246
							19	1456
<b>ResNet101V2</b>	0.8635	0.9397	0.8327	0.6943	0.7985	0.7171	654	288
							42	1433
<b>ResNet152V2</b>	0.8771	0.9272	0.8544	0.7431	0.8250	0.7427	700	242
							55	1420
<b>InceptionV3</b>	0.8713	0.9376	0.8432	0.7176	0.8130	0.7324	676	266
							45	1430
<b>InceptionResNetV2</b>	0.8577	0.9359	0.8267	0.6815	0.7887	0.7049	642	300
							44	1431
<b>DenseNet121</b>	0.8093	0.8860	0.7826	0.5860	0.7054	0.5997	552	390
							71	1404
<b>DenseNet169</b>	0.8395	0.8991	0.8154	0.6624	0.7628	0.6629	624	318
							70	1405
<b>DenseNet201</b>	0.8448	0.9717	0.8029	0.6200	0.7570	0.6865	584	358
							17	1458
<b>MobileNet</b>	0.9156	0.9590	0.8940	0.8185	0.8832	0.8240	771	171
							33	1442
<b>MobileNetV2</b>	0.9090	0.8824	0.9260	0.8843	0.8834	0.8087	833	109
							111	1364
<b>NASNetMobile</b>	0.7530	0.9078	0.7202	0.4076	0.5626	0.4893	384	558
							39	1436
<b>NASNetLarge</b>	0.7815	0.8750	0.7539	0.5127	0.6466	0.5413	483	459
							69	1406

Table 8  
AUC and Objective Function Value of selected CNN architecture and transfer learning models

Model Name	AUC	Objective Function Value
C <sub>13</sub>	0.9927	5.9335
Xception	0.9887	2.5788
VGG-16	0.9860	1.1493
VGG-19	0.9894	0.9585
ResNet50	0.8237	1.4257
ResNet101	0.8281	0.8993
ResNet152	0.8614	0.6494
ResNet50V2	0.8629	1.5700
ResNet101V2	0.8328	1.1504
ResNet152V2	0.8529	0.9385
InceptionV3	0.8435	1.6928
InceptionResNetV2	0.8258	1.1776
DenseNet121	0.7689	1.0954
DenseNet169	0.8074	1.1126
DenseNet201	0.8042	0.9466
MobileNet	0.8980	2.1720
MobileNetV2	0.9045	2.2787
NASNetMobile	0.6906	1.1417
NASNetLarge	0.7329	0.5594

While considering all the parameters, Xception, VGG16, and VGG19 were ahead of our C<sub>13</sub>, but when it comes to computational cost and training time, our C<sub>13</sub> beat all the models. Our CNN model had less training time than transfer learning models. C<sub>13</sub> gained high accuracy with minimal loss in less time, which resulted in proposing architecture for the classification of weeds among soybean with low computational cost.

Our selected C<sub>13</sub> performed outstandingly in every metric calculation and had the highest objective function value of 5.9335, and the area under the curve was 0.9927, which is very high. C<sub>13</sub> architecture had 251,730 parameters which were very less when compared to all transfer learning models. Testing of the model was done on 2417 images and where True Negative = 890, True Positive = 1402, False Negative = 52, and False Positive = 73 are shown in

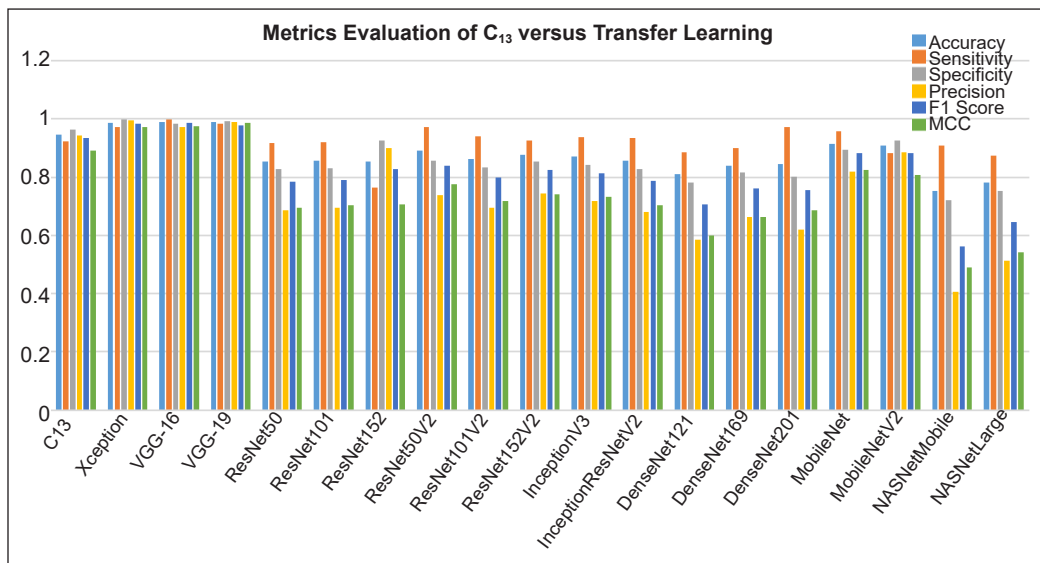


Figure 9. Graphical representation of metrics evaluation of C<sub>13</sub> versus transfer learning

Figure 11. All the metrics were almost 90%, indicating our model was performing well and was excellent compared to all other transfer learning models in distinguishing between weeds and soybean leaves. These values are very high and far ahead of other proposed works in the related work section.

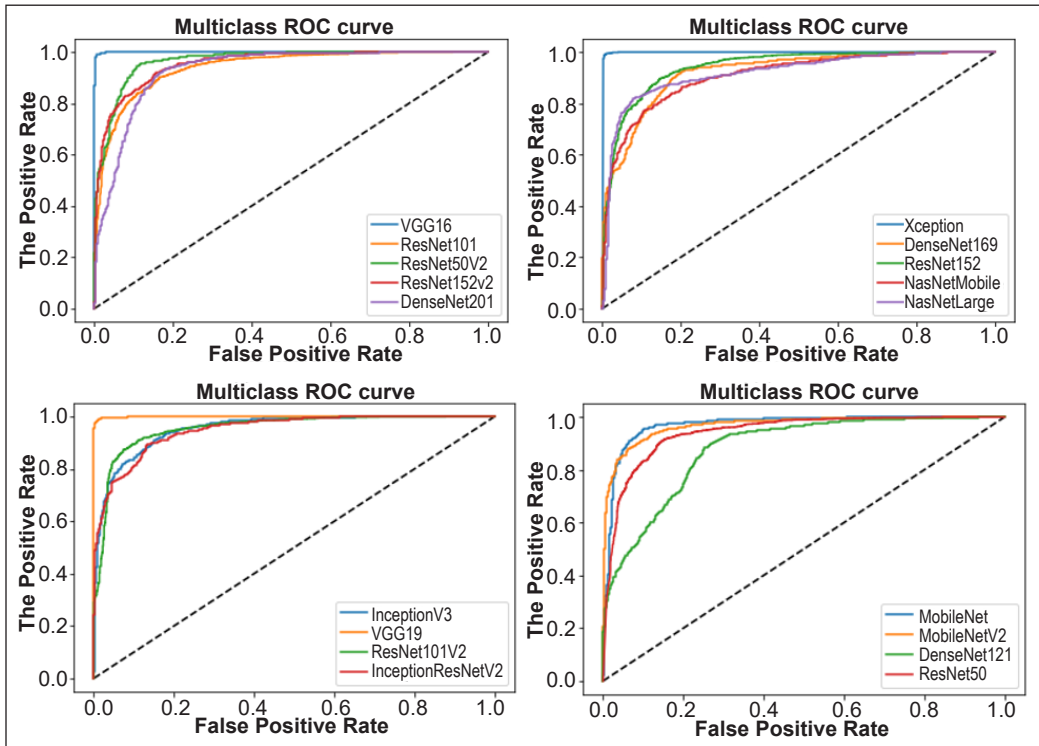


Figure 10. Receiver-operating characteristics (ROC) curve for all transfer learning models. The area under the curve is given in Table 7.

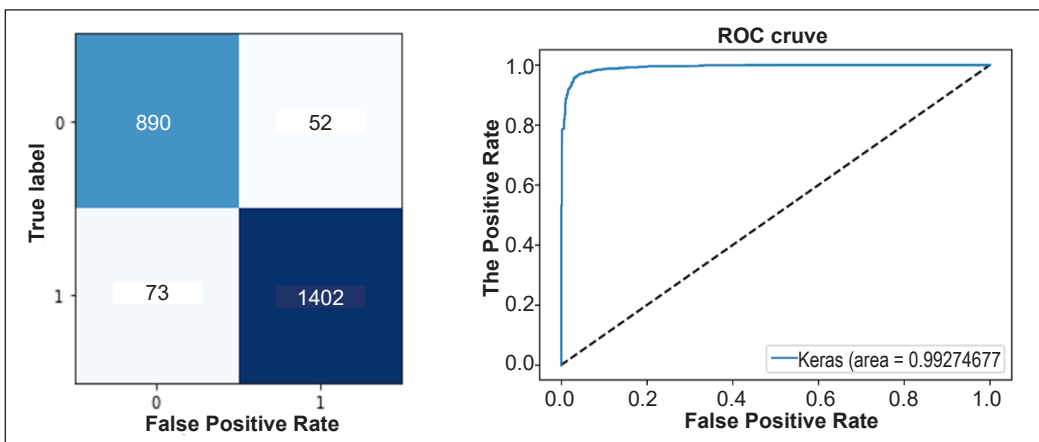


Figure 11. (L)The confusion matrix for  $C_{13}$  (see Table 7). (R) The receiver-operating characteristics (ROC) curve for  $C_{13}$  architecture. The area under the curve of  $C_{13}$  was 0.9927 units.

## CONCLUSION AND FUTURE DIRECTION

Our research helps provide a detailed analysis of CNNs and transfer learning models and find an optimal architecture for detecting weeds from soybean crops. Based on Objective Function Value, we have selected the ideal model  $C_{13}$  for comparison with various transfer learning models in metrics evaluation which can easily reduce the computational cost. The best architecture was selected, and our proposed  $C_{13}$  outshines every domain as it has the least computational cost, which will help in easy training, faster detection rate, accurate classification, and reliability. As we compared our architecture with various architectures, we found that heavy parameterized transfer learning models like VGG-16 and VGG-19 have achieved very high accuracy. However, they lag in OFV calculation due to more training time, leading to a high computational cost. NASNetMobile performed poorly while building relationships with the dataset. So as learned from the findings in research work, we recommend that simpler architectures are good and reliable for learning, and they can perform much better than complex ones. We admit that  $C_{13}$  architecture performed well and can perform much better and gain a higher accuracy and stability by adjusting some hyper-parameters.

Our next goal is to propose another efficient model for classifying weeds from various crops. Some changes in the parameters of  $C_{13}$  can provide better results. More complex datasets can be used for weed detection and classification. The transfer learning technique, i.e., EfficientNet, can also be implemented to find a more stable and reliable model. As weeds have various categories, various complex models can be proposed for better detection. These techniques can work efficiently with few hyper-parameters tuning, leading to low computational cost as weed detection needs high accuracy. Our architecture had minimal computational cost as all the domains were considered for evaluating and detecting weeds among soybean leaves.

## ACKNOWLEDGMENT

The author wishes to acknowledge no conflict of interest in publishing the paper. The author wants to thank Prof. Mahendra Kumar Gourisaria for always supporting and motivating nature. The author also acknowledges and thank Dr. Tanupriya Choudhury for his all-time support.

## REFERENCES

- Ahmad, A., Saraswat, D., Aggarwal, V., Etienne, A., & Hancock, B. (2021). Performance of deep learning models for classifying and detecting common weeds in corn and soybean production systems. *Computers and Electronics in Agriculture*, 184, Article 106081. <https://doi.org/10.1016/j.compag.2021.106081>
- Alfaras, M., Soriano, M. C., & Ortín, S. (2019). A fast machine learning model for ECG-based heartbeat classification and arrhythmia detection. *Frontiers in Physics*, 7, Article 103. <https://doi.org/10.3389/fphy.2019.00103>

- Al-Timemy, A. H., Khushaba, R. N., Mosa, Z. M., & Escudero, J. (2021). An efficient mixture of deep and machine learning models for covid-19 and tuberculosis detection using x-ray images in resource-limited settings. In D. Oliva, S. A. Hassan & A. Mohamed (Eds.) *Artificial Intelligence for COVID-19* (Vol. 358, pp. 77-100). Springer. [https://doi.org/10.1007/978-3-030-69744-0\\_6](https://doi.org/10.1007/978-3-030-69744-0_6)
- Aravind, K. R., & Raja, P. (2020). Automated disease classification in (Selected) agricultural crops using transfer learning. *Automatika*, 61(2), 260-272. <https://doi.org/10.1080/00051144.2020.1728911>
- Asad, M. H., & Bais, A. (2020). Weed detection in canola fields using maximum likelihood classification and deep convolutional neural network. *Information Processing in Agriculture*, 7(4), 535-545. <https://doi.org/10.1016/j.inpa.2019.12.002>
- Badage, A. (2018). Crop disease detection using machine learning: Indian agriculture. *International Research Journal of Engineering and Technology (IRJET)*, 5(9), 866-869.
- Chandra, S., Gourisaria, M. K., GM, H., Konar, D., Gao, X., Wang, T., & Xu, M. (2022). Prolificacy assessment of spermatozoan via state-of-the-art deep learning frameworks. *IEEE Access*, 10, 13715-13727. <https://10.1109/ACCESS.2022.3146334>
- Chen, L., & Yuan, Y. (2018). Agricultural disease image dataset for disease identification based on machine learning. In J. Li, X. Meng, Y. Zhang, W. Cui & Du, Z. (Eds.), *International Conference on Big Scientific Data Management* (Vol. 11473, pp. 263-274). Springer. [https://doi.org/10.1007/978-3-030-28061-1\\_26](https://doi.org/10.1007/978-3-030-28061-1_26)
- Ferreira, A. D. S., Freitas, D. M., da Silva, G. G., Pistori, H., & Folhes, M. T. (2017). Weed detection in soybean crops using ConvNets. *Computers and Electronics in Agriculture*, 143, 314-324. <https://doi.org/10.1016/j.compag.2017.10.027>
- Etienne, A., & Saraswat, D. (2019). Machine learning approaches to automate weed detection by UAV-based sensors. In *Autonomous Air and Ground Sensing Systems for Agricultural Optimization and Phenotyping IV, International Society for Optics and Photonics* (Vol. 11008, Article 110080R). SPIE Digital Library. <https://doi.org/10.1117/12.2520536>
- Gourisaria, M. K., Harshvardhan, G. M., Agrawal, R., Patra, S. S., Rautaray, S. S., & Pandey, M. (2021). Arrhythmia detection using deep belief network extracted features from ECG signals. *International Journal of E-Health and Medical Communications (IJEHMC)*, 12(6), 1-24. <https://doi.org/10.4018/ijehmc.20211101.oa9>
- Harshvardhan, G. M., Sahu, A., Gourisaria, M. K., Singh, P. K., Hong, W. C., Singh, V., & Balabantaray, B. K. (2022). On the dynamics and feasibility of transferred inference for diagnosis of invasive ductal carcinoma: A perspective. *IEEE Access*, 10, 30870-30889. <https://doi.org/10.1109/ACCESS.2022.3159700>
- Khalajzadeh, H., Mansouri, M., & Teshnehlab, M. (2014). Face recognition using a convolutional neural network and simple logistic classifier. In V. Snásel, P. Krömer, M. Köppen & G. Schaefer (Eds.), *Soft Computing in Industrial Applications* (Vol. 223, pp. 197-207). Springer. [https://doi.org/10.1007/978-3-319-00930-8\\_18](https://doi.org/10.1007/978-3-319-00930-8_18)
- Rajagopalan, N., Narasimhan, V., Vinjimoor, S. K., & Aiyer, J. (2021). Retracted article: Deep CNN framework for retinal disease diagnosis using optical coherence tomography images. *Journal of Ambient Intelligence and Humanized Computing*, 12, 7569-7580. <https://doi.org/10.1007/s12652-020-02460-7>

- Sannigrahi, A., Singh, V., Gourisaria, M. K., & Srivastava, R. (2021). Diagnosis of skin cancer using feature engineering techniques. In *2021 3rd International Conference on Advances in Computing, Communication Control and Networking (ICAC3N)* (pp. 405-411). IEEE Publishing. <https://doi.org/10.1109/ICAC3N53548.2021.9725420>
- Sarah, S., Singh, V., Gourisaria, M. K., & Singh, P. K. (2021). Retinal disease detection using CNN through optical coherence tomography images. In *2021 5th International Conference on Information Systems and Computer Networks (ISCON)* (pp. 1-7). IEEE Publishing. <https://doi.org/10.1109/ISCON52037.2021.9702480>
- Singh, V., Gourisaria, M. K., GM, H., Rautaray, S. S., Pandey, M., Sahni, M., Leon-Castro, & Espinoza-Audelo, L. F. (2022a). Diagnosis of intracranial tumors via the selective CNN data modeling technique. *Applied Sciences*, *12*(6), Article 2900. <https://doi.org/10.3390/app12062900>
- Singh, V., Gourisaria, M. K., GM, H., & Singh, V. (2022b). Mycobacterium tuberculosis detection using CNN ranking approach. In T. K. Gandhi, D. Konar, B. Sen & Sharma, K. (Eds.), *Advanced Computational Paradigms and Hybrid Intelligent Computing*, (Vol. 1373, pp. 583-596). Springer. [https://doi.org/10.1007/978-981-16-4369-9\\_56](https://doi.org/10.1007/978-981-16-4369-9_56)
- Soystats. (2020). *International: World soybean production*. The American Soybean Association. <http://soystats.com/international-world-soybean-production/>
- Tang, J., Wang, D., Zhang, Z., He, L., Xin, J., & Xu, Y., (2017). Weed identification based on K-means feature learning combined with the convolutional neural network. *Computers and Electronics in Agriculture*, *135*, 63-70. <https://doi.org/10.1016/j.compag.2017.01.001>
- Sivakumar, A. N. V., Li, J., Scott, S., Psota, E., Jhala, A. J., Luck, J. D., & Shi, Y. (2020). Comparison of object detection and patch-based classification deep learning models on mid-to late-season weed detection in UAV imagery. *Remote Sensing*, *12*(13), Article 2136. <https://doi.org/10.3390/rs12132136>
- Yu, J., Sharpe, S. M., Schumann, A. W., & Boyd, N. S. (2019). Deep learning for image-based weed detection in turfgrass. *European Journal of Agronomy*, *104*, 78-84. <https://doi.org/10.1016/j.eja.2019.01.004>





## Failure Behavior and Mechanism of Pultruded Kenaf/Glass Hybrid Composite Under Compressive Impact Loading

Muhammad Fauzinizam Razali, Sareh Aiman Hilmi Abu Seman\*, Mohd Syakirin Rusdi and Megat Naiman Megat Anorhisham

*School of Mechanical Engineering, Universiti Sains Malaysia, 14300 Nibong Tebal, Pulau Pinang, Malaysia*

### ABSTRACT

A substantial amount of kenaf fiber research has been carried out recently to incorporate more sustainable materials into the production process. For many years, scientists have studied the properties of kenaf and the hybrid composites it may form. Composites made from kenaf and synthetic fibers were the focus of the majority of the study. Similarly, the researchers discovered mechanical characteristics as a fundamental truth. Despite this, earlier research on particular properties has not permitted using kenaf composites for load-bearing purposes. Nevertheless, kenaf composites can significantly influence car exteriors and other vital applications, even if their impact characteristics are only studied in other materials science disciplines. Due to this, dynamic failure behavior and mechanism of unidirectional kenaf and kenaf/glass hybrid composite compressive response were examined. Therefore, both composite specimens were loaded compressively under static and dynamic loading at a strain rate range of 0.1/s to 1700/s. The results showed that the failure behavior and mechanism of kenaf and kenaf/glass hybrid composite were different under static and dynamic loadings. Shear banding failure occurred at 60 degrees for kenaf composites. In contrast, kenaf/glass composites were fractured longitudinally along the fiber direction under static loading. Glass fibers in hybrid composites were more vulnerable to damage under microscopic analysis because they carried most loads. Consequently, the kenaf fibers in hybrid composites were less damaged than those in kenaf composites, which had fiber breakage, fiber splitting, and fiber-matrix debonding.

### ARTICLE INFO

#### Article history:

Received: 26 January 2022

Accepted: 22 April 2022

Published: 09 November 2022

DOI: <https://doi.org/10.47836/pjst.31.1.25>

#### E-mail addresses:

[mefauzinizam@usm.my](mailto:mefauzinizam@usm.my) (Muhammad Fauzinizam Razali)

[sarehaiman@usm.my](mailto:sarehaiman@usm.my) (Sareh Aiman Hilmi Abu Seman)

[syakirin@usm.my](mailto:syakirin@usm.my) (Mohd Syakirin Rusdi)

[megatnaiman6169@gmail.com](mailto:megatnaiman6169@gmail.com) (Megat Naiman Megat Anorhisham)

\* Corresponding author

*Keywords:* Compressive loading, failure behavior and mechanism, high strain rate, kenaf/glass composite

## INTRODUCTION

The usefulness of composite structural material, such as a hybrid combination of synthetic and natural fibers, is greatly enhanced because natural fibers are abundantly available and significantly less expensive. Furthermore, the growth in the market for hybrid fiber composites is encouraging research and development to provide even better utilization of natural fiber resources by improving its mechanical properties. However, the mechanical properties of natural fiber composite are significantly lower than synthetic fiber composite, which limits the application of natural fiber composite for structural purposes. Nevertheless, natural fibers are preferable when applied to improve composite materials since their lower manufacturing costs help to reduce the overall cost of composite fabrication while maintaining material properties.

Since the 1990s, the use of natural fiber composites has been the subject of a number of research investigations, most notably in the automobile (Ravishankar et al., 2019), household, and construction industries (Onuwe et al., 2018). The problem with natural fiber is that it is not as strong or as water-resistant as synthetic fiber. So, mixing natural and synthetic fibers to boost mechanical performance and repel moisture is highly beneficial. Several experiments with different combinations of natural and synthetic fibers are being conducted in the automotive, packaging, aerospace, and sports industries to apply secondary structures in their respective fields (Safri et al., 2018).

The mechanical properties of hybrid composite materials have been researched extensively using various research methodologies. For example, Zhang et al. (2013) studied the response of flax/glass composite under tensile loading. The tensile properties of the composite improved as the proportion of glass fiber rose. In a similar study, Sanjay and Yogesha (2018) found that mechanical characteristics strengthened when glass fiber was partially incorporated into the woven jute/kenaf/glass fiber hybrid composite.

Mishra et al. (2003) examined the tensile properties of glass/sisal and glass/pineapple leaf fiber reinforced polyester composites. Tensile strength was improved by hybridization in these composite materials. Using a woven combination of kenaf and glass fibers, Subramaniam et al. (2019) explored the characteristics of tension and quasi-static indentation in composite metal laminate made of metal woven fabric with similar fiber weight fractions and diverse fiber stacking sequences. Composites with glass fiber in the topmost layers showed great resistance to indentation and tensile strength when compared to composites that were not hybrid.

Carbon/flax fiber reinforced epoxy hybrid composites were analyzed by Sarasini et al. (2016) to find out the characteristics of low-velocity impact damage. Regarding the enhanced energy absorption capabilities of flax fibers, the hybrids showed to have greater fracture propagation resistance because of it. Kenaf/X-ray/epoxy hybrid composites also possess a surprisingly good energy absorption when impacted by hemispherical projectiles,

as discovered by Azmi et al. (2019). However, an impact force of 800N and an energy of 135 Joules are no match for this hybrid composite's impressive shock resistance.

Composites made from kenaf/glass and kenaf/epoxy, when impacted at 9J, had significant crack lengths of 52.92 and 100.61 millimeters, respectively. Kenaf/glass hybrid composites were resilient to impact because of the incorporated woven glass and kenaf. In the meantime, 16.02 mm damage to the glass/epoxy composite was measured (Majid et al., 2018). Other studies have shown that 25% kenaf and 75% glass fiber composites perform nearly identical to 100% glass fiber composites in terms of mechanical properties. Under low-speed testing, the kenaf/glass fiber hybrid composite, stacked up to 10 layers, could absorb 40J (Ismail et al., 2019).

Matrix cracking, delaminations, fiber fracture, and infiltration have all been observed due to low-velocity impact (Ahmad Nadzri et al., 2020). In all laminate kenaf/epoxy and hybrid composites studied by Majid et al. (2018), matrix cracking was found to be the primary source of damage. Woven kenaf fibers showed an interesting behavior as they acted as a mechanism to arrest the spread of matrix cracking and to confine its propagation through the weft and warp directions, as opposed to crack propagation along the radial direction under low-velocity impact loading.

Despite significant effort, little is known about the hybridization effect of glass fibers in the pultruded natural/synthetic fiber reinforced hybrid composites in the face of high impact loading, and much less about the specific failure behavior and mechanism. It is, therefore, necessary to investigate the static and dynamic mechanical responses of pultruded kenaf/glass hybrid composites to comprehend their potential application range.

## METHODOLOGY

The pultruded kenaf and kenaf/glass hybrid composites in this study were made of kenaf fiber with tex number 1400, E-glass unidirectional glass fibers and unsaturated polyester were produced through a pultrusion process with a diameter of 12.7 mm. Benzoyl peroxide (BPO) was utilized as an initiator, calcium carbonate ( $\text{CaCO}_3$ ) was used as a filler, and a powdered release agent was used in the resin combination. As a result, kenaf composite was produced with 80% fiber volume fraction. In contrast, the kenaf/glass hybrid composite was produced with a kenaf to glass fiber ratio of roughly 1:1 (Figure 1).

For dynamic and quasi-static uniaxial compression tests, kenaf

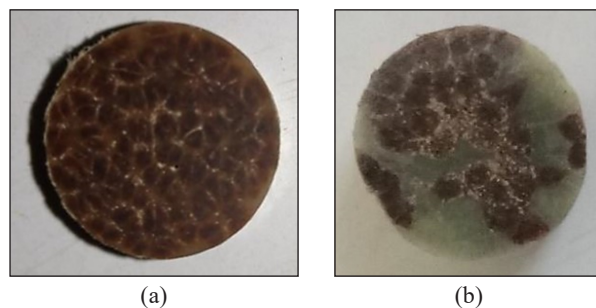


Figure 1. Pultruded specimens: (a) kenaf; and (b) kenaf glass hybrid composites

and kenaf/glass hybrid composite cylindrical specimens with a diameter of 12.7 mm were utilized. Abu Seman et al. (2019) employed the ideal slenderness ratio of 0.5 for the split Hopkinson pressure bar (SHPB) test. According to ASTM standard E9–89, a slenderness ratio of 1.5 was preferred for static tests, which resulted in the specimen in Figure 1. The lubricant was added to the contact field to help reduce the end friction between the sample and compression plates. The surface was ground to achieve maximum contact and remove any possible additional stress.

A Universal Testing Machine (UTM) was used to conduct the static compressive tests that identified the mechanical properties of the kenaf composites. In order to ensure that the moving head center is vertically above the specimen center, the specimen is positioned centrally between the two compression plates. A correct preload was provided at the crosshead location, where the device's loading mechanism arrives to prepare the specimen for a certain value before a test may be confirmed. The specimens were put under load until they reached a certain level of strain, and their load-bearing ability was measured. The displacement data points for each specimen were then calculated into stress-strain curves.

An SHPB constructed of steel bar (diameter of 12 mm) at the School of Aerospace Engineering, Universiti Sains Malaysia (USM), was used for the dynamic characterization of kenaf and kenaf/glass composites. The SHPB compression test setup is shown in Figure 2. SHPB functions on the elastic wave theory principle. The incident bar, transmission bar, and striker bar make up the SHPB. Compressed air moves the striking bar inside the barrel up to 2 bars. The cylindrical composite sample is placed between the transmission bars during the test. When the striking bar hits the incident bar, a rectangular compressive wave with continuous amplitude is generated. The incident bar, specimen and transmission bar then propagate that wave. Wave propagation partially reflects the tensile pulse at the boundary between the specimen and the incident bar. The data acquisition system (DAQ) collects and calibrates the voltage pulses generated by pressure gauges. The stress and strain generated by a dynamic equilibrium in the specimen at different times were then estimated with the elastic wave theory.

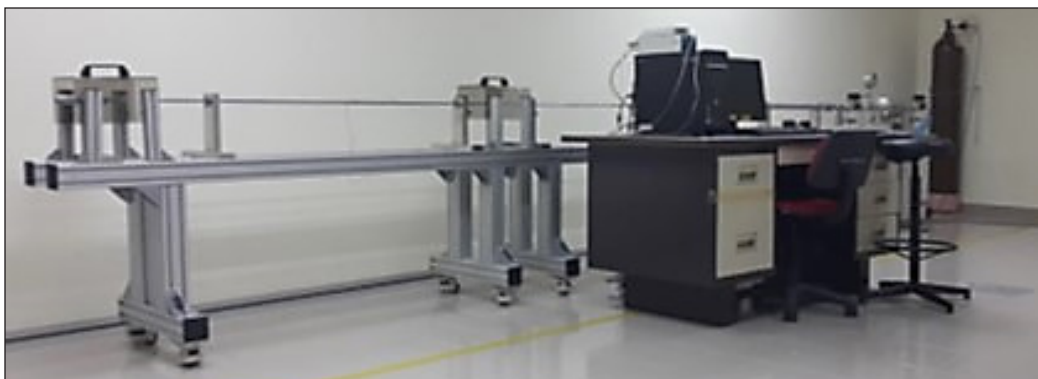


Figure 2. Split Hopkinson pressure bar

The specimen's strain rate, strain, and stress histories can be derived from a one-dimensional stress-wave analysis performed on the bars as shown in Equations 1 to 3:

$$\dot{\varepsilon} = \frac{C_0}{L_s} [\varepsilon_i(t) - \varepsilon_r(t) - \varepsilon_t(t)] \quad [1]$$

$$\varepsilon = \frac{C_0}{L_s} \int_0^t [\varepsilon_i(t) - \varepsilon_r(t) - \varepsilon_t(t)] \quad [2]$$

$$\sigma = \frac{A_0}{2A_s} E_0 [\varepsilon_i(t) - \varepsilon_r(t) - \varepsilon_t(t)] \quad [3]$$

$\varepsilon_i(t)$ ,  $\varepsilon_r(t)$ , and  $\varepsilon_t(t)$  are incident, reflected, and transmitted strain pulses,  $A_0$ ,  $E_0$  and  $C_0$  are bars cross-sectional area, Young's modulus and wave speed,  $A_s$  and  $L_s$  are the specimen's initial cross-sectional area and length.

Under conditions of homogeneous stress in the specimen, pulses become Equation 4:

$$[\varepsilon_i(t) + \varepsilon_r(t) = \varepsilon_t(t)] \quad [4]$$

Equations 1 to 3 can be simplified as Equations 5 to 7:

$$\dot{\varepsilon} = -2 \frac{C_0}{L_s} \varepsilon_r(t) \quad [5]$$

$$\varepsilon = -2 \frac{C_0}{L_s} \int_0^t \varepsilon_r(t) dt \quad [6]$$

$$\sigma = \frac{A_0}{A_s} E_0 \varepsilon_r(t) \quad [7]$$

As a result, the stress-strain data can be extracted from the collected strain gauge signals in an SHPB experiment.

With the Hitachi S-3700N scanning electron microscope (SEM), microscopic images of all specimens that suffered damage are captured at resolutions of up to 500  $\mu\text{m}$  to uncover different post-compression failures. Prior to SEM analysis, a carbon layer was applied to the samples using a sputter coater. For macroscopic pictures, a standard camera was used to document the damage behavior of the kenaf and kenaf/glass composites at low and high strain rates.

## RESULTS AND DISCUSSION

In the fiber direction of both composites, uniaxial static and dynamic compressive experiments have been carried out. Strain data captured by the strain gauge mounted on the incident and transmitter bars of SHPB during high strain rate testing of kenaf and

kenaf/glass composite is shown in Figure 3. The incident reflected and transmitted strain pulses are denoted as I, R and T, respectively. Those pulses have been extracted and used in Equations 5 to 7 to calculate the stress-strain curves of both composites. Stress-strain curves of kenaf and kenaf/glass composites were then compared under static and dynamic loadings (Figures 4 and 5).

Under static loading, for the kenaf composite, the initial straight section of the curve up to the yield point represents the specimen’s elastic responses. The yield point signals the beginning of inelastic behavior, where the curve displays stress hardening before its maximum stress is reached. The highest stress on the graph was the ultimate stress when the specimen collapsed after the maximum load-bearing capacity was surpassed. Strain

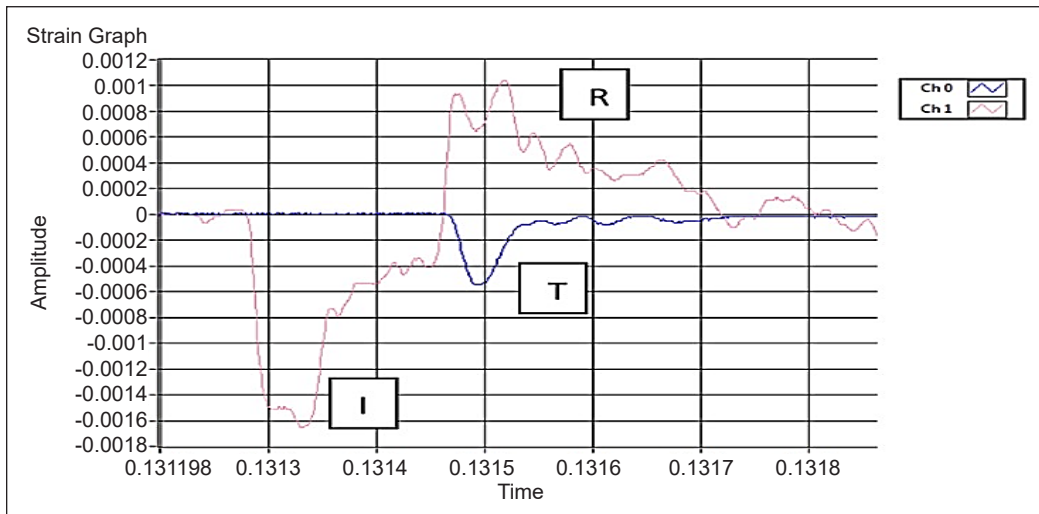


Figure 3. Incident, reflected and transmitted data obtained from SHPB

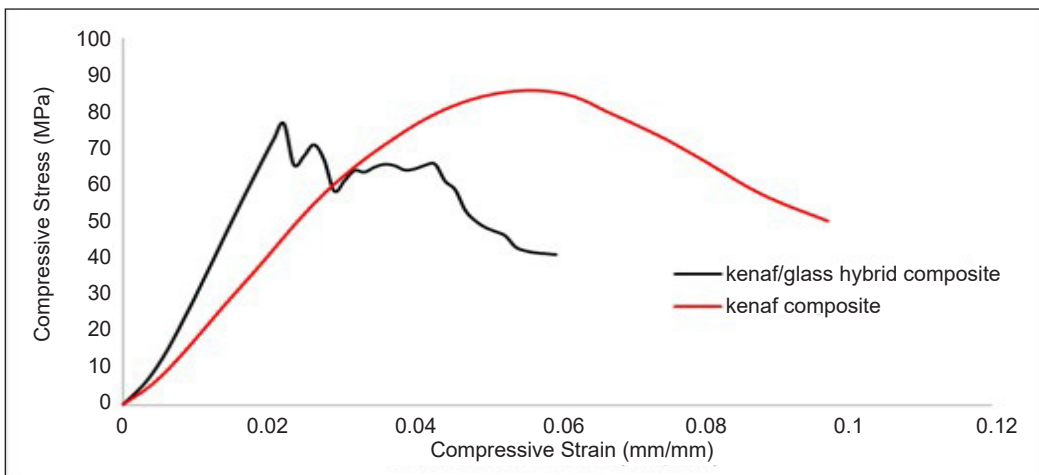


Figure 4. Stress-strain curves of kenaf and kenaf glass hybrid composite under static loading

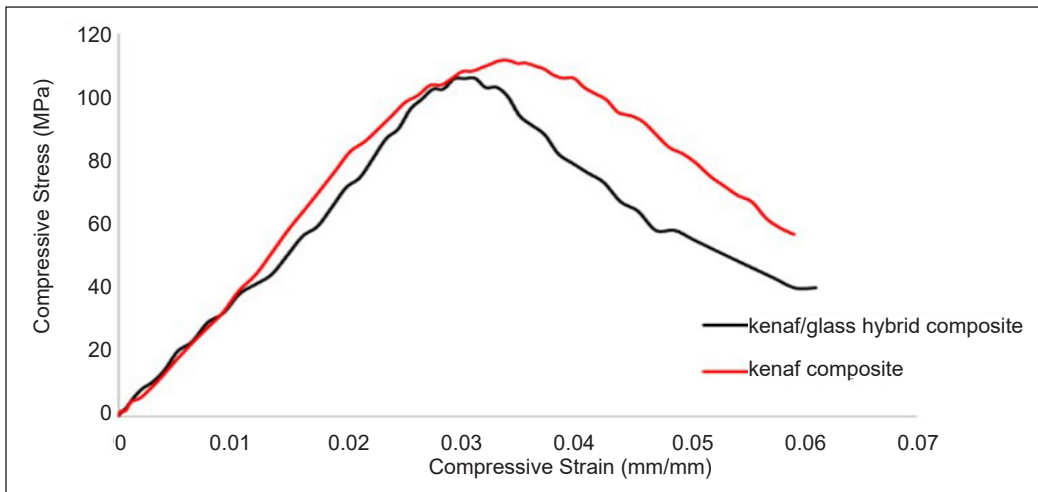


Figure 5. Stress-strain curves of kenaf and kenaf glass hybrid composite under dynamic loading

softening then takes place up to the residual strength of the specimen. Dewan et al. (2013) also observed similar stress-strain curves showing elastic-plastic behavior for a natural jute/polyester composite.

The kenaf/glass hybrid composite demonstrated different stress-strain curve behavior. After the initial straight section of the curve up to the yield point, no stress hardening region is observed. Nonetheless, after the maximum load-bearing capacity was surpassed, the specimen fractured brittlely, especially by the glass fibers. However, as shown in the stress-strain curves (Figure 4), even though some glass fibers failed, kenaf fibers could carry the applied load until the second maximum stress was achieved. Ashraf et al. (2021) also reported a similar stress-strain curve for a flax/glass hybrid composite that demonstrated elastic-brittle and dual fracture site behavior.

Under dynamic loading, the shape of stress-strain curves for kenaf and kenaf/glass composites are just slightly different. It is because loads were applied instantaneously on the fibers, and all fibers have deformed uniformly throughout the specimens. Nonetheless, for the kenaf/glass composite, it did not show any strain hardening region before maximum stress was reached. It happened because the glass fibers in the hybrid composite handled most of the load when subjected to dynamic loading (Figure 5).

Failure stress and strain of kenaf and kenaf/glass hybrid composites are shown in Table 1. As shown in Table 1, the failure stress of the kenaf/glass hybrid composite was slightly lower than the kenaf composite under both static and dynamic loadings. The slight reduction in failure stress can be explained by the low bonding strength between kenaf and glass fibers in the hybrid composite (Figures 6 and 7). According to Goutianos et al. (2018), the inter-fiber bond density and strength would have a greater impact on both Young's modulus and strength of the fiber-reinforced composites but only a modest



impact on the strain to failure. Post failure SEM images of hybrid composites after static and impact loading showed that the interface between kenaf/glass fibers would be the stress concentration area that contributed to the strength degradation. Tamrakar et al. (2021) noted a minor decline in flexural strength in their study when 12.5% of kenaf fibers were added to the kenaf/glass hybrid composite. Additionally, adding glass fibers to the hybrid composite has reduced the elongation capability, reflected in the failure strain reduction of as high as 60% when loaded statically. Sharba et al. (2016) also found similar outcomes where the addition of glass fibers in the kenaf woven hybrid composite did not significantly change the compressive strength (78MPa to 88MPa) but noticeably changed the failure strain from 1.8% to 0.8%.

Microscopically, distinct types of failure were shown between kenaf and kenaf/glass composites when compressed under static and impact loading (Figures 6 and 7). Matrix cracking was dominant for the kenaf composite, while fiber-matrix debonding was observed for the kenaf/glass composite when loaded statically. As explained before, the low bonding strength between kenaf and glass fibers would be the main culprit for the low failure strength of the hybrid composite. Glass fibers in hybrid composites were more vulnerable

Table 1  
Effect of strain rate on composites' mechanical properties and failure behavior

Loading rate	Specimen	Failure stress (MPa)	Failure Strain (mm/mm)	Type of failures
Static	Kenaf	86	0.056	Matrix cracking, shear banding
	Kenaf/glass	77	0.022	Fibres-matrix debonding, Glass fibres fracture, longitudinal splitting
Dynamic	Kenaf	111	0.034	Fibres-matrix debonding, Matrix cracking, shear splitting
	Kenaf/glass	106	0.031	Glass fibres fracture, kenaf fibres splitting, shear splitting

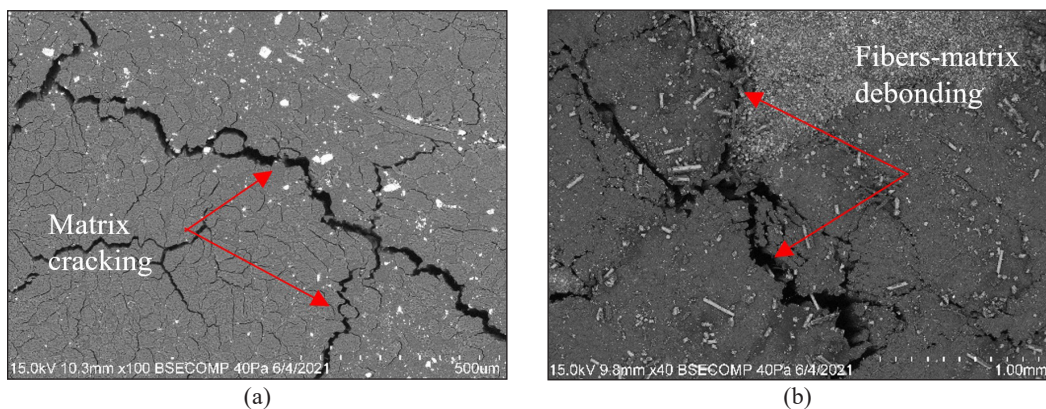


Figure 6. SEM images of specimens' surfaces: (a) kenaf; and (b) kenaf glass composites under static loading

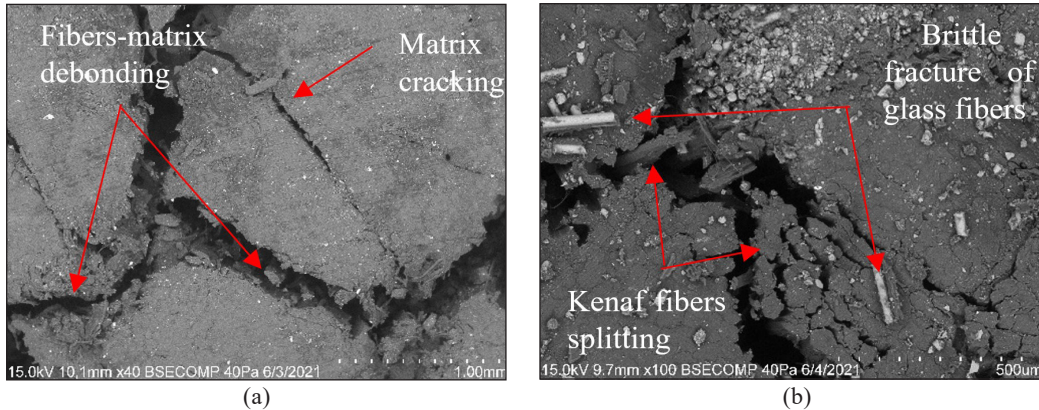


Figure 7. SEM images of specimens' surfaces; (a) kenaf; and (b) kenaf glass composites under dynamic loading

to degradation during dynamic loading because they carried most of the stresses. As a result, there were less fiber breakage, split fibers, and fiber-matrix debonding on kenaf fibers in the hybrid composites than on the kenaf composite specimens.

Different failure behaviors were observed macroscopically when kenaf and kenaf/glass hybrid compressed under static and impact loading, as listed in Table 1. Shear banding failure occurred at  $60^\circ$  for the kenaf composite, while the kenaf/glass hybrid composite failed with longitudinal splitting along the fiber's direction (Figure 8) under static loading. Matrix cracking is the first step of damage caused by quasi-static loading. When a greater external load is applied, the number of cracks increases, resulting in a second failure type known as shear banding. Matrix cracking was discovered to generate shear banding when strong transverse shear loads at the surrounding matrix surface affect the matrix surface and later evolve into a weak interfacial bond that leads to fiber fracture and fiber pullout. Under dynamic loading, both specimens were seen to fail, with longitudinal fibers splitting along the direction of the fibers, which occurred mostly in the outer region (Figure 9). Fiber splitting occurs when the hoop stress or normal stress in the direction perpendicular to the

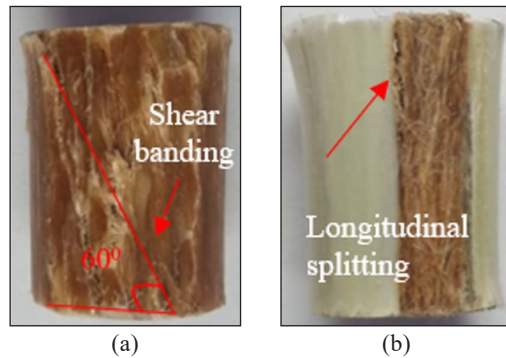


Figure 8. Failure of: (a) kenaf; and (b) kenaf glass hybrid composite, under static loading

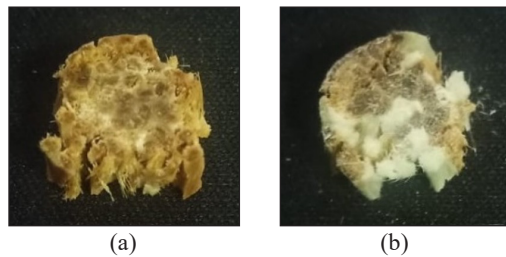


Figure 9. Failure of: (a) kenaf; and (b) kenaf glass hybrid composite, under dynamic loading

axis of cylindrical symmetry reaches the maximum allowed stress value. In the same way, exceeding hoop stresses can lead to fiber fracture in radial. (Rahul et al., 2019). Lee and Waas (1999) have also identified from their experiments that longitudinal fiber splitting, or brooming is the most common form of failure for glass fiber composites in the 10% to 30% fiber volume fraction range.

## CONCLUSION

This study has been performed on kenaf and kenaf/glass hybrid composite under two different strain-rate conditions to identify the effect of glass fiber hybridization on the overall failure behavior and mechanism of hybrid composites. The stress-strain curves behavior was more affected by the glass hybridization when compressed statically than when specimens failed at several points before completely fracturing. Hybridization resulted in a 5% reduction in failure stress and a 60% reduction in failure strain when the strain rate ranged from 0.02 to 1400/s. Through the hybridization of glass fibers, which added some stiffness, the failure mechanism of kenaf composite has been changed from shear banding failure to longitudinal splitting, which is observed along the fiber direction. Under microscopic observation, fiber-matrix debonding and interface debonding between fibers were dominant in the hybrid composite, which would be the main cause of low failure strength.

## ACKNOWLEDGEMENT

The authors want to thank the USM Short Term Grant 304/PMEKANIK/6315493 for supporting this research.

## REFERENCES

- Ashraf, W., Ishak, M. R., Zuhri, M. Y. M., Yidris, N., & Ya'acob, A. M. (2021). Experimental investigation on the mechanical properties of a sandwich structure made of flax/glass hybrid composite facesheet and honeycomb core. *International Journal of Polymer Science*, 2021, Article 8855952. <https://doi.org/10.1155/2021/8855952>
- Azmi, A. M. R., Sultan, M. T. H., Jawaid, M., Shah, A. U. M., Nor, A. F. M., Majid, M. S. A., Muhamad, S., & Talib, A. R. A. (2019). Impact properties of kenaf fibre/X-ray films hybrid composites for structural applications. *Journal of Materials Research and Technology*, 8(2), 1982-1990. <https://doi.org/10.1016/j.jmrt.2018.12.016>
- Dewan, M. W., Hossain, M. K., Hosur, M., & Jeelani, S. (2013). Thermomechanical properties of alkali treated jute-polyester/nanoclay biocomposites fabricated by VARTM process. *Journal of Applied Polymer Science*, 128(6), 4110-4123. <https://doi.org/10.1002/app.38641>

- Goutianos, S., Mao, R., & Peijs, T. (2018). Effect of inter-fibre bonding on the fracture of fibrous networks with strong interactions. *International Journal of Solids and Structures*, 136-137, 271-278. <https://doi.org/10.1016/j.ijsolstr.2017.12.020>
- Ismail, M. F., Sultan, M. T. H., Hamdan, A., Shah, A. U. M., & Jawaid, M. (2019). Low velocity impact behaviour and post-impact characteristics of kenaf/glass hybrid composites with various weight ratios. *Journal of Materials Research and Technology*, 8(3), 2662-2673. <https://doi.org/10.1016/j.jmrt.2019.04.005>
- Lee, S. H., & Waas, A. (1999). Compressive response and failure of fiber reinforced unidirectional composites. *International Journal of Fracture*, 100, 275-306. <https://doi.org/10.1023/A:1018779307931>
- Majid, D. L., Jamal, Q., & Manan, N. (2018). Low-velocity impact performance of glass fiber, kenaf fiber, and hybrid glass/kenaf fiber reinforced epoxy composite laminates. *BioResources*, 13(4), 8839-8852. <https://doi.org/10.15376/biores.13.4.8839-8842>
- Mishra, S., Mohanty, A. K., Drzal, L. T., Misra, M., Parija, S., Nayak, S. K., & Tripathy, S. S. (2003). Studies on mechanical performance of biofibre/glass reinforced polyester hybrid composites. *Composites Science and Technology*, 63(10), 1377-1385. [https://doi.org/10.1016/S0266-3538\(03\)00084-8](https://doi.org/10.1016/S0266-3538(03)00084-8)
- Nadzri, S. N. Z. A., Sultan, M. T. S., Shah, A. U. M., Safri, S. N. A., & Basri, A. A. (2020). A review on the kenaf/glass hybrid composites with limitations on mechanical and low velocity impact properties. *Polymers*, 12(6), Article 1285. <https://www.mdpi.com/2073-4360/12/6/1285>
- Onuwe, J., Ogunbode, E., Yatim, J., & Ali, S. (2018). An overview of kenaf fibre as a bio composites material in fabrication process for sustainable construction. *Environmental Technology & Science Journal*, 9(1), 134-144.
- Rahul, V., Alokita, S., Jayakrishna, K., Kar, V. R., Rajesh, M., Thirumalini, S., & Manikandan, M. (2019). Structural health monitoring of aerospace composites. In M. Jawaid, M. Thariq, & N. Saba (Eds.), *Structural Health Monitoring of Biocomposites, Fibre-Reinforced Composites and Hybrid Composites* (pp. 33-52). Woodhead Publishing. <https://doi.org/10.1016/B978-0-08-102291-7.00003-4>
- Ravishankar, B., Nayak, S. K., & Kader, M. A. (2019). Hybrid composites for automotive applications - A review. *Journal of Reinforced Plastics and Composites*, 38(18), 835-845. <https://doi.org/10.1177/0731684419849708>
- Safri, S. N. A., Sultan, M. T. H., Jawaid, M., & Jayakrishna, K. (2018). Impact behaviour of hybrid composites for structural applications: A review. *Composites Part B: Engineering*, 133, 112-121. <https://doi.org/10.1016/j.compositesb.2017.09.008>
- Sanjay, M., & Yogesha, B. (2018). Studies on hybridization effect of jute/kenaf/E-glass woven fabric epoxy composites for potential applications: Effect of laminate stacking sequences. *Journal of Industrial Textiles*, 47(7), 1830-1848. <https://doi.org/10.1177/1528083717710713>
- Sarasini, F., Tirillò, J., D'Altilia, S., Valente, T., Santulli, C., Touchard, F., Chocinski-Arnault, L., Mellier, D., Lampani, L., & Gaudenzi, P. (2016). Damage tolerance of carbon/flax hybrid composites subjected to low velocity impact. *Composites Part B: Engineering*, 91, 144-153. <https://doi.org/10.1016/j.compositesb.2016.01.050>
- Seman, S. A. H. A., Ahmad, R., & Akil, H. M. (2019). Experimental and numerical investigations of kenaf natural fiber reinforced composite subjected to impact loading. *Polymer Composites*, 40(3), 909-915. <https://doi.org/10.1002/pc.24758>

- Sharba, M. J., Leman, Z., Sultan, M. T. H., Ishak, M. R., & Hanim, M. A. A. (2016). Tensile and compressive properties of woven kenaf/glass sandwich hybrid composites. *International Journal of Polymer Science*, 2016, Article 1235048. <https://doi.org/10.1155/2016/1235048>
- Subramaniam, K., Malingam, S. D., Feng, N. L., & Bapokutty, O. (2019). The effects of stacking configuration on the response of tensile and quasi-static penetration to woven kenaf/glass hybrid composite metal laminate. *Polymer Composites*, 40(2), 568-577. <https://doi.org/10.1002/pc.24691>
- Tamrakar, S., Kiziltas, A., Mielewski, D., & Zander, R. (2021). Characterization of kenaf and glass fiber reinforced hybrid composites for underbody shield applications. *Composites Part B: Engineering*, 216, Article 108805. <https://doi.org/10.1016/j.compositesb.2021.108805>
- Zhang, Y., Li, Y., Ma, H., & Yu, T. (2013). Tensile and interfacial properties of unidirectional flax/glass fiber reinforced hybrid composites. *Composites Science and Technology*, 88, 172-177. <https://doi.org/10.1016/j.compscitech.2013.08.037>



## A Comparative Study on Dengue-Related Knowledge, Attitude, and Practice in Hotspot and Non-Hotspot Areas in Selangor

Siti Nor Izani Mustapha<sup>1</sup>, Shamarina Shohaimi<sup>1\*</sup>, Mohd Bakri Adam<sup>2</sup>, Meenakshii Nallappan<sup>1</sup>, Abdul Hafiz Ab Rahman<sup>3</sup> and Nader Salari<sup>4</sup>

<sup>1</sup>Department of Biology, Faculty of Science, Universiti Putra Malaysia, 43400 UPM, Serdang, Selangor, Malaysia

<sup>2</sup>Institute of Mathematical Research, Universiti Putra Malaysia, 43400 UPM, Serdang, Selangor, Malaysia

<sup>3</sup>Faculty of Social Sciences and Humanities, Universiti Kebangsaan Malaysia, 43600 UKM, Bangi, Selangor, Malaysia

<sup>4</sup>Department of Biostatistics, School of Public Health, Kermanshah University of Medical Sciences, Iran

### ABSTRACT

Dengue fever is a deadly vector-borne disease. Prevention strategies without specific drugs or vaccines emphasise community involvement in dengue vector control. Identifying dengue-related knowledge, attitudes, and behaviours is critical to developing more effective intervention strategies. A cross-sectional study compared the knowledge, attitudes, and practices on dengue in selected dengue hotspots and non-hotspot areas in Selangor, Malaysia. A self-administered questionnaire was distributed among 320 randomly selected residents. Data were analysed using an independent t-test and Spearman's rank-order correlation. Despite having a good understanding of the dengue virus, most respondents (83.1%) from both hotspot and non-hotspot areas were unaware that a person could be infected with the virus more than once in their lifetime, and 62.8% agreed that dengue patients could recover without treatment. Most respondents (76.9%) agreed that buying mosquito repellent is

a waste of money, and most reported not sleeping under the insecticide net at night (74.7%). Respondents from dengue hotspot areas had significantly higher attitude scores ( $32.00 \pm 4.60$ ) compared to those of non-hotspot regions ( $28.78 \pm 5.51$ ),  $t(307) = 5.674$ ,  $p < 0.05$ . There was a significant positive correlation between knowledge and attitude scores ( $r_s = 0.214$ ,  $p < 0.01$ ), between knowledge and practices ( $r_s = 0.563$ ,  $p < 0.01$ ), and attitude and practices ( $r_s = 0.374$ ,  $p < 0.01$ ). In addition to the high levels of knowledge

### ARTICLE INFO

#### Article history:

Received: 07 February 2022

Accepted: 07 June 2022

Published: 09 November 2022

DOI: <https://doi.org/10.47836/pjst.31.1.26>

#### E-mail addresses:

aniemustapha@gmail.com (Siti Nor Izani Mustapha)

shamarina@upm.edu.my (Shamarina Shohaimi)

bakri@upm.edu.my (Mohd Bakri Adam)

meenakshii@upm.edu.my (Meenakshii Nallappan)

abhafizrahman@gmail.com (Abdul Hafiz Ab Rahman)

n.salari@kums.ac.ir (Nader Salari)

\* Corresponding author

and practice, attitudes toward dengue must be improved to implement proper prevention measures.

*Keywords:* Attitude, dengue, hotspot area, knowledge, practice, Selangor

---

## INTRODUCTION

Dengue is a mosquito-borne viral disease that affects tropical and subtropical countries in the Americas, Southeast Asia, Africa, the Western Pacific, and the Eastern Pacific (Rodenhuis-Zybert et al., 2010). Dengue virus (DENV) is spread between hosts by female *Aedes aegypti* and *Aedes albopictus* mosquitoes (Kamal et al., 2018). Previously known as break-bone fever, the infection can cause asymptomatic to mild dengue fever (DF) (Jordan et al., 2020; Tantawichien, 2012).

Since there are no specific dengue drugs, controlling the mosquito populations has become a major priority. In Malaysia, dengue control is based on rapid reactive vector management, which includes source reduction, space spraying, and larviciding (Saadatian-Elahi et al., 2021). Although these measures effectively reduce mosquito populations, community understanding and acceptance are required to ensure their effectiveness. Therefore, a knowledge, attitudes, and practices survey was conducted among residents of the hotspot and non-hotspot areas to understand better what residents know, believe, and do. Understanding the knowledge, attitude, and practices will provide valuable information for resource allocation, planning, and implementing dengue prevention interventions (Andrade et al., 2020).

An earlier study conducted in 2016 by Ghani et al. (2019) compared the knowledge, attitude, and practices related to dengue among communities in dengue hotspots and non-hotspot areas of Selangor. An area with a dengue outbreak lasting over 30 days is classified as a dengue hotspot. In the study, Ghani et al. (2019) found that respondents living in non-hotspot areas had better knowledge and attitude, which may have contributed to the decrease in dengue cases from 2016 until 2018, as reported by the Ministry of Health Malaysia. However, in the 25<sup>th</sup> week of 2019, 59,615 cases were reported nationwide, up 96.2% from the same period the previous year (Ministry of Health Malaysia, 2019). In addition, 117 hotspot areas were reported, 92 of which were in Selangor. The increase in the number of cases and hotspot locations necessitated this study to determine the present state of dengue knowledge, attitudes and practises among people living in hotspot and non-hotspot areas.

## METHODOLOGY

### Study Setting

A descriptive cross-sectional survey was designed and conducted among selected residents in dengue hotspot and non-hotspot areas in Selangor, Malaysia, from July to September



2019. Selangor is located on the west coast of Peninsular Malaysia and had a population of 6.53 million in 2019 (Department of Statistics Malaysia, 2020). Selangor was chosen because it has had the most dengue cases in recent years.

This study included eight dengue hotspots and eight non-hotspots in Selangor. Areas with dengue outbreaks for 30 days or more were classified as hotspots, while areas without dengue outbreaks for 30 days or more were classified as non-hotspots. In contrast to a previous study conducted by Ghani et al. (2019), the study sites (Table 1) were chosen at random using SPSS Version 22 from the Malaysian Crisis Preparedness Resource Centre's (CRPC) list of dengue hotspot areas provided on the iDengue Remote Sensing website dated June 26, 2019 (Week 26) (Malaysian Remote Sensing Agency, 2019).

### Study Design and Respondents

A self-administered questionnaire was used to assess the level of dengue KAP in 16 selected hotspot and non-hotspot areas in Selangor from July to September 2019. The inclusion criteria for respondents include adults aged 18 and above living in Petaling District, Selangor and Malaysian. One hundred sixty respondents were selected in hotspot areas and 160 in non-hotspot areas. Each participant received a consent letter and a brief explanation. The respondents had the right to withdraw from the survey at any time. They could also ask questions if they did not understand them. Each survey session lasted 15 minutes, and the enumerator collected the completed questionnaire on the spot.

Table 1

*Selected sampling sites of dengue hotspot and non-hotspot areas in Selangor, June 26, 2019*

Dengue hotspot areas	Dengue non-hotspot areas
Apartment Baiduri, Shah Alam	Seksyen 2, Shah Alam
Dataran Otomobil, Shah Alam	Seksyen 11, Shah Alam
Palm Spring Condominium, Petaling Jaya	Mutiara Damansara, Petaling Jaya
Ridzuan Condominium, Petaling Jaya	Desa Mentari, Petaling Jaya
Pangsapuri Perdana, Shah Alam	Taman Tadisma, Shah Alam
Kampung Bukit Sungai Puteh, Ampang Jaya	Taman Lembah Jaya, Ampang Jaya
Mentari Court, Petaling Jaya	SS 9, Petaling Jaya
Gugusan Dedap, Petaling Jaya	Gugusan Semarak, Petaling Jaya
Kampung Baru Hicom, Shah Alam	Taman Sri Muda, Shah Alam

### Instrument

The questionnaire was based on published studies on dengue-related knowledge, attitude, and practice (KAP). The questionnaire used in this study differed from that used in the study conducted by Ghani et al. (2019). The questionnaire used in the present study consisted of four parts. Part 1 consisted of 20 closed-ended questions about dengue knowledge (yes/

no), while Part 2 consisted of 14 closed-ended questions about dengue attitude. “Strongly disagree,” “disagree,” “agree,” and “strongly agree” were the options for dengue attitudes. Part 3 had ten closed-ended questions about dengue prevention practices. The respondents could select “no” or “yes” for each item. Finally, part 4 included nine closed-ended questions to collect respondents’ socio-demographic data. Putting the socio-demographic items at the end of the questionnaire encourages respondents to fill it out because some may find them intrusive and threatening, affecting their performance on the other KAP items (Parmenter & Wardle, 2000).

The questionnaire was pretested among 200 residents of Petaling District to ensure its clarity. The data was entered into SPSS version 22 and tested for reliability. The Cronbach’s alpha coefficient for dengue knowledge was 0.70, dengue attitude was 0.824, and dengue prevention practices were 0.702. These values reflect the measuring questionnaire’s high reliability and internal consistency (Flynn et al., 1990; Streiner, 2003).

### Sampling and Data Collection

A total of 320 respondents were recruited using a systematic random sampling method to participate in this study. The sample size was calculated using Cochran’s formula in Equation 1 (Cochran, 1977).

$$n_o = \frac{z^2pq}{d^2} = \frac{1.960^2 \times (0.296 \times 0.704)}{0.050^2} = 320 \quad (1)$$

where

$n_o$  = the required sample size,

$z = 1.960$  (standard normal score at 95% confidence interval)

$p = 0.296$  (estimated prevalence present in the population) (Othman et al., 2019)

$q = 1 - p$

$d =$  an acceptance error of 5%

Respondents were approached in the selected residential areas. The enumerators chose one qualified respondent for every three houses they passed, yielding 320 eligible respondents (Ghani et al., 2019). This method was used to ensure that everyone in the population had an equal chance of being chosen (Acharya et al., 2013).

### Data Handling and Analysis

Before data entry into SPSS, collected questionnaires were checked for appropriateness and completeness of responses (Diema et al., 2019). For the analyses to assess the level of knowledge, correct responses were scored as one, and wrong responses were scored as 0. The scores ranged from 0 to 20, and each response was classified into three levels based on Bloom’s cut-off point: good knowledge level (16 to 20), fair knowledge level

(12 to 15), and poor knowledge level ( $\leq 11$ ). Attitude towards dengue was measured by a four-point Likert scale that ranged from 1 (strongly disagree) to 4 (strongly agree). The scores ranged from 14 to 56, and each response was classified into three levels according to Bloom's cut-off point: good attitude level (45 to 56), fair attitude level (34 to 44), and poor attitude level ( $\leq 33$ ). For practice, each positive response was scored one, and the negative response was scored 0. The scores ranged from 0 to 10, and respondents' practice levels were defined as good practice level (9 to 11), fair practice level (7 to 8), and poor practice level ( $\leq 6$ ) based on Bloom's cut-off point.

The data was entered and analysed by using SPSS version 22. Descriptive analysis was done to calculate frequencies and percentages of socio-demographic characteristics of the respondents and the proportion of the correct answer for each item for every domain. An Independent t-test was used to compare the mean of knowledge, attitude, and practice scores between non-hotspot and hotspot areas Spearman's rank-order correlation was conducted to examine the relationship between knowledge, attitude, and practice scores.

### **Ethical Considerations**

The National Institutes approved the study of Health Malaysia Medical Research Ethics Committee (Reference No. KKM.NIHSEC.P18-1250 (6)) on June 20, 2018. Human participant protection procedures were adopted. The respondents were fully informed of the study's purpose, the questions to be asked, the data collection process and the data use before consenting to participate. The consent was verbal, as most people dislike signing documents (Khun & Manderson, 2007). The respondent's identity was protected. After collection, the data is entered into a computer only the researchers can access.

## **RESULTS**

### **Socio-Demographic Characteristics of Respondents**

Table 2 provides information on the socio-demographic characteristics of 320 respondents from Selangor enrolled in this study. Females constituted the majority of the recruited respondents (70.7%). In this study, the age was categorised according to the timeline of generations. Respondents aged 43 to 54 years formed the majority (46.7%), and only a small percentage of the respondents were aged 18 to 21 and above 73 years, both at 2.2%. Most respondents were married (87.4%), while the rest were single (7.7%), divorced (3.9%), and widowed (1.0%). Nearly three-quarters of the respondents were Malay (73.5%), followed by Chinese (18.5%) and Indian (8.0%). Most respondents were employed, accounting for 70.2% of the total sample (Table 3). For many respondents, secondary school was their highest educational attainment (70.0%). Over half of the respondents earned between RM3000 and RM5999 per month on average, which suggests that they are well off (53.9%). Nearly a third of the respondents said that at least one family member had been

Table 2  
Socio-demographic characteristics of respondents

Characteristics	Frequency (N=320)	Percentage (%)
Gender		
Male	93	29.3
Female	224	70.7
Age group		
18-21 years	7	2.2
22-42 years	123	38.8
43-54 years	148	46.7
55-73 years	32	10.1
>73 years	7	2.2
Marital status		
Single	24	7.7
Married	271	87.4
Divorce	12	3.9
Widowed	3	1.0
Race		
Malay	230	73.5
Chinese	58	18.5
Indian	25	8.0
Occupation		
Employed	221	70.2
Retired	34	10.8
Housewife	40	12.7
Student	9	2.9
Unemployed	11	3.5
Education level		
Tertiary education	67	21.1
Secondary education	222	70.0
Primary education	27	8.5
Informal education	1	0.3
Household average monthly income		
≤RM999	7	2.3
RM1000-RM2999	105	34.1
RM3000-RM5999	166	53.9
≥RM6000	30	9.7
Previous dengue infection (own self)		
Yes	57	18.0
No	260	82.0
Previous dengue infection (family member)		
Yes	93	29.5
No	222	70.5

RM indicates Ringgit Malaysia

diagnosed with dengue fever (29.5%). Only a very small percentage of the respondents had been exposed to dengue before (18.0%).

### Dengue-Related Knowledge

Table 3 presents the results of the Chi-square test of item-by-item analysis of respondents' knowledge of dengue. Respondents from dengue hotspots and non-hotspot areas showed comparable knowledge about the causal agent of dengue; dengue could affect all age groups and the capability of *Aedes* mosquitoes to transmit dengue. Most respondents from non-hotspot areas knew that dengue could be transmitted through blood transfusion, and it was significantly different from respondents in hotspot areas,  $p < 0.05$ . Surprisingly, only 24.4% of the respondents knew that a person could be infected with dengue more than once. A significant association was found between respondents' knowledge and hotspot and non-hotspot areas,  $p < 0.05$ .

Respondents from the hotspot and non-hotspot areas showed significant differences in knowledge about the characteristics of *Aedes* mosquitoes, with more respondents from hotspots being able to identify the features of *Aedes* mosquitoes with black and white stripes on their legs and bodies,  $p < 0.05$ . Most respondents (93.8%) knew that *Aedes* mosquitoes could not breed in stagnant dirty water, whereas only 6.3% of respondents answered incorrectly for this item. Both respondents from the hotspot (93.1%) and non-hotspot areas (93.1%) showed similar knowledge of mosquito peak biting times between dawn and dusk.

Table 3  
*Item-by-item analysis of respondents' knowledge of dengue*

Variables	Hotspot, n (%)	Non-hotspot n (%)	Total n (%)	p-value
<b>Knowledge of dengue transmission</b>				
Dengue is caused by the virus				
Yes	142 (88.8)	149 (93.1)	291 (90.9)	0.173
No	18 (11.3)	11 (6.9)	29 (9.1)	
Dengue affects all age group				
Yes	158 (98.8)	158 (98.8)	316 (98.8)	1.000
No	2 (1.3)	2 (1.3)	4 (1.3)	
<i>Aedes</i> mosquito can transmit dengue				
Yes	157 (98.1)	158 (98.8)	315 (98.4)	0.652
No	3 (1.9)	2 (1.3)	5 (1.6)	
Blood transfusion can transmit dengue				
Yes	125 (78.1)	141 (88.7)	266 (83.4)	0.011*
No	35 (21.9)	18 (11.3)	53 (16.6)	
A person can only get dengue once in their lifetime				
Yes	133 (83.1)	109 (68.1)	242 (75.6)	0.002*
No	27 (16.9)	51 (31.9)	78 (24.4)	
<b>Knowledge of dengue vector</b>				
<i>Aedes</i> mosquito has black and white stripes on its leg and body				
Yes	155 (96.9)	140 (87.5)	295 (92.2)	0.002*
No	5 (3.1)	20 (12.5)	25 (7.8)	
<i>Aedes</i> mosquito breeds in stagnant dirty water				
Yes	6 (3.8)	14 (8.8)	20 (6.3)	0.065
No	154 (96.3)	146 (91.3)	300 (93.8)	
<i>Aedes</i> mosquito bites/feeds during dawn and dusk				
Yes	148 (93.1)	149 (93.1)	297 (93.1)	0.988
No	11 (6.9)	11 (6.9)	22 (6.9)	
<b>Knowledge of dengue symptoms</b>				
Having a fever reaching 40°C				
Yes	147 (91.9)	141 (88.1)	288 (90.0)	0.264
No	13 (8.1)	19 (11.9)	32 (10.0)	
Consistent headache				
Yes	149 (93.1)	152 (95.0)	301 (94.1)	0.478
No	11 (6.9)	8 (5.0)	19 (5.9)	
Muscle and joint pain				
Yes	151 (94.4)	148 (92.5)	299 (93.4)	0.498
No	9 (5.6)	12 (7.5)	21 (6.6)	
Small and red pinhead-like rashes appear on the body				
Yes	139 (86.9)	123 (76.9)	262 (81.9)	0.020*
No	21 (13.1)	37 (23.1)	58 (18.1)	
Pain behind the eyes				
Yes	141 (88.1)	126 (78.8)	267 (83.4)	0.024*
No	19 (11.9)	34 (21.3)	53 (16.6)	

Table 3 (continue)

Variables	Hotspot, n (%)	Non-hotspot n (%)	Total n (%)	p-value
<b>Nausea and vomit</b>				
Yes	142 (88.8)	124 (77.5)	266 (83.1)	0.007*
No	18 (11.3)	36 (22.5)	54 (16.9)	
<b>Knowledge of dengue treatment</b>				
There is a vaccine to prevent dengue				
Yes	13 (8.1)	27 (16.9)	40 (12.5)	0.018*
No	147 (91.9)	133 (83.1)	280 (87.5)	
There is medication for dengue				
Yes	22 (13.8)	25 (15.6)	47 (14.7)	0.636
No	138 (86.3)	135 (84.4)	273 (85.3)	
<b>Knowledge of dengue prevention</b>				
Removing standing water can prevent mosquitoes to breed				
Yes	157 (98.1)	145 (90.6)	302 (94.4)	0.004*
No	3 (1.9)	15 (9.4)	18 (5.6)	
Covering water-filled containers can prevent mosquitoes to breed				
Yes	156 (97.5)	147 (92.5)	303 (95.0)	0.039*
No	4 (2.5)	12 (7.5)	16 (5.0)	
Insecticide spray can kill adult mosquitoes				
Yes	157 (98.1)	153 (95.6)	310 (96.9)	0.199
No	3 (1.9)	7 (4.4)	10 (3.1)	
Larvicide such as Abate is used to kill mosquito larvae				
Yes	158 (98.8)	152 (96.2)	310 (97.5)	0.147
No	2 (1.3)	6 (1.9)	8 (2.5)	

\*Indicates a significant difference as a p-value less than 0.05

Most respondents who live in both areas have correctly identified the dengue symptoms. Both respondents from the hotspot and non-hotspot areas had comparable knowledge about dengue symptoms, such as body temperature as high as 40°C, consistent headache, and muscle and joint pain. On the other hand, a significantly higher percentage of respondents from hotspot areas knew that skin rash, pain behind the eyes, nausea, and vomiting were symptoms of dengue fever than respondents from non-hotspot areas ( $p < 0.05$ ).

Responses to the item 'there is a vaccine to prevent dengue' differed significantly between the hotspot and non-hotspot areas,  $p < 0.05$ . More respondents from hotspot areas (91.9%) knew that the dengue vaccine is unavailable in Malaysia to prevent dengue infection compared to respondents from non-hotspot areas (83.1%). In addition, respondents from the hotspot and non-hotspot areas had similar knowledge about the absence of specific medication to treat dengue.

Regarding knowledge on dengue prevention, the responses to each item were statistically significant between the hotspot and non-hotspot areas except for the item 'insecticide spray can kill adult mosquito' and 'larvicide such as Abate is used to kill

mosquito larvae. More respondents from hotspot areas knew that removing standing water and covering water-filled containers could prevent mosquitoes from breeding than respondents from non-hotspot areas,  $p < 0.05$ . Respondents from the hotspot and non-hotspot areas have comparable knowledge about insecticides capable of killing adult mosquitoes and larvicides such as Abate to kill mosquito larvae.

### **Attitudes Towards Dengue Disease**

Table 4 shows the results of an item-by-item analysis of attitude related to dengue using the Chi-square test. The responses to each item were statistically significant between the hotspot and non-hotspot areas except for the responses to the item 'spending money to buy mosquito repellent is a waste' and 'preventing dengue is government's responsibility'. Most respondents from hotspot areas believed that they were at risk of getting dengue and that anyone could be infected by dengue, compared to respondents from non-hotspot areas. More than 90.0% of the respondents from hotspot areas agreed and strongly agreed that dengue is a life-threatening disease and can be prevented compared to respondents from non-hotspot areas. Surprisingly, only a few respondents (13.7%) disagreed and strongly disagreed that eliminating mosquito breeding sites could reduce the mosquito population, and most of them were from non-hotspot areas. Most respondents (93.8%) from hotspot areas agreed and strongly agreed that avoiding mosquito bites could prevent dengue, 14.4% higher than respondents from non-hotspot areas. Health authorities often implement dengue campaigns to educate the community about the dengue-related issue. In this study, a higher percentage of the respondents from hotspot areas agreed and strongly agreed that the dengue campaign is beneficial compared to respondents from non-hotspot areas.

A total of 31 respondents from non-hotspot areas agreed and strongly agreed that fogging is enough to prevent dengue, 5.6% lower than the total percentage of respondents from hotspot areas that answered 'agreed' and 'strongly agreed'. Most respondents from the hotspot and non-hotspot areas agreed and strongly agreed that spending money to buy mosquito repellent is a waste. Likewise, less than half of the respondents from the hotspot and non-hotspot areas agreed and strongly agreed that preventing dengue is the government's responsibility (40.9%).

More respondents from hotspot areas (90.6%) agreed and strongly agreed that the public plays an important role in preventing dengue compared to respondents from non-hotspot areas (69.4%). In addition, more respondents from hotspot areas (78.1%) strongly agreed that they could prevent dengue compared to respondents from non-hotspot areas (58.1%). Overall, only 23.2% of the respondents from the hotspot and non-hotspot areas disagreed and strongly disagreed that a dengue-infected person could recover without any treatment. Regarding vaccination, 267 respondents from the hotspot and non-hotspot areas agreed and strongly agreed that vaccination is important to prevent dengue.



Table 4  
Item-by-item analysis of respondents' attitudes on dengue

Variables	Hotspot n (%)	Non-hotspot n (%)	Total n (%)	p-value
Anyone can get dengue				
<i>Strongly agree</i>	37 (23.1)	10 (6.3)	47 (14.7)	<0.001*
<i>Agree</i>	100 (62.5)	106 (66.3)	206 (64.4)	
<i>Disagree</i>	19 (11.9)	39 (24.4)	58 (18.1)	
<i>Strongly disagree</i>	4 (2.5)	6 (3.1)	9 (2.9)	
I am at risk of getting dengue				
<i>Strongly agree</i>	27 (16.9)	10 (6.3)	37 (11.6)	0.001*
<i>Agree</i>	117 (73.1)	123 (76.9)	240 (64.4)	
<i>Disagree</i>	13 (8.1)	27 (16.9)	40 (12.5)	
<i>Strongly disagree</i>	3 (1.9)	0 (0.0)	3 (0.9)	
Dengue is a life-threatening disease				
<i>Strongly agree</i>	47 (29.4)	21 (13.1)	68 (21.3)	<0.001*
<i>Agree</i>	101 (63.1)	107 (66.9)	208 (65.0)	
<i>Disagree</i>	11 (6.9)	26 (16.3)	37 (11.6)	
<i>Strongly disagree</i>	1 (0.6)	6 (3.8)		
Dengue can be prevented				
<i>Strongly agree</i>	117 (73.1)	91 (56.9)	208 (65.0)	<0.001*
<i>Agree</i>	36 (22.5)	33 (20.6)	69 (21.6)	
<i>Disagree</i>	6 (3.8)	36 (22.5)	42 (13.1)	
<i>Strongly disagree</i>	1 (0.6)	0 (0.0)	2 (0.6)	
Eliminating mosquito breeding sites can reduce mosquito				
<i>Strongly agree</i>	115 (71.9)	93 (58.1)	208 (65.0)	<0.001*
<i>Agree</i>	37 (23.1)	31 (19.4)	68 (21.3)	
<i>Disagree</i>	8 (5.0)	34 (21.3)	42 (13.1)	
<i>Strongly disagree</i>	0 (0.0)	2 (1.3)	2 (0.6)	
Avoiding mosquito bites can prevent dengue				
<i>Strongly agree</i>	120 (75.0)	97 (60.6)	217 (67.8)	0.001*
<i>Agree</i>	30 (18.8)	30 (18.8)	60 (18.8)	
<i>Disagree</i>	10 (6.3)	27 (16.9)	37 (11.6)	
<i>Strongly disagree</i>	0 (0.0)	6 (3.8)	6 (1.9)	
Dengue campaign is beneficial				
<i>Strongly agree</i>	121 (75.6)	96 (60.0)	217 (67.8)	0.007*
<i>Agree</i>	25 (15.6)	31 (19.4)	56 (17.5)	
<i>Disagree</i>	11 (6.9)	21 (13.1)	32 (10.0)	
<i>Strongly disagree</i>	3 (1.9)	12 (7.5)	15 (4.7)	
Fogging is enough to prevent dengue				
<i>Strongly agree</i>	24 (15.0)	31 (19.4)	55 (17.2)	0.014*
<i>Agree</i>	34 (21.3)	18 (11.3)	52 (16.3)	
<i>Disagree</i>	9 (5.6)	21 (13.1)	30 (9.4)	
<i>Strongly disagree</i>	93 (58.1)	90 (56.3)	183 (57.2)	
Spending money to buy mosquito repellent is a waste				
<i>Strongly agree</i>	125 (78.1)	121 (75.6)	246 (76.9)	0.893
<i>Agree</i>	26 (16.3)	31 (19.4)	57 (17.8)	
<i>Disagree</i>	5 (3.1)	4 (2.5)	9 (2.8)	
<i>Strongly disagree</i>	4 (2.5)	4 (2.5)	8 (2.5)	

Table 4 (continue)

Variables	Hotspot n (%)	Non-hotspot n (%)	Total n (%)	p-value
Preventing dengue is the government's responsibility				
<i>Strongly agree</i>	35 (21.9)	40 (25.0)	75 (23.4)	0.191
<i>Agree</i>	24 (15.0)	32 (20.0)	56 (17.5)	
<i>Disagree</i>	9 (5.6)	3 (1.9)	12 (3.8)	
<i>Strongly disagree</i>	92 (57.5)	85 (53.1)	177 (55.3)	
The public played an important role in preventing dengue				
<i>Strongly agree</i>	124 (77.5)	88 (55.0)	212 (66.3)	<0.001*
<i>Agree</i>	21 (13.1)	23 (14.4)	44 (13.8)	
<i>Disagree</i>	9 (5.6)	29 (18.1)	38 (11.9)	
<i>Strongly disagree</i>	6 (3.8)	20 (12.5)	26 (8.1)	
I am capable of preventing dengue				
<i>Strongly agree</i>	125 (78.1)	93 (58.1)	218 (68.1)	<0.001*
<i>Agree</i>	27 (16.9)	37 (23.1)	64 (20.0)	
<i>Disagree</i>	8 (5.0)	26 (16.3)	34 (10.6)	
<i>Strongly disagree</i>	0 (0.0)	4 (2.5)	4 (1.3)	
Dengue patients can recover without any treatment				
<i>Strongly agree</i>	103 (64.4)	98 (61.3)	201 (62.8)	0.001*
<i>Agree</i>	25 (15.6)	20 (12.5)	45 (14.1)	
<i>Disagree</i>	20 (12.5)	41 (25.6)	61 (19.1)	
<i>Strongly disagree</i>	12 (7.5)	1 (0.6)	13 (4.1)	
Vaccination is important to prevent dengue				
<i>Strongly agree</i>	121 (75.6)	87 (54.4)	208 (65.0)	0.001*
<i>Agree</i>	21 (13.1)	38 (23.8)	59 (18.4)	
<i>Disagree</i>	11 (6.9)	23 (14.4)	34 (10.6)	
<i>Strongly disagree</i>	7 (4.4)	12 (7.5)	19 (5.9)	

\*Indicates a significant difference as a p-value less than 0.05

## Practices Against Dengue

Table 5 summarises the Chi-square test of item-by-item analysis of practice against dengue transmission. Respondents from the hotspot and non-hotspot areas demonstrated significant differences in practising dengue prevention measures except for wearing long pants and long-sleeve shirts while outdoors, cleaning refrigerator trays once a week, and covering water-filled containers indoors and outdoors, participating in neighbourhood clean-up activities and using insecticide spray to kill mosquitoes. Regarding avoiding mosquito contact, only 81 out of 320 respondents used insecticide bed nets while sleeping at night. Of these, 57 respondents were from non-hotspot areas, while the remaining 24 were from hotspot areas. In addition, most respondents from the hotspot and non-hotspot areas took personal measures against dengue by using mosquito repellent on their bodies (79.1%) and wearing long pants and long-sleeve shirts while outdoors (87.2%). On the other hand, more respondents from hotspot areas reported that they properly disposed of their household garbage, removed standing water inside and outside their houses, cleaned refrigerator

trays once a week, covered water-filled containers indoors and outdoors, participated in neighbourhood clean-up activities, open windows and doors during fogging activity, used Abate to kill mosquito larvae, and used insecticide spray to kill the adult mosquito.

Table 5  
*Item-by-item analysis of respondents' practice on dengue*

Variables	Hotspot (%)	Non-hotspot n (%)	Total n (%)	p-value
I sleep under an insecticide net at night				
Yes	24 (7.5)	57 (17.8)	81 (25.3)	< 0.001*
No	136 (42.5)	103 (32.2)	239 (74.7)	
I use mosquito repellent on my body				
Yes	119 (37.2)	134 (41.9)	253 (79.1)	0.039*
No	41 (12.8)	26 (8.1)	67 (20.9)	
I wear long pants and long sleeve shirt while outdoors				
Yes	134 (41.9)	145 (45.3)	279 (87.2)	0.066
No	26 (8.1)	15 (4.7)	41 (12.8)	
I properly dispose of household garbage				
Yes	154 (48.1)	142 (44.4)	296 (92.5)	0.011*
No	6 (1.9)	18 (5.6)	24 (7.5)	
I remove standing water indoor and outdoor				
Yes	153 (47.8)	137 (42.8)	290 (90.6)	0.002*
No	7 (2.2)	23 (7.2)	30 (9.4)	
I clean the refrigerator tray once a week				
Yes	150 (46.9)	144 (45.0)	294 (91.9)	0.220
No	10 (3.1)	16 (5.0)	26 (8.1)	
I cover water-filled containers indoor and outdoor				
Yes	147 (45.9)	138 (43.1)	285 (89.1)	0.107
No	13 (4.1)	22 (6.9)	35 (10.9)	
I participate in neighbourhood clean-up activities				
Yes	146 (45.6)	139 (43.4)	285 (89.1)	0.210
No	14 (4.4)	21 (6.6)	35 (10.9)	
I open windows and doors during fogging activity				
Yes	152 (47.5)	132 (41.3)	284 (88.8)	< 0.001*
No	8 (2.5)	28 (8.8)	36 (11.3)	
I use Abate to kill mosquito larvae				
Yes	152 (47.5)	139 (43.4)	291 (90.9)	0.011*
No	8 (2.5)	21 (6.6)	29 (9.1)	
I use insecticide spray to kill mosquitoes				
Yes	155 (48.4)	149 (46.6)	304 (95.0)	0.124
No	5 (1.6)	11 (3.4)	16 (5.0)	

\*Indicates a significant difference as a p-value less than 0.05

### Mean Knowledge, Attitude, and Practice Scores

The results of the independent t-test used to compare the mean of knowledge, attitude, and practice scores between respondents who live in dengue hotspot areas and those who do not live in hotspot areas are shown in Table 6. The findings indicate that respondents who live in hotspot areas had statistically significantly higher attitude scores ( $32.00 \pm 4.60$ ) compared to those who live in non-hotspot areas ( $28.78 \pm 5.51$ ),  $t(307) = 5.674$ ,  $p < 0.05$ . On the other hand, no significant differences were found between areas with knowledge scores and practice scores. Respondents who live in hotspot areas seemed to have slightly better knowledge and good practices of dengue prevention measures; however, this was not statistically significant.

### Correlation between Dengue Knowledge, Attitude, and Practice Scores

This study uses Spearman's rank-order correlation to examine the relationship between knowledge, attitude, and practice scores. As shown in Table 7, there was a positive correlation between knowledge and attitude scores ( $r_s = 0.214$ ,  $p < 0.01$ ), between knowledge and practices ( $r_s = 0.563$ ,  $p < 0.01$ ), and attitude and practices ( $r_s = 0.374$ ,  $p < 0.01$ ), which were statistically significant.

Table 6

*Comparison of mean knowledge, attitude, and practice between respondents living in dengue hotspot and non-hotspot areas*

KAP score	Hotspot area	Non-hotspot area	P-value
Knowledge	16.48±0.99	16.25±1.34	0.120
Attitude	32.00±4.60	28.78±5.51	<0.05*
Practice	9.29±1.25	9.10±1.21	0.175

\*Indicates a significant difference as a p-value less than 0.05

Table 7

*Correlation between dengue knowledge, attitude, and practice scores of respondents in Selangor*

Variables	Spearman's correlation	P-value
Knowledge & attitudes	0.214	<0.01**
Knowledge & practices	0.563	<0.01**
Attitude & practices	0.374	<0.01**

\*\*Indicates a significant association as the p-value is less than 0.01

## DISCUSSION

A survey was conducted to assess dengue knowledge, attitudes, and practices among the residents of dengue hotspots and non-hotspot areas in Selangor. It was found that the level of knowledge about dengue among respondents from both areas was high. It is suggested

that the dengue campaigns implemented through various platforms in the country have effectively disseminated dengue-related information.

In the present study, many respondents knew that the virus is the causative agent of dengue fever, most of whom were from hotspot areas. It may be due to the health education programs implemented by the Ministry of Health Malaysia, which often focuses on the *Aedes* mosquitoes instead of the virus (Leong, 2014; Naing et al., 2011). It should be noted that knowledge of *Aedes* mosquitoes is more important because, at the moment, the best ways to prevent the spread of dengue are to control the *Aedes* mosquito population and avoid mosquito bites (Leong, 2014; Roiz et al., 2018). According to the findings, almost all respondents from both areas knew that *Aedes* mosquitoes are the dengue vector. It could be due to a public education campaign using the slogan ‘No *Aedes*, No Dengue.’

Most surveyed respondents from both areas knew that dengue fever could affect all age groups. This knowledge is expected to encourage people to take preventive measures and seek medical treatment immediately if their family members develop dengue symptoms, especially for those aged 0–4 years, because they are at high risk of being infected with dengue. According to Woon et al. (2018), the incidence rate for children aged 0 to 4 was 176.6 per 1,000 in 2013. Despite having a high level of knowledge, most respondents, particularly those living in hotspot areas, were unaware that a person could contract dengue more than once in their lifetime. Because they are more susceptible to dengue infection, it is critical to disseminate important information about dengue, particularly because someone diagnosed with dengue has a second chance of being infected with heterologous serotypes. Secondary infection should be avoided by maintaining proper prevention practices, as it has been reported to be more severe than primary infection (Soo et al., 2016).

In terms of the dengue vector, most respondents from hotspot areas had significantly better knowledge of the physical characteristics of *Aedes* mosquitoes. It could be due to dengue education talks or exhibitions displaying dengue-related information, such as replicas of adult *Aedes* mosquitoes, which were held in conjunction with cleanliness activities in hotspot areas. Another reason for this is educational advertisements on television or social media that feature the image of an *Aedes* mosquito. Furthermore, most respondents in both areas knew that *Aedes* mosquitoes breed in clean stagnant water rather than dirty water. In Malaysia, the weather is hot and humid all year, with rain, which can create breeding grounds for *Aedes* mosquitoes if rainwater stagnates in artificial containers (Tang, 2019). *Aedes aegypti* and *Aedes albopictus* lay their eggs in various containers, including tanks, buckets, gutters, and air conditioner drip trays, all of which can be found in or around the home. As a result, identifying potential breeding grounds may assist people in keeping their homes clean by removing unused containers that can hold water, emptying water-filled containers, and treating stored water with larvicides.

Most respondents from both areas were knowledgeable about *Aedes* mosquito feeding habits. However, a small percentage of the respondents were unaware that *Aedes* mosquitoes

are most active at dawn and dusk and are more likely to bite humans during these times. Therefore, it can lead to poor protection practices, such as being outside in the early morning and late afternoon and increasing mosquito contact. The most commonly recognised symptoms were high fever, headache, muscle pain, and joint pain. Surprisingly, less than a fifth of respondents living in non-hotspot areas were aware that dengue also causes skin rashes, back pain, nausea, and vomiting.

Compared to those who live in dengue hotspot areas, respondents from the non-hotspot area may have had less experience with infection or have witnessed close relatives contract dengue, limiting their knowledge of dengue symptoms. It is suggested that dengue education campaigns emphasise the symptoms of dengue that many people are unaware of and can be used to determine whether a person has dengue fever or a common fever. The ability of an individual to recognise dengue symptoms is critical to avoid confusion with similar illnesses such as influenza and initiate treatment promptly (Karimah Hanim et al., 2017; Khun & Manderson, 2007). It could contribute to a decrease in dengue cases and deaths.

Many respondents were aware of the lack of an effective dengue vaccine and specific dengue medications. With this knowledge, it is hoped that the community will keep their homes clean and free of mosquito breeding grounds, thereby reducing mosquito populations. Additionally, the current study established that respondents from both areas possessed a high level of knowledge regarding dengue prevention. It could be a result of frequent dengue campaigns emphasising dengue prevention practices. Additionally, this could account for respondents' improved dengue prevention practices, as knowledge about dengue was found to correlate positively with practices. In other words, it can be asserted that increased community awareness of dengue fever has resulted in improved dengue prevention practices.

The study found that respondents, particularly those living in dengue hotspot areas, have a favourable attitude toward dengue. Having a high level of knowledge about dengue may be one of the reasons, as this study discovered a positive correlation between knowledge and attitude. For instance, knowing that dengue can infect people of all ages may have led them to believe that everyone, including themselves, has a chance of contracting dengue. Although they are aware that there is no vaccine to prevent the spread of dengue, they continue to believe and feel that dengue can be prevented. Additionally, the respondents agreed that eradicating mosquito breeding grounds and avoiding mosquito bites can help protect them from dengue infection. It may increase people's awareness of the importance of protecting themselves and their families by implementing preventive activities in their residential areas to eradicate mosquitoes and prevent dengue infections that can be fatal. While most respondents, particularly those from hotspot areas, believed it was their responsibility to prevent dengue, some believed it was the government's sole responsibility. According to Lisut (2018), one of the primary reasons it is difficult to eradicate *Aedes* mosquitoes is the expectation that others will prevent dengue. As a result, such attitudes

must be corrected, as the government is incapable of always locating and eliminating mosquito breeding grounds in every home, especially when doing so would be costly.

Most respondents thought the dengue campaign was beneficial because it educated the public about dengue and instilled a sense of responsibility to protect their families, neighbours, and themselves from dengue infections and care for their environment. However, most respondents agreed that fogging is insufficient to prevent dengue in this study. Aung et al. (2016) reported a similar finding in Terengganu and suggested that this could be due to increased dengue cases despite frequent fogging activities. Fogging is not the primary method of combating dengue; it is only used when a dengue case is detected in each area (Kumarasamy, 2006). According to the findings of this study, respondents from both urban and rural areas believed that purchasing mosquito repellents was a waste of money. This study also dispelled the myth that dengue patients can improve independently. Health messages should emphasise the importance of seeking treatment to avoid harmful self-treatment practices (Hamid et al., 2015), which may be dangerous for them, particularly those suffering from dengue haemorrhage fever. Additionally, the respondent believed vaccination was critical for preventing dengue infection. It is hoped that with the advancement of technology, an effective dengue vaccine will be developed to prevent dengue fever, thereby resolving the dengue burden.

The survey respondents demonstrated poor practices regarding using insecticide nets at night, with respondents from hotspot areas exhibiting the worst practices. Several studies conducted in the dengue-prone area of Selangor revealed similar findings. For example, in a study by Said et al. (2018), respondents stated that sleeping with a bed net can be uncomfortable. Additionally, most respondents from non-hotspot areas engaged in basic personal protective behaviours to avoid mosquito bites, such as applying mosquito repellent to the body and wearing long pants and long-sleeve shirts outdoors.

Over 80.0% of respondents in both areas claimed to practise some form of environmental measure to reduce the mosquito population, such as properly disposing of household garbage, removing standing water in and around their home, cleaning the refrigerator frequently, and covering water-filled containers indoors and outdoors. Additionally, most of them said they engaged in cleanliness activities to maintain a clean-living environment. However, most respondents, particularly those from hotspot areas, are still unaware of fogging activity when they do not open their windows and doors when health authorities perform it. Over 90% of respondents reported using some form of insecticide, such as Abate, to kill mosquito larvae in water containers or insecticide spray to kill adult mosquitoes. Most respondents' widespread use of Abate as a precautionary measure, particularly those from hotspot areas, may be due to overall awareness of Abate's ability to disrupt the development of immature mosquitoes in water containers. According to Noor and Suddin (2017), health professionals will provide Abate free of charge to the



public, particularly during dengue outbreaks, which may contribute to the prevalence of abate use among them. Additionally, Hairi et al. (2003) suggested that this could result from aggressive media advertising regarding the use of insecticides.

This study also found positive correlations between knowledge and attitude and between knowledge and practice, indicating that the translation of knowledge to attitude and practice was good among the respondents. Previous studies in Malaysia also reported that the higher a person's knowledge of dengue, the better their attitude towards dengue and the more likely they are to adopt proper prevention practices (Mohamad et al., 2014; Naing et al., 2011; Noor & Suddin, 2017). In addition, a significant positive correlation between attitudes and practices was observed. Previous studies have shown that people with better attitudes were more likely to practice proper dengue prevention measures (Suwanbamrung et al., 2021).

There are some limitations of the present study. All information was obtained through self-report, and it could not be verified whether the reported practice followed actual practice. Also, while enumerators were trained in conducting the survey, errors may occur when different enumerators explain the question differently when asked by the respondents, which may influence the responses.

## CONCLUSION

In conclusion, residents in both hotspot and non-hotspot areas of Selangor, Malaysia, have a high level of knowledge about dengue. Nonetheless, continuous appropriate education is critical to ensuring that the community has accurate information about dengue. For instance, a sizable proportion of respondents in this study were unaware that they could contract dengue more than once; thus, dispelling any doubts about this risk is critical to ensuring that they do not become complacent and continue to practise preventive measures in their daily lives even if they have previously been infected. Additionally, this study reveals that respondents' attitudes toward dengue were significantly lower in non-hotspot areas. It is hoped that this information will assist authorities in designing and improving existing intervention programmes to be more effective and foster a more positive attitude toward dengue among residents of non-hotspot areas, which may influence the pattern of prevention practices.

## ACKNOWLEDGEMENT

The authors would like to express their gratitude to the Malaysian Ministry of Health's Medical Research and Ethics Committee for providing ethical approval for this study. We would also like to thank the Malaysian Ministry of Higher Education for funding this project under the Fundamental Research Grant Scheme (FRGS), grant number 01-01-17-1919FR. Finally, we want to thank everyone who volunteered to participate in this study.

## REFERENCES

- Acharya, A. S., Prakash, A., Saxena, P., & Nigam, A. (2013). Sampling: Why and how of it? *Indian Journal of Medical Specialties*, 4(2), 330-333.
- Andrade, C., Menon, V., Ameen, S., & Praharaj, S. K. (2020). Designing and conducting knowledge, attitude, and practice surveys in psychiatry: Practical guidance. *Indian Journal of Psychological Medicine*, 42(5), 478-481.
- Aung, M. M. T., Hassan, A. B., Kadarman, N. B., Hussin, T. M., Barman, A., Ismail, S. B., & Hashim, S. E. (2016). Knowledge, attitude, practices related to dengue fever among rural population in Terengganu, Malaysia. *Malaysian Journal of Public Health Medicine*, 16(2), 15-23.
- Cochran, W. (1977). *Sampling Techniques*. John Wiley & Sons.
- Department of Statistics Malaysia. (2020). *Selangor*. [https://www.dosm.gov.my/v1/index.php?r=column/colone&menu\\_id=eGUyTm9RcEVZSllmYW45dmpnZHh4dz09](https://www.dosm.gov.my/v1/index.php?r=column/colone&menu_id=eGUyTm9RcEVZSllmYW45dmpnZHh4dz09)
- Diema, K. K., Amu, H., Konlan, K. D., & Japiong, M. (2019). Awareness and malaria prevention practices in a rural community in the Ho Municipality, Ghana. *Interdisciplinary Perspectives on Infectious Diseases*, 2019, Article 9365823. <https://doi.org/10.1155/2019/9365823>
- Flynn, B. B., Sakakibara, S. S., Schroeder, R. G., Bates, K. A., & Flynn, E. J. (1990). Empirical research methods in operations management. *Journal of Operations Management*, 9(2), 250-284. [https://doi.org/10.1016/0272-6963\(90\)90098-X](https://doi.org/10.1016/0272-6963(90)90098-X)
- Ghani, N., Shohaimi, S., Hee, A., Chee, H. Y., Emmanuel, O., & Ajibola, L. A. (2019). Comparison of knowledge, attitude, and practice among communities living in hotspot and non-hotspot areas of dengue in Selangor, Malaysia. *Tropical Medicine and Infectious Disease*, 4(1), Article 37. <https://doi.org/10.3390/tropicalmed4010037>
- Hairi, F., Ong, C. H. S., Suhaime, A., Tsung, T. W., Ahmad, M. A. A., Sundaraj, C., & Soe, M. M. (2003). A knowledge, attitude and practices (KAP) study on dengue among selected rural communities in the Kuala Kangsar District. *Asia-Pacific Journal of Public Health*, 15(1), 37-43. <https://doi.org/10.1177/101053950301500107>
- Hamid, M., Lugova, H., Mon, A., & Knight, V. (2015). Awareness and practice related to dengue infection among military cadets in Malaysia. *Journal of Behavioral Health*, 4(2), 39-43. <https://doi.org/10.5455/JBH.20150311072802>
- Hanim, A. A. K., Razman, M. R., Jamalludin, A. R., Nasreen, E. H., Phyu, H. M., SweSwe, L., & Hafizah, P. (2017). Knowledge, attitude and practice on dengue among adult population in Felda Sungai Pancing Timur, Kuantan, Pahang. *IJUM Medical Journal Malaysia*, 16(2). <https://doi.org/10.31436/imjm.v16i2.318>
- Jordan, S., Martindale, A. W., Heuss, A., Miller, D., Tamse, J., & Hall, B. L. (2020). A physical model for exploring drug design to treat break-bone fever. *The FASEB Journal*, 34(S1), 1-1. <https://doi.org/10.1096/fasebj.2020.34.s1.06940>
- Kamal, M., Kenawy, M. A., Rady, M. H., Khaled, A. S., & Samy, A. M. (2018). Mapping the global potential distributions of two arboviral vectors *Aedes aegypti* and *Ae. albopictus* under changing climate. *PLOS One*, 13(12), Article e0210122. <https://doi.org/10.1371/journal.pone.0210122>

- Khun, S., & Manderson, L. (2007). Community and school-based health education for dengue control in rural Cambodia: A process evaluation. *PLoS Neglected Tropical Diseases*, *1*(3), Article e143. <https://doi.org/10.1371/journal.pntd.0000143>
- Kumarasamy, V. (2006). Dengue fever in Malaysia: Time for review. *Medical Journal of Malaysia*, *61*(1), 1-3.
- Leong, T. K. (2014). Knowledge, attitude and practice on dengue among rural communities in Rembau and Bukit Pelanduk, Negeri Sembilan, Malaysia. *International Journal of Tropical Disease & Health*, *4*(7), 841-848.
- Lisut, O. (2018, August 21). Sikap harapkan orang lain punca sukar hapus Aedes [The attitude of expecting others is the reason it is difficult to remove Aedes]. *Berita Harian*. <https://www.bharian.com.my/rencana/komentar/2018/08/464462/sikap-harapkan-orang-lain-punca-sukar-hapus-aedes>
- Malaysian Remote Sensing Agency. (2019). *Senarai lokaliti hotspot* [Hotspot locality list]. <https://idengue.mysa.gov.my/pdf/statistik.pdf#page=3>
- Ministry of Health Malaysia. (2019). *Senarai kenyataan akhbar demam denggi dan chikungunya* [List of dengue fever and chikungunya press releases]. [https://www.moh.gov.my/index.php/database\\_stores/store\\_view/17?items=25&page=5](https://www.moh.gov.my/index.php/database_stores/store_view/17?items=25&page=5)
- Mohamad, M., Selamat, M. I., & Ismail, Z. (2014). Factors associated with larval control practices in a dengue outbreak prone area. *Journal of Environmental and Public Health*, *2014*, Article 459173. <https://doi.org/10.1155/2014/459173>
- Naing, C., Ren, W. Y., Man, C. Y., Fern, K. P., Qiqi, C., Ning, C. N., & Ee, C. W. S. (2011). Awareness of dengue and practice of dengue control among the semi-urban community: A cross-sectional survey. *Journal of Community Health*, *36*, 1044-1049. <https://doi.org/10.1007/s10900-011-9407-1>
- Noor, M. N., & Suddin, L. S. (2017). Larviciding practice for prevention and control of dengue among urban community. *Brunei International Medical Journal*, *13*(2), 58-63.
- Othman, H., Karim, N., Rashid, N. A. A., Abas, M. B. H., Sahani, M., Hod, R., Daud, F., Nordin, S. A., & Nor, N. A. M. (2019). Applying the health belief model for the assessment of community knowledge, attitude and prevention practices following a dengue epidemic in a township in Selangor, Malaysia. *International Journal of Community Medicine and Public Health*, *6*(3), 958-970. <http://dx.doi.org/10.18203/2394-6040.ijcmph20190578>
- Parmenter, K., & Wardle, J. (2000). Evaluation and design of nutrition knowledge measures. *Journal of Nutrition Education*, *32*(5), 269-277. [https://doi.org/10.1016/S0022-3182\(00\)70575-9](https://doi.org/10.1016/S0022-3182(00)70575-9)
- Rodenhuis-Zybert, I. A., Wilschut, J., & Smit, J. M. (2010). Dengue virus life cycle: Viral and host factors modulating infectivity. *Cellular and Molecular Life Sciences*, *67*, 2773-2786. <https://doi.org/10.1007/s00018-010-0357-z>
- Roiz, D., Wilson, A. L., Scott, T. W., Fonseca, D. M., Jourdain, F., Müller, P., Velayudhan, R., Corbel, V. (2018). Integrated Aedes management for the control of Aedes-borne diseases. *PLOS Neglected Tropical Diseases*, *12*(12), Article e0006845. <https://doi.org/10.1371/journal.pntd.0006845>
- Saadatian-Elahi, M., Alexander, N., Möhlmann, T., Langlois-Jacques, C., Suer, R., Ahmad, N. W., Mudin, R. N., Ariffin, F. D., Baur, F., Schmitt, F., Richardson, J. H., Rabilloud, M., & Hamid, N. A. (2021). Measuring the effectiveness of integrated vector management with targeted outdoor residual spraying and

- autodissemination devices on the incidence of dengue in urban Malaysia in the iDEM trial (intervention for Dengue Epidemiology in Malaysia): Study protocol for a cluster randomised controlled trial. *Trials*, 22(1), 1-16. <https://doi.org/10.1186/s13063-021-05298-2>
- Said, M. F. F, Abdullah, H., & Ghafar, N. A. (2018). Dengue prevention practices among community in dengue hotspot area. *International Journal of Community Medicine and Public Health*, 5(11), 4664-4669. <http://dx.doi.org/10.18203/2394-6040.ijcmph20184553>
- Soo, K. M., Khalid, B., Ching, S. M., & Chee, H. Y. (2016). Meta-analysis of dengue severity during infection by different dengue virus serotypes in primary and secondary infections. *PLoS One*, 11(5), Article e0154760. <https://doi.org/10.1371/journal.pone.0154760>
- Streiner, D. L. (2003). Starting at the beginning: An introduction to coefficient alpha and internal consistency. *Journal of Personality Assessment*, 80(1), 99-103. [https://doi.org/10.1207/S15327752JPA8001\\_18](https://doi.org/10.1207/S15327752JPA8001_18)
- Suwanbamrung, C., Saengsuwan, B., Sangmanee, T., Thrikaew, N., Srimoung, P., & Maneerattanasak, S. (2021). Knowledge, attitudes, and practices towards dengue prevention among primary school children with and without experience of previous dengue infection in southern Thailand. *One Health*, 13, Article 100275. <https://doi.org/10.1016/j.onehlt.2021.100275>
- Tang, K. H. D. (2019). Climate change in Malaysia: Trends, contributors, impacts, mitigation and adaptations. *Science of The Total Environment*, 650(2), 1858-1871. <https://doi.org/10.1016/j.scitotenv.2018.09.316>
- Tantawichien, T. (2012). Dengue fever and dengue haemorrhagic fever in adolescents and adults. *Paediatrics and International Child Health*, 32(sup1), 22-27. <https://doi.org/10.1179/2046904712Z.00000000049>
- Woon, Y. L., Hor, C. P., Lee, K. Y., Anuar, S. F. Z. M., Mudin, R. N., Ahmad, M. K. S., Komari, S., Amin, F., Jamal, R., Chen, W. S., Goh, P. P., Yeap, L., Lim, Z. R., & Lim, T. O. (2018). Estimating dengue incidence and hospitalisation in Malaysia, 2001 to 2013. *BMC Public Health*, 18(1), Article 946. <https://doi.org/10.1186/s12889-018-5849-z>

*Review Article*

## Review of Window Performance in A Hot and Humid Climate

Zinnirah Wellun<sup>1</sup>, Wardah Fatimah Mohammad Yusoff<sup>1,2\*</sup>, Mohd Farid Mohamed<sup>1</sup>,  
Mohd Khairul Azhar Mat Sulaiman<sup>1</sup> and Mohammad Rasidi Mohammad Rasani<sup>3</sup>

<sup>1</sup>Department of Architecture and Built Environment, Faculty of Engineering and Built Environment, Universiti Kebangsaan Malaysia, 43600 UKM, Bangi, Selangor, Malaysia

<sup>2</sup>Centre for Engineering Education Research, Faculty of Engineering and Built Environment, Universiti Kebangsaan Malaysia, 43600 UKM, Bangi, Selangor, Malaysia

<sup>3</sup>Department of Mechanical and Manufacturing Engineering, Faculty of Engineering and Built Environment, Universiti Kebangsaan Malaysia, 43600 UKM, Bangi, Selangor, Malaysia

### ABSTRACT

Incorrect implementation of window parameters, such as configuration, position, and size, cause an unpleasant indoor environment. The authors reviewed window performance in a hot and humid climate in this paper. Articles were screened in detail to determine eligibility, compiled, and organised according to Preferred Reporting Items for Systematic Reviews and Meta-Analyses (PRISMA) requirements. The articles included in this review concerned natural ventilation and window performance in a hot and humid climate. Keywords or topics were reviewed and focused on indoor environment comfort. The results demonstrated that sliding windows were unfavourable openings that were nevertheless in demand. This review was performed to guide consumers, designers, and the market of the built environment industry.

*Keywords:* Hot humid climate, indoor environment, PRISMA, sliding window, window

### ARTICLE INFO

*Article history:*

Received: 13 February 2022

Accepted: 28 June 2022

Published: 09 November 2022

DOI: <https://doi.org/10.47836/pjst.31.1.27>

*E-mail addresses:*

p102441@siswa.ukm.edu.my (Zinnirah Wellun)

wardahyusoff@ukm.edu.my (Wardah Fatimah Mohammad Yusoff)

faridmohamed@ukm.edu.my (Mohd Farid Mohamed)

m.khairulazhar@ukm.edu.my (Mohd Khairul Azhar Mat Sulaiman)

rasidi@ukm.edu.my (Mohammad Rasidi Mohammad Rasani)

\* Corresponding author

### INTRODUCTION

A hot and humid climate features high solar radiation and humidity throughout the year. Malaysia has such a climate and records temperatures up to 40°C during the northeast and 32°C during the southwest monsoon (Kamal et al., 2017). This climate has remained unchanged for a decade and is expected to remain until 2099 (Tarmizi et al., 2019).

In humans, high temperatures cause increased thermal discomfort, decreased consciousness, tiredness, serious headaches, and dizziness (Sung et al., 2014; Bidet et al., 2020). Furthermore, compared to lower temperatures, high indoor temperatures exceeding 37°C cause a substantially higher heart rate and dehydration rate (Y. Chen et al., 2020), which affect physiological and psychological performance (Fan et al., 2019). The recommended range of thermal comfort is between 22.5°C and 25.5°C (Caetano et al., 2017), while 26.3°C and 26.9°C were suggested for coastal regions and rainforest regions, respectively (Guevara et al., 2021). For sedentary activity, the neutral temperature for thermal comfort can increase to 30°C (Wijewardane & Jayasinghe, 2008).

Higher air velocity can escalate the neutral temperature for thermal comfort. Environmental issues drive sustainable design, and health risks are caused by the absence of environmental design criteria or energy storage. They have become the highest priority in the built environment by focusing on green architecture. Cooling the indoor environment consumes high energy due to improper design or user carelessness in the form of energy wastage inside the building (Masood et al., 2017). Hence, renewable energy sources like the sun and wind should be utilised optimally with green design to achieve sustainable development. The sun and wind, which provide heat and airflow, are important parameters affecting indoor air quality and human comfort. Applying natural ventilation can achieve satisfactory comfort and a healthy indoor environment. Enhancing air velocity increases the occupant's sweat evaporation with thorough ventilation (Castillo & Huelsz, 2017). Considering the excellent air circulation (Kim & Kim, 2018), natural ventilation provides fresh air and reduces future health problems.

The indoor environment, human comfort, and natural ventilation are closely related (Cuce et al., 2019). Studies have been performed on temperatures in a hot and humid climate and building occupants' reactions to a hot and humid environment, eventually leading to research on how sustainable design aids building designers and consumers in choosing the right building component design, such as window configuration, for achieving indoor thermal comfort. A suitable window configuration exerted a positive effect on indoor thermal comfort (Zhao & Du, 2020). In this study, the authors examined the most common window types in the market and reviewed their performance. The results reveal the worst window type according to performance so that consumers can choose the best window to fit the function of their building.

## **METHODS**

The Preferred Reporting Items for Systematic Reviews and Meta-Analyses (PRISMA) guideline (Page et al., 2021) was used for compiling related articles. The PRISMA 2020 guideline is a systematic procedure that guides authors in searching articles from available databases. The PRISMA simplifies the article search by identifying the databases to be used, namely, Scopus, Web of Science, and grey literature. Grey literature is unindexed by

primary database sources but is also considered an important information source (Osayande & Christopher, 2012).

In this study, the two main keywords were ‘natural ventilation’ and ‘hot humid climate’, followed by ‘solar,’ ‘opening,’ and the synonyms for ‘window,’ ‘airflow,’ ‘wind flow,’ and ‘air velocity.’ Next, openings (important building components that affect indoor airflow) and windows were divided into design, parameters, arrangement, dimension, position, and size criteria to widen the search.

The early stage of article compilation was crucial to finding and achieving the correct focus topic and yielded 994 articles. The 994 articles were screened by excluding articles based on year (2015–2021), subject area (engineering, energy), document type (article), and language (English). Articles that did not feature the criteria above were excluded and filtered out.

Article eligibility was tested by checking each article that remained after the exclusion process and yielded 135 articles. The full text of the articles underwent eligibility testing to exclude unrelated articles. Subsequently, the exclusion and eligibility testing were repeated, and the articles were finalised and analysed by categorising the information needed. Fewer than 100 articles that were included in this review underwent final screening. The screening continued until articles on sliding windows focused on residential buildings were identified.

## RESULTS

### Window Type

The articles included in this study focused on natural ventilation in a hot and humid climate. The included articles were on sliding and pivoted windows (Hossain et al., 2017); sliding, double, and quadruple cut-up sliding windows, fixed and projected windows (Kim et al., 2019); sliding window opening (de Faria et al., 2018); side-hung, top-hung, bottom-hung, and sliding windows (Liu & Lee, 2020; Liu & Lee, 2019); two window bands with a single opening (Tena-Colunga & Liga-Paredes, 2020); fixed, louvre, sliding, and double-hung windows (Z. Chen et al., 2020); sliding windows (Yoon et al., 2020); and sliding, horizontal rectangle windows, and louvre windows (Kitagawa et al., 2021).

Nine articles focused on naturally ventilated conditions: glazing (Kim et al., 2019) and the optimal positioning of the building opening (Yoon et al., 2020). The other articles on natural ventilation featured investigation of the cooling ventilation process (Hossain et al., 2017; de Faria et al., 2018; Kitagawa et al., 2021), hot–cold season (Z. Chen et al., 2020), the performance of indoor ventilation in relation to window design (Liu & Lee, 2019), window-opening degree (Liu & Lee, 2020), and window frames (Tena-Colunga & Liga-Paredes, 2020).

Most of the included studies involved square window openings. Thermal comfort was studied in the articles on square windows with no external shading (Zomorodian &



Tahsildoost, 2017) and typical square windows (Elshafei et al., 2017), while an article on square wind-deflector windows and energy and window rating (Orouji et al., 2019) examined indoor–outdoor temperature and airflow to improve the convection process (Lin et al., 2021). Finally, an article on ordinary square double-glazed windows examined the economic cost of energy efficiency, thermal comfort, and daylight usage (Yılmaz & Yılmaz, 2021).

In the other articles on square window openings, window parameters (Zhai et al., 2019), influence of opening position (Xing et al., 2018), windows of different sizes (Rizal et al., 2020), and triple-glazed air supply windows (Bastien, 2019) were investigated. In this study, the different ratios from square to rectangular shapes (Rizal et al., 2020) were used as a reference in addition to the window parameter (Zhai et al., 2019) and window arrangement topics (Bastien, 2019). Furthermore, airflow patterns (Nalamwar et al., 2017) and volume flux (Derakhshan & Shaker, 2017) were investigated in relation to square windows. Vertical and square windows of various designs were studied, particularly concerning energy savings and cost, effect on the environment, and thermal comfort stimulated by window parameters (Elghamry & Hassan, 2020).

The second most frequently compiled shape-related window opening was rectangular window openings with vertical or horizontal orientation. One study on horizontal window openings focused on the ideal window parameters by investigating sunlight quality and energy intake (Maleki & Dehghan, 2020). Decreased energy intake was observed by determining the ideal window design variables (Foroughi et al., 2018). The topics compiled for horizontal window openings were fluctuation of cross-ventilation and flow field (Hawendi & Gao, 2018), stimulated and distributed wind speed (F. B. Chen et al., 2020), the microscopic change rate of the air (O’Sullivan & Kolokotroni, 2017), window position on the building façade (Hammad et al., 2019), porosities with several wind angles (Gautam et al., 2019) thermochromic glazing (Liang et al., 2018), and sunlight balance with energy performance (Pilechiha et al., 2020).

In the compiled articles, both horizontal and vertical window openings were studied. Moreover, natural ventilation was investigated to identify the effect of window-to-wall ratio position variables (Hamdani et al., 2017), window size, building orientation (Manigandan et al., 2018), and composite shear wall performance by determining the effects of the opening position and number (Badarloo & Jafari, 2018).

In three studies on vertical rectangular window openings, the water flow window configuration effect was examined, focusing on the distribution effects on thermal flow attribution of header design (Chow & Lyu, 2017), high-performance windows (Li & Tang, 2020), and energy performance analyses (Li et al., 2021). One study involved a water flow test with horizontal windows focusing on energy-saving capability (Li et al., 2020). Another two studies used ordinary vertical window openings to investigate indoor thermal

conditions by studying passive design (Amir et al., 2018) and various window-to-wall ratios (Sacht & Lukiantchuki, 2017).

Topics on the effect of window ratio–position to air and temperature distribution (Vadugapalayam et al., 2017; Abed et al., 2018) and direction with wind speed (Stamatopoulos et al., 2019) were studied. In one study on energy saving, vertical window openings were favourable for smart windows (Wu et al., 2018) and were also used for an opening experiment on tsunami flow (Moon et al., 2020).

The window-to-wall ratio was investigated in a total of 518 simulated window configurations (Marino et al., 2017), while the fenestration system (Mousa et al., 2017), window area luminance (Amirkhani et al., 2018), indoor-outdoor air movement comparison (Wahab et al., 2018), window configuration on energy performance (Altun & Kiliç, 2019), residential energy usage (Mori et al., 2020), and thermal investigation (Koohsari & Heidari, 2020) were studied in relation to various window opening types. These studies involved field measurements (Wahab et al., 2018), surveys (Mori et al., 2020), and computer simulations (Marino et al., 2017; Mousa et al., 2017; Amirkhani et al., 2018; Altun & Kiliç, 2019). One study on energy-saving windows ignored the window type utilised (Bayoumi, 2017), while two studies on natural ventilation in a hot and humid climate focused on defining the perfect window design by various attributions adapted (Hwang & Lee, 2018) and producing a guidance tool for windowmakers focusing on the adaptation procedures related to cost, product quality, and the indoor environment (Arranz et al., 2018).

In one study that did not specify the window shape, air change performance was investigated in an L-shaped room (Rabanillo-Herrero et al., 2020). Other studies investigated the energy efficiency of operable louvres (Scheuring & Weller, 2020) and triple-glazed fluidic windows (Su et al., 2021). In thermal performance studies, experiments were performed on multi-azimuthal windows (Barea et al., 2017). Two studies involved investigations of metacage windows (Fusaro et al., 2020) and acoustic metawindow frames (Fusaro et al., 2021) for simultaneous noise reduction and natural ventilation. Acoustic metamaterial windows were investigated in relation to ventilated tunables (Kumar et al., 2020). An investigation of thermal behaviour in hot and cold seasons did not report a specific smart window shape (El Khattabi et al., 2018). The authors of a study on basic window frames focused on the frame surface temperature (Nota et al., 2017), while a study of wood–aluminium window frames involved an investigation of the thermal properties related to the window-to-wall ratio (Misiopcecki et al., 2018). In studies on ordinary window design, improvement in human satisfaction was investigated using artificial intelligence (Karan & Asadi, 2019) and shaded glazed window parameters of different shapes for decreasing energy cooling usage (El Dakdoky, 2019).

In one study on window shapes related to natural ventilation in a hot and humid climate, the authors investigated wind fields after residential building renovating typical

house windows (Enteria & Cuartero-Enteria, 2017). In another study on centre pivot windows, bioclimatic design productiveness was identified in relation to temperature and relative humidity (Jamaludin et al., 2017). Finally, typical punch windows were studied to investigate human satisfaction with discomfort, glare and lighting acceptableness (Amirkhani et al., 2017).

## **Window Performance**

This section focused on the variables categorised into single-sided and cross-ventilation conditions. Related variables, such as airflow, focused on the patterns or exchange rates, wind flow, wind speed, or velocity in relation to the types of opening and ventilation. Some articles discussed more than one variable, which included pressure difference, solar gain, temperature, building location, building group layout and orientation, internal space arrangement, and opening design.

The airflow studies involved media that included building models, generic isolated buildings, window simulation models, teaching spaces of a school building, residential buildings, including traditional dwellings, and office buildings. Some airflow studies were conducted in cross-ventilation conditions involving horizontal openings (Shetabivash, 2015; Kosutova et al., 2019), vertical openings (Manolesos et al., 2018), side-hung and bottom-hung casements (Cruz & Viegas, 2016), and vertical openings (doors) along with horizontal windows (Tan & Deng, 2020). Inlet opening affected cross-ventilation and indoor flow patterns (Shetabivash, 2015) while opening the upper part of a façade resulted in the largest velocities in a building (Kosutova et al., 2019). The side-hung and bottom-hung casement studies reported consistent discharge coefficients (Cruz & Viegas, 2016).

Airflow rate measurement was considered an improvement method for future studies. Vertical openings and horizontal windows resulted in greater indoor thermal operative temperature stability by preventing overventilation (Tan & Deng, 2020). The mean absolute deviation of the indoor operative temperature from the neutral operative temperature recorded a reduction exceeding 30%. An airflow study on single-sided ventilation involving the 'Mashrabiya' lattice window reported up to 3.5 m/s velocity for single-sided ventilation due to the oblique windward direction of 3 m/s velocity (Elwan, 2020). An investigation of residential building openings and air change rate concluded that the total number of openings (either window or door) was the important first-order predictor of living area air change rates. Increased attic–outdoor temperature differences caused increased airflow from the living area to the attic (Liu et al., 2018).

The included articles also involved studies on single-sided and cross-ventilation conditions due to window opening and closing patterns. One study featured a critical evaluation of passive energy-saving techniques on a hypothetical building refurbishment involving replacing old windows and the need for specific adaptive measures to improve

indoor environmental quality (Carlos, 2017). A study on the effect of classroom openings on natural ventilation performance involved an investigation of the ventilation angle and evaluating the performance of natural ventilation using the air–age ratio. The authors reported that outside corridor ventilation was 35.55% better compared to the inside corridor, and large rooms had 30.85% better ventilation than small rooms (Yang et al., 2019).

One study investigated the ventilation behaviour of a double-skin façade building model with a square opening. There were no significant changes for cavity space division into smaller parts, while an additional channel on the northern part of the model was very efficient and directly affected the functionality of the façade (Nasrollahi & Salehi, 2015).

In studies on air velocity, the authors focused on horizontal openings in single-sided and cross-ventilation of residential buildings. Compared to the solid model, porous models demonstrated an average wind velocity at the opening that was 1.54–1.64 times larger with the lowest mean age of air (Saadatjoo et al., 2018). Moreover, various opening patterns were investigated in the natural ventilation of a traditional neighbourhood. The authors reported that night ventilation was the most effective passive cooling in vernacular dwellings in the hot season compared to daytime and full-day ventilation. This strategy reduced the highest indoor temperature while improving thermal conditions for the following day (Michael et al., 2017).

In one article, wind speed for single-sided ventilation was investigated in traditional buildings in Huizhou, China. The analysis demonstrated that the traditional dwellings exhibited good natural ventilation during the summer due to the patio attribution (Huang et al., 2017). In another study, natural ventilation behaviour was investigated with simulation modelling. The model predicted the mass flow rate and heat removed by ventilation with a high level of agreement with the experimental data (Dama et al., 2017). Other than air velocity, the occupants' experiences with air were also investigated, where heritage buildings in Baixa Pombalina, Lisbon, Portugal, were studied using a questionnaire. During the summer, the climate played a major role in controlling the thermal performance of the Baixa buildings (Nunes de Freitas & Guedes, 2015).

One article investigated the building location, building group layout orientation, internal space arrangement, and opening design of traditional dwellings with various openings. Traditional dwellings featured good adaptation to the local climate even during the summer, while thermal simulation revealed unsatisfactory indoor thermal comfort in the cold season (Gou et al., 2015). Building models for the window-to-wall ratio of inlets and outlets resulted in potential good performance of cross-ventilation for the indoor thermal environment and achieved comfort conditions.

An indoor temperature reduction of 4% to 8% was achieved even with less favourable conditions during the hot season. Due to the directly proportional relationship between airflow rate and indoor temperature with inlet and outlet size, larger inlets and outlets

provided higher flow rates with proper orientation (Aldawoud, 2016). A single-sided ventilation simulation with a vertical and horizontal opening used pulsating and eddy penetration flow. The model could predict the total flow rate of single-sided natural ventilation in buildings driven by wind pressure. Small openings demonstrated a total flow rate driven by pulsating flow, while larger openings were mainly caused by the mean flow (Zhou et al., 2017).

## **DISCUSSION**

The articles included in this review demonstrated that fewer studies were performed on sliding windows in relation to indoor environments, specifically studies that focused on hot and humid climates, thus resulting in little information on the performance of sliding windows and whether such windows exerted good or detrimental effects on the indoor environments of certain buildings. Substantial industrial and consumer decisions on utilising or choosing window designs that crucially affect the indoor environment are limited to certain sources, such as seller brochures, the internet, and personal experience. Hence, the findings may assist developers and consumers in making the correct decision.

### **Sliding Windows**

In addition to the studies included in this review, previous studies related to sliding windows mainly focused on airborne particles (Sadrizadeh et al., 2018), window orientation with its position related to natural ventilation (Liu & Lee, 2019), and air pollution (Wang et al., 2020). Another study of window types, including sliding windows, focused on single-opening wind-driven natural ventilation (Ruan & Li, 2012), and cross-ventilation was characterised in a study of a classroom with different window and opening types (Nitawichit et al., 2008).

### **Performance of Sliding Windows in Residential Buildings**

The most recent field measurement conducted in a residential building demonstrated that sliding windows resulted in low indoor air velocity, high indoor air temperature, and heat accumulation between the window glass (Wellun et al., 2021). This main finding encouraged further investigations of sliding windows, which are still being utilised in residential buildings. However, the low performance of sliding windows may lead to an unpleasant indoor environment and high electricity consumption for indoor cooling.

Table 1 depicts a summary of sliding window performance in residential buildings. Sliding windows were the most unfavourable windows for reducing energy consumption for cooling. In residential buildings in Hong Kong, window design affected ventilation performance by surface regression. The most favourable window type was the side-hung window, followed by the top-hung and sliding windows. A mathematical model was used

Table 1  
*Summary of sliding window performances*

Reference	Aim	Space or window type	Conclusion
Liu and Lee (2019)	Evaluated the influence of window type on ventilation performance.	<ul style="list-style-type: none"> <li>• Residential building</li> <li>• Sliding window</li> </ul>	Sliding windows performed poorly in terms of energy consumption for cooling.
Wang et al. (2020)	Sheltering efficiency of houses equipped with ventilation systems.	<ul style="list-style-type: none"> <li>• Residential building</li> <li>• Sliding window</li> </ul>	Ultrafine particles remained the main challenge in particle penetration into indoor space.
de Faria et al. (2018)	Evaluating natural ventilation systems for cooling potential to deliver comfort while reducing the energy demand of the building.	<ul style="list-style-type: none"> <li>• Multi-storey residential building</li> <li>• Sliding window</li> </ul>	Enlarged window sizes improved ventilation but resulted in an unavoidable increase in heat gain due to glazed area enlargement.
Liu and Lee (2020)	Influence of window opening degree of residential buildings.	<ul style="list-style-type: none"> <li>• Residential building</li> <li>• Side-hung, top-hung, bottom-hung, and sliding windows</li> </ul>	Sliding windows performed the worst compared to other windows.

to determine favourable to unfavourable windows, in which ventilation performance sensitivity depended on wind alteration, followed by ventilation mode, window type, and window orientation. The results demonstrated that ventilation mode was evaluated by air change per hour, where side-hung and top-hung windows achieved 124% and 97% higher ventilation, respectively than sliding windows for maximum air change per hour (Liu & Lee, 2019).

Studying particle penetration into indoor space through windows remains challenging. Particles < 69 mm could penetrate window cracks, while particles between 69 and 100 mm were captured due to the large diffusion effect, which focused on the universal household sliding window. Moreover, an increased ventilation system should be considered to enhance air purification effectively (Wang et al., 2020).

Increasing the total hours over a year for natural ventilation in removing heat gains was achieved by enlarging the free area of the windows by a factor of three in addition to purpose-provided openings for ventilation and fan utilisation. Unfortunately, the window area enlargement resulted in a larger glazed area. The increased heat gain was unavoidable and worsened when the façade faced the direction of solar radiation. Nonetheless, outer louvred shutters could be utilised to avoid overheating on glazed surfaces (de Faria et al., 2018).

The window opening degree also influenced the air change rate per hour. An acceptable opening degree range was 0.6–0.9 for maximum natural ventilation usage. Sliding windows were the worst design preference for single-sided ventilation, with an optimum window opening degree of 0.9. Conversely, with a window opening degree of 0.7, side-hung windows were the best design preference for cross-ventilation (Liu & Lee, 2020).



Sliding windows also yielded low performance in non-residential buildings. Wind-driven natural ventilation performance is an important criterion for optimising the wind direction to achieve window position effectiveness, ideally considering outdoor conditions. Sliding window data provided information on how the window should be positioned correctly to achieve optimised performance. In addition, the information suggested a maximum cooling effect for natural ventilation (Yoon et al., 2020).

Sliding windows were reported as an unfavourable window type for air ventilation. Air entry in the working area of a building was restricted and limited the potential of ventilation to lower the indoor air temperature. In Bangladeshi garment factories, changing sliding windows to pivoted windows potentially decreased overheating by as much as 15% and by as low as 2% of working hours in three different work areas (Hossain et al., 2017). However, sliding windows resulted in the worst air mass flow rate compared to the three other windows tested in a single room opening. At  $\geq 45^\circ$ , the air mass flow rate neared zero. At a wind direction of  $0^\circ$ , the sliding window and conventional side-hung window produced the lowest air mass flow rate compared to the up-down folio window and the multi-sash mid-pivoted folio window with vertical deflectors (Ruan & Li, 2012).

## CONCLUSION

The study of sliding window openings is important as they are still used in buildings despite research data demonstrating their unfavourable behaviour and effects on indoor environments. Research information does not educate building designers or consumers on how the sliding window is one of the most unfavourable designs. The reason building designers still utilise the sliding window is unknown but might be due to economical cost and ease of installation. In addition to a detailed investigation of glass behaviour, the questions above should be answered in research soon. Ultimately, the research can be developed into a combined investigation of sliding windows and glass behaviour in the indoor environment.

## ACKNOWLEDGEMENT

The authors want to express gratitude to the Ministry of Higher Education Malaysia (MOHE), which granted research funding, namely the Fundamental Research Grant Scheme (FRGS/1/2019/TK10/UKM/02/4 - Air flow characteristics and behaviour around openings with various types of shading elements), as well as the National University of Malaysia that also provided research grant GUP-2019-017.

## REFERENCES

- Abed, F. M., Ahmed, O. K., & Ahmed, A. E. (2018). Effect of climate and design parameters on the temperature distribution of a room. *Journal of Building Engineering*, 17, 115-124. <https://doi.org/10.1016/j.job.2018.02.007>



- Aldawoud, A. (2016). Windows design for maximum cross-ventilation in buildings. *Advances in Building Energy Research*, 11(1), 67-86. <https://doi.org/https://doi.org/10.1080/17512549.2016.1138140>
- Altun, A. F., & Kiliç, M. (2019). Influence of window parameters on the thermal performance of office rooms in different climate zones of Turkey. *International Journal of Renewable Energy Research*, 9(1), 226-243.
- Amir, A., Mohamed, M. F., Sulaiman, M. K. A. M., & Yusoff, W. F. M. (2018). Comparative assessment of passive design strategies for improving indoor thermal comfort of low-cost house in hot-humid climate of Malaysia. *International Journal of Civil Engineering and Technology*, 9(11), 1500-1514.
- Amirkhani, M., Garcia-Hansen, V., Isoardi, G., & Allan, A. (2017). An energy efficient lighting design strategy to enhance visual comfort in offices with windows. *Energies*, 10(8), Article 1126. <https://doi.org/10.3390/en10081126>
- Amirkhani, M., Garcia-Hansen, V., Isoardi, G., & Allan, A. (2018). Innovative window design strategy to reduce negative lighting interventions in office buildings. *Energy and Buildings*, 179, 253-263. <https://doi.org/10.1016/j.enbuild.2018.09.006>
- Arranz, B., Bedoya-Frutos, C., & Vega-Sánchez, S. (2018). Proposal of a product indicator as a tool for a comprehensive assessment of windows. *Archnet-IJAR*, 12(1), 266-279.
- Badarloo, B., & Jafari, F. (2018). A numerical study on the effect of position and number of openings on the performance of composite steel shear walls. *Buildings*, 8(9), Article 121. <https://doi.org/10.3390/buildings8090121>
- Barea, G., Ganem, C., & Esteves, A. (2017). The multi-azimuthal window as a passive solar system: A study of heat gain for the rational use of energy. *Energy and Buildings*, 144, 251-261. <https://doi.org/10.1016/j.enbuild.2017.03.059>
- Bastien, D. (2019). Natural ventilation with a supply air window and motorized skylight: A field study. *IOP Conference Series: Materials Science and Engineering*, 609(3), Article 032005. <https://doi.org/10.1088/1757-899X/609/3/032005>
- Bayoumi, M. (2017). Impacts of window opening grade on improving the energy efficiency of a façade in hot climates. *Building and Environment*, 119, 31-43. <https://doi.org/10.1016/j.buildenv.2017.04.008>
- Bidel, F., Sahlabadi, A. S., Jafari, M. J., & Khodakarim, S. (2020). Evaluation of the effect of heat stress on cognitive performance and physiological parameters of the students. *Iran Occupational Health*, 17(1), 893-907.
- Caetano, D. S., Kalz, D. E., Lomardo, L. L. B., & Rosa, L. P. (2017). Evaluation of thermal comfort and occupant satisfaction in office buildings in hot and humid climate regions by means of field surveys. *Energy Procedia*, 115, 183-194. <https://doi.org/10.1016/j.egypro.2017.05.017>
- Carlos, J. S. (2017). The impact of refurbished windows on Portuguese old school buildings. *Architectural Engineering and Design Management*, 13(3), 185-201. <https://doi.org/10.1080/17452007.2016.1274252>
- Castillo, J. A., & Huelsz, G. (2017). Indoor comfort evaluation by natural ventilation in hot climates: Heat Balance Index. *Proceedings of 33rd PLEA International Conference: Design to Thrive, PLEA 2017*, 3(2006), 4909-4916.
- Chen, F. B., Wang, X. L., Zhao, Y., Li, Y. B., Li, Q. S., Xiang, P., & Li, Y. (2020). Study of wind loads and wind speed amplifications on high-rise building with opening by numerical simulation and wind tunnel test. *Advances in Civil Engineering*, 2020, Article 8850688. <https://doi.org/10.1155/2020/8850688>

- Chen, Y., Tao, M., & Liu, W. (2020). High temperature impairs cognitive performance during a moderate intensity activity. *Building and Environment*, 186, Article 107372. <https://doi.org/10.1016/j.buildenv.2020.107372>
- Chen, Z., Hammad, A. W. A., Kamardeen, I., & Haddad, A. (2020). Optimising window design on residential building facades by considering heat transfer and natural lighting in nontropical regions of Australia. *Buildings*, 10(11), 1-27. <https://doi.org/10.3390/buildings10110206>
- Chow, T. T., & Lyu, Y. (2017). Effect of design configurations on water flow window performance. *Solar Energy*, 155, 354-362. <https://doi.org/10.1016/j.solener.2017.06.050>
- Cruz, H., & Viegas, J. C. (2016). On-site assessment of the discharge coefficient of open windows. *Energy and Buildings*, 126, 463-476. <https://doi.org/10.1016/j.enbuild.2016.05.051>
- Cuce, E., Sher, F., Sadiq, H., Cuce, P. M., Guclu, T., & Besir, A. B. (2019). Sustainable ventilation strategies in buildings: CFD research. *Sustainable Energy Technologies and Assessments*, 36, Article 100540. <https://doi.org/10.1016/j.seta.2019.100540>
- Dama, A., Angeli, D., & Larsen, O. K. (2017). Naturally ventilated double-skin façade in modeling and experiments. *Energy and Buildings*, 144, 17-29. <https://doi.org/https://doi.org/10.1016/j.enbuild.2017.03.038>
- de Faria, L., Cook, M. J., Loveday, D., Angelopoulos, C., Manu, S., & Shukla, Y. (2018, December 1). Sizing natural ventilation systems for cooling: The potential of NV systems to deliver thermal comfort while reducing energy demands of multi-storey residential buildings in India. In *PLEA 2018 - Smart and Healthy within the Two-Degree Limit: Proceedings of the 34th International Conference on Passive and Low Energy Architecture*. Hong Kong, China.
- Derakhshan, S., & Shaker, A. (2017). Numerical study of the cross-ventilation of an isolated building with different opening aspect ratios and locations for various wind directions. *International Journal of Ventilation*, 16(1), 42-60. <https://doi.org/10.1080/14733315.2016.1252146>
- El Dakdoky, S. (2019). Impact of plan shape and window parameters on performance efficiency of office buildings. *Journal of Engineering and Applied Science*, 66(2), 199-219.
- El Khattabi, E. M., Mharzi, M., Zouini, M., & Valančius, K. (2018). Comparative study of various thermal analyses of smart windows in cubic building design. *Journal of Engineering Science and Technology Review*, 11(5), 86-92. <https://doi.org/10.25103/jestr.115.10>
- Elghamry, R., & Hassan, H. (2020). Impact of window parameters on the building envelope on the thermal comfort, energy consumption and cost and environment. *International Journal of Ventilation*, 19(4), 233-259. <https://doi.org/10.1080/14733315.2019.1665784>
- Elshafei, G., Negm, A., Bady, M., Suzuki, M., & Ibrahim, M. G. (2017). Numerical and experimental investigations of the impacts of window parameters on indoor natural ventilation in a residential building. *Energy and Buildings*, 141, 321-332. <https://doi.org/10.1016/j.enbuild.2017.02.055>
- Elwan, M. M. (2020). The role of traditional Lattice window “Mashrabiya” in delivering single-sided ventilation-A CFD study. *International Journal of Engineering Trends and Technology*, 68(9), 154-161. <https://doi.org/10.14445/22315381/IJETT-V68I9P221>

- Enteria, N. A., & Cuartero-Enteria, O. L. (2017). CFD evaluation on the pre- and post- Renovation, and windows and doors opening, of a typical, walled, detached family house in the Philippines. *Infrastructures*, 2(4), Article 16. <https://doi.org/10.3390/infrastructures2040016>
- Fan, X., Liu, W., & Wargocki, P. (2019). Physiological and psychological reactions of sub-tropically acclimatized subjects exposed to different indoor temperatures at a relative humidity of 70%. *Indoor Air*, 29(2), 215-230. <https://doi.org/10.1111/ina.12523>
- Foroughi, R., Mostavi, E., & Asadi, S. (2018). Determining the optimum geometrical design parameters of windows in commercial buildings: Comparison between humid subtropical and humid continental climate zones in the United States. *Journal of Architectural Engineering*, 24(4), Article 04018026. [https://doi.org/10.1061/\(asce\)ae.1943-5568.0000329](https://doi.org/10.1061/(asce)ae.1943-5568.0000329)
- Fusaro, G., Yu, X., Kang, J., & Cui, F. (2020). Development of metacage for noise control and natural ventilation in a window system. *Applied Acoustics*, 170, Article 107510. <https://doi.org/10.1016/j.apacoust.2020.107510>
- Fusaro, G., Yu, X., Lu, Z., Cui, F., & Kang, J. (2021). A metawindow with optimised acoustic and ventilation performance. *Applied Sciences*, 11(7), Article 3168. <https://doi.org/10.3390/app11073168>
- Gautam, K. R., Rong, L., Zhang, G., & Abkar, M. (2019). Comparison of analysis methods for wind-driven cross ventilation through large openings. *Building and Environment*, 154, 375-388. <https://doi.org/10.1016/j.buildenv.2019.02.009>
- Gou, S., Li, Z., Zhao, Q., Nik, V. M., & Scartezzini, J. L. (2015). Climate responsive strategies of traditional dwellings located in an ancient village in hot summer and cold winter region of China. *Building and Environment*, 86, 151-165. <https://doi.org/10.1016/j.buildenv.2014.12.003>
- Guevara, G., Soriano, G., & Mino-Rodriguez, I. (2021). Thermal comfort in university classrooms: An experimental study in the tropics. *Building and Environment*, 187, Article 107430. <https://doi.org/10.1016/j.buildenv.2020.107430>
- Hamdani, M., Bekkouche, S. M. A., Cherier, M. K., Benouaz, T., & Belarbi, R. (2017). Study on effects of window with an external shutters for natural ventilation for buildings in hot climates. In *Proceedings of 2016 International Renewable and Sustainable Energy Conference, IRSEC 2016*, (pp. 780-784). IEEE Publishing. <https://doi.org/10.1109/IRSEC.2016.7983905>
- Hammad, A., Akbarnezhad, A., Grzybowska, H., Wu, P., & Wang, X. (2019). Mathematical optimisation of location and design of windows by considering energy performance, lighting and privacy of buildings. *Smart and Sustainable Built Environment*, 8(2), 117-137. <https://doi.org/10.1108/SASBE-11-2017-0070>
- Hawendi, S., & Gao, S. (2018). Impact of windward inlet-opening positions on fluctuation characteristics of wind-driven natural cross ventilation in an isolated house using LES. *International Journal of Ventilation*, 17(2), 93-119. <https://doi.org/10.1080/14733315.2017.1356054>
- Hossain, M. M., Lau, B., Wilson, R., & Ford, B. (2017). Effect of changing window type and ventilation strategy on indoor thermal environment of existing garment factories in Bangladesh. *Architectural Science Review*, 60(4), 299-315. <https://doi.org/10.1080/00038628.2017.1337557>
- Huang, Z., Wu, Z., Yu, M., & Dong, Y. (2017). The Measurement of natural ventilation in Huizhou traditional dwelling in summer. *Procedia Engineering*, 205, 1439-1445. <https://doi.org/10.1016/j.proeng.2017.10.350>

- Hwang, J. H., & Lee, H. (2018). Parametric model for window design based on prospect-refuge measurement in residential environment. *Sustainability*, *10*(11), Article 3888. <https://doi.org/10.3390/su10113888>
- Jamaludin, A. A., Hussein, H., Keumala, N., & Mohd Ariffin, A. R. (2017). Post occupancy evaluation of residential college building with bioclimatic design strategies in tropical climate condition of Malaysia. *Jurnal Teknologi*, *79*(4), 113-122. <https://doi.org/10.11113/jt.v79.5607>
- Kamal, S. N. O., Salim, D. A., Fouzi, M. S. M, Khai, D. T. H., & Yusof, M. K. Y. (2017). Feasibility study of turbine inlet air cooling using mechanical chillers in Malaysia climate. *Energy Procedia*, *138*, 558-563. <https://doi.org/10.1016/j.egypro.2017.10.159>
- Karan, E., & Asadi, S. (2019). Intelligent designer: A computational approach to automating design of windows in buildings. *Automation in Construction*, *102*, 160-169. <https://doi.org/10.1016/j.autcon.2019.02.019>
- Kim, H. J., & Kim, J. S. (2018). Design methodology for street-oriented block housing considering daylight and natural ventilation. *Sustainability*, *10*(9), Article 3154. <https://doi.org/10.3390/su10093154>
- Kim, S. H., Jeong, H., & Cho, S. (2019). A Study on changes of window thermal performance by analysis of physical test results in Korea. *Energies*, *12*(20), Article 3822. <https://doi.org/10.3390/en12203822>
- Kitagawa, H., Asawa, T., Kubota, T., Trihamdani, A. R., Sakurada, K., & Mori, H. (2021). Optimization of window design for ventilative cooling with radiant floor cooling systems in the hot and humid climate of Indonesia. *Building and Environment*, *188*, Article 107483. <https://doi.org/10.1016/j.buildenv.2020.107483>
- Koohsari, A. M., & Heidari, S. (2020). Optimizing window size by integrating energy and lighting analyses considering occupants' visual satisfaction. *Built Environment Project and Asset Management*, *11*(4), 673-686. <https://doi.org/10.1108/BEPAM-02-2020-0034>
- Kosutova, K., van Hooff, T., Vanderwel, C., Blocken, B., & Hensen, J. (2019). Cross-ventilation in a generic isolated building equipped with louvers: Wind-tunnel experiments and CFD simulations. *Building and Environment*, *154*, 263-280. <https://doi.org/10.1016/j.buildenv.2019.03.019>
- Kumar, S., Xiang, T. B., & Lee, H. P. (2020). Ventilated acoustic metamaterial window panels for simultaneous noise shielding and air circulation. *Applied Acoustics*, *159*, Article 107088. <https://doi.org/10.1016/j.apacoust.2019.107088>
- Li, C., Lyu, Y., Li, C., & Qiu, Z. (2020). Energy performance of water flow window as solar collector and cooling terminal under adaptive control. *Sustainable Cities and Society*, *59*, Article 102152. <https://doi.org/10.1016/j.scs.2020.102152>
- Li, C., & Tang, H. (2020). Evaluation on year-round performance of double-circulation water-flow window. *Renewable Energy*, *150*, 176-190. <https://doi.org/10.1016/j.renene.2019.12.153>
- Li, C., Tang, H., Tan, J., Li, C., Yang, Y., & Zeng, F. (2021). Numerical simulation on year-round performance of water-flow window with different shading control modes. *Building Services Engineering Research and Technology*, *42*(2), 157-174. <https://doi.org/10.1177/0143624420970397>
- Liang, R., Sun, Y., Aburas, M., Wilson, R., & Wu, Y. (2018). Evaluation of the thermal and optical performance of thermochromic windows for office buildings in China. *Energy and Buildings*, *176*, 216-231. <https://doi.org/10.1016/j.enbuild.2018.07.009>

- Lin, H. T., Guu, Y. H., & Hsu, W. H. (2021). Design and fabrication of a novel window-type convection device. *Applied Sciences*, 11(1), Article 267. <https://doi.org/10.3390/app11010267>
- Liu, T., & Lee, W. L. (2019). Using response surface regression method to evaluate the influence of window types on ventilation performance of Hong Kong residential buildings. *Building and Environment*, 154, 167-181. <https://doi.org/10.1016/j.buildenv.2019.02.043>
- Liu, T., & Lee, W. L. (2020). Influence of window opening degree on natural ventilation performance of residential buildings in Hong Kong. *Science and Technology for the Built Environment*, 26(1), 28-41. <https://doi.org/10.1080/23744731.2019.1659026>
- Liu, Y., Misztal, P. K., Xiong, J., Tian, Y., Arata, C., Nazaroff, W. W., & Goldstein, A. H. (2018). Detailed investigation of ventilation rates and airflow patterns in a northern California residence. *Indoor Air*, 28(4), 572-584. <https://doi.org/10.1111/ina.12462>
- Maleki, A., & Dehghan, N. (2020). Optimization of energy consumption and daylight performance in residential building regarding windows design in hot and dry climate of Isfahan. *Science and Technology for the Built Environment*, 27(3), 351-366. <https://doi.org/10.1080/23744731.2020.1812294>
- Manigandan, S., Gunasekar, P., Devipriya, J., Anderson, A., & Nithya, S. (2018). Energy-saving potential by changing window position and size in an isolated building. *International Journal of Ambient Energy*, 39(5), 462-466. <https://doi.org/10.1080/01430750.2017.1318782>
- Manolesos, M., Gao, Z., & Bouris, D. (2018). Experimental investigation of the atmospheric boundary layer flow past a building model with openings. *Building and Environment*, 141, 166-181. <https://doi.org/10.1016/j.buildenv.2018.05.049>
- Marino, C., Nucara, A., & Pietrafesa, M. (2017). Does window-to-wall ratio have a significant effect on the energy consumption of buildings? A parametric analysis in Italian climate conditions. *Journal of Building Engineering*, 13, 169-183. <https://doi.org/10.1016/j.jobbe.2017.08.001>
- Masood, O. A. I., Al-Hady, M. I. A., & Ali, A. K. M. (2017). Applying the principles of green architecture for saving energy in buildings. *Energy Procedia*, 115, 369-382. <https://doi.org/10.1016/j.egypro.2017.05.034>
- Michael, A., Demosthenous, D., & Philokyprou, M. (2017). Natural ventilation for cooling in Mediterranean climate: A case study in vernacular architecture of Cyprus. *Energy and Buildings*, 144, 333-345. <https://doi.org/10.1016/j.enbuild.2017.03.040>
- Misiopecki, C., Bouquin, M., Gustavsen, A., & Jelle, B. P. (2018). Thermal modeling and investigation of the most energy-efficient window position. *Energy and Buildings*, 158, 1079-1086. <https://doi.org/10.1016/j.enbuild.2017.10.021>
- Moon, W. C., Lau, T. L., & Puay, H. T. (2020). Experimental investigations of tsunami loading on internal wall of a building with various openings and wall configurations. *Coastal Engineering*, 158, Article 103691. <https://doi.org/10.1016/j.coastaleng.2020.103691>
- Mori, H., Kubota, T., Antaryama, I. G. N., & Ekasiwi, S. N. N. (2020). Analysis of window-opening patterns and air conditioning usage of urban residences in tropical southeast Asia. *Sustainability*, 12(24), Article 10650. <https://doi.org/10.3390/su122410650>

- Mousa, Y., Lang, W. A., W., & Auer, T. (2017). Numerical assessment of the efficiency of fenestration system and natural ventilation mechanisms in a courtyard house in hot climate. *Building Simulation*, 10, 737-754. <https://doi.org/10.1007/s12273-017-0357-0>
- Nalamwar, M. R., Parbat, D. K., & Singh, D. P. (2017). Study of effect of windows location on ventilation by CFD simulation. *International Journal of Civil Engineering and Technology*, 8(7), 521-531.
- Nasrollahi, N., & Salehi, M. (2015). Performance enhancement of double skin facades in hot and dry climates using wind parameters. *Renewable Energy*, 83, 1-12. <https://doi.org/10.1016/j.renene.2015.04.019>
- Nitatwichit, C., Khunatorn, Y., & Tippayawong, N. (2008). Investigation and characterization of cross ventilating flows through openings in a school classroom. *Journal of the Chinese Institute of Engineers, Transactions of the Chinese Institute of Engineers, Series A/Chung-Kuo Kung Ch'eng Hsueh K'an*, 31(4), 587-603. <https://doi.org/10.1080/02533839.2008.9671413>
- Nota, R., Jochim, S., & Bad'ura, R. (2017). Impact of the schape of the casement on the inside surface temperature at wood-aluminium windows, *Acta Facultatis Xylogologiae Zvolen*, 59(2), 115-126. <https://doi.org/10.17423/afx.2017.59.2.11>
- Nunes de Freitas, P., & Guedes, M. C. (2015). The use of windows as environmental control in "Baixa Pombalina's" heritage buildings. *Renewable Energy*, 73, 92-98. <https://doi.org/10.1016/j.renene.2014.08.029>
- O'Sullivan, P. D., & Kolokotroni, M. (2017). A field study of wind dominant single sided ventilation through a narrow slotted architectural louvre system. *Energy and Buildings*, 138, 733-747. <https://doi.org/10.1016/j.enbuild.2016.11.025>
- Orouji, P., Vakili, A., Behrouz, M. K., Jafari, H. H., Eslami, M. R., Vahidnia, M., Sadegh, R. M., & Rezaie, M. (2019). Methodology of standardizing the energy labeling and rating of window fenestration in IRAN. *Sustainable Energy Technologies and Assessments*, 33, 24-33. <https://doi.org/10.1016/j.seta.2019.02.009>
- Osayande, O., & Christopher, O. (2012). Grey Literature acquisition and management: Challenges in academic libraries in Africa. *Library Philosophy and Practice (e-journal)*.
- Page, M. J., McKenzie, J. E., Bossuyt, P. M., Boutron, I., Hoffmann, T. C., Mulrow, C. D., Moher, D. (2021). The PRISMA 2020 statement: An updated guideline for reporting systematic reviews. *The BMJ*, 372(n71). <https://doi.org/10.1136/bmj.n71>
- Pilechiha, P., Mahdavinejad, M., Pour Rahimian, F., Carnemolla, P., & Seyedzadeh, S. (2020). Multi-objective optimisation framework for designing office windows: Quality of view, daylight and energy efficiency. *Applied Energy*, 261, Article 114356. <https://doi.org/10.1016/j.apenergy.2019.114356>
- Rabanillo-Herrero, M., Padilla-Marcos, M. Á., Feijó-Muñoz, J., Gil-Valverde, R., & Meiss, A. (2020). Ventilation efficiency assessment according to the variation of opening position in L-shaped rooms. *Building Simulation*, 13, 213-221. <https://doi.org/10.1007/s12273-019-0566-9>
- Rizal, Y., Robandi, I., & Yuniarno, E. M. (2020). Daylight factor distribution optimization based on sky component on the room for window openings. *International Journal of Innovative Computing, Information and Control*, 16(1), 15-28. <https://doi.org/10.24507/ijicic.16.01.15>



- Ruan, F., & Li, N. (2012). Comparison of wind-driven natural ventilation for different windows in a room with a single opening. *International Journal of Ventilation*, 11(2), 193-204. <https://doi.org/10.1080/14733315.2012.11683981>
- Saadatjoo, P., Mahdavejad, M., & Zhang, G. (2018). A study on terraced apartments and their natural ventilation performance in hot and humid regions. *Building Simulation*, 11, 359-372. <https://doi.org/10.1007/s12273-017-0407-7>
- Sacht, H., & Lukiantchuki, M. A. (2017). Windows size and the performance of natural ventilation. *Procedia Engineering*, 196, 972-979. <https://doi.org/10.1016/j.proeng.2017.08.038>
- Sadrizadeh, S., Pantelic, J., Sherman, M., Clark, J., & Abouali, O. (2018). Airborne particle dispersion to an operating room environment during sliding and hinged door opening. *Journal of Infection and Public Health*, 11(5), 631-635. <https://doi.org/10.1016/j.jiph.2018.02.007>
- Scheuring, L., & Weller, B. (2020). An investigation of ventilation control strategies for louver windows in different climate zones. *International Journal of Ventilation*, 3-4, 226-235. <https://doi.org/10.1080/14733315.2020.1777018>
- Shetabivash, H. (2015). Investigation of opening position and shape on the natural cross ventilation. *Energy and Buildings*, 93, 1-15. <https://doi.org/10.1016/j.enbuild.2014.12.053>
- Stamatopoulos, P., Drosatos, P., Nikolopoulos, N., & Rakopoulos, D. (2019). Determination of a methodology to derive correlations between window opening mass flow rate and wind conditions based on CFD results. *Energies*, 12(9), Article 1600. <https://doi.org/10.3390/en12091600>
- Su, L., Fraaß, M., & Wondraczek, L. (2021). Design guidelines for thermal comfort and energy consumption of triple glazed fluidic windows on building level. *Advanced Sustainable Systems*, 5(2), Article 2000194. <https://doi.org/10.1002/adsu.202000194>
- Sung, W. P., Chen, R., Chang, H. C., & Zhao, Y. K. (2014). Living comfortable strategies for offices in Taiwan's hot-humid climate. *Applied Mechanics and Materials*, 457-458, 1498-1502. <https://doi.org/10.4028/www.scientific.net/AMM.457-458.1498>
- Tan, Z., & Deng, X. (2020). An optimised window control strategy for naturally ventilated residential buildings in warm climates. *Sustainable Cities and Society*, 57, Article 102118. <https://doi.org/10.1016/j.scs.2020.102118>
- Tarmizi, A. H. A., Rahmat, S. N., Karim, A. T. A., & Tukimat, N. N. A. (2019). Climate change and its impact on rainfall. *International Journal of Integrated Engineering*, 11(1), 170-177.
- Tena-Colunga, A., & Liga-Paredes, A. E. (2020). Approximation of lateral stiffness for walls with two bands of openings considering slab stiffness effects. *Journal of Building Engineering*, 30, Article 101310. <https://doi.org/10.1016/j.jobbe.2020.101310>
- Vadugapalayam, R., Sivanathan, S., & Muthu, R. (2017). Experimental investigation on single-sided transient natural ventilation driven by buoyancy. *Thermal Science*, 21(suppl. 2), 489-496. <https://doi.org/10.2298/TSCI17S2489V>
- Wahab, I. A., Ismail, L. H., Abdullah, A. H., Rahmat, M. H., & Salam, N. N. A. (2018). Natural ventilation design attributes application effect on indoor natural ventilation performance of a double storey single



- unit residential building. *International Journal of Integrated Engineering*, 10(2), 7-12. <https://doi.org/10.30880/ijie.2018.10.02.002>
- Wang, W., Kato, N., Kimoto, S., Matsui, Y., & Yoneda, M. (2020). Simulation and evaluation of sheltering efficiency of houses equipped with ventilation systems. *Building and Environment*, 168, Article 106491. <https://doi.org/10.1016/j.buildenv.2019.106491>
- Wellun, Z., Yusoff, W. F. M., Mohamed, M. F., Mat Sulaiman, K. A., & Rasani, M. R. M. (2021). Field measurement of indoor environment of a room with single-sided sliding glass opening. *Journal of Physics: Conference Series*, 2053, Article 012017. <https://doi.org/10.1088/1742-6596/2053/1/012017>
- Wijewardane, S., & Jayasinghe, M. T. R. (2008). Thermal comfort temperature range for factory workers in warm humid tropical climates. *Renewable Energy*, 33(9), 2057-2063. <https://doi.org/10.1016/j.renene.2007.11.009>
- Wu, M., Shi, Y., Li, R., & Wang, P. (2018). Spectrally selective smart window with high near-infrared light shielding and controllable visible light transmittance. *ACS Applied Materials and Interfaces*, 10(46), 39819-39827. <https://doi.org/10.1021/acsami.8b15574>
- Xing, F., Mohotti, D., & Chauhan, K. (2018). Experimental and numerical study on mean pressure distributions around an isolated gable roof building with and without openings. *Building and Environment*, 132, 30-44. <https://doi.org/10.1016/j.buildenv.2018.01.027>
- Yang, L., Liu, X., Qian, F., & Du, S. (2019). Ventilation effect on different position of classrooms in “line” type teaching building. *Journal of Cleaner Production*, 209, 886-902. <https://doi.org/10.1016/j.jclepro.2018.10.228>
- Yılmaz, Y., & Yılmaz, B. Ç. (2021). A weighted multi-objective optimisation approach to improve based facade aperture sizes in terms of energy, thermal comfort and daylight usage. *Journal of Building Physics*, 44(5), 435-460. <https://doi.org/10.1177/1744259120930047>
- Yoon, N., Piette, M. A., Han, J. M., Wu, W., & Malkawi, A. (2020). Optimization of window positions for wind-driven natural ventilation performance. *Energies*, 13(10), Article 2464. <https://doi.org/10.3390/en13102464>
- Zhai, Y., Wang, Y., Huang, Y., & Meng, X. (2019). A multi-objective optimization methodology for window design considering energy consumption, thermal environment and visual performance. *Renewable Energy*, 134, 1190-1199. <https://doi.org/10.1016/j.renene.2018.09.024>
- Zhao, J., & Du, Y. (2020). Multi-objective optimization design for windows and shading configuration considering energy consumption and thermal comfort: A case study for office building in different climatic regions of China. *Solar Energy*, 206, 997-1017. <https://doi.org/10.1016/j.solener.2020.05.090>
- Zhou, J., Ye, C., Hu, Y., Hemida, H., Zhang, G., & Yang, W. (2017). Development of a model for single-sided, wind-driven natural ventilation in buildings. *Building Services Engineering Research and Technology*, 38(4), 381-399. <https://doi.org/10.1177/0143624417699658>
- Zomorodian, Z. S., & Tahsildoost, M. (2017). Assessment of window performance in classrooms by long term spatial comfort metrics. *Energy and Buildings*, 134, 80-93. <https://doi.org/10.1016/j.enbuild.2016.10.018>

## Predicting Students' Inclination to TVET Enrolment Using Various Classifiers

Chia Ming Hong<sup>1\*</sup>, Chee Keong Ch'ng<sup>1</sup> and Teh Raihana Nazirah Roslan<sup>2</sup>

<sup>1</sup>Department of Decision Science, School of Quantitative Sciences, Universiti Utara Malaysia, 06010 UUM, Sintok, Kedah, Malaysia

<sup>2</sup>Othman Yeop Abdullah Graduate School of Business, Universiti Utara Malaysia, 50300 UUM, Kuala Lumpur, Malaysia

### ABSTRACT

Technical and Vocational Education and Training (TVET) is an education system that delivers necessary information, skills, and attitudes related to work or self-employment. However, the TVET program is not preferred by most Malaysian students due to several factors such as students' interest, parental influence, employers' negative impression, facility in vocational institutions, inexperienced TVET instructors, and society's negative perception. Consequently, it raises the issue of skilled workers shortage. The gravest threat will be far-reaching, pushing our economy into depreciation. Therefore, it is important to identify the students' traits and interests before conducting further investigation to turn and thrive in this phenomenon. This study aims to utilise several classifiers (Decision Tree, Neural Network, Logistic Regression and Naïve Bayes) to predict students' inclination to join TVET programmes. A total of 428 secondary school students from Kedah, Malaysia, are chosen as our survey respondents. The best classifier is determined according to the lowest misclassification rate. The findings revealed that the Decision Tree-based Gini Index with three branches prevail against other classifiers with a misclassification rate

of 0.1938. Therefore, the classifier could act as a steer for the Kedah Department of Education (DOE), related parties, and the TVET agency in implementing effective strategies to enliven and inspire students to join TVET programs.

### ARTICLE INFO

#### Article history:

Received: 08 March 2022

Accepted: 27 April 2022

Published: 09 November 2022

DOI: <https://doi.org/10.47836/pjst.31.1.28>

#### E-mail addresses:

carmenhongcm@gmail.com (Chia Ming Hong)

chee@uum.edu.my (Chee Keong Ch'ng)

raihana@uum.edu.my (Teh Raihana Nazirah Roslan)

\* Corresponding author

**Keywords:** Decision tree, logistic regression, Naïve Bayes, neural network, technical and vocational education and training

## INTRODUCTION

The Fourth Industrial Revolution 4.0 (IR 4.0) is rapidly transforming and changing the skills demanded by the industry. The readiness of Technical and Vocational Education and Training (TVET) institutions to produce a high-quality workforce and high-value competing manufacturers is vital for developing human capital to make Malaysia a high-income and developed nation (Sulaiman & Salleh, 2016; Yaakob, 2017). Therefore, the government should enforce the TVET program by coordinating different resources from various agencies. The education system must provide the opportunity to learn from basic to advanced levels across various institutional and work settings and focus on students' understanding of industrial processes and enormous technical skills. Previously, several efforts have been implemented by the Malaysian government to attract more students to enrol in TVET. For instance, the government had allocated RM30 million under Malaysia Budget 2019, RM5.9 billion under Malaysia Budget 2020 and RM 6 billion under Malaysia Budget 2021 to boost the quality of TVET (Sivanandam et al., 2019; Rajaendram, 2020). Currently, there are 36 polytechnics, 98 community colleges, 80 vocational colleges, 676 public-accredited vocational centres, and 642 private accredited vocational centres in Malaysia. It indicated that the government aims to produce a top-notch workforce towards becoming a fully industrialised, developed, and high-income nation.

Although the number of TVET institutions has been increasing, most school leavers are unaware of the advantages of TVET (Sabang, 2017; Azizi, 2018). One of the benefits of being a TVET graduate is that the average employability rate of TVET graduates is as high as 96% in the industry (Ismail et al., 2021). It shows that most TVET graduates can secure a job after they graduate. Other than that, TVET can equip students with specific skills to face the working environment so they will not have any difficulties in their work (Karim, 2018). However, despite our government's recognition of TVET certification, students still resist vocational education, resulting in low enrolment, which is far from the expected number (KRI, 2018; Aziz, 2019). According to the Malaysia Human Resource Minister, the government expects at least 35% of skilled workers in the industry, but currently, there are only 28% skilled workers (Aziz, 2019). As a result, the number of skilled workers is still far from reaching the market demands. Several adverse factors to the TVET program are identified, such as students' interest, parental influence, employers' negative impression, facility in vocational institutions, inexperienced TVET instructors, society's negative perception, government policy, and expensive education costs (Hong et al., 2021).

In investigating the palpable phenomenon, the mentioned factors can assist in developing models which aim to study the students' inclination using data mining approaches. It uses statistical study techniques to extract the data pattern and transform the information into an easily understandable structure for future usage (Sahu et al., 2011). There has been a surge

of interest in using data mining techniques to tackle educational research issues, specifically Educational Data Mining (EDM). EDM has emerged rapidly in becoming an important field to reveal hidden yet meaningful data patterns in educational institutions. It is widely applied in many areas, such as the prediction of students' enrolment, the performance of students and teachers in school, and students' dropout rates.

Several kinds of research related to the prediction of students' enrolment in EDM have been performed using data mining techniques such as Decision Tree, Logistic Regression, Neural Network and Naïve Bayes (Khan & Choi, 2014; Raju & Schumacker, 2015; Hung et al., 2020; Messele & Addisu, 2020). However, there is a lack of a predictive model discussing students' enrolment in vocational education institutions. Most previous studies focus on the student's performance using data mining approaches. Specifically, most researchers only apply one data mining approach in their data analysis (Babu et al., 2020; Messele & Addisu, 2020; Herlambang et al., 2019). Therefore, the main objective of this study is to utilize and compare several data mining approaches, namely Decision Tree, Neural Network, Logistic Regression and Naïve Bayes, to investigate the students' inclination to TVET enrolment. This study is unique in addressing the current TVET challenges in Malaysia. So far, no specific model has been developed to help the government identify students' tendency to join TVET even though huge grants and funds have been allocated (as stated in MOHE's Malaysia Education Blueprint (Higher Education) and Malaysia Budget).

## LITERATURE REVIEW

### Sustainable Development Goals (SDGs)

Sustainable Development Goals (SDGs) are important to ensure that all people worldwide can enjoy endless peace and prosperity. Some goals are closely related to the TVET field. For example, Goal 4 is for quality education, and Goal 5 is for gender equality. SDGs ensure that all students receive a high standard of education and encourage them to continue studying throughout their lives (Mustapha, 2015). By 2030, all people will have affordable, high-quality technical, vocational and tertiary education. Other than the quality of education, SDGs also emphasise long-term economic growth, increased productivity, and encourage the development of new technologies (Berawi, 2019; Imaz & Sheinbaum, 2017). Consequently, there will be demand for TVET workers who act as the experts in creating technological products. In addition, sustainable industrialization is one of the goals to be achieved in SDGs. To fulfil this, TVET workers play an important role because they are trained to handle, manage and upgrade new technologies. However, the resistance issues of young generations to TVET remain unchanged.

## TVET Issues

In Malaysia, most students are still reluctant to enrol in TVET programs due to some factors. Students' interests, vocational talent, demographic background, and personality are the main components in determining the students' tendency in enrolling TVET (Ismail & Hassan, 2013). However, negative social perceptions toward TVET, such as labelling TVET students as low achievers in school, cause intense impediments (Abdul-Aziz et al., 2020; Ismail & Hassan, 2013; Amedorme & Fiagbe, 2013). Consequently, this leads to poor perception from parents' perspectives (Hussin et al., 2017; Koya, 2019). Likewise, the employer is one factor that discourages students from choosing TVET because of the TVET graduates' qualification issues (Cheong & Lee, 2016; Chan, 2018).

Furthermore, TVET instructors who are inexperienced, and lacking in information, communication, and technology (ICT) and English skills can affect students' inclination to TVET (Ismail et al., 2017; Ismail & Hassan, 2013). According to Amin (2016), currently, there are two accreditation bodies (Malaysian Qualification Agency and Department for Skill Development), which confuses the graduates in choosing the right accreditation channel. Certain employers only accept accreditation from the Malaysian Qualification Agency. As a result, students may be perplexed when choosing a course with many certification agencies. Education cost is also one of the barriers for students to pursue their education in TVET institutions because technical education is costly, and the allocation from the government is not enough to cover the cost (TheStart, 2019). Lastly, poor facilities in technical institutions can sway away students' interest too—for instance, poor equipment, unfunctional air conditioners, and cramped classrooms (Bakar, 2011).

## Introduction to Data Mining Approaches

This study uses descriptions, and related equations for several popular data mining approaches: Decision Tree, Neural Network, Logistic Regression, and Naïve Bayes.

**Decision Tree.** Researchers widely apply a Decision Tree for prediction and classification due to its simplicity and transparency (Salal et al., 2019; Yamini & Ramakrishna, 2015). It is a tree-like structure that consists of a root node, internal node, and leaf node. The root node is also the parent node, which does not have incoming edges. Branches connect the root node with the internal node, which has outgoing and incoming edges. Nodes with no outgoing edges are known as leaf nodes (Rokach & Maimon, 2015).

Several algorithms are involved in inducing a Decision Tree, such as ID3, C4.5 CART, and CHAID algorithms. The differences between those algorithms depend on the splitting criteria. Entropy and Gini index are the most commonly used splitting criteria (Breiman, 1996). Entropy is the way to measure the impurity in the sample. It ranges from 0 to 1. The Equation 1 of Entropy is displayed below:

$$\text{Entropy, } H(x) = - \sum p(x) \log_2 p(x) \quad (1)$$

where  $x$  = random variable;  $p(x)$  = the possibility of result  $x$  in variable  $x$ .

If the entropy value equals 0, it is defined as the sample is completely homogeneous. Next, Gini Index calculates the likelihood of a randomly chosen feature being wrongly categorised. Equation 2 of the Gini Index is displayed below:

$$\text{Gini Index} = 1 - \sum [p(x)]^2 \quad (2)$$

where  $p(x)$  = the possibility of result  $x$  of variable  $x$ .

The Gini Index ranges from 0 to 1, with 0 as classification purity and 1 as the random distribution of elements among different classes.

**Artificial Neural Network (ANN).** An Artificial Neural Network (ANN) is a copy of the human brain. It consists of processing units known as neurons (Kelvin, 1997). It is a tool to discover data patterns and tackle recurring problems in certain areas. A bias value will be added along with the input,  $x_i$  (Zakaria et al., 2014). Weight,  $w_i$  is the strength of the processing ability of input. The product of weight and input is the strength of the signal. To activate the neurons, one commonly used activation function is the sigmoid function (Kukreja et al., 2016). It is important to understand how neural network solves complex problems. Equation 3 is shown below:

$$f(x) = \frac{1}{1 + e^{-\text{sum}}} \quad (3)$$

where  $\text{sum} = \sum_{i=0}^n x_i w_i$ .

The value of the sigmoid function is ranged between 0 and 1. The structure of ANN includes the input layer, hidden layer, and output layer. The input layer begins the flow, which receives the input data to be processed in the ANN system. The hidden layer is between the input layer and an output layer which can be zero or more than one. It is used for the transformation of input to enter the network. Finally, the output layer shows the output classification that maps the input pattern (Islam et al., 2019).

**Logistic Regression.** Logistic regression is another approach used to model the probability of a binary or dichotomous dependent variable. For example, if the predicted value probability is less than 0.5 will be assigned to group 0; group 1 otherwise. The advantages of logistic regression are that it is relatively fast compared to other supervised classification techniques and allows the evaluation of multiple explanatory variables by extension of the basic principles. The specified form of the logistic regression model can be written as Equation 4:

$$p = \frac{1}{1 + e^{-(b_0 + b_1 X_1 + b_2 X_2 + \dots + b_p X_p)}} \tag{4}$$

where  $p$  = target variable;  $X_i$  = independent variable;  $b_i$  = parameter of the model.

The value will always be positive, ranging from 0 to 1.

**Naïve Bayes.** Naïve Bayes is a simple probability classifier applying Bayes' theorem with strong independent assumptions. Bayes' theorem was developed by a mathematician named Thomas Bayes in the 1740s. It is suitable for classification, although the output is more than two classes. For the categorical input, frequencies are used, while for the continuous input, the Gaussian density function or probability density function is used to calculate the probability (Berrar, 2018; Gandhi, 2018). For example, Equation 5 of Naïve Bayes is displayed below:

$$P(a|b) = \frac{p(b|a) p(a)}{p(b)} \tag{5}$$

where  $P(a|b)$  = objective;  $p(a|b)$  = probability of occurrence of  $b$  given  $a$ ;  $p(a)$  = probability of an in the sets of data;  $p(b)$  = probability of occurrence of  $b$ .

Naïve Bayes allows you to calculate the posterior probability,  $P(a|b)$  from  $p(a)$ ,  $p(b)$  and  $p(a|b)$ . As mentioned, the Gaussian density function deals with the continuous input (Gandhi, 2018). Equation 6 is shown below:

$$f(x) = \frac{1}{\sigma\sqrt{2\pi}} e^{-\frac{(x-\mu)^2}{2\sigma^2}} \tag{6}$$

where  $\sigma$  = standard deviation;  $\mu$  = mean.

Besides, there are three types of Naïve Bayes algorithms, namely, Multinomial Naïve Bayes, Bernoulli Naïve Bayes and Gaussian Naïve Bayes. Multinomial Naïve Bayes is used for the discrete data. Text classification is one of the problems in this algorithm. For example, counting how often the word occurs in the paper. For Bernoulli's Naïve Bayes, it is used when the vectors are binary. For example, it is "0 or 1" or "yes or no." The table of parameters for each method is displayed in Table 1.

Table 1  
*Parameters for each method*

No	Method	Parameters
1	Decision Tree	Tree depth, number of features
2	Artificial Neural Network	Number of hidden layers, number of hidden nodes
3	Logistic Regression	Maximum likelihood estimation
4	Naïve Bayes	Prior probabilities of the class, portion of the largest variance of the features



### Application of Data Mining in TVET

Data mining approaches are widely applied in the vocational education field. For example, Matei et al. (2018) used the Decision Tree model to examine the trend of Romanians to choose general or vocational education. To study the individuals' choices, factors such as age, education level, gender, and income range, were collected from the respondents from all regions in Romania through a survey form. The variables were split using the Gini Index, and the age variable was the most important factor. In addition, Babu et al. (2020) compared 16 Decision Tree models in predicting students' performance in their examinations. A Decision Tree with Gini Index was chosen as the best tree. Therefore, the model could be used as a reference for teachers to improve their quality of teaching work.

Next, ANN is useful in classifying and recognising data patterns. Previously, ANN was used to predict the academic achievement of vocational school students in their science subjects such as Physics, Chemistry, and Biology. The independent variables were the variables that influenced students' academic achievement, whereas the dependent variable was set as the mean score of students in those three subjects. Each subject had a different factor that contributed the most to affecting students' achievement. For example, for Physics and Chemistry subjects, the factor of "class size" had the highest significance, while for the Biology subject, the factor of "enthusiasm for Biology" had the highest significance (Yağcı & Çevik, 2017). Neural Network was also used to predict the student's acceptance of the vocational school's learning management system (LMS). A few factors act as important predictors, such as performance expectation, effort expectation, societal influence, and facilitating conditions. Of those factors, the most important factor was "performance expectation", which was defined as the trust in improving performance with the help of technology (Ozkan et al., 2020).

Next, Logistic Regression was widely used to solve education issues. For example, Karim and Maat (2019) applied Logistic Regression to develop a Student Employability Skills (SES) model for TVET students in Malaysia. Multinomial Logistic Regression was used in solving the problem because the dependent variables were more than two. The findings revealed that education level, mother's occupation, and job status were the essential variables that led to high SES. Therefore, the model was useful to perform the prediction for the students' employment after they graduated from school. Other than that, the researchers used Logistic Regression to determine if the "family background" variable would influence the students' intentions to enrol in TVET. Fathers' education, mothers' education, and family income were included as the variables in this study. According to the findings, students' enrolment into TVET was influenced by two significant factors: their fathers' education and family income (Assunção et al., 2019).

Lastly, Naïve Bayes was widely applied in real-world problems such as spamming of email, face recognition software, and text classification. Previously, the researchers

applied Naïve Bayes, which were based on 10-fold-cross validation and percentage split to discover TVET students' performance. It was found that factors such as age, sex, sector, type of employment, training experience, level, the purpose of assessment, and category of the candidate were found to affect students' academic performance (Messele & Addisu, 2020). Naïve Bayes was also implemented to predict the vocational students' learning achievement. For the input, there were many variables such as age, gender, parent's education and occupation, the reason for choosing a school, duration to reach school, study duration, previous class failure, and health. In this paper, the researchers classified the students' achievement into five categories "very good," "good," "fair," "poor", and "failed." The created model had a moderate accuracy which could be a guide for reference in the future (Herlambang et al., 2019).

Despite many data mining approaches widely discussed in educational fields, little attention has been paid to incorporating various classifiers in past research, especially in the TVET issue. Therefore, this study aims to develop several classification models to predict the students' inclination to TVET enrolment in future. The models are compared based on their performances. The model that reaches the highest accuracy will be selected as our predictive model.

## **MATERIALS AND METHOD**

### **Questionnaire Design**

The questionnaire structure is developed based on the previous study by Trudis (2014). Some modifications have been made to that questionnaire to match our suitability. After that, the Cronbach-alpha test is used to measure the reliability of the questionnaire. From the test, the alpha value is 0.612, which means that this questionnaire can be accepted (Ursachi et al., 2015).

### **Data Collection Process**

In the data collection process, 428 students were selected from secondary schools in Kedah, Malaysia. The reason for choosing secondary school students is because this group is eligible for tertiary education soon. The widespread recognition that tertiary education is a major driver of economic competitiveness in an increasingly knowledge-driven global economy. Therefore, the post-secondary school students' opinions are vital, particularly in the TVET course, as it promotes competency-based education and training linked to industry needs. The techniques used to select those respondents are disproportionate stratified sampling with equal allocation and simple random sampling.

Disproportionate stratified sampling is carried out according to the 9 District Education Office (PPD) and 36 State Legislative Assembly (DUN) to justify the number of samples selected in this study. Subsequently, simple random sampling is used to choose the location

in each DUN. For example, three DUN are under PPD Baling: Bayu, Kuala Ketil and Kupang. Therefore, one of them is randomly selected as our targeted location.

After deciding on all the schools, an appointment will be made with the representative. Questionnaires are distributed to students after the briefing. The flowchart of the data collection process is shown in Figure 1.

**Process of Development of Data Mining Approaches**

The process flow of this study is presented in Figure 2, and the explanations of each part are discussed.

**Input Data.** For the input data, the variables in the questionnaire are used to conduct the data analysis. There are 15 input variables and 1 output variable. For the ordinal type variables, the answers use the 5 Likert Scales, where 1 represents strongly disagree, 2 represents disagree, 3 represents not sure, 4 represents agree, and 5 represents strongly agree. The input values applied are based on the Likert scale values. Table 2 shows the role and description of each variable.

**Data Pre-Processing.** In the pre-processing data phase, the data undergoes a few steps, such as data cleaning, data integration, and data reduction, to ensure the data is clean before performing analysis. The most frequent values replace missing values in the dataset.

**Data Partitioning.** Data is split according to the 70:30 rule (Nguyen et al., 2021; Liu & Cocca, 2017). The training set (299 instances) is used to develop the model, whereas the test set (129 instances) is used to evaluate its performance.

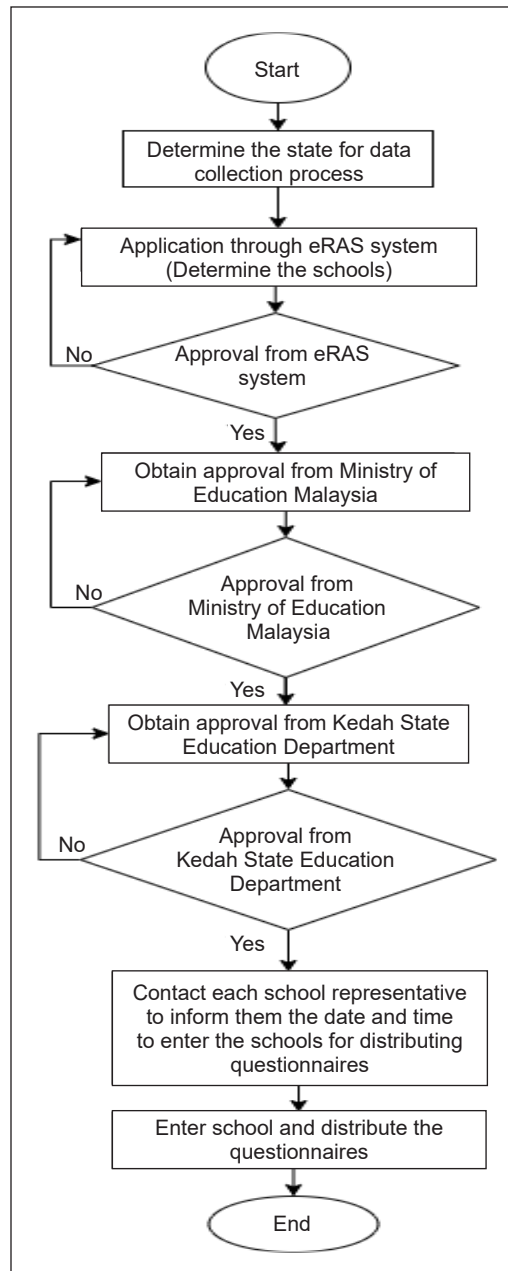


Figure 1. Data collection flowchart

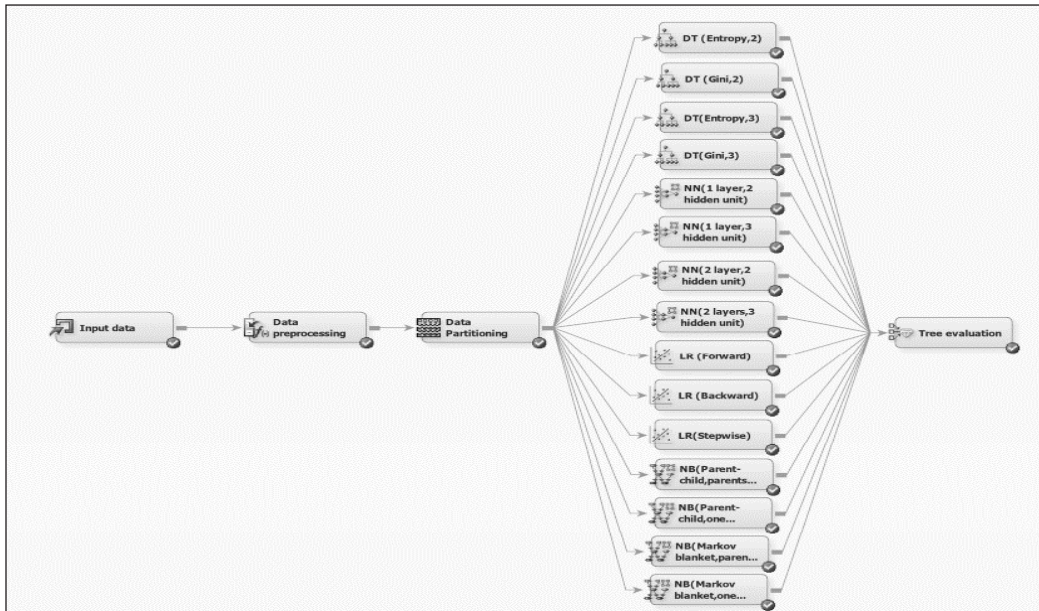


Figure 2. Process flow diagram

Table 2  
Role and description for each variable

Variables	Role	Type	Description
AcademicSubjMoreImportant	Input	Ordinal	Students' agreement towards the academic subject is more important than the vocational subject.
FamilyInvolved	Input	Nominal	Students having family members who had joined TVET
FatherEducation	Input	Nominal	The highest education of the student's father.
FatherJob	Input	Nominal	The occupation of the student's father
Gender	Input	Nominal	Gender of student
HeardTVET	Input	Nominal	The students had heard the information about TVET before.
InterestedTVET	Output	Nominal	The student feels interested in joining TVET after Form 5.
MotherEducation	Input	Nominal	The highest education of the student's mother.
MotherJob	Input	Nominal	The occupation of the student's mother.
PlanAfterForm5	Input	Nominal	The plan of the student after completion of secondary school.
Stream	Input	Nominal	The stream of students in their secondary school.
TVETBright	Input	Ordinal	With the level of agreement towards students who get a TVET certification, people will think they have a bright future.
TVETStudHigherJobChance	Input	Ordinal	The level of agreement toward TVET students will have a higher chance of getting a job compared to those who do not.

Table 2 (continue)

Variables	Role	Type	Description
TVETStudHighSalary	Input	Ordinal	The level of agreement toward TVET students has a high salary.
VocationalSubjStatus	Input	Ordinal	The level of agreement towards the vocational subject has a high status.
VocationalCourseInteresting	Input	Ordinal	The level of agreement towards vocational courses is interesting.

**Models Construction.** Four types of Data Mining models were developed in this study: Decision Tree, Neural Network, Logistic Regression, and Naïve Bayes. Decision Tree mainly focuses on splitting criteria and the number of branches; Artificial Neural Network relies on the number of nodes and layers; Logistic Regression specifies different entry methods for different subsets of variables; Naïve Bayes uses conditional probabilities. Table 3 shows the type of models constructed in this study.

Table 3  
Types of models constructed

No	Model	Criteria
1	Decision Tree	Entropy, 2 branches
		Gini, 2 branches
2	Artificial Neural Network	Entropy, 3 branches
		Gini, 3 branches
		1 layer, 2 hidden units
		1 layer, 3 hidden units
3	Logistic Regression	2 layers, 2 hidden units
		2 layers, 3 hidden units
		Forward
		Backwards
4	Naïve Bayes	Stepwise
		Parent-child structure, parents set
		Parent-child structure, 1 parent
		Markov-blanket structure, parents set
		Markov-blanket structure, 1 parent

**Tree Evaluation.** Several aspects need to be considered to measure the accuracy of the model. These aspects are in the confusion matrix, as shown in Table 4.

True Negative (TN) is the number of correct predictions where the actual class is “no”, and True Positive (TP) is the number

Table 4  
Confusion matrix

Confusion matrix	Predicted	
	No	Yes
Actual No	True Negative (TN)	False Positive (FP)
Actual Yes	False Negative (FN)	True Positive (TP)

of correct predictions where the actual class is “yes.” False Negative (FN) is the number of predictions where the actual class is “yes,” but it is predicted as “no.” The last one is False Positive (FP), which means the actual class is “no” but wrongly predicted as “yes.” The four parameters are used to calculate accuracy, which aims to evaluate the models’ performance. For example, Equation 7 of the misclassification rate is given as below:

$$\text{Misclassification rate} = \frac{\text{FP} + \text{FN}}{\text{TP} + \text{TN} + \text{FP} + \text{FN}}. \quad (7)$$

The model with the lowest misclassification rate is considered the best model.

## RESULTS AND DISCUSSIONS

### Descriptive Analysis of Input Variables

The descriptive analysis of input variables is identified and discussed in Table 5.

Table 5  
*Descriptive analysis of input variables*

No	Variables	Outputs
1	AcademicSubjMoreImportant	Strongly disagree: 6; Disagree: 59; Not sure: 134; Agree: 151; Strongly agree: 78
2	FamilyInvolved	Yes: 64; No: 364
3	FatherEducation	Degree: 26; Diploma: 38; Foundation/ A-level/ Matriculation: 7; No Complete Secondary School: 51; Postgraduate: 13; SPM: 271; STPM: 22
4	FatherJob	Agriculture: 37; Clerical/ Civil Service: 128; Construction: 10; Manufacturing: 6; Others: 49; Professional: 3; Retail: 6; Self-employed: 167; Unemployed: 22
5	Gender	Female: 246; Male: 182
6	HeardTVET	Yes: 117; No: 311
7	MotherEducation	Degree: 26; Diploma: 37; Foundation/ A-level/ Matriculation: 11; No Complete Secondary School: 54; Postgraduate: 19; SPM: 257; STPM: 24
8	MotherJob	Agriculture: 4; Clerical/ Civil Service: 102; Manufacturing: 4; Others: 30; Professional: 4; Retail: 6; Self-employed: 120; Unemployed: 158
9	PlanAfterForm5	Form 6: 30; Matriculation: 26; Polytechnic: 91; Skill Training Centre: 74; University/ Private College: 163; Work: 44
10	Stream	Account: 65; Arts: 114; Business: 70; Catering: 5; Economy: 2; ICT: 24; Landscape: 3; Literature: 71; Science: 46; Technical: 17; Vocational: 11
11	TVETBright	Strongly disagree: 4; Disagree: 17; Not sure :142; Agree: 207; Strongly agree: 58
12	TVETStudHigherJobChance	Strongly disagree: 4; Disagree: 27; Not sure :158; Agree: 158; Strongly agree: 81

Table 5 (continue)

No	Variables	Outputs
13	TVETStudHighSalary	Strongly disagree: 2; Disagree: 13; Not sure :187; Agree: 162; Strongly agree: 64
14	VocationalSubjStatus	Strongly disagree: 5; Disagree: 17; Not sure :136; Agree: 220; Strongly agree: 50
15	VocationalCourseInteresting	Strongly disagree: 2; Disagree: 9; Not sure :55; Agree: 264; Strongly agree: 98

### Evaluation and Description of the Model

Table 6 shows the evaluation of the models from training data (70%) and testing data (30%).

Table 6  
Evaluation of the models

No	Models	Training data (70%)		Testing data (30%)		Number of depths	Number of features used
		Number of misclassified instances	Misclassification rate	Number of misclassified instances	Misclassification rate		
1	Decision Tree (Entropy,2 branches)	56	0.1873	31	0.2403	6	9
2	Decision Tree (Gini,2 branches)	52	0.1739	27	0.2093	6	12
3	Decision Tree (Entropy, 3 branches)	38	0.1271*	31	0.2403	6	11
4	Decision Tree (Gini, 3 branches)	43	0.1438	25	0.1938*	6	15
5	Neural Network (1 hidden layer, 2 hidden units)	53	0.1773	32	0.2481	Not applicable	
6	Neural Network (1 hidden layer, 3 hidden units)	50	0.1672	32	0.2481	Not applicable	
7	Neural Network (2 hidden layers, 2 hidden units)	63	0.2107	38	0.2946	Not applicable	
8	Neural Network (2 hidden layers, 3 hidden units)	53	0.1773	33	0.2558	Not applicable	
9	Logistic Regression (Forward)	58	0.1940	27	0.2093	Not applicable	
10	Logistic Regression (Backward)	58	0.1940	27	0.2093	Not applicable	
11	Logistic Regression (Stepwise)	58	0.1940	27	0.2093	Not applicable	
12	Naïve Bayes (Parent-child,Set of parents)	63	0.2107	33	0.2558	Not applicable	
13	Naïve Bayes (Parent-child,One parent)	71	0.2375	39	0.3023	Not applicable	



Table 6 (continue)

No	Models	Training data (70%)		Testing data (30%)		Number of depths	Number of features used
		Number of misclassified instances	Misclassification rate	Number of misclassified instances	Misclassification rate		
14	Naïve Bayes (Markov-Blanket,Set of parents)	62	0.2074	26	0.2016	Not applicable	
15	Naïve Bayes (Markov-Blanket,One parent)	95	0.3177	39	0.3023	Not applicable	

\* Means lowest misclassification rate

The output shows that Decision Tree-based Entropy with three splitting branches obtained the lowest misclassification rate in training data which is 0.1271. However, the high misclassification rate (0.2403) reflects that this model is not fit enough as the best predictive model. On the contrary, the Decision Tree-based Gini Index with three branches outperformed all models by possessing the least misclassification rate (0.1938). Also, medium size but blanket all features earned a magnificent triumph over other models. The importance values of each feature and the tree diagram are displayed in Table 7 and Figure 3.

Table 7  
Importance value for the variable

Variable	Importance value
VocationalCourseInteresting	1.0000
PlanAfterForm5	0.6335
AcademicSubjMoreImportant	0.4042
Stream	0.3810
MotherEducation	0.3254
FatherJob	0.2343
Gender	0.2255
TVETStudHighSalary	0.1964
FatherEducation	0.1896
MotherJob	0.1752
VocationalSubjStatus	0.1548
TVETBright	0.1413

Table 7 shows that “VocationalCourseInteresting” has the highest importance value which is 1.0000, followed by “PlanAfterForm5” (0.6335), “AcademicSubjMoreImportant” (0.4042), “Stream” (0.3810), “MotherEducation” (0.3254), “FatherJob” (0.2343), “Gender” (0.2255), “TVETStudHighSalary” (0.1964), “FatherEducation” (0.1896), “MotherJob” (0.1752), “VocationalSubjStatus” (0.1548), and “TVETBright” (0.1413).

The examples of rules for Node 13 and Node 18 are discussed in Table 8. The findings show that the variable VocationalCourseInteresting plays the most critical role in students’ desire to enrol in TVET. Students who feel a vocational course is interesting are more likely to enrol in TVET following high school. As a result, the government should work with school teachers and TVET instructors to develop practical and relevant techniques for making TVET more engaging. It can be accomplished by bringing more technical teaching

Predicting TVET Inclination Using Various Classifiers

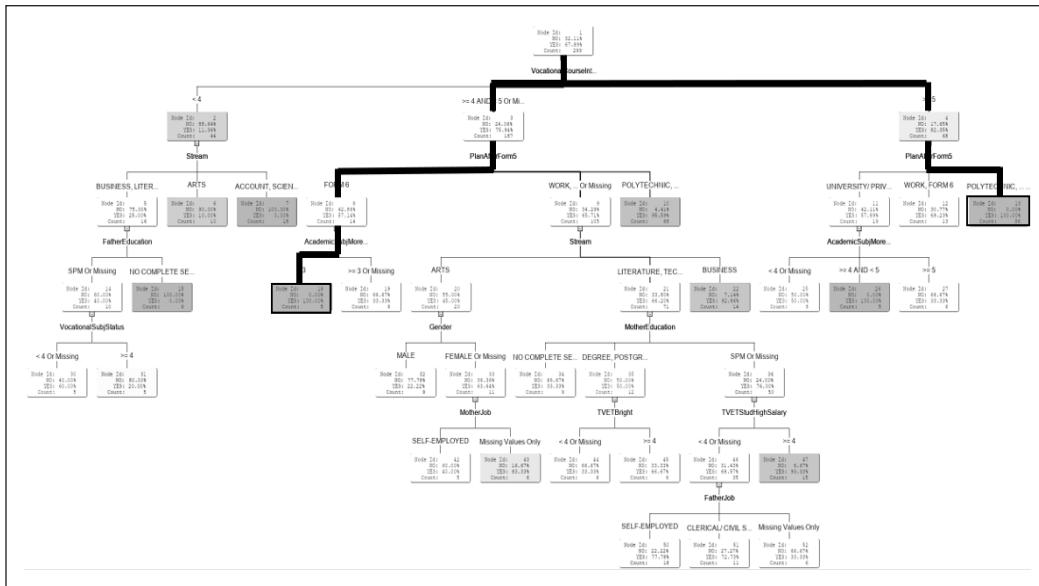


Figure 3. Decision Tree-based Gini Index with three branches

Table 8  
Rules of nodes

Node	Rules
Node = 13	if VocationalCourseInteresting = 5 and PlanAfterForm5 is one of Polytechnic, Skill Training Centre or missing then Predicted: InterestedTVET=Yes = 100%
Node = 18	if VocationalCourseInteresting = 4 or missing and PlanAfterForm5 is one of: Form 6 and AcademicSubjMoreImportant=1, 2 then Predicted: InterestedTVET=Yes = 100%

tools into vocational schools, such as interactive whiteboards, 3D printing devices, mobile devices, and so on. Furthermore, the government should provide training or short courses for TVET instructors to prepare them adequately for teaching. Aside from that, students' plans after Form 5 are the second key factor influencing their desire to enrol in TVET. As a result, it is critical to understand the children's educational paths following secondary school. As a result, teachers and parents play an important role in helping students grasp their post-secondary goals.

**CONCLUSION**

The stigma associated with Technical and Vocational Education and Training (TVET) has led to a low number of students applying to pursue their studies in this field in Kedah Malaysia. The backgrounds, characteristics, and misperceptions of students against TVET make it dull and still unpopular even though our government has put much effort such as

huge appropriation, institutions, training, campaign and facilities to engage more students to join the vocational program. Therefore, this study implemented several predictive models to discover the significant factors and predict the tendency of secondary students to join the TVET program. The Decision Tree-based Gini Index with three splitting branches has prevailed against 14 prominent models. Structural transparency, flexibility, and robustness led to enormous popularity among practitioners or researchers, especially those less proficient in data mining approaches. In conjunction with the model, Kedah DOE, related parties, and the TVET agency could have uncovered the core problem whilst implementing proper strategies to reshape the perception and policy of TVET education. Promoting TVET should not be a privilege for some to profiteer but a birth right for all Malaysians to be equitably competitive, regardless of gender, race, religion, and creed, in an increasingly challenging world economy.

## ACKNOWLEDGEMENTS

This research was supported by Ministry of Higher Education (MoHE) of Malaysia through Fundamental Research Grant Scheme (FRGS/1/2020/SSIO/UUM/02/18).

## REFERENCES

- Abdul-Aziz, S. N., Zulkifli, N., Nashir, I. M., & Karim, N. A. H. (2020). Pull and push factors of students' enrolment in the TVET programme at community colleges in Malaysia. *Journal of Technical Education and Training*, 12(1), 68-75. <https://doi.org/10.30880/jtet.2020.12.01.007>
- Amedorme, S., & Fiagbe, Y. (2013). Challenges facing technical and vocational education in Ghana. *International Journal of Scientific & Technology Research*, 2(6), 253-255.
- Amin, J. M. (2016). *Quality assurance of the qualification process in TVET: Malaysia country*. TVET Online Asia. [http://tvvet-online.asia/wp-content/uploads/2020/03/mohd-amin\\_tvvet7.pdf](http://tvvet-online.asia/wp-content/uploads/2020/03/mohd-amin_tvvet7.pdf)
- Assunção, M. V. D., Araújo, A. G., & Almeida, M. R. (2019). The influence of family background on the access to technical and vocational education. *Journal of Public Administration*, 53(3), 542-559. <https://doi.org/10.1590/0034-761220170352x>
- Aziz, A. (2019, July 24). Govt struggles to overcome vocational education misconception. *The Malaysian Reserved*. <https://themalaysianreserve.com/2019/07/24/govt-struggles-to-overcome-vocational-education-misconception/>
- Azizi, N. A. (2018, Jun 29). Ubah stigma terhadap TVET [Change the stigma against TVET]. *Berita Harian Online*. <https://www.bharian.com.my/berita/wilayah/2018/06/443161/ubah-stigma-terhadap-tvvet>
- Babu, C., Varghese, R., & Manimozhi. (2020). Predicting student's performance using educational data mining. *International Journal of Scientific Research in Computer Science Applications and Management Studies*, 9(1), 1-4.
- Bakar, A. R. (2011). *Roles of technical and vocational education and training (TVET)*. UPM Press.

- Berawi, M. A. (2019). The role of industry 4.0 in achieving sustainable development goals. *International Journal of Technology*, 10(4), 644-647. <https://doi.org/10.14716/ijtech.v10i4.3341>
- Berrar, D. (2018). Bayes' theorem and naïve bayes classifier. *Encyclopedia of Bioinformatics and Computational Biology*, 1, 403-412.
- Breiman, L. (1996). Technical note: Some properties of splitting criteria. *Machine Learning*, 24, 41-47.
- Chan, Y. S. (2018, November 23). We need to change perception of TVET. *The Star Online*. <https://www.thestar.com.my/opinion/letters/2018/11/23/we-need-to-change-perception-of-tvet>
- Cheong, K., & Lee, K. (2016). Malaysia's education crisis- Can TVET help? *Malaysian Journal of Economic Studies*, 53(1), 115-134. <https://doi.org/10.1787/888933003668>
- Gandhi, R. (2018). *Naïve Bayes classifier*. Towards Data Science. <https://towardsdatascience.com/naive-bayes-classifier-81d512f50a7c>
- Herlambang, A. D., Wijoyo, S. H., & Rachmadi, A. (2019). Intelligent computing system to predict vocational high school student learning achievement using naive bayes algorithm. *Journal of Information Technology and Computer Science*, 4(1), 15-25. <https://doi.org/10.25126/jitecs.20194169>
- Hong, C. M., Ch'ng, C. K., & Roslan, T. R. N. (2021). Students' tendencies in choosing technical and vocational education and training (TVET): Analysis of the influential factors using analytic hierarchy process. *Turkish Journal of Computer and Mathematics Education (TURCOMAT)*, 12(3), 2608-2615. <https://doi.org/10.17762/turcomat.v12i3.1262>
- Hung, H. C., Liu, I. F., Liang, C. T., & Su, Y. S. (2020). Applying educational data mining to explore students' learning patterns in the flipped learning approach for coding education. *Symmetry*, 12(2), Article 213. <https://doi.org/10.3390/sym12020213>
- Hussin, A., Mohamad, M., Hassan, R., & Omar, A. (2017). Technical vocational education training branding from perspective of stakeholder (parent) in Malaysia. *Advanced Science Letters*, 23(2), 1216-1219. <https://doi.org/10.1166/asl.2017.7543>
- Imaz, M., & Sheinbaum, C. (2017). Science and technology in the framework of the sustainable development goals. *World Journal of Science, Technology and Sustainable Development*, 14(1), 2-17. <https://doi.org/10.1108/WJSTSD-04-2016-0030>
- Islam, M., Chen, G. R., & Jin, S. Z. (2019). An overview of neural network. *American Journal of Neural Networks and Applications*, 5(1), 7-11. <https://doi.org/10.11648/j.ajjna.20190501.12>
- Ismail, A., & Hassan, R. (2013). Issues and challenges of technical and vocational education & training in Malaysia for knowledge worker driven. In *National Conference on Engineering Technology* (pp. 1-11). ResearchGate. <https://doi.org/10.13140/2.1.4555.2961>
- Ismail, J., Chik, C. T., & Hemdi, M. A. (2021). TVET graduate employability: Mismatching traits between supply and demand. *International Journal of Academic Research in Business and Social Sciences*, 11(13), 223-243. <https://doi.org/10.6007/IJARBS/v11-i13/8522>
- Ismail, K., Nopiah, Z. M., Rasul, M. S., & Leong, P. C. (2017). Malaysian teachers' competency in technical vocational education and training: A review. In A. G. Abdullah, T. Aryanti, A. Setiawan & M. Alias (Eds.), *Regionalization and Harmonization in TVET* (pp. 59-64). Taylor & Francis Group.

- Karim, M. A. (2018, September 5). TVET, a relevant choice. *New Straits Times*. <https://www.nst.com.my/education/2018/09/408470/tvet-relevant-choice>
- Karim, Z. I. A., & Maat, S. M. (2019). Employability skills model for engineering technology students. *Journal of Technical Education and Training*, 11(2), 79-87. <https://doi.org/10.30880/jtet.2019.11.02.008>
- Kelvin, G. (1997). *An introduction to neural networks*. UCL Press
- Khan, I. A., & Choi, J. T. (2014). An application of educational data mining (EDM) technique for scholarship prediction. *International Journal of Software Engineering and Its Applications*, 8(12), 31-42.
- Koya, Z. (2019, July 4). TVET courses are not for those who are academically weak, Kula tells parents. *The Star Online*. <https://www.thestar.com.my/news/nation/2019/07/04/tvet-courses-are-not-for-those-who-are-academically-weak-kula-tells-parents>
- KRI. (2018). *The school-to-work transition survey of young Malaysians*. Khazanah Research Institute. [http://www.krinstitute.org/assets/contentMS/img/template/editor/20181205\\_SWTS\\_Main%20Book.pdf](http://www.krinstitute.org/assets/contentMS/img/template/editor/20181205_SWTS_Main%20Book.pdf)
- Kukreja, H., Bharath, N., Siddesh, C. S., & Kuldeep, S. (2016). An introduction to artificial neural network. *International Journal of Advance Research And Innovative Ideas In Education*, 1(5), 27-30.
- Liu, H., & Cocea, M. (2017). Semi-random partitioning of data into training and test sets in granular computing context. *Granula Computing*, 2, 357-386. <https://doi.org/10.1007/s41066-017-0049-2>
- Matei, M. M. M., Mocanu, C., & Zamfir, A. M. (2018). Educational paths in Romania: Choosing general or vocational education. *HOLISTICA*, 9(2), 127-136. <https://doi.org/10.2478/hjbpa-2018-0016>
- Messele, A., & Addisu, M. (2020). A model to determine factors affecting students academic performance: The case of Amhara region agency of competency, Ethiopia. *International Research Journal of Science and Technology*, 1(2), 75-87. <https://doi.org/10.46378/irjst.2020.010202>
- Mustapha, R. B. (2015). Green and sustainable development for TVET in Asia. *The International Journal of Technical and Vocational Education*, 11(2), 133-142.
- Nguyen, Q. H., Ly, H. B., Ho, L. S., Al-Ansari, N., Le, H. V., Tran, V. Q., Prakash, I., & Pham, B. T. (2021). Influence of data splitting on performance of machine learning models in prediction of shear strength of soil. *Mathematical Problems in Engineering*, 2021, Article 4832864. <https://doi.org/10.1155/2021/4832864>
- Ozkan, U. B., Cigdem, H., & Erdogan, T. (2020). Artificial neural network approach to predict lms acceptance of vocational school students. *Turkish Online Journal of Distance Education*, 21(3), 156-169. <https://doi.org/10.17718/tojde.762045>
- Rajaendram, R. (2020, November 6). Budget 2021: Association welcomes bigger allocation for TVET sector. *The Star Online*. <https://www.thestar.com.my/news/nation/2020/11/06/budget-2021-association-welcomes-bigger-allocation-for-tvet-sector>
- Raju, D., & Schumacker, R. (2015). Exploring student characteristics of retention that lead to graduation in higher education using data mining models. *Journal of College Student Retention: Research, Theory & Practice*, 16(4), 563-591. <https://doi.org/10.2190/CS.16.4.e>
- Rokach, L., & Maimon, O. (2015). *Data mining with decision trees theory and applications*. World Scientific Publishing Co. Pte. Ltd.

- Sabang, A. (2017, September 2). Kesedaran TVET perlu dipertingkatkan [Awareness of TVET needs to be improved]. *Utusan Borneo Online*. <https://www.utusanborneo.com.my/2017/09/02/kesedaran-tvet-perlu-dipertingkatkan>
- Sahu, H., Shirma, S., & Gondhalakar, S. (2011). A brief overview on data mining survey. *International Journal of Computer Technology and Electronics Engineering*, 1(3), 114-121.
- Salal, Y. K., Abdullaev, S. M., & Kumar, M. (2019). Educational data mining: Student performance prediction in academic. *International Journal of Engineering and Advanced Technology*, 8(4C), 54-59.
- Sivanandam, H., Rahim, R., Carvalho, M., & Tan, T. (2019, October 11). Budget 2020: Every single sen for education will be used properly, says Maszlee. *The Star Online*. <https://www.thestar.com.my/news/nation/2019/10/11/budget-2020-every-single-sen-for-education-will-be-used-properly-says-maszlee>
- Sulaiman, N. L., & Salleh, K. M. (2016). The development of technical and vocational education and training (tvvet) profiling for workforce management in Malaysia: Ensuring the validity and reliability of TVET data. *Man In India*, 96, 2825-2835.
- TheStart. (2019, October 12). Thanks, but RM5.9bil not enough for TVET. *The Star Online*. <https://www.thestar.com.my/news/nation/2019/10/12/thanks-but-rm59bil-not-enough-for-tvet>
- Trudis, H. (2014). *Secondary school students' perceptions of vocational education in Barbados*. <https://docslib.org/doc/7204149/secondary-school-students-perceptions-of-vocational-education-in-barbados>
- Ursachi, G., Horodnic, I. A., & Zait, A. (2015). How reliable are measurement scales? External factors with indirect influence on reliability estimators. *Procedia Economics and Finance*, 20, 679-686. [https://doi.org/10.1016/S2212-5671\(15\)00123-9](https://doi.org/10.1016/S2212-5671(15)00123-9)
- Yaakob, H. (2017). Technical and vocational education & training (TVET) institutions towards statutory body: Case study of Malaysian polytechnic. *Advanced Journal of Technical and Vocational Education*, 1(2), 07-13. <https://doi.org/10.26666/rmp.ajtve.2017.2.2>
- Yağcı, A., & Çevik, M. (2017). Predictions of academic achievements of vocational and technical high school students with artificial neural networks in science courses (physics, chemistry and biology) in Turkey and measures to be taken for their failures. *SHS Web Conference*, 37, Article 1057. <https://doi.org/10.1051/shsconf/20173701057>
- Yamini, O., & Ramakrishna, S. (2015). A study on advantages of data mining classification techniques. *International Journal of Engineering Research & Technology*, 4(9), 969-972.
- Zakaria, M., AL-Shebany, M., & Sarhan, S. (2014). Artificial neural network: A brief overview. *International Journal of Engineering Research and Applications*, 4(2), 7-12.





## Water Quality Assessment and Characterization of Rivers in Pasir Gudang, Johor via Multivariate Statistical Techniques

Muhammad Syafiq Mohamad Desa<sup>1</sup>, Mohd Aeddy Sulaiman<sup>2</sup> and Shantakumari Rajan<sup>1\*</sup>

<sup>1</sup>Centre of Environmental Health & Safety, Faculty of Health Sciences, Universiti Teknologi MARA, UiTM Cawangan Selangor, 42300 Puncak Alam, Selangor, Malaysia

<sup>2</sup>Environmental and Safety Unit, Department of Public Health and Environmental, Level 15 Menara Aqabah, Majlis Bandaraya Pasir Gudang, Jalan Bandar, 81700 Pasir Gudang, Johor, Malaysia

### ABSTRACT

In Pasir Gudang, an accelerated industry-based economy has caused a tremendous increase and diversity of water contamination. The application of multivariate statistical techniques can identify factors that influence water systems and is a valuable tool for managing water resources. Therefore, this study presents spatial evaluation and the elucidation of inordinate complex data for 32 parameters from 25 sampling points spanning 20 rivers across Pasir Gudang, summing up to 1500 observations between 2015-2019. Hierarchical cluster analysis with the K-means method grouped the rivers into two main clusters, i.e., proportionately low polluted rivers for Cluster 1 (C1) and high polluted rivers for Cluster 2 (C2), based on the similitude of water quality profiles. The discriminant analysis applied to the cluster resulted in a data reduction from 32 to 7 parameters (Cl, Cd, S, OG, temperature, BOD, and pH) with a 99.5% correct categorization in spatial analysis. Hence, element complexity was reduced to a few criteria accountable for large water quality differences between C1 and C2. The principal component analysis produced 6 and 7 principal components after rotation for C1 and C2, respectively, where total variance was 62.48% and 66.85%. In addition, several sub-clusters were identified; two from C1 and three from C2, based on the principal contributing components. These results show that the functionality

of multivariate techniques can be effectively used to identify spatial water characteristics and pollution sources. The outcomes of this study may benefit legislators in managing rivers within Pasir Gudang.

### ARTICLE INFO

#### Article history:

Received: 15 March 2022

Accepted: 21 June 2022

Published: 09 November 2022

DOI: <https://doi.org/10.47836/pjst.31.1.29>

#### E-mail addresses:

[muhdsyafiqdesa@gmail.com](mailto:muhdsyafiqdesa@gmail.com) (Muhammad Syafiq Mohamad Desa)

[aeddy@mbpg.gov.my](mailto:aeddy@mbpg.gov.my) (Mohd Aeddy Sulaiman)

[shanta@uitm.edu.my](mailto:shanta@uitm.edu.my) (Shantakumari Rajan)

\* Corresponding author

**Keywords:** Cluster analysis, discriminant analysis, water quality assessment

## INTRODUCTION

Developing countries worldwide are facing alarming environmental issues; one of the significant issues is the decline of surface water quality due to pollution. Rivers are amongst the most vulnerable surface water bodies because of their capacity as reservoirs for all surface contaminants. Moreover, due to rapid development, the surface water quality of the river has deteriorated over time owing to its role in carrying off discharge from municipal and industrial wastewater with additional run-off from the agricultural sector. The main functions of rivers are common as a supply for drinking water, irrigation, and various other industrial purposes in addition to recreation.

Since the early 1980s, Malaysia has rapidly transformed from an agriculture-based economy to an industrial-based economy. Industrialization has provided many benefits in terms of economic growth in Malaysia, but these have occurred at the expense of the environment (Samsudin et al., 2017), as a great number of anthropogenic activities end up in water bodies. Overall, river water pollution in Malaysia generally is surging as the percentage of clean rivers has decreased to 47% in 2016 compared to 58% in the previous year, and polluted rivers increased from 7% to 10% in 2016 (Department of Environment, 2016). Ultimately, a recent case happened in March 2019 that had a high impact on Malaysian citizens; the case of pollution in the Kim Kim River involved untreated factory waste being illegally and directly discharged into the river body (Academy of Sciences Malaysia, 2019). As a result, several toxic gases, such as methane xylene, acrylonitrile and toluene, were emitted following the interaction of the chemicals concerned with water and air, causing this crisis to be unique as the water pollution subsequently caused air pollution (Chai, 2020). As a result, pollutants were removed from the 1.5 km stretch of Sungai Kim Kim, where chemicals were expected to cost approximately RM 6.5 million (The Straits Times, 2019).

Alkarkhi et al. (2008) stated that industrialization is the main factor in ecosystems' pollution. Unsustainable factories are the real culprit as pollutants are discharged into rivers and lakes with minimal treatment. Water demand in Malaysia for the year 2020 was approximately 53% for domestic and industrial usage, while the remaining 47% for agricultural activities. It is predicted that by 2050, water demand in Malaysia will increase by 103% for domestic, industrial, and agriculture (Ishak & Ismail, 2020). Malaysia may clearly face a huge problem in water supply if there is a lack of comprehension of the water data assessment and practical decisions in water quality management. Improving water resource capacity and maintaining excellent standards can specifically mitigate health and water supply issues. However, a water quality issue in the country is related to catchment protection, pollution and flooding control management, and legislation weaknesses. Generally, a holistic cognition of water quality monitoring and analysis is needed to curb the current situation from deteriorating further.

Water quality monitoring programs are conducted by several government agencies such as the Department of Environment, Ministry of Health and Local Authorities. These observing projects regularly appraise and estimate physicochemical boundaries with limit values suggested by national or worldwide bodies (Bhuiyan et al., 2011). These programs will eventually produce large complex data sets over time, requiring efficient analysis to be fully understood. Therefore, applying appropriate statistical methodology when analyzing water quality data is essential to draw valid conclusions and provide useful advice in water management (Uddin et al., 2021). Nevertheless, data analysis using multivariate techniques has been proven to be one of the legitimate methods. Multivariate techniques can analyze complex water data sets in a straightforward way for better interpretation. Many elements in multivariate statistical methods such as Cluster Analysis (CA), Principal Component Analysis (PCA), and Discriminant (DA) help understanding the complex data sets, such as those created by long-term water quality monitoring programs, allowing a better view of the temporal and spatial variations in water quality (Shrestha & Kazama, 2007). Studies have shown that multivariate statistical analysis is useful for assessing spatial water quality variations in a river. For example, a multivariate analysis of the Kinta River's water quality parameters in Perak revealed rock weathering along the riverbanks and untreated wastewater as the main pollution source (Isiyaka & Juahir, 2015). This analysis output provided valuable information for decision-making in river management.

In this study, collaboration with the Pasir Gudang City Council (PGCC) was developed to understand better water surface analysis across rivers in areas under the PGCC administration. These rivers are being monitored as Pasir Gudang is a hub for many industry types such as chemical-based (oleochemical, plastic production, petrochemicals), heavy engineering, logistics and small and medium enterprises. Therefore, multivariate statistical methods can classify the rivers into clusters based on the type and concentration of pollutants present. Identifying clustering patterns is based on identifying similarities between the rivers and would enable enhanced management of this region. Therefore, this study focused on applying multivariate techniques such as CA, PCA, and DA to determine the major pollutants affecting the water quality of the rivers in this locality and to identify the presence of river clusters according to their water quality characteristics.

## **MATERIALS AND METHODS**

### **Study Area**

Pasir Gudang is a significant industrial and port city located in the southwestern part of Johor Bahru district, Johor, Malaysia (Abdullah et al., 2012). There are 25 sampling points scattered across the Pasir Gudang region (Table 1). Most of the sampling points focus on downstream areas covering 20 different rivers. Some of these rivers are the main water sources for the Sultan Iskandar reservoir, which is used for residential and industrial water supply and irrigation.

**Water Quality Data**

The archive data set obtained from PGCC covers water quality data from 2015-2019, where water samples were collected monthly by PGCC personnel from each sampling point. All sampling bottles were acid-washed, cleaned, and dried before use. The samples were placed in an ice box and transported to the laboratory for further analysis. A certified laboratory carried out all analyses except temperature, measured in situ. The data set comprises 32 parameters summarised in Table 2 and the analytical methods used (APHA, 2016).

**Data Analysis**

The data sets were analyzed using Statistical Package for the Social Sciences (SPSS) version 26. Cluster analysis (CA) was used to classify rivers into clusters based on their similarities (exposure level pattern). It will give optimal grouping and combine hierarchical and K-means clustering. The hierarchical method applied Ward’s method

Table 1  
*Sampling points and rivers*

Sampling point	River
P1	Masai (A)
P2	Masai (B)
P3	Masai (C)
P4	Kim Kim
P5	Kopok
P6	Kong Kong
P7	Tiga
P8	Perapat
P9	Cupak
P10	Hujung
P11	Tengah
P12	Laloh
P13	Tukang Batu (A)
P14	Tukang Batu (B)
P15	Perembi
P16	Buluh
P17	Selangkah
P18	Kopok Baru
P19	Serai
P20	Redan
P21	Air Puteh
P22	Tiram (A)
P23	Tiram (B)
P24	Tiram (C)
P25	Penderam

Table 2  
*Water quality parameters and analytical methods*

No.	Parameter	Analytical Method
1	Silver	APHA 3111 B
2	Aluminum	APHA 3111 D
3	Ammoniacal-Nitrogen (AN)	APHA 4500 – NH <sub>3</sub> C/ NH <sub>3</sub> B
4	Arsenic	APHA 3114 B
5	Boron	APHA 4500 – B B
6	Barium	APHA 3111 D
7	Biochemical Oxygen Demand (BOD)	APHA 5210 B/ APHA 4500- OG
8	Cadmium	APHA 3111 B
9	Cyanide	APHA 4500 – CN C&E and Merek Method 14429
10	Chemical Oxygen Demand (COD)	APHA 5220 C
11	Chromium (III)	APHA 3500 - Cr B
12	Chromium (IV)	APHA 3500 – Cr B

Table 2 (continue)

No.	Parameter	Analytical Method
13	Copper	APHA 3111 B
14	Fluoride	APHA 4500 - F D
15	Iron	APHA 3111 B
16	Formaldehyde	Macherey Nagel Nano color Formaldehyde
17	Mercury	APHA 3112 B
18	Manganese	APHA 3111 B
19	Nickel	APHA 3111 B
20	Oil & Grease (OG)	APHA 5520 B
21	Lead	APHA 3111 B
22	pH	APHA 4500 – H <sup>+</sup> B
23	Phenol	APHA 5530 B & APHA 5530 D
24	Selenium	APHA 3114 B
25	Tin	APHA 3114 B
26	Total Suspended Solids (TSS)	APHA 2540 D
27	Zinc	APHA 3111 B
28	Chloride	APHA 4500 - CI B
29	Chlorine	APHA 4500 – CI B
30	Sulfide	APHA 4500 -S <sup>2</sup> -F
31	Temperature	In-situ
32	Color	APHA 2120 F

with squared Euclidean distances as a similarity measure. The data sets were treated by -1 to 1 scale transformation. At the same time, K-means can portray each cluster's mean exposure toward water parameters predetermined by the hierarchical method. Combining hierarchical and K-means results are used to identify river clusters and interpreted into a useful grouping. Parameters that did not have a stored data value for the observation and were recorded as not detected were set at zero during the data cleaning stage before the analysis.

Discriminant analysis (DA) was used to calculate the mathematical weights for each score of variables (water quality parameters) and reflects it to scores on each variable (32 parameters), where it can differentiate clusters obtained from CA. This analysis can produce a discriminant function (DF) depending on the number of groups/clusters from CA (Singh et al., 2005), whereby the DF is made of parameters that can distinguish between clusters in this study. The DA was applied using a stepwise method where all variables are reviewed and evaluated to determine which one contributes most to the discrimination between groups.

Principal component analysis (PCA) is a dimensionality reduction method that uses fewer variables to explain most of the variation in the original data and converts many

highly correlated variables into independent or unrelated variables (Li et al., 2017). Principal components (PC) provide information on the most meaningful parameters. Hence, the PCs can unveil more hidden vital parameters related to possible pollution sources based on spatial aspects. Only parameters with loading factors of more than 0.5 meet the requirements to clarify each cluster's water quality variation pattern. Principally, varimax rotations were applied to PCs with eigenvalues of more than one. Factors with eigenvalues > 1 explained total variation in the data than individual water quality variables. PCA was carried out separately for each cluster to describe the covariance relationship among variables for each cluster individually.

## RESULTS AND DISCUSSION

### Site Similarity and Clustering

Phenol, cyanide, chlorine and selenium concentration for Masai (A), Masai (B), Masai (C), Kim Kim, Kopok, Kong Kong, Tiga, Prapat, Cupak, Hujung, Tengah, Laloh, Tukang Batu (A), Tukang Batu (B), Perembi, Buluh, Selangkah, Kopok Baru, Serai, Redan, Air Puteh, Tiram (A), Tiram (B), Tiram (C), and Penderam Rivers were below detection limits in all samples between the years 2015-2019. Most water quality parameters are classified in groups I to III according to the National Water Quality Standards for Hg, As, Sn, Ag, Cl<sub>2</sub>, Phenol, Cd, Pb, Zn, Al, S, CN, Cr<sup>3</sup>, Cr<sup>6</sup>, Ni, Fe, and Ba. Class I to III are considered fit for being biologically viable and have economic value. Various physico-chemical parameters, such as F, Cu, BOD, and AN, are in class IV. At the same time, only COD falls under class V. Water within class IV, and V is limited to irrigation use only (class IV) or has no economic value or other benefits (class V). The mean values of water quality parameters was arranged in the order, Cl > COD > TSS > BOD > pH > AN > F > Fe > B > Zn > OG > Mn > S > Cu > Pb > As > Ni > Sn > Cr<sup>6+</sup> > Al > Cd > Formaldehyde > Cr<sup>3+</sup> > Ag > Ba > Hg.

The spatial variation of water quality mainly depends on the different water quality parameters. The clustering pattern showed that the data set could be divided into two common groups where the dendrogram derived yielded two main clusters (Figure 1). The confirmed clusters subjected to K-means analysis yielded Cluster 2 as a considerably bigger cluster than Cluster 1. There was sufficient internal homogeneity within the clusters and external heterogeneity between the clusters to show 2 main clusters as the stations in these groups have similar and natural backgrounds of the water quality characteristics (McKenna, 2003). The analysis outcome grouped 11 rivers into cluster 1, consisting of Kim Kim, Kopok, Perapat, Kong Kong, Cupak, Hujung, Tengah, Laloh, Air Puteh, and Penderam River, while the remaining 14 rivers comprised cluster 2 (Tiram A, B, C, Redan, Masai A, B, C, Tukang Batu A, B, Perembi, Buluh, Selangkah, Kopok Baru, and Serai River).

The differences in water quality characteristics between clusters 1 and 2 show a clear and distinct line for most parameters such as BOD, COD, TSS, AN, Cr<sup>6+</sup>, As, Mn, Ni,

Sn, Zn, B, Fe, F, OG, and Color (Table 3). These parameters are highly affiliated with anthropogenic discharges related to industrialization, commercialization and residential activities (Khatri & Tyagi, 2015), becoming important factors influencing surface water quality (Hussain et al., 2008). According to Phiri et al. (2005), indiscriminate disposal of municipal solid waste in river systems cause an increase in BOD, COD, TDS, TSS, and toxic metals such as Cd, Cr, Ni and Pb. Degraded streams and rivers that drain urbanized landscapes often have higher nutrient loads and contaminant concentrations, as well as altered stream morphology and reduced biodiversity (Meyer et al., 2005). In contrast, cluster 1 is highly correlated with water quality parameters such as B, Cl<sup>-</sup>, and S suggesting a strong correlation with natural factors such as weathering of the parent rock. Cl<sup>-</sup>, S, and B can be classified as conductivity ions commonly present when surface runoff is in solid form (Isiyaka & Juahir, 2015). The cluster mapping in Figure 2 clearly illustrates that cluster 1

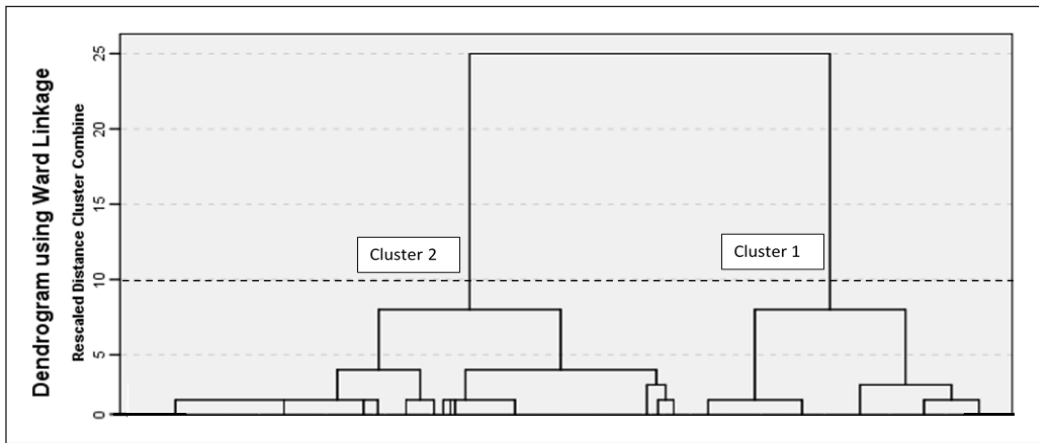


Figure 1. Dendrogram of river clusters

Table 3  
Final cluster centers of water quality parameters

	Cluster 1	Cluster 2
pH	7.53	6.91
Temperature (°C)	28.32	28.54
BOD (mg/L)	5.77	10.60
COD (mg/L)	103.46	139.68
TSS (mg/L)	17.63	25.50
AN (mg/L)	0.65	3.09
Hg (mg/L)	ND	ND
Cd (mg/L)	ND	ND
Cr <sup>3+</sup> (mg/L)	ND	ND
Cr <sup>6+</sup> (mg/L)	ND	0.01
As (mg/L)	ND	0.03



Table 3 (continue)

	Cluster 1	Cluster 2			
Pb (mg/L)	0.03	0.03			
Cu (mg/L)	0.04	0.04			
Mn (mg/L)	0.05	0.08			
Ni (mg/L)	0.01	0.03			
Sn (mg/L)	ND	0.01			
Zn (mg/L)	0.16	0.24			
B (mg/L)	0.32	0.26			
Fe (mg/L)	0.40	0.48			
Ag (mg/L)	ND	ND			
Al (mg/L)	ND	ND			
Se (mg/L)	ND	ND			
Ba (mg/L)	ND	ND			
F (mg/L)	0.80	0.87			
Cl (mg/L)	15871	1416			
Cl <sub>2</sub> (mg/L)	ND	ND			
S (mg/L)	0.08	0.03	Number of cases in each cluster		
OG (mg/L)	0.10	0.15			
Formaldehyde (mg/L)	ND	ND	Cluster	1	560.0
Phenol (mg/L)	ND	ND		2	940.0
CN (mg/L)	ND	ND	Valid		1500.0
Color (ADM)	16.5	29.1	Missing		0.0

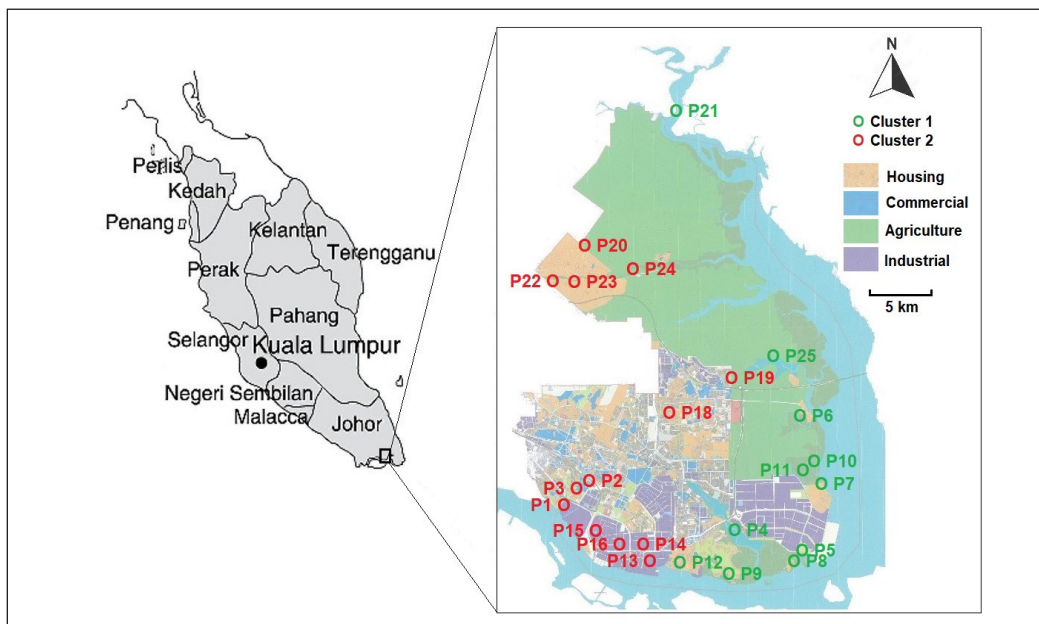


Figure 2. The geographic locations of river clusters overlay the area's general land use area  
 Source. GeoJohor

(green) focuses more on rivers associated with low agricultural activities and undeveloped land. In contrast, cluster 2 (red) is highly connected with pollution loading from urban human activities. Studies have shown that changes in landscape patterns induced by human activities have major impacts on river conditions (Allan, 2004; Bhat et al., 2006; Hopkins, 2009). Cluster analysis has provided a practical grouping system for the rivers under PGCC surveillance, which can be used to construct gilt-edged spatial observation at a lower cost.

### Identification of Discriminating Parameters and Pollution Sources

Based on clusters generated from the CA, water quality parameters were analyzed in the stepwise method using discriminate analysis. The DA identified 7 parameters that can discriminate against the naturally occurring cluster. Since there are two clusters, only one Differentiate Function (DF) appeared in DA. Wilk's Lambda test showed that DF is statistically significant,  $p < 0.05$ . The same value, also parallel with Wilk's Lambda test, is the canonical value at 0.925 near the value of 1, indicating it is very strong, indicating that the clustering result of CA was reliable, proving that the water quality had significant spatial variation. The DF produced can be labeled as a natural factor that can measure score using Equation 1. The main contributing parameters to the equation are Cl<sup>-</sup>, Cd, OG, BOD, Temperature, S and pH, which suggests that these parameters are important for differentiation among the clusters. The equation can determine the cluster membership of new cases using cluster centroids. In this study, the centroids of cluster 1 and cluster 2 were 3.148 and -1.875, respectively. Cl<sup>-</sup> has the highest contribution value in differentiating the two river clusters with a value of 1.023, as there was a much larger divergence between average Cl<sup>-</sup> values between clusters. In comparison, other parameters contributed less to explaining the variation between the two clusters. The relative contribution of all water quality parameters in differentiating the two clusters can be arranged in the order, Cl<sup>-</sup> > Cd > OG > BOD > Temperature > S > pH.

$$DF = 1.023(Cl) + 0.132(Cd) + 0.096(OG) - 0.085(BOD) - 0.083(Temperature) + 0.075(S) - 0.066(pH) \quad (1)$$

The classification matrix showed that 99.5% of the cases were correctly classified (Table 4). The result from DA showed significant differences between the two clusters, which are expressed as one discriminant function.

Principle component analysis was applied to the water quality data for both clusters to identify the spatial sources of pollution and constitution patterns. In order to pin down the source of pollution, only loading factors of >0.5 qualify to clarify the variation of the water quality pattern of each cluster; hence only 17 water quality parameters were measured out of 32 in cluster 1. The data scored 0.703 in the Kaiser-Meyer-Olkin (KMO) measure

of sampling adequacy test, which was considered middling (Kim & Muller, 1987). Six Principal Components (PCs) were obtained with eigenvalues larger than 1, and the total percentage variance was explained as 62.48%. While for cluster 2, there were 18 parameters used in PCA with a KMO test value of 0.692, which was considered mediocre (Kim & Muller, 1987). The total PCs obtained were seven, with a total percentage of variance explained at 66.85%. The water quality parameters excluded in analysis with values <0.5 were Mn, Fe, Ag, Sn and Hg for cluster 1 and S, Cd, Mn, Sn, Formaldehyde, Ag, Al, and Cu for cluster 2, respectively.

6 PCs explain the variability of river water quality from 2015-2019 for cluster 1 (Table 5). Accumulation of 6 factors explains about 62.48% of total variance after rotation.

These 6 factors can unfold the pattern in the characteristics of the examined parameters and point out major possible sources of pollution. In cluster 1, PC1, with 17.84% of the total variance, has strong positive loadings on Pb, B, and F but moderate loadings for Cd. Pb and Cd are normal components in industry effluent (Rosli et al., 2015), while B and F can be generated from urban runoff from aquaculture and

Table 4  
Percentage of correctly classified cluster variables

	Cluster K-means	Predicted Group Membership		
		1	2	Total
Count	1	556	4	560
	2	4	936	940
%	1	99.3	0.7	100.0
	2	0.4	99.6	100.0

a. 99.5% of original grouped cases correctly classified

Table 5  
Principle components loading of Cluster 1

	PC1	PC2	PC3	PC4	PC5	PC6
Pb (mg/L)	0.882					
F (mg/L)	0.831					
B (mg/L)	0.792					
Cd (mg/L)	0.704					
COD (mg/L)		0.879				
BOD (mg/L)		0.836				
TSS (mg/L)		0.652				
OG (mg/L)			0.768			
Color (ADM)			0.677			
Temperature (°C)			0.518			
Cu (mg/L)				0.718		
pH				-0.559		
AN (mg/L)					0.857	
Zn (mg/L)					0.591	
S (mg/L)						0.763
Ni (mg/L)						0.676

residential activities. The PC2 with 12.75 % variance shows strong COD, BOD, and TSS loading. These parameters represent anthropogenic input in most cases, where industrial effluent or residential discharge can contribute to elevated levels of either or both BOD and COD. The positive loading on TSS can be from soil erosion or earthworks. It can happen when there is significant interference from human activities toward rivers, such as water dredging, diversion and channelization (Hua et al., 2016).

In PC3, which contributes 10.007% of the variance, the components have strong positive loading for OG with medium loading for color and temperature. Oil contaminated wastewater comes from various sources such as the petrochemical industry, oil refinery, crude oil production, compressor condensates, metal processing, lubricant and cooling agents, vegetable oil industries, food processing industries, car washing and restaurants (Lan et al., 2009). The largest source of oily wastewater produced is during the oil extraction processes in most oil mills and the mill effluents such as palm oil mill effluent. Additionally, residential sources of OG are from kitchen greywater, which has been reported as the highest contributor to oil and grease in domestic greywater (Alade et al., 2011). PC4 has a positive loading of Cu and negative loading of pH, showing an inverse proportional relationship contributing 7.525% of the variance. The concentration of Cu is below the standard level set within the National Water Quality Standards of Malaysia, with a mean of 0.0255 mg/L. The low values of Cu indicate that there is no significant source of pollution, and the presence of this element is due to the weathering of rocks (Hussain et al., 2017) and soil (Kumar et al., 2013), where leaching has contributed to Cu presence in the water.

PC5, with a variance of 7.317%, has a strong loading of AN and Zn. Municipal, industrial, and agricultural activities generate AN discharge into environmental resources. Therefore, these parameters are attributed to products from anthropogenic activities with urban impacts. Meanwhile, PC6 has the lowest percent of variance with 7.044%, strong positive loading of S and moderate loading of Ni. The mean concentration of Ni (0.0063 mg/L) is below the standard of the NWQS, whereas sulfur concentration has a value of 0.0764 mg/L and is considered above class II and III. The source of nickel is possibly due to weathering of rocks, soil erosion, and vegetation as natural occurrences like metamorphic rocks with high Ni can add up the element in the water profile (Al-Badaii et al., 2016). In contrast, S content is highly likely derived from surface runoff from agricultural activities and soil erosion (Bhuiyan et al., 2011). Overall, for cluster 1, it can be concluded that two sub-clusters exist; sub-cluster A (P4, P5, P8, P9 & P12) associated with anthropogenic activities and sub-cluster B (P6, P7, P19, P11, P21 & P25) associated with nature factors (Figure 3).

7 PCs explain the variability of river water quality for cluster 2, whereby the accumulation of 7 factors explains 66.85% of total variance after rotation (Table 6). PC1 specified 16.38% variance after rotation with strong positive loading of As, Cr<sup>6+</sup>, and Pb. These parameters are derived mainly from industrial activities such as industrial processes,

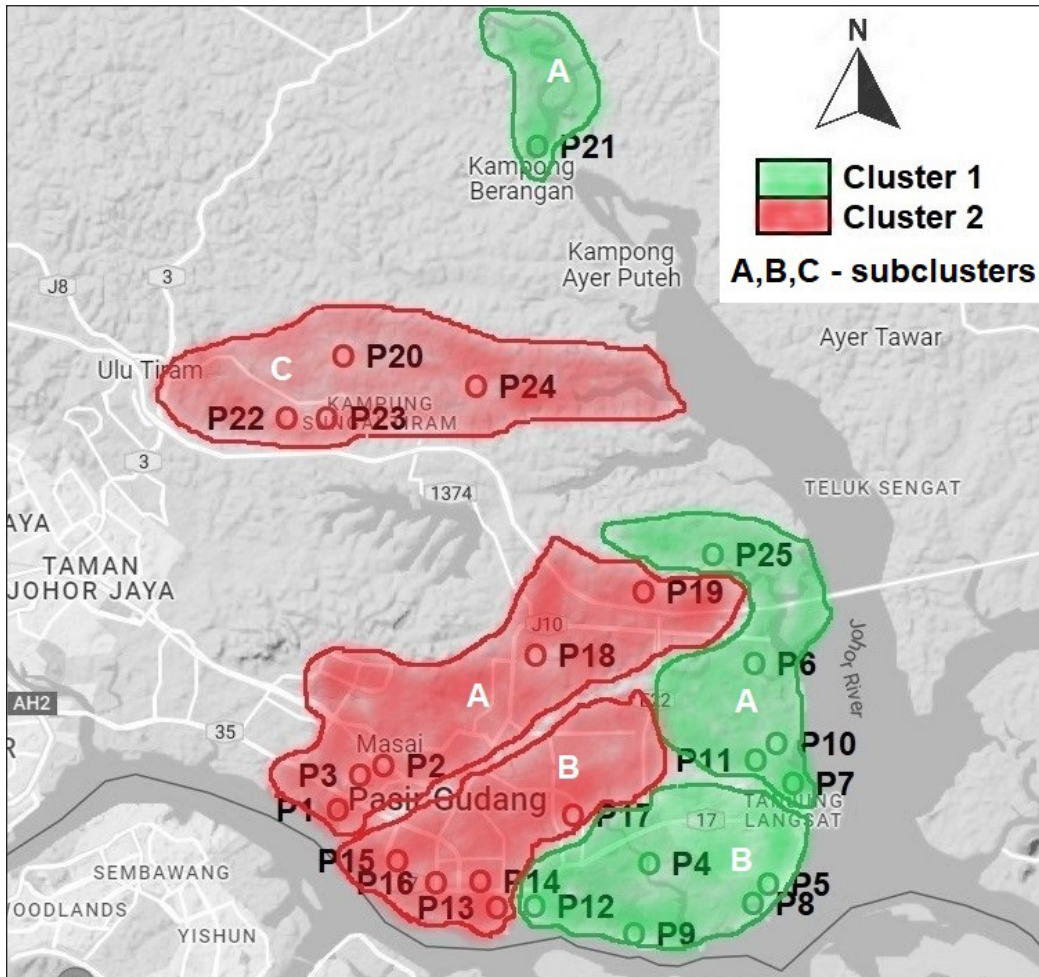


Figure 3. Sub-clustering of rivers within the main cluster pattern

including mining, burning of fossil fuels, metal waste recycling activities, and cement manufacturing (Zhang et al., 2010). For PC2, the percent of the variance is 12.594, with a positive loading for B, COD, BOD, and temperature. The relationship between B, COD and BOD are directly proportional; however, they are inversely proportional to temperature. Boron is widely used in metal processing for containers of high-temperature reactions and electrodes. The loading of COD and BOD can signify the combination of effluent from industries, sewage, commercial area, and small and medium enterprises (Halder & Islam, 2015).

In PC3, valued at 10.834% of the variance, the composition showed two strong positive loadings for OG and color. The sources for these parameters are the same as for PC3 for cluster 1. PC4 scored 8.130% of the variance with strong positive loading for Cl<sup>-</sup> and moderate loading for pH. Additionally, chloride, which is only commonly high during rainy

seasons due to weathering, may become abnormally high due to sand mining activities along rivers. Meanwhile, for PC5, it scored a percentage of variance at 6.626 alongside strong positive loading for Ni and moderate loading for Fe. Commonly both elements can be sourced from natural and anthropogenic factors; however, in this study, the influence is more due to anthropogenic sources based on concentration levels.

PC6 contributed 6.122 % of the variance and consisted of strong positive loading for  $\text{Cr}^{3+}$  and moderate loading for F only. Natural sources of chromium are rare and are mainly associated with industrial effluent derived from the production of corrosion inhibitors and pigments (Oliveira, 2012). As for F, this element is commonly present in water, and in this study, the mean concentration is below NWQS only at 0.87 mg/L. Finally, the last PC7 has a percent variance of 5.899 scores and is strongly associated with Zn, whereby sources are related to mining, industries, and residential land use. Therefore, cluster 2 can be divided into three main sub-clusters that are all contributed by anthropogenic activities; sub-cluster A (P1, P2, P3, P18 & P19), sub-cluster B (P13, P14, P15, P16 & P17), and sub-cluster C (P20, P22, P23 & P24) (Figure 3).

Table 6  
*Principle components loading of Cluster 2*

	PC1	PC2	PC3	PC4	PC5	PC6	PC7
As (mg/L)	0.994						
$\text{Cr}^{6+}$ (mg/L)	0.994						
Pb (mg/L)	0.987						
B (mg/L)		0.726					
COD (mg/L)		0.711					
BOD (mg/L)		0.705	0.515				
Temperature ( $^{\circ}\text{C}$ )		-0.593					
OG (mg/L)			0.768				
Color (ADM)			0.766				
$\text{Cl}^{-}$ (mg/L)				0.774			
pH				0.716			
Ni (mg/L)					0.796		
Fe (mg/L)					0.508		
$\text{Cr}^{3+}$ (mg/L)						0.774	
F (mg/L)						0.638	
Zn (mg/L)							0.928

## CONCLUSION

Multivariate techniques (cluster analysis, discriminant analysis, and principal component analysis) were successfully applied to appraise the spatial variation of water quality across rivers under PGCC surveillance. CA grouped the sampling stations into two main



clusters based on similar water characteristics, representing low and high anthropogenic activities. DA revealed significant data reduction, giving seven parameters (Cl, Cd, S, OG, temperature, BOD, and pH) with 99.5 % correct assignation. The PCA extracted principal components for cluster 1, in which the major sources of pollution are a mix of anthropogenic and natural factors, while cluster 2 was affected by anthropogenic activities only. Therefore, multivariate techniques are important in environmental management for authorities and decision-makers to develop an optimal strategy for reducing sampling stations. Based on these findings, authorities can design optimal sampling stations and reduce experimental analysis costs. Additionally, these methods are important to avoid misinterpreting environmental monitoring data contamination due to uncertainties. A comprehensive approach to the land use pattern in tandem with onsite assessment is needed to decipher the sources of pollution and discharges into the rivers. These techniques can assist by providing an enhanced view of selecting which rivers should be focused on for remediation.

## ACKNOWLEDGEMENTS

The authors wish to express their sincere recognition to the Pasir Gudang City Council for providing raw data.

## REFERENCES

- Abdullah, J., Ahmad, Z., Shah, R. N. H. R. A., & Anor, N. (2012). Port city development and quality of life in Pasir Gudang Port, Johor, Malaysia. *Procedia-Social and Behavioral Sciences*, 35, 556-563. <https://doi.org/10.1016/j.sbspro.2012.02.122>
- Academy of Sciences Malaysia. (2019). *ASM Report: Lessons from Sungai Kim Kim, Pasir Gudang*. Academy of Sciences Malaysia. <https://www.akademisains.gov.my/asm-publication/lessons-from-sungai-kim-kim-pasir-gudang/>
- Alade, A. O., Jameel, A. T., Muyubi, S. A., Karim, M. I. A., & Alam, M. Z. (2011). Removal of oil and grease as emerging pollutants of concern (EPC) in wastewater stream. *IIUM Engineering Journal*, 12(4), 161-169.
- Al-Badaai, F., Halim, A. A., & Shuhaimi-Othman, M. (2016). Evaluation of dissolved heavy metals in water of the Sungai Semenyih (Peninsular Malaysia) using environmetric methods. *Sains Malaysiana*, 45(6), 841-852.
- Alkarkhi, A. F. M., Ahmad, A., & Easa, A. M. (2008). Assessment of surface water quality of selected estuaries of Malaysia: Multivariate statistical techniques. *The Environmentalist*, 29(3), 255-262.
- Allan, J. D. (2004). Landscapes and riverscapes: The influence of land use on stream ecosystems. *Annual Review of Ecology, Evolution, and Systematics*, 35, 257-284.
- APHA. (2005) *Standard methods for the examination of water and wastewater* (21st Ed.). American Public Health Association/American Water Works Association/Water Environment Federation. <https://www.standardmethods.org/doi/book/10.2105/SMWW.2882>



- Bhat, S., Jacobs, J. M., Hatfield, K., & Prenger, J. (2006). Relationships between stream water chemistry and military land use in forested watersheds in Fort Benning, Georgia. *Ecological Indicators*, 6(2), 458-466. <https://doi.org/10.1016/j.ecolind.2005.06.005>
- Bhuiyan, M. A., Rakib, M. A., Dampare, S. B., Ganyaglo, S., & Suzuki, S. (2011). Surface water quality assessment in the central part of Bangladesh using multivariate analysis. *KSCE Journal of Civil Engineering*, 15(6), 995-1003.
- Chai, L. G. (2020). The river water quality before and during the Movement Control Order (MCO) in Malaysia. *Case Studies in Chemical and Environmental Engineering*, 2, Article 100027. <https://doi.org/10.1016/j.cscee.2020.100027>
- Department of Environment. (2016). River Water Quality. *Malaysia Environmental Quality Report*. <https://enviro2.doe.gov.my/ekmc/digital-content/laporan-kualiti-alam-sekeliling-2016-2/>
- Halder, J. N., & Islam, M. N. (2015). Water pollution and its impact on human health. *Journal of Environment and Human*, 2(1), 36-46.
- Hopkins, R. L. (2009). Use of landscape pattern metrics and multiscale data in aquatic species distribution models: A case study of a freshwater mussel. *Landscape Ecology*, 24(7), 943-955. <https://doi.org/10.1007/s10980-009-9373-5>
- Hua, A. K., Kusin, F. M., & Praveena, S. M. (2016). Spatial variation assessment of river water quality using environmetric techniques. *Polish Journal of Environmental Studies*, 25(6), 2411-2421. <https://doi.org/10.15244/pjoes/64082>
- Hussain, J., Husain, I., Arif, M., & Guota, N. (2017) Studies on heavy metal contamination in Godavari River basin. *Applied Water Science*, 7(8), 4539-4548. <https://doi.org/10.1007/s13201-017-0607-4>
- Hussain, M., Ahmed, S. M., & Abderrahman, W. (2008). Cluster analysis and quality assessment of logged water at an irrigation project, eastern Saudi Arabia. *Journal of Environmental Management*, 86(1), 297-307. <https://doi.org/10.1016/j.jenvman.2006.12.007>
- Ishak, A. M., & Ismail, M. A. (2020). Tool for water resources management. *Journal of Water Resources Management*, 34, 447-462.
- Isiyaka, H. A., & Juahir, H. (2015). Analysis of surface water pollution in the Kinta River using multivariate technique. *Malaysian Journal of Analytical Sciences*, 19(5), 1019-1031.
- Khatri, N., & Tyagi, S. (2015). Influences of natural and anthropogenic factors on surface and groundwater quality in rural and urban areas. *Frontiers in Life Science*, 8(1), 23-39. <https://doi.org/10.1080/21553769.2014.933716>
- Kim, J. O., & Mueller, C. W. (1987). *Introduction to factor analysis: What it is and how to do it*. Sage Publications.
- Kumar, R. N., Solanki, R., & Kumar, J. N. (2013). Seasonal variation in heavy metal contamination in water and sediments of river Sabarmati and Kharicut canal at Ahmedabad, Gujarat. *Environmental Monitoring and Assessment*, 185(1), 359-368.
- Lan, W. U., Gang, G. E., & Jinbao, W. A. N. (2009). Biodegradation of oil wastewater by free and immobilized *Yarrowia lipolytica* W29. *Journal of Environmental Sciences*, 21, 237-242.

- Li, H., Liu, J., Liu, R., Xiong, N., Wu, K., & Kim, T. (2017). A dimensionality reduction-based multi-step clustering method for robust vessel trajectory analysis. *Sensors*, 17(8), Article 1792. <https://doi.org/10.3390/s17081792>
- Meyer, J. L., Paul, M. J., & Taulbee, W. K. (2005). Stream ecosystem function in urbanizing landscapes. *Journal of the North American Benthological Society*, 24(3), 602-612.
- Oliveira, H. (2012). Chromium as an environmental pollutant: Insights on induced plant toxicity. *Journal of Botany*, 2012, Article 375843. <https://doi.org/10.1155/2012/375843>
- Phiri, O., Mumba, P., Moyo, B. H. Z., & Kadewa, W. (2005). Assessment of the impact of industrial effluents on water quality of receiving rivers in urban areas of Malawi. *International Journal of Environmental Science & Technology*, 2(3), 237-244. <https://doi.org/10.1007/BF03325882>
- Rosli, S. N., Aris, A. Z., & Majid, N. M. (2015). Spatial variation assessment of Malacca River water quality using multivariate statistical analysis. *Malaysian Applied Biology*, 44(1), 13-18.
- Samsudin, M. S., Azid, A., Khalit, S. I., Saudi, A. S. M., & Zaudi, M. A. (2017). River water quality assessment using APCS-MLR and statistical process control in Johor River basin, Malaysia. *International Journal of Advanced and Applied Sciences*, 4(8), 84-97. <https://doi.org/10.21833/ijaas.2017.08.013>
- Shrestha, S., & Kazama, F. (2007). Assessment of surface water quality using multivariate statistical techniques: A case study of the Fuji River Basin, Japan. *Environmental Modelling and Software*, 22, 464-475. <http://dx.doi.org/10.1016/j.envsoft.2006.02.001>
- Singh, K. P., Malik, A., Singh, V. K., Mohan, D., & Sinha, S. (2005). Chemometric analysis of groundwater quality data of alluvial aquifer of Gangetic plain, North India. *Analytica Chimica Acta*, 550, 82-91. <https://doi.org/10.1016/j.aca.2005.06.056>
- The Straits Times. (2019, March 21). Cleaning up toxic river Sungai Kim Kim in Pasir Gudang to cost S\$2.16 million. *The Straits Times*. <https://www.straitstimes.com/asia/se-asia/cleaning-up-toxic-river-sungai-kim-kim-in-pasir-gudang-to-cost-s216-million>
- Uddin, M. G., Nash, S., & Olbert, A. I. (2021). A review of water quality index models and their use for assessing surface water quality. *Ecological Indicators*, 122, Article 107218. <https://doi.org/10.1016/j.ecolind.2020.107218>
- Zhang, H., Cui, B., Xiao, R., & Zhao, H. (2010). Heavy metals in water, soils and plants in riparian wetlands in the Pearl River Estuary, South China. *Procedia Environmental Sciences*, 2, 1344-1354. <https://doi.org/10.1016/j.proenv.2010.10.145>

## Ammonia-Nitrogen Reduction in Low Strength Domestic Wastewater by Polyvinyl Alcohol (PVA) Gel Beads

Nordin Sabli\* and Norzarina Zakaria

*Department of Chemical & Environmental Engineering, Faculty of Engineering, Universiti Putra Malaysia, 43400 UPM, Serdang, Selangor, Malaysia*

### ABSTRACT

This study aimed to evaluate the efficacy of polyvinyl alcohol (PVA) gel beads as an immobilized biofilm carrier to enhance the reduction rate of Ammonia-Nitrogen ( $\text{NH}_3\text{-N}$ ) and Chemical Oxygen Demand (COD) in domestic wastewater. Laboratory scale reactors were developed to assess the reduction levels of ammonia-nitrogen and COD with and without PVA gel beads using optimal and non-optimal treatment mode settings based on operation procedures from the sewage treatment plant in Taman Kajang Utama, Selangor. The treatment method used is an activated sludge sequencing batch reactor with a treatment cycle duration of 288 minutes. The findings showed the ammonia-nitrogen reduction by non-optimal treatment mode is more effective, with a reduced rate of 62.96% to 65.71% compared to optimal treatment mode with a reduced rate of 30.94% and treatment without PVA gel beads (optimal and non-optimal) with a reduced rate of 32.41% to 47.85%. The ammonia-nitrogen reduction rate using PVA gel beads for non-optimal treatment mode was significantly increased from 17.86% to 18.82% and complied with ammonia-nitrogen reduction parameter 10mg/L, Standard A of Environmental Quality (Sewage) Regulations 2009 (EQSR 2009). The rate of COD reduction using the non-optimal treatment mode was also more stable, with a reduced rate of 70.68%. It was also found that the COD reduction

rate using PVA gel beads for the non-optimal mode was better than the optimal mode, which was 70.68% compared to 42.0%, and both treatment modes complied with COD reduction parameters 120mg/L, Standard A of EQSR 2009.

### ARTICLE INFO

*Article history:*

Received: 09 February 2022

Accepted: 22 April 2022

Published: 27 December 2022

DOI: <https://doi.org/10.47836/pjst.31.1.30>

*E-mail addresses:*

nordin\_sab@upm.edu.my (Nordin Sabli)

aqidra12@gmail.com (Norzarina Zakaria)

\* Corresponding author

*Keywords:* Ammonia-nitrogen, biofilm carrier, COD, domestic wastewater, polyvinyl alcohol (PVA)

## INTRODUCTION

According to Malaysian Sewerage Industry Guideline (MSIG) Volume IV, 2009, all domestic sewage treatment plants (STP) in Malaysia are designed to treat the incoming biodegradable organic loading Biochemical Oxygen Demand (BOD) of 250mg/L and Chemical Oxygen Demand (COD) of 500mg/L of influent values (Services, 2016). Nonetheless, preliminary studies and previous data records show that Malaysia's biodegradable organic loading of sewage is low and fluctuating, which the influent measured COD concentration can reach as low as 50–150mg/L and the BOD reading can reach as low as 40–70 mg/L (Hanafiah et al., 2019). The ammonia-nitrogen reduction can be accomplished through the nitrification and denitrification processes, for which most STPs in Malaysia are either designed or upgraded. The efficiency of ammonia-nitrogen reduction is determined by several variables, including the amount of biodegradable organic material loaded into the STP. This low concentration is most likely the result of dilution or infiltration through the sewerage conveyance system. Infiltration occurs due to poor pipe jointing, cracks, aging pipe, and other factors (Suruhanjaya Perkhidmatan Air Negara, 2016). When the organic matter content of the wastewater influent is low, especially the carbon source, the denitrification process by denitrification bacteria is hampered. The process of converting nitrite ions ( $\text{NO}_2^-$ ) and nitrate ions ( $\text{NO}_3^-$ ) into harmless nitrogen gas ( $\text{N}_2$ ) is inhibited, which impedes the ammonia-nitrogen reduction process. The high concentration of  $\text{NO}_3^-$  and  $\text{NO}_2^-$  ions released into the receiving water body does not meet the ammonia-nitrogen reduction parameter 10mg/L, Standard A of Environmental Quality (Sewage) Regulations 2009 (EQSR 2009) and it would disrupt the receiving water quality and aquatic ecosystem (Rahimi et al., 2020). To address water quality degradation by improving water quality, the Government spent approximately RM26.3 billion from the 8th Malaysia Plan to the 11th Malaysia Plan (2001–2020) to modernize sewerage facilities and infrastructure. Therefore, this study is relevant and essential for further analysis and proposing suitable and practical solutions for optimizing and removing ammonia-nitrogen from low-strength domestic wastewater.

## MATERIALS AND METHODS

### **Biological Treatment Process by Sequencing Batch Reactor Without Polyvinyl Alcohol (PVA) Gel Beads**

For this study, optimum and non-optimum treatment mode settings were adopted from the actual operation of the sewage treatment plant (STP) in Taman Kajang Utama, Selangor, as shown in Table 1. Taman Kajang Utama STP is operated by using sequencing batch reactor (SBR) process in continuous feed configuration targeting pollutants removal as specified under Standard A, EQSR 2009 (EQA 1974), and it received the same influent as the lab-scale reactor (though in continuous feed vs semi-batch feed) with similar operating

conditions. Originally, the Taman Kajang Utama STP was designed to operate in non-optimal treatment settings. However, for energy-saving measures, the plant operator has optimized the operation of the current sewage treatment system by minimizing the use of blowers during the aeration phase while at the same time maintaining the effluent quality that meets the Standard A effluent discharge.

Table 1  
*Summary of the biological wastewater treatment process in Taman Kajang Utama, Selangor*

Treatment mode (Optimum)	Treatment duration (minutes)	Treatment mode (Non-optimum)	Treatment duration (minutes)
Aeration	72	Aeration	120
Denitrification - idling	48	Denitrification - idling	0
Denitrification - stir	48	Denitrification - stir	48
Settling	48	Settling	48
Discharged	72	Discharged	72
Total Treatment Time	288	Total Treatment Time	288

One lab-scale reactor with 5L capacity (4L raw sewage taken from the secondary screen chamber of Taman Kajang Utama STP and 1L of seed sludge (MLSS) taken from SBR tank No. 2 of Taman Kajang Utama STP was fed into the reactor) was developed to run an ammonia-nitrogen and COD reduction simulation using an activated sludge sequencing batch reactor. The simulation of the sequencing batch reactor was conducted based on two scenarios as per Table 2.

Table 2  
*Experiment set-up by a sequencing batch reactor*

Scenario	Treatment Setting	Remarks
<b>1<sup>st</sup> Scenario</b>	Optimum	The total simulation time is 288 minutes. Raw sewage (low concentration) was taken from Taman Kajang Utama STP to run the simulation
Low COD and NH <sub>3</sub> -N concentration at the beginning of the treatment process	Non-optimum	
<b>2<sup>nd</sup> Scenario</b>	Optimum	<ul style="list-style-type: none"> <li>The total simulation time is 288 minutes, and raw sewage (low concentration) was taken from Taman Kajang Utama STP to run the simulation</li> <li>1.2 g glucose (C<sub>6</sub>H<sub>12</sub>O<sub>6</sub>) was added to the raw sewage at the beginning of the treatment process.</li> </ul>
High COD and low NH <sub>3</sub> -N concentration at the beginning of the treatment process	Non-optimum	

The low concentration of incoming raw sewage (consists of Biochemical Oxygen Demand (BOD), COD, Ammonia-Nitrogen, oil & grease, total organic carbon, and alkalinity, among others) and activated sludge were collected from the same sewage

treatment plant for this experiment. In this experiment, 1.2g glucose ( $C_6H_{12}O_6$ ) was added to the raw sewage collected from Taman Kajang Utama, Selangor, at the beginning of the treatment process to increase the concentration of COD to play a vital role as a carbon source, especially in the denitrification process. Ventilation and stirring were used in the treatment process depending on the mode of treatment to be performed. The  $NH_3-N$  and COD parameter were observed

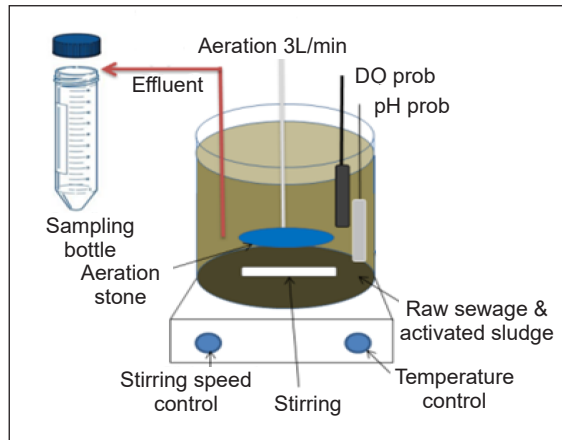


Figure 1. Schematic of a laboratory-scale reactor

and tested by American Public Health Association (APHA) standard method. Dissolved oxygen (DO), pH, and temperature were also measured during the operation of the lab-scale reactor. The setup of a lab-scale reactor is shown in Figure 1. The experiment observed that the pH range was between 6.0–7.5, and the temperature range was kept at 25–28°C with no alteration to the parameters. DO content was maintained at 4.71–7.10 mg/L

The COD and  $NH_3-N$  reduction efficiency (%) was determined by using the following Equation 1 (Kim et al., 2021):

$$\text{COD and } NH_3-N \text{ reduction efficiency (\%)} = \frac{C_o - C_e}{C_o} \times 100 \quad (1)$$

Where  $C_o$ : initial COD and  $NH_3-N$  concentration, mg/L;  $C_e$ : final equilibrium COD and  $NH_3-N$  concentration, mg/L

### Biological Treatment Process by Sequencing Batch Reactor with Polyvinyl Alcohol (PVA) Gel Beads-Preparation of Synthetic Wastewater

This experiment developed two different size reactor tanks with 5L and 4L capacity. A 3L and 2.4L synthetic wastewater (60% of reactor capacity) with various compounds and compositions were prepared, contained (per lit):  $C_6H_{12}O_6$  500mg,  $NH_4Cl$  122mg,  $K_2HPO_4$  22mg,  $MgSO_4$  50mg,  $FeSO_4 \cdot 7H_2O$  40mg,  $NaCl$  15mg,  $CaCO_3$  100mg, EDTA 6mg and  $Na_2HPO_4$  15mg (Tuyen et al., 2018). This experiment used  $C_6H_{12}O_6$  and  $NH_4Cl$  chemical reagents as COD and ammonia sources. In addition, a 1L and 0.8L activated sludge (20% of reactor capacity) was collected from SBR Tank No. 2 at Taman Kajang Utama, Selangor sewage treatment plant, and 1L and 0.8L of PVA gel beads (16%–20% of total reactor volume) were added to the reactor tank and mixed with synthetic wastewater (Wang et al., 2018). PVA gel beads with 3–4mm diameter in a spherical shape with a

density of  $1.025\text{g/cm}^3$ , a surface area of  $2,500\text{--}3,000\text{ m}^2/\text{m}^3$  and network  $10\text{--}20\text{-micron}$  pores were purchased from Kuraray Co. Ltd., Japan. The experiment with PVA gel beads was performed for low COD and  $\text{NH}_3\text{-N}$  concentrations at the beginning of the treatment process. The low concentration of raw sewage represents the actual state of domestic wastewater characteristics in Malaysia.

### Experiment Start-Up Process with Polyvinyl Alcohol (PVA)-Gel Beads

All substances were mixed and continuously aerated (24 hours) in a 5L and 4L single reactor to promote microbial growth in highly porous PVA gel beads and to adapt bacteria to organic matter. The startup phase for microbial growth in synthetic wastewater took about 28 days (acclimatization phase). During this phase,  $1.2\text{L--}1.5\text{L}$  synthetic wastewater in the reactor was replaced with new synthetic wastewater at certain interval days until the startup phase stabilized with a consistent reduction rate of COD and  $\text{NH}_3\text{-N}$ . On day 29, the synthetic wastewater was replaced with  $1.6\text{L--}2.0\text{L}$  raw sewage collected from Taman Kajang Utama, Selangor, to acclimate the microbial growth in PVA gel beads with actual domestic sewage. This startup process continued until day 34, when the bacteria had reached the stationary phase and were ready to be used for the study until the reduction rate of COD and  $\text{NH}_3\text{-N}$  became consistent and stable at  $60\text{--}70\%$  at the end of the acclimatization period. The  $\text{NH}_3\text{-N}$  and COD parameter were observed for 34 days startup phase and tested by American Public Health Association (APHA) standard method. Similarly, pH, dissolved oxygen (DO), and temperature were also measured for 34 days startup phase using digital portable devices, namely, Eutech Instruments Cyberscan pH 300 and Hanna multiparameter DO meter-HI2040. The overall timeline of the startup phase is shown in Figure 2.

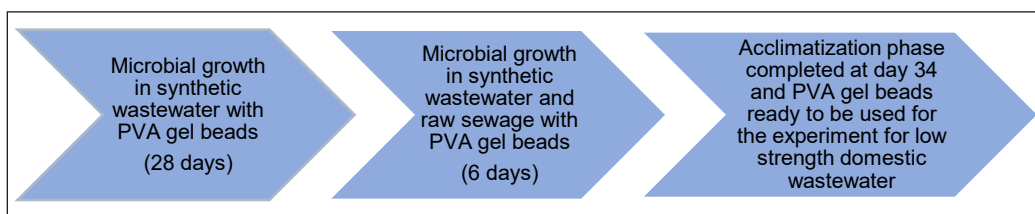


Figure 2. Overall timeline for the startup phase of microbes with PVA gel beads

## RESULTS AND DISCUSSION

### Biological Treatment Process by Sequencing Batch Reactor Without Polyvinyl Alcohol (PVA) Gel Beads

The summary of COD and  $\text{NH}_3\text{-N}$  reduction performance without PVA gel beads is shown in Table 3. The graph of ammonia-nitrogen and COD reduction performance without PVA gel beads for low COD and  $\text{NH}_3\text{-N}$  concentration at the beginning of the treatment process (optimum and non-optimum treatment setting) is shown in Figures 3 and 4.



Table 3  
*COD and NH<sub>3</sub>-N reduction efficiency without PVA gel beads*

Scenario	Treatment Setting	Temp (°C)	pH	COD Reduction Rate	NH <sub>3</sub> -N Reduction Rate	C/N ratio
<b>1<sup>st</sup> Scenario</b> Low COD and NH <sub>3</sub> -N concentration at the beginning of the treatment process	Optimum	25.0 to 27.7	6.52 to 7.50	55.95% to 86.14%	32.41% to 44.30%	2.62 to 2.89
	Non-Optimum	25.8 to 27.8	6.87 to 7.59	58.65% to 84.30%	44.14% to 47.85%	6.37 to 10.05
<b>2<sup>nd</sup> Scenario</b> High COD and low NH <sub>3</sub> -N concentration at the beginning of the treatment process (1.2 g glucose (C <sub>6</sub> H <sub>12</sub> O <sub>6</sub> ) was added)	Optimum	25.8 to 27.5	6.85 to 7.65	33.48% to 59.46%	11.68% to 26.20%	20.34 to 24.92
	Non-optimum	25.0 to 27.5	6.87 to 7.67	64.52% to 65.32%	53.03% to 55.50%	21.6 to 22.77

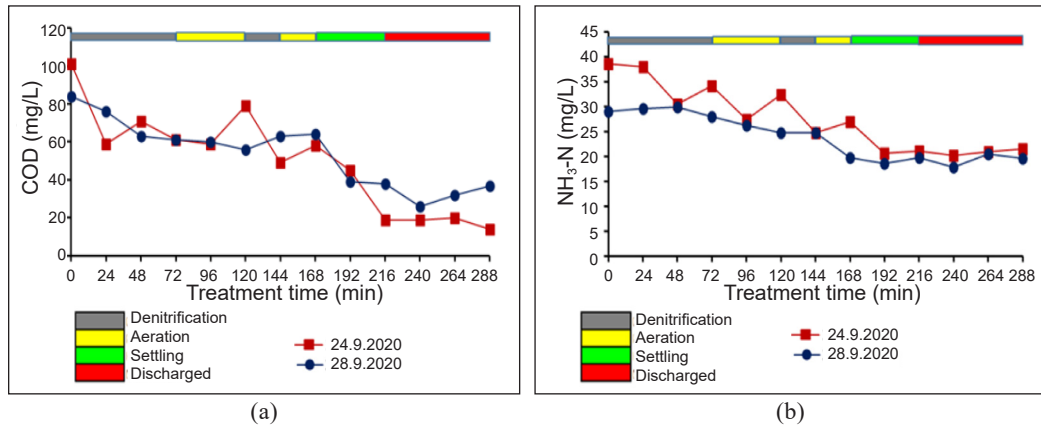


Figure 3. Graph of (a) COD analysis and (b) NH<sub>3</sub>-N analysis for optimum mode treatment

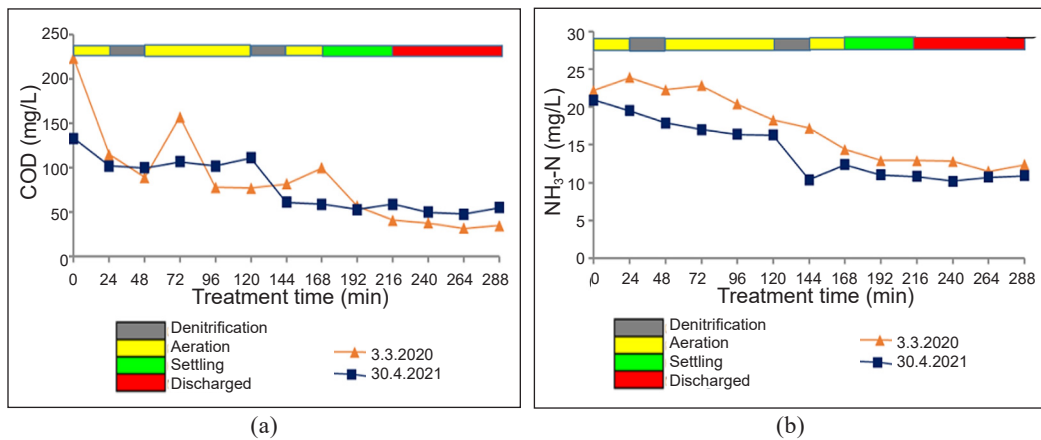


Figure 4. Graph of (a) COD analysis and (b) NH<sub>3</sub>-N analysis for non-optimum mode treatment

The graph of ammonia-nitrogen and COD reduction performance without PVA gel beads for high COD and NH<sub>3</sub>-N concentration at the beginning of the treatment process (optimum and non-optimum treatment setting) is shown in Figures 5 and 6.

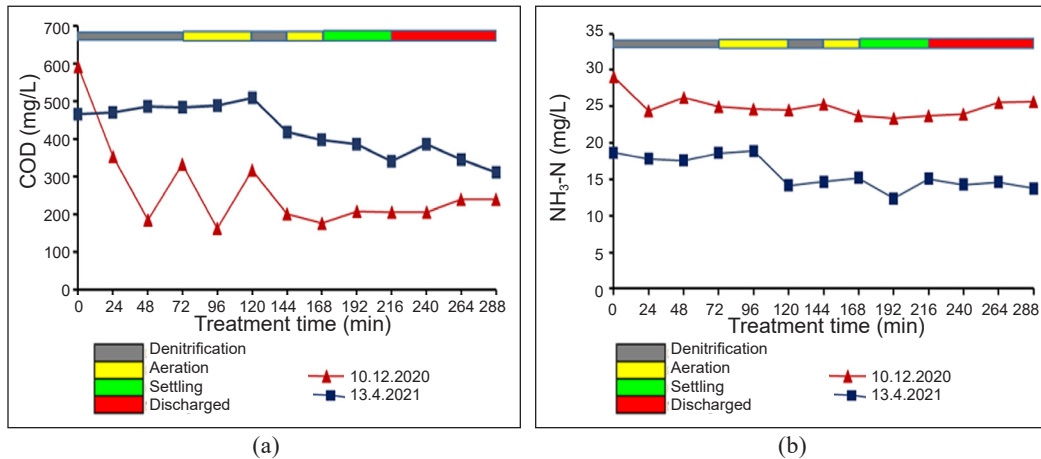


Figure 5. Graph of (a) COD analysis and (b) NH<sub>3</sub>-N analysis for optimum mode treatment

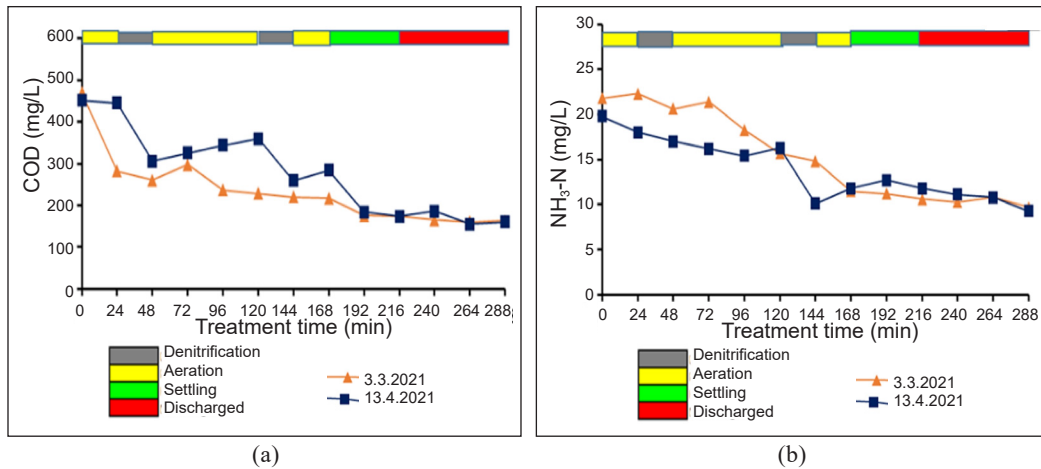


Figure 6. Graph of A) COD analysis and B) NH<sub>3</sub>-N analysis for non-optimum mode treatment

### Reduction Efficiency of Ammonia-Nitrogen Without PVA Gel-Beads

The experiments showed that nitrification and denitrification were the primary biological nitrogen reduction processes. The C/N ratio, variation of carbon sources, DO concentrations, and the number of intermittent aeration sequences affect the ammonia-nitrogen reduction in these experiments. However, other factors, such as temperature and pH, will also be discussed in this section.

As shown in Table 3, under the first scenario of the optimum mode setting, the ratio of carbon to ammonia-nitrogen nitrogen (C/N) is between 2.62 to 2.89 with a 32.41% to 44.30% reduction, while for the non-optimum mode setting, the C/N ratio is between 6.37 to 10.05 with 44.14% to 47.85% reduction, respectively. The influent for both treatment settings presented a low organic matter (COD) concentration of 84 to 223mg/L. Even though the experiment failed to achieve the required effluent discharge standard of 10mg/L, the non-optimum mode has shown better performance than the optimum mode setting. In the second scenario, it was observed that the C/N ratio for the optimum mode setting is between 20.34 to 24.92 with an 11.68% to 26.20% reduction, and for the non-optimum mode, the setting is between 21.6 to 22.77 with 53.03% to 55.50% reduction. The COD/N ratios were pretty high due to the addition of glucose to the fed wastewater. The influent for both treatment settings presented a high organic matter (COD) concentration of 451 to 592mg/L. The non-optimum mode setting has shown better performance than the optimum mode setting and met the required effluent discharge standard of 10mg/L.

In contrast, the optimum mode setting failed to achieve the desired effluent discharge limit. Therefore, it can be summarized that the low C/N ratio in the first scenario represents low organic matter (COD) in the substrate, and the high C/N ratio in the second scenario represents high organic matter (COD) in the substrate. In the denitrification process, heterotrophic bacteria perform biological denitrification and require a biodegradable organic carbon source as an electron donor.

Thus, the availability of organic carbon as an electron donor (typically written as biodegradable chemical oxygen demand (bCOD)) determines the denitrification potential of wastewater. According to Sun et al. (2010), in simultaneous nitrification and denitrification (SND), the optimal C/N ratio, in which the nitrification and denitrification reactions are balanced, was found to be 11.1. Water Environment Federation (2007) highlighted that 8.6 mg of COD is required to eliminate 1 mg of nitrate-nitrogen from wastewater. Moreover, it was found in the previous study that COD (readily biodegradable COD) (rbCOD) in tropical countries like Malaysia has low soluble COD content and high slowly biodegradable COD (sbCOD) content. Thus, the low rbCOD content was insufficient to reach the complete denitrification process (How et al., 2020). In the first scenario, it can be seen that the average C/N ratios are all below 11.1. Thus, the denitrification process is not in the best condition due to the lack of carbon sources for the denitrification process in the deep biofilm. In the second scenario, 1.2g glucose was added to increase the COD concentrations in the existing domestic sewage to investigate the effect of external carbon sources on nitrogen reduction performance. It was observed that the reduction rate of  $\text{NH}_3\text{-N}$  has increased and improved in non-optimum mode as compared with the optimum mode and the first scenario experiment. Therefore, it can be concluded that the nitrogen reduction in the second scenario under non-optimum mode is supported by adding an external carbon source from

glucose in deep biofilm to facilitate denitrification. In addition, the average C/N ratio is above 11.1, thus improving the nitrogen reduction in this experiment.

In the SND process, due to diffusional limitations, the dissolved oxygen (DO) concentration gradients within the microbial biofilms (typical floc size: 100 to 150 $\mu$ m diameter, optimum floc size: 80 to 100 $\mu$ m diameter) form different populations throughout the biofilm: the nitrifying regions are located in high DO concentration zones, while the denitrifying regions are located in lower concentration zones (Bueno et al., 2018; Sun et al., 2010). Khanitchaidecha et al. (2015) reported that the rate of nitrification could be accelerated by increasing the DO concentration in the reactor tank. As a result, in this study, the reactor tank was aerated at a higher air flow rate of 3L/min with a DO of 5–7mg/L intermittently. However, it impacts the denitrification process since the increased air flow rate and DO concentration resulted in increased oxygen retention in the anaerobic stage, lowering denitrification activity and nitrogen reduction efficiency.

According to Jimenez et al. (2011), previous studies have found that DO concentrations for nitrification in SND should be higher than 1.0 mg/L, and the most recommended value is 2.0 mg/L or less to produce higher nitrification rates. Low DO concentrations may result in a low nitrification rate, affecting TN removal. When DO concentrations are high, it may lead to low denitrification rates due to the reduction of anoxic zones. How et al. (2018) reported low COD concentration in sewage may have contributed to active nitrification in low DO conditions by minimizing oxygen competition between heterotrophs and nitrifiers. At low DO concentrations, the microbial community structure of the nitrifying sludge is expected to be different from a standard high DO nitrifying community. Active nitrification in low DO settings has been associated with increased oxygen affinity in both ammonia-oxidizing bacteria (AOB) and nitrite-oxidizing bacteria (NOB).

Therefore, the SND process's effectiveness depends on the proper DO concentrations range for both kinetic reactions, nitrification, and denitrification in the same reactor (Li et al., 2007). On the other hand, the higher ammonia-nitrogen reduction rate in non-optimal mode was attributed to a longer aeration process of 120 minutes (5 cycles of intermittent aeration) compared to 72 minutes (3 cycles of intermittent aeration) in optimum mode. The ample time taken and the optimum intermittent aeration sequences to supply DO concentration during the nitrification process have increased the conversion rate of  $\text{NH}_4^+$  to  $\text{NO}_3\text{-N}$ , lowering the  $\text{NH}_3\text{-N}$  concentrations in the reactor. Despite having an optimal C/N ratio of 11.1 in the denitrification process, sufficient aeration time also plays an important role in nitrogen reduction in these experiments. The DO concentration and the effective time taken to supply DO concentration during nitrification are crucial for the growth of nitrifying bacteria in the nitrification process. It is probably due to the nitrifiers requiring enough time to react with the ammonia, and they (autotrophic bacteria) grow slower in the nitrification process compared with denitrifiers (heterotrophic bacteria) in the denitrification process (Curtin et al., 2011; Rusalleda Beylier et al., 2011).

As discussed earlier, other factors influencing biological nitrogen reduction are temperature and pH reading. In these experiments, temperature and pH readings were measured at 6.52–7.59 and 25.0 to 27.8°C for the first scenario. While in the second scenario, temperature and pH readings were measured at 6.85–7.67 and 25.0 to 27.5°C, respectively. Alkalinity in the form of calcium carbonate ( $\text{CaCO}_3$ ) in raw wastewater serves as a carbon source for nitrifiers to perform well in the nitrification process. Typically, 0.454kg of ammonia requires 3.239kg of alkalinity ( $\text{CaCO}_3$ ) to oxidize to nitrate. Nitrification is a chemical reaction that results in the formation of acids. This acid production, together with the consumption of calcium carbonate during nitrification, can lower the pH of the nitrifiers, causing nitrifying bacteria to develop at a slower rate (Trygar, 2009). In nitrification, the optimum pH range is 6.8 to 8.0 (Curtin et al., 2011); for denitrification, the pH range is 6.5 to 7.5. Based on both scenarios, the pH reading is within the optimum range and has not significantly affected the nitrogen reduction process. According to Curtin et al. (2011), to maintain a stable population of nitrifiers, the temperature must be higher than 7°C. At liquid temperatures between 25–28°C (Rodziewicz et al., 2019), nitrification reaches its maximum rate. For denitrification, the optimal temperature is between 20–35°C (Ni et al., 2017). Hence, the experiments' temperatures of nitrification and denitrification were within an optimal range.

### **Reduction Efficiency of COD Without PVA Gel-Beads**

The study was conducted to analyze the reduction efficiency of organic matter (COD). In the first scenario, COD concentrations decreased at a higher reduction rate of 55.95% to 86.14%. They met the required discharge limit of 120mg/L, whereas, in the second scenario, COD concentrations decreased at a lower reduction rate of 33.48% to 65.32%. However, under the non-optimum mode, the COD concentration was reduced in the second scenario more than in the optimal mode. In the suspended growth process, microorganisms are thoroughly mixed with organic matter (COD), stimulating their growth by allowing them to consume the organic matter as food. Individual bacteria clump together (floculate) to form an active mass of microbes (biologic floc) termed activated sludge as they proliferate and are mixed by air agitation. Air is introduced to mix the activated sludge with the wastewater, and oxygen is provided for the microorganisms to break down the organic matter.

Mixed liquor is the mixture of activated sludge and wastewater in the reactor tank. From the first scenario, it was envisaged that sufficient food (organic matter) and oxygen supplied to suspended microbes facilitated the reduction of organic matter in the wastewater. The concentration of MLSS/MLVSS in the mixture is also found to be in the appropriate quantity for effective treatment. Hence, there is no significant difference in performance for both optimal and non-optimal modes under the first scenario. In the second scenario, due to the addition of 1.2g glucose, the poor performance of organic matter reduction was observed, especially under the optimal setting. It is most likely due to the high loading of

organic matter (COD) into the system, low MLSS/MLVSS concentrations to consume the organic matter as food, and inadequate aeration period to supply oxygen to break down the organic matter. In addition, the adaptation of microorganisms with the additional organic matter has also led to ineffective treatment, affecting the microbes' ability to degrade the organic matter (Herlina et al., 2019). However, in non-optimal settings, reduction effectiveness is higher than in optimal settings, and this could be due to a longer aeration process of 120 minutes (5 cycles of intermittent aeration) compared to 72 minutes (3 cycles of intermittent aeration) in the optimal setting, which facilitated organic matter reduction.

**Biological Treatment Process by Sequencing Batch Reactor with Polyvinyl Alcohol (PVA) Gel Beads**

The summary of COD and NH<sub>3</sub>-N reduction performance with PVA gel beads is shown in Table 4.

Table 4  
COD and NH<sub>3</sub>-N reduction efficiency with PVA gel beads

Scenario	Treatment Setting	Temp (°C)	pH	COD Reduction Rate	NH <sub>3</sub> -N Reduction Rate	C/N ratio
<b>1<sup>st</sup> Scenario</b>	Optimum	24.0 to 26.1	7.00 to 7.59	42.02%	30.94%	8.56
Treatment with PVA gel-beads	Non - Optimum	25.0 to 27.0	6.78 to 7.69	70.68%	62.96% to 65.71%	8.8 to 11.26
Low COD and NH <sub>3</sub> -N concentration at the beginning of the treatment process						

The graph of ammonia-nitrogen and COD reduction performance with PVA gel beads for low COD and NH<sub>3</sub>-N concentration at the beginning of the treatment process (optimum treatment and non-optimum setting) is shown in Figures 7 and 8. Figure 9 depicts the color of new PVA gel beads (white) and used PVA gel beads (yellowish), and Figure 10 depicts the lab-scale reactor with PVA gel beads.

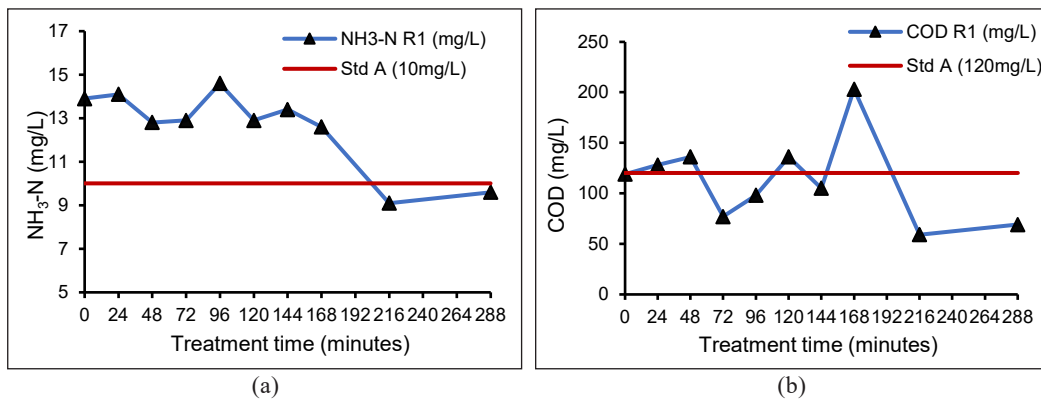


Figure 7. Graph of (a) NH<sub>3</sub>-N analysis and (b) COD analysis for optimum mode treatment



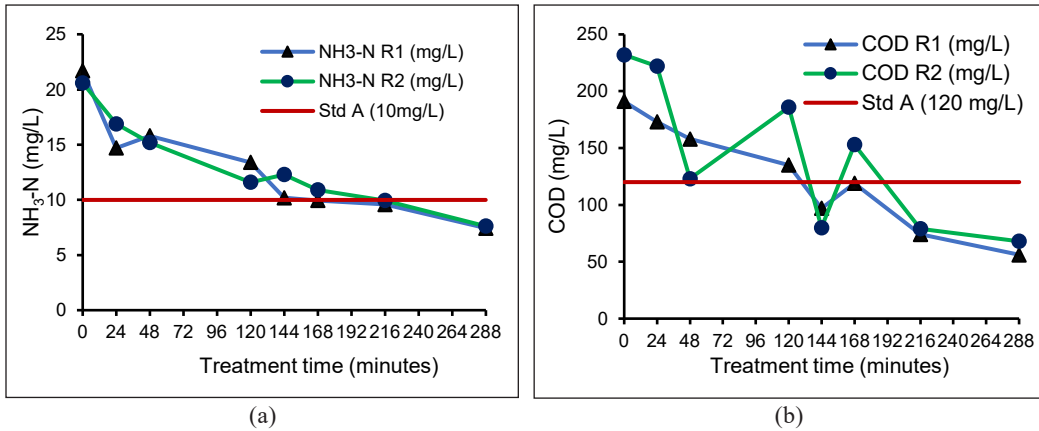


Figure 8. Graph of (a) NH<sub>3</sub>-N analysis and (b) COD analysis for non-optimum mode treatment



Figure 9. A) Unused PVA gel beads (white color) and B) used PVA gel beads (yellowish color) after a lab-scale experiment



Figure 10. Lab scale-reactor with PVA gel beads

### Reduction Efficiency of Ammonia-Nitrogen Nitrogen with PVA Gel Beads

According to the experiment's results, under optimal setting, the C/N ratio is at 8.56, while under a non-optimal setting, the C/N ratio ranges from 8.8 to 11.26. Thus, the C/N ratio is within the optimal condition of 11.1 for nitrification and denitrification to perform well in SND as the reactions were balanced. Furthermore, an analysis of a lab-scale reactor under non-optimal conditions revealed that the nitrogen reduction efficiency significantly improved when PVA gel beads were added to the reactor. The NH<sub>3</sub>-N reduction performance, on average, was increased by 17.86% to 18.82% under the same treatment setting. The improvement of ammonia-nitrogen nitrogen reduction with PVA gel beads indicated that the active core and highly porous immobilized biofilm carriers developed an efficient denitrification microreactor. Each PVA gel bead with high specific surface areas provided an anoxic microenvironment when placed in an aerobic reactor (Li et al., 2021). On the



other hand, the microbes (living cells) are contained in a porous polymeric matrix that allows substrate molecules to diffuse in and product molecules to diffuse out (Pham & Tho Bach, 2014).

However, it is contrary to the optimal setting in which the reduction rate is not in the best performance. As discussed in the previous section, the ineffective treatment was most likely associated with high DO concentrations throughout the treatment process and less intermittent aeration sequences during the nitrification process. Zhang et al. (2021) highlighted that different DO concentrations significantly affect the activity of various functional microorganisms in the reactor, making it one of the most significant elements. As DO rises, the population of ammonium-oxidizing bacteria (AOB) and nitrite-oxidizing bacteria (NOB) rises, affecting nitrifying and denitrifying activities. DO can significantly affect the proportions of aerobic and anaerobic zones within the biofilm and the microbial community structure, thus making it the most critical parameter for improving the SND rate. It is suggested that DO concentration should be controlled at an optimal range, within 2.0 to 5.0mg/L in the aerobic phase, as reported by Jimenez et al. (2011), to maintain a suitable operational condition. Another factor that promotes effective nitrogen reduction is the concentration of organic loading (COD) in the raw sewage as a carbon source during the denitrification process. The best results of nitrogen reduction were found in a non-optimal setting as the influent COD level was relatively higher than the COD level in the optimal setting. The concentration of ammonia entering the treatment system, which will affect the growth of bacteria in the nitrification process (Rodríguez-Gómez et al., 2021), also affects the nitrogen reduction process.

As shown in Figure 9, the color of the new PVA gel beads was white and turned yellowish after 1 month of acclimatization. According to Jin et al. (2016), the color of PVA was yellowish after 1 month cultivation period, and after 5 months of treatment, the color of matured PVA gel beads was black. It is supported by another study by Khanh et al. (2011), where the matured black color of PVA gel beads was used in wastewater treatment. Another study found a similar finding in which the color of PVA gel beads turned from white to yellowish after 1 month of operation and became red-brown after 3 months. During the 3 months of operation, the reduction rate of  $\text{NH}_3\text{-N}$  and COD were 70-80%, respectively. The change of color represents that microbial growth increased with the proportionality of time (Wang et al., 2018). Hence, the color changes in PVA gel beads in this study were still in the culture process, and the ammonia-nitrogen reduction rate increased with increasing acclimatization time. These findings are supported by the reduction levels of  $\text{NH}_3\text{-N}$  and COD of 60–70% during the startup phase. Therefore, it is suggested that the acclimatization period with the domestic wastewater should be extended until the reduction efficiency of  $\text{NH}_3\text{-N}$  and COD reaches a minimum of 70-80% and becomes stable prior to undertaking the sequencing operation based on the optimum and non-optimum setting.

As discussed previously, temperature and pH readings influenced the nitrogen reduction process. In these experiments, temperature and pH readings were measured at 7.14–7.59 and 24.0 to 26.3°C in an optimal setting, while temperature and pH measurements in the non-optimal configuration were 6.78–7.69°C and 25.0–27.0°C, respectively. Thus, as observed in both treatment settings, the pH value and temperature are within the ideal ranges of 6.8 to 8.0 in nitrification and 6.5 to 7.5 in denitrification and 25–28°C, respectively. Moreover, the total volumetric capacity of PVA gel beads in the range of 5 to 15% allows hydraulic capacity to enter the system more than 50 to 70% volumetric capacity for other carriers (Singh et al., 2016).

### **Reduction Efficiency of COD with PVA Gel Beads**

Similar to ammonia-nitrogen nitrogen, the reduction rate of COD in a non-optimal setting has shown a high effect than in the optimal setting. During the experiment, the COD influent ranged from 119 to 232 mg/L. The COD reduction rate under the optimal setting was only 42.0%, while the COD reduction rate under the non-optimal setting was measured at 70.68%. In addition, an analysis of a lab-scale reactor with PVA gel beads under non-optimal conditions revealed that the COD reduction efficiency was stable and consistent. The gap in COD reduction efficiency without PVA gel beads is between 25–30%. This condition demonstrated that the treatment efficiency was inconsistent even though the reduction rate could achieve higher than 80%. The consistent and stable COD reduction rate with PVA gel beads is likely due to the microbes being preserved in their native form by encapsulation within a membrane, inhibiting leakage and protecting the microbes from adverse conditions.

Thus, PVA gel beads allow microbes to grow quickly and steadily on the media and in the inner part of the media resulting in non-flocculent biomass with fewer self-oxidizing protozoans and metazoans (Rajpal et al., 2021). In addition, these results show that the system can handle variable organic loading, thus delivering consistent results of organic matter removal (Singh et al., 2016). When microbes are confined or curbed within a semi-permeable membrane, tiny substrate molecules can diffuse while product molecules can diffuse out (Bouabidi et al., 2019; Krishnamoorthi et al., 2015). At the same time, this treatment has both biofilms in the carrier and freely suspended biomass in the same reactor. Unlike treatment without the carrier, the gap in COD reduction efficiency is likely due to microbes growing freely in suspended conditions and not being protected from the adverse environmental situation and easily washout from the reactor (El-Naas et al., 2013). However, more experiments need to be performed for this study to establish the findings. Other factors that affect microbes' proliferation are pH and temperature. According to Herlina et al. (2019), the anaerobic process is most effective in the pH range of 6.5–7.5, while the aerobic process is most effective in the pH range of 6.5–8.5. Furthermore, the

microbes can proliferate at the best temperature of 25–35°C. These experiments' average pH readings and temperature were 7.23 and 25.69°C, respectively. Thus, from the observation, the pH and temperature were in the optimal range and facilitated microbial growth in the reactor.

In addition, it was observed in non-optimal settings that reduction effectiveness is higher than in optimal settings. It is likely due to more intermittent aeration sequences with a total aeration period of 120 minutes vs. 72 minutes in an optimal setting, facilitating organic matter degradation. The trend of COD reduction performance with PVA gel beads at optimal configuration is similar to the COD reduction without PVA gel beads. Based on these trends, it can be concluded that the COD reduction with more intermittent aerobic sequences significantly improved the reduction of organic compounds.

## CONCLUSION

Based on the study performed, it is proven that PVA gel beads as an immobilized carrier are able to treat low-medium concentrations of domestic wastewater in Malaysia. Wastewater treatment using this carrier can increase the reduction level of nitrogen and organic matter. In addition, it can be used as an alternative option to enhance existing biological wastewater treatment systems without involving major construction works, thus reducing the capital cost of building a new sewage treatment plant or upgrading the existing sewage treatment plant. It can be concluded that the reduction efficiency of ammonia-nitrogen and COD with PVA gel beads under a non-optimal setting is better than with PVA gel beads under the optimal setting and meets the required effluent discharge, Standard A of Environmental Quality (Sewage) Regulations 2009. The nitrogen reduction improved significantly, and organic matter reduction showed a more stable performance than wastewater treatment without PVA gel beads. The results showed that the combination of attached and suspended biomass was superior to the freely suspended biomass for nitrification and denitrification of wastewater. The color change of PVA gel beads from white to yellowish after one month of operation indicates that a colony of microbes was growing in the highly inner porous carriers.

## ACKNOWLEDGEMENTS

This study was supported by Sewerage Services Department, Malaysia and Environmental Engineering (EE) & Environmental Technology Management (ETM) project fund.

## REFERENCES

- Bouabidi, Z. B., El-Naas, M. H., & Zhang, Z. (2019). Immobilization of microbial cells for the biotreatment of wastewater: A review. *Environmental Chemistry Letters*, 17, 241-257. <https://doi.org/10.1007/s10311-018-0795-7>

- Bueno, R. F., Piveli, R. P., Campos, F., & Sobrinho, P. A. (2018). Simultaneous nitrification and denitrification in the activated sludge systems of continuous flow. *Environmental Technology*, 39(20), 2641-2652. <https://doi.org/10.1080/09593330.2017.1363820>
- Curtin, K., Duerre, S., Fitzpatrick, B., Meyer, P., & Ellefson, N. (2011). *Biological nutrient removal*. Minnesota Pollution Control Agency. <https://www.pca.state.mn.us/sites/default/files/wq-wwtp8-21.pdf>
- El-Naas, M. H., Mourad, A. H. I., & Surkatti, R. (2013). Evaluation of the characteristics of polyvinyl alcohol (PVA) as matrices for the immobilization of *Pseudomonas putida*. *International Biodeterioration and Biodegradation*, 85, 413-420. <https://doi.org/10.1016/j.ibiod.2013.09.006>
- Hanafiah, Z. M., Mohtar, W. H. M. W., Hasan, H. A., Jensen, H. S., Abdullah, M. Z., & Husain, H. (2019). Diversification of temporal sewage loading concentration in tropical climates. *IOP Conference Series: Earth and Environmental Science*, 264, Article 012026. <https://doi.org/10.1088/1755-1315/264/1/012026>
- Herlina, N., Turmuzi Lubis, M., Husin, A., & Putri, I. (2019). Studies on decreasing chemical oxygen demand (COD) on artificial laundry wastewater using anaerobic-aerobic biofilter dipped with bio ball media. *MATEC Web of Conferences*, 276, Article 06015. <https://doi.org/10.1051/mateconf/201927606015>
- How, S. W., Lim, S. Y., Lim, P. B., Aris, A. M., Ngoh, G. C., Curtis, T. P., & Chua, A. S. M. (2018). Low-dissolved-oxygen nitrification in tropical sewage: An investigation on potential, performance and functional microbial community. *Water Science and Technology*, 77(9), 2274-2283. <https://doi.org/10.2166/wst.2018.143>
- How, S. W., Sin, J. H., Wong, S. Y. Y., Lim, P. B., Aris, A. M., Ngoh, G. C., Shoji, T., Curtis, T. P., & Chua, A. S. M. (2020). Characterization of slowly-biodegradable organic compounds and hydrolysis kinetics in tropical wastewater for biological nitrogen removal. *Water Science and Technology*, 81(1), 71-80. <https://doi.org/10.2166/wst.2020.077>
- Jimenez, J., Dursun, D., Dold, P., Bratby, J., Keller, J., & Parker, D. (2011). Simultaneous nitrification-denitrification to meet low effluent nitrogen limits: Modeling, performance and reliability. *Proceedings of the Water Environment Federation*, 2010(15), 2404-2421. <https://doi.org/10.2175/193864710798158968>
- Jin, Y., Wang, D., & Zhang, W. (2016). Treatment of high-strength ethylene glycol wastewater in an expanded granular sludge blanket reactor: Use of PVA-gel beads as a biocarrier. *SpringerPlus*, 5, Article 856. <https://doi.org/10.1186/s40064-016-2409-9>
- Khanh, D., Quan, L., Zhang, W., Hira, D., & Furukawa, K. (2011). Effect of temperature on low-strength wastewater treatment by UASB reactor using poly (vinyl alcohol)-gel carrier. *Bioresource Technology*, 102(24), 11147-11154. <https://doi.org/10.1016/j.biortech.2011.09.108>
- Khanitchaidecha, W., Nakaruk, A., Koshy, P., & Futaba, K. (2015). Comparison of simultaneous nitrification and denitrification for three different reactors. *BioMed Research International*, 2015, Article 901508. <https://doi.org/10.1155/2015/901508>
- Kim, E. J., Kim, H., & Lee, E. (2021). Influence of ammonia stripping parameters on the efficiency and mass transfer rate of ammonia removal. *Applied Sciences*, 11(1), Article 441. <https://doi.org/10.3390/app11010441>
- Krishnamoorthi, S., Banerjee, A., & Roychoudhury, A. (2015). Immobilized enzyme technology: Potentiality and Prospects Review. *Enzymology and Metabolism*, 1(1), 1-11.

- Li, H., Liu, Q., Yang, P., Duan, Y., Zhang, J., & Li, C. (2021). Encapsulation of microorganisms for simultaneous nitrification and denitrification in aerobic reactors. *Journal of Environmental Chemical Engineering*, 9(4), Article 105616. <https://doi.org/10.1016/j.jece.2021.105616>
- Li, J., Peng, Y., Gu, G., & Wei, S. (2007). Factors affecting simultaneous nitrification and denitrification in an SBBR treating domestic wastewater. *Frontiers of Environmental Science and Engineering in China*, 1, 246-250. <https://doi.org/10.1007/s11783-007-0042-0>
- Ni, B. J., Pan, Y., Guo, J., Viridis, B., Hu, S., Chen, X., & Yuan, Z. (2017). Denitrification processes for wastewater treatment. In I. Moura, J. J. G. Moura, S. R. Pauleta & L. B. Maia (Eds.), *Metalloenzymes in Denitrification: Applications and Environmental Impacts* (pp. 368-418). The Royal Society of Chemistry. <https://doi.org/10.1039/9781782623762-00368>
- Pham, D. V., & Bach, L. T. (2014). Immobilized bacteria by using PVA (Polyvinyl alcohol) crosslinked with Sodium sulfate. *International Journal of Science and Engineering*, 7(1), 41-47. <https://doi.org/10.12777/ijse.7.1.41-47>
- Rahimi, S., Modin, O., & Mijakovic, I. (2020). Technologies for biological removal and recovery of nitrogen from wastewater. *Biotechnology Advances*, 43, Article 107570. <https://doi.org/10.1016/j.biotechadv.2020.107570>
- Rajpal, A., Srivastava, G., Bhatia, A., Singh, J., Ukai, Y., & Kazmi, A. A. (2021). Optimization to maximize nitrogen removal and microbial diversity in PVA-gel based process for treatment of municipal wastewater. *Environmental Technology and Innovation*, 21, Article 101314. <https://doi.org/10.1016/j.eti.2020.101314>
- Rodríguez-Gómez, L. E., Rodríguez-Sevilla, J., Hernández, A., & Álvarez, M. (2021). Factors affecting nitrification with nitrite accumulation in treated wastewater by oxygen injection. *Environmental Technology*, 42(5), 813-825. <https://doi.org/10.1080/09593330.2019.1645742>
- Rodziewicz, J., Ostrowska, K., Janczukowicz, W., & Mielcarek, A. (2019). Effectiveness of nitrification and denitrification processes in biofilters treating wastewater from de-icing airport runways. *Water (Switzerland)*, 11(3), Article 630. <https://doi.org/10.3390/w11030630>
- Ruscalleda Beylier, M., Balaguer, M. D., Colprim, J., Pellicer-Nàcher, C., Ni, B. J., Smets, B. F., Sun, S. P., & Wang, R. C. (2011). Biological nitrogen removal from domestic wastewater. *Comprehensive Biotechnology*, 6, 329-340. <https://doi.org/10.1016/B978-0-08-088504-9.00533-X>
- Services, N. W. C. (2016). Section 3 sewage characteristics and effluent discharge requirements. *Malaysian Sewage Industry Guidelines*, 4, 27-34.
- Singh, N. K., Singh, J., Bhatia, A., & Kazmi, A. A. (2016). A pilot-scale study on PVA gel beads based integrated fixed film activated sludge (IFAS) plant for municipal wastewater treatment. *Water Science and Technology*, 73(1), 113-123. <https://doi.org/10.2166/wst.2015.466>
- Sun, S. P., Nàcher, C. P. I., Merkey, B., Zhou, Q., Xia, S. Q., Yang, D. H., Sun, J. H., & Smets, B. F. (2010). Effective biological nitrogen removal treatment processes for domestic wastewaters with low C/N ratios: A review. *Environmental Engineering Science*, 27(2), 111-126. <https://doi.org/10.1089/ees.2009.0100>
- Suruhanjaya Perkhidmatan Air Negara. (2016). *Section 2 Planning, Material and Design*. <https://www.span.gov.my/article/view/malaysian-sewerage-industry-guidelines-msig>

- Trygar, R. (2009). *Nitrogen Control in Wastewater Treatment Plants* (2nd Ed.). TREECo Center.
- Tuyen, N. V., Ryu, J. H., Yae, J. B., Kim, H. G., Hong, S. W., & Ahn, D. H. (2018). Nitrogen removal performance of anammox process with PVA-SA gel bead crosslinked with sodium sulfate as a biomass carrier. *Journal of Industrial and Engineering Chemistry*, 67, 326-332. <https://doi.org/10.1016/j.jiec.2018.07.004>
- Water Environment Federation. (2007). *Chapter 22: Biological nutrient removal processes*. <https://enviro2.doe.gov.my/ekmc/wp-content/plugins/download-attachments/includes/download.php?id=200697>
- Wang, Y., Liu, Y., Feng, M., & Wang, L. (2018). Study of the treatment of domestic sewage using PVA gel beads as a biomass carrier. *Journal of Water Reuse and Desalination*, 8(3), 340-349. <https://doi.org/10.2166/wrd.2017.181>
- Zhang, S., Chen, J., Yuan, J., & Wang, G. (2021). Response of simultaneous nitrification-denitrification to do increments in continuously aerated biofilm reactors for aquaculture wastewater treatment. *Water Practice and Technology*, 16(4), 1067-1077. <https://doi.org/10.2166/wpt.2021.062>

## Effects of Various Doses of *Saccharomyces cerevisiae* on the Growth, Survival Rate, and Blood Profile of Saline Red Tilapia (*Oreochromis spp.*) in the Semi-Intensive Culture Conditions

Istiyanto Samidjan<sup>1\*</sup>, Diana Rachmawati<sup>1</sup>, Safar Dody<sup>2</sup> and Putut Har Riyadi<sup>3</sup>

<sup>1</sup>Department of Aquaculture, Faculty of Fisheries and Marine Sciences, Diponegoro University, Semarang, Central Java 50275, Indonesia

<sup>2</sup>Research Center for Oceanography, National Research and Innovation Agency, Pademangan, Jakarta 14430, Indonesia

<sup>3</sup>Department of Fisheries Product Technology, Faculty of Fisheries and Marine Sciences, Diponegoro University, Semarang, Central Java 50275, Indonesia

### ABSTRACT

The availability of good feeding on fish performance is needed to improve the poor aquaculture condition. The study examines the effects of *Saccharomyces cerevisiae* supplementation on the growth, survival rate, and blood profile of saline red tilapia in the semi-intensive culture. Sixty saline red tilapia ( $4.58 \pm 0.09$  g) were divided into five groups and received standard feed with supplementation of *S. cerevisiae* at different doses: (A-E) 0, 5, 10, 15, and 20 g/kg feed. *S. cerevisiae* was sprayed onto the feed and given to fish three times/day for 49 days. The efficiency of feed utilization (EFU), feed conversion ratio (FCR), the protein efficiency ratio (PER), relative growth rate (RGR), survival rate (SR), and blood profiles were examined. The water quality parameters were also evaluated, including temperature, pH, dissolved oxygen, NH<sub>3</sub>, and salinity. Data were analyzed using ANOVA followed by the Duncan test. The supplementation of 10 g/kg *S. cerevisiae* could significantly ( $p < 0.05$ ) increase EFU (85.13%), PER (3.76), RGR (4.53%), and survival

rate (97.53%), and decrease FCR (1.42) of the saline red tilapia. All doses of *S. cerevisiae* significantly ( $p < 0.05$ ) increased the number of hematocytes (34.68, 35.96, 34.14, and 34.52%, respectively) and hemoglobin (12.98, 13.58, 12.73, and 12.67%, respectively) of fish. The highest number of erythrocytes and leucocytes was found in dose 10 g/kg feed. All water parameters were stable during the study.

### ARTICLE INFO

#### Article history:

Received: 13 February 2022

Accepted: 20 June 2022

Published: 27 December 2022

DOI: <https://doi.org/10.47836/pjst.31.1.31>

#### E-mail addresses:

istiyanto\_samidjan@yahoo.com (Istiyanto Samidjan)

dianarachmawati1964@gmail.com (Diana Rachmawati)

safa001@brin.go.id (Safar Dody)

putut.riyadi@live.undip.ac.id (Putut Har Riyadi)

\* Corresponding author



Therefore, *S. cerevisiae* can be used as a feed supplement for red tilapia fish to increase the growth, survival rate, and blood profile of the saline red tilapia.

*Keywords:* Immune system, *Saccharomyces cerevisiae*, saline red tilapia, semi-intensive intensive

---

## INTRODUCTION

Saline red tilapia (*Oreochromis* spp.) is a cultivated fish species in Kendal Regency, Central Java Province, Indonesia. The increase in sea level, seawater intrusion, and seawater flooding into the rice field was due to climate change and global warming. Those caused a rise in brackish water areas and need special treatment to support aquaculture. The Kendal Regency has a high potential for aquaculture since the regency has a long shoreline (42.2 km) and a huge area of brackish water ponds (1,002.23 km<sup>2</sup>) (Ayuniar & Hidayat, 2018). In 2018, the total production of Nile tilapia in the Kendal Regency was approximately 142 tons, with a total value of Rp. 2,342,385 (Statistics of Jawa Tengah Province, 2018). However, the saline red tilapia aquaculture in Kendal Regency has yet to develop because of the low growth of the fish and the use of traditional or extensive methods with high production costs. In addition, the use of standard fish feed pellet, which contains 35% protein, 5% fat, 6–8% fiber, 13% ash, and 12% water, has not been efficient yet and has not been able to increase the fish's immune system. One of the alternative solutions to solve this problem is the supplementation of *Saccharomyces cerevisiae* into the feed.

*Saccharomyces cerevisiae* is a yeast or single-celled fungus microorganism widely found on ripe fruits and the bark of oaks. The yeast is round to an oval with 5–10 µm in size. The optimum temperature for *S. cerevisiae* culture condition is 30–35°C. *S. cerevisiae* is one of the most commonly used yeast species in aquaculture to maintain the health of fish species. *S. cerevisiae* has higher amino acid contents, such as methionine and cysteine, which could enhance the immune response in several fish (Agboola et al., 2021). In addition, *Saccharomyces cerevisiae* can increase growth (Rawung & Manoppo, 2014), enzyme activities in the digestive system (Tewary & Patra, 2011), feed and protein digestibility to improve feed efficiency (Manoppo & Kolopita, 2015), protein digestibility, the efficiency of feed utilization and growth (Rachmawati et al., 2019a; Rachmawati et al., 2019b) and disease resistance of the fish (Sheikhzadeh et al., 2012). Moreover, *S. cerevisiae* can produce peptidase, protease, and amylase, and the availability of these enzymes in the fish's digestive system can raise enzyme activities. Therefore, it can boost the breakdown of complex nutrients into a simpler forms of the nutrient. As a result, feed nutrients can easily be absorbed by the fish's digestive system (Sitohang et al., 2012).

The supplementation of *S. cerevisiae* in the feed improved non-specific immune response and growth (Sheikhzadeh et al., 2012). In addition, the supplementation of *S. cerevisiae* in the feed could increase the growth, immune system, and disease resistance

of *Oncorhynchus mykiss*. Rachmawati et al. (2019a) and Rahmawati et al. (2019b) also reported that the *S. cerevisiae*-supplemented feed could increase growths and survival rates of *Pangasius hypothalamus* and *Barbonymus gonionotus*. Abdel-Tawwab et al. (2010), Abu-Elala et al. (2013), and Manoppo and Kolopita (2016) suggested that the *S. cerevisiae*-supplemented feed can boost non-specific immune response and growth of tilapia (*Oreochromis niloticus*).

Meanwhile, the information on the *S. cerevisiae* incorporated feed for saline red tilapia was scarce. The red saline tilapia cultivation in Kendal Regency has yet to be maximally developed because of the high mortality. The availability of good feeding with a great impact on fish performance is needed to improve the poor aquaculture condition in Tilapia fish. The study of the effect of *S. cerevisiae* on the growth performance of saline red tilapia is still needed. Therefore, the present study aims to examine the growth, survival rate, and blood of saline red tilapia (*Oreochromis* spp.) in a semi-intensive culture.

## MATERIALS AND METHODS

### Fish Sample

This study was conducted from January until March 2021. The saline red tilapia with an average weight of  $4.58 \pm 0.09$  g/fish was obtained from the fish farmer association of saline red tilapia in the Village of Pidodo Kulon, Palebon Sub-district, Kendal Regency, Central Java, Indonesia. The fish were selected based on uniformity, defect-free, high activity level, and healthy. Fish were then acclimated in 1 m<sup>3</sup> of 15 floating cages and fed for seven days. The temperature was 26–32°C during the experimental period. The dissolved oxygen, pH, NH<sub>3</sub> concentration, and salinity were 4.46–4.95 mg/l, 7.5–7.53, 0.002%, and 20 ppt, respectively. After acclimation, the fish fasted for one day to rest their digestive organs and detoxification (Rachmawati et al., 2017).

### Feed Preparation with *S. cerevisiae* as Diet Supplement

The standard fish feed (Infiniti, Cargill™) was a commercial pellet purchased from PT. Cargill Indonesia, Pasuruan, East Java, Indonesia. *S. cerevisiae* was purchased from Indrasari Chemical Store, Semarang, Central Java, Indonesia. The standard fish feed was a pellet containing 35% protein, 5% fat, 6–8% fiber, 13% ash, 12% water content, and 272.56 Kcal DE/kg (Rachmawati et al., 2018). The standard feed was supplemented with *S. cerevisiae* in various doses, including 0 g/kg feed (A), 5 g/kg feed (B), 10 g/kg feed (C), 15 g/kg feed (D), and 20 g/kg feed (E). The doses of *S. cerevisiae* were chosen based on Razak et al. (2017). First, *S. cerevisiae* was weighed and thoroughly mixed with 100 ml sterilized water. Then, the mixture was sprayed onto the feed. The dried *S. cerevisiae* incorporated feed was bagged using plastic bags and stored at 4°C (Manoppo & Kolopita,

2015). The proximate method was used based on the Association of Official Analytical Chemists to analyze the nutrient contents in the feed, including protein (%), fat (%), Nitrogen Free Extract (NFE) (%), energy (kcal), and ratio E/P (AOAC, 2019). The results of the proximate analysis are displayed in Table 1.

Table 1  
*The results of the proximate feed analysis*

Parameter	Treatments				
	A	B	C	D	E
Protein (%)	30.00	31.13	32.09	31.53	31.23
Fat (%)	10.76	10.64	10.66	10.53	10.53
Nitrogen Free Extract (NFE) (%)	34.34	34.34	34.40	34.50	34.50
Energy(kcal)	273.15	285.29	286.80	285.89	285.19
Ratio of Energy/protein (E/P)	9.10	9.16	9.21	9.22	9.13

Note. (A). 0 g/kg feed; (B). 5 g/kg feed, (C). 10 g/kg feed, (D). 15 g/kg feed, (E). 20 g/kg feed

### Semi-Intensive Culture

The study was conducted in the fish farmer association of saline red tilapia in Pidodo Kulon, Palebon Sub-district, Kendal Regency, Central Java, Indonesia. The fish was cultivated in 1 m<sup>3</sup> of 15 floating cages. The saline tilapia was used at a density of 60 fish per m<sup>2</sup>, with a total of 900 fish, with each cage filled with 60 red saline tilapia. Fifteen floating cages were assembled on the raft and randomly planted. Before cultivating the fish, the seawater as media culture was channeled into the pond until the salinity reached 20 ppt and 85 cm depth. The growth and water quality observation was conducted every seven days. The fish was fed at a fixed feeding rate of 3%/biomass fish weight/day. In addition, the fish were fed with experimental feed three times per day for 49 days.

### Observed Parameters

The efficiency of feed utilization (EFU), the feed conversion ratio (FCR), the protein efficiency ratio (PER), the relative growth rate (RGR), and the survival rate (SR) were calculated based on Equations 1 to 5:

$$EFU = 100 (\text{final weight} - \text{initial weight}) / (\text{the amount of feed consumed}) \quad (1)$$

$$RGR = 100(W_t - W_0) / (W_0 \times T) \quad (2)$$

Where  $W_0$  and  $W_t$  are the initial and final weight, respectively, and  $T$  is the number of days in the feeding period.

$$FCR = 100 [\text{feed intake (g)} / \text{weight gain (g)}] \quad (3)$$

$$\text{PER} = 100 [\text{weight gain (g)}/\text{protein intake (g)}] \quad (4)$$

$$\text{SR} = 100 (\text{final count}/\text{initial count}) \quad (5)$$

The blood profile of saline red tilapia (hematocyte, hemoglobin, erythrocyte, and leukocytes) was analyzed based on Mohammed et al. (2013).

### Water Quality

The water quality was evaluated based on the previous method by Rachmawati et al. (2019a). The observation of the water quality included physical and chemical characteristics of the water. The water temperature was examined based on the method of HANNA: HI. 8633. pH, dissolved oxygen, ammonia content, and salinity were observed using Jenway 3510, Jenway 970, American Water Works Association, and refractometer (ATAGO S-10, Japan) (APHA, 2017).

### Data Analysis

The study was an experimental method with a completely randomized design with five treatments and three repetitions in each treatment. Data were analyzed using analysis of variance (ANOVA) and then tested using the Duncan test (Steel et al., 1996).  $P < 0.05$  was used as a statistical difference. A polynomial orthogonal test was used to examine the optimum doses of *S. cerevisiae*. Data analysis was performed using Maple v. 12.0. The water quality was descriptively explained.

## RESULTS AND DISCUSSION

The supplementation of *S. cerevisiae* at a dose of 5–20 g/kg feed (group B–E) resulted in higher values of EFU (60.73–85.13%) than in group A (50.27%) (Table 2). The increase in EFU values was due to the supplementation of *S. cerevisiae* which could increase the efficiency of feed utilization of saline red tilapia. The suggested process was as follows: first, *S. cerevisiae* increased digestive enzyme activities. The enzyme activities could break down the complex feed into a simpler form. The simpler nutrients were easier to absorb, and it could increase the efficiency of feed utilization. The addition of bread yeast (*S. cerevisiae*) in the feed could increase the feed digestibility of *Cyprinus carpio* L (Razak et al., 2017). *Saccharomyces cerevisiae* also can be used as a growth promoter and immunomodulator in *Labeo rohita* (Ham.) fish (Tewary & Patra, 2011). Manoppo and Kolopita (2016) also revealed that bread yeast (*S. cerevisiae*) could increase the resistance of Carp (*Cyprinus carpio* L) against *Aeromonas hydrophila*. Therefore, *S. cerevisiae* can improve the feed efficiency and the better growth of the fish.

Table 2

The results of the efficiency of feed utilization (EFU), the feed conversion ratio (FCR), the protein efficiency ratio (PER), the relative growth rate (RGR), the survival rate (SR), of saline red tilapia

Parameters	Treatments				
	A	B	C	D	E
Initial weight (g)	4.58±0.09 <sup>a</sup>	4.35±0.07 <sup>a</sup>	4.43±0.15 <sup>a</sup>	4.52±0.06 <sup>a</sup>	4.48±0.04 <sup>a</sup>
Final weight(g)	40.27±0.17 <sup>c</sup>	62.27±0.24 <sup>c</sup>	88.69±0.15 <sup>a</sup>	73.19±0.15 <sup>b</sup>	55.37±0.12 <sup>d</sup>
EFU (%)	50.27±0.48 <sup>d</sup>	62.67±0.59 <sup>c</sup>	85.13±0.17 <sup>a</sup>	73.49±0.64 <sup>b</sup>	60.73±0.59 <sup>c</sup>
FCR	2.23±0.14 <sup>c</sup>	2.05±0.18 <sup>d</sup>	1.42±0.31 <sup>a</sup>	1.96±0.29 <sup>b</sup>	2.19±0.27 <sup>c</sup>
RGR (%)	2.15±0.36 <sup>d</sup>	2.36±0.21 <sup>c</sup>	4.53±0.29 <sup>a</sup>	3.53±0.46 <sup>b</sup>	2.57±0.38 <sup>c</sup>
PER	2.04±0.46 <sup>c</sup>	2.58±0.28 <sup>b</sup>	3.76±0.23 <sup>a</sup>	2.93±0.24 <sup>b</sup>	2.37±0.13 <sup>b</sup>
SR (%)	68.33±2.64 <sup>d</sup>	78.42±2.75 <sup>c</sup>	97.53±2.29 <sup>a</sup>	82.33±2.35 <sup>b</sup>	73.33±247 <sup>c</sup>

Note. (A). 0 g/kg feed; (B). 5 g/kg feed, (C). 10 g/kg feed, (D). 15 g/kg feed, (E). 20 g/kg feed. EFU: efficiency of feed utilization, FCR: feed conversion ratio, PER: protein efficiency ratio, RGR: relative growth rate, SR: survival rate. Values with the same superscript in the column show insignificant

The highest value of EFU was observed in group C (85.13%), followed by group D (73.49%), B (62.67%), E (60.73%), and A (50.27%) (Table 2). Therefore, the supplementation of *S. cerevisiae* in the feed at 10 g/kg (group C) resulted in the highest value of EFU. Therefore, it was suggested that the dose was the effective amount of *S. cerevisiae* to boost the efficiency of feed utilization. Welker et al. (2007) stated that *S. cerevisiae* could improve enzyme production in the digestive system and then raise digestibility, nutrient absorption, and efficiency of feed utilization. Abdel-Tawwab et al. (2010) revealed that supplementing an *S. cerevisiae*-enriched diet for six weeks could improve feed utilization and increase serum glucose, lipids, and protein of Galilee tilapia (*Sarotherodon galileaus*). Rachmawati et al. (2019a) also demonstrated that the addition of *S. cerevisiae* in the feed affected the specific growth rate (SGR), apparent digestibility coefficient of protein (ADCp), and survival rate (SR) of the *Pangasius hypothalamus*. Figure 1 showed that the relationship between the *S. cerevisiae* supplementation and EFU was in a quadratic pattern with  $Y = -0.2412x^2 + 5.4588x + 48.05$  and  $R^2 = 0.8621$ . Therefore, the optimum dose of *Saccharomyces cerevisiae* supplementation in the feed was 10 g/kg, resulting in the highest value of EFU (85.13%).

The results showed that the *S. cerevisiae* enriched feed significantly ( $P < 0.05$ ) influenced on FCR of saline red tilapia.

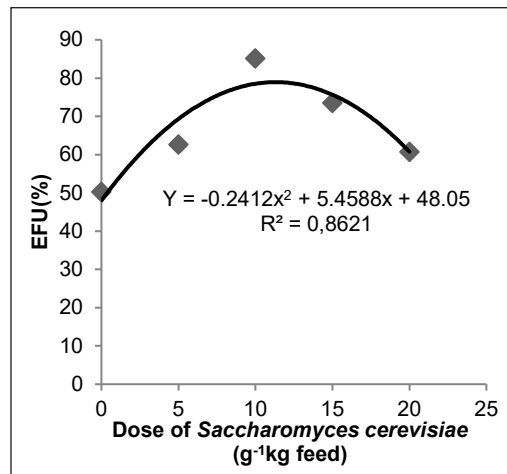


Figure 1. The relationship between the *S. cerevisiae* supplementation in the feed and (efficiency of feed utilization) EFU of saline red tilapia

According to Abu-Elala et al. (2013), *S. cerevisiae* contained mannaoligosaccharidae that could increase the feed conversion ratio in *Oreochromis niloticus*. The extract of *S. cerevisiae* wall is a natural immunostimulant and catalysator for growth (Abu-Elala et al., 2013). Table 2 showed that the lowest value of FCR was found in group C (10 g/kg feed), with a value of 1.42, followed by groups D (1.96), B (2.05), E (2.19), and A (2.23). The low value of FCR in group C (10 g/kg feed) was thought that the dose was the right amount of *S. cerevisiae* to support the optimum efficiency of feed utilization and decreased the value of FCR. The saline red tilapia fed with the dose of 10 g/kg feed (group C) had the highest value of EFU and the lowest value of FCR (Table 1).

Abdel-Tawwab et al. (2010) and Razak et al. (2017) revealed that *S. cerevisiae* enriched feed could increase feed efficiency and decreases feed conversion ratio. Moreover, Tovar et al. (2002) showed that *S. cerevisiae* in the feed caused a decrease in the feed conversion ratio. The low value of FCR and the increase of EFU showed that the fish could effectively and efficiently use the feed to grow. The values of FCR determined the effectiveness of the feed that is inversely proportional to the value of EFU. Goda et al. (2012) revealed that the growth performance and feed utilization efficiency of Nile tilapia (*Oreochromis niloticus*) fingerlings were increased after receiving *S. cerevisiae*. Figure 2 indicates the quadratic relationship between *S. cerevisiae* supplementation and FCR was  $Y = 0.0057x^2 - 0.1171x + 2.2883$  and  $R^2 = 0.6724$ . The optimum dose of *S. cerevisiae* from the equation could be calculated as 10 g/kg feed with an FCR value of 1.42.

The saline red tilapia fed supplemented with *S. cerevisiae* at 5-20 g/kg feed had higher values of PER (2.37–3.76) than 0 g/kg feed (1.96). The supplementation of *S. cerevisiae* in the feed significantly ( $P < 0.05$ ) affected PER. It was indicated that *S. cerevisiae* could boost the digestibility of the protein and the maximum feed utilization influenced the protein efficiency ratio. The highest value of PER (3.76) was obtained in group C (10 g/kg feed), which indicated that the dose was the effective dose of *S. cerevisiae* to increase protein digestibility and efficiency of feed utilization. Abdel-Tawwab et al. (2010) reported that *S. cerevisiae* improved the growth performance and resistance to Copper (Cu) addition by increasing PER and EU (energy utilization). This effect on tilapia growth and feed utilization might be caused by spermine and spermidine produced and released by yeast in the fish digestive tract.

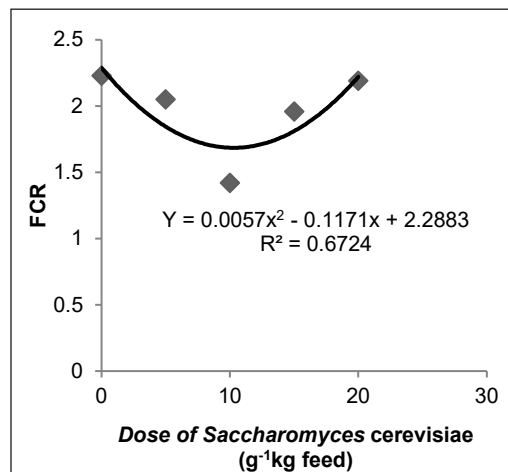


Figure 2. The relationship between the *S. cerevisiae* supplementation in the feed and feed conversion ratio (FCR) of saline red tilapia



This compound could increase the proliferation and regeneration of gut tissue. Moreover, Abu-Elala et al. (2013) stated that *S. cerevisiae* produced protease enzymes to improve the protein efficiency ratio and inhibit the bacterial toxin. Tovar et al. (2002) compared the use of *Debaryomyces hansenii* (yeast from the fish gut) and *S. cerevisiae* to improve fish digestive enzyme activity in sea bass (*Dicentrarchus labrax*) larvae. The supplementation of *S. cerevisiae* X2180 did not trigger gut maturation in sea bass compared with *D. hansenii* because *S. cerevisiae* produces a low polyamine than *D. hansenii* (Tovar et al., 2002).

Figure 3 showed that the relationship between the supplementation of *S. cerevisiae* in the feed and PER was in the quadratic form:  $Y = -0.012x^2 + 0.2608x + 1.9326$ ;  $R^2 = 0.7913$ . The optimum dose of *Saccharomyces cerevisiae* obtained from the equation was 10 g/kg feed with a PER value of 3.76%. The higher dose of *S. cerevisiae* (20 g/kg feed) exhibited a low weight gain, EFU, and a high FCR than other doses of *S. cerevisiae*. Therefore, this dose was not optimal for increasing the weight and decreasing the FCR value.

In our study, the supplementation of *S. cerevisiae* in the feed significantly ( $P < 0.05$ ) affected the RGR value. *S. cerevisiae* increased feed and protein digestibility and the protein efficiency ratio, which supported the growth of the saline red tilapia. Manoppo and Kolopita (2015) claimed that 10 kg of *S. cerevisiae* could improve the growth of Nile Tilapia by increasing weight gain. At the same time, Rajagukguk et al. (2017) revealed that the highest growth of Nile Tilapia was found in fish fed with 20% of yeast. Furthermore, 2% of *S. cerevisiae* supplementation improved growth performances and food efficiency ratio in three-spot cichlid fish (*Cichlasoma trimaculatum*) (Mohammadi et al., 2016).

The saline red tilapia fed with the dose of 10 g/kg feed (group C) had the highest value of RGR (4.53%/day), followed by the group D (3.53%/day), E (2.57%/day), B (2.36%/day) and A (2.15%/day). The 10 g/kg feed (group C) was an effective dose of *S. cerevisiae* to increase digestive enzyme activities; therefore, the feed digestibility and efficiency of feed utilization were optimum to support fish growth. Moreover, the protein content in group C (10 g/kg feed) was higher (32.09%) than in group D (31.53%), E (31.23%), B (31.13%), and A (30%). Thus, the need for protein could be fulfilled for the saline red tilapia growth. Adding *S. cerevisiae* to the feed increased the feeding pattern, improving growth and feed. Huyben et al. (2017) also reported that supplementing *S. cerevisiae*

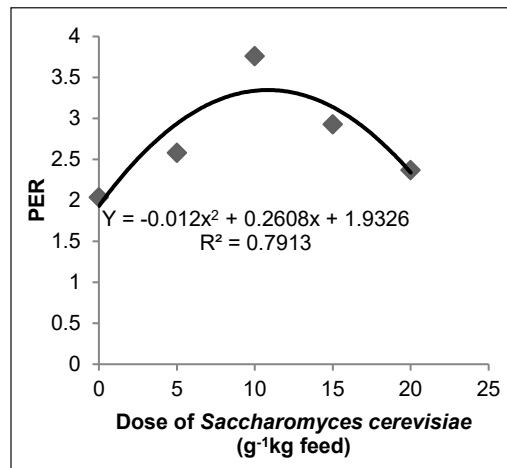


Figure 3. The relationship between the *S. cerevisiae* supplementation in the feed and protein efficiency ratio (PER) of saline red tilapia



and *Wickerhamomyces anomalous* was good for rainbow trout (*Oncorhynchus mykiss*) fish growth because it contains raw protein and amino acids to support fish growth and changed the fish gut microbiota. The study showed that the saline red tilapia fed with the dose of 10 g/kg feed (group C) had the highest values of RGR (4.53%/day), EFU (85.13%), and PER (4.53). Rawung and Manoppo (2014) revealed that the supplementation of 10 g of yeast cells/kg pellet for three weeks exhibited the highest total leukocyte and phagocytosis activity of Nile tilapia. Figure 4 showed that the relationship between the *S. cerevisiae* enriched feed and RGR was quadratic:  $Y = -0.0157x^2 + 0.3551x + 1.8389$ ;  $R^2 = 0.6538$ . From the equation, the optimum dose of *S. cerevisiae* was 10 g/kg feed with the RGR value of 4.53%/day.

The supplementation of *S. cerevisiae* in the feed significantly ( $P < 0.05$ ) affected the survival rate of the saline red tilapia. Table 2 demonstrated that the saline red tilapia fed with *S. cerevisiae* had higher survival rates (78.42–97.53%) than without adding *S. cerevisiae* (68.33%). The saline red tilapia fed with 10 g/kg feed of *Saccharomyces cerevisiae* (group C) had the highest survival rate. It was suggested that group C exhibited the highest resistance to the disease compared to other treatments. *Saccharomyces cerevisiae* contained  $\beta$ -glucan as an immunostimulant that can improve the immune system in the fish; therefore, the fish was disease-prone and had a high survival rate (Manoppo & Kolopita, 2015).  $\beta$ -glucan could increase the phagocytosis of granulocytes, macrophages, and dendritic cells, which plays a role as effector cells against the pathogen (Rodrigues et al., 2020). The relationship between the *S. cerevisiae* supplementation in the feed and SR of saline red tilapia was in the quadratic form:  $Y = -0.2071x^2 + 4.4205x + 66.85$ ;  $R^2 = 0.7959$  (Figure 5). The optimum dose of *Saccharomyces cerevisiae* from the equation was 10 g/kg feed with an SR value of 97.53%.

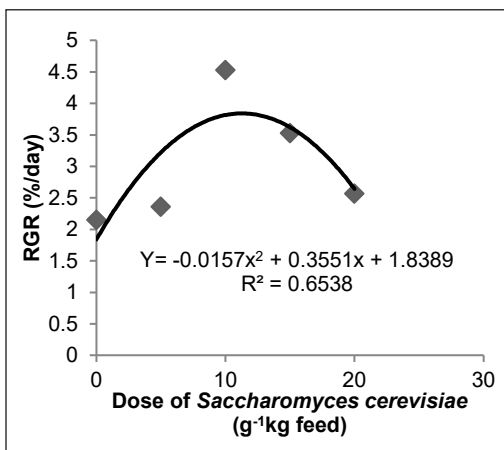


Figure 4. The relationship between the *S. cerevisiae* supplementation in the feed and relative growth rate (RGR) of saline red tilapia

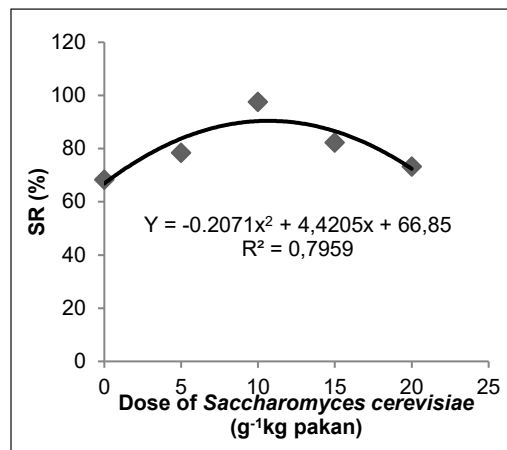


Figure 5. The relationship between the *S. cerevisiae* supplementation in the feed and survival rate (SR) of saline red tilapia

Table 3 indicated that the saline red tilapia fed with the supplementation of *S. cerevisiae* in the feed had higher values of Hematocyte (%), Hemoglobin (G%), Erythrocyte (cell/mm<sup>3</sup>), and Leukocyte (cell/mm<sup>3</sup>) compared to the fish fed without supplementation. Abu-Elala et al. (2013) revealed that the saline red tilapia fed with *S. cerevisiae* incorporated feed for two months could significantly increase the amount of erythrocyte, hemoglobin, and leukocytes in the *O. niloticus* (Abu-Elala et al., 2013). Furthermore, adding *S. cerevisiae* to the catfish feed for one week exhibited high amounts of red and white blood cells compared to feeding without *S. cerevisiae* (Welker et al., 2007). Enhancing leukocytes is important to recognize and eliminate pathogens in fish bodies. The major action of  $\beta$ -glucan contained in yeast could increase the proliferation of leukocytes, including neutrophils, monocytes, natural killer cells, and macrophages. This action is mediated by binding activity between  $\beta$ -glucan with a specific receptor in the membrane of leukocytes (Dectin-1 and CR3), promoting T cell activation and antibody production by B cells. The binding between  $\beta$ -glucan and their receptor also resulted in ROS and NO production, which then enhanced the destruction of pathogenic agents (Rodrigues et al., 2020). Other studies revealed that using prebiotic mannan oligosaccharide (MOS) and *Bacillus subtilis*, isolated or combined (synbiotic), could improve growth performance, body index, intestine morphometry, and carcass composition in Nile tilapia (de Azedevo et al., 2016).

Table 3  
Blood profiles of saline red tilapia after receiving *S. cerevisiae* in their feed

Parameters	Treatments				
	A	B	C	D	E
Hematocyte (%)	29.15 <sup>b</sup>	34.68 <sup>a</sup>	35.96 <sup>a</sup>	34.14 <sup>a</sup>	34.52 <sup>a</sup>
Hemoglobin (%)	12.05 <sup>b</sup>	12.98 <sup>a</sup>	13.58 <sup>a</sup>	12.73 <sup>a</sup>	12.67 <sup>a</sup>
Erythrocyte (cell/mm <sup>3</sup> )	1.95 × 10 <sup>6</sup> <sup>a</sup>	2.95 × 10 <sup>6</sup> <sup>b</sup>	3.25 × 10 <sup>6</sup> <sup>c</sup>	3.05 × 10 <sup>6</sup> <sup>b</sup>	3.07 × 10 <sup>6</sup> <sup>b</sup>
Leukocyte (cell/mm <sup>3</sup> )	87.537 <sup>a</sup>	153.875 <sup>b</sup>	155.012 <sup>d</sup>	154.959 <sup>c</sup>	153.528 <sup>b</sup>

Note. (A). 0 g/kg feed; (B). 5 g/kg feed, (C). 10 g/kg feed, (D). 15 g/kg feed, (E). 20 g/kg feed. Values with the same superscript in the same row show insignificant

Table 4  
Water quality parameters on the saline red tilapia culture

Treatment	Water Quality				
	Temperature (°C)	pH	Dissolve Oxygen (DO) (mg/l)	NH <sub>3</sub> (%)	Salinity (ppt)
A	26 - 32	7.50 - 7.53	4.46 - 4.95	0.002 - 0.002	20
B	27 - 32	7.34 - 7.48	4.27 - 4.76	0.002 - 0.002	20
C	28 - 31	7.36 - 7.50	4.37 - 4.83	0.002 - 0.002	20
D	27 - 32	7.35 - 7.49	4.48 - 4.92	0.002 - 0.002	20
E	27 - 31	7.29 - 7.38	4.35 - 4.87	0.002 - 0.002	20

Note. (A). 0 g/kg feed; (B). 5 g/kg feed, (C). 10 g/kg feed, (D). 15 g/kg feed, (E). 20 g/kg feed

The observation of water quality parameters during the study is demonstrated in Table 4. The results showed that all water quality parameters, including temperature, pH, Dissolve Oxygen (DO), NH<sub>3</sub>, and salinity, were stable for the saline red tilapia culture during the study (Table 4). Therefore, it was indicated that water quality was still viable for the red tilapia in semi-intensive culture.

## CONCLUSION

The results showed that the supplementation of 10 g/kg *S. cerevisiae* in the feed exhibited the highest EFU, PER, and RGR and decreased FCR, which supported the high survival rate of the saline red tilapia. Therefore, *S. cerevisiae* can be used as a feed supplement for red tilapia fish to increase the growth, survival rate, and blood profile of the saline red tilapia. In addition, *S. cerevisiae* has improved feed utilization by reducing the food necessary for animal growth and decreasing production costs.

## ACKNOWLEDGEMENTS

We are grateful for the unconditional support of Mr. Achmad Syifa, the head of the fish farmer association of saline red tilapia in the Village of Pidodo Kulon, Palebon Sub-district, Kendal Regency, Central Java, Indonesia. We are truly thankful and appreciate his efforts. We could have never made it without him.

## REFERENCES

- Abdel-Tawwab, M., Mousa, M. A. A., & Mohammed, M. A. (2010). Use of live baker's yeast, *Saccharomyces cerevisiae*, in practical diet to enhance the growth performance of galilee tilapia, *Sarotherodon galilaeus* (L.), and its resistance to environmental copper toxicity. *Journal of the World Aquaculture Society*, 41(S2), 214-223. <https://doi.org/10.1111/j.1749-7345.2010.00361.x>
- Abu-Elala, N., Marzouk, M., & Moustafa, M. (). Use of different *Saccharomyces cerevisiae* biotic forms as immune-modulator and growth promoter for *Oreochromis niloticus* challenged with some fish pathogens. *International Journal of Veterinary Science and Medicine*, 1(1), 21-29. <https://doi.org/10.1016/j.ijvsm.2013.05.001>
- Agboola, J. O., Overland, M., Skrede, A., & Hansen, J. O. (2021). Yeast as major protein-rich ingredient in aquafeeds: A review of the implications for aquaculture production. *Reviews in Aquaculture*, 13(2), 949-970. <https://doi.org/10.1111/raq.12507>
- AOAC. (2019). *Official methods of analyses* (21st Ed.). Association of Official Analytical Chemists Inc <https://www.aoc.org/official-methods-of-analysis-21st-edition-2019/>
- APHA (2017). *Standard methods for the examination of water and wastewater* (23rd Ed.). American Water Works Association. [https://beta-static.fishersci.com/content/dam/fishersci/en\\_US/documents/programs/scientific/technical-documents/white-papers/apha-water-testing-standard-methods-introduction-white-paper.pdf](https://beta-static.fishersci.com/content/dam/fishersci/en_US/documents/programs/scientific/technical-documents/white-papers/apha-water-testing-standard-methods-introduction-white-paper.pdf)

- Ayuniar, L. N., & Hidayat, J. W. (2018). The profile quality of pond In Kendal Regency to diversification aquaculture. *Proceedings of E3S Web of Conferences*, 31(08025), 1-5. <https://doi.org/10.1051/e3sconf/20183108025>
- de Azevedo, R. V., Filho, J. C. F., Pereira, S. L., Cardoso, L. D., Andrade, D. R., & Júnior, M. V. (2016). Dietary mannan oligosaccharide and *Bacillus subtilis* in diets for Nile tilapia (*Oreochromis niloticus*). *Acta Scientiarum*, 38(4), 347-353. <http://dx.doi.org/10.4025/actascianimsci.v38i4.31360>
- Goda, A. M. A., Mabrouk, H. A. H. H., Wafa, M. A. E., & El-Afifi, T. M. (2012). Effect of using baker's yeast and exogenous digestive enzymes as growth promoters on growth, feed utilization and hematological indices of Nile Tilapia, *Oreochromis niloticus* fingerling. *Journal of Agricultural Science and Technology*, B(2), 15-28.
- Huyben, D., Nyman, A., Vidakovic, A., Passoth, V., Moccia, R., Kiessling, A., Dicksved, J., & Lundh, T. (2017). Effect of dietary inclusion of the yeasts *Saccharomyces cerevisiae* and *Wickerhamomyces anomalus* on gut microbiota of rainbow trout. *Aquaculture*, 473, 528-537. <http://dx.doi.org/10.1016/j.aquaculture.2017.03.024>
- Manoppo, H., & Kolopita, M. E. F. (2015). Pengimbuhan ragi roti dalam pakan meningkatkan respons imun nonspesifik dan pertumbuhan ikan Nila [Supplementation of baker's yeast in feed enhance nonspecific immune response and growth of Nile tilapia]. *Jurnal Veteriner*, 16(2), 204-211.
- Manoppo, H., & Kolopita, M. E. F. (2016). Use of bread yeast (*Saccharomyces cerevisiae*) as immunostimulant to increase resistance of carp (*Cyprinus carpio* L) against *Aeromonas hydrophila* bacterial infection. *Jurnal Budidaya Perairan*, 4(3), 37-47. <https://doi.org/10.35800/bdp.4.3.2016.14945>
- Mohammadi, F., Mousavi, S. M., Zakeri, M., & Ahmadmoradi, E. (2016). Effect of dietary probiotic, *Saccharomyces cerevisiae* on growth performance, survival rate and body biochemical composition of three spot cichlid (*Cichlasoma trimaculatum*). *AACL Bioflux*, 9(3), 451-457.
- Mohammed, H., Olivares-Fuster, O., Lafrentz, S., & Arias, C. R. (2013). New attenuated vaccine against columnaris disease in fish: Choosing the right parental strain is critical for vaccine efficacy. *Vaccine*, 31(45), 5276-80. <https://doi.org/10.1016/j.vaccine.2013.08.052>
- Rachmawati, D., Istiyanto, S., & Elfitasari, T. (2018). Effect of the phytase enzyme addition in the artificial feed on digestibility of feed, feed conversion ratio and growth of gift tilapia saline fish (*Oreochromis niloticus*) nursery stadia I. *IOP Conference Series Earth and Environmental Science*, 116(012009), 1-12. <http://dx.doi.org/10.1088/1755-1315/116/1/012009>
- Rachmawati, D., Istiyanto, S., & Mel, M. (2017). Effect of phytase on growth performance, feed utilization efficiency and nutrient digestibility in fingerlings of *Chanos chanos* (Forsskal 1775). *Philippine Journal of Science*, 146(3), 237-245.
- Rachmawati, D., Istiyanto, S., Ristiawan A. N., & Susilowati, T. (2019a). Effects of *Sacharomyces cereviceae* incorporated diet on growth performance, apparent digestibility coefficient of protein and survival rate of catfish (*Pangasius hypothalamus*). *Aquacultura Indonesiana*, 20(1), 8-14. <http://dx.doi.org/10.21534/ai.v20i1.136>
- Rachmawati, D., Johannes, H., Istiyanto, S., Vivi, E. H., & Windarto, S. (2019b). The effects of *Saccharomyces cerevisiae*-enriched diet on feed usage efficiency, growth performance and survival rate in Java barb (*Barbonymus gonionotus*). *AACL Bioflux*, 12(5), 1841-1849.

- Rajagukguk, B. B., Lumenta, C., & Mokolensang, J. F. (2017). Pemanfaatan ragi (*Saccharomyces cerevisiae*) pada formulasi pakan dalam meningkatkan pertumbuhan ikan Nila (*Oreochromis niloticus*) [Utilization of yeast (*Saccharomyces cerevisiae*) in feed formulations in increasing the growth of tilapia (*Oreochromis niloticus*)]. *Jurnal Budidaya Perairan*, 5(3), 44-49. <https://doi.org/10.35800/bdp.5.3.2017.17887>
- Rawung, M. E., & Manoppo, H. (2014). Penggunaan ragi roti (*Saccharomyces cerevisiae*) secara in situ untuk meningkatkan respon kebal non-spesifik ikan nila (*Oreochromis niloticus*) [In situ use of baker's yeast (*Saccharomyces cerevisiae*) to enhance the non-specific immune response of tilapia (*Oreochromis niloticus*)]. *Jurnal Perikanan and Kelautan*, 2(2), 7-14. <https://doi.org/10.35800/bdp.2.2.2014.4901>
- Razak, A. P., Kreckhoff, R. L., & Watung, J. C. (2017). Administrasi oral imunostimulan ragi roti (*Saccharomyces cerevisiae*) untuk meningkatkan pertumbuhan ikan mas (*Cyprinus carpio* L.) [Oral administration of *Saccharomyces cerevisiae* as immunostimulant to increase growth of carp, *Cyprinus Carpio* L.]. *Jurnal Budidaya Perairan*, 5(2), 27-36. <https://doi.org/10.35800/bdp.5.2.2017.16637>
- Rodrigues, M. V., Zanuzzo, F. S., Koch, J., de Oliveira, C., Sima, P., & Vetricka, V. (2020). Development of fish immunity and the role of  $\beta$ -Glucan in immune responses. *Molecules*, 25(22), Article 5378. <https://doi.org/10.3390/molecules25225378>
- Sheikhzadeh, A. E., Heidrich, M., Pashaki, A. K., Nofouzi, K., Farshabi, M. A., & Akbari, M. (2012). Hilyses®, fermented *Saccharomyces cerevisiae*, enhances the growth performance and skin non-specific immune parameters in rainbow trout (*Oncorhynchus mykiss*). *Fish and Shellfish Immunology*, 32(6), 1083-1087. <https://doi.org/10.1016/j.fsi.2012.03.003>
- Sitohang, R. V., Herawati, T., & Lili, W. (2012). Pengaruh pemberian dedak hasil fermentasi ragi (*Saccharomyces cerevisiae*) terhadap pertumbuhan biomass *Daphnia* sp [The Effect of fermented yeast bran (*Saccharomyces cerevisiae*) on biomass growth of *Daphnia* sp.]. *Jurnal Perikanan and Kelautan*, 3(1), 65-72.
- Statistics of Jawa Tengah Province. (2018). *Production and production value of aquaculture by regency/municipality and main commodity in Jawa Tengah Province, 2018*. <https://jateng.bps.go.id/statistable/2020/07/22/1953/produksi-dan-nilai-produksi-perikanan-budidaya-menurut-kabupaten-kota-dan-komoditas-utama-di-provinsi-jawa-tengah-2018x.html>
- Steel, R. G. D., Torrie, J. H., & Dickey, D. A. (1996). *Principles and procedures of statistics* (3rd Ed.). McGraw Hill International Book Company, Inc.
- Tewary, A., & Patra, B. C. (2011). Oral administration of baker's yeast (*Saccharomyces cerevisiae*) acts as a growth promoter and immunomodulator in *Labeo rohita* (Ham.). *Journal of Aquaculture Research & Development*, 2(1), 1-7. <https://doi.org/10.4172/2155-9546.1000109>
- Tovar, D., Zambonino, J., Cahu, C., Gatesoupe, F. J., Va'zquez-Ju'arez, R., & Le'sel, R. (2002). Effect of live yeast incorporation in compound diet on digestive enzyme activity in sea bass (*Dicentrarchus labrax*) larvae. *Aquaculture*, 204(1-2), 113-123. [https://doi.org/10.1016/S0044-8486\(01\)00650-0](https://doi.org/10.1016/S0044-8486(01)00650-0)
- Welker, T. L., Lim, C., Yildirim-Aksoy, M., Shelby, R., & Klesius, P. H. (2007). Immune response and resistance to stress and Edwardsiella ictaluri challenge in channel catfish, *Ictalurus punctatus*, fed diets containing commercial whole-cell yeast or yeast subcomponents. *Journal of the World Aquaculture Society*, 38(1), 24-35. <https://doi.org/10.1111/j.1749-7345.2006.00070.x>



*Review Article*

## **Chitosan Nanocomposites as Wound Healing Materials: Advances in Processing Techniques and Mechanical Properties**

**Temitope T. Dele-Afolabi<sup>1,2</sup>, Azmah Hanim Mohamed Ariff<sup>1,3\*</sup>, Oluwatosin J. Ojo-Kupoluyi<sup>4</sup> and Ebenezer Oluwatosin Atoyebi<sup>5,6</sup>**

<sup>1</sup>*Department of Mechanical and Manufacturing Engineering, Faculty of Engineering, Universiti Putra Malaysia, UPM, Serdang, Selangor, 43400, Malaysia*

<sup>2</sup>*Department of Mechanical Engineering, Faculty of Engineering, Ajayi Crowther University, Oyo, Nigeria*

<sup>3</sup>*Research Center Advanced Engineering Materials and Composites, (AEMC), Faculty of Engineering, Universiti Putra Malaysia, 43400 Serdang, Selangor, Malaysia*

<sup>4</sup>*Department of Sugar Engineering, Nigeria Sugar Institute, Km.18, Ilorin-Kabba Highway, Ilorin, Nigeria*

<sup>5</sup>*Department of Biomedical Engineering, College of Engineering and Technology, Achievers University, Owo, Nigeria*

<sup>6</sup>*Department of Biomedical Engineering, University of Ibadan, Ibadan, Nigeria*

### **ABSTRACT**

This review discusses the increasing potential of chitosan nanocomposites as viable materials capable of targeting these debilitating factors. This review focuses on various techniques used to process chitosan nanocomposites and their mechanical properties. Chitosan nanocomposites are regarded as highly effective antimicrobials for the treatment of chronic wounds. Chitosan nanocomposites, such as chitosan/polyethylene and oxide/silica/ciprofloxacin, demonstrate efficient antibacterial activity and exhibit no cytotoxicity against Human Foreskin Fibroblast Cell Lines (HFF2). Other studies have also showcased the capacity of chitosan nanocomposites to accelerate and improve tissue

regeneration through increment in the number of fibroblast cells and angiogenesis and reduction of the inflammation phase. The layer-by-layer technique has benefits, ensuring its suitability in preparing chitosan nanocomposites for drug delivery and wound dressing applications. While the co-precipitation route requires a cross-linker to achieve stability during processing, the solution-casting route can produce stable chitosan nanocomposites without a cross-

#### ARTICLE INFO

*Article history:*

Received: 24 March 2022

Accepted: 30 June 2022

Published: 27 December 2022

DOI: <https://doi.org/10.47836/pjst.31.1.32>

*E-mail addresses:*

tt.dele-afolabi@acu.edu.ng (Temitope T. Dele-Afolabi)

azmah@upm.edu.my (Azmah Hanim Mohamed Ariff)

damex052001@yahoo.com (Oluwatosin J. Ojo-Kupoluyi)

eoatoyebi1@gmail.com (Ebenezer Oluwatosin Atoyebi)

\* Corresponding author



linker. By using the solution casting method, fillers such as multi-walled carbon nanotubes (MWCNTs) and halloysite nanotubes (HTs) can be uniformly distributed in the chitosan, leading to improved mechanical properties. The antibacterial effects can be achieved with the introduction of AgNPs or ZnO. With the increasing understanding of the biological mechanisms that control these diseases, there is an influx in the introduction of novel materials into the mainstream wound care market.

*Keywords:* Chitosan nanocomposite, mechanical properties, processing techniques, tissue regeneration, wound healing

---

## INTRODUCTION

Chitosan is a natural co-polymer of the deacetylated derivative of chitin units ( $\beta$ -(1 $\rightarrow$ 4)-linked D-glucosamine) as well as the non-deacetylated units (N-acetyl-D-glucosamine) (Islam et al., 2017; Liu et al., 2018). It is widely studied owing to its multifaceted applications and multitasking ability, besides its significant benefits, including biodegradability, biocompatibility, and non-toxicity (Singh et al., 2013; Islam et al., 2013). Chitin is the second most abundant biopolymer after cellulose, and its application in wound treatment is an incredible breakthrough, which is by virtue of its excellent attributes (Dai et al., 2011). To accelerate the healing process, the wound dressings, which have a crucial part in the wound healing niche, must possess certain important features, such as the ability to prevent bleeding and dehydration of the wound, ensure a suitable moist environment, protect the wound against external contamination, allow gas permeation and fluid exchanges, absorb exudates from the wound area, thermal isolation, biocompatibility, non-toxicity, and a non-allergenic profile (Zhong et al., 2010; Gu et al., 2009). Chitosan nanocomposites with various reinforcements, fabricated through simple and economically viable techniques, are one of the most used wounds dressing materials due to their enhanced and exceptional wound healing capability (Figure 1).

Based on these features, Lu et al. (2012) processed chitosan-polyvinyl alcohol (PVA)/graphene nanofibers using the electrospinning technique and investigated the prospects of these membranes in healing skin wounds in mice and rabbits. They discovered that the wound areas decreased significantly after five days, and a complete recovery was achieved at the end of 10 days. On the other hand, the wound areas were still evident when membranes without graphene were employed. Aguzzi et al. (2014) produced chitosan/montmorillonite nanocomposites loaded with silver sulfadiazine for a similar purpose. Through microstructural analysis, it was revealed that the silver sulfadiazine was successfully loaded into the nanocomposite structure. X-ray diffraction (XRD) analysis detected no free drug in the composite. It shows that intercalated nanocomposites can be produced with uniform drug and/or polymer molecule distribution.

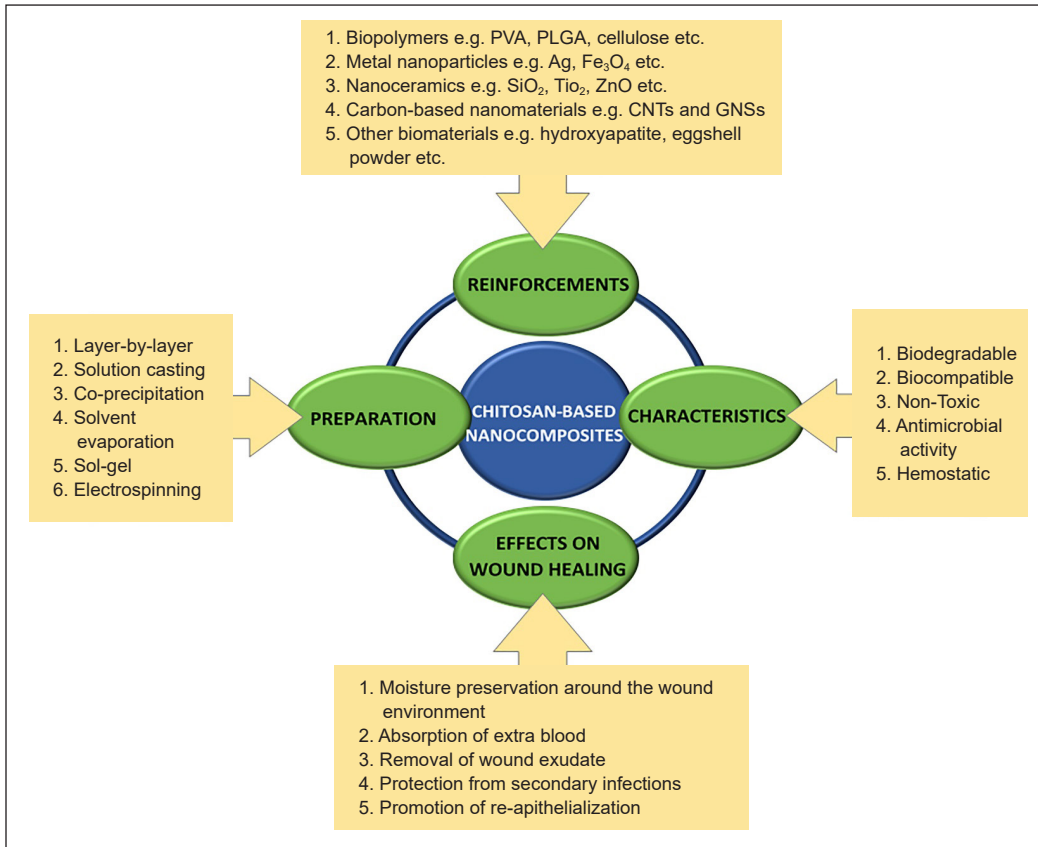


Figure 1. Overview of chitosan nanocomposite

In a similar study, Lu et al. (2017) produced a microporous chitosan-Ag/ZnO composite dressing that demonstrated enhanced antibacterial and wound healing activities. Both the surface and interior of the microporous chitosan-Ag/ZnO dressing possessed interconnected porous structures with a pore size in the range of 50–150  $\mu\text{m}$ . After investigating for several days, the authors further observed that the *in vivo* wound healing ability of the CS-Ag/ZnO-0.5 composite surpassed those of ZnO ointment gauze, CS, and CS-ZnO-0.5 composites. Furthermore, compared to other types of dressing, the application of CS-Ag/ZnO-0.5 composite dressing resulted in smoother-grown skin with small scabs (Figure 2). In addition, an investigation of the antibacterial activity of the CS-Ag/ZnO-0.5 composite dressings on mice wounds was conducted, and only a small number of bacterial colonies were observed, which was owed to the outstanding antibacterial property of silver (Ag) and zinc oxide (ZnO).

Li et al. (2019) investigated collagen/chitosan gel composite enhanced with Oligoarginine (CPP: Cell-Penetrating Peptide). They discovered that the gel composite successfully suppressed *Staphylococcus aureus* growth, reflecting its excellent wound

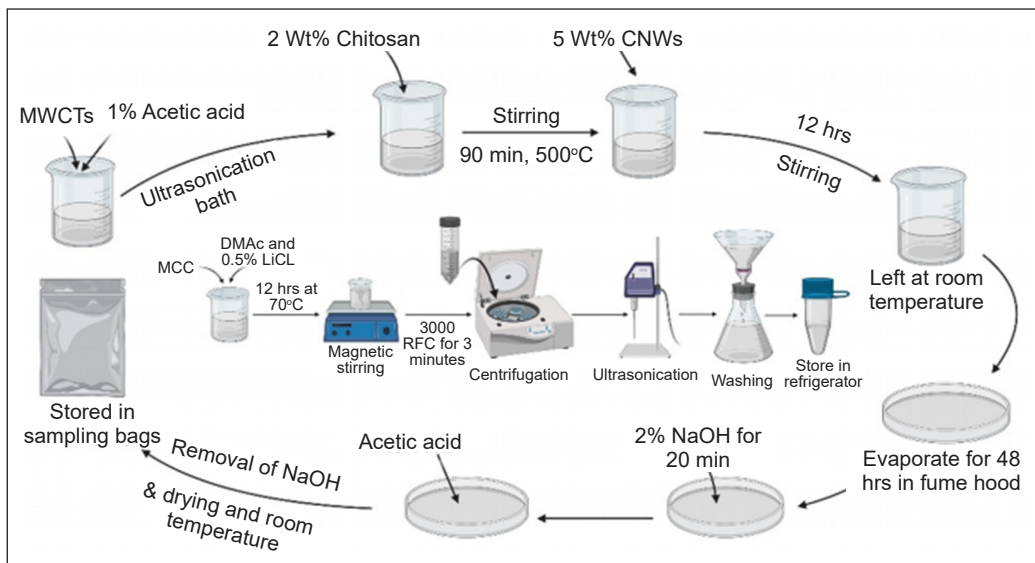


Figure 2. Schematic illustration of preparation of CS/CNWs/MWCNTs nanocomposites (Thou et al., 2021)

healing capability without substantial cytotoxicity. Furthermore, the results of the histopathological analysis revealed that the collagen/chitosan/CPP gel composites had great potential in promoting cutaneous wound healing by enhancing granulation tissue formation, increasing collagen deposition, and promoting angiogenesis in the wound tissue. In another study, chitosan and protein isolate composite hydrogels were developed for controlled carotenoid delivery and wound healing (Hamdi et al., 2020). The authors also developed models to investigate the *vivo* healing ability of the composite hydrogels in rats. It was observed that using the composite hydrogels loaded with carotenoids as topical patches accelerated the wound healing process and ultimately achieved full healing.

In another investigation, it was reported that biocomposite films containing chitosan, polyvinyl alcohol, polyvinyl pyrrolidone, and HMDACS (hexamethylene 1, 6-di(aminocarboxysulfonate)) cross-linker exhibited excellent antibacterial activity against *Escherichia coli* and *Staphylococcus aureus*, making the biocomposite films a promising wound dressing material (Rahmani et al., 2020). In a related study, a composite dressing composed of collagen, chitosan, and alginate (CCA) exhibited no substantial cytotoxicity and remarkably promoted hemocompatibility (Xie et al., 2018). The authors concluded that the CCA composite dressing could prevent seawater immersion and enhance wound healing, in addition to having reliable biosecurity.

Selecting the best route to develop chitosan nanocomposites is crucial to ensure their structural reliability, performance integrity, and resultant properties. Due to their solubility in acidic media, several techniques have been proposed to process stand-alone and reinforced chitosan nanomaterials and enhance their inherent properties. Furthermore,

these materials should have excellent mechanical properties to ensure their sustainability and ability to perform under various working conditions. This review highlights the research progress related to the processing techniques of chitosan nanocomposites and their mechanical properties.

## **PROCESSING ROUTES FOR DEVELOPING CHITOSAN NANOCOMPOSITES**

As the demand for chitosan nanocomposites in various applications continues to increase, researchers have proposed various processing techniques to meet these demands. The selection and suitability of these fabrication techniques depend on the industrial requirement, cost-effectiveness, simplicity, and reproducibility. The commonly used techniques for processing chitosan nanocomposites are comprehensively discussed in the following sub-sections.

### **Layer-By-Layer Method**

The layer-by-layer (LBL) is a simple, cost-effective, and multipurpose technique. In this technique, substrates combine and modify properties of various materials to achieve specific unique functions (Gulaczyk et al., 2003). The materials are deposited layer by layer using substrates that have strong interactions with them, which makes the technique attractive for processing nanocomposites (Podsiadlo et al., 2007). The layers of deposited materials interact via electrostatic interactions, covalent bonding, and bio-specific interactions. Furthermore, using the LBL technique ensures the efficient distribution of particles and interaction between components while reinforcing the chitosan nanocomposite matrix with other materials to achieve the desired structure and function.

Siqueira et al. (2006) assembled metallophthalocyanines with chitosan (Ch) in nanostructured films through an electrostatic LBL route. The procedure comprised the preparation of chitosan and metallophthalocyanine solutions at room temperature and the fabrication of the films. The silicon and Au-coated glass substrates were dipped alternately in the chitosan and metallophthalocyanine solutions and subsequently rinsed and dried under nitrogen (N<sub>2</sub>) gas. The fabricated films possessed high stability with 0.8 and 0.75 reversible redox peaks and could detect low dopamine concentrations. The redox peaks reflected the high anodic and cathodic currents in the bilayer. It was concluded that this technique enables the incorporation of various nanoparticles and metallophthalocyanine molecules into LBL films and the modification of the films. This technique may find applicability in bioanalytical and other fields.

In a similar study by de Mesquita et al. (2010), cellulose nanowhiskers (CNW) and chitosan (CS) composites were assembled on a glass or quartz substrate via the LBL route. It was concluded that the processing route could be extended and used to develop

various biopolymers, which can fabricate novel biobased nanocomposites applicable in biomedical fields such as drug delivery. This conclusion was drawn from observing the homogenous distribution and strong interaction between the cellulose whiskers and chitosan nanocomposites. In addition, the LBL technique ensured that the hydrogen bond and electrostatic interaction between CS and CNW were matched for proper adherence, which is one of the important features of a wound dressing material.

Li et al. (2013) developed chitosan (CS) and cellulose in nanocrystal form (CNs) on an amorphous poly (ethylene terephthalate) substrate (glass slides and silicon wafers) via the LBL technique and analyzed their oxygen-barrier properties. The CS/CNs nanocomposite was revealed to have a low oxygen permeability coefficient and a less superior oxygen barrier property compared to the composites with the LBL and inorganic coatings. Another significant advantage of the LBL technique is the prospect of designing/producing high-performance materials with high precision. It also allows the analysis of the interface between components to understand better the resultant properties of the multilayered thin films (Pinto et al., 2017). For example, the analysis of the morphology and thickness of the interface between fabricated carbon dots and chitosan biopolymer suggested that both parameters can be tailored and reproduced by controlling the biopolymer solution and the number of dips while employing the LBL technique.

Huang et al. (2012c) investigated the effect of the number of deposited bilayers and the composition of coating bilayers on their morphology and antibacterial activities. The bilayers were produced via the LBL technique, in which the negatively charged electrospun cellulose acetate (CA) fibrous mats were combined with positively charged lysozyme (LY)–chitosan–organic rectorite (OREC). It was reported that the various deposition conditions significantly influenced the morphology of the LBL film-coated fibrous mats, especially when the bilayers were doubled to increase deposition thickness. It created big junctions, and the addition of OREC significantly impeded the growth of *Escherichia coli* and *Staphylococcus aureus*. OREC is known to possess high absorption ability. Therefore it can easily absorb onto surfaces and suppress the proliferation of bacteria. The authors concluded that the scope of the LBL approach could be expanded and exploited by developing and analyzing the structure and surface properties of 3D LBL materials, which could be suitable for various applications such as antimicrobial wound dressing and tissue engineering.

In a recent study, Huang et al. (2019) deposited chitosan (CS) and tannic acid (TA) composite on non-fibrous mats to study its antibacterial activity against *Escherichia coli* and *Staphylococcus aureus*. The antibacterial activity of the LBL cellulose-CS/TA mats was observed to increase significantly with the increasing number of coatings. Furthermore, the antibacterial activity against *S. aureus* was reported to be higher due to the higher sensitivity of the bacteria as compared to that of *E. coli*. Conclusively, the LBL technique

was suggested as a prominent and reliable technique to fabricate films for drug delivery application and as wound dressing materials as it does not alter the substrates' size and shape. Furthermore, the LBL route ensures efficient contact and interaction between bacteria and LBL film coating. Apart from the non-flexibility of chitosan polymer, which was regarded as a drawback in the processing of LBL films with clay nanosheets (Liu et al., 2009), the LBL technique can be considered an appropriate method for preparing chitosan nano-multilayer films as it eliminates the disadvantages that include low stability and poor absorption.

### **Solution Casting Method**

Solution casting is a popular technique due to its simplicity and versatility. It has been extensively employed to produce antibacterial chitosan films for biomedical applications. Tripathi et al. (2011) stated that this technique is superior because the film can be formed without a cross-linker. In preparing chitosan-silver oxide nanocomposite film via solution casting, silver-oxide nanoparticles were prepared by adding trisodium citrate into silver nitrate ( $\text{AgNO}_3$ ) to obtain black precipitates before filtering and rinsing. The prepared silver-oxide solution was added to the chitosan solution (1% w/v in 1% acetic acid) and stirred for two hours. The mixed solution was later cast onto glass plates and dried for 48 hours to obtain the desired composite films. The analysis results suggested that the silver oxide nanoparticles in the chitosan matrix improved the antimicrobial activity; hence, it was deemed suitable for wound healing.

In a much more recent and related study that aimed to explain and comprehensively describe the versatility of the solution casting technique, Thou et al. (2021) investigated the influence of functionalized multi-walled carbon nanotubes (f-MWCNTs) and untreated multi-walled carbon nanotubes (Un-MWCNTs) on the structure and properties of chitosan matrix mixed with cellulose nanowhiskers (CS/CNWs) produced via solution casting. The step-by-step processing of CS/CNWs/MWCNTs composite was carried out by adding 0.5% f-MWCNTs and Un-MWCNTs to the acetic acid solution. First, the mixture underwent dispersion treatment for one hour, and then 2 wt.% chitosan powder was added. Next, the mixture was stirred before 5 wt.% CNWs were added, after which a homogenous mixture was formed through continuous stirring. Subsequently, the homogenous mixture was cast on a petri dish and left to dry until a nanocomposite film was formed. The schematic description of the process is presented in Figure 2. The results revealed that f-MWCNTs and un-MWCNTs were adequately dispersed in the CS/CNWs aqueous solution. Nevertheless, the f-MWCNTs-reinforced composite possessed better mechanical properties, which was in line with the findings by Celebi and Kurt (2015).

Darder et al. (2006) stated that one of the important factors to be considered in evaluating the properties of nanocomposites is the dispersion of nanofillers, and a suitable



solution casting technique can result in a good dispersion in the chitosan matrix. To further support this statement, Huang et al. (2012a) introduced sepiolite into chitosan poly (vinyl alcohol) (PVA) nanocomposite via solution casting. The reinforcement with sepiolite was observed to have significantly enhanced the mechanical properties of the nanocomposite due to the intermolecular hydrogen bonds between the sepiolite, PVA, and chitosan. Similarly, Huang et al. (2012b) prepared nanocomposite films by reinforcing chitosan (CS) and poly (vinyl alcohol) (PVA) with halloysite nanotubes (HTs) via solution casting. With the aid of a field emission scanning electron microscope (FESEM) to analyze the morphology of the samples, it was revealed that the processing technique could guarantee better miscibility, which in turn enhances the mechanical properties and water resistance of the nanocomposite film. Another notable benefit of the solution casting technique is that it can produce circular and translucent membranes containing chitosan, as reported by De Silva et al. (2013).

The excellent water vapor and oxygen permeability of biocompatible chitosan and poly (vinyl pyrrolidone)/Nanocellulose (CPN) composite were discovered by Poonguzhali et al. (2017). The composite could maintain a moist environment over the wound bed, which was also expected to prevent further contaminations. Patel et al. (2018) prepared Lupeol-entrapped chitosan-gelatin hydrogel (LCGH) films via solution casting. After the equilibrium water content (EWC) and water vapor transmission rate (WVTR) were determined, the results revealed that the prepared LCGH films were ideal for wound healing with an EWC of 85.40% and WVTR of  $2228 \pm 31.8$ . In addition, the antibacterial activity of the Lupeol was maintained, as assessed via the disc diffusion method. It shows that this processing route has flexibility, and the LCGH film can be a suitable delivery system for the sustained release of Lupeol for enhanced wound healing.

The interaction between the positively charged chitosan molecules and negatively charged microbial cell membranes can disturb the metabolism of bacteria strains. At the same time, the large surface area of the nanocellulose facilitates the adsorption of *Staphylococcus aureus* and *Pseudomonas aeruginosa*. In a more recent study, Rahmani et al. (2020) prepared chitosan (CS), polyvinyl alcohol (PVA), and polyvinyl pyrrolidone (PVP) composite via solution casting. The electrostatic forces between CS and charged microbial cell membrane inhibited the activity of *Escherichia coli* and *Staphylococcus aureus*. The flexibility of the solution casting technique plays an important role in the modification of chitosan nanocomposites in the way that the thickness of the composite films can be controlled by customizing the amount of solution used during processing (Fan et al., 2012). While solution casting is a popular technique to prepare materials suitable for wound healing and food packaging applications, its major shortcoming is the possibility of retaining solvents during processing. Therefore, it is mostly not recommended for tissue engineering applications due to the possibility of toxicity of the produced composite (Boccaccini & Ma, 2014).



## Co-Precipitation Method

Co-precipitation is another method that has been utilized by researchers, with significant achievements in producing reinforced chitosan nanocomposites with desired functionality. Unlike the solution casting technique, the co-precipitation method utilizes a cross-linker to achieve stability during processing. The technique has been recognized as an accomplished and economical means to mass-produce nanomaterials (Chen et al., 2008; Raoufi, 2013). In a study by Yamaguchi et al. (2001), the co-precipitation method was used to prepare chitosan/hydroxyapatite (CS/HAp) composites. In the initial preparation stage, 3 wt.% chitosan aqueous solution was prepared by dissolving chitosan powder in 1 wt % acetic acid and adding 8.5 wt %  $H_3PO_4$  solution. Subsequently, the chitosan/ $H_3PO_4$  solution was mixed with  $Ca(OH)_2$  suspension to obtain a slurry, which was then aged for 24 hours. The procured precipitate was filtered, washed, and compressed into a cylindrical form under a pressure of 20 MPa. Varma et al. (1999) explored several processing routes to develop CS/Hap composite. They stated that the co-precipitation technique's drawbacks included the powder mixtures' dissatisfactory homogeneity and the noticeable inflammation of the samples. Nonetheless, this technique enabled the production of samples with mechanical flexibility and significant homogeneity.

The route was further used by Sreedhar et al. (2007) to develop HAp/Carboxymethyl chitosan (CMCh) nanocomposites to explain the excellent thermal stability of the nanocomposite, which resulted from the strong interaction that existed within the prepared samples. Agglomerate-free  $Fe_3O_4$ -gold-chitosan nanoparticles with improved morphology were highlighted in the study by Salehizadeh et al. (2012). The excellent morphology was achieved using formaldehyde as a cross-linker to ensure stability and improve gelation properties in the nanocomposites. Zhang et al. (2012) produced chitosan-coated magnetite ( $Fe_3O_4/CS$ ) nanocomposites, where the co-precipitation reaction was facilitated by applying a magnetic field. Analysis of the magnetite crystallinity revealed that the magnetic field improved the morphology of the synthesized  $Fe_3O_4/CS$  nanocomposites. The study by Li et al. (2016) further emphasized the benefits of cross-linker in the co-precipitation technique. The results proved the improvement in the properties and conductivity of methanol fuels by adding glutaraldehyde cross-linker into chitosan, reinforced with quaternized poly (vinyl alcohol). The cross-linker significantly reduced the particle size and enhanced deacetylation during processing.

As previously mentioned, the selection of the processing route to develop reinforced nanocomposites is sometimes based on the desired properties of the nanocomposites. Therefore, Türkeş & Açıkel (2020) prepared pure halloysite nanotubes and chitosan nanocomposites (MHNT-CTN) for the adsorption of methylene blue via the co-precipitation technique by developing suitable magnetic properties of MHNT-CTN. In another study, the immersion of chitosan-capped ZnO nanoparticles (NCCZO NPs) after a certain period

exhibited good resistance against tubeworms and barnacle formation due to the hydroxyl and amine functional groups (El-saied & Ibrahim, 2020). Hence it can be summarized that the co-precipitation route utilizes a cross-linker to obtain a better morphology, stability, and a physical cross-linking network of molecular chain arrangements with hydrogen bonding. Additionally, the route is also known to be cost-effective and flexible.

### **Solvent Evaporation Method**

Solvent evaporation is a prominent method used for the preparation of biodegradable nanoparticles. According to Gundloori et al. (2019), the technique involves emulsifying polymer in an aqueous phase and dispersion in a volatile solvent such as chloroform, dichloromethane, or ethyl acetate. The authors further stated that the nanoparticles are produced by evaporating the solvent using a high-temperature vacuum or continuous stirring. One of the benefits of this technique is that the parameters, such as particle size, can be tailored by adjusting the evaporation temperature or rate and the stirring rate. In addition, it is perceived that microspheres morphology can be regulated by applying the solvent evaporation method to achieve a targeted purpose.

The properties of bionanocomposites can sometimes depend largely on the evolution of the interactions between the functional groups of polymers and surface hydroxyl groups. Chrissafis et al. (2008) prepared organic/inorganic hybrids by dispersing fumed silica nanocomposites in poly (vinyl pyrrolidone) (PVP), chitosan, or poly (vinyl alcohol) (PVA) bionanocomposites via solvent evaporation method. This route can prevent the agglomeration of nanoparticles in the prepared bionanocomposites. Denkbas et al. (2004) found that the success rate of the prepared Norfloxacin-loaded chitosan sponges for wound healing purposes was directly proportional to the release rate. It is worth noting that the sponges were able to protect the wound from infections by releasing the loaded antibiotics at predetermined release rates. In the research conducted by El Achaby et al. (2014), it was revealed that the existence of spaces between the sheets and substrates in graphene oxide-reinforced chitosan/polyvinylpyrrolidone polymer improved the strength and toughness of the bionanocomposites, owing to the wrinkled and folded structure of sheets. This modification was accomplished using the solvent evaporation technique, which was chosen to increase the thickness of the graphene oxide sheets.

In a related study, Wu et al. (2011) investigated the interfacial compatibility between multi-walled carbon nanotubes and chitosan nanocomposites (MWCNT/CS) to improve the properties of reinforced chitosan nanocomposites. The authors introduced covalent and ionic linkages into the MWCNT/CS nanocomposites to increase the interaction between the nanocomposites and further initiate chemical interactions to join poly (styrene sulfonic acid) to the surface of the MWCNTs. Due to the nanostructure of chitin nanofillers, which

were used to reinforce chitosan during solvent evaporation, the growth of *A. niger* fungus on the biocomposite films could be impeded (Salaberria et al., 2015). Ifuku et al. (2009) used a similar biocomposite produced through a simple grinding treatment to act as an anti-fungus material. The size and structure of reinforced chitosan biocomposite were modified during processing.

The application of the emulsion solvent evaporation technique has facilitated the fabrication of drug delivery systems with tremendous efficiency. Wang et al. (2017) fabricated biodegradable poly (lactic-co-glycolic acid) (PLGA)-chitosan core-shell nanocomposites as drug carriers. Modifications were done on the nanocomposites by stabilizing the hydrophilic PLGA core with aqueous-phase chitosan to ensure their solubility. This process guaranteed a safe procedure to develop a monodisperse polymer-based drug carrier. To further address the growing interest in a low-cost and effective wound dressing material that has the capability of inhibiting bacterial activities, Santos et al. (2019) developed chitosan and eggshell powder composites with reduced film permeability via solvent evaporation. The authors attributed this significant feature to the presence of remarkable cell viability in the material. To demonstrate the versatility of the solvent evaporation route, Aslam et al. (2021) fabricated copper oxide-reinforced chitosan nanocomposite (CCNC), which was applicable for sensing devices or microelectronics. Analysis results implied a successful fabrication of multifunctional composite films, and the step-by-step procedure is presented in Figure 3. With the solvent evaporation technique, good homogeneous nanocomposites can be produced with improved mechanical properties.

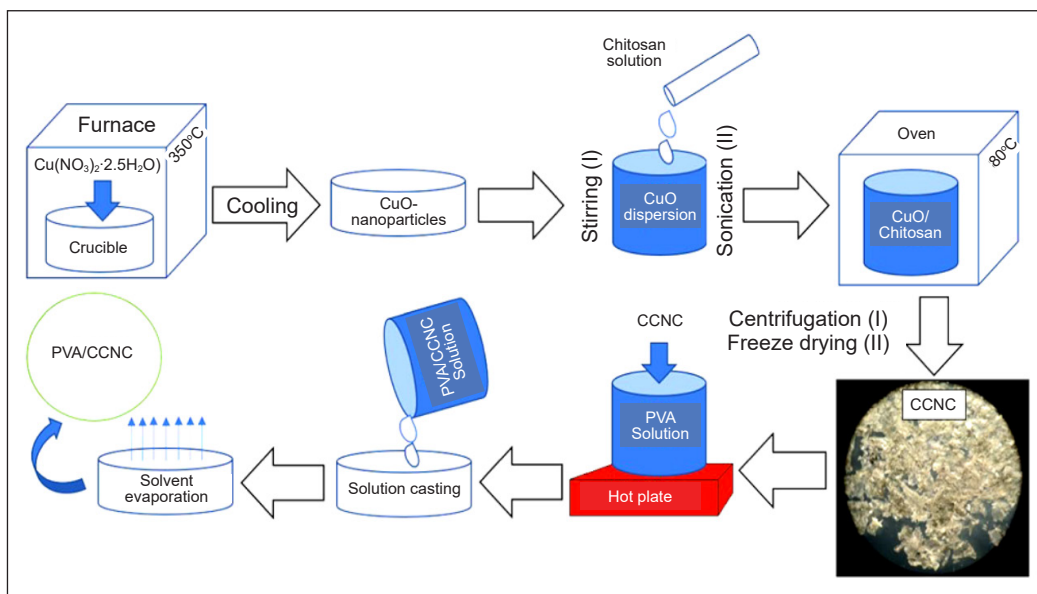


Figure 3. Schematic process of the formation of CuO/chitosan nanocomposites (Aslam et al., 2021)

## Sol-Gel Method

Sol-gel is a versatile wet-chemical technique commonly utilized to process ceramic and glassy materials. The procedure is described as a steady evolution of the solution to form a gel-like network, inside which liquid and solid phases are embedded. Two stages must take place to process nanomaterials, namely hydrolysis of precursor in acidic and basic media and poly-condensation of the hydrolyzed mixture. In other words, the sol-gel technique is an approach to modify the surface of the substrates and has the benefit of producing nanocomposites with large surface areas and stable surfaces (Yilmaz & Soylak, 2020).

During processing, the complete dissolution of chitosan and silica in acid and alkaline solutions must be avoided. Therefore, the prepared hybrids should chelate with Cu(II) and Fe(III) ions to a large degree through the sol-gel technique. This method resolved the solubility of chitosan in a weak acid medium while preparing chitosan/silica (CS/Si) via the sol-gel method. Results from the study also indicated the existence of hydrogen bonding within the molecular chain of chitosan and the dispersion of  $\text{SiO}_2$ , which provide enhanced optical properties to the nanocomposite (Lai et al., 2006). The study by Packirisamy et al. (2019) supported this claim. Furthermore, it was reported that the increase in chelation in ZnO/CS nanocomposite increased the number of dead bacteria and inhibited the growth of *E. Coli*. The schematic diagram of the sol-gel chemical process shown in Figure 4 presents the various ZnO-CS nanocomposites synthesized in the study.

Compared to the blending method, applying the sol-gel method resulted in excellent permeation flux and separation factor in chitosan/titanium oxide composite under similar conditions, owing to the formation of hydrogen and titanoxane bonds within the nanocomposite (Yang et al., 2009). In a related study, to emphasize further the importance of the high surface area in nanocomposites fabricated via the sol-gel technique, Kavitha et al. (2013) reported that a surface area around (114-265  $\text{m}^2/\text{g}$ ) and high purity in titania-chitosan nanocomposite significantly controlled swelling and degradation rate which in turn improved cell growth during implantation and tissue engineering.

In a study by Budnyak et al. (2015), a chitosan-silica composite was synthesized. The composite possessed an excellent morphology due to the high number of available adsorption sites and large surface area, significantly

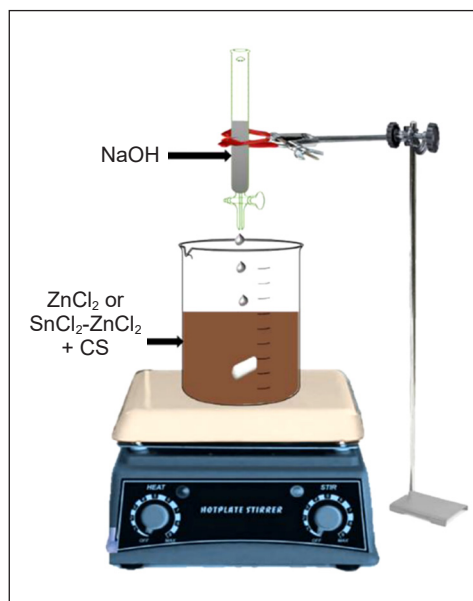


Figure 4. Sol-gel chemical reaction (Packirisamy et al., 2019)

increasing the oxoanions adsorption capacity. It demonstrates the benefit of the sol-gel technique. Furthermore, the sol-gel method could easily be expanded to incorporate organic functionality and hybrid inorganic-organic sol-gels due to its bi-network forming process and the ability to synthesize composite at low temperatures (Budnyak et al., 2016). An excellent homogeneity and cross-link between CS/PEG/E102 and the calcium silicate matrix gave rise to good antibacterial properties of the nanocomposites (Youssef et al., 2017). Owing to a high reaction rate, good biocompatibility, and surface morphology, the prepared chitosan-cl-poly (AA)/ZrPO<sub>4</sub> composite exhibited excellent antibacterial activity against *Pseudomonas aeruginosa*, *Escherichia coli*, and *Staphylococcus aureus* (Sharma et al., 2020). Saravanan et al. (2018) employed the sol-gel coupled with precipitation method to study the crystallinity and bandgap of TiO<sub>2</sub>/CS nanocomposite. The analysis performed on the nanocomposite revealed that it possessed good crystallinity and low bandgap, which makes it applicable as an environmental catalyst for textile effluents.

As the sol-gel technique enables the simultaneous synthesis of two or more nanoparticles of different sizes, Rezvani et al. (2018) fabricated Fe<sub>3</sub>O<sub>4</sub>/CS nanocomposites at low temperatures. Improved oil recovery was achieved by virtue of the stable nanocomposites in the suspensions and modified interfacial properties. In another study, a chitosan-doped hybrid/nano-TiO<sub>2</sub> sol-gel coated surface displayed a uniform nanoparticle homogeneity, which resulted in the formation of adherent, crack-free corrosion-resistant coating for aluminum metals (Balaji & Sethuraman, 2017). Hammad et al. (2019) stated that the formation and growth of calcium aluminosilicate (CAS) particles in the chitosan (CS) matrix is a significant factor that increases structural strength in CS/CAS composite doped with aluminum oxide, which can be efficiently utilized as CO<sub>2</sub> gas capturing material at moderate temperatures.

In conclusion, the sol-gel technique is labeled as eco-friendly. Furthermore, it possesses exceptional advantages over other methods as the composition of the nanomaterials can be controlled to achieve excellent homogeneity at the molecular level, and the composite can be produced at low processing temperatures. Table 1 summarizes various processing routes' main highlights and significance in preparing reinforced chitosan nanocomposites and their antibacterial activities.

### **Electrospinning Method**

In recent years, the electrospinning technique has been widely utilized in producing nanofibers. It is a technique that involves the application of electrical voltage to a polymer solution. As a result, the physical and chemical properties of the nanofibers can be modified at the nanoscale level; thus, stronger, more durable, and more elastic fibers can be produced (Schiffman & Schauer, 2008; Meng et al., 2010). The production of nanofibers via the electrospinning process relies on the aggregation of fine fibers from polymer solutions

Table 1  
Significance of different processing routes on the morphology and antibacterial activity of chitosan nanocomposites

Composite	Processing route	Key observations	Bacteria specimens	Ref.
Films of chitosan with tetrasulfonated metallophthalocyanines containing (NiTsPc), (CuTsPc) and (FeTsPc)	Electrostatic layer-by-layer (LBL)	<ul style="list-style-type: none"> <li>The prepared chitosan films were found to be highly stable and suitable for detecting dopamine concentration</li> <li>Applicable in bioanalytical fields</li> <li>Homogeneity in particle distribution and strong interaction between nanocomposites</li> <li>The processing route is suggested to be applicable in food packaging and biomedical fields</li> </ul>	—	Siqueira et al. (2006)
Cellulose nanowhiskers and Chitosan	LBL	<ul style="list-style-type: none"> <li>The use of various deposition conditions influenced the morphology</li> <li>Improvement in the degree of antibacterial activity</li> </ul>	—	de Mesquita et al. (2010)
Cellulose acetate + lysozyme-chitosan-organic rectorite + sodium alginate	LBL	<ul style="list-style-type: none"> <li>An increase in the number of coatings significantly increased antibacterial activity</li> <li>High antibacterial activity in <i>S. aureus</i> due to its sensitivity</li> </ul>	<i>Escherichia coli</i> and <i>Staphylococcus aureus</i>	Huang et al. (2012c)
Chitosan and tannic deposited on non-fibrous mats	LBL	<ul style="list-style-type: none"> <li>The processing route can achieve film formation without a cross-linker</li> <li>The amino group of chitosan interacted with negatively charged microbial cell membranes leading to leakage in proteinaceous and other intracellular constituents of the microorganisms</li> <li>Bacteria activity was impeded due to the synergistic of AgNO<sub>3</sub> and chitosan</li> <li>Good dispersion in chitosan matrix and sepiolite</li> <li>Improved intermolecular hydrogen bonds between chitosan (PVA) and sepiolite</li> </ul>	<i>Escherichia coli</i> and <i>Staphylococcus aureus</i>	Huang et al. (2019)
Chitosan + silver oxide nanocomposite	Solution casting		<i>Bacillus subtilis</i>	Tripathi et al. (2011)
Chitosan poly(vinyl alcohol) (PVA) nanocomposite and sepiolite	Solution casting		—	Huang et al. (2012a)



Table 1 (continue)

Composite	Processing route	Key observations	Bacteria specimens	Ref.
Chitosan and poly(vinyl pyrrolidone)/nanocellulose (CPN)	Solution casting	<ul style="list-style-type: none"> <li>Excellent water vapor and oxygen permeability of CPN maintained a moist environment over the wound bed</li> <li>The high surface area of nanocellulose aided the adsorption of bacteria microorganisms</li> </ul>	<i>Staphylococcus aureus</i> and <i>Pseudomonas aeruginosa</i>	Poonguzhali et al. (2017)
Chitosan + PVA + PVP	Solution casting	<ul style="list-style-type: none"> <li>Strong electrostatic forces between chitosan and charged microbial cell membrane inhibited bacteria activity</li> </ul>	<i>Escherichia coli</i> and <i>Staphylococcus aureus</i>	Rahmani et al. (2020)
Chitosan + hydroxyapatite (HAp)	Co-precipitation	<ul style="list-style-type: none"> <li>Mechanical flexibility and significant homogeneity</li> </ul>	—	Yamaguchi et al. (2001)
Fe <sub>3</sub> O <sub>4</sub> -gold-chitosan	Co-precipitation	<ul style="list-style-type: none"> <li>Better morphology and agglomerate-free nanoparticles due to the use of formaldehyde as cross-linker</li> </ul>	—	Salehizadeh et al. (2012)
Chitosan + quarternized poly(vinyl alcohol)	Co-precipitation	<ul style="list-style-type: none"> <li>Enhanced properties, including conductivity of methanol fuels due to the addition of glutaraldehyde</li> <li>Enhanced deacetylation</li> </ul>	—	Li et al. (2016)
Halloysite nanotubes + chitosan nanocomposites (MHNT-CTN)	Co-precipitation	<ul style="list-style-type: none"> <li>Suitable magnetic properties of (MHNT-CTN)</li> </ul>	—	Türkeş et al. (2020)
Chitosan nanocomposites + ZnO nanoparticles	Co-precipitation	<ul style="list-style-type: none"> <li>The presence of hydroxyl and amine functional groups of (MHNT-CTN) resulted in good resistance to bacteria formation</li> </ul>	<i>Tubeworms</i> and <i>barnacles</i>	El-saied et al. (2020)
Multi-walled carbon nanotubes + chitosan nanocomposites (MWCNT/CS)	Solvent evaporation	<ul style="list-style-type: none"> <li>The solvent evaporation route demonstrated a good interaction between nanoparticles which initiated chemical reactions to improve properties</li> </ul>	—	Wu et al. (2011)
Chitin nanofillers + chitosan (CS/CHNC) and (CS/CHNF)	Solvent evaporation	<ul style="list-style-type: none"> <li>The size and shape of chitin nanofillers influenced the inhibition of the activity of the bionanocomposite</li> </ul>	A. Niger	Salaberria et al. (2015)



Table 1 (continue)

Composite	Processing route	Key observations	Bacteria specimens	Ref.
Poly(lactic-co-glycolic acid) (PLGA) - chitosan	Solvent evaporation	<ul style="list-style-type: none"> <li>The solubility of PLGA caused by the aqueous-phase chitosan ensured a safe procedure to develop a monodisperse polymer-based drug carrier</li> </ul>		Wang et al. (2017)
Chitosan + eggshell powder	Solvent evaporation	<ul style="list-style-type: none"> <li>Reduction in the permeability of the films of chitosan and eggshell powder</li> <li>The presence of remarkable cellular viability impeded bacteria activities</li> </ul>		Santos et al. (2019)
Chitosan + silica	Sol-gel	<ul style="list-style-type: none"> <li>Due to excellent hydrogen bonding within the molecular chain of CS and the dispersion of SiO<sub>2</sub>, an enhanced optical property of the nanocomposite was achieved</li> </ul>		Lai et al. (2006)
ZnO + CS	Sol gel	<ul style="list-style-type: none"> <li>Increased chelation of ZnO/CS resulted in the death of bacteria cells and inhibited the growth of <i>Escherichia coli</i></li> </ul>	<i>Escherichia coli</i>	Packirisamy et al. (2019)
Titania + chitosan	Sol gel	<ul style="list-style-type: none"> <li>High surface area and purity controlled swelling and degradation rate, which improved cell growth during implantation</li> </ul>	—	Kavitha et al. (2013)
Chitosan polyethylene glycol (PEG) + calcium silicate + modifier (zinc oxide nanoparticles and tartrazine dye)	Sol-gel	<ul style="list-style-type: none"> <li>Significant homogeneity and cross-linking yielded good antibacterial activities</li> <li>Application in optical and biomedical fields</li> <li>ZnO-NPs are embedded into microbes to interact and bond to the cellular enzyme microbes to inhibit the growth of microbes</li> </ul>	<i>Staphylococcus aureus</i> , <i>Pseudomonas aeruginosa</i> (bacteria), <i>Candida albicans</i> , and <i>Aspergillus niger</i> (fungi)	Youssef et al. (2017)
Chitosan-cl-poly (AA)/ZrPO <sub>4</sub>	Sol gel	<ul style="list-style-type: none"> <li>The sol-gel route demonstrated a high reaction rate, and good surface morphology resulted in antibacterial activity</li> </ul>	<i>Pseudomonas aeruginosa</i> , <i>Escherichia coli</i> , <i>Staphylococcus aureus</i> and <i>Vibrio fischeri</i>	Sharma et al. (2020)

Table 1 (continue)

Composite	Processing route	Key observations	Bacteria specimens	Ref.
Chitosan+affinin+AgNP	Electrospinning	<ul style="list-style-type: none"> <li>• Composite nanofibers showed no defects and exhibited homogeneously dispersed orientation</li> <li>• The greater surface area of the nanofiber mats offered significant improvement to the antibacterial activity of the composites</li> </ul>	<i>E. coli</i> <i>P. aeruginosa</i>	Bedolla-Cazares et al. (2016)
Chitosan+PVA+AgNP	Electrospinning	<ul style="list-style-type: none"> <li>• The fibers exhibited optimum mechanical properties and bactericidal activity</li> </ul>		Wang et al. (2018)
Chitosan+Ultra-high molecular weight polyethylene oxide	Electrospinning	<ul style="list-style-type: none"> <li>• Improved benefits in terms of antibacterial and osseo-conductive properties.</li> <li>• Lesser swelling upon immersion in water.</li> </ul>		Qasim et al.(2018)
Chitosan+PVA	Electrospinning	<ul style="list-style-type: none"> <li>• Improved antibacterial activity against <i>S. aureus</i> and <i>P. aeruginosa</i></li> </ul>	<i>S. aureus</i> <i>P. aeruginosa</i>	Abbaspour et al. (2015)
Chitosan+Polyethylene oxide+AgNP	Electrospinning	<ul style="list-style-type: none"> <li>• Improved antibacterial activity against <i>E. coli</i> and <i>S. aureus</i></li> </ul>	<i>E. coli</i> <i>S. aureus</i>	Wang et al. (2015)

through electrostatic forces. The critical components of an electrospinning setup are (i) a high-voltage power supply, (ii) a spinneret and a grounded collecting plate, and (iii) a plate or rotating mandrel (Figure 5) (Zafar et al., 2016).

The electrospinning process of chitosan/ultra-high molecular weight polyethylene oxide (CH-UHMWPEO) solutions was reported by Qasim et al. (2018). The major advantages of the produced fibers were the high chitosan and low PEO contents, which led to lesser swelling upon immersion in water. In addition, increasing the CH content improved the antibacterial and osseo-conductive properties. A great deal of research was carried out to enhance the stability, regenerative property, and antimicrobial property against *Staphylococcus aureus* and *Escherichia coli* of electrospun CH-PEO fibers combined with poly(hexamethylene biguanide) hydrochloride (PHMB) or silver nitrate nanoparticles (Dilamian et al., 2013; Penchev et al., 2010). These fiber-based scaffolds exhibited promising potential as wound dressings to prevent infections and accelerate healing.

In another study, nano-silver particles added to electrospun CH/PEO fibers demonstrated antibacterial activity against *S. aureus* and *E. coli*, which are the dominant organisms that cause wound infections (Wang et al., 2015). Similarly, electrospun chitosan/polyvinyl alcohol (CH-PVA) fibers incorporated with mafenide acetate exhibited antibacterial activity against *S. aureus* and *P. aeruginosa* (Abbaspour et al., 2015). Elsewhere, fibers with silver nanoparticles were produced through the in-situ reduction of  $AgNO_3$  into a chitosan-polyvinyl alcohol mixture (CS/PVA: 1/10, w/w), which was dissolved in lactic acid (Wang et al., 2018). It was observed in the study that the optimum mechanical properties and bactericidal activity were exhibited by the fibers with the least content of nanoparticles, which complied with the high surface-to-volume ratio resulting from their low dimension.

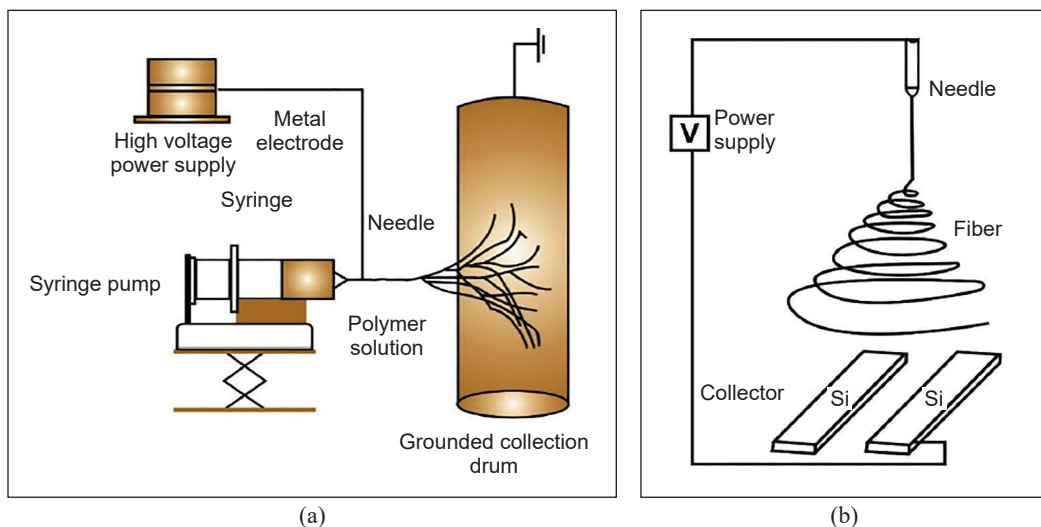


Figure 5. (a) Electrospinning equipment plate or rotating mandrel, and (b) aligned collection plates for electrospun nanofibers (Zafar et al., 2016)

In a study by Dobrovolskaya et al. (2018), composite nanofibers based on chitosan and chitin nanofibrils were prepared. The fibers were spun from an aqueous solution containing chitin nanofibrils and underwent ultrasound treatment for 40 minutes. The nanoparticle concentrations were in the range of 1 to 30 wt% with respect to chitosan. The electrospinning of the fibers was performed by employing the NANON-01A setup. The solution was fed into the setup by an injection pump via a spinneret electrode operating in an electric field at a voltage of 18 kV. A distance of 0.2 m was set between the spinneret electrode and the collector electrode, where the fibers were deposited. The effectiveness of the electrospinning technique in producing chitosan nanocomposites with silver nanoparticles from the  $\text{AgNO}_3$ -affinin complex was studied by Bedolla-Cazares et al. (2017) (Figure 6). The chitosan/AgNP composite solution, prepared via chemical reduction, was dried at  $74^\circ\text{C}$  for eight hours to evaporate the solvent. The resulting films were re-dissolved in a TFA- $\text{CH}_2\text{Cl}_2$  mixture to produce 12 wt% solutions, which were later processed in a NaBond® electrospinning unit to produce nanofiber mats.

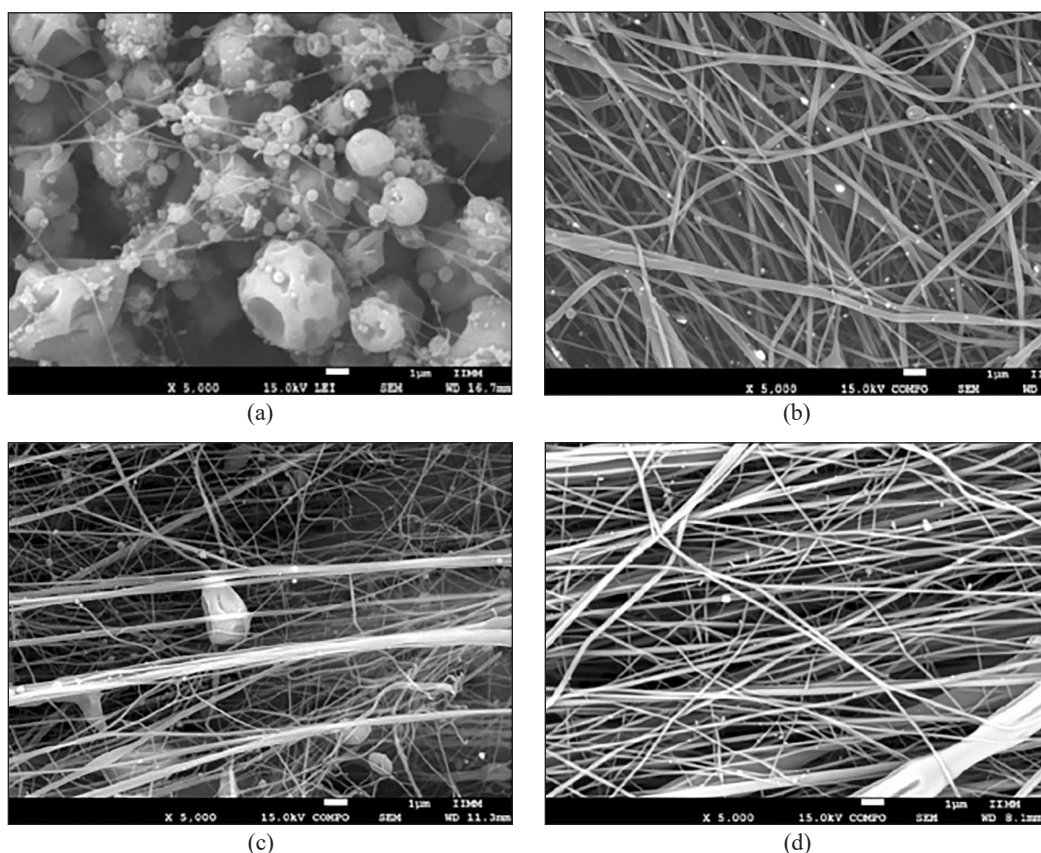


Figure 6. Electrospun nanofibers from (a) Chitosan/affinin, (b) Chitosan/ $\text{AgNO}_3$  (after reduction), (c) Chitosan/affinin +  $\text{AgNO}_3$  added independently (after reduction), (d) Chitosan/ $[\text{Ag}_2\text{-(affinin)}](\text{NO}_3)_2$  complex (after reduction) (Bedolla-Cazares et al., 2017)

In work by Haider and Park (2009), as-spun nanofibers were neutralized using potassium carbonate to prevent fibrous structure loss when the fibers come into contact with neutral or weak basic aqueous solutions (Haider & Park, 2009). As seen in Figure 6(c), the introduction of  $\text{AgNO}_3$  into the chitosan/affinin mixture promoted the production of nanofibers. Nevertheless, large agglomerates were still evident. This drawback was overcome when the affinin was complexed with  $\text{AgNO}_3$ . Figure 6(d) shows that the CTS/affinin/ $\text{AgNP}$  composite nanofibers were successfully formed without defects and with a more homogeneously dispersed orientation. The antibacterial activity test results show that *E. coli* and *P. aeruginosa* exhibited limited activity in the inhibition zones of the thin composite films produced with affinin and  $\text{AgNP}$ . Due to the greater surface area of the nanofiber mats, the antibacterial activity of pure chitosan and composite combinations was significantly enhanced.

## MECHANICAL PROPERTIES OF CHITOSAN NANOCOMPOSITES

Chitosan is a polysaccharide obtained from the exoskeletons of arthropods, crustaceans, insect cuticles, plants, and the cell wall of fungi. On the one hand, the natural origin of chitosan endows it with good hemostatic, antibacterial, and non-toxic properties, in addition to biocompatibility, biodegradability, and bio-inertness. These properties make it suitable for composite materials in wound healing and other biological applications which involve direct contact with physiological fluids. On the other hand, poor mechanical properties of unreinforced chitosan constitute a major setback, especially in structural and load-bearing applications such as tissue engineering. It is because of the destruction of the chitin multiscale fibrillar structure during its conversion to chitosan, which affects further processing and exploitation. Chitosan is often combined with other materials to form bio-based blends with improved properties to overcome this setback. Thereby, their advantageous innate properties could still be exploited. This section highlights the mechanical properties of various chitosan blends.

### Tensile Properties

Generally, pure chitosan film has low tensile strength due to its low crystallinity (Li et al., 2021). Therefore, combining chitosan with other materials, such as polylactic acid (PLA), is often beneficial. For example, Elsayy et al. (2016) studied the mechanical properties of PLA nanocomposites prepared by reinforcing PLA with chitosan nanoparticles (CSNP) at a proportion between 0 and 5%. The presence of chitosan nanoparticles in the nanocomposites produced progressive improvement in tensile strength. It was also reported that reinforcing PLA with chitosan nanoparticles altered the tensile strength at the breaking point, which increased progressively with an increase in the proportion of the reinforcement. Based

on these findings, it is possible to further improve the tensile strength of pure PLA by increasing the proportion of chitosan.

In related research, Boonkong et al. (2013) investigated the suitability of deacetylated chitosan blended with various proportions of polylactic acid (PLA) and polycaprolactone (PCL) as wound dressings. As Khan et al. (2000) established, good wound dressing devices must be flexible yet stiff enough to withstand blood pressure from wounds. The chitosan-PLA-PCL blends possessed these features. PLA enhanced the strength, while PCL increased the flexibility and elasticity of the biocomposite. The mechanical properties of the blend, namely tensile strength, young's modulus, and percentage elongation, were studied using Universal Testing Machine (UTM) according to the ASTM D 882 standard. The temperature and humidity were 25°C and 50%, respectively, whereas the crosshead speed and load cell were set at 12.5 mm/min and 5.0kN, respectively. The study revealed that 60 wt% chitosan, 28 wt% PLA, and 12 wt% PC produced a blend with improved tensile and adhesive strengths and superior swelling and water vapor transmission rate. It was assumed that the improved mechanical properties could enhance the surface interaction between the film and wound tissues to promote a faster healing process, especially when the film was loaded with drugs for controlled delivery. This assumption was confirmed by performing a blood clotting test on the blend (60% chitosan, 28% PLA, and 12% PCL) loaded with doxycycline (0.03 g) and monosodium glutamate MSG (0.1 g). The test results revealed an outstanding blood clotting capability of the biocomposite. Moreover, the *in vitro* study of this film blend showed that it could prevent hemolysis and bacterial infection.

Aside from synthetic materials such as PLA, blending chitosan with other materials of natural origin, which possess properties that can improve the mechanical properties of the blend, such as tensile and compressive strength, can be beneficial. One such material is natural silk, which possesses high crystallinity and good mechanical properties. However, it is also regarded as one of the toughest natural materials (Li et al., 2021; Zhang et al., 2015). The complex hierarchical structure of silk, which includes high molecular weight,  $\beta$ -sheet crystal, and fibrillar structures, is the underlying reason for its excellent mechanical properties, making it a good reinforcement candidate for chitosan (Keten et al., 2010; Vollrath & Knight, 2001).

In a study by Li et al. (2021), silk nanofibrils solution (SNF), which was obtained from silkworms, was combined with chitosan (CS) solution based on the weight percentage to obtain various blends of SNF-CS biocomposites, which mechanical properties were tested. The study revealed that reinforcing chitosan films with 25 to 75 wt% SNF significantly improved their tensile strength from 29.3 to 40.1 MPa (Figure 7). Nevertheless, a decrease in the compressive strength of the composite films was observed when the weight percentage of SNF was further increased. It suggests that a high proportion of nanofiber in the nanocomposite may weaken the interfacial binding force, leading to a reduction in the



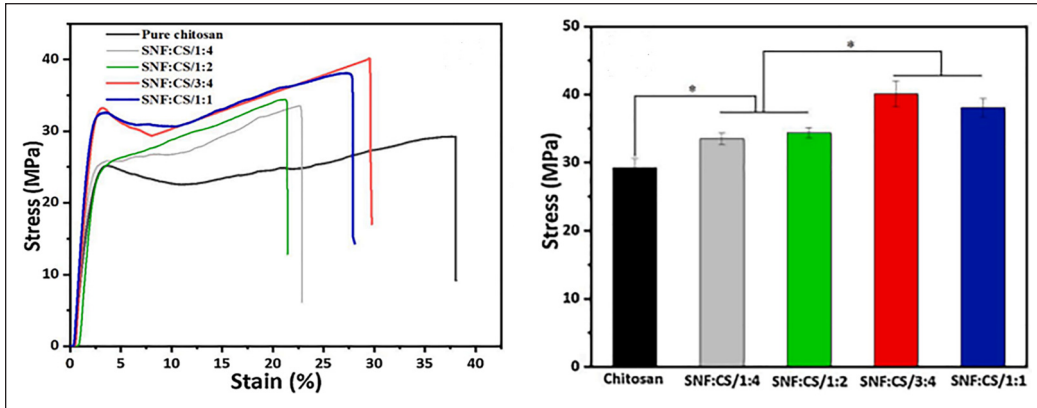


Figure 7. Stress-strain curve of Silk nanofibril-Chitosan nanocomposite (Li et al., 2021)

mechanical properties of the matrix phase, which in turn inhibits further improvement in the tensile properties. In addition, a decrease in elongation at fracture was observed after the SNF loading was increased. It indicates that decreasing the SNF loading increases the brittleness of the chitosan nanocomposites.

Like other bio-based materials, chitosan processing methods could influence its mechanical properties and wound healing capabilities. It was confirmed in a study in which chitosan films were prepared by dissolving them in two solvents: lactic acid (LA) and acetic acid (AA). The mechanical properties of Chitosan-AA and Chitosan-LA biofilms were compared with those of a commercial Omiderm film. Both films exhibited superior mechanical and bioadhesive properties as compared to Omiderm film. More importantly, compared to Chitosan-AA film, Chitosan-LA film possessed lower tensile strength with longer elongation at fracture, which endowed it with better flexibility, remarkable softness, and superior pliable properties. As a result, Chitosan-LA was more bioadhesive and hence, more applicable to wound healing and skin burn management than Omiderm and Chitosan-AA films. In addition, due to its flexibility, Chitosan-LA film had good permeability to water vapor, was non-irritant, and did not induce any adverse reaction on the skin. These are the expected characteristics of a typical wound management construct (Khan et al., 2000).

### Compressive Properties

Biocomposites are a blend of various materials, and their compressive properties are expected to differ from one blend to another, depending on the materials involved. Research has shown that chitosan forms electrostatic conjugates with other negatively charged polymers (natural or synthetic) because it is either neutral or negatively charged in an acidic medium. Therefore, it has led researchers to conjugate chitosan with various polymers. One such research involved reinforcing PLA (95% L-lactide and 5% meso-lactide) dried at 50-60°C under vacuum using an electric air convection heater, with varying



proportions of chitosan powder particles  $\leq 25\mu\text{m}$ . The compressive test results revealed that the compressive strength of the biocomposite could be increased by increasing the proportion of chitosan reinforcement (Singh et al., 2020).

Developing porous scaffolds from biomaterials has been the main focus in wound healing and tissue engineering applications, especially biomaterials of natural origins, such as silk nanofibrils-Chitosan (SNF-CS) biocomposite (Wang et al., 2013). In weight-bearing applications such as meniscal tissue regeneration, the 3D scaffolds are mostly subjected to compression. Therefore, the need to study the mechanical properties of porous scaffolds under compression is even greater. Several researchers have suggested that the presence of biopolymer nanofibrils such as chitin nanocrystals in nanocomposites increases the compressive strength and the modulus of chitosan scaffolds (Dresvyanina et al., 2020; Yin et al., 2019; Liu et al., 2016). Furthermore, tissue scaffolds mimic the natural extracellular matrix of the biological system, which is usually in wet conditions due to the contact with physiological fluids, for instance, in wound healing applications. Several biochemical processes and cellular activities occur in this moist environment, including cell migration, signaling, differentiation, growth, survival, and other conditions that keep the extracellular matrix in good health. Because of this, it is necessary to examine the behavior of tissue scaffolds in wet and dry conditions to give an idea of their suitability in various *in vivo* conditions.

In work involving silk nanofibril-chitosan porous scaffolds, Li et al. (2021) reported significant improvement in the mechanical properties of SNF/CS nanocomposites scaffold, with 75% of the SNF/CF scaffold in the wet state as compared to pure chitosan scaffolds. Furthermore, the modulus of elasticity in compression and the strength at 0.6 strain had improved remarkably, indicating that the chitosan scaffolds can be successfully reinforced with SNF for use under wet conditions. It verifies that the porous scaffolds' mechanical properties, especially the compressive properties, are strongly affected by the nanofiber ratio and the solid content.

### **Impact Strength and Nanoindentation**

An investigation of the impact strength of biocomposite material could provide insight into its ability to retain its structural integrity after being loaded by a suddenly applied force. It usually entails mounting a test specimen tightly and hitting it with a pendulum at a known impact force. For example, Elsayy et al. (2016) conducted an Izod impact test on PLA reinforced with chitosan nanoparticles. The presence of 1 and 3% chitosan nanoparticles in the PLA-CSNP composite significantly enhanced its impact strength. However, increasing the chitosan reinforcement to 5% decreased the impact strength of the biocomposite. It suggests that PLA should be moderately reinforced with chitosan nanoparticles to produce composites suitable for applications requiring an impact strength higher than pure PLA.

Wang et al. (2005) used the continuous stiffness measurement (CSM) technique with a tri-sided pyramidal diamond indenter to examine the mechanical behavior of biopolymer chitosan-montmorillonite nanocomposites at the nanoscale level. It involved pressing the nanoindenter into a 60 µm thick chitosan test specimen and clay nanocomposites film at a strain rate of 0.05 1/s up to a depth of 3000 nm. The authors reported that clay-reinforced nanocomposites had higher moduli than non-reinforced composites. Furthermore, it was observed that increasing the clay concentration increased the modulus profile and stiffness of the nanocomposites. In addition, reinforced nanocomposites exhibited a higher hardness profile than their unreinforced counterparts. Hence, it can be concluded that the hardness and elastic modulus of chitosan nanocomposites can be enhanced by increasing the clay concentration.

Similarly, Zhu et al. (2011) utilized the atomic force microscopy nanoindentation process to investigate the hardness and modulus of soft tissue scaffolds made from chitosan. It involved pressing spherical indenters with diameters of 5 and 10 µm for investigating nano hardness and modulus of indentation, respectively, on two chitosan nanofilms produced by reinforcing cross-linked and non-cross-linked chitosan with graphene and fullerene of varying proportions. They reported that improved hardness was the result of increasing the nanofillers proportion. The mechanical properties of various blends of materials with chitosan are summarized in Table 2.

Table 2  
*Mechanical properties of different chitosan nanocomposites*

Composite	Mechanical Test	Key observations	Ref.
Chitosan film-silk nanofibrils	Tensile	Silk nanofibrils reinforcement improved the tensile strength of the chitosan film up to 40.1 MPa.	Li et al. (2021)
Chitosan-polylactic acid	Tensile	Improved tensile strain (ductility) with increasing reinforcement from 1-3%.	Elsawy et al. (2016)
Chitosan-polylactic acid-polycaprolactone	Tensile	Superior tensile and adhesive strengths were exhibited at 60 % chitosan, 28 % polylactic acid, and 12 % polycaprolactone	Boonkong et al. (2013)
Chitosan film-silk nanofibrils	Compressive	Improved compressive modulus of elasticity and strength at 0.6 strain	Li et al. (2021)
Chitosan-polylactic acid	Compressive	Enhanced compressive strength with rising content of reinforcement.	Singh et al. (2020)
Chitosan-polylactic acid	Impact	Improved impact strength was achieved by up to 3 % of reinforcement addition.	Elsawy et al. (2016)
Chitosan-montmorillonite	Nanoindentation	Reinforced chitosan film exhibited a higher hardness profile relative to the unreinforced counterpart.	Wang et al. (2005)
Chitosan scaffold	Nanoindentation	Improved hardness with increasing addition of nanofillers	Zhu et al. (2011)

## CONCLUSION

This paper provides a comprehensive insight into the currently known processing techniques of chitosan nanocomposites and highlights their potential as viable wound healing material. The performance of chitosan nanocomposites is largely related to the homogenous distribution of fillers within their polymeric matrix. The successful distribution creates an excellent chitosan/filler interface, which often creates a high specific interfacial area required to achieve the full potential of the developed nanocomposites. Among the processing techniques reviewed in this paper, the LBL is the most reliable technique for drug delivery applications. The particles are homogeneously distributed and could interact effectively to ensure contact between the bacteria and LBL film. Through the solution casting method, fillers such as MWCNTs and HTs can be homogeneously dispersed in the chitosan, resulting in enhanced mechanical properties of the composites. The antibacterial effects can be achieved with the introduction of AgNPs or ZnO. Sol-gel is notably environmentally friendly, and the nanomaterial composition can be controlled to achieve remarkable homogeneity. Future studies are crucial to give insights into various cost-effective processing techniques. A comprehensive characterization of chitosan nanocomposites can ascertain their conformity to existing standards in the clinical setting.

## ACKNOWLEDGEMENTS

The Research Management Center of Universiti Putra Malaysia (UPM/GP-IPB/2020/9688700) supported this study.

## REFERENCES

- Abbaspour, M., Makhmalzadeh, B. S., Rezaee, B., Shoja, S., & Ahangari, Z. (2015). Evaluation of the antimicrobial effect of chitosan/polyvinyl alcohol electrospun nanofibers containing mafenide acetate. *Jundishapur Journal of Microbiology*, 8(10), Article e24239. <https://doi.org/10.5812/jjm.24239>
- Aguzzi, C., Sandri, G., Bonferoni, C., Cerezo, P., Rossi, S., Ferrari, F., Caramella, C., & Viseras, C. (2014). Solid state characterisation of silver sulfadiazine loaded on montmorillonite/chitosan nanocomposite for wound healing. *Colloids and Surfaces B: Biointerfaces*, 113, 152-157. <https://doi.org/10.1016/j.colsurfb.2013.08.043>
- Aslam, M., Raza, Z. A., & Siddique, A. (2021). Fabrication and chemo-physical characterization of CuO/chitosan nanocomposite-mediated tricomponent PVA films. *Polymer Bulletin*, 78(4), 1955-1965. <https://doi.org/10.1007/s00289-020-03194-4>
- Balaji, J., & Sethuraman, M. G. (2017). Chitosan-doped-hybrid/TiO<sub>2</sub> nanocomposite based sol-gel coating for the corrosion resistance of aluminum metal in 3.5% NaCl medium. *International Journal of Biological Macromolecules*, 104, 1730-1739. <https://doi.org/10.1016/j.ijbiomac.2017.03.115>
- Bedolla-Cázares, F., Hernández-Marcelo, P. E., Gómez-Hurtado, M. A., Rodríguez-García, G., Del Río, R. E., López-Castro, Y., García-Merinos, J. P., Torres-Valencia, J. M., & González-Campos, J. B. (2017).

- Silver nanoparticles from AgNO<sub>3</sub>-affinin complex synthesized by an ecofriendly route: Chitosan-based electrospun composite production. *Clean Technologies and Environmental Policy*, 19(3), 897-906. <https://doi.org/10.1007/s10098-016-1285-x>
- Boccaccini, A. R., & Ma, P. X. (Eds.). (2014). *Tissue Engineering Using Ceramics and Polymers*. Elsevier.
- Boonkong, W., Petsom, A., & Thongchul, N. (2013). Rapidly stopping hemorrhage by enhancing blood clotting at an opened wound using chitosan/poly(lactic acid)/polycaprolactone wound dressing device. *Journal of Materials Science: Materials in Medicine*, 24(6), 1581-1593. <https://doi.org/10.1007/s10856-013-4864-y>
- Budnyak, T. M., Pylypchuk, I. V., Tertykh, V. A., Yanovska, E. S., & Kolodynska, D. (2015). Synthesis and adsorption properties of chitosan-silica nanocomposite prepared by sol-gel method. *Nanoscale Research Letters*, 10(1), 1-10. <https://doi.org/10.1186/s11671-014-0722-1>
- Budnyak, T. M., Yanovska, E. S., Kołodyńska, D., Sternik, D., Pylypchuk, I. V., Ischenko, M. V., & Tertykh, V. A. (2016). Preparation and properties of organomineral adsorbent obtained by sol-gel technology. *Journal of Thermal Analysis and Calorimetry*, 125(3), 1335-1351. <https://doi.org/10.1007/s10973-016-5581-9>
- Celebi, H., & Kurt, A. (2015). Effects of processing on the properties of chitosan/cellulose nanocrystal films. *Carbohydrate Polymers*, 133, 284-293. <https://doi.org/10.1016/j.carbpol.2015.07.007>
- Chen, C., Liu, P., & Lu, C. (2008). Synthesis and characterization of nano-sized ZnO powders by direct precipitation method. *Chemical Engineering Journal*, 144(3), 509-513. <https://doi.org/10.1016/j.cej.2008.07.047>
- Chrissafis, K., Paraskevopoulos, K. M., Papageorgiou, G. Z., & Bikiaris, D. N. (2008). Thermal and dynamic mechanical behavior of bionanocomposites: Fumed silica nanoparticles dispersed in poly (vinyl pyrrolidone), chitosan, and poly (vinyl alcohol). *Journal of Applied Polymer Science*, 110(3), 1739-1749. <https://doi.org/10.1002/app.28818>
- Dai, T., Tanaka, M., Huang, Y. Y., & Hamblin, M. R. (2011). Chitosan preparations for wounds and burns: Antimicrobial and wound-healing effects. *Expert Review of Anti-Infective Therapy*, 9(7), 857-879. <https://doi.org/10.1586/eri.11.59>
- Darder, M., López-Blanco, M., Aranda, P., Aznar, A. J., Bravo, J., & Ruiz-Hitzky, E. (2006). Microfibrillar chitosan - Sepiolite nanocomposites. *Chemistry of Materials*, 18(6), 1602-1610.
- de Mesquita, J. P., Donnici, C. L., & Pereira, F. V. (2010). Biobased nanocomposites from layer-by-layer assembly of cellulose nanowhiskers with chitosan. *Biomacromolecules*, 11(2), 473-480. <https://doi.org/10.1021/cm0523642>
- Denkbaş, E. U. R. B., Öztürk, E., Özdemir, N., Keçecioğlu, K., & Agalar, C. (2004). Norfloxacin-loaded chitosan sponges as wound dressing material. *Journal of Biomaterials Applications*, 18(4), 291-303.
- De Silva, R. T., Pasbakhsh, P., Goh, K. L., Chai, S. P., & Ismail, H. J. P. T. (2013). Physico-chemical characterisation of chitosan/halloysite composite membranes. *Polymer Testing*, 32(2), 265-271. <https://doi.org/10.1016/j.polymertesting.2012.11.006>

- Dilamian, M., Montazer, M., & Masoumi, J. (2013). Antimicrobial electrospun membranes of chitosan/poly (ethylene oxide) incorporating poly (hexamethylene biguanide) hydrochloride. *Carbohydrate Polymers*, 94(1), 364-371. <https://doi.org/10.1016/j.carbpol.2013.01.059>
- Dobrovolskaya, I. P., Yudin, V. E., Popryadukhin, P. V., Ivan'kova, E. M., Shabunin, A. S., Kasatkin, I. A., & Morgantie, P. (2018). Effect of chitin nanofibrils on electrospinning of chitosan-based composite nanofibers. *Carbohydrate Polymers*, 194, 260-266. <https://doi.org/10.1016/j.carbpol.2018.03.074>
- Dresvyanina, E. N., Grebennikov, S. F., Elokhoyskii, V. Y., Dobrovolskaya, I. P., Ivan'kova, E. M., Yudin, V. E., Heppe, K., & Morganti, P. (2020). Thermodynamics of interaction between water and the composite films based on chitosan and chitin nanofibrils. *Carbohydrate Polymers*, 245, Article 116552. <https://doi.org/10.1016/j.carbpol.2020.116552>
- El Achaby, M., Essamlali, Y., El Miri, N., Snik, A., Abdelouahdi, K., Fihri, A., Zahouily, M., & Solhy, A. (2014). Graphene oxide reinforced chitosan/polyvinylpyrrolidone polymer bio-nanocomposites. *Journal of Applied Polymer Science*, 131(22), 1-11. <https://doi.org/10.1002/app.41042>
- El-saied, H. A. A., & Ibrahim, A. M. (2020). Effective fabrication and characterization of eco-friendly nano chitosan capped zinc oxide nanoparticles for effective marine fouling inhibition. *Journal of Environmental Chemical Engineering*, 8(4), Article 103949. <https://doi.org/10.1016/j.jece.2020.103949>
- Elsawy, M. A., Saad, G. R., & Sayed, A. M. (2016). Mechanical, thermal, and dielectric properties of poly (lactic acid)/chitosan nanocomposites. *Polymer Engineering & Science*, 56(9), 987-994. <https://doi.org/10.1002/pen.24328>
- Fan, J., Shi, Z., Ge, Y., Wang, Y., Wang, J., & Yin, J. (2012). Mechanical reinforcement of chitosan using unzipped multiwalled carbon nanotube oxides. *Polymer*, 53(2), 657-664. <https://doi.org/10.1016/j.polymer.2011.11.060>
- Gu, S. Y., Wang, Z. M., Ren, J., & Zhang, C. Y. (2009). Electrospinning of gelatin and gelatin/poly (l-lactide) blend and its characteristics for wound dressing. *Materials Science and Engineering: C*, 29(6), 1822-1828. <https://doi.org/10.1016/j.msec.2009.02.010>
- Gulaczyk, I., Kręglewski, M., & Valentin, A. (2003). The N-N stretching band of hydrazine. *Journal of Molecular Spectroscopy*, 220(1), 132-136. [https://doi.org/10.1016/S0022-2852\(03\)00106-1](https://doi.org/10.1016/S0022-2852(03)00106-1)
- Gundloori, R. V., Singam, A., & Killi, N. (2019). Nanobased intravenous and transdermal drug delivery systems. In S. S. Mohapatra, S. Ranjan, N. Dasgupta, R. K. Mishra & S. Thomas (Eds.), *Applications of Targeted Nano Drugs and Delivery Systems* (pp. 551-594). Elsevier. <https://doi.org/10.1016/B978-0-12-814029-1.00019-3>
- Haider, S., & Park, S. Y. (2009). Preparation of the electrospun chitosan nanofibers and their applications to the adsorption of Cu (II) and Pb (II) ions from an aqueous solution. *Journal of Membrane Science*, 328(1-2), 90-96. <https://doi.org/10.1016/j.memsci.2008.11.046>
- Hamdi, M., Feki, A., Bardaa, S., Li, S., Nagarajan, S., Mellouli, M., & Nasri, R. (2020). A novel blue crab chitosan/protein composite hydrogel enriched with carotenoids endowed with distinguished wound healing capability: In vitro characterization and in vivo assessment. *Materials Science and Engineering: C*, 113, Article 110978. <https://doi.org/10.1016/j.msec.2020.110978>

- Hammad, A. B. A., Elnahrawy, A. M., & Youssef, A. M. (2019). Sol gel synthesis of hybrid chitosan/calcium aluminosilicate nanocomposite membranes and its application as support for CO<sub>2</sub> sensor. *International Journal of Biological Macromolecules*, 125, 503-509. <https://doi.org/10.1016/j.ijbiomac.2018.12.077>
- Huang, D., Mu, B., & Wang, A. (2012). Preparation and properties of chitosan/poly (vinyl alcohol) nanocomposite films reinforced with rod-like sepiolite. *Materials Letters*, 86, 69-72. <https://doi.org/10.1016/j.matlet.2012.07.020>
- Huang, D., Wang, W., Kang, Y., & Wang, A. (2012). A chitosan/poly (vinyl alcohol) nanocomposite film reinforced with natural halloysite nanotubes. *Polymer Composites*, 33(10), 1693-1699. <https://doi.org/10.1002/pc.22302>
- Huang, J., Cheng, Y., Wu, Y., Shi, X., Du, Y., & Deng, H. (2019). Chitosan/tannic acid bilayers layer-by-layer deposited cellulose nanofibrous mats for antibacterial application. *International Journal of Biological Macromolecules*, 139, 191-198. <https://doi.org/10.1016/j.ijbiomac.2019.07.185>
- Huang, W., Xu, H., Xue, Y., Huang, R., Deng, H., & Pan, S. (2012). Layer-by-layer immobilization of lysozyme-chitosan-organic rectorite composites on electrospun nanofibrous mats for pork preservation. *Food Research International*, 48(2), 784-791. <https://doi.org/10.1016/j.foodres.2012.06.026>
- Ifuku, S., Nogi, M., Abe, K., Yoshioka, M., Morimoto, M., Saimoto, H., & Yano, H. (2009). Preparation of chitin nanofibers with a uniform width as  $\alpha$ -chitin from crab shells. *Biomacromolecules*, 10(6), 1584-1588. <https://doi.org/10.1021/bm900163d>
- Islam, A., Riaz, M., & Yasin, T. (2013). Structural and viscoelastic properties of chitosan-based hydrogel and its drug delivery application. *International Journal of Biological Macromolecules*, 59, 119-124. <https://doi.org/10.1016/j.ijbiomac.2013.04.044>
- Islam, S., Bhuiyan, M. A., & Islam, M. N. (2017). Chitin and chitosan: structure, properties and applications in biomedical engineering. *Journal of Polymers and the Environment*, 25(3), 854-866. <https://doi.org/10.1007/s10924-016-0865-5>
- Kavitha, K., Sutha, S., Prabhu, M., Rajendran, V., & Jayakumar, T. (2013). In situ synthesized novel biocompatible titania-chitosan nanocomposites with high surface area and antibacterial activity. *Carbohydrate Polymers*, 93(2), 731-739. <https://doi.org/10.1016/j.carbpol.2012.12.031>
- Keten, S., Xu, Z., Ihle, B., & Buehler, M. J. (2010). Nanoconfinement controls stiffness, strength and mechanical toughness of  $\beta$ -sheet crystals in silk. *Nature Materials*, 9(4), 359-367. <https://doi.org/10.1038/nmat2704>
- Lai, S. M., Yang, A. J. M., Chen, W. C., & Hsiao, J. F. (2006). The properties and preparation of chitosan/silica hybrids using sol-gel process. *Polymer-Plastics Technology and Engineering*, 45(9), 997-1003. <https://doi.org/10.1080/03602550600726269>
- Li, F., Biagioni, P., Finazzi, M., Tavazzi, S., & Piergiovanni, L. (2013). Tunable green oxygen barrier through layer-by-layer self-assembly of chitosan and cellulose nanocrystals. *Carbohydrate Polymers*, 92(2), 2128-2134. <https://doi.org/10.1016/j.carbpol.2012.11.091>
- Li, L., Yang, H., Li, X., Yan, S., Xu, A., You, R., & Zhang, Q. (2021). Natural silk nanofibrils as reinforcements for the preparation of chitosan-based bionanocomposites. *Carbohydrate Polymers*, 253, Article 117214. <https://doi.org/10.1016/j.carbpol.2020.117214>



- Li, M., Han, M., Sun, Y., Hua, Y., Chen, G., & Zhang, L. (2019). Oligoarginine mediated collagen/chitosan gel composite for cutaneous wound healing. *International Journal of Biological Macromolecules*, *122*, 1120-1127. <https://doi.org/10.1016/j.ijbiomac.2018.09.061>
- Li, P. C., Liao, G. M., Kumar, S. R., Shih, C. M., Yang, C. C., Wang, D. M., & Lue, S. J. (2016). Fabrication and characterization of chitosan nanoparticle-incorporated quaternized poly (vinyl alcohol) composite membranes as solid electrolytes for direct methanol alkaline fuel cells. *Electrochimica Acta*, *187*, 616-628. <https://doi.org/10.1016/j.electacta.2015.11.117>
- Liu, H., Wang, C., Li, C., Qin, Y., Wang, Z., Yang, F., & Wang, J. (2018). A functional chitosan-based hydrogel as a wound dressing and drug delivery system in the treatment of wound healing. *RSC Advances*, *8*(14), 7533-7549. <https://doi.org/10.1039/C7RA13510F>
- Liu, M., Zheng, H., Chen, J., Li, S., Huang, J., & Zhou, C. (2016). Chitosan-chitin nanocrystal composite scaffolds for tissue engineering. *Carbohydrate Polymers*, *152*, 832-840. <https://doi.org/10.1016/j.carbpol.2016.07.042>
- Liu, Y. L., Chen, W. H., & Chang, Y. H. (2009). Preparation and properties of chitosan/carbon nanotube nanocomposites using poly (styrene sulfonic acid)-modified CNTs. *Carbohydrate Polymers*, *76*(2), 232-238. <https://doi.org/10.1016/j.carbpol.2008.10.021>
- Lu, B., Li, T., Zhao, H., Li, X., Gao, C., Zhang, S., & Xie, E. (2012). Graphene-based composite materials beneficial to wound healing. *Nanoscale*, *4*(9), 2978-2982. <https://doi.org/10.1039/C2NR11958G>
- Lu, Z., Gao, J., He, Q., Wu, J., Liang, D., Yang, H., & Chen, R. (2017). Enhanced antibacterial and wound healing activities of microporous chitosan-Ag/ZnO composite dressing. *Carbohydrate Polymers*, *156*, 460-469. <https://doi.org/10.1016/j.carbpol.2016.09.051>
- Meng, D., Erol, M., & Boccaccini, A. R. (2010). Processing technologies for 3D nanostructured tissue engineering scaffolds. *Advanced Engineering Materials*, *12*(9), B467-B487. <https://doi.org/10.1002/adem.201080019>
- Packirisamy, R. G., Govindasamy, C., Sanmugam, A., Venkatesan, S., Kim, H. S., & Vikraman, D. (2019). Synthesis of novel Sn<sub>1-x</sub>Zn<sub>x</sub>O-chitosan nanocomposites: Structural, morphological and luminescence properties and investigation of antibacterial properties. *International Journal of Biological Macromolecules*, *138*, 546-555. <https://doi.org/10.1016/j.ijbiomac.2019.07.120>
- Patel, S., Srivastava, S., Singh, M. R., & Singh, D. (2018). Preparation and optimization of chitosan-gelatin films for sustained delivery of lupeol for wound healing. *International Journal of Biological Macromolecules*, *107*, 1888-1897.
- Penchev, H., Paneva, D., Manolova, N., & Rashkov, I. (2010). Hybrid nanofibrous yarns based on N-carboxyethylchitosan and silver nanoparticles with antibacterial activity prepared by self-bundling electrospinning. *Carbohydrate Research*, *345*(16), 2374-2380. <https://doi.org/10.1016/j.carres.2010.08.014>
- Pinto, T. D. S., Alves, L. A., de Azevedo Cardozo, G., Munhoz, V. H., Verly, R. M., Pereira, F. V., & de Mesquita, J. P. (2017). Layer-by-layer self-assembly for carbon dots/chitosan-based multilayer: Morphology, thickness and molecular interactions. *Materials Chemistry and Physics*, *186*, 81-89. <https://doi.org/10.1016/j.matchemphys.2016.10.032>



- Podsiadlo, P., Kaushik, A. K., Arruda, E. M., Waas, A. M., Shim, B. S., Xu, J., Nandivada, H., Pumpllin, B. G., Lahann, J., Ramamoorthy, A., & Kotov, N. A. (2007). Ultrastrong and stiff layered polymer nanocomposites. *Science*, *318*(5847), 80-83. <https://doi.org/10.1126/science.1143176>
- Poonguzhali, R., Basha, S. K., & Kumari, V. S. (2017). Synthesis and characterization of chitosan-PVP-nanocellulose composites for in-vitro wound dressing application. *International Journal of Biological Macromolecules*, *105*, 111-120. <https://doi.org/10.1016/j.ijbiomac.2017.07.006>
- Qasim, S. B., Zafar, M. S., Najeeb, S., Khurshid, Z., Shah, A. H., Husain, S., & Rehman, I. U. (2018). Electrospinning of chitosan-based solutions for tissue engineering and regenerative medicine. *International Journal of Molecular Sciences*, *19*(2), Article 407. <https://doi.org/10.3390/ijms19020407>
- Rahmani, H., Najafi, S. H. M., Ashori, A., Fashapoyeh, M. A., Mohseni, F. A., & Torkaman, S. (2020). Preparation of chitosan-based composites with urethane cross linkage and evaluation of their properties for using as wound healing dressing. *Carbohydrate Polymers*, *230*, Article 115606. <https://doi.org/10.1016/j.carbpol.2019.115606>
- Raoufi, D. (2013). Synthesis and microstructural properties of ZnO nanoparticles prepared by precipitation method. *Renewable Energy*, *50*, 932-937. <https://doi.org/10.1016/j.renene.2012.08.076>
- Rezvani, H., Riazi, M., Tabaei, M., Kazemzadeh, Y., & Sharifi, M. (2018). Experimental investigation of interfacial properties in the EOR mechanisms by the novel synthesized Fe<sub>3</sub>O<sub>4</sub>@ Chitosan nanocomposites. *Colloids and Surfaces A: Physicochemical and Engineering Aspects*, *544*, 15-27. <https://doi.org/10.1016/j.colsurfa.2018.02.012>
- Salaberria, A. M., Diaz, R. H., Labidi, J., & Fernandes, S. C. (2015). Preparing valuable renewable nanocomposite films based exclusively on oceanic biomass - Chitin nanofillers and chitosan. *Reactive and Functional Polymers*, *89*, 31-39. <https://doi.org/10.1016/j.reactfunctpolym.2015.03.003>
- Salehzadeh, H., Hekmatian, E., Sadeghi, M., & Kennedy, K. (2012). Synthesis and characterization of core-shell Fe<sub>3</sub>O<sub>4</sub>-gold-chitosan nanostructure. *Journal of Nanobiotechnology*, *10*(1), 1-7. <https://doi.org/10.1186/1477-3155-10-3>
- Santos, K. O., Barbosa, R. C., da Silva Buriti, J., Bezerra Junior, A. G., de Sousa, W. J. B., de Barros, S. M. C., de Oliveira, R. J., & Fook, M. V. L. (2019). Thermal, chemical, biological and mechanical properties of chitosan films with powder of eggshell membrane for biomedical applications. *Journal of Thermal Analysis and Calorimetry*, *136*(2), 725-735. <https://doi.org/10.1007/s10973-018-7666-0>
- Saravanan, R., Aviles, J., Gracia, F., Mosquera, E., & Gupta, V. K. (2018). Crystallinity and lowering band gap induced visible light photocatalytic activity of TiO<sub>2</sub>/CS (Chitosan) nanocomposites. *International Journal of Biological Macromolecules*, *109*, 1239-1245. <https://doi.org/10.1016/j.ijbiomac.2017.11.125>
- Schiffman, J. D., & Schauer, C. L. (2008). A review: Electrospinning of biopolymer nanofibers and their applications. *Polymer Reviews*, *48*(2), 317-352. <https://doi.org/10.1080/15583720802022182>
- Sharma, G., Naushad, M., Kumar, A., Kumar, A., Ahamad, T., & Stadler, F. J. (2020). Facile fabrication of chitosan-cl-poly (AA)/ZrPO<sub>4</sub> nanocomposite for remediation of rhodamine B and antimicrobial activity. *Journal of King Saud University-Science*, *32*(2), 1359-1365. <https://doi.org/10.1016/j.jksus.2019.11.028>

- Singh, A., Sinsinbar, G., Choudhary, M., Kumar, V., Pasricha, R., Verma, H. N., Singh, S. P., & Arora, K. (2013). Graphene oxide-chitosan nanocomposite based electrochemical DNA biosensor for detection of typhoid. *Sensors and Actuators B: Chemical*, *185*, 675-684. <https://doi.org/10.1016/j.snb.2013.05.014>
- Singh, S., Singh, G., Prakash, C., Ramakrishna, S., Lamberti, L., & Pruncu, C. I. (2020). 3D printed biodegradable composites: An insight into mechanical properties of PLA/chitosan scaffold. *Polymer Testing*, *89*, Article 106722. <https://doi.org/10.1016/j.polymertesting.2020.106722>
- Siqueira, J. R., Gasparotto, L. H., Crespilho, F. N., Carvalho, A. J., Zucolotto, V., & Oliveira, O. N. (2006). Physicochemical properties and sensing ability of metallophthalocyanines/chitosan nanocomposites. *The Journal of Physical Chemistry B*, *110*(45), 22690-22694. <https://doi.org/10.1021/jp0649089>
- Sreedhar, B., Aparna, Y., Sairam, M., & Hebalkar, N. (2007). Preparation and characterization of HAP/carboxymethyl chitosan nanocomposites. *Journal of Applied Polymer Science*, *105*(2), 928-934. <https://doi.org/10.1002/app.26140>
- Khan, T. A., Peh, K. K., & Ch'ng, H. S. (2000). Mechanical, bioadhesive strength and biological evaluations of chitosan films for wound dressing. *Journal of Pharmaceutical Sciences*, *3*(3), 303-311.
- Thou, C. Z., Khan, F. S. A., Mubarak, N. M., Ahmad, A., Khalid, M., Jagadish, P., Walvekar, R., Abdullah, E. C., Khan, S., Khan, M., Hussain, S., Ahmad, I., & Algarni, T. S. (2021). Surface charge on chitosan/cellulose nanowhiskers composite via functionalized and untreated carbon nanotube. *Arabian Journal of Chemistry*, *14*(3), 103022. <https://doi.org/10.1016/j.arabjc.2021.103022>
- Tripathi, S., Mehrotra, G. K., & Dutta, P. K. (2011). Chitosan-silver oxide nanocomposite film: Preparation and antimicrobial activity. *Bulletin of Materials Science*, *34*(1), 29-35. <https://doi.org/10.1007/s12034-011-0032-5>
- Türkeş, E., & Açıknel, Y. S. (2020). Synthesis and characterization of magnetic halloysite-chitosan nanocomposites: Use in the removal of methylene blue in wastewaters. *International Journal of Environmental Science and Technology*, *17*(3), 1281-1294. <https://doi.org/10.1007/s13762-019-02550-w>
- Varma, H. K., Yokogawa, Y., Espinosa, F. F., Kawamoto, Y., Nishizawa, K., Nagata, F., & Kameyama, T. (1999). Porous calcium phosphate coating over phosphorylated chitosan film by a biomimetic method. *Biomaterials*, *20*(9), 879-884. [https://doi.org/10.1016/S0142-9612\(98\)00243-9](https://doi.org/10.1016/S0142-9612(98)00243-9)
- Vollrath, F., & Knight, D. P. (2001). Liquid crystalline spinning of spider silk. *Nature*, *410*(6828), 541-548. <https://doi.org/10.1038/35069000>
- Wang, D., Lu, Q., Wei, M., & Guo, E. (2018). Ultrasmall Ag nanocrystals supported on chitosan/PVA nanofiber mats with bifunctional properties. *Journal of Applied Polymer Science*, *135*(28), 46504. <https://doi.org/10.1002/app.46504>
- Wang, H. M., Chou, Y. T., Wen, Z. H., Wang, Z. R., Chen, C. H., & Ho, M. L. (2013). Novel biodegradable porous scaffold applied to skin regeneration. *PloS One*, *8*(6), Article e56330. <https://doi.org/10.1371/journal.pone.0056330>
- Wang, J., Law, W. C., Chen, L., Chen, D., & Tang, C. Y. (2017). Fabrication of monodisperse drug-loaded poly (lactic-co-glycolic acid)-chitosan core-shell nanocomposites via pickering emulsion. *Composites Part B: Engineering*, *121*, 99-107. <https://doi.org/10.1016/j.compositesb.2017.03.032>

- Wang, S. F., Shen, L., Tong, Y. J., Chen, L., Phang, I. Y., Lim, P. Q., & Liu, T. X. (2005). Biopolymer chitosan/montmorillonite nanocomposites: preparation and characterization. *Polymer Degradation and Stability*, *90*(1), 123-131. <https://doi.org/10.1016/j.polymdegradstab.2005.03.001>
- Wang, X., Cheng, F., Gao, J., & Wang, L. (2015). Antibacterial wound dressing from chitosan/polyethylene oxide nanofibers mats embedded with silver nanoparticles. *Journal of biomaterials applications*, *29*(8), 1086-1095. <https://doi.org/10.1177/0885328214554665>
- Wu, T., Pan, Y., Bao, H., & Li, L. (2011). Preparation and properties of chitosan nanocomposite films reinforced by poly (3, 4-ethylenedioxythiophene)-poly (styrenesulfonate) treated carbon nanotubes. *Materials Chemistry and Physics*, *129*(3), 932-938. <https://doi.org/10.1016/j.matchemphys.2011.05.030>
- Xie, H., Chen, X., Shen, X., He, Y., Chen, W., Luo, Q., Ge, W., Yuan, W., Tang, X., Hou, D., Jiang, D., Wang, Q., Liu, Y., Liu, Q., & Li, K. (2018). Preparation of chitosan-collagen-alginate composite dressing and its promoting effects on wound healing. *International Journal of Biological Macromolecules*, *107*, 93-104. <https://doi.org/10.1016/j.ijbiomac.2017.08.142>
- Yamaguchi, I., Tokuchi, K., Fukuzaki, H., Koyama, Y., Takakuda, K., Monma, H., & Tanaka, J. (2001). Preparation and microstructure analysis of chitosan/hydroxyapatite nanocomposites. *Journal of Biomedical Materials Research*, *55*(1), 20-27. [https://doi.org/10.1002/1097-4636\(200104\)55:1<20::AID-JBM30>3.0.CO;2-F](https://doi.org/10.1002/1097-4636(200104)55:1<20::AID-JBM30>3.0.CO;2-F)
- Yang, D., Li, J., Jiang, Z., Lu, L., & Chen, X. (2009). Chitosan/TiO<sub>2</sub> nanocomposite pervaporation membranes for ethanol dehydration. *Chemical Engineering Science*, *64*(13), 3130-3137. <https://doi.org/10.1016/j.ces.2009.03.042>
- Yilmaz, E., & Soylak, M. (2020). Functionalized nanomaterials for sample preparation methods. In C. M. Hussain (Ed.), *Handbook of Nanomaterials in Analytical Chemistry* (pp. 375-413). Elsevier. <https://doi.org/10.1016/B978-0-12-816699-4.00015-3>
- Yin, K., Divakar, P., & Wegst, U. G. (2019). Plant-derived nanocellulose as structural and mechanical reinforcement of freeze-cast chitosan scaffolds for biomedical applications. *Biomacromolecules*, *20*(10), 3733-3745. <https://doi.org/10.1021/acs.biomac.9b00784>
- Youssef, A. M., El-Nahrawy, A. M., & Hammad, A. B. A. (2017). Sol-gel synthesis and characterizations of hybrid chitosan-PEG/calcium silicate nanocomposite modified with ZnO-NPs and (E102) for optical and antibacterial applications. *International Journal of Biological Macromolecules*, *97*, 561-567. <https://doi.org/10.1016/j.ijbiomac.2017.01.059>
- Zafar, M., Najeeb, S., Khurshid, Z., Vazirzadeh, M., Zohaib, S., Najeeb, B., & Sefat, F. (2016). Potential of electrospun nanofibers for biomedical and dental applications. *Materials*, *9*(2), Article 73. <https://doi.org/10.3390/ma9020073>
- Zhang, F., You, X., Dou, H., Liu, Z., Zuo, B., & Zhang, X. (2015). Facile fabrication of robust silk nanofibril films via direct dissolution of silk in CaCl<sub>2</sub>-formic acid solution. *ACS Applied Materials & Interfaces*, *7*(5), 3352-3361. <https://doi.org/10.1021/am508319h>
- Zhang, W., Jia, S., Wu, Q., Wu, S., Ran, J., Liu, Y., & Hou, J. (2012). Studies of the magnetic field intensity on the synthesis of chitosan-coated magnetite nanocomposites by co-precipitation method. *Materials Science and Engineering: C*, *32*(2), 381-384. <https://doi.org/10.1016/j.msec.2011.11.010>

- Zhong, S. P., Zhang, Y. Z., & Lim, C. T. (2010). Tissue scaffolds for skin wound healing and dermal reconstruction. *Wiley Interdisciplinary Reviews: Nanomedicine and Nanobiotechnology*, 2(5), 510-525. <https://doi.org/10.1002/wnan.100>
- Zhu, Y., Dong, Z., Wejinya, U. C., Jin, S., & Ye, K. (2011). Determination of mechanical properties of soft tissue scaffolds by atomic force microscopy nanoindentation. *Journal of Biomechanics*, 44(13), 2356-2361. <https://doi.org/10.1016/j.jbiomech.2011.07.010>



## Brain Tumour Region Extraction Using Novel Self-Organising Map-Based KFCM Algorithm

Peddamalla Gangadhara Reddy<sup>1\*</sup>, Tirumala Ramashri<sup>1</sup> and Kayam Lokesh Krishna<sup>2</sup>

<sup>1</sup>Department of ECE, Sri Venkateswara University College of Engineering, S.V. University, Tirupati, A.P., India

<sup>2</sup>Department of ECE, S.V. College of Engineering, Tirupati, A.P., India

### ABSTRACT

Medical professionals need help finding tumours in the ground truth image of the brain because the tumours' location, contrast, intensity, size, and shape vary between images because of different acquisition methods, modalities, and the patient's age. The medical examiner has difficulty manually separating a tumour from other parts of a Magnetic Resonance Imaging (MRI) image. Many semi- and fully automated brain tumour detection systems have been written about in the literature, and they keep improving. The segmentation literature has seen several transformations throughout the years. An in-depth examination of these methods will be the focus of this investigation. We look at the most recent soft computing technologies used in MRI brain analysis through several review papers. This study looks at Self-Organising maps (SOM) with K-means and the kernel Fuzzy c-means (KFCM) method for segmenting them. The suggested SOM networks were first compared to K-means analysis in an experiment based on datasets with well-known cluster solutions. Later, the SOM is combined with KFCM, reducing time complexity and producing more accurate results than other methods. Experiments show that skewed data improves networks' performance with more SOMs. Finally, performance measures in real-time datasets are analysed using machine learning approaches. The results show that the proposed algorithm has good sensitivity and better accuracy than k-means and other state-of-art methods.

### ARTICLE INFO

#### Article history:

Received: 30 March 2022

Accepted: 28 June 2022

Published: 27 December 2022

DOI: <https://doi.org/10.47836/pjst.31.1.33>

#### E-mail addresses:

[gangadharareddy.p@gmail.com](mailto:gangadharareddy.p@gmail.com) (Peddamalla Gangadhara Reddy)

[rama.jaypee@gmail.com](mailto:rama.jaypee@gmail.com) (Tirumala Ramashri)

[kayamlokesh78@gmail.com](mailto:kayamlokesh78@gmail.com) (Kayam Lokesh Krishna)

\* Corresponding author

*Keywords:* Brain tumour segmentation, feature extraction, kernel FCM, K-means, medical imaging, self-organising map

### INTRODUCTION

MRI utilises radio waves and a magnetic field to create precise pictures of the brain and brain stem. It is a painless and safe

procedure. Because it does not utilise radiation, magnetic resonance imaging differs from computed tomography. An MRI scan may detect cysts, tumours, haemorrhages, oedema, and structural brain abnormalities. A brain MRI may help patients to find the cause of their symptoms, like persistent headaches, dizziness, paralysis, or seizures. Additionally, it can diagnose chronic nervous system illnesses such as multiple sclerosis. At times, an MRI may provide a more detailed image of the brain than an ultrasound Computed Tomography (CT) scan or X-ray (Zhang & Sejdić, 2019).

The most efficient segmentation approach relied on a grey-level information process in which organs with comparable intensities make it challenging to determine the tumour's location. Kohonen developed an unsupervised SOM neural network using a competitive learning method with an automated topological mapping procedure that reduces the number of dimensions to one or two (Şişik & Eser, 2020). Thus far, the picture segmentation method provided by the SOM neural network has been more attractive. On the other hand, an automated SOM neural network classification method generates feature vectors that help with the colour picture segmentation process (Kumar et al., 2019).

When used in image segmentation, SOM neural networks used two-stage classification algorithms that employed a predetermined noise reduction (Garcia-Lamont et al., 2018). The automated ideal cluster centre was obtained using a fuzzy clustering algorithm with a SOM neural network. An unsupervised segmentation technique supports a trained network that performs dimension reduction. SOM segmentation using fuzzy clustering is compared to an Efficient Graph (EG)-based segmentation approach in the centre initialisation procedure (Kumar et al., 2018 & Sandhya et al., 2019). Halder's research team suggested a SOM neural network with modal analysis and mutational aggregation for automatic classification. However, it is not self-contained and requires a mapping technique and dimension reduction (Garcia-Lamont et al., 2018). Segmentation is more efficient using the 2D discrete wavelet transform with the Moving Average SOM (MASOM) method, as it ensures the least human involvement in modifying the variables that initiate the segmentation process. This technique combines clustering with a self-organising map to achieve successful MRI image segmentation, as shown in Figure 1. This method has the main drawback of using additional computing time during the segmentation procedure.

Tumours in the brain are made up of aberrant cells that develop quickly and that the body cannot manage. Brain tumours continue to develop at an accelerated rate, and their appearance determines whether they are benign or malignant. The skull is a static bone structure. As a result, the skull cannot grow, and the tumour begins to push on the brain once it has formed. Primary brain cancers occur when tumours originate in the brain.

On the other hand, cancer develops in other body areas and spreads to the brain (Anaraki et al., 2019), and it is considered secondary or metastatic. Tumours in the brain may spread at varying rates. The tumour's location determines the rate at which it grows. The tumour's



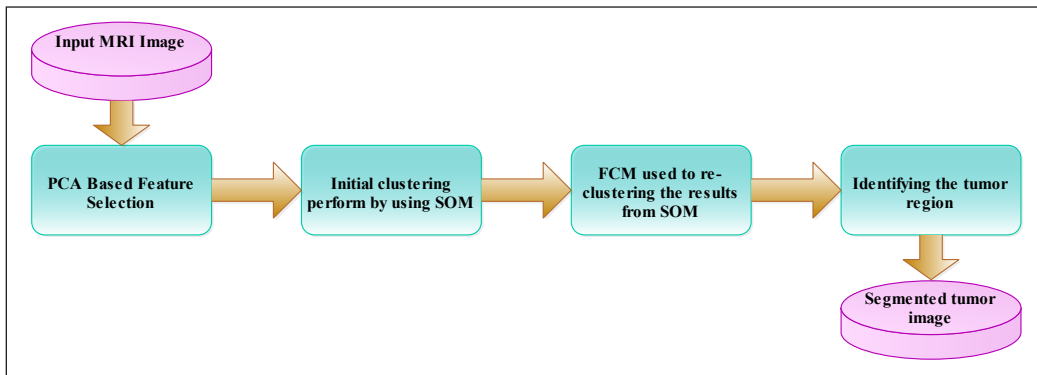


Figure 1. The basic segmentation flow for SOM based clustering algorithm

location is also critical in terms of neurological impairment. Simultaneously, tumour therapy depends on the size, location, and kind of tumour (Mohan & Subashini, 2019 & Tarhini & Shbib, 2020). The research attempted to bring some benchmark segmentation methods in medical image analysis, which have been thoroughly studied. To segment medical images used, the fuzzy C-means method, a new FCM method that heavily relies on the neighbourhood means to determine the goal function. The enhanced FCM algorithm revealed non-local information in the neighbour function (Song et al., 2022). The modified genetic algorithm crossover and mutation process are used to process the input picture by the algorithm, which is used to make the final segmentation result. Particle Swarm Optimization (PSO)-FCM and a region-growing algorithm are used to get more precise tumour detection at the cost of longer processing times. A modified fuzzy K-means method based on bacteria foraging optimisation takes less time to provide segmentation results (Vishnuvarthanan et al., 2017 & Sandhya et al., 2020). The semi-supervised method is the moving average SOM algorithm to get excellent segmentation results with little human involvement. A SOM neural network utilising dynamic spanning trees needs a longer learning time to give excellent segmentation results. For MR brain imaging, the SOM-based fuzzy K means (FKM) method aids in detecting tumour heterogeneity (Mohan & Subashini, 2018). The author recommends using the Brain Extraction Tool (BET) when preparing medical pictures that heavily rely on human interaction. The SOM-based Learning Vector Quantization (LVQ) method aids in analysing MRI brain images using the method to obtain the image segmentation results may be generated quickly and with little input from the user (Vijh et al., 2020 & Ejaz et al., 2020). Helmy and El-Taweel (2016) introduce the pulse-coupled neural network method, which is unquestionably a step forward in supervised clustering. The SOM method uses a modified pulse-coupled neural network to build an automatic cluster centre. On the other hand, the Entropy Gradient Segmentation-Self Organization Map (EGS-SOM) method uses the genetic algorithm to determine the cluster centre's location (Al-Dmour & Al-Ani, 2018). It uses the statistical feature to execute the clustering

operation in a unique SOM-based FCM technique. A novel hybrid segmentation technique to produce performance-oriented segmentation based on Different clustering methods (Ejaz et al., 2020). A comparative analysis of parameters like sensitivity and selectivity resulted in K-means, Gaussian Mixture Model (GMM) and FCM algorithms (Baid et al., 2017). An effective brain tumour classification and segmentation for identifying the tumour and non-tumour cells in the brain (Krishnakumar & Manivannan, 2021).

A brain tumour segmentation approach is proposed based on an extreme learning machine and significantly fast and robust fuzzy C-means clustering algorithms (BTS-ELM-FRFCM) running on Raspberry Pi (PI) hardware (Şişik & Eser, 2020). The algorithm combines Region of Interest (ROI), Region Growing and Morphological Operation, and FCM (Sheela & Suganthi, 2020). Computer-aided robotic research technology is incorporated to effectively diagnose the brain tumour at the initial stage with improved accuracy (Balamurugan et al., 2021). The Neural Network architecture does leaf image clustering, self-organising map (SOM), and K-Means algorithm for generating the sub-images by clustering the pixels based on the colours (Kumar et al., 2019), the basic features such as entropy, mean, and standard deviation are extracted from each sub-images. A novel weighted spatial kernel FCM clustering for segmenting the region of interest in the medical image (Kumar et al., 2018).

An automatic brain tumour MRI Data segmentation framework proposed a combined segmentation model based on VNet, integrating the SE and AG modules. By using volume input, three-dimensional convolution is used to process MRI images, get excellent segmentation results, and have the potential clinical application (Guan et al., 2021). A deep multi-task learning framework utilises a decoder for v-net for better segmentation which works on multiple datasets (Huang et al., 2021). A novel network structure with Multi-Encoder with different modalities greatly improves the segmentation performance. Network (ME-Net), a new architecture composed of four encoders performing on the Multimodal Brain Tumour Segmentation Challenge (BraTS) 2020 dataset and compared it with the results of other teams participating in the challenge. The results show that our model has a promising performance for brain tumour segmentation (Zhang et al., 2021). A fully automated method of detection and segmentation of the abnormal tissue associated with a brain tumour (tumour core and oedema) from Fluid Attenuated Inversion Recovery (FLAIR) Magnetic Resonance Imaging (MRI). Results demonstrate the high detection and segmentation performance of the proposed method using ERT classifier, which is a faster and more reproducible method of brain tumour detection and delineation to aid patient management (Soltaninejad et al., 2018).

GAN is a neural network that can translate an image from one domain to another using unpaired data. It alleviates the problem posed by a lack of paired datasets since there is a vast amount of unpaired image data. On the other hand, the main advantage of using a

SOM is that the data is easily interpreted and understood. Furthermore, the reduction of dimensionality and grid clustering makes it easy to observe similarities in the data.

The Supervoxels method demonstrates promising results in the segmentation of brain tumours. Multimodal MRI images increase the segmentation accuracy, which gives a faster and more reproducible method of brain tumour detection (Soltaninejad et al., 2018).

Any researcher interested in classification should not use an unsupervised learning scheme like K-means or SOM because data clusters may not match class distributions. Instead, learning vector quantisers (LVQ) or SVMs should be applied. If applying any unsupervised learning for those problems with a post-labelling, the accuracy might not be the best because the unsupervised learning goal differs from classification.

## METHODS

MRI brain tumour images were segmented using algorithms like K-Means, Fuzzy C-Means, Kernel Fuzzy C-Means, and Self-Organising Map techniques. These strategies will be briefly explored in the following sections (Mohan & Subashini, 2018).

### K-Means Clustering

Samples are divided into  $k$  clusters with the closest cluster centroid using K-Means clustering (Osman & Alzahrani, 2018) as a vector quantisation technique. Assume that the  $n$  input vectors  $x_1, x_2, \dots, x_n$  are real-valued and  $d$ -dimensional. Then,  $C_1, C_2, \dots, C_k$  represent the  $k$  clusters in which these sample vectors have been divided. As stated in Equation 1, this method minimises the cluster sum. In this case, let  $\mu_i$  represent the average of the  $C_i$  samples.

$$\arg \min_c \sum_{i=1}^k \sum_{x \in C_i} \|x - \mu_i\|^2 \quad [1]$$

To get the solution for  $x$  in Equation 1, we must solve for  $x$  in Equation 2.

$$\arg \min_c \sum_{i=1}^k \frac{1}{2|C_i|} \sum_{x,y \in C_i} \|x - y\|^2 \quad [2]$$

When using the conventional K-Means technique, accuracy improved with the iterative refinement method (Asliyan & Atbakan, 2020). The K-means algorithm considers two stages, like initial and updated stages. In other words, we will say that the initial set of K-means is made up of  $m_1(1), m_2(1), \dots, m_k(1)$ .

The first step is to compute the distances between the samples and the means using the least squared Euclidean distance and then place each sample in the cluster to which it is closest. In this case, sample  $x$  is placed precisely in cluster  $C(t)$ , the number of iterations is  $t$ , and clusters are  $i$ , respectively, as shown in Equation 3.

$$C_i(t) = \left\{ x: \|x - m_i(t)\|^2 \leq \|x - m_j(t)\|^2, 1 \leq j \leq k \right\} \quad [3]$$

In the update step, we obtain the means ( $m_i$ ) of all clusters' samples according to Equation 4.

$$m_i(t + 1) = \frac{1}{C_i(t)} \sum_{x_j \in C_i(t)} x_j \quad [4]$$

A standard K-means algorithm consists of the steps shown below:

- (1) Set the number of clusters to  $k$  and create them randomly or generate cluster centres ( $k$ ).
- (2) Use Euclidean distance to define every location here to the cluster centre that is closest to it.
- (3) Use the new data to figure out which cluster centres should be added.
- (4) Repeat procedures (2) and (3) as necessary until the convergence criteria are satisfied.

### Fuzzy C-Means Clustering

Fuzzy C-Means is a technique for unsupervised clustering that divides data into  $k$  groups (Ren et al., 2019; Sheela & Suganthi, 2020). Dunn invented this technique in 1973, and Bezdek refined it in 1981, intending to minimise an objective function as stated in Equation 5.

$$\arg \min_c \sum_{i=1}^n \sum_{j=1}^c \mu_{ij}^m |x_i - c_j|^2 \quad [5]$$

where  $m$  is a positive integer larger than 1,  $x_i$  is the  $i^{\text{th}}$  dimension of  $d$ -dimensional measured data,  $c_j$  is the cluster's  $d$ -dimension centre, and  $\mu_{ij}$  is the degree of membership of  $x_i$  in cluster  $j$ . Membership  $\mu_{ij}$  and cluster centres  $c_j$  are changed in each iteration, as illustrated in Equations 6 and 7.

$$\mu_{ij} = \frac{1}{\sum_{k=1}^c \left\{ \frac{\|x_i - c_j\|}{\|x_i - c_k\|} \right\}^{(2/m-1)}} \quad [6]$$

$$c_j = \frac{\sum_{i=1}^n \mu_{ij}^m x_i}{\sum_{i=1}^n \mu_{ij}^m} \quad [7]$$

If  $xy=0$ , the iteration is complete.  $\delta$  is a real number between 0 and 1, and there are  $t$  iterations.

### Self-Organising Map (SOM)

SOM is an instance of a self-organising map (Şişik & Eser, 2020). It is an unsupervised artificial neural network. Additionally, SOM employs competitive learning and dimension reduction. As shown in Figure 2, it creates a map representing the input space in a low-dimensional manner. In the 1980s, Kohonen invented this technique, and Kohonen Map got its name for this reason.

### Proposed SOM-KFCM

Our proposed method trains a SOM neural network on colour picture characteristics with and without a saliency map. All these steps are done to ensure that the output prototype vectors are filtered and aggregated using a k-means-based image segmentation assessment index. The method also has preprocessed and post-processing stages. Figure 3 depicts a comprehensive flowchart of the SOM-KFCM technique. This same flowchart is used for the SOM-Kmeans technique. The main difference here is that KFCM contains a saliency map module, but Kmeans does not have a saliency map.

**Self-Organising Map.** Unsupervised artificial neural networks like SOM, initially proposed by Kohonen, are extensively utilised (Song et al., 2021). In most cases, the map is a collection of prototype vectors representing node units in a two-dimensional space, although nodes may also be in a single or multiple spaces. For example, a neighbourhood function connects apartments to the apartments next door. Initialisation techniques for prototype

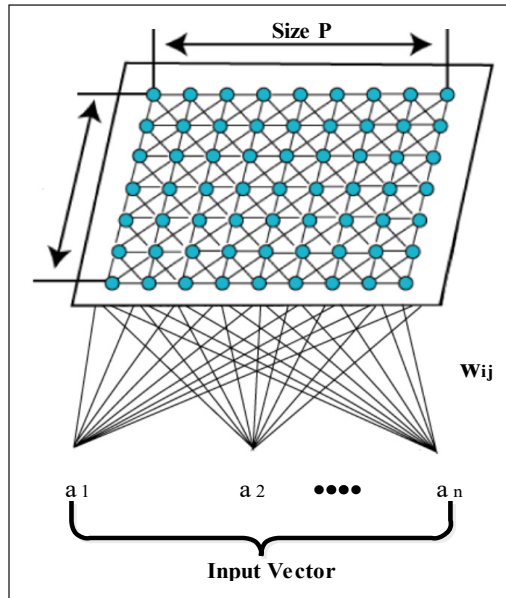


Figure 2. Fundamental architecture for SOM

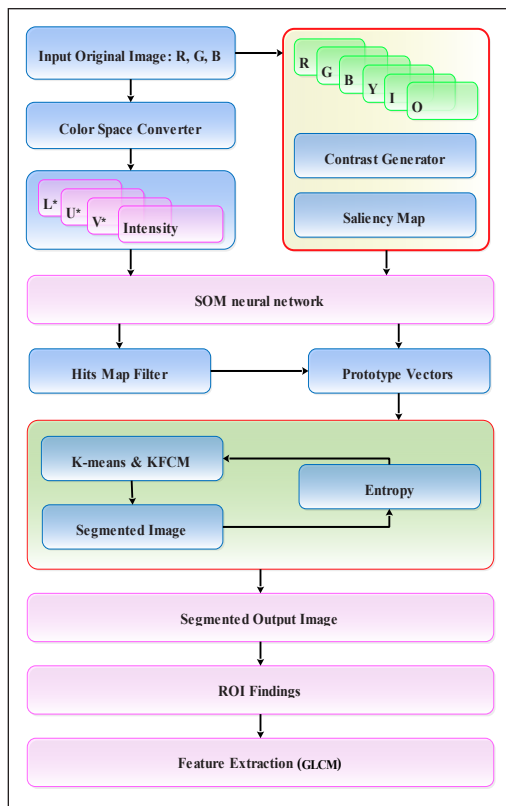


Figure 3. Architecture of SOM-KFCM technique

vectors are random and linear, then “folded” in a two-dimensional space. After that, they are trained sequentially or in batches using randomly chosen input samples and then updated based on the neighbours’ results. Once trained, the prototype velocities become stable and “unfold” in the two-dimensional space map. It is very uncommon for SOM to include capabilities like seeing a system’s topology and the ability to represent many different input patterns (such as those with  $p$  samples and  $m$  dimensions) using a minimal number of nodes. The nodes map is among SOM’s most significant features, representing the input patterns that are topologically close to one other in the output space.

According to Kohonen, a prototype vector  $w_i =$  exists for each node  $i$  [20-21]. ( $w_{i1}, w_{i2}, \dots, w_{im}$ ). The similarity rule chooses a winning node,  $c$ , for each input sample  $x$ . This node is represented by Equation 8.

$$c = \arg \min_i \{\|x - w_i\|\} \tag{8}$$

in other words, the same thing can be written as in Equation 9

$$\{\|x - w_i\|\} = \min_i \{\|x - w_i\|\} \tag{9}$$

where  $\|\cdot\|$  denotes the Euclidean distance between two points. Equation 10 updates the weights of the winning node  $c$  (prototype vector) and its neighbours’ nodes.

$$w_i(t + 1) = w_i(t) + h_{ci}(t)[x(t) - w_i(t)] \tag{10}$$

Equation 11 shows the winning node  $c$  neighbourhood function  $h_{ci}$ , and  $t$  is the current training iteration with input sample  $x(t)$  utilised. For example, the learning rate  $\alpha(t)$  and the neighbourhood function  $h$  reduce the iteration time and the distance between each source and destination node.

$$h_{ci}(t) = \alpha(t)(\|r_c - r_i\|, t) \tag{11}$$

where  $r_i$  and  $r_c$  are the locations of the winning nodes  $i$  and  $c$  in the topological map, respectively, and  $\alpha(t)$  is the learning rate.

This method is efficient even if the model vectors’ initial values do not match the data distribution. Because the previous strategy does not include a learning rate parameter, it has no convergence issue, and the asymptotic values of  $w_i$  are more stable than the original approach. Generally, a few repeats of this approach are sufficient (Vijh et al., 2020).

Each input sample has a maximum output node. When the input sample “hits” the node, it affects it. The more input samples a node has, the more hits it may return. Nodes in a 2-dimensional SOM map represent the structure of a multidimensional space inside

input feature patterns. SOM groups the nodes to organise the input feature patterns (pixels for an image).

Proposed SOM Algorithm:

- 1) SOM neurons' weights are set to random values at the start of the simulation.
- 2) The training data set randomly selects an input vector,  $x$ .
- 3) No distances exist between the input vector and any neurons or units. Therefore, the winning neuron is the one with the shortest distance.
- 4) When a winning neuron is found, its area is computed.
- 5) The weights of nearby neurons affected by the winning neuron (including the winning neuron) are shown by Equation 12. In other words, the input vector is becoming closer to the neurons.

$$w_v(t + 1) = w_v(t) + \beta(u, v, t)[x - w_v(t)] \quad [12]$$

Step 2 should be repeated as many times as iterations in  $N$ .

The current iteration,  $t$ , is assumed to be the iteration,  $v$  is the neuron index in the map,  $W_v$  is the current weight vector of the neuron  $v$ , and  $\beta(u, v, t)$  is the neighbourhood function.

**Kernel-FCM Clustering Algorithm.** The FCM method outperforms the Hard C-Mean (HCM) algorithm in terms of clustering accuracy. By incorporating the kernel approach into clustering, this study may successfully address the drawbacks of the FCM methodology. The Kernel FCM works by nonlinearly mapping the input model space  $R^s$  to high-dimensional feature space and then performing FCM clustering in high-dimensional feature space. The Mercer condition is the most extensively used nonlinear transformation. Usually, base kernel functions are polynomial and radial. A feature space is  $X = \{x_1, x_2, \dots, x_n\} \subset R^q$ , i.e., dataset  $R^s$  is mapped to a feature space  $R^q$ , where  $c$ , the number of classes to be separated is  $2 \leq c \leq N$ , and now the goal function is:

$$J_{km}(U, V) = \sum_{i=1}^c \sum_{j=1}^N \mu_{ij}^m \|\psi(x_j) - \psi(v_i)\|^2 = \sum_{i=1}^c \sum_{j=1}^N \mu_{ij}^m d_{kij}^2(x_j - v_i) \quad [13]$$

$$K=1,2,3,\dots,N \text{ and } i=1,2,3,\dots,c$$

In Equation 13,  $m$  denotes the control index of fuzzy, and  $\mu_{ij}$  is the membership degree of the  $j^{\text{th}}$  data pair  $i$ . The Euclid distance between  $R^q$  and the two vectors  $x_i$  and  $x_j$  may be expressed using the kernel function  $K$  in this chosen Equation 14.

$$d_{kij} = [K(x_i, x_i) - 2K(x_i, x_j) + K(x_j, x_j)]^{1/2} \quad [14]$$

When the Lagrange multiplier optimisation technique is used to solve Equations 15 and 16, the resulting objective function is as follows:



$$\mu_{ij} = \frac{\left(1/d_{kij}^2(x_j, v_i)\right)^{1/m-1}}{\sum_{i=1}^c \left(1/d_{kij}^2(x_j, v_i)\right)^{1/m-1}} \tag{15}$$

$$v_i = \frac{\left(1/d_{kij}^2(x_j, v_i)\right)^{1/m-1}}{\sum_{i=1}^N (\mu_{ij}^m K(x_j, v_i))} \tag{16}$$

The iteration is over when the last partition matrices U and V are found. Furthermore, KFCM can group a lot of different types of data. The only thing it does not give is how the classes work together. When the size of the data set changes a lot, the impact of clustering is not as significant as it could be.

## RESULTS AND DISCUSSION

The methodology of the proposed method was described above, and the results are shown in Tables 1 to 4 and Figure 4. Table 1 compares the proposed SOM-based Kmeans and KFCM algorithm’s average picture quality parameter values to those of other conventional image segmentation algorithms, which aids in verifying the algorithm’s efficiency.

Figure 4a shows the input images used to train the SOM neural network. An 8 x 8 map construction may be used to generate an efficient pixel classification procedure, and this map is provided as input to the KFCM method by the SOM. Consequently, a significant incentive for the re-clustered procedure to achieve the automated cluster centre is categorisation derived from the map structure. Finally, the scanned and segmented images identified the tumour and lesion areas.

SOM-based KFCM algorithm provides excellent segmentation; compared to the suggested SOM-based K-means method, an enlarged cyst tumour in the right hepatic lobe may be easily detected in Figures 4b and 4c. The proposed SOM-based K-means and KFCM method successfully segment the brain, lungs and liver, demonstrating the usefulness of identifying the tumour area. The work in this paper identifies brain tumours only. We mainly consider brain tumour segmentation as it is also suitable for other tumour segmentation, like support for lung and liver segmentation.

The results of the comparison of K-means and the KFCM method are shown in Tables 1, 2 and 3 in terms of simulated, statistical, and quality performance. Glioma and metastatic bronchogenic carcinoma patients’ brain tumours are shown in Figures 4b and 4c. The suggested SOM-based KFCM algorithm m’s input picture is shown in Figure 4a. The suggested technique clearly distinguished the tumour’s precise location and the surrounding grey and white matter.

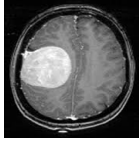
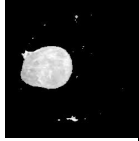

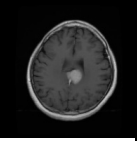
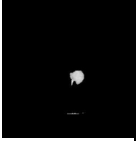
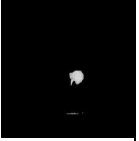
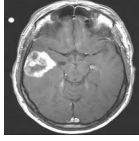
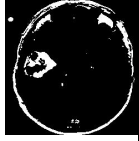
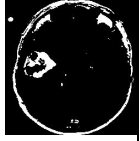
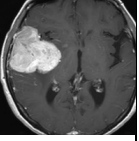
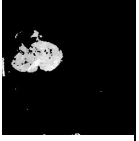

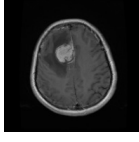
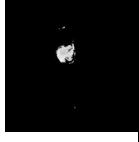

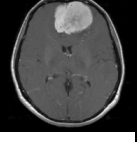
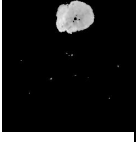

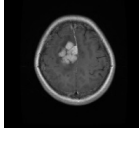
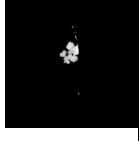
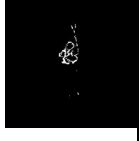
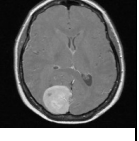
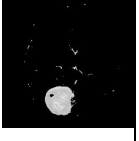
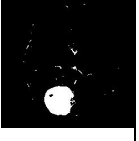
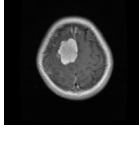
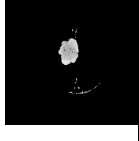

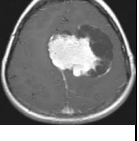
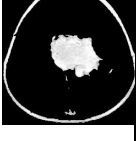

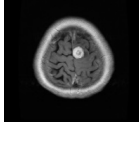


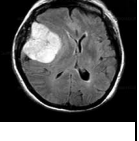
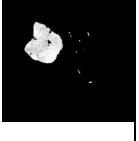

S. No	4a. Input images	4b. K-means tumor images	4c. KFCM tumor images	S. No	4a. Input images	4b. K-means tumor images	4c. KFCM tumor images
1				7			
2				8			
3				9			
4				10			
5				11			
6				12			

Figure 4. Segmented tumour detection and feature extraction results

A comparison of competing soft computing methods is shown in Tables 1 and 2, where the average values of evaluation parameters are shown. Compared to other conventional algorithms, the suggested SOM-based KFCM method has an average performance value Energy returns the sum of squared elements in the GLCM Range is [0 1], and the Energy is 1 for a constant image.

Table 3 demonstrates that the statistical metrics of Laplacian operators are similar to the ideal values. Measurement of Diagonal Laplacian (LAPD) focus yields somewhat improved results. For example, Mean Square Error (MSE) is a standard and fundamental metric for assessing distortion. There is a difference between the processed picture and

Table 1  
Simulated performance analysis

Images	SOM K-means				SOM-KFCM					
	Tumour Area	No. of Pixels	r_cr	r_bpp	n_cr	n_bpp	r_cr	r_bpp	n_cr	n_bpp
Flair_1	0.0968	6050	7.5170	1.0643	7.6107	1.0512	0.0916	0.9967	9.2046	0.8691
Flair_2	0.6076	37972	1.6049	4.9848	4.1569	1.9245	0.0884	0.9180	4.4307	1.8056
Flair_3	0.0128	803	45.6739	0.1752	9.8022	0.8161	0.0128	0.1752	9.8022	0.8161
Flair_4	0.0133	831	42.9141	0.1864	10.8713	0.7359	0.0064	0.0941	13.6461	0.5862
Flair_5	0.0227	1416	26.7776	0.2988	11.2469	0.7113	0.0117	0.1564	12.9963	0.6156
Flair_6	0.0192	1198	30.7650	0.2600	10.6781	0.7492	0.0210	0.2836	13.6580	0.5857
Flair_7	0.0082	515	67.9984	0.1176	10.5662	0.7571	0.0962	0.7822	8.6672	0.9230
Flair_8	0.0639	3991	10.9652	0.7296	6.4954	1.2316	0.0938	1.0811	5.2069	1.5364
T1_1	0.0519	3246	13.1438	0.6086	7.6676	1.0433	0.0165	0.1859	8.8903	0.8999
T1_2	0.0377	2354	18.0548	0.4431	8.3959	0.9528	0.0381	0.4485	8.3332	0.9600
T1_3	0.1500	9374	5.1773	1.5452	4.2875	1.8659	0.1416	1.4495	5.5427	1.4434
T1_4	0.0539	3366	12.6555	0.6321	8.6480	0.9251	0.0568	0.6714	6.6887	1.1961
T1_5	0.0963	6017	7.2026	1.1107	5.3920	1.4837	0.0343	0.4169	6.2587	1.2782
T1_6	0.0481	3009	14.3490	0.5575	13.0560	0.6127	0.0491	0.5714	13.0751	0.6118
T1_7	0.0177	1105	34.7120	0.2305	8.0915	0.9887	0.0931	0.8370	5.5873	1.4318
T1_8	0.0655	4095	10.6422	0.7517	6.5747	1.2168	0.0660	0.7583	6.5795	1.2159
T2_1	0.0109	680	58.6157	0.1365	8.4230	0.9498	0.0103	0.1270	11.4174	0.7007
T2_2	0.0118	740	47.8828	0.1671	11.9410	0.6700	0.0092	0.1289	16.1496	0.4954
T2_3	0.0104	648	55.3762	0.1445	13.3203	0.6006	0.0103	0.1433	13.3118	0.6010
T2_4	0.0136	853	41.8088	0.1913	11.1208	0.7194	0.0132	0.1849	11.1228	0.7192
T2_5	0.0157	979	38.7441	0.2065	12.2619	0.6524	0.0350	0.4413	16.6132	0.4815
T2_6	0.1394	8712	6.0914	1.3133	8.4356	0.9484	0.0133	0.1787	13.4958	0.5928
T2_7	0.0139	871	42.5996	0.1878	10.9917	0.7278	0.0133	0.1787	13.4958	0.5928
T2_8	0.0178	1110	34.1198	0.2345	10.5680	0.7570	0.0180	0.2381	10.5501	0.7583

\* cr - compression ratio, bpp - bits per pixel

Table 2  
*Statistical features analysis*

Images	SOM K-means				SOM-KFCM			
	Contrast	Correlation	Energy	Homogeneity	Contrast	Correlation	Energy	Homogeneity
Flair_1	0.19994	0.97675	0.99820	0.99643	0.20309	0.97518	0.82885	0.99637
Flair_2	2.16158	0.90728	0.98204	0.96140	1.37913	0.82609	0.81081	0.97537
Flair_3	0.12595	0.89907	0.97197	0.99775	0.12595	0.89907	0.97197	0.99775
Flair_4	0.13854	0.89267	0.97084	0.99753	0.26292	0.58188	0.98183	0.99531
Flair_5	0.18892	0.91328	0.99170	0.99663	0.34951	0.69311	0.96968	0.99376
Flair_6	0.45026	0.75658	0.98534	0.99196	0.47073	0.76772	0.94913	0.99159
Flair_7	0.05825	0.92756	0.98240	0.99896	0.92257	0.89216	0.80694	0.98353
Flair_8	0.37706	0.93570	0.98727	0.99327	0.38886	0.95340	0.82186	0.99306
T1_1	0.16531	0.96587	0.89778	0.99705	0.42350	0.73520	0.95879	0.99244
T1_2	0.25819	0.98759	0.92199	0.99539	0.26606	0.92620	0.92103	0.99525
T1_3	1.00601	0.99747	0.72406	0.98204	0.98082	0.91793	0.73649	0.98249
T1_4	0.19837	0.96043	0.89367	0.99646	0.21411	0.95937	0.88809	0.99618
T1_5	0.38729	0.95464	0.81794	0.99308	0.74073	0.77236	0.91870	0.98677
T1_6	0.13697	0.96962	0.90521	0.99755	0.13539	0.97053	0.90347	0.99758
T1_7	0.33376	0.99868	0.95836	0.99404	1.94117	0.76615	0.79255	0.96534
T1_8	0.15901	0.97360	0.87385	0.99716	0.17003	0.97196	0.87279	0.99696
T2_1	0.05510	0.99480	0.97727	0.99902	0.04880	0.95121	0.97859	0.99913
T2_2	0.05353	0.99535	0.97542	0.99904	0.04723	0.94716	0.98080	0.99916
T2_3	0.07557	0.98251	0.97786	0.99865	0.07557	0.92457	0.97801	0.99865
T2_4	0.14799	0.98883	0.96996	0.99736	0.13539	0.89423	0.97112	0.99758
T2_5	0.28181	0.98424	0.96332	0.99497	0.40618	0.87790	0.92389	0.99275
T2_6	1.07685	0.99087	0.73777	0.98077	0.07557	0.94146	0.97212	0.99865
T2_7	0.08974	0.97363	0.97058	0.99840	0.07557	0.94146	0.97212	0.99865
T2_8	0.12910	0.98478	0.96234	0.99769	0.13539	0.92228	0.96169	0.99758

the original, known as the MSE value. Significantly better outcomes are obtained with significantly greater MSE. As a result, Peak-Signal-to-Noise-Ratio (PSNR) is one of the most widely-used quality indicators in reconstructing consistency. In other words, a more significant PSNR number indicates a better reconstruction. Calculate the error by squaring the difference between the predicted and actual values and averaging it across the dataset. MSE is also known as Quadratic loss, as the penalty is not proportional to the error but

Table 3  
Quality performance analysis

Images	SOM K-Means						SOM-KFCM							
	Accuracy	Sensitivity	Specificity	Dice	Jacquard	MSE	PSNR	Accuracy	Sensitivity	Specificity	Dice	Jacquard	MSE	PSNR
Flair_1	0.861	0.843	0.866	0.764	0.882	0.319	53.124	0.986	0.995	0.304	0.180	0.545	0.098	58.274
Flair_2	0.597	0.597	0.748	0.597	0.988	17.435	35.751	0.869	0.871	0.225	0.126	0.430	0.202	55.106
Flair_3	0.908	0.986	0.845	0.731	0.882	1.280	47.093	0.875	0.999	0.072	0.037	0.671	0.038	62.313
Flair_4	0.914	0.994	0.826	0.703	0.893	1.843	45.510	0.717	0.996	0.044	0.023	0.715	0.041	61.996
Flair_5	0.922	0.986	0.820	0.694	0.908	1.565	46.219	0.760	0.967	0.091	0.047	0.758	0.053	60.957
Flair_6	0.909	0.905	0.786	0.647	0.910	0.867	48.784	0.781	0.999	0.164	0.090	0.776	0.048	61.318
Flair_7	0.899	0.970	0.839	0.722	0.873	2.669	43.901	0.742	0.996	0.427	0.271	0.714	0.076	59.331
Flair_8	0.291	0.122	0.210	0.117	0.856	4.468	41.664	0.953	0.928	0.788	0.650	0.956	0.093	58.465
T1_1	0.900	0.961	0.906	0.828	0.838	5.123	41.069	0.945	0.996	0.059	0.031	0.444	0.088	58.705
T1_2	0.860	0.892	0.861	0.756	0.830	5.824	40.513	0.515	0.972	0.133	0.071	0.497	0.132	56.964
T1_3	0.158	0.158	0.272	0.158	0.968	12.423	37.222	0.926	0.796	0.752	0.603	0.947	0.142	56.652
T1_4	0.876	0.845	0.854	0.746	0.899	5.260	40.955	0.935	0.996	0.237	0.135	0.613	0.081	59.083
T1_5	0.293	0.122	0.210	0.117	0.856	0.520	51.009	0.888	0.727	0.310	0.184	0.894	0.132	56.960
T1_6	0.898	0.893	0.837	0.720	0.900	5.533	40.736	0.878	0.988	0.259	0.149	0.703	0.055	60.765
T1_7	0.941	0.946	0.914	0.842	0.938	2.854	43.611	0.937	0.998	0.416	0.263	0.710	0.082	59.048
T1_8	0.800	0.860	0.833	0.714	0.719	5.498	40.763	0.850	0.996	0.194	0.107	0.411	0.078	59.226
T2_1	0.850	0.975	0.804	0.673	0.792	1.373	46.789	0.860	0.998	0.044	0.023	0.555	0.032	63.069
T2_2	0.926	0.955	0.873	0.775	0.915	1.621	46.066	0.991	0.928	0.056	0.029	0.688	0.028	63.764
T2_3	0.909	0.982	0.831	0.710	0.887	3.119	43.225	0.699	0.996	0.062	0.032	0.696	0.047	61.464
T2_4	0.913	0.994	0.825	0.702	0.893	0.482	51.331	0.724	0.972	0.089	0.047	0.720	0.039	62.268
T2_5	0.932	0.975	0.803	0.671	0.925	0.975	48.274	0.832	0.796	0.299	0.176	0.826	0.039	62.268
T2_6	0.888	0.889	0.775	0.633	0.888	0.461	51.524	0.713	0.999	0.084	0.044	0.709	0.043	61.816
T2_7	0.914	0.997	0.833	0.714	0.891	0.487	51.292	0.813	0.996	0.084	0.044	0.709	0.043	61.816
T2_8	0.916	0.997	0.830	0.710	0.895	0.467	51.474	0.930	0.928	0.118	0.063	0.725	0.047	61.478

Table 4  
Performance evaluation of different MRI segmentation techniques

Techniques	Sensitivity	Accuracy	Specificity	Dice	Jacquard	MSE	PSNR	FOM
<b>Proposed</b>								
SOM - K-means	0.827	0.913	0.758	0.644	0.884	3.436	45.329	0.77
SOM-KFCM	0.951	0.974	0.221	0.143	0.684	0.073	60.129	0.319
<b>Tarhini &amp; Shbib (2020)</b>								
Threshold	0.852	0.888	0.768	-	-	-	-	-
GLCM	0.721	0.814	0.667	-	-	-	-	-
SVM	0.912	0.721	0.899	-	-	-	-	-
CV model	85.868	0.849	82.65489	0.718	-	-	-	-
SOM	89.96	0.908	89.68526	0.801	-	-	-	-
<b>Sandhya et al. (2020)</b>								
FCM	87.86	0.864	84.85698	0.709	-	-	-	-
PSO	89.86	0.898	87.08646	0.797	-	-	-	-
ANN	90.96	0.916	91.31465	9.636	-	-	-	-
SOM ACM	97.36	0.981	95.91567	0.877	-	-	-	-
<b>Sandhya et al. (2019)</b>								
CV model	82.649	0.849	85.864	0.718	-	-	-	-
SOM	89.68	0.908	91.454	0.801	-	-	-	-
SOM ACM	95.91	0.981	97.358	0.877	-	-	-	-
<b>Şişik &amp; Eser (2020)</b>								
ELM-FRFCM	-	-	-	0.905505	0.841055	-	-	0.911115
SVM	-	-	-	0.187975	0.15142	-	-	0.158715
FCM	-	-	-	0.280995	0.176455	-	-	0.206845
SOM	-	-	-	0.28124	0.17214	-	-	0.219145
<b>Ejaz et al. (2020)</b>								
SOM K-means	-	-	-	0.988182	0.981818	0.04612	20.7352	-
SOM-FCM	-	-	-	0.973455	0.930636	0.2036	20.7464	-
<b>Asliyan &amp; Afbakan (2020)</b>								
K-Means	-	0.93	-	-	-	-	-	-
Fuzzy C-Means	-	0.92	-	-	-	-	-	-
SOM	-	0.88	-	-	-	-	-	-
Otsu	-	0.91	-	-	-	-	-	-
K-Means+Otsu	-	0.94	-	-	-	-	-	-

to the square of the error. Squaring the error gives higher weight to the outliers, which results in a smooth gradient for small errors. Optimisation algorithms benefit from this penalisation for large errors as it helps find the optimum values for parameters. MSE will never be negative since the errors are squared.

Table 4 shows the comparison with state-of-the-art different MRI segmentation algorithms. The proposed segmentation techniques provide a higher Peak single-to-noise ratio, and it has a minimum mean square error. The overall accuracy of the proposed SOM-Kernal FCM techniques provides an accuracy of 95.1% when compared to the other deep learning-based segmentation techniques. Here we take different image quality analyses of different images and compare the proposed method results with the recent techniques. In addition, our proposed work considers more features and compares them with the state-of-the-art SOTA methods. These are explained in Table 4.

## CONCLUSION

The proposed novel SOM-based KFCM technique for tumour segmentation identification was compared to other segmentation algorithms like K-means and FCM. The SOM-based KFCM segmentation method performs better than conventional methods, especially the SOM K-means method. The suggested method outperforms the KFCM and SOM-based KFCM techniques in PSNR. To summarise, the DOI value generated by the recommended approach is much greater than the traditional procedure. On the other hand, the proposed SOM-based KFCM method can identify tumours and segment tissues with high accuracy. Furthermore, the suggested methodology's operation may be improved, allowing it to segment noisy multimodal images.

## ACKNOWLEDGEMENT

The authors thank the faculty members ECE department at the S.V. University College of Engineering, Tirupati, Andhra Pradesh, India, for their encouragement and cooperation.

## REFERENCES

- Al-Dmour, H., & Al-Ani, A. (2018). A clustering fusion technique for MR brain tissue segmentation. *Neurocomputing*, 275, 546-559. <https://doi.org/10.1016/j.neucom.2017.08.051>
- Anaraki, A. K., Ayati, M., & Kazemi, F. (2019). Magnetic resonance imaging-based brain tumor grades classification and grading via convolutional neural networks and genetic algorithms. *Biocybernetics and Biomedical Engineering*, 39(1), 63-74. <https://doi.org/10.1016/j.bbe.2018.10.004>
- Asliyan, R., & Atbakan, İ. (2020). Automatic brain tumor segmentation with K-means, fuzzy c-means, self-organizing map and otsu methods. *Selçuk-Teknik Dergisi*, 19(4), 267-281.
- Balamurugan, K. M., Singh, P., & Ramalingam, V. (2021). A novel approach for brain tumor detection by self-organizing map (SOM) using adaptive network based fuzzy inference system (ANFIS) for robotic



- systems. *International Journal of Intelligent Unmanned Systems*, 10(1), 98-116. <https://doi.org/10.1108/IJUS-08-2020-0038>
- Baid, U., Talbar, S., & Talbar, S. (2017). Comparative study of k-means, gaussian mixture model, fuzzy c-means algorithms for brain tumor segmentation. *Advances in Intelligent Systems Research*, 137, 592-597.
- Ejaz, K., Rahim, M. S. M., Bajwa, U. I., Chaudhry, H., Rehman, A., & Ejaz, F. (2020). Hybrid segmentation method with confidence region detection for tumor identification. *IEEE Access*, 9, 35256-35278. <https://doi.org/10.1109/ACCESS.2020.3016627>
- Garcia-Lamont, F., Cervantes, J., López, A., & Rodriguez, L. (2018). Segmentation of images by color features: A survey. *Neurocomputing*, 292, 1-27. <https://doi.org/10.1016/j.neucom.2018.01.091>
- Guan, X., Yang, G., Ye, J., Yang, W., Xu, X., Jiang, W., & Lai, X. (2021). *3D AGSE-VNet: An automatic brain tumor MRI data segmentation framework*. ArXiv e-prints.
- Helmy, A. K., & El-Taweel, G. S. (2016). Image segmentation scheme based on SOM-PCNN in frequency domain. *Applied Soft Computing*, 40, 405-415. <https://doi.org/10.1016/j.asoc.2015.11.042>
- Huang, H., Yang, G., Zhang, W., Xu, X., Yang, W., Jiang, W., & Lai, X. (2021). A deep multi-task learning framework for brain tumor segmentation. *Frontiers in Oncology*, 11, Article 690244. <https://doi.org/10.3389/fonc.2021.690244>
- Krishnakumar, S., & Manivannan, K. (2021). Effective segmentation and classification of brain tumor using rough K means algorithm and multi kernel SVM in MR images. *Journal of Ambient Intelligence and Humanized Computing*, 12(6), 6751-6760.
- Kumar, K. A., Kumar, B. M., Veeramuthu, A., & Mynavathi, V. S. (2019). Unsupervised machine learning for clustering the infected leaves based on the leaf-colors. In D. K. Mishra, X. S. Yang & A. Unal (Eds.), *Data Science and Big Data Analytics* (pp. 303-312). Springer.
- Kumar, S. A., Harish, B. S., & Shivakumara, P. (2018). A novel fuzzy clustering based system for medical image segmentation. *International Journal of Computational Intelligence Studies*, 7(1), 33-66.
- Mohan, G., & Subashini, M. M. (2018). MRI based medical image analysis: Survey on brain tumor grade classification. *Biomedical Signal Processing and Control*, 39, 139-161.
- Mohan, G., & Subashini, M. M. (2019). Medical imaging with intelligent systems: A review. In A. K. Sangaiah (Ed.), *Deep Learning and Parallel Computing Environment for Bioengineering Systems* (pp. 53-73). Academic Press.
- Osman, A. H., & Alzahrani, A. A. (2018). New approach for automated epileptic disease diagnosis using an integrated self-organization map and radial basis function neural network algorithm. *IEEE Access*, 7, 4741-4747.
- Ren, T., Wang, H., Feng, H., Xu, C., Liu, G., & Ding, P. (2019). Study on the improved fuzzy clustering algorithm and its application in brain image segmentation. *Applied Soft Computing*, 81, Article 105503. <https://doi.org/10.1016/j.asoc.2019.105503>
- Sandhya, G., Kande, G. B., & Satya, S. T. (2019). An efficient MRI brain tumor segmentation by the fusion of active contour model and self-organizing-map. *Journal of Biomimetics, Biomaterials and Biomedical Engineering*, 40, 79-91. <https://doi.org/10.4028/www.scientific.net/JBBBE.40.79>

- Sandhya, G., Kande, G. B., & Savithri, T. S. (2020). Tumor segmentation by a self-organizing-map based active contour model (SOMACM) from the brain MRIs. *IETE Journal of Research*, 1-13. <https://doi.org/10.1080/03772063.2020.1782780>
- Sheela, C., & Suganthi, G. J. M. T. (2020). Morphological edge detection and brain tumor segmentation in magnetic resonance (MR) images based on region growing and performance evaluation of modified fuzzy C-means (FCM) algorithm. *Multimedia Tools and Applications*, 79(25), 17483-17496. <https://doi.org/10.1007/s11042-020-08636-9>
- Şişik, F., & Eser, S. E. R. T. (2020). Brain tumor segmentation approach based on the extreme learning machine and significantly fast and robust fuzzy C-means clustering algorithms running on Raspberry Pi hardware. *Medical Hypotheses*, 136, Article 109507. <https://doi.org/10.1016/j.mehy.2019.109507>
- Soltaninejad, M., Yang, G., Lambrou, T., Allinson, N., Jones, T. L., Barrick, T. R., Howe, F. A., & Ye, X. (2018). Supervised learning based multimodal MRI brain tumour segmentation using texture features from supervoxels. *Computer Methods and Programs in Biomedicine*, 157, 69-84. <https://doi.org/10.1016/j.cmpb.2018.01.003>
- Song, Q., Wu, C., Tian, X., Song, Y., & Guo, X. (2022). A novel self-learning weighted fuzzy local information clustering algorithm integrating local and non-local spatial information for noise image segmentation. *Applied Intelligence*, 52(6), 6376-6397. <https://doi.org/10.1007/s10489-021-02722-7>
- Tarhini, G. M., & Shbib, R. (2020). Detection of brain tumor in MRI images using watershed and threshold-based segmentation. *International Journal of Signal Processing Systems*, 8(1), 19-25. <https://doi.org/10.18178/ijsp.8.1.19-25>
- Vijh, S., Sharma, S., & Gaurav, P. (2020). Brain tumor segmentation using OTSU embedded adaptive particle swarm optimization method and convolutional neural network. In J. Hemanth, M. Bhatia & O. Geman (Eds.), *Data Visualization and Knowledge Engineering* (pp. 171-194). Springer. [https://doi.org/10.1007/978-3-030-25797-2\\_8](https://doi.org/10.1007/978-3-030-25797-2_8)
- Vishnuvarthanan, A., Rajasekaran, M. P., Govindaraj, V., Zhang, Y., & Thiyagarajan, A. (2017). An automated hybrid approach using clustering and nature inspired optimization technique for improved tumor and tissue segmentation in magnetic resonance brain images. *Applied Soft Computing*, 57, 399-426. <https://doi.org/10.1016/j.asoc.2017.04.023>
- Zhang, W., Yang, G., Huang, H., Yang, W., Xu, X., Liu, Y., & Lai, X. (2021). ME-Net: multi-encoder net framework for brain tumor segmentation. *International Journal of Imaging Systems and Technology*, 31(4), 1834-1848. <https://doi.org/10.1002/ima.22571>
- Zhang, Z., & Sejdíć, E. (2019). Radiological images and machine learning: Trends, perspectives, and prospects. *Computers in Biology and Medicine*, 108, 354-370. <https://doi.org/10.1016/j.compbiomed.2019.02.017>

*Review Article*

## Reliability Components of Online Teaching and Learning Tools in Lesotho Higher Education Institutions: A Systematic Review

Musa Adekunle Ayanwale\*, Paseka Andrew Mosia, Rethabile Rosemary Molefi and Liapeng Shata

*Department of Educational Foundations, Faculty of Education, National University of Lesotho, Lesotho*

### ABSTRACT

Electronic learning is a techno approach that brings new opportunities for teaching and learning in many fields of education compared to the traditional classroom environment. However, there is a dearth of research on its effectiveness in practicality and whether it is dependable enough during teaching and learning. Thus, this systematic review aims to provide evidence from numerous findings on the reliability components (such as functionality, probability of success, environment, and duration) of online teaching and learning (OTL) tools in Lesotho higher education institutions (HEIs), focusing on functionality and probability of success only. A review of online learning tools includes Thuto, Google Meet, Google Classroom, Zoom, Moodle, and Microsoft Teams. Technology adoption models and Siemens' theory of connectivism underpin this review. The review covered 18 articles between 2015 and 2021. Scopus, Google Scholar, ProQuest, and EBSCO were used for data search. In addition, selected studies were reviewed by experts in Educational Technology at the National University of Lesotho. Some factors were found to hinder the functionality and success of OTL tools, including lack of internet connectivity, electricity, and gadgets. As a result of this review, OTL tools are effective to some extent in terms of functionality and likelihood of success. However, the weaknesses of the e-learning tools outweigh the strengths of Lesotho HEIs. Consequently, only using OTL tools could hamper the quality of higher education in Lesotho. In HEIs, blended learning and continuous training on e-learning tools should be introduced for effective teaching and learning.

#### ARTICLE INFO

*Article history:*

Received: 09 April 2022

Accepted: 12 July 2022

Published: 27 December 2022

DOI: <https://doi.org/10.47836/pjst.31.1.34>

*E-mail addresses:*

ma.ayanwale@nul.ls (Musa Adekunle Ayanwale)

pa.mosia@nul.ls (Paseka Andrew Mosia)

rethabile68@gmail.com (Rethabile Rosemary Molefi)

shataliapeng01@gmail.com (Liapeng Shata)

\* Corresponding author

*Keywords:* Higher education institutions, online learning tools, online teaching, and learning, reliability components

## INTRODUCTION

Learning has recently extended mainly from the traditional face-to-face encounter in the classroom to the virtual environment. E-learning education, called online learning, takes place over the internet. Aderson (2016), Mpungose (2020b), and Sadiku et al. (2018) asserted that due to its flexibility, online teaching and learning (OTL) accommodates and engages different students in the comfort of their own space and time. One of the reasons for offering online courses is that it is easy and convenient for students to complete a higher degree. Dhull and Sakshi (2017) opine that it also helps students learn at their own pace and convenience. The key to successfully implementing OTL is taking student characteristics into account. It implies that strategies that work for conventional full-time students may not be effective for adult students with full-time jobs and family responsibilities. These students (the former) are mostly practically-oriented with a keen interest in tools and technologies (Sadiku et al., 2018).

More importantly, the introduction of OTL has proven to be challenging in sub-Saharan African countries (such as Zimbabwe, Ghana, Namibia, South Africa, Zambia, and Lesotho) due to internet access, poor connectivity, exorbitant data bundle, and frequent power interruptions (Henaku, 2020; Tamrat & Teferra, 2020; Makumane, 2021). In addition, the literature highlights more deficiencies in effective online implementation, such as the weakness of online teaching infrastructure, teachers' inexperience, the information gap, and the complex environment at home (Ali, 2020; Murgatroid, 2020). Nonetheless, OTL has consistently focused on education research for decades. Moreover, with the upsurge of Coronavirus (COVID-19) worldwide, it became even more relevant since the global decision to shut down higher education institutions (HEIs) was rational to keep social distancing to stop its spread. As a result, countries worldwide, including Lesotho HEIs, migrated to OTL immediately. However, for online learning to run smoothly, Dhull and Sakshi (2017) and Makumane (2021) argue that digital technologies, such as text and video communication applications, cloud-based video conferencing services, and learning management systems (LMS), must be accessible to students and their teachers or lecturers. For instance, the National University of Lesotho used online learning tools such as Zoom, Google Meet, and Thuto for effective teaching, learning, and assessment processes since the outbreak of COVID-19.

Lesotho is currently a progressive country to better its educational system by teaching its inhabitants. The Curriculum Assessment Policy (CAP) mandates show that the country is committed to being better in the future. CAP's goals can illustrate this to provide pupils with the knowledge, attitudes, and skills they will need to adapt to socio-economic and technological changes. It also aims to promote aesthetic and creative skills through different forms of literary work and promote a sense of cooperation and service to others (Ministry of Education and Training, 2008). The policy also emphasizes modern educational pedagogies

that can help students develop creativity, independence, and survival skills. For all these to be achieved, the policy acknowledges that the new trend should be a shift from teaching to assisting learning; from facts to knowledge production by students; and from information memory to information analysis, synthesis, evaluation, and application; from knowledge acquisition to development of knowledge, skills, values, and attitudes.

Conversely, the resources to help facilitate this new innovative kind of learning are inadequate, particularly in the context of Lesotho. For instance, many students originate from rural areas and vulnerable families, and learning through e-learning poses a serious challenge because of their socio-economic background (Hlojeng & Makura, 2020). Several students come from poverty-stricken families and can barely afford data units or buy a smartphone and a laptop. Besides that, the country itself has poor infrastructure for OTL. Many areas do not have access to electricity, and schools and homes lack Information Communication Technology (ICT) infrastructure like the accessibility of Wi-Fi facilities. Moreover, schools are not capacitated enough with computers to allow students to learn.

Through the above-captured scenario, this study found it very significant to check the effectiveness of online learning tools used in Lesotho's HEIs. Most previous studies on e-learning have rarely examined the effectiveness of e-learning tools in Lesotho. The digital divide (DD)—the gap between those who have and do not have access to computers and the internet—significantly limits the probability of using Lesotho OTL tools. Nevertheless, it is undeniable that digital technologies have great potential to elevate the education systems in developing countries. Thus, this study reviewed the reliability components of online and teaching tools in Lesotho's HEIs. The purpose of the study is to establish the extent to which e-learning tools are effective, looking at their functionality and probability of success only. The study is poised to use the following questions to guide the review. These include how accessible is teaching and learning offered through online tools. Are instructors and students trained for online teaching and learning? Moreover, are the online learning and teaching tools user-friendly? As a result, the preceding questions will aid in evaluating e-learning tools' functionality and probability of success and delve deep into understanding the phenomenon being studied.

### **The Underpinning Theory**

To reach out to rapidly evolving knowledge, George Siemens has proposed a new theory called Connectivism. This hypothesis is more concerned with decentralizing information and networking (Siemens, 2005; Mpungose, 2020b). Learners can access material through digital devices from anywhere and at any time. As they do so, they connect or, to put it in another way, network with other people through online platforms. As a result, the inference is that learning with connectivism is more at learners' disposal. This theory provides a lens into looking deeper at the effectiveness of e-learning tools. That is, as much as the

information is decentralized, it is accessible to everyone, everywhere. The connectivism also blends well with the technology adoption model. This model's strength lies in its simplicity. It has only two constructs; the perceived usefulness and ease of predicting the extent of adopting new technologies at each individual's level (Lai, 2017). This model postulates that it can be beneficial if people find technology easy to use. This theory helps see the actual problem, for instance, students' and instructors' attitudes towards e-learning tools—how they relate to the devices. For example, old-aged lecturers may find it challenging to navigate e-learning tools and need to relate better. However, the reliability of e-learning may be effective for the youth since they find it easy and interesting to maneuver—thus, a good relationship between a child and a tool. As a result, this review is underpinned by Siemens' theory of connectivism and technology adoption model.

## MATERIALS AND METHODS

Inclusion and exclusion criteria for screening relevant studies employed the assistance of two educational technology experts at NUL to review selected studies. The inclusion criteria were based on online learning articles published between 2015 and 2021. The rationale for choosing this period is that the researchers were looking for the most recent publications and literature that discussed reliability components of e-learning, those written in English only, those that collected data from e-learning evaluation, and finally, full-text articles. In addition, articles were excluded if their focus was not on the Lesotho context, were not written in English, and their year of publication was before 2015. Finally, the abstracts, editorial comments, and editor letters were excluded. Figure 1 presents the flowchart of the systematic review.

### Search Strategy

Systematic reviews use an explicit search strategy to guide studies' inclusion and exclusion criteria in a review. This study used electronic and manual searches. A comprehensive search through international

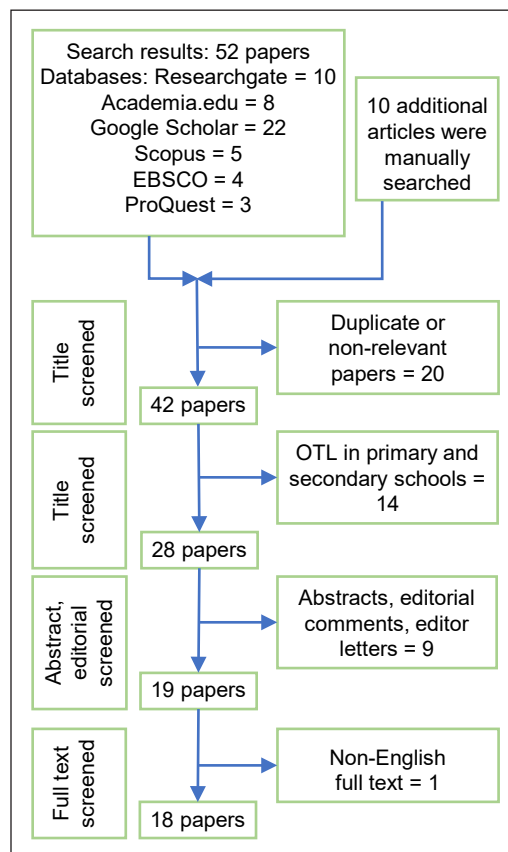


Figure 1. Flowchart of the systematic literature review

databases: ProQuest, Google Scholar, Scopus, EBSCO, and general internet search engines such as Google search bibliographic database identified a dataset of 52 articles from which 11 academic papers met the inclusion criteria for OTL in Lesotho. Also, online academic sites like Researchgate and academia.edu have used the four most relevant articles for this review while using these databases. These were considered appropriate because they give more relevant results with stable information. Finally, they are the most popular educational databases to which the study belongs. This review included the following search terms in electronic search: online teaching and learning, online learning tools, reliability of OTL in any field of education in Lesotho, and the effectiveness of online learning tools. Academic papers from which five were manually searched met the inclusion criteria of OTL in Lesotho.

### **Selection of Studies**

Following the objective of this study, which sought to examine the effectiveness of OTL in Lesotho, this study employed a qualitative content analysis method. Findings derived from 18 articles were analysed qualitatively. It used the interpretivism approach to seek the deeper meaning of research. Interpretivism is a paradigm in which researchers do not predict people's actions. Instead, it describes how people make sense of their worlds and create meaning in their actions (Creswell & Poth, 2017). This review used this paradigm to focus on the effectiveness of OTL in HEIs. This paradigm gives an in-depth understanding of reflections and the reasons that inform them about using OTL tools. Only articles on OTL, e-learning and technological learning were included. The literature review in this study was limited to articles published in academic journals between 2015 and 2021. Articles published in the English Language were selected for the review.

## **RESULTS AND DISCUSSION**

Of the 18 studies included in this review, they were all conducted in Africa. Table 1 summarises the articles included in this review. It shows the author, year of publication, paper title, type of paper, participants, and the results.

There are several factors to be considered for effective OTL, such as internet connectivity, data availability for learning, availability of e-resources for learning, students' attitudes, lecturers' and students' knowledge and skills on the usage of e-resources (Henaku, 2020; Makafane & Chere-Masopha, 2021; Mashinini, 2020; Oketch-Oboto, 2021). The findings below reveal the determining factors for effective OTL, as aforementioned. It is done to gather enough information from the literature to conclude whether OTL is reliable in Lesotho's HEIs.



Table 1  
Summary of the articles included in this review

Authors	Year of publication	Paper title	Type of paper	Participants	Findings
Makumane	2021	Students' perceptions of the use of LMS at a Lesotho university amidst the COVID-19 pandemic	interpretive case study	10	Students' unique experiences with the LMS proved to have a bearing on the content acquired and the efficiency of technological knowledge in attaining goals.
Oketch-Oboth	2021	Online learning challenges, stress experience, and coping strategies among university students during the lockdown due to the COVID-19 pandemic	questionnaire	90 male and 70 female students	Students were concerned with the uncondusive learning environment, internet connectivity problems, inadequate training on online learning platforms, unreliable power supply, cost of internet bundles, and lack of online learning equipment like laptops.
Makafane and Chere-Masophia	2021	COVID-19 Crisis: Challenges of Online Learning in one University in Lesotho.	qualitative approach	12 undergraduate students in the Faculty of Education	The findings of this study suggest that the challenges that the students experienced were mainly influenced by their attributes, pedagogical issues, and how the university supported them
Maphosa	2020	Using the MyLSU app to enhance student engagement and promote a smart town at a rural university in Zimbabwe	design science research	220 participants	The app was usable and easy to learn, and they would recommend it to others and agreed that they could use it without assistance. The results show that the app promoted student engagement and promoted concepts of a smart town
Henaku	2020	COVID-19: Online Learning Experience of College Students: A Case of Ghana	Systematic review	21 studies	Students from Asia and Africa had an unfavorable view of online learning during Covid-19.
Mpfungose	2020b	The emergent transition from face-to-face to online learning in a South African University in the context of the Coronavirus pandemic	qualitative research	26	The Digital divide hinders students from realizing the full potential of e-learning. However, lecturers still want students to submit assessment tasks and engage with Moodle learning management system course activities.
Sepiriti	2021	investigating the effects of using the Thuto learning management system	Qualitative inquiry	NUL students	Thuto LMS is ideal during the Covid-19 era since learning still happens but has many challenges.

Table 1 (continue)

Authors	Year of publication	Paper title	Type of paper	Participants	Findings
Letseka et al.	2018	The Challenges of E-learning in South Africa.	Quantitative research	None	Modern technological devices in the form of information and communication technologies (ICTs) and access to the Internet are perceived to be ubiquitous.
Pete and Soko	2020	Preparedness for Online Learning in the Context of COVID-19 in Selected Sub-Saharan African Countries	Qualitative research: questionnaires	2,341 respondents (855 lecturers and learners from Ghana, 842 from Kenya, and 644 from South Africa)	There was an extremely low level of satisfaction with the internet connection, cost, and reliability
Mataka et.al	2020b	UNIVERSITIES IN PANDEMONIUM AS COVID-19 WREAK HAVOC: A CASE OF TWO CONVENTIONAL UNIVERSITIES IN SOUTHERN Africa	Qualitative research Surveys	Students, lecturers, administrators	Lack of preparedness in institutions became a source of confusion and uncertainty among students.
Mpungose	2020a	Beyond limits: Lecturers' reflections on Moodle uptake in South African universities	qualitative case study	31 lecturers	The study revealed that the top-down imposition of mandatory Moodle implementation was resisted by lecturers, hindering uptake, and maximum potential took time to measure.
Mashimini	2020	COVID-19 and National University of Lesotho: Experiences and Challenges	questionnaire	50 NUL students	THUTO network system experienced overloads; some lecturers had to be trained on its use, some students could not access it due to a lack of connection at their homes, and others could not afford data for access even after partnerships with some service providers to zero-rate access
Mpungose	2021	Students' Reflections on the Use of the Zoom Video Conferencing Technology for Online Learning at a South African University	An interpretive qualitative case study	26 students	The study found that Internet access was a major challenge. While most students enjoyed synchronous Zoom discussions, they could not use other Zoom functions for effective engagement.

Table 1 (continue)

Authors	Year of publication	Paper title	Type of paper	Participants	Findings
Dube	2020	Rural Online Learning in the Context of COVID-19 in South Africa: Evoking an Inclusive Education Approach	Participatory action research	Ten students and five teachers	Many rural learners are excluded from teaching and learning due to a lack of resources to connect to the internet, the learning management system, and low-tech software.
Hussaini et al.	2020	Effectiveness of Google Classroom as a Digital Tool.	Survey research design	198 students	Google Classroom effectively improves students' access and attentiveness towards learning, knowledge, and skills gained through Google Classroom, makes to be active learners; however, a poor network hinders students from effectively utilizing Google Classroom, thus submitting late.
Amponsah et al.	2021	Academic experiences of "zoom-Fatigue" as a virtual streaming phenomenon during the COVID-19 pandemic	exploratory multiple-case study design	Eight academics	It was found that the participants viewed video conferencing during the COVID-19 lockdown period as an exhausting experience. However, a second major finding revealed that the participants were empowered with digital literacy skills to use video conferencing effectively. The current findings add to a growing body of literature on video conferencing, focusing on Zoom fatigue.
Awad et al.	2019	Evaluating learning management system usage at a small university	Survey and data log generated from event logs	25% sample of the faculty and 15% of students	Efficiency and saving time are essential benefits of any LMS. However, these are only some benefits, and many argue they are not the most important. To fully utilize Blackboard or any LMS, it is crucial to take advantage of the many tools they boast, especially those that improve student interaction and increase engagement.
Mafa	2018	Capabilities of Google Classroom as a Teaching and Learning Tool in Higher Education	A quantitative questionnaire	36 third-year healthcare service management learners	Google Classroom is compelling in educating and learning; thus, it improves teaching and learning.

## **Addressing the Probability of Success of Online Teaching and Learning Tools as a Reliability Component**

**How Accessible are the Teaching and Learning Offered Through Online Tools?** It is apparent that in the context of Lesotho, the quality of education is negatively obstructed in HEIs like Limkokwing University of Creative Technology (LUCT), National University of Lesotho (NUL), Lesotho Agricultural College (LAC) as well as Centre for Accounting Studies (CAS). Many students come from disadvantaged families that cannot even buy data or a laptop and phone for their children to access the internet for teaching and learning. Maphosa (2021) indicated that most respondents clarified that one of the main drawbacks of online learning is that it is costly in terms of data. This is in congruence with teachers' views in Tanzania, who revealed that their main challenge is internet costs to deliver online content (Maphosa, 2021; Mfaume, 2019). Also, Mashinini (2020) agrees that sometimes students need more data to sustain them throughout the allocated time of the meeting. Similarly, Henaku's (2020) results disclose that participants highlighted that using OTL tools is financially draining, and the cost may negatively affect accessibility.

Most students in the above-captured HEIs complained that data bundles are costly, especially if one has to use Zoom and Google Meet for all lectures. This notion is supported by Oketch-Oboth (2021), that most students indicated that bundles were too expensive at the time. Likewise, Dube (2020) participants reported that data is too expensive and beyond reach for many who stayed in rural communities. Moreover, a survey conducted by Mataka et al. (2020a) indicated that students have smartphones but accessing data for daily learning activities is costly. They argued that the charges for data are exorbitant, significantly worse if one is online for a long time. The issue of data cost is further revealed by Mataka et al. (2020b), where parents stated their main worry is the data costs required for students to access the OTL tools.

### **Internet Connectivity**

Because of poor infrastructure in remote villages, network speed and stability is poor. Therefore, learning through e-learning poses a severe challenge to students from such areas since tools like Zoom require strong internet. It slows down students' participation, which leads to poor understanding and process of learning, consequently negatively impacting the educational development of Lesotho. In Henaku's (2020) study, participants indicated that learning through Zoom and Google meet was problematic due to poor mobile networks. This network problem sometimes takes a long time before an audio or video can be downloaded, and when it is downloaded, many questions have already been asked, which confuses students. In addition, students have to download Google Meet before joining the class. Because of network problems, some students could not download Google Meet and failed to join the class. Henaku (2020) further portrays that students have difficulties

accessing Zoom because of network problems at their places, thus leading them to miss what teachers taught or ideas shared by other students. The issue of internet connectivity as a primary concern to most students is further addressed by Oketch-Oboth (2021), where the majority of students indicated that they were experiencing poor internet connectivity while a minority of students did not have accessible internet services at home.

Mpungose (2020b) studied 26 HEIs students in South Africa who were used as a sample to examine their experiences transitioning from face-to-face classroom to e-learning; the results remarked that students encountered the problem of internet connectivity. It is due to the digital divide limiting most students from effective e-learning, particularly those staying in remote areas and with low socio-economic status. For instance, a student confirmed this by stating that she only checked her emails from the community library with internet access because there is no internet access and network service at her homestead. Internet access plays a significant part in observing effective e-learning, but this can never be achieved if students have limited or no access to the internet. For more clarity, another student asserted that submitting was impossible because of a lack of internet access at home. This statement proves that assessing students online is difficult if the students have no access to the internet.

For this reason, most students become nervous when their instructors demand them to submit their work within the required time when they do not have internet access. The study of Dube (2020) also revealed that despite online learning being one of the best ways of learning, the unavailability of internet connectivity in some rural areas hampers innovation. For instance, one of the participants posited that it is difficult to access online learning materials. This position is further sustained by Hussaini et al. (2020), where students indicated that they find it challenging to submit their assignments on time because of the poor network in the university. They further state that there is no free functional Wi-Fi in the school.

Conversely, Letseka et al. (2018) findings disclosed that most students who participated in accessing and using MyUnisa learning management system had ample access to the internet, and only a minority of students did not. Most students accessed it from home and work. Pete and Soko (2020) remark that assessing the following online tools, Moodle, Google Classroom, and Zoom in Ghana, South Africa, and Kenya's universities reveals that internet services were affordable and adequate for students and lecturers. They were accessed at campus and the workplace, implying that respondents accessed them free of charge. Letseka et al. (2018) and Pete and Soko's (2020) views are much similar to the NUL postgraduate students who can access the Wi-Fi in the university. Still, the internet connection is terrible, so bad that they miss important information from the lecturer. Pete and Soko (2020) further portray this argument that as much as the internet services were affordable and adequate, lecturers and students were asked about the extent to which they are satisfied with an internet connection, and most respondents expressed dissatisfaction.

In addition, most respondents were dissatisfied with these tools' internet speed and stability. They discovered that platforms like Zoom require a strong internet connection, so the video is affected, which calls for internet providers to strengthen their signals and develop e-learning platforms (Pete & Soko, 2020).

### **Teachers' and Students' Knowledge and Skills in the Usage of e-Resources**

Mpungose (2020a) conducted case study research on 31 South African lecturers from two universities and tested their efficiency using the Moodle learning management system. Results revealed that lack of training on using Moodle LMS hindered smooth online teaching and learning since students depended on lecturers for curriculum dissemination and supplementation of other relevant materials that needed to be uploaded by the lecturers. Most lecturers claimed they knew how to use Moodle LMS lesson activity theoretically, but practically it became a problem for them to apply it successfully. They even added that they attend Moodle LMS workshops only once a year. Others added that they failed to upload quizzes for grading because of inadequate training on the system. Mpungose's (2021) findings disclose that students had inadequate knowledge of using hardware and software resources for learning. One of the participants noted that they did not know that they had to download the Zoom app before joining the meeting. The participant said he only realized that Zoom was plugged in on the Moodle LMS while submitting his assignment. Most participants in their first year of studies agreed that training would improve the use of Zoom and other technological resources. Another student indicated she could be given training manuals; she can practice different functions of all Zoom and Moodle.

Mpungose's (2020b) explorative case study reveals that students were not prepared thoroughly by their lecturers to study online, to add to inadequate training on online learning tools. His participants opined that the sudden shutdown had hindered effective ways to be trained to access lectures online. Additionally, they lamented that they were not told which online platform would be used for online lectures. Furthermore, on the lack of facilitators' training for e-resources, Makafane and Chere-Masopha (2021) highlight that students in their study explained that their lecturers had turned the University LMS (Thuto) as a platform for dumping unexplained lecture notes and assignments. Their findings further indicate that the university was not doing enough to support online learning, particularly by making digital infrastructure and resources available and accessible to ensure that students were not disadvantaged. Following, Makafane and Chere-Masopha's (2021) findings pointed out that though the content taught through Thuto is comprehensive, communication is difficult because students have to make an appointment first. In addition, some concepts could be better elaborated to clarify some concepts on other platforms that do not limit self-expression, such as WhatsApp and Zoom.

The study by Henaku (2020) further indicates that students felt they needed adequate training on the e-learning platforms such as Zoom, Google Meets, and WhatsApp. Furthermore, Mataka et al. (2020a) discovered that using Zoom and other platforms that allow virtual meetings will be a severe drawback because not all students will participate in OTL. Lecturers also noted their main concern of training online platforms to reach the students because some need to learn how to use them (Mataka et al., 2020a). Dube (2020) further portrays this issue by reporting that most rural teachers in South Africa could not access online learning tools, thus hampering effective and efficient learning and teaching processes.

The World Bank (2020) also highlights that only a few classroom teachers have been trained in online instructional approaches and tools. As reported in Mpungose (2021), a case study finding on 26 students revealed that students were not equipped with functional knowledge and skills to use hardware and software resources (tools) for online teaching and learning. Some first-year students' reflections are that access is a challenge because they are not given the laptops promised to them since the first semester. One student noted that she did not know how to use OTL tools or even have a smartphone.

Meanwhile, Mpungose (2020a) disclosed that there were those lecturers who found online learning platforms convenient to use. For instance, one lecturer explained that he uses Moodle LMS to facilitate student discussion. His entire informal assessment task uses Moodle LMS resources because he asserts that results are readily displayed for students' feedback. In addition, Amponsah et al. (2021) findings reveal that many zoom and Teams video conferencing technology participants affirmed they had pre-requisite digital literacy skills and information about online teaching. They said Teams is a video conferencing approach, a spontaneous online teaching experience. One participant outlined that her experience with Zoom or Teams as online tools has improved her knowledge base with technology.

Similarly, another participant pointed out that Teams had positively impacted his knowledge of using these and other online tools. In addition to LMS convenience, Maphosa's (2021) study results in the 2021 survey disclosed that online teaching was easy for most respondents. Awad et al. (2019) showed that most faculty members found online learning easy to use. For Maphosa (2021), survey results reveal that a higher percentage of teachers approved that online learning, primarily through WhatsApp, supported and promoted collaborative learning and interaction between students and teachers and between students. In contrast, a lower percentage disagreed, and the lowest percentage vehemently opposed.

The study by Mafa (2018) demonstrates that students can work, read, and do their schoolwork in harmony or without being pushed by their schoolmates using Google Classroom. He further shows that students can individually respond to the teacher's



instructions in their own space and time. Since learning never stops, it goes past classroom contacts; for this reason, students are encouraged to learn online through Google Classroom, and a greater part of them are confirmed to be encouraged to utilise Google Classroom in their learning. The views asserted above are much similar to opinions from some of the HEIs in Lesotho, which argue Teams app used in one of the HEIs in Lesotho is easily accessible for students to receive and send their schoolwork using this app.

### **Availability of Devices for Learning**

Mpungose (2021) study revealed the inaccessibility of hardware resources and the internet for learning. A participant commented: “e-learning is frustrating me when I am home because I do not have necessary resources like laptops and Wi-Fi access ... my uncle is abusive in the house since he is not taking alcohol and not smoking because of lockdown regulations.” Mpungose (2021) further posited that most of the participants stayed in remote areas, which implies a lack of accessibility to the internet. The study indicates that all the first-year students agreed with the above statement. A third-year student said: “I do not have a laptop and smartphone ... I cannot afford data bandwidth for internet access....” Mpungose’s (2020a) results on 26 students studying curriculum studies disclosed that affordability to possess hardware learning resources like laptops, phones, and others is difficult because of the socio-economic divide (poor socio-economic background).

Hence, most students depend entirely on the university to supply such resources for effective e-learning. A student asserted that they were promised laptops at the beginning of the academic calendar, but all in vain. Because of this, one had to resort to a smartphone for learning. Similarly, another student emphasized that the total lockdown will negatively affect her, for they are not given money to support them. She will not have money to access hotspot spaces like community libraries as she stays in remote areas. Additionally, this view of the total shutdown creating inconvenience for some students is incongruent with another participant who maintains that she would not have money for transport to go and come back from home. In other words, closing traditional lectures create bedlam since she does not have the necessary learning equipment.

However, another student posits that access to all the necessary resources leads to effective e-learning: “... at home, I have access to Wi-Fi, laptop, and other resources ... we are just informed to use Moodle LMS and Zoom for e-learning.” It denotes that lecturers do not consider whether students have access to electronic learning resources. Furthermore, some students’ challenge is the lack of laptops or smartphones for Google Classroom; consequently, they have to depend on their friends to attend classes (Hussaini et al., 2020). They conclude that all these reasons challenge students to use Google Classroom efficiently and accessibly as an OTL tool.

## **Students' Attitudes Towards LMS**

Because of boredom, many HEIs students attend Zoom VCT, Google Meet, and Teams classes in Lesotho deteriorate until a few consistent students are left to attend the class. As a result, students are not actively engaged in learning and teaching; sometimes, they are just passive members who log in to their WhatsApp and Facebook accounts. As presented in Mpungose's (2021) survey, lengthy lectures can cause fatigue, with students losing focus or concentration. All participants agreed with the observation that they ended up checking their Facebook posts while the lecturer was sharing the screen with them [presenting the lecture] because there were no activities given to do. Similarly, another participant said: "I also don't see people's faces ... I don't feel like I am in class." In other words, students on a Zoom platform seem to be deprived of connectedness with their lecturers and learner autonomy; they do not feel as if they are in a real classroom (face-to-face) context.

Furthermore, some students do not join Zoom using the video function and use audio to save data. Most students highlighted that listening to the voice-only limits the interaction with the lecturer and other students on the platform, and they get bored. Some students leave the lecture early due to challenges with internet access. It is proved by another participant who stated: "I only come in for the first 30 minutes in the first lecture to save data bundle for other lectures."

Amponsah et al. (2021) reveal that learning management systems tend to cause fatigue to facilitators and students in the teaching and learning platform. For example, many participants regarded joining video conferences for longer than an hour, viewing and listening to the speakers' declaring points on issues as an 'online-taxing exercise.' Some also said it is physically and emotionally draining during video conferencing. Moreover, the participants voiced that they lost focus on ideas during the discussion because they were exhausted and could not listen or participate.

## **Addressing Functionality as a Reliable Component of Online Learning and Teaching Tool**

**Are Online Teaching and Learning Tools User-Friendly?** Another line of thought on OTL's functionality demonstrates faculty members' insufficient information technology (IT) knowledge and the deficiency of electronic devices. Sepiriti's (2021) findings reveal that Thuto, an OTL tool used at the National University of Lesotho (NUL), is inaccessible. The study remarked that Thuto does not accommodate all students at once, and it goes offline frequently, thus, limiting students' participation; it is not easily accessible during the weekends. He further indicates that it is slow and unreliable while writing assignments so much that students miss their deadlines, and for that matter, they are penalized. At the same time, the problem is created by Thuto and not their human errors. Conversely, Makumane (2021) argues that Thuto LMS is viewed as a professional platform to which every lecturer

and student alike has access, promoting professional and structured communication, reliable record-keeping, and students following specific steps to access the content. The findings from Makumane (2021) and Sepiriti (2021) juxtapose the disconnect between the failures of Thuto as an LMS and the “unexamined” ideals for which it was mounted, hence the significance of the current study.

Google Classroom allows the facilitator to give a broad scope of assets for instruction and learning (Mafa, 2018). Many students agree that Google Classroom has numerous easy-to-use features which are provided by this learning management system, such as the capacity to download notes, assignments, and records, upload videos and audio, transfer files, and finally, permit one to see posts and notifications from either the facilitator or the learner. In accord with Mafa (2018), the findings discovered by Hussaini et al. (2020) portray that the majority of people claim it is easy and accessible to learn through Google Classroom, meaning that it is an effective strategy that enhances students’ ability to think and access to learning material. Furthermore, knowledge and skills are magnified through Google Classroom as students’ participation in class improves. Participants claimed that Google Classroom should be incorporated into teaching and learning as it would significantly improve students’ academic performance. Therefore, Google Classroom positively impacts students’ knowledge and skills (Hussaini et al., 2020).

The other positive comments about Zoom and Microsoft Teams are that participants acquire new digital skills. One participant stated that Microsoft Teams as a video-conferencing tool was introduced to them at a university continuous professional development session. With two follow-up sessions he attended this year, he improved his skills digitally. With the skills acquired through the sessions, he incorporates them with his students during the COVID-19 lockdown. Another female participant shared that she can now organise and chair Zoom meetings through the training she has acquired from the university. Finally, she has trained other faculty members to use video conferencing.

Nonetheless, as cited by Amponsah et al. (2021), so that people do not annoy others in LMS like Zoom and Teams, it is important to mute the microphones unless one wants to give their views to the session (Hines & Sun, 2020; Jiang, 2020). Besides muting the microphone and videos, another point is that people should not murmur behind gadgets (Hines & Sun, 2020). They also touched on arranging spaces so that disruptions would be minimised. It implies that the nature of these LMS can be quite disturbing, especially during synchronous online learning, if managed poorly. University of South Africa (Unisa) also uses satellite broadcast, which is revealed to be less interactive than video conferencing but more cost-effective. Also, students can see their lecturer, but the lecturer cannot. One of the disadvantages of satellite broadcasts is that they encourage passive viewing instead of active viewing. Moreover, students cannot control the medium and cannot stop the flow of information to ask questions and request clarification (Letseka et al., 2018).

More so, Amponsah et al. (2021) reported that the connection breaks up and causes poor sound and video conferencing quality, disturbing hearing. For instance, a participant illustrated that she was troubled by people's behaviour at her first Team meeting. Again, people did not mute their microphones, which disturbed the whole meeting. The worst part is that their many words simultaneously always echoed in her ears. In most interview sessions, people always expressed opinions by repeating 'what are you saying' and 'you are breaking up.' Most participants posted that their dissatisfaction with poor presentations, poor sound, and high noise levels were disturbing and broke their concentration. One participant alluded that she hated sitting in meetings because poor-quality presentations or background noise affected her concentration.

## **IMPLICATIONS AND SUGGESTIONS**

It is pretty evident from the existing literature that in as much as the use of OTL tools plays a valuable role in facilitating the dissemination of knowledge to learners, there are some factors affecting its functionality and probability of success which have been noted in the results such as internet connectivity, lack of infrastructure, electricity, gadgets to be used for OTL. Therefore, this implies that there could be a broadened digital divide between learners and lecturers regarding the tools' accessibility since it has to be accessible if it is functional. Therefore, it could pose some threats to a certain extent, hindering the progression and success of teaching and learning in HEIs. Therefore, for students who are disadvantaged and from poor social backgrounds, the situation can turn around if the government of Lesotho can provide subsidies to students, allowing them to access e-learning resources at low or no costs. Similarly, Lesotho telecommunication companies must assist learners by providing them free Wi-Fi since most lecturers in Lesotho HEIs do not prepare for different student situations. Alternatively, educational systems could consider blended learning platforms to address this digital divide among students so that the learning process does not slow down and negatively impacts the educational development of Lesotho. Furthermore, it could assist teachers and learners who find it difficult or struggle while using online devices. Besides that, it is advisable to have policies designed for OTL explaining step-by-step how to use e-learning and e-teaching resources.

The findings also illustrate that because of boredom, many students' Zoom VCT classes' attendance deteriorates daily until a few consistent students are left to attend the class. Therefore, the content delivered in this learning environment is wasted; the outcomes are unfavorable. One could imagine what this implies to the country's educational development if these learning conditions are left just as they are. Therefore, it would be advisable for lecturers to engage students actively in an online platform and maintain the same level of interaction as face-to-face to avoid losing focus in class. It is also wise for students to practice listening skills for effective learning.

Most students from NUL reported that Thuto LMS is inaccessible, especially on weekends, and constantly offline. On the same note, participants in Teams and Zoom VCT protested poor sound quality, break-ups in connectivity, and low quality of video conferencing. Another problem revealed from the literature is that online platforms encourage passive viewing instead of active viewing. Similarly, this indicates that these tools have limitations regarding their functionality and probability of success. These limitations pose a threat of depleting educational progress among Basotho learners, especially in this global pandemic, where students feel compelled to use online learning tools to avoid infection. However, adequate training of lecturers and learners in properly using hardware and software resources can remedy this threat. In addition, the institutions could draw policies regarding e-learning and e-teaching to guide lecturers and students in properly using the devices.

As much as OTL tools have limitations, it can still be reasoned that it has some positive impacts. The functionality and probability of success component of OTL tools are, to some degree, dependable since it provides features that enable learners to download notes, assignments, records, videos, and audio. As argued in the findings, OTL is easy to use and promotes collaborative learning and interaction, which sharpens one's knowledge base with technologies. One of the online learning tools, Moodle, quickly displays students' results for students feedback. Similarly, Google Classroom is an effective tool that develops students' thoughtfulness and easy access to lecture materials. Again, Google Classroom improves students' interest in learning while other students' level of participation in class activities is also believed to be enhanced by this approach. It concludes that Google Classroom positively affects students' knowledge and skills. Thuto LMS is also viewed as a professional platform to which every teacher and student has access, promoting professional and structured communication and reliable record-keeping. Students follow specific steps to access the content.

The advantages outlined above can be crucial in Lesotho's context because e-learning tools can efficiently deliver courses as the resources can be easily accessed anywhere and in unconstrained times. Again, because online learning tools promote collaboration amongst learners, students can interact with their friends from all over the country through group discussions and private chats. Suppose online learning tools increase participation in class activities. In that case, it portrays that more students will be able to comprehend the concepts taught through these tools, which leads to improved performance and maintains effective and quality education in Lesotho. Subsequently, one could argue that the functionality and probability of success of OTL tools are reliable.

## CONCLUSION

This review investigated the reliability of Lesotho's OTL tools. The qualitative content analysis method used the interpretivism approach to conduct this study. This approach sought the deeper meaning of the information we gathered. It is also important to note that this study informs the users or institute administrators of strategies for the effective implementation of online learning. Further, it checks the reliability of online tools, thus informing future researchers of recent findings. Therefore, based on the findings extracted from the articles, it was concluded that OTL tools are reliable regarding the probability of success and their functionality. However, many shortcomings outweigh the strengths, implying that the education quality in Lesotho could be hampered if lecturers only rely on OTL tools. Therefore, blended learning is advisable, especially for students from disadvantaged families who cannot buy data or gadgets needed for OTL. In addition, students and lecturers should be trained in using the tools for effective teaching and learning. We acknowledge a few limitations in this review. It did not analyse all the reliability components of OTL tools. Therefore, further research is recommended, covering a broader scope of reliability components for the generalisability of the findings.

## ACKNOWLEDGEMENT

The authors acknowledged all the previous works used in this review.

## REFERENCES

- Aderson, T. (2016). Theories for learning with emerging technologies. *Emerging Technologies in Distance Education*, 7(1), 7-23.
- Ali, W. (2020). online and remote learning in higher education institutes: A necessity in light of COVID-19 pandemic. *Higher Education Studies*, 10(3), 16-25. <https://doi.org/10.5539/HES.V10N3P16>
- Amponsah, S., Van Wyk, M. M., & Kolugu, M. K. (2021). Academic experiences of "zoom-fatigue" as a virtual streaming phenomenon during the COVID-19 pandemic. *International Journal of Web-Based Learning and Teaching Technologies*, 17(6), 1-16. <https://doi.org/10.4018/IJWLTT.287555>
- Awad, M., Salameh, K., & Leiss, E. L. (2019). Evaluating learning management system usage at a small university. *ACM International Conference Proceeding Series*, 1(4), 98-102. <https://doi.org/10.1145/3325917.3325929>
- Creswell, J., & Poth, C. (2017). *Qualitative inquiry and research design: Choosing among five approaches*. SAGE Publications.
- Dhull, I., & Sakshi, A. (2017). Online learning. *International Education & Research Journal*, 3(8), 32-34.
- Dube, B. (2020). Rural online learning in the context of COVID-19 in South Africa: Evoking an inclusive education approach. *Multidisciplinary Journal of Educational Research*, 10(2), 135-157. <https://doi.org/10.447/remie.2020.5607>



- Henaku, E. A. (2020). COVID-19: Online learning experience of college students: A case of Ghana. *International Journal of Multidisciplinary Sciences and Advanced Technology*, 1(2), 54-62. <https://doi.org/10.12691/education-9-7-1>
- Hines, A., & Sun, P. (2020). *Zoom fatigue: how to make video calls less tiring*. The Conversation. <https://theconversation.com/zoom-fatigue-how-to-make-video-calls-less-tiring-137861>
- Hlojeng, M. A., & Makura, A. H. (2020, October 5-6). *Out-of-school factors contributing towards academic underachievement of vulnerable learners in lesotho high schools*. In *Proceedings of ADVED 2020 - 6th International Conference on Advances in Education* (pp. 429-438). Virtual-Online. <https://doi.org/10.47696/ADVED.2020101>
- Hussaini, I., Ibrahim, S., Wali, B., Libata, I., & Musa, U. (2020). Effectiveness of Google classroom as a digital tool. *International Journal of Research and Innovation in Social Science*, 4(4), 51-54.
- Jiang, M. (2020). *The reason zoom calls drain your energy*. BBC Worklife. [https://www.counsellingresources.co.nz/uploads/3/9/8/5/3985535/the\\_reason\\_zoom\\_calls\\_drain\\_your\\_energy.pdf](https://www.counsellingresources.co.nz/uploads/3/9/8/5/3985535/the_reason_zoom_calls_drain_your_energy.pdf)
- Lai, P. C. (2017). The literature review of technology adoption models and theories for the novelty technology. *Journal of Information Systems and Technology Management*, 14(1), 21-38. <https://doi.org/10.4301/S1807-17752017000100002>
- Letseka, M., Letseka, M. M., & Pitsoe, V. (2018). The challenges of e-learning in South Africa. *Trends in E-Learning*, 1(3), 2-19. <https://doi.org/10.5772/intechopen.74843>
- Mafa, K. R. (2018). Capabilities of Google classroom as a teaching and learning tool in higher education. *Journal of Science Technology & Engineering*, 5(5), 30-34.
- Makafane, D. T., & Chere-Masopha, J. (2021). COVID-19 crisis: Challenges of online learning in one University in Lesotho. *African Perspectives of Research in Teaching & Learning*, 5(1), 1-13.
- Makumane, M. A. (2021). Students' perceptions on the use of LMS at a Lesotho University amidst the COVID-19 pandemic. *African Identities*, 2021(1), 1-18. <https://doi.org/10.1080/14725843.2021.1898930>
- Maphosa, V. (2021). Teachers' perspectives on remote-based teaching and learning in the COVID-19 era: Rethinking technology availability and suitability in Zimbabwe. *European Journal of Interactive Multimedia and Education*, 2(1), 1-11. <https://doi.org/10.30935/ejimed/9684>
- Mashinini, V. (2020). COVID-19 and National University of Lesotho: Experiences and challenges. *International Journal of Education and Research*, 8(9), 157-180.
- Mataka, T. W., Mukurunge, T., & Bhila, T. (2020a). Universities in pandemonium as COVID 19 wreak havoc: A case of two conventional universities in Southern Africa. *International Journal of All Research Writings*, 1(11), 71-78.
- Mataka, W. T., Mukurunge, T., & Bhila, T. (2020b). Virtual teaching and learning: a sad reality of the "haves" and "have nots", the teacher's voice in Zimbabwe during COVID 19 pandemic. *International Journal of All Research Writings*, 1(12), 8-14.
- Mfaume, H. (2019). Awareness and use of a mobile phone as a potential pedagogical tool among secondary school teachers in Tanzania Hamisi Mfaume Dar es Salaam University College of Education, Tanzania.



- International Journal of Education and Development Using Information and Communication Technology*, 15(2), 154-170.
- Ministry of Education and Training. (2008). *Curriculum and assessment policy framework: Education for individual and social development*. [https://planipolis.iiep.unesco.org/sites/default/files/ressources/lesotho\\_curriculum\\_and\\_assessment\\_policy\\_framework.pdf](https://planipolis.iiep.unesco.org/sites/default/files/ressources/lesotho_curriculum_and_assessment_policy_framework.pdf)
- Mpungose, C. B. (2021). Students' reflections on the use of the Zoom video conferencing technology for Online learning at a South African University. *International Journal of African Higher Education*, 8(1), 159-178. <https://doi.org/10.6017/ijahc.v8i1.13371>
- Mpungose, C. B. (2020a). Beyond limits: Lecturers' reflections on Moodle uptake in South African universities. *Education and Information Technologies*, 25(6), 1-20. <https://doi.org/10.1007/s10639-020-10190-8>
- Mpungose, C. B. (2020b). Emergent transition from face-to-face to online learning in a South African University in the context of the Coronavirus pandemic. *Humanities and Social Sciences Communications*, 7(1), 1-9. <https://doi.org/10.1057/S41599-020-00603-X>
- Murgatroid, S. (2020). *COVID-19 and Online Learning*. ResearchGate. <https://doi.org/10.13140/RG.2.2.31132.85120>
- Oketch-Oboto, J. W. (2021). Online learning challenges, stress experience and coping strategies among university students during the lockdown due to COVID-19 pandemic international practice. *Journal of Pedagogy, Andragogy and Heutagogy in Academic*, 2(1), 15-27.
- Pete, J., & Soko, J. J. (2020). Preparedness for online learning in the context of COVID-19 in selected Sub-Saharan African Countries. *Asian Journal of Distance Education*, 15(2), 37-47.
- Sadiku, M. N. O., Adebo, P. O., & Musa, S. M. (2018). Online teaching and learning. *International Journal of Advanced Research in Computer Science and Software Engineering*, 8(2), 73-75. <https://doi.org/10.23956/ijarsse.v8i2.549>
- Sepiriti, S. (2021). Investigating the effects of using thuito learning management system. *International Journal of Online and Distance Learning*, 2(1), 1-11. <https://doi.org/10.47604/ijodl.1336>
- Siemens, G. (2005). Connectivism a learning theory for the digital age. *International Journal of Instructional Technology & Distance Learning*, 2, 3-10.
- Tamrat, W., & Teferra, D. (2020). COVID-19 poses a serious threat to higher education. *University World News*, 1(4), 1-2.
- World Bank. (2020). *Remote learning and COVID-19. The use of educational technologies at scale across an education system as a result of massive school closings in response to the COVID-19 pandemic to enable distance education and online learning*. World Bank. <https://www.unapcict.org/resources/ictd-infobank/remote-learning-and-covid-19-use-educational-technologies-scale-across-education-system-result-massive-school-closings>

## **Alternative Design of One-Sided Shewhart Control Charts for the Multivariate Coefficient of Variation**

**XinYing Chew**

*School of Computer Sciences, Universiti Sains Malaysia, 11800 USM, Penang*

### **ABSTRACT**

The control charting technique is an approach to quality control and was implemented in various industries. There are many control charts, where the coefficient of variation control chart was one of the common charts and greatly used in Statistical Process Control. Since most processes are multivariate, the multivariate coefficient of variation charts has received great attention in the past few years. However, the existing multivariate coefficient of variation control charts was evaluated in terms of the average run length criterion, which may misinterpret the actual performance of the charts. This paper designs an alternative for the Shewhart multivariate coefficient of variation chart by considering the median run length and expected median run-length criteria to circumvent this problem. The research on the multivariate coefficient of variation chart is very limited in the existing literature by considering the median run length criterion. This proposed chart in this paper can minimize this research gap. The formulas and algorithms of the proposed chart are presented. The outputs of the proposed charts are shown by examining the different upward and downward process shifts. Additionally, the sample sizes, the process shifts, and the variation of the run-length distribution are investigated for their effects on the proposed chart. The findings

reveal that the run-length distribution's variation is inversely proportional to the shift size. Furthermore, it shows that the variation decreases if the shift size increases.

### ARTICLE INFO

#### *Article history:*

Received: 15 April 2022

Accepted: 20 June 2022

Published: 27 December 2022

DOI: <https://doi.org/10.47836/pjst.31.1.35>

#### *E-mail address:*

[xinying@usm.my](mailto:xinying@usm.my) (XinYing Chew)

*Keywords:* Control chart, median run length, multivariate coefficient of variation, statistical process control

## INTRODUCTION

The control chart is frequently used in Statistical Process Control for detecting the processed signal. Implementing the control chart aims to improve the quality of processes in various domains such as healthcare, manufacturing, and service (Mim et al., 2019). The traditional control chart was used to monitor the process location and dispersion. Note that the process mean needs to be constant, and the process standard deviation is not correlated to the mean (Khaw & Chew, 2019). Shewhart  $\bar{X}$  was proposed to monitor the process mean, while  $R$  and  $S$  charts are commonly used for process variability. In the past two decades, the coefficient of variation (CV) chart has been widely applied in different domains, where the most common domains are manufacturing, healthcare, finance, and service. The CV can be defined as the ratio of the standard deviation to the mean, and it can be used when the mean and standard deviation of the data are highly correlated. For example, Chanda et al. (2018) investigated the CV obtained from Vegetarian Indices with the millable stalk of sugarcane varieties and plant population. Huang and Tang (2007) proposed a new infrared device for the CV in yarns. Shriberg et al. (2003) used the CV as a diagnostic marker for childhood apraxia of speech, while Alharbi et al. (2019) combined the CV and normalized-difference vegetative index to predict the plant populations in corn. The CV of the endothelial cell area was examined by Doughty and Aakre (2008). The CV is also recently applied in the chemical reactor process (Mahmood & Abbasi, 2021) and continuous glucose monitoring (Mo et al., 2021), respectively.

Kang et al. (2007) were the first researchers to develop the Shewhart CV chart. It could be applied for monitoring the process in which the traditional  $\bar{X}$  and  $R$  charts could not function well. Most traditional charts focus on monitoring the process's mean or standard deviation. However, in some processes, such as the healthcare process, the mean and the standard deviation are not independent, where the mean is not constant and/or the standard deviation is a function of the mean. In such processes, the use of traditional charts is dubious. In these conditions, it is better to monitor the CV. Over the years, many intermediate and advanced CV charts have been discussed by using different strategies, such as exponentially weighted moving average (EWMA) (Zhang et al., 2014; Castagliola et al., 2011), CUSUM (Tran & Tran, 2016), synthetic (Calzada & Scariano, 2013; Chew et al., 2021), run rules (Castagliola et al., 2013), adaptive schemes (Khaw et al., 2017; Castagliola et al., 2015; Yeong et al., 2018) and variable sample size run sum (Yeong et al., 2022). Those proposed charts provided better performance in detecting small and moderate shifts. However, at the same time, the computational difficulties and costs increased.

All preceding charts are used for monitoring the univariate process. In real-life applications, most process monitoring is in multivariate conditions, containing at least two quality characteristics. Yeong et al. (2016) introduced a CV chart in a multivariate case called a multivariate coefficient of variation (MCV). The proposed chart only performs

well when detecting large process shifts. Khaw et al. (2019) and Chew et al. (2020) proposed a synthetic MCV and run rules MCV charts to improve the detection of small and moderate shifts. The results show that the synthetic MCV chart outperformed the Shewhart MCV and run rules MCV charts for detecting small and moderate MCV shifts. However, the drawback of the synthetic MCV chart is its weak efficiency in detecting downward shifts. The adaptive schemes were incorporated into the Shewhart MCV chart to improve performance. Those are variable sampling interval MCV (Nguyen et al., 2019), variable sample size MCV (Khaw et al., 2021), variable sample size and sampling interval MCV (Khaw et al., 2018), and variable parameter MCV charts (Chew et al., 2019). Comparing those adaptive charts reveals that the variable parameter MCV chart provides the best performance detecting small to large shifts in different shift sizes and ranges. More recently, Giner-Bosch et al. (2019) recommended the MCV-squared EWMA chart. More recently, Adegoke et al. (2022) suggested an MCV chart for high-dimensional processes, while Ng et al. (2022) investigated the MCV chart in terms of economic criterion.

To date, the design of the existing MCV charts is based on the average run length (ARL) criterion. According to Khoo et al. (2012), the ARL performance measure should not be the only measure as it could potentially cause the chart's misinterpretation. In addition, the ARL performance measure may not be practically effective due to the inconsistency and excessive variations of the run-length distribution (Zhou et al., 2012). Zhou et al. (2012) stated that the run-length distribution's percentile effectively summarizes the run-length behavior and provides more information on the control chart. Therefore, the 50<sup>th</sup> percentile, also called median run length (MRL), is considered more practical in designing the control chart.

In contrast, the fifth (5%) and 95<sup>th</sup> (95%) percentiles can be used with the MRL for investigating the skewness and spread of the run-length distribution (Chakraborti, 2007). Some of the research works on control charts could be found using MRL. For example, Teoh et al. (2017) proposed a variable sample size chart for monitoring the process mean based on the MRL criterion. The results revealed that the proposed chart performed better than the Shewhart chart. This study is then adopted by Lim et al. (2019) for recommending a variable sample size univariate CV chart. The distribution of CV is investigated in this study. Yeong et al. (2021) recently adopted the side-sensitive synthetic scheme to the CV chart. The proposed chart is more sensitive than the variable sample size CV chart detecting small and moderate CV shifts. With the salient properties of the MRL performance measure, this paper proposes two one-sided Shewhart MCV charts based on the MRL and expected median run length (EMRL). MRL is the median number of samples (subgroups) that must be plotted on a chart until it produces the first out-of-control signal (Montgomery, 2013). MRL could be used as a performance measure in detecting the shift size  $\tau$ , whereas the EMRL is used for detecting the shift range.

In the current literature, the research on MCV charts based on MRL is very limited. Therefore, only the synthetic MCV chart of Lee et al. (2020) based on MRL is introduced. Although the advanced chart, the synthetic MCV chart, performed better than the Shewhart MCV chart, this proposed chart can be used by the practitioner who likes to implement an intermediate-type chart in the process monitoring. This intermediate framework is simple yet effective in terms of costs and time. However, the synthetic MCV chart was not investigated in terms of EMRL, which is required to be used when the exact shift size could not be defined in certain processes. Additionally, the synthetic chart is ineffective in detecting the downward process shifts. The downward process shifts are crucial since it shows process improvement. The proposed chart circumvents these drawbacks as it has been developed and can effectively detect the upward and downward process shifts in the MRL and EMRL criteria. Figure 1 illustrates the graphical view of the proposed upward and downward charts. This paper's organization is shown as follows: The properties and distribution of the Shewhart MCV chart are discussed in Methods. Methods also enumerated the formulas and algorithms of MRL and EMRL. Then, the outputs of the proposed chart are shown in the Results and Discussion. Lastly, the concluding remarks and recommendations will be presented in Conclusion.

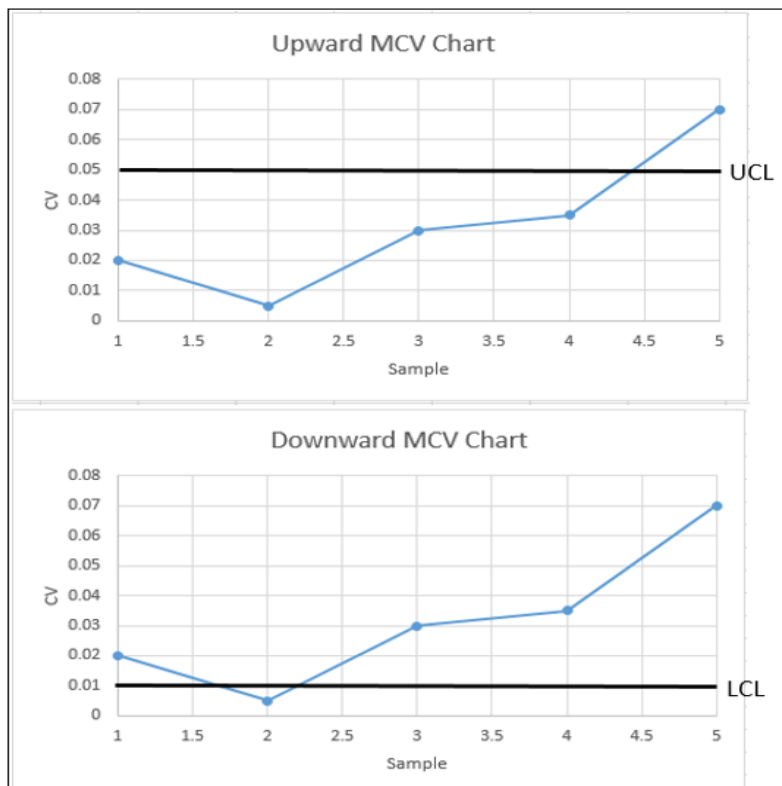


Figure 1. Graphical view of the Shewhart MCV charts

**METHODS**

According to Voinov and Nikulin (1996), suppose that we have a random sample size of  $a$ , i.e.,  $X_1, X_2, \dots, X_a$  from a  $b$ -variate normal distribution with a mean vector  $\mu$  and covariance matrix  $\Sigma$ , it gives  $X \sim N_b(\mu, \Sigma)$ , where  $X_i^T = (X_{i1}, X_{i2}, \dots, X_{ib})$ , for  $1 \leq i \leq a$  and  $\mu^T = (\mu_1, \mu_2, \dots, \mu_b)$ . The MCV statistic for the population can be denoted as  $\gamma = (\mu^T \Sigma^{-1} \mu)^{-1/2}$ . The sample MCV can assume  $\gamma, \hat{\gamma}$  if  $\mu$  and  $\Sigma$  are unknown. Thus,  $\hat{\gamma} = (\bar{X}^T S^{-1} \bar{X})^{-1/2}$  can be obtained by substituting  $\mu$  and  $\Sigma$  to  $\bar{X}$  and  $S$ . Note that  $\bar{X}$  is the sample mean vector while  $S$  is the sample covariance matrix. The  $\bar{X}$  and  $S$  are defined as  $\bar{X} = 1/a \Sigma X_i$  and  $S = 1/(a - 1) \Sigma (X_t - \bar{X})(X_t - \bar{X})^T$ , respectively. Here,  $\bar{X}$  and  $S$  are not correlated.

Based on Wijsman’s theorem (1957), Yeong et al. (2016) gave  $\hat{\gamma}$  distribution.  $\bar{X}$  is normally distributed with mean  $\mu$  and covariance matrix  $(1/a)\Sigma$ , i.e.,  $\bar{X} \sim N_b(\mu, (1/a)\Sigma)$ . At the same time,  $S$  has a Wishart distribution with  $(a - 1)$  degree of freedom and covariance matrix  $(1/(1 - a))\Sigma$ , which gives  $S \sim W_b(a - 1, (1/(a - 1))\Sigma)$ . By letting  $T^2 = a\bar{X}^T S^{-1} \bar{X}$ , it provides  $T^2/(a - 1) \cdot (a - b)/b \sim F_{b, a-b}(\delta)$ , which can be defined as a noncentral  $F$  distribution. Here,  $a$  refers to sample size, and  $b$  is the number of quality characteristics. Note that it is with  $b$  and  $a - b$  degrees of freedom and noncentrality parameter  $\delta = a\mu^T \Sigma^{-1} \mu$ . From  $\hat{\gamma} = (\bar{X}^T S^{-1} \bar{X})^{-1/2}$ , it can be further derived as by adding  $a$  to both sides. By adopting, it gives Equation 1

$$\left(\frac{\sqrt{a}}{\hat{\gamma}}\right)^2 \cdot \frac{a-b}{b} = \frac{a(a-b)}{(a-1)b\hat{\gamma}^2} \sim F_{b, a-b}(\delta). \tag{1}$$

Since  $\delta = a\mu^T \Sigma^{-1} \mu$  and it can also be formulated as  $\frac{a}{\gamma^2}$ , where  $\gamma$  is the MCV, as mentioned in the early paragraph. The cumulative distribution function (CDF) of  $\hat{\gamma}$  can be derived as Equation 2

$$\begin{aligned} F_{\hat{\gamma}}(x|a, b, \delta) &= P(\hat{\gamma} \leq x) = P\left(\frac{1}{\hat{\gamma}} \geq \frac{1}{x}\right) = P\left(\frac{a(a-b)}{(a-1)b\hat{\gamma}^2} \geq \frac{a(a-b)}{(a-1)bx^2}\right) \\ &= 1 - F_F\left(\frac{a(a-b)}{(a-1)bx^2} \mid b, a-b, \delta\right) \end{aligned} \tag{2}$$

where  $F_F(\cdot | a, a - b, \delta)$  is the noncentral  $F$  distribution. Note that it is with  $b$  and  $a - b$  degrees of freedom and noncentrality parameter  $\delta$ .

To formulate the inverse CDF of  $\hat{\gamma}$ , Yeong et al. (2016) let  $F_{\hat{\gamma}}^{-1}(\alpha|a, b, \delta) = y$  gives  $F_{\hat{\gamma}}^{-1}(y|a, b, \delta) = \alpha$ . Then, Equation 3 gives

$$1 - F_F\left(\frac{a(a-b)}{(a-1)by^2} \mid b, a-b, \delta\right) = \alpha. \tag{3}$$

Then, it gives Equation 4

$$\frac{a(a-b)}{(a-1)by^2} = F_F^{-1}(1 - \alpha|b, a - b, \delta). \tag{4}$$

With some algebraic manipulations, it provides Equation 5 as follows:

$$y = \sqrt{\frac{a(a-b)}{(a-1)b} \left[ \frac{1}{F_F^{-1}(1-\alpha|b, a-b, \delta)} \right]}, \tag{5}$$

Since  $F_{\hat{\gamma}}^{-1}(\alpha|a, b, \delta) = y$ , then the inverse CDF of can be derived in Equation 6

$$F_{\hat{\gamma}}^{-1}(\alpha|a, b, \delta) = \sqrt{\frac{a(a-b)}{(a-1)b} \left[ \frac{1}{F_F^{-1}(1-\alpha|b, a-b, \delta)} \right]}, \tag{6}$$

where  $F_F(\cdot | a, a - b, \delta)$  is the inverse CDF of the noncentral  $F$  distribution. Note that it is with  $b$  and  $a - b$  degrees of freedom and noncentrality parameter  $\delta$ . The distribution of  $\hat{\gamma}$  is only considered true when  $b < a$  due to the positive degree of freedom. Next,  $\delta = a\mu^T \Sigma^{-1} \mu$  as mentioned in the early paragraph, it is equivalent to  $\delta = a/(\tau\gamma_0)^2$ , where the shift size  $\tau = 1$  in the in-control process and  $\gamma_1 = \tau\gamma_0$  is an out-of-control MCV when  $\tau \neq 1$ . When  $\tau \neq 1$ , the values of  $\tau > 1$  and  $0 < \tau < 1$  are for an increase and decrease MCV shifts, respectively.

According to Yeong et al. (2016), the root mean square method can be applied when the in-control sample MCV, i.e.,  $\hat{\gamma}_0$ , is unknown. Then, the formula can be obtained as Equation 7:

$$\hat{\gamma}_0 = \sqrt{\frac{1}{m} \sum_{i=1}^m \hat{\gamma}_t^2}, \tag{7}$$

where  $m$  is the number of in-control Phase I samples. The two one-sided Shewhart MCV charts consist of two independent charts: the upward Shewhart MCV chart for detecting the increase of the process MCV shifts and the downward Shewhart MCV chart for detecting the decrease of the process MCV shifts. The upward chart has an upper control limit (UCL), while the downward chart has a lower control limit (LCL). The chart will detect an out-of-control signal if the sample MCV falls beyond the LCL and UCL. Therefore, the practitioner needs to identify the assignable cause(s) immediately to bring the process back to normal. By setting the Type I error probability ( $\alpha$ ), the UCL and LCL's formulas are shown in Equations 8 and 9.

$$\text{UCL} = F_{\hat{\gamma}}^{-1}(1 - \alpha|a, b, \delta_0), \tag{8}$$

for the increasing case and

$$\text{LCL} = F_{\hat{\gamma}}^{-1}(\alpha|a, b, \delta_0), \tag{9}$$



for the decreasing case. Note that  $\delta_0 = a/\gamma_0^2$  and  $\alpha = 1/ARL_0$ . The  $ARL_0$  is the in-control ARL value, where the  $ARL_0$  value is specified by the practitioner, depending on the current process system. For example, if the  $ARL_0$  is set as 370, then the  $\alpha$  value will be computed as  $\alpha = 1/370 = 0.0027$ .

As mentioned above, the process is out-of-control when the sample falls above the UCL of the upward Shewhart MCV chart and below the LCL of the downward Shewhart MCV chart. Thus, the probabilities that the upward and downward Shewhart MCV charts for detecting an out-of-control signal are  $Q = Pr(\hat{y} > UCL)$  and  $Q = Pr(\hat{y} < LCL)$ , respectively. Subsequently, the ARL and expected ARL (EARL) are shown in Equations 10 and 11:

$$ARL = \frac{1}{Q} \tag{10}$$

and

$$EARL = \int_{\tau_{min}}^{\tau_{max}} d\tau, ARL_1 f_{\tau}(\tau) \tag{11}$$

where  $ARL_1$  is an out-of-control ARL and  $f_{\tau}(\tau)$  denotes the probability density function (PDF) of  $\tau$ . According to Yeong et al. (2016), the EARL is a better performance measure for the case when  $\tau$  unable to be specified by the practitioner. In the interval  $(\tau_{max}, \tau_{min})$ , the  $\tau_{min}$  is the lower bound of  $\tau$ , whereas the  $\tau_{max}$  is the upper bound of  $\tau$ , subject to  $\tau_{max}, \tau_{min}$ .

The limits of the charts are known constants if the plotted statistics are independent (Montgomery, 2013). Thus, the probability mass function (PMF), that is,  $f_{RL}(l)$  and CDF, that is,  $F_{RL}(l)$  of the run length (RL) for the Shewhart MCV chart, can be obtained as  $f_{RL}(l) = P(RL = l) = \alpha(1 - \alpha)^{l-1}$  and  $F_{RL}(l) = P(RL \leq l) = 1 - (1 - \alpha)^l$ , respectively, where  $l \in \{1, 2, 3, \dots\}$ . According to Gan (1993), the  $(100\theta)^{th}$  percentile of the run-length distribution can be denoted as the value  $l_{\theta}$  such as in Equation 12

$$P(RL \leq l_{\theta} - 1) \leq \theta \text{ and } P(RL \leq l_{\theta}) > \theta. \tag{12}$$

where  $0 < \theta < 1$ . Then, the percentiles of the run-length distribution of the upward and downward Shewhart MCV charts can be computed such that MRL, by setting  $\theta = 0.5$  in Equation (12), that is,  $P(RL \leq MRL - 1) \leq 0.5$  and  $P(RL \leq MRL) > 0.5$ . Note that the practitioner can specify the in-control MRL ( $MRL_0$ ) based on the current process system. When the shift size  $\tau$  is unknown, the EMRL can be used as the performance measure. For the computation of EMRL, the formula is shown in Equation 13

$$EMRL = \int_{\tau_{min}}^{\tau_{max}} d\tau, MRL f_{\tau}(\tau) \tag{13}$$

where the in-control EMRL ( $EMRL_0$ ) is equal to the  $MRL_0$  and  $f_{\tau}(\tau)$  is the PDF of  $\tau$ .

## RESULTS AND DISCUSSION

Tables 1, 2, and 3 present the  $(\vartheta_{0.05}, \text{MRL}_1, \vartheta_{0.95})$  values for the upward and downward Shewhart MCV charts for monitoring the upward and downward MCV shifts, respectively, when  $b \in \{2, 3, 4\}$ ,  $a \in \{5, 10, 15\}$ ,  $\gamma_0 \in \{0.1, 0.5\}$ ,  $\tau \in \{1.1, 1.2, 1.3, 1.4, 1.5\}$  (for the upward case) and  $\tau \in \{0.5, 0.6, 0.7, 0.8, 0.9\}$  (for the downward case) and the  $\text{MRL}_0$  value is specified as 250 (when  $\tau = 1.0$ ). Note that the values of sample size  $a$  and the quality characteristics  $b$  were adopted from Yeong et al. (2016) and Khatun et al. (2019). The spread and variation of the run-length distribution can be measured by referring to the difference of the values between  $\vartheta_{0.05}$  and  $\vartheta_{0.95}$ , where  $\vartheta_{0.05}$  and  $\vartheta_{0.95}$  are the 5<sup>th</sup> and 95<sup>th</sup> percentiles of the run-length distribution, respectively. The results reveal that the larger shift  $\tau$  gives smaller  $(\vartheta_{0.05}, \text{MRL}_1, \vartheta_{0.95})$  values with any change of the  $b$ ,  $\gamma_0$ , and  $n$  values. For example, in Table 1, for  $b = 2$ ,  $\gamma_0 = 0.1$  and  $a = 10$ , the  $\text{MRL}_1 \in \{(6, 81, 347), (2, 18, 76), (1, 7, 30)\}$  when upward shift  $\tau \in \{1.1, 1.3, 1.5\}$  whereas the  $\text{MRL}_1 \in \{(15, 190, 820), (8, 97, 417), (3, 38, 163)\}$  when downward shift  $\tau \in \{0.9, 0.7, 0.5\}$ .

The run-length distribution's variation is inversely proportional to the shift size. It shows that the variation decreases if the shift size increases. One of the examples is shown in Table 2; for  $b = 3$ ,  $\gamma_0 = 0.5$ , and  $a = 5$ , the different values between  $\vartheta_{0.05}$  and  $\vartheta_{0.95}$  are (454, 143, 69) when  $\tau \in \{1.1, 1.3, 1.5\}$  (for upward shift) and (887, 557, 296) when  $\tau \in \{0.9, 0.7, 0.5\}$  (for downward shift). The  $(\vartheta_{0.05}, \text{MRL}_1, \text{and } \vartheta_{0.95})$  values have a minimal decrease trend for detecting the downward shift with a small sample size value,  $a = 5$ . For example, in Table 3, for  $b = 4$ ,  $\gamma_0 = 0.1$ , and  $a = 5$ , the decreased percentage of the  $\text{MRL}_1$  value from  $\tau = 0.9$  to  $\tau = 0.5$  is 46% while the decreased percentages when  $a = 10$  and 15 are 92% and 98%, respectively. Generally, the  $(\vartheta_{0.05}, \text{MRL}_1, \text{and } \vartheta_{0.95})$  values increase when  $b$  and  $\gamma_0$  values increase. An example is presented in Tables 1, 2, and 3, for  $b \in \{2, 3, 4\}$ ,  $a = 5$  and  $\tau = 1.1$ , the  $\text{MRL}_1 \in \{(81, 97), (91, 107), (107, 123)\}$ , when  $\gamma_0 \in \{0.1, 0.5\}$ .

In terms of the  $\text{EMRL}_1$  criterion, Tables 4, 5, and 6 present the values for the upward and downward Shewhart MCV charts, for monitoring the upward and downward MCV shift ranges, respectively, when  $b \in \{2, 3, 4\}$ ,  $a \in \{5, 10, 15\}$ ,  $\gamma_0 \in \{0.1, 0.5\}$ ,  $(\tau \max_{\min} \epsilon) \in \{(1.0, 2.0), (1.3, 2.0), (1.5, 2.0)\}$  (for the upward case) and  $(\tau \max_{\min} \epsilon) \in \{(0.3, 1.0), (0.5, 1.0), (0.7, 1.0)\}$  (for the downward case) and the  $\text{EMRL}_0$  value is set equal to the  $\text{MRL}_0$  value, that is 250. Generally, the detected trend on the effect of  $b$ ,  $a$ , and  $\gamma_0$  values is nothing different from the case of  $\text{MRL}_1$ . However, it shows that the run-length distribution's variation for the downward shift ranges is larger than the run-length distribution's, regardless of the  $b$ ,  $\gamma_0$ , and  $a$  values. For instance, in Table 4, when  $b = 2$ ,  $a = 5$ , and  $\gamma_0 = 0.1$ , the run-length distribution's variation of the downward shift range  $(\tau \max_{\min} \epsilon) (0.5, 1.0)$  is 531.23 while the upward shift range  $(\tau \max_{\min} \epsilon) (1.0, 2.0)$  is 111.12. Note that the shift ranges (0.5, 1.0) and (1.0, 2.0) are considered very practical in the real industry (Castagliola et al., 2011).

Table 1

$(\vartheta_{0.05}, MRL_1, \vartheta_{0.95})$  values of the two one-sided Shewhart MCV charts, for the case  $b = 2$ ,  $a \in \{5, 10, 15\}$ ,  $\gamma_0 \in \{0.1, 0.5\}$ ,  $\tau \in \{0.5, 0.6, 0.7, 0.8, 0.9, 1.1, 1.2, 1.3, 1.4, 1.5\}$  and  $MRL_0 = 250$

$\tau$	$\gamma_0 = 0.1$	$\gamma_0 = 0.5$
$a = 5$		
0.5	3, 38, 163	3, 38, 164
0.6	5, 63, 273	5, 63, 272
0.7	8, 97, 417	8, 97, 416
0.8	11, 140, 602	11, 138, 597
0.9	15, 190, 820	15, 191, 825
1.1	6, 81, 347	8, 97, 418
1.2	3, 35, 148	4, 48, 204
1.3	2, 18, 76	2, 27, 117
1.4	1, 11, 45	2, 18, 75
1.5	1, 7, 30	1, 13, 53
$a = 10$		
0.5	1, 5, 18	1, 5, 20
0.6	1, 12, 50	1, 13, 53
0.7	3, 29, 126	3, 30, 129
0.8	5, 67, 287	5, 66, 284
0.9	10, 135, 583	10, 134, 576
1.1	5, 55, 237	6, 71, 307
1.2	2, 19, 79	3, 29, 122
1.3	1, 9, 35	2, 14, 61
1.4	1, 5, 19	1, 9, 36
1.5	1, 3, 12	1, 6, 23
$a = 15$		
0.5	1, 2, 6	1, 2, 7
0.6	1, 5, 18	1, 5, 20
0.7	1, 14, 58	1, 14, 59
0.8	4, 41, 177	3, 39, 168
0.9	9, 113, 489	8, 103, 445
1.1	4, 43, 183	5, 58, 248
1.2	1, 13, 53	2, 20, 87
1.3	1, 5, 22	1, 10, 40
1.4	1, 3, 12	1, 6, 22
1.5	1, 2, 7	1, 4, 14

Table 2

$(\vartheta_{0.05}, MRL_1, \vartheta_{0.95})$  values of the two one-sided Shewhart MCV charts, for the case  $b = 3, a \in \{5, 10, 15\}, \gamma_0 \in \{0.1, 0.5\}, \tau \in \{0.5, 0.6, 0.7, 0.8, 0.9, 1.1, 1.2, 1.3, 1.4, 1.5\}$  and  $MRL_0 = 250$

$\tau$	$\gamma_0 = 0.1$	$\gamma_0 = 0.5$
$a = 5$		
0.5	6, 69, 297	6, 70, 301
0.6	8, 98, 422	8, 99, 426
0.7	10, 131, 563	10, 132, 567
0.8	13, 168, 724	13, 168, 723
0.9	16, 207, 891	16, 209, 903
1.1	7, 91, 391	8, 107, 462
1.2	4, 42, 180	5, 56, 242
1.3	2, 23, 98	3, 34, 146
1.4	2, 14, 60	2, 23, 98
1.5	1, 10, 41	2, 17, 71
$a = 10$		
0.5	1, 6, 26	1, 7, 28
0.6	2, 16, 67	2, 17, 70
0.7	3, 36, 156	3, 37, 158
0.8	6, 76, 329	6, 76, 325
0.9	11, 144, 620	11, 143, 614
1.1	5, 59, 252	6, 75, 324
1.2	2, 21, 88	3, 31, 134
1.3	1, 10, 40	2, 16, 68
1.4	1, 5, 22	1, 10, 41
1.5	1, 4, 14	1, 7, 27
$a = 15$		
0.5	1, 2, 7	1, 2, 8
0.6	1, 5, 22	1, 6, 23
0.7	2, 16, 68	2, 16, 68
0.8	4, 46, 197	4, 43, 186
0.9	9, 119, 513	8, 109, 468
1.1	4, 45, 192	5, 60, 258
1.2	1, 14, 57	2, 22, 93
1.3	1, 6, 24	1, 10, 43
1.4	1, 3, 13	1, 6, 24
1.5	1, 2, 8	1, 4, 16

Table 3

$(\vartheta_{0.05}, MRL_1, \vartheta_{0.95})$  values of the two one-sided Shewhart MCV charts, for the case  $b = 4$ ,  $a \in \{5, 10, 15\}$ ,  $\gamma_0 \in \{0.1, 0.5\}$ ,  $\tau \in \{0.5, 0.6, 0.7, 0.8, 0.9, 1.1, 1.2, 1.3, 1.4, 1.5\}$  and  $MRL_0 = 250$

$\tau$	$\gamma_0 = 0.1$	$\gamma_0 = 0.5$
$a = 5$		
0.5	9, 122, 526	10, 131, 564
0.6	12, 149, 644	12, 156, 673
0.7	13, 175, 754	14, 180, 778
0.8	15, 201, 868	16, 204, 878
0.9	17, 225, 970	17, 229, 990
1.1	8, 107, 461	10, 123, 530
1.2	5, 55, 238	6, 71, 306
1.3	3, 33, 141	4, 46, 199
1.4	2, 22, 92	3, 33, 141
1.5	2, 15, 65	2, 25, 106
$a = 10$		
0.5	1, 9, 38	1, 10, 41
0.6	2, 22, 92	2, 22, 95
0.7	4, 46, 197	4, 46, 197
0.8	7, 88, 380	7, 87, 375
0.9	12, 153, 661	12, 153, 658
1.1	5, 63, 270	6, 80, 334
1.2	2, 23, 98	3, 34, 147
1.3	1, 11, 46	2, 18, 77
1.4	1, 6, 25	1, 11, 47
1.5	1, 4, 16	1, 8, 31
$a = 15$		
0.5	1, 2, 9	1, 3, 10
0.6	1, 7, 27	1, 7, 28
0.7	2, 19, 80	2, 19, 79
0.8	4, 51, 220	4, 48, 206
0.9	10, 125, 539	9, 114, 493
1.1	4, 47, 202	5, 63, 270
1.2	2, 15, 62	2, 23, 99
1.3	1, 6, 26	1, 11, 47
1.4	1, 4, 14	1, 7, 27
1.5	1, 2, 9	1, 4, 17

Table 4

$(E\vartheta_{0.05}, EMRL_1, E\vartheta_{0.95})$  values of the two one-sided Shewhart MCV charts, for the case  $b = 2, a \in \{5, 10, 15\}, \gamma_0 \in \{0.1, 0.5\}, (\tau_{max_{min}} \in) \{(0.3, 1.0), (0.5, 1.0), (0.7, 1.0), (1.0, 2.0), (1.3, 2.0), (1.5, 2.0)\}$  and  $EMRL_0 = 250$

$(\tau_{max_{min}})$	$\gamma_0 = 0.1$	$\gamma_0 = 0.5$
$a = 5$		
(0.3, 1.0)	7.61, 96.57, 420.90	7.61, 96.47, 420.32
(0.5, 1.0)	9.84, 125.68, 541.07	8.84, 125.98, 542.66
(0.7, 1.0)	12.95, 167.40, 722.03	12.82, 166.73, 719.32
(1.0, 2.0)	2.60, 26.65, 113.72	2.93, 33.61, 143.56
(1.3, 2.0)	1.05, 6.25, 24.71	1.25, 10.46, 43.83
(1.5, 2.0)	1.00, 4.07, 15.63	1.00, 7.32, 30.12
$a = 10$		
(0.3, 1.0)	4.47, 52.60, 238.93	4.38, 52.37, 237.85
(0.5, 1.0)	5.81, 71.77, 317.32	5.72, 71.39, 315.63
(0.7, 1.0)	8.67, 111.06, 477.52	8.57, 109.71, 471.99
(1.0, 2.0)	2.08, 18.74, 79.92	2.34, 23.86, 101.57
(1.3, 2.0)	1.00, 2.69, 10.29	1.01, 5.10, 19.70
(1.5, 2.0)	1.00, 1.82, 5.99	1.00, 3.31, 12.41
$a = 15$		
(0.3, 1.0)	3.70, 42.01, 193.12	3.48, 39.80, 182.16
(0.5, 1.0)	4.68, 56.88, 256.35	4.47, 54.46, 244.51
(0.7, 1.0)	7.17, 91.05, 393.88	6.83, 86.27, 372.57
(1.0, 2.0)	1.85, 15.67, 66.01	2.12, 19.84, 83.54
(1.3, 2.0)	1.00, 1.77, 6.20	1.00, 3.21, 12.36
(1.5, 2.0)	1.00, 1.25, 3.75	1.00, 2.13, 7.64

Table 5

$(E\vartheta_{0.05}, EMRL_1, E\vartheta_{0.95})$  values of the two one-sided Shewhart MCV charts, for the case  $b = 3, a \in \{5, 10, 15\}, \gamma_0 \in \{0.1, 0.5\}, (\tau_{max_{min}} \in) \{(0.3, 1.0), (0.5, 1.0), (0.7, 1.0), (1.0, 2.0), (1.3, 2.0), (1.5, 2.0)\}$  and  $EMRL_0 = 250$

$(\tau_{max_{min}})$	$\gamma_0 = 0.1$	$\gamma_0 = 0.5$
$a = 5$		
(0.3, 1.0)	9.57, 122.04, 526.11	9.57, 122.81, 529.84
(0.5, 1.0)	11.72, 151.33, 652.63	11.85, 153.24, 659.99
(0.7, 1.0)	14.25, 188.35, 812.95	14.35, 188.89, 814.78
(1.0, 2.0)	2.78, 30.46, 130.06	3.25, 38.65, 165.16
(1.3, 2.0)	1.17, 8.27, 33.69	1.40, 14.05, 59.10
(1.5, 2.0)	1.00, 5.54, 22.12	1.10, 10.22, 42.25
$a = 10$		
(0.3, 1.0)	4.66, 57.12, 258.07	4.68, 57.01, 257.60
(0.5, 1.0)	6.11, 77.91, 342.67	6.05, 77.82, 340.83
(0.7, 1.0)	9.26, 118.66, 510.99	9.19, 117.31, 505.26
(1.0, 2.0)	2.12, 19.85, 84.13	2.52, 25.27, 107.39
(1.3, 2.0)	1.00, 3.05, 11.78	1.05, 5.54, 22.74
(1.5, 2.0)	1.00, 2.01, 7.05	1.00, 3.72, 14.60
$a = 15$		
(0.3, 1.0)	3.74, 43.97, 202.12	3.63, 41.67, 190.67
(0.5, 1.0)	4.98, 59.72, 268.37	4.76, 57.07, 255.77
(0.7, 1.0)	7.55, 94.95, 410.73	7.08, 90.09, 388.48
(1.0, 2.0)	1.88, 16.11, 68.18	2.12, 20.37, 86.76
(1.3, 2.0)	1.00, 1.87, 6.89	1.00, 3.59, 13.45
(1.5, 2.0)	1.00, 1.25, 4.09	1.00, 2.43, 8.33



Table 6

values of the two one-sided Shewhart MCV charts, for the case  $b = 4$ ,  $a \in \{5, 10, 15\}$ ,  $\gamma_0 \in \{0.1, 0.5\}$ ,  $(\tau_{max_{min}} \epsilon) \in \{(0.3, 1.0), (0.5, 1.0), (0.7, 1.0), (1.0, 2.0), (1.3, 2.0), (1.5, 2.0)\}$  and  $EMRL_0 = 250$

$(\tau_{max_{min}})$	$\gamma_0 = 0.1$	$\gamma_0 = 0.5$
$a = 5$		
(0.3, 1.0)	12.44, 161.48, 696.08	12.83, 167.38, 722.30
(0.5, 1.0)	14.12, 185.83, 801.75	14.74, 191.94, 827.81
(0.7, 1.0)	16.23, 213.75, 922.54	16.45, 216.25, 932.47
(1.0, 2.0)	3.25, 37.64, 160.67	3.96, 47.56, 203.77
(1.3, 2.0)	1.40, 12.81, 53.86	2.05, 21.11, 89.67
(1.5, 2.0)	1.05, 8.93, 37.05	1.64, 15.95, 67.71
$a = 10$		
(0.3, 1.0)	5.16, 63.13, 283.50	5.08, 63.04, 282.84
(0.5, 1.0)	6.88, 85.88, 374.46	6.76, 85.79, 372.81
(0.7, 1.0)	9.94, 128.07, 550.78	9.94, 126.53, 545.17
(1.0, 2.0)	2.24, 20.90, 89.15	2.59, 26.81, 114.32
(1.3, 2.0)	1.00, 3.60, 13.74	1.05, 6.39, 26.29
(1.5, 2.0)	1.00, 2.35, 8.24	1.00, 4.37, 17.33
$a = 15$		
(0.3, 1.0)	3.95, 46.27, 212.28	3.78, 43.92, 200.62
(0.5, 1.0)	5.08, 62.89, 281.90	4.88, 60.08, 268.82
(0.7, 1.0)	7.84, 99.56, 429.86	7.62, 94.44, 406.90
(1.0, 2.0)	1.95, 16.70, 70.83	2.24, 21.30, 90.03
(1.3, 2.0)	1.00, 2.13, 7.40	1.00, 3.72, 14.80
(1.5, 2.0)	1.00, 1.35, 4.49	1.00, 2.62, 9.16

## CONCLUSION

No attempt has been made to investigate the Shewhart MCV chart based on MRL and EMRL in the current literature. This paper proposes the two one-sided Shewhart MCV charts for monitoring the upward and downward MCV shifts and shift ranges based on MRL and EMRL. In the existing literature, the ARL performance measure should not be the only measure as it could potentially cause the chart's misinterpretation. The ARL performance measure may not be practically effective due to the inconsistency and excessive variations of the run-length distribution. It shows the importance of this study, in which the proposed charts can circumvent the drawbacks of using ARL, and at the same time, the biased performance of the two-sided MCV chart can be resolved. Additionally, the proposed

charts can be used by the practitioner who likes to implement an intermediate-type chart in the process monitoring. This intermediate framework is simple yet effective in terms of costs and time. The proposed charts provided the results based on the  $MRL_1$  and  $EMRL_1$  criteria. The variation and spread of the run-length distribution are discussed by referring to the run-length distribution's 5<sup>th</sup> and 95<sup>th</sup> percentiles. The effects of different parameter combinations on the proposed chart's performance are the sample size  $a$ , the number of quality characteristics  $b$ , the in-control MCV value  $\gamma_0$ , the MCV shifts (for MRL), and the MCV shift ranges (for EMRL) are investigated. The proposed charts can be investigated in the future by including measurement errors. It can help the practitioner obtain more accurate results when implementing the proposed charts in real-life manufacturing, healthcare, service, and finance processes.

## ACKNOWLEDGMENT

The Universiti Sains Malaysia supports this work, Short Term Grant [Grant Number: 304 / PKOMP / 6315616], with the project entitled "New Coefficient of Variation Control Charts based on Variable Charting Statistics in Industry 4.0 for the Quality Smart Manufacturing and Services."

## REFERENCES

- Adegoke, N. A., Dawod, A., Adeoti, O. A., Sanusi, R. A. & Abbasi, S. A. (2022). Monitoring the multivariate coefficient of variation for high dimensional processes. *Quality and Reliability Engineering International*, 38(5), 2606-2621. <https://doi.org/10.1002/qre.3094>
- Alharbi, S., Raun, W. R., Arnall, D. B., & Zhang, H. (2019). Prediction of maize (*Zea mays* L.) population using normalized-difference vegetative index (NDVI) and coefficient of variation (CV). *Journal of Plant Nutrition*, 42, 673-679. <https://doi.org/10.1080/01904167.2019.1568465>
- Calzada, M. E., & Scariano, S. M. (2013). A synthetic control chart for the coefficient of variation. *Journal of Statistical Computation and Simulation*, 83, 853-867. <https://doi.org/10.1080/00949655.2011.639772>
- Castagliola, P., Achouri, A., Taleb, H., Celano, G., & Psarakis, P. (2013). Monitoring the coefficient of variation using control charts with run rules. *Quality Technology & Quantitative Management*, 10, 75-94. <https://doi.org/10.1080/16843703.2013.11673309>
- Castagliola, P., Achouri, A., Taleb, H., Celano, G., & Psarakis, P. (2015). Monitoring the coefficient of variation using a variable sample size control chart. *The International Journal of Advanced Manufacturing Technology*, 80, 1561-1576. <https://doi.org/10.1007/s00170-015-7084-4>
- Castagliola, P., Celano, G., & Psarakis, S. (2011). Monitoring the coefficient of variation using EWMA charts. *Journal of Quality Technology*, 43, 249-265. <https://doi.org/10.1080/00224065.2011.11917861>
- Chakraborti, S. (2007). Run-length distribution and percentiles: The Shewhart  $\bar{X}$  chart with unknown parameters. *Quality Engineering*, 19, 119-127. <https://doi.org/10.1080/08982110701276653>

- Chanda, S., Kanke, Y., Dalen, M., Hoy, J., & Tubana, B. (2018). Coefficient of variation from vegetarian index for sugarcane population and stalk evaluation. *Agrosystems, Geosciences & Environment*, *1*, 1-9. <https://doi.org/10.2134/age2018.07.0016>
- Chew, M. H., Yeong, W. C., Talib, M. A., Lim, S. L., & Khaw, K. W. (2021). Evaluating the steady-state performance of the synthetic coefficient of variation chart. *Pertanika Journal of Science and Technology*, *29*(3), 2149-2173. <https://doi.org/10.47836/pjst.29.3.20>
- Chew, X. Y., Khaw, K. W., & Yeong, W. C. (2020). The efficiency of run rules schemes for the multivariate coefficient of variation: A Markov chain approach. *Journal of Applied Statistics*, *47*, 460-480. <https://doi.org/10.1080/02664763.2019.1643296>
- Chew, X. Y., Khoo, M. B. C., Khaw, K. W., Yeong, W. C., & Chong, Z. L. (2019). A proposed variable parameter control chart for monitoring the multivariate coefficient of variation. *Quality and Reliability Engineering International*, *35*, 2442-2461. <https://doi.org/10.1002/qre.2536>
- Doughty, M. J., & Aakre, B. M. (2008). Further analysis of assessments of the coefficient of variation of corneal endothelial cell areas from specular microscopic images. *Clinical and Experimental Optometry*, *91*, 438-446. <https://doi.org/10.1111/j.1444-0938.2008.00281.x>
- Gan, F. F. (1993). An optimal design of EWMA control charts based on median run length. *Journal of Statistical Computation and Simulation*, *45*, 169-184. <https://doi.org/10.1080/00949659308811479>
- Giner-Bosch, V., Tran, K. P., Castagliola, P., & Khoo, M. B. C. (2019). An EWMA control chart for the multivariate coefficient of variation. *Quality and Reliability Engineering International*, *35*, 1515-1541. <https://doi.org/10.1002/qre.2459>
- Huang, C. C., & Tang, T. (2007). Development of a new infrared device for monitoring the coefficient of variation in yarns. *Journal of Applied Polymer Science*, *106*, 2342-2349. <https://doi.org/10.1002/app.25441>
- Kang, C. W., Lee, M. S., Seong, Y. J., & Hawkins, D. M. (2007). A control chart for the coefficient of variation. *Journal of Quality Technology*, *39*, 151-158. <https://doi.org/10.1080/00224065.2007.11917682>
- Khatun, M., Khoo, M. B. C., Lee, M. H., & Castagliola, P. (2019). One-sided control charts for monitoring the coefficient of variation in short production runs. *Transactions of the Institute of Measurement and Control*, *41*, 1712-1728. <https://doi.org/10.1177/0142331218789481>
- Khaw, K. W., & Chew, X. Y. (2019). A re-evaluation of the run rules control charts for monitoring the coefficient of variation. *Statistics, Optimization & Information Computing*, *7*, 716-730. <https://doi.org/10.19139/soic-2310-5070-717>
- Khaw, K. W., Chew, X. Y., Lee, M. H., & Yeong, W. C. (2021). An optimal adaptive variable sample size scheme for the multivariate coefficient of variation. *Statistics, Optimization & Information Computing*, *9*, 681-693. <https://doi.org/10.19139/soic-2310-5070-996>
- Khaw, K. W., Chew, X. Y., Yeong, W. C., & Lim, S. L. (2019). Optimal design of the synthetic control chart for monitoring the multivariate coefficient of variation. *Chemometrics and Intelligent Laboratory Systems*, *186*, 33-40. <https://doi.org/10.1016/j.chemolab.2019.02.001>
- Khaw, K. W., Khoo, M. B. C., Castagliola, P., & Rahim, M. A. (2018). New adaptive control charts for monitoring the multivariate coefficient of variation. *Computers & Industrial Engineering*, *126*, 595-610. <https://doi.org/10.1016/j.cie.2018.10.016>

- Khaw, K. W., Khoo, M. B. C., Yeong, W. C., & Wu, Z. (2017). Monitoring the coefficient of variation using a variable sample size and sampling interval control chart. *Communications in Statistics - Simulation and Computation*, *46*, 5772-5794. <https://doi.org/10.1080/03610918.2016.1177074>
- Khoo, M. B. C., Wong, V. H., Wu, Z., & Castagliola, P. (2012). Optimal design of the synthetic chart for the process mean based on median run length. *IIE Transactions*, *44*, 765-779. <https://doi.org/10.1080/0740817X.2011.609526>
- Lee, M. H., Lim, V. Y. C., Chew, X. Y., Lau, M. F., Yakub, S., & Then, P. H. H. (2020). Design of the synthetic multivariate coefficient of variation chart based on the median run length. *Advances in Mathematics: Scientific Journal*, *9*, 7397-7406. <https://doi.org/10.37418/amsj.9.9.86>
- Lim, S. L., Yeong, W. C., Khoo, M. B. C., Chong, Z. L., & Khaw, K. W. (2019). An alternative design for the variable sample size coefficient of variation chart based on the median run length and expected median run length. *International Journal of Industrial Engineering: Theory, Applications, and Practice*, *26*, 199-220. <https://doi.org/10.23055/ijietap.2019.26.2.4085>
- Mahmood, T., & Abbasi, S. A. (2021). Efficient monitoring the coefficient of variation with an application to chemical reactor process. *Quality and Reliability Engineering International*, *37*, 1135-1149. <https://doi.org/10.1002/qre.2785>
- Mim, F. N., Saha, S., Khoo, M. B. C., & Khatun, M. (2019). A side-sensitive modified group runs control chart with auxiliary information to detect process mean shifts. *Pertanika Journal of Science and Technology*, *27*(2), 847-866.
- Mo, Y., Ma, X., Lu, J., Shen, Y., Wang, Y., Zhang, L., Lu, W., Zhu, W., Bao, Y., & Zhou, J. (2021). Defining the target value of the coefficient of variation by continuous glucose monitoring in Chinese people with diabetes. *Journal of Diabetes Investigation*, *12*, 1025-1034. <https://dx.doi.org/10.1111%2Fjdi.13453>
- Montgomery, D. C. (2013). *Statistical quality control: A modern introduction*. John Wiley & Sons, Inc.
- Ng, W. C., Khoo, M. B. C., Chong, Z. L., & Lee, M. H. (2022). Economic and economic-statistical designs of multivariate coefficient of variation chart. *REVSTAT-Statistical Journal*, *20*, 117-134. <https://doi.org/10.57805/revstat.v20i1.366>
- Nguyen, Q. T., Tran, K. P., Heuchenne, H. L., Nguyen, T. H., & Nguyen, H. D. (2019). Variable sampling Interval Shewhart control charts for monitoring the multivariate coefficient of variation. *Applied Stochastics Models in Business and Industry*, *35*, 1253-1268. <https://doi.org/10.1002/asmb.2472>
- Shriberg, L. D., Green, J. R., Campbell, T. F., Mcsweeny, J. L., & Scheer, A. R. (2003). A diagnostic marker for childhood apraxia of speech: The coefficient of variation ratio. *Clinical Linguistic & Phonetics*, *17*, 575-595. <https://doi.org/10.1080/0269920031000138141>
- Teoh, W. L., Chong, J. K., Khoo, M. B. C., Castagliola, P., & Yeong, W. C. (2017). Optimal designs of the variable sample size  $\bar{X}$  chart based on median run length and expected median run length. *Quality and Reliability Engineering International*, *33*, 121-134. <https://doi.org/10.1002/qre.1994>
- Tran, P. H., & Tran, K. P. (2016). The efficiency of CUSUM schemes for monitoring the coefficient of variation. *Applied Stochastic Models in Business and Industry*, *32*, 870-881. <https://doi.org/10.1002/asmb.2213>

- Voinov, V. G., & Nikulin, M. S. (1996). *Unbiased estimator and their applications, multivariate case* (2nd Ed.). Kluwer Publishing.
- Wijsman, R. A. (1957). Random orthogonal transformations and their use in some classical distribution problems in multivariate analysis. *The Annals of Mathematical Statistics*, 28, 415-423. <https://doi.org/10.1214/AOMS%2F1177706969>
- Yeong, W. C., Khoo, M. B. C., Teoh, W. L., & Castagliola, P. (2016). A control chart for the multivariate coefficient of variation. *Quality and Reliability Engineering International*, 32, 1213-1225. <https://doi.org/10.1002/qre.1828>
- Yeong, W. C., Lee, P. Y., Lim, S. L., Ng, P. S., & Khaw, K. W. (2021). Optimal designs of the side sensitive synthetic chart for the coefficient of variation based on median run length and expected median run length. *PLoS ONE*, 16, Article e0255366. <https://doi.org/10.1371/journal.pone.0255366>
- Yeong, W. C., Lim, S. L., Khoo, M. B. C., & Castagliola, P. (2018). Monitoring the coefficient of variation using a variable parameter chart. *Quality Engineering*, 30, 212-235. <https://doi.org/10.1080/08982112.2017.1310230>
- Yeong, W. C., Tan, Y. Y., Lim, S. L., Khaw, K. W., & Khoo, M. B. C. (2022). A variable sample size run sum coefficient of variation chart. *Quality and Reliability Engineering International*, 38, 1869-1885. <https://doi.org/10.1002/qre.3057>
- Zhang, J., Li, Z., Chen, B., & Wang, Z. (2014). A new exponentially weighted moving average control chart for monitoring the coefficient of variation. *Computers & Industrial Engineering*, 78, 205-212. <https://doi.org/10.1016/j.cie.2014.09.027>
- Zhou, Q., Zou, C., Wang, Z., & Jiang, W. (2012). Likelihood-based EWMA charts for monitoring Poisson count data with time-varying sample sizes. *Journal of the American Statistical Association*, 107, 1049-1062. <https://doi.org/10.1080/01621459.2012.682811>

# REFEREES FOR THE PERTANIKA JOURNAL OF SCIENCE & TECHNOLOGY

Vol. 31 (1) Jan. 2023

The Editorial Board of the Pertanika Journal of Science and Technology wishes to thank the following:

Abd Rahman Abdul Rahim  
(UTM, Malaysia)

Bhatia Amit  
(Amity University, India)

Kwong Qi Jie  
(UiTM, Malaysia)

Abraham Aworinde  
(Covenant University, Nigeria)

Che Zulzikrami Azner Abidin  
(UniMAP, Malaysia)

Lee Foo Wei  
(UTAR, Malaysia)

Agus Arsad  
(UTM, Malaysia)

Chua Han Bing  
(Curtin University, Malaysia)

Lee Teang Shui  
(UPM, Malaysia)

Ahmad Zhafran Ahmad Mazlan  
(USM, Malaysia)

Dayang Azra Awang Mat  
(UNIMAS, Malaysia)

Lim Wei Jer  
(Southern University College, Malaysia)

Ahmed Jalal Khan Chowdhury  
(IIUM, Malaysia)

Dzati Athiar Ramli  
(USM, Malaysia)

Low Kah Hin  
(UM, Malaysia)

Amnorzahira Amir  
(UiTM, Malaysia)

Edi Syams Zainudin  
(UPM, Malaysia)

Mahadimenakbar Mohd. Dawood  
(UMS, Malaysia)

Anuar Mikdad Muad  
(UKM, Malaysia)

Guang Yang  
(Imperial College London, UK)

Mai Mariam Mohamed  
Aminuddin  
(UTeM, Malaysia)

Anusha Achuthan  
(USM, Malaysia)

Gupta Surbhi  
(Amity University, India)

Maizatul Hayati Mohamad Yatim  
(UPSI, Malaysia)

Aqilah Baseri Huddin  
(UKM, Malaysia)

Halimatun Sakdiah Zainuddin  
(UPM, Malaysia)

Maz Jamilah Masnan  
(UniMAP, Malaysia)

Aslina Baharum  
(UMS, Malaysia)

Hazlina Hamdan  
(UPM, Malaysia)

Mohan Reddy Moola  
(Curtin University, Malaysia)

Aweng Eh Rak  
(UMK, Malaysia)

Hazrul Abdul Hamid  
(USM, Malaysia)

Mohd Firrdhaus Mohd  
Sahabuddin  
(UM, Malaysia)

Ayu Haslija Abu Bakar  
(UCSI University, Malaysia)

Iman Rousta  
(Yazd Universirt, Iran)

Mohd Hafis Sulaiman  
(UPM, Malaysia)

Aziah Daud  
(USM, Malaysia)

John Paul Tan Yusiong  
(UP, Philippines)

Mohd Hudzari Haji Razali  
(UiTM, Malaysia)

Azizan As'arry  
(UPM, Malaysia)

Joseph Babalola Agboola  
(University of Lagos, Nigeria)

Mohd Tahir Ismail  
(USM, Malaysia)

Azura Ishak  
(UKM, Malaysia)

Khairul Hamimah Abas  
(UTM, Malaysia)

Mohd Yusoff Ishak (UPM, Malaysia)	Rafidah Hanim Shueb (USM, Malaysia)	Shumpei Iehata (UMT, Malaysia)
Muthu Krishnan (KIT, India)	Raja Muhammad Zuha Raja Kamal Bashah (UKM, Malaysia)	Siti Hasnah Kamarudin (UiTM, Malaysia)
Muzalwana Abdul Talib <sup>†</sup> (UM, Malaysia)	Raja Rina Raja Ikram (UTeM, Malaysia)	Siti Nur Aliaa Roslan (UPM, Malaysia)
Nazatul Syadia Zainordin (UPM, Malaysia)	Razali Yaakob (UPM, Malaysia)	Sok Li Lim (UM, Malaysia)
Nik Raihan Nik Yusoff (UMK, Malaysia)	Riza Wirawan (ITB, Indonesia)	Teoh Sian Hoon (UiTM, Malaysia)
Noor Diyana Osman (USM, Malaysia)	Rosdi Daud (UMP, Malaysia)	Wan Mohd Rauhan Wan Hussin (UMT, Malaysia)
Noradila Nordin (UUM, Malaysia)	Roshida Abdul Majid (UTM, Malaysia)	Wan Mohd Zahiruddin Wan Mohammad (USM, Malaysia)
Norashikin Mohd Fauzi (UMK, Malaysia)	Saadah Hasan (UPM, Malaysia)	Wong Seng Yue (UM, Malaysia)
Norhafiz Azis (UPM, Malaysia)	Saadi Ahmad Kamaruddin (UUM, Malaysia)	Yap Soon Poh (UM, Malaysia)
Norharyati Harum (UTeM, Malaysia)	Saidatul Shima Jamari (UMP, Malaysia)	Yeong Wai Chung (UM, Malaysia)
Norshita Mat Nayan (UKM, Malaysia)	Sariah Saalah (UMS, Malaysia)	Zainab Ngaini (UNIMAS, Malaysia)
Norsyafina Roslan (UKM, Malaysia)	Sathya Shankara Sharma (MIT, India)	Zanariah Hashim (UTM, Malaysia)
Nurulnadwan Aziz (UiTM, Malaysia)	Sharifah Rahmah Syed Muhammad (UMT, Malaysia)	Zarirah Mohamed Zulperi (UPM, Malaysia)
Ooi Boon Yaik (UTAR, Malaysia)		

---

IIUM – International Islamic University Malaysia  
 ITB – Bandung Institute of Technology  
 KIT – Kalaignarkarananidhi Institute of Technology  
 MIT – Manipal Institute of Technology  
 UiTM – Universiti Teknologi MARA  
 UKM – Universiti Kebangsaan Malaysia  
 UM – Universiti Malaya  
 UMP – Universiti Malaysia Pahang  
 UMS – Universiti Malaysia Sabah  
 UMT – Universiti Malaysia Terengganu

---

UniMAP – Universiti Malaysia Perlis  
 UNIMAS – Universiti Malaysia Sarawak  
 UP – University of the Philippines  
 UPM – Universiti Putra Malaysia  
 UPSI – University Pendidikan Sultan Idris  
 USM – Universiti Sains Malaysia  
 UTAR – Universiti Tunku Abdul Rahman  
 UTeM – Universiti Teknikal Malaysia Melaka  
 UTM – Universiti Teknologi Malaysia  
 UUM – Universiti Utara Malaysia

---

While every effort has been made to include a complete list of referees for the period stated above, however if any name(s) have been omitted unintentionally or spelt incorrectly, please notify the Chief Executive Editor, *Pertanika* Journals at [executive\\_editor.pertanika@upm.edu.my](mailto:executive_editor.pertanika@upm.edu.my)

Any inclusion or exclusion of name(s) on this page does not commit the *Pertanika* Editorial Office, nor the UPM Press or the university to provide any liability for whatsoever reason.



<i>Review Article</i>	
Review of Window Performance in A Hot and Humid Climate	457
<i>Zinnirah Wellun, Wardah Fatimah Mohammad Yusoff, Mohd Farid Mohamed, Mohd Khairul Azhar Mat Sulaiman and Mohammad Rasidi Mohammad Rasani</i>	
Predicting Students' Inclination to TVET Enrolment Using Various Classifiers	475
<i>Chia Ming Hong, Chee Keong Ch'ng and Teh Raihana Nazirah Roslan</i>	
Water Quality Assessment and Characterization of Rivers in Pasir Gudang, Johor via Multivariate Statistical Techniques	495
<i>Muhammad Syafiq Mohamad Desa, Mohd Aeddy Sulaiman and Shantakumari Rajan</i>	
Ammonia-Nitrogen Reduction in Low Strength Domestic Wastewater by Polyvinyl Alcohol (PVA) Gel Beads	511
<i>Nordin Sabli and Norzarina Zakaria</i>	
Effects of Various Doses of <i>Saccharomyces cerevisiae</i> on the Growth, Survival Rate, and Blood Profile of Saline Red Tilapia ( <i>Oreochromis spp.</i> ) in the Semi-Intensive Culture Conditions	529
<i>Istiyanto Samidjan, Diana Rachmawati, Safar Dody and Putut Har Riyadi</i>	
<i>Review Article</i>	
Chitosan Nanocomposites as Wound Healing Materials: Advances in Processing Techniques and Mechanical Properties	543
<i>Temitope T. Dele-Afolabi, Azmah Hanim Mohamed Ariff, Oluwatosin J. Ojo- Kupoluyi and Ebenezer Oluwatosin Atoyebi</i>	
Brain Tumour Region Extraction Using Novel Self-Organising Map-Based KFCM Algorithm	577
<i>Peddamalla Gangadhara Reddy, Tirumala Ramashri and Kayam Lokesh Krishna</i>	
<i>Review Article</i>	
Reliability Components of Online Teaching and Learning Tools in Lesotho Higher Education Institutions: A Systematic Review	595
<i>Musa Adekunle Ayanwale, Paseka Andrew Mosia, Rethabile Rosemary Molefi and Liapeng Shata</i>	
Alternative Design of One-Sided Shewhart Control Charts for the Multivariate Coefficient of Variation	615
<i>XinYing Chew</i>	

Timekeeping and Immediate Monitoring of Employees by Consistently Advocating Time Consciousness and Honesty Using Enhanced Attendance Monitoring System (TIME CATCH Using EAMS) <i>Ronald Bautista Rivera, Maricar Bulan Asis and Oscar Gacutan Bangayan</i>	291
ESS-IoT: The Smart Waste Management System for General Household <i>Shen Yuong Wong, Huashuo Han, Kin Meng Cheng, Ah Choo Koo and Salman Yussof</i>	311
<i>Review Article</i>	
Some Abiotic and Biotic Factors Influencing Firefly Population Abundance in Southeast Asia: A Review <i>Nurhafizul Abu Seri, Azimah Abd Rahman and Nur Faeza Abu Kassim</i>	327
Optimization of the Formulation of Sago Starch Edible Coatings Incorporated with Nano Cellulose Fiber (CNF) <i>Rahmiyati Kasim, Nursigit Bintoro, Sri Rahayoe and Yudi Pranoto</i>	351
<i>Short Communication</i>	
Latent and Manifest Variables of PLS-SEM Model in the Decision Making of PIKNET Sound Wave-Based Attractor Innovation by Fishermen in Bulak Sub-District, Surabaya, Indonesia <i>Nurul Rosana, Nuddin Harahab, Gatot Ciptadi, Andi Kurniawan, Suryadhi, Safriudin Rifandi, Amirul Mukminin and Viv Djanat Prasita</i>	373
The Effect of Varying the HCl Solution on the Purity, Morphological, and Electrical Properties of Silicon Dioxide Extracted from Rice Straw <i>Nazopatul Patonah Har, Endah Kinarya Palupi, Rofiqul Umam, Aminullah, Md Wahadoszamen, Irmansyah and Irzaman</i>	389
Weed Detection in Soybean Crop Using Deep Neural Network <i>Vinayak Singh, Mahendra Kumar Gourisaria, Harshvardhan GM and Tanupriya Choudhury</i>	401
Failure Behavior and Mechanism of Pultruded Kenaf/Glass Hybrid Composite Under Compressive Impact Loading <i>Muhammad Fauzinizam Razali, Sareh Aiman Hilmi Abu Seman, Mohd Syakirin Rusdi and Megat Naiman Megat Anorhisham</i>	425
A Comparative Study on Dengue-related Knowledge, Attitude, and Practice in Hotspot and Non-Hotspot Areas in Selangor <i>Siti Nor Izani Mustapha, Shamarina Shohaimi, Mohd Bakri Adam, Meenakshii Nallappan, Abdul Hafiz Ab Rahman and Nader Salari</i>	437

Real-Time Traffic Sign Recognition Using Deep Learning <i>Ananya Belagodu Shivayogi, Nehal Chakravarthy Matasagara Dharmendra, Anala Maddur Ramakrishna and Kolala Nagaraju Subramanya</i>	137
<i>Review Article</i>	
A Systematic Review on an Optimal Dose of Disaster Preparedness Intervention Utilizing Health Belief Model Theory <i>Mohd Tariq Mhd Noor, Hayati Kadir Shahar, Mohd Rafee Baharudin, Sharifah Norkhadajah Syed Ismail, Rosliza Abdul Manaf, Salmiah Md Said, Jamilah Ahmad and Sri Ganesh Muthiah</i>	149
<i>Review Article</i>	
A Review: Requirements Prioritization Criteria Within Collaboration Perspective <i>Tan Amelia and Rozlina Mohamed</i>	161
Contamination and Human Health Risk Assessment of Toxic Trace Elements in Drinking Water of Gilgit-Baltistan, Pakistan <i>Syed Jarar Hussain, Shaukat Ali, Javid Hussain, Salar Ali, Jamal Hussain, Manzoor Hussain and Ittehad Hussain</i>	187
Development of Flood Hazard Index (FHI) of the Kelantan River Catchment Using Geographic Information System (GIS) Based Analytical Hierarchy Process (AHP) <i>Zulkarnain Hassan and Ain Nihla Kamarudzaman</i>	203
<i>Review Article</i>	
Fibre-Reinforced Soil Mixed Lime/Cement Additives: A Review <i>Sakina Tamassoki, Nik Norsyahariati Nik Daud, Mohammad Nazir Nejabi and Mohammad Jawed Roshan</i>	217
Technology Adoption for STEM Education in Higher Education: Students' Experience from Selected Sub-Saharan African Countries <i>Jumoke Iyabode Oladele, Musa Adekunle Ayanwale and Mdutshekelwa Ndlovu</i>	237
Towards Designing a Framework for Adaptive Gamification Learning Analytics in Quranic Memorisation <i>Siti Hasrinafasya Che Hassan, Syadiah Nor Wan Shamsuddin and Nor Hafizi Yusof</i>	257
<i>Review Article</i>	
A Review of Optical Ultrasound Imaging Modalities for Intravascular Imaging <i>Munyaradzi Charles Rushambwa, Rimer Suvendi, Thanyani Pandelani, Rajkumar Palaniappan, Vikneswaran Vijejan and Fizza Ghulam Nabi</i>	279

**Pertanika Journal of Science & Technology**  
**Vol. 31 (1) Jan. 2023**

**Content**

Foreword <i>Mohd Sapuan Salit</i>	i
Real-Time Monitoring of Oil Temperature in Distribution Power Transformer by Using Internet of Things <i>Shafrida Sahrani, Nur Darina Ahmad, Ramizi Mohamed, Mohd Aizam Talib and Chaw Jun Kit</i>	1
A Study on Features of Different Tone Quality in a Kenong Set <i>Ahmad Faudzi Musib, Sinin Hamdan and Saiful Hairi Othman</i>	17
Computational Analysis of Polymer Melt Filling in a Medical Mold Cavity During the Injection Molding Process <i>Muhammad Khalil Abdullah, Mohd Syakirin Rusdi, Mohd Zulkifly Abdullah, Abdus Samad Mahmud, Zulkifli Mohamad Ariff, Khor Chu Yee and Mohd Najib Ali Mokhtar</i>	33
Blade Fault Localization with the Use of Vibration Signals Through Artificial Neural Network: A Data-Driven Approach <i>Ngui Wai Keng, Mohd Salman Leong, Mohd Ibrahim Shapiai and Lim Meng Hee</i>	51
<i>Case Study</i> Structural Comparison of Naturally Aspirated and Turbocharged Diesel Engine for Steel and Aluminium Made Radiator: A Finite Element Study <i>Asad Munir, Muhammad Fauzinizam Razali, Nasir Iqbal and Muhammad Tahir Amin</i>	69
The Impacts of Passive Design Strategies on Building Indoor Temperature in Tropical Climate <i>Maryam Qays Oleiwi and Mohd Farid Mohamed</i>	83
Study of Metabolic Flux Distribution in Rice ( <i>Oryza sativa</i> ) Cultures for Starch Production <i>Nur Aqila Syafiq Abdul Nuri, Noor Illi Mohamad Puad, Muhammad Yusuf Abduh and Azlin Suhaida Azmi</i>	109
Prediction of Daily Air Pollutants Concentration and Air Pollutant Index Using Machine Learning Approach <i>Nurul A'isyah Mustakim, Ahmad Zia Ul-Saufie, Wan Nur Shaziayani, Norazian Mohamad Noor and Sofianita Mutalib</i>	123



Pertanika Editorial Office, Journal Division,  
Putra Science Park,  
1st Floor, IDEA Tower II,  
UPM-MTDC Center,  
Universiti Putra Malaysia,  
43400 UPM Serdang,  
Selangor Darul Ehsan  
Malaysia

<http://www.pertanika.upm.edu.my>  
Email: [executive\\_editor@upm.edu.my](mailto:executive_editor@upm.edu.my)  
Tel. No.: +603- 9769 1622

**PENERBIT**  
**UPM**  
UNIVERSITI PUTRA MALAYSIA  
**PRESS**

<http://www.penerbit.upm.edu.my>  
Email: [penerbit@upm.edu.my](mailto:penerbit@upm.edu.my)  
Tel. No.: +603- 9769 8851

